INTERNATIONAL SERIES IN PHYSICS

F. K. RICHTMYER, CONSULTING EDITOR

A STUDY OF CRYSTAL STRUCTURE AND ITS APPLICATIONS

INTERNATIONAL SERIES IN PHYSICS

LEE A. DuBRIDGE, *Consulting Editor*

Bacher and Goudsmit—ATOMIC ENERGY STATES

Bitter—INTRODUCTION TO FERROMAGNETISM

Clark—APPLIED X-RAYS

Condon and Morse—QUANTUM MECHANICS

Curtis—ELECTRICAL MEASUREMENTS

Davey—CRYSTAL STRUCTURE AND ITS APPLICATIONS

Edwards—ANALYTIC AND VECTOR MECHANICS

Eldridge—THE PHYSICAL BASIS OF THINGS

Hardy and Perrin—THE PRINCIPLES OF OPTICS

Harnwell—PRINCIPLES OF ELECTRICITY AND ELECTROMAGNETISM

Harnwell and Livingood—EXPERIMENTAL ATOMIC PHYSICS

Houston—PRINCIPLES OF MATHEMATICAL PHYSICS

Hughes and DuBridge—PHOTOELECTRIC PHENOMENA

Hund—HIGH-FREQUENCY MEASUREMENTS

Hund—PHENOMENA IN HIGH-FREQUENCY SYSTEMS

Kemble—THE FUNDAMENTAL PRINCIPLES OF QUANTUM MECHANICS

Kennard—KINETIC THEORY OF GASES

Koller—THE PHYSICS OF ELECTRON TUBES

Morse—VIBRATION AND SOUND

Muskat—THE FLOW OF HOMOGENEOUS FLUIDS THROUGH POROUS MEDIA

Pauling and Goudsmit—THE STRUCTURE OF LINE SPECTRA

Richtmyer and Kennard—INTRODUCTION TO MODERN PHYSICS

Ruark and Urey—ATOMS, MOLECULES AND QUANTA

Seitz—THE MODERN THEORY OF SOLIDS

Slater—INTRODUCTION TO CHEMICAL PHYSICS

Slater and Frank—INTRODUCTION TO THEORETICAL PHYSICS

Smythe—STATIC AND DYNAMIC ELECTRICITY

Stratton—ELECTROMAGNETIC THEORY

White—INTRODUCTION TO ATOMIC SPECTRA

Williams—MAGNETIC PHENOMENA

Dr. F. K. Richtmyer was consulting editor of the series from its inception in 1929 until his death in 1939.

A STUDY OF CRYSTAL STRUCTURE AND ITS APPLICATIONS

BY

WHEELER P. DAVEY, PH.D.

Research Professor of Physics and Chemistry, School of Chemistry and Physics, The Pennsylvania State College

FIRST EDITION

McGRAW-HILL BOOK COMPANY, INC.

NEW YORK AND LONDON

1934

COPYRIGHT, 1934, BY THE
McGRAW-HILL BOOK COMPANY, INC.

PRINTED IN THE UNITED STATES OF AMERICA

All rights reserved. This book, or parts thereof, may not be reproduced in any form without permission of the publishers.

THE MAPLE PRESS COMPANY, YORK, PA.

PREFACE

This book is written primarily for those who have the maturity and training to be expected of a college graduate in a modern curriculum in physics, physical chemistry and chemical physics, chemistry, or metallurgy.* The purpose of the book is to put such a person in possession of enough knowledge of the theory and technique of crystal analysis to enable him to read the literature intelligently and to do independent experimental work. The book does not attempt to be an encyclopedia of the theory of crystal analysis, nor is it a summary of the data to be found in the literature. Both of these needs have already been taken care of excellently by others. On the other hand, it presupposes a knowledge of the physics of x-rays and of x-ray equipment such as is reviewed in the first few chapters of G. L. Clark's "Applied X-rays."

The text, in its present form, is primarily the result of over fourteen semesters of classes of my own in crystal analysis at The Pennsylvania State College. The topics chosen for discussion, the order of presentation, and the specific illustrations used are those found by experience to meet the purpose of the book as stated above. The references given to the literature are not intended to be complete, but are intended to enable the reader to find easily those articles which fit the purpose of the book either because of content or because of the method of presentation, irrespective of the date of publication. In order to carry out the aim of the book the subject matter is made to fall under three main heads:

Necessary preliminary information about diffraction, crystal structure, etc.
Methods of crystal analysis.
Applications in physics, chemistry, and metallurgy of some of the information gained from studies in crystal structure.

In so far as possible, each chapter has been written in such a way as to require only an elementary knowledge of the content of the preceding chapters. The three main divisions of the book may therefore be taken up for serious study in any order that may best fit the needs of the individual reader, and in most cases the order of chapters within a division may be altered at will to suit the individual needs of students with highly specialized training.

* The text may be adapted to the needs of college seniors by omitting the following: (*a*) that portion of Chap. III which deals with the general equation for interplanar spacings; (*b*) the mathematical portion of the discussion of projection diagrams in Chap. IV; (*c*) Chaps. VII to X, XIV, and XV; (*d*) the last portion of Chap. XVI, which deals with diffraction effects in gases.

The first two main portions of the book are intended to enable the student to go into the laboratory and actually do experimental work on the structure of crystals, using well-recognized, standard methods of procedure. The third portion of the book is intended to point the way toward the use of crystal structure technique as a tool in still other fields of knowledge, and to aid the student in reading the growing body of literature written in the language of crystal structure. It is not to be expected that the reader with highly specialized training in some field of work will be entirely satisfied with that portion of the third part which deals with his specialty. Either he will find that the treatment of his own field is too elementary, or that it is too fragmentary or too one-sided. I hope, however, that this third portion is complete enough to fit in with the aim of the book and that it will help the student to find that body of information and to acquire those (sometimes unorthodox) viewpoints which will aid him in reading and in assaying the literature.

WHEELER P. DAVEY.

STATE COLLEGE, PA.
June, 1934.

ACKNOWLEDGMENTS

I have had the good fortune to have Mr. M. L. Fuller of the Research Division of the New Jersey Zinc Company give the benefit of his experience by writing Appendix I and a portion of Chap. XVII, and to have Dr. W. P. Jesse of the Research Laboratory of the General Electric Company write Chap. VII. To both of these men I wish to express my deepest gratitude. It is a pleasure, too, to express my thanks to Prof. W. L. Bragg and to Prof. A. H. Compton for permission to use their work and the work of their students as a basis for writing portions of Chaps. X, XI, and XVI; to The American Society for Steel Treating for permission to base Chap. XII on a paper of mine presented before the society [*Trans. Amer. Soc. Steel Treating*, **21**, 965–966 (1933)]; to Sir William H. Bragg for permission to use the Astbury and Yardley Tables in compiling Tables I to XXXII of Appendix III; to Prof. P. Niggli for permission to quote Table XLI of Appendix III from *Zeitschrift für Krystallographie;* and to E. C. Sanders, Editor of the *General Electric Review*, for permission to make use of material which I published in the Review many years ago under the encouragement of Dr. W. R. Whitney and Dr. W. D. Coolidge. It is also a pleasure to thank The Chemical Catalog Company for Figs. 17*a* and 17*b* of Chap. IV; J. B. Bernal for Figs. 17 and 18, and E. G. Cox for Fig. 20 of Chap. VII; C. W. Siller for the drawings of the point-groups in Chap. VIII; H. M. Cyr and L. C. Copeland for Figs. 1 to 4 of Chap. XII; F. E. Haworth for Fig. 6 of Appendix I; J. O. Wilhelm for the orthorhombic charts of Appendix II; and D. McLachlan for the projection charts of Appendix IV.

It is too much to expect that a book of this sort will be entirely free from errors. That it is as free as it is from errors of fact is due largely to the kind and helpful criticisms and corrections of many friends who have read various portions of the manuscript. Among these may be mentioned especially

H. V. Anderson, Lehigh University
E. A. Anderson, Research Division, New Jersey Zinc Company
W. L. Bragg, University of Manchester
G. L. Clark, University of Illinois
M. L. Fuller, Research Division, New Jersey Zinc Company
O. R. Grawe, Missouri School of Mines
C. B. Hollabaugh, Research Laboratory, Hercules Powder Company
A. P. Honess, The Pennsylvania State College
W. P. Jesse, Research Laboratory, General Electric Company
E. R. Jette, Columbia University

J. S. Marsh, Alloys of Iron Research of the Engineering Foundation
C. C. Murdock, Cornell University
W. W. Nicholas, Bureau of Standards
R. T. Phelps, Colorado School of Mines
O. L. Roberts, Research Laboratory, Atlantic Refining Company
A. E. Ruark, University of Pittsburgh
F. A. Steele, Research Division, New Jersey Zinc Company
R. W. G. Wyckoff, Rockefeller Institute for Medical Research

Much of the tedious labor of checking the proof has been borne by my wife and son and by the following graduate students: George R. Dean, Walter J. Haring, William E. McCormick, and Irwin Olcott.

For all expressions of opinion, for all statements of unorthodox theory, and for such errors of fact as may be found in the book, the author must assume full responsibility.

It is an especial pleasure to acknowledge the cooperation of successive classes in crystal analysis in the Graduate School of The Pennsylvania State College who have taken an active interest in helping to make the book self-consistent and in insuring the presentation of the subject in teachable form. If they have learned a tenth as much in studying the text as their teacher has learned in writing it, they have been amply repaid.

CONTENTS

PAGE

CHAPTER XVIII

CHAPTER XIX

APPENDIX I

APPENDIX II

APPENDIX III

APPENDIX IV

A STUDY OF CRYSTAL STRUCTURE AND ITS APPLICATIONS

CHAPTER I

THE THEORY OF DIFFRACTION OF X-RAYS BY A CRYSTAL

Practically all rigid solids except the glasses and possibly certain waxes are composed of crystals. It is known to every metallurgist that metals and their alloys exist in the form of crystals, and the crystalline state of most chemical compounds is universally accepted. Even cellulose, of which wood and cotton are largely composed, shows real evidence of crystallinity. It is therefore evident that any study of the properties of materials will be very largely a study of the crystalline state of matter. There is the same difference between crystalline and noncrystalline substances that there is between an army and a mob, for a crystal represents an organized array of atoms all arranged in definite rows with regular spacings between rows, while the atoms in a noncrystalline substance have a chaotic, hit-and-miss placing.

It has long been known that the mechanical and chemical properties of crystals depend markedly upon the direction in the crystal in which these properties are measured. It was early taken for granted that this was caused by the various rows of atoms acting as units so that the effect of one atom was added to that of its neighbor in a perfectly systematic way. For a long time this picture was necessarily rather hazy, for no means were at hand to measure the distances between the atoms in the various rows and the distances between rows. These distances are so minute that if an ordinary pinhead were magnified until its diameter became 100 miles, the distance between centers of adjacent atoms would be about one inch. Such measurements can now be made easily to within 1 part in 1,000 by means of the diffraction of x-rays. In other words, x-rays furnish us with a micrometer by which we can measure without difficulty a distance of 10^{-8} cm. with an accuracy of $\frac{1}{10}$ per cent.

A micrometer of this sort differs from an ordinary micrometer not only in the exceedingly small distances which it measures but also in the fact that these distances lie hidden in the body of the crystal itself. As is the case with other micrometers, the measurement of a small

distance is accomplished by measuring a relatively large distance (in this case, several centimeters) which is related to the desired distance by some known law. It will therefore be necessary to consider in detail the law of diffraction of x-rays and how this law may be made to relate large, easily measurable distances to the distances between atoms in crystals. In short, we must first study the theory of our micrometer.

Such a study must be combined with other information on the spatial relationships which are possible inside a crystal. This will then enable us to see how the interatomic distances in a crystal may be used to determine the arrangement in space of the atoms of which the crystal is composed. The knowledge, thus gained, of the structure of crystals is the starting point for a rapidly growing body of information which is of considerable theoretical and practical importance. From a knowledge of the structure of crystals it is possible to obtain information as to the sizes and shapes of atoms and ions, and to find valuable hints as to the mechanism of chemical combinations. Evidence is found leading to fundamental ideas in the theory of solid solutions and the inner structure of alloys, so that a more rational explanation may be made of certain metallurgical phenomena. Evidence may also be obtained of the effect of mechanical working on the orientation of crystals in metals, so that we may hope some time in the future to roll and draw metal better than we can today. This short résumé shows that a study of crystal structure is not only of interest to the so-called "pure scientist" working in physics, chemistry, and physical chemistry, but that it gives much promise of practical results to the metallographer and through him to almost every branch of industry.

DIFFRACTION OF X-RAYS

It was stated in the foregoing that the "micrometer" used in measuring interatomic distances is based upon the diffraction of x-rays. When x-rays of a given wave length strike a substance, part of the radiation is scattered so that it appears at every possible angle to the incident beam. If the scattering substance is a crystal, the scattered radiation is much more intense at certain angles than at others, *i.e.*, the x-rays are diffracted through definite angles. These angles depend upon the wave length of the x-rays employed and upon the arrangement and spacing of the atoms in the crystal. The distances measured in determining these angles and the relative intensities of the x-ray beams at these angles form the basis of study in x-ray crystallography.

Bragg's Law.—It is shown in elementary texts on physics that ordinary light can be diffracted from a plane grating. A crystal acts toward x-rays like a family of plane gratings placed one above the other. The introduction of *height* in addition to *width between lines* changes the final form of the diffraction law considerably. It may be shown experi-

mentally that this changes the diffraction law from the form found in texts on physical optics to the form known as Bragg's law:

$$n\lambda = 2d \sin \theta \tag{1}$$

where λ is the wave length of the x-rays and θ is the grazing angle of incidence between the x-ray beam and the diffracting family of atomic planes in the crystal. The experimental fact of the diffraction of x-rays according to Bragg's law may be explained either on the basis of the classical spreading-wave theory[1,2] or on the basis of the quantum theory.[3,4] A consideration of the two types of explanation shows that they give identical results.

Diffraction of a Spreading Wave.—According to the spreading-wave theory, x-rays and ordinary light are both thought of as being trains of

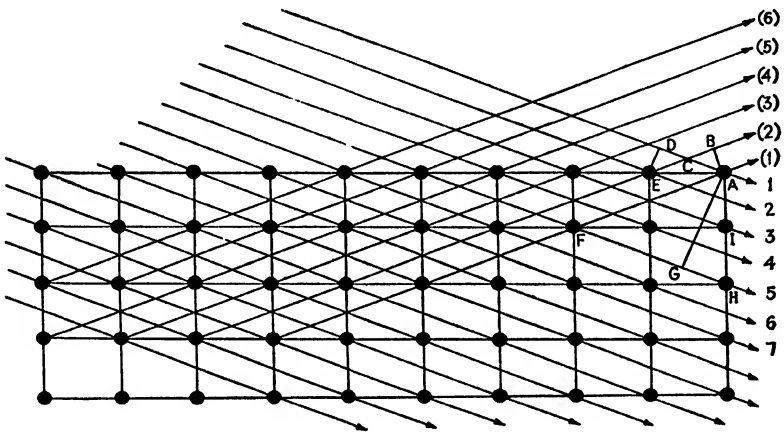

FIG. 1.—Diffraction of a plane wave by a crystal.

electromagnetic waves which tend to spread out in all directions from their source, *i.e.*, they tend to advance on a spherical wave front. The difference between ordinary light and x-rays is, according to this theory, merely a matter of wave length. The distance "from crest to crest" of an x-ray is supposed to be about one ten-thousandth as great as the corresponding distance for visible light.

Let the network of dots in Fig. 1 represent the atoms of a crystal, and let the crystal receive x-rays from a source sufficiently distant so that the wave fronts may be considered to be planes. Let the arrows 1, 2, 3 . . . represent normals to these wave fronts, and let the arrows (1), (2), (3) . . . represent the corresponding normals for the first order of the diffracted beam. Experimentally, it is found that the grazing angles of incidence and emergence are equal, *i.e.*, that $DAE = BEA$. Let AG be drawn perpendicular to FH. The path of the beam 5 to

the point G is equal in length to the path of the beam 1 to the point A. The difference in path length between the beam 1 at A and the beam 5 diffracted from F to A is GH, since FH is equal to FA. GH is equal to AH sin GAH. But the angle GAH is equal to the grazing angle of incidence DAE. Since AH is twice AI, *i.e.*, it is twice the interplanar distance d of the crystal, and since DAE is the grazing angle θ, we know the waves diffracted along (1) from incident beams 1 and 5 will meet in phase if

$$n\lambda = 2d \sin \theta \tag{1}$$

where n is any whole number and λ is the wave length of the x-rays employed. The integer represented by n is called the "order" of diffraction and is the number of wave lengths difference in the two paths. Similar beams such as (2), (3), (4) . . . will be in phase with beam (1); for let ED and AB be perpendicular respectively to 1 and (2). Then, since $BEA = DAE$, we have the two right triangles with an acute angle and hypotenuse of one equal to an acute angle and hypotenuse of the other. Therefore, the path EB equals the path DA, which is the condition for beams (1) and (2) being in phase with each other. In a similar manner it may be shown that (1) and (3), (1) and (4), etc., are all in phase.

It is therefore possible to have a whole wave front of diffracted x-rays emerging from a crystal at an angle equal to the angle of incidence, provided this angle is related to the wave length of the x-rays and the interplanar distance of the crystal in the manner shown by Eq. (1). It may be shown that, if the crystal were infinitely thick and offered no absorption to the x-rays, there could be no first-order diffracted beam at any other angle; for no matter what other angle we choose for diffraction from a given point in the crystal, there will be some other point which can send out a wave in the same direction which will meet the first wave a half wave length out of phase. Experimentally, it is found that it is sufficient if the crystal is about 10^3 molecules thick. If the crystals are too thin, the diffracted beam tends to widen because of incomplete interference at angles other than that which is equal to the angle of incidence.

The diffraction of x-rays by a crystal may be shown analytically as follows. The three-dimensional diffraction grating of a crystal may be regarded as composed of three sets of unidimensional gratings, each one of which consists of a row of atoms parallel to one of the three axes of the crystal. Let the interatomic distances along the three axes be x_1, y_1, and z_1. Let the directions of the incident and diffracted beams be expressed by their direction cosines α_1, β_1, γ_1 and α_2, β_2, γ_2, respectively. Then the conditions for diffraction along these three sets of linear gratings are

$$\begin{aligned} x_1(\alpha_2 - \alpha_1) &= e\lambda \\ y_1(\beta_2 - \beta_1) &= f\lambda \\ z_1(\gamma_2 - \gamma_1) &= g\lambda \end{aligned} \tag{2}$$

where e, f, and g are integers representing the order of the diffracted beam from each of the gratings.* In the simplest case, that of a cubic crystal, $x_1 = y_1 = z_1 = a$, the edge of the unit-cube. Remembering that

$$\alpha_1^2 + \beta_1^2 + \gamma_1^2 = \alpha_2^2 + \beta_2^2 + \gamma_2^2 = 1$$

we have by squaring and adding

$$2 - 2(\alpha_1\alpha_2 + \beta_1\beta_2 + \gamma_1\gamma_2) = \left(\frac{\lambda}{x_1}\right)^2 (e^2 + f^2 + g^2)$$

But, since, by a well-known theorem in trigonometry,

$$\alpha_1\alpha_2 + \beta_1\beta_2 + \gamma_1\gamma_2 = \cos\phi$$

where ϕ is the angle between the incident and the diffracted beams, and since

$$2(1 - \cos\phi) = 4\sin^2\frac{\phi}{2}$$

we have

$$2\sin\frac{\phi}{2} = \frac{\lambda}{x_1}\sqrt{e^2 + f^2 + g^2} \tag{3}$$

We may therefore calculate the angle of deviation ϕ from the wave length λ, the grating space x_1, and the orders of the diffraction patterns of the three sets of linear gratings.

* To arrive at the equation for diffraction by one of these three sets of linear gratings, consider a series of diffraction centers equally spaced along the line XX'. On striking the diffraction center A', the beam A will be diffracted in the direction $A'A''$. In the same way the beam B will be diffracted in the direction $B'B''$. Now, the path AA'' is longer than the path BB''. Diffraction can occur only if the difference in path length is equal to a whole number of wave lengths. To obtain a value for this path difference, drop the perpendiculars $A'G$ and $B'H$. The difference in the path lengths of AA'' and BB'' is given by $(A'H - GB')$. But $A'H$ is $A'B'$ cos $B'A'H$ and GB' is $A'B'$ cos $A'B'G$. Cos $B'A'H$ is, by definition, the direction cosine, α_2. Cos $A'B'G$ is, by definition, the direction cosine, α_1. The distance $A'B'$ is the interatomic distance x_1. We may therefore write as the condition for diffraction along the X-axis

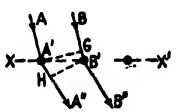

$$x_1(\alpha_2 - \alpha_1) = e\lambda$$

where e is an integer. Similarly for diffraction by the linear gratings along the Y- and Z-axes,

$$\begin{aligned} y_1(\beta_2 - \beta_1) &= f\lambda \\ z_1(\gamma_2 - \gamma_1) &= g\lambda \end{aligned}$$

Equation (3), derived in this way, may be regarded as typical of the viewpoint of Laue at the time of his discovery of x-ray diffraction. It may be expressed in terms of the more useful Bragg viewpoint as follows: A plane of atoms in a crystal is most commonly defined by its "Miller indices,"* which are the reciprocals of the intercepts of the plane upon the X-, Y-, and Z-axes, respectively. For instance, the (1 0 0) plane cuts the X-axis at unit distance and is parallel to the other two axes; it is the edge of a cube or of some other symmetrical figure. The (3 2 1) plane cuts the X-axis at $\frac{1}{3}$, the Y-axis at $\frac{1}{2}$, and the Z-axis at unity. It is customary to express these reciprocal intercepts in terms of their lowest prime numbers, so that, if the reciprocal intercepts are given as h, k, l, the actual reciprocal intercepts will be nh, nk, and nl, where n is any integer. If, therefore, we choose such a plane of atoms that

$$\begin{aligned} e &= nh \\ f &= nk \\ g &= nl \end{aligned}$$

we may regard the diffracted beam of Eq. (3) to be a diffracted beam of the nth order from the plane $(h\,k\,l)$.† Equation (3) may therefore be written

$$2 \sin \frac{\phi}{2} = \frac{\lambda}{x_1} n \sqrt{h^2 + k^2 + l^2}$$

or

$$n\lambda = 2 \frac{x_1}{\sqrt{h^2 + k^2 + l^2}} \cdot \sin \frac{\phi}{2} \tag{4}$$

It will be shown in Chap. III that $x_1/\sqrt{h^2 + k^2 + l^2}$ is the distance between successive $(h\,k\,l)$ planes. It is the d of Eq. (1).

The grazing angle of incidence (or the angle of diffraction) is $\phi/2$ and is the θ of Eq. (1). It is therefore evident that Eqs. (4) and (1) are identical. If, instead of confining ourselves to the cubic system, we had taken any other crystal system, we should have arrived at a new expression in the denominator of Eq. (4) which would represent

* Miller indices are treated at greater length in the next chapter.

† It should be noted that this substitution of nh, nk, and nl for e, f, and g, is only done as a matter of convenience in the study of crystal structure. A tiny crystallite may be so small that it does not contain representatives of many of the atomic planes found in larger crystals of the same substance yet it is theoretically capable of giving a diffraction pattern corresponding to every linear grating in the crystal. The changes to be made in Eq. (4) in such cases will be obvious. In the case of the crystallite, there will be a very rapid falling off in the sharpness and intensity of the diffracted beams with increasing angle of diffraction. For most practical purposes the effect is therefore somewhat the same as we should have had if diffraction had occurred only from individual families of planes which were actually present in the crystal.

the distance d between successive planes for that crystal system. Equation (1) is therefore perfectly general and applies to all types of crystals.

Diffraction of a Quantum.—In the preceding section on Diffraction of a Spreading Wave we have regarded an x-ray as a train of spherical waves of short wave length spreading out from a point source. The picture of an x-ray from the standpoint of the quantum theory may be given sufficiently well for our present purpose by regarding it as a wave train of very small cross-section (possibly of the order of 10^{-25} sq. cm.) proceeding out in a straight line from its source.[5] Any x-ray beam with which we ordinarily deal is supposed to contain an enormous number of these quanta coming out in all directions from the "focal spot" on the anode of an x-ray tube. In many ways, the whole bundle of quanta acts much like a train of spreading spherical waves, but the mechanism by which diffraction must be explained is quite different for quanta from that for spreading spherical waves.

According to the quantum theory, it is a characteristic of a quantum that its energy E determines the frequency of its waves, *i.e.*,

$$E = h\nu = \frac{hc}{\lambda} \tag{5}$$

where ν is the frequency, λ the wave length, c the velocity of light, and h is a proportionality constant known as "Planck's constant." If for any reason a quantum loses a portion of its energy, it must decrease the frequency of its waves until the new frequency multiplied by Planck's constant gives a product equal to the energy still remaining in the quantum. Since the wave has energy and has a definite velocity c it may be said (at least figuratively) to have mass and therefore momentum. It may be shown that the momentum of a quantum is*

$$M = \frac{h\nu}{c} = \frac{h}{\lambda} \tag{6}$$

The ordinary law of conservation of momentum which holds for the impact of material bodies is assumed to hold for the impact of quanta on atoms and electrons. It is further assumed that a quantum can give up momentum to an atom or electron in definite units. Since h has the dimensions of a momentum multiplied by a length,† it is assumed that the quantum unit of momentum is h/l where l is any length which may be shown to have a physical meaning in the diffracting substance.

* The kinetic energy of the electrostatic vector of the quantum is $\frac{1}{2}mc^2$. The kinetic energy of the electromagnetic vector of the quantum is also $\frac{1}{2}mc^2$. The total kinetic energy E of the x-ray quantum is therefore, mc^2. Its momentum M, is, by definition, mc. Evidently, then, $M = E/c = h\nu/c$.

† h has the dimensions $\frac{\text{energy}}{\text{frequency}} = ML^2T^{-1}$. Momentum has the dimensions mass $\times$ velocity $= MLT^{-1}$.

Let a quantum of x-rays fall upon a crystal as shown in Fig. 2, so as to make a grazing angle θ_1. At some point in its path it may hit an electron belonging to one of the atoms of the crystal and be deflected so that it emerges at an angle θ_2. The momentum transferred to the crystal in a direction parallel to the X-axis is

$$\frac{h\nu}{c}(\cos\theta_1 - \cos\theta_2) = n_1\frac{h}{x_1} \tag{7}$$

where the interatomic distance x_1 is the only length in the X-direction which has any physical meaning, and where n_1 is any positive integer including zero. Similarly, the momentum transferred in the Y-direction is

$$\frac{h\nu}{c}(\sin\theta_1 - \sin\theta_2) = n_2\frac{h}{y_1} \tag{8}$$

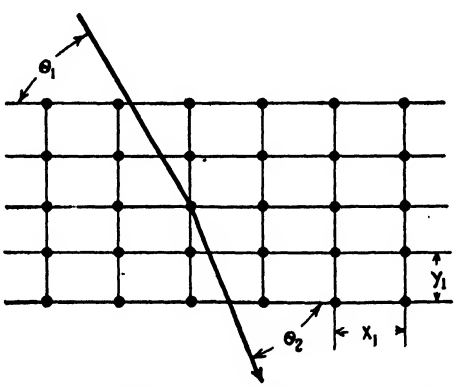

FIG. 2.—Diffraction of a quantum by a crystal.

If n_1 and n_2 are both zero, there is no transfer of momentum and no change in direction, so that the quantum passes on through until it hits an electron in some other atom. If n_1 is zero and n_2 is not zero, then $\cos\theta_1$ equals $\cos\theta_2$ but $\sin\theta_1$ does not equal $\sin\theta_2$. This means that $\sin\theta_1$ must be equal to $-\sin\theta_2$. Equation (8) therefore becomes

$$\frac{2h\nu}{c}\sin\theta_1 = n_2\frac{h}{y_1} \tag{9}$$

or

$$n_2\lambda = 2y_1\sin\theta_1 \tag{10}$$

which is identical with Eq. (1) for diffraction from the X-Z planes. Similarly, if n_2 is zero but n_1 is not zero,

$$n_1\lambda = 2x_1\sin(90° - \theta_1) \tag{11}$$

which represents diffraction from the Y-Z planes. Equations (10) and (11) may therefore be written in the form of Eq. (1)

$$n\lambda = 2d \sin \theta \qquad (1)$$

If n_1 and n_2 are both integers other than zero, Eqs. (7) and (8) give the same law of diffraction for still other families of planes in the crystal.

Exceptions to the Simple Form of Bragg's Law.—Equation (1) does not correlate all the known facts on the diffraction of x-rays. It is therefore necessary to extend the simple theories on which Eqs. (1), (10), and (11) were founded. It is found experimentally that, for a given crystal, Eq. (1) gives slightly higher values for wave lengths when n is small (1 or 2) than when n is larger. In the same way, if the wave length is assumed to be known, the first few lines in the diffraction pattern appear to be caused by interplanar spacings in the crystal which are slightly larger than those calculated from the second order of these same lines. This effect is explained as being caused by certain electrons in the atom having natural periods of vibration close to that of the incident beam of x-rays, thus giving the effect of a refractive index less than unity.[6]

Davis and v. Nardroff[7] have determined the refractive index of pyrites for four wave lengths and have compared their results with calculations based on the Lorentz dispersion formula

$$1 - \mu = \frac{e^2}{2\pi m}\left(\frac{n_1}{\nu^2 - \nu_1^2} + \frac{n_2}{\nu^2 - \nu_2^2} + \cdots\right)$$

where μ is the index of refraction, ν is the frequency of the incident beam, and n_1, n_2, . . . are the number of electrons per unit of volume having natural frequencies ν_1, ν_2, . . . , and e and m, as usual, represent the charge and mass of an electron. Their calculated and experimental values are compared in Table I.

When the planes of atoms from which the rays are diffracted are parallel to the surface of the crystal (as is the case when a cleavage face

TABLE I.—INDEX OF REFRACTION OF PYRITES CRYSTAL FOR X-RAYS

λ	$1 - \mu$, experimental	$1 - \mu$, calculated
0.6311Å.	2.82×10^{-6}	2.64×10^{-6}
0.7078	3.33	3.29
1.389	13.2	13.5
1.537	17.6	17.6

is used), the error caused by refraction is very small. For instance, the bending is only about three seconds of arc for the $K\alpha$ rays of Mo from

a cleavage face of calcite. This bending increases as the angle between the atomic planes and the crystal surface is increased. It is greater the shorter the wave length of x-rays employed. This is illustrated by the data of Table II from Davis and v. Nardroff for pyrites. Additional data on glass, tin, silver, selenium, and zinc have been published by Doan[8]

TABLE II.—EFFECT OF ANGLE AND WAVE LENGTH ON THE ANGLE OF BENDING OF X-RAYS

λ	Angle between crystal surface and atomic planes	Angle of bending of x-rays	$1 - \mu$, experimental	Weighted mean $1 - \mu$
0.7078Å.	0° 0′ 0″	3.6″	4.6×10^{-6}	
	6° 31′ 57.5″	39 ″	3.26×10^{-6}	
	7° 18′ 39″	159 ″	3.37×10^{-6}	3.33×10^{-6}
0.6311Å.	0° 0′ 0″	3 ″	3.87×10^{-6}	
	6° 31′ 57.5″	160 ″	2.82×10^{-6}	2.82×10^{-6}

and by Edwards,[9] and on aluminum by Davis and Slack.[10] For further details see a review of the subject by Bergen Davis in the *Journal of the Franklin Institute.*[11]

Because of the refraction of the rays, Bragg's law must be applied not to the original direction of the incident beam but to the direction of the refracted beam inside the crystal. It is hardly necessary to make this correction in the determination of the configuration of atoms in a crystal, since it affects only the exact size of the unit-crystal. Where the exact size of the unit-crystal is important (see Chap. VI), the experimental technique may be made such as to make the correction unnecessary.

PRIMARY AND SECONDARY STANDARDS FOR THE DETERMINATION OF *d* IN EQ. (1)

Equation (1) gives the relation between the wave length of x-rays and the interplanar spacing for diffraction at a given grazing angle. In order to determine one of these quantities by means of this equation it is necessary to know the other. Using the method of W. H. and W. L. Bragg[12] we may determine the dimensions of the unit-crystal* of NaCl as follows: A study of the diffraction patterns of NaCl and KCl shows that these patterns may be accounted for if these salts crystallize as simple cubes of ions, with the alkali and halogen ions occupying alternate

* The *unit-crystal* is the smallest crystal which can show the symmetry characteristics of the crystal. When the symmetry is cubic, the unit-crystal is called the *unit-cube;* when it is rhombohedral it is called the *unit-rhombohedron*, etc. The term "unit-crystal" is also sometimes applied loosely, as here, to represent the smallest portion of the crystal capable of showing the configuration of atoms.

corners of the cubes.* Since this is the simplest structure which accounts for the experimental facts, it will be adopted as the structure of NaCl. Each corner of one of the elementary cubes (unit-cubes) of the crystal contributes $\frac{1}{8}$ atom to the cube. The mass of the unit-cube of NaCl is therefore

$$[\tfrac{1}{8}A_{\mathrm{Na}} + \tfrac{1}{8}A_{\mathrm{Cl}}]m = \tfrac{1}{2}[A_{\mathrm{Na}} + A_{\mathrm{Cl}}]m$$

where A_{Na} = atomic weight of Na = 22.997.
A_{Cl} = atomic weight of Cl = 35.458.
m = mass in grams associated with one unit of atomic weight.

The factor m is most easily found as e/F, where e is the charge on the electron and F is the Faraday constant in electrolysis. Millikan[13] gives e as 4.774×10^{-10} absolute electrostatic unit (abs. e.s.u.) of charge or 1.591×10^{-19} absolute coulomb. The maximum error is about 0.1 per cent. Vinal and Bates[14] give F as 96,500 absolute coulombs with a maximum error of 0.01 per cent. The factor m is therefore 1.649×10^{-24} gram (g.).† This makes the mass of the unit-cube of NaCl equal to 4.820×10^{-23} g. If we divide the mass of the unit-cube of NaCl by the density, we obtain the volume of the unit-cube. From this we can calculate at once the length of the edge of the unit-cube.

Many values for the density of NaCl may be found in the literature. These differ among themselves considerably, partly due to impurities in the salt used by some of the workers and partly due to the difficulty of growing large crystal aggregates of NaCl free from voids or to the equally great difficulty of growing large single crystals of NaCl free from strains which, by reason of the dislocation of the atoms, tend to lower the effective density. The density of NaCl is given twice in the "International Critical Tables."[15,16] In Vol. I it is given as $d_4^{20} = 2.163$. In Vol. III it is given as

$$\begin{aligned} d_4^{20} &= 2.1680(1 - 20 \times 11.2 \times 10^{-5} - 400 \times 0.5 \times 10^{-7}) \\ &= 2.1631 \end{aligned}$$

This second value considers the work of the most careful workers up to the end of 1925, and we shall accept it as being the most reliable value obtainable by direct experiment. If we consider it to be in error by as much as 0.004, *i.e.*, 0.2 per cent, it has the largest percentage error of any of the items which enter into our calculations of volume. Even if the error in the value of m happens to affect the final result in the same direction as the error in the value of d, our value for the volume of the unit-cube of NaCl can be in error only by 0.3 per cent. This would give an uncertainty of only 0.1 per cent in our value for the edge of the

* See Fig. 7, Chap. V.

† This factor is given by R. T. Birge, *Phys. Rev. Supplement*, Vol. 1, No. 1 (1929) as $1.6489_8 \pm 0.0016 \times 10^{-24}$.

unit-cube. Denoting the length of the edge of the unit-cube by a_0, we would therefore have

$$a_{0_{NaCl}} = \sqrt[3]{\frac{4.820 \pm 0.005 \times 10^{-23}}{2.163 \pm 0.004}} = 2.814 \pm 0.002 \times 10^{-8} \text{ cm.}$$

It is, however, hardly possible that the above value of the density can be in error by more than ± 0.001, so that we may narrow down our value to

$$a_{0_{NaCl}} = 2.814 \pm 0.001 \times 10^{-8} \text{ cm.}$$

This agrees, within the precision of the underlying data, with the value 2.814×10^{-8} cm. used by Duane in his *Bulletin of the National Research Council* (November, 1920).

The density of calcite can be measured with greater accuracy than the density of NaCl since calcite can be obtained in large single crystals which are quite free from strains. For this reason, in the unit-rhombohedron of calcite whose faces are parallel to the cleavage planes, the distance between successive atomic planes which are parallel to the faces* is taken as the primary standard of length in all crystal-analysis work. The true value of the edge of the unit-cube of NaCl is determined from this as a secondary standard.[17,18,19] Optically clear calcite may contain Mn or Mg. Since both $MnCO_3$ and $MgCO_3$ have higher densities than those listed for calcite, it is clear that the lower the value reported in the literature, the more likely it is that the calcite was of high purity. Birge[20] gives as the best experimental value for the density of calcite, $d_{20} = 2.7102 \pm 0.0004$ g. per cubic centimeter. The interaxial angle of the cleavage rhombohedron of calcite is 101° 55′,[21,22] so that the volume of the unit-rhombohedron is $1.09630 \pm 0.00007 \times \left(a_{0_{CaCO_3}}\right)^3$ where $\left(a_{0_{CaCO_3}}\right)^3$ is the grating space of calcite. The molecular weight of $CaCO_3$ is[20]

$$\begin{array}{r} 40.075 \pm 0.005 \\ 12.003 \pm 0.001 \\ 48.000 \pm 0.000 \\ \hline 100.078 \pm 0.006 \end{array}$$

* As was pointed out by Wyckoff [*Amer. Jour. Sci.*, **50**, 317 (1920)] this is not the true theoretical unit of structure. It does, however, afford an easy way of visualizing the spacing between successive cleavage planes of calcite, *i.e.*, the crystal analyst's fundamental unit of length. It is, perhaps, only fair to say that crystal analysts practically never actually use calcite as a comparison standard (see Chap. VI) in measurements of interplanar spacings. Either they use NaCl ($a_0 = 2.814$Å.) or they arbitrarily adopt some measured wave length which they find in the literature or in some book such as Siegbahn's. The discrepancies introduced are usually of only academic interest.

It will be shown in a later chapter that a unit-rhombohedron, which for our present purposes may be considered as the unit of structure of calcite, contains one-half a molecule. Therefore

$$d_{20} = 2.7102 = \frac{\frac{1}{2} \times 100.078 \times 1.64898 \times 10^{-24}}{1.09630 a_0^3}$$

so that at 20°C.,

$$a_{0_{CaCO_3}} = 3.0283 \pm 0.0010 \times 10^{-8} \text{ cm.} \tag{12}$$

This is the primary standard of length used in all crystal-structure work. Diffraction experiments,[17,23] of which those of Siegbahn are probably the most accurate, show that the ratio

$$\frac{\text{Grating space of calcite}}{\text{Grating space of NaCl}} = 1.076417$$

(= $\log^{-1} 0.0319806$). This requires us to adopt for the true grating space of NaCl at 20°C. the value

$$a_{0_{NaCl}} = 2.8135 \pm 0.0010 \times 10^{-8} \text{ cm.}$$

This value again agrees, within the precision of the underlying data, with the value 2.8140×10^{-8} cm. proposed by Duane.[24] Since a large fraction of the published data is given in terms of Duane's value, it has become customary to consider the secondary standard of distance for crystal-structure work as

$$a_{0_{NaCl}} = 2.8140 \pm 0.0010 \times 10^{-8} \text{ cm.} \tag{13}$$

CdO crystallizes with the same type of structure as NaCl, but the crystals are more perfect and yield unusually sharp maxima in the diffraction pattern. For the same exposure time a much wider range of diffracted beams can be photographed from CdO than from NaCl. CdO has therefore been suggested[25] as a tertiary standard for practical laboratory work.

Both for spectroscopically pure CdO and for the "commercially pure" CdO containing traces of CO_2 and ZnO,

$$a_{0_{CdO}} = 4.681 \pm 0.002 \times 10^{-8} \text{ cm.} \tag{14}$$

It will be shown in a later chapter that it is sometimes convenient to have a standard of length in terms of the grating space of some element of higher atomic weight. For this reason the edges of the unit-cubes of Cu, W, and Au have been set up as additional tertiary standards,[26,27] with the following values at room temperature (approximately 20°C.):

$$a_{0_{Cu}} = 3.608 \pm 0.002 \times 10^{-8} \text{ cm.} \quad (15)$$

$$a_{0_{W}} = 3.155 \pm 0.001 \times 10^{-8} \text{ cm.} \quad (16)$$

$$a_{0_{Au}} = 4.065 \pm 0.004 \times 10^{-8} \text{ cm.} \quad (17)$$

Perhaps the best justification for the simple crystal structures assumed in the foregoing is the fact that wave lengths of x-rays, determined from Eq. (1) with the aid of these values of a_0, agree, within one quarter of a per cent, with the results of calculations based on the quantum theory[19] and with the results of diffraction of x-rays by a slit[28,29,30] and by a ruled grating.[31,32] Altogether the evidence forms a wonderfully coordinated body of experimental facts.

THE INTENSITY OF THE DIFFRACTED BEAM

The intensity of the diffracted beam will depend upon (1) the temperature, (2) the absorption of x-rays in the diffracting crystal, (3) the absorption of x-rays by non-diffracting material in the path of the beam, (4) the perfection of the crystal, (5) the wave length of the x-rays which are diffracted, (6) the distribution of electrons in the atoms of which the crystal is composed, and (7) the angle of diffraction.

1. The higher the temperature of a crystal, the less efficient it will be as a diffractor of x-rays. This is not surprising, for, although the heat motion will not alter the configuration of the mean positions of the atoms in the crystal, it will alter the fraction of the total number of atoms which at any one instant are arranged in a truly orderly array. The atoms which, at a given instant, are not in their mean positions do not diffract the x-rays with the correct phase. The resultant diffracted beam is therefore weaker than it would have been at absolute zero. This effect was predicted by Debye[33] and has since been studied by several workers.[34] Theory and experiment agree that the effect of temperature may be accounted for by inserting into some formula for the intensity of a diffracted beam a factor of the form

$$D = e^{-B \sin^2 \theta} \quad (18)$$

where θ is, as always, the angle between the incident beam of x-rays and the diffracting planes of atoms in the crystal. The quantity B has been a subject for debate. It can be determined experimentally for any given substance over a definite temperature range (for instance, at room temperature it is 6.44 for NaCl[35]), but the theoretical expression for B depends upon the assumptions adopted in building up a theory of heat motions.*

* If we assume the Maxwell-Boltzmann equation, then

$$B = \frac{16\pi^2 kT}{f\lambda^2}$$

in which λ is the wave length of x-rays used, f is the force per unit displacement on the atom, T is the absolute temperature, and k is the Boltzmann constant. If we assume

2. By the absorption of x-rays in the diffracting crystal is meant here the absorption which would be present even if the atoms of the crystal could be caused to take up chaotic (truly amorphous) positions which would prevent diffraction. For any one wave length, this simple sort of absorption follows the ordinary optical law

$$I = I_0 e^{-\mu x}$$

in which I is the intensity of x-rays after absorption by a thickness x, I_0 is the intensity of the incident x-rays, and e is the base of natural logarithms; μ is called the "coefficient of absorption."

Consider two crystals of the same material which are made to diffract x-rays of the same wave length from the same type of atomic planes. It is evident that both crystals will have the same grazing angle of incidence between the x-ray beam and the diffracting plane. But if both crystals do not have precisely the same exterior shape, it is possible that one will offer a longer path to the x-rays than the other, and the additional absorption along the longer path will cause it to give off a weaker diffracted beam. This effect was found by B. Davis and his coworkers to be important in their study of the refraction effects noted earlier in this chapter.

In the Laue method of crystal analysis, which will be discussed in Chap. IV, different wave lengths of x-rays are used simultaneously, and each diffracts at a different angle. In such a case the intensity of the diffracted beam depends not only upon the coefficient of absorption of the crystal for each wave length used but also upon the length of the path through the crystal for each of the diffracted beams.

3. In all experimental work in crystal structure great care is taken to have as little extraneous absorbing material as possible in the path of the x-rays. This extraneous material ordinarily includes the walls of the x-ray tube, the air in the path of the beam, and either the window of an ionizing chamber or the light-tight envelope of a photographic film. In the case of the powder method of crystal analysis, which will be discussed in Chap. VI, it also includes (1) those crystal fragments

---

Debye's theory of specific heat, as modified by Born and Karman, and assume the absence of energy at absolute zero,

$$B = \frac{6h^2T}{\mu k\lambda^2\Theta^2} \cdot \phi\left(\frac{\Theta}{T}\right)$$

where h is Planck's constant, T is the absolute temperature, μ is the mass of an atom, k is Boltzmann's constant, λ is the wave length of the x-rays, Θ is a temperature which is characteristic of the crystal, and $\phi(\Theta/T)$ is some function of (Θ/T).

If we assume the existence of a zero-point energy,

$$B = \frac{6h^2}{\mu k\lambda^2\Theta}\left\{\frac{1}{4} - \frac{\phi(\Theta/T)}{\Theta/T}\right\}$$

which do not happen to be oriented at the correct angle to diffract the x-ray beam from the atomic plane under consideration and (2) usually also some container (such as a glass or celluloid tube) for the powdered crystal.

4. Consider a perfect crystal in the path of a "monochromatic" x-ray beam, and let it be so oriented that no atomic planes are at the correct angle for diffraction. Its coefficient of absorption for the x-ray beam will then be the same as if the material had been amorphous instead of crystalline. If now we orient the crystal so that some one family of atomic planes diffracts the x-ray beam, the energy of the incident beam in the interior will be decreased by the energy diffracted by the surface planes of atoms. The result is the same as if the coefficient of absorption of the crystal had been suddenly increased when the correct orientation for diffraction had been reached. This effect is called "primary extinction."[36] It is evident that, if the crystal is made up of atoms of any but the very lightest elements, and if x-rays of ordinary wave length are used, the combined effect of absorption and of primary extinction will cause most of the diffracted wave to come from a relatively thin layer near the surface. Primary extinction, then, has to do with the effect of the diffracting process on the amplitude of a single diffracted wave coming from a perfect crystal. It is the loss in energy of an x-ray beam as it progresses through a perfect crystal caused by the diffraction of the energy by that crystal.

Now consider an imperfect crystal made up of a mosaic of very tiny crystals whose orientations, although not identical, are so nearly the same that the aggregate looks like a single crystal even under the microscope.* If a beam of monochromatic rays strikes such a crystal at the correct angle for diffraction for some of the tiny crystals, it will also strike adjacent tiny crystals which, by reason of their slightly different orientation, cannot diffract the rays but will permit them to pass through freely subject only to the ordinary laws of absorption. The interior of such an imperfect crystal is therefore able to receive and diffract x-rays some of which would never have reached it except for the imperfections of the crystal. The diffracted beam therefore represents the resultant of a multitude of diffracted beams, all practically in phase with each other, each originating from its own tiny crystal. The intensity of this resultant diffracted wave is not so great as would be expected on the basis of the ordinary laws of absorption, for the incident beam will be weakened by the primary extinction of those tiny crystals near the surface which happen to be at the correct orientation to diffract the wave length present in the beam. This loss in intensity of the incident beam is called "secondary extinction."[36] It is the loss in energy of an x-ray beam as it progresses through an imperfect crystal

* It will be shown in Chap. XII that imperfection is the natural state of a crystal.

and is caused by the summation of the primary extinctions in all the tiny perfect crystals which contribute toward the diffracted beam from the aggregate which we have called an imperfect crystal.

Theoretical formulas for the intensity of the diffracted beam have been derived for the two extreme cases: (*a*) an ideally perfect crystal, and (*b*) an ideally imperfect crystal. Experiment shows that all crystals belong somewhere between these two ideal states, for the intensities of their diffracting beams lie between the two intensities calculated for (*a*) and (*b*). The subject of imperfections in crystals will be taken up more fully in a later chapter. It will be sufficient to point out here that very few crystals have been found which even begin to approach ideal perfection. Nearly all crystals approach more or less closely the state of ideal imperfection. Probably the three most perfect crystals known are the crystals of calcite examined by B. Davis and W. M. Stempel[37] and B. Davis and H. Purks,[38] and the diamond examined by H. Mark.[39]

5. The theoretical formula[36] for the amplitude of the wave diffracted by an ideally perfect crystal includes in the numerator the square of the wave length. The corresponding formula for the intensity of the wave diffracted by an ideally imperfect crystal[36] includes in the numerator the cube of the wave length. We may therefore assume that the efficiency of diffraction for most crystals varies approximately as the cube of the wave length of x-rays used, but that in exceptional cases (as in the case of some calcite or diamond) it will vary approximately as the square of the wave length.

6. It is assumed that, when x-rays are diffracted, the actual diffracting centers are the electrons which compose the extranuclear portion of the atoms in the crystal. Whether we assume these electrons to be stationary (static-atom theory) or whether we assume them to be in motion around the nucleus (Bohr-Sommerfeld theory, etc.), it is hard to escape the conclusion that the x-rays diffracted from one electron must be somewhat out of phase with the x-rays diffracted by some other electron in the same atom. The total intensity of any beam of x-rays diffracted by a crystal would be expected to depend upon the distribution of electrons in the atoms of which the crystal is composed. In a later chapter we shall discuss the use of intensities in the determination of crystal structure and the attempt to use this as a tool in the investigation of atomic structure.

SUMMARY

The outstanding experimental facts of the diffraction of x-rays may be accounted for by Bragg's law on the basis of either the spreading-wave or the quantum theory of x-rays, and the apparent exceptions to the law may be satisfactorily explained. In terms of the densities

and the structures of certain crystals it is possible to set up trustworthy standards of length for use with Bragg's law. The factors have been discussed which affect the intensities of diffracted x-ray beams.

We must now study the different systems of crystals and the calculation of their various interplanar spacings so that we may have at our disposal all of the information necessary for a preliminary investigation of crystal structure.

References

1. W. H. and W. L. Bragg, "X-Rays and Crystal Structure," Chap. II, George Bell & Sons, London, 1915.
2. P. P. Ewald, "Krystalle und Roentgenstrahlen," Julius Springer, Berlin, 1923.
3. Wm. Duane, *Proc. Nat. Acad. Sci.*, **9**, 158 (1923).
4. A. H. Compton, *Proc. Nat. Acad. Sci.*, **9**, 359 (1923).
5. W. P. Davey, *Jour. Franklin Inst.*, **197**, 439, 629 (1924).
6. C. G. Darwin, *Phil. Mag.*, **27**, 315 (1914).
   W. Stentrom, Doctor's Dissertation, Lund (1919).
   E. Hjalmar, *Zeit. Physik*, **7**, 341 (1921).
   B. Davis and H. M. Terrill, *Proc. Nat. Acad. Sci.*, **8**, 357 (1922).
   P. P. Ewald, *Zeit. Physik*, **30**, 1 (1924).
7. B. Davis and R. v. Nardroff, *Proc. Nat. Acad. Sci.*, **10**, 60, 384 (1924), and in private communication.
   R. v. Nardroff, *Phys. Rev.*, **24**, 143 (1924).
   C. C. Hatley, *Phys. Rev.*, **24**, 486 (1924).
8. R. L. Doan, *Phil. Mag.*, **4**, 100 (1927).
9. H. W. Edwards, *Phys. Rev.*, **30**, 91 (1927).
10. B. Davis and C. M. Slack, *Phys. Rev.*, **27**, 18 (1926).
11. B. Davis, *Jour. Franklin Inst.*, **204**, 29 (1927).
12. W. H. and W. L. Bragg, *Proc. Roy. Soc.*, **88**, 428 (1913).
13. R. A. Millikan, *Phys. Rev.*, **2**, 109 (1913); *Phil. Mag.*, **34**, 1 (1917).
14. G. W. Vinal and S. J. Bates, *Bull. Bur. Standards*, **10**, 425 (1914).
15. "International Critical Tables," Vol. I, p. 150, McGraw-Hill Book Company, Inc., New York, 1926.
16. "International Critical Tables," Vol. III, p. 43.
17. M. Siegbahn, *Phil. Mag.*, **37**, 601 (1919).
18. Wm. Duane, *Bull. Nat. Research Council*, Vol. 1, No. 6, p. 383 (1920).
19. L. W. McKeehan, *Science*, **56**, 757 (1922).
20. R. T. Birge, *Phys. Rev. Supplement*, Vol. 1, No. 1 (1929).
21. P. Groth, *Chemische Krystallographie*, **2**, 204 (1908).
22. H. S. Uhler, *Phys. Rev.*, **12**, 39 (1918).
23. H. S. Uhler and C. D. Cooksey, *Phys. Rev.*, **10**, 645 (1917).
    A. H. Compton, H. N. Beets, and O. K. De Foe, *Phys. Rev.*, **25**, 625 (1925).
24. Wm. Duane, *Bull. Nat. Research Council*, **1**, 383 (1920).
25. M. L. Fuller, *Phil. Mag.*, **8**, 585 (1929). See also J. Brentano and J. Adamson, *Phil. Mag.*, **7**, 507 (1929).
26. W. P. Davey, *Phys. Rev.*, **25**, 753 (1925); **26**, 736 (1925).
27. R. A. Patterson, *Phys. Rev.*, **26**, 56 (1925).
28. Haga and Wind, *Wied. Ann.*, **68**, 884 (1899).
29. B. Walter, *Ann. Physik*, **75**, 189 (1924).
30. I. I. Rabinov, *Proc. Nat. Acad. Sci.*, **11**, 222 (1925).
31. A. H. Compton and R. L. Doan, *Proc. Nat. Acad. Sci.*, **11**, 598 (1925).

32. J. THIBAUD, *Compt. rend.*, **182**, 55 (1926).
33. P. DEBYE, *Verh. deut. phys. Ges.*, **15**, 678, 738, 857 (1913); *Ann. Physik*, **43**, 49 (1913).
34. W. H. BRAGG, *Phil. Mag.*, **27**, 881 (1914).
C. G. DARWIN, *Phil. Mag.*, **27**, 315 (1914).
L. BRILLOUIN, *Ann. physique*, **17**, 88 (1922).
I. BACKHURST, *Proc. Roy. Soc.*, **102**, 340 (1922).
G. E. M. JAUNCEY, *Phys. Rev.*, **20**, 405, 421 (1922).
H. FAXEN, *Zeit. Physik*, **17**, 266 (1923).
L. WALLER, *Zeit. Physik*, **17**, 398 (1923).
E. H. COLLINS, *Phys. Rev.*, **24**, 152 (1924).
R. W. JAMES, *Phil. Mag.*, **49**, 585 (1925); *Manchester Phil. Soc., Mem.* **71**, 9 (1926–1927).
R. W. JAMES and E. M. FIRTH, *Proc. Roy. Soc.*, **117**, 62 (1927).
I. WALLER and R. W. JAMES, *Proc. Roy. Soc.*, **117**, 214 (1927).
35. W. L. BRAGG, C. G. DARWIN, and R. W. JAMES, *Phil. Mag.*, **1**, 897 (1926).
36. C. G. DARWIN, *Phil. Mag.*, **27**, 315, 675 (1914).
W. L. BRAGG, R. W. JAMES, and C. H. BOSANQUET, *Phil. Mag.*, **41**, 309 (1921); **42**, 1 (1921); **44**, 433 (1922).
C. G. DARWIN, *Phil. Mag.*, **43**, 800 (1922).
W. L. BRAGG, C. G. DARWIN, and R. W. JAMES, *Phil. Mag.*, **1**, 897 (1926).
See also:
E. WAGNER and H. KULENKAMPFF, *Ann. Physik*, **68**, 369 (1922).
O. L. SPONSLER, *Phys. Rev.*, **23**, 662 (1924).
R. J. HAVIGHURST, *Proc. Nat. Acad. Sci.*, **12**, 375 (1926).
M. v. LAUE, *Zeit. Kryst.*, **64**, 115 (1926).
J. BRENTANO, *Phil. Mag.*, **4**, 620 (1927).
37. B. DAVIS and W. H. STEMPEL, *Phys. Rev.*, **17**, 608 (1921).
38. B. DAVIS and H. PURKS, *Phys. Rev.*, **34**, 181 (1929).
39. H. MARK, *Naturwissenschaften*, **13**, 1042 (1925).
W. EHRENBERG, P. P. EWALD, and H. MARK, *Zeit. Kryst.*, **66**, 547 (1928).

CHAPTER II

CRYSTAL LATTICES

THE SIX SYSTEMS OF CRYSTALS

If a crystal such as rock salt (NaCl) is crushed, it is found that the fragments have the same angles between their faces that the original crystal had. Other crystals such as calcite ($CaCO_3$) give fragments which, although having angles between the faces different from the original, are all alike in shape and show the same symmetry characteristics as the original crystal. When these crystal fragments are again crushed the resulting particles all have the same shape as the original

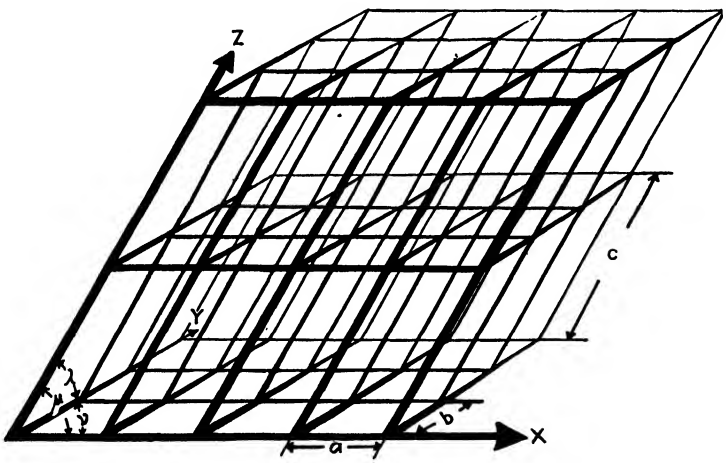

FIG. 1.—A space lattice.

fragments, and measurement shows that the angles between their faces are identical with the angles between the corresponding faces of the original fragments. Experiments of this sort indicate that the external form of a crystal results from a systematic arrangement of the atoms of which it is composed. As a result of studies on x-ray diffraction patterns of crystals, this assumption is now universally accepted. A large portion of the work of a crystal analyst consists in the determination of these systematic arrangements of the atoms in crystals. Only rarely, however, is such work an end in itself. It is usually a tool which aids in the attainment of some other end, such as a study of the nature of chemical combinations, the construction of temperature-constitution

diagrams, a study of the nature of alloys, the identification of materials, or the correlation of crystal structure with physical properties.

As an aid in visualizing the configuration of atoms in a crystal let us consider a three-dimensional lattice-work, such as is shown in Fig. 1, built up of imaginary straight lines in such a way that they outline a group of imaginary symmetrical prisms (for instance, cubes, hexagonal prisms, or rhombohedra), all of equal size and all in close contact with their neighbors. In the simplest cases (which are the only ones treated in this chapter) we may imagine atoms placed at each of the intersections of the lattice lines, or placed at some position (such as the body-center of a cube) which may be easily defined by reference to the lattice intersections. In more complicated cases (see Chap. VIII) whole groups of atoms may be placed so that some reference point in each group lies at a lattice point.

A three-dimensional lattice-work of imaginary lines such as we have described is called a *space-lattice.** Only 14 types of space-lattices are possible. They fall into six systems, called the triclinic, monoclinic, orthorhombic, tetragonal, cubic, and hexagonal systems. A space-lattice must have its imaginary lines parallel, respectively, to each of three definite directions corresponding more or less roughly to the directions of length, width, and height. Three of these lines which meet at a common point are chosen as reference lines, and are called the X-axis, Y-axis, and Z-axis, respectively. The distance between successive intersections of the lines of the space-lattice along the X-axis is called a. The corresponding distances along the Y- and the Z-axes are called b and c, respectively. If the angles between the Y- and Z-axes, X- and Z-axes, and X- and Y-axes are called λ, μ, and ν, respectively, we may define the six systems of space-lattices as follows:

Triclinic system:

$$\lambda \neq \mu \neq \nu$$
$$a \neq b \neq c$$

Monoclinic† system:

$$\lambda = \mu = 90°$$
$$\nu \neq 90° \neq 120°$$
$$a \neq b \neq c$$

Orthorhombic system:

$$\lambda = \mu = \nu = 90°$$
$$a \neq b \neq c$$

* The terms *point-group* and *space-group* are defined in Chap. VIII.

† Crystallographers ordinarily use the convention that $\lambda = \nu = 90°$. In crystal-structure work the departure from convention is justified because, if $\lambda = \mu = 90°$, the hexagonal system becomes a special case of the monoclinic system, thus facilitating the derivation of the equation for interplanar spacings in the hexagonal system.

Tetragonal system:

$$\lambda = \mu = \nu = 90°$$
$$a = b \neq c$$

Cubic system:

$$\lambda = \mu = \nu = 90°$$
$$a = b = c$$

Hexagonal system:

$$\lambda = \mu = 90°$$
$$\nu = 120°$$
$$a = b \neq c$$

Axial Ratio.—When a, b, and c are not all equal, it is customary to take the value of b as the basis of measurement, expressing a and c in terms of b by means of the ratios $A(=a/b)$ and $C(=c/b)$, respectively. These ratios are called the "axial ratios" of the crystal. A crystal belonging to the triclinic, monoclinic, or orthorhombic system would have two axial ratios, namely, A and C. A crystal belonging to the tetragonal or hexagonal system would have only one designated axial ratio, namely, C, since $A = 1$. A cubic crystal obviously has no designated axial ratio, since for a cubic crystal $A = C = 1$ by definition.

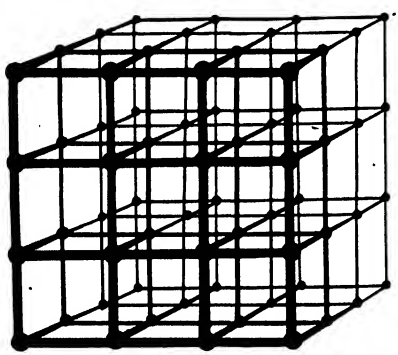

FIG. 2.—Simple cubic lattice.

Cubic Lattices.—Since the cubic lattices are the easiest to visualize, we shall describe them in some detail as an introduction to a more general discussion of space-lattices. The simplest possible cubic lattice is illustrated in Fig. 2. It is called a "simple cubic lattice." A chemical element crystallizing on such a lattice would have to have one atom at each of the lattice intersections.

Actually there are no elements which are simple cubic, but certain compounds such as KCl give all the x-ray diffraction effects of a simple cubic element. The K^+ and Cl^- ions occupy alternate intersections of a simple cubic lattice and both have the same number of electrons (18) outside the nucleus so that their diffracting powers are practically identical. From an x-ray diffraction standpoint, therefore, KCl simulates a simple cubic chemical element.

A simple cubic crystal may be thought of as being built up of unit-cubes so placed together that each one shares its corners, edges, and faces with its neighbors. It is at once evident that this structure requires

each atom in the interior of the crystal to belong equally to eight cubes at once so that, if the lattice were of infinite extent, it would require an average of one atom per unit-cube.

Not all cubic crystals have this simple structure. Additional atoms may be placed in symmetrical positions in the lattice to give more or less complicated structures which still retain many of the cubic characteristics of the simple cubic crystal. For instance, an additional atom may be placed at the center of each unit-cube. Such a unit-cube, shown in Fig. 3, is called a "body-centered cube." It is evident that, if this lattice were of infinite extent, it would require two atoms per unit-cube. A body-centered cubic lattice may be thought of as composed of two interpenetrating simple cubic lattices so placed with respect to each other that the corners of the unit-cubes of one lattice lie at the centers of the unit-cubes of the other lattice.

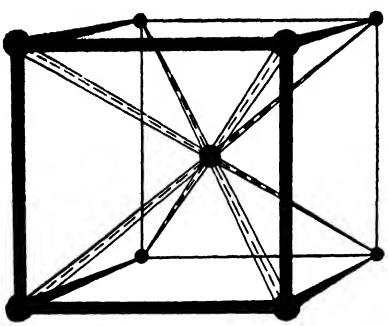

FIG. 3.—A unit-cube from a body-centered cubic lattice.

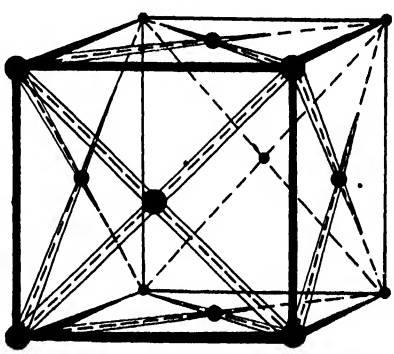

FIG. 4.—A unit-cube from a face-centered cubic lattice.

A more complicated form is the "face-centered" cubic lattice shown in Fig. 4. The unit-cube has an atom at each corner as in the simple cube and, in addition, has an atom at the center of each face. As before, the eight atoms at the corners contribute a total of one atom to the unit-cube. The atoms at the centers of the faces each belong to two unit-cubes, so that these six atoms contribute a total of three atoms to the unit-cube. The face-centered cubic lattice therefore has a grand total of four atoms per unit-cube. Such a lattice may be thought of as composed of four interpenetrating simple cubic lattices.

A still more complicated structure is the "diamond" cubic structure—so called because it represents the arrangement of the carbon atoms in the diamond. This structure is most easily described as composed of two interpenetrating face-centered cubic lattices of equal size, placed so that the corners of the unit-cubes of one lattice lie on the body-diagonals of the other lattice, at a distance from the end of the diagonal equal to one-fourth the length of the diagonal. The effect is that of

putting four additional atoms inside a face-centered cube. These additional atoms are shown in Fig. 5, but for the sake of clearness only the corners of the unit face-centered cube are shown. The complete unit diamond cube is shown in Fig. 6, which is a superposition of Figs. 4 and 5.

All dimensions of a cubic crystal are expressed in terms of the length of the edge of its unit-cube. The origin of coordinates is put at the center of one atom, and the coordinate axes are chosen so as to pass along the edges of the unit-cubes. If we start at the origin and travel along the X-axis of a simple cubic lattice, every time we go a distance equal to the edge of the unit-cube, or an exact integral multiple of that distance, we shall reach the center of an atom. In other words, we shall come to

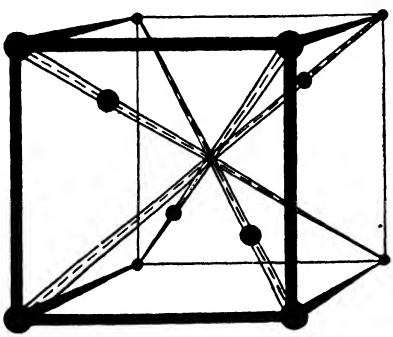

FIG. 5.—Structure of the interior of the unit-cube of a diamond cubic structure.

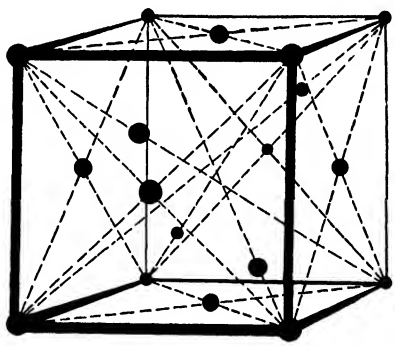

FIG. 6.—A unit-cube of a diamond cubic structure.

the center of an atom every time we have traversed an exact number of the units of length which are characteristic of that particular simple cubic lattice. Similar statements might be made in connection with the Y- and the Z-axes. All this may be expressed in very convenient form by means of a system of generalized coordinates. Let m be any integer (including zero) used to express distances along the X-axis in terms of the edge of the unit-cube. Obviously m may be either positive or negative. Similarly, let n and p be corresponding integers used to express distances along the Y- and Z-axes, respectively. Then the position of any atom in a simple cubic lattice is given by the generalized coordinates

$$m, \quad n, \quad p$$

The corresponding generalized coordinates for the atoms of a body-centered cube are:

$$\begin{array}{lll} m, & n, & p \\ m + \tfrac{1}{2}, & n + \tfrac{1}{2}, & p + \tfrac{1}{2} \end{array}$$

For a face-centered cube they are:

$m,$	$n,$	p
$m + \frac{1}{2},$	$n + \frac{1}{2},$	p
$m + \frac{1}{2},$	$n,$	$p + \frac{1}{2}$
$m,$	$n + \frac{1}{2},$	$p + \frac{1}{2}$

For a diamond cube they are:

$m,$	$n,$	p ·
$m + \frac{1}{2},$	$n + \frac{1}{2},$	p ·
$m + \frac{1}{2},$	$n,$	$p + \frac{1}{2}$ ·
$m,$	$n + \frac{1}{2},$	$p + \frac{1}{2}$ ·
$m + \frac{1}{4},$	$n + \frac{1}{4},$	$p + \frac{1}{4}$ ·
$m + \frac{3}{4},$	$n + \frac{3}{4},$	$p + \frac{1}{4}$ ·
$m + \frac{3}{4},$	$n + \frac{1}{4},$	$p + \frac{3}{4}$ ·
$m + \frac{1}{4},$	$n + \frac{3}{4},$	$p + \frac{3}{4}$ ·

It is a fundamental characteristic of a space-lattice that, no matter what atom of the crystal we start with, the same system of motions of translation will lead us to its immediate neighbors. For instance, let us choose any atom on a simple cubic lattice as a starting point. Then a motion of translation along the X-axis of one unit of length (*i.e.*, the edge of the unit-cube) and similar motions along the Y- and Z-axes will bring us to the three atoms of the simple cube which lie closest to our starting point. Starting now with *any* one of these three newly located atoms, we may repeat our system of three motions of translation, and we shall at once find three other atoms. This process may be repeated indefinitely. If the repetition is carried out systematically, using each newly found atom as a starting point, we shall eventually reach every atom in the crystal. If we represent the motions of translation along the edges of the unit-cube parallel to the X-, Y-, and Z-axes by $2\tau_x$, $2\tau_y$, and $2\tau_z$, we may completely describe a simple cubic lattice by the three primitive translations

$$2\tau_x; \qquad 2\tau_y; \qquad 2\tau_z$$

for, by starting from a single point in space, we can reconstruct the whole crystal.*

Similarly, the four primitive translations

$$2\tau_x; \qquad 2\tau_y; \qquad 2\tau_z; \qquad \tau_x, \tau_y, \tau_z$$

completely describe a body-centered cubic lattice. The first three translations lead us to the atoms at the three nearest corners of the unit-

* It is evident from the above that we can start from any one atom of a simple cube and proceed *directly* to any other atom by motions of translation of $m(2\tau_x)$; $n(2\tau_y)$; $p(2\tau_z)$.

cube, and the three components of translation, τ_x, τ_y, τ_z, taken as a single operation, lead us to the atom at the body-center of the unit-cube. If we repeat these four characteristic translations, starting with *any* of the four newly located atoms, we at once find four other atoms, and the process may be repeated indefinitely. It is a consequence of the possibility of starting with any atom, that it rests only with the point of view of the observer whether a given atom lies at the corner or at the body-center of a unit-cube. This is illustrated in two dimensions in

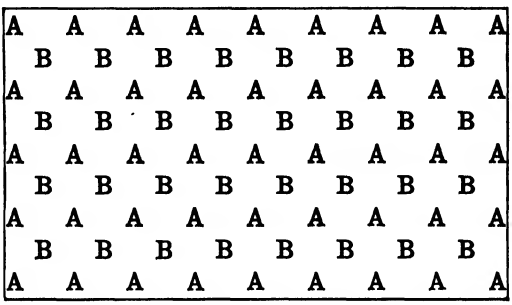

FIG. 7.—The corners of the squares may be at either A or B.

Fig. 7. It is evident that we may consider the figure to be made up of squares with **A** at the corners and **B** at the centers, or we may consider equally well that the squares all have **B** at the corners and **A** at the centers.

A face-centered cube may be defined in terms of the three translations

$$\tau_y\tau_z; \qquad \tau_z\tau_x; \qquad \tau_x\tau_y$$

If we start with an atom at the corner of a unit-cube, these three primitive translations lead us to the atoms at the centers of three adjacent faces. Starting with any of these atoms, a repetition of the three primitive translations will lead us to one atom at one of the corners of the unit-cube and to two others which lie on centers of the faces of the unit-cube. It is a consequence of this picture that one observer may choose one atom as being at the corner of a unit-cube and a second observer may choose his origin of coordinates so that that same atom lies at the center of one of the faces of his unit-cube. If the configuration of atoms in space had not been such as to permit this absolutely random choice of starting point, then our three-dimensional framework of imaginary lines would not have been entitled to the designation "space-lattice."

Considerations of this sort were responsible for the use of the word *structure* instead of *lattice* in giving the generalized coordinates of a diamond cube. Trial shows that it is not possible to write primitive translations for a diamond cube such that any atom may be picked at random as an origin of coordinates. The best we can do is to consider the diamond cube as being made up of two separate interpenetrating

face-centered cubic lattices. Any atom may be picked at random as a starting point for finding the location of all the other atoms *on its own lattice*, but the translations for one face-centered cubic lattice will never lead us to any of the atoms of the other face-centered cubic lattice. To reach these remaining atoms, we must make a fresh start with one of the atoms on the second lattice. In this connection it will be noted that the eight generalized coordinates given for the diamond cube include the four which were previously given for a face-centered cube. The remaining four are the coordinates of a second face-centered cube and differ from the first four in that their origin of coordinates has been shifted to the point $\frac{1}{4}, \frac{1}{4}, \frac{1}{4}$.

The Fourteen Space-lattices.—So far we have discussed only the cubic space-lattices. Each of the six systems of crystals has one or more space-lattices. Their primitive translations are all listed in Table I, along with the customary code symbol for each lattice.[1] The triclinic

TABLE I.—THE FOURTEEN SPACE-LATTICES

Serial No.	Symbol	Primitive translations
Triclinic system:		
1. Simple	Γ_{tr}	$2\tau_x;\ 2\tau_y;\ 2\tau_z$
Monoclinic system:		
2. Simple	Γ_m	$2\tau_x;\ 2\tau_y;\ 2\tau_z$
3. Side-centered	Γ_m'	$2\tau_x;\ \tau_y, \tau_z;\ \tau_y, -\tau_z$*
Orthorhombic system:		
4. Simple	Γ_o	$2\tau_x;\ 2\tau_y;\ 2\tau_z$
5(*a*). Base-centered	$\Gamma_o'(a)$	$\tau_x, \tau_y;\ \tau_x, -\tau_y;\ 2\tau_z$
5(*b*). Side-centered	$\Gamma_o'(b)$	$2\tau_x;\ \tau_y, \tau_z;\ \tau_y, -\tau_z$
6. Face-centered	Γ_o''	$\tau_y, \tau_z;\ \tau_z, \tau_x;\ \tau_x, \tau_y$
7. Body-centered	Γ_o'''	$2\tau_x;\ 2\tau_y;\ 2\tau_z;\ \tau_x, \tau_y, \tau_z$
Tetragonal system:		
8(*a*). Simple	$\Gamma_t(a)$	$2\tau_x;\ 2\tau_y;\ 2\tau_z$
8(*b*). Base-centered	$\Gamma_t(b)$	$\tau_x, \tau_y;\ \tau_x, -\tau_y;\ 2\tau_z$
9(*a*). Face-centered	$\Gamma_t'(a)$	$\tau_y, \tau_z;\ \tau_z, \tau_x;\ \tau_x, \tau_y$
9(*b*). Body-centered	$\Gamma_t'(b)$	$2\tau_x;\ 2\tau_y;\ 2\tau_z;\ \tau_x, \tau_y, \tau_z$
Cubic system:		
10. Simple	Γ_c	$2\tau_x;\ 2\tau_y;\ 2\tau_z$
11. Face-centered	Γ_c'	$\tau_y, \tau_z;\ \tau_z, \tau_x;\ \tau_x, \tau_y$
12. Body-centered	Γ_c''	$2\tau_x;\ 2\tau_y;\ 2\tau_z;\ \tau_x, \tau_y, \tau_z$
Hexagonal system:		
13. Rhombohedral	Γ_{rh}	$2\tau_x;\ 2\tau_y;\ 2\tau_z$ (rhombohedral axes)
14. Hexagonal	Γ_h	$2\tau_x;\ 2\tau_y;\ 2\tau_z$ (hexagonal axes)

* By τ_y, τ_z is meant a translation τ_y along the *Y*-axis followed by one of length τ_z along the *Z*-axis. The translation $\tau_y, -\tau_z$ is similar except that τ_z is here taken in the $-z$-direction. These are written by Schoenflies as $\tau_y + \tau_z$ and $\tau_y - \tau_z$, respectively (see reference 1).

system has only the simple lattice Γ_{tr}. The monoclinic system has the simple Γ_m and the side-centered Γ_m' lattices. The orthorhombic system

has the simple Γ_o, the base-centered $\Gamma_o'(a)$, the side-centered $\Gamma_o'(b)$ (which is the same thing as a base-centered orthorhombic lattice turned over on its side), the face-centered Γ_o'', and the body-centered Γ_o''' lattices. The tetragonal system has the simple $\Gamma_t(a)$ and the face-centered $\Gamma_t'(a)$ lattices. It also has what appears at first sight to be a base-centered lattice $\Gamma_t(b)$. This is really the simple tetragonal lattice with the X- and Y-axes rotated 45° about the Z-axis. In the orthorhombic system the simple lattice and the base-centered lattices were different from each other because of the different units of length along the X- and the Y-axes. Since these two units of length are equal in the tetragonal system, the simple lattice and the base-centered lattice become indistinguishable except in terms of the point of view of the observer. Similarly, the only distinction between the face-centered lattice $\Gamma_t'(a)$ and the body-centered lattice $\Gamma_t'(b)$ lies in the observer's choice of axes. The cubic system has three lattices, the simple Γ_c, the face-centered Γ_c', and the body-centered Γ_c''. The hexagonal system has two simple lattices, Γ_{rh}, called the "rhombohedral lattice," and Γ_h, called the "simple triangular lattice," which are referred to rhombohedral (triclinic with all three angles equal and with all three units of measure equal, *i.e.*, a kind of distorted cubic) axes and to hexagonal axes, respectively. The reader will undoubtedly feel that still other space-lattices should be possible. Trial shows, however, that every such additional lattice becomes one of the 14 listed in Table I if only the lattice is looked at from some different direction or if some other three rows of atoms are picked for the principal crystallographic axes. Such duplicates as are given in Table I [such as 5(*a*), 5(*b*)] will be found useful in Chap. VIII.*

We have already seen in the case of the cubic system that space-lattices may be put together to form still more complicated structures; for instance, the diamond cube was found to be composed of two face-centered cubic lattices. Similar illustrations may be found in other crystal systems. For instance, two simple triangular lattices may be put together to form a hexagonal close-packed structure whose generalized coordinates are:†

$$\begin{array}{lll} m, & n, & pC \\ m + \frac{1}{3}, & n + \frac{2}{3}, & (p + \frac{1}{2})C \end{array}$$

* In any crystal system the shape of the unit-prism is determined by the X-, Y-, and Z-axes and by the axial ratios. Thus, in the cubic system, the unit of structure is a cube; in the tetragonal system it is a tetragonal prism; in the orthorhombic system it is an orthorhombic prism. The unit-prism in the hexagonal system has for its base a rhombus whose sides make an angle of 120°, *i.e.*, the base may be thought of as being made up of two equilateral triangles having a common side. The altitude of the unit-prism is the distance between adjacent atoms on the Z-axis.

† The axial ratio C appears in the coordinates for the Z-axis in order to reduce all the spacings to a common linear unit of measure.

Three simple triangular lattices may be put together to form a rhombohedral structure which is identical with the rhombohedral lattice. From this point of view the generalized coordinates of a rhombohedron would be

$$\begin{array}{lll} m, & n, & pC \\ m + \frac{1}{3}, & n + \frac{2}{3}, & (p + \frac{1}{3})C \\ m + \frac{2}{3}, & n + \frac{1}{3}, & (p + \frac{2}{3})C \end{array}$$

From the point of view of the rhombohedral lattice (Γ_{rh}), the generalized coordinates would be

$$m, \qquad n, \qquad p$$

NAMES OF THE ATOMIC PLANES

A glance at Fig. 1 shows that the atoms of which a crystal is composed must lie in layers, or planes. It is possible to have a large number of such planes all parallel to each other. For instance, let us start with the atomic plane in Fig. 1 which passes through the origin of coordinates and which contains both the Y- and Z-axes. There will be as many other atomic planes parallel to this as may be permitted by the size of the crystal. The number of such parallel planes may easily run into the millions. But we might just as well have started with an atomic plane passing through the origin and containing the X- and Z-axes, or the X- and Y-axes. It is evident that here again we may have an enormous number of planes, all parallel to each other. But these planes are clearly different in both direction and spacing from those which are parallel to the Y- and Z-axes. Each of these groups of parallel planes constitutes a "family." Figure 8 shows by means of a two-dimensional analogy that there must be a large number of families of planes in any crystal, and that any given atom lies in some one member of each family of planes. Conversely, every family of planes contains every atom in the crystal. Since the number of atoms involved is the total number in the crystal irrespective of the particular family of planes under consideration, we have the general rule that *in a given crystal, the atomic*

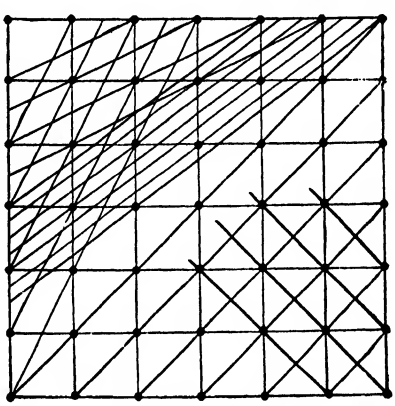

FIG. 8.—Two-dimensional analogy showing various families of planes.

*population per unit area of a plane is directly proportional to the interplanar distance.**

The oldest and, at first sight, most logical method of naming planes is the method devised by C. E. Weiss, formerly a professor in the University of Berlin. According to this scheme, each plane is named in terms of its intercepts on the X-, Y-, and Z-axes, *i.e.*, in terms of the distance which it cuts off on each of the three axes. The unit of length along each of the three axes is the distance between adjacent atoms along that axis. In other words, the units of measure along the X-, Y-, and Z-axes are the distances called a, b, and c in the discussions of crystal systems and axial ratios at the beginning of this chapter. It is inherent in the nature of a space-lattice that each of the successive planes in the same family will have an intercept along a given axis which is a multiple or a submultiple of the same small integer.† The smallest three integers which serve the purpose constitute the name of the family of planes according to the Weiss system. Although the Weiss system has all the advantage of clearness of visualization, it has the fatal disadvantage of not being well suited to some of the calculations which every crystal analyst has to make.

It will be shown in Chap. III that all ordinary calculations of the distances between adjacent planes of the same family require the use of numbers which are proportional to the reciprocals of the Weiss intercepts. This has resulted in the almost universal adoption of a nomenclature first used by Grassmann‡ of Stettin, Germany, and used in 1839 by Prof. W. H. Miller of Cambridge University. This nomenclature employs integers which are proportional to the reciprocals of the three Weiss intercepts. The work of Miller attracted such attention that the reciprocal designations are universally known among crystallographers as "Miller indices." If the three actual intercepts of a given family of planes, expressed in ordinary units of measure such as centimeters, are x, y, and z, then the Miller indices h, k, l are the three smallest integers which are proportional to a/x, b/y, and c/z, respectively, where a, b, and c are the distances between adjacent atoms along the X-, Y-, and Z-axes. These quantities, a, b, and c, are, as before, identical with the units of measure mentioned in the discussions of crystal systems and axial ratio at the beginning of this chapter. The use of a, b, and c, along with the

* This rule applies rigorously in the case of all elements and binary compounds. In the case of compounds containing radicals and in the case of most organic compounds, certain exceptions must be made which will be self-evident in the light of Chap. VIII and Appendix III.

† This law was first stated in somewhat different language by the Abbe René Hauy in 1782 as a result of a brilliant study of the exterior forms of crystals.

‡ Apparently these symbols were invented independently by Plücker in 1828. When applied to three dimensions they are called by mathematicians "nonhomogeneous space coordinates."

values of the "actual" intercepts, means that the Miller indices are the three smallest integers which are proportional to the reciprocals of the Weiss intercepts of a plane.

For purposes of illustration, let us confine ourselves to the cubic system, so that $a = b = c = 1$. Consider the family of parallel planes whose intercepts are

1,	$1\frac{1}{3}$,	$1\frac{1}{5}$
2,	$2\frac{2}{3}$,	$2\frac{2}{5}$
3,	1,	$3\frac{3}{5}$
4,	$1\frac{1}{3}$,	$4\frac{4}{5}$

The smallest integers which are proportional to the reciprocals of these numbers are 1, 3, 5. The planes are, therefore, all said to belong to the (1 3 5) family.

The parentheses around the Miller indices make them apply to a whole family of parallel planes rather than just to some one individual plane. Thus the (1 0 0), (0 1 0), and (0 0 1) planes in a cube are the three families of planes which are parallel to the cube faces. When an index is taken in a negative direction along an axis, a minus sign is placed over the index. It is evident that the $(\bar{1}\,0\,0)$ planes of a cube are parallel to the (1 0 0) planes and are a part of the (1 0 0) family. Similarly, the $(0\,\bar{1}\,0)$ and $(0\,0\,\bar{1})$ planes belong to the (0 1 0) and the (0 0 1) families. In general, two sets of Miller indices refer to the same family of planes if each of the indices of one set has the opposite sign to the corresponding index of the other set.

In the case of a cubic lattice, the (1 0 0), (0 1 0), and (0 0 1) planes may be given the common designation of {1 0 0} since they cannot be distinguished from each other. Such a group of families of planes is called a "form." In a tetragonal space-lattice the plane-families (1 0 0) and (0 1 0) are indistinguishable and belong to the form {1 0 0} because $a = b$. Since the unit of measure, c, along the Z-axis is different from a and b, the family (0 0 1) cannot be a member of the form {1 0 0}. In an orthorhombic space-lattice, (1 0 0), (0 1 0), and (0 0 1) are all different, since $a \neq b \neq c$. They cannot be given a common designation and there can be no common form. The eight types of octohedral planes of a cube are (1 1 1), $(\bar{1}\,1\,1)$, $(1\,\bar{1}\,1)$, $(1\,1\,\bar{1})$, $(\bar{1}\,\bar{1}\,1)$, $(\bar{1}\,1\,\bar{1})$, $(1\,\bar{1}\,\bar{1})$, and $(\bar{1}\,\bar{1}\,\bar{1})$. These are representatives of the four families (1 1 1), $(\bar{1}\,1\,1)$, $(1\,\bar{1}\,1)$, $(1\,1\,\bar{1})$, which constitute the form {1 1 1}.

Zone Axes.—Since the planes of a space-lattice are planes of atoms, it follows that the intersections of the planes must be rows of atoms. Conversely, every row of atoms must be the line of intersection for two or more atomic planes. A row of atoms, considered from this viewpoint, is called a "zone axis." The larger the number of planes of

small Miller indices which intersect at a given zone axis, the more important is that zone axis. In a cubic lattice, the most important zone axes are those parallel to the X-, Y-, and Z-axes. For instance, any row of atoms parallel to the Z-axis belongs equally to some member of each of the (1 0 0), (1 1 0), (2 1 0), (3 2 0), etc., families of planes. For this reason, the X-, Y-, and Z-axes are often called the "principal axes."

Consider a plane on a cubic space-lattice and let its Miller indices be h_1, k_1, l_1. If some plane parallel to this plane passes through the origin of coordinates, the position of any atom lying in the plane and having coordinates x, y, z is subject to the equation of the plane:

$$h_1x + k_1y + l_1z = 0$$

If $h_2k_2l_2$ is some other plane intersecting the plane $h_1k_1l_1$ and also containing the atom $x\,y\,z$, we have the additional equation

$$h_2x + k_2y + l_2z = 0$$

The equation of the line which represents the intersection of these two planes, and which passes through the atom $x\,y\,z$, is therefore

$$\frac{x}{k_1l_2 - l_1k_2} = \frac{y}{l_1h_2 - h_1l_2} = \frac{z}{h_1k_2 - k_1h_2}$$

The three denominators are called the "indices of the zone" and are usually written $[u\,v\,w]$ where

$$\begin{aligned} u &= k_1l_2 - l_1k_2 \\ v &= l_1h_2 - h_1l_2 \\ w &= h_1k_2 - k_1h_2 \end{aligned}$$

For an orthorhombic crystal:

$$\begin{aligned} u &= k_1\frac{l_2}{C} - \frac{l_1}{C}k_2 \\ v &= \frac{l_1}{C}\cdot\frac{h_2}{A} - \frac{h_1}{A}\cdot\frac{l_2}{C} \\ w &= \frac{h_1}{A}k_2 - k_1\frac{h_2}{A} \end{aligned}$$

The Miller indices of a plane containing two zone axes $[u_1v_1w_1]$ and $[u_2v_2w_2]$ are:

$$\begin{aligned} h &= v_1w_2 - w_1v_2 \\ k &= w_1u_2 - u_1w_2 \\ l &= u_1v_2 - v_1u_2 \end{aligned}$$

In the cubic system, the indices of a given zone axis are numerically the same as the indices of the family of planes which is perpendicular to

that zone axis. For instance: in a cube, the [1 0 0] axis is perpendicular to the (1 0 0) plane; the [0 1 0] axis is perpendicular to the (0 1 0) plane; the [1 $\bar{1}$ 1] axis is perpendicular to the (1 $\bar{1}$ 1) plane; etc.

Indices in the Hexagonal System.—We have defined a hexagonal space-lattice as having two axes at an angle of 120° to each other and a third axis perpendicular to the plane of the other two. When considered from the standpoint of external symmetry, crystals having hexagonal lattices must be assigned a total of four axes, the first three of which are mutually 120° apart. These lie in a plane which is perpendicular to the fourth axis. From this standpoint the atomic planes would have four indices of the Miller type, called the Bravais-Miller indices. The third index is always equal to $-(h + k)$. Since it does not enter into the calculations of interplanar spacings it is often discarded by crystal analysts,[2] and its place is taken by a dot, thus: (1 0 · 0).

A rhombohedron may be considered as being made up of three interpenetrating hexagonal space-lattices, or it may be considered to be a distorted cube for which the three interaxial angles λ, μ, ν are equal. The indices of the atomic planes in a rhombohedron may therefore be referred either to the Bravais-Miller indices of the hexagonal space lattice Γ_h or to the true Miller indices of a distorted cubic lattice Γ_{rh}. The Bravais-Miller indices $(HK \cdot L)$ are related to the Miller indices (hkl) by the following equations:

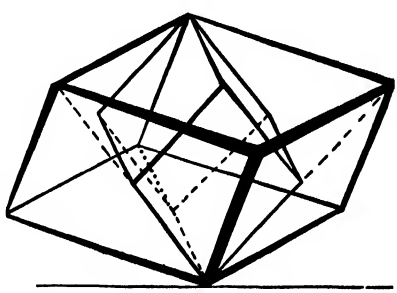

FIG. 9.—Two sets of rhombohedral axes.

$$
\begin{aligned}
h &= 2H + K + L \\
k &= K - H + L \\
l &= -2K - H + L \\
H &= h - k \\
K &= k - l \\
L &= h + k + l
\end{aligned}
$$

When a rhombohedron is considered as being a distorted cube, a second set of rhombohedral axes may be used which have the directions of the face-diagonals of the original rhombohedron. This is shown in Fig. 9. Indices h', k', l' for the new rhombohedral axes may be calculated from the indices for the original rhombohedral axes by means of the formulas:

$$
\begin{aligned}
h' &= k + l \\
k' &= h + l \\
l' &= h + k
\end{aligned}
$$

Interrelations between Lattices.—There are certain crystal forms of especial interest in that they may be regarded as belonging to either of two crystal systems. For instance, if a model of a face-centered cube is held so that one of its body-diagonals is vertical, a triangular arrangement of the "atoms" is at once evident, and it is seen that the structure may be regarded as a rhombohedron whose axial ratio, referred to hexagonal axes, is 2.45. Similarly, a simple cube is a rhombohedron of axial ratio 1.225, and a body-centered cube is a rhombohedron of axial ratio 0.612. A body-centered cube is a face-centered tetragonal prism of axial ratio $1/\sqrt{2}$, and a face-centered cube is a body-centered tetragonal prism of axial ratio $\sqrt{2}$. Any body-centered tetragonal prism of axial

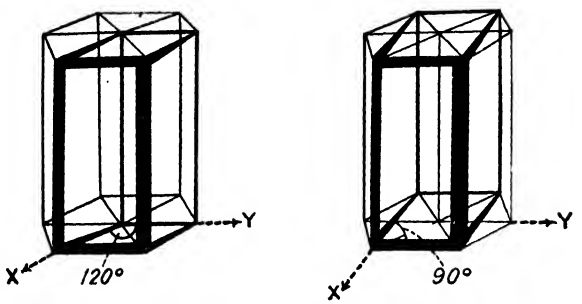

FIG. 10.—(*a*) Hexagonal axes; (*b*) orthohexagonal axes.

ratio C may be considered as being a face-centered tetragonal prism of axial ratio $C/\sqrt{2}$; or a face-centered tetragonal prism of axial ratio C may be called a body-centered tetragonal prism of axial ratio $C\sqrt{2}$. A simple triangular lattice of axial ratio C may be regarded as an orthorhombic lattice of a special sort whose axial ratios are $\sqrt{3}$ and C. A large number of crystals have their axial ratios at or near these critical values

It is sometimes convenient to consider a hexagonal structure in terms of orthohexagonal axes of reference instead of in terms of the customary hexagonal axes. The relation between these axes is shown in Fig. 10. If the Bravais-Miller hexagonal indices are (HKL) and if the orthohexagonal indices are (pqr), then

$$p = K + 2H \qquad H = \frac{p - q}{2}$$

$$q = K \qquad K = q$$

$$r = L \qquad L = r$$

Similarly the orthohexagonal indices (pqr) may be transformed into the regular Miller indices (hkl) of a rhombohedron by the equations

$$h = 2p + 2r \qquad p = 2h - k - l$$
$$k = -p + 3q + 2r \qquad q = k - l$$
$$l = -p - 3q + 2r \qquad r = h + k + l$$

DENSITIES OF CRYSTALS

Since the determinations of the standard grating spaces of calcite and rock salt are made in terms of the densities of single crystals and the mass in grams of the unit of structure, it is evident that a density for crystalline materials may be calculated in terms of the dimensions of the unit of crystal structure as determined by x-ray methods. Such calculated values are subject to whatever errors there may be in the determination of the standard substances. This error seems to be considerably greater than is usually supposed, not because of an inability to make more refined x-ray measurements, but because the crystals of the same substance do not exactly duplicate each other, due to the effect of traces of impurities on the interplanar distances and due to fragmentation of the crystal. Measurements of the size of the unit of structure may be easily duplicated for the crystals of most materials to within $\frac{1}{10}$ per cent, using different crystals of the same substance from different sources. This gives a limit of duplicatability to density measurements from x-ray data of $\frac{3}{10}$ per cent. Densities calculated in this way agree in a general way with those found by direct measurement. They rarely agree exactly, even when both density measurements are made on the same sample of material. This is probably because the material used for direct measurement contains a small amount of intercrystalline material whose density can hardly be expected to be that of the crystals. The extreme limits of accuracy are illustrated by the case of CsI as measured by Clark and Duane.[3] The salt was of atomic-weight purity. The density of one of the crystals, as calculated from x-ray measurements was 4.513, while the density of the whole sample was found by Baxter and Wallace[4] to be 4.509.

The density of a crystal may be calculated from the equation:

$$\text{Density} = \frac{\text{weight}}{\text{volume}}$$

The weight is the product of the atomic or molecular weight of the chemical unit of which the crystal is composed, times the number of such units per unit-crystal, times the factor 1.649×10^{-24} which changes units of atomic weight into grams. The volume is the volume of the unit-crystal.

In the cubic system the density of the crystal is, therefore,

$$\rho = n\frac{M \times 1.649 \times 10^{-24}}{a_0^3} \qquad (1)$$

where M = mass of the chemical unit of which the crystal is composed, *i.e.*, of the "molecule," expressed in units of atomic weight.

a_0 = edge of the unit-cube in centimeters.

$\mathbf{n}$ = number of points associated with a unit-cube in the crystal lattice. $\mathbf{n}$ is 1 for a simple cube, 2 for a body-centered cube, 4 for a face-centered cube, and 8 for a diamond cube.

It was stated in Chap. I that crystals like NaCl could be pictured as being simple cubes with positive and negative ions occupying alternate corners of the cubes. Such a picture gives for NaCl a value for a_0 of 2.814×10^{-8} cm. and requires that the weight of the unit-cell be calculated in terms of the average weight of the Na and Cl; *i.e.*, M is $\frac{1}{2}(23.000 + 35.458) = 29.229$ and $\mathbf{n}$ is unity. According to the theory of space-groups (Chap. VIII), these structures should be thought of as being face-centered cubic with one positive ion and one negative ion both associated with a position on the face-centered cubic lattice. This would give for NaCl a value for a_0 of 5.628×10^{-8} cm. instead of 2.814×10^{-8} cm.; would require M to be $23.000 + 35.458 = 58.458$; and would make $\mathbf{n} = 4$. Obviously the two sets of calculations yield identical answers.

In the tetragonal system the density is obviously

$$\rho = \mathbf{n}\frac{M \times 1.649 \times 10^{-24}}{C a_0^3} \tag{2}$$

In the hexagonal system the density is

$$\rho = \mathbf{n}\frac{M \times 1.649 \times 10^{-24}}{\frac{1}{2}\sqrt{3} C a_0^3} \tag{3}$$

where a_0 = edge of the rhombus which serves as the base of the unit prism.

$\mathbf{n} = 1$ for a simple triangular lattice, 2 for a hexagonal close-packed structure (see page 28), and 3 for a rhombohedral lattice referred to hexagonal axes.

The value of a_0 in Eq. (3) is most easily found as $2d/\sqrt{3}$ for the $(1\,0\cdot 0)$ planes or as $2d$ for the $(1\,1\cdot 0)$ planes.

SUMMARY

The six crystal systems and the 14 space-lattices have been described, and the method of naming the atomic planes has been explained. The interrelationships between certain crystal structures have been discussed briefly, and the calculations of the densities of crystals have been touched upon. We must now take up the calculation of the interplanar spacings of various types of crystals, so that we may be in possession of the minimum information necessary to a solution of the simpler crystal structures.

References

1. R. W. G. Wyckoff, The Analytical Expression of the Results of the Theory of Space Groups, *Carnegie Inst. Pub.* 318, (1922, 1930). See also Schoenflies, "Krystallsysteme und Krystallstruktur" (Leipzig, 1891).
2. A. W. Hull and W. P. Davey, *Phys. Rev.*, **17**, 549 (1921).
   W. P. Davey, *Gen. Elec. Rev.*, **25**, 565 (1922).
3. Clark and Duane, *Proc. Nat. Acad. Sci.*, **9**, 117, 126, 131, 398 (1923); *Science*, **58**, 400 (1923); *Jour. Optical Soc. Amer.*, **7**, 455 (1923).
4. Baxter and Wallace, *J. Amer. Chem. Soc.*, **38**, 96 (1916).

CHAPTER III

THE CALCULATION OF INTERPLANAR SPACINGS

Reference has already been made to the importance of the calculation of the distance between adjacent atomic planes belonging to the same plane-family. The formula used in making these calculations is derived[1] by a simple mathematical device composed of three steps as follows: (1) A well-known theorem in solid analytic geometry gives us the perpendicular distance from any point to a plane. (2) In terms of (1) we can calculate at once the perpendicular distance from an atom situated at the point $x_1y_1z_1$ in one plane of the $(h\,k\,l)$ family to some other $(h\,k\,l)$ plane which is used as a reference plane; a similar calculation gives us the perpendicular distance between the reference plane and some other atom at the point $x_2y_2z_2$. (3) If, now, the two atoms $x_1y_1z_1$ and $x_2y_2z_2$ lie in parallel $(h\,k\,l)$ planes, then the difference between the two calculated distances is the interplanar spacing of those two $(h\,k\,l)$ planes. For the triclinic system of crystals, the formula is quite complex. It becomes successively simpler for the monoclinic, hexagonal, orthorhombic, tetragonal, and cubic systems. Because of the simplicity of the formula for the cubic system it will be derived first, and its application will be shown for the various ordinary types of cubic crystals. The general formula for the triclinic system will then be derived, and it will be shown that the simpler formulas for the other crystal systems may be regarded as special cases of the general triclinic formula.

INTERPLANAR SPACINGS IN A CUBIC CRYSTAL

Let ABC in Fig. 1 be a plane in a cubic crystal, and let its intercepts be $OA = 1/h$, $OB = 1/k$, and $OC = 1/l$. Let R be the center of the atom at the point $x_1y_1z_1$, and let RP be a perpendicular dropped from the point R to the plane. RP is therefore the distance d_1 which we must determine in step 1 of our calculations. Let the point O be chosen as the origin of coordinates, and let the line OH be a perpendicular to the plane from the point O.

Step 1. If we start from the point R and travel by any route so as to return again to R, then the projections of the various portions of the path on some one straight line must add up to zero. We then choose as our path the route $RP + PO + OE + ED + DR$ because it includes the coordinates of the point R, namely $x_1 = OE$, $y_1 = ED$, $z_1 = DR$. We shall take our projections on the line OH, which is parallel

to RP; the projection of RP on an extension of OH is therefore RP itself, *i.e.*, it is the distance d_1 whose value we wish to find in step 2.

Step 2. If the arrows in Fig. 1 are taken to indicate the direction of positive quantities along the three axes, we have

$0 = -d_1$ — projection of PO on OH + projection of OE on OH + projection of ED on OH + projection of DR on OH.

The projection of PO on OH is OH itself, because P and H both lie in the plane ABC, and the plane ABC is perpendicular to OH.

The projection of OE on OH is $OE \times OH/OA = OH \cdot hx_1$.

The projection of ED on OH is $ED \times OH/OB = OH \cdot ky_1$.

The projection of DR on OH is $DR \times OH/OC = OH \cdot lz_1$.

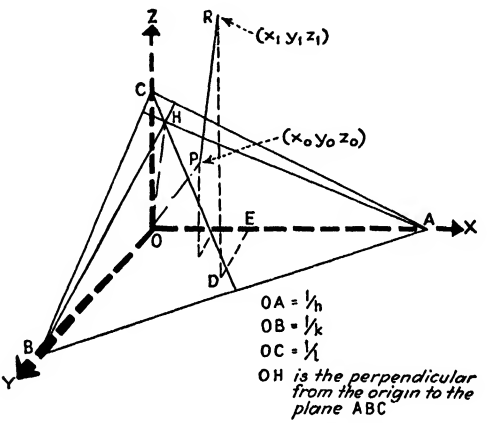

FIG. 1.—Calculation of interplanar spacings in a cubic lattice.

Therefore,

$$d_1 = -OH + OH \cdot hx_1 + OH \cdot ky_1 + OH \cdot lz_1 = (hx_1 + ky_1 + lz_1 - 1)OH$$

In order that d_1 may be expressed completely in terms of only the coordinates of the point R and the Miller indices of the plane ABC, we must express OH in terms of h, k, and l. This can be done by taking advantage of the fact that the sum of the squares of the three direction cosines of a line is equal to unity.

$$\left(\frac{OH}{OA}\right)^2 + \left(\frac{OH}{OB}\right)^2 + \left(\frac{OH}{OC}\right)^2 = 1$$

$$(OH)^2\left\{\left(\frac{1}{OA}\right)^2 + \left(\frac{1}{OB}\right)^2 + \left(\frac{1}{OC}\right)^2\right\} = 1$$

$$(OH)^2(h^2 + k^2 + l^2) = 1$$

$$OH = \frac{1}{\sqrt{h^2 + k^2 + l^2}}$$

Therefore,

$$d_1 = \frac{hx_1 + ky_1 + lz_1 - 1}{\sqrt{h^2 + k^2 + l^2}} \tag{1}$$

Similarly, the distance from the point $x_2 y_2 z_2$ to the plane is

$$d_2 = \frac{hx_2 + ky_2 + lz_2 - 1}{\sqrt{h^2 + k^2 + l^2}} \tag{2}$$

Step 3. If the two points $x_1 y_1 z_1$ and $x_2 y_2 z_2$ are so chosen that they lie in two planes of the same family as the plane ABC, then the interplanar spacing for those two planes is

$$d = d_1 - d_2 = \frac{s}{\sqrt{h^2 + k^2 + l^2}} \tag{3}$$

where

$$\begin{aligned} s &= (hx_1 + ky_1 + lz_1 - 1) - (hx_2 + ky_2 + lz_2 - 1) \\ &= h(x_1 - x_2) + k(y_1 - y_2) + l(z_1 - z_2) \end{aligned}$$

The two planes are properly chosen for the calculation of interplanar spacings when s is the smallest increment in the numerator of Eq. (1) which regularly repeats itself. The numerator s is called the "periodicity" of the plane-family $(h\,k\,l)$. For any given crystal, the calculation of the interplanar spacings involves a study of the periodicities of the planes.

In a simple cubic lattice, the generalized atomic coordinates have been shown in Chap. II to be

$$m \quad n \quad p$$

This means that for a simple cube, the quantities x_1, y_1, z_1 of Eq. (1) are all integers. By properly choosing these integers, the numerator of Eq. (1) can be made equal to any integer, either positive or negative, including zero; that is, the numerators of Eq. (1) are members of the series

$$\cdots\cdots -3, -2, -1, 0, 1, 2, 3, \cdots\cdots$$

This is illustrated for the (874) planes in Table I. The periodicity is evidently unity, and so we have the following rule:

For a simple cubic lattice the value of s in Eq. (3) *is always unity.*

In a body-centered cubic lattice, the generalized atomic coordinates have been shown in Chap. II to be

$$\begin{array}{lll} m, & n, & p \\ m + \tfrac{1}{2}, & n + \tfrac{1}{2}, & p + \tfrac{1}{2} \end{array}$$

This means that we may have two sorts of numerators for Eq. (1). The first sort will be composed only of integers as in the case of the simple

cube. The second sort of numerator will be the sum, diminished by unity, of three products

$$h(m + \tfrac{1}{2})$$
$$k(n + \tfrac{1}{2})$$
$$l(p + \tfrac{1}{2})$$

TABLE I.—TABULATION OF SUCCESSIVE NUMERATORS OF EQ. (1) FOR THE (874) PLANES OF A SIMPLE CUBIC LATTICE $(hkl) = (874)$

Sample values of			Numerator of Eq. (1) = $hx_1 + ky_1 + lz_1 - 1$	s
$m = x_1$	$n = y_1$	$p = z_1$		
1	− 1	0		
− 3	3	1		
− 1	− 1	4	0	
0	3	−5		
13	−13	−3		
				1
− 1	2	−1		
0	− 2	4		
2	− 2	0	1	
− 2	2	1		
				1
0	1	−1		
3	− 3	0		
0	− 3	6	2	
− 4	5	0		
				1
1	0	−1		
− 1	0	3		
− 3	4	0	3	
4	− 4	0		
				1
Etc.	Etc.	Etc.	Etc.	

TABLE II.—CALCULATIONS OF PERIODICITY FOR A BODY-CENTERED CUBIC LATTICE

Generalized atomic coordinates	Numerator of Eq. (1) (i = integer)			
	Indices all odd	Indices all even	One odd index	One even index
m, n, p	i	i	i	i
$m + \tfrac{1}{2}$, $n + \tfrac{1}{2}$, $p + \tfrac{1}{2}$	$i + \tfrac{1}{2}$	i	$i + \tfrac{1}{2}$	i
Number of integers	1	2	1	2
Number of integers + ½	1	0	1	0
Periodicity = s	½	1	½	1

If h, k, and l are all odd numbers,* or if only one of them is odd, the numerators of the second sort will all be integers plus $\frac{1}{2}$. Since the two sorts of integers must occur with equal frequency we can, by properly choosing the integers m, n, and p, show that the numerators of Eq. (1) are members of a series

$$-2, -1\frac{1}{2}, -1, -\frac{1}{2}, 0, \frac{1}{2}, 1, 1\frac{1}{2}, 2,$$

The periodicity is evidently $\frac{1}{2}$, and the value of s in Eq. (3) is therefore $\frac{1}{2}$. If h, k, and l are all even numbers, or if only one of them is even, the numerators of the second sort will all be integers and the periodicity s must be unity. We therefore have the following rule:

For a body-centered cubic lattice, if all the indices of a family of planes are odd, or if only one of them is odd, $s = \frac{1}{2}$; *otherwise* $s = 1$.

The generalized atomic coordinates for a face-centered cubic lattice show that there will be four sorts of numerators for Eq. (1) and that these four sorts will occur with equal frequency. The numerators of the first sort are like those of the simple cube. The remaining three sets of numerators are each the sum, diminished by unity, of three products:

$$\begin{cases} h(m + \frac{1}{2}) \\ k(n + \frac{1}{2}) \\ lp \end{cases}$$

$$\begin{cases} h(m + \frac{1}{2}) \\ kn \\ l(p + \frac{1}{2}) \end{cases}$$

$$\begin{cases} hm \\ k(n + \frac{1}{2}) \\ l(p + \frac{1}{2}) \end{cases}$$

If only one index is odd, or if only two indices are odd, two of the three last sorts of numerators will each give a sum which is an integer plus $\frac{1}{2}$. The other numerator will be like the numerator of the first sort, for it will be an integer. We therefore have integers and integers plus $\frac{1}{2}$ occurring with equal frequency as numerators in Eq. (1). By properly choosing the integers m, n, and p, we have the series

$$-2, -1\frac{1}{2}, -1, -\frac{1}{2}, 0, \frac{1}{2}, 1, 1\frac{1}{2}, 2,$$

The periodicity is evidently $\frac{1}{2}$; that is, s in Eq. (3) is $\frac{1}{2}$. A similar discussion for all indices odd, or all indices even, shows that for such cases s in Eq. (3) is unity. We have, therefore, the following rule:

* Zero is an even number.

For a face-centered cubic lattice if only one or two indices are odd, $s = \frac{1}{2}$; *otherwise* $s = 1$.

For a diamond cube, if only one index is odd, $s = \frac{1}{4}$; *if only two indices are odd, or if the indices are even but not divisible by* 4, $s = \frac{1}{2}$; *otherwise* $s = 1$.*

TABLE III.—CALCULATIONS OF PERIODICITY FOR A FACE-CENTERED CUBIC LATTICE

Generalized atomic coordinates	Numerator of Eq. (1) (i = integer)			
	Indices all odd	Indices all even	One odd index, say h	One even index, say h
m, n, p	i	i	i	i
$m + \frac{1}{2}$, $n + \frac{1}{2}$, p	i	i	$i + \frac{1}{2}$	$i + \frac{1}{2}$
$m + \frac{1}{2}$, n, $p + \frac{1}{2}$	i	i	$i + \frac{1}{2}$	$i + \frac{1}{2}$
m, $n + \frac{1}{2}$, $p + \frac{1}{2}$	i	i	i	i
Number of integers	4	4	2	2
Number of integers + $\frac{1}{2}$	0	0	2	2
Periodicity = s	1	1	$\frac{1}{2}$	$\frac{1}{2}$

It has been stated that the interplanar distance could be found by studying the periodicity in the numerator of Eq. (3). This is well illustrated in the case of the (1 1 1) plane in the diamond cube (see Figs 5 and 6 of Chap. II). If the indices of a family of planes are all multiplied by 2, so as to give indices $2h$, $2k$, $2l$, then Eq. (3) gives a spacing of half that found for the planes $(h\,k\,l)$. The interplanar spacing of planes $(h\,k\,l)$ would give, therefore, with a given wave length of x-rays, a diffraction pattern of the second order at the same angle as the first-order pattern of the $(2h\,2k\,2l)$ planes. The third-order pattern of $(h\,k\,l)$ is at the same angle as the first order of $(3h\,3k\,3l)$, etc. Planes whose indices contain a common factor may or may not be present in a crystal. For instance, the (2 0 0) plane is present in body-centered, face-centered, and diamond cubes, but not in the simple cubic lattice. As was explained in Chap. II, such a plane, when actually present, is commonly called by the simpler indices; thus the (4 4 4) plane is called merely the (1 1 1) plane except when for some reason it is necessary to distinguish between the two.

It is evident from the generalized coordinates of the atoms in the diamond cubic structure that the distances from a given atom to successive (1 1 1) planes are

* A detailed list of values of s under various conditions of symmetry will be found in Appendix III.

$$\frac{0}{\sqrt{3}}, \frac{3/4}{\sqrt{3}}, \frac{1}{\sqrt{3}}, \frac{1\,3/4}{\sqrt{3}}, \frac{2}{\sqrt{3}}, \frac{2\,3/4}{\sqrt{3}}, \ldots$$

This means that (1 1 1) planes in a diamond cube show a periodicity such that the spacings are alternately $\frac{3/4}{\sqrt{3}}$ and $\frac{1/4}{\sqrt{3}}$. Such a structure may be thought of as being composed of two families of (1 1 1) planes, the

TABLE IV.—CALCULATIONS OF PERIODICITY FOR A DIAMOND CUBIC STRUCTURE

Generalized atomic coordinates	Numerator of Eq. (1) (i = integer)				
	Indices all odd	Indices all even but not divisible by 4	Indices all even and divisible by 4	One odd index, say h	One even index, say h
$m,\ n,\ p$	i	i	i	i	i
$m+1/2,\ n+1/2,\ p$	i	i	i	$i+1/2$	$i+1/2$
$m+1/2,\ n,\ p+1/2$	i	i	i	$i+1/2$	$i+1/2$
$m,\ n+1/2,\ p+1/2$	i	i	i	i	i
$m+1/4,\ n+1/4,\ p+1/4$	$i+3/4$	$i+1/2$	i	$i+1/4$	i
$m+3/4,\ n+3/4,\ p+1/4$	$i+3/4$	$i+1/2$	i	$i+3/4$	$i+1/2$
$m+3/4,\ n+1/4,\ p+3/4$	$i+3/4$	$i+1/2$	i	$i+3/4$	$i+1/2$
$m+1/4,\ n+3/4,\ p+3/4$	$i+3/4$	$i+1/2$	i	$i+1/4$	i
Number of integers	4	4	8	2	4
Number of integers + 1/4	0	0	0	2	0
Number of integers + 1/2	0	4	0	2	4
Number of integers + 3/4	4	0	0	2	0
Periodicity = s	1	1/2	1	1/4	1/2

members of each family having an interplanar distance of $1/\sqrt{3}$. If x-rays of a given wave length strike the (1 1 1) planes at the appropriate angle of incidence, diffraction of the first order will occur from both these two families of planes. The two diffracted beams will not be exactly in phase with each other, but they will be nearly enough in phase to give a resultant of considerable intensity. The rule for s as given for the diamond cubic structure is therefore worded so that $s = 1$ for the (1 1 1) plane.

In the case of the diffracted beam of the second order, the periodicity of the (1 1 1) planes in the diamond cube is such as to present interesting complications. The two families of (1 1 1) planes are so spaced with respect to each other that the distance between adjacent members of the two families is $\frac{1}{4}(1/\sqrt{3})$, thus giving the effect of a family of (4 4 4) planes (see Fig. 2). The diffracted beam of the second order from the (1 1 1) planes [first order from a fictitious family of (2 2 2)

planes] is destroyed by interference with the first-order beam from these (4 4 4) planes, so that this beam is absent from the diffraction pattern of a diamond cube. The effect is the same as if the spacing of these fictitious (2 2 2) planes had been made half as great. The rule for s is therefore so worded as to make $s = \frac{1}{2}$ for the (2 2 2) plane.

The denominators of the equations for the various space-lattices of any one crystal system are all alike when expressed in terms of the symbols h, k, and l. In the cubic system these denominators are the square roots of numbers each of which is the sum of three squares, *i.e.*, $h^2 + k^2 + l^2$. There are no denominators equal to the square roots of 7, 15, 23, 28, 31, etc., because no three perfect squares will add up to give these numbers.

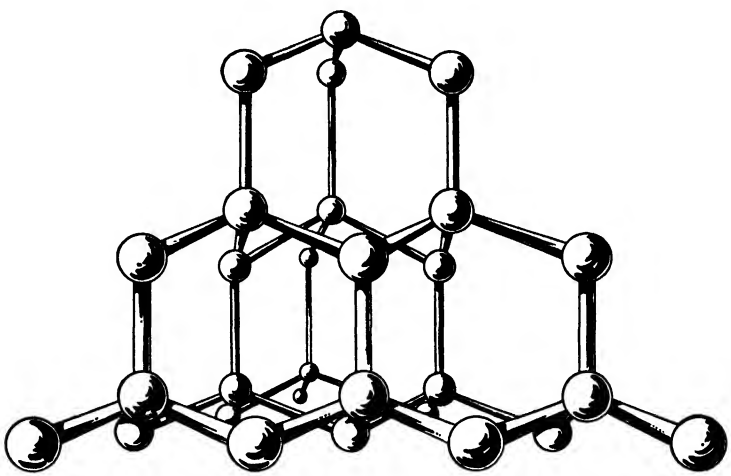

FIG. 2.—Diamond cubic structure showing (1 1 1) planes. (The body-diagonal of the cube is vertical.)

Taking the edge of the unit-cube as unity, the interplanar spacings for a simple cube, body-centered cube, face-centered cube, and diamond cube are shown in Table V. It is strongly recommended that the reader calculate these values himself; in no other way can he gain the intimate familiarity with these calculations which is necessary to a good working knowledge of the subject.

Tetragonal and Orthorhombic Lattices.—Just as the structure of a crystal having cubic symmetry is accounted for by assuming that the atoms lie on some sort of an imaginary cubic framework, in the same way it is assumed that in crystals belonging to the tetragonal system the atoms lie on an imaginary tetragonal framework. The bases of the prisms of which this framework is composed are squares. The vertical sides (direction of the Z-axis) may be either longer or shorter

than the sides of the base, depending upon the material of which the crystal is composed.

TABLE V.—INTERPLANAR SPACINGS IN TYPICAL CUBIC CRYSTALS

Miller indices h, k, l	$h^2 + k^2 + l^2$ for simple cube	Number of families of planes	Interplanar spacings, including the fictitious spacings for various orders of diffraction $n = 2$, $n = 3$, etc. (Edge of unit cube = 1.0000)			
			Simple cube	Body-centered cube	Face-centered cube	Diamond cube
100	1	3	1.0000	.....	.....	.....
110	2	6	0.7071	0.7071	.....	.....
111	3	4	0.5774	.....	0.5774	0.5774
100	4	3	($n = 2$) 0.5000	0.5000	0.5000	.....
210	5	12	0.4472	.....	.....	.....
211	6	12	0.4082	0.4082	.....	.....
110	8	6	($n = 2$) 0.3536	($n = 2$) 0.3536	0.3536	0.3536
221	9	12	0.3333	.....	.....	.....
100	9	3	($n = 3$) 0.3333	.....	.....	.....
310	10	12	0.3162	0.3162	.....	.....
311	11	12	0.3015	.....	0.3015	0.3015
111	12	4	($n = 2$) 0.2887	0.2887	($n = 2$) 0.2887	.....
320	13	12	0.2773	.....	.....	.....
321	14	24	0.2673	0.2673	.....	.....
100	16	3	($n = 4$) 0.2500	($n = 2$) 0.2500	($n = 2$) 0.2500	0.2500
410	17	12	0.2425	.....	.....	.....
322	17	12	0.2425	.....	.....	.....
411	18	12	0.2357	0.2357	.....	.....
110	18	6	($n = 3$) 0.2357	($n = 3$) 0.2357	.....	.....
331	19	12	0.2294	.....	0.2294	0.2294
210	20	12	($n = 2$) 0.2236	0.2236	0.2236	.....
421	21	24	0.2182	.....	.....	.....
332	22	12	0.2132	0.2132	.....	.....
211	24	12	($n = 2$) 0.2041	($n = 2$) 0.2041	0.2041	0.2041
430	25	12	0.2000	.....	.....	.....
100	25	3	($n = 5$) 0.2000	.....	.....	.....
431	26	24	0.1961	0.1961	.....	.....
510	26	12	0.1961	0.1961	.....	.....
511	27	12	0.1924	.....	0.1924	0.1924
111	27	4	($n = 3$) 0.1924	.....	($n = 3$) 0.1924	($n = 3$) 0.1924
520	29	12	0.1857	.....	.....	.....
432	29	24	0.1857	.....	.....	.....
521	30	24	0.1826	0.1826	.....	.....
110	32	6	($n = 4$) 0.1768	($n = 4$) 0.1768	($n = 2$) 0.1768	($n = 2$) 0.1768
530	34	12		0.1715	.....	.....
433		12		0.1715	.....	.....
531	35	24		.....	0.1690	0.1690
100	36	3		($n = 3$) 0.1667	($n = 3$) 0.1667	.....
221		12		0.1667	0.1667	.....
611	38	12		0.1622	.....	.....
532		24		0.1622	.....	.....
310	40	12		($n = 2$) 0.1581	0.1581	0.1581
541	42	24		0.1543	.....	.....
533	43	12		.....	0.1525	0.1525
311	44	12		0.1508	($n = 2$) 0.1508	.....
631	46	24		0.1474	.....	.....
111	48	4		($n = 2$) 0.1443	($n = 4$) 0.1443	($n = 4$) 0.1443
110	50	6		($n = 5$) 0.1414	.....	.....
710		12		0.1414	.....	.....
543		24		0.1414	.....	.....
711	51	12		.....	0.1400	0.1400
551		12		.....	0.1400	0.1400
320	52	12		0.1387	0.1387	.....
211	54	12		($n = 3$) 0.1361	.....	.....
552		12		0.1361	.....	.....
721		24		0.1361	.....	.....
321	56	24		($n = 2$) 0.1336	0.1336	0.1336
730	58	12		0.1313	.....	.....
553	59	12		.....	0.1302	0.1302
731		24		.....	0.1302	0.1302
732	62	24		0.1270	.....	.....
651		24		0.1270	.....	.....
100	64	3		($n = 4$) 0.1250	($n = 4$) 0.1250	($n = 2$) 0.1250
741	66	24		0.1231	.....	.....
811		12		0.1231	.....	.....
554		12		0.1231	.....	.....
733	67	12		.....	0.1222	0.1222
410	68	12		0.1213	0.1213	.....
322		12		0.1213	0.1213	.....

It was stated in Chap. II that the dimensions of a tetragonal crystal are ordinarily expressed in terms of the lengths of the edges of the unit tetragonal prism. If the edges of the base of the unit-prism are called a and b, and if the altitude is c, then $a = b \neq c$. The unit of length along the Z-axis is therefore different from the unit of length along the X- and Y-axes. The ratio of these two units of length $c/a = C$ is called the "axial ratio" (see Chap. II). The advantage in using an axial ratio is that it permits the use of equations for calculating interplanar distances which closely resemble those used in the cubic lattices. Corresponding to Eq. (1) for a cubic lattice, we have for the distance from any atom to the plane $(h\,k\,l)$:

$$d_1 = \frac{hx_1 + ky_1 + lz_1 - 1}{\sqrt{h^2 + k^2 + (l/C)^2}} \tag{4}$$

Similarly, Eq. (3) is replaced by

$$d = \frac{s}{\sqrt{h^2 + k^2 + (l/C)^2}} \tag{5}$$

Crystals belonging to the orthorhombic system are assumed to have their atoms arranged on an imaginary framework such that the unit-prism has rectangles for bases and sides. The edges of this unit-prism along the X-, Y-, and Z-axes are a, b, and c, respectively, and $a \neq b \neq c$. Such crystals have two axial ratios, $a/b = A$ and $c/b = C$, and Eqs. (1) and (3) become

$$d_1 = \frac{hx_1 + ky_1 + lz_1 - 1}{\sqrt{(h/A)^2 + k^2 + (l/C)^2}} \tag{6}$$

$$d = \frac{s}{\sqrt{(h/A)^2 + k^2 + (l/C)^2}} \tag{7}$$

THE GENERAL EQUATION FOR THE INTERPLANAR SPACINGS OF CRYSTALS

In the three crystal systems so far considered, the X-, Y-, and Z-axes were mutually perpendicular to each other. In crystals which, because of the symmetry of their exteriors, are assigned to the hexagonal, monoclinic, or triclinic systems, this restriction no longer holds. If we call the angles between the Y-Z, X-Z, and X-Y axes λ, μ, and ν, respectively, then (see Chap. II);

In the hexagonal system, $\lambda = \mu = 90°$, $\nu = 120°$, and $a = b \neq c$

In the monoclinic system, $\lambda = \mu = 90°$, ν may have any value except 90° or 120°, and $a \neq b \neq c$

In the triclinic system, $\lambda \neq \mu \neq \nu$ and $a \neq b \neq c$

We shall now derive the general equation for the distance from a point to a plane and see how it may be applied to each of the six systems of crystals.

Figure 1 may be used to represent the case of the triclinic system if we imagine that the X-, Y-, and Z-axes are not at right angles to each other. The plane ABC represents any plane (hkl). The line OH is still perpendicular to the plane (hkl). Its length may be represented by p.*

In deriving Eq. (1) for the cubic system we had the equivalent of the expression

$$d_1 = hx_1p + ky_1p + lz_1p - p \tag{8a}$$

Since

$$\frac{h}{A}p = \cos\alpha$$
$$kp = \cos\beta$$
$$\frac{l}{C}p = \cos\gamma$$

we may write this expression in a more general form which is better suited to the triclinic system,

$$d_1 = x_1A\cos\alpha + y_1\cos\beta + z_1C\cos\gamma - p \tag{8b}$$

Since α, β, and γ are now the angles between the line OH and the triclinic axes, it remains to express $\cos\alpha$, $\cos\beta$, and $\cos\gamma$ by means of functions of λ, μ, and ν, so that they may be made to relate directly to a triclinic lattice. These new values must then be substituted into Eq. (8b).

On the line which corresponds to OH of Fig. 1, take a point situated a unit-distance from O and call its triclinic coordinates e, f, g. Projecting the coordinates of this point on the triclinic X-, Y-, and Z-axes in succession, we obtain

$$-\cos\alpha + e + f\cos\nu + g\cos\mu = 0$$
$$-\cos\beta + e\cos\nu + f + g\cos\lambda = 0$$
$$-\cos\gamma + e\cos\mu + f\cos\lambda + g = 0$$

We then have

$$\cos\alpha = \frac{h}{A}p = e + f\cos\nu + g\cos\mu \tag{9}$$

$$\cos\beta = kp = e\cos\nu + f + g\cos\lambda \tag{10}$$

$$\cos\gamma = \frac{l}{C}p = e\cos\mu + f\cos\lambda + g \tag{11}$$

* Care must be taken not to confuse this symbol with the generalized coordinate of Chap. II.

Equations (9), (10), and (11) may be readily solved for e, f, and g by the method of determinants* with the following results:

$$e = \frac{\begin{vmatrix} \frac{h}{A}p & \cos\nu & \cos\mu \\ kp & 1 & \cos\lambda \\ \frac{l}{C}p & \cos\lambda & 1 \end{vmatrix}}{\begin{vmatrix} 1 & \cos\nu & \cos\mu \\ \cos\nu & 1 & \cos\lambda \\ \cos\mu & \cos\lambda & 1 \end{vmatrix}} \tag{12}$$

$$f = \frac{\begin{vmatrix} 1 & \frac{h}{A}p & \cos\mu \\ \cos\nu & kp & \cos\lambda \\ \cos\mu & \frac{l}{C}p & 1 \end{vmatrix}}{\begin{vmatrix} 1 & \cos\nu & \cos\mu \\ \cos\nu & 1 & \cos\lambda \\ \cos\mu & \cos\lambda & 1 \end{vmatrix}} \tag{13}$$

$$g = \frac{\begin{vmatrix} 1 & \cos\nu & \frac{h}{A}p \\ \cos\nu & 1 & kp \\ \cos\mu & \cos\lambda & \frac{l}{C}p \end{vmatrix}}{\begin{vmatrix} 1 & \cos\nu & \cos\mu \\ \cos\nu & 1 & \cos\lambda \\ \cos\mu & \cos\lambda & 1 \end{vmatrix}} \tag{14}$$

Remembering that the point whose coordinates are e, f, g is at unit-distance from the point O, we have

$$e\cos\alpha + f\cos\beta + g\cos\gamma = 1 \tag{15}$$

Equation (15) may be written

$$e\frac{h}{A}p + fkp + g\frac{l}{C}p = 1 \tag{16}$$

* In the notation of determinants, the expression

$$\begin{vmatrix} a & d & g \\ b & e & h \\ c & f & i \end{vmatrix}$$

is interpreted to mean $(aei + bfg + cdh) - (ceg + fha + ibd)$.

Equation (16) may obviously be used to connect Eqs. (12), (13), and (14) as follows:

$$\frac{\frac{h}{A}p\begin{vmatrix} \frac{h}{A}p & \cos\nu & \cos\mu \\ kp & 1 & \cos\lambda \\ \frac{l}{C}p & \cos\lambda & 1 \end{vmatrix} + kp\begin{vmatrix} 1 & \frac{h}{A}p & \cos\mu \\ \cos\nu & kp & \cos\lambda \\ \cos\mu & \frac{l}{C}p & 1 \end{vmatrix} + \frac{l}{C}p\begin{vmatrix} 1 & \cos\nu & \frac{h}{A}p \\ \cos\nu & 1 & kp \\ \cos\mu & \cos\lambda & \frac{l}{C}p \end{vmatrix}}{\begin{vmatrix} 1 & \cos\nu & \cos\mu \\ \cos\nu & 1 & \cos\lambda \\ \cos\mu & \cos\lambda & 1 \end{vmatrix}} = 1$$

This may be simplified to

$$\frac{\frac{h}{A}p^2\begin{vmatrix} \frac{h}{A} & \cos\nu & \cos\mu \\ k & 1 & \cos\lambda \\ \frac{l}{C} & \cos\lambda & 1 \end{vmatrix} + kp^2\begin{vmatrix} 1 & \frac{h}{A} & \cos\mu \\ \cos\nu & k & \cos\lambda \\ \cos\mu & \frac{l}{C} & 1 \end{vmatrix} + \frac{l}{C}p^2\begin{vmatrix} 1 & \cos\nu & \frac{h}{A} \\ \cos\nu & 1 & k \\ \cos\mu & \cos\lambda & \frac{l}{C} \end{vmatrix}}{\begin{vmatrix} 1 & \cos\nu & \cos\mu \\ \cos\nu & 1 & \cos\lambda \\ \cos\mu & \cos\lambda & 1 \end{vmatrix}} = 1$$

Solving for p:

$$p = \frac{1}{\left[\frac{\frac{h}{A}\begin{vmatrix} \frac{h}{A} & \cos\nu & \cos\mu \\ k & 1 & \cos\lambda \\ \frac{l}{C} & \cos\lambda & 1 \end{vmatrix} + k\begin{vmatrix} 1 & \frac{h}{A} & \cos\mu \\ \cos\nu & k & \cos\lambda \\ \cos\mu & \frac{l}{C} & 1 \end{vmatrix} + \frac{l}{C}\begin{vmatrix} 1 & \cos\nu & \frac{h}{A} \\ \cos\nu & 1 & k \\ \cos\mu & \cos\lambda & \frac{l}{C} \end{vmatrix}}{\begin{vmatrix} 1 & \cos\nu & \cos\mu \\ \cos\nu & 1 & \cos\lambda \\ \cos\mu & \cos\lambda & 1 \end{vmatrix}}\right]^{1/2}} \tag{17}$$

This value of p may then be substituted in Eq. (8a), which may be written in the form

$$\begin{aligned} d_1 &= hx_1p + ky_1p + lz_1p - p \\ &= (hx_1 + ky_1 + lz_1 - 1)p \end{aligned} \tag{8a}$$

Our final value for d_1 then becomes

$$d_1 = \frac{hx_1 + ky_1 + lz_1 - 1}{\left[\frac{\frac{h}{A}\begin{vmatrix} \frac{h}{A} & \cos\nu & \cos\mu \\ k & 1 & \cos\lambda \\ \frac{l}{C} & \cos\lambda & 1 \end{vmatrix} + k\begin{vmatrix} 1 & \frac{h}{A} & \cos\mu \\ \cos\nu & k & \cos\lambda \\ \cos\mu & \frac{l}{C} & 1 \end{vmatrix} + \frac{l}{C}\begin{vmatrix} 1 & \cos\nu & \frac{h}{A} \\ \cos\nu & 1 & k \\ \cos\mu & \cos\lambda & \frac{l}{C} \end{vmatrix}}{\begin{vmatrix} 1 & \cos\nu & \cos\mu \\ \cos\nu & 1 & \cos\lambda \\ \cos\mu & \cos\lambda & 1 \end{vmatrix}}\right]^{1/2}} \tag{18}$$

Application of the General Equation.—No simplification of Eq. (18) is possible for the triclinic lattices, because $\lambda \neq \mu \neq \nu$ and $a \neq b \neq c$.

Since, for the monoclinic lattices, $\lambda = \mu = 90°$, *i.e.*, since

$$\cos \lambda = \cos \mu = 0$$

we have

$$d_1 = \frac{hx_1 + ky_1 + lz_1 - 1}{\sqrt{\left(\frac{h}{A}\right)^2 - 2\frac{h}{A}k \cos \nu + k^2 + \left(\frac{l}{C}\right)^2 (1 - \cos^2 \nu)}} \Big/ \sqrt{1 - \cos^2 \nu}$$

$$d_1 = \frac{hx_1 + ky_1 + lz_1 - 1}{\sqrt{\frac{\left(\frac{h}{A}\right)^2 - 2\frac{h}{A}k \cos \nu + k^2}{\sin^2 \nu} + \left(\frac{l}{C}\right)^2}} \tag{19}$$

For the orthorhombic lattices, $\lambda = \mu = \nu = 90°$ so that

$$\cos \lambda = \cos \mu = \cos \nu = 0$$

and

$$d_1 = \frac{hx_1 + ky_1 + lz_1 - 1}{\sqrt{(h/A)^2 + k^2 + (l/C)^2}} \tag{20}$$

For the tetragonal lattices, $\lambda = \mu = \nu = 90°$ and $a = b \neq c$ so that

$$d_1 = \frac{hx_1 + ky_1 + lz_1 - 1}{\sqrt{h^2 + k^2 + (l/C)^2}} \tag{21}$$

For the cubic lattices, Eq. (18) evidently reduces to Eq. (1) for $\lambda = \mu = \nu = 90°$ and $a = b = c$, and we have

$$d_1 = \frac{hx_1 + ky_1 + lz_1 - 1}{\sqrt{h^2 + k^2 + l^2}} \tag{22}$$

For the hexagonal system, $\lambda = \mu = 90°$, $\nu = 120°$, $a = b \neq c$, so that we have

$$d_1 = \frac{hx_1 + ky_1 + lz_1 - 1}{\sqrt{\frac{4}{3}(h^2 + hk + k^2) + (l/C)^2}} \tag{23}$$

If a rhombohedron is considered as a distorted cube in which

$$\lambda = \mu = \nu \neq 90° \qquad \text{and} \qquad a = b = c,$$

we have

$$d_1 = \frac{(hx_1 + ky_1 + lz_1 - 1)\sqrt{1 + 2 \cos^3 \lambda - 3 \cos^2 \lambda}}{\sqrt{(h^2 + k^2 + l^2) \sin^2 \lambda + 2(hk + hl + kl)(\cos^2 \lambda - \cos \lambda)}} \tag{24}$$

The complexity of Eq. (24) as compared with Eq. (23) accounts for the tendency among crystal analysts when using the powder method of analysis to calculate the interplanar spacings of rhombohedra on the basis of the hexagonal system. The Z-axis of the hexagonal lattice is the body-diagonal of the rhombohedron which passes through the trihedral angle for which $\lambda = \mu = \nu$.

In the orthorhombic system of lattices it rests with the experimenter which of the axes is picked as the Z-axis. He has nothing but his own personal preference to guide him,* for the angles between the axes are all identical. A similar situation is found in the case of a rhombohedron considered as a distorted cube. It is to be expected, therefore, that the rules for periodicity which we have derived for the cubic lattice will also hold for these lattices. Otherwise the periodicity for a given plane would depend upon the experimenter's accidental choice, and the interplanar spacings in the crystal would change merely because some axis happened to be called by a different name. Such an absurd result is impossible if the same rules for periodicity apply to all crystal systems having $\lambda = \mu = \nu$.

In the case of the triclinic system, all the axes are distinguishable from each other since $\lambda \neq \mu \neq \nu$, and the periodicity is necessarily always unity.

For the hexagonal and monoclinic systems, the experimenter has no choice as to which is the Z-axis; the matter is decided for him by the angles between the axes. This means that for these two crystal systems, the Z-axis is set apart as being crystallographically different, *i.e.*, distinguishable, from the other axes. This introduces certain complications in the determination of s in Eqs. (19) and (23), for measurements along this peculiar axis are to be regarded differently from measurements along the X- and Y-axes. This may be illustrated by considering the case of the hexagonal close-packed structure, for which the generalized atomic coordinates are

$$\begin{array}{lll} m, & n, & pC \\ m + \tfrac{1}{3}, & n + \tfrac{2}{3}, & (p + \tfrac{1}{2})C \end{array}$$

In Eq. (23) half the numerators will be of the form

$$hx_1 + ky_1 + lz_1C - 1$$

and the other half will be of the form

$$h(x_1 + \tfrac{1}{3}) + k(y_1 + \tfrac{2}{3}) + l(z_1 + \tfrac{1}{2})C - 1$$

Neglecting the -1 which does not affect the value of s, each of the two sorts of numerators of Eq. (23) may be considered to be composed of

* See Chap VIII for certain exceptions.

two terms, one of which is the sum of two quantities that deal with measurements along the X- and Y-axes and the other of which deals with measurements along the peculiar Z-axis. If the values of h and k are such as to yield successive terms, $\frac{1}{3}h + \frac{2}{3}k$, which differ from each other by unity, then the periodicity of the planes in the family (hkl) will depend upon the successive values of $\frac{1}{2}lC$. Similarly, if $\frac{1}{2}lC$ yields successive terms which differ from each other by unity, then the periodicity of the planes will depend upon the successive values of

$$(\tfrac{1}{3}h + \tfrac{2}{3}k).$$

The reader should make for himself tables corresponding to Tables II, III, and IV to aid in a thorough understanding of the above.

A rhombohedron, considered from the standpoint of hexagonal axes, has the generalized coordinates

m,	n,	pC
$m + \frac{1}{3}$,	$n + \frac{2}{3}$,	$(p + \frac{1}{3})C$
$m + \frac{2}{3}$,	$n + \frac{1}{3}$,	$(p + \frac{2}{3})C$

In the case of a rhombohedron, the derivation of the rule for the value of s in Eq. (23) is left as an exercise for the reader.

A consideration of the generalized atomic coordinates gives the following rules for the value of s in Eq. (23):

Simple triangular lattice: s is always unity.

Hexagonal close-packed structure: If the difference between h and k is a multiple of 3, then if l is odd, $s = \frac{1}{2}$; otherwise $s = 1$.

Rhombohedral structure referred to hexagonal axes (see Chap. II): If the difference between h and k is a multiple of 3, then if l is a multiple of 3, $s = 1$, but if l is not a multiple of 3, $s = \frac{1}{3}$; if the difference between h and k is not a multiple of 3, then if l is a multiple of 3, $s = \frac{1}{3}$, but if l is not a multiple of 3, then $s = 1$.

In the application of these rules, it should be remembered that zero is a multiple of 3.

SUMMARY

We have taken up the calculation of the interplanar spacings of cubic crystals. Using this as an introduction, we have derived the general formula for interplanar spacings of crystals, and we have shown how the periodicity of the planes (which enters into our formulas for interplanar spacings) may be determined for the various types of crystals. We are now ready to take up the simplest cases of crystal analysis by the Laue, Bragg, powder, and rotation methods. This will be done in the next four chapters.

Reference

1. A. W. Hull, *Phys. Rev.*, **10**, 661 (1917).

CHAPTER IV

THE LAUE METHOD OF CRYSTAL ANALYSIS

X-RAY SPECTRA AND THEIR APPLICATION TO CRYSTAL ANALYSIS

The beam of x-rays given off by an x-ray tube contains waves of every possible wave length, from the longest x-rays which can emerge from the glass of the tube with appreciable intensity down to a limit which is determined only by the voltage across the x-ray tube. This limiting wave length λ_0 may be calculated at once from the peak voltage across the tube by the "quantum equation,"

$$\lambda_0 = \frac{hc}{E_1 e} \tag{1}$$

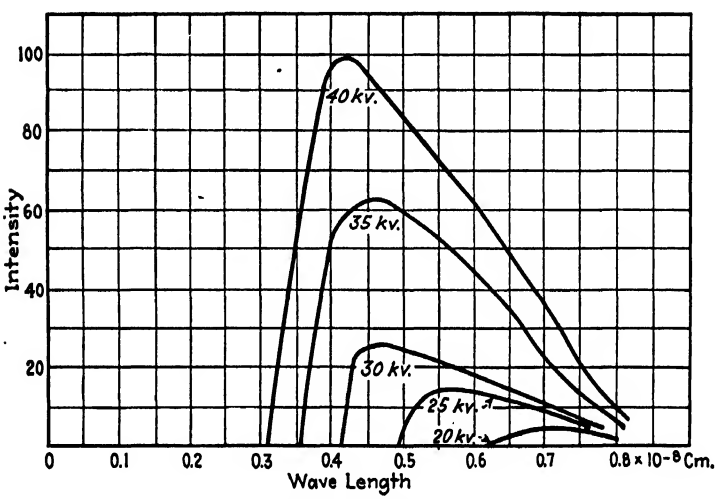

FIG. 1.—Spectrum of white x-rays. (*Hull.*)

where h = proportionality constant (Planck's constant) = 6.55×10^{-27} erg sec.

c = velocity of light = 3×10^{10} cm. per second.

E_1 = potential difference across the x-ray tube in absolute electromagnetic units = volts $\times 10^8$.

e = charge on the electron in absolute electromagnetic units = 1.591×10^{-20} e.m.u.

Since e, h, and c are all constants, Eq. (1) may be written

$$\lambda_0 = 1.234 \times 10^{-4} E_2^{-1} \tag{2}$$

where E_2 is the potential difference across the x-ray tube in volts. By analogy with visible light, a beam of x-rays which contains all possible wave lengths within the limits given above is usually called a beam of "white" x-rays. For every element there are groups of wave lengths which are characteristic of that element. These groups are called the K, L, M, . . . series. The target of an x-ray tube emits all the wave lengths of a given one of its characteristic series with relatively large intensities when the voltage across the tube exceeds the quantum limit for the shortest wave length of that series. The result is that these

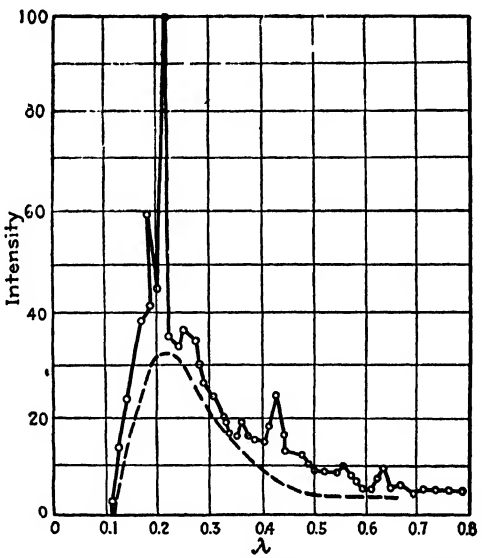

FIG. 2.—Characteristic x-ray spectrum of tungsten superimposed on white spectrum. (*Hull.*)

characteristic rays are superimposed on the white x-rays. X-ray spectra are illustrated in Figs. 1 and 2, taken from articles by A. W. Hull in "X-ray Studies of the Research Laboratory," General Electric Company. The voltages calculated from Eq. (2) which are necessary to produce characteristic rays from the various elements are given in Table I.

These peculiarities of x-ray spectra have all been utilized by one or another of the various methods of x-ray crystal analysis. The Laue method uses the white rays. The Bragg and powder methods use one of the characteristic wave lengths. Each of these methods has its own advantages and disadvantages for various kinds of work. It will therefore be worth our while to take up each in turn.

TABLE I.—POTENTIAL DIFFERENCE IN KILOVOLTS ACROSS THE X-RAY TUBE REQUIRED TO EXCITE SPECTRAL LINES CHARACTERISTIC OF VARIOUS ELEMENTS*

	K	*L*	*M*	*N*		*K*	*L*	*M*	*N*
92 U	115	21.7	5.54	1.44	47 Ag	25.5	3.79	0.72	0.10
90 Th	109	20.5	5.17	1.33	46 Pd	24.4	3.64	0.67	0.08
83 Bi	90.1	16.4	4.01	0.96	45 Rh	23.2	3.43	0.62	0.07
82 Pb	87.6	15.8	3.85	0.89	44 Ru	22.1	3.24	0.59	0.06
81 Tl	85.2	15.3	3.71	0.86	42 Mo	20.0	2.87	0.51	0.06
80 Hg	82.9	14.8	3.57	0.82	41 Nb	19.0	2.68	0.48	0.05
79 Au	80.5	14.4	3.43	0.79	40 Zr	18.0	2.51	0.43	0.05
78 Pt	78.1	13.9	3.30	0.71	39 Yt	17.0	2.36		
77 Ir	76.0	13.4	3.17	0.67	38 Sr	16.1	2.19		
76 Os	73.8	13.0	3.05	0.64	37 Rb	15.2	2.05		
74 W	69.3	12.1	2.81	0.59	35 Br	13.5	1.77		
73 Ta	67.4	11.7	2.71	0.57	34 Se	12.7	1.64		
72 Hf	65.4	11.3	2.60	0.54	33 As	11.9	1.52		
71 Lu	63.4	10.9	2.50	0.51	32 Ge	11.1	1.41		
70 Yb	61.4	10.5	2.41	0.50	31 Ga	10.4	1.31		
69 Tm	59.5	10.1	2.31	0.47	30 Zn	9.65	1.20		
68 Er	57.5	9.73	2.22	0.45	29 Cu	8.86			
67 Ho	55.8	9.38	2.13	0.43	28 Ni	8.29			
66 Dy	53.8	9.03	2.04	0.42	27 Co	7.71			
65 Tb	52.0	8.70	1.96	0.40	26 Fe	7.10			
64 Gd	50.3	8.37	1.88	0.38	25 Mn	6.54			
63 Eu	48.6	8 04	1.80	0.36	24 Cr	5.98			
62 Sm	46.8	7.73	1.72	0.35	23 Va	5.45			
60 Nd	43.6	7.12	1.58	0.32	22 Ti	4.95			
59 Pr	41.9	6.83	1.51	0.30	21 Sc	4.49			
58 Ce	40.3	6.54	1.43	0.29	20 Ca	4.03			
57 La	38.7	6.26	1.36	0.27	19 K	3.59			
56 Ba	37.4	5.99	1.29	0.25	17 Cl	2.82			
55 Cs	35.9	5.71	1.21	0.23	16 S	2.46			
53 I	33.2	5.18	1.08	0.19	15 P	2.14			
52 Te	31.8	4.93	1.01	0.17	14 Si	1.83			
51 Sb	30.4	4.69	0.94	0.15	13 Al	1.55			
50 Sn	29.1	4.49	0.88	0.13	12 Mg	1.30			
49 In	27.9	4.28	0.83	0.12	11 Na	1.07			
48 Cd	26.7	4.07	0.77	0.11					

* M. SIEGBAHN, "Spektroskopie der Röentgenstrahlen," Julius Springer, 1924.

THE LAUE DIFFRACTION PATTERN

If a crystal is placed in the path of white x-rays it will, in general, diffract some of the x-rays, for, no matter what plane of atoms in the crystal may be inclined to the beam, there will be some wave length present which will require just that grazing angle of incidence for diffraction from that family of planes. In other words, for any values of d and θ in Eq. (1) of Chap. I there will be found in the beam some value of λ such that diffraction can occur, provided only that the voltage across

the x-ray tube is high enough to produce that wave length. Since the atoms of a crystal have an orderly arrangement in all three dimensions in space, it follows that diffraction of x-rays will occur from many families of atomic planes at once, each family picking out the wave length which it can diffract at the angle at which it finds itself. This is illustrated diagrammatically in Fig. 3. The sort of diffraction pattern obtained is illustrated in Fig. 4 first published in the original work of Friedrich, Knipping, and Laue.[1]

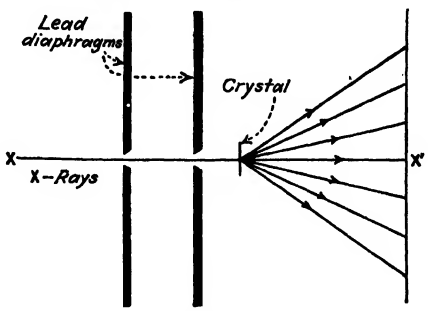

FIG. 3.—Diffraction of white x-rays by a single stationary crystal.

When the primary beam passes along an axis of symmetry of the crystal, the Laue pattern consists of a series of "spots" whose loci are ellipses which pass through the "central image" made by the primary

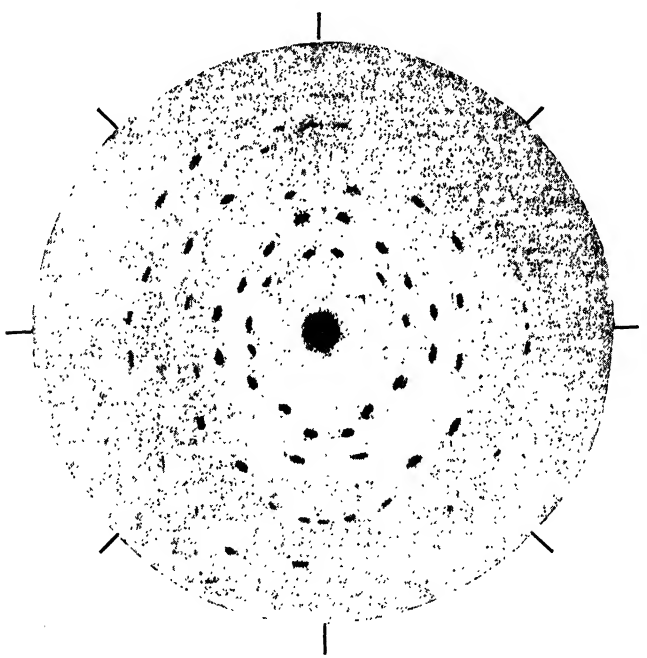

FIG. 4.—Laue diffraction pattern of zinc blende. The rays pass through the crystal parallel to one of the cubic axes.

beam, and which are symmetrically placed around it. This is shown in Fig. 5. W. L. Bragg's explanation of the elliptical shape of these loci is as follows.[2] Let the primary beam approach the crystal in the direc-

tion of one of its axes, for instance, the Z-axis in Fig. 6. It will pass through the crystal at O and strike the photographic plate at P, producing the central image. If the line OQ is the direction of some row of atoms in the crystal, *i.e.*, if it is a zone axis, then OQ is necessarily the intersection of several atomic planes. If one of these happens to lie in the YOQ plane, the diffracted beam will make a spot on the photographic plate at R. Other atomic planes passing through OQ will cause diffracted beams whose locus is the surface of a cone whose altitude is along OQ and whose generators lie along OR and OP. The intersection of this cone with the photographic plate is an ellipse.

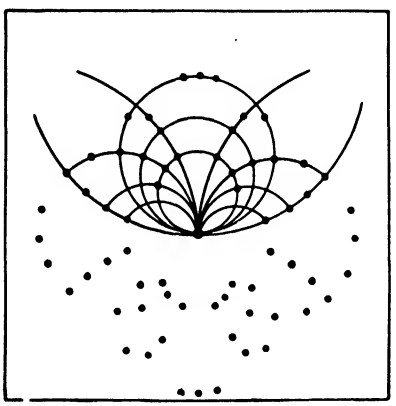

FIG. 5.—Elliptical loci of spots of Laue pattern.

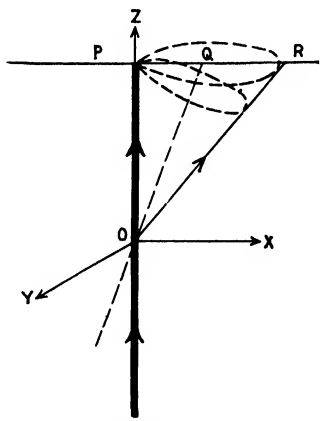

FIG. 6.—Bragg's explanation of elliptical loci.

PROJECTION DIAGRAMS

In the Laue method a crystal is used such that its faces, and therefore its crystallographic axes, may be identified by ordinary crystallographic methods. This implies that the type of crystal structure must be assumed to be that found by the ordinary crystallographic measurements of the angles between faces, for, if the faces of the specimen crystal are wrongly identified, the simple procedure given in this chapter becomes very much more complicated. We shall assume, therefore, that the crystal is mounted so that one of its principal faces is perpendicular, or nearly perpendicular, to the direction of the incident primary x-ray beam.

The identification of the plane-families associated with the spots in the Laue diffraction pattern is very laborious when a strictly analytical method is used. Labor is lessened greatly by the use of graphical methods in which each of the plane-families in the crystal is represented by a single point in a plane called the "plane of projection." Such a scheme permits us to study the orientations of planes in a three-dimensional crystal by graphical methods in two dimensions.

Although, of course, there are many ways by which a point may be made to represent a plane, the simplest and most common method is as follows: Construct a sphere using as a center some point (*i.e.*, atomic center) in one of the planes of the crystal. From this central point erect a perpendicular to the plane. This perpendicular acts like a pointer and

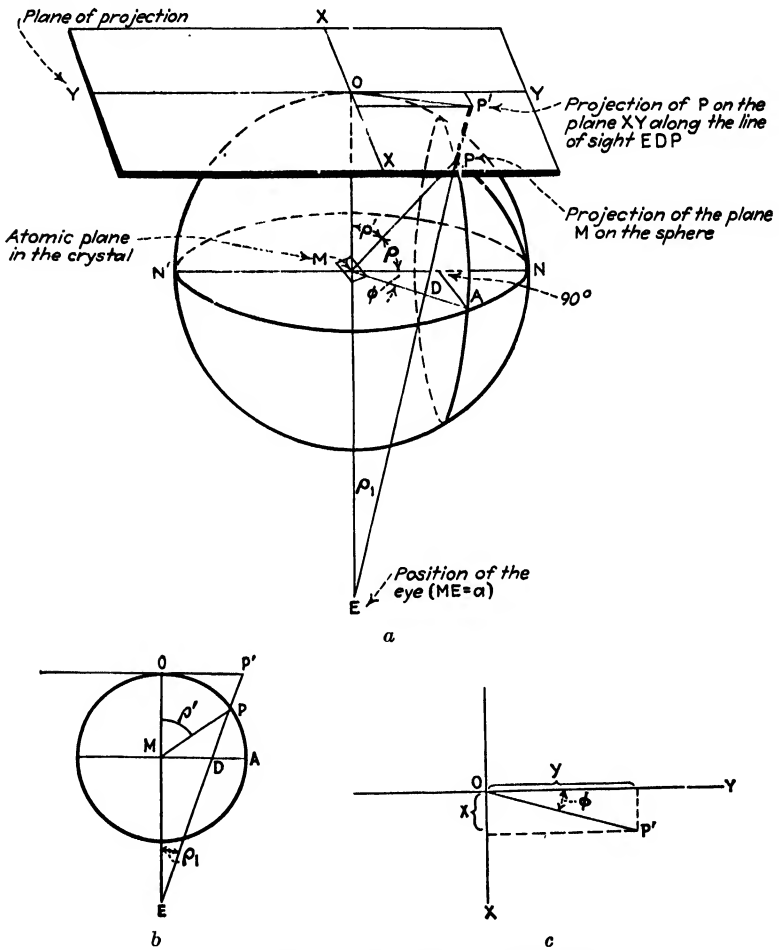

FIG. 7.—Projection of a point on a small circle.

its intersection with the surface of the sphere is a point which shows by its position the orientation of the plane. By merely erecting the necessary perpendiculars, we may have a separate point on the surface of the sphere for each family of planes in the crystal; for instance, we may have points for (1 0 0), (0 1 0), (0 0 1), (1 1 0), (0 1 1), (1 0 1), ($\bar{1}$ 1 0), (0 $\bar{1}$ 1), ($\bar{1}$ 0 1), (1 1 1), (1 1 $\bar{1}$), (1 $\bar{1}$ 1), ($\bar{1}$ 1 1), etc. The number of points which we place on the surface of the sphere will be limited only by the number of

plane-families in the crystal whose orientations we may happen to wish to show. We have, then, a method by which each plane in the crystal can be represented by a single point. It remains to transfer all these points systematically to a single plane so that our three-dimensional crystal may be represented in two dimensions. This is done by (1) setting up a plane called the "plane of projection" (see Fig. 7*a*), (2) erecting a perpendicular *OME* to this plane through the center of the sphere, (3) placing the eye at some specified place on this line *OME*, and (4) marking the points on the plane of projection where the eye "sees" the various points on the surface of the sphere. The schemes of projection in common use among crystallographers differ among themselves only in the location of the plane of projection and in the position of the eye of the observer.

In order that we may understand how these variables affect the configuration of points in the final projection, we shall take up first the general equations for the projection of a point from the surface of the sphere to the plane of projection. We shall then consider the application of the general equations to the special cases of those projections, the gnomonic and the stereographic, which are most used by crystal analysts. These and still other types of projection have been discussed in an article by F. E. Wright[3] to which the reader is referred for a complete mathematical résumé of the subject.

In the general case (see Fig. 7*a*) let *MN* and *MO* be the equatorial radius and the polar radius, respectively, of the sphere whose center is the point *M* in the crystal plane. Both *MN* and *MO* lie in the plane of the paper. Let *MP* be the perpendicular erected to the crystal plane at *M*. The point *P* lies above the plane of the paper. *MP* makes an angle ρ with the equatorial radius *MN* and an angle ρ' with the polar radius *MO*. Let the plane of projection *XY* be perpendicular to the line *MO* so that all lines in the plane passing through the point *O* are perpendicular to *OM*. Let the eye of the observer be at the point *E* on the extension of the line *OM*, and let *a* be the distance from the eye to the center *M* of the sphere. Let the line of sight *EDP* cut the equatorial plane at *D*, making an angle ρ_1 with *EMO*, and let *P'* be the projection on the plane *XY* *along the line of sight* of the point *P*. The coordinates of *P'* in the plane of projection are x and y. Since the plane *EOP'* makes an angle ϕ with *MN*, the line *OP'* will make an angle ϕ with the *Y*-axis as shown in Fig. 7*c*.

The derivation of the general equations of projection may now be considered in two parts: (1) the case where the point *P* lies on a small circle of the sphere of projection such that the small circle is parallel to *OME* of Fig. 7 and perpendicular to the equatorial diameter *NN'* and to the *Y*-axis of the plane of projection; (2) the case where the point *P* lies on a great circle of the sphere of projection.

Case 1: P Lies on a Small Circle.—In Fig. 7*a* the plane of PMA is perpendicular to the plane of AMN so that by imagining a great circle drawn through P and A we would have a right spherical triangle PAN. Then:

The spherical angle $PAN = 90°$
The central angle subtended by $AN = \phi$
The central angle subtended by $AP = 90° - \rho'$
The central angle subtended by $PN = \rho$

and

$$\cos \rho = \cos \phi \cdot \cos (90° - \rho')$$
$$\cos \rho = \cos \phi \cdot \sin \rho' \tag{3}$$

In the triangle EMP (see both Figs. 7*a* and 7*b*)

MP = radius of the sphere = 1
ME = distance from the eye to the center of the sphere = a
$\angle MPE = \angle PMO - \angle PEM = \rho' - \rho_1$

$$\frac{ME}{MP} = \frac{\sin (\rho' - \rho_1)}{\sin \rho_1} = \frac{a}{1}$$

$$a = \frac{\sin (\rho' - \rho_1)}{\sin \rho_1} = \frac{\sin \rho' \cos \rho_1 - \cos \rho' \sin \rho_1}{\sin \rho_1}$$

$$a = \sin \rho' \cdot \cot \rho_1 - \cos \rho' \tag{4}$$

Since

$$OP' = \sqrt{x^2 + y^2} \text{ (see Figs. 7}a \text{ and 7}c\text{)}$$

and since

$$OE = 1 + a \text{ (see Figs. 7}a \text{ and 7}b\text{)}$$

we have

$$\cos \phi = \frac{y}{\sqrt{x^2 + y^2}} \tag{5}$$

and

$$\tan \rho_1 = \frac{\sqrt{x^2 + y^2}}{1 + a} \tag{6}$$

By combining Eqs. (3) and (4) we find that

$$\cos \rho \cdot \cot \rho_1 = a \cos \phi + \sqrt{\cos^2 \phi - \cos^2 \rho}$$

for, if, from Eq. (3),

$$\sin \rho' = \frac{\cos \rho}{\cos \phi}$$

then

$$\cos \rho' = \sqrt{1 - \frac{\cos^2 \rho}{\cos^2 \phi}} = \frac{\sqrt{\cos^2 \phi - \cos^2 \rho}}{\cos \phi}$$

and

$$a + \cos \rho' = a + \frac{\sqrt{\cos^2 \phi - \cos^2 \rho}}{\cos \phi}$$
$$= \frac{a \cos \phi + \sqrt{\cos^2 \phi - \cos^2 \rho}}{\cos \phi}$$

But from (4),

$$a + \cos \rho' = \sin \rho' \cdot \cot \rho_1$$

so that

$$\sin \rho' \cdot \cot \rho_1 = \frac{a \cos \phi + \sqrt{\cos^2 \phi - \cos^2 \rho}}{\cos \phi}$$

But if (3) is multiplied by $\cot \rho_1$,

$$\cos \rho \cdot \cot \rho_1 = \cos \phi \cdot \sin \rho' \cdot \cot \rho_1$$

or

$$\sin \rho' \cdot \cot \rho_1 = \frac{\cos \rho \cot \rho_1}{\cos \phi}$$

Therefore

$$\cos \rho \cot \rho_1 = a \cos \phi + \sqrt{\cos^2 \phi - \cos^2 \rho} \tag{7}$$

By combining Eqs. (5), (6), and (7) we obtain the general equation for the projection of a point lying on a small circle of the sphere. This equation will involve only ρ, x, and y, for from (6) we have

$$\cot \rho_1 = \frac{1}{\tan \rho_1} = \frac{1 + a}{\sqrt{x^2 + y^2}}$$

and from (5) we have

$$\cos \phi = \frac{y}{\sqrt{x^2 + y^2}}$$

so that substitution in (7) gives

$$\frac{1 + a}{\sqrt{x^2 + y^2}} \cos \rho = \frac{ay}{\sqrt{x^2 + y^2}} + \sqrt{\frac{y^2}{x^2 + y^2} - \cos^2 \rho}$$

$$(1 + a) \cos \rho = ay + \sqrt{y^2 - (x^2 + y^2) \cos^2 \rho} \tag{8}$$

This is the general equation for the projection of a point lying on a small circle of the sphere when the small circle is perpendicular to the Y-axis of the plane of projection.

Case 2: P Lies on a Great Circle.—The designation of points and angles in Fig. 8 corresponds to that used in Fig. 7. Let us choose a great circle whose diameter RR' (Fig. 8) is parallel to the X-axis of the plane of projection. Then the plane of the great circle $RPKR'$ is per-

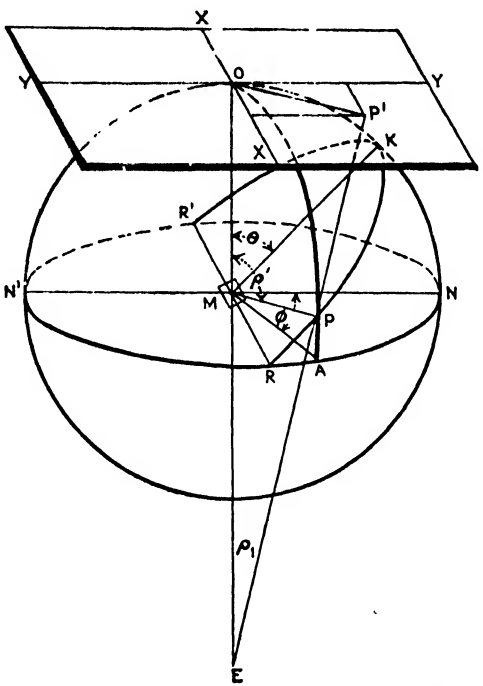

FIG. 8.—Projection of a point on a great circle.

pendicular to the plane of the great circle $OKNN'$. In the right spherical triangle POK,

The spherical angle $PKO = 90°$

The central angle subtended by $OK = \theta$

The central angle subtended by $OP = \rho'$

The angle POK is measured by the central angle ϕ which is subtended by AN

The cosine of an acute angle subtended by one leg of a right spherical triangle in terms of functions of the angles subtended by the other leg and by the hypotenuse is

$$\cos \phi = \cot \rho' \tan \theta$$

or

$$\tan \theta = \cos \phi \tan \rho' \tag{9}$$

In the plane triangle EMP (see both Figs. 7*a* and 7*b*) Eq. (4) still applies:

$$a = \sin \rho' \cot \rho_1 - \cos \rho' \tag{4}$$

By combining Eqs. (4) and (9) we may eliminate the functions of ρ' thus:

$$\tan \rho' = \frac{\tan \theta}{\cos \phi}$$

$$\frac{\sin \rho'}{\cos \rho'} = \frac{\tan \theta}{\cos \phi}$$

$$\sin \rho' = \frac{\tan \theta \cos \rho'}{\cos \phi}$$

Since, by a well-known theorem,

$$\cos \rho' = \frac{1}{\sqrt{1 + \tan^2 \rho'}}$$

we have

$$\cos \rho' = \frac{1}{\sqrt{1 + \dfrac{\tan^2 \theta}{\cos^2 \phi}}}$$

$$\cos \rho' = \frac{\cos \phi}{\sqrt{\cos^2 \phi + \tan^2 \theta}}$$

so that

$$\sin \rho' = \frac{\tan \theta}{\cos \phi} \cos \rho' = \frac{\tan \theta}{\cos \phi} \cdot \frac{\cos \phi}{\sqrt{\cos^2 \phi + \tan^2 \theta}}$$

$$\sin \rho' = \frac{\tan \theta}{\sqrt{\cos^2 \phi + \tan^2 \theta}}$$

Substituting these values of $\sin \rho'$ and $\cos \rho'$ in Eq. (4), we have

$$a = \frac{\tan \theta}{\sqrt{\cos^2 \phi + \tan^2 \theta}} \cot \rho_1 - \frac{\cos \phi}{\sqrt{\cos^2 \phi + \tan^2 \theta}}$$

or

$$a \sqrt{\cos^2 \phi + \tan^2 \theta} = \tan \theta \cot \rho_1 - \cos \phi$$

From Fig. 7*c*,

$$\cos \phi = \frac{y}{\sqrt{x^2 + y^2}}$$

and from Fig. 7*b*,

$$\tan \rho_1 = \frac{\sqrt{x^2 + y^2}}{1 + a}$$

so that

$$a\sqrt{\frac{y^2}{x^2 + y^2} + \tan^2 \theta} = \tan \theta \frac{1 + a}{\sqrt{x^2 + y^2}} - \frac{y}{\sqrt{x^2 + y^2}}$$

or

$$a\sqrt{y^2 + (x^2 + y^2) \tan^2 \theta} = (1 + a) \tan \theta - y \qquad (10)$$

This is the general equation for the projection of a point lying on a great circle of the sphere when the great circle is parallel to the X-axis of the plane of projection. Since the final form of the equation includes no angles but θ, and since the directions which we chose as the directions of the X- and Y-axes were entirely arbitrary, it follows that Eq. (10) will apply to the projection of any point lying on the upper half of any given great circle of the sphere. By assigning definite positions to the plane of projection along the line EO, and by assigning definite values to $a(=ME)$, we may obtain the special equations for the various types of projection in common use. Of the various projections (gnomonic, stereographic, orthographic, and Wright) ordinarily used by mineralogists and crystallographers the first two have found direct application in crystal analysis. It will therefore be of interest to derive their special equations as a means of studying the properties of their projected figures.

GNOMONIC PROJECTION

In this projection (see Fig. 9*a*) the eye is considered to be at the center of the sphere of projection, and the plane of projection is tangent to the sphere at the pole O. The points E and M therefore coincide, so that $a = 0$, and $\rho' = \rho_1$. Equation (8) for the point on the small circle then becomes

$$\begin{aligned} \cos \rho &= \sqrt{y^2 - (x^2 + y^2) \cos^2 \rho} \\ \cos^2 \rho &= y^2 - (x^2 + y^2) \cos^2 \rho \\ y^2(1 - \cos^2 \rho) &= (1 + x^2) \cos^2 \rho \\ y^2 &= (1 + x^2) \frac{\cos^2 \rho}{1 - \cos^2 \rho} \\ y^2 &= (1 + x^2) \cot^2 \rho \end{aligned} \qquad (11a)$$

which is the equation of an hyperbola. Substitution of $a = 0$ in Eq. (10) for the great circle gives immediately

$$y = \tan \theta \qquad (11b)$$

which is the equation of a straight line for any single value of θ. Equation (11a) shows that if the plane LL' of Fig. 9a is rotated about NN' as an axis, its gnomonic projection P' will sweep out an arc of an hyperbola in the plane of projection. When P' falls on the Y-axis of the plane of projection, ρ of (11a) equals $90° - \theta$ of (11b). Equation (11b) shows that, for successive values of ρ, the intersections of the hyperbolas with the Y-axis will lay off lengths on the Y-axis which will be proportional to tan θ. This will come up later in our discussion of the gnomonic rotation net. Equation (11b) also shows that when θ is kept constant, then y is constant so that if the plane LL' of Fig. 9a is rotated about an axis which is normal to the great circle $RPKR'$ (Fig. 8) at its center M, then the gnomonic projection of the plane will sweep out a straight line on the

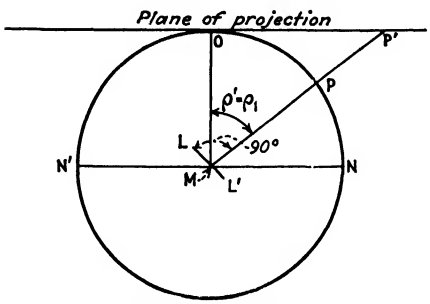

FIG. 9a.—Gnomonic projection of the plane LL'.

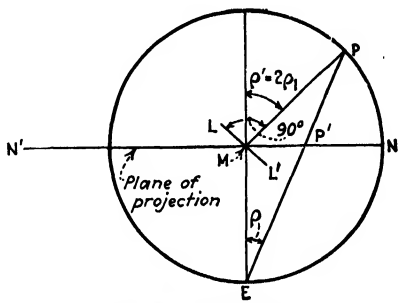

FIG. 9b.—Stereographic projection of the plane LL'.

plane of projection. This means that in the gnomonic projection all zone axes are represented by straight lines. Herein lies the great value of the gnomonic projection to the crystal analyst. It has the defect that the plane of projection would have to extend to infinity in all directions in order to represent one hemisphere of the reference sphere.

STEREOGRAPHIC PROJECTION

This projection (Fig. 9b) differs from the gnomonic not only in the location of the eye but also in the location of the plane of projection. The eye is placed at the lower pole E of the reference sphere, and the plane of projection is made to coincide with the equatorial plane of the reference sphere. This gives us $a = 1$ and $\rho' = 2\rho_1$. Since the plane of projection is no longer tangent to the reference sphere but now coincides with the equatorial plane, the coordinates of our projected points will be only half as large as those in our general Eqs. (8) and (10). If x' and y' are the coordinates on the equatorial plane and x and y are the corresponding coordinates of a point projected on the tangent plane, then

$$x = 2x'$$
$$y = 2y'$$

Equation (8) for the projection of a point which lies on a small circle of the reference sphere becomes

$$\left(y' - \frac{1}{\cos \rho}\right)^2 + x'^2 = \tan^2 \rho$$

for, remembering that $a = 1$,

$$2 \cos \rho - y = \sqrt{y^2 - (x^2 + y^2) \cos^2 \rho}$$
$$4 \cos^2 \rho - 4y \cos \rho + y^2 = y^2 - (x^2 + y^2) \cos^2 \rho$$
$$4y = \cos \rho \cdot (4 + x^2 + y^2)$$
$$8y' = \cos \rho \cdot (4 + 4x'^2 + 4y'^2)$$
$$2y' = \cos \rho \cdot (1 + x'^2 + y'^2)$$
$$2y' \cos \rho = \cos^2 \rho + x'^2 \cos^2 \rho + y'^2 \cos^2 \rho$$

Since $\cos^2 \rho = 1 - \sin^2 \rho$,

$$y'^2 \cos^2 \rho - 2y' \cos \rho + 1 + x'^2 \cos^2 \rho = \sin^2 \rho$$
$$y'^2 - 2y' \frac{1}{\cos \rho} + \frac{1}{\cos^2 \rho} + x'^2 = \frac{\sin^2 \rho}{\cos^2 \rho}$$
$$\left(y' - \frac{1}{\cos \rho}\right)^2 + x'^2 = \tan^2 \rho \qquad (12a)$$

which is the equation of a circle.

Equation (10) for the projection of a point which lies on a great circle of the reference sphere becomes

$$(y' + \cot \theta) + x'^2 = \frac{1}{\sin^2 \theta} = \csc^2 \theta$$

for, since $a = 1$, Eq. (10) will read

$$2 \tan \theta - y = \sqrt{y^2 + (x^2 + y^2) \tan^2 \theta}$$
$$4 \tan^2 \theta - 4y \tan \theta + y^2 = y^2 + (x^2 + y^2) \tan^2 \theta$$
$$4 - 4y \cot \theta = x^2 + y^2$$
$$y^2 + 4y \cot \theta + x^2 = 4$$
$$y^2 + 4y \cot \theta + 4 \cot^2 \theta + x^2 = 4 + 4 \cot^2 \theta$$
$$(y + 2 \cot \theta)^2 + x^2 = 4(1 + \cot^2 \theta) = 4 \frac{1}{\sin^2 \theta} = (2 \csc \theta)^2$$
$$(y' + \cot \theta)^2 + x'^2 = \frac{1}{\sin^2 \theta} = \csc^2 \theta \qquad (12b)$$

which is the equation of a circle.

The stereographic projection represents one hemisphere of the reference sphere in a circle of unit radius and will represent the whole reference

sphere if the plane of projection is of infinite extent. It is angle true; all zone lines are circular arcs. These properties make the stereographic projection useful to the crystal analyst in picturing "preferred orientations" of crystals in mechanically worked metals. This subject will be taken up in a later chapter.

IDENTIFICATION OF SPOTS IN THE LAUE PATTERN BY MEANS OF THE GNOMONIC PROJECTION

The gnomonic projection is so widely used in connection with the Laue method that it will be worth while to describe it more fully from the standpoint of the crystal analyst. The method of identification of the Laue spots is illustrated in Fig. 10. The primary beam of x-rays passes through the crystal at O and strikes the photographic plate at P. On

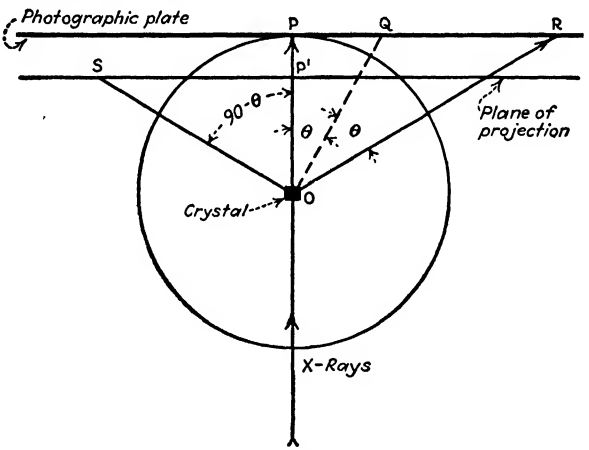

FIG. 10.—Gnomonic projection of a Laue spot.

its way through the crystal at O it will strike some atomic plane. Let us assume that this atomic plane is perpendicular to the plane of the paper and that it passes through the zone axis OQ. A perpendicular drawn to this plane at O will strike the plane of projection at S. Then S is the gnomonic projection of this plane of the crystal. The distance from the spot on the photographic film at R to the central image at P is $PR = PO \tan 2\theta$. The distance from the primary x-ray beam to S is $P'S = P'O \tan (90° - \theta)$. In practice, PO is usually 4 or 5 cm. and $P'O$ is usually 5 cm. Convenient tables for gnomonic projection have been published by Wyckoff.[4] They are reproduced here as Tables II and III. The data of Table II or III may be marked off on a paper or celluloid rule (Fig. 11). A silver print is then made of the original negative of the Laue pattern. This print is pasted at the center of a sheet of drawing paper, and a pin is passed through the common starting point P' of the two scales on the rule and through the middle of the central spot on the print. The rule

TABLE II.—DATA FOR PREPARING GNOMONIC RULER WHEN THE DISTANCE FROM CRYSTAL TO PLATE IS 4 CM.

Left side of ruler, centimeters	Right side of ruler, centimeters	Left side of ruler, centimeters	Right side of ruler, centimeters
1.20	34.06	3.40	13.60
1.25	32.77	3.50	13.31
1.30	31.57	3.60	13.03
1.35	30.45	3.70	12.77
1.40	29.42	3.80	12.52
1.45	28.45	3.90	12.29
1.50	27.58	4.00	12.07
1.55	26.74	4.10	11.86
1.60	25.96	4.20	11.67
1.65	25.23	4.30	11.48
1.70	24.55	4.40	11.30
1.75	23.90	4.50	11.13
1.80	23.29	4.60	10.97
1.85	22.73	4.70	10.82
1.90	22.19	4.80	10.68
1.95	21.67	4.90	10.54
2.00	21.18	5.00	10.40
2.05	20.72	5.10	10.28
2.10	20.28	5.20	10.15
2.15	19.86	5.30	10.04
2.20	19.47	5.40	9.93
2.25	19.09	5.50	9.82
2.30	18.72	5.60	9.71
2.35	18.38	5.70	9.62
2.40	18.05	5.80	9.52
2.45	17.74	5.90	9.43
2.50	17.44	6.00	9.34
2.55	17.14	6.10	9.26
2.60	16.87	6.20	9.18
2.65	16.60	6.30	9.10
2.70	16.35	6.40	9.02
2.75	16.10	6.50	8.95
2.80	15.86	6.60	8.88
2.85	15.63	6.70	8.81
2.90	15.42	6.80	8.74
2.95	15.20	6.90	8.68
3.00	15.00	7.00	8.61
3.10	14.61		
3.20	14.25		
3.30	13.92		

TABLE III.—DATA FOR PREPARING GNOMONIC RULER WHEN THE DISTANCE FROM CRYSTAL TO PLATE IS 5 CM.

Left side of ruler, centimeters	Right side of ruler. centimeters	Left side of ruler centimeters	Right side of ruler, centimeters
1.10	46.0	3.30	16.65
1.15	44.0	3.35	16.44
1.20	42.3	3.40	16.24
1.25	40.6	3.45	16.05
		3.50	15.86
1.30	39.1		
1.35	37.7	3.55	15.68
1.40	36.4	3.60	15 50
1.45	35.2	3.65	15.33
1.50	34.06	3.70	15.16
		3.75	14.99
1.55	33.01	3.80	14.84
1.60	32.02	3.85	14.69
1.65	31.10	3.90	14.54
1.70	30.24	3.95	14.40
1.75	29.41	4.00	14.26
1.80	28.65	4.10	13.98
1.85	27.92	4.20	13.73
1.90	27.23	4.30	13.48
1.95	26.58	4.40	13.25
2.00	25.96	4.50	13.02
2.05	25.38	4.60	12.82
2.10	24.82	4.70	12.62
2.15	24.29	4.80	12.43
2.20	23.78	4.90	12.25
2.25	23.29	5.00	12.07
2.30	22.84	5.10	11.90
2.35	22.39	5.20	11.74
2.40	21.97	5.30	11.59
2.45	21.57	5.40	11.44
2.50	21.18	5.50	11.30
2.55	20.81	5.60	11.17
2.60	20.45	5.70	11.04
2.65	20.11	5.80	10.91
2.70	19.78	5.90	10.79
2.75	19.47	6.00	10.67
2.80	19.16	6.10	10.56
2.85	18.87	6.20	10.45
2.90	18.58	6.30	10.35
2.95	18.31	6.40	10.25
3.00	18.05	6.50	10.15
3.05	17.80	6.60	10.06
3.10	17.55	6.70	9.97
3.15	17.32	6.80	9.88
3.20	17.09	6.90	9.80
3.25	16.87	7.00	9.72

then enables the experimenter to mark down directly on the drawing paper the point which is the gnomonic projection for the plane-family corresponding to any given Laue spot.

The gnomonic projections of the Laue patterns of rutile (Fig. 12), and of rhodochrosite (Fig. 13), illustrate how the names of the various atomic

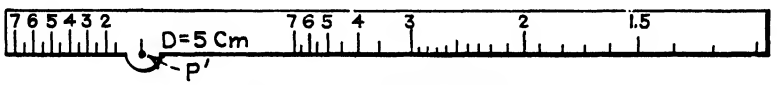

FIG. 11.—The Wyckoff scale.

planes are related to the corresponding points of the projection. Let us assume for simplicity that the crystal belongs to the cubic system and that the x-rays strike it in the direction of the Z-axis. The positions of the X- and Y-axes are known from the external symmetry of the crystal.

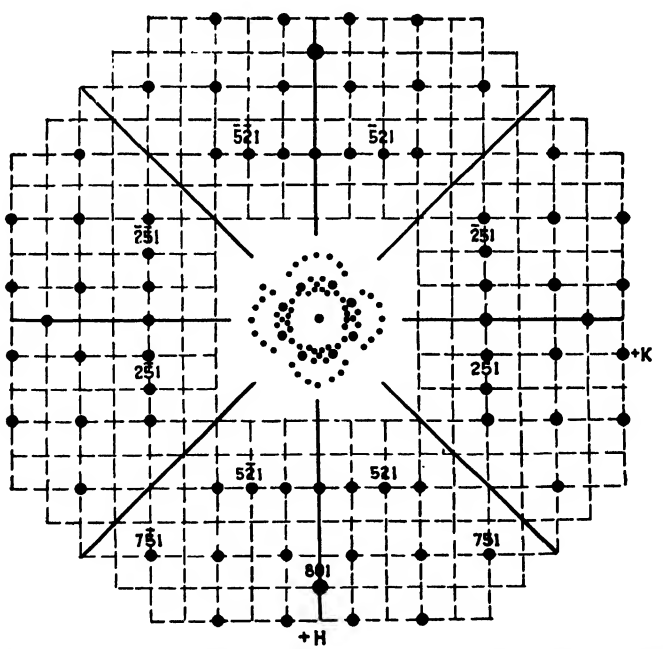

FIG. 12a.—Gnomonic projection of Laue pattern of rutile (TiO_2). Primary beam parallel to the Z-axis. (*Wyckoff*). TiO_2 is face-centered tetragonal with an axial ratio $C = 0.455$, *i.e.*, body-centered tetragonal with $C = 0.644$.

Figure 14 gives the gnomonic projections of typical planes which lie parallel to the Y-axis. It is evident that S_1, which is the gnomonic projection of the plane Q_1OY, is exactly as far from the central image P' as is the crystal O, and that $P'S_1 = S_1S_2 = S_2S_3$. This means that if the plane of projection is $P'O$ cm. from the crystal, then the gnomonic

projections which fall in the direction of the X-axis are all $P'O$ cm. apart from each other. Similarly, the gnomonic projections which fall in the direction of the Y-axis are $P'O$ cm. apart. The gnomonic projection of a cubic crystal is therefore based on a network of squares whose sides are equal to the distance from the crystal to the plane of projection. The indices of the planes whose projections fall at the intersections of this network may be read off directly in terms of the coordinates of their projections on the network, remembering that the l index (reciprocal

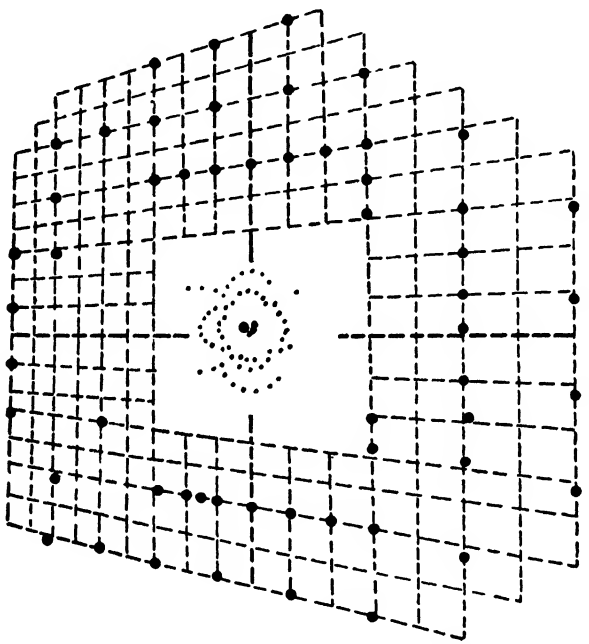

FIG. 12b.—Gnomonic projection of Laue pattern of rutile primary beam at an angle to the Z-axis. (*Wyckoff.*)

of the intercept of the plane on the Z-axis) is necessarily unity. Indices of other planes whose projections do not fall on the network may be determined by first expressing them as fractions and then by changing them to the lowest possible corresponding integers. For instance in Fig. 13, the projection of plane $(1\,\bar{2}\cdot 2)$ is first found as $(\frac{1}{2}\,\bar{1}\cdot 1)$; the projection of plane $(4\,\bar{3}\cdot 4)$ is first found as $(1\,\bar{\frac{3}{4}}\cdot 1)$, etc.

If the crystal is tetragonal, and the primary beam of x-rays is made to pass parallel to the Z-axis (*i.e.*, parallel to the axis which has a different unit of length from the other two), then the gnomonic pattern will be built up of a network of squares as in the case of a cubic crystal, but with this difference—the sides of the squares are no longer equal to the distance from the crystal to the plane of projection but to this distance

multiplied by the axial ratio C of the crystal. It has been already stated in Chap. II that any body-centered tetragonal crystal may be regarded as a face-centered tetragonal crystal by dividing the axial ratio by $\sqrt{2}$. For this reason the network of Fig. 12*a* may be replaced by a square network placed at 45° to the one shown in the drawing. If the primary

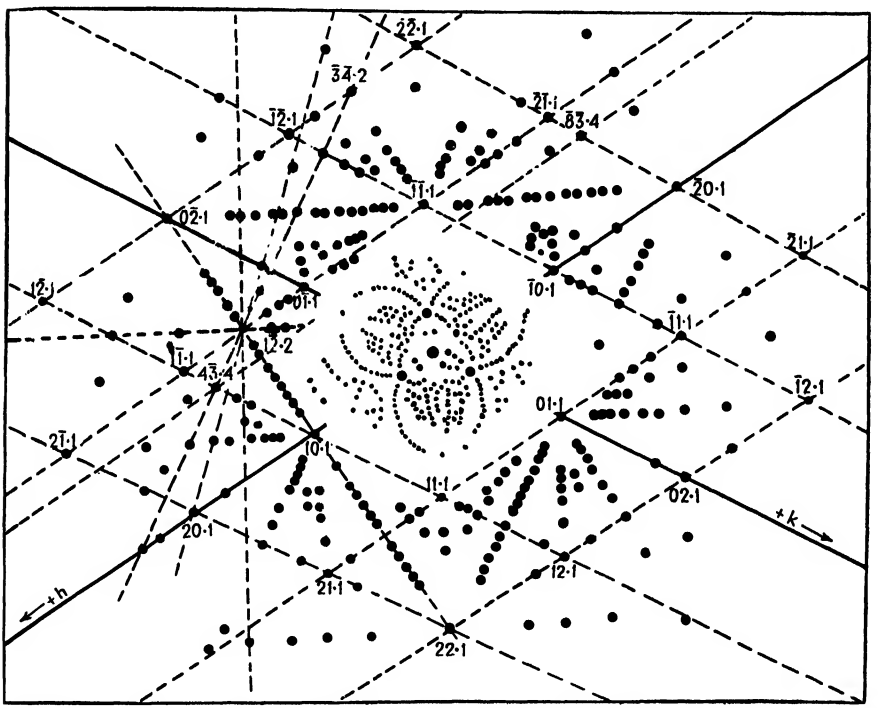

FIG. 13.—Gnomonic projection of Laue pattern of rhodochrosite ($MnCO_3$). Primary beam approximately normal to the basal (1 1 1) plane. (*Wyckoff.*)

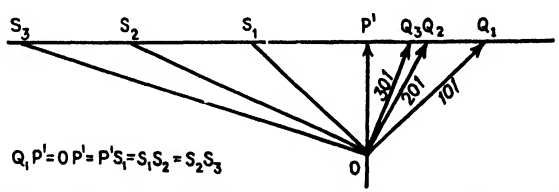

FIG. 14.—Gnomonic projection in the X-Y plane for a cubic crystal. A similar projection may be made in the X-Z or the Y-Z plane.

beam of x-rays is made to pass parallel to the X- or Y-axis, then the gnomonic network will be composed of rectangles. One side of the rectangles will be equal to the distance from the crystal to the plane of projection. The other side will be this distance divided by the axial ratio C. If the crystal is orthorhombic, the lengths of the sides of the

rectangles in the network will have the same ratio to each other as the reciprocals of the corresponding axial ratios in the crystal.

If the crystal is a rhombohedron or has a triangular close-packed structure, and if the primary beam of x-rays passes parallel to the Z-axis of the hexagonal lattice, then the gnomonic network will consist of parallelograms whose sides make an angle of 120° (see Fig. 13). This angle corresponds to the angle between the X- and Y-axes. The network therefore names the planes of the crystal in terms of the reciprocals of the intercepts on the hexagonal system of axes. As was stated in Chap. II, the hexagonal indices for the rhombohedral lattice may be transformed, if desired, into indices referred to the edges of the rhombohedron by the equations

$$\begin{aligned} h &= 2H + K + L \\ k &= -H + K + L \\ l &= -H - 2K + L \end{aligned}$$

where H, K, L are the indices in terms of the hexagonal axes and h, k, l are the indices in terms of the edges of the rhombohedron.

If the crystal is monoclinic and the primary beam is parallel to the Z-axis, the network is composed of parallelograms whose angle is determined by the angle between the X- and Y-axes. If the x-ray beam is parallel to the X- or Y-axis, the network is rectangular but is displaced so that the origin of coordinates is not at the center of the projection. If the crystal is triclinic, the network is composed of parallelograms whose origin of coordinates is not at the center of the projection.

If the primary beam of x-rays is not quite parallel to one of the axes of the crystal, the gnomonic projection is slightly distorted as in Fig. 12*b*, but for angles less than 10° the distortion does not usually prevent the easy identification of atomic planes. However, it is not always desirable to have the primary x-ray beam approximately parallel to one of the crystal axes. It will be shown later in this chapter, and again in Chap. IX, that it is sometimes necessary to compare the intensities of Laue spots from two families of planes having nearly the same interplanar spacing. In such cases both spots must appear on the same photographic film and are preferably at the same distance from the central image. This sometimes requires the crystal to be oriented so that one of its axes makes a considerable angle with the incident beam. The identification of the resulting points in the gnomonic projection can be made easily by the graphical method of the "rotation net" described by Wyckoff.[4]

Figure 15 shows the geometrical relationships which underlie the rotation net. Let the crystal be situated at the point O, and let an imaginary sphere be drawn with the point O as a center. The radius of the sphere is taken as OP', *i.e.*, it is the distance from the crystal to the plane of projection $ABCD$; it is identical with OP' of Figs. 10 and 14, and

with MO of Fig. 9a. Let us consider the crystal to be so placed at O that one of its axes coincides with OP'. If, now, the crystal is rotated through some angle $90° - \phi_1$ about the line EF as an axis, the point P' will move along the circumference of the great circle $GP'H$ and the line OP' extended will touch the plane $ABCD$ at some point whose distance from the original position of P' is OP' cot ϕ_1. This is consistent with Eq. (11b) in which $90° - \phi_1 = \theta$ and OP' is taken as unity. A plane passed through EF and the new position of OP' will intersect the plane $ABCD$ in a straight line which is parallel to MN and which is distant OP' cot ϕ_1 from it. Now let the line OKS_1 be perpendicular to some plane $(h\,k\,l)$ in the crystal. The point of intersection of this line with the plane

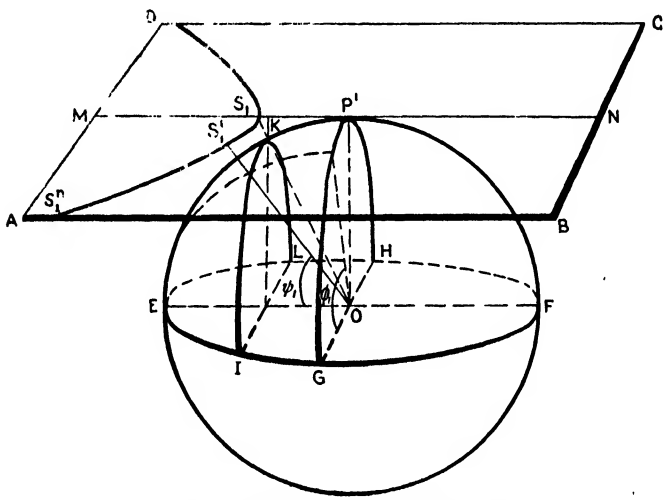

FIG. 15.—The theory of the gnomonic rotation net.
(EF corresponds to RR' of Fig. 8.)

$ABCD$ is therefore the gnomonic projection of the plane $(h\,k\,l)$. As the crystal is rotated about the line EF, the line OKS_1 marks off the small circle IKL on the sphere and the extension of OKS_1 marks out on the plane $ABCD$ the hyperbola $S_1S_1'S_1''$ as predicted by Eq. (11a). If, therefore, the angular rotation of the crystal is represented on $ABCD$ by straight lines parallel to the axis of rotation, then the corresponding locations of the Laue spots will be shown by the intersections of these straight lines with the hyperbolas. This gives the gnomonic rotation net shown in Fig. 16.

Each experimenter should make for himself a gnomonic rotation net, calculated for the same value of OP' for which his Wyckoff rule was made, *i.e.*, 5 cm. These drawings will be more satisfactory if they are traced on tracing cloth. The coordinates of the projection of the Laue spots in the plane $ABCD$ are:

x-coordinate (perpendicular to MN of Fig. 15) $= OP' \cot \phi_1$
y-coordinate (parallel to MN) $= \cot \psi_1 \csc \phi_1 \cdot OP'$ (13)

The center of the rotation net corresponds to the point P' of Figs. 10, 14, and 15 for a crystal having orthogonal axes. It is the position of the photographic record of the primary x-ray beam on the silver print which was pasted on the sheet of drawing paper preparatory to making the gnomonic projection if the primary beam is parallel to one of the axes.

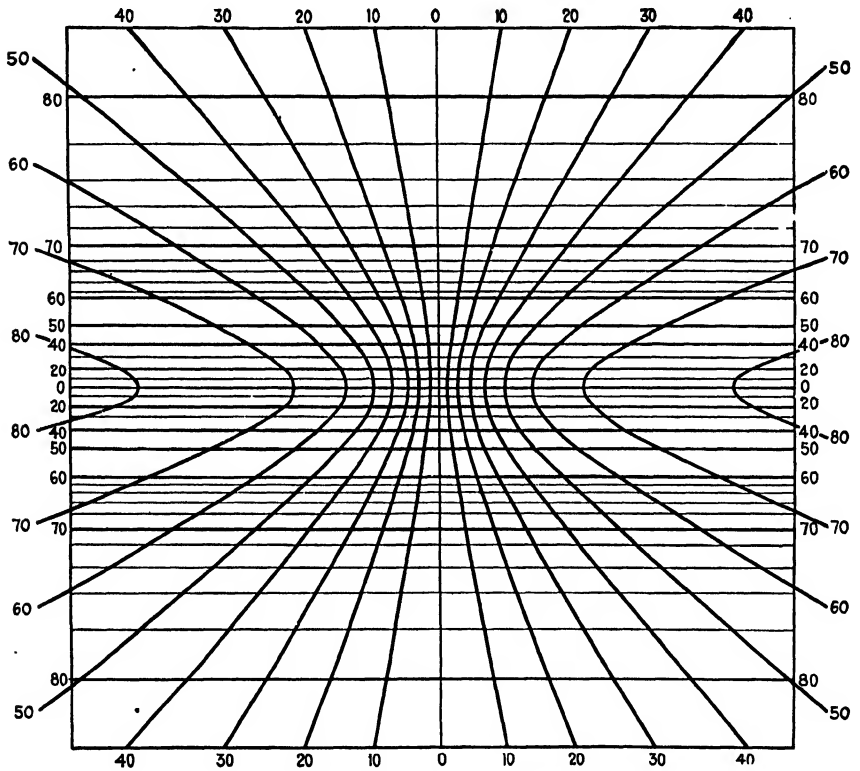

FIG. 16.—The gnomonic rotation net.

If we have a Laue pattern of a crystal taken with the primary x-ray beam parallel to one of the axes of the crystal, we can, by the following procedure, draw at once the gnomonic projection of the pattern which would have been obtained if the primary beam had made some predetermined angle ϕ_1 with that crystal axis;

a. Make a copy of the original gnomonic projection on tracing cloth or tracing paper.

b. Place this over the rotation net so that the point representing the primary beam lies at the center P' of the net.

c. Orient the drawing so that the desired axis of rotation of the crystal is parallel to the line *MN*.

d. Move each point of the original projection along its own hyperbola until its angular reading on the x-coordinates has been increased by $90° - \phi_1$.

The new positions of the points will give the gnomonic projection which would have been found if the Laue pattern had been taken with the new orientation of the crystal. The center of the new projection will be the gnomonic projection of the plane (hkl) of the crystal which would have been perpendicular to the primary beam, *i.e.*, the plane which in the new orientation would have been perpendicular to the primary

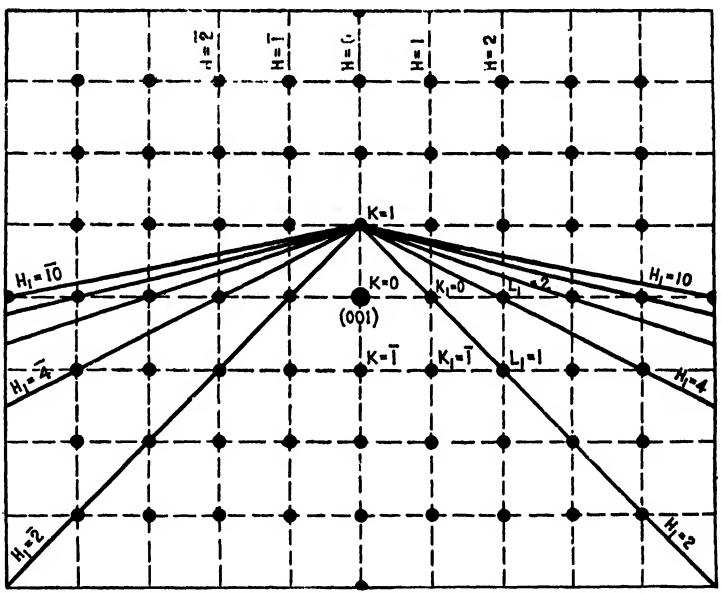

FIG. 17*a*.—Gnomonic projection for a cubic crystal when the primary beam passes parallel to a principal axis. (*Wyckoff*.[6])

beam is represented as lying parallel to the plane of the new projection. Since the orientation of the crystal is known for the actual Laue pattern, and since the angular rotation of the crystal is known, it follows that the plane which corresponds to the center of the new diagram is also known. When the primary x-ray beam does not pass parallel to one of the principal axes of a cubic crystal, it should be noted that the l index is no longer unity for points lying at the corners of squares in the projection. This is brought out in Fig. 17, in which h, k, and l refer to indices of spots which lie on straight lines in the original gnomonic projection (primary beam parallel to the crystal axis) and h_1, k_1, and l_1 refer to indices of spots which lie on straight lines in the gnomonic projection of the crystal after rotation. The changes to be made in the above

procedure when the original Laue pattern is taken with the primary beam not parallel to a crystal axis will be obvious. In such a case the technique is much more tedious than the simple procedure just outlined.

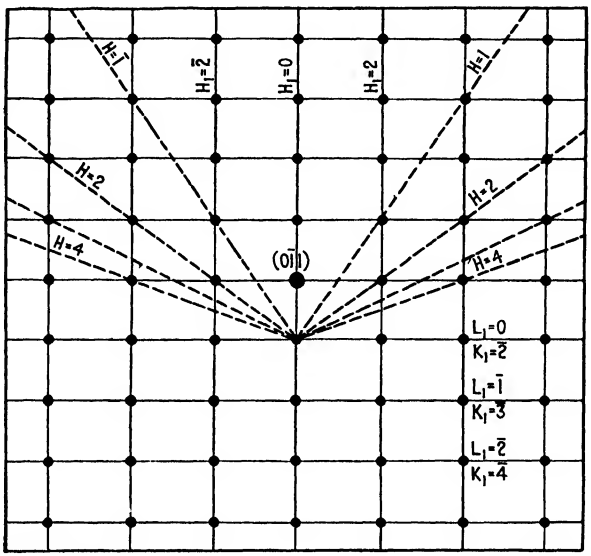

FIG. 17*b*.—Gnomonic projection for the same cubic crystal when the primary beam is normal to the (0 $\bar{1}$ 1) planes. (*Wyckoff*.[6])

INTERPRETATION OF THE LAUE PATTERN

Once the "spots" of the Laue pattern have been identified in terms of the atomic planes which produced them, there remains the problem of using these spots to determine the structure of the crystal. The simplest case is that of a crystal of an element, for, since all its atoms are alike, their diffracting powers under similar conditions may be assumed to be all alike. Let us assume for the purpose of illustration that a given element has a simple cubic structure, although actually no such element is known. Then, from Eq. (3) of Chap. III, we can calculate the relative distances between its various families of planes in terms of the edge of the unit-cube. Every such plane should be represented by a spot in the Laue pattern and is shown in its proper place in the gnomonic projection, provided only that a suitable wave length from the primary beam is available for producing the spot on the photographic film. If, however, the crystal is body-centered cubic, certain planes are only half as far apart as they would be if the crystal were simple cubic. An instance of this is the (1 1 1) plane. If the crystal is body-centered cubic, no gnomonic projection of spots will be found at $h = 1$, $k = 1$; $h = \bar{1}$, $k = 1$; $h = 1$, $k = \bar{1}$; $h = \bar{1}$, $k = \bar{1}$. The same will apply to every plane for which the numerator of Eq. (3) of Chap. III

is ½. Similarly, the Laue pattern of a face-centered cube (or some other division of the cubic system) is characterized by the absence of spots of those planes for which the numerator of the equation differs from unity. The same sort of procedure may be applied in the case of other crystal systems.

It is of course evident that for such comparatively simple structures the various families of planes which differ only in the sign of their indices will act similarly; that is, if the (1 1 1) position in the gnomonic network is vacant, then the $(\bar{1}\,1\,1)$, $(1\,\bar{1}\,1)$, and $(1\,1\,\bar{1})$ positions are also vacant. Otherwise some other and possibly more complicated structure must be found which is consistent with the Laue pattern and its gnomonic projection. This implies also that it must be consistent with the symmetry of the crystal as determined by ordinary crystallographic methods. The theory of space-groups, which will be treated more fully in Chap. VIII, lists the 230 ways in which points can be arranged symmetrically in space. Some of these 230 space-groups have the symmetry characteristics of the triclinic system of crystallization; others belong to the monoclinic system; still others to the orthorhombic system; etc. The 230 space-groups are listed in Chap. VIII and in Appendix III according to the crystal systems to which they belong. By reason of its systematic listing of the various geometrical configurations possible for different symmetries, the theory of space-groups is useful as a means of insuring that no possible interpretation of the crystal structure is overlooked which might be consistent with the Laue pattern. The application of the theory of space-groups to the interpretation of Laue patterns will be taken up in considerable detail in Chap. IX. We shall, therefore, consider here only in a general way how this theory may be used as an aid in determining the structure of a crystal by the Laue method. The general procedure described will of course apply to the crystals of either elements or compounds.

In general, when using the theory of space-groups, the method of determining the structure of a crystal from the gnomonic projection of its Laue pattern consists of three steps which are briefly as follows:

1. The selection of the type of symmetry,* *i.e.*, the system of crystallization, required by the exterior of the crystal. This limits the possible marshaling of atoms (or molecules) to those space-groups which are consistent with this symmetry.

2. The determination of the dimensions of the unit-crystal and from these the determination of the number of atoms (or molecules) in the unit-crystal. It will be shown in Chap. IX how this serves to limit further the number of possible space-groups found in 1.

3. The selection from the structures found in 2 of the one which is most consistent with the Laue pattern. This requires the use of Eq. (16) or (17) and involves certain

* This always limits us to some one crystal system and in most cases to some one division of a crystal system.

assumptions which may not be rigorously true but which are on the whole consistent with existing data. This step, too, is given in full in Chap. IX.

For most crystals, the first step may be taken with the aid of any good crystallography text.*

The crystallographic system to which the crystal belongs determines the general shape of the unit-crystal. For instance, if the crystal belongs to the cubic system, the unit-crystal is necessarily a cube; if it belongs to the tetragonal system, the unit-crystal is a right prism all of whose sides are rectangles and whose bases are squares; etc. In some cases a choice is possible between two or more unit-crystals for the same substance. For instance, it has already been shown that a rhombohedral crystal may be regarded as having as its unit-crystal a so-called "rhomboid prismatic" structure whose base is an equilateral parallelogram with 120° and 60° angles (*i.e.*, two equilateral triangles with one side in common), or it may be regarded as having a unit-crystal of rhombohedral shape.

The second step in the solution of the crystal structure requires data not obtainable from a single Laue pattern. Two procedures are open:

1. The voltage across the x-ray tube may be lowered step by step for successive Laue patterns until some spot disappears. From the quantum relation given in Eq. (2) the wave length can be calculated which gave rise to that spot, and thus the interplanar spacing corresponding to the spot can be calculated by the aid of Bragg's law.

2. One of the faces of the crystal may be rotated slowly in the path of a beam of x-rays consisting essentially of a single, known wave length. The angles at which diffraction occurs are noted, and from them not only can the order of diffraction n of Bragg's law be determined but also the interplanar distance d can at once be calculated.

From the value of d found by either of these two methods for some plane of known Miller indices we can determine the edge of the unit of structure by the aid of the equations of Chap. III, assuming the simplest possible lattice in the crystal system, *i.e.*, simple cube, simple "rhomboid prism," (*i.e.*, the unit of structure for the simple triangular lattice), etc. The volume of this simple model of the unit-crystal is then calculated, and its mass is determined (at least approximately) in terms of the published data for the density of the crystal. From the molecular weight of the substance of which the crystal is composed and the fact that one unit of atomic weight is equal to 1.649×10^{-24} g., the number of molecules per unit crystal is at once found. It is the **n** of Eqs. (1) to (3) in Chap. II. From this and the chemical symbol of the substance of which the crystal is composed, it is possible to find at once the number of atoms of each kind in the unit-crystal. A check may be obtained upon the unit-crystal assumed above by calculating the value of $n\lambda$ from Bragg's

* GROTH, "Chemische Krystallographie," Leipzig, 1906, is probably the most complete to date.

law for each spot in the Laue pattern, using in each case the value of d determined above for the planes which gave rise to the spot and the value of θ given by the Laue pattern. In no case may the value of $n\lambda$ calculated in this way be less than the minimum of wave length [λ_0 of Eq. (1)] present in the x-ray beam. The distribution in space of the atoms in the unit-crystal is, of course, limited to those space-groups which are consistent with the data so far obtained. In other words, we have a limited number of possibilities for the coordinates of the various atoms of which the crystal is composed.

There now remains the third step in the solution by which, as far as is possible, the choice of coordinates for the atoms is further narrowed down by a consideration of the intensities of the various diffracted beams. These intensities are usually estimated roughly in terms of the blackness of the spots in the Laue pattern. Using the language of the wave theory of radiation, the amplitude of the beam of x-rays diffracted from any given family of planes in the crystal will be the vector sum of the amplitudes of the wavelets sent out from each of the planes in that family. This problem is then really the old problem of adding together wave motions which have the same wave length, but which differ in both phase and amplitude.*

It is well known that in such a problem the square of the resultant amplitude may be expressed in terms of the sum of the squares of two numbers which represent, respectively, the sum of the components, taken 90° apart, *i.e.*, taken along the X- and Y-axes of reference, of the amplitudes of all the constituent wavelets. The X- and Y-components of each wavelet are, respectively,

$$a \cos \Delta$$

and

$$a \sin \Delta$$

where a is the amplitude of the wavelet and Δ is the phase angle between the wavelet and some phase standard. When we are dealing with only two wavelets one of them may be taken as the standard of phase, and the phase angle Δ becomes the difference in phase between the two wavelets. If we represent by X the sum of all the terms corresponding to $a \cos \Delta$ for all the wavelets, and by Y the sum of all the terms corresponding to $a \sin \Delta$ for all the wavelets, then the resultant amplitude R is given by

$$R^2 = X^2 + Y^2 \tag{14}$$

* In this connection see A. Schuster, "The Theory of Optics," Chap. I, Edward Arnold, London, 1909, 1919. The same problem in another guise appears in alternating-current work.

To find the values of X and Y we must know both the amplitude and the phase of every constituent wavelet. The amplitude of the wavelet diffracted from a given plane of atoms in the crystal depends upon many factors, but for any given order of diffraction from a single family of planes we are here concerned with only one, namely, the effect of the kind of atoms in each individual plane. It is assumed that the amplitude of a wavelet diffracted from any single plane is proportional to the atomic or ionic number N of the atoms or ions which compose the plane.* This assumption is consistent with our fundamental ideas on the diffraction of x-rays. It appears to have some experimental justification, for, as the Braggs have pointed out, the two fluorine ions ($2N = 2 \times 10 = 20$) in CaF_2 seem to have about the same diffracting power as the calcium ion,

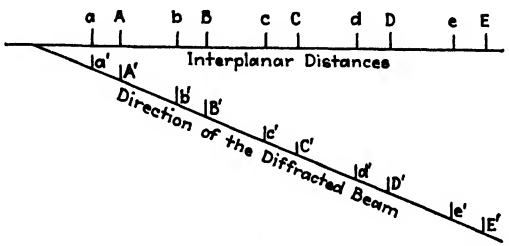

FIG. 18.—Projection of interplanar spacings in the direction of the diffracted beam.

for which N is 18. This assumption does not, in its ordinary form, include any effect of the distribution of the electrons in space, so it is not quite consistent with the experimental fact[5] that Na^+ ($N = 11 - 1$) and F^- ($N = 9 + 1$) differ slightly in diffracting power. It is, however, sufficiently accurate to enable one to distinguish between the various possible alternatives of crystal structure found in actual practice at least in the case of comparatively simple structures. It therefore remains only to express the phase difference between the wavelets diffracted from successive atomic planes in the same family in terms of the coordinates of the various atoms in the unit-crystal.

Let the lines a, A, b, B, etc., of Fig. 18 represent the members of some family of planes in a crystal. Let the lines a', A', b', B', etc., represent the projections of these planes in the direction of the diffracted beam. If the crystal had had the simplest structure for the crystallographic system to which it belongs (in the case of the cubic system

* It can be shown that the intensity of the diffracted beam will depend a great deal upon the degree of perfection or imperfection of the crystal. The statements in this chapter apply most rigorously to an "ideally imperfect" crystal, *i.e.*, to a crystal which is a fine-grained mosaic of perfect crystals. In this connection see the discussion of primary and secondary extinction in Chap. I; see also Chap. XII. For the effect of the structures of the atoms of which the crystal is composed, see Chaps. X and XI.

this is simple cubic; in the case of the hexagonal system it is simple triangular, etc.), the successive members of the family would have been at a, b, c, etc., and nowhere else. In such a case the distances $a'b'$, $b'c'$, etc., would have to be such that a wavelet from a would meet the wavelet from b exactly in phase, otherwise there would have been no diffracted beam. In circular measure the length of a sine wave is 2π (see any standard text in optics). The phase difference between these wavelets, expressed in circular measure in the usual way, is therefore $2\pi n$, where n is the order of diffraction. The phase difference between the wavelets from a, b, c, etc., and A, B, C, etc., is

$$\Delta = 2\pi n \frac{a'A'}{a'b'} = 2\pi n \frac{aA}{ab}$$

At this point let us limit ourselves temporarily to the cubic system. The distance ab is the interplanar distance in a simple cube. In terms of the edge of the unit-cube, by Eq. (3) of Chap. III,

$$ab = \frac{1}{\sqrt{h^2 + k^2 + l^2}}$$

The distance from atomic plane a to atomic plane A is

$$aA = bB = \frac{(hx_1 + ky_1 + lz_1 - 1) - (hx_2 + ky_2 + lz_2 - 1)}{\sqrt{h^2 + k^2 + l^2}}$$

where $x_1y_1z_1$ and $x_2y_2z_2$ are the coordinates of atoms in the two planes. Now, if one of these planes is considered to pass through the origin of coordinates, $x_2 = y_2 = z_2 = 0$, and

$$aA = bB, \quad \cdots = \frac{hx_1 + ky_1 + lz_1}{\sqrt{h^2 + k^2 + l^2}}$$

then

$$\frac{aA}{ab} = \frac{\dfrac{hx_1 + ky_1 + lz_1}{\sqrt{h^2 + k^2 + l^2}}}{\dfrac{1}{\sqrt{h^2 + k^2 + l^2}}}$$

$$\frac{aA}{ab} = hx_1 + ky_1 + lz_1$$

The phase difference between wavelets from a and A, b and B, etc., is therefore

$$\Delta = 2\pi n(hx_1 + ky_1 + lz_1) \tag{15}$$

If the crystal had belonged to any other than the cubic system, the result would have been the same, because the denominators of both portions

of the complex fraction necessarily are identical and cancel out. Remembering our assumption as to the dependence of the amplitude of the wavelets upon the atomic number, we have for the two components of each wavelet in the X- and Y-directions of Eq. (14):

$$N \cos 2\pi n(hx_1 + ky_1 + lz_1)$$

and

$$N \sin 2\pi n(hx_1 + ky_1 + lz_1)$$

For a given family of planes, X and Y will each contain as many such terms as there are kinds of atomic planes in the unit-crystal which belong to that family. Since the intensity of the spot in the Laue pattern is proportional to R^2 of Eq. (14), it is proportional to

$$[\Sigma N_1 \cos 2\pi n(hx_1 + ky_1 + lz_1) + \Sigma N_2 \cos 2\pi n(hx_2 + ky_2 + lz_2) + \cdots]^2 + [\Sigma N_1 \sin 2\pi n(hx_1 + ky_1 + lz_1) + \Sigma N_2 \sin 2\pi n(hx_2 + ky_2 + lz_2) + \cdots]^2 \quad (16)$$

The values of N_1, N_2, etc., are known from the chemical constitution of the crystal. The theory of space-groups gives all the possible coordinates $x_1y_1z_1$, $x_2y_2z_2$, etc., either directly or in terms of an undetermined distance from some known position in the unit-crystal. In one case the coordinates are substituted directly in Eq. (16) as a means of choosing between the alternative structures offered by the theory of space-groups. In the other case various numerical values are substituted systematically for the undetermined distance until one is found which gives the correct intensity. For every test made in this way the calculated intensity for the various planes must be compared with the actual intensity as shown by the blackness of the spots in the Laue pattern. Since the intensity of the diffracted beam depends markedly on the angle of diffraction, we have only two alternatives: (1) We must take various Laue patterns with such orientations as will put the spots which we wish to compare at the same distance from the image of the central beam; or (2) we must correct the observed intensity for the angle of diffraction. The first alternative necessitates either taking many Laue patterns of the same crystal or the use of the gnomonic rotation net. In some cases this makes the Laue method rather laborious and time consuming. The second alternative can be taken by means of an empirical approximate method, proposed by Wyckoff,[6] by which the relative intensities of all the spots may be calculated in terms of the so-called "normal decline" of intensity with increase in angle. The calculations differ from those of Eq. (16) by the factor $(d_{hkl}/n)^{2.35}$, where d_{hkl} is the interplanar distance and n is the order of diffraction. Equation (16) then becomes

$$R^2 = \left(\frac{d_{hkl}}{n}\right)^{2.35} \{[\Sigma N_1 \cos 2\pi n(hx_1 + ky_1 + lz_1) + \Sigma N_2 \cos 2\pi n (hx_2 + ky_2 + lz_2) + \cdots]^2 + [\Sigma N_1 \sin 2\pi n(hx_1 + ky_1 + lz_1) + \Sigma N_2 \sin 2\pi n(hx_2 + ky_2 + lz_2) + \cdots]^2\} \quad (17)$$

When Eq. (17) is used the intensities of the various spots may ordinarily be compared without regard to the spacings of their atomic planes.

SUMMARY

The Laue method may be summarized by saying that a single stationary crystal is used and the x-ray beam employed contains all possible wave lengths from those barely able to pass through the x-ray bulb and crystal down to the quantum limit imposed by the voltage across the x-ray tube. The diffraction pattern obtained is interpreted by means of a gnomonic projection to give the Miller indices of the planes which diffract the x-rays. The data thus obtained may be used to aid in eliminating some of the possibilities permitted by the theory of space-groups. Further discussion of the Laue method must be postponed until after we have taken up the theory of space-groups in Chap. VIII. The discussion will be resumed in Chap. IX.

References

1. Friedrich, Knipping, and Laue, *Sitzb. bayer. Akad. Wiss., math-physik. Klasse,* **303,** 363 (1912); *Ann. Physik,* **41,** 971 (1913).
2. W. L. Bragg, *Proc. Roy. Soc.,* **89,** 248 (1913).
3. F. E. Wright, *Carnegie Inst. Pub.* 680; *Amer. Mineral.,* **14,** 251 (1929).
   See also:
   V. Goldschmidt, "Über Projektion und Krystallberechnung," 1887.
   H. E. Boeke, "Die gnomonische Projektion," Berlin, 1913.
   R. Rinne, *Ber. Verh. K. sächs. Ges. Wiss.,* Leipzig, **67,** 303 (1915).
   C. Palache, *Amer. Mineral.,* **5,** 67 (1920).
   R. W. G. Wyckoff, *Amer. Jour. Sci.,* **50,** 317 (1920).
4. R. W. G. Wyckoff, *Amer. Jour. Sci.,* **50,** 317 (1920). See also R. W. G. Wyckoff, "The Structure of Crystals," Chemical Catalog Company, New York, 1924
5. W. P. Davey, *Phys. Rev.,* **21,** 143 (1923).
6. R. W. G. Wyckoff, "The Structure of Crystals," Chemical Catalog Company, New York, 1924.

CHAPTER V

THE BRAGG METHOD OF CRYSTAL ANALYSIS

We have seen how in the Laue method of crystal analysis the chain of evidence leading to the structure of a crystal is furnished mainly by the symmetry characteristics of the crystal, x-ray diffraction being used only to supply those links which would otherwise be missing from that chain. In other words, the Laue method makes x-ray diffraction play only the rôle of an assistant to the older crystallographic methods. In the Bragg method[1] emphasis is placed on the x-ray diffraction data, and symmetry considerations are used to supplement these data. The Bragg method of crystal analysis uses a single crystal. X-rays of known wave lengths are used so that from the angles of diffraction the corresponding interplanar spacings may be calculated at once from Bragg's law, which is Eq. (1) of Chap. I. These interplanar spacings together with the relative intensities of different orders of the diffracted beams constitute the x-ray data used by the Bragg method in determining the structure of the crystal.

EXPERIMENTAL TECHNIQUE OF THE BRAGG METHOD

The x-ray tube is operated at such a voltage as to produce a large proportion of characteristic rays from the anode (see Fig. 2 of Chap. IV). This bundle of characteristic rays contains more than one wave length, for instance the K spectrum of Mo contains the following four wave lengths:[2] $\alpha_1 = 0.7121$Å., $\alpha_2 = 0.7078$Å., $\beta = 0.6312$Å., $\gamma = 0.6197$Å.*

* The following designations and wave lengths are taken from the "International Critical Tables," McGraw-Hill Book Company, Inc., New York. The wave length of β given above is the average of 0.6315 and 0.6310.

System of names					Relative intensity	Wave length in Ångströms ($= 10^{-8}$ cm.)
Siegbahn	De Broglie and Dauvillier	Davis and Purks	Sommerfeld	Difference		
α_2	α_2	α_2	α'	$K - L_{21}$	50	0.712105
α_1	α_1	α_1	α	$K - L_{22}$	100	0.707831
β_3	β_1'	β_2	β'	$K - M_{21}$	35	0.631543
β_1	β_1	β_1	β	$K - M_{22}$		0.630978
β_2	γ_1	γ	γ	$K - M_{21,23}$	15	0.619698
β_4	..	..	..	$K - O_{21,22}$	Very weak	0.61825

In some cases the beam may be made nearly monochromatic by means of filters. ● For example, the β and γ lines of the K spectrum of Mo may be almost completely absorbed by Zr which is especially transparent to the α doublet of MoK.[3] The characteristic rays most used in the Bragg method are those of Fe, Cu, Mo, and Rh. The proper filters are, respectively, Mn, Ni, Zr, and Ru. Fe and Cu possess the advantage of giving large angles of diffraction because of their long wave lengths, but the rays have such small penetrating ability that the x-ray tube must have a special window of Lindemann glass, very thin pyrex, aluminum foil, or thin mica to let out the rays. When this window is fastened to the glass of the x-ray tube with sealing wax, the tube can only be operated on the pump. Glass windows are free from this objection. Tubes with Mo or Rh anodes do not require such transparent windows. Of these two, Mo is most used because of the relative abundance of Zr for filtering material. Since absorption of x-rays is essentially an atomic property, it is easiest to use the Zr in the form of a compound with some atom or atoms of low atomic number such as ZrO_2, $ZrSiO_4$, $Zr(NO_3)_4$, etc. Experience shows that 0.036 g. of Zr atoms per square centimeter is sufficient to reduce the white rays and the β and γ lines of MoK to a negligible amount when the x-ray tube is operated at a voltage of 30 kv. r.m.s. or less. In this way the x-ray beam is composed mainly of the α_1 and α_2 lines.

It is essential to the fullest success of the Bragg method that the intensities of the diffracted beams be measured with a fair degree of accuracy. For this reason the ionization chamber is preferred to the photographic film as a means of detecting and measuring the x-rays. The ionization chamber may be a metal tube filled with air in which an insulated electrode inside runs parallel with the axis of the tube but at some distance from it. If the air in the chamber is replaced by C_2H_5Br or CH_3I, the insulation should be preferably of quartz to prevent corrosion by the gas, and the port of entry for the x-rays is rendered gas-tight by a thin mica or aluminum window fastened in place with sealing wax. The use of cellophane or pyroxylin windows is not advised as they tend to become brittle under the action of the x-rays. The ionization current is measured in the usual way by either an electroscope, an electrometer, or an appropriate vacuum-tube circuit of high amplification, care being taken that the voltage between the electrodes is sufficient to catch every ion that is produced. For further details on the construction and use of ionization chambers the reader is referred to any standard book on the conduction of electricity through gases.

The arrangement of the apparatus is shown in Fig. 1. The x-ray beam is defined by the two slits S_1 and S_2. These slits are usually made of lead or gold. The slit S_3 is made wide enough so that it is not grazed by the main beam, but narrow enough to intercept any rays diffracted by the material of which S_2 is made. A slit S_4, in front of the ionization chamber

I, insures that only one diffracted beam enters the chamber at any given setting of the chamber. The filtering material used to render the x-rays substantially monochromatic is best placed next to S_4, so that it will not only filter out undesirable wave lengths coming directly from the x-ray tube but also at the same time tend to filter out any secondary, *i.e.*, characteristic, rays from the crystal under examination.

The crystal is mounted on a crystal holder as in Fig. 2, so that any face may be oriented so as to lie parallel to the x-ray beam. This crystal

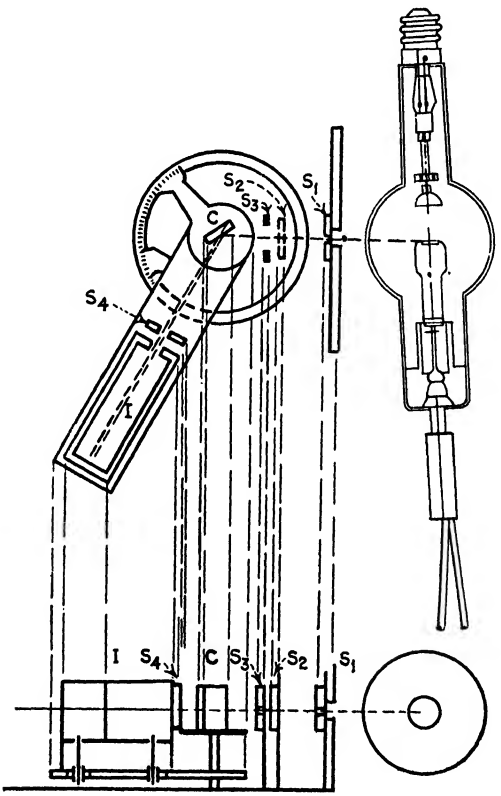

FIG. 1.—Diagram of Bragg apparatus.

holder is clamped to a table which may be rotated about a vertical axis. The crystal is so adjusted in the crystal holder that this axis of rotation passes through a zone axis of the crystal. The advantage of this is that diffraction can then be obtained from each of several atomic planes by merely rotating the crystal table as a whole. The more important the zone axis, the greater is this advantage. Usually a zone axis is easy to find, for it may be located from two or more natural faces of the crystal. If only one natural face is developed, the second atomic plane (corre-

sponding to a second face) must be found by means of its diffracted x-ray beam, using cut-and-try methods.

If the crystal is very small, it will itself limit the x-ray beam sufficiently and the slits may be opened up to any reasonable width. In such a case it is only necessary to see to it that by some suitable means, such as a template, the crystal face to be investigated lies directly over the axis of rotation. For larger crystals, or for crystals in the form of flat flakes or broad needles, the x-ray beam must be defined by the slits S_1 and S_2. In such a case the following technique is recommended:

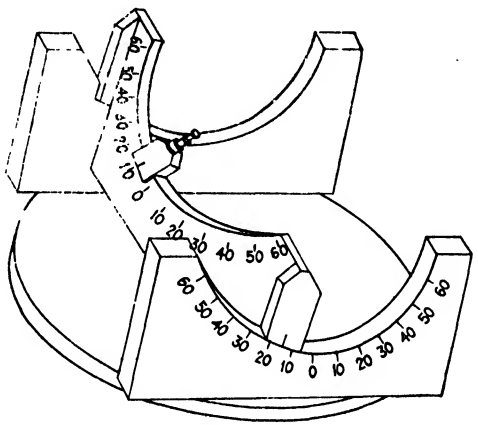

FIG. 2.—Crystal holder for use with the Bragg method of crystal analysis.

1. The crystal holder is clamped on its table so that the diffracting face of the crystal is in the axis of rotation. The accuracy of the setting will become evident in the subsequent adjustments.

2. Turn on the x-ray tube, and darken the room. Open slits S_1, S_2, and S_3 wide and place a fluorescent screen in a holder, behind the crystal table to show up the x-ray beam. It is best to place a piece of black paper somewhere in the path of the x-ray beam to cut off the visible light which comes through the slits.

3. Turn the crystal table until the face of the crystal is parallel to the direction of the x-ray beam.

4. Close up the side of S_3 opposite the crystal until the line on the fluorescent screen becomes very narrow. If, in operation 1, the crystal face was not properly set parallel to the axis of rotation of the crystal table, the line on the fluorescent screen instead of being of uniform width will be tapering, thus indicating the direction and magnitude of the tilt.

5. If the crystal table is slowly rotated back and forth, through a small angle, it will be observed that at a certain angle the line on the fluorescent screen appears. As the table is rotated still more so that the crystal face becomes more nearly parallel to the x-ray beam, the line on the screen grows toward a maximum intensity. It disappears again when the crystal reaches the limiting angle on the opposite side. The width of the x-ray beam grazing the crystal face at the moment when the two are parallel can be made as small as desired by closing down the slit, thus decreasing the limiting angle through which the crystal table can be turned while the line still shows on the fluorescent screen.

6. Turn the crystal table through an angle of 180°, thus bringing the diffracting face of the crystal on the opposite side of the axis of rotation.

7. The second side of slit S_3 is now closed down as in 4 and 5. If the diffracting face of the crystal is not on the axis of rotation, it will be found that either

a. The limiting angle is relatively large when the line on the fluorescent screen is very narrow showing that the crystal face is displaced behind the axis of rotation, or,

b. When the adjustment of the second side of S_3 is finished, it will be found that the slit is still considerably open, showing that the crystal face is displaced so that the axis of rotation goes through the body of the crystal instead of lying in the crystal face.

8. Still keeping the crystal holder clamped to the crystal table, remove the crystal table from its mounting and move the fluorescent screen to the place where the end of the ionization chamber would have to be to register the primary, *i.e.*, undeviated, x-ray beam. This will show the position and width of the primary beam, which is the criterion of the width of the slit adjustment.

9. Close up one side of slit S_1 until the line on the fluorescent screen becomes narrowed; then slowly open it again until the full width of the line appears and no farther. Do the same with the other side of slit S_1. Repeat with S_2. Then increase the width of S_3 slightly, taking care to move both sides of the slit by the same amount.

10. Replace the crystal table on its mounting.

11. Rotate the crystal until the diffracting face is again parallel with the x-ray beam as shown by the fluorescent screen.

12. Note the angular reading on the scale of the crystal table. This is the zero of reference.

13. Adjust the orientation of the crystal face to the required angle with respect to the x-ray beam.

Caution: In all work involving adjustments of any sort while the x-ray tube is in operation, great care must be taken to keep the hands and all other parts of the body out of the path of the x-ray beam. The danger of x-ray burns is discussed briefly in Appendix I.

It is a matter of experience that few crystals will diffract Mo characteristic rays at grazing angles of incidence of less than 3°. The crystal face is therefore set at an angle of about 3° to the primary x-ray beam, and the slit S_4 is opened up as widely as possible. The ionization chamber is slowly turned from an angle of about 6° to an angle of 12° or more. If some atomic plane which passes through the chosen zone axis happens to lie at the correct angle to the x-ray beam, a diffracted beam will be found. Otherwise the table on which the crystal is mounted is turned slightly, and the ionization chamber is again slowly swept past. This is repeated if necessary until some plane is found which is so oriented as to show first-order diffraction of the wave length of x-rays employed in the primary beam. The slit S_4 is then narrowed down so as to be at least as narrow as the x-ray beam, and the ionization chamber is moved past, step by step. At each step a reading of the ionization current is made. The angle is noted at which the maximum ionization current is found. The crystal is then rotated so that the same family of planes diffracts on the other side of the primary beam and the angle of maximum ionization current is again noted. Halfway between these two positions is the cor-

rect zero through which the undeviated beam passes after barely grazing the axis of rotation of the crystal. Half the angular distance between the two ionization maxima is therefore the angular deviation of the x-ray beam; it is the angle ϕ of Eq. (3) of Chap. I, or twice the angle θ of Eq. (1) of Chap. I. It is twice the grazing angle of incidence of the x-ray beam on the atomic plane in the crystal.

INTERPRETATION OF THE DIFFRACTION PATTERN

From Eq. (1) of Chap. I the interplanar spacing d is calculated, and parallel lines, such as ABC, DEF, GHI, etc., of Fig. 3 are drawn to scale to represent the atomic planes which produce the diffracted beam. The crystal is then turned through an angle ψ such that another family of planes shows first-order diffraction of the x-ray beam, and the interplanar spacing d' is calculated. A new set of parallel lines such as AP, BQ, CR, etc., of Fig. 3 are now drawn to scale so as to make an angle ψ with the first set of lines. Then the intersections of these lines represent possible positions for atoms in the crystal. The plot suggests other angles at which the crystal may be set in order to find first-order diffracted beams. The interplanar distances found at these angles are then drawn on the plot, for example, AEI, GKO, MQ of Fig. 3. These interplanar distances will be multiples or submultiples of the distances predicted by the plot. This helps to determine the projection of the atomic arrangement in the plane of the plot, for now atoms are in general to be expected only at positions corresponding to the points where three lines intersect. The greater the number of planes examined which pass through the given zone axis, the greater is the certainty with which the projection of the crystal lattice may be drawn. A similar procedure for some other zone axis gives still other plots whose planes are at known angles to that of the first plot. From plots of this sort an idea can be gained as to the general type of the framework on which the crystal is built. The greater the number of plots made for a given crystal, the more certainly are the positions of the various atoms known.

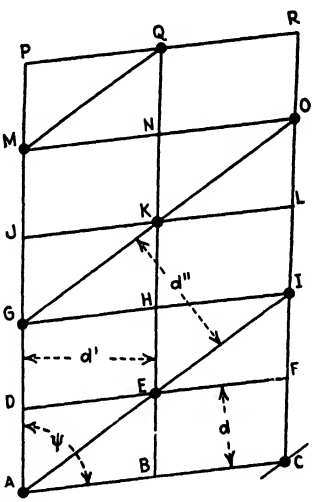

FIG. 3.—A Bragg plot.

In some cases, at least, the certainty of the positions assigned to the atoms may be greatly increased by considering the intensities of the different orders of diffraction for each of the planes. These intensities may be most accurately compared by making special measurements

for the purpose.[4,5] The ionization chamber is set at the correct angle to receive the first-order diffraction from some family of planes, as determined by the procedure outlined above. The slit S_4 (Fig. 1) is then opened up so that the opening is considerably wider than the width of the diffracted beam and the crystal is swept past the diffracting angle at a uniform rate. The total amount of ionization produced in the chamber is taken as a measure of the intensity of the diffracted beam. The ionization chamber is then set at a little less than twice the angle so as to receive the second-order diffraction from the same family of planes as before. The crystal is again swept past the diffracting angle at the same rate as before, and the total ionization is again read. This is repeated for such other orders as may be desired. If a crystal is warped, or if it is "imperfect" so that it is a mosaic of small crystals all having nearly the same orientation (see Chap. I), one portion of a family of planes will make a slightly different angle with the incident beam from some other portion, so that there will appear to be a range of settings instead of just one correct setting of the crystal for each family of planes. The procedure just given has the advantage that it frees the final result from this effect. There will still be present, however, errors caused by absorption, temperature changes, the dimensions of the crystal, etc. (see Chap. I). These are usually of relatively small importance in the interpretation of the structure of simple crystals by the Bragg method, and they will therefore not be discussed further at this point.

If all the atoms in the crystal have equal diffracting power, and if they are arranged according to some elementary lattice (simple cubic, simple triangular, simple tetragonal, etc.), then every intersection on the plot will be the projection of the position of some atom in the crystal, and each order of diffraction will be less intense than the next lower order. For instance, in KCl the ions of K^+ and Cl^- are arranged on a simple cubic lattice. Their ionic numbers are equal, so that they have nearly identical diffracting powers and KCl acts toward x-rays much like an element which is simple cubic. The first-order diffracted beam is more intense than the second order; the second order is more intense than the third order, etc. The normal rate of decline of intensity with increasing order of diffraction is given by W. L. Bragg[1,6] for such cases as approximately:

$$\text{First order : second order : third order} = 100 : 20 : 7$$

This has since been given[1] as

$$\text{First order : second order : third order} = 100 : 18.7 : 6.25$$

Extreme accuracy in the measurement of these intensities is rarely necessary because the intensities vary so markedly with changes in the type of crystal structure. For most work the essential point is

to determine whether or not some one order of diffraction is entirely absent, or, if all the orders of diffraction are present up to the limit of the crystal and the wave length of the x-rays, to know which of two orders of diffraction is more intense and to determine to within a few per cent what their relative intensities are. If the structure is more complicated, the intensities of successive orders of diffraction do not decrease regularly. For instance, even though all the atoms in diamond (see Figs. 5 and 6 of Chap. II) are of the same element and may therefore be supposed to have the same diffracting power, the second-order diffraction from the (1 1 1) planes is missing, although the third and fourth orders are present. This is interpreted as meaning that the (1 1 1) planes are arranged in pairs (see the discussion of the diamond cubic structure in Chap. III) such that the distance between the members of a pair is one-fourth the distance between corresponding planes in two adjacent pairs as in Fig. 4.

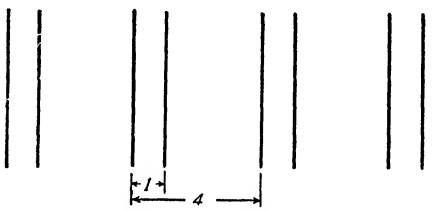

FIG. 4.—Spacing of (1 1 1) planes in diamond.

The general method of interpreting the data on the intensities of various orders of diffraction from a single family of planes is as follows. An arrangement of atomic planes is assumed and the relative intensities of the different orders of diffraction are calculated in terms of the amplitudes and phase relationships of the waves from the different planes of the family. The calculated intensities are compared with those found by experiment, and, if necessary, the procedure is repeated until a marshaling of planes is found such that the calculated and experimental results are sufficiently in agreement.

In order to illustrate one method of making these calculations let us suppose that the crystal is composed of equal numbers of each of two kinds of atoms A and B whose atomic numbers are N_A and N_B, respectively, and let the atomic planes under consideration have a spacing d as calculated from the diffraction pattern. Two possibilities are open: either (1) each plane in the family contains both A and B and these planes are spaced a distance of d apart (see Fig. 5), or (2) there are alternate planes of A and of B so spaced that the A-planes are a distance of d apart from each other and the B-planes are a distance d from each other, while A and B are spaced a distance apart $\frac{1}{m}d$ (see Fig. 6). In the first case the waves from the A atoms and those from the B atoms are necessarily in phase, and the amplitude of the resultant wave is the sum of the amplitudes of the waves sent out by the two sets of atoms. These amplitudes must be linked up in some way with the atomic number.

The Braggs[1] assume as a first approximation that the electrons in the atoms vibrate so nearly in phase with each other that the amplitude of each wavelet is proportional to the number of electrons in the atom which sends out the wavelet, *i.e.*, to the atomic number. Since the ionization chamber measures intensities rather than amplitudes, we must deal with the square of the resultant amplitudes. In terms of Bragg's

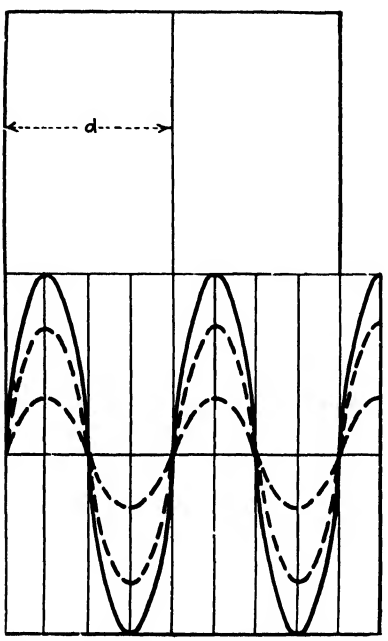

FIG. 5.—Resultant wave from planes each of which contains two kinds of atoms.

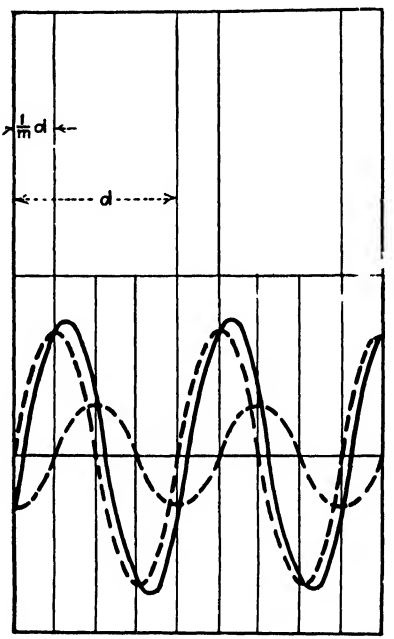

FIG. 6.—Resultant wave from planes of one kind of atoms alternating with planes of another kind of atoms.

assumption we must therefore consider the intensity of an x-ray beam diffracted from a plane containing both A and B atoms as being

$$I = (N_A + N_B)^2 \tag{1}$$

(using units for I such that the factor of proportionality is unity). In the second case the waves from the A- and B-planes are out of phase by an angle ω such that for the first order of diffraction

$$\frac{\omega_1}{2\pi} = \frac{\frac{1}{m}d}{d} = \frac{1}{m}$$

for the second order,

$$\frac{\omega_2}{2\pi} = \frac{2}{m}$$

for the third order,

$$\frac{\omega_3}{2\pi} = \frac{3}{m}$$

Therefore

$$\begin{aligned} \omega_1 &= \frac{2\pi}{m} \\ \omega_2 &= \frac{4\pi}{m} \\ \omega_3 &= \frac{6\pi}{m} \\ \omega_n &= \frac{2n\pi}{m} \end{aligned} \tag{2}$$

In terms of the assumption mentioned above, in which the amplitudes of the wavelets are taken to be proportional to the atomic numbers, the vector sum of the amplitudes of the wavelets from A and B is proportional to

$$(N_A^2 + 2N_AN_B \cos \omega + N_B^2)^{1/2}$$

thus giving a resultant wave whose intensity is

$$I' = N_A^2 + 2N_AN_B \cos \omega + N_B^2 \tag{3}$$

(again using units for I such that the factor of proportionality is unity). Let the intensities of successive orders of diffraction for the first case be I_1, I_2, I_3, etc. Their ratios as experimentally determined by W. L. Bragg have already been given. The corresponding intensities I_1', I_2', I_3', etc., for the second case, will differ for every possible combination of values for N_A and N_B and for every possible value of $1/m$. They are most easily calculated in terms of I_1, I_2, I_3, etc., so that we have, from Eqs. (1), (2), and (3),

$$I_n' = I_n \frac{N_A^2 + 2N_AN_B \cos \dfrac{2\pi n}{m} + N_B^2}{(N_A + N_B)^2} \tag{4}$$

If there are p atoms of A and q atoms of B in the chemical formula for the crystal, then N_A will have to be replaced by pN_A and N_B by qN_B.

This line of reasoning has been applied by the Braggs to the case of the (1 0 0) planes of zinc blende (ZnS) on the assumption that the Zn and S are present in the crystal as atoms so that $N_{Zn} = 30$ and $N_S = 16$. All methods of crystal analysis agree that zinc blende has a diamond cubic structure. The Zn forms a face-centered cubic lattice like Fig. 4 of Chap. II, and the S occupies the four inside positions of Fig. 5 of Chap. II. This causes the (1 0 0) planes to be composed alternately of Zn and S. Let us assume first that, contrary to fact, each (1 0 0) plane

contains both Zn and S. Then the ratio of the intensities of the first two orders of diffraction should correspond to the "normal rate of decline," *i.e.*, $I_1 : I_2 = 100 : 18.7$. Experimentally they are in the ratio of 52:100. Obviously the assumed structure is incorrect. Let us now assume that the Zn and S lie in alternate planes. Equation (4) does not lend itself readily to a direct solution for $1/m$, but various values of $1/m$ may be tried in the equation until one is found which gives the experimental intensities. Suppose that the value on trial for $1/m$ is $\frac{1}{2}$. Then for the first order, n of Eq. (4) is 1 and

$$I_1' = I_1 \frac{(30 - 16)^2}{(30 + 16)^2} = 0.0926 I_1$$

For the second order, $n = 2$ and

$$I_2' = I_2 \frac{(30 + 16)^2}{(30 + 16)^2} = I_2$$

Therefore

$$\frac{I_1'}{I_2'} = 0.0926 \frac{I_1}{I_2}$$

But by experiment

$$\frac{I_1}{I_2} = \frac{100}{18.7}$$

Therefore

$$\frac{I_1'}{I_2'} = 0.0926 \frac{100}{18.7} = \frac{49.5}{100}$$

which agrees very well with the experimental ratio of 52:100.

If, instead of taking the zinc and sulphur as atoms, we had made the more plausible assumption that they exist in the zinc blende in the form of ions, then in Eqs. (3) and (4) we should have had $N_{Zn^{++}} = 28$ and $N_{S^{--}} = 18$, and I_1'/I_2' would have been 25.4/100. This is still sufficiently close to the experimental value of 52/100 to enable us to say that the Zn^{++} and S^{--} lie in alternate layers, for the value of the normal rate of decline for planes containing both Zn^{++} and S^{--} would have to be something like that for KCl, namely 100/18.7—over ten times the experimental value for the (1 0 0) planes of ZnS.

It is not surprising that our calculated ratio for the intensities of different orders of diffraction does not agree more closely with the experimental value. We have already seen in Chap. I that most crystals are exceedingly imperfect, *i.e.*, they are made up of a mosaic of crystal fragments which simulates a single crystal. The more imperfect the crystal, the more energy is concentrated in the diffracted x-ray beam of the first order. This gives the effect of increasing the normal rate of decline of intensity for successive orders of diffraction. In other words,

I_2/I_1 is smaller, *i.e.*, I_1/I_2 is greater the more imperfect the crystal which is taken as a standard. We must remember, then, that the experimental values of the ratio of the intensities of different orders of diffraction are always open to some suspicion, for they will depend largely upon the degree of perfection of the individual crystal used in the experiment.* For instance, as a result of experiments made under different conditions, two values, 52/100 and 27.2/100, are reported[1,7] in the literature for

$$\frac{\text{Intensity of second order from (1 1 1) of NaCl}}{\text{Intensity of first order from (1 1 1) of NaCl}}$$

Bragg and his associates have shown that it is possible to substitute a suitable specimen of a powdered crystal for the single crystal which we have assumed so far in our discussion of the Bragg method. This makes the measurements of intensity correspond to an ideally imperfect crystal and removes the source of the difficulties we have just considered.

Calcite offers an extreme example of the effect of the degree of perfection of a crystal on the rate of decline of intensity with order of diffraction. Calcite crystals have been tested[8] which show a coefficient of maximum diffraction as high as 44 per cent of that to be expected from a perfect crystal. For such a crystal the ratio I_2/I_1 should be much higher than for an imperfect crystal, like KCl. It will be shown in Chap. X that for imperfect crystals the intensity of the diffracted beam is proportional to the quantity F^2 where F is the "structure factor" and has to do with the number and configuration of electrons in the components of the crystal. For perfect crystals the intensity is proportional to F. We may therefore assume for perfect and nearly perfect crystals that the intensity of the diffracted beam from a given plane of atoms or ions is approximately proportional to the electron population of that plane, *i.e.*, to the sum of the atomic or ionic numbers of the various atoms or ions in that plane. Since for low atomic weights the atomic numbers are roughly proportional to the atomic weights, we may take as an alternative approximation that the intensity of the diffracted beam from a given plane in a crystal is proportional to the mass of that plane.

W. H. Bragg has given some interesting evidence[9] that this approximation can be used to good advantage in the case of calcite. The structure of calcite ($CaCO_3$) has been worked out[6] from its x-ray diffraction pattern supplemented by symmetry considerations. It is simple rhombohedral with Ca^{++} and CO_3^{--} at alternate corners of the rhombohedron. This structure has since been confirmed[10] by the Laue method.

* The intensity will also depend considerably upon the configuration of electrons in the atoms of the crystal. This effect is discussed in Chap. X. It is not important in the case of the comparatively simple structures taken up in this chapter, but it is very important in the case of complicated structures. The method of Chap. X may be regarded as an extension of the Bragg method.

The interplanar spacing of the (1 1 1) planes (referred to rhombohedral axes) is just double that of the ($\bar{2}$ 1 1) planes. The second-order diffracted beam of (1 1 1) therefore falls at the same angle as the first-order beam from ($\bar{2}$ 1 1) so that their intensities may be compared without any error due to angle. The (1 1 1) planes occur in alternate layers of Ca^{++} and CO_3^{--}. In the second order their effects are additive, so Bragg assigns a diffracting power equal to the mass of $CaCO_3 = 40 + 12 + 48 = 100$. The ($\bar{2}$ 1 1) planes are composed of Ca + C + O(= 68) with other planes of O lying between them. The effect of those O planes is considered to be negligible. The ratio of the masses of the two planes is 100:68. The ratio of intensities from experiment is 100:66. If we had used ionic numbers instead of atomic weights, we should, of course, have obtained practically the same results.

$$Ca^{++} = 18,$$
$$CO_3^{--} = 2 + 3 \times 10 = 32,$$

giving a value of 50 for the second-order beam from (1 1 1). $Ca^{++} = 18$, $CO = 2 + 10 = 12$, giving a value of 30 for the first order of ($\bar{2}$ 1 1). These are in the ratio of 100:60, which probably agrees with the experimental ratio to within the accuracy of the data.

Equation (4) takes no account of changes in intensity caused by (*a*) absorption of x-rays in the crystal, (*b*) temperature, (*c*) size of the crystal, and (*d*) angle of diffraction. Equation (4) is no more unsatisfactory in these respects than the more cumbersome Eq. (16) of Chap. IV given in the discussion of the Laue method. Except for the empirical proportionality factor $(d/n)^{2.35}$ mentioned in that discussion, the two equations rest on the same assumption, namely, that the amplitude of an x-ray beam diffracted by an atom is proportional to the first power of its atomic number.

The discrepancies which have been noted above are not so serious as they might seem at first sight. As has been mentioned before, it is often sufficient to know only that certain lines in the diffraction pattern are more intense than certain other lines. Equation (4) is therefore an exceedingly useful equation. The cumulative evidence of even relative intensities is of great weight, and, if the lines are so chosen as to represent several orders of diffraction for every family of planes belonging to two or three important zone axes, the chance of a false interpretation is very small indeed.

If the crystal contains only one kind of atoms, *i.e.*, if it is a chemical element, then this equation may be assumed to be independent of any assumptions as to the effect of atomic number on the amplitude of the component wavelets. In such a case it gives a value of $1/m$ whose accuracy is limited chiefly by the structure of the atoms of the element, by the accuracy (not reproducibility) of the intensity measurements

of the different orders of diffraction, and by the accuracy to which the intensity ratios are known for the simple structure. The value of $1/m$ so obtained will be very close to that required by some structure which is consistent with the symmetry characteristics of the crystal. It may in this way serve as a criterion between two structures which are equally consistent with the symmetry of the crystal. The true value of $1/m$ may often be found directly from the atomic coordinates of the theory of space-groups. When the theory of space-groups permits an undetermined parameter, its value may be obtained approximately in terms of intensities of diffraction or in terms of the optical properties of the crystal (see Chap. XIV).

If the crystal contains two or more kinds of atoms, *i.e.*, if it is a chemical compound, Eq. (4) is still useful but not always to the same extent as in the case of an element. By expressing the fact that atoms of high atomic number diffract x-rays more strongly than atoms of low atomic number, it makes it possible to determine in most cases whether a family of planes is composed of planes which are all exactly alike or whether it is made up of alternate layers of A and B. The equation shows that if the crystal planes under consideration are composed alternately of A and B, it is difficult to distinguish between the composition of nearly equally spaced planes if the atomic numbers N_A and N_B are nearly equal. The equation is also insensitive if N_A is very large and N_B very small; in such cases the Bragg plots give no hint as to the complete solution of the crystal structure, for they tend to show only the positions of A. The exact determination of the location of B is therefore left in such cases to considerations of symmetry. As in the case of the Laue method, the theory of space-groups, especially as given by Wyckoff[11] and by Astbury and Yardley,[12] is useful in this connection as a means of insuring that no possibilities have been overlooked. Considerations of electrostatic equilibrium, cleavage, and etch figures are sometimes valuable in helping to decide between alternative structures offered by the theory of space-groups.

The Structure of the Common Alkali Halides.—So far the Bragg method has been described only in general terms. Specific examples have been given only when necessary to make some special point clear or to justify some particular assumptions. The method as a whole will now be illustrated by specific examples. Since, historically, the structures of the common alkali halides were first determined by the Bragg method, it will be of interest to take them up first, using, as typical examples, NaCl, KCl, and KI. These compounds are composed of equal numbers of atoms (or more correctly, ions) of an alkali metal and a halogen. From their external symmetry they are all classed as cubic crystals.

When a single crystal of KCl is examined by the Bragg method, it is found that the plots indicate a marshaling of diffracting centers at the

corners of a simple cubic lattice-work. Although the plots assign a simple cubic structure to KCl, they do not show whether a whole "molecule" of KCl is to be found at each corner of the unit-cube or whether half the corners will contain K^+ and half Cl^-. In either case, Eqs. (3) and (4) would give identical answers for any family of planes, for the ionic numbers of K^+ and Cl^- are identical. We may therefore assume that the ratios of the intensities of different orders of diffraction for any given family of planes in KCl will be practically identical with the corresponding ratios for any other family of planes in the crystal of KCl. This is borne out by experiment, and these ratios are therefore called the "normal rate of decline" of intensity with order of diffraction. As has been stated before, it is approximately

$$\text{First order : second order : third order} = 100 : 18.7 : 6.25$$

The Bragg plots use only the first-order diffracted beam. They show a face-centered cubic marshaling of diffracting centers for NaCl and for KI. For the (1 0 0) and (1 1 0) planes of both these salts the intensities of the first three orders of diffraction tend to follow the same normal law of decline as the planes of KCl.

For instance, the intensity of diffraction from the (1 0 0) planes of NaCl is[7]

First order	100.00 per cent
Second order	19.90
Third order	4.87
Fourth order	0.79
Fifth order	0.116

For the (1 1 0) planes it is, in the same units,

First order	50.4	100 per cent
Second order	6.10	12
Third order	0.71	1.4

This indicates that the (1 0 0) and (1 1 0) planes are composed of equal numbers of alkali and halogen ions. Otherwise these planes would not show the normal rate of decline as nearly as they do.

The (1 1 1) planes of NaCl and KI, however, do not follow this normal law. For NaCl the intensities expressed in the same units as before are

First order	9.00	100 per cent
Second order	33.1	100 per cent
Third order	0.58	6.4
Fourth order	2.82	8.5
Fifth order	0.137	1.5

The odd orders alone, or the even orders alone, from the (1 1 1) planes have a rate of decline comparable to that of the successive orders of

diffraction from the (1 1 0) planes. This indicates that the (1 1 1) planes of NaCl (and the same thing holds with KI) occur in pairs, the Bragg plots showing only the locations of the planes containing the ions of higher atomic number in each case.

All these conditions are satisfied if we assume that NaCl and KI each have a simple cubic structure in which alkali and halogen ions occupy alternate corners as in Fig. 7. Such a structure places each kind of ions on a face-centered cubic lattice.* The simple cube is obtained by the interpenetration of the two face-centered lattices. Each of the (1 0 0) and (1 1 0) planes if extended to infinity is composed of equal numbers of alkali and halogen ions. The (1 1 1) planes occur as alternate layers of alkali and halogen ions.

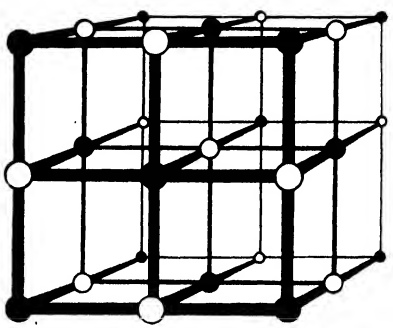

FIG. 7.—Structure of unit-cube of NaCl, KCl, and KI. Dark circles represent the alkali ion, light circles represent the halogen ion.

Because of the close similarity of NaCl, KCl, and KI in physical and chemical properties, and because of the similarity in their crystal habits, we are at once tempted to assume that KCl has an arrangement of ions in space like that assigned to NaCl and KI. Because the K^+ and Cl^- ions have equal ionic numbers, and therefore approximately equal diffracting powers, the two face-centered cubes of K^+ and of Cl^- would be indistinguishable from each other, so that the effect, as far as the diffraction of x-rays is concerned, would be that of a simple cubic lattice.

If the structures assumed above are correct, they must be consistent with the known densities of the three salts. In Chap. I the wave length of MoK_α was calculated in terms of the density of NaCl and the structure given above. Using this value of the wave length, the edges of the unit simple cubes of KCl and KI are found experimentally to be[13] 3.138 ± 0.003Å. and 3.525 ± 0.004Å., respectively. That is, the edges of the unit face-centered cubes are 6.276 ± 0.006Å. and 7.050 ± 0.008Å., respectively. In terms of the simple cubic picture, the density of KCl must equal the mass of its unit-cube divided by the volume of that cube [see Eq. (1) of Chap. II]. Since K^+ and Cl^- occupy alternate corners of the cube, the average mass per crystallographic point must be used, *i.e.*,

$$\frac{39.10 + 35.46}{2} \times 1.649 \times 10^{-24} \text{ g.}$$

This gives a density of 1.990 ± 0.006 as compared with 1.987 determined

* The simple cubic picture is easiest to visualize, but the face-centered picture conforms to the theory of space-groups (Chap. VIII) and is therefore to be preferred.

in the usual way.* A similar calculation gives the density of KI as 3.125 ± 0.009 as compared with 3.123, determined in the ordinary way. The agreement is within the experimental error. This, together with the fact that all other methods of crystal analysis lead to the same structure for these salts, gives such a high degree of probability to the solution that any objection to its correctness must be regarded as purely academic.

A warning should be given against assuming that, just because the crystals of two chemically similar substances both belong to the cubic system, the substances have the same crystal structure. For instance,

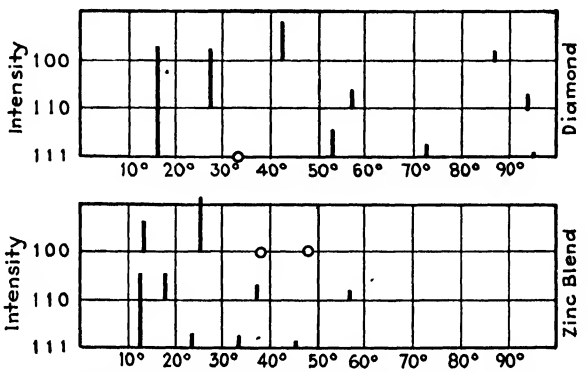

FIG. 8.—Intensities of different orders of diffraction from (1 0 0), (1 1 0) and (1 1 1) planes of diamond and zinc blende. (*Bragg.*)

all the alkali halides have physical and chemical similarities, and they all belong to the cubic system. Of these, CsI, CsBr, and CsCl crystallize as body-centered cubic lattices of ions. CsF and all the Rb, K, Na, and Li halides crystallize as simple cubic lattices of ions. The ammonium halides may have either of these structures depending upon the temperature. It is therefore evident that in every case the results of x-ray diffraction must be shown to be similar before any weight can be placed upon physical, chemical, and crystallographic similarities.

The Structure of Diamond, Zinc Blende, and Fluorite.—Just as a correlation of the diffraction patterns of NaCl, KCl, and KI served to give the key to the interpretation of all three, so the structure of diamond, zinc blende (sometimes called sphalerite, ZnS), and fluorite (CaF_2) are best considered together. The diffraction patterns of the (1 0 0), (1 1 0),

* In terms of the face-centered cubic picture, the mass of the unit of structure for KCl becomes

$$4(39.10 + 35.46) \times (1.649 \times 10^{-24}) \text{ g.}$$

and the density is

$$\frac{(4)\ (39.10 + 35.46)(1.649 \times 10^{-24})}{(6.276 \times 10^{-8})^3} = 1.990$$

and (1 1 1) planes of the first two of these crystals are shown[1] diagrammatically in Fig. 8. The (1 0 0) and (1 1 0) planes of a diamond show a progressive decrease in the intensity of successive orders of diffraction which is much like the rate of normal decline. The pattern from the (1 1 1) planes is of the same general sort, except that the second order is almost entirely absent. The intensities are approximately:

(1 0 0) planes:		
First order	8	100 per cent
Second order	2	25
(1 1 0) planes:		
First order	12	100 per cent
Second order	2½	21
Third order	1	8
(1 1 1) planes:		
First order	24	100 per cent
Second order	0	0
Third order	4	17
Fourth order	1¾	7
Fifth order	0¾	3

The Bragg plots show the diamond crystal to be of the face-centered cubic type. Assuming all the atoms in diamond to be alike, we must account for the absence of the second-order diffraction from the (1 1 1) planes in terms of the marshaling of the atoms in space. This means that in Eq. (4), N_A and N_B are the same, and we must find a value for $1/m$ such that the intensity for the second order will come out to be zero. In other words, cos $4\pi/m$ must be -1; *i.e.*, $4\pi/m = 180°$ and $1/m = \frac{1}{4}$. We now have to imagine a face-centered cubic crystal structure such that the (1 1 1) planes come in pairs, the members of a pair being one-fourth as far apart as the corresponding planes of two successive pairs (see Fig. 4). Such a structure has already been shown in Fig. 6 of Chap. II.

Each order of diffraction for the (1 0 0) and (1 1 0) planes is less intense than the next lower order, so that in a qualitative way these planes follow the rate of normal decline. The agreement is, however, far from quantitative. This may be explained by the fact that diamond is an unusually perfect crystal,[14] so that it should probably be calculated like calcite. In any case, Bragg's interpretation of the structure of diamond, as it is described above, is consistent with the ordinary crystallographic properties of diamond and with its density. The structure has since been confirmed by both the Laue and the powder methods and is as well established as any crystal structure so far investigated.

The Bragg plots (which, it will be remembered, use only the first-order diffraction) show zinc blende to be founded on a face-centered cubic lattice. The intensities of the different orders of diffraction are shown in Fig. 8. They are not those to be expected from Eq. (4) for an ordinary

face-centered cube. The density shows that, considered only as a face-centered cube, a whole "molecule" of ZnS must be associated with each point. This is interpreted to mean that the ions of Zn^{++} are arranged on a face-centered cubic lattice, and that we must find additional places in this lattice-work for the S^{--} ions. If we place the Zn^{++} ions on a face-centered cubic lattice, there are two simple ways of symmetrically placing an equal number of S^{--} ions either of which places the S^{--} on a second face-centered cubic lattice. In the first way, the two face-centered cubic lattices are displaced with respect to each other along a cube axis so that the corners of the S^{--} cube come at the centers of the edges of the Zn^{++} cube. This is the structure already found above for NaCl, KCl, KI, etc., and illustrated in Fig. 7. In the second way, the two face-centered cubes are displaced with respect to each other along the body-diagonal, so that the corners of the S^{--} cube come one-fourth of the way along the body-diagonal of the Zn^{++} cube. This is the structure already found for diamond and illustrated in Figs. 4, 5, and 6 of Chap. II. We must make a choice between these two structures for zinc blende, and the choice is to be made on the basis of the relative intensities of the different orders of diffraction for the various planes of atoms in the crystal. The intensities shown in Fig. 8 are approximately:

(1 0 0) planes:	
First order	6
Second order	12
Third order	0
Fourth order	0
(1 1 0) planes:	
First order	7
Second order	3
Third order	1
(1 1 1) planes:	
First order	17
Second order	2½
Third order	2½
Fourth order	1

It is at once evident that, for the first and third of the three families of planes cited, these intensities do not correspond at all with those for the same family of planes in NaCl. The intensities of the various orders of diffraction from the (1 0 0) planes are like those of the (1 1 1) planes of NaCl. It has already been shown in the discussion of Eq. (4) that they are what might be expected of alternate layers of Zn^{++} and S^{--}. This is consistent with the second of the two tentative structures given above for zinc blende. This is brought out more clearly in Fig. 9. The construction lines show that each S^{--} ion lies at the center of a tetrahedron of Zn^{++} whose vertex is the corner of the face-centered cube of Zn^{++}

and whose base is determined by the three Zn^{++} ions at the centers of the adjacent faces. Such a structure causes the S^{--} ions to form (1 0 0) planes midway between the (1 0 0) planes of Zn^{++}, in this way reducing by interference the intensity of the odd orders of diffraction. It introduces no new (1 1 0) planes so that the various orders of diffraction from (1 1 0) tend to show the normal rate of decline. It gives (1 1 1) planes of S^{--} close to similar planes of Zn^{++} so that the distance between S^{--} and Zn^{++} planes is one-fourth that between the nearest Zn^{++} planes. It will be remembered that this type of lattice caused the (1 1 1) planes of diamond to lose their second-order diffraction, for the two sets of planes had equal diffracting power. Since the S^{--} has less diffracting power than Zn^{++}, the second-order diffraction of the (1 1 1) planes of zinc blende is not entirely wiped out but is so greatly weakened that it is no more intense than the third order.

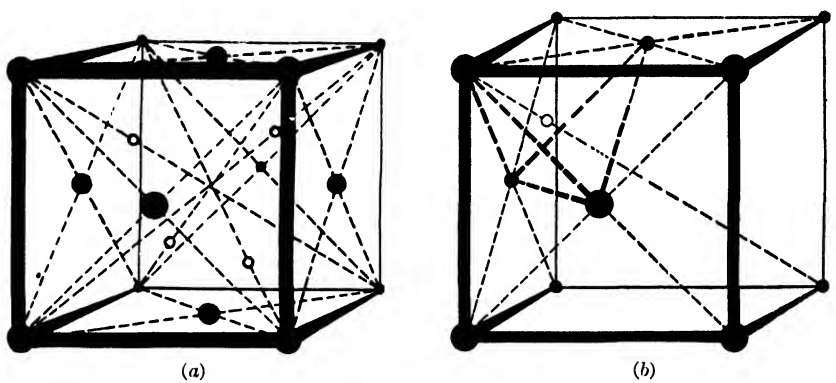

(*a*) (*b*)

FIG. 9.—Structure of unit-cube of zinc blende (ZnS). Dark circles represent the Zn^{++}; light circles represent the S^{--}.

The relative intensities of the various orders of diffraction from the (1 0 0), (1 1 0), and (1 1 1) planes of fluorite (CaF_2) are practically identical with those for diamond. Here again the Bragg plots, founded on interplanar distances calculated from first-order diffractions, indicate a face-centered cubic structure. The density shows that we are to place the Ca^{++} on the points of this face-centered cubic lattice and find other, symmetrically located, positions in the lattice for $2F^-$ such that the intensities of the various orders of diffraction may be accounted for. Since the cleavage is just like that of diamond, we shall at once try the diamond type of lattice, putting the F^- at the centers of tetrahedra of Ca^{++}. In order to get enough F^- into the lattice to conform to the chemical formula CaF_2, all these tetrahedra must contain F^-. This gives (1 0 0) planes composed alternately of Ca^{++} and $2F^-$. Since the ionic number of Ca^{++} is $20 - 2 = 18$ and the ionic number of F^- is $9 + 1 = 10$, it is evident that the sum of the diffracting powers of the F^- planes is very nearly the same as that of the Ca^{++} planes. The rela-

tive intensities of the various orders of diffraction from the (1 0 0) planes should therefore be practically the same as in diamond. The (1 1 0) planes are composed of both Ca^{++} and F^-, so they tend to give the normal rate of decline as in diamond. The (1 1 1) planes have a plane of F^- on each side of each plane of Ca^{++} and situated one-fourth as far from it as the next plane of Ca^{++}. This means that there are two F^- planes between each two Ca^{++} planes, and that the distance between the two F^- planes is half that between adjacent Ca^{++} planes. The result is that the second-order diffraction from the Ca^{++} planes is almost completely destroyed by interference with the first-order beam from the two F^- planes. The relative intensities of the diffracted beams from the (1 1 1) planes are therefore practically the same as in diamond. The structure of fluorite just described is shown in Figs. 10 and 11.

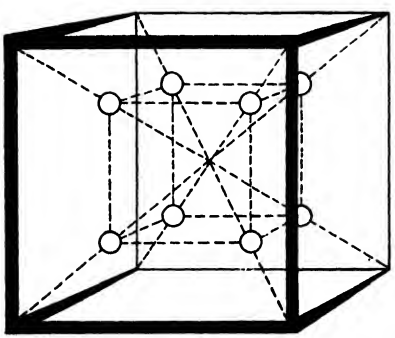

FIG. 10.

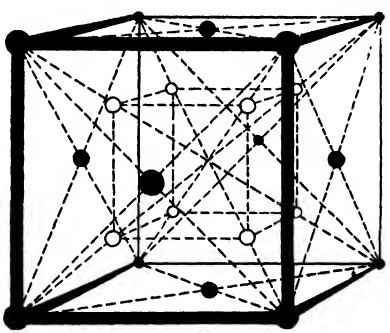

FIG. 11.

FIG. 10.—Inner structure of the unit-cube of fluorite (CaF_2). The light circles represent F^-. The Ca^{++} is on a face-centered cubic lattice like Fig. 4, Chap. II. When these two figures are superimposed to give the complete structure of fluorite, we have Fig. 11.

FIG. 11.—Structure of the unit-cube of fluorite (CaF_2). Dark circles represent Ca^{++}; light circles represent F^-.

The Structure of the Calcite Group.—The Bragg plots for calcite (Iceland spar, $CaCO_3$) show it to be a face-centered rhombohedral lattice. A rhombohedron may be considered to be a cube which has been stretched or compressed along the direction of one of its body-diagonals. Although the angles between the three axes are all equal, they are no longer 90°. If the body-diagonal of the cube has been stretched, these angles are less than 90°. If it has been compressed they are more than 90°. For calcite the angle between any two axes of reference is 101° 54′. The Bragg plots give the data for a rhombohedron directly in terms of these rhombohedral axes so that in the following discussion these axes will be employed rather than the axes of the hexagonal system.

In a face-centered cube the distance between successive (1 0 0) planes is one-half the edge of the unit-cube, because the atoms at the centers of the faces introduce planes half way between the faces of the cube. Similarly,

the interplanar spacing d_{100} ($= 3.03 \times 10^{-8}$ cm.) of the face-centered rhombohedron is half the distance between the sides of the unit-rhombohedron. The density of calcite, measured in the usual way, is 2.7102. This density is consistent with a structure for calcite in which a whole "molecule" of $CaCO_3$ is associated with each point of a face-centered rhombohedral lattice. Using a precise determination of the density of a particular sample of calcite, A. H. Compton[15] finds for that sample that $d_{100} = 3.029 \times 10^{-8}$ cm. This value has since been given by Birge[16] as 3.028×10^{-8} cm., which is the value now universally accepted as the primary standard for all crystal structure and wave-length work.* It has since been confirmed by Bearden.[17] Just as in the case of NaCl, it was necessary to find the location of Na^+ in the lattice in terms of the intensity of the various orders of diffraction, so in the case of calcite we assume from the Bragg plots that the CO_3^{--} radicals (ionic number 32) are marshaled on a face-centered rhombohedral lattice and we assign places in that lattice to the Ca^{++} (ionic number 18) in terms of the relative intensities of the diffracted beams. As in the case of NaCl, the various orders of diffraction from the (1 0 0) and (1 1 0) planes, referred to the rhombohedral axes, tend to show the normal rate of decline of intensity, indicating that these planes contain equal numbers of Ca^{++} and CO_3^{--} ions. For the (1 1 1) planes the relative intensities are approximately:

First order	9 per cent
Second order	29
Third order	0
Fourth order	6

showing that these planes are made up alternately of Ca^{++} and CO_3^{--}.

Bragg has pointed out[1] that if this is the case, it should be possible to find a carbonate which will show a simple rhombohedral structure of ions on the Bragg plots, just as KCl shows a simple cubic structure of K^+ and Cl^-. The ionic numbers of the positive and negative ions of a series of salts having the calcite structure are:

$$\begin{aligned} Na : NO_3 &= 10:32 \\ Ca : CO_3 &= 18:32 \\ Mn : CO_3 &= 23:32 \\ Fe : CO_3 &= 24:32 \end{aligned}$$

Bragg's experimental data for diffraction from the (1 1 1) planes of these salts are given in Fig. 12. It is evident from this figure that the nearer the two ions are in ionic number, the more nearly equal are their diffracting powers. For $NaNO_3$ the preponderance of x-ray intensity from the NO_3^- is so great that the intensity of the first order of diffraction is greater than that of the second order. For $MnCO_3$ and $FeCO_3$ the

* See, however, footnote on p. 12.

interference is so nearly complete that the first-order diffraction is practically extinguished. $ZnCO_3$ has a "calcite" structure and is an even better example, for its ionic numbers are 28:32. If the interference between Zn^{++} and CO_3^{--} is sufficiently complete, it will make the first-order diffraction from the (1 1 1) planes correspond to the distance between adjacent Zn^{++} and CO_3^{--} planes. This distance is half that between successive CO_3^{--} planes, so that if we are correct in assuming the diffracting power of CO_3^{--} to be 32 (see, however, Chaps. X and XI) the (1 1 1) spacings will appear to be half what they would have been if the interference betweeen Zn^{++} and CO_3^{--} had not been complete. The Bragg plots for $ZnCO_3$ may therefore be expected to show a simple rhombohedral lattice, just as for KCl they showed a simple cubic structure.

We have now located the Ca^{++} and the CO_3^{--} radical in the calcite lattice. There remains the problem of showing the locations of the three

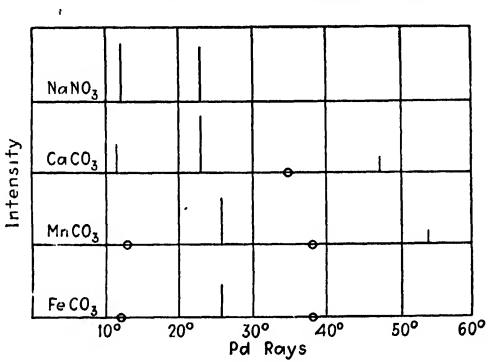

FIG. 12.—Intensities of different orders of diffraction from the (1 1 1) planes of $NaNO_3$, $CaCO_3$, $MnCO_3$, and $FeCO_3$. (*Bragg.*)

oxygens with respect to the carbon. Bragg's solution to this problem, using intensity and symmetry considerations, is given in Fig. 13. The oxygens are placed at the corners of an equilateral triangle with the carbon at the center. In successive (1 1 1) planes of CO_3^{--} these triangles are rotated by 60°. In this way the average amount of oxygen along any one of the hexagonal axes is kept the same as along any other axis, thus giving complete crystallographic similarity to each end of each axis. This not only gives a symmetrical crystal but is also in accord with the fact that the etch figures are supposed to be identical on all (1 0 0) faces of a calcite crystal when an optically inactive etching reagent is used. The details of Bragg's solution for the positions of the oxygens must be postponed until after we have studied the theory of space-groups in Chap. VIII.

SUMMARY

The Bragg method of crystal analysis may be summed up by saying that it interprets as much of the structure of a crystal as possible in

terms of the angles of diffraction of x-rays of known wave length and in terms of the intensities of the diffracted beams. The nature of the method is such that the results are necessarily consistent with the

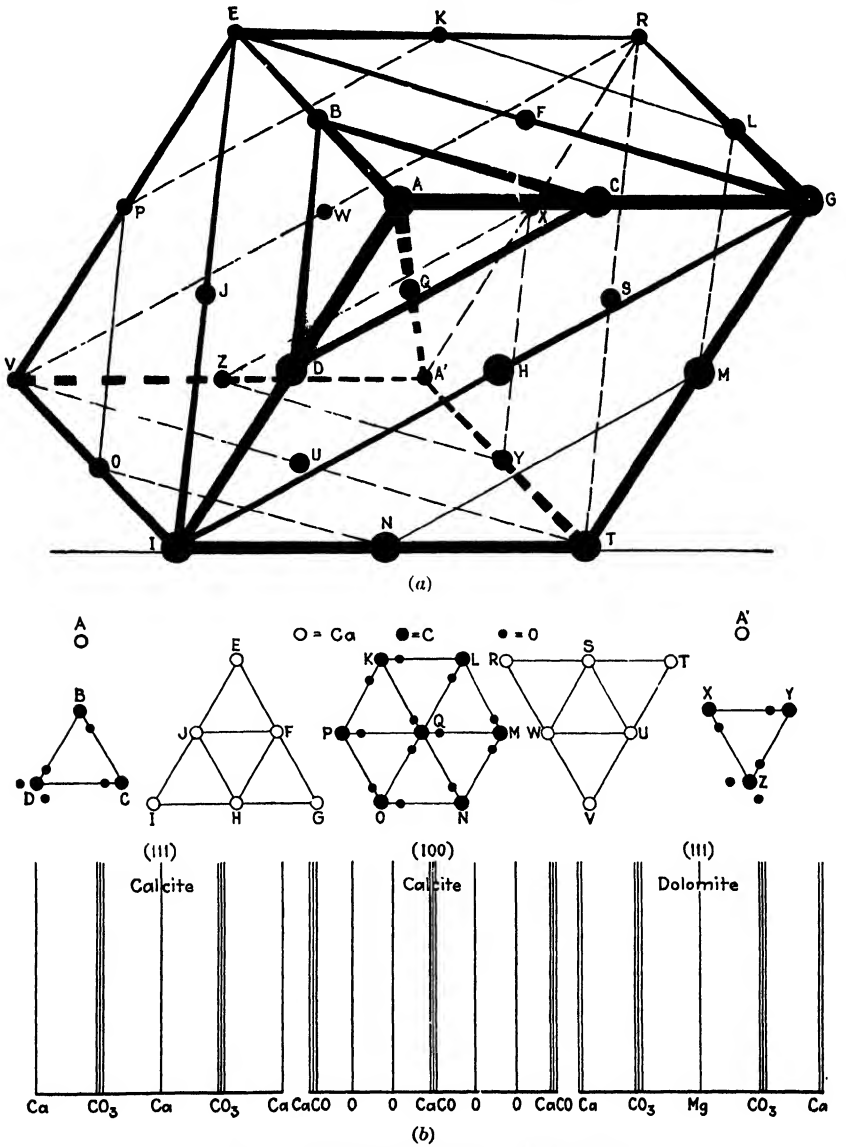

FIG. 13.—Structure of calcite. (*After Bragg.*)

symmetry of the crystal and often include implicitly the results of the theory of space-groups. The theory of space-groups as such is used as a primary tool in determining possible positions of atoms in the crystal

only when x-ray methods are inapplicable or do not give a unique solution of the structure.

References

1. W. H. and W. L. Bragg, "X-rays and Crystal Structure," Bell and Sons, London, 1915.
2. Wm. Duane, *Bull. Nat. Research Council*, No. 6 (1920).
3. A. W. Hull, *Phys. Rev.*, **10**, 661 (1917).
4. C. G. Darwin, *Phil. Mag.*, **43**, 800 (1922).
5. A. H. Compton, *Phys. Rev.*, **9**, 29; **10**, 95 (1917).
6. W. L. Bragg, *Proc. Roy. Soc.*, **89**, 468 (1914).
7. W. L. Bragg, R. W. James, and C. H. Bosanquet, *Phil. Mag.*, **41**, 309 (1921).
8. B. Davis and W. M. Stempel, *Phys. Rev.*, **17**, 608 (1921).
9. W. H. Bragg, *Trans. Roy. Soc.*, **215**, 253 (1915).
10. R. W. G. Wyckoff, *Amer. Jour. Sci.*, **50**, 317 (1920).
11. R. W. G. Wyckoff, The Analytical Expression of the Results of the Theory of Space Groups, *Carnegie Inst. Pub.* 318.
12. W. T. Astbury and K. Yardley, *Trans. Roy. Soc.*, **224**, 221 (1924).
13. W. P. Davey, *Phys. Rev.*, **21**, 143 (1923).
14. H. Mark, *Naturwissenschaften*, **13**, 1042 (1925).
    W. Ehrenberg, P. P. Ewald, and H. Mark, *Zeit. Kryst.*, **66**, 547 (1928).
15. A. H. Compton, H. N. Beets, and O. K. DeFoe, *Phys. Rev.*, **25**, 625 (1925).
16. R. T. Birge, *Phys. Rev. Supplement*, Vol. I, No. 1 (1929).
17. J. A. Bearden, *Phys. Rev.*, **38**, 2089 (1931).

CHAPTER VI

THE POWDER METHOD OF CRYSTAL ANALYSIS

THE POWDER METHOD

This method was devised independently by A. W. Hull[1] and by P. Debye and P. Scherrer.[2] Just as the Laue and Bragg methods were named after the men who first employed them, so in naming this method an attempt was made to honor those who originated it by calling it the "Hull-Debye-Scherrer method." The awkwardness of this name has been responsible for the widespread use of the descriptive title "powder method." This method uses a beam of essentially monochromatic x-rays as does the Bragg method, but, instead of using single crystals, it uses crystals which have been crushed to such a fine powder that the fragments have a random or chaotic orientation. Such a powder requires no rotation, for, since every atomic plane is present in every possible orientation, there must be some individuals from each family of planes which are oriented at the correct angle to diffract the monochromatic x-ray beam. If the volume of powder used is large enough and the fragments are sufficiently small, there will be, for any given family of planes, many individuals correctly oriented, so that, as far as the general appearance of a line in a photograph of the diffraction pattern is concerned, the combined effect for any one plane is much the same as might be expected from a large single crystal having the same orientation. Experimentally it is found that in most cases the powder is fine enough if it will go through 200-mesh bolting cloth. The openings in such cloth are of the order of 0.06 mm. This does not mean that perfect crystals of 0.06 mm. in diameter would show a truly random orientation. It does mean that most crystals are imperfect enough (*i.e.*, consist of a sufficiently complex mosaic of crystal fragments having nearly the same orientation), so that the actual crystal fragments will show a truly random orientation if the aggregates are not more than 0.06 mm. in diameter. The powdered crystal is of sufficient amount if it will fill a cylindrical container ¾ mm. or less in diameter and about 10 mm. long, *i.e.*, if the total volume is about 5 cu. mm. Since every atomic plane in the powdered crystal has some representatives at the correct angle for diffraction, the whole diffraction pattern may be photographed simultaneously.

The powder method may be used with any crystalline substance. It is the only method which can be used with that large class of substances

which cannot be obtained easily in the form of perfect crystals of appreciable size. This class includes not only most metals and their alloys but also a large number of compounds. For instance, the writer wished to study the crystal structure of calcium selenide (CaSe). As this was not an article of commerce, it had to be made for the occasion by heating weighed lumps of metallic calcium and selenium in a hard-glass tube which had previously been evacuated and sealed off. For some unknown reason the reaction took place with explosive violence, shattering the glass tube to small bits. These bits were gathered, and on the concave side of each was found a thin layer of dark scale. This was scraped off and found to be composed of crystals of CaSe. Crystallization had taken place during the time in which the explosion took place, thus giving rise to extremely minute crystals. They were examined by the powder method with complete success, although they were obviously quite unsuited for either the Laue or Bragg methods.

EXPERIMENTAL TECHNIQUE OF THE POWDER METHOD

A typical arrangement of x-ray tube, slits, and specimen is shown diagrammatically in Fig. 1. Slits S_1 and S_2 serve to define the x-ray beam. S_3 cuts off any diffraction pattern from the crystals on the edge of S_2. The specimen of powdered crystal is at C. In the type of apparatus illustrated, the width of the specimen is less than that of the x-ray beam, so that the effective width of the beam is determined by the width of the specimen. The diffraction pattern is recorded on the photographic film P. The filter F renders the rays practically monochromatic (see Chap. V). The trap T not only prevents overexposure from the undeviated beam but also by its shape prevents fogging the film by rays scattered by the trap from the primary beam. A septum in the film-holder allows two diffraction patterns to be taken on the same photographic film.

Ordinarily, if the specimen is a salt or some other brittle type of crystal, it is crushed in an agate mortar. If the specimen is a metal, it may be reduced to filings using only light pressure on a very fine, clean file. The powder or filings are then sieved through a clean 200-mesh silk bolting cloth. This powder may be mounted in any of several ways. Probably the most common method is to load it into a thin-walled glass tube of not more than 0.6 mm. internal diameter. Care must be taken that the glass contains only elements of low atomic weight. Lead-free lime glass, such as is made for x-ray bulbs by the Vineland Flint Glass Works (Vineland, N. J.), or pyrex glass tubes, are suitable. They may be drawn down easily from larger sized tubing. The Corning glass, known as 707 BM, from the Corning Glass Works (Corning, N. Y.) is especially good. Ordinary hard glass usually contains a little lead and is too opaque to the x-rays. In some cases celluloid tubes may be used to advantage.

These tubes may be loaded rapidly and with little danger of breakage by means of the following technique: (1) A plug of cotton is pushed into the tube to a point midway between the ends, using as a ramrod a piece

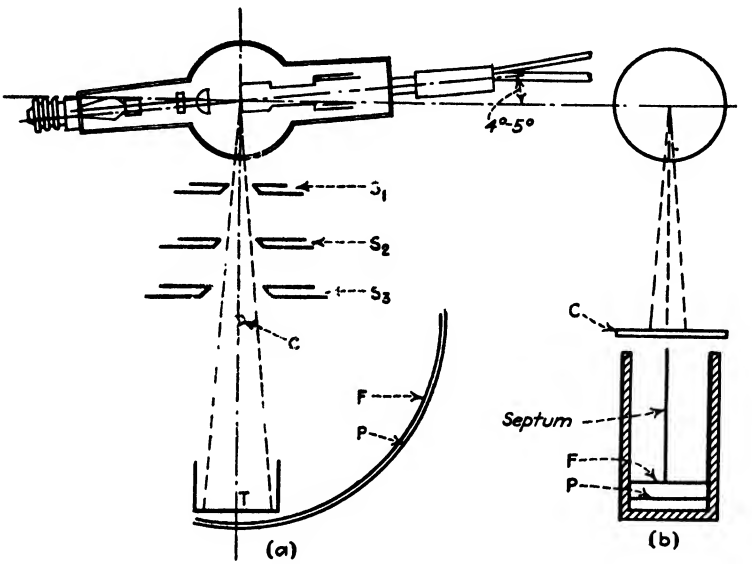

FIG. 1.—Typical apparatus for the powder method: (*a*) View from top; (*b*) view from side.

of 10-mil wire of platinum, molybdenum, tungsten, or other non-corrosive material. The plug should not be longer than the width of the septum in the film-holder (see Fig. 1*b*). (2) The open end of the tube is scraped along the bowl of the mortar containing the crushed crystal, starting at

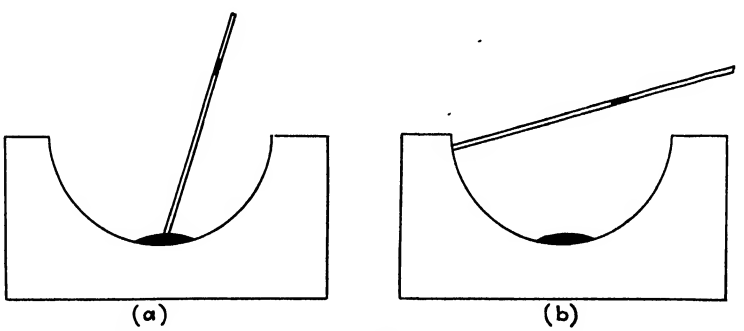

FIG. 2.—Filling a specimen tube: (*a*) Beginning of stroke; (*b*) end of stroke.

the bottom and ending at the top (see Fig. 2*a* and *b*). (3) The lower end of the tube is then held vertically between the thumb and index finger of one hand and the thumbnail is tapped with a pencil. This causes the powder to drop into the tube. In some cases it is better to hold the cen-

tral portion of the tube vertically between the thumb and index finger of one hand and with the other hand draw the corner of a fine triangular file lightly across the side of the specimen tube. During this operation the file should rest on the thumb of the hand which holds the tube. (4) These operations are repeated until enough powder has been collected to extend from the septum to a point beyond the edge of the x-ray beam. A second piece of cotton is then inserted to keep the powder in place. (5) The whole procedure is repeated in loading some other crystal into the other half of the specimen tube. The first powdered crystal to be loaded is some substance used as a comparison standard, usually NaCl (a_0 = 2.814Å.)* which is the secondary standard for interplanar distances (see Chap. I). The second substance is the one under investigation. The two ends of the tube are then plugged with sealing wax with the aid of an electrically heated nichrome hairpin, and an identification tag is waxed on. Care must be taken that no sealing wax is on that part of the tube exposed to x-rays, for in such a case the inorganic filler in the wax will produce a diffraction pattern of its own. If the powdered crystal is slightly hygroscopic, the agate mortar must be kept heated to about 100°C. on a hot plate during the loading operation. A full-size diagram of the loaded tube is shown in Fig. 3.

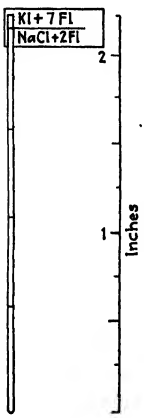

Fig. 3.—Diagram of filled specimen tube.

These specimen tubes increase the time of exposure by reason of their absorption of energy from the x-ray beam, and they have a tendency to scatter the x-rays causing some general blackening on the photographic film. To obviate these difficulties, a method has been devised by Morse[3] which consists of casting the powder in place in the form of cylinders approximately 0.6 mm. in diameter and 15 mm. long in the center of the cassette. The method is especially adapted for use with apparatus in which the specimen is held vertically. It is hardly applicable to other types of apparatus. Figure 4 shows a cross-section of the mold used. A little shellac is used to make the base [marked (1) in the figure] tacky, so that the foot of the cylinder will adhere to it. The position of the mold (2) is governed by the nut (3) by means of lugs which project through slots in the stem (4). This mold is screwed down tight by means of the nut (3) and filled from the top with the powdered specimen material. If necessary to make it mold properly, the powder may be mixed with a little gum tragacanth. Care must be taken to prevent so much pressure as would cause orientation of the crystal fragments. When the mold is full, the plunger (5) is attached firmly to the stem (4) by the set

* On the basis of a simple cubic picture, a_0 = 2.814Å. On the basis of the theoretically correct face-centered cubic picture, a_0 = 5.628Å.

screw (6), thus holding the molded specimen from the top. The mold (2) is then raised by means of the nut (3) on the thread of (4). The plunger (5) is then carefully removed and the mold (2) is taken off, leaving the powder cylinder without any container, standing vertically on its support.

The act of crushing or filing introduces strains into many crystals. If the strains exceed the elastic limit, the crystals may even be broken up into aggregates of smaller fragments without introducing cracks at the newly formed fragment boundaries. It has already been stated in Chap. III that for very small crystal size the intensity of the diffracted beam drops off very sharply, as the angle of diffraction is increased. The diffraction pattern of an overstrained crystal has therefore only a limited number of lines of measurable intensity. A second effect is the widening of those few lines which can appear in the diffraction pattern. This is due to the failure of Bragg's law for extremely small particle size.

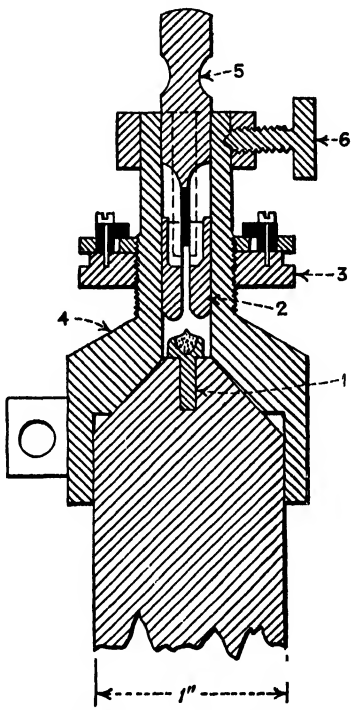

FIG. 4.—Mold for forming specimens.

The effect of strains which do not exceed the elastic limit is to distort the atomic planes, thus introducing the effect of slightly variable interplanar spacings. This results in a widening* of the lines and may even result in seriously weakening the intensities of the lines from those planes in the crystal whose interplanar distance is small. It has already been explained in Chap. V that the nearest convenient approach to monochromatic x-rays gives a beam containing two wave lengths, called α_1 and α_2 which differ from each other by less than 1 per cent. Each of these is diffracted by the crystal powder independently of the other, so that if the angle of diffraction, θ, is large enough (about 21° or more for a specimen in a cylindrical container about 0.6 mm. in diameter when Mo rays are used), and if the crystals in the powder are large enough, each "line" of the diffraction pattern should be a doublet. If the crystal

* In this connection see the article by W. A. Wood, *Phil. Mag.*, **15**, 533 (1933). An attempt is made to differentiate between the effects of fine grain and of lattice distortion on the x-ray diffraction pattern of a metal. A method is suggested for calculating the proportionate contribution of each factor to the broadening of the x-ray line.

FIG. 5a.—Diffraction pattern of strained (upper half) and unstrained tungsten (lower half).

FIG. 5b.—Diffraction pattern of strain-free silicon-iron. (*Courtesy of Prof. E. R. Jette.*)

fragments in the powder have become too greatly strained, each line of these doublets is widened out until the lines of the doublet tend to become merged into a single line of rather hazy outline. The total energy of the diffracted beam from these planes is spread out over a larger area of the photographic film so that the line is less black on the film than it otherwise would be, thus giving the effect of a decrease in the intensity of the diffracted beam. This may be illustrated by an experiment with tungsten. A tungsten incandescent lamp was burned for 4 hr. at its rated voltage in order to anneal the filament thoroughly. The filament was then removed and crushed to a powder in an agate mortar. Half of this powder was then reannealed in hydrogen at the same temperature as before. Diffraction patterns of the two portions were taken side by side on the same film. They are shown in Fig. 5*a*. Unfortunately the temperature at which a crystalline material becomes annealed is the temperature at which crystal growth begins to become appreciable. A fine example of a diffraction pattern of strain-free iron is shown in Fig. 5*b*.

While the primary beam is traversing the specimen, it suffers absorption. Still further absorption occurs in each of the diffracted beams on their way out from the specimen. If the specimen is mounted as shown in Fig. 1, the optimum thickness of crystalline material is approximately

$$t = \frac{1}{\mu} \qquad (1)$$

where μ is the linear coefficient of absorption of the crystal for the wave length of x-rays used.[1] This may be shown as follows:

If the original intensity of the incident primary beam is I_0, the intensity after passing through a distance x is reduced to

$$I_1 = I_0 e^{-\mu x}$$

The initial intensity δI_2 of a diffracted beam from a layer in a crystal of thickness δx in the direction of the incident beam, the layer being at a distance x below the surface of the specimen, must be proportional to δx and to I_1, so that

$$\delta I_2 = kI_1 \delta x = kI_0 e^{-\mu x} \delta x$$

The path of the diffracted beam to the surface of the crystalline material may be expressed approximately as $(t - x)$ where t is the thickness of the specimen in the direction of the incident beam. The intensity I_3 of the emergent diffracted beam is therefore approximately

$$\begin{aligned} I_3 &= \int_0^t kI_0 e^{-\mu x} e^{-\mu(t-x)} dx \\ &= \int_0^t kI_0 e^{-\mu t} dx \\ &= kI_0 t e^{-\mu t} \end{aligned}$$

This will be a maximum if $dI_3/dt = 0$, *i.e.*, when

$$t = \frac{1}{\mu}$$

It is obviously not convenient to use specimen tubes of different diameter for different crystalline materials. The same effect may be obtained, however, using tubes of constant diameter, by diluting the powdered crystal with some amorphous material of low opacity to the x-rays. Gum tragacanth is sufficiently amorphous for this purpose. For many crystalline materials the diffraction pattern is so strong in comparison with that from cellulose that cornstarch or flour may be used as a diluent. Cornstarch is better than flour for specimens containing small quantities of iodides, because most wheat flour is bleached with chlorine. The chlorine in the flour tends to decompose the iodide. In general, the higher the atomic number, the greater is the coefficient of absorption of the crystal. For this reason, from the standpoint of Eq. (1), crystals composed of elements of high atomic number should be very greatly diluted. There are, however, practical limits to the amount of dilution, for a point is soon reached where there are not enough crystal fragments present in the material which can be packed into a specimen tube to give a truly chaotic orientation. Table I gives an empirical schedule, used by the writer, for diluting powdered crystals. It applies best to specimen tubes 0.6 mm. in diameter and is for use with

Mo rays. At each end of the horizontal rows of Table I will be found a number. This represents the number of volumes of diluting material to be mixed with one volume of an element at that end of the row. If the crystal is a compound, the weighted average is taken of the dilutions for the elements in the compound, the weights being proportional to the number of atoms of the element in the chemical formula for the compound.

TABLE I.—EMPIRICAL DILUTIONS OF POWDERED MATERIAL

Volume of diluting material	Group 0	1	2	3	4	5	6	7	8	Volume of diluting material
0	He(2)	H(1) Li(3)	Be(4)	B(5)	C(6)	N(7)	O(8)	F(9)		0
1 3	Ne(10) A(18)	Na(11) K(19)	Mg(12) Ca(20)	Al(13) Sc(21)	Si(14) Ti(22)	P(15) V(23)	S(16) Cr(24)	Cl(17) Mn(25)	Fe(26) Co(27) Ni(28)	3 5
5 6	Kr(36)	Cu(29) Rb(37)	Zn(30) Sr(38)	Ga(31) Yt(39)	Ge(32) Zr(40)	As(33) Cb(41)	Se(34) Mo(42)	Br(35) Ma(43)	Ru(44) Rh(45) Pd(46)	6 "
7 8 9–10	Xe(54)	Ag(47) Cs(55)	Cd(48) Ba(56)	In(49) La(57)	Sn(50)	Sb(51) Ta(73)	Te(52) W(74)	I(53) Re(75)	Os(76) Ir(77) Pt(78)	8 10
					Rare earths					
10	Nt(86)	Au(79) Va(87)	Hg(80) AcX(88) ThX Ra Mth	Tl(81) Ac(89) Mth_2	Pb(82) RdAc(90) Rth Io Th Ux_1	Bi(83) Ux_2(91)	Po(84) U_1(92) U_2	Am(85)		10

In certain cases it is desirable to avoid the use of the glass specimen tube, and yet it is not convenient, or sometimes not even possible, to press the specimen into a cylinder by means of a mold. If the specimen is not hygroscopic and is not readily oxidized in the air, the powdered crystal may be mixed with an amorphous adhesive such as gum tragacanth and pressed up into a thin slab having a flat edge. This slab may then be mounted with its edge at C, Fig. 6, so as to make a very slight angle with the primary beam. The edges of the lines in the diffraction pattern are sharpened if the specimen material is pasted on the edge of some opaque amorphous material like lead glass. In some cases it is possible to substitute for the slab and lead glass a strip of thin cardboard which has a layer of the powder stuck on its edge. The crystals of mechanically worked metals are usually quite small. If the specimen to be examined is a thin sheet of metal having a straight edge, it may be mounted in the same manner as the slab described above. Most metals are sufficiently opaque to the x-rays used in crystal analysis so that the lead glass backing is unnecessary. If for some reason there is objection to using an edge, the sheet may be bent over a mandrel and the bent portion may be used as the specimen. It should be remembered, however, that the bending will alter the sizes and orientations of the crystals of

the metal. If the metal is in the form of a thin wire, it may be stretched out in the path of the beam so as to take the place of the specimen tube of Fig. 1. This is one of the most desirable methods of mounting a specimen when no other diffraction pattern is to be taken on the same film for purposes of comparison. If a comparison pattern is desired, the wire and the comparison standard may be mounted along the same straight line on the edge of an amorphous holder such as a slab of pressed gum tragacanth or a sheet of glass, or the wire and the comparison standard may be inserted in opposite ends of a glass or celluloid specimen tube.

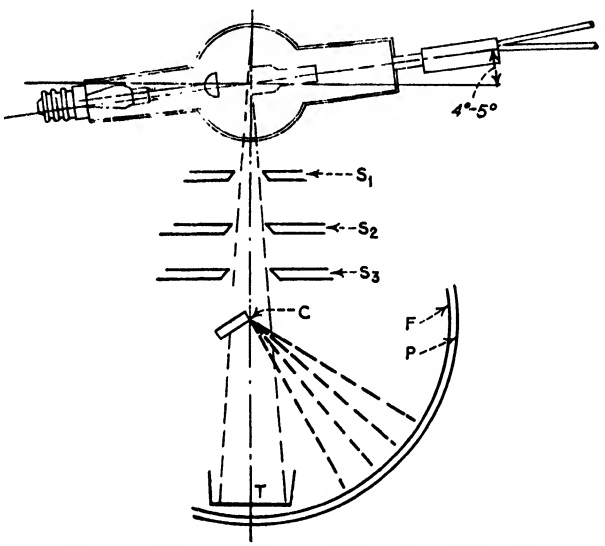

FIG. 6.—Powder method applied to a pressed block.

If the wire is of very fine diameter, it is best to use several lengths side by side. For 5-mil wire, six or seven lengths are sufficient.

If it is desired to investigate the surface of a flat sheet, such as a sheet of rolled metal, the x-ray beam may be defined by a narrow slit of about 0.020 in. width, and the surface of the sheet may be placed at an angle of about 5° to the beam. The width of each of the diffracted beams is obviously determined largely by the projection of the irradiated portion of the surface in the direction of the diffracted beam. The x-ray beam should therefore be as narrow as is consistent with a reasonable speed of taking the diffraction pattern, and the surface of the foil should make as large an angle as possible with the x-ray beam without blocking out part of the diffraction pattern. Considerations of this sort were responsible for the recommendations just given for slit width and angle.

If the specimen is transparent to the x-rays but, like some textile fibers, difficult to mold into a cylindrical shape, it may be pressed in a

hydraulic press between two metal plates to give a reasonably flat slab. A very dilute glue solution may be used if necessary to bind the fibers or particles together. The slab may then be mounted at right angles to the x-ray beam. In such a case the beam must be defined by a narrow slit of about 0.020 in. width, and the slab should be thick enough to present an adequate amount of specimen to the rays. For cotton or wood fiber, the slab, pressed to a hard mass, should be about $\frac{1}{16}$ in. thick.

St. John[4] has applied the principle of the "Seemann slit"[5] to powdered crystals. The specimen is a pressed slab of powdered crystal diluted

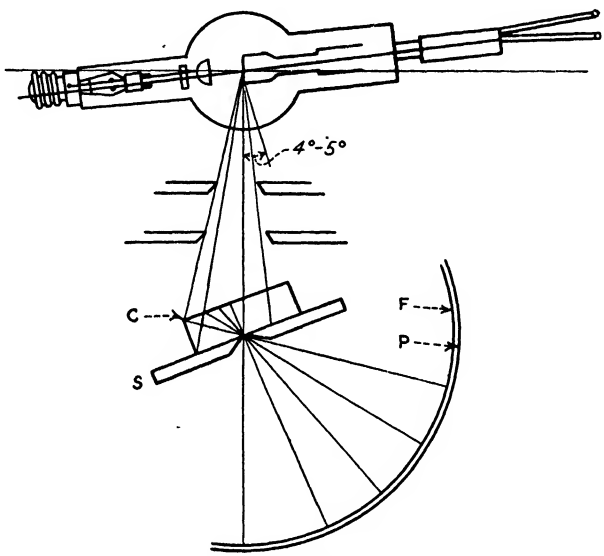

FIG. 7.—St. John's application of a Seemann slit.

with gum tragacanth. Since the reciprocal of the dilution is made proportional to the thickness t of Eq. (1), the dilution must be roughly proportional to the coefficient of absorption μ. An x-ray beam passes a pair of slits (Fig. 7) and falls upon the specimen slab. A narrow slit adjacent to the slab permits x-rays to pass to the photographic film. Each of the diffracted beams comes from a different part of the slab so that homogeneity of the slab is essential. It is important too that the x-ray beam be used only at a small angle from the face of the target so that all parts of the slab are irradiated uniformly. For any given line in the diffraction pattern the effect is the same as if all the crystalline material in the path of the x-rays composing that line had been crowded up into the specimen tube of Fig. 1. The advantage of the scheme is that the glass specimen tube is eliminated, thus avoiding variations in the general fog on the photographic film caused by variations in the

thickness of the glass wall of the specimen tube. The slits cause the lines on the diffraction pattern to be very clean and sharp without the necessity of preparing a specimen with a narrow edge. The scheme is, of course, as unsuited to hygroscopic substances or to substances which tend to oxidize in the air as is the scheme of Fig. 6.

H. Seemann,[6] H. Bohlin,[7] W. H. Bragg,[8] and J. Brentano[9] have described methods in which thin layers of powder are used in such a way as to focus the diffracted x-rays rather sharply upon a photographic film. The methods all depend upon the geometrical principle that two angles inscribed in the same circle are equal if they subtend the same arc. Let a photographic film be placed on the arc ABC of the circle

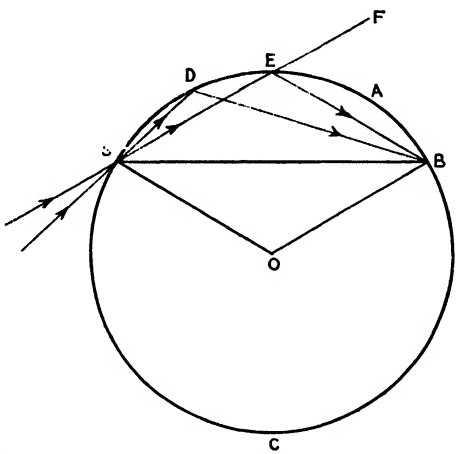

FIG. 8.—The focusing method of crystal-powder analysis. The divergence of the incident beam is considerably exaggerated in the figure. The angle $FEB = 2\theta$.

$ABCDE$ of Fig. 8, and let a crystal powder be pressed into an arc $SDEA$ of the same circle. Let a fine slit S be placed on the circumference of the circle so that a divergent beam of monochromatic x-rays falls on the powdered crystal. Then all the particles of the powder which find themselves oriented at the correct angle for diffraction from some given family of planes will, irrespective of their position on the arc $SDEA$, diffract the x-rays to the same point on the photographic film. For example, the angles SDB and SEB are equal because they both are inscribed in the same circle and both subtend the same arc BCS. Therefore $180° - \angle SDB = 180° - \angle SEB$. But $180° - \angle SEB = \angle FEB = 2\theta$, where θ is the grazing angle of incidence mentioned in Bragg's law. Therefore, if, in a crystal fragment lying in the arc $SDEA$ at D, a given family of planes can diffract x-rays to B, then in a second fragment the same family of planes similarly situated in the arc at any point E can also diffract the same wave length of x-rays to B.

Since $2\theta = 180° - \angle SEB$, it must also equal $\angle EBS + \angle ESB$. The angle EBS subtends the arc SDE, and the angle ESB subtends the arc EAB, so that the sum of the inscribed angles EBS and ESB subtends the arc $SDEAB$ and is measured by half of that arc. In other words, 2θ is measured by half the arc $SDEAB$. Since the central angle SOB is measured by the arc $SDEAB$, we have

$$2\theta = \frac{1}{2}\angle SOB = \frac{l}{2R}$$

where l is the length of the arc $SDEAB$, and R is the radius of curvature of the photographic film ($=OB$).

It is essential that the slit S be very fine, otherwise the effect is the same as if the point S were moved to the left, away from the circumference of the circle. The wider the slit S, the less sharp is the focus at B. A scheme due to Brentano[9] minimizes this effect, especially over small angular ranges. It can be applied to large angular ranges with some loss in the speed of photographing the diffraction pattern.

It will be shown later on in this chapter that, if the length of the slit is too great, one side of the line which represents the diffracted beam on the photographic film will be distorted. The straight side of the line represents the true position of the diffracted beam. The straight side lies away from the slit, so that, if 2θ is less than 90°, it lies on the side toward C of Fig. 8; and, if 2θ is greater than 90°, it lies on the side toward A. When 2θ is 90°, the chord SB becomes the diameter of the circle; the line is then of minimum width, and both edges are straight. The sample of powdered crystal must, of course, be thin. Otherwise, diffracted beams coming from behind the surface will be far enough off the arc $SDEA$ to decrease the sharpness of the focus. The more transparent the crystal is to the wave length of x-rays employed, the more important is the thinness of the layer of powder. In using specimens of metal foil it is necessary to make sure that the surface of the foil lies accurately on the arc $SDEA$ without any wrinkles.

For the sake of simplicity the rest of this chapter is written in terms of the type of apparatus shown in Fig. 1. The few changes necessary to make it apply to the other types which have just been described will be obvious.

THE DIFFRACTION PATTERN AND ITS INTERPRETATION

It is inherent in the powder method that all the families of atomic planes in the specimen send out their diffracted beams simultaneously. A single photographic film may therefore be made to record the whole diffraction pattern or as much of it as may be desired. Each family of planes in the powdered crystal produces a line on the film for its first-order diffracted beam and additional lines for such other orders of

diffraction as may be given by the crystal, provided only that $n\lambda/2d$ is less than unity (see Bragg's law). The photographic record of the diffraction pattern is therefore a series of lines whose angular distances from the "zero line" (photographic record of the undeviated beam) are characteristic of the various interplanar spacings in the crystal. From these angular distances, and the wave length of the x-rays, the interplanar spacings may be calculated at once from Bragg's law.

Knowing the interplanar spacings, it is possible, at least in the case of the simpler crystal systems, to find by systematic cut-and-try methods

TABLE II.—DISTANCES BETWEEN ROWS IN A SIMPLE RECTANGULAR (TWO-DIMENSIONAL) LATTICE

Distance between rows, feet	Ratio from experiment (50.0 = 1.00)	Ratio from experiment (25.0 = 1.00)	Ratio calculated for simple rectangular lattice (A = 2.00)	Miller indices for rows in simple rectangular lattice
50.0	1.00	2.00	2.000	1,0
25.0	0.50	1.00	1.000	0,1
22.3	0.44	0.87	0.894	1,1
17.7	0.35	0.71	0.707	2,1
13.9	0.27	0.55	0.555	3,1
12.1	0.24	0.48	0.485	1,2
11.2	0.22	0.45	0.447	4,1
10.0	0.20	0.40	0.400	3,2
9.3	0.18	0.37	0.372	5,1
8.2	0.16	0.33	0.329	1,3
7.9	0.16	0.32	0.316	2,3 6,1
7.8	0.15	0.31	0.312	5,2
6.9	0.14	0.28	0.277	4,3
	0.13	0.27	0.275	7,1

an arrangement of atoms in space which will account for the observed interplanar distances. The situation may be visualized by the following illustrations in two dimensions. If the trees of an orchard are planted according to some systematic geometrical scheme, they will appear to be in rows whose direction and distance apart will depend upon the position of the observer with respect to the orchard. Now suppose that the reader had never seen the orchard but had been supplied with data giving the distance apart of these various rows of trees, and suppose that it is required to draw a map to scale showing the positions of the trees in the orchard. It would be necessary to list the data in a column in the order of the size of the numbers, starting with the largest number at the top of the column. In a parallel column a corresponding list would be made of the ratios of the several distances to the largest dis-

tance, as in Table II. Some geometrical configuration of trees must now be assumed, and the ratios of distances required by that configuration must be compared with the tabulated ratios. If they do not agree, a new configuration must be assumed and its ratios compared with those listed from the data. The first column of Table II shows that the orchard has its trees at the corners of imaginary rectangles whose sides are in the ratio of 2:1, for such a configuration gives calculated ratios of spacings identical with those from the tabulated experimental data. It is evident that the imaginary unit-rectangles are 50 ft. long and 25 ft. wide.*

Suppose the distances between rows had been those listed in the first column of Table III. Certain of the ratios in the second column

TABLE III.—DISTANCE BETWEEN ROWS IN A CENTERED RECTANGULAR (TWO-DIMENSIONAL) LATTICE

Distance between rows, feet	Ratio from experiment (25.0 = 1.00)	Ratio calculated for a centered rectangular lattice (A = 2.00)	Miller indices for rows in centered rectangular lattice
25.0	1.00	1.000	1,0
22.2	0.89	0.894	1,1
13.7	0.55	0.555	3,1
12.5	0.50	0.500	0,1
9.2	0.37	0.372	5,1
8.8	0.35	0.353	2,1
8.2	0.33	0.329	1,3
6.9	0.27	0.275	7,1

are identical with those of the second and third columns of Table II. Such an accidental agreement of a portion of the data cannot be taken to mean that the plan of the orchard of Table III is a simple rectangle, for, if *every* experimental ratio is not duplicated, within the precision of the data, in the columns of calculated ratios, the solution cannot be valid. The third column of Table III shows that *every* experimental ratio is duplicated in the ratios calculated for a centered rectangle for which A = 2.00. The actual distances in Table III may be accounted for if the unit-rectangles are 50 ft. long and 25 ft. wide. A comparison of the third and fourth columns of Table III with the fourth and fifth columns of Table II shows that the effect of the additional trees has not been to produce rows in new directions in the orchard; all that has

* In crystallographic language we have a two-dimensional analogy to an orthorhombic crystal for which a = 50, b = 25, and A = 2.00. The distances between the various rows of trees can be calculated from Eq. (6) of Chap. III, remembering that l is zero. For the simple rectangular lattice the periodicity is of course always unity. For the centered rectangular lattice the periodicity is unity when both indices are odd; if only one index is odd, the periodicity is ½.

been done is to cut in half the distances between those rows which have one even Miller index.

The interpretation of the diffraction pattern of a powdered crystal is much like the foregoing illustration except that there are three dimensions to be considered instead of two, and the data include fictitious distances d/n caused by lines in the diffraction pattern corresponding to the second, third, etc., order of diffraction. In the cubic system it is easy, with the aid of the information given in Chap. III, to make reference tables of interplanar distances taking the edge of the unit-cube as the unit of length. Such a table is illustrated by Table V of Chap. III. The fictitious distances are listed in the table as though they actually existed, so that the table corresponds to all the interplanar distances calculated from the diffraction pattern just as truly as Tables II and III

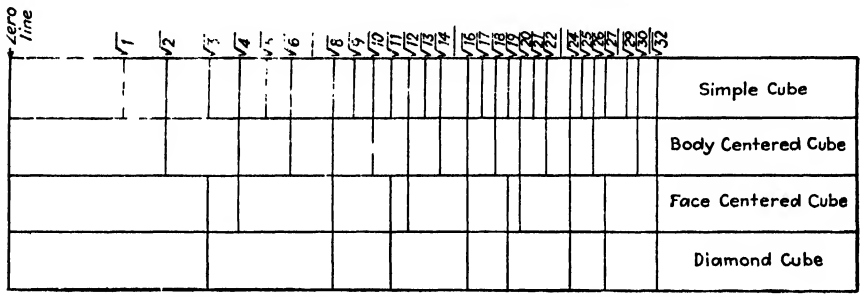

FIG. 9.—Effect on diffraction pattern of complicating the crystal structure.

correspond to all the distances measured in the orchards. An inspection of Table V of Chap. III shows that the pattern for a simple cubic crystal contains every possible line which can be produced by a crystal having cubic symmetry. When the crystal structure is made more complicated by placing additional atoms in symmetrical positions in the simple cube without changing the dimensions of the cube, the effect is not to add more lines but to wipe out certain lines from the simple cubic pattern. This is brought out in Fig. 9 which is plotted from Table V of Chap. III. The actual diffraction patterns will differ from those of Fig. 9, for in Fig. 9 the distance from each line to the zero line is made proportional to $\sqrt{h^2 + k^2 + l^2}$, while in the actual pattern the distance from each line to the zero line is the length of the arc corresponding to twice the θ in Bragg's law. In terms of the actual diffraction pattern, therefore, Fig. 9 is considerably compressed on the right-hand end.

It was shown in Chap. III that each spacing for a simple cube is the reciprocal of the square root of the sum of three squares. These spacings therefore decrease in regular fashion for the first six lines of the diffraction pattern. There is, however, no line corresponding to $1/\sqrt{7}$, for no three squares can add up to 7. Similar breaks may be found at $1/\sqrt{15}$, $1/\sqrt{23}$, $1/\sqrt{28}$, etc. If therefore a diffraction pattern is found to have

six lines regularly spaced, followed by a vacant place where the seventh line might be expected, it should be tested quantitatively at once to see if the ratios of spacings correspond to those of a simple cube. The spacings for the first six planes of a body-centered cube decrease in a regular way like those of a simple cube. In fact, if, in Table V of Chap. III, instead of using as a unit of measure the edge of the unit-cube, we had used the largest interplanar spacing calculated from the diffraction pattern of a body-centered cube, *i.e.*, the (1 1 0) planes, we should have found exactly the same ratios as in the simple cube. The fundamental reason for this is that for the body-centered cube the numerator of Eq. (3) of Chap. III is unity only when the denominator is the square root of an even number. The diffraction pattern of a body-centered cube differs markedly, however, from that of a simple cube in that there is no break in the regularity of spacing of the lines until after the thirteenth line. The diffraction pattern of a face-centered cube has the first nine lines grouped so as to form three repetitions of "a pair followed by a single line." The tenth line, corresponding to the spacing $1/\sqrt{27}$, would be the first line of the next pair except that the second line of the pair would correspond to a spacing $1/\sqrt{28}$ which cannot exist. The sequence of "pair and one" is continued for three more groups after which it is broken up again by missing lines. The diffraction pattern of a diamond cube consists of a single line followed by a succession of pairs.

GRAPHICAL METHODS OF INTERPRETATION

The quantitative examination of the diffraction pattern of a cubic crystal is easiest made with the aid of a slide rule. If the slide of an ordinary slide rule is turned so that the numbers are upside down, and the ends of the scales are made to register with each other (Fig. 10), it will be found that readings on the lower scale of the body of the slide rule are opposite the reciprocals of their squares on the inverted slide. If the slide is pushed along, any two readings on the lower scale of the body of the rule have the same ratio as the reciprocals of the square roots of the corresponding readings on the lower (adjacent) scale of the inverted slide. The interplanar distances of a crystal, as calculated from the diffraction pattern with the aid of Bragg's law, are therefore plotted on the lower scale of the body of the slide rule, using a soft lead pencil. The interplanar distances usually measured from the diffraction pattern range for most inorganic crystals from 2 or 3Å. down to about 0.6 or 0.7Å. At 1.00Å. the plot runs off the left-hand end of the scale and must be continued at the right-hand end. The inverted slide is pushed along until 1 is opposite the pencil mark corresponding to the greatest interplanar distance. Suppose the next pencil mark is found opposite 2, the next opposite 3, etc. Taking note of the reading on the slide which is opposite 1.00 at the left-hand end of the fixed scale, move the slide

back until this reading is opposite 1.00 at the right-hand end of the fixed scale (see Fig. 11). If *all* the remaining pencil marks also come opposite integers on the slide, the crystal is simple cubic, for its interplanar distances have the same ratios as those listed in the fourth column of Table V of Chap. III. If an exact match is not obtained the slide is moved back until 2 on the inverted slide is opposite the pencil mark corresponding to the greatest interplanar distance. Then if *all* the pencil marks are

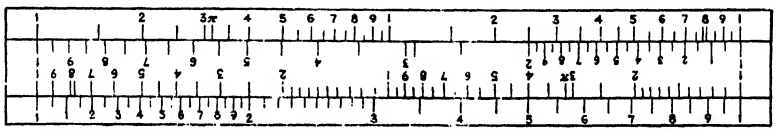

FIG. 10.—Slide rule arranged for quantitative study of diffraction patterns of cubic crystals.

opposite even numbers on the inverted slide, the crystal is body-centered cubic. If an exact match is still not found the slide is moved back until 3 on the inverted slide is opposite the first pencil mark, and the pattern, as plotted out on the body of the rule, is examined to see whether every pencil mark is opposite an integer on the inverted slide. If so, a comparison with the ratios given in Table V of Chap. III will show whether the diffraction pattern is characteristic of a face-centered or of a diamond cube. A similar procedure may be employed for still other types of cubic crystals. In all cases, if an exact match is obtained within the

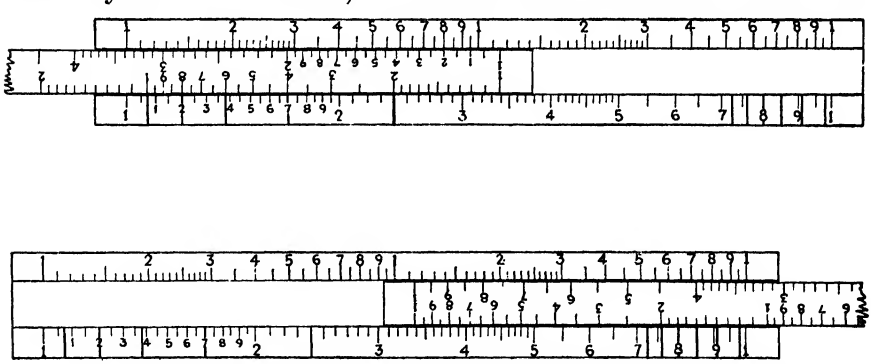

FIG. 11.—Slide rule marked with a body-centered cubic diffraction pattern.

limits set by the accuracy of the data, the reading on the lower scale of the body of the slide rule opposite 1 on the slide is the length in Ångström units (10^{-8} cm.) of the edge of the unit-cube. It is important that the match be exact within the precision of the experimental data. If any lines in the experimental diffraction pattern are unaccounted for, either the solution is invalid or it must be shown that the specimen consists of a mechanical mixture of two crystals such that every line is accounted for.

The usefulness of the slide rule in the solution of diffraction patterns of cubic crystals is due to the fact that the distances engraved on the inverted slide are proportional to the logarithms of successive values of d

in Eq. (3) of Chap. III. Since the scale on the body of the slide rule on which the experimental interplanar distances are plotted is also logarithmic, a direct comparison can be made between the two sets of ratios without further reference to the absolute values of the interplanar distances. This principle has been used[10] in the development of a series of semilogarithmic charts for the rapid solution of the diffraction patterns of crystals belonging to the tetragonal and hexagonal systems. The logarithms of d from Eq. (5) of Chap. III and from the corresponding equation derived from Eq. (23) of Chap. III were plotted as functions of the axial ratio C. For any given value of C the lines of the chart have the same relation to the theoretical ratios of distances in the tetragonal or hexagonal systems of crystals that the readings on the inverted slide of the slide rule had for the cubic system. The experimental data are plotted to the same logarithmic scale on the edge of a piece of paper. This plot corresponds to the pencil-mark plot on the lower scale of the body of the slide rule. Such charts were made and published at first only for the simple, body-centered, and face-centered tetragonal lattices for the simple triangular, and rhombohedral lattices and for the hexagonal close-packed structure. Although the diffraction pattern must be plotted as log d, the scale of abscissas was shown in terms of d itself, just as on a slide rule, in order to facilitate the work of plotting the pattern. A specimen chart is reproduced in Fig. 12. Figure 13 illustrates the use of a chart of this sort in the interpretation of experimental data on cadmium obtained by Hull.[10,11]

This method of interpretation is also applicable to diffraction patterns of crystals belonging to the orthorhombic system, and an extensive set of simple orthorhombic charts has been published by J. O. Wilhelm.[12] A series of charts for the tetragonal, hexagonal, and orthorhombic systems is given in Appendix II. Obviously the number of charts required for the monoclinic system would be prohibitive. Of course, if the axial ratios and angles are known for some monoclinic or triclinic crystal from ordinary crystallographic measurements, the theoretical interplanar distances may be calculated at once, plotted on the inverted slide of a slide rule, and compared with the experimental pattern plotted on the bottom scale of the rule. Then a consideration of what lines, if any, are missing may give a clew to the degree of complexity of the inner structure of the unit-crystal.

In cases where the charts of Appendix II contain lines whose spacings are too close for accurate reading, the graphical methods of Bjurström[13] may be used. Bjurström combines the equations of Chap. III with Bragg's law and writes the results in the form:

$$\sin^2\theta = K_1(h^2 + k^2) + K_3l^2 \qquad \text{(tetragonal system)}$$

$$\sin^2\theta = K_1(h^2 + K_2k^2) + K_3l^2 \qquad \text{(orthorhombic system)}$$

$$\sin^2\theta = K_1(h^2 + hk + k^2) + K_3l^2 \qquad \text{(hexagonal system)}$$

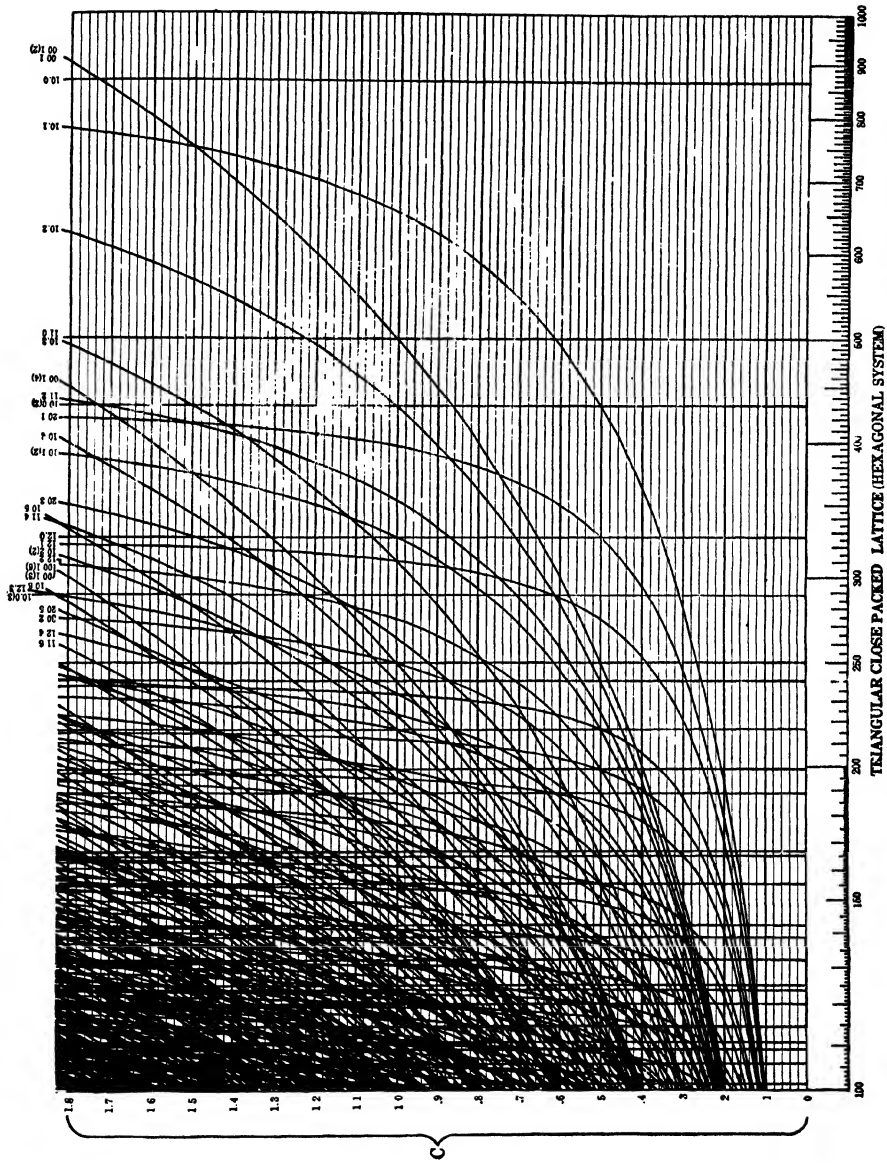

FIG. 12.—Semilogarithmic chart for the solution of diffraction patterns of hexagonal close-packed structures.

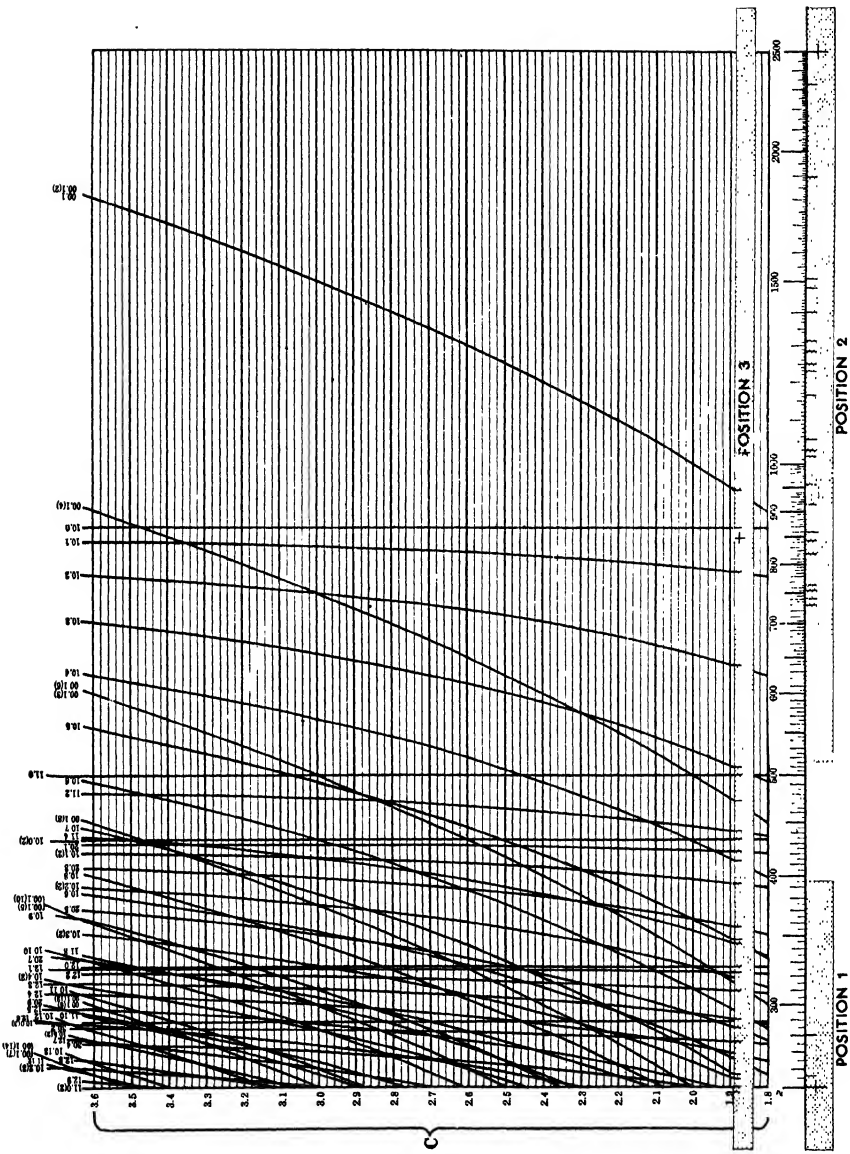
POSITION 3
POSITION 2
POSITION 1
c

where θ is as usual the grazing angle of incidence of the x-rays; h, k, and l are the Miller indices; and K_1, K_2, and K_3 are constants. For the pur-

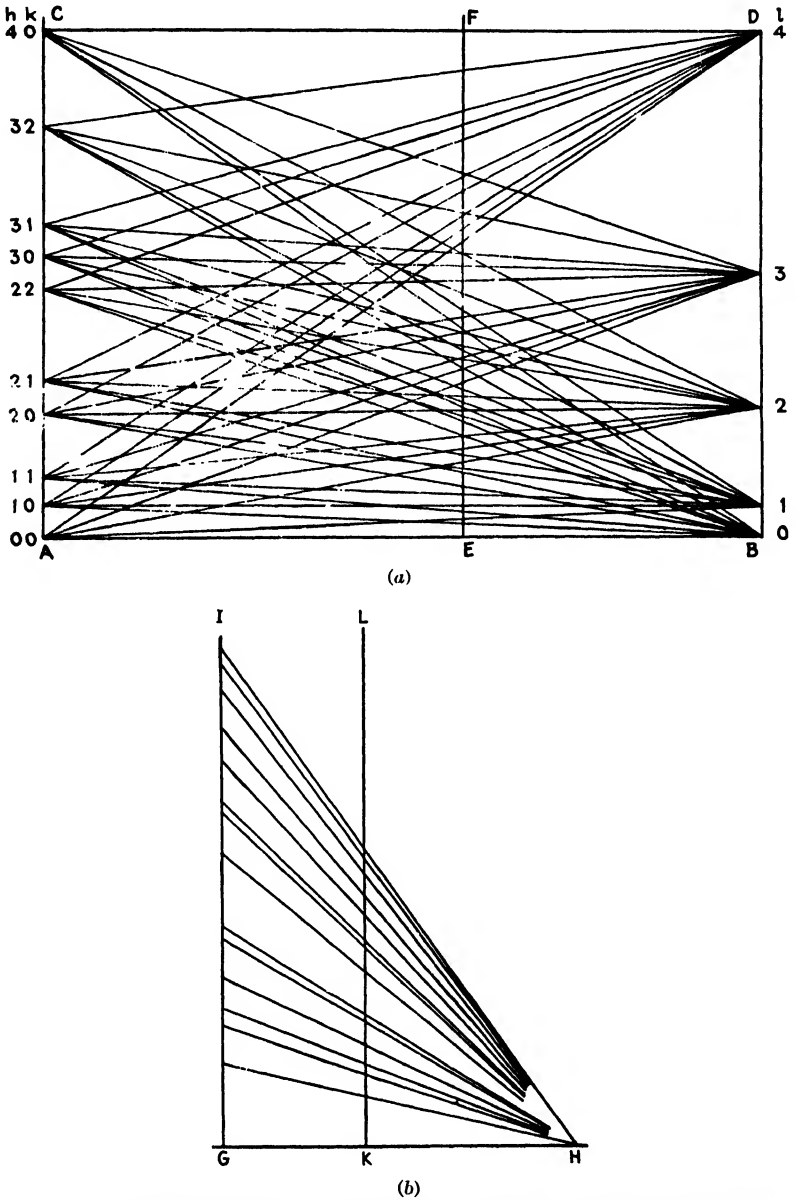

FIG. 14.—Bjurström's graphical solution for tetragonal and hexagonal crystals.

poses of crystal analysis, these equations may be treated graphically as follows.

To find the Miller indices corresponding to the powder pattern of a tetragonal crystal, construct a figure like Fig. 14*a*. In this figure, AC is perpendicular to AB. Points are marked off on AC whose distances from A are proportional to $(h^2 + k^2)$, and other points are marked off on BD whose distances from B are proportional to 1^2, 2^2, 3^2, 4^2, etc. Every point on AC is then connected to every point on BD by a straight line. It is evident that any line, EF, drawn perpendicular to AB will be cut by these lines at points whose distances from E are proportional to the quantity $K_1(h^2 + k^2) + K_3l^2$. If, therefore, the values of $\sin^2 \theta$ of the tetragonal lattice under investigation could be laid off from E on EF on a suitable scale, and if EF could be moved parallel to itself along the chart, then at the position where $AE:EB = K_1:K_3$, every point

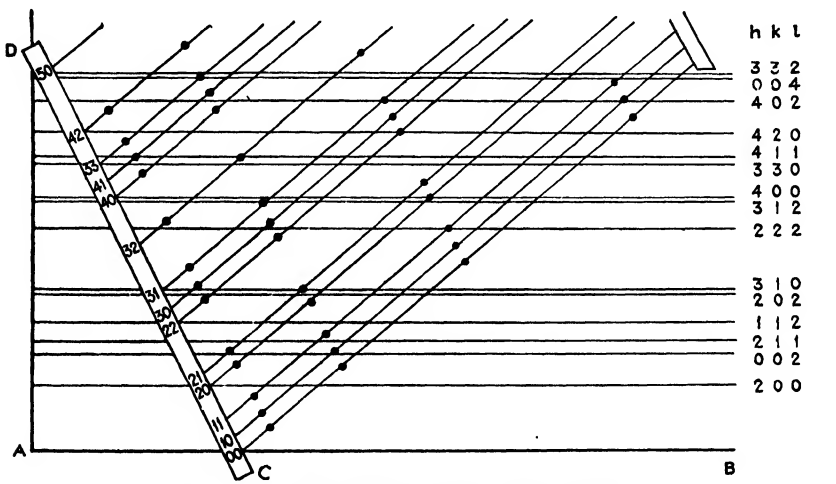

FIG. 15.—Bjurström's rule-and-string method.

marked off on EF would fall on the intersection of EF with some crossline whose indices correspond to the indices of the diffracting planes in the tetragonal crystal. Up to this point the correct scale for plotting the points on EF is unknown. This scale may be found as follows. Let the experimental values of $\sin^2 \theta$ be plotted on a large scale (larger than EF) on the line GI which is perpendicular to GH of Fig. 14*b*. If these points are connected to some common point H on GH, then every line KL parallel to GI will be cut at points corresponding to those on GI, and GI and KL will differ only in the scale of measurement. Let Fig. 14*b* be laid on Fig. 14*a* so that GH and AB coincide, and let Fig. 14*b* be slid back and forth on Fig. 14*a* until some imaginary vertical line shows the same intersection points on both figures. Now let this line be drawn on Fig. 14*a*; it is the line represented by KL and EF. Not only is the ratio of the constants K_1 and K_3 known from the position of this line, but also

the indices of all the diffracting planes can be read off directly on AC and BD.

The equation for the hexagonal system can, of course, be treated in the same way except that the distances marked off on AC must correspond to $(h^2 + hk + k^2)$.

Another type of procedure is illustrated in Fig. 15. It applies not only to the tetragonal and hexagonal systems but also to the orthorhombic system. It has the disadvantage of being a little hard to manipulate. For the tetragonal and hexagonal systems, straight lines are drawn parallel to AB of Fig. 15 such that their distances from AB are proportional to $\sin^2 \theta$. Points are marked off on the edge of a ruler CD whose distances from a point 00 are proportional to $(h^2 + k^2)$ or to $(h^2 + hk + k^2)$. From these points parallel threads are stretched to a second ruler which is kept parallel to CD. On these threads points are marked whose distances from the edge of the ruler CD are proportional to the numbers 1^2, 2^2, 3^2, 4^2, etc. The ruler CD is placed so that 00 falls on AB, and by trial the angle of inclination of the ruler and that of the threads are varied* until each of the horizontal lines falls across a point either on the ruler or on a thread. Since the points on the ruler correspond to $(h^2 + k^2)$ or $(h^2 + hk + k^2)$, and the points on the threads correspond to 1^2, 2^2, 3^2, 4^2, etc.,† it follows that the indices for the horizontal lines can be read off directly. For the orthorhombic system the scheme has to be changed slightly. If the distances of the threads from the point 00 are made proportional to 1^2, 2^2, 3^2, 4^2, etc., and if the points marked on the threads are also spaced proportional to 1^2, 2^2, 3^2, 4^2, etc., then we can use the threads and ruler to find a series of diffraction lines whose values of $\sin^2 \theta$ satisfy the equation

$$\sin^2 \theta = K_1 h^2 + K_2 k^2$$

or

$$\sin^2 \theta = K_1 h^2 + K_3 l^2$$

or

$$\sin^2 \theta = K_2 k^2 + K_3 l^2$$

If several such series of diffraction lines can be found, the constants K_1 and K_2; K_1 and K_3; or K_2 and K_3 should be evaluated for each series. If the same value appears in two series, it must be proved whether or not this and the other constants of these two series are the three lattice constants K_1, K_2, and K_3.

Still other graphical schemes are described by Bjurström for which the reader is referred to reference 13.

* This corresponds to varying K_1 and K_3, respectively.

† The intersection of the threads with the edge of the ruler corresponds to 0^2.

Owen and Preston[14] have published a chart for the interpretation of hexagonal close-packed structures in which $\log \frac{1}{d}$ and $\log \frac{1}{C}$ are the coordinates. This has the advantage of including a wide range of axial ratios on a single chart, although at some sacrifice in the accuracy with which the axial ratio may be determined. In using their chart, which is shown in Fig. 16, it should be noted that the scale of abscissas is expressed in terms of the logarithm of $1/d$ and not in terms of d directly as in the case of the semilogarithmic chart of Fig. 12. When no filter is used to

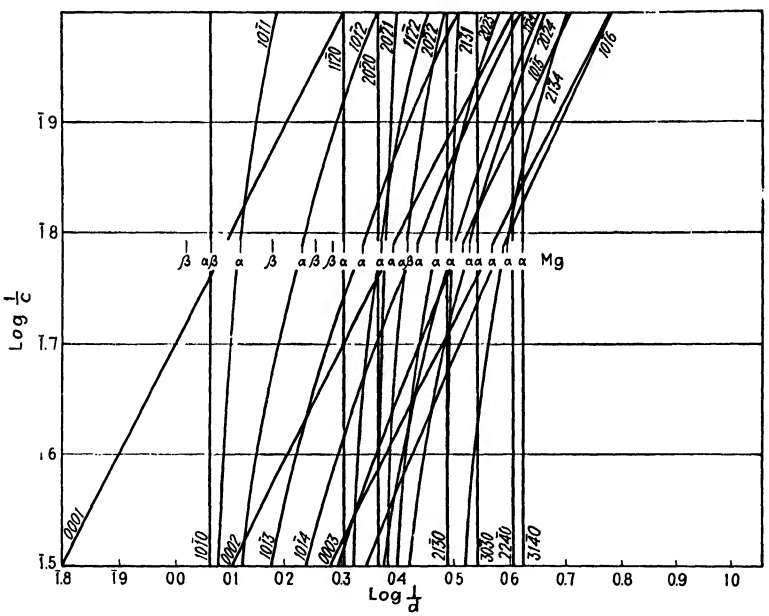

FIG. 16.—Owen and Preston's chart for hexagonal close-packed structures.

give a single wave length of x-rays, the ionization chamber or photographic plate shows two diffraction patterns superimposed, one produced by the "α doublet," the other by the "β line" of the x-ray beam. If the scale of abscissas is taken as log sin θ instead of $\log \frac{1}{d}$ it is evident that the angles of diffraction for the β line can be plotted directly on the same strip of paper as the angles for the α doublet. Either of these patterns may then be used independently of the other. Figure 16 shows some of the β pattern for Mg crystals plotted along with the α pattern.

Ewald[15] has published an incomplete chart of a rhombohedral lattice, regarding it as a distorted cube and using the rhombohedral axes of Eq. (24) of Chap. III. Several lines are missing, but the chart shown in Fig. 17 serves to illustrate how, instead of an axial ratio, the angle μ

between the axes may be used in the interpretation of rhombohedral structures. Like Owen and Preston, Ewald plots log $\frac{1}{d}$ or log sin θ as abscissas. An additional scale has been added in Fig. 17 giving the abscissas in terms of $1/d$ directly. The use of the plot is illustrated by Debye's diffraction pattern of "pseudo-graphite." Ewald's equations

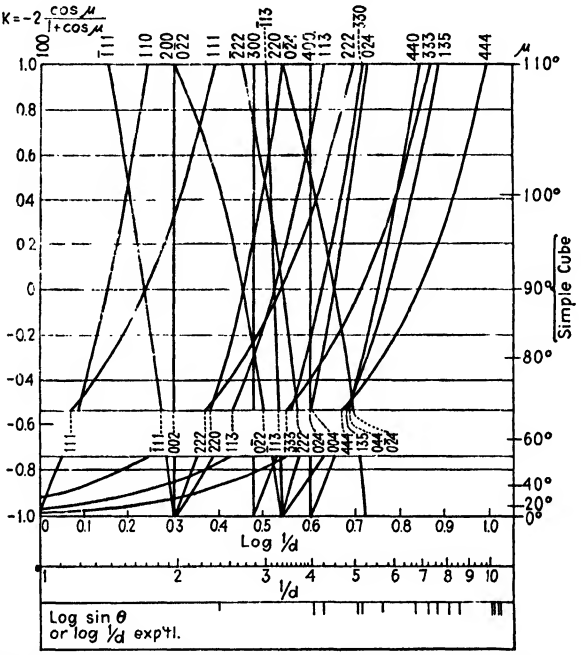

FIG. 17.—Interpretation of diffraction pattern of pseudo-graphite by means of Ewald's chart.

differ from Eq. (24) of Chap. III as they are based on the idea of a "reciprocal lattice" (see Chap. VII). His chart therefore uses

$$k = -2\frac{\cos \mu}{1 + \cos \mu}$$

as ordinates. The corresponding values of the angle μ are given on a separate scale of ordinates.

Owen and Preston[14] have also proposed a graphical solution of the diffraction patterns of cubic crystals. They write Bragg's law in the form

$$n\lambda = 2ka \sin \theta$$

where a is the edge of the unit-cube and k is a constant for any given family of planes for some one value of the wave length λ. This may be written

$$\frac{n}{a} = \frac{2k}{\lambda} \sin \theta$$

showing that for any given wave length of x-rays the relation between n/a and sin θ may be represented graphically by a family of straight lines passing through the origin. Their charts for body-centered and face-centered cubes are shown in Figs. 18 and 19, using the Mo characteristic rays $\lambda_\alpha = 0.710$Å. and $\lambda_\beta = 0.631$Å.

It should be emphasized that no matter what scheme is used for interpreting a diffraction pattern, the solution must be verified by:

a. Showing that it is consistent with the known density of the crystal;

b. Showing that the order of the intensities of the lines in the pattern can be calculated from the proposed crystal structure. This latter point will be taken up more fully later on in this chapter in the discussion of the Structure of Arsenic.

Number of Lines Required.—No matter what method is used for the interpretation of diffraction patterns, too much emphasis cannot be placed upon the necessity for having a sufficiently large number of lines in the diffraction pattern. It has already been shown that the ratios between the interplanar distances for the first six lines of a simple cubic pattern are the same as for a body-centered cubic pattern. Many other instances will be found from the semilogarithmic charts given in Appendix II, where the first few lines are often identical for widely different crystal structures. Such diffraction patterns can be differentiated from each other only when lines are present in sufficient number.

In most cases the diffraction pattern should be investigated through an angle corresponding to an interplanar distance of 0.7Å. In the case of some crystal structures, such as the face-centered cubic, an angle corresponding to 0.8Å. is sufficient. The number of lines in a diffraction pattern of a powder is greater the shorter the wave length of x-rays employed, since the smallest interplanar distance which will diffract the rays is, from Bragg's law,

$$d = \tfrac{1}{2}\lambda$$

The longer wave lengths, such as are characteristic of Fe and Cu, give more accurate determinations of the larger interplanar spacings, and in special cases, such as investigations of the structure of organic compounds, have considerable real advantage for such purposes. The wave length for Fe is too long to give enough lines for the satisfactory solution of crystal structures of many inorganic substances, even when the x-rays are bent through an angle $2\theta = 180°$. The wave length for Cu requires 180° for an interplanar distance of 0.77Å. Both wave lengths are so long as to require a special window on the x-ray bulb, and this in turn has until recently necessitated operating the tube while connected to the pump. The objections to operating on the pump are obvious to any one

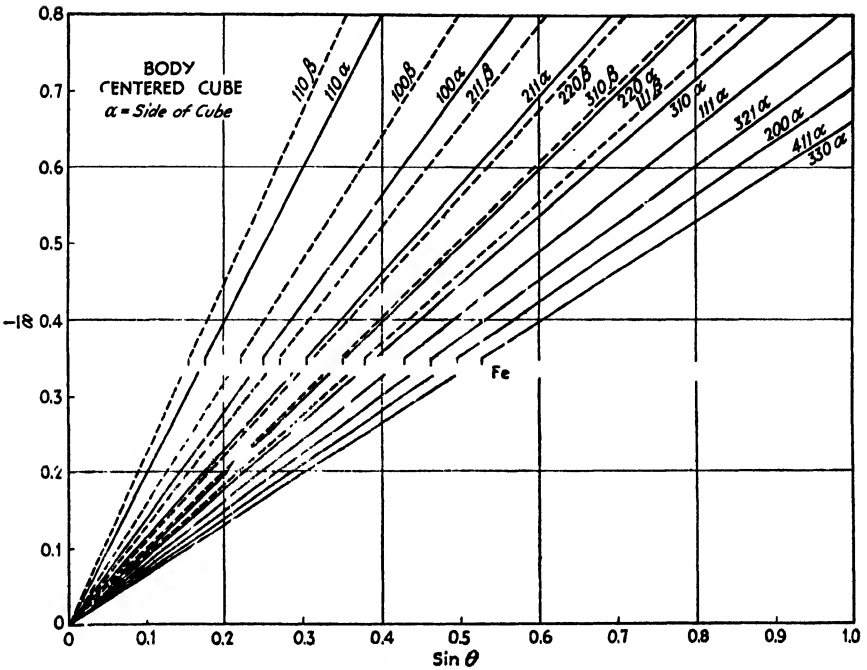

FIG. 18.—Owen and Preston's chart for body-centered cubic lattice.

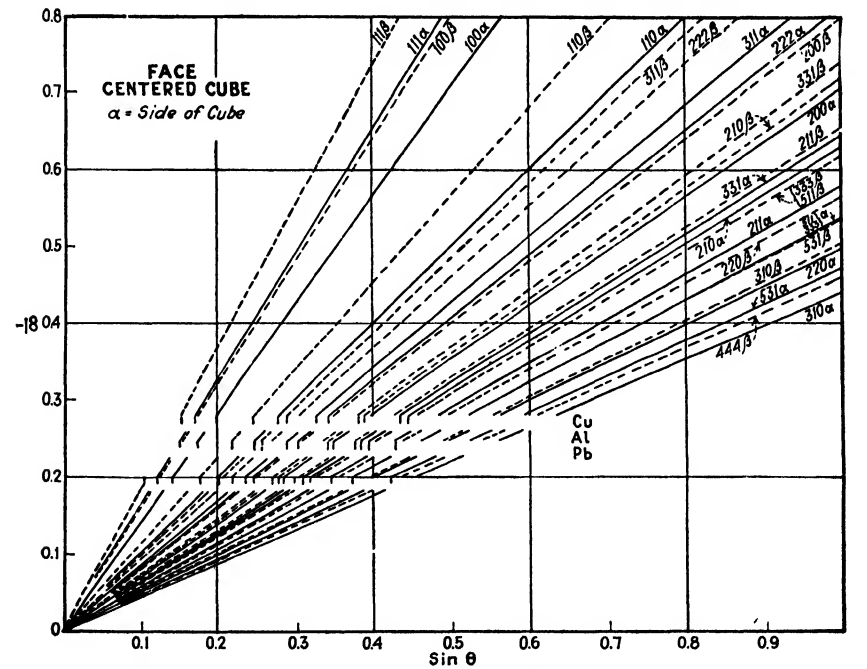

FIG. 19.—Owen and Preston's chart for face-centered cubic lattice.

who has ever tried it.* The very short wave lengths such as are characteristic of W, $\lambda = 0.2$Å., give angles of diffraction which are so small as to interfere seriously with accuracy of measurement, especially on a photographic film. An interplanar distance of 0.7Å. bends these rays through an angle 2θ of about 16°. The upper left-hand corner of Fig. 12 shows that, in extreme cases at least, there is a practical limit to the number of lines in a diffraction pattern which are useful in solving a crystal structure by the ordinary graphical methods, so that we are led to the conclusion that the short wave lengths from W, Pt, etc., are ordinarily of little value in making a complete crystal analysis by the powder method. They are sometimes useful in studying the constitution diagrams of alloys when a well-known phase may often be identified by two or three lines. The wave lengths which are characteristic of Mo, Rh, or Ag are sufficiently penetrating to permit the use of an all-glass x-ray bulb which has been pumped out once for all and sealed off from the pump. An interplanar distance of 0.7Å. corresponds to an angle 2θ of about 60° for Mo rays. This means that, if a photographic film is bent on an arc of 8 in. radius, interplanar distances of 2.0Å. can be determined to ¼ per cent and distances of 1.6Å. or less can be determined easily to $\frac{1}{10}$ per cent. Greater accuracy is rarely useful because the traces of impurities ordinarily found in even "chemically pure" materials seem to make variations from sample to sample of the order of $\frac{1}{10}$ per cent in the parameters of crystals from different sources. For instance, the edge of the unit-cube of 99.9 per cent Ag is 4.058 ± 0.004Å., while the value for 99.999 per cent Ag is 4.079 ± 0.004Å.[16] Considerations of this sort, coupled with the fact that the x-ray tube itself imposes certain limitations upon the choice of a target material and therefore indirectly upon the choice of a filtering material, have led users of the powder method in this country; when investigating inorganic materials, to the almost exclusive use of MoK_α rays, a radius of curvature of the photographic film of 8 in., and an exposure time sufficient to show a diffraction pattern throughout an arc of at least 60°. When investigating organic materials either Mo or Cu rays are used, depending upon the circumstances of the experiment.

STRUCTURES OF TYPICAL SUBSTANCES

The Structure of Typical Alkali Halides.—It will be of interest to illustrate the powder method by showing the interpretation of the diffraction patterns of some of the same crystals by which the Bragg method was illustrated. Figures 20, 21, and 22 show the diffraction patterns of KCl, NaCl, and KI, respectively.

* The most serious of these objections may be removed by inserting a carboy or tank between the high-vacuum pump and the backing pump with a stopcock between the carboy and the backing pump.

The pattern of KCl shows six lines whose spacings decrease in regular fashion. Where a seventh line might be expected, there is an empty space. This corresponds to the description already given for the diffrac-

FIG. 20.—Diffraction pattern of KCl.

FIG. 21.—Diffraction pattern of NaCl.

FIG. 22.—Diffraction pattern of KI.

tion pattern of a simple cubic crystal. Trial shows that the interplanar distances corresponding to the various lines of the pattern have, quantitatively, the same ratios as are listed in Table V of Chap. III for a simple cubic lattice. In a simple cubic crystal there are three families of (1 0 0)

planes, parallel, respectively, to the three axes of the crystal (see Table V of Chap. III). There are six families of (1 1 0) planes corresponding to the six possible directions for face-diagonals. There are four families of (1 1 1) planes perpendicular, respectively, to the four directions for the body-diagonals of the cube. The chance of a (1 1 0) plane being turned at the correct angle for diffraction is therefore double that of a (1 0 0) plane. The chance of a (1 1 1) plane being turned at the correct angle is $1\frac{1}{3}$ times that of a (1 0 0) plane, etc. Other things being equal, the x-ray beam diffracted from the (1 1 0) planes of the powdered crystal should, therefore, be twice as intense as that from the (1 0 0) planes. The beam from the (1 1 1) planes should be $1\frac{1}{3}$ times as intense, etc. If we remember that the intensity of the diffracted beam falls off as the angle of diffraction increases, it is evident from Fig. 20 that the relative intensities of the lines actually do correspond to the numbers of families of the various planes in the crystal.* We therefore are justified in assuming that KCl is built up on a simple cubic lattice. A calculation of density made in accordance with Eq. (1) of Chap. II shows at once that, on the average, *half* a "molecule" of KCl is situated at each corner of the unit-cube. Since the ionic numbers of K^+ and Cl^- are equal, their diffracting powers should be practically equal; so we conclude at once that they occupy alternate corners of the cube.

The diffraction pattern of NaCl is that already described as characteristic of a face-centered cubic lattice. A calculation of density shows that a whole "molecule" of NaCl must be associated with each point in the face-centered cubic lattice. It will be noticed from Fig. 21 that those planes for which the Miller indices are all odd† produce lines in the diffraction pattern which are much weaker than the others. If these relatively faint lines are disregarded, the remaining lines form, quantitatively, a diffraction pattern of a simple cubic lattice whose cube-edge is half that of the face-centered cube. A calculation of density for such a cube‡ shows that, on the average, *half* a "molecule" of NaCl would have to be associated with each point of the simple cubic lattice, *i.e.*, Na^+ and Cl^- might be assumed to occupy alternate corners of the simple

* These intensities will depend also upon the degree of imperfection of the crystal, and comparisons between theory and experiment must be carefully scrutinized to make sure that they apply to crystals having the same degree of imperfection. In this connection see Chaps. X and XI.

† Second-order diffraction is considered, as before, as being a first-order beam coming from fictitious planes whose Miller indices are all double those for the actual first-order diffraction. Such indices are therefore all even. Third-order diffraction is considered as coming from fictitious planes whose indices are three times those for the actual first-order diffraction.

‡ In order to avoid reasoning in a circle we must calculate our interplanar spacings for NaCl in terms of wave lengths obtained by experiments with ruled gratings such as were used by A. H. Compton, or by considerations of quantum theory.

cube. Such a structure would place the Na^+ and Cl^- on two interpenetrating face-centered cubic lattices as in Fig. 7 of Chap. V.

This model gives alternate planes of Na^+ and Cl^- for each of those families of planes whose Miller indices are all odd and gives planes composed of both Na^+ and Cl^- for the other families of planes. If now we assume, as we have already done all along in discussing the Laue and Bragg methods, that Cl^- (ionic number 18) diffracts x-rays more strongly than Na^+ (ionic number 10), then the small intensities of the diffracted rays from the (1 1 1), (3 1 1), (3 3 1), (5 1 1), (3 3 3) . . . planes will be accounted for, for their amplitudes in each case will be the *difference* between the amplitudes of the beams sent out by the planes of Na^+ and of Cl^-. Similar reasoning leads to a structure of the NaCl type for KI. In this case the lines from the planes of odd indices are relatively stronger than for NaCl because of the greater difference in the ionic numbers of K^+ and I^-.

CsI, CsBr, and CsCl show much the same sort of progression in their diffraction patterns. Cs^+ and I^- have the same ionic number and are therefore assumed to have equal diffracting power. The diffraction pattern of CsI is that of a body-centered cube. It is concluded from the density that half a "molecule" of CsI is situated at each point of the body-centered cubic lattice. This is consistent with having the Cs^+ ions occupy the corners of the unit-cube and the I^- ions occupy the body-centers, or *vice versa*. CsBr shows a simple cubic pattern, the strong lines of which form a body-centered cubic pattern. CsCl shows a similar sort of pattern except that the lines which are weak for CsBr are stronger, thus accentuating the simple cubic pattern. These facts may be accounted for by assuming for CsCl and CsBr the same structure which we have assumed for CsI. It should be noted that, if we are to follow the theory of space-groups rigorously, we must describe these structures as being simple cubic with a whole "molecule" (Cs^+ and halogen) associated with each point of the simple cube. We shall learn in Chap. VIII the methods of designating structures in accordance with the theory of space-groups. For our present purposes it is sufficient to describe the structure as a body-centered cube with Cs^+ at the corners and halogen ions at the body-centers.

The Structure of Diamond, Zinc Blende, and Fluorite.—Hull has obtained[1] a very complete powder-diffraction pattern of diamond using MoK_α rays and a photographic film mounted in a complete circle except for a small porthole through which the incident beam entered. The glass tube containing the crushed diamond was at the center of the circle. In this way he was able to photograph every one of the 25 lines which are theoretically possible within an angle of 172° on each side of the incident beam. There should be two more lines between 172° and 180°, but the fog from the incident beam made it impossible to see them clearly.

Hull's data are tabulated in Table IV. Along with his experimental data are given the interplanar distances calculated with the aid of Eq. (3) of Chap. III from Bragg's value for the edge of the unit-cube. Every experimental spacing is accounted for, and there are no theoretical spacings left unaccounted for. The chance of any structure, other than that of Fig. 6 of Chap. II, accounting completely for 25 consecutive interplanar spacings is so remote as to be negligible.

The powder pattern of zinc blende is that of a face-centered cube with strong lines such as to give a diamond cubic pattern if taken alone.

TABLE IV.—HULL'S DIFFRACTION DATA FOR DIAMOND

Miller indices	Number of cooperating planes	Spacing of planes in Ångstroms		Estimated intensity of line
		Experimental	Theoretical	
111	4	2.05	2.06	1.00
110	6	1.26	1.26	0.50
311	12	1.072	1.075	0.40
100	3	0.885	0.890	0.10
331	12	0.813	0.817	0.25
211	12	0.721	0.728	0.40
111 (3) 511	4 12	0.680	0.683	0.20
110 (2)	6	0.625	0.630	0.10
531	24	0.597	0.602	0.20
310	12	0.558	0.563	0.15
533	12	0.538	0.543	0.06
111 (4)	4	0.507	0.513	0.03
711 551	12 12	0.496	0.498	0.08
321	24	0.473	0.476	0.20
731 553	24 12	0.462	0.463	0.15
100 (2)	3	0.442	0.445	0.005
733	12	0.432	0.435	0.003
411 110 (3)	12 6	0.417	0.420	0.12
751 111 (5)	24 4	0.409	0.411	0.08
210	12	0.397	0.397	0.05
753 911	24 12	0.389	0.391	0.08
332	12	0.378	0.379	0.05
931	24	0.372	0.373	0.05
211 (2)	12	0.363	0.363	0.07
933 755 771 311 (3)	12 12 12 12	0.358	0.358	0.20

The dimensions of the face-centered and diamond cubes are identical. The density shows that a whole "molecule" of ZnS is associated with each point of the face-centered lattice, but that on the average only half a "molecule" is located at each point of the diamond lattice. These facts lead at once to the structure of Fig. 9 of Chap. V.

The diffraction pattern of fluorite is that of a diamond cube, and the intensities of the lines are practically the same as in the pattern of diamond. The density shows that, on the average, one Ca^{++} or two F^- ions must be associated with each "point" in the diamond lattice. By placing the two F^- ions as in Figs. 10 and 11 of Chap. V, the diffraction pattern, the density, and the ordinary crystallographic properties of fluorite are all satisfied.

The Structure of Quartz.—The low-temperature form of quartz offers an interesting example of the possibilities of the powder method. Its diffraction pattern is that of a simple triangular lattice. The side of the equilateral triangle is $a_0 = 4.903$Å. The height of the unit-prism is $c_0 = 5.393$Å., giving an axial ratio $C = 1.10$. Equation (3) of Chap. II gives the density as 0.89 instead of the actual density of 2.69. Evidently the crystal has three times as many SiO_2 molecules as it would have if there were only a single SiO_2 at each point of a simple triangular lattice. This means that the crystal must be composed of three interpenetrating simple triangular lattices. The symmetry of the crystal leads us at once to believe that the unit-triangle of each of the basal $(0\,0\cdot 1)$ planes may be derived from those of the plane below by a rotation of 120° together with a vertical shift of $C/3$ along the Z-axis. Since a rhombohedral lattice is composed of three simple triangular lattices equally spaced along the Z-axis, it is natural to guess that quartz might be rhombohedral; but a comparison of the actual diffraction pattern with that calculated for a rhombohedron of the same axial ratio shows that this guess is wrong. It is therefore necessary to assume that, although the quartz is made up of three interpenetrating lattices equally spaced along the Z-axis, yet these are differently situated with respect to each other along the X- and Y-axes than they would have been if the crystal were rhombohedral. The approximate locations of the Si and O on the X- and Y-axes have been determined by McKeehan.[17] His work illustrates the possibilities of the powder method so well that the results are given below in some detail.

It will be remembered from the discussion of the Laue method in Chap. IV that the resultant R of waves which have the same wave length but which differ in phase and amplitude is given by

$$R^2 = (X^2 + Y^2) \tag{2}$$

where R is the amplitude of the resultant wave and X and Y are two numbers which represent, respectively, the sum of the components, taken

90° apart, of the amplitudes of the constituent waves. Equation (16) of Chap. IV gave for X and Y, respectively:

$$\begin{aligned} X = \quad & \Sigma N_1 \cos 2\pi n(hx_1 + ky_1 + lz_1) \\ & + \Sigma N_2 \cos 2\pi n(hx_2 + ky_2 + lz_2) \\ & + \cdots\cdots\cdots\cdots\cdots \end{aligned}$$

and

$$\begin{aligned} Y = \quad & \Sigma N_1 \sin 2\pi n(hx_1 + ky_1 + lz_1) \\ & + \Sigma N_2 \sin 2\pi n(hx_2 + ky_2 + lz_2) \\ & + \cdots\cdots\cdots\cdots\cdots \end{aligned} \tag{3}$$

where N_1, N_2, etc., are the atomic or ionic numbers of atoms or ions in the crystal, n is the order of diffraction, h, k, and l are the Miller indices of the atomic plane, and $x_1y_1z_1$, $x_2y_2z_2$, *etc.*, are the coordinates of the various atoms in the plane $(h\,k\,l)$.

The intensity of a beam of homogeneous radiation is proportional to the square of the amplitude of the waves in that beam, *i.e.*,

$$I = K_1R^2 = K_1(X^2 + Y^2) \tag{4}$$

For a single crystal the factor of proportionality between the intensity of the x-ray beam and the square of the amplitude of the waves was shown in Chap. IV to be of the form

$$K_1 = \left(\frac{d_{hkl}}{n}\right)^g$$

where d_{hkl} is the interplanar distance and g is an exponent given by Wyckoff as 2.35. McKeehan uses Eq. (4), but, since he is dealing with powdered crystals, his value of K_1 is different from that just given above. The intensity of the diffracted beam of a finely powdered crystal falls off more rapidly with the angle than when a single crystal is used. This necessitates an increase in the exponent g. The intensity of the diffracted beam is proportional to the number f of families of cooperating planes in the crystal which can diffract at the given angle, so that it is necessary to introduce f as a factor. McKeehan therefore writes Eq. (4) in the form:

$$I = f\left(\frac{d_{hkl}}{n}\right)^3 (X^2 + Y^2) \tag{5}$$

The values of f and d depend upon the plane chosen for investigation, *i.e.*, upon the values of h, k, and l. It is assumed that the silicon and oxygen are present as ions in the crystal, thus giving Si^{++++} an ionic number $N_1 = 10$ and each O^{--} an ionic number $N_2 = 10$. This assumption is consistent with chemical theory and with calculations on the optical properties of quartz. Various values of $x_1y_1z_1$, $x_2y_2z_2$, etc., are systematically substituted in the X- and Y-terms and the relative inten-

sities of diffracted beams are calculated for various atomic planes in the crystal. McKeehan used the six planes having the largest interplanar spacings, d, in the crystal. The values of $x_1y_1z_1$, etc., which gave calculated intensities most nearly in agreement with results of experiment, were assumed to be the values of the true coordinates of the atoms. The value calculated for I from Eq. (5) is very sensitive to small changes in the values of $x_1y_1z_1$, etc., so that a change in the coordinates of 0.1Å. from the preferred values gives a calculated result of the wrong order of magnitude.

At first it might seem that an infinite number of choices was possible for the value of each coordinate, so that the chance of finding the right values would be negligibly small. It is at this point that the symmetrical characteristics of the crystal are again useful. These impose two limitations on the choice of coordinates:

1. In each molecule the two O^{--} centers are equidistant from the Si^{++++} center, so that the three ion-centers lie at the corners of an isosceles triangle.

2. Each Si^{++++} center is equidistant from the two O^{--} centers in adjacent molecules, the Si^{++++} centers of which belong to simple triangular lattices which are different from each other and from that of the Si^{++++} center under consideration.

The reasons for these two limitations will be more clear to the reader after a study of Chaps. VIII and IX.

It is a matter of experience that the distance of closest approach of atomic centers in crystals usually lies between 1.5 and 3.5Å. In the neighborhood of Si and O this range is between 1.5 and 2.5Å. This serves to reduce the number of choices of coordinates still further.

Bragg's values for the parameters of quartz are

$$a_0 = 4.89\text{Å}.$$
$$c_0 = 5.375\text{Å}.$$

In terms of these values for the unit-crystal, McKeehan finds that the following values of $x_1y_1z_1$, $x_2y_2z_2$, etc., give the best agreement with the results of experiment.

Coordinates of ion-centers, grouped by molecules:

$Si^{++++}(0, 0, 0)$
$O^{--}(0.325a, -0.016a, 0)$, $(-0.325a, -0.341a, 0)$
$Si^{++++}(0.603a, 0.206a, 0.333c)$
$O^{--}(0.619a, 0.547a, 0.333c)$, $(0.944a, 0.222a, 0.333c)$
$Si^{++++}(0.397a, 0.603a, 0.667c)$
$O^{--}(0.056a, 0.278a, 0.667c)$, $(0.381a, 0.928a, 0.667c)$

Angles at ion-centers between lines to adjacent ion-centers:

At Si^{++++} between lines to O^{--} of same molecule = 115° 14′
At Si^{++++} between lines to O^{--} of adjacent molecules = 111° 28′
At O^{--} between lines to Si^{++++} of same molecule and to Si^{++++} of adjacent molecules = 137° 50′

Distance between Si^{++++} and O^{--} centers of the same molecule = 1.631Å.; of adjacent molecules = 2.176Å.

These coordinates give three equally spaced horizontal layers of ions as described above. A plan of each of these three layers is shown in Fig. 23*a*, *b*, and *c*. Figure 24 shows these plans superimposed, thus giving a view of a quartz crystal looking down from the top.

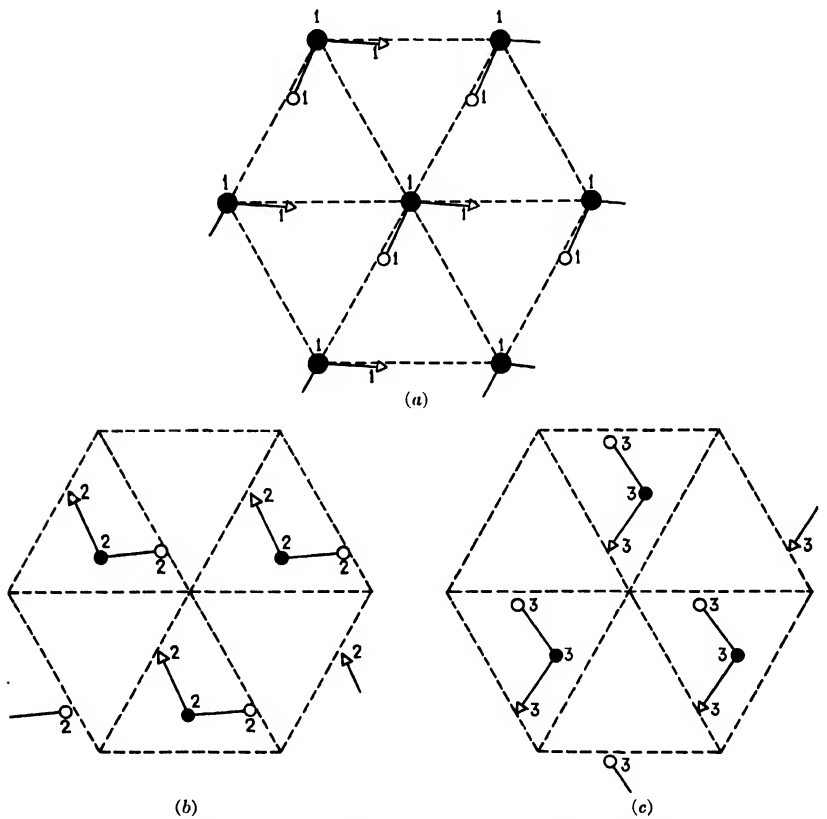

FIG. 23.—Plan views of successive (0 0 · 1) planes of McKeehan's quartz.

A second approximation to the correct atomic coordinates has been suggested by Gibbs[18] from a consideration of the diffracted beams from the (0 0 · 1) planes. Diffraction from these planes is very weak, and the first three orders of diffraction have about the same intensity. This is easiest accounted for by assuming each basal plane to be split up into three others: a plane of Si^{++++} sandwiched in between two planes of O^{--}. Gibbs spaces these planes so that the Z-axis of the unit-crystal is divided into approximately equal parts. The spacings differ from the value $C/3$ used by McKeehan only enough to give a weak third-order diffraction.

Such an arrangement of basal planes, if confirmed, would alter some of the interionic distances in McKeehan's model somewhat, because it would rotate each SiO_2 group slightly about an axis running in the plane containing Si^{++++} from the center of the Si^{++++} to the screw axis of symmetry* of the unit-structure. This would have the effect of lifting all the O^{--} marked with a circle in Fig. 23 and depressing the O^{--} marked with a triangle, or *vice versa.*

But in spite of such a change, the structure of quartz differs from the structure of all other compounds described up to this point. In all the crystals so far described the unit-particle has been a single ion. Such crystals have nothing which may properly be called a "chemical molecule." For instance each Na^+ in NaCl is equally spaced from six Cl^- and each Cl^- is equally spaced from six Na^+. A given Na^+ can hardly be said to "belong" to one of the six Cl^- more than to any of the other five. Such a crystal is an *ionic crystal,* for it is merely a systematic assembly of ions. In quartz each Si^{++++} has two O^{--} which are slightly closer to it at room temperature than to any other Si^{++++}, so that the molecule of SiO_2 has a real existence in the quartz crystal. Such a crystal is a *molecular crystal.* At elevated temperatures it is to be expected that this slight inequality in spacing will be overcome from instant to instant for individual ions because of their increased freedom of motion. This means that at elevated temperatures quartz should take on the properties of an ionic crystal and should become electrically conducting. It is a matter of ordinary laboratory experience that this is indeed the case.

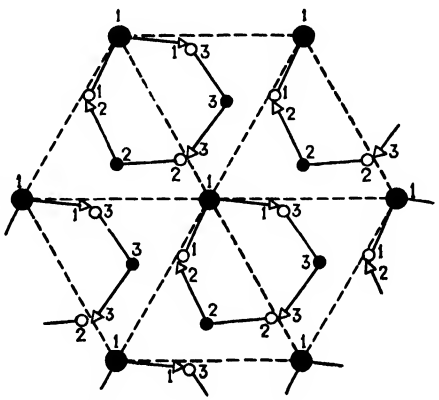

FIG. 24.—Superposition of Figs. 23*a*, *b*, and *c*.

The Structure of Arsenic.—The powder method is also well illustrated by Bradley's solution[19] of the structure of arsenic. The diffraction pattern is that of a rhombohedron whose axial ratio (in the hexagonal system) is $C = 2.81$. Such a rhombohedron may be easiest thought of as a face-centered cube which has been stretched along a body-diagonal. The crystal must contain two interpenetrating rhombohedra of this type in order to give the proper density.

The symmetry of the crystal demands that the Z-axes (hexagonal system) of the two rhombohedra lie in the same straight line. This means that, if we think of these rhombohedra as distorted cubes, then

* A screw axis of symmetry is defined completely in Chap. VIII.

the body-diagonal of one will lie in the same straight line as the body-diagonal of the other. Such a displacement is much like what we have in NaCl. So far we have considered the face-centered lattice of Cl^- to be displaced along the cube-edge of the Na^+ lattice until the corner of the Cl^- cube was halfway along the edge of the Na^+ cube. A glance at Fig. 7 of Chap. V shows that exactly the same result could have been obtained by displacing the Cl^- lattice along the body-diagonal of the Na^+ cube until the corner of the Cl^- cube was halfway along the body-diagonal of the Na^+ cube. Either kind of displacement leads to the generalized ionic coordinates (see Chap. II),

Na^+		
m,	n,	p
$m + \frac{1}{2}$,	$n + \frac{1}{2}$,	p
$m + \frac{1}{2}$,	n,	$p + \frac{1}{2}$
m,	$n + \frac{1}{2}$,	$p + \frac{1}{2}$
Cl^-		
$m + \frac{1}{2}$,	$n + \frac{1}{2}$,	$p + \frac{1}{2}$
$m + 1$,	$n + 1$,	$p + \frac{1}{2}$
$m + 1$,	$n + \frac{1}{2}$,	$p + 1$
$m + \frac{1}{2}$,	$n + 1$,	$p + 1$

where m, n, and p are any integers, including zero.* The two face-centered rhombohedra (distorted face-centered cubes) of arsenic must be related to each other in much the same way, except that the corner of one cannot lie exactly at the center of the body-diagonal of the other. If it did lie exactly at the center we would have a distorted simple cube, and the diffraction pattern would have to be different from what it actually is. If we use rhombohedral axes so as to correspond to the cubic axes of our NaCl analogy, the generalized atomic coordinates must be

m,	n,	p
$m + \frac{1}{2}$,	$n + \frac{1}{2}$,	p
$m + \frac{1}{2}$,	n,	$p + \frac{1}{2}$
m,	$n + \frac{1}{2}$,	$p + \frac{1}{2}$
$m + \frac{1}{2} + x$,	$n + \frac{1}{2} + x$,	$p + \frac{1}{2} + x$
$m + 1 + x$,	$n + 1 + x$,	$p + \frac{1}{2} + x$
$m + 1 + x$,	$n + \frac{1}{2} + x$,	$p + 1 + x$
$m + \frac{1}{2} + x$,	$n + 1 + x$,	$p + 1 + x$

The displacement of $\frac{1}{2} + x$ along each of the three axes is equivalent to a displacement along the body-diagonal to some point other than the center. By the use of the coordinate x, it is unnecessary to use the factor

* Since m, n, and p are integers, $m + 1$, $n + 1$, and $p + 1$ are also integers. Since m, n, and p are *any* integers, it follows that $m + 1$, $n + 1$, and $p + 1$ may be written as m, n, and p when making generalizations.

$1/m$ which was employed in Chap. V in our discussion of the Bragg method. Of course it is possible, if desired, to calculate the value of $1/m$ for any given family of planes from the value of x and the angles between the (rhombohedral) axes of the arsenic crystal.

Bradley used a slightly simpler, but less general, scheme for calculating the atomic coordinates of arsenic than was used by McKeehan for quartz. McKeehan used Eqs. (3) and (5), which give the resultant of two or more waves which differ from each other in both amplitude and phase. These equations resolve each of the waves along the X- and Y-axes and add up the components along each axis, thus giving two vectors at right angles to each other, which are, in general, of different magnitude. The square of the resultant of these two vectors is expressed in the usual way by Eq. (5) as the sum of the squares of the two vectors. Assuming that all the atoms of arsenic are alike and therefore have equal diffracting power, Bradley had to deal with only two wave trains of equal amplitude A in each beam of the diffraction pattern. Let ψ be the phase angle between these two wave trains (Fig. 25). The resultant R is evidently

$$2A \cos \frac{\psi}{2} = 2A\sqrt{\frac{1}{2}(1 + \cos \psi)}$$

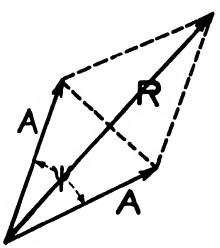

FIG. 25.—Resultant of two vectors equal in magnitude but different in phase.

Since the intensity I of the wave is proportional to the square of the amplitude, we may use K_2 as a factor of proportionality and write

$$I = K_2R^2 = K_2(2A^2)(1 + \cos \psi)$$
$$I = K_2A^2(2 + 2 \cos \psi) \qquad (6)$$

An empirical expression for the factor of proportionality has already been given in the discussion of McKeehan's structure of quartz, namely,

$$K_1 = f\left(\frac{d_{hkl}}{n}\right)^q$$

This may be turned into the form used by Bradley. Bragg's law may be written:

$$\frac{2d_{hkl}}{n\lambda} = \frac{1}{\sin \theta}$$

If λ is kept constant, this becomes

$$k\frac{d_{hkl}}{n} = \frac{1}{\sin \theta}$$

If we choose our units of intensity so that k is unity, then

$$\left(\frac{d_{hkl}}{n}\right)^q = \left(\frac{1}{\sin \theta}\right)^q$$

Following Bragg, Bradley uses $g = 2$, so that he has

$$K_2 = \frac{f}{\sin^2 \theta}$$

where θ is the angle of grazing incidence as in Bragg's law.

The value of ψ of Eq. (6) is found in terms of the atomic coordinates in the following way: For the sake of simplicity we shall assume, at first, a cubic structure instead of the rhombohedral structure of arsenic. We shall continue to use the symbol d_{hkl} to represent the interplanar spacings as calculated for the $(h\,k\,l)$ family by the methods of Chap. III and shall use the symbol d' to represent the distance between adjacent planes of this same $(h\,k\,l)$ family. In the case of Fig. 18 of Chap. IV, d_{hkl} would represent the spacings ab or AB, and d' would represent the spacings aA or bB. By Eq. (3) of Chap. III,

$$d' = \frac{(hx_1 + ky_1 + lz_1 - 1) - (hx_2 + ky_2 + lz_2 - 1)}{\sqrt{h^2 + k^2 + l^2}}$$

In terms of the generalized atomic coordinates of arsenic this distance is

$$d' = \frac{h(x + \tfrac{1}{2}) + k(x + \tfrac{1}{2}) + l(x + \tfrac{1}{2})}{\sqrt{h^2 + k^2 + l^2}} \tag{7}$$

Since

$$d_{hkl} = \frac{s}{\sqrt{h^2 + k^2 + l^2}}$$

Eq. (7) becomes

$$d' = \frac{(x + \tfrac{1}{2})(h + k + l)d_{hkl}}{s} \tag{8}$$

where s is the periodicity of the $(h\,k\,l)$ planes (see Chap. III).

Obviously all expressions which are characteristic of the 90° angles of a cubic structure have disappeared and Eq. (8) will hold for a rhombohedron.

When

$$2d_{hkl} \sin \theta$$

is an exact multiple of the wave length used in the experiment, complete "constructive interference" occurs [see discussion of Eq. (15) in Chap. IV]. This corresponds to an angular distance of $2\pi n$. Then

$$\frac{2d' \sin \theta}{2d_{hkl} \sin \theta} = \frac{\psi}{2\pi n} = \frac{(x + \tfrac{1}{2})(h + k + l)d_{hkl}(2 \sin \theta)}{sd_{hkl}(2 \sin \theta)} \tag{9}$$

Therefore the phase difference between x-ray waves diffracted from corresponding planes in the two face-centered lattices of arsenic will be

$$\psi = \frac{2\pi n}{s}\left(x + \frac{1}{2}\right)(h + k + l)$$

If we follow the usual convention of incorporating the order of diffraction n with the indices so that the nth-order diffraction from (hkl) is considered as a first-order beam from a fictitious plane $(nh\,nk\,nl)$, we have

$$\psi = \frac{2\pi}{s}\left(x + \frac{1}{2}\right)(nh + nk + nl) \tag{10}$$

Substituting for ψ and K_2 in Eq. (6), we have

$$I = \frac{f\Lambda^2}{\sin^2\theta}\left[2 + 2\cos\left\{\frac{2\pi}{s}\left(x + \frac{1}{2}\right)(nh + nk + nl)\right\}\right] \tag{11}$$

It is now necessary to solve Eq. (11) for the various beams diffracted from the crystal using successive values for x, remembering that x must always be a positive fraction. For each value assumed for x there must be made a tabulation of the calculated *order of intensities* of the various lines in the diffraction pattern. This is done by numbering the lines in the order of their calculated intensities, calling the most intense line 1, the second most intense line 2, etc. In a parallel column is listed the experimental order of intensities, and in still another column is listed the "error," *i.e.*, the difference between the calculated and the experimental orders of the intensities. For any assumed value of x the sum of all the errors, irrespective of sign, is taken as a measure of the incorrectness of the assumed value of x. Such a tabulation for one value of x ($x = 0.0488$) is shown in Table V. The use of *order of intensity* instead of *absolute intensity* avoids many pitfalls connected with some of the assumptions on which the calculations are based, for, although certain changes in these assumptions may result in great changes in the calculated intensities, they rarely affect seriously the order of these intensities. (In this connection see Chap. X.)

Bradley saved a great deal of labor in the calculation of x by first getting approximate values which served to show the limits within which his calculations could be made profitably. The line $(\bar{3}\,1\,1)$ entirely disappears in the first order. The factor $(nh + nk + nl)$ in Eq. (11) becomes -1. Since s is unity the only way to make I negligibly small is to make the term

$$2\cos\{2\pi(x + \tfrac{1}{2})(-1)\}$$

have a value approximately equal to -2. This, in turn, requires us to make x very small. The line $(2\,0\,0)$ is by far the brightest on the photographic film. If x were 0.25, Eq. (11) would contain the term

$$2\cos\{2\pi(0.75)(2)\} = 2\cos\{3\pi\} = -2$$

so that the calculated intensity of the diffracted beam would be zero. It is evident, then, that x must be much less than 0.25, if we are to account for the high intensity of this line. The line $(2\,2\,0)$ is the third strongest

in the diffraction pattern. It would disappear for $x = 0.125$ or 0.375, so that x must be considerably less than 0.125. Lines (4 4 2) and (4 4 4)

TABLE V.—BRADLEY'S DIFFRACTION DATA FOR ARSENIC

	I	II	III	IV	V	VI
	d/n (observed) $\times 10^{-8}$ cm.	d/n (calculated)* $\times 10^{-8}$ cm.	hkl (trigonal axes)	Order of intensity observed	Order of intensity calculated	Error
1	3.555	3.525	1 1 1	19	19	..
2	3.18	3.118	1 $\bar{1}$ 1	25	24	1
3	2.780	2.777	2 0 0	1	1	..
4	2.054	2.054	2 2 0	3	3	..
5	1.891	1.886	2 $\bar{2}$ 0	2	2	..
6	1.781	1.790	3 1 1	4	9	5
7	1.764	1.764	2 2 2			
8	1.662	1.662	3 $\bar{1}$ 1	12	15	3
		1.614	$\bar{3}$ 1 1	..	26	..
9	1.562	1.559	2 $\bar{2}$ 2	8	7	1
10	1.387	1.388	4 0 0	5	4	1
11	1.368	1.368	3 3 1			
12	1.286	1.291	3 3 $\bar{1}$	7	8	1
		1.287	4 2 0			
13	1.223	1.227	4 2 2	23	23	..
		1.226	3 $\bar{3}$ 1			
14	1.201	1.201	4 $\bar{2}$ 0	6	5	1
15	1.182	1.177	3 3 3	21	21	..
16	1.119	1.119	4 $\bar{2}$ 2	9	6	3
17	1.107	1.109	5 1 1			
18	1.089	1.088	$\bar{4}$ 2 2	14	14	..
19	1.068	1.066	5 $\bar{1}$ 1	15	15	..
20	1.041	1.039	3 $\bar{3}$ 3	20	22	2
		1.038	$\bar{5}$ 1 1			
21	1.023	1.027	4 4 0	24	25	1
		1.005	4 4 2	..	28	..
22	0.998	0.997	5 3 1	10	10	..
23	0.955	0.955	5 3 $\bar{1}$	16	13	3
24	0.942	0.943	4 4 0	18	18	..
25	0.929	0.9265	6 0 0	11	11	..
		0.9265	4 4 $\bar{2}$			
26	0.922	0.9215	5 3 3			
27	0.908	0.910	5 $\bar{3}$ 1	22	20	2
		0.902	6 2 0			
		0.902	$\bar{5}$ 3 1			
28	0.891	0.895	6 2 2	13	12	1
		0.892	4 $\bar{4}$ 2			
		0.882	4 4 4	..	27	..
29	0.854	0.856	6 $\bar{2}$ 0	17	17	..
				Total error.....		25

* These interplanar spacings are calculated with the aid of Eq. (23) of Chap. III, using for C the value of 2.81 obtained from the charts and for $a_0/2$ the most probable value (2.799Å.) calculated from the data of column 1.

are absent. The smallest values of x giving zero intensities in Eq. (11) are $x = 0.05$ and $x = 0.15$ for (4 4 2) and $x = 0.0417$ and $x = 0.125$ for

(4 4 4). A value in the neighborhood of $x = 0.04$ or 0.05 will obviously fit in with all these facts. Bradley actually calculated from $x = 0.025$ to $x = 0.075$.

When the calculations have been made and tabulated, a plot is made, as in Fig. 26, which shows the value of x for which the total error is a minimum. The error can never be zero, partly because of the difficulties in measuring the observed intensities accurately. The value of x used in Table V is the one for the minimum of the plot. It is strongly advised that the reader repeat the calculations necessary for Fig. 26, in order that he may obtain a really workable knowledge of the powder method.

It was brought out in Chap. II that many lattices might be considered to belong to one of two or more crystal structures, depending only upon the point of view. Arsenic is an excellent example of this. We have already considered it as being made up of two slightly distorted face-centered cubes, *i.e.*, as two interpenetrating face-centered rhombohedra with rhombohedral (distorted cubic) axes of reference. One of these face-centered rhombohedra is shown in Fig. 27*a*. The two together are shown in Fig. 27*b*. The edge AB of the unit face-centered rhombohedron is $a_1 = 5.598$Å. and $x = 0.0488a_1$. The angle between any two of the axes is $\alpha = 84° 36'$. Such a structure may also be referred to a second set of rhombohedral axes which lie along the face-diagonals of the rhombohedra described above. Since α is less than 90°, the longer of the face-diagonals must be used. The edges of the new rhombohedra lie along these new axes and have a length equal to half the face-diagonals of the old rhombohedra. The long body-diagonals of the new rhombohedra are identical with the long body-diagonals of the corresponding old rhombohedra. From this point of view, arsenic is built up of two interpenetrating simple rhombohedra. One of these is shown in Fig. 28*a*. A portion of the other is shown in Fig. 28*b*. The side AG is $a_2 = 4.145$ and x becomes $0.054a_2$. A structure similar to arsenic has been described in the literature as being made up of two interpenetrating fragmentary simple rhombohedra whose axes are identical with those of the face-centered rhombohedra described above. The edges are parallel to the edges of the face-centered rhombohedra but are only half as long. Each of these fragmentary simple rhombohedra has half its corners missing so that if x had been zero the combined structure would have been a complete simple rhombohedron. From this viewpoint arsenic is built up of

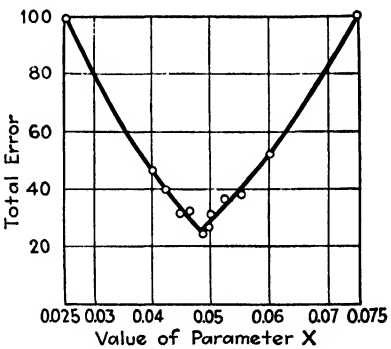

FIG. 26.—Graphical method of determining x for arsenic.

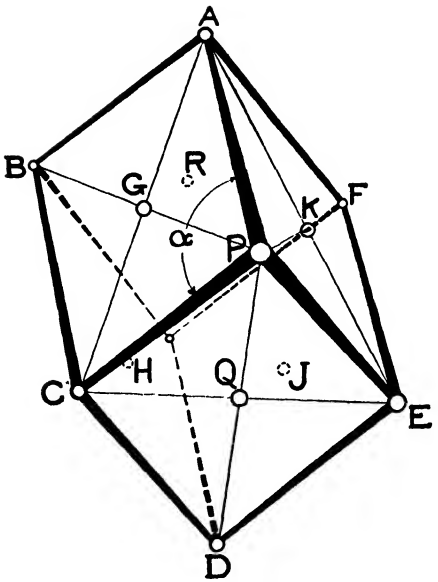

(*a*)

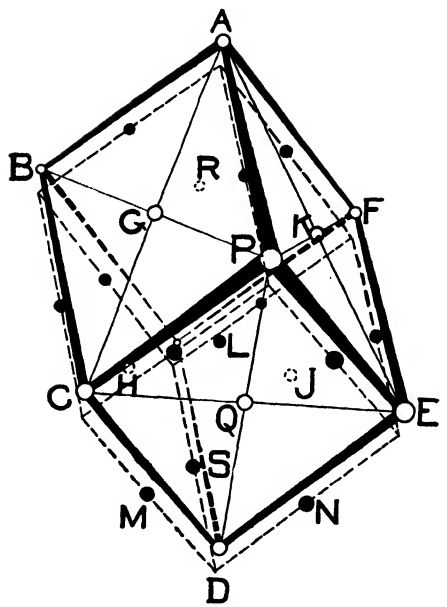

(*b*)

FIG. 27.—(*a*) Structure of arsenic. One of the two face-centered rhombohedra. (*b*) Structure of arsenic. Both of the face-centered rhombohedra.

two interpenetrating fragmentary simple rhombohedra of side $a_3 = 2.80$Å. and $x = 0.097a_3$. If now the origin of coordinates of the original face-centered rhombohedron of arsenic is shifted to any one of the three adjacent corners of the unit-structure, the crystal appears as a special case of the triclinic system (see Chap. II), in which all three axes are of equal length and two of the three axes make equal angles with each other. Two of these three structures turn out to be duplicates, so that for every rhombohedral structure so far described for arsenic we have two possible face-centered triclinic lattices. Lastly, any rhombohedron may be thought of as being built up of three interpenetrating simple triangular lattices, and thus it may be considered to belong to the triangular (hexagonal) system. The diffraction pattern of arsenic is an exact match with the theoretical pattern for a rhombohedron such that

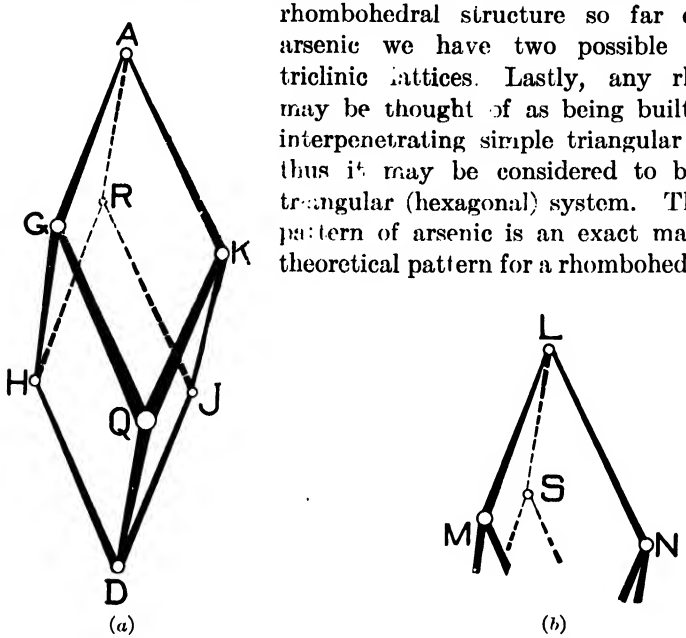

(*a*) (*b*)

FIG. 28.—(*a*) Structure of arsenic. One of the simple rhombohedra. (*b*) Structure of arsenic. A portion of the second rhombohedron.

the side of the unit-triangle is 3.75Å. and the axial ratio is 2.81. This axial ratio is somewhat larger than that for a face-centered cube (considered as a rhombohedron, a face-centered cube has an axial ratio of 2.45), so that the rhombohedron is built upon a face-centered cubic lattice which has been stretched along its body-diagonal. This therefore agrees with the first interpretation given of the structure of arsenic. The density shows that arsenic is composed of two interpenetrating face-centered rhombohedra. If the simple rhombohedra of Fig. 28 are considered from the point of view of the triangular (hexagonal) system, they lead to the same size of unit-triangle and the same axial ratio as are given above.

Altogether we have seen how the structure of arsenic can be expressed, without undue complication, in any one of seven different ways. Such an embarrassing freedom of choice in the description of a crystal structure sometimes makes it a little hard to correlate the various statements in

the literature. This is one of the reasons why models of crystal structure, built to scale, are indispensable to workers in this subject.

PRECISION MEASUREMENTS OF CRYSTAL PARAMETERS

We have seen how, by means of x-ray diffraction, it is possible to determine the arrangement of atoms and of ions in crystals. If this were the whole object of our study, there would be little incentive to make precision measurements of the dimensions of unit-crystals. It will appear, however, in later chapters that the study of crystal structure is usually undertaken as a tool for the investigation of phenomena in other branches of science—it is a means to an end. The attainment of that end often necessitates a measurement of the dimensions of a unit-crystal to within 1 part in 1,000, *i.e.*, $\frac{1}{10}$ per cent. It will therefore be necessary to take up in detail the methods to be employed and the sources of error to be avoided in making such measurements.

The diffraction pattern is usually recorded on a photographic film bent into the arc of a circle whose center is the specimen of powdered crystal (see Fig. 1). The grazing angle of diffraction θ of Bragg's law, may then be determined for any line in the diffraction pattern directly in terms of the distance L from that line to the shadow of the specimen on the zero line (photographic record of the undeviated beam), for

$$2\theta = \frac{L}{R} \text{ radians} = \frac{360L}{2\pi R} \text{ deg.}$$

where R is the radius of curvature of the film. Bragg's law then becomes

$$d = \frac{n\lambda}{2} \cdot \frac{1}{\sin \frac{360}{4\pi} \cdot \frac{L}{R}} = \frac{n\lambda}{2 \sin \frac{28.65L}{R}} \tag{12}$$

The value of λ is fixed by the material used as a target in the x-ray tube.* Because diffraction of the second, third, . . . , nth order may always be considered as a first-order diffraction from fictitious planes having an interplanar spacing of $\frac{1}{2}$, $\frac{1}{3}$, . . . , $1/n$ of the actual spacing, n is taken as unity. Our discussion of precision measurements of d or of the edge a of the unit of structure in the crystal must necessarily, therefore, center about the measurements of L and R. If a flat plate is substituted for the curved film, the value of θ, and therefore of d, may be measured in terms of L' (analogous to L) and the perpendicular distance R' from the specimen to the sensitive surface of the photographic plate. In such a case the discussion of L and R which follows may be readily altered to make it apply to L' and R'.

* Tables of characteristic wave lengths are given by Wm. Duane, *Nat. Research Council Bull.* 6 (1920); M. de Broglie, "Les rayons X," 1922; M. Siegbahn, "Spektroskopie der Röntgenstrahlen," 1924.

It is customary, when examining a diffraction pattern, to hold the film so that the zero line (photographic record of the undeviated beam) is on the left, and most apparatus used in examining diffraction patterns is designed in accordance with that custom. It will therefore be assumed, for the sake of simplicity, that this custom is followed by the reader. It was explained earlier in this chapter that, if the source of x-rays were a geometrical point and if the slit system were merely a series of infinitesimal pinholes, the lines of the diffraction pattern would be arcs of circles whose common center would be the spot caused by the zero beam. Since the source of x-rays is actually a spot of finite size, its projection is a line whose length is several times its width. The slits are usually rectangular in outline. Each line of the diffraction pattern therefore represents the envelope of an infinite number of circles, all of the same radius and all tangent to the same straight line at successive points along its length. The shape of the lines is therefore roughly that of some portion of the cross-section of a plano-concave lens. Over an arc of 90°, the straight edge is on the side away from the zero line. This effect is most noticeable at the left-hand end of the pattern where the radius of the component circles is least. This is plainly brought out in Fig. 21.

When the specimen is in the form of a thin sheet, (for instance, when studying the structure of the edge of a safety-razor blade), the zero line is cut off sharply by a well-defined shadow from the specimen. In conformity with Fig. 6 it will be assumed that it is the left-hand half of the zero beam that is cut off, and that the photographic film is mounted so as to record the diffraction pattern to the right of the zero line. Then, if the edge of the specimen is at the center of the arc on which the film is bent, there is little chance for error in the measurement of R. L is then taken as the distance from the edge of the shadow of the specimen to the straight edge of the line in the diffraction pattern. It is difficult to determine accurately the position of this edge for such lines as do not show complete resolution of the α_1 and α_2 wave lengths of the K doublet. For all other lines in the diffraction pattern this value of L is free from objection, (*a*) if there is no widening of the line caused by halation of the film, (*b*) if the crystals are not so small that Bragg's law starts to break down to the ordinary diffraction equation for light thus broadening the line, and (*c*) if there is neither stretching nor shrinking of the film.

When the specimen is mounted in a tube whose center is the center of curvature of the film, as shown in Fig. 1, the measurement of R and L is not so simple. Let us first assume that the specimen is infinitely transparent to the x-rays. Then, R would be measured from the center of the specimen tube. Such a specimen could not throw a shadow on the zero line, but the measurement of L would have to be made from the center of the narrowest portion of the given line in the diffraction pattern to the center of where the shadow would have been in the zero line if the

specimen had not been infinitely transparent. If, instead, we assume that the specimen is infinitely opaque to the x-rays, the diffracted beams would all come from the right- and left-hand surfaces (Fig. 1). This would give the effect of two separate specimens, one on each side of the center of curvature of the film. Because of the opacity of the specimen the left-hand edge would give no diffraction pattern on the film to the right of the specimen, and the right-hand edge would be the source of the only diffraction pattern recorded on the film. Equation (12) does not hold rigorously for such a condition but gives too large values of L and therefore too small values of d. It would have to be modified to account for the eccentricity of the edge of the specimen. All actual specimens fall between these two extremes and act as though they were made up of two specimens each of which has its own equivalent center of diffraction. The more transparent the substance is to the x-rays, the closer these two equivalent centers will approach the actual center of the specimen. It might be supposed that the difficulty could be avoided by using a photographic film only on the right-hand side of the zero beam and placing the edge of the specimen at the center of curvature of the film. All measurements of L would then have to be made from the right-hand edge of the shadow to the right-hand edges of the lines in the diffraction pattern. Experimentally it is hard to place the specimen with sufficient accuracy, and the shadow cast by specimens of low atomic number is often too faint to give a sharp outline.

Both of these objections may be obviated by using a calibrating substance, so that its diffraction pattern serves as a comparison standard for the pattern under investigation. There are two ways in which the calibrating substance may be mounted: (1) It may be mixed directly with the substance to be investigated,[20,21] so that the equivalent centers of diffraction of the two coincide. Such a procedure is possible only in those cases where there is no chemical action between the two substances and no tendency for one to form a solid solution with the other during the process of mixing the two powders. (2) The calibrating substance may be put in one end of the specimen tube and the substance to be investigated at the other end.[22,23] In this case the film-holder must be provided with a septum as illustrated in Fig. 1, in order to separate the two diffraction patterns. Both substances must be diluted with an amorphous material until they have approximately the same efficiency of diffraction. Empirically it is found that, when this condition is fulfilled, the equivalent centers of diffraction of the two substances practically coincide. In the absence of more complete knowledge the use of the table of dilutions as given in Table I is recommended. That this gives results which may be depended upon in ordinary practice to 0.1 per cent is shown by the following:[24] A specimen tube of very fine bore (about 0.3 mm. diameter) was loaded at one end with NaCl which had been

mixed with an equal volume of flour. The other end was loaded with W powder (99.999 per cent pure) which had been passed through a 200-mesh sieve and which had been mixed with 10 times its own volume of flour as recommended in Table I. The diffraction pattern gave the lattice parameter $a = 3.155 \pm 0.001$Å. A second tube of somewhat greater bore (about 0.6 mm. diameter) was loaded with a mixture of 1 volume of the same lot of W and 10 volumes of NaCl. The diffraction pattern gave a lattice parameter $a = 3.157 \pm 0.003$Å. The first value gives a density 19.32. The second gives a density 19.28. The best determination of the density of W by ordinary methods[25] is 19.3. The lattice parameter of pure gold (99.99 per cent) has been determined[13] in terms of NaCl as $a = 4.065$Å., and the density agrees within the experimental error with that for pure gold. Using this gold as a comparison standard, the lattice parameter of W is 3.155Å. The results are shown graphically in Fig. 29, which will be referred to in greater detail later. The agreement between the final results for the two methods of using NaCl is striking. The high atomic number of W would lead one to expect that its equivalent diffracting center in the specimen tube would be much closer to the surface than that of NaCl. This would unquestionably have been so if the W had been uniformly dispersed throughout the tube. The favorable results shown above are caused by the fact that, instead of being coated on to each particle of flour, the W was scattered through the flour in the form of a powder so that the x-rays found relatively free paths by which to enter and emerge from it. It is doubtful if such good agreement could have been found if the specimen tube had exceeded 0.7 or 0.8 mm. in diameter, for larger tube diameters tend to be incompatible with the existence of free paths for the x-ray beam. It is mainly for this reason that, in the discussion of the technique of preparing the specimen, it was recommended that the diameter of the specimen tube should not exceed 0.6 mm.

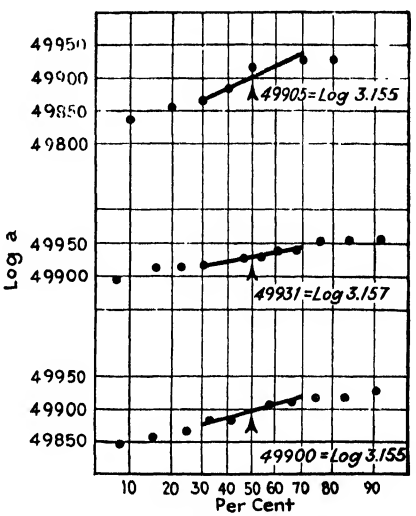

FIG. 29.—Probability curves of the lattice parameter of tungsten: Top Graph; W plus 10 flour. Calibration made in terms of NaCl plus 1 flour at other end of specimen tube. Middle graph; W plus 10 NaCl. Calibration made in terms of NaCl mixed with W in the specimen tube. Bottom Graph; W plus 10 flour. Calibration made in terms of Au plus 10 flour at other end of specimen tube.

The use of a calibrating substance avoids any accurate measurement of R. In making measurements of L, whatever procedure is adopted for

one of the diffraction patterns must be employed for the other. For instance, the measurements may be made from the right-hand edge of the shadow of the specimen to the right-hand edges of the lines in the pattern. This presupposes that there is no widening of the lines caused by very small particle size, halation of the film, etc., and that the α_1 and α_2 lines are completely resolved. If these conditions have been fulfilled, the

TABLE VI.—THEORETICAL VALUES OF INTERPLANAR SPACINGS FOR NaCl CONSIDERED AS A SIMPLE CUBE (a = 2.814Å.)

$h^2 + k^2 + l^2$	Plane	Theoretical simple cubic spacings for NaCl (a = 2.814Å.)
1	100	2.814
2	110	1.990
3	111	1.625
4	100 (2)	1.407
5	210	1.259
6	211	1.149
8	110 (2)	0.995
9	100 (3) 221	0.938
10	310	0.890
11	311	0.848
12	111 (2)	0.812
13	320	0.781
14	321	0.752
16	100 (4)	0.703
17	410 322	0.682
18	110 (3) 411	0.663
19	331	0.646
20	210 (2)	0.629
21	421	0.614
22	332	0.599

reading at the right-hand edge represents the position of the lines from an infinitely narrow specimen whose zero-line shadow falls on the right-hand edge of the actual shadow. It is usually much easier, especially if the lines are faint, to measure L from the center of the shadow on the zero line to the center of the lines of the diffraction pattern. The previous discussion of the shape of these lines makes it plain that the center of the line should be taken at its narrowest width. For instance, in Fig. 5, the lines of the upper pattern should be measured close to the top. The lines of the lower pattern should be measured at the middle of their length.

The calibrating substance is usually NaCl. It is the secondary standard for crystal-lattice measurements, and it is easily obtainable in a high state of purity. Its diffraction pattern is fairly well spread out over the film, so that all parts, especially those corresponding to the larger interplanar spacings, are easily calibrated. The theoretical interplanar spacings of NaCl in terms of $a = 2.814$Å. (*i.e.*, in terms of the simple

TABLE VII.—THEORETICAL VALUES OF INTERPLANAR SPACINGS FOR CdO, CONSIDERED AS A FACE-CENTERED CUBE ($a = 4.681$Å.)

$h^2 + k^2 + l^2$	Plane	Theoretical spacing
3	1 1 1	2.704
4	1 0 0 (1)(2)	2.340
8	1 1 0 (1)(2)	1 655
11	3 1 1	1.411
12	1 1 1 (2)	1.352
16	1 0 0 (2)(4)	1.170
19	3 3 1	1.074
20	2 1 0 (1)(2)	1.074
24	2 2 1 (1)(2)	0.955
27	{5 1 1 / 1 1 1 (3)}	0.901
32	1 1 0 (2)(4)	0.827
35	5 3 1	0.791
36	{1 0 0 (3)(6) / 2 2 1 (1)(2)}	0.780
40	3 1 0 (1)(2)	0.740
43	5 3 3	0.714
44	3 1 1 (2)(4)	0.706
48	1 1 1 (4)	0.676
51	{7 1 1 / 5 5 1}	0.655
52	3 2 0 (1)(2)	0.649
56	3 2 1 (1)(2)	0.626
59	{5 5 3 / 7 3 1}	0.609
64	1 0 0 (4)(8)	0.585
67	7 3 3	0.572

cubic pattern of strong lines) are given for reference in Table VI. The use of CdO as a calibrating material has been suggested by Brentano and Adamson[26] and by Fuller.[27] The advantage of CdO lies chiefly in the fact that the lines have larger intensities at large diffracting angles than do the lines of NaCl. This facilitates the calibration of films of low intensity. The interplanar spacings for CdO are given in Table VII.

The chance of not having the equivalent center of diffraction of the calibration standard coincide with that of the substance under investigation is lessened if the two materials themselves have about the same

opacity to the x-rays. Patterson[28] has proposed "conductivity copper" as a new secondary standard for use with substances like Cr, Fe, and Ni. Such copper is easily obtained and seems to be uniform from sample to sample. In terms of NaCl = 2.814Å., the lattice parameter of Cu[23] is 3.605 ± 0.002Å. In terms of W = 3.155Å., it is 3.600 ± 0.003 where ± refers to the combined uncertainty of the values for W and Cu. For substances of high atomic number, the W from a Mazda lamp filament might be used as a calibration standard, as it is of high and uniform purity and may be easily obtained. Of the values for its lattice parameter given above, the first, $a = 3.155 \pm 0.001$Å., is to be preferred because of the high degree of reproducibility in the readings on the diffraction pattern from which the measurements were made. The uncertainty of measurements made with derived standards like Cu or W is the sum of the uncertainty of the value for the derived standard plus the uncertainty of measurement of the substance under investigation. Therefore, if derived standards are to be used, it is important that their lattice parameters be established within narrow limits so that the precision of the final results, expressed in terms of NaCl, may not suffer too seriously.

TABLE VIII.—DATA FROM FILM 805 FOR DETERMINING THE LATTICE PARAMETER OF PURE W

NaCl			W				
Experimental	Theoretical	Correction	Plane	Intensity	Experimental	Corrected	log a
2.82Å.	2.814Å.	.....	110	*S*	2.23Å.	.....	.....
1.995	1.990	−0.005	100	*W*	1.579	1.577Å.	49 886
1.627	1.625	−0.002	211	*M*	1.290	1.289	49 932
1.409	1.407	−0.002	110 (2)	*W*	1.117	1.116	49 920
1.260	1.259	−0.001	310	*M*	0.998	0.997	49 870
1.150	1.149	−0.001	111	*F*	0.912	0.912	49 958
0.996	0.995	−0.001	321	*W*	0.842	0.842	49 837
0.938	0.938	0.000	100 (2)	*VF*	0.788	0.788	49 859
0.890	0.890	0.000	{411	*W*	0.744	0.744	49 920
0.848	0.848	0.000	110 (3)}				
.....	0.812	0.000	210	*F*	0.706	0.706	49 931
0.780	0.780	0.000					

So far we have discussed the measurement of the distances, L, from the zero line to various lines in the diffraction pattern. After the various readings of L for the calibrating pattern have been taken, they must be translated into measurements of interplanar spacings by Eq. (12). A calibration curve is drawn showing the corrections which must be applied to change these values into the theoretically correct values. This correction curve is then applied directly to the interplanar spacings

calculated from the diffraction pattern of the substance under investigation. This procedure may be illustrated by giving the data[23] from our film 805 for the lattice parameter of pure W. The calibration material was NaCl. The interplanar distances of NaCl, as determined from the pattern, are listed in the first column of Table VIII. The corresponding theoretical distances are listed in the second column. The third column gives the correction which must be added to each experimental value to change it to the correct value. Figure 30 shows these corrections plotted against interplanar distances so that interpolations may be made easily. The large experimental error in reading diffraction patterns too near the zero line makes it useless to attempt to correct readings for interplanar spacings of more than 2.00Å. when MoK_α rays are used. The experimental values of W, given in column 6 of Table VIII, are corrected by means of Fig. 30 thus giving the readings of column 7. Each of these

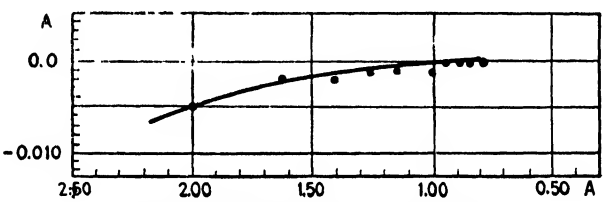

FIG. 30.—Correction curve for film 805.

corrected readings is then multiplied by the reciprocal of the appropriate structure constant from Table II of Chap. III, so that each reading smaller than 2.00Å. is made to give a value for the edge a of the unit-cube. This is easiest done by the use of five-place logarithms. The last column of Table VIII gives the values of log a so obtained. For convenience of reference, Table IX gives the cologarithms of the structure constants for the common types of cubic crystals.

It remains to find from all of these values the true value of the edge of the unit-cube. This is usually done graphically. The operation is carried out in terms of the logarithms such as are listed in Table VIII, partly as a matter of convenience and partly as an aid to the investigator in drawing his graph without prejudice for any particular final answer. The various logarithms from Table VIII are first arranged in ascending numerical order as shown in Table X. If there are p logarithms, the mth one is interpreted as showing that $\frac{100\,m}{p+1}$ per cent of the values are equal to, or smaller than, that logarithm. If the logarithms are then plotted against their corresponding percentages the result is an approximation to the integral of a probability curve, and the larger p is the closer the approximation will be. This may be illustrated in terms of life-insurance statistics. Suppose we choose a large group of men all of the same age, and suppose we plot, year by year, the number who die during the year

TABLE IX.—COLOGARITHMS OF THE STRUCTURE CONSTANTS FOR THE COMMON TYPES OF CUBES

Planes	$h^2 + k^2 + l^2$ for simple cube	$\log \sqrt{h^2 + k^2 + l^2}$			
		Simple cube	Body-centered cube	Face-centered cube	Diamond cube
100	1	0.00000	.....	.....	.....
110	2	0.15051	0.15051	.....	.....
111	3	0.23856	.....	0.23856	0.23856
100	4	0.30103	0.30103	0.30103	.....
210	5	0.34948	.....	.....	.....
211	6	0.38907	0.38907	.....	.....
110	8	0.45154	0.45154	0.45154	0.45154
221 100	9	0.47712	.....	.....	.....
310	10	0.50000	0.50000	.....	.....
311	11	0.52069	.....	0.52069	0.52069
111	12	0.53959	0.53959	0.53959	.....
320	13	0.55697	.....	.....	.....
321	14	0.57306	0.57306	.....	.....
100	16	0.60206	0.60206	0.60206	0.60206
410 322	17	0.61523	.....	.....	.....
411 110	18	0.62763	0.62763	.....	.....
331	19	0.63937	.....	0.63937	0.63937
210	20	0.65051	0.65051	0.65051	.....
421	21	0.66111	.....	.....	.....
332	22	0.67121	0.67121	.....	.....
211	24	0.69010	0.69010	0.69010	0.69010
430 100	25	0.69897	.....	.....	.....
431 510	26	0.70748	0.70748	.....	.....
511 111	27	0.71568	.....	0.71568	0.71568
520 432	29	0.73120	.....	.....	.....
521	30	0.73856	0.73856	.....	.....
110	32	0.75257	0.75257	0.75257	0.75257
441 522	33	0.75925	.....	.....	.....
530 433	34	0.76574	0.76574	.....	.....
531	35	0.77203	.....	0.77203	0.77203
100 221	36	0.77815	0.77815	0.77815	.....
611 532	38	———	0.78987	.....	.....
310	40	———	0.80103	0.80103	0.80103
533	43	———	.....	0.81673	0.81673
311	44	———	0.82172	0.82172	.....
631	46	———	0.83138	.....	.....
111	48	———	0.84062	0.84062	0.84062
543 110 710	50	———	0.84948	.....	.....
711 551	51	———	.....	0.85378	0.85378
320	52	———	0.85800	0.85800	.....
211 552 721	54	———	0.86619	.....	.....
321	56	———	0.87409	0.87409	0.87409
730	58	———	0.88171	.....	.....
553 731	59	———	.....	0.88542	0.88542
651 732	62	———	0.89619	.....	.....
100	64	———	0.90309	0.90309	0.90309
741 811 554	66	———	0.90975	.....	.....
733	67	———	.....	0.91303	0.91303
410 322	68	———	0.91625	.....	.....

against the length of life. The result is a probability curve, the peak of which gives the most probable length of life of the men in the group. If, instead, we plot, year by year, the total number who have died from the beginning of the test through to the end of the year, we have the integral of a probability curve. Instead of plotting the actual number of men, it is preferable to plot the percentage of the original number. If there were an infinite number of men in the test, it is evident that the center of symmetry of the curve would come at the 50 per cent point. If there are only p men in the test, the plot may be made on the basis of $p + 1$, thus making the peak come at the 50 per cent point of abscissas. The mth point on the curve then represents $\frac{100m}{p+1}$ per cent of the total number of men who were dead at the end of m years. Such a curve may easily be made into a straight line by expanding the abscissas symmetrically on both sides of the 50 per cent point in accordance with the equation for the probability integral. Coordinate paper of this kind has been fully described elsewhere by Hazen[29] and by Whipple.[30]*

TABLE X.—DIFFRACTION DATA OF W (TABLE VIII) ARRANGED FOR PLOTTING ON PROBABILITY PAPER

Per Cent ($p + 1 = 10$)	log a
10	0.49837
20	0.49859
30	0.49870
40	0.49886
50	0.49920
60	0.49920
70	0.49931
80	0.49932
90	0.49958

In Table X we have $p = 9$ values for the logarithm of the edge of the unit-cube of pure W. The first value ($m = 1$) indicates that, if p were infinity, 10 per cent $\left(= \frac{100\,m}{p+1}\right)$ of the values would be approximately 0.49837 or less; similarly, 20 per cent would be 0.49859 or less; etc. In the case of the insurance data the number of men necessary to give a smooth curve would be rather large. In the case of x-ray diffraction data taken with MoK rays on a film bent over an arc of 8 in. radius, the degree of reproducibility is such that if $p =$ or >8 the graph represents very closely the integral of a true probability curve between the 30 and 70 per cent abscissas. The upper curve of Fig. 29 is the probability integral, plotted on "probability paper," for the data of Tables VIII and X.

* This type of plotting paper is printed in tablet form by the Stationery Department of the General Electric Company. It is known as "FN-384 probability paper."

Hazen uses a somewhat different formula for finding the decimal position of the mth term. Expressed in terms of the symbols we have just used, his expression is $\frac{2m-1}{2p}$. This divides the abscissas into p equal spaces and requires that the position of plotting be at the center of each space.

The two methods give almost identical graphs especially in the important range of 30 to 70 per cent on the axis of abscissas. The use of logarithms makes either of these methods of plotting exceedingly sensitive, without using too open a scale of ordinates. For instance, the interplanar distance 1.116Å. in Table VIII, corresponding to 50 per cent in Table X, gives a point in the upper curve of Fig. 29 which appears to be considerably above the straight line. If this value is decreased by only 0.1 per cent, *i.e.*, if it is reduced to 1.115Å., the point would be as far below the graph as it now is above it. The probability method is to be preferred to the ordinary method of averaging in that it automatically weights the most concordant values; yet it does not completely disregard the less concordant values, for they have their effect in producing a shift of the whole graph to the left or right. The greater the consistency of the data the more nearly horizontal will be the graph. For any given scale of ordinates the slope of the straight line of the graph is a measure of the probability of the correctness of the final answer. It is easy by this method to measure different diffraction patterns of the same sample, or patterns of different samples having identical composition, or a single pattern at intervals of several months, and to have no final result differ from the mean of all of them by more than 0.1 per cent. If proper precautions are taken to insure that the calibration standard and the crystal under investigation have the same equivalent center of diffraction, and if the crystal fragments are free enough from strain to give clear lines in the diffraction pattern, the accuracy of the final result should be greater than 0.1 per cent. It rarely happens, however, that materials are duplicated either in nature or in the arts with sufficient precision to justify the assumption that two specimens from different sources are identical. Even slight amounts of impurities may make considerable change in the lattice parameter. For instance,[23] the lattice parameter of 99.999 per cent Ag is 4.079Å.; that of 99.9 per cent Ag plus 0.1 per cent Cu is 4.058Å. In other words, a difference of 0.1 per cent in composition in this case makes a difference of 0.5 per cent in the lattice parameter. For most "pure" metals and their compounds the effect of a small amount of impurity is much less than this. For instance,[23] the lattice parameter of 99.999 per cent Au is 4.065Å.; that of "24-carat" gold is 4.073Å. Iron of high purity from one source gave 2.858Å.; from another source 2.855Å. This effect of impurities is not surprising when it is remembered that, if the impurity comprises only 0.1 per cent

of the total number of atoms in a simple cube, the atoms of the impurity are on the average only 10 atoms apart, while the range of atomic influence is given by surface-tension experiments as about 200 atomic diameters.

All this makes it seem that it is usually inadvisable to assign lattice parameters with a precision better than 0.1 per cent except for some one individual specimen or for specimens which have been subjected to a thorough chemical analysis. Refined table salt (NaCl), conductivity copper, and Mazda lamp filaments are three notable exceptions. In some cases, especially in metallographic work, it is also necessary to make sure that the physical state of each specimen is known. When additional precision can be justified in the case of a cubic crystal, diffracting angles close to 180° may be used. Diffraction patterns taken at these large angles are sometimes given the technical name of "back reflections" in the literature.

Several investigators[21,31,32,33,34,35] have discussed the sources of error which are to be taken into account in measuring the lattice parameter of an individual specimen. They all agree that the chief source of error lies in the lack of absolute coincidence of the center of curvature of the photographic film and the equivalent center of diffraction. Several rules and formulas are to be found in the literature for the correction of this error. These all lead to essentially the same result (to within 0.1 per cent) as is given by the procedure recommended at the beginning of this chapter. Methods may be found in the literature by which it is claimed that a lattice parameter may be determined to within less than 0.01 per cent, using lines whose spacings are all greater than 0.6Å. The scheme is to include in the formula an arbitrary constant which is intended to represent the distance from the center of curvature of the photographic film to the equivalent center of diffraction. A value is then selected for this constant such that all the lines in this pattern are caused to give as nearly as possible the same value of the lattice parameter. It is easy to show that such "accuracy" is illusory. To obtain a lattice parameter from a film to within 0.01 per cent it is necessary to be able to calculate the interplanar spacings for individual lines with an accuracy of a few hundredths of one per cent. For purposes of illustration it will be assumed that the individual lines are to be read to 0.01 per cent. If, using MoK rays, the radius of curvature of the photographic film is 8 in. (20.32 cm.), the line corresponding to an interplanar distance of 2.00Å. would have to be located to within 0.0003 in. (0.007 mm.) to give a precision of 0.01 per cent; for 1.00Å. it would have to be determined to within 0.0006 in. (0.015 mm.); for 0.50Å. it would have to be determined to within 0.001 in. (0.025 mm.). The difficulty of locating either the center or the edge of a line on the clearest possible diffraction pattern to within 0.001 in. or even to 0.003 in. is apparent to any one who has ever tried it. No amount of calculation will increase the precision of a

final result beyond that determined by the accuracy of the experimental data. It is therefore evident that if a lattice parameter is to be measured with MoK rays to 0.01 per cent from a single film, or even from two or three films, only those lines must be used which correspond to interplanar distances of 0.50Å. or less.

It has already been stated that the axial ratio of a hexagonal, tetragonal, or orthorhombic crystal may be read off from the charts of Appendix II. M. L. Fuller and the author have devised a method[36] by which

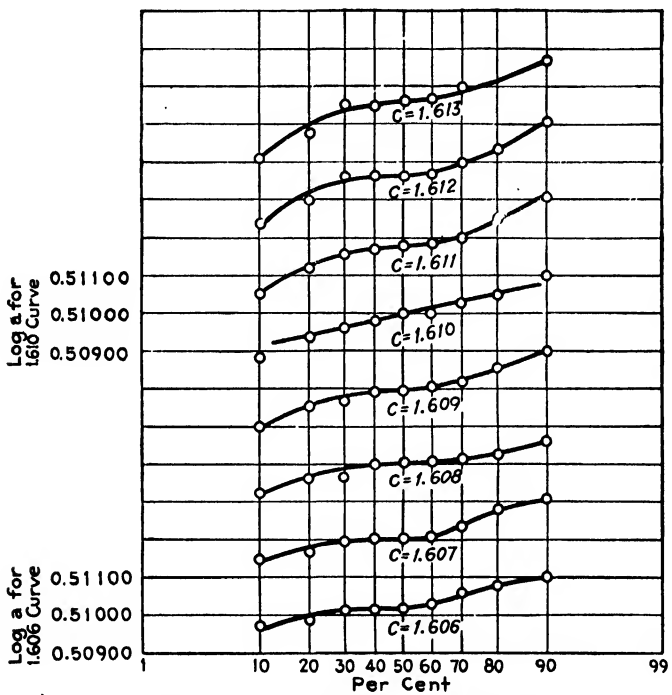

FIG. 31.—Graphical method for finding the axial ratio of ZnO.

the precision of such measurements may be considerably increased. The axial ratio is found approximately from the semilogarithmic charts of Appendix II. A group of seven or eight values approximating this axial ratio is selected and, for each of these axial ratios, values of log a are calculated from each of the observed interplanar spacings.

The values of log a for each axial ratio are plotted on probability paper according to the method described above, one curve for each axial ratio. That curve based on the most probably correct axial ratio will be closest to being a straight line. All others on either side of it will be progressively farther from being a straight line, because they will necessarily be poorer approximations to true probability curves. The sensitiveness of the method is illustrated in the case of zinc oxide. The

semilogarithmic charts of Appendix II give an axial ratio of 1.61 from these data, hence a series of axial ratios from 1.606 to 1.613 were selected for the calculations. The curves plotted from these data are shown in Fig. 31. The origin of coordinates is shifted for each curve in order to avoid overlapping of the curves. The ordinates for two of the curves are indicated on the figure. There is no doubt that the points of the 1.610 curve come closest to being in a straight line between the 30 and 70 per cent points. The value of log a at the 50 per cent point of this straight line will give the most probably correct value of a.

The unit-cell dimensions of zinc oxide of extremely high purity are, therefore, $a = 3.235 \pm 0.003$Å.; $c = 5.209 \pm 0.005$Å.; $C = c/a = 1.610 \pm 0.001$. This value of the axial ratio is slightly higher than the value 1.608 accepted by Bragg[37] and by Weber[38] and considerably higher than the value 1.596 obtained by Barth.[39]

This method seems to give results reliable to the third decimal place for C. Under very special and carefully controlled conditions a higher accuracy of data can sometimes be justified. In such cases a Seemann-Bohlin focusing cassette can be used, of large enough radius to give, with proper precautions, a very high accuracy of data. With such data the method just described is not sufficiently sensitive. Instead, equations must be set up for the interplanar spacings corresponding to the various lines in the diffraction pattern. For hexagonal and tetragonal crystals each equation will have two variables, one for the edge a (or b) of the unit of structure along the X- (or Y-) axis, and one for the axial ratio C. These equations may be solved by taking them in pairs, so that each pair yields a value of a (or b) and a value for C. Examination of the equations will show that certain pairs of planes yield results for axial ratio which are much more sensitive than others. These are the pairs which should be used in determining the axial ratio. Of course the accuracy of the result can be increased if a wave length of x-rays can be used which will cause the desirable pairs of planes to give back reflections.

SUMMARY

Like the Bragg method, the powder method of crystal analysis interprets as much of the structure of a crystal as possible in terms of the diffraction data. Great emphasis is placed on the cumulative evidence given by the interplanar spacings of many families of planes arranged in the order of their magnitude and on the relative intensities of the lines in the diffraction pattern. The symmetry characteristics of the crystal are used to supplement the x-ray data. So far as is known to the author, no complete solution of crystal structure by the powder method has been found to be inconsistent with the results of other methods. It is a method which is applicable to a large number of

materials whose analysis offers the greatest hope of immediate usefulness to science and industry.

References

1. A. W. Hull, Paper before *Amer. Phys. Soc.*, October, 1916; *Phys. Rev.*, **9**, 84, 564 (1917); **10**, 661 (1917).
2. P. Debye and P. Scherrer, *Nachr. Kgl. Ges. Wiss. Göttingen* (1915–1916); *Phys. Zeit.*, **17**, 277 (1916); **18**, 291–301 (1917).
3. J. K. Morse, *Jour. Optical Soc. Amer. and Rev. Sci. Instr.*, **16**, 360 (1928).
4. A. St. John, paper read at meeting of Amer. Assoc. Adv. Sci., Jan. 1, 1925.
5. H. Seemann, *Phys. Zeit.*, **20**, 169 (1919).
6. H. Seemann, *Ann. Physik*, **59**, 455 (1919).
7. H. Bohlin, *Ann. Physik*, **61**, 421 (1920).
8. W. H. Bragg, *Proc. Phys. Soc. London*, **33**, 222 (1921).
9. J. Brentano, *Arch. sci. phys. nat.*, (5), **1**, 550 (1919); *Proc. Phys. Soc. London*, **37**, 184 (1925).
10. A. W. Hull and W. P. Davey, *Phys. Rev.*, **17**, 549 (1921).
    W. P. Davey, *Gen. Elec. Rev.*, **25**, 565 (1922).
    See also Fairbanks, "Laboratory Investigations of Ores," Chap. II, McGraw-Hill Book Company, Inc., New York, 1928.
11. A. W. Hull, *Phys. Rev.*, **17**, 571 (1921).
12. J. O. Wilhelm, *Trans. Roy. Soc. Canada*, **21**, 1 (1927).
13. T. Bjurström, *Zeit. Physik*, **69**, 346 (1931).
14. E. A. Owen and G. D. Preston, *Proc. Phys. Soc. London*, **35**, 101 (1923).
15. P. P. Ewald, "Krystalle und Röntgenstrahlen," Julius Springer, Berlin, 1923.
16. W. P. Davey, *Trans. Amer. Soc. Steel Treating*, **6**, 375 (1924); *Phys. Rev.*, **25**, 753 (1925).
17. L. W. McKeehan, *Phys. Rev.*, **21**, 206, 503 (1923).
18. R. E. Gibbs, *Proc. Roy. Soc.*, A, **107**, 561 (1925).
19. A. J. Bradley, *Phil. Mag.*, **47**, 657 (1924).
20. H. Ott, *Sitzb. bayer. Akad. Wiss., math.-naturw. Abt.*, **31**, 7 (1924).
21. R. J. Havighurst, E. Mack, and F. C. Blake, *Jour. Amer. Chem. Soc.*, **46**, 2368 (1924).
22. W. P. Davey, *Phys. Rev.*, **19**, 538 (1922); **21**, 143 (1923).
23. W. P. Davey, *Phys. Rev.*, **25**, 753 (1925).
24. W. P. Davey, *Phys. Rev.*, **26**, 736 (1925).
25. C. G. Fink, *Trans. Amer. Electrochem. Soc.*, **17**, 229 (1910).
26. J. Brentano and J. Adamson, *Phil. Mag.*, **7**, 507 (1929).
27. M. L. Fuller, *Phil. Mag.*, **8**, 585 (1929).
28. R. A. Patterson, *Phys. Rev.*, **26**, 56 (1925).
29. Allen Hazen, *Trans. Amer. Soc. Civil Eng.*, **77**, 1539 (1914).
30. G. G. Whipple, *Jour. Franklin Inst.*, **182**, 37, 205 (1916).
31. A. J. Bijl and N. H. Kolkmeijer, *Koninklijke Akad. Wetenschappen Amsterdam*, **21**, 494 (1919).
32. A. Hadding, *Centralbl. Mineral., Geol.*, p. 631 (1921).
33. L. W. McKeehan, *Jour. Franklin Inst.*, **193**, 231 (1922).
34. F. Kirchner, *Ann. Physik*, **69**, 59 (1922).
35. Phebus and Blake, *Phys. Rev.*, **25**, 107 (1925).
36. M. L. Fuller, *Science*, **70**, 196 (1929).
37. W. L. Bragg, *Phil. Mag.*, **39**, 647 (1920).
38. L. Weber, *Zeit. Kryst.*, **57**, 398–403 (1922).
39. Tom Barth, *Norsk. Geol. Tids.*, **9**, 317–319 (1927).

CHAPTER VII

THE ROTATING-CRYSTAL METHOD*

There has been developed in Germany and in England a method[1,2,3,4,5] of crystal analysis in which the necessary diffraction data are obtained either by oscillating or by rotating a single crystal in a beam of monochromatic x-rays. The interpretation of the diffraction pattern so produced involves certain geometrical considerations which make this method very powerful especially in the case of crystals of complex structure. It is with the experimental technique and with the theory and details of the interpretation that this chapter has to do.

APPARATUS AND EXPERIMENTAL TECHNIQUE

Apparatus.—When a large crystal is used, the x-ray beam must be defined sharply by a set of slits. If the crystal is small enough to be

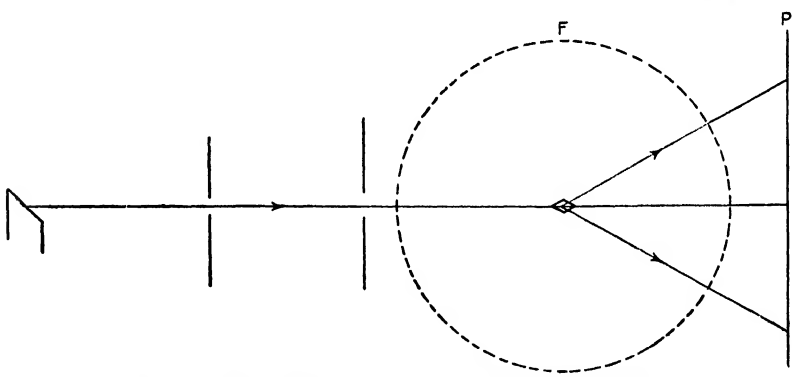

FIG. 1.—Schematic diagram of rotating crystal apparatus.

completely bathed in the beam passing through the slit system, it will itself define the beam. A schematic diagram of the apparatus is shown in Fig. 1. The diffraction pattern may be registered either upon a photographic plate P perpendicular to the x-ray beam or upon a film F in a cylindrical camera the axis of which coincides with the axis of rotation of the crystal. Figure 2 shows the Bernal type of apparatus arranged for use with a photographic plate. The cylindrical camera C, which is interchangeable with the plate-holder on the apparatus, may be seen at the right of the figure. The small crystal D is attached to a fine glass

*By Dr. W. P. Jesse, Research Laboratory, General Electric Co., Schenectady, N. Y.

fiber with a tiny drop of clear nitrocellulose lacquer, and the fiber is mounted in a mass of plasticine on the crystal holder. The holder is equipped with a pair of goniometer arcs A at right angles with each other. These greatly facilitate any adjustments necessary to bring some given crystallographic axis in the crystal into coincidence with the axis of rotation. The crystal may also be centered accurately on the rotation axis by a double cross-slide arrangement S with centering screws. A small lead cup in the center of the plate-holder prevents the direct x-ray beam

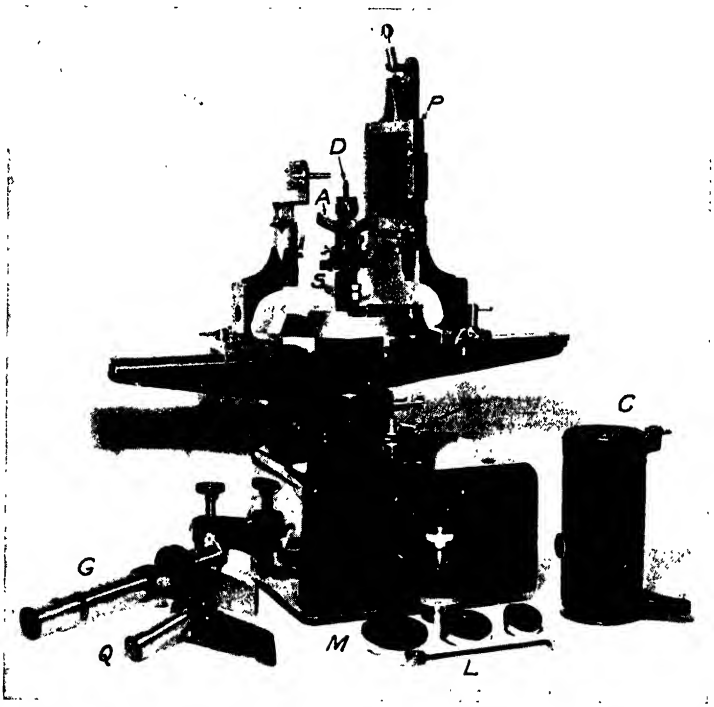

FIG. 2.—Rotating crystal apparatus designed by J. D. Bernal for W. G. Pye and Company after instruments in use at the Royal Institution.

from striking the plate and causing general fogging from scattered radiation. This cup may be removed for an instant at the end of an exposure to obtain on the plate a record of the central spot due to the undeviated beam.

Rotation and Oscillation Photographs.—In crystal analyses by this method, either of two types of photographs may be obtained. The first of these, the "complete-rotation" photograph, involves the uniform turning of the crystal through a series of complete revolutions. In the apparatus shown in Fig. 2 this rotation is accomplished by a clockwork drive which rotates the crystal spindle by means of a belt and pulley T. A complete rotation of the crystal gives rise to the symmetrical photo-

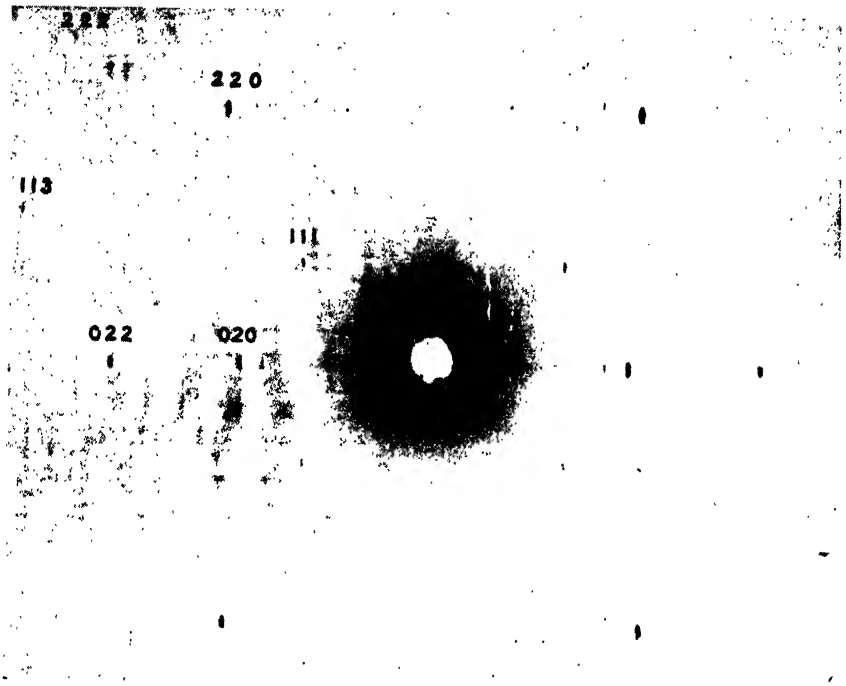

FIG. 3.—Rotation photograph of a crystal of rock salt about a cube-edge. X-ray beam of copper radiation perpendicular to the rotation axis and to a flat photographic plate.

FIG. 4.—Rotation photograph of a monoclinic crystal of diphenyl about the [1 0 0] axis. Unfiltered copper radiation. Flat photographic plate.

graphs of Figs. 3, 4, 5, and 6. In the general case each set of planes in the crystal diffracts four times during the rotation. The four resulting

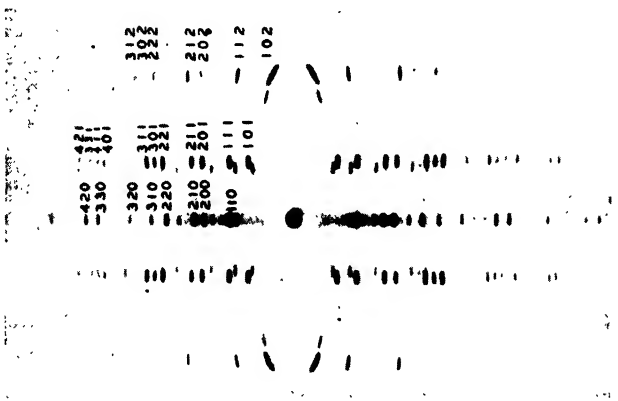

FIG. 5.—Rotation photograph of a tetragonal crystal of urea about the [001] axis. Unfiltered copper radiation. Cylindrical film.

diffracted beams are distributed in a rectangular pattern about the center point of the photograph.

Sometimes it is useful to investigate the diffracted beams as the crystal turns through a more limited angular range. In such a case the second type of photograph, called an "oscillation" photograph, may be employed.

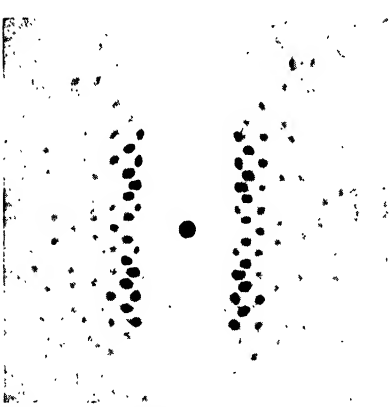

FIG. 6.—Rotation photograph of a monoclinic crystal of stilbene about an axis perpendicular to the (010) face. Copper radiation filtered through nickel. Cylindrical film.

Instead of being given a continuous rotation, the crystal is made to oscillate back and forth with a constant angular speed throughout a chosen angular range. Such a range may be 5°, 10°, 15°, or even larger according to circumstances. The rocking motion is imparted to the spindle of the crystal holder through a lever arm the end of which is always in contact with a heart-shaped cam. This cam, shown in Fig. 7, is so designed that, turning with uniform speed, it gives to the rocker arm a uniform angular motion, which is imparted to the crystal spindle. Three such cams, *M*, are shown in the foreground of Fig. 2. They give to the crystal an oscillation range of 5°, 10°, and 15°, respectively. Any one of these cams may replace the driving pulley *T*. The rocker arm, *L* of Fig. 2, is clamped on the lower end of the crystal-spindle shaft so that its sharp edge rests against the surface of the cam. The oscillation

range may be set quite precisely by reference to the horizontal graduated azimuth circles on the instrument. A typical oscillation photograph is shown in Fig. 24. It will be noted that such a photograph lacks the symmetry shown by the complete-rotation photographs.

Adjustment of the Crystal.—A small "perfect single" crystal should be chosen with dimensions of the order of 0.1 to 0.5 mm. If the crystal is too small, the task of setting becomes difficult and tedious. On the other hand, if the crystal is too large, the geometrical shape of the crystal, the increased absorption, and the nonhomogeneity of the x-ray beam over the large cross-sectional area, all tend to alter the relative intensities of the diffracted beams from planes of widely different orientation in the crystal.

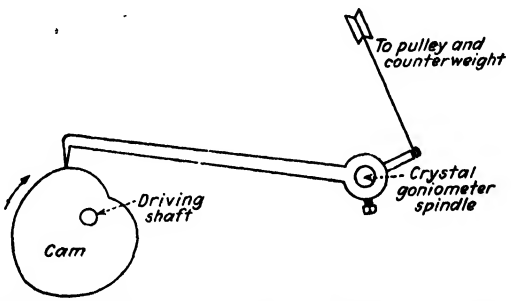

FIG. 7.—Cam and lever arrangement for rocking a crystal at a uniform angular speed.

Rotation and oscillation photographs are generally taken with the axis of rotation of the crystal in coincidence with some principal crystallographic axis. The easiest method of making such an adjustment will depend upon the crystal used. When the crystal is needle-like in shape, the long axis may be brought into coincidence with the rotation axis by viewing the crystal from the side with a short-focus telescope and by making adjustments on the goniometer until the long axis of the crystal coincides with the vertical crosshair of the telescope. When the axis of rotation is a zone axis of a crystal with well-developed zonal faces, the setting may be made best by transferring the goniometer arcs to an optical goniometer and then setting the crystal by the usual optical method. The apparatus shown in Fig. 2 is fitted with a telescope G and collimator Q which may replace the x-ray slit system and the plate-holder assembly. Hence in this instrument the optical adjustment just described may be made with the crystal in place.

In case no optical goniometer is available, a satisfactory setting by optical methods may still be accomplished in the following manner. An improvised eyepiece is made by fastening, at an angle to the outer face of the pinhole system, a thin microscope cover slide as shown in Fig. 8. A parallel beam of light directed through the pinhole system

strikes the crystal face and is reflected back. When some face of the crystal is exactly perpendicular to the beam, the reflected beam passes back through the pinholes, is partially reflected by the coverglass G, and is seen by the eye at A. The crystal is adjusted by means of the goniometer arcs until, on rotation, each of its zone faces gives a tiny flash of light observable at A; then the zone axis is parallel to the axis of rotation. Of course any attempt at such an adjustment presupposes that the beam through the slit system is accurately perpendicular to the axis of rotation of the instrument. If such is not the case, the slit system must first be adjusted by a method similar to the above except that the crystal is replaced by a small plane parallel glass plate silvered on both surfaces.

In case the crystal does not have well-defined bright faces so that an optical method of setting may be used, then an accurate setting must

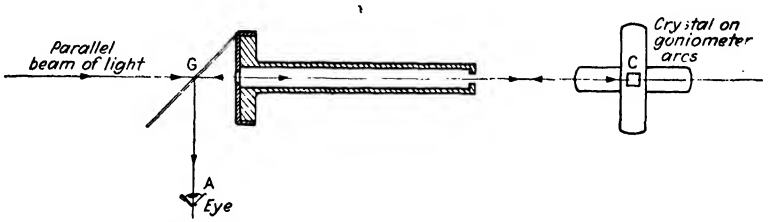

FIG. 8.—Optical method for adjustment of crystal.

be made by means of x-rays. Laue photographs are of great help here. Frequently the small angle through which the crystal must be turned for a perfect setting may be determined by observing the angle between the trace of a plane of symmetry on the Laue photograph and a true horizontal or vertical line on the photographic plate. Two successive oscillation photographs[6] with a known change of setting on the goniometer arcs will also give information leading to the desired setting. Such methods, however, may become very complicated.

Assuming that, by one of the above methods, the desired crystallographic axis has been set accurately parallel to the rotation axis, then the only further adjustment necessary is the exact centering of the crystal on the axis of rotation. This is done easily by means of the cross-slide arrangement, S of Fig. 2, use being made of a short-focus telescope equipped with a vertical crosshair.

Calibration of Apparatus.—If the distance from the crystal to the photographic plate (or the radius of the circular camera) is unknown, it must be determined before rotation photographs of unknown crystals can be interpreted. This calibration is easily accomplished by photographing the diffraction pattern of a calcite rhombohedron or a bit of mica and computing the distance involved from the known grating space of the crystal used.

Choice of Wave Length.—For most rotation photographs a long-wave-length radiation, such as the K radiation from copper, is generally most convenient since it tends to give a well spread-out pattern. This is especially important in the investigation of organic crystals where the interplanar distances are quite large. When using copper radiation the β lines may be suppressed by a filter of nickel 0.001 in. thick. Such filtering is, however, rarely necessary since the β lines cause little confusion on the photographs.* If the crystal absorbs the copper radiation too strongly, some more penetrating radiation may be used, such as that from molybdenum.

THE THEORY OF THE ROTATION PHOTOGRAPH

The rotation diagrams of Figs. 3, 4, and 5 all show, grouped on the central horizontal line, the sort of diffraction pattern which has already been described in connection with the powder method (Chap. VI). It is the sort of pattern that would have been obtained by the continuous rotation of a crystal in the Bragg method (Chap. V) if a stationary photographic film had been substituted for the ionization chamber. Such diffracted beams are produced by planes parallel to the rotation axis. Planes which are not parallel to the axis give rise to still other diffraction patterns because, at certain points in their rotation, the angle at which the x-ray beam meets the oblique plane will be exactly that required by Bragg's law, *i.e.*, $n\lambda = 2d \sin \theta$. At such points diffraction will take place. Diffraction spots from such planes may be found grouped in horizontal lines or curves above and below the central horizontal lines of Figs. 3, 4, and 5. In general, any oblique plane passes through four such points during the course of a complete revolution. In the special case in which the axis of rotation is parallel to a crystallographic axis or is perpendicular to a crystal face, the array of spots on the photograph is on definitely ordered curves. Such an orderly array is comparatively easy of interpretation and will now be considered in detail.

Assume a crystal lattice, such as is shown in Fig. 1 of Chap. II, to be mounted so that one of the crystallographic axes coincides with the axis of rotation. For simplicity let us choose the Z-axis. Let A and B of Fig. 9 be neighboring atoms at the lattice points along the Z-axis, the distance between them being the primitive translation c. As the crystal lattice is rotated in the x-ray beam, the limitations upon the diffracted beam are those discussed in the derivation of Eq. (2) of Chap. I. There

* It will be noted from Figs. 3, 4, and 5 that, except in the case of the equatorial line, the fainter lines caused by diffraction of the β wave length fall in layers different from the lines caused by the α wave length. These fainter layers of lines fall somewhat closer to the origin, since λ has a smaller value for the β wave length. This is brought out more fully in the discussion of Eq. (2).

it was shown that the condition for diffraction from a linear grating is given by an equation of the form

$$z_1(\gamma_2 - \gamma_1) = g\lambda$$

Hence, in the notation of Fig. 9, the condition for diffraction is

$$c(\cos \delta + \cos \phi) = n\lambda \tag{1}$$

where n is an integer (equivalent to g, above) representing the order of diffraction by the line grating. For the usual case where the direction of

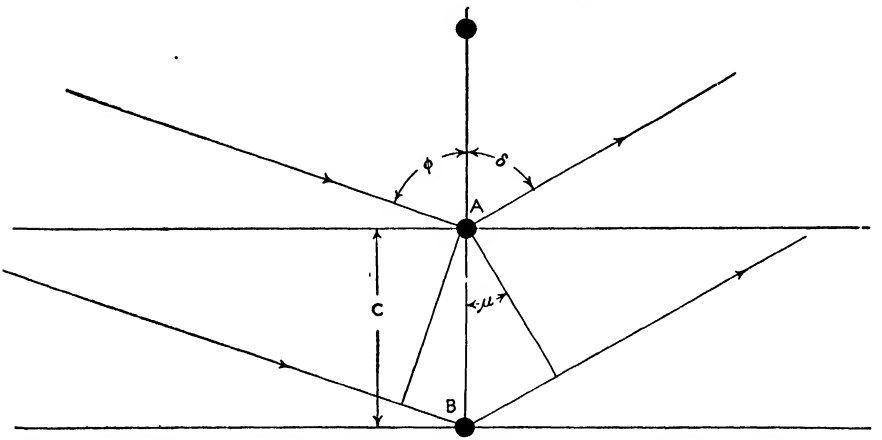

FIG. 9.—Diffraction of x-rays by crystal lattice elements spaced regularly along the rotation axis.

the x-ray beam is perpendicular to the rotation axis, ϕ becomes 90° and Eq. (1) simplifies to

$$c \cos \delta = c \sin \mu = n\lambda \tag{2}$$

For various orders of diffraction n assumes values such as 0, 1, 2, 3, etc., giving rise to the series of equations

$$\left.\begin{aligned} \cos \delta_0 &= \sin \mu_0 = 0 \\ \cos \delta_1 &= \sin \mu_1 = \frac{\lambda}{c} \\ \cos \delta_2 &= \sin \mu_2 = \frac{2\lambda}{c} \\ \cos \delta_3 &= \sin \mu_3 = \frac{3\lambda}{c} \\ \cos \delta_n &= \sin \mu_n = \frac{n\lambda}{c} \end{aligned}\right\} \tag{3}$$

Such equations, for a constant wave length, give the loci of all possible diffracted rays as the crystal turns. These loci are elements of a series of cones, shown in Fig. 10, of which the half-apex angles are given by δ_0, δ_1,

δ_2, etc. Any element of each of the cones makes an angle μ_0, μ_1, μ_2, etc., respectively, with the horizontal plane.

For the crystal which we are considering, the central horizontal plane contains, according to Eq. (3), all diffracted beams of order of zero for the linear grating along the Z-axis. The grating distance c must therefore appear in the zero order for all these beams. Hence the Miller indices of all planes giving diffracted beams in the horizontal plane must be

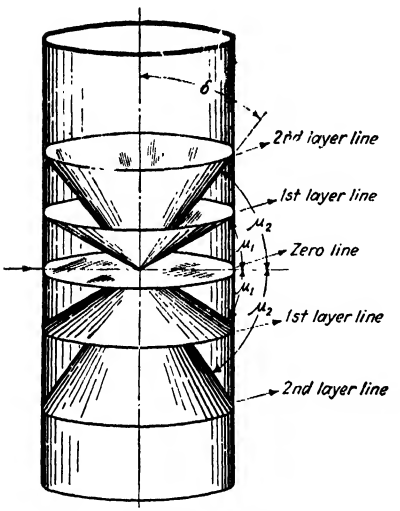

FIG. 10.—X-ray diffraction by a rotating crystal and the formation of layer lines on a cylindrical film.

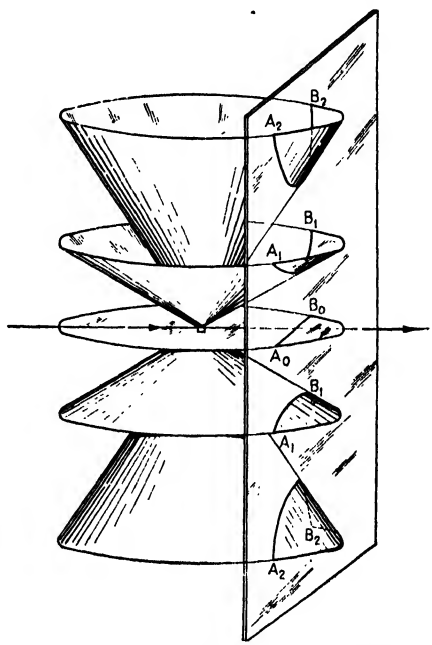

FIG. 11.—The intersection of diffracting cones with a photographic plate, placed perpendicular to the x-ray beam.

represented by $(h\,k\,0)$. Similarly all x-rays diffracted by planes of indices $(h\,k\,1)$ lie on the first-order cone defined by

$$\mu_1 = \sin^{-1}\frac{\lambda}{c} \tag{4}$$

and in general all beams diffracted from planes of indices $(h\,k\,n)$ lie on the nth-order cone defined by

$$\mu_n = \sin^{-1}\frac{n\lambda}{c} \text{ (see Fig. 5)} \tag{5}$$

Figure 11 shows that the intersections of such cones with a plane photographic plate placed perpendicular to the incident x-ray beam consist of a system of hyperbolas A_1B_1 and A_2B_2 on either side of a central straight line A_0B_0. Figure 12 shows that for a cylindrical film the axis

of which coincides with the rotation axis the intersections of the cones with the cylindrical surface give a series of circles (see Fig. 10) which become straight lines when the film is flattened out. The central line is termed the "equatorial" or "zero" line. The succeeding lines are termed the first, second, third, etc., "layer" lines. Throughout this chapter the term "layer line" will be used broadly to include the corresponding hyperbolas on the plane photographic plate.

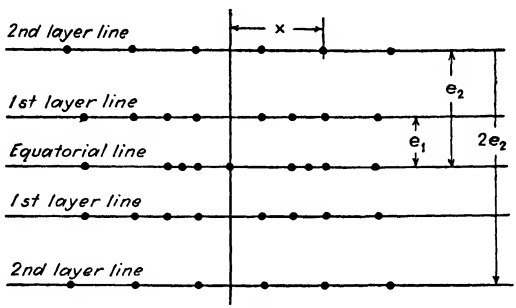

FIG. 12.—Schematic rotation diagram on a cylindrical film.

Dimensions of the Unit-crystal.—From the theory so far presented it will be seen that measurements of the positions of layer lines on the photograph may be used to determine the spacing between equivalent positions along the crystallographic axis about which the crystal has been rotated. Thus the primitive translation along the Z-axis of the crystal lattice is given by Eq. (3) to be

$$\frac{n\lambda}{\sin \mu_n} \tag{6}$$

where the values of μ_1, μ_2, μ_3, etc., are determined from the layer lines of the photograph taken with rotation about the Z-axis. Similarly, the primitive translations may be found along the X- and the Y-axes. Hence, to determine the true dimensions of a unit-crystal, it is necessary only to measure a rotation photograph about each coordinate axis of the crystal which has a distinctive primitive translation.

When a cylindrical film is used, the angle μ_n is found from the spacing of the layer lines by the equation

$$\tan \mu_n = \frac{e_n}{R} \tag{7}$$

where e_n is half the measured distance from the nth layer line above to the nth layer line below the equatorial line, and where R is the radius of the cylindrical film.

For the case of a plane photographic plate perpendicular to the x-ray beam, the value of sin μ_n may be calculated conveniently from Fig. 13 as

$$\sin \mu_n = \frac{B}{\sqrt{A^2 + B^2 + D^2}}$$

or

$$\sin \mu_n = \sin 2\theta \cos \psi \tag{8}$$

where $\tan 2\theta = r/D$ and $\cos \psi = B/r$. D is the perpendicular distance from crystal to plate, and $2A$, $2B$, and $2r$ are measured on the photograph, as shown in Fig. 13, between positions of the four spots corresponding to diffracted beams from a single plane. ψ is the angle shown in the figure

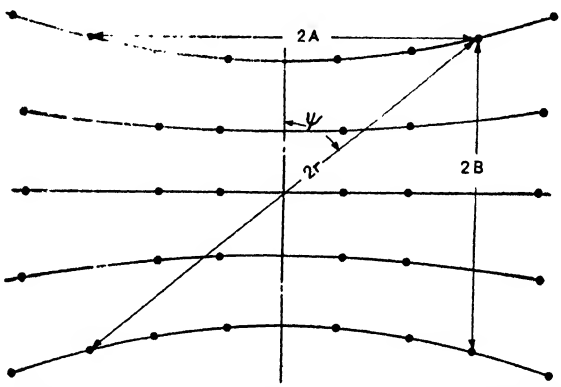

FIG. 13.—Schematic rotation diagram on a plane photographic plate.

and 2θ is, as usual, the angle at the crystal between the incident and diffracted x-ray beams.

The rotating-crystal method is superior to any other x-ray method in its ability to determine the dimensions of the true unit of structure of a crystal. In other methods, where diffracted beams are observed from only a limited number of planes, one may mistake diffraction of the second order for first-order diffraction from a unit-crystal having only half the true dimension. In the case of the rotation method, such a mistake is much less likely to occur since the rotation about a coordinate axis brings together on a single layer line diffracted beams from planes having a common intercept on the rotation axis (*i.e.*, a common Miller index) but having widely different orientations. With such a wide variety of planes it becomes quite unlikely that whole layer lines will be missed on the diagram even though they may be quite faint. Such possible faint layer lines should be looked for carefully, especially in the higher orders where they appear to best advantage, since to miss such lines involves assigning to the unit-crystal a dimension only half the true one.

The very simple diagram of the sodium chloride crystal rotated about its cube-edge (Fig. 3) illustrates this principle. If one were to consider the stronger hyperbolas on the diagram as those of first-order diffraction, then the edge of the unit-cube would have to be given as 2.81Å. A closer inspection, however, brings out a faint intermediate hyperbola. Assuming this to be the first-order hyperbola and the strong one to be the second-order hyperbola, the edge of the unit-cube would be calculated to be 5.63Å. This is the true unit-crystal for sodium chloride, *i.e.*, the unit which repeats itself in space throughout the whole crystal. (In this connection see Chaps. I, V, IX.)

Assignment of Indices to Spots on Rotation Diagrams.—In the determination of the dimensions of the unit-crystal, use was made only of the spacings of the layer lines, and no attempt was made to identify any individual spot on the diagram as proceeding from a plane of a given set of indices. To go further with the analysis of the crystal, such identification is necessary. The methods of accomplishing this will now be discussed.

We know the crystal system and symmetry from optical goniometric measurements (and possible Laue patterns), and we know the size and shape of the unit-crystal from the x-ray measurements which we have just discussed. This information enables us to pick the appropriate equation for interplanar spacings from Chap. III. The seemingly most straightforward method of assigning indices would be to follow the general procedure adopted in the case of the powder method, namely to calculate the interplanar spacings corresponding to the equation and to compare these calculated values with values obtained from direct measurement of the photograph. Such a method is perfectly valid, though at times laborious. When a plane photographic plate is used, the interplanar spacing for a given family of planes may be calculated at once exactly as in the case of the powder method in terms of the distance of the diffraction spot from the central spot.

The equations are (see Fig. 13):

$$\left.\begin{aligned} \tan 2\theta &= \frac{r}{D} \\ n\lambda &= 2d \sin \theta \end{aligned}\right\} \tag{9}$$

When a cylindrical film is used, the geometrical relations are shown in Fig. 14. C is the center of the rotating crystal, F a section of the cylindrical film, and R the radius of the camera. The direct x-ray beam passes through the crystal and makes the central spot at O. At some point in the course of the rotation, a given plane diffracts x-rays along the line CS and causes the spot S on the film. The angle 2θ between the incident ray CO and the diffracted ray CS is given by the relation

$$\cos 2\theta = \cos \phi \cos \mu \tag{10}$$

where ϕ is the horizontal angle measured between CO and CS', the projection of CS upon the equatorial plane. On the film, ϕ and μ are measured by the relations

$$\left.\begin{aligned}\phi &= \frac{\text{arc } OS'}{R} = \frac{x}{R}\\ \tan \mu &= \frac{e}{R}\end{aligned}\right\} \tag{11}$$

From measurements of e and x (Fig. 12) on the film the values of ϕ and μ are obtained, and hence the value of θ can be found from Eq. (10).

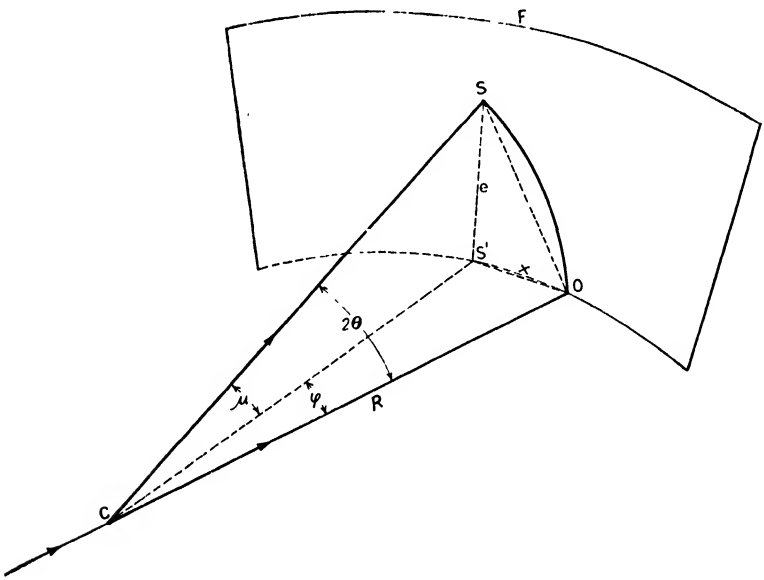

FIG. 14.—Geometrical relations for a cylindrical film.

Knowing θ, the interplanar spacing corresponding to the spot in question may be determined from Bragg's law. The computations are somewhat simplified in that the value of e is constant for a given layer line on the film if the crystal is properly set. This permits a single value of tan μ to serve for all the spots on a given layer line. For the equatorial line, $\mu = 0$ and cos $\mu = 1$, so that Eq. (10) reduces to

$$2\theta = \phi = \frac{x}{R} \tag{12}$$

which is the relation for the powder photograph using a cylindrical film.

In this manner it is possible to prepare a list of the interplanar spacings corresponding to all the spots on the rotation photograph. A comparison of this list with a list calculated from the equation used from Chap. III will, by the closeness of the check between the values, fix the Miller

line, respectively. The closeness of check between columns 3 and 5 identifies the diffraction spots listed in column 3. It will be seen that certain diffraction spots, *viz.*, (1 0 0), (3 0 0), (4 0 0), (4 1 0) on the equatorial line, (3 2 1) on the first layer line, and (4 2 2) on the second layer line, are apparently missing on the photograph. The absence of such spots is frequently of importance in the determination of the space-group, (see Chap. VIII and Appendix III). Especial care should be taken to determine whether important spots are truly missing, merely faint, or perhaps only beyond the range of the photograph.

The method of assigning indices which has just been outlined is essentially the same as that employed in Chap. VI for the powder method. There are, however, two limitations for the planar indices for the rotating crystal which make the assignment much more certain than in the powder method. The first of these, already mentioned, is that one index remains constant over a given layer line when the crystal is rotated about a coordinate axis.* Such a relation obviously rules out a large number of planes which might otherwise have to be considered. The second limitation, which applies only to rotations about a coordinate axis which is orthogonal to the other two, is illustrated in Fig. 5 for the case of the rotation of urea about the Z-axis. It will be noted that except for spots far from the center of the diagram there is a tendency for spots characterized by a constant value of hk on the various layer lines to lie almost vertically above one another. Thus spot (2 0 1) lies directly above (2 0 0); (2 1 1) above (2 1 0); and (2 1 2) above (2 1 1). Such lines of constant hk are termed "row lines" in contrast to the layer lines. The row lines are not truly vertical lines, especially at the edges of the photograph. Thus, in Fig. 5, (4 2 1) is not directly above (4 2 0) nor is (1 0 2) just above (1 0 1). The accurate trace of such row lines is given in Fig. 20 for the plane photographic plate and in Fig. 21 for the cylindrical film. The general shape of these curves enables one to know approximately where to look for the spot corresponding to a plane of a given index when the spot with a related index has been located. This serves as a rough check on the correctness of the indices assigned.

The whole method just outlined of indexing the diffraction spots on a rotation photograph is very satisfactory for rotation photographs involving comparatively few spots. When the number of spots on a single photograph becomes of the order of 100 or 200, then the computations involved become much too laborious for such a large number of spots and a graphical method is to be preferred. Of several such methods probably the most satisfactory is one due to Bernal.[5] An account of this method will be outlined in later sections of this chapter.

* More generally, for a rotation about any zone axis $[u\,v\,w]$ the indices of all diffraction spots on a given layer line satisfy the equation $hu + kv + lw = n$, where n is an integer corresponding to the order of the layer line.

THE RECIPROCAL LATTICE

The Concept of the Reciprocal Lattice.—Before taking up a discussion of Bernal's graphical method it will be necessary to make a digression and consider certain phases of a concept which has been most helpful in the study of crystal structure, especially in the case of the rotation method. This is the concept of the "reciprocal lattice" (often called in this chapter by the simple term "lattice") first developed by Ewald.[8] Suppose O in Fig. 15 to be the origin of a lattice network and let O be situated in one of the atomic planes of a crystal. Let d be the interplanar distance from O to the adjacent plane A. With the origin as center, let a sphere be described of radius equal to an arbitrary constant K. The plane A may then be represented by a point A' which lies on the perpendicular from O

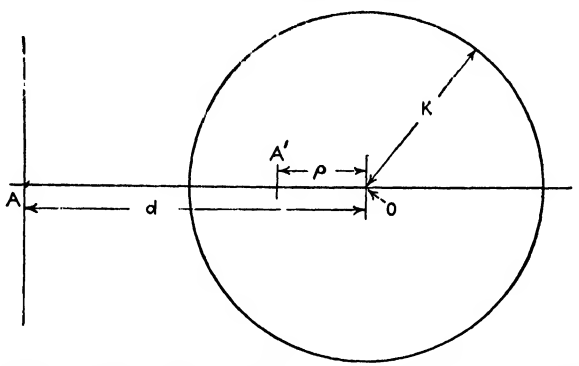

FIG. 15.—Diagram of the relation between a crystal plane and the corresponding point in the reciprocal lattice.

to the plane A and whose distance from O is given by $\rho = K^2/d$. Thus the greater the interplanar distance d, the closer to O does the corresponding point representation lie. Similarly for any other plane of interplanar spacing d', there is a corresponding point with distance $\rho' = K^2/d'$ which is its representation. Following such a procedure, it is possible to build up from a given crystal lattice a space array of points, each point representing a plane in the old lattice. The total array of points builds a new lattice which is called the "reciprocal" of the old lattice. If the same method of representation is reapplied to the planes of the new lattice, the original lattice is again obtained. Each of the two lattices is thus reciprocal to the other.

If a lattice, built up from the unit vectors $\bar{a}$, $\bar{b}$, and $\bar{c}$ with corresponding angles α, β, γ, is transformed into its reciprocal by the process described above, the unit vectors $\bar{a}^*$, $\bar{b}^*$, $\bar{c}^*$ of the new reciprocal lattice are defined in terms of the old by the vector equations

$$\begin{aligned} \bar{a} \cdot \bar{a}^* &= K^2 \\ \bar{b} \cdot \bar{a}^* &= 0 \\ \bar{c} \cdot \bar{a}^* &= 0 \end{aligned} \qquad (14)$$

and their cyclical transformations. These relations between the two systems may be put into convenient form thus:

$$\bar{a}^* = K^2 \frac{\bar{b} \times \bar{c}}{\bar{a}(\bar{b} \times \bar{c})} \tag{15}$$

a vector of scalar magnitude $K^2 \frac{bc \sin \alpha}{V}$ and in direction perpendicular to the plane bc.

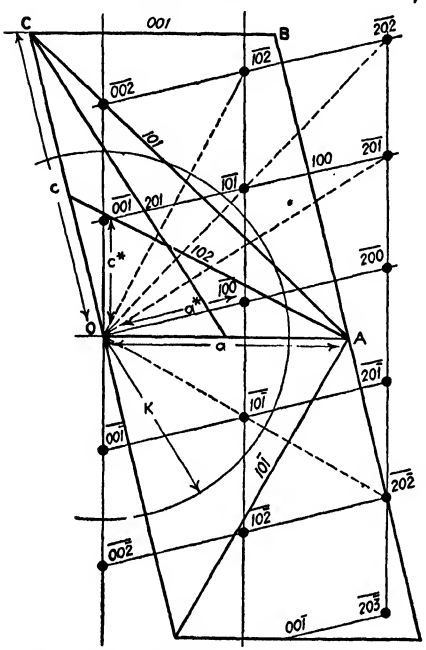

FIG. 16.—Projection of a monoclinic crystal lattice on the central plane perpendicular to the b-axis. The corresponding reciprocal lattice is also shown.

$$\bar{b}^* = K^2 \frac{\bar{c} \times \bar{a}}{\bar{b}(\bar{c} \times \bar{a})} \tag{16}$$

a vector of scalar magnitude

$$K^2 \frac{ca \sin \beta}{V}$$

and in direction perpendicular to the plane ac.

$$\bar{c}^* = K^2 \frac{\bar{a} \times \bar{b}}{\bar{c}(\bar{a} \times \bar{b})} \tag{17}$$

a vector of scalar magnitude

$$K^2 \frac{ab \sin \gamma}{V}$$

and in direction perpendicular to the plane ab.

V is here the volume of the unit-crystal, and a, b, and c are the scalar values of the unit vectors $\bar{a}$, $\bar{b}$, and $\bar{c}$.

A graphical representation in two dimensions of the relation between the two reciprocal lattices is given in Fig. 16. The diagram represents the projection of a monoclinic lattice upon a plane through the origin perpendicular to the b-axis.* The trace of the sphere of radius K appears in the diagram as a circle. The projection $OABC$ of the original unit-crystal and the projections of the original $(h\,0\,l)$ planes are

* There are two conventions for the naming of axes in the monoclinic system: (*a*) the one used by Wyckoff in his "Analytical Expression of the Results of the Theory of Space Groups" (and therefore used in most of this book), in which the X- and Y-axes are at some angle to each other, not 90° or 120°, and in which the Z-axis is perpendicular to the plane of the X- and Y-axes; (*b*) the one used by British and German crystal analysts, by mineralogists and crystallographers, and in Chap. XI of this book, in which the a- and c-axes correspond to the X- and Y-axes, respectively, and in which the b-axis corresponds to the Z-axis. Figure 16 is lettered in accordance with this latter convention. This means that a plane which would be called the $(2\bar{3}0)$ plane according to the Wyckoff convention is called the $(20\bar{3})$ plane in Fig. 16.

shown by heavy lines. The black circles represent the lattice points in the corresponding reciprocal lattice. In Fig. 16 the indices of the planes of the original lattice are designated in the usual way; those in the reciprocal lattice have a bar above them thus, $(\bar{2}0\bar{1})$. It should be noted that each plane of indices $(h\,0\,l)$ has as its counterpart in the reciprocal lattice a point of the same indices $(\overline{h\,0\,l})$. This point lies on the perpendicular from the origin to the plane $(h\,0\,l)$. Its distance ρ from the origin is related to the interplanar spacing of the $h\,0\,l$ planes by the equation

$$\rho_{h\,0\,l} = \frac{K^2}{d_{\overline{h\,0\,l}}} \tag{18}$$

A reciprocal monoclinic lattice such as is shown in Fig. 16 would be completed in space by a third vector $\bar{b}^*$ perpendicular to the ac plane. Thus the $\bar{b}$- and $\bar{b}^*$-axes coincide in direction for this type of lattice. Each reciprocal point $(h1\,l)$ lies directly above its corresponding $(h\,0\,l)$ point and lies in a plane which is situated a distance b^* from the $(h\,0\,l)$ plane. Similarly the $(h\bar{1}\,l)$ reciprocal points lie in a plane which is b^* below the $(h\,0\,l)$ plane. A three-dimensional diagram of a reciprocal network derived from an orthorhombic lattice is shown in Fig. 22. Because of the orthogonal relations, $\bar{a}^*$ coincides in direction with $\bar{a}$, $\bar{b}^*$ with $\bar{b}$, and $\bar{c}^*$ with $\bar{c}$.

The Reciprocal Lattice and the Diffraction of X-rays.—Since the reciprocal lattice is only a geometrical concept, a real physical picture of the diffraction of x-rays by such a lattice is impossible. Bragg's law, however, makes it possible to build a picture of the geometrical relations governing a point in the reciprocal lattice when diffraction by the real lattice plane takes place. If, in the equation $\lambda = 2\frac{d}{n}\sin\theta$, the value of d/n in terms of the reciprocal lattice is substituted, *i.e.*, $d/n = K^2/\rho$, then

$$\lambda = 2\frac{K^2}{\rho}\sin\theta \tag{19}$$

A representation of the geometrical conditions which this equation implies is given in Fig. 17.

Let the origin of the diffracting crystal lattice be at the point O, and let the normal to the advancing x-ray wave front be XO. Any system of crystal planes of spacing d in a position to diffract the oncoming x-ray beam must make an angle θ with XO. Let P be the reciprocal lattice representation of such a system of diffracting planes. Then PO is a perpendicular to the diffracting planes and, when n is taken as 1, $\rho = K^2/d$. Let the plane $XCBB'$ be drawn through the point P perpendicular to PO. The original ray XO makes then an angle θ with the plane $XCBB'$. The diffracted ray OC makes an angle 2θ with XO. The plane $XCBB'$

cuts the line of travel of the incident and diffracted rays, respectively, at X and C, where $XO = OC$.* From Fig. 17, $\rho = XO \sin \theta$. By comparison with Eq. (19), $XO = 2K^2/\lambda$. Since the angle XPO must always be $\pi/2$, the equation $\rho = XO \sin \theta$ is that of a sphere drawn on a diameter $XO = 2K^2/\lambda$. Hence the locus of all points in the reciprocal lattice which are in a position to diffract is the surface of a sphere of diameter $2K^2/\lambda$. The concept of this "sphere of diffraction" (often called in the literature the "sphere of reflection") is due first to Ewald.[8] The graphical treatment of the problem here follows the method of Bernal.[5]

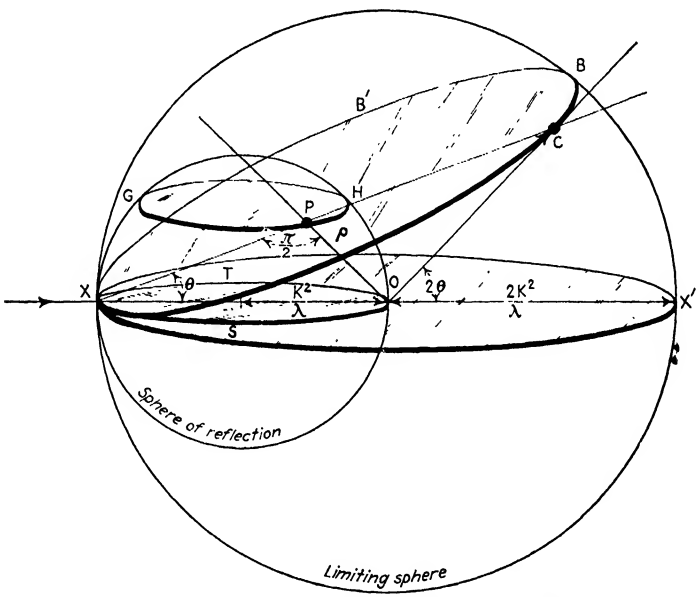

FIG. 17.—Diagram illustrating the geometrical conditions for "diffraction" by a point in a reciprocal lattice. (*After Bernal.*)

So far in our discussion there has been no restriction on the value of K^2. Bernal introduced the simplification of making K^2 equal to λ, the wave length of the x-rays used. The radius of the sphere of diffraction then becomes unity. Such a simplification will be adopted in this discussion at this point. If the crystal is assumed to revolve about a rotation axis which is perpendicular to the incident beam, then any point P in the reciprocal lattice rotates also and diffraction for the corresponding plane will occur as such a point passes, in the course of this rotation, through the surface of the sphere of diffraction. This will, in general, occur twice during a complete rotation, once as P cuts the surface entering the sphere and again as it cuts the surface in leaving the sphere.

* In ΔXOC, $\angle X'OC = \angle OCX + \angle CXO = 2\theta$ (exterior $\angle$ of Δ = sum of two opposite interior angles). Since $\angle CXO = \theta$, then $\angle OCX$ is also θ and ΔOCX is isosceles. Hence, $OX = OC$, so that X and C lie on a sphere of radius $OX = 2K^2/\lambda$.

Since P of indices $(h\,k\,l)$ has its negative counterpart P' of indices $(\bar{h}\,\bar{k}\,\bar{l})$ centrosymmetrically situated with regard to the origin of the reciprocal lattice, P' also cuts the surface of the sphere of diffraction in two similar points below the equatorial plane. This geometrical construction thus accounts for four diffraction spots which are observed from a given plane on the rotation photograph. When P and P' lie in the central equatorial plane in the reciprocal lattice, they cut through the sphere at the same points so that there are but two spots on the equatorial (center) line of the photograph. If, during the rotation of the lattice about a given

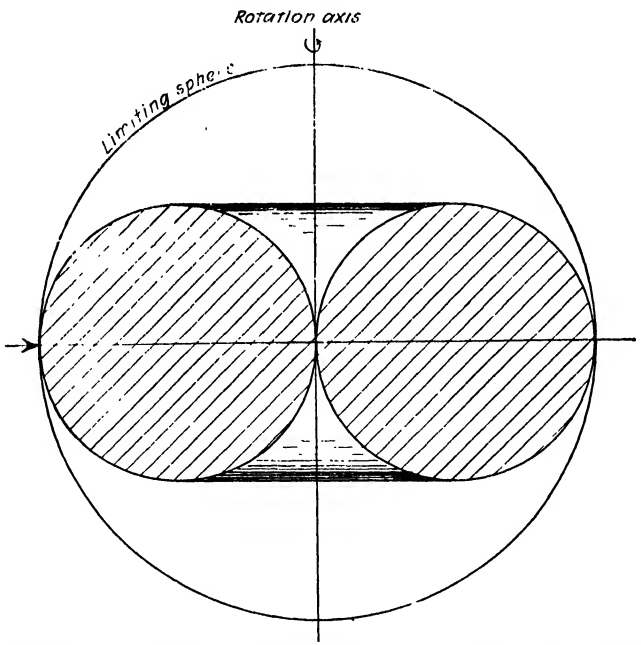

FIG. 18.—Cross-section through the torus formed by the rotation of the sphere of diffraction. (*After Bernal.*)

rotation axis, P is in such a position that it cannot touch the surface of the sphere of diffraction, then no diffraction is possible during this rotation for the crystal plane represented by P.

Since the question is one of relative motion, it is immaterial in the geometrical construction whether we consider the x-ray beam stationary and the crystal rotating, or whether we consider the crystal stationary and the x-ray beam to revolve about the rotation axis in the opposite sense. If we adopt this latter view, then the sphere of diffraction, rotating with the x-ray beam, traces out a ring-shaped solid figure (shown in projection in Fig. 18), called by mathematicians a "torus," within the volume of which lie all the points in the reciprocal lattice which can give diffraction spots during the course of the rotation about this particu-

lar axis. For the investigation of planes outside of the region included in this torus, rotation photographs about some other axis must be employed so that these points of the reciprocal lattice may fall inside of the new torus corresponding to the new rotation axis.

Whatever the rotation axis, there are some planes which must lie outside the region of possible diffraction for a given x-ray wave length. The points P for such planes obviously lie outside the "limiting sphere" of Figs. 17 and 18, whose radius is $2K^2/\lambda$ (or 2, if K^2 is put equal to λ). These are, of course, the planes whose grating spaces are so small that in Bragg's law $2d$ becomes less than $n\lambda$ so that $\sin\theta$ acquires physically impossible values greater than unity.

The Relation between Coordinates in the Reciprocal Lattice and the Corresponding Diffraction Spots on the Rotation Photograph.—The

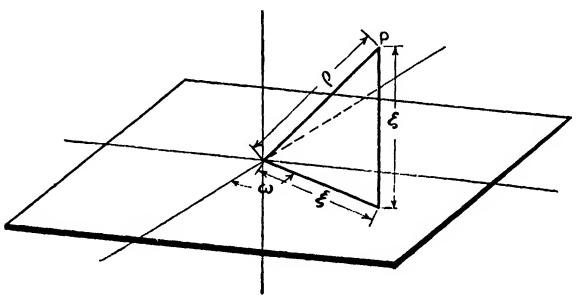

FIG. 19.—Cylindrical coordinates for the point P in reciprocal space.

position of the point P in reciprocal space may be expressed best in terms of cylindrical coordinates ξ, ζ, ω, as shown in Fig. 19. The axis of the coordinate system is chosen to coincide with the axis of rotation of the crystal. The origin of coordinates lies at the center of the crystal and coincides with the origin of the reciprocal lattice network. ξ is the coordinate which measures the radial distance of the point P, while ζ measures the distance of P above or below a central plane through the origin perpendicular to the axis of rotation. ω, measuring the azimuth angle of rotation of the crystal, is indeterminate in the case of a complete rotation and may be neglected for the moment in the discussion.

The problem now is to relate these coordinates ξ and ζ in the reciprocal lattice to the coordinates of the diffraction spots corresponding to P on the photographic plate or circular film. Trigonometric equations for this purpose have been worked out[5] somewhat as in the case of Eqs. (9), (10), (11), and (12). These equations are, however, very laborious to use for the large number of diffraction spots commonly occurring on a photograph, and a graphical method is usually employed. Figures 20 and 21 represent charts for the plate and cylindrical film, respectively. Such charts, when reduced to the proper scales on a piece of photographic film, can be laid over the photograph and the values of ξ and ζ correspond-

ing to all the diffraction spots can be read off directly and listed. The lines of constant ζ on the charts have the form of the familiar layer lines on the photograph, namely, a system of hyperbolas for the photo-

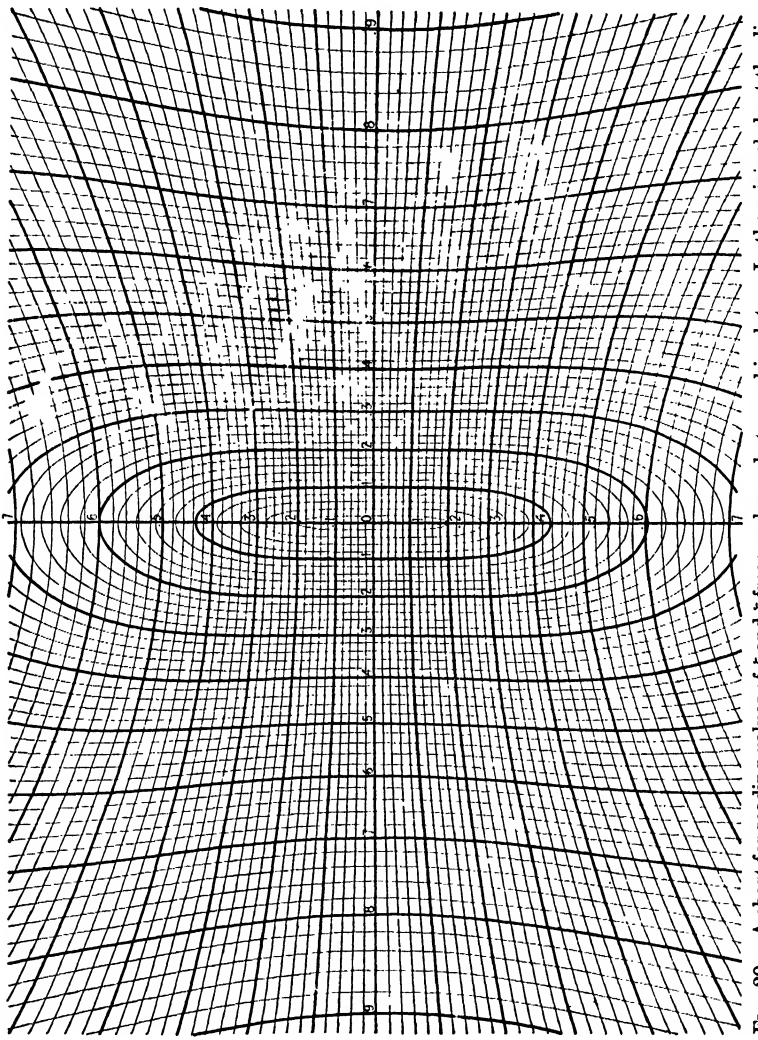

FIG. 20.—A chart for reading values of ξ and ζ from a plane photographic plate. In the original chart the distance from crystal to plate is 10 cm. The length of the original chart is 11 in. (*After Bernal.*)

graphic plate and straight lines for the cylindrical film. All diffraction spots on a given layer line have a constant value of ζ as read on the chart. Assume that, for any given layer line on the photograph, ζ has a given value ζ_a. Then all planes contributing spots to this layer line have their representations in the reciprocal lattice as lattice points lying in the same geometrical plane. This plane is perpendicular to the rota-

tion axis and at a distance ζ_a above or below a similar plane through the origin. Thus in Fig. 22 the reciprocal lattice points in the basal plane A_0B_0 correspond to diffraction spots on the equatorial line of the photograph. Lattice points in A_1B_1 and $A_1'B_1'$ give rise to spots on the first layer lines, respectively above and below the equatorial lines. A_2B_2 and $A_2'B_2'$ correspond to the second layer lines above and below on the photograph. The complex curves of constant ξ on the chart correspond to the row lines previously mentioned. Such lines in the reciprocal

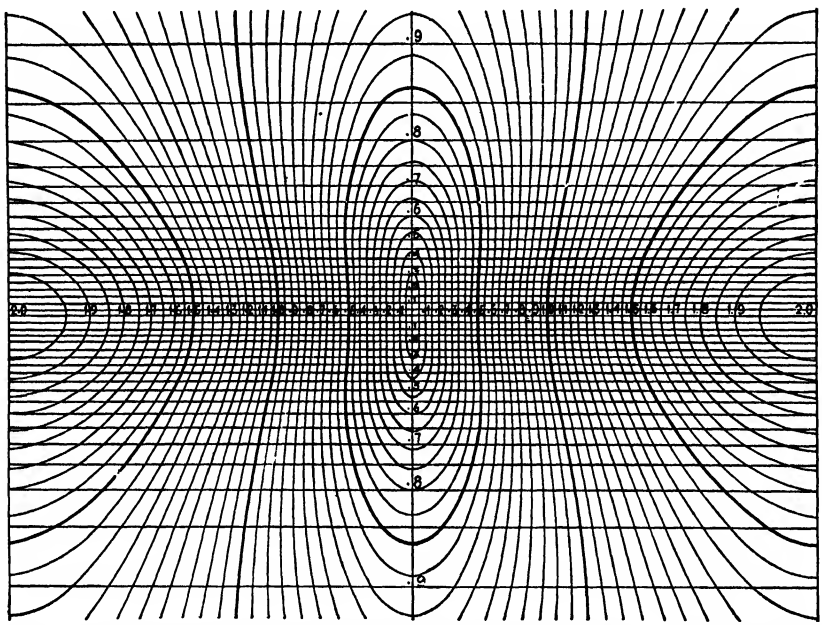

FIG. 21.—A chart for reading values of ξ and ζ from a cylindrical film. In the original the radius of the camera is 5 cm. The length of the original chart is $12\frac{5}{16}$ in. (*After Bernal.*)

lattice are parallel to the rotation axis, for example, the line between points $(\bar{2}\,1\,\bar{1})$ and $(\bar{2}\,1\,1)$ in Fig. 22.

ASSIGNMENT OF INDICES BY THE GRAPHICAL METHOD

The steps in the use of the charts are briefly as follows:

1. The primitive translations for the crystal are determined from the requisite number of rotation photographs.
2. The scalar values a^*, b^*, c^* of the unit-vectors $\bar{a}^*$, $\bar{b}^*$, $\bar{c}^*$ are determined for the reciprocal lattice.
3. By means of the chart the values of ξ and ζ are read from a photograph and listed.
4. This list is compared with a list of values of ξ and ζ obtained from the reciprocal lattice for all possible diffracting planes, and the agreement between the two sets of values is used to index the diffraction spots.

We shall now discuss these steps for the special cases of orthogonal, monoclinic, triclinic, and hexagonal crystals.

Case of an Orthogonal Crystal.—In the case of such a crystal there is the simplification that the reciprocal unit-vectors $\bar{a}^*$, $\bar{b}^*$, $\bar{c}^*$ coincide in direction, respectively, with the vectors $\bar{a}$, $\bar{b}$, $\bar{c}$ of the original lattice.

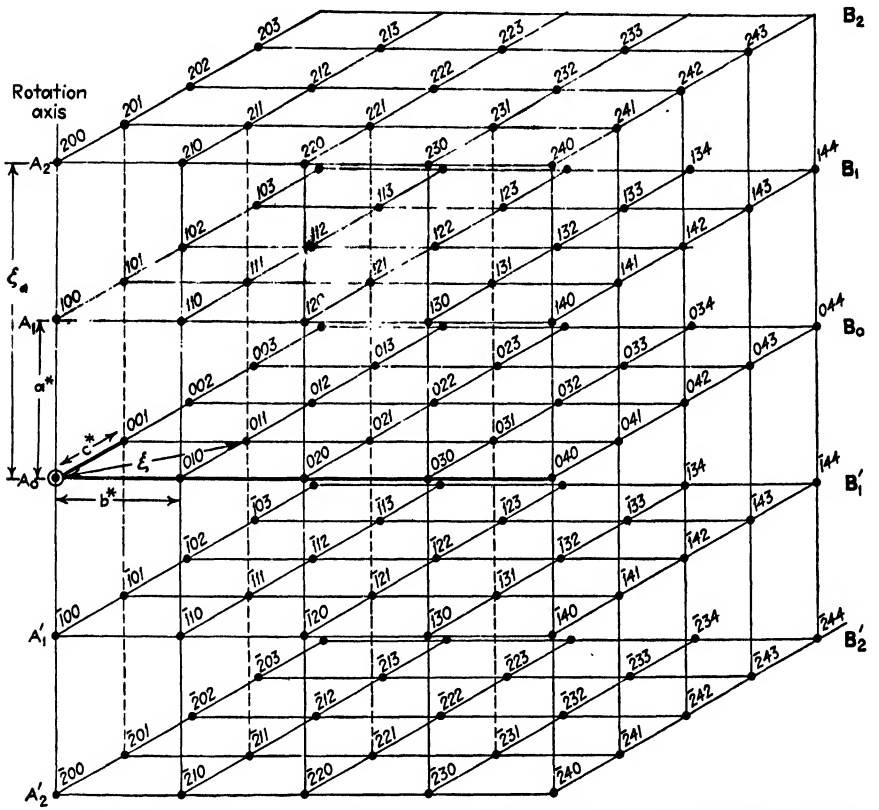

FIG. 22.—Diagram of the reciprocal lattice derived from an orthorhombic crystal lattice. (For the sake of simplicity in the drawing, the bars are omitted from the designations of the points.)

If a rotation photograph is taken about each of the axes X, Y, and Z,* then the dimensions of the unit-crystal, a, b, and c, along each of these axes can be determined as already described in the discussion of Eq. (6). From the values of a, b, and c the values of a^*, b^*, and c^* may be determined at once from the relation:

* Strictly speaking, the axes are called X, Y, and Z, and the unit-distances in the crystal along these axes are called a, b, and c, respectively. Crystallographers often use a, b, and c to represent not only the distances but also the axes along which these distances are measured.

$$\left.\begin{aligned} a^* &= \frac{K^2}{a} = \frac{\lambda}{a} \\ b^* &= \frac{K^2}{b} = \frac{\lambda}{b} \\ c^* &= \frac{K^2}{c} = \frac{\lambda}{c} \end{aligned}\right\} \tag{20}$$

More easily still, a^*, b^*, and c^* may be determined graphically by reading from the chart the values ζ_a, ζ_b, and ζ_c for the layer lines of the rotation diagrams. If ζ_a is the mean value of ζ for the nth layer line as read from the chart from the a-axis rotation photograph, then

$$\left.\begin{aligned} a^* &= \frac{\zeta_a}{n} \\ \text{Similarly,} \quad b^* &= \frac{\zeta_b}{n} \\ \text{from the } b\text{-axis rotation photograph.} \quad c^* &= \frac{\zeta_c}{n} \\ \text{from the } c\text{-axis rotation photograph.} \end{aligned}\right\} \tag{21}$$

From these values of a^*, b^*, and c^* the reciprocal lattice may be constructed. In an orthogonal system, only a basal network is necessary for the determination of the value of ξ and ζ for the various lattice points. This basal network is repeated for the upper layers since for rotations about coordinate axes in an orthogonal system the lattice points lie on lines parallel to the rotation axis, *i.e.*, on lines of constant ξ. This is brought out in Fig. 22. From such a network, laid off to scale, the values of ξ for all the reciprocal lattice points may be measured with sufficient accuracy. A comparison of such values with the corresponding values of ξ from, let us say, the a-axis rotation photograph, identifies the diffraction spots on the diagram. Analytically, of course, for the a-axis rotation,

$$\begin{aligned} \xi^2 &= k^2 b^{*2} + l^2 c^{*2} \\ \zeta &= h a^* \end{aligned} \tag{22}$$

The simplicity of this graphical method, as compared with the analytical method of Eq. (2), may be illustrated by a redetermination of the indices of the diffraction spots on the rotation photograph of urea (Fig. 5). The results are shown in Table II. In the second and third columns are recorded the values of ξ and ζ for each diffraction spot on the photograph as read directly from the chart. The values of ζ for the first and second layer lines give at once the value of $c^* = 0.330$. Similarly, the rotation photograph about the a-axis gives the value $a^* = 0.273$. Since the

crystal is tetragonal, we have then $a^* = b^* = 0.273$; and the basal network for the c-axis rotation consists of a network of squares of side $a^* = 0.273$. From this network the values of ξ in the fifth column are calculated analytically or are scaled graphically. A comparison of the calculated and observed values identifies the various diffracting planes.

TABLE II.—FINDING INDICES OF DIFFRACTION SPOTS BY THE GRAPHICAL METHOD FOR THE c-AXIS ROTATION OF A CRYSTAL OF UREA

Intensity	Values of coordinates from chart for various diffraction spots		Radiation	Values from reciprocal network for possible planar diffraction spots		Indices of diffracting plane
	ξ	ζ		ξ	ζ	
Equatorial line						
m	0.350	0	β			
vs	0.390	0	α	0.389	0	(110)
w	0.500	0	β			
vs	0.555	0	α	0.546	0	(200)
vs	0.620	0	α	0.614	0	(210)
w	0.710	0	β			
s	0.780	0	α	0.778	0	(220)
ms	0.875	0	α	0.864	0	(310)
m	1.000	0	α	0.988	0	(320)
w	1.055	0	β			
w	1.115	0	β			
s	1.170	0	α	1.167	0	(330)
s	1.235	0	α	1.226	0	(420)
				0.273	0	(100)
				0.819	0	(300)
				1.092	0	(400)
				1.128	0	(410)
First layer line						
vs	0.280	±0.330	α	0.273	±0.330	(101)
vs	0.395	±0.330	α	0.389	±0.330	(111)
s	0.550	±0.330	α	0.546	±0.330	(201)
m	0.610	±0.330	α	0.614	±0.330	(211)
s	0.780	±0.330	α	0.778	±0.330	(221)
m	0.830	±0.330	α	0.819	±0.330	(301)
s	0.875	±0.330	α	0.864	±0.330	(311)
w	1.110	±0.330	α	1.092	±0.330	(401)
vw	1.140	±0.330	α	1.128	±0.330	(411)
vw	1.170	±0.330	α	1.167	±0.330	(331)
mw	1.240	±0.330	α	1.226	±0.330	(421)
				0.988	±0.330	(321)
Second layer line						
vs	0.275	±0.660	α	0.273	±0.660	(102)
ms	0.390	±0.660	α	0.389	±0.660	(112)
w	0.550	±0.660	α	0.546	±0.660	(202)
m	0.620	±0.660	α	0.614	±0.660	(212)
w	0.780	±0.660	α	0.778	±0.660	(222)
vw	0.825	±0.660	α	0.819	±0.660	(302)
w	0.870	±0.660	α	0.864	±0.660	(312)
w	1.000	±0.660	α	0.988	±0.660	(322)
vw	1.100	±0.660	α	1.092	±0.660	(402)
vw	1.140	±0.660	α	1.128	±0.660	(412)
vw	1.160	±0.660	α	1.167	±0.660	(332)
				1.226	±0.660	(422)

Case of a Monoclinic Crystal.—For a monoclinic crystal which is rotated about its b-axis the situation is similar to the orthogonal case. The basal network is repeated for the upper layer lines so that the values of ξ are the same for the various layers. Since the basal network is not orthogonal, it must be drawn through a range of at least 180° to include the ξ's for all the combinations of positive and negative values of h and l. Such a network is shown in Fig. 25. In the monoclinic case, Eqs. (21) become:

$$\left.\begin{aligned} b^* &= \frac{\zeta_b}{n} \\ a^* &= \frac{\zeta_a}{n \sin \beta} \\ c^* &= \frac{\zeta_c}{n \sin \beta} \end{aligned}\right\} \tag{23}$$

where β is the angle between the a- and c-axes, and ζ_a, ζ_b, and ζ_c are, respectively, the values for the nth layer line on the a-, b-, c-axis rotation photographs. Analytically,

$$\left.\begin{aligned} \xi^2 &= h^2a^{*2} + l^2c^{*2} - 2hla^*c^* \cos \beta \\ \zeta &= kb^* \end{aligned}\right\} \tag{24}$$

The rotation photographs about the a- and c-axes of a monoclinic crystal are seldom used for the general identification of planes corresponding to diffraction spots. They are, of course, necessary in the determination of the dimensions of the unit-crystal. In the case of rotation about the a- or the c-axis, the row lines of constant ζ vanish and the computation of the values of ξ is more awkward than in the case of rotation about the perpendicular b-axis. If for any reason it becomes desirable to determine in a monoclinic crystal a large number of diffraction spots which do not appear to advantage on the b-axis rotation photograph, then, rather than use an a- or a c-axis rotation, it is often more advantageous to take a rotation photograph about the a^*- or the c^*-axis. Reference to Fig. 16 shows that a rotation about a^* is equivalent to a rotation about a normal to the b-c plane. Similarly, a rotation about c^* is equivalent to a rotation about a normal to the a-b plane. In such a photograph the layer lines disappear and the spots are spread more uniformly over the whole photograph, on row lines of constant ξ. This greater distribution renders the overlapping of spots less probable. Such a photograph is shown in Fig. 6.

Case of a Triclinic Crystal.—The interpretation of rotation photographs for crystals of the triclinic system requires somewhat the same procedure as for monoclinic crystals. The interpretation is, however, much more complicated. For a full treatment of the interpretation the reader is referred to the literature on the subject.[5]

Case of a Hexagonal Crystal.—For crystals belonging to the hexagonal system the interpretation of the rotation photographs is much simplified by the use of orthohexagonal coordinates (see Fig. 10, Chap. II), by which the hexagonal space-lattice is expressed in terms of three mutually perpendicular axes of unit-length: a, $a\sqrt{3}$, c.

USE AND INTERPRETATION OF OSCILLATION PHOTOGRAPHS

So far we have considered only the interpretation of complete rotation photographs. In some cases such interpretations result in ambiguities, and the rotation photograph must be supplemented by one or more oscillation photographs. Quite often in crystals of complex structure, especially in organic crystals with their large interplanar spacings, the diffracted beams on the layer lines overlap and difficulties arise in the assignment of indices with any degree of certainty. The oscillation photograph, because of its more limited range of possible diffractions, leads to a correct determination of the indices in such cases. Because of the possibility of greatly increased intensity of the recorded diffraction spots, the oscillation photograph is also of great use in bringing out weak spots which might be overlooked on the less intense rotation photograph. Such weak spots may be very important in the determination of the space-group.

In making the oscillation photograph, the motion of the crystal is limited to a turning to and fro through a definite small arc. Any diffraction spots which may appear upon the photographic plate or film can come only from planes in the crystal which pass through a diffracting position as the crystal moves within this given arc. In order that such planes may be determinable, it becomes necessary to know the orientation of the crystal with regard to the direction of the primary x-ray beam. This is usually accomplished by bringing one known vertical face of the crystal exactly perpendicular to the x-ray beam. The exact method to be employed will depend upon the nature of the crystal and the form of the apparatus. Where bright, well-developed crystal faces exist, one of the optical methods described at the beginning of this chapter is particularly suitable. With the crystal in this known position, the position of the pointer on the fixed azimuth circle of the instrument is read. The orientation of the crystal with regard to the direction of the beam may then be determined at any phase of the rotation by means of a new reading on the azimuth circle.

From the known orientation of the crystal it is not difficult to determine graphically what planes will pass through a diffracting position during an oscillation over a given range. It was shown in the discussion of Fig. 17 that diffraction can take place only when the point in the reciprocal lattice representing the plane in question intersects the surface

of Ewald's sphere of diffraction. It was also shown to be quite logical to assume that the reciprocal lattice network remains stationary while the x-ray beam and the sphere of diffraction revolve about the rotation axis in the opposite sense. The solid figure cut out in space by the surface of the sphere was found to be a torus and all the points in the reciprocal lattice which can diffract during the complete rotation were found to lie within the torus. Instead of moving through a complete revolution, the x-ray beam in the oscillation photograph moves through only a small angle with regard to the stationary reciprocal lattice. The solid figure thus cut out by the spherical surface consists of two cup-shaped solids. The interiors of these include all points of the reciprocal lattice which can diffract within the oscillation limits.

Figure 23 illustrates a 30° oscillation about the a-axis of the orthorhombic lattice pictured in Fig. 22. Figure 23a shows as a great circle the trace of the sphere of diffraction on the basal plane through the origin. Let XO be the direction of the beam and let $S'OT$ be the intersection of the sphere with the plane at the beginning of the oscillation. If the crystal moves counterclockwise about the axis O, this is equivalent to a clockwise rotation of the x-ray beam through the same angle XOX' with regard to a stationary lattice. The final position of the great circle at the end of the oscillation is SOT'. The surface of the sphere has therefore swept out on the basal plane the two portions which are shaded in the figure, and all the lattice points lying in the plane and included within the two shaded lunes have passed through a diffracting position. Their diffraction spots are to be found on the equatorial line of the oscillation photograph. The points in the lune $MSOS'$ will diffract to the right of the central spot and those in the lune $MTOT''$ will diffract to the left.

A plane surface, parallel to the basal plane of the reciprocal lattice and at a distance ζ above or below it, will have as its intersection with the sphere of diffraction a circle of smaller radius, corresponding to the circle GH in Fig. 17. The radius of the circle may be determined graphically from an auxiliary diagram as shown in Fig. 23b. The values of r_1 and r_2, scaled from this diagram, give at once the radii of the circles of intersection of plane surfaces at distances ζ_1 and ζ_2 above the central plane. The construction for determining the possible diffracting planes for the second layer line for the given oscillation of the reciprocal lattice is shown in Fig. 23c. The shaded lunes, embracing fewer points than in the case of the basal plane, enclose all possible diffracting points in the reciprocal lattice for the second layer line. If the oscillation is about a coordinate crystal axis, orthogonal to the other two, the same basal network may be used throughout for the equatorial line and all layer lines. The only change is that of one Miller index in going from one layer line to another. This is brought out in Figs. 23a and c.

Figure 24 is an oscillation photograph of a crystal of monoclinic stilbene about the *b*-axis. The (100) face was first set perpendicular

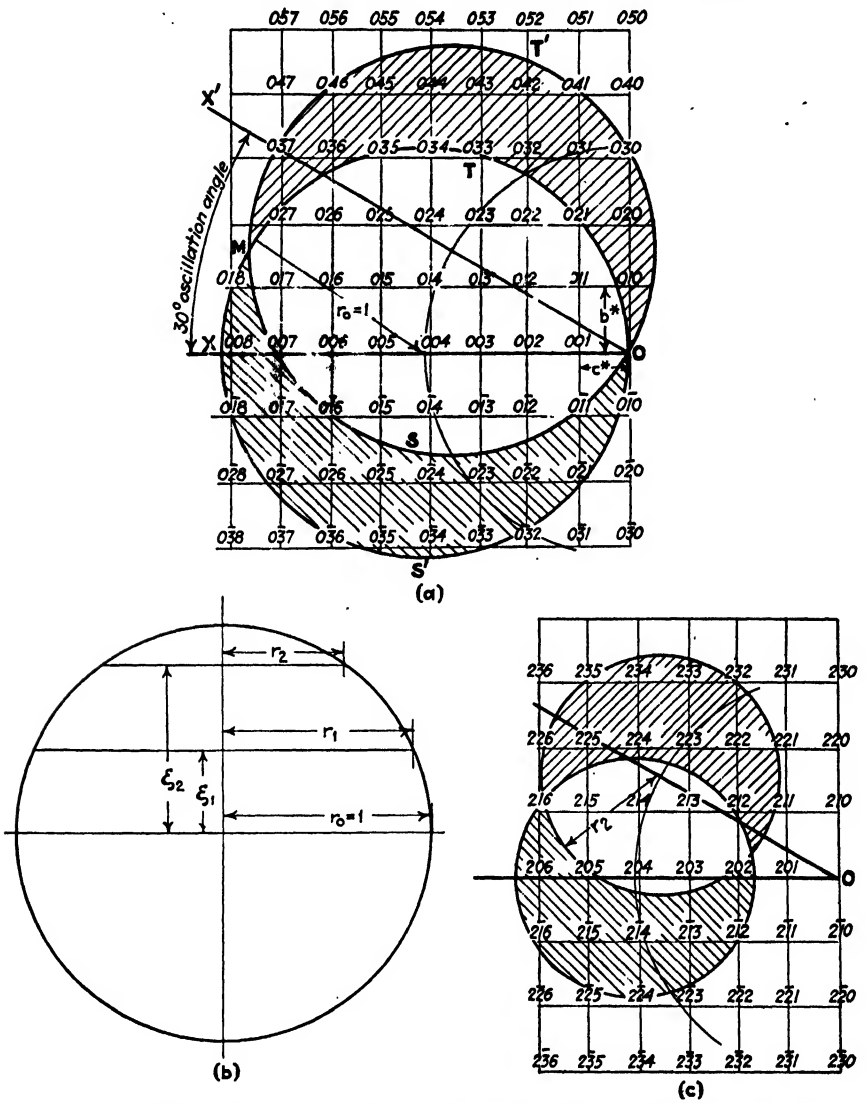

FIG. 23.—Diagrams for the determination of possible diffracting planes for the oscillation photograph of an orthorhombic crystal. (*a*) Network for the basal plane; (*b*) auxiliary diagram; (*c*) network for the second layer line.

to the x-ray beam by the optical methods already described. This setting is equivalent to putting the a^*-axis parallel to the x-ray beam. Figure 25 represents the construction to determine the possible diffracting planes for an oscillation where the crystal is rocked from 71° to

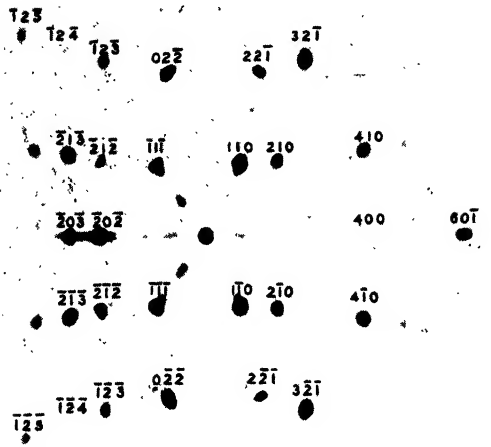

FIG. 24.—Oscillation photograph of monoclinic stilbene about the *b*-axis. Copper radiation with nickel filter. Beam perpendicular to flat photographic plate.

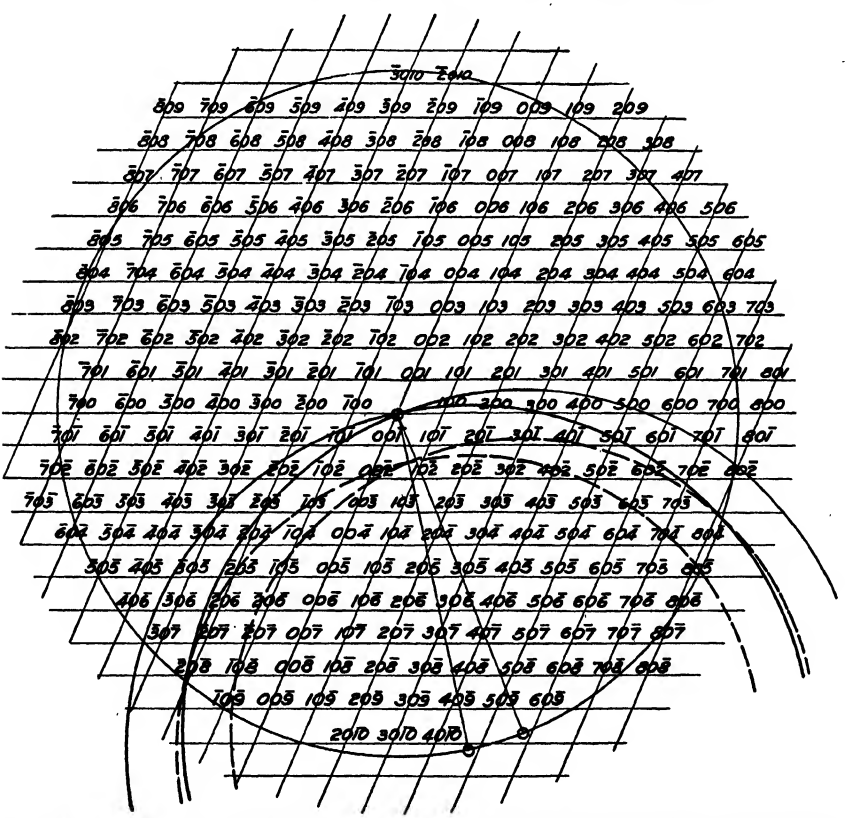

FIG. 25.—Construction necessary to determine possible diffracting planes; limiting rocking angles 71° and 81°.

81° with respect to the original setting. The basal network, constructed as previously described, serves for the equatorial line and the two layer lines visible on the photograph. To avoid complication of the diagram the arcs are drawn only for the equatorial line and the second layer line. Table III shows the process of identification of the diffraction spots actually observed. It should be noted that a few points just outside

TABLE III.—FINDING INDICES OF DIFFRACTION SPOTS ON OSCILLATION PHOTOGRAPH OF STILBENE ABOUT THE *b*-AXIS

Left of center					Right of center				
Planes	Possible spots		Spots read		Planes	Possible spots		Spots read	
	ξ	ζ	ξ	ζ		ξ	ζ	ξ	ζ
Equatorial line									
$\bar{1}0\bar{1}$*	0.202	0			300*	0.404	0		
200	0.403	0	0.405	0	400	0.538	0	0.540	0
$\bar{2}0\bar{3}$*	0.489	0	0.495	0	500	0.674	0		
$\bar{3}0\bar{3}$*	0.605	0			$50\bar{1}$*	0.636	0		
$\bar{3}0\bar{4}$	0.692	0			$60\bar{1}$	0.769	0	0.780	0
$\bar{3}0\bar{5}$	0.784	0			$70\bar{1}$	0.904	0		
Second layer line									
$0\,2\,\bar{2}$ $0\,\bar{2}\,\bar{2}$	0.210	±0.535	0.210	±0.535	$2\,2\,\bar{1}$ $2\,\bar{2}\,\bar{1}$	0.246	±0.535	0.250	±0.535
$\bar{1}\,2\,\bar{3}$ $\bar{1}\,\bar{2}\,\bar{3}$	0.388	±0.535	0.390	±0.535	$3\,2\,\bar{1}$ $3\,\bar{2}\,\bar{1}$	0.376	±0.535	0.380	±0.535
$\bar{1}\,2\,\bar{4}$ $\bar{1}\,\bar{2}\,\bar{4}$	0.489	±0.535	0.495	±0.535	$4\,2\,\bar{1}$ $4\,\bar{2}\,\bar{1}$	0.492	±0.535		
$\bar{1}\,2\,\bar{5}$ $\bar{1}\,\bar{2}\,\bar{5}$ *	0.593	±0.535	0.600	±0.535	$5\,2\,\bar{2}$ $5\,\bar{2}\,\bar{2}$	0.618	±0.535		
$\bar{2}\,2\,\bar{5}$ $\bar{2}\,\bar{2}\,\bar{5}$	0.682	±0.535			$6\,2\,\bar{2}$ $6\,\bar{2}\,\bar{2}$	0.744	±0.535		
$\bar{2}\,2\,\bar{6}$ $\bar{2}\,\bar{2}\,\bar{6}$	0.778	±0.535			$6\,2\,\bar{3}$ $6\,\bar{2}\,\bar{3}$	0.738	±0.535		
					$7\,2\,\bar{3}$ $7\,\bar{2}\,\bar{3}$	0.863	±0.535		

the area of possible diffraction have been included in the table of possible diffracting planes and marked with an asterisk (*). This is to allow for small inaccuracies of setting of the crystal and for possible distortions in the crystal itself, both of which may cause diffraction spots to appear on the photograph although the corresponding calculated points on the diagram are as far as 1° of rotation away from the diffracting zone.

With the oscillation method just described, one is able to determine only within the oscillation limits the exact position in the turning of the crystal at which any given diffraction occurs. The Weissenberg x-ray goniometer,[9] a very ingenious device in which the cylindrical recording

film moves up and down parallel to the axis as the crystal turns, enables one to read the exact angular distance traversed by the crystal between the recording of any two diffraction spots on the film. A purely schematic diagram of the instrument is given in Fig. 26. A photograph of the actual instrument is shown in Fig. 27. The crystal can be oscillated through any desired range up to 180° by means of the motor-driven wheel *W*. The direction of rotation is automatically reversed by the proper electrical contacts. As the wheel *W* turns, it winds or unwinds a chain which, passing over a pulley *P* moves the wheeled carriage bearing the cylindrical film *F*. The film thus moves up and down parallel to the axis of rotation in exact synchronism with the to-and-fro angular oscillation of the crystal about the rotation axis. Any series of diffraction spots which would ordinarily be registered upon a single layer line is thus drawn out by the motion of the film into a spiral array of spots distributed over the whole surface of the film. A cylindrical shield *S* pierced with a slot *L* is inserted over the stationary head *H* of Fig. 27 between the crystal and the film. This shield prevents the register-

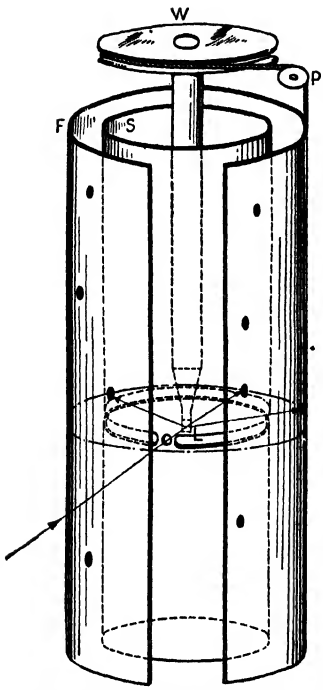

FIG. 26.—Schematic diagram of Weissenberg x-ray goniometer.

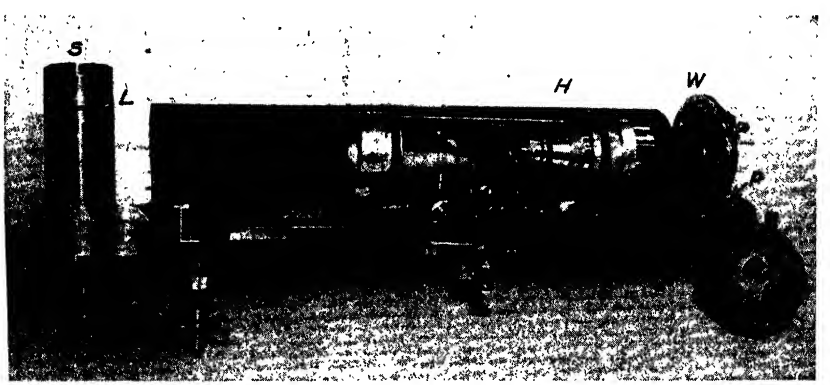

FIG. 27.—Photograph of Weissenberg-Bohm x-ray goniometer.

ing of more than one layer line at an exposure. Confusion of spots from several layer lines upon the same film is thus avoided.

If the linear vertical travel of the camera film for a half-revolution is d, then $d/180$ is the linear distance moved per degree of revolution of the crystal. The dimensions of the instrument are such that $d/180$ is exactly 1 mm. Hence the linear distance in millimeters, measured parallel to the axis of the camera, between any two diffraction spots on the film gives at once the angular distance turned through by the crystal between the two corresponding diffracting positions. The

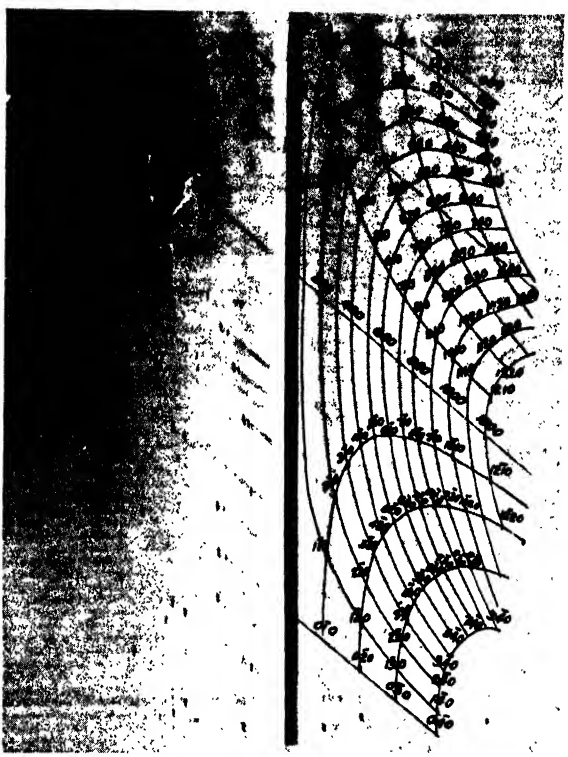

FIG. 28.—Weissenberg photograph of monoclinic *p*-dichlorobenzene rotated about the *c*-axis with a superimposed network for interpretation. Unfiltered copper radiation.

Weissenberg camera film thus gives not only the measurement of the grating spacings of the planes involved, but it also gives the possibility of measuring directly the angular relations between any two diffracting planes in the crystal. The instrument is thus, as its name suggests, the x-ray counterpart of the optical goniometer. For the details of the goniometer determination in the most general case of the angle between any two diffracting planes in the crystal, the reader is referred to the references already cited.[9]

The Weissenberg camera may be used to good advantage in the indexing of diffraction spots which are so thickly clustered on layer lines

as to require otherwise a large number of oscillation photographs. Certain relations in the Weissenberg diagram aid in the ready identification of the various diffraction spots. This is illustrated by Fig. 28 which shows a Weissenberg diagram of the zero line of monoclinic *p*-dichlorobenzene rotated about the *c*-axis. One half of the diagram is overlaid with a network showing the relation of the diffraction spots to each other on the diagram. It will be noted that the spots can be made to lie upon two intersecting families of curves. Curves of the one family are characterized by a constant value of the h index along each curve, while the k index remains constant along each individual curve of the second family. The value of l is, of course, zero throughout the diagram. Successive orders of any given plane lie upon the same straight line. These lines are made more apparent by the streaks due to the general radiation. The diffraction spots due to the β wave length are displaced along these streaks toward the central line of the diagram and thus are easily distinguished. As would be expected from the rectangular nature of the basal network in such a rotation, the Weissenberg diagram exhibits symmetry with regard to the lines representing diffraction spots of nomenclature $(h\,0\,0)$ and $(0\,k\,0)$. The diagram has a center of symmetry at each of the points where such lines cross the central line of the figure. Such points serve as convenient datum points for measuring angular relations between planes.

In case of any doubt as to the correctness of the indices assigned to any spot, a measurement of angle with regard to the datum point together with a measurement of ξ (see Figs. 19 and 21) serves to fix the diffraction spot on the reciprocal basal network.

INTENSITY RELATIONS FOR DIFFRACTION SPOTS ON ROTATION PHOTOGRAPHS

After the dimensions of the unit-crystal have been determined and the space-group* fixed for a given crystal, the last and most difficult step consists in fixing the positions of the various atoms in the crystal cell. Such a determination makes use either quantitatively or qualitatively of the observed intensities of a large number of diffraction spots from many crystal families of planes. In using the rotation photograph for this purpose it must be borne in mind that all diffraction spots are not recorded with equal advantage on a rotation plate or film. In addition to the general factors affecting intensity of diffraction, such as polarization of the beam, absorption by the crystal, and the intensity variations dependent upon the perfection of the crystal, there are two further purely geometrical factors which are of especial importance in rotation photographs.

* See Chaps. VIII and IX.

The first of these factors depends upon the number of times during the rotation that any given type of plane* makes a record on the film. Since such records are superimposed during the course of a complete rotation, the total blackening on the film will depend upon the symmetry of the crystal and also upon the position of the plane with respect to the rotation axis. Thus, in general, a single plane in a crystal of lowest symmetry gives rise, as we have seen, to four spots on the film. When this plane is parallel to the rotation axis, the number of spots is reduced to two, and each spot on the equatorial line is the result of two diffracted beams—one from the "forward" and one from the "back" side of the plane. Because of the symmetry relations in various crystal systems there will be also the possibility, for certain rotation axes, of the superposition of the diffraction spots from planes symmetrically situated with regard to one another. Hence, when the complete rotation photograph is used as a basis for estimating the relative intensities of the various diffraction spots, care must be taken to evaluate each spot on the film as the composite of the proper number of superimposed diffracted beams.

The second factor to be considered is that even in the case of an oscillation photograph, where each spot on the photograph is the result of one single planar diffraction, certain spots may be greatly intensified because of their positions on the film. This follows from the fact that, owing to such causes as the divergence of the x-ray beam and the imperfection of the crystal, no plane diffracts sharply only at the precise angle θ required by Bragg's law. The plane really diffracts throughout an angular range α which may be expressed as lying between the limits of the angle θ and a slightly larger angle $(\theta + \alpha)$. (See first part of Chap. X.) For any given plane the intensity recorded on the photograph will be directly proportional to the time during which the plane remains in this diffracting range α while the crystal is rotating. The time of passage through the diffracting zone is constant for all planes which are parallel to the rotation axis but increases from plane to plane as the normal to the diffracting plane makes a smaller and smaller angle with the rotation axis. Equation (25) states[10,11] that the variation in intensity I of a diffraction spot is inversely proportional to the rate of change of the diffracting angle θ as the crystal rotates. In terms of the angle μ for the given layer line, we have

$$I = C\left(\frac{1}{\frac{d\theta}{dt}}\right) = k\frac{1}{\sqrt{1 - \left(\frac{\sin \mu}{\sin 2\theta}\right)^2}} \tag{25}$$

* The word "plane" is used here to represent a whole family of parallel atomic planes, not just some one individual plane.

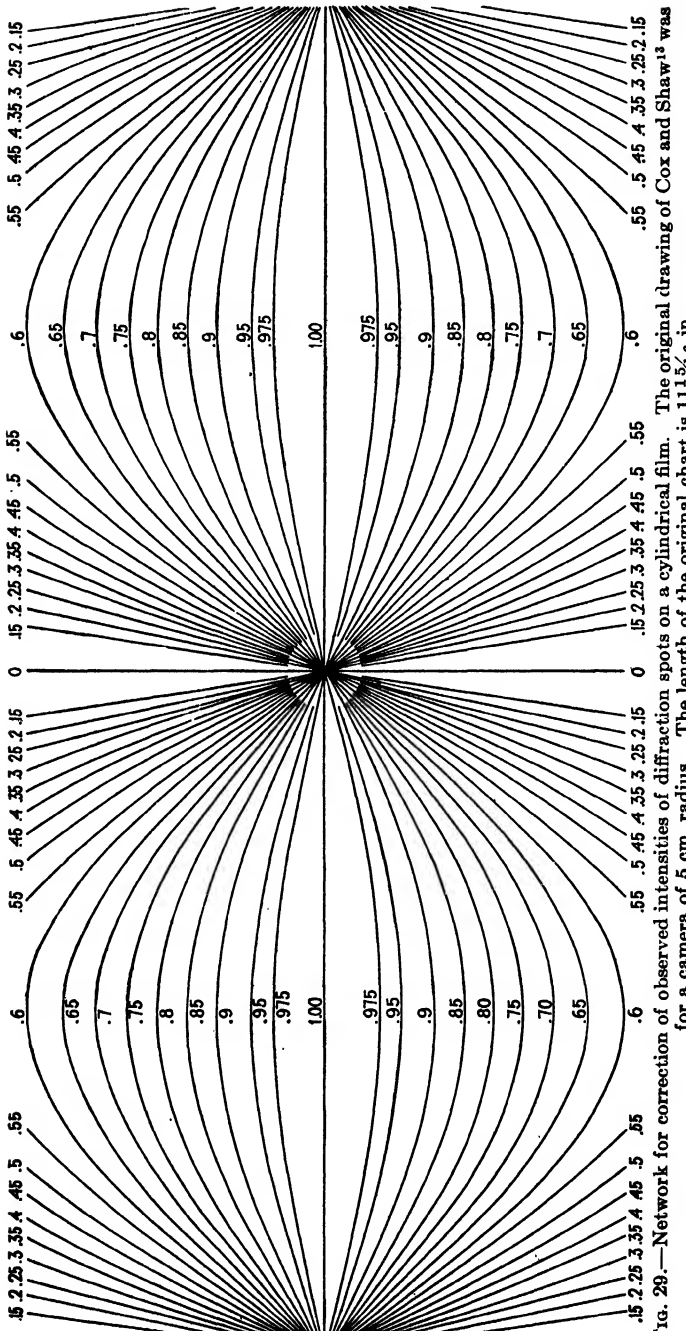

FIG. 29.—Network for correction of observed intensities of diffraction spots on a cylindrical film. The original drawing of Cox and Shaw[13] was for a camera of 5 cm. radius. The length of the original chart is $11\frac{15}{16}$ in.

where C and k are proportionality constants. For all planes parallel to the axis of rotation, $\sin \mu = 0$ and $I = k$. The spots on the layer lines arise from planes having a somewhat longer time of passage than for spots in the equatorial plane so that their intensities are correspondingly enhanced. Especially where $\sin \mu$ is almost equal to $\sin 2\theta$ (*i.e.*, for spots near the vertical center line of the photograph) the intensities of the recorded spots may be enormously increased.

The correction chart[11] in Fig. 29 shows lines of constant intensity for a cylindrical camera. Marked on each line is the correction factor by which the intensity of a diffraction spot falling on that line must be multiplied to reduce it to the same relative terms as the spots on the equatorial line where the factor is unity. For most regions on the film the judgment of the intensities of the spots needs no great correction, but for spots near the vertical axis the estimated intensities may be five or six times too great. Such enhancement may be observed in the four spots of the (1 0 2) plane in the rotation photograph of urea shown in Fig. 5. The apparent intensity of diffraction from such planes must always be discounted heavily, and a more accurate judgment of the true intensity of diffraction must be found, if necessary, from the spots of rotation photographs about other axes.

SUMMARY

In this chapter the rotation method of crystal analysis has been considered. A brief account of the experimental method has been given, and the underlying theory has been discussed. A rather extended account of graphical methods of interpreting the photographs has been presented since without such methods interpretation becomes impossibly laborious.

It has been shown that the rotation method offers unique advantages in the determination of the dimensions of the true unit-crystal and certain other advantages in the solution of crystal structures. It is not, however, to be supposed that any one method is to be used exclusively in the analysis of a crystal. The Laue method is indispensable in determining symmetry relations, and the ionization spectrometer (see Chaps. V, X, XI) is still the most accurate instrument for determining the intensities of diffracted beams. Information gained by the rotation method should be supplemented by such methods and by the results of the theory of space-groups.

We must now interrupt our discussion of experimental methods (Chaps. IV, V, VI, and VII) in order to take up in considerable detail the theory of space-groups and its application to the various methods of crystal analysis which we have so far studied. After having rounded out in this way (Chaps. VIII and IX) our knowledge of the easier methods, we shall be ready to study in Chaps. X and XI an extension of the Bragg

method which makes it the most powerful of all for the precise determination of atomic positions in the crystal cell.

References

1. E. Schiebold, *Fortschritte Mineral., Kryst. Petrog.*, **11**, 113 (1927). Most complete account of method.
2. M. Polanyi, *Zeit. Physik*, **7**, 149 (1921).
3. M. Polanyi, and K. Weissenberg, *Zeit. Physik*, **9**, 123 (1922); *Zeit. Physik*, **10**, 44 (1922).
4. H. Seemann, *Phys. Zeit.*, **20**, 169 (1919).
5. J. D. Bernal, *Proc. Roy. Soc.*, **A, 113**, 117–160 (1927).
6. J. D. Bernal, *Proc. Roy. Soc.*, **A, 113**, 133 (1927); *Proc. Roy. Soc.*, **A, 106**, 749 (1924).
7. Groth, *Chemische Krystallographie*, **3**, 539. For x-ray analysis: Mark and Weissenberg, *Zeit. Physik*, **16**, 1 (1923).
8. P. P. Ewald, *Zeit. Kryst.*, **56**, 129 (1921).
9. K. Weissenberg, *Zeit. Physik*, **23**, 229 (1924).
   J. Bohm, *Zeit. Physik*, **39**, 557 (1926).
10. H. Ott, *Zeit. Physik*, **22**, 201 (1924).
11. Cox and Shaw, *Proc. Roy. Soc.*, **A, 127**, 71–88 (1930).

CHAPTER VIII

THE THEORY OF SPACE-GROUPS

We have already seen in Chap. II that crystals may be considered to be built on an imaginary three-dimensional framework or space-lattice, and we have become accustomed in Chaps. IV, V, VI, and VII to the idea of having atoms or ions at the intersection points of such an imaginary lattice work. We must now extend this picture so as to include the possibility of having *groups* of atoms or ions associated with each point of the lattice. Obviously the symmetry of the configuration of atoms or ions in a given group must be consistent with the symmetry of the lattice on which the groups are placed. We shall therefore have to consider the various ways in which points may be placed in symmetrical configurations, and then we shall have to find the coordinates of these points after they have been placed on an appropriate space-lattice.

SYMMETRY MACHINES

In order to visualize the grouping of points in symmetrical configurations, let us consider an imaginary set of machines which we may call "symmetry machines." It will be the function of each symmetry machine to lay down points in space in such a way that the whole group of points will have some predetermined symmetry characteristics. There are five possible types of simple symmetry machines:

1. Cyclic axis.
2. Screw axis.
3. Mirror.
4. Glide-mirror.
5. Inverter.

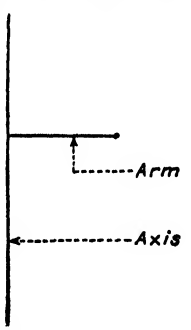

FIG. 1.—Cyclic axis.

1. Cyclic Axis.—This consists of an imaginary axis having an arm as shown in Fig. 1. Imagine that the end of this arm is able to lay down a "point" every time the axis stops rotating. Then, if the axis is a single-fold axis, the arm will lay down a point every time it has rotated through an angle of 2π. All these points coincide so that we really have only one "point," no matter how many times the axis is rotated. The operations of all cyclic axes are represented by the general symbol C. The operation of a single-fold cyclic axis is represented by C_1. It is represented in greater detail by $\{A(2\pi)\}$, where A represents the rotation of the cyclic axis and (2π) is the angle through which it

must rotate before the end of the arm can lay down a point. Figure 2*a* represents a single-fold cyclic axis passing vertically through the paper at A and shows the single point P which the end of the arm is able to lay down.

If the cyclic axis is a 2-fold axis, the end of the arm can lay down a point every half-revolution. The operation of such an axis is represented by the symbol C_2. It is represented in greater detail by the symbol $\{A(2\pi/2)\}$. Figure 2*b* represents a 2-fold cyclic axis passing vertically through the paper at A and shows the two points P_1 and P_2 which the end of the arm has laid down. Similarly, we may have 3-fold, 4-fold, and 6-fold axes (see Fig. 2*c*, *d*, *e*).* In general symbols, $C_n = \{A(2\pi/n)\}$.

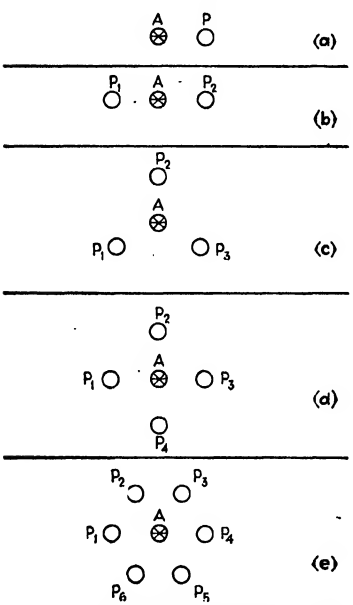

FIG. 2.—Points laid down by 1-fold, 2-fold, 3-fold, 4-fold, and 6-fold cyclic axes which pass vertically through the paper at A. Point-groups C_1, C_2, C_3, C_4, C_6.

2. Screw Axes.—If we imagine an axis to be threaded like a screw so that rotation is accompanied by a motion of translation parallel to the direction of the axis, then that axis is called a "screw axis." Just as in the case of the cyclic axis we can have 1-fold, 2-fold, 3-fold, 4-fold, and 6-fold screw axes (see Fig. 3). The symbol for the operation of a screw axis is $\bar{C}_n$, where $n = 1, 2, 3, 4$, or 6. Its operation is given in greater detail by

$$\bar{C}_n = \left\{\bar{A}\left(\frac{2\pi}{n}\right)\right\}$$

3. Mirror.—Imagine an infinitely thin plane mirror which is polished on both sides so as to reflect light from both its surfaces. Such a mirror may be placed so that the plane of the mirror is perpendicular to a cyclic axis or to a screw axis. The image of every point will lie as far below (or above) the mirror as the point itself is above (or below) the mirror. This operation is technically known as "Spiegelung" (reflection). Since the cyclic axis is commonly imagined as being vertical, the mirror is horizontal and the symmetry operation is given by the symbol S_h.

*A 5-fold, 7-fold, 8-fold, etc., axis would have no crystallographic significance because its points could not be duplicated indefinitely in all directions to form crystals without leaving voids where the fundamental structures would not fit together. This may be illustrated in two dimensions by saying that a floor cannot be laid with five-sided tiles nor with any tiles of more than six sides and still have each tile in contact with its neighbors on all its sides. Still other structures which have no crystallographic significance will be found later in this chapter.

Similarly, a mirror may be placed vertically so that the cyclic axis lies in the reflecting plane. The image of every point is now as far behind (or in front of) the mirror as the point itself is in front of (or behind) it. This operation is given by the symbol S_v. When the action of a horizontal mirror is combined with the action of some other symmetry machine such as C_n, the combination is represented by C_{nh} or C_n^h. Similarly, a combination of S_v with C_n is represented by C_{nv} or C_n^v. It is evident that a mirror may be called a *plane of symmetry*. This term is often used in crystallographic literature.

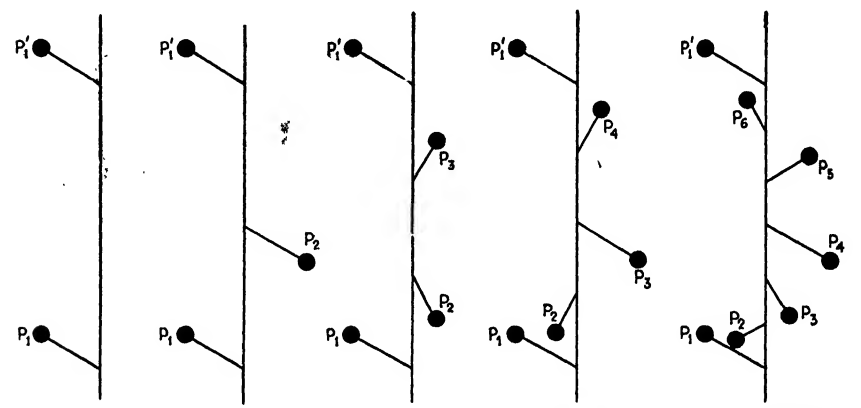

FIG. 3.—Perspective view of the action of 1-fold, 2-fold, 3-fold, 4-fold, and 6-fold screw axes. Point-groups C_1, C_2, C_3, C_4, C_6.

4. Glide-mirror.—Imagine a magic mirror which has the property not only of reflecting the image of a point in the ordinary way but also of shifting that image by a motion of translation over a definite distance parallel to the plane of the mirror. Such a symmetry machine is called a "glide-mirror" or a glide-plane of symmetry. The reflection-translation must be specified by giving the position of the glide-mirror and the length and direction of the motion of translation, for instance, $S_a(\tau_s)$.

5. Inverter.—An inverter is a machine which operates on a given point, or configuration of points, by means of a reference point called a "center of symmetry." The machine draws an imaginary line from each of the original points to the center of symmetry and then extends each of these lines for an equal distance behind the center of symmetry. The center of symmetry therefore bisects each of these imaginary lines. At the end of each extended line the machine lays down a point. This operation is called an "inversion" and is denoted by the symbol I or i. The combined action of I and some other symmetry machine such as C_n is represented by C_{ni} or C_n^i.

POINT-GROUPS

Symmetry machines may be used either singly or in combination with each other. It is evident that certain configurations of points may be obtained in more than one way. For instance, a 2-fold cyclic axis C_2 will produce the same effect as C_v; $\overline{C}_1$ gives identically the same configuration of points as S_h; $\overline{C}_2$ gives identically the same configuration of points as I.

If we list the results of the operations of each of the symmetry machines acting alone, and the results of the operations of the various possible combinations of machines, we shall find a large number of duplications similar to those pointed out above. Counting each configuration only once, and excluding configurations which have no crystallographic significance, we have a total of 32 configurations of points. These are called the 32 point-groups. It is possible, because of the large number of duplicate results obtained by combining various symmetry machines, to dispense with certain of the machines entirely. For instance, it is easy to obtain all of the 32 point-groups by the use of only the cyclic axis, the screw axis, the mirror, and the inverter. It is possible to obtain them all by using only the cyclic axis and the inverter.[2] It will be worth our while to study in detail one of the several possible systematic schemes by which the 32 point-groups may be built up by the action of symmetry machines.

A point-group may be designated by the same symbol which designates the machine or combination of machines which produced it. Five point-groups, C_1, C_2, C_3, C_4, and C_6, may be obtained by the use of a single cyclic axis by the operation $C_n = \{A(2\pi/n)\}$, where n may be 1, 2, 3, 4, or 6. They have already been illustrated in Fig. 2.

Four more groups, D_2, D_3, D_4, and D_6, may be obtained by a combination of an n-fold cyclic axis with n 2-fold axes which are all symmetrically arranged in a plane which is perpendicular to the n-fold axis. The value of n may be 1, 2, 3, 4, or 6, but, when $n = 1$, the point-group becomes identical with C_2. Obviously, C_2 and D_1 yield groups composed of only two points each, so that the two groups can differ only in terms of the orientation of the lines which join the points. This leaves four *new* groups as a result of the combination of symmetry machines. This particular combination of cyclic axes may be given the name of "dihedral combination" and the four point-groups produced by the four dihedral combinations are called the "dihedral groups" (German, Diëdergruppen). The operation of a dihedral combination is given by

$$D_n = \left\{A\left(\frac{2\pi}{n}\right), U\right\}$$

where U (German, Umklappung) represents the operations of the n 2-fold axes. The n-fold axis is called the "principal" axis. The n 2-fold

axes are called the "secondary" axes. Figure 4 shows the secondary axes when $n = 2$, 3, 4, and 6. From these the reader may obtain the configurations of points corresponding to D_2, D_3, D_4, and D_6. The special case for $n = 2$ is given the name of the "quadratic group," Q (German, Vierergruppe, V).

One additional point-group is obtained by adding to the three 2-fold axes of the quadratic group four 3-fold axes as follows: Let the quadratic

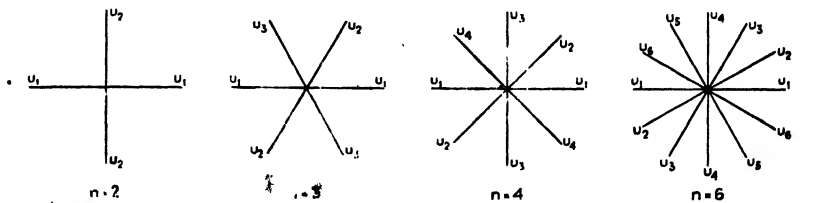

FIG. 4.—Secondary axes of dihedral combinations. The principal axis in each case is perpendicular to the paper. These yield the point-groups $D_2 = V$, D_3, D_4, D_6.

axes U, V, W of Fig. 5 pass through the centers of the edges of a tetrahedron; then the four 3-fold axes A, A_1, A_2, A_3 must be made to pass from the point of intersection of the three 2-fold axes to the four corners of the tetrahedron. This point-group is called the tetrahedral group (symbol T).

The octahedral group (symbol O) is produced by three 4-fold cyclic axes which are mutually at right angles to each other (like the altitudes of a cube), four 3-fold cyclic axes which correspond to the body-diagonals

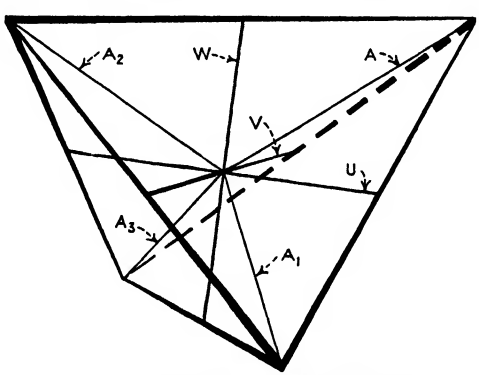

FIG. 5.—The tetrahedral point-group T.

of the cube, and six 2-fold axes which are parallel to the face-diagonals of the cube. All 13 axes pass through a common point which corresponds to the body-center of the cube.

Point-groups $\bar{C}_1$ and $\bar{C}_2$ are obtained by the use of single-fold and 2-fold screw axes of symmetry, respectively. $\bar{C}_1$ is evidently identical with C_1^h and with C_1^v. Since the configuration of points represented by

$\bar{C}_1$ may also be obtained by using a combination of cyclic axis and mirror, it is sometimes expressed by the symbol C_s, or S_1. $\bar{C}_2$ is identical with C_1^i. The effect of a 2-fold screw axis is the same as the composite action of a 2-fold cyclic axis and a horizontal mirror, so that $\bar{C}_2 = S_2$.

Point-group S_4 is arrived at by the composite action of a 4-fold cyclic axis and a horizontal mirror. This composite action must be carefully distinguished from the successive action which is indicated by the symbol C_n^h. The operations symbolized by S_4 are as follows:

1. Let the arm of a cyclic axis deposit a point with the coordinates xyz.

2. Reflect this point in the horizontal mirror. Since the mirror lies in the X-Y plane, the reflection will lie at $xy\bar{z}$. Move the arm along the axis until its end coincides with $xy\bar{z}$, rotate the arm through 90°, and lay down a second point. The coordinates of the second point will therefore be $\bar{y}x\bar{z}$.

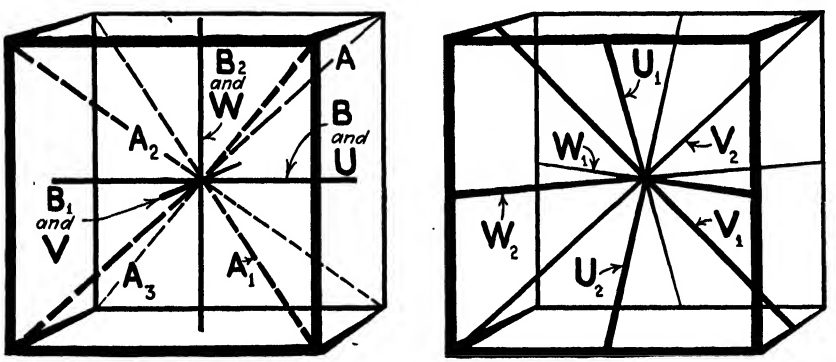

FIG. 6.—The octahedral point-group O.

3. Reflect the second point in the mirror. This reflection will lie at $\bar{y}xz$. Move the arm along the axis as before, rotate it through 90°, and lay down a third point. The coordinates of the third point will be $\bar{x}\bar{y}z$.

4. Reflect the third point in the mirror. This reflection will lie at $\bar{x}\bar{y}\bar{z}$. Move the arm along the axis as before, rotate it through 90°, and lay down a fourth point. The coordinates of the fourth point will be $y\bar{x}\bar{z}$.

It is evident that in the two point-groups S_1 and S_2 the composite action of the cyclic axis and the mirror produces the same configuration of points as is obtained by the successive actions indicated by C_1^h and $\bar{C}_2$, respectively.

The three types of point-groups, C_n^h, C_n^v, and C_n^i, are easiest discussed together because of the duplications which they present. They call, respectively, for the successive action of an n-fold cyclic axis and a horizontal mirror, an n-fold cyclic axis and a vertical mirror, and an n-fold cyclic axis and an inverter. When $n = 1$, C_1^h and C_1^v are identical in configuration and differ only in orientation (see Fig. 7).* We have

* For simplicity Fig. 7 shows only the special case in which the point lies directly on the end of the arm of the cyclic axis. In the general case, the point would be

already seen that C_1^h is identical with $\bar{C}_1$, and that C_1^i is identical with $\bar{C}_2$. Similarly, $C_2^h = C_2^i$; $C_4^h = C_4^i$; $C_6^h = C_6^i$. When $n = 3$ there are no duplications. We therefore have the point-groups $C_2^h = C_2^i$, C_3^h, $C_4^h = C_4^i$, $C_6^h = C_6^i$, C_2^v, C_3^v, C_4^v, C_6^v, and C_3^i.

Six more point-groups may be obtained by adding a mirror to the various dihedral combinations. When the mirror is horizontal, we obtain the groups $D_2^h = V^h(= Q^h)$, D_3^h, D_4^h, D_6^h. When the mirror is vertical and lies in the X-Z or Y-Z plane, no new configurations of points are

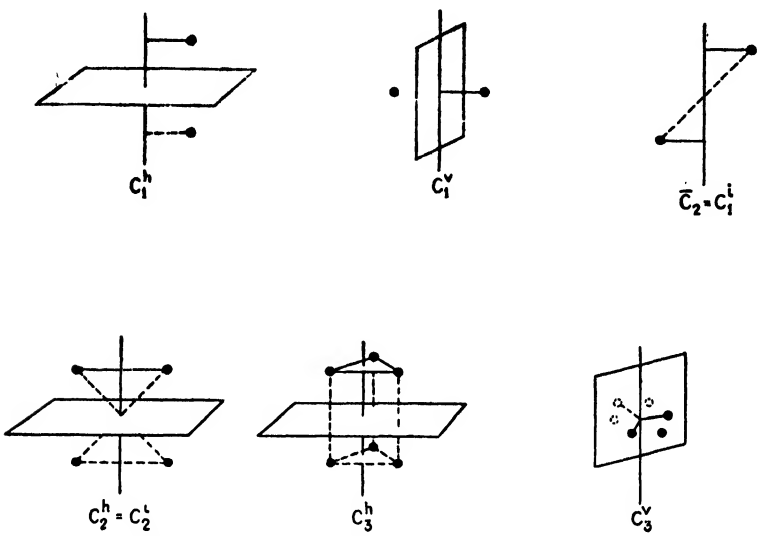

FIG. 7.—The action of the mirror and the inverter.

obtained. When the mirror is vertical and bisects the angle between the X- and Y-axes, the resulting configurations have no crystallographic significance except when $n = 2$ or 3. These give rise to the point-groups $D_2^d = V^d(= Q^d)$ and D_3^d in which the superscript d indicates the operation of a diagonal-vertical mirror.

By adding a horizontal mirror to the combination of symmetry machines which produced the tetrahedral point-group T, we obtain the point-group T^h; if we replace the horizontal mirror by a diagonal-vertical mirror,* we obtain the point-group T^d. By the addition of a

arrived at by going from the end of the arm along two directions such that, when the arm is parallel to the X-axis, these other two directions are parallel to the Y- and Z-axes respectively. These three distances together, then, represent the coordinates of the point. (The general case is employed in Fig. 10, p. 238.)

* This mirror contains the Z-axis and passes through a line which is at 45° to the X- and Y-axes.

TABLE I.—THE

	Schoenflies	Hilton I	Hilton II	Wyckoff	Schoenflies	Dana
	Triclinic system					
1	C_1	C_1	A	$1C$	Hemihedry	Asymmetric
2	$\bar{C}_2 = S_2 = C^i$	c_1	a	$1Ci$	Holohedry	Normal
	Monoclinic system					
3	$\bar{C}_1 = C_1^h = C_s$	c_2	b	$2c$	Hemihedry	Clinohedral
4	C_2	C_2	B	$2C$	Hemimorphic hemihedry	Hemimorphic
5	C_2^h	Γ_2	B_a	$2Ci$	Holohedry	Normal
	Orthorhombic system					
6	$D_2 = V = Q$	D	C	$2D$	Enantiomorphic hemihedry	Sphenoidal
7	C_2^v	δ_2	c	$2e$	Hemimorphic hemihedry	Hemimorphic
8	$D_2^h = V^h = Q^h$	Δ	C_a	$2Di$	Holohedry	Normal
	Tetragonal system					
9	C_4	C_4	D	$4C$	Tetartohedry	Pyramidal hemimorphic
10	S_4	c_4	d	$4c$	Tetartohedry of the second sort	Tetartohedral
11	D_4	D_4	DB	$4D$	Enantiomorphic hemihedry	Trapezohedral
12	C_4^h	Γ_4	D_a	$4Ci$	Paramorphic hemihedry	Pyramidal
13	C_4^v	δ_4	D_b	$4e$	Hemimorphic hemihedry	Hemimorphic
14	$D_2^d = V^d = Q^d$	d_4	dB	$4d$	Hemihedry of the second sort	Sphenoidal
15	D_4^h	Δ_4	d_a	$4Di$	Holohedry	Normal
	Cubic system					
16	T	T	T	T	Tetartohedry	Tetartohedral
17	O	O	o	O	Enantiomorphic hemihedry	Plagihedral
18	T_h	Θ	T_a	Ti	Paramorphic hemihedry	Pyritohedral

32 POINT-GROUPS

Groth (Groth-Goldirew)	Friedel	Miers (Miers-Phillips)	
Asymmetric pedial (monohedral)	Hémiédrie	Asymmetric	1
Pinacoidal	Holoédrie	Centrosymmetric	2
Domatic (dihedral anaxial)	Antihémiédrie	Equatorial (planar)	3
Sphenoidal (dihedral axial)	Hémiédr. holoaxe	Digonal polar (digonal alternating)	4
Prismatic	Holoédrie	Digonal equatorial	5
Rhombic bisphenoidal (rhombic tetrahedral)	Hémiédr. holoaxe	Digonal holoaxial	6
Rhombic pyramidal	Antihémiédrie	Didigonal polar (didigonal alternating)	7
Rhombic bipyramidal (rhombic dipyramidal)	Holoédrie	Didigonal equatorial	8
Tetragonal pyramidal	Tétartoédrie quat.	Tetragonal polar	9
Tetragonal bisphenoidal (tetragonal tetrahedral)	Tétartoédrie sphen.	Tetragonal alternating	10
Tetragonal trapezohedral	Hémiédrie holoaxe	Tetragonal holoaxial	11
Tetragonal bipyramidal (tetragonal dipyramidal)	Parahémiédrie	Tetragonal equatorial	12
Ditetragonal pyramidal	Antihémiédrie quat.	Ditetragonal polar	13
Didigonal scalenohedral (tetragonal scalenohedral)	Antihémiédrie sphen.	Ditetragonal alternating	14
Ditetragonal bipyramidal (ditetragonal dipyramidal)	Holoédrie	Ditetragonal equatorial	15
Tetrahedral pentagonal dodecahedral (pentagonal tritetrahedral)	Tétartoédrie	Tesseral polar	16
Pentagonal icositetrahedral (pentagonal trioctohedral)	Hémiédrie holoaxe	Tesseral holoaxial	17
Diacisdodecahedral (or pyritohedral hemihedral) (didodecahedral)	Parahémiédrie	Tesseral central	18

TABLE I.—

	Schoenflies	Hilton I	Hilton II	Wyckoff	Schoenflies	Dana
19	T_d	θ	T_b	*Te*	Hemimorphic hemihedry	Tetrahedral
20	O_h	Ω	O_a	*Oi*	Holohedry	Normal
	Hexagonal system					
	Rhombohedral division					
21	C_3	C_3	*E*	3*C*	Rhombohedral tetartohedry	24 (trigonal tetartohedral)
22	D_3	D_3	*EB*	3*D*	Enantiomorphic hemihedry	Trapezohedral
23	C_{3v}	δ_3	E_b	3*e*	Hemimorphic hemihedry	Rhombohedral hemimorphic (ditrigonal pyramidal)
24	C_{3i}	Γ_3	*e*	3*Ci*	Hexagonal tetartohedry of the second sort	Trirhombohedral
25	D_{3d}	Δ_3	*eB*	3*Di*	Rhombohedral holohedry	Rhombohedral
	Hexagonal division					
26	C_{3h}	c_6	*f*	6*c*	Trigonal paramorphic hemihedry	23 (trigonal bipyramidal hemihedral)
27	D_{3h}	d_6	*fB*	6*d*	Trigonal holohedry	Trigonotype
28	C_6	C_6	*F*	6*C*	Hexagonal tetartohedry	Pyramidal hemimorphic
29	D_6	D_6	*FB*	6*D*	Enantiomorphic hemihedry	Trapezohedral
30	C_{6h}	Γ_6	F_a	6*Ci*	Paramorphic hemihedry	Pyramidal
31	C_{6v}	δ_6	F_b	6*e*	Hemimorphic hemihedry	Hemimorphic
32	D_{6h}	Δ_6	*fC*	6*Di*	Hexagonal holohedry	Normal

horizontal mirror to the combination of symmetry machines which produced the octahedral point-group *O*, we obtain O^h.

We have now described all of the 32 point-groups in terms of a systematic use of the symmetry machines. The Schoenflies system which we have used is, however, by no means the only possible system. For instance, if we had used only cyclic axes and the inverter, we should have arrived at the same 32 point-groups, but in this case the operations

(*Concluded*)

Groth (Groth-Böldirew)	Friedel	Miers (Miers-Phillips)	
Hexacistetrahedral (hexte-trahedral)	Antihémiédrie	Ditesseral polar	19
Hexacisoctahedral (hexoc-tahedral)	Holoédrie	Ditesseral central	20
Trigonal pyramidal	Tétartoédrie	Trigonal polar	21
Trigonal trapezohedral	Hémiédrie holoaxe	Trigonal holoaxial	22
Ditrigonal pyramidal	Antihémiédrie	Ditrigonal polar	23
Trigonal rhombohedral	Parahémiédrie	Hexagonal alternating	24
Ditrigonal scalenohedral (dihexagonal scalenohedral)	Holoédrie	Dihexagonal alternating	25
Trigonal bipyramidal (trigonal dipyramidal)	Antitétartoédr. trigon.	Trigonal equatorial	26
Ditrigonal bipyramidal (ditrigonal dipyramidal)	Antihémiédr. trigon.	Ditrigonal equatorial	27
Hexagonal pyramidal	Tétartoédrie sen.	Hexagonal polar	28
Hexagonal trapezohedral	Hémiédrie holoaxe	Hexagonal holoaxial	29
Hexagonal bipyramidal (hexagonal dipyramidal)	Parahémiédrie	Hexagonal equatorial	30
Dihexagonal pyramidal	Antihémiédrie sen.	Dihexagonal polar	31
Dihexagonal bipyramidal (dihexagonal dipyramidal)	Holoédrie	Dihexagonal equatorial	32

of these symmetry machines would have led to a set of symbols[2] (not widely used in this country) as follows:

1. Groups (C_n or nC), which have a single n-fold axis of symmetry.
2. The dihedral groups (D_n or nD), which have a principal axis and 2-fold rotation axes perpendicular to it.
3. Groups (C_n^i or nCi), which combine an n-fold axis with a center of symmetry lying in it.

4. Groups (D_n^i or nDi), which contain the axes of the dihedral groups nD with centers of symmetry situated at the intersection of these axes.

5. Groups (nc), which contain a single n-fold axis of rotary inversion.

6. Groups (nd), which combine an n-fold principal axis of rotary inversion with perpendicular 2-fold axes.

7. Groups (ne), which consist of an n-fold principal rotation axis and perpendicular 2-fold axes of rotary inversion.

8. The groups T and O and the groups Ti, Te, and Oi, obtained by adding inversions and axes of rotary inversion to them.

Unfortunately almost every pioneer in this work seems to have worked out his own set of names or symbols for the 32 point-groups. Efforts at simplification have resulted in the confusion of additional symbols.[3] Table I gives a tabulation of the 11 sets of names and symbols most commonly found in the literature. The point-groups characteristic of each crystal system are listed in the order of their symmetry with the least symmetrical group first in each case. Of the four sets of symbols listed in the table it is recommended that only the Schoenflies and the Wyckoff be used. The Wyckoff symbols are by far the easiest to set up in type. The Schoenflies symbols have the great advantage of world-wide use.

COORDINATES OF THE 32 POINT-GROUPS

It is now necessary to find the coordinates of each of the point-groups. This is done by starting with a point having the coordinates xyz and finding for each point-group the new coordinates which result from the actions of the appropriate symmetry machines. Each point-group evidently has the symmetry characteristics of some one of the six crystal systems (see Table I). The 32 point-groups will be discussed in the order of ascending symmetry for each crystal system. Each point-group will be named according to the Schoenflies system of symbols, which we have already studied in detail in this chapter, except that the superscript symbols will be written along with the subscript symbols; *i.e.*, we shall use C_{2h} instead of C_2^h, etc. The reason for this change will be obvious when we take up the study of the symbols for the 230 space-groups at the end of this chapter. The Schoenflies symbol will be followed by the Wyckoff symbol in parentheses. In giving the coordinates of points in the following discussion, we shall follow the ordinary conventions used by crystal analysts, *viz.*, (1) the *letters* x, y, and z refer respectively to three *distances* which are fixed by the arm of the axis (C_n or $\bar{C}_n$) of a symmetry machine, and (2) when these three letters are put together to form the symbol for the coordinates of a point, the first letter gives the distance corresponding to the x-coordinate, the second letter gives the distance corresponding to the y-coordinate, and the third letter gives the distance corresponding to the z-coordinate.

Triclinic System[4]

1. *Point-group* C_1 (1*C*).—This point-group has the lowest possible symmetry, for it consists of only a single point. If a single-fold cyclic axis starts with a point at xyz, it must lay down all its other points on precisely the same spot. The operation is therefore an identity (symbol, 1).

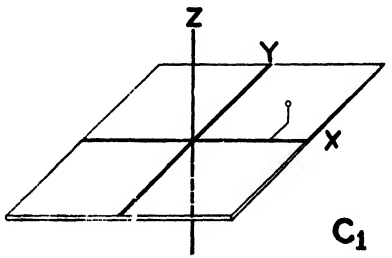

Operations of symmetry; 1

Coordinates of equivalent points; xyz

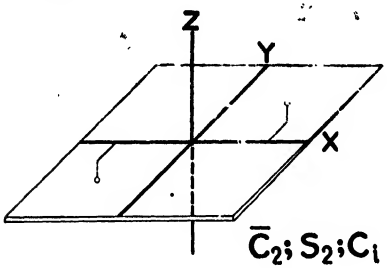

2. *Point-group* $\bar{C}_2 = S_2 = C_i$ (1*Ci*).—Using the inverter to obtain this point-group, we have two operations, the identity and the inversion.

Operations of symmetry;

1 I

Coordinates of equivalent points;

xyz $\bar{x}\bar{y}\bar{z}$

Monoclinic Syst

3. *Point-group* $\bar{C}_1 = C_{1h} (= C_s)$ (2*c*).—A horizontal mirror (*i.e.*, a mirror lying in the *X*-*Y* plane) cannot change the x- or y-coordinates of a point but will reverse the sign of the z-coordinates.

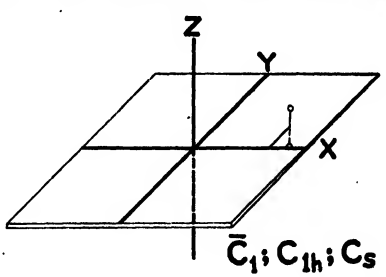

Operations of symmetry;

1 S_h

Coordinates of equivalent points;

xyz $xy\bar{z}$

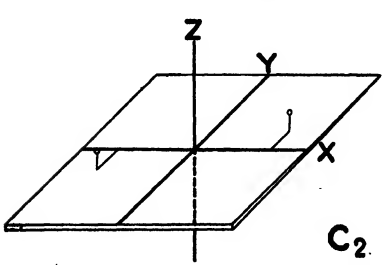

4. *Point-group* C_2 (2*C*).—A 2-fold cyclic axis changes the signs of the x- and y-coordinates but does not alter the z-coordinates.

Operations of symmetry;

1 $A(\pi)$

Coordinates of equivalent points;

xyz $\bar{x}\bar{y}z$

* Based on the convention that the *Z*-axis is perpendicular to the *X*-*Y* plane.

5. *Point-group* C_{2h} $(2Ci)$.—This contains four points, two from the operation of the 2-fold cyclic axis and two from the operation S_h on each of the first two points.

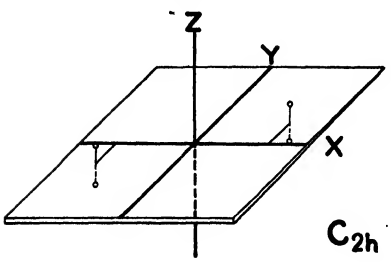

Operations of symmetry;

$1 \qquad A(\pi) \qquad S_h \qquad A(\pi)S_h$

Coordinates of equivalent points;

$xyz \qquad \bar{x}\bar{y}z \qquad xy\bar{z} \qquad \bar{x}\bar{y}\bar{z}$

Orthorhombic System[4]

6. *Point-group* $V = Q = D_2$ $(2D)$.—We have three mutually perpendicular 2-fold cyclic axes whose operations are denoted by

$U = A(\pi)$ for the X-axis.
$V = A(\pi)$ for the Y-axis.*
$W = A(\pi)$ for the Z-axis.

After the operation U is completed, restore the original state and then perform operation V. After the operation V is completed, restore the original state and perform operation W.

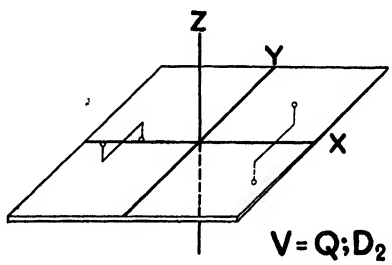

Operations of symmetry;

$1 \qquad U \qquad V \qquad W$

Coordinates of equivalent points;

$xyz \qquad x\bar{y}\bar{z} \qquad \bar{x}yz \qquad \bar{x}\bar{y}z$

7. *Point-group* C_{2v} $(2e)$.—A vertical mirror in the Y-Z plane will reverse the sign of the x-coordinate. A vertical mirror in the X-Z plane will similarly reverse the sign of the y-coordinate. It is evident that the same sets of coordinates are obtained in either case.

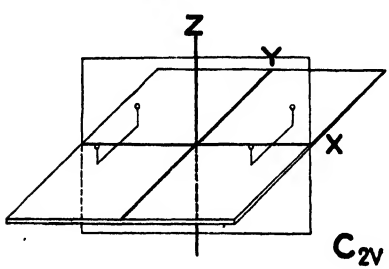

Operations of symmetry;

$1 \qquad A(\pi) \qquad S_v \qquad A(\pi)S_v$

Coordinates of equivalent points;

$xyz \qquad \bar{x}\bar{y}z \qquad x\bar{y}z \qquad \bar{x}yz$

* The operation V should be carefully distinguished from the German designation V of the point-group. It is unfortunate that the two have the same symbol in existing literature. To try to introduce a new set of symbols would only complicate matters.

8. *Point-group* $V_h = Q_h$ (2*Di*).—The effect of the horizontal mirror is to reverse the sign of the z-coordinates.

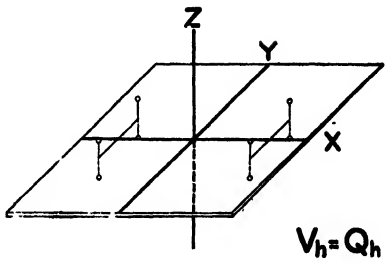

Operations of symmetry;

1	U	V	W
S_h	US_h	VS_h	WS_h

Coordinates of equivalent points;

xyz	$x\bar{y}\bar{z}$	$\bar{x}y\bar{z}$	$\bar{x}\bar{y}z$
$xy\bar{z}$	$x\bar{y}z$	$\bar{x}yz$	$\bar{x}\bar{y}\bar{z}$

Tetragonal System[4]

9. *Point-group* C_4 (4*C*).—The 4-fold cyclic axis interchanges the x- and y-coordinates and reverses the sign of the new x-coordinates every time the axis revolves through $\pi/2$.

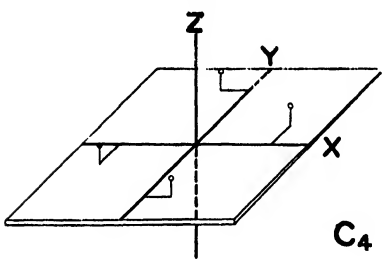

Operations of symmetry;

$$1 \quad A\left(\frac{\pi}{2}\right) \quad A(\pi) \quad A\left(\frac{3\pi}{2}\right)$$

Coordinates of equivalent points;*

xyz	$\bar{y}xz$	$\bar{x}\bar{y}z$	$y\bar{x}z$

10. *Point-group* S_4 (4*c*).—This point-group requires the composite action of a horizontal mirror and a 4-fold cyclic axis. It should be remembered that the operation of S_h on S_h results in a nullification of the reflection.

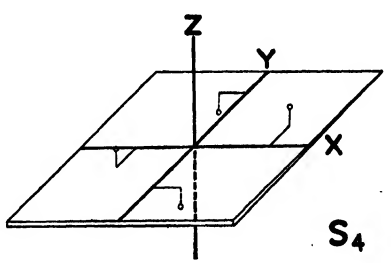

Operations of symmetry;

$$1 \quad A\left(\frac{\pi}{2}\right)S_h \quad A(\pi) \quad A\left(\frac{3\pi}{2}\right)S_h$$

Coordinates of equivalent points;

xyz	$\bar{y}x\bar{z}$	$\bar{x}\bar{y}z$	$y\bar{x}\bar{z}$

11. *Point-group* D_4 (4*D*).—Figure 4 shows that the four 2-fold secondary axes in the X-Y plane are 45° apart. The 4-fold principal axis lays down four points. If these are operated on by any one of the

* It has already been stated that the letters x, y, z represent *lengths*. Their position in the sequence of coordinates indicates the axis to which they refer The first of the three letters is the coordinate measured along the X-axis; the second letter is the y-coordinate; the third letter is the z-coordinate.

four secondary axes, the configuration of points is identical with that obtained by the use of any one of the remaining secondary axes. If we choose the secondary axis which coincides with the X-axis, then $D_4 = \{C_4 U\}$.

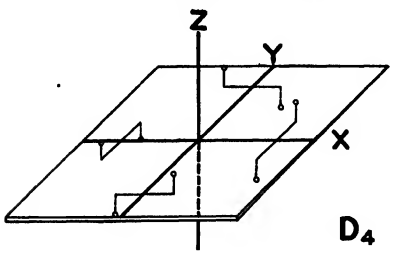

Operations of symmetry;

$$1 \quad A\left(\frac{\pi}{2}\right) \quad A(\pi) \quad A\left(\frac{3\pi}{2}\right)$$
$$U \quad A\left(\frac{\pi}{2}\right)U \quad A(\pi)U \quad A\left(\frac{3\pi}{2}\right)U$$

Coordinates of equivalent points;

xyz	$\bar{y}xz$	$\bar{x}\bar{y}z$	$y\bar{x}z$
$x\bar{y}\bar{z}$	$\bar{y}\bar{x}\bar{z}$	$\bar{x}yz$	$yx\bar{z}$

12. *Point-group* C_{4h} $(4Ci)$.—The horizontal mirror changes the sign of the z-coordinate.

Operations of symmetry;

$$1 \quad A\left(\frac{\pi}{2}\right) \quad A(\pi) \quad A\left(\frac{3\pi}{2}\right)$$
$$S_h \quad A\left(\frac{\pi}{2}\right)S_h \quad A(\pi)S_h \quad A\left(\frac{3\pi}{2}\right)S_h$$

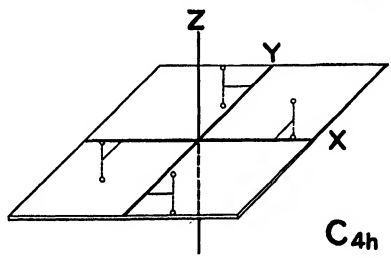

Coordinates of equivalent points;

xyz	$\bar{y}xz$	$\bar{x}\bar{y}z$	$y\bar{x}z$
$xy\bar{z}$	$\bar{y}x\bar{z}$	$\bar{x}\bar{y}\bar{z}$	$y\bar{x}\bar{z}$

13. *Point-group* C_{4v} $(4e)$.—As in the case of point-group C_{2v} it makes no difference whether the mirror is in the X-Z or Y-Z plane.

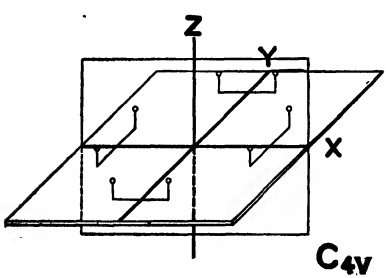

Operations of symmetry;

$$1 \quad A\left(\frac{\pi}{2}\right) \quad A(\pi) \quad A\left(\frac{3\pi}{2}\right)$$
$$S_v \quad A\left(\frac{\pi}{2}\right)S_v \quad A(\pi)S_v \quad A\left(\frac{3\pi}{2}\right)S_v$$

Coordinates of equivalent points;

xyz	$\bar{y}xz$	$\bar{x}\bar{y}z$	$y\bar{x}z$
$x\bar{y}z$	$\bar{y}\bar{x}z$	$\bar{x}yz$	yxz

14. *Point-group* $V_d = Q_d$ $(4d)$.—The diagonal mirror interchanges the x- and y-coordinates.

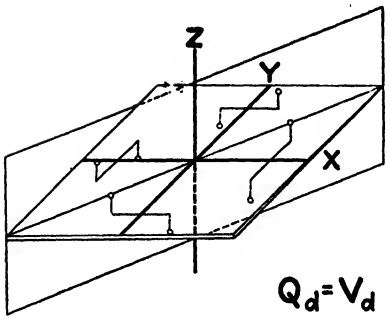

Operations of symmetry;

1	U	V	W
S_d	US_d	VS_d	WS_d

Coordinates of equivalent points;

xyz	$x\bar{y}\bar{z}$	$\bar{x}y\bar{z}$	$\bar{x}\bar{y}z$
yxz	$\bar{y}x\bar{z}$	$y\bar{x}\bar{z}$	$\bar{y}\bar{x}z$

15. *Point-group D_{4h}* ($4Di$).—This point-group contains not only the eight points of D_4 but, besides, a second set of eight points laid down by the horizontal mirror.

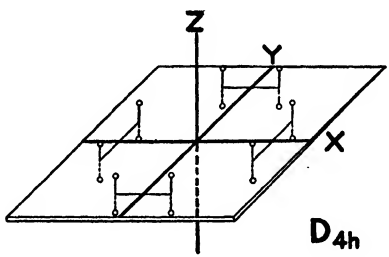

Operations of symmetry;

1	$A\left(\frac{\pi}{2}\right)$	$A(\pi)$	$A\left(\frac{3\pi}{2}\right)$
U	$A\left(\frac{\pi}{2}\right)U$	$A(\pi)U$	$A\left(\frac{3\pi}{2}\right)U$
S_h	$A\left(\frac{\pi}{2}\right)S_h$	$A(\pi)S_h$	$A\left(\frac{3\pi}{2}\right)S_h$
US_h	$A\left(\frac{\pi}{2}\right)S_hU$	$A(\pi)S_hU$	$A\left(\frac{3\pi}{2}\right)S_hU$

Coordinates of equivalent points;

xyz	$\bar{y}xz$	$\bar{x}\bar{y}z$	$y\bar{x}z$
$x\bar{y}\bar{z}$	$\bar{y}\bar{x}\bar{z}$	$\bar{x}y\bar{z}$	$yx\bar{z}$
$xy\bar{z}$	$\bar{y}x\bar{z}$	$\bar{x}\bar{y}\bar{z}$	$y\bar{x}\bar{z}$
$x\bar{y}z$	$\bar{y}\bar{x}z$	$\bar{x}yz$	yxz

CUBIC SYSTEM[4]

16. *Point-group T* (T).—The points in this group require the combined operations of the three 2-fold axes and the four 3-fold axes shown

in Fig. 5. First, one of the 3-fold axes A is operated as shown in the first vertical column. Then the original position is restored, the Umklappung operation U is employed about the X-axis, and the second 3-fold axis A_1 is operated. The original position is again restored, the Umklappung operation V is employed about the Y-axis, and the third 3-fold axis A_2 is operated. The original position is again restored, the Umklappung operation W is employed about the Z-axis, and the fourth 3-fold axis A_3 is operated.

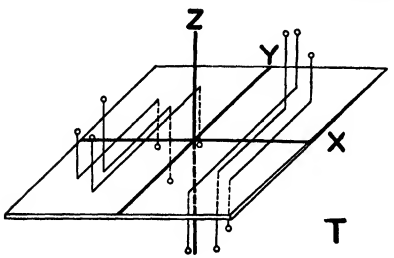

Operations of symmetry;

1	U	V	W
$A\left(\frac{2\pi}{3}\right)$	$A_1\left(\frac{2\pi}{3}\right)$	$A_2\left(\frac{2\pi}{3}\right)$	$A_3\left(\frac{2\pi}{3}\right)$
$A\left(\frac{4\pi}{3}\right)$	$A_1\left(\frac{4\pi}{3}\right)$	$A_2\left(\frac{4\pi}{3}\right)$	$A_3\left(\frac{4\pi}{3}\right)$

Coordinates of equivalent points;

xyz	$x\bar{y}\bar{z}$	$\bar{x}y\bar{z}$	$\bar{x}\bar{y}z$
zxy	$\bar{z}x\bar{y}$	$\bar{z}\bar{x}y$	$z\bar{x}\bar{y}$
yzx	$\bar{y}\bar{z}x$	$y\bar{z}\bar{x}$	$\bar{y}z\bar{x}$

17. *Point-group O* (O).—The 2-fold axes U, V, W of Fig. 5 are now 4-fold in Fig. 6, so that to the operations 1 and U in point-group T we must now add $B(\pi/2)$ and $B(3\pi/2)$; to the operations 1, V we must add $B_1(\pi/2)$ and $B_1(3\pi/2)$; and to the operations 1, W we must add $B_2(\pi/2)$ and $B_2(3\pi/2)$. We still have the same 3-fold axes as in point-group T. In addition we have six 2-fold axes (see Fig. 6) whose operations are U_1, U_2, V_1, V_2, W_1, W_2.

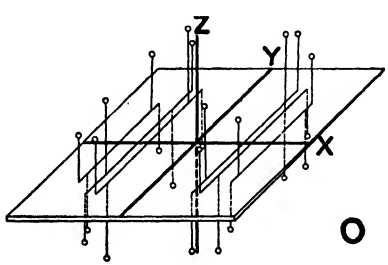

Operations of symmetry;

All 12 operations of point-group T and, in addition,

$B\left(\frac{\pi}{2}\right)$	$B\left(\frac{3\pi}{2}\right)$	$B_1\left(\frac{\pi}{2}\right)$	$B_1\left(\frac{3\pi}{2}\right)$	$B_2\left(\frac{\pi}{2}\right)$	$B_2\left(\frac{3\pi}{2}\right)$
U_1	U_2	V_1	V_2	W_1	W_2

Coordinates of equivalent points;

All 12 coordinate positions of T and, in addition,

$\bar{y}\bar{x}\bar{z}$	$y\bar{x}z$	$\bar{y}xz$	$yx\bar{z}$
$\bar{x}\bar{z}\bar{y}$	$\bar{x}zy$	$xz\bar{y}$	$x\bar{z}y$
$\bar{z}\bar{y}\bar{x}$	$zy\bar{x}$	$z\bar{y}x$	$\bar{z}yx$

The order of writing these coordinates has been changed from the order given above for the additional operations of symmetry so as to make it conform to the treatment of Wyckoff.[1]

18. *Point-group* T_h (*Ti*).—This point-group uses all the symmetry machines of T and has, in addition, the horizontal mirror. The same effect may be had by adding an inverter to T. In other words,

$$T_h = \{T, S_h\} = \{2, I\}.$$

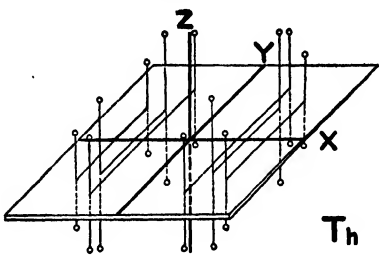

The additional coordinates are listed in the logical order for $\{T, S_h\}$.

Operations of symmetry;

All 12 operations of point-group T and, in addition, 12 more, each of which is a mirror image (S_h) of one of the original 12.

Coordinates of equivalent points;

All 12 coordinate positions of T and, in addition,

$xy\bar{z}$	$x\bar{y}z$	$\bar{x}yz$	$\bar{x}\bar{y}\bar{z}$
$zx\bar{y}$	$\bar{z}xy$	$\bar{z}\bar{x}\bar{y}$	$z\bar{x}y$
$yz\bar{x}$	$\bar{y}\bar{z}\bar{x}$	$y\bar{z}x$	$\bar{y}zx$

19. *Point-group* T_d (*Te*).—The coordinates are those of point-group T and, in addition, those produced by the diagonal mirror. The additional points are listed in the logical order for a mirror which bisects the angle between the X- and Y-axes. These same points would have been obtained if the mirror had bisected the angle between the Y- and X-axes, but the logical order for writing down these points would have been different.

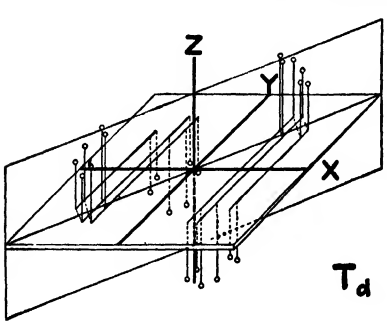

Operations of symmetry;

All 12 operations of point-group T and 12 more from the action of S_d.

Coordinates of equivalent points;

All 12 coordinate positions of T and, in addition,

yxz	$\bar{y}x\bar{z}$	$y\bar{x}\bar{z}$	$\bar{y}\bar{x}z$
xzy	$x\bar{z}\bar{y}$	$\bar{x}\bar{z}y$	$\bar{x}z\bar{y}$
zyx	$\bar{z}\bar{y}x$	$\bar{z}y\bar{x}$	$z\bar{y}\bar{x}$

20. *Point-group* O_h (*Oi*).—The point-group O has already been described as including the 12 points of point-group T and 12 additional points due to the operation of $B(\pi/2)$, . . . , U_1, U_2 . . . Obviously, then, the horizontal mirror of O_h will add to these 24 points of O the 12 additional points listed under T_h and an additional set of 12 points which are the mirror image, S_h (*i.e.*, with the sign of the z-coordinate reversed) of the points listed under point-group O as being due to the operations of $B(\pi/2)$, . . . , U_1, U_2 . . . Inspection shows that this fourth group of 12 points is identical with the 12 listed under T_d.

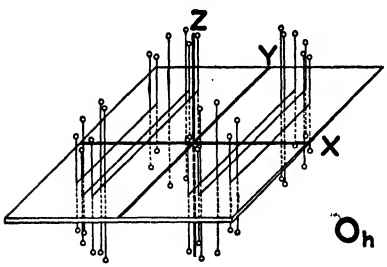

Operations of symmetry;

$$O_h = \{O, S_h\} = \{O, I\}$$

Coordinates of equivalent points;

All the 48 sets of coordinates listed under point-groups T, O, T_h, and T_d.

Hexagonal System[4]

It was stated in Chap. II that a rhombohedron could be considered in terms of equal rhombohedral (distorted cubic) axes or in terms of

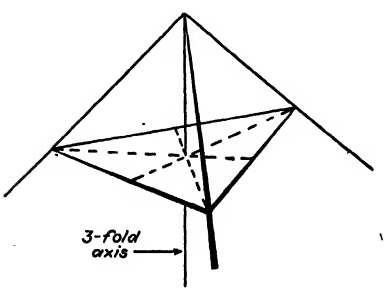

Fig. 8.—The three rhombohedral axes of a rhombohedron.

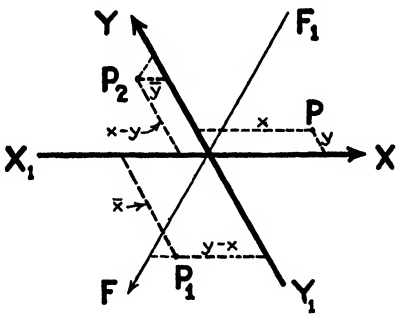

Fig. 9.—The X- and Y-hexagonal axes.

hexagonal axes. Figure 8 shows the rhombohedral axes, symmetrically placed about a vertical 3-fold axis. This 3-fold axis becomes the Z-axis when the rhombohedron is considered as a hexagonal structure (Fig. 9); in such a case the rhombohedron becomes a special case of the monoclinic system in which the angle ν between the X- and Y-axes is 120°. An extra axis may be placed in the X-Y plane in such a way that its positive direction makes an angle of 120° with the positive directions of both the X- and the Y-axes. Such an axis is inherent in the effect of the 3-fold

and 6-fold principal hexagonal axes of the hexagonal system. It was shown in Chap. III that this extra axis is not necessary in the calculation of interplanar spacings. This extra axis is, however, inherent in the symmetries of some of the point-groups of the hexagonal system. Coordinates of point-groups in the rhombohedral division of the hexagonal system are listed in terms of both the rhombohedral axes (I) and the hexagonal axes (II). Coordinates of point-groups in the hexagonal division are listed only in terms of hexagonal axes.

RHOMBOHEDRAL DIVISION

21. *Point-group* C_3 (3*C*).
Operations of symmetry;

$$1 \quad A\left(\frac{2\pi}{3}\right) \quad A\left(\frac{4\pi}{3}\right)$$

Coordinates of equivalent points;

I. xyz zxy yzx
II. xyz $y-x, \bar{x}, z$ $\bar{y}, x-y, z$

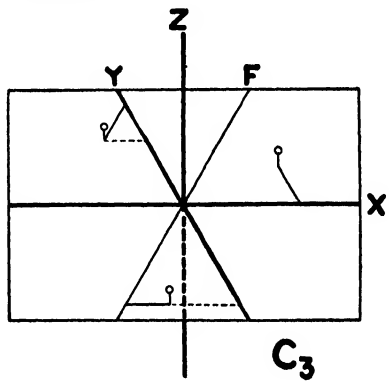

22. *Point-group* D_3 (3*D*).—This point-group has a principal 3-fold axis and three secondary 2-fold axes. These 2-fold axes may coincide with the three horizontal hexagonal axes of the X-Y plane or may lie

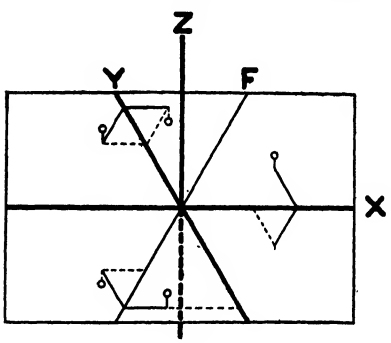

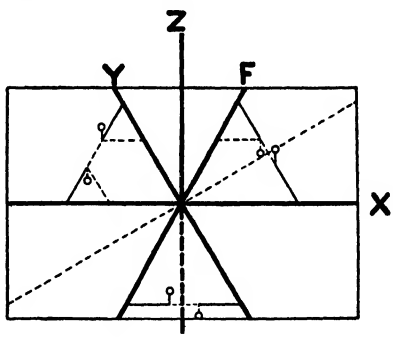

midway between them, thus making an angle of 30° to these axes. All three of the secondary axes produce identical end results on the three points laid down by the principal axis. When the secondary axes coincide with the three horizontal hexagonal axes, the rotation about one of them is symbolized by U_a. When the secondary axes make an

angle of 30° to the horizontal hexagonal axes, the rotation about one of them is symbolized by U_a. This gives rise to two different sets of coordinates for the six equivalent points when hexagonal axes are employed.

Operations of symmetry;

$$D_3 = \{C_3, U\}$$

Coordinates of equivalent points;

I. $xyz \quad zxy \quad yzx \quad \bar{y}\bar{x}\bar{z} \quad \bar{x}\bar{z}\bar{y} \quad \bar{z}\bar{y}\bar{x}$

II. When $D_3 = \{C_3, U_a\}$;

$xyz \quad y-x, \bar{x}, z \quad \bar{y}, x-y, z \quad x-y, \bar{y}, \bar{z} \quad yx\bar{z} \quad \bar{x}, y-x, \bar{z}$

II. When $D_3 = \{C_3, U_s\}$;

$xyz \quad y-x, \bar{x}, z \quad \bar{y}, x-y, z \quad y-x, y, \bar{z} \quad \bar{y}\bar{x}\bar{z} \quad x, x-y, \bar{z}$

23. *Point-group* C_{3v} (3*e*).—When hexagonal axes are used, the vertical mirror may lie in a plane determined by the Z-axis and any one

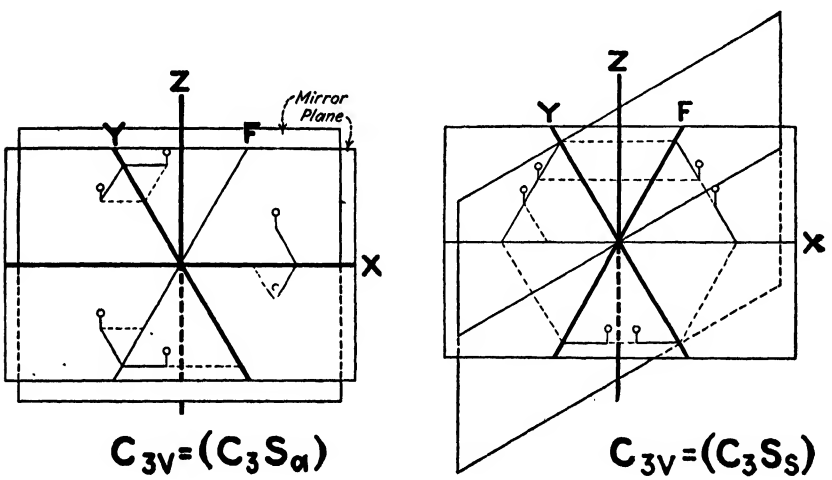

$C_{3V}=(C_3S_a)$ $C_{3V}=(C_3S_S)$

of the three horizontal hexagonal axes. The effect of the mirror is the same no matter which horizontal hexagonal axis is used. The mirror may, however, lie in a plane determined by the Z-axis and a line which bisects one of the angles between the horizontal hexagonal axes. The effect of the mirror is the same no matter which angle is bisected. We therefore have two sets of coordinates for the six equivalent points when hexagonal axes are employed. The operation of the mirror is symbolized by S_a and S_s for the two positions, respectively.

Operations of symmetry;

$$C_{3v} = \{C_3, S_v\}$$

Coordinates of equivalent points;

I. $xyz \quad zxy \quad yzx \quad yxz \quad xzy \quad zyx$

II. When $C_{3v} = \{C_3 S_a\}$;

$xyz \quad y-x, \bar{x}, z \quad \bar{y}, x-y, z \quad x-y, \bar{y}, z \quad yxz \quad \bar{x}, y-x, z$

II. When $C_{3v} = \{C_3 S_s\}$;

$xyz \quad y-x, \bar{x}, z \quad \bar{y}, x-y, z \quad y-x, y, z \quad \bar{x}\bar{y}z \quad x, x-y, z$

24. *Point-group* C_{3i} $(3Ci)$.
Operations of symmetry;

$$C_{3i} = \{C_3, I\}$$

Coordinates of equivalent points;

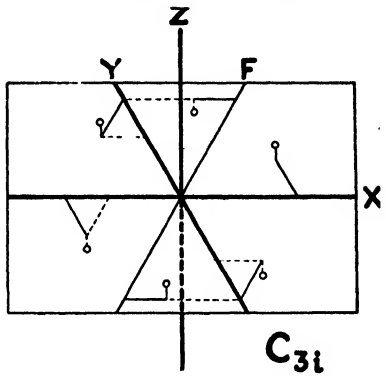

I $xyz \quad zxy \quad yzx$
$\bar{x}\bar{y}\bar{z} \quad \bar{z}\bar{x}\bar{y} \quad \bar{y}\bar{z}\bar{x}$

II. $xyz \quad y-x, \bar{x}, z \quad \bar{y}, x-y, z$
$\bar{x}\bar{y}\bar{z} \quad x-y, x, \bar{z} \quad y, y-x, \bar{z}$

25. *Point-group* D_{3d} $(3Di)$.—Since with hexagonal axes there are two possible sets of coordinates for the point-group D_3, there must be two possible sets of coordinates for D_{3d}.

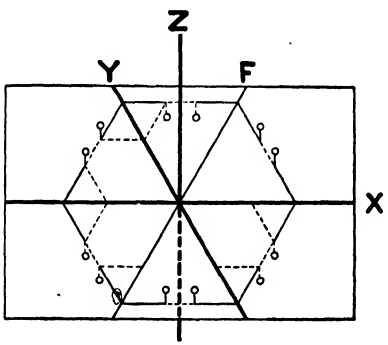

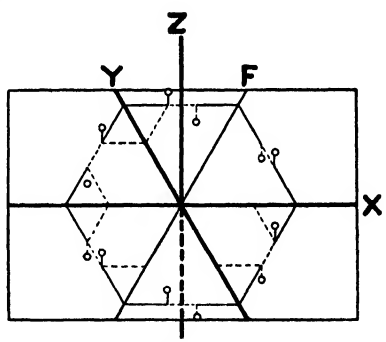

Operations of symmetry;

$$D_3 = \{D_3, S_d\} = \{D_3, I\} = \{C_3, U, S_d\} = \{C_3, U, I\}$$

Coordinates of equivalent points;

I. $xyz \quad zxy \quad yzx \quad \bar{y}\bar{x}\bar{z} \quad \bar{x}\bar{z}\bar{y} \quad \bar{z}\bar{y}\bar{x}$
$\bar{x}\bar{y}\bar{z} \quad \bar{z}\bar{x}\bar{y} \quad \bar{y}\bar{z}\bar{x} \quad yxz \quad xzy \quad zyx$

II. When $D_{3d} = \{C_3, U_a, I\}$;

$xyz \quad y-x, \bar{x}, z \quad \bar{y}, x-y, z \quad x-y, \bar{y}, \bar{z} \quad yx\bar{z} \quad \bar{x}, y-x, \bar{z}$
$\bar{x}\bar{y}\bar{z} \quad x-y, x, \bar{z} \quad y, y-x, \bar{z} \quad y-x, y, z \quad \bar{y}\bar{x}z \quad x, x-y, z$

II. When $D_{3d} = \{C_3, U_s, I\}$;

$xyz \quad y-x, \bar{x}, z \quad \bar{y}, x-y, z \quad y-x, y, \bar{z} \quad \bar{y}\bar{x}\bar{z} \quad x, x-y, \bar{z}$
$\bar{x}\bar{y}\bar{z} \quad x-y, x, \bar{z} \quad y, y-x, \bar{z} \quad x-y, \bar{y}, z \quad yxz \quad \bar{x}, y-x, z$

HEXAGONAL DIVISION

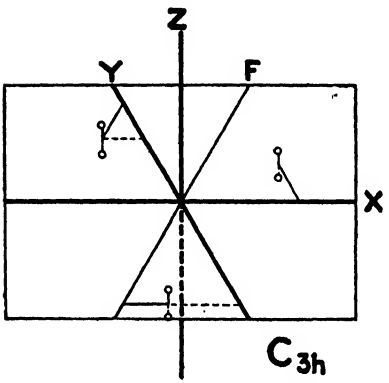

26. *Point-group* C_{3h} (6*c*).
Operations of symmetry;

$$C_{3h} = \{C_3, S_h\}$$

Coordinates of equivalent points;

$xyz \quad y-x, \bar{x}, z \quad \bar{y}, x-y, z$

$xy\bar{z} \quad y-x, \bar{x}, \bar{z} \quad \bar{y}, x-y, \bar{z}$

27. *Point-group* D_{3h} (6*d*).—Since there were two sets of possible coordinates for D_3, there must be two sets for D_{3h}.
Operations of symmetry;

$$D_{3h} = \{D_3 S_h\} = \{C_3, U, S_h\}$$

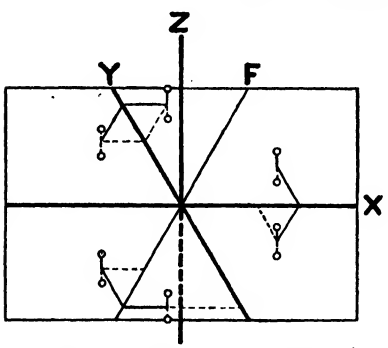

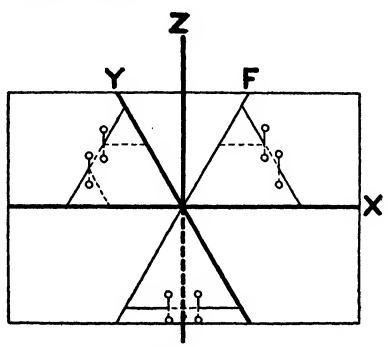

Coordinates of equivalent points;
When $D_{3h} = \{C_3, U_a, S_h\}$;

$xyz \quad y-x, \bar{x}, z \quad \bar{y}, x-y, z \quad x-y, \bar{y}, \bar{z} \quad yx\bar{z} \quad \bar{x}, y-x, \bar{z}$
$xy\bar{z} \quad y-x, \bar{x}, \bar{z} \quad \bar{y}, x-y, \bar{z} \quad x-y, \bar{y}, z \quad yxz \quad \bar{x}, y-x, z$

When $D_{3h} = \{C_3, U_s, S_h\}$;

xyz $y-x, \bar{x}, z$ $\bar{y}, x-y, z$ $y-x, y, \bar{z}$ $\bar{y}\bar{x}\bar{z}$ $x, x-y, \bar{z}$
$xy\bar{z}$ $y-x, \bar{x}, \bar{z}$ $\bar{y}, x-y, \bar{z}$ $y-x, y, z$ $\bar{y}\bar{x}z$ $x, x-y, z$

28. *Point-group* C_6 (6*C*).
Operations of symmetry;

$$1 \quad A\left(\frac{\pi}{3}\right) \quad A\left(\frac{2\pi}{3}\right)$$
$$A(\pi) \quad A\left(\frac{4\pi}{3}\right) \quad A\left(\frac{5\pi}{3}\right)$$

Coordinates of equivalent points;

xyz $\bar{y}, x-y, z$ y $x, \bar{x}, z$
$\bar{x}\bar{y}z$ $\bar{y}, x-y, z$ $x-y, x, z$

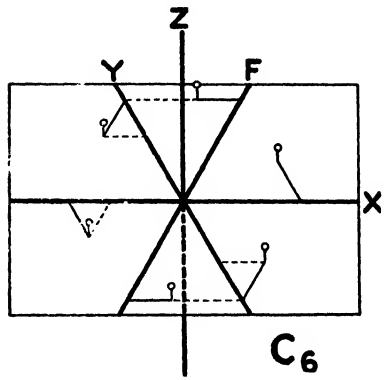

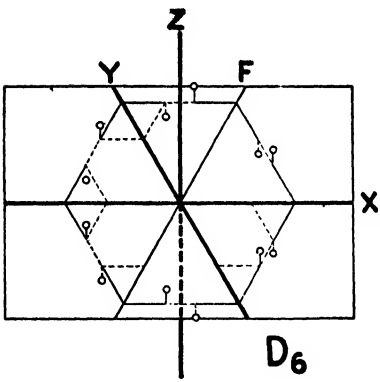

29. *Point-group* D_6 (6*D*).—The six secondary axes all lie in the X-Y plane. The first coincides with the X-axis; the third with the Y-axis; etc. The operation of every one of these secondary axes gives identically the same result as the operation of any other.

Operations of symmetry;

$$D_6 = \{C_6, U\}$$

Coordinates of equivalent points;

xyz $y, y-x, z$ $y-x, \bar{x}, z$ $\bar{x}\bar{y}z$ $\bar{y}, x-y, z$ $x-y, x, z$
$\bar{x}, y-x, \bar{z}$ $y-x, y, \bar{z}$ $yx\bar{z}$ $x, x-y, \bar{z}$ $x-y, \bar{y}, \bar{z}$ $\bar{y}\bar{x}\bar{z}$

30. *Point-group* C_{6h} (6*Ci*).
Operations of symmetry;

$$C_{6h} = C_6 S_h$$

Coordinates of equivalent points;

xyz $y, y-x, z$ $y-x, \bar{x}, z$
$xy\bar{z}$ $y, y-x, \bar{z}$ $y-x, \bar{x}, \bar{z}$

$\bar{x}\bar{y}z$ $\bar{y}, x-y, z$ $x-y, x, z$
$\bar{x}\bar{y}\bar{z}$ $\bar{y}, x-y, \bar{z}$ $x-y, x, \bar{z}$

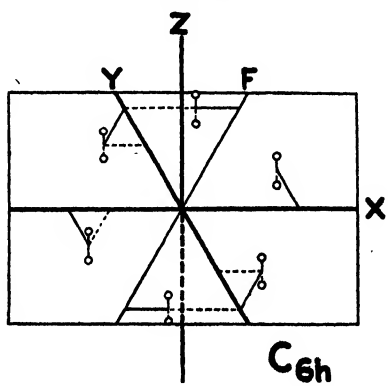

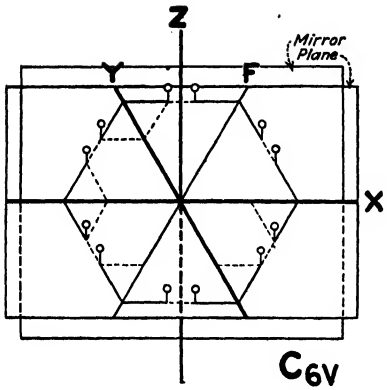

31. *Point-group* C_{6v} (6*e*).
Operations of symmetry;

$$C_{6v} = \{C_6, S_v\}$$

Coordinates of equivalent points;

xyz	$y, y-x, z$	$y-x, \bar{x}, z$
$\bar{x}\bar{y}z$	$\bar{y}, x-y, z$	$x-y, x, z$
$\bar{x}, y-x, z$	$y-x, y, z$	yxz
$x, x-y, z$	$x-y, \bar{y}, z$	$\bar{y}\bar{x}z$

32. *Point-group* D_{6h} (6*Di*).
Operations of symmetry;

$$D_{6h} = \{D_6, S_h\} = \{C_6, U, S_h\}$$

Coordinates of equivalent points;

xyz	$y, y-x, z$	$y-x, \bar{x}, z$
$\bar{x}, y-x, \bar{z}$	$y-x, y, \bar{z}$	$yx\bar{z}$
$\bar{x}\bar{y}\bar{z}$	$\bar{y}, x-y, \bar{z}$	$x-y, x, \bar{z}$
$x, x-y, z$	$x-y, \bar{y}, z$	$\bar{y}\bar{x}z$
$\bar{x}\bar{y}z$	$\bar{y}, x-y, z$	$x-y, x, z$
$x, x-y, \bar{z}$	$x-y, \bar{y}, \bar{z}$	$\bar{y}\bar{x}\bar{z}$
$xy\bar{z}$	$y, y-x, \bar{z}$	$y-x, \bar{x}, \bar{z}$
$\bar{x}, y-x, z$	$y-x, y, z$	yxz

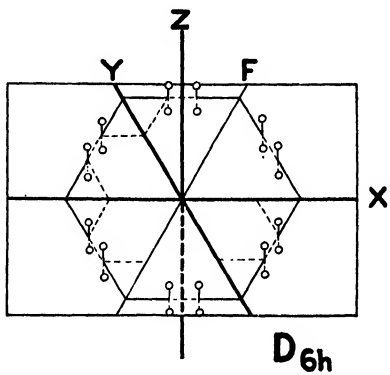

SPACE-GROUPS

We have up to this point listed the coordinates of each of the 32 point-groups. It now remains to place each of these groups in turn at the "lattice points" (which may in general be visualized as intersection points) of such of the various space-lattices (see Chap. II) as have appropriate symmetry characteristics. The combined configuration of points which results from a superposition of a point-group on a space-lattice is a "space-lattice point-group" or, in shorter and more convenient terminology a "space-group."

Except in the simplest cases the perspective drawings representing these space-groups are hopelessly complicated, so that the coordinates of each of the points in a space-group are most conveniently determined analytically as the algebraic sum of the coordinates of the point-group and the primitive translations (or multiples of the primitive translations) of the space-lattices. The case of point-group C_{2h} placed on the simple monoclinic lattice Γ_m (see Table II) is shown in Fig. 10*a* and *b*. The point A is arrived at from the origin O by the primitive translation $2r_x$.

TABLE II.—PRIMITIVE TRANSLATIONS OF THE FOURTEEN SPACE-LATTICES

Lattice	Symbol	Primitive translations	Coordinates of typical points
Triclinic system:			
1. Simple	Γ_{tr}	$2\tau_x;\ 2\tau_y;\ 2\tau_z$	O, (000)
Monoclinic system:			
2. Simple	Γ_m	$2\tau_x;\ 2\tau_y;\ 2\tau_z$	O, (000)
3. Side-centered	Γ_m'	$2\tau_x;\ \tau_y, \tau_z;\ \tau_x, -\tau_z$	O, (000) P, $(0, \tau_y, \tau_z)$
Orthorhombic system:			
4. Simple	Γ_o	$2\tau_x;\ 2\tau_y;\ 2\tau_z$	O, (000)
5(a). Base-centered	$\Gamma_o'(a)$	$\tau_x\ \tau_y;\ \tau_x, -\tau_y;\ 2\tau_z$	O, (000) P_1, $(\tau_x, \tau_y, 0)$
5(b). Side-centered	$\Gamma_o'(b)$	$2\tau_x;\ \tau_y, \tau_z;\ \tau_y, -\tau_z$	O, (000) P, $(0, \tau_y, \tau_z)$
6. Face-centered	Γ_o''	$\tau_y, \tau_z;\ \tau_z, \tau_x;\ \tau_x, \tau_y$	O, (000) P, $(0, \tau_y, \tau_z)$ P_1, $(\tau_x, \tau_y, 0)$ P_2, $(\tau_x, 0, \tau_z)$
7. Body-centered	Γ_o'''	$2\tau_x;\ 2\tau_y;\ 2\tau_z;\ \tau_x, \tau_y, \tau_z$	O, (000) P_3, (τ_x, τ_y, τ_z)
Tetragonal system:			
8(a). Simple	$\Gamma_t(a)$	$2\tau_x;\ 2\tau_y;\ 2\tau_z$	O, (000)
8(b). Base-centered	$\Gamma_t(b)$	$\tau_x, \tau_y;\ \tau_x, -\tau_y;\ 2\tau_z$	O, (000) P_1, $(\tau_x, \tau_y, 0)$
9(a). Face-centered	$\Gamma_t'(a)$	$\tau_y, \tau_z;\ \tau_z, \tau_x;\ \tau_x, \tau_y$	O, (000) P, $(0, \tau_y, \tau_z)$ P_1, $(\tau_x, \tau_y, 0)$ P_2, $(\tau_x, 0, \tau_z)$
9(b). Body-centered	$\Gamma_t'(b)$	$2\tau_x;\ 2\tau_y;\ 2\tau_z;\ \tau_x, \tau_y, \tau_z$	O, (000) P_3, (τ_x, τ_y, τ_z)
Cubic system:			
10. Simple	Γ_c	$2\tau_x;\ 2\tau_y;\ 2\tau_z$	O, (000)
11. Face-centered	Γ_c'	$\tau_y, \tau_z;\ \tau_z, \tau_x;\ \tau_x, \tau_y$	O, (000) P, $(0, \tau_y, \tau_z)$ P_1, $(\tau_x, \tau_y, 0)$ P_2, $(\tau_x, 0, \tau_z)$
12. Body-centered	Γ_c''	$2\tau_x;\ 2\tau_y;\ 2\tau_z;\ \tau_x, \tau_y, \tau_z$	O, (000) P_3, (τ_x, τ_y, τ_z)
Hexagonal system:			
13. Rhombohedral	Γ_{rh}	$2\tau_x;\ 2\tau_y;\ 2\tau_z$	O, (000)
14. Hexagonal	Γ_h	$2\tau_x;\ 2\tau_y;\ 2\tau_z$	O, (000)

O represents the corner of the unit-prism which is used as the origin of coordinates; P, the center of a side; P_1, the center of the base; P_2, the center of an end; P_3, the body-center; $2\tau_x$, $2\tau_y$, and $2\tau_z$ represent the lattice parameters along the X-, Y-, and Z-axes, respectively. By τ_y, τ_z is meant a translation of τ_y along the Y-axis followed by one of length τ_z along the Z-axis.

Since the coordinates of the four points of C_{2h}, referred to A as the origin, are xyz, $\bar{x}\bar{y}z$, $x\bar{y}\bar{z}$, $\bar{x}y\bar{z}$, it is evident that the coordinates referred to O as the origin must be $x+2\tau_x, y, z$; $2\tau_x-x, \bar{y}, z$; $x+2\tau_x, y, \bar{z}$; $2\tau_x-x, \bar{y}, \bar{z}$. Similarly the coordinates of the four points to be placed about A_1, B, C, D, E, etc., may be determined. In general symbols, if m, n, and p

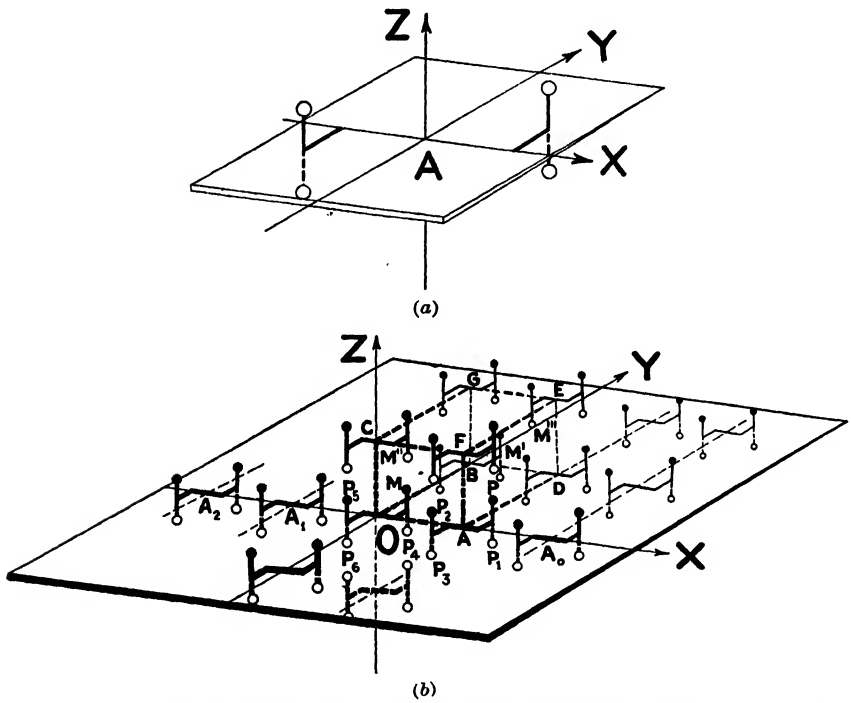

FIG. 10(*a*).—The point-group C_{2h}. (*b*) The point-group C_{2h} on the simple monoclinic lattice Γm, giving the space-group C_{2h}^1. For convenience of reference this figure is lettered to correspond to Fig. 15, p. 28, of Wyckoff.[1]

are any integers, including zero, the generalized coordinates of the points of this space-group are:

$$\begin{array}{lll} 2m\tau_x + x & 2n\tau_y + y & 2p\tau_z + z \\ 2m\tau_x - x & 2n\tau_y - y & 2p\tau_z + z \\ 2m\tau_x + x & 2n\tau_y + y & 2p\tau_z - z \\ 2m\tau_x - x & 2n\tau_y - y & 2p\tau_z - z \end{array}$$

It was pointed out in Chap. II that it is inherent in the symmetry characteristics of a space-lattice that any lattice point may be used as the starting point for constructing the whole lattice. It is customary to use the point in the point-group corresponding to A in Fig. 10*b* as the starting point in building up the crystal lattice. In this way a crystal structure may be built up by hanging some point-group on succes-

sive points of the appropriate space-lattice in such a way that the centers of gravity* of the various repetitions of the point-group correspond to the lattice-points A, A_1, B, C, D, E, etc., of Fig. 10*b*, and so that the point-groups are properly oriented with respect to the space-lattice. A still more complicated type of crystal may be built up by hanging on the lattice points, not one of the simple 32 point-groups, but an aggregate of points which is derived from a simple point-group and which has, taking the aggregate as a whole, the symmetry corresponding to the simple point-group. These aggregates of points are derived from the simple point-groups by adding to the translations of the space-lattice the operation of either an n-fold screw axis or a glide-mirror. Portions of the following tabulations of the 230 possible space-groups will serve to make this more clear.

The 230 space-groups are ordinarily tabulated in such a way that all the space-groups in a given crystal system which require the same symmetry machine are listed together. The nomenclature for space-groups is in about as chaotic a condition as that for the point-groups. Every attempt at simplification has so far resulted in just one more set of symbols which have to be correlated with those previously in use. For the sake of uniformity in the literature it was only natural to have hoped that only the Schoenflies system would remain in common use since it has been so widely used in both the English and German languages. However, the "International Critical Tables" (1926) are written in terms of the Wyckoff symbols,† and in 1929–1930 an international committee decided to adopt still a new set of symbols (the Hermann-Mauguin) which it hoped might find for itself a place in the literature of the future to the exclusion of all other systems. The number of systems to be learned is therefore increased by still one more. Appendix III gives the Hermann-Mauguin symbols which correspond to the various Schoenflies symbols. A glance at this table shows how poorly the Hermann-Mauguin symbols are adapted to ready reference. They follow no system by which they may be readily indexed and still retain

* "Center of gravity" is here applied to the center of the configuration of points, all points being given the same weight.

† Space-groups are listed in the "International Critical Tables" by writing the Wyckoff symbol (see Table I) for the point-group followed by the Schoenflies serial number for the listing within that point-group, thus C_{2v}^{10} becomes $2e - 10$. The Hermann system gives first the Schoenflies symbol for the point-group; then the Hermann symbol for the space-lattice; then such additional information in code form as may be needed to completely identify the space-group. Thus C_2p2 means point-group C_2 on the simple monoclinic lattice p, in which the Z-axis is a 2-fold axis. The Hermann symbols for the 230 space-groups are listed along with the corresponding Schoenflies symbols in Wyckoff,[1] "The Analytical Expression of the Results of the Theory of Space-Groups" (2d ed.) to which the reader is referred for further details. It should be noted that these Hermann symbols are quite different from the Hermann-Mauguin symbols.

any logical crystallographic grouping. For purpose of tabulation they must be placed after the corresponding Schoenflies symbols. A single usable system, widely represented in the literature, even though it is not ideal, is better than a variety of systems each of which approaches ideality in some one or more directions.[3] Considerations of this sort are responsible for the use of the Schoenflies system in the discussion of space-groups in this chapter. In this system each space-group formed with the aid of a given point-group is designated by the Schoenflies symbol for the point-group (see Table I), to which is added, in the exponent position, a number which distinguishes that space-group from others formed with the aid of the same point-group. Thus C_{2v}^{10} is the tenth space-group listed by Schoenflies as being derived from the point-group C_{2v}.

The 230 space-groups are listed together for reference in Tables I to XXXII of Appendix III in tabular form giving (1) the serial number of the space-group;* (2) the Schoenflies space-group symbol; (3) the Schoenflies code for the derivation of the space-group; (4) the space-lattice; (5) the number, n, of asymmetric molecules required to produce the symmetry of the structure; (6) Astbury and Yardley's statement of the value of s of Eqs. (3), (5), (7), etc., of Chap. III; (7) the value of p, where n/p is the number of molecules of symmetry p required to produce the symmetry of the structure.†

The following discussion is intended to aid the reader in visualizing the derivation of each of the 230 space-groups as given in the accompanying tabulations‡ and to serve as a guide in the use of the tables of space-groups in Appendix III.

A. Triclinic System (Space-groups 1 to 2)

I. *Triclinic Hemihedry; Asymmetric.*—The point-group C_1 is placed at each lattice point of Γ_{tr}:

1. $C_1^1 \quad C_1\Gamma_{tr} \quad \Gamma_{tr}$

II. *Triclinic Holohedry; Centrosymmetric.*—The point-group C_i is placed at each lattice point of Γ_{tr}:

2. $C_i^1 \quad C_i\Gamma_{tr} \quad \Gamma_{tr}$

The triclinic lattice is the most general of all lattices. All the primitive translations are independent of each other in both magnitude and direc-

* It should be noted that the serial number is not a characteristic property of the space-group; it will vary from author to author. Its justification lies in making cross reference easier between tables in reading a given author.

† A discussion of the symmetries of ions and molecules will be given in Chap. XIX. The eighth column in the tabulations of Appendix III relates to material presented in Chap. XIX.

‡ In these tabulations the serial number of the space-group is followed by the space-group symbol, its derivation, and the symbol of the space-lattice to which it belongs.

tion. C_i^1 differs from C_1^1 by having a center of symmetry. Unfortunately, in the Laue method, the x-rays themselves always introduce into the diffraction-pattern the effect of a center of symmetry in the crystal. It is therefore impossible on the basis of the symmetry of the Laue pattern alone to distinguish between C_1^1 and C_i^1, and a complete solution of the crystal structure by the Laue method can be made only by bringing in other data to supplement the x-ray data. Tables A of Appendix III show that space-group C_1^1 permits the presence of only one chemical "molecule" per unit of structure; space-group C_i^1 requires the presence of two asymmetric molecules or of one molecule which possesses a center of symmetry. When a second molecule is present, its position is not definitely fixed by space-group C_i^1. The periodicity, s, of the planes (see Chap. III) in triclinic crystals must, therefore, always be unity. This means that the powder method will yield no fractional values of s which will help distinguish between C_1^1 and C_i^1. If the density of the crystal requires two molecules per unit of structure, (*i.e.*, requires that n of Appendix III be 2), we can safely assign the crystal to space-group C_i^1. If, however, the density requires only one "molecule" per unit of structure, the crystal might belong to C_1^1 if the molecule is asymmetric, or to C_i^1 if the molecule has a center of symmetry. Any choice between these two crystal structures must then be made in the light of still other data such as the external symmetry of the crystal, etch figures made under the proper precautions,[5] or some chemical evidence as to the nature of the "molecule."

B. Monoclinic System (Space-groups 3 to 15)

III. *Monoclinic Hemihedry; Equatorial.*—We shall designate the configuration obtained by putting the point-group C_1 on the space-lattice Γ_m by the symbol of this lattice alone, *i.e.*, Γ_m. Similarly the configuration obtained by putting C_1 on Γ_m' will be represented merely by Γ_m'. Space-groups C_s^m are obtained by combining one or the other of these with a horizontal reflection S_h (*i.e.*, a mirror in the X-Y plane) or with a horizontal glide-mirror $S_h(\tau)$. τ is the primitive translation of the glide-mirror in the X-Y plane. It may be taken parallel to either the X- or the Y-axis, *i.e.*, it may be either τ_x or τ_y.*

3.	C_s^1	Γ_m, S_h	Γ_m
4.	C_s^2	Γ_m, $S_h(\tau)$	Γ_m
5.	C_s^3	Γ_m', S_h	Γ_m'
6.	C_s^4	Γ_m', $S_h(\tau)$	Γ_m'

IV. *Monoclinic Hemimorphic Hemihedry; Digonal Polar.*—The point-group C_2 differs from C_1 in having a 2-fold cyclic axis, $A(\pi)$. We may

* The Z-axis is here the principal axis of the crystal. It corresponds to the b-axis of ordinary crystallographic practice. The X-Y plane of this book and of Wyckoff's tables is the a-c plane of ordinary crystallographic practice.

therefore designate the configuration obtained by putting the point-group C_2 on the space-lattice Γ_m by the symbol $C_2^1 = \Gamma_m, A(\pi)$. Similarly the configuration obtained by putting C_2 on Γ_m' will be represented by $\Gamma_m', A(\pi)$. Configurations belonging to the same class of symmetry can be obtained by replacing C_2 by $\bar{C}_2$. The translation components τ of these screw axes are one-half the lattice parameter along the Z-axis of the crystal.

7.	C_2^1	$\Gamma_m, A(\pi)$	Γ_m
8.	C_2^2	$\Gamma_m, \bar{A}(\pi) = \Gamma_m, A(\pi, \tau_z)$	Γ_m
9.	C_2^3	$\Gamma_m', A(\pi) = \Gamma_m', A(\pi, \tau_z)$	Γ_m'

V. *Monoclinic Holohedry; Digonal Equatorial.*—The first three of this family of six space-groups can be obtained by combining the operations of a horizontal mirror with the operations which led to the three members of the C_2 family of space-groups. Three more are obtained by substituting a horizontal glide-mirror for the simple horizontal mirror.

10.	C_{2h}^1	$C_2^1, S_h = \Gamma_m, A(\pi), S_h$	Γ_m
11.	C_{2h}^2	$C_2^2, S_h = \Gamma_m, A(\pi, \tau)S_h$	Γ_m
12.	C_{2h}^3	$C_2^3, S_h = \Gamma_m', A(\pi), S_h$	Γ_m'
13.	C_{2h}^4	$C_2^1, S_h(\tau) = \Gamma_m, A(\pi), S_h(\tau)$	Γ_m
14.	C_{2h}^5	$C_2^2, S_h(\tau) = \Gamma_m, A(\pi, \tau), S_h(\tau)$	Γ_m
15.	C_{2h}^6	$C_2^3, S_h(\tau) = \Gamma_m', A(\pi), S_h(\tau)$	Γ_m'

Inspection of a model shows that there are three ways of regarding the lattice Γ_m' all of which require that one edge of the chosen unit of structure be perpendicular to the other two. It may be considered as: (*a*) a body-centered monoclinic lattice; (*b*1) a monoclinic lattice with points at the centers of the (1 0 0) faces; (*b*2) a monoclinic lattice with points at the centers of the (0 0 1) faces; (*c*) a face-centered monoclinic lattice. Figure 11 shows that these are merely three ways of looking at the same structure.

These three subdivisions appear in the tabulations for the monoclinic system in Appendix III wherever the Γ_m' lattice is used. For instance, the unit of structure of C_s^2 contains two molecules, the second of which can be obtained from the first by a reflection S_h plus a definite translation (τ) in the X-Y plane. The translation may be parallel to the X-axis, τ_x; or to the Y-axis, τ_y. If we choose the position of any characteristic point A of the first molecule as our origin of coordinates, and if we use the crystallographic axes as axes of coordinates, then the coordinates of the corresponding point B in the second molecule are either

$$\left(\frac{a}{2}, v, 0\right) \text{ or } \left(0, v, \frac{c}{2}\right) \text{ or } \left(\frac{a}{2}, v, \frac{c}{2}\right)$$

where v is indeterminate. The particular coordinates to be used depend only on the choice of the unit of structure, for all three sets of coordinates

represent the same space-group. Subdivision (*a*) makes the periodicity s equal to one-half if the second molecule B occupies the position $(a/2, v, 0)$; subdivision (*b*) makes $s = \frac{1}{2}$ when B is at $(0, v, c/2)$; subdivision (*c*) makes $s = \frac{1}{2}$ when B is at $(a/2, v, c/2)$.

We have already seen in our discussion of the triclinic system that it is not always possible by x-ray diffraction methods alone to distinguish between certain space-groups even though they may be formed with the aid of different point-groups. Still other illustrations may be found in the other crystal systems. For instance, in the monoclinic system the tabulations in Appendix III show that the rules for $s = \frac{1}{2}$ are the

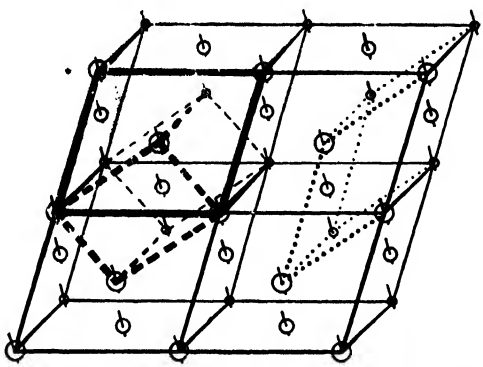

FIG. 11.—Dashed lines, body-centered monoclinic lattice. Dotted lines, monoclinic lattice with one pair of opposite rectangular faces centered. Full lines, face-centered monoclinic lattice.

same for C_s^2 and for C_{2h}^4. If it is found that there are four "molecules" per unit of structure, and if the lattice is Γ_m, it is reasonable to assume that the point-group is C_{2h}^4. If, however, there are only two "molecules" per unit of structure, then there are two possibilities open: either the molecules may be asymmetric so that the crystal belongs to space-group C_s^2, or the molecules may have a 2-fold symmetry (by reason of an axis of symmetry or a center of symmetry) so that the crystal belongs to the space-group C_{2h}^4. If the external symmetry of the crystal, or the symmetry shown by deep etching under the proper precautions,[5] shows that the crystal is monoclinic holohedral (digonal equatorial) and belongs to space-group C_{2h}^4, it is still not possible by x-ray diffraction methods to decide whether the molecule has an axis of symmetry or a center of symmetry or both.

C. ORTHORHOMBIC SYSTEM (Space-groups 16 to 74)

The orthorhombic space-groups are based on:

a. The simple orthorhombic lattice, Γ_o.

b. The orthorhombic lattice with points at the centers of one pair of opposite faces, Γ_o'.

c. The face-centered orthorhombic lattice, Γ_o''.
d. The body-centered orthorhombic lattice, Γ_o'''.

VI. *Orthorhombic Enantiomorphic Hemihedry; Digonal Holoaxial.*—The quadratic point-group $V(=Q)$ has already been described as being made up of a 2-fold principal cyclic axis, C_2, and two 2-fold secondary cyclic axes, each represented by C_2, which are at right angles to each other and to the principal axis. In the simplest possible case of the space-group V^m, the effect is that of placing three space-groups C_2^1 (for which the angle between the X- and Y-axes is given the special value of 90°) so that their axes are parallel to the X-, Y-, and Z-axes, respectively, of an orthorhombic space-lattice. Still other groups, all having this same class of symmetry, can be formed by substituting space-groups C_2^2 or C_2^3 in place of one or more of the C_2^1 groups. These all lead to the following:

16.	V^1	C_2^1, C_2^1, C_2^1	Γ_o
17.	V^2	C_2^1, C_2^1, C_2^2	Γ_o
18.	V^3	C_2^2, C_2^2, C_2^1	Γ_o
19.	V^4	C_2^2, C_2^2, C_2^2	Γ_o
20.	V^5	C_2^3, C_2^3, C_2^2	$\Gamma_o'(a)$ (see Table II)
21.	V^6	C_2^3, C_2^3, C_2^1	$\Gamma_o'(a)$
22.	V^7	C_2^3, C_2^3, C_2^3	Γ_o''
23.	V^8	C_2^3, C_2^3, C_2^3	Γ_o'''
24.	V^9	C_2^3, C_2^3, C_2^3	Γ_o'''

These last two space-groups, V^8 and V^9, differ only in the manner of the distribution of their axes. A complete picture of the difference between these groups may be obtained by studying the coordinates of the points as listed by Wyckoff in his "Analytical Expression of the Results of the Theory of Space-Groups."[1]

VII. *Orthorhombic Hemimorphic Hemihedry; Didigonal Polar.*—In the monoclinic space-group C_2^m, the axes of all the C_2 point-groups are parallel to each other. If we put all three crystallographic axes at right angles to each other, the crystal is no longer monoclinic but is orthorhombic. We shall choose the crystallographic axis which is parallel to the axes of the C_2 point-groups as the Z-axis of the orthorhombic lattice. Then we can form the C_{2v}^m space-groups by adding to these C_2^m groups a vertical mirror or a vertical glide-mirror. Obviously there are three possible positions for the mirror (or glide-mirror): (1) it may be placed in the X-Z or Y-Z planes; (2) it may be placed midway between pairs of adjacent X-Z or Y-Z planes; (3) it may be placed diagonally so as to lie in the (1 1 0) or ($\bar{1}$ 1 0) plane. These three cases are designated by S, S_m, and S_d, respectively. The choice of which of the two horizontal crystallographic axes is X and which is Y rests entirely with the observer, so that

the space-groups based on S and S_m are completely described by assuming that the mirror (or glide-mirror) may be located by reference to the X-Z plane alone.

25.	C_{2v}^1	C_2^1, S	Γ_o
26.	C_{2v}^2	C_2^2, S	Γ_o
27.	C_{2v}^3	$C_2^1, S(\tau_z)$	Γ_o
28.	C_{2v}^4	$C_2^1, S(\tau_x)$	Γ_o
29.	C_{2v}^5	$C_2^2, S(\tau_x)$	Γ_o
30.	C_{2v}^6	$C_2^1, S(\tau_x + \tau_z)$	Γ_o
31.	C_{2v}^7	$C_2^2, S(\tau_x + \tau_z)$	Γ_o
32.	C_{2v}^8	$C_2^1, S_m(\tau_x)$	Γ_o
33.	C_{2v}^9	$C_2^2, S_m(\tau_x)$	Γ_o
34.	C_{2v}^{10}	$C_2^1, S_m(\tau_x + \tau_z)$	Γ_o
35.	C_{2v}^{11}	C_2^1, S_d	$\Gamma_o'(a)$ (see Table II)
36.	C_{2v}^{12}	C_2^2, S_d	$\Gamma_o'(a)$
37.	C_{2v}^{13}	$C_2^1, S_d(\tau_z)$	$\Gamma_o'(a)$
38.	C_{2v}^{14}	C_2^3, S	$\Gamma_o'(b)$
39.	C_{2v}^{15}	$C_2^3, S(\tau_z)$	$\Gamma_o'(b)$
40.	C_{2v}^{16}	$C_2^3, S(\tau_x)$	$\Gamma_o'(b)$
41.	C_{2v}^{17}	$C_2^3, S(\tau_x + \tau_z)$	$\Gamma_o'(b)$
42.	C_{2v}^{18}	C_2^3, S	Γ_o''
43.	C_{2v}^{19}	$C_2^3, S_m\frac{1}{2}(\tau_x + \tau_z)$	Γ_o''
44.	C_{2v}^{20}	C_2^3, S_d	Γ_o'''
45.	C_{2v}^{21}	$C_2^3, S_d(\tau_z)$	Γ_o'''
46.	C_{2v}^{22}	$C_2^3, S_d(\tau_x)$	Γ_o'''

VIII. *Orthorhombic Holohedry; Didigonal Equatorial.*—This family of space-groups can be obtained by combining a horizontal mirror or a

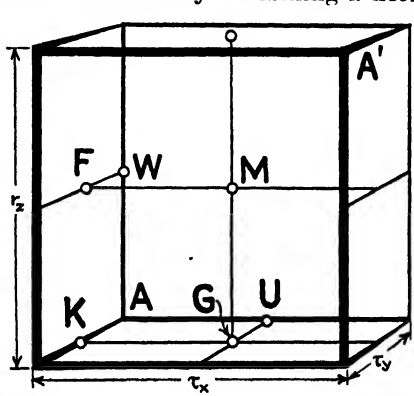

FIG. 12.—Inversion points and mirrors for tabulations VIII, XIV to XIX.

horizontal glide-mirror with the space-groups V^m. They are more easily visualized as combinations of $\bar{V}^m$ with various inversions. These inver-

sion points are shown in Fig. 12 and are represented by subscripts to the inversion symbol, thus I_m.

47.	$V_h^1 = D_{2h}^1$	V^1, I	Γ_o
48.	V_h^2	V^1, I_m	Γ_o
49.	V_h^3	V^1, I_w	Γ_o
50.	V_h^4	V^1, I_g	Γ_o
51.	V_h^5	V^2, I	Γ_o
52.	V_h^6	V^2, I_m	Γ_o
53.	V_h^7	V^2, I_u	Γ_o
54.	V_h^8	V^2, I_k	Γ_o
55.	V_h^9	V^3, I	Γ_o
56.	V_h^{10}	V^3, I_m	Γ_o
57.	V_h^{11}	V^3, I_k	Γ_o
58.	V_h^{12}	V^3, I_w	Γ_o
59.	V_h^{13}	V^3, I_g	Γ_o
60.	V_h^{14}	V^3, I_f	Γ_o
61.	V_h^{15}	V^4, I	Γ_o
62.	V_h^{16}	V^4, I_g	Γ_o
63.	V_h^{17}	V^5, I	$\Gamma_o'(a)$ (see Table II)
64.	V_h^{18}	V^5, I_u	$\Gamma_o'(a)$
65.	V_h^{19}	V^6, I	$\Gamma_o'(a)$
66.	V_h^{20}	V^6, I_m	$\Gamma_o'(a)$
67.	V_h^{21}	V^6, I_u	$\Gamma_o'(a)$
68.	V_h^{22}	V^6, I_f	$\Gamma_o'(a)$
69.	V_h^{23}	V^7, I	Γ_o''
70.	V_h^{24}	V^7, I_m	Γ_o''
71.	V_h^{25}	V^8, I	Γ_o'''
72.	V_h^{26}	V^8, I_w	Γ_o'''
73.	V_h^{27}	V^9, I	Γ_o'''
74.	V_h^{28}	V^9, I_g	Γ_o'''

The following discussion of x-ray studies of orthorhombic crystals assumes that the space-lattice of the crystal has been found, employing the methods described in Chaps. IV, V, VI, and VII. The tabulations of the orthorhombic system in Appendix III show that quite frequently the values of the periodicity, s, will be the same for space-groups formed with the aid of different point-groups, for instance, see C_{2v}^4, V_h^{5}*; C_{2v}^1, V^1, V_h^1; etc. Here, as in the monoclinic system, x-ray diffraction data alone will not decide between such space-groups without the assistance of other evidence such as the symmetry of the exterior of the crystals, etch figures, physical properties, etc. If, in addition to the space-lattice, we can decide upon the class of symmetry, *i.e.*, upon the point-group, then we can distinguish between the various space-groups derived from

* Note that we have complete freedom of choice of axes in V and V_h.

that point-group (V^8 and V^9 excepted) entirely in terms of the values found for s. For example, x-ray diffraction methods should distinguish between space-groups belonging to the V point-group in the case of crystals which show $s = \frac{1}{2}$ for one or more of the axial planes and which show at the same time $s = 1$ for all other planes in the axial zones. Similarly, x-ray methods should distinguish between crystals belonging to the V_h point-group for which $s = \frac{1}{2}$ in all three axial zones and other crystals belonging to the same point-group which show $s = \frac{1}{2}$ for the general planes $(h\,k\,l)$. In practically every case reported in the literature the unit of structure appears to contain the minimum number of molecules rather than an integral multiple of that number.

We have seen that in space-groups derived from the C_{2v} point-group, the Z-axis is taken parallel to the 2-fold axis. This means that the glide-planes must be parallel to (1 0 0) and (0 1 0) but not to (0 0 1). The X- and Y-axes are not determined by convention as is the Z-axis. We may therefore interchange h and k in the tabulations of Appendix III for point-group C_{2v}, care being taken that the changes are all consistent. For instance, if the structure contains one plane of symmetry and one glide-plane of symmetry as in C_{2v}^2, the glide-plane may be taken arbitrarily parallel to (1 0 0), as was done in making the tabulation; this makes $s = \frac{1}{2}$ for $(0\,k\,l)$ when l is odd. But we may, instead, take (0 1 0) as the glide-plane. This would make $s = \frac{1}{2}$ for $(h\,0\,l)$ when l is odd. Similar alternatives are possible in C_{2v}^4, C_{2v}^5, C_{2v}^6, C_{2v}^7, C_{2v}^9, C_{2v}^{12}, etc. For instance, if it is found experimentally that $s = \frac{1}{2}$ for $h0l$ when l is odd [instead of $(0\,k\,l)$ as listed in the tabulation], then we must use (0 1 0) for the glide-plane of symmetry in the crystal instead of (1 0 0) as listed in the tabulation.

As was shown in Table II, there are two possible cases of Γ_o', one in which the pair of centered faces is (0 0 1), as in C_{2v}^{11}, etc., the other in which the centered faces are (1 0 0) as in C_{2v}^{14}, etc.

D. Tetragonal System (Space-groups 75 to 142)

IX. *Tetragonal Tetartohedry; Tetragonal Polar.*—The space-groups C_4^m can be derived by putting 4-fold cyclic axes or 4-fold screw axes on the tetragonal lattices Γ_t and Γ_t'.

75.	C_4^1	$A\left(\frac{\pi}{2}\right)$, Γ_t	Γ_t
76.	C_4^2	$A\left(\frac{\pi}{2}, \frac{\tau_z}{2}\right)$, Γ_t	Γ_t
77.	C_4^3	$A\left(\frac{\pi}{2}, \tau_z\right)$, Γ_t	Γ_t
78.	C_4^4	$A\left(\frac{\pi}{2}, \frac{3\tau_z}{2}\right)$, Γ_t	Γ_t

79. C_4^5 $A\left(\frac{\pi}{2}\right)$, Γ_t' Γ_t'

80. C_4^6 $A\left(\frac{\pi}{2}, \frac{\tau_z}{2}\right)$, Γ_t' Γ_t'

X. *Tetragonal Tetartohedry of the Second Sort; Tetragonal Alternating.*—The space-groups S_4^m are obtained by making all three angles between the crystallographic axes of C_2^m exactly 90° and combining with them a rotary reflection $\bar{A}$, *i.e.*, a screw axis of symmetry. The axis $\bar{A}$ is made to coincide with the axis of C_2.

81. S_4^1 $C_2^1, \bar{A}$ Γ_t

82. S_4^2 $C_2^3, \bar{A}$ Γ_t'

XI. *Tetragonal Enantiomorphic Hemihedry; Tetragonal Holoaxial.*—

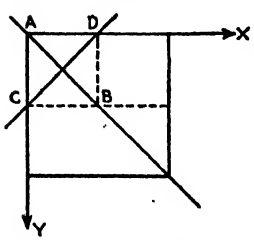

FIG. 13.—Axes of Umklappung for D_{2d}^m and mirrors for C_{4v}^m.

It was stated earlier in this chapter that the point-group D_n is obtained by combining the 4-fold cyclic axis C_4 with an Umklappung U which represents the operation of n 2-fold axes all of which lie in the X-Y plane. In forming the space-groups D_4^m the symmetry requires only one axis of Umklappung. This single 2-fold axis may be either in the line AB of Fig. 13, in which case it is called U_s, or in the line CD, in which case it is called U_c. D_4^m may therefore be obtained by combining C_4^m with U_s or with U_c.

83. D_4^1 C_4^1, U_s Γ_t

84. D_4^2 C_4^1, U_c Γ_t

85. D_4^3 C_4^2, U_s Γ_t

86. D_4^4 C_4^2, U_c Γ_t

87. D_4^5 C_4^3, U_s Γ_t

88. D_4^6 C_4^3, U_c Γ_t

89. D_4^7 C_4^4, U_s Γ_t

90. D_4^8 C_4^4, U_c Γ_t

91. D_4^9 C_4^5, U_s Γ_t'

92. D_4^{10} C_4^6, U_s Γ_t'

XII. *Tetragonal Paramorphic Hemihedry; Tetragonal Equatorial.*—These space-groups can be obtained by combining C_4^m with an inversion. There are two possible inversions. In the first, I, the center of symmetry lies on the 4-fold axis of C_4; in the second, I_1, it lies at the center point of a line joining two adjacent axes of C_4.

93. C_{4h}^1 C_4^1, I Γ_t

94. C_{4h}^2 C_4^3, I Γ_t

95. C_{4h}^3 C_{4v}^1, I_1 Γ_t

96.	C_{4h}^{4}	C_4^3, I_1	Γ_t
97.	C_{4h}^{5}	C_4^5, I	Γ_t'
98.	C_{4h}^{6}	C_4^6, I_1	Γ_t'

XIII. *Tetragonal Hemimorphic Hemihedry; Ditetragonal Polar.*—The space-groups of this class are obtained by combining the operations for space-groups C_4^m with vertical mirrors or glide-mirrors. Mirrors which cut the X-Y plane in the direction of AB, Fig. 13, are represented by S_a; mirrors cutting the X-Y plane in the direction of CD are represented by S_c.

99.	C_{4v}^{1}	C_4^1, S_a	Γ_t
100.	C_{4v}^{2}	C_4^1, S_c	Γ_t
101.	C_{4v}^{3}	C_4^3, S_a	Γ_t
102.	C_{4v}^{4}	C_4^3, S_c	Γ_t
103.	C_{4v}^{7}	$C_4^1, S_a(\tau_z)$	Γ_t
104.	C_{4v}^{8}	$C_4^1, S_c(\tau_z)$	Γ_t
105.	C_{4v}^{7}	$C_4^3, S_a(\tau_z)$	Γ_t
106.	C_{4v}^{8}	$C_4^3, S_c(\tau_z)$	Γ_t
107.	C_{4v}^{9}	C_4^5, S_a	Γ_t'
108.	C_{4v}^{10}	$C_4^5, S_a(\tau_z)$	Γ_t'
109.	C_{4v}^{11}	C_4^6, S_c	Γ_t'
110.	C_{4v}^{12}	$C_4^6, S_c(\tau_z)$	Γ_t'

XIV. *Tetragonal Hemihedry of the Second Sort; Ditetragonal Alternating.*—The space-groups of this class are obtained by combining the operations for space-groups V^m with the operation of a mirror or of a glide-mirror. A mirror in the plane $WMGA$ of Fig. 12 is represented by S_d; a mirror in the parallel plane through F and K is represented by S_{d1}.

111.	$V_d^1 = D_{2d}^1$	V^1, S_d	Γ_t
112.	V_d^2	$V^1, S_d(\tau_z)$	Γ_t
113.	V_d^3	V^3, S_d	Γ_t
114.	V_d^4	$V^3, S_d(\tau_z)$	Γ_t
115.	V_d^5	V^6, S_d	$\Gamma_t(b)$
116.	V_d^6	$V^6, S_d(\tau_z)$	$\Gamma_t(b)$
117.	V_d^7	$V^6, S_{d1}\left(\frac{\tau_x+\tau_y}{2}\right)$	$\Gamma_t(b)$
118.	V_d^8	$V^6, S_{d1}\left(\frac{\tau_x+\tau_y}{2}+\tau_z\right)$	$\Gamma_t(b)$
119.	V_d^9	V^7, S_d	$\Gamma_t'(b)$
120.	V_d^{10}	$V^7, S_d(\tau_z)$	$\Gamma_t'(b)$
121.	V_d^{11}	V^8, S_d	Γ_t'
122.	V_d^{12}	$V^9, S_d\left(\frac{\tau_x}{2}, \frac{\tau_y}{2}, \frac{\tau_z}{2}\right)$	Γ_t'

XV. *Tetragonal Holohedry; Ditetragonal Equatorial.*—The space-groups of this class are most easily obtained by combining the operations for space-groups D_4^m with an inversion. Four such inversions, I, I_w, I_g, I_m, are possible about the points A, W, G, and M of Fig. 12.

123.	D_{4h}^1	D_4^1, I	Γ_t
124.	D_{4h}^2	D_4^1, I_w	Γ_t
125.	D_{4h}^3	D_4^1, I_g	Γ_t
126.	D_{4h}^4	D_4^1, I_m	Γ_t
127.	D_{4h}^5	D_4^2, I	Γ_t
128.	D_{4h}^6	D_4^2, I_w	Γ_t
129.	D_{4h}^7	D_4^2, I_g	Γ_t
130.	D_{4h}^8	D_4^2, I_m	Γ_t
131.	D_{4h}^9	D_4^5, I	Γ_t
132.	D_{4h}^{10}	D_4^5, I_w	Γ_t
133.	D_{4h}^{11}	D_4^5, I_g	Γ_t
134.	D_{4h}^{12}	D_4^5, I_m	Γ_t
135.	D_{4h}^{13}	D_4^6, I	Γ_t
136.	D_{4h}^{14}	D_4^6, I_w	Γ_t
137.	D_{4h}^{15}	D_4^6, I_g	Γ_t
138.	D_{4h}^{16}	D_4^6, I_m	Γ_t
139.	D_{4h}^{17}	D_4^9, I	Γ_t'
140.	D_{4h}^{18}	D_4^9, I_w	Γ_t'
141.	D_{4h}^{19}	D_4^{10}, I_g	Γ_t'
142.	D_{4h}^{20}	D_4^{10}, I_m	Γ_t'

The tabulations of the tetragonal space-groups given in Appendix III are somewhat more complicated than those given above. The reason for this is as follows: It was shown in Chap. II that there are only two possible tetragonal space-lattices, namely Γ_t and Γ_t'. It was brought out in Chaps. II, III, and IV, and again in Table II of this chapter, that the first of these, Γ_t, may be regarded at will as being either a simple tetragonal lattice $\Gamma_t(a)$ (corresponding to the simple orthorhombic lattice Γ_o), or an end-centered tetragonal lattice $\Gamma_t(b)$ (*i.e.*, with the square faces centered, thus corresponding to the end-centered or side-centered orthorhombic lattice Γ_o'). Similarly it was shown that Γ_t' may be regarded at will as being a face-centered tetragonal lattice $\Gamma_t'(a)$ (corresponding to Γ_o'') or a body-centered tetragonal lattice $\Gamma_t'(b)$ (corresponding to Γ_o'''). For each of these two lattices the various crystal forms may be described according to either alternative, so that both are given in the tetragonal tabulations of Appendix III except for the space-groups derived from $D_{2d} = V_d$. In the $D_{2d} = V_d$ class, the axial planes are always taken as bisecting the angles between the symmetry planes of the crystal, so that only one of the alternatives is possible with Γ_t and only one with Γ_t'. To avoid confusion, the example of Astbury and

Yardley is followed in Appendix III and the orthorhombic lattice with which the actual tetragonal lattice may be compared is inserted in parentheses in the space-lattice column. In order to facilitate reference to Astbury and Yardley,[1] $\Gamma_t(a)$ and $\Gamma_t'(b)$ are listed in Appendix III as the "first alternatives" of Γ_t and Γ_t', respectively. $\Gamma_t(b)$ and $\Gamma_t'(a)$ are listed as the "second alternatives."*

In using the tetragonal tabulations of Appendix III it should be kept in mind that in the tetragonal system the form $\{1\,0\,0\}$ includes both the $(1\,0\,0)$ and the $(0\,1\,0)$ planes. Similarly the form $\{0\,k\,l\}$ includes both the $(0\,k\,l)$ and the $(h\,0\,l)$ planes; that is, the X- and Y-axes are indistinguishable from each other. For example, C_{4v} 1) reads "½ for $\{0\,k\,l\}$ if $(k + l)$ is odd." This means not only that the periodicity s is ½ for $\{0\,k\,l\}$ if $(k + l)$ is odd, but also that s is also ½ for $\{h\,0\,l\}$ if $(h + l)$ is odd.

It has already been pointed out that when a crystal is examined by the Laue method with "white" x-rays, there is imposed upon the diffraction pattern the effect of a center of symmetry. In the tetragonal system the addition of a center of symmetry to the seven classes of space-groups reduces them to two, one showing full C_{4h} symmetry and the other showing full D_{4h} symmetry. Consequently, by the use of the Laue method, we can readily discriminate between the space-groups derived from S_4, C_4, and C_{4h}, on the one hand, and space-groups derived from $D_{2d}(=V_d)$, C_{4v}, D_4, and D_{4h} on the other hand. Such a partitioning of the seven classes of tetragonal space-groups may be useful when the value of the periodicity s is the same for certain space-groups which are derived from different point-groups.

E. Cubic System (Space-groups 143 to 178)

XVI. *Cubic Tetartohedry; Tesseral Polar.*—The space-groups belonging to this class of symmetry can be obtained by combining with the symmetry operations leading to certain of the V^m space-groups the operation of a 3-fold axis, A_3. In the case of T^2 this 3-fold axis must lie in the diagonal $A'A$ of Fig. 12. For the other T^m space-groups any of the body-diagonals of Fig. 12 may be used.

143.	T^1	V^1, A_3	Γ_c
144.	T^2	V^7, A_3	Γ_c'
145.	T^3	V^8, A_3	Γ_c''
146.	T^4	V^4, A_3	Γ_c
147.	T^5	V^9, A_3	Γ_c''

* It should be noted that the diagrams given at the end of their article by Astbury and Yardley[1] correspond to alternative (1); the diagrams corresponding to alternative (2) may be made by interchanging the (1 1 0) and (1 0 0) planes.

XVII. *Cubic Enantiomorphic Hemihedry; Tesseral Holoaxial.*—The space-groups of this class can be formed by combining the operation of a 2-fold axis with the operations leading to space-groups T^m.

The 2-fold axis is parallel to KU of Fig. 14. If it passes through the point A, it is denoted by U; if it passes through M, it is denoted by

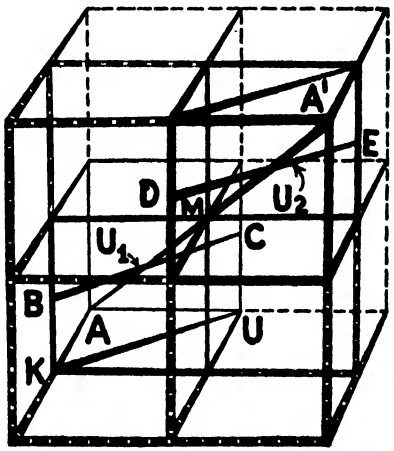

FIG. 14.—The 2-fold axes of space-groups O^m.

U_m; if it lies in the line BC, which bisects AM, it is denoted by U_1; if it lies in the line DE, which bisects MA', it is denoted by U_2.

148.	O^1	T^1, U	Γ_c
149.	O^2	T^1, U_m	Γ_c
150.	O^3	T^2, U	Γ_c'
151.	O^4	T^2, U_m	Γ_c'
152.	O^5	T^3, U	Γ_c''
153.	O^6	T^4, U_1	Γ_c
154.	O^7	T^4, U_2	Γ_c
155.	O^8	T^5, U	Γ_c''

XVIII. *Cubic Paramorphic Hemihedry; Tesseral Central.*—In the discussion of point-group T_h it was stated that T_h could be obtained by combining a horizontal mirror with the symmetry combination used to form T and that the horizontal mirror could be replaced by an inverter. Space-groups T_h^m can therefore be formed by combining the operation of S_h or I with T^m. When the inverter is used, the center of symmetry is at A or M of Fig. 12. The two inversions are denoted by I and I_m, respectively.

156.	T_h^1	T^1, I	Γ_c
157.	T_h^2	T^1, I_m	Γ_c
158.	T_h^3	T^2, I	Γ_c'

159.	T_h^4	T^2, I_m	Γ_c'
160.	T_h^5	T^3, I	Γ_c''
161.	T_h^6	T^4, I	Γ_c
162.	T_h^7	T^5, I	Γ_c''

XIX. *Cubic Hemimorphic Hemihedry; Ditesseral Polar.*—The space-groups having this class of symmetry can be obtained by combining with the operations of T^m the operation of a diagonal mirror or of a diagonal glide-mirror. The mirror or glide-mirror lies in a (1 1 0) plane of the cube (*WMGA* of Fig. 12).

163.	T_d^1	T^1, S_d	Γ_c
164.	T_d^2	T^2, S_d	Γ_c'
165.	T_d^3	T^3, S_d	Γ_c''
166.	T_d^4	$T^1, S_d(\tau)$	Γ_c
167.	T_d^5	$T^2, S_d(\tau)$	Γ_c'
168.	T_d^6	$T^5, S_d(\tau)$	Γ_c''

XX. *Cubic Holohedry; Ditesseral Central.*—The space-groups in this class can be obtained by combining the operation of a horizontal mirror

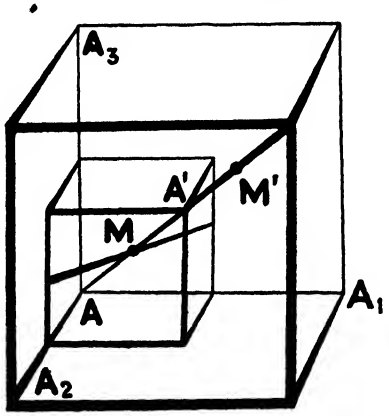

FIG. 15.—The centers of inversion of space-groups O_h^m.

S_h with the operations leading to the space-groups O^m. The horizontal mirror may be replaced by inverters I, I', I_m, and I_m' whose centers of inversion are at A, A', M, and M' of Fig. 15.

169.	O_h^1	O^1, I	Γ_c
170.	O_h^2	O^1, I_m	Γ_c
171.	O_h^3	O^2, I	Γ_c
172.	O_h^4	O^2, I_m	Γ_c
173.	O_h^5	O^3, I	Γ_c'
174.	O_h^6	O^3, I'	Γ_c'
175.	O_h^7	O^4, I_m	Γ_c'

176.	O_h^8	O^4, I_m'	Γ_c'
177.	O_h^9	O^5, I	Γ_c''
178.	O_h^{10}	O^8, I	Γ_c''

Only three space-lattices have cubic symmetry. The first of these, Γ_c, is the simple cubic lattice corresponding to Γ_o and Γ_t but with all its edges equal in length. The face-centered cubic lattice Γ_c' corresponds to Γ_o''. It is not possible in the cubic system for one pair of opposite faces to be centered and not the other two pairs (like Γ_o'), since every cubic crystal must have four 3-fold axes of symmetry perpendicular to the $\{1\,1\,1\}$ planes; in other words, the X-, Y-, and Z-axes must be indistinguishable not only in length but in every other respect. The body-centered cubic lattice Γ_c'' corresponds to Γ_o''' except that all its edges are equal.

Since the three cubic axes are indistinguishable, the form $\{h\,k\,0\}$ includes all the three axial zones just as the form $\{1\,0\,0\}$ includes all the axial planes. This must be remembered in referring to the tabulations of cubic space-groups in Appendix III. For example, when we read "T_h^2; $s = \frac{1}{2}$ for $\{h\,k\,0\}$ if $(h + k)$ is odd," we must remember that s will be $\frac{1}{2}$ for any plane in an axial zone if the sum of the indices is odd, so that our statement will apply not only to $(h\,k\,0)$ but also to $(h\,0\,k)$, $(0\,h\,k)$, $(k\,h\,0)$, $(k\,0\,h)$, $(\bar{h}\,k\,0)$, etc.; or to take a specific example, our statement applies not only to $(1\,2\,0)$, but also to $(1\,0\,2)$, $(0\,1\,2)$, $(2\,1\,0)$, $(2\,0\,1)$, $(\bar{1}\,2\,0)$, etc.

In the cubic system, white x-rays yield two types of Laue diffraction patterns, because adding a center of symmetry to each of the five classes of space-groups reduces them to two, one possessing full T_h symmetry and one possessing full O_h symmetry. It follows that Laue diffraction patterns can distinguish between the T and T_h classes on the one hand and the T_d, O, and O_h classes on the other hand. But no x-ray methods alone can distinguish between, say, T^1 and T_h^1 if there are 12, 6, or 1 molecules per unit of structure, nor between T_d^1, O^1, or O_h^1 if there are 24, 12, 6, or 1 molecules per unit of structure.

F. Hexagonal System (Space-groups 179 to 230)

RHOMBOHEDRAL DIVISION

XXI. *Rhombohedral Tetartohedry; Trigonal Polar.*—The space-groups of this symmetry class are obtained by combining a 3-fold axis $A(2\pi/3)$ or screw axis with the lattices Γ_h and Γ_{rh}. The screw axis is parallel to the Z-axis.

179.	C_3^1	$A\left(\frac{2\pi}{3}\right)$, Γ_h	Γ_h
180.	C_3^2	$A\left(\frac{2\pi}{3}, \frac{2\tau_z}{3}\right)$, Γ_h	Γ_h

181. C_3^3 $A\left(\frac{2\pi}{3}, \frac{4\tau_z}{3}\right), \Gamma_h$ Γ_h

182. C_3^4 $A\left(\frac{2\pi}{3}\right), \Gamma_{rh}$ Γ_{rh}

XXII. *Rhombohedral Enantiomorphic Hemihedry; Trigonal Holoaxial.*—The space-groups of this class are formed by combining a 2-fold axis U with the operations leading to space-groups C_3^m. When the 2-fold axis lies along the Y-axis of a system of hexagonal coordinates, it is

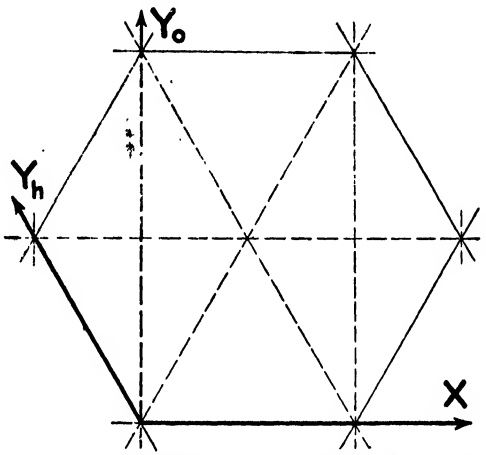

FIG. 16.—The X-Y plane of the hexagonal and orthohexagonal systems of coordinates (see also Chap. II, Fig. 10).

denoted by U_a; when it lies along the Y-axis of a system of orthohexagonal coordinates (see Fig. 16), it is denoted by U_b.

183. D_3^1 C_3^1, U_b Γ_h
184. D_3^2 C_3^1, U_a Γ_h
185. D_3^3 C_3^2, U_b Γ_h
186. D_3^4 C_3^2, U_a Γ_h
187. D_3^5 C_3^3, U_b Γ_h
188. D_3^6 C_3^3, U_a Γ_h
189. D_3^7 C_3^4, U_b Γ_{rh}

XXIII. *Rhombohedral Hemimorphic Hemihedry; Ditrigonal Polar.*—The space-groups of this class are formed by combining a vertical mirror or glide-mirror with the operations leading to C_3^m. The mirror S_a lies in the Y-axis of hexagonal coordinates; the mirror S_b liés in the Y-axis of orthohexagonal coordinates (see Fig. 16).

190. C_{3v}^1 C_3^1, S_b Γ_h
191. C_{3v}^2 C_3^1, S_a Γ_h
192. C_{3v}^3 $C_3^1, S_b(\tau_z)$ Γ_h

193.	C_{3v}^4	$C_3^1, S_a(\tau_z)$	Γ_h
194.	C_{3v}^5	C_3^4, S_a	Γ_{rh}
195.	C_{3v}^6	$C_3^4, S_a(\tau_z)$	Γ_{rh}

XXIV. *Hexagonal Tetartohedry of the Second Sort* (*Rhombohedral Paramorphic Hemihedry*); *Hexagonal Alternating.*—These space-groups are obtained by combining an inversion with C_3^m.

196.	C_{3i}^1	C_3^1, I	Γ_h
197.	C_{3i}^2	C_3^4, I	Γ_{rh}

XXV. *Rhombohedral Holohedry; Dihexagonal Alternating.*—The space-groups of this class can be obtained by a diagonal mirror with D_3^m. The mirror may be replaced by an inverter for which the center of symmetry may be at the intersection of a 3-fold axis and a 2-fold axis (I) or half way between successive intersections (I').

198.	D_{3d}^1	D_3^1, I	Γ_h
199.	D_{3d}^2	D_3^1, I'	Γ_h
200.	D_{3d}^3	D_3^2, I	Γ_h
201.	D_{3d}^4	D_3^2, I'	Γ_h
202.	D_{3d}^5	D_3^7, I	Γ_{rh}
203.	D_{3d}^6	D_3^7, I'	Γ_{rh}

HEXAGONAL DIVISION

XXVI. *Trigonal Paramorphic Hemihedry; Trigonal Equatorial.*—This space-group is obtained by combining a horizontal mirror with the operations of C_3^1.

204.	C_{3h}^1	C_3^1, S_h	Γ_h

XXVII. *Trigonal Holohedry; Ditrigonal Equatorial.*—The space-groups in this class are formed by combining a horizontal mirror with the operations of D_3^m. The mirror may lie in a plane which contains the 2-fold axis (S_h) or it may lie midway between two such adjacent planes (S_m).

205.	D_{3h}^1	D_3^1, S_h	Γ_h
206.	D_{3h}^2	D_3^1, S_m	Γ_h
207.	D_{3h}^3	D_3^2, S_h	Γ_h
208.	D_{3h}^4	D_3^2, S_m	Γ_h

XXVIII. *Hexagonal Tetartohedry; Hexagonal Polar.*—The space-groups in this class are formed by combining a 6-fold axis $A(\pi/3)$ or a 6-fold screw axis with the hexagonal lattice.

209.	C_6^1	$A\left(\frac{\pi}{3}\right), \Gamma_h$	Γ_h

210.	C_6^2	$A\left(\frac{\pi}{3}, \frac{\tau_z}{3}\right)$, Γ_h	Γ_h
211.	C_6^3	$A\left(\frac{\pi}{3}, \frac{5\tau_z}{3}\right)$, Γ_h	Γ_h
212.	C_6^4	$A\left(\frac{\pi}{3}, \frac{2\tau_z}{3}\right)$, Γ_h	Γ_h
213.	C_6^5	$A\left(\frac{\pi}{3}, \frac{4\tau_z}{3}\right)$, Γ_h	Γ_h
214.	C_6^6	$A\left(\frac{\pi}{3}, \tau_z\right)$, Γ_h	Γ_h

XXIX. *Hexagonal Enantiomorphic Hemihedry; Hexagonal Holoaxial.*—The space-groups of this class can be derived by combining a 2-fold axis U_a with the operations of C_6^m. The 2-fold axis lies along the X-axis of Fig. 16.

215.	D_6^1	C_6^1, U_a	Γ_h
216.	D_6^2	C_6^2, U_a	Γ_h
217.	D_6^3	C_6^3, U_a	Γ_h
218.	D_6^4	C_6^4, U_a	Γ_h
219.	D_6^5	C_6^5, U_a	Γ_h
220.	D_6^6	C_6^6, U_a	Γ_h

XXX. *Hexagonal Paramorphic Hemihedry; Hexagonal Equatorial.*—The space-groups of this class can be derived by combining a horizontal mirror with the operations of C_6^m.

221.	C_{6h}^1	C_6^1, S_h	Γ_h
222.	C_{6h}^2	C_6^6, S_h	Γ_h

XXXI. *Hexagonal Hemimorphic Hemihedry; Dihexagonal Polar.* The space-groups of this class are obtained by combining a vertical mirror or a vertical glide-mirror with the operations of C_6^m. The mirror S_a lies in the X-axis of Fig. 16. Its operations produce the effect of a second mirror in the orthohexagonal Y-axis.

223.	C_{6v}^1	C_6^1, S_a	Γ_h
224.	C_{6v}^2	$C_6^1, S_a(\tau_z)$	Γ_h
225.	C_{6v}^3	C_6^6, S_a	Γ_h
226.	C_{6v}^4	$C_6^6, S_a(\tau_z)$	Γ_h

XXXII. *Hexagonal Holohedry; Dihexagonal Equatorial.*—The space-groups in this class are easiest obtained by combining an inversion with the operations of D_6^m. The center of symmetry lies in the 6-fold axis, either at its intersection with a 2-fold axis or midway between two such adjacent planes. The two possible inversions are denoted by I and I', respectively.

227.	D^1_{6h}	D^1_6, I	Γ_h
228.	D^2_{6h}	D^1_6, I'	Γ_h
229.	D^3_{6h}	D^6_6, I	Γ_h
230.	D^4_{6h}	D^6_6, I'	Γ_h

General Remarks on the Hexagonal System.—We have seen from Table II that, although the hexagonal division of this system is based entirely on the hexagonal lattice, the rhombohedral division is based on both the hexagonal and the rhombohedral lattices. The hexagonal lattice Γ_h is identical with a simple monoclinic lattice (see Chap. II) for which the X- and Y-axes make an angle of 120° and for which $a = b$. In other words, it is a distorted simple tetragonal lattice for which the angle between the X- and Y-axes has been increased to 120°. The rhombohedral lattice Γ_{rh} is a simple cube which has been compressed or elongated along its body-diagonal. This body-diagonal then becomes the unique 3-fold axis of the rhombohedron. The rhombohedral lattice occurs as an alternative to the hexagonal lattice in C_3, C_{3i}, C_{3v}, D_3, and D_{3d}. This introduces a peculiar difficulty in the examination of crystals belonging to any of these five point-groups, for such crystals are usually referred to the Miller axes (distorted cubic axes) irrespective of whether the basic lattice is rhombohedral or hexagonal. These rhombohedral axes are no more suitable for the description of a crystal which is based on the hexagonal lattice than the Bravais-Miller hexagonal axes would be in describing a true rhombohedral crystal. This difficulty may be avoided by reserving the Miller (rhombohedral) axes for the true rhombohedral crystals and the Bravais-Miller hexagonal axes for the crystals which are based on the hexagonal axes. The following discussion, adapted from Astbury and Yardley,[1] shows how this may be done.

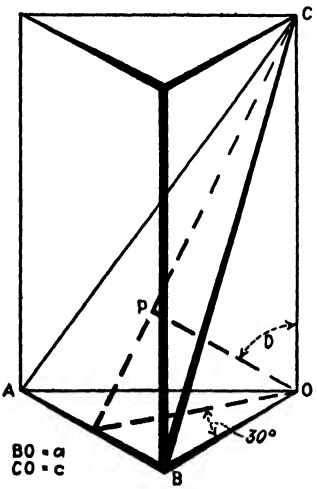

FIG. 17.—Simple trigonal pyramid.

It is not completely possible by examination of the external form alone to find out on which of the two lattices the crystal under examination is built, but, in general, a crystal tends to betray its basic lattice in its external form or "habit." In rhombohedral ("trigonal") crystals based on Γ_h we should expect simple trigonal prisms and pyramids, while in those based on Γ_{rh} the development of rhombohedra is more likely. Consider now a crystal developed as a simple trigonal pyramid only (see Fig. 17). A face of this pyramid would be taken as the parametral plane and for Γ_h would correspond to ABC in Fig. 17. For Γ_{rh} it

would correspond to an extended rhombohedral face such as $\underline{W}MN$ of Fig. 18. In the first the ratio $c/a = OC/OA$; and, in the second, $c/a = O\underline{W}/O\underline{X}$. If the lattice is Γ_h, the crystallographic and experimental values of c/a will agree in the simplest case (C_3^1, say), but should the lattice be really rhombohedral (C_3^4) the observed ratio will be

$$\frac{2}{3}\frac{c}{2a} = \frac{c}{3a}$$

Unfortunately this is only the simplest case, and such a test would not distinguish immediately between C_3^2 (or C_3^3), in which there are screw

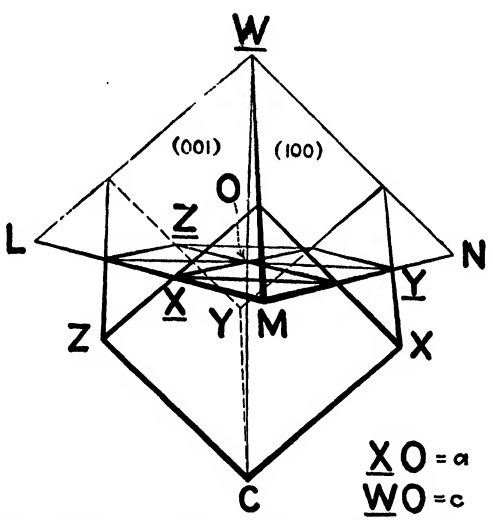

FIG. 18.—Rhombohedron showing relation between rhombohedral axes and hexagonal axes.

axes of translation $2\tau_z/3$, and C_3^4 which is based on a simple rhombohedral lattice.

There are, however, always certain planes which can be used as an aid in identifying the underlying space-lattice. Such planes are the prism faces $(1\bar{2}1)$ or $(10\bar{1}0)$ and $(1\bar{1}0)$ or $(11\bar{2}0)$. A glance at the tables shows that the spacings of these planes are unaffected by the dispositions of the molecules. Figure 18 shows the relation between the rhombohedral axes (parallel to CX, CY, CZ) and the hexagonal axes ($O\underline{X}$, $O\underline{Y}$, $O\underline{Z}$, $O\underline{W}$). The volume of the rhombohedron is $4a^2c/\sqrt{3}$, while the volume of the corresponding hexagonal cell is $a^2c\sqrt{3}/2$; the ratio between the two is $\frac{8}{3}$. Thus the dimensions of a rhombohedron with $\frac{8}{3}$ molecules per cell will correspond crystallographically to those of a hexagonal cell with one molecule per cell, that is, the dimensions in the two cases are based on the same values of c and a.

Suppose now in a given rhombohedral (trigonal) crystal the chosen parametral plane is the true parametral plane of either Γ_h or Γ_{rh}. The possible numbers (N, say) of molecules per cell can be obtained from the tables, and from the above we know that the dimensions of a rhombohedron containing $8N/3$ molecules per cell will correspond to the dimensions of a hexagonal cell of N molecules per cell. Hence we can calculate and compare the corresponding spacings of these two corresponding cells. For the hexagonal cell, $d_{10\bar{1}0} = a\sqrt{3}/2$ and $d_{11\bar{2}0} = a/2$; but for the corresponding rhombohedral cell, $d_{1\bar{2}1} = a/\sqrt{3}$ and $d_{1\bar{1}0} = a$. Thus in a rhombohedral crystal based on a hexagonal lattice, but referred by convention to rhombohedral axes, provided that the crystallographic parametral plane is the same as the parametral plane of the hexagonal lattice, we can detect the hexagonal lattice by testing the $(1\bar{2}1)$ and the $(1\bar{1}0)$ of a rhombohedron containing $8N/3$ molecules per cell, where N is either equal to n, the number of asymmetric molecules given by the class, or to some submultiple of n. We shall find that the observed spacing of $(1\bar{2}1)$ is $\frac{3}{2}$ times that calculated for a simple lattice, while for $(1\bar{1}0)$ it is $\frac{1}{2}$ the calculated value. Additional information is afforded (*a*) by the (1 1 1), the observed spacing of which is normally $\frac{3}{2}$ times the calculated but which by a thirding or halving may be reduced to $\frac{1}{2}$ or $\frac{3}{4}$ times the calculated value; and (*b*) by the (1 0 0), the observed spacing of which is normally $\frac{1}{2}$ the calculated value but which by a halving may be reduced to $\frac{1}{4}$ of the calculated value.

If the above treatment leads to anomalous results, the inference is that the crystallographic parametral plane does not correspond to the true parametral plane of the lattice, in which case it is necessary to repeat the examination using the face of another general form $\{hkl\}$ as parametral plane and making the new "angular element" D equal to the angle between (hkl) and (1 1 1).* (Note that $c/a = \tan D \cos 30°$.) When agreement is found, the crystallographic nomenclature should be abandoned and the crystal referred to the true structural axes.

Another difficulty, similar to the one discussed above, arises in the examination of crystals based on Γ_h from the frequent discrepancy between the conventional relations between crystallographic axes and elements of symmetry and the true structural relations. For instance, in the C_{3v} and D_{3h} classes, the conventional crystallographic axes (rhombohedral, since the class is trigonal) lie *in* the symmetry planes, and the hexagonal axes derived from these are perpendicular to the symmetry planes. Thus these derived hexagonal axes correspond to the true structural axes in groups C_{3v}^1 and C_{3v}^3 but are perpendicular to them in groups C_{3v}^2 and C_{3v}^4. In the two last mentioned, the crystallographic angle D, equal to the angle between (1 0 0) and (1 1 1), is not the true

* In the symbols of crystallography, $D = (hkl) \wedge (1\,1\,1)$.

structural angular element (D_0, say). The two are connected by the equations $c/a = \tan D_0 \cdot \cos 30° = \tan D \sin 30°$, where c and a refer to the true structural values. It must be distinctly understood that all the tabulated data of Appendix III refer exclusively to the true structural axes, *i.e.*, to the edges of the true unit-cell. If there is any discrepancy between the conventional and structural axes, it is necessary to first localize this difficulty, as far as is theoretically possible, and then apply the tabulated results. This sort of problem occurs in many of the crystal classes in addition to those belonging to this system,[6] and no general rules for guidance can be offered. With regard to other classes of the systems now being discussed it should be noticed that in the classes D_3 and D_{3d} crystallographers always take the 2-fold axes as hexagonal axes, whereas the true structural axes may be parallel or perpendicular to the 2-fold axes. By referring to the tables it will be found that only in a very limited number of cases is it possible without complete examination to distinguish between groups in which the true structural hexagonal axes lie in the symmetry planes (C^2_{3v}, C^4_{3v}, D^3_{3h}, D^4_{3h}) and the corresponding groups in which they are perpendicular to the symmetry planes (C^1_{3v}, C^3_{3v}, D^1_{3h}, D^2_{3h}). For example, we can distinguish between C^1_{3v} and C^2_{3v} if there are two molecules only per cell, for then the molecule itself must possess a 3-fold axis and this is only possible in C^2_{3v}; but the tables alone do not distinguish between them if there are one, three, or six molecules per cell. Similar considerations hold with regard to the pairs of groups in which the true hexagonal axes are parallel and perpendicular, respectively, to the 2-fold axes of the structure (D^2_3 and D^1_3; D^4_3 and D^3_3; D^6_3 and D^5_3; D^3_{3d} and D^1_{3d}; D^4_{3d} and D^2_{3d}).

In Laue photographs of crystals belonging to these two systems classes C_3 and C_{3i} appear as C_{3i}; C_{3v}, D_3, and D_{3d} appear as D_{3d}; C_{3h}, C_6, and C_{6h} appear as C_{6h}; D_{3h}, D_6, C_{6v}, and D_{6h} appear as D_{6h}; thus the twelve classes are reduced to four.

A method of detecting the underlying lattice, based on the study of Laue diagrams has been suggested by Wyckoff. It will be discussed in Chap. IX.

Derivation of Coordinates.—We have shown how the 230 space-groups may be arrived at. It remains to show how to obtain the coordinates for the points in each of these space-groups. The process may be illustrated in terms of the space-group C^1_{2h} which has already been pictured in Fig. 10*b*. Figure 10*b* shows the monoclinic unit-prism (or unit-cell) *OAFCGBDE*. This contains the points M, M', M'', and M''', whose coordinates are:

$x,$	$y,$	z
$2\tau_x - x,$	$2\tau_y - y,$	z
$x,$	$y,$	$2\tau_z - z$
$2\tau_x - x,$	$2\tau_y - y,$	$2\tau_z - z$

Since it is inherent in a space-lattice that any point may be used as the starting point in building up the lattice, we may move this unit-prism bodily so that the point O lies at its center. Instead of the original points M, M', M'', and M''', the unit-prism now contains the four points M, P_4, P_5, and P_6 whose coordinates

$$xyz, \quad \bar{x}\bar{y}z, \quad xy\bar{z}, \quad \bar{x}\bar{y}\bar{z}$$

are the simplest possible since they do not involve τ_x, τ_y, and τ_z. These simple coordinates will be used to typify the coordinates of all the points in the crystal, for the crystal itself is merely an endless succession of unit-prisms so placed as to share all their edges and faces with their neighbors.

It is evident from Fig. 10*b* that the space-group C_{2h}^1 cannot possibly contain more than four equivalent points, but it is easy to imagine how it might contain only two points or even only one point.

(1) The point xyz will coincide with the point $\bar{x}\bar{y}z$, when $x = \bar{x}$, $y = \bar{y}$, and $z = z$; that is, when $x = 0$ or $a/2$, $y = 0$ or $b/2$, and $z = wc$, where w is any fractional part of c. (a, b, and c are the units of measure along the X-, Y-, and Z-axes, respectively, as in Chap. II.) These same conditions will cause the points $xy\bar{z}$ and $\bar{x}\bar{y}\bar{z}$ to coincide so that the original four equivalent points have become two.

(2) The points xyz and $xy\bar{z}$ will coincide when $x = x$, $y = y$, and $z = \bar{z}$; that is, when $x = ua$, $y = vb$, and $z = 0$ or $c/2$. u and v are any fractional parts of a and b, respectively. These same conditions will cause the points $\bar{x}\bar{y}z$ and $\bar{x}\bar{y}\bar{z}$ to coincide so that again the original four equivalent points have become two.

(3) The points xyz and $\bar{x}\bar{y}\bar{z}$ will coincide when $x = \bar{x}$, $y = \bar{y}$, and $z = \bar{z}$; that is, when $x = 0$ or $a/2$, $y = 0$ or $b/2$, $z = 0$ or $c/2$. These same conditions will cause the points $\bar{x}\bar{y}z$ and $xy\bar{z}$ to coincide with xyz, so that the original four points have become one. These values of x, y, and z lead to the following possible coordinates of points, expressed in terms of fractions of a, b, and c.

(1) When $x = 0$, $y = 0$, and $z = w$, we obtain $00w$ and $00\bar{w}$
When $x = 0$, $y = \frac{1}{2}$, and $z = w$, we obtain $0\frac{1}{2}w$ and $0\frac{1}{2}\bar{w}$
When $x = \frac{1}{2}$, $y = 0$, and $z = w$, we obtain $\frac{1}{2}0w$ and $\frac{1}{2}0\bar{w}$
When $x = \frac{1}{2}$, $y = \frac{1}{2}$, and $z = w$, we obtain $\frac{1}{2}\frac{1}{2}w$ and $\frac{1}{2}\frac{1}{2}w$
(2) When $x = u$, $y = v$, and $z = 0$, we obtain $uv0$ and $\bar{u}\bar{v}0$
When $x = u$, $y = v$, and $z = \frac{1}{2}$, we obtain $uv\frac{1}{2}$ and $\bar{u}\bar{v}\frac{1}{2}$
(3) When $x = 0$, $y = 0$, and $z = 0$, we obtain 000
When $x = \frac{1}{2}$, $y = 0$, and $z = 0$, we obtain $\frac{1}{2}00$
When $x = 0$, $y = \frac{1}{2}$, and $z = 0$, we obtain $0\frac{1}{2}0$
When $x = 0$, $y = 0$, and $z = \frac{1}{2}$, we obtain $00\frac{1}{2}$
When $x = 0$, $y = \frac{1}{2}$, and $z = \frac{1}{2}$, we obtain $0\frac{1}{2}\frac{1}{2}$
When $x = \frac{1}{2}$, $y = 0$, and $z = \frac{1}{2}$, we obtain $\frac{1}{2}0\frac{1}{2}$

When $x = \frac{1}{2}$, $y = \frac{1}{2}$, and $z = 0$, we obtain $\frac{1}{2}\frac{1}{2}0$
When $x = \frac{1}{2}$, $y = \frac{1}{2}$, and $z = \frac{1}{2}$, we obtain $\frac{1}{2}\frac{1}{2}\frac{1}{2}$

It is evident that any further attempt to consolidate points by trying to make the equivalent points of (1) or (2) coincide leads to coordinates already listed under (3). We may therefore list as the possible coordinates of equivalent points of C_{2h}^1 in the order given by Wyckoff, giving to each set of coordinates the standard Wyckoff code letter:

One equivalent position:

(*a*) 000	(*e*) $0\frac{1}{2}\frac{1}{2}$
(*b*) $00\frac{1}{2}$	(*f*) $\frac{1}{2}0\frac{1}{2}$
(*c*) $\frac{1}{2}00$	(*g*) $\frac{1}{2}\frac{1}{2}0$
(*d*) $0\frac{1}{2}0$	(*h*) $\frac{1}{2}\frac{1}{2}\frac{1}{2}$

Two equivalent positions:*

(*i*) $00w$; $00\bar{w}$	(*l*) $\frac{1}{2}\frac{1}{2}w$; $\frac{1}{2}\frac{1}{2}\bar{w}$
(*j*) $0\frac{1}{2}w$; $0\frac{1}{2}\bar{w}$	(*m*) $uv0$; $\bar{u}\bar{v}0$
(*k*) $\frac{1}{2}0w$; $\frac{1}{2}0\bar{w}$	(*n*) $uv\frac{1}{2}$; $\bar{u}\bar{v}\frac{1}{2}$

Four equivalent positions:

(*o*) xyz; $\bar{x}\bar{y}z$; $xy\bar{z}$; $\bar{x}\bar{y}\bar{z}$

If this same procedure is followed for all the rest of the 230 space-groups we shall arrive at a tabulation of all the coordinates (expressed in their simplest forms) possible for equivalent points in crystals. Such a tabulation has been made by R. W. G. Wyckoff. It has been published as *Publication* 318 by the Carnegie Institution of Washington under the name of "The Analytical Expression of the Results of the Theory of Space-groups" (2d ed.). This book should be in the hands of every crystal analyst. It is used in crystal analysis as a convenient table of reference to the same extent that a table of logarithms is used in trigonometry.

For convenience of reference in Chap. IX, the numbers of equivalent points which can be associated with each of the various point-groups are tabulated† in Appendix III. These values may be picked off from the space-group tables of Wyckoff, or they may be found from the values of n and p given in the Astbury and Yardley tables of Appendix III.

* It is customary in writing these coordinates to use u when there is only one undetermined (*i.e.*, variable or adjustable) coordinate, so that $00w$ would appear as $00u$, etc.

† This tabulation follows the form of similar tables in Wyckoff but uses the order of Table I of this chapter and of the Astbury and Yardley tables of Appendix III.

References

1. The subject matter of this chapter is given in somewhat different form in considerable detail by R. W. G. Wyckoff in his book, "The Analytical Expression of the Results of the Theory of Space-groups," published as *Publication* 318 (2d ed.) by the *Carnegie Institution* of Washington. This book should be owned by every student who expects to do research in crystal structure. A portion of the subject matter is based on an excellent article by W. T. Astbury and K. Yardley in *Phil. Trans. Roy. Soc. London*, **A, 224,** 221 (1924).

   The original sources are:

   Bravais, *Jour. école polytech.*, **19,** 127 (1850); **20,** 102 (1851).

   Jordan, *Annali di matematica pura ed applicata*, (2), 167, 215, 322 (1869).

   Sohncke, "Entwickelung einer Theorie der Krystallstruktur," Leipzig, 1879. See also *Report* of the British Association, pp. 297–337 (1901).

   Schoenflies, "Krystallsysteme und Krystallstruktur," Leipzig, 1891.

   Barlow, *Zeit. Kryst.*, **23,** 1 (1894).

   Federov, *Zeit. Kryst.*, **24,** 209 (1895), and previous (Russian) articles.

2. R. W. G. Wyckoff, *Amer. Jour. Sci.*, **6,** 288 (1923).
   H. Hilton, *Mineralog. Mag.*, **14,** 261 (1907).

3. In this connection see Niggli, Krystallographische und strukturtheoretische Grundbegriffe, "Handbuch der Experimentalphysik," Vol. VII (1), p. 86.

4. The six crystal systems are briefly described from the standpoint of space-lattices in the first three paragraphs of Chap. II.

5. A. P. Honess, "The Nature, Origin, and Interpretation of Etch Figures of Crystals," John Wiley & Sons, Inc., New York, 1927. See also *Penn. State Coll. Mineral Ind. Expt. Sta., Bull.* 3.

6. W. T. Astbury, *Proc. Roy. Soc.*, **A, 104,** 219 (1923).

CHAPTER IX

THE APPLICATION OF THE THEORY OF SPACE-GROUPS

In Chaps. IV, V, VI, and VII we carried our discussions of the methods of crystal analysis up to the point where a knowledge of the theory of space-groups was required. We are now in a position to complete those discussions with the aid of Chap. VIII and Appendix III. This will be done by giving in detail the determination of the structures of rock salt (NaCl), of calcite ($CaCO_3$), and of tricalcium aluminate ($3CaO.Al_2O_3$). We shall use in the first two with the Laue method and the third with the powder method. In the light of these illustrations, further applications of the theory of space-groups should be obvious.

DETERMINATION OF THE STRUCTURE OF NaCl BY THE LAUE METHOD

It was stated in Chap. IV that a typical investigation of crystal structure by the Laue method consists of three steps:

1. The selection of the type of symmetry required by the exterior of the crystal. This limits the possible marshaling of atoms (or molecules) to those space-groups which are consistent with this symmetry.

2. The determination of the dimensions of the unit-crystal and from these the determination of the number of atoms (or molecules) in the unit-crystal. This serves to limit further the number of space-groups found in 1.

3. The selection from the structures found in 2 of the one (or ones) which can be shown to be most consistent with the Laue pattern.

Step 1. NaCl crystallizes in the cubic system. The crystals show a cubic exterior when the salt is pure; certain impurities tend to bring out the {1 1 1} faces at the expense of the {1 0 0} faces. Etch figures on the crystals of the salt in its ordinary state of purity show hemihedral symmetry, but deep etching on extremely pure crystals shows holohedral symmetry.[1,2,3] NaCl must therefore be assigned to the symmetry class O_h. Any attempt to assign a definite space-group in the O_h class must depend upon the results of steps 2 and 3.

Step 2. The determination of the number **n** of "molecules" of NaCl in a unit-cube may be made in various ways depending upon what we are willing to take as a starting point. We shall discuss three ways of determining **n** which do not include the lines of reasoning used in Chaps. V and VI for the Bragg and powder methods.

a. We may assume that the wave length of characteristic x-rays may be determined approximately by measurements of the angle of diffraction from a ruled grating.[4,5] Within the precision of these measurements

of wave length we can make an absolute determination of the lattice parameter of NaCl by using a technique like that employed in the Bragg or powder methods (see Chaps. V and VI). Such a measurement does not involve a solution of the structure of the crystal; the work is only carried far enough to give the length of the edge of the unit-cube.* Knowing the density of NaCl we can now solve Eq. (1) of Chap. II for the number **n** of molecules of NaCl per unit-cube. Evidently this number should be an exact whole number, but, because of the nature of the wave-length data obtained from ruled gratings, **n** will differ somewhat from a true integer. It will, however, be so much closer to 4.00 than to 3.00 or to 5.00 that there can be no doubt but that there are four "molecules" of NaCl per unit-cube.†

b. We may assume that the value of the wave length of the x-rays used in step 2 is given in terms of the calcite standard. This wave length enables us to find directly the length of the edge of the unit-cube of NaCl. By substituting this value into Eq. (1) of Chap. II we arrive at a value for **n** which is within experimental error (about 0.3 per cent) of 4.00.

c. Since we know from step 1 that NaCl has the symmetry of the O_h family of space-groups, we may list for each of the O_h space-groups the possible values of **n** and of $\mathbf{n}/p$ (see Table XXXVII of Appendix III).‡ It is a matter of experience that small values of **n** or of $\mathbf{n}/p$ are much more probable than are large values. We therefore have a series of values

* Strictly speaking, this statement is not necessarily true. The exact state of affairs may be illustrated as follows. If we assume that we are dealing with a cubic crystal and that the interplanar spacing d_{100} represents the length of the edge of the unit-cube, then our calculated value of **n** represents the exact facts. But the crystal may be actually body-centered cubic, or face-centered cubic, or some other cubic structure such that the d_{100} spacing is half the cube edge. In such a case the true spacing of d_{100} would give a diffracted beam at an angle equal to that corresponding to the second-order diffraction from the simple cubic spacing; *i.e.*, it would correspond to d/n, where n is the order of diffraction and d is the interplanar spacing for the simple cube. This will not affect our final result, for such a value for d_{100} gives not only one-eighth the volume but also one-eighth the number of "molecules," so that the number of "molecules" in the actual unit-crystal is the same as before. It is evident that, so long as we do not run into fractional numbers of "molecules" per unit of structure, we are justified in terms of the end result in pretending that our measurements represent the actual parameter of the crystal.

† This value of 4.00 may then be substituted back into Eq. (1) of Chap. II so as to give, with the density, the true value of the lattice parameter of NaCl. The same answer may of course be obtained by using, in the manner described above, some characteristic wave length determined by the quantum relation. The parameter of calcite, determined in much this same way, is now our primary standard of length in crystal analysis.

‡ It will be shown in Chap. XIX that for ionic compounds, in which there is no true "molecule," p cannot be regarded as an index of "molecular symmetry," but the quotient $\mathbf{n}/p$ still represents a possible value of **n** in Eq. (1) of Chap. II.

such as 1, 2, 4, 6, 8, 12, etc., each of which may be tried in turn with each of the O_h space-groups, using the procedure outlined below. Trial will show that only the value 4 will survive the final test of step 3.

We shall therefore assume for the purposes of this discussion that we have settled on the value of 4.00 as the number of "molecules" of NaCl in the unit-cube.* We now have to place four Na^+ ions and four Cl^- ions in a unit-cube which has a symmetry corresponding to the O_h space-groups.

This gives five possibilities open for Na^+:[6]

(1) All four Na^+ ions occupy positions in the unit-cube which are crystallographically indistinguishable. For instance, any one of the four might serve equally well as a corner of the unit-cube. In crystallographic language, all four Na^+ ions are "indistinguishable," "equivalent," "alike," or "of one sort." This may be denoted by the symbol 4.

(2) Three of the Na^+ ions are equivalent to each other, and the fourth is crystallographically distinguishable from the three others. This may be denoted by the symbol 3-1.

(3) Two of the Na^+ ions are equivalent to each other, and the other two are equivalent to each other, but one pair is crystallographically different from the other pair. This might be expressed by saying that two were of one sort and two of a second sort. Such a condition of affairs may be denoted by the symbol 2-2.

(4) Two of the Na^+ ions are equivalent to each other, but the other two are crystallographically distinguishable from this pair and from each other. This may be denoted by 2-1-1.

(5) All four of the Na^+ ions are crystallographically different from one another. This may be denoted by the symbol 1-1-1-1. The same five possibilities may be assumed for the Cl^- ions. This gives us 25 cases which must be considered, namely:

Na^+	4	4	4	4	4
Cl^-	4	3-1	2-2	2-1-1	1-1-1-1
Na^+	3-1	3-1	3-1	3-1	3-1
Cl^-	4	3-1	2-2	2-1-1	1-1-1-1
Na^+	2-2	2-2	2-2	2-2	2-2
Cl^-	4	3-1	2-2	2-1-1	1-1-1-1

* In accordance with modern physicochemical theory, we assume that there are no true "molecules" of NaCl but that we have instead a crystal made up of Na^+ and Cl^- ions. Although it turns out that crystal-structure methods alone cannot distinguish between an orderly geometrical assemblage of Na and Cl atoms and a similar assemblage of ions, still the results are not at all inconsistent with the ionic pictures. It would be unthinkable chemically to picture NaCl as being made up of neutral Na and Cl atoms, and the crystal structure data are quite inconsistent with the picture of NaCl "molecules." This leaves us with Na^+ and Cl^- ions as the only remaining alternative.

Na^+	2-1-1	2-1-1	2-1-1	2-1-1	2-1-1
Cl^-	4	3-1	2-2	2-1-1	1-1-1-1
Na^+	1-1-1-1	1-1-1-1	1-1-1-1	1-1-1-1	1-1-1-1
Cl^-	4	3-1	2-2	2-1-1	1-1-1-1

These 25 possibilities must now be considered in the light of Table XXXVII of Appendix III.

Na+4, *Cl*−4. This combination is possible, since Table XXXVII of Appendix III shows that we can have two complete sets of positions of four points each in both space-groups O_h^4 and O_h^5. In each of these space-groups one of the sets of coordinates may be used for Na^+ and the other for Cl^-. Reference to Wyckoff's tables[1] shows that for O_h^4 we have the coordinates

Na^+	(or Cl^-)	$\frac{1}{4}\frac{1}{4}\frac{1}{4}$;	$\frac{1}{4}\frac{3}{4}\frac{3}{4}$;	$\frac{3}{4}\frac{1}{4}\frac{3}{4}$;	$\frac{3}{4}\frac{3}{4}\frac{1}{4}$
Cl^-	(or Na^+)	$\frac{3}{4}\frac{3}{4}\frac{3}{4}$;	$\frac{3}{4}\frac{1}{4}\frac{1}{4}$;	$\frac{1}{4}\frac{3}{4}\frac{1}{4}$;	$\frac{1}{4}\frac{1}{4}\frac{3}{4}$

and for O_h^5

Na^+	(or Cl^-)	000;	$0\frac{1}{2}\frac{1}{2}$;	$\frac{1}{2}0\frac{1}{2}$;	$\frac{1}{2}\frac{1}{2}0$
Cl^-	(or Na^+)	$\frac{1}{2}\frac{1}{2}\frac{1}{2}$;	$\frac{1}{2}00$;	$0\frac{1}{2}0$;	$00\frac{1}{2}$

These two sets of coordinates represent the same configurations of Na^+ and Cl^-, for they can be made identical by shifting the origin of coordinates of O_h^4 to the point $\frac{1}{4}\frac{1}{4}\frac{1}{4}$. For our purposes they may therefore both be expressed by the coordinates for space-group O_h^5.

Na+4, *Cl*−3-1. Table XXXVII of Appendix III shows that O_h^1 is the only space-group in the O_h class which permits us to have three equivalent points. But O_h^1 does not permit of four equivalent points, so that the grouping Na^+4, Cl^-3-1 is impossible. Similarly the grouping Na^+3-1, Cl^-4 is impossible.

Na+4, *Cl*−2-2. Table XXXVII of Appendix III shows four space-groups each of which permits of *one* "set" of two equivalent points, but there is no space-group in the O_h class which permits of *two* sets of two equivalent points each. Na^+4, Cl^-2-2 is therefore impossible. Similarly Na^+2-2, Cl^-4 and all other groupings containing 2-2 are impossible.

Na+4, *Cl*−2-1-1. Table XXXVII of Appendix III shows no possibility in any of the O_h space-groups of having 2-1-1.

Na+4, *Cl*−1-1-1-1. Table XXXVII of Appendix III shows one space-group which permits of *two* sets of one point each, but there is no space-group which permits of *four* sets of one point each. Na^+4, Cl^-1-1-1-1 is, therefore, impossible. Similarly all other groupings containing 1-1-1-1 are impossible.

Na+3-1, *Cl*−4. See Na^+4, Cl^-3-1.

Na+3-1, *Cl*−3-1. Space-group O_h^1 permits us to have *two* sets of three equivalent points each, and *two* sets of one point each. We may therefore use one of the sets in each case for Na^+ and the other for Cl^-. There

is nothing which requires us to choose which of the two sets of three equivalent points shall go with a given set of a single point. We have therefore two possible configurations of Na^+ and Cl^-. Reference to Wyckoff's tables shows that we may have

Na^+	(or Cl^-)	000	and	$0\frac{1}{2}\frac{1}{2}$,	$\frac{1}{2}0\frac{1}{2}$,	$\frac{1}{2}\frac{1}{2}0$
Cl^-	(or Na^+)	$\frac{1}{2}\frac{1}{2}\frac{1}{2}$	and	$\frac{1}{2}00$,	$0\frac{1}{2}0$,	$00\frac{1}{2}$

or

Na^+	(or Cl^-)	000	and	$\frac{1}{2}00$,	$0\frac{1}{2}0$,	$00\frac{1}{2}$
Cl^-	(or Na^+)	$\frac{1}{2}\frac{1}{2}\frac{1}{2}$	and	$0\frac{1}{2}\frac{1}{2}$,	$\frac{1}{2}0\frac{1}{2}$,	$\frac{1}{2}\frac{1}{2}0$

The first of these is identical with the coordinates listed for O_h^5 and is therefore also indistinguishable from O_h^4.

Na+3-1, *Cl*−2-2. See Na+4, Cl−2-2.
Na+3-1, *Cl*−2-1-1. See Na+4, Cl−2-1-1.
Na+3-1, *Cl*−1-1-1-1. See Na+4, Cl−1-1-1-1.
Na+2-2, *Cl*−4. See Na+4, Cl−2-2.
Na+2-2, *Cl*−3-1. See Na+4, Cl−2-2.
Na+2-2, *Cl*−2-2. See Na+4, Cl−2-2.
Na+2-2, *Cl*−2-1-1. See Na+4, Cl−2-1-1.
Na+2-2, *Cl*−1-1-1-1. See Na+4, Cl−2-2; also Na+4, Cl−1-1-1-1.
Na+2-1-1, *Cl*−4. See Na+4, Cl−2-1-1.
Na+2-1-1, *Cl*−3-1. See Na+4, Cl−2-1-1.
Na+2-1-1, *Cl*−2-2. See Na+4, Cl−2-1-1.
Na+2-1-1, *Cl*−2-1-1. See Na+4, Cl−2-1-1.
Na+2-1-1, *Cl*−1-1-1-1. See Na+4, Cl−2-1-1.
Na+1-1-1-1, Cl−4. See Na+4, Cl−1-1-1-1.
Na+1-1-1-1, *Cl*−3-1. See Na+4, Cl−1-1-1-1.
Na+1-1-1-1, *Cl*−2-2. See Na+4, Cl−1-1-1-1.
Na+1-1-1-1, *Cl*−2-1-1. See Na+4, Cl−2-1-1.
Na+1-1-1-1, *Cl*−1-1-1-1. See Na+4, Cl−1-1-1-1.

We have now covered all the possibilities permitted by the theory of space-groups for a crystal of the holohedral class of cubic symmetry with four "molecules" per unit-cube. The end result has been that we have two sets of coordinates for Na^+ and Cl^-:

Na^+	(or Cl^-)	000;	$0\frac{1}{2}\frac{1}{2}$;	$\frac{1}{2}0\frac{1}{2}$;	$\frac{1}{2}\frac{1}{2}0$
Cl^-	(or Na^+)	$\frac{1}{2}\frac{1}{2}\frac{1}{2}$;	$\frac{1}{2}00$;	$0\frac{1}{2}0$;	$00\frac{1}{2}$

and

Na^+	(or Cl^-)	000;	$\frac{1}{2}00$;	$0\frac{1}{2}0$;	$00\frac{1}{2}$
Cl^-	(or Na^+)	$\frac{1}{2}\frac{1}{2}\frac{1}{2}$;	$0\frac{1}{2}\frac{1}{2}$;	$\frac{1}{2}0\frac{1}{2}$;	$\frac{1}{2}\frac{1}{2}0$

both of which are equally probable in the light of the theory of space-groups. If any criterion is to be found at all by which we may distinguish between these two sets of ionic coordinates, it must be furnished by step 3 in our analysis.

Step 3. Equations (14) and (16) of Chap. IV stated that the intensity of a "spot" in the Laue pattern is proportional to

$$\begin{aligned} R^2 = X^2 + Y^2 = [&\Sigma N_1 \cos 2\pi n(hx_1 + ky_1 + lz_1) \\ &+ \Sigma N_2 \cos 2\pi n(hx_2 + ky_2 + lz_2) \\ &+ \cdots\cdots\cdots\cdots\cdots]^2 \\ &+ [\Sigma N_1 \sin 2\pi n(hx_1 + ky_1 + lz_1) \\ &+ \Sigma N_2 \sin 2\pi n(hx_2 + ky_2 + lz_2) \\ &+ \cdots\cdots\cdots\cdots\cdots]^2 \end{aligned} \tag{1}$$

N_1, N_2 . . . are the atomic (or ionic) numbers of the atoms (or ions) in the crystal; n is the order of the diffracted beam; h, k, l are the Miller indices of the diffracting plane; $x_1y_1z_1$, $x_2y_2z_2$, etc., are the various possible atomic (or ionic) coordinates of atoms (or ions) 1, 2, etc. We substitute into this expression the coordinates of Na^+ and Cl^- as given, first by O_h^5, and then as given by those coordinates for O_h^1 which did not make O_h^1 merely a repetition of O_h^5. In this substitution N_1 becomes N_{Na^+} and N_2 becomes N_{Cl^-}, x_1, y_1, z_1 become in turn the various possible coordinates of Na^+, and x_2, y_2, z_2 become in turn the various possible coordinates of Cl^-.

For O_h^5 Eq. (1) becomes

$$\begin{aligned} R^2 = &\left\{N_{Na^+}\left[\cos 2\pi n(0) + \cos 2\pi n\left(\frac{k}{2}+\frac{l}{2}\right) + \cos 2\pi n\left(\frac{h}{2}+\frac{l}{2}\right)\right.\right. \\ &\left.\left. + \cos 2\pi n\left(\frac{h}{2}+\frac{k}{2}\right)\right] + N_{Cl^-}\left[\cos 2\pi n\left(\frac{h}{2}+\frac{k}{2}+\frac{l}{2}\right) + \cos 2\pi n\left(\frac{h}{2}\right)\right. \right. \\ &\left.\left. + \cos 2\pi n\left(\frac{k}{2}\right) + \cos 2\pi n\left(\frac{l}{2}\right)\right]\right\}^2 + \left\{N_{Na^+}\left[\sin 2\pi n(0)\right.\right. \\ &\left.\left. + \sin 2\pi n\left(\frac{k}{2}+\frac{l}{2}\right) + \sin 2\pi n\left(\frac{h}{2}+\frac{l}{2}\right) + \sin 2\pi n\left(\frac{h}{2}+\frac{k}{2}\right)\right]\right. \\ &\left. + N_{Cl^-}\left[\sin 2\pi n\left(\frac{h}{2}+\frac{k}{2}+\frac{l}{2}\right) + \sin 2\pi n\left(\frac{h}{2}\right) + \sin 2\pi n\left(\frac{k}{2}\right)\right.\right. \\ &\left.\left. + \sin 2\pi n\left(\frac{l}{2}\right)\right]\right\}^2 \end{aligned}$$

Since the sine of an integral multiple of π is zero, the second term of our equation is zero.

When n is even, our equation reduces to

$$R = N_{Na^+}[4] + N_{Cl^-}[4]$$

so that the diffracted beams of even order are all strong.

When n is odd, if h, k, and l are all odd,

$$R = N_{Na^+}[4] + N_{Cl^-}[-4]$$

and these diffracted beams are all weak.

When n is odd, if h, k, and l are one odd and two even,

$$R = N_{Na^+}[0] + N_{Cl^-}[0]$$

and these diffracted beams are absent.

When n is odd, if h, k, and l are two odd and one even,

$$R = N_{Na^+}[0] + N_{Cl^-}[0]$$

and these diffracted beams are absent.

If, therefore, NaCl crystallizes with the structure O_h^5 the diffraction pattern will show strong second-order diffractions for all its crystal planes, but the only first-order diffracted beams will be from planes whose indices are all odd and these beams will all be weak in intensity. The Laue pattern, as interpreted by the gnomonic projection, shows that NaCl diffracts x-rays in exactly this way. O_h^5 therefore remains a possible structure for NaCl. We must now try out O_h^1 in the same way in order to see whether it, too, remains a possible structure for NaCl.

For O_h^1 our equation becomes

$$\begin{aligned} R^2 = \Big\{ & N_{Na^+}\Big[\cos 2\pi n(0) + \cos 2\pi n\Big(\frac{h}{2}\Big) + \cos 2\pi n\Big(\frac{k}{2}\Big) + \cos 2\pi n\Big(\frac{l}{2}\Big)\Big] \\ & + N_{Cl^-}\Big[\cos 2\pi n\Big(\frac{h}{2}+\frac{k}{2}+\frac{l}{2}\Big) + \cos 2\pi n\Big(\frac{k}{2}+\frac{l}{2}\Big) + \cos 2\pi n\Big(\frac{h}{2}+\frac{l}{2}\Big) \\ & + \cos 2\pi n\Big(\frac{h}{2}+\frac{k}{2}\Big)\Big]\Big\}^2 + \Big\{N_{Na^+}\Big[\sin 2\pi n(0) + \sin 2\pi n\Big(\frac{h}{2}\Big) \\ & + \sin 2\pi n\Big(\frac{k}{2}\Big) + \sin 2\pi n\Big(\frac{l}{2}\Big)\Big] + N_{Cl^-}\Big[\sin 2\pi n\Big(\frac{h}{2}+\frac{k}{2}+\frac{l}{2}\Big) \\ & + \sin 2\pi n\Big(\frac{k}{2}+\frac{l}{2}\Big) + \sin 2\pi n\Big(\frac{h}{2}+\frac{l}{2}\Big) + \sin 2\pi n\Big(\frac{h}{2}+\frac{k}{2}\Big)\Big]\Big\}^2 \end{aligned}$$

Here again the second term of our equation is zero.

When n is even, our equation reduces to

$$R = N_{Na^+}[4] + N_{Cl^-}[4]$$

so that the diffracted beams of even order are all strong.

When n is odd, if h, k, and l are all odd,

$$R = N_{Na^+}[-2] + N_{Cl^-}[2]$$

and these diffracted beams are all weak.

When n is odd, if h, k, and l are one odd and two even,

$$R = N_{Na^+}[2] + N_{Cl^-}[-2]$$

and these diffracted beams are present but weak. In this respect O_h^1 differs from O_h^5.

When n is odd, if h, k, and l are two odd and one even,

$$R = N_{Na^+}[0] + N_{Cl^-}[0]$$

and these beams are absent.

The Laue pattern, as interpreted by its gnomonic projection, shows that the first-order beams are absent from planes having one odd and two even indices so that space-group O_h^1 is eliminated as a possible structure for NaCl.

We have, therefore, completed step 3 and have found that the structure of NaCl can be represented only by assuming that four Na^+ and four Cl^- ions are marshaled on the space-group O_h^5 with the following coordinates:

Na^+	(or Cl^-)	000;	$0\frac{1}{2}\frac{1}{2}$;	$\frac{1}{2}0\frac{1}{2}$;	$\frac{1}{2}\frac{1}{2}0$
Cl^-	(or Na^+)	$\frac{1}{2}\frac{1}{2}\frac{1}{2}$;	$\frac{1}{2}00$;	$0\frac{1}{2}0$;	$00\frac{1}{2}$

and that it cannot be accounted for on the basis of any other coordinates. We have, therefore, arrived at a unique solution for the structure of NaCl. It is identical with that already given by the Bragg and powder methods in Chaps. V and VI.

DETERMINATION OF THE STRUCTURE OF CALCITE BY THE LAUE METHOD

Step 1. For calcite this step is more complicated than was the corresponding step for NaCl. Calcite has the external symmetry of the D_{3d} class, rhombohedral division of the hexagonal system. Table XXV of Appendix III shows that in the D_{3d} class of symmetry we must choose between space-groups which are built on a hexagonal lattice and other space-groups built on a rhombohedral lattice. We can make this choice in terms of the indices of the spots of the Laue pattern as determined by the gnomonic projection.

It was shown in Chap. II that the Bravais-Miller indices $(H\,K\,L)$ were the natural indices for the hexagonal axes and that the Miller indices $(h\,k\,l)$ were the natural indices for the rhombohedral axes. These two sets of indices are connected by the equations:

$$\begin{aligned} h &= 2H + K + L \\ k &= K - H + L \\ l &= -2K - H + L \end{aligned}$$

It is inherent in crystal structure that planes having the greatest interplanar spacings must have small indices. If planes of a rhombohedral lattice which have small Miller indices are referred to hexagonal axes and are expressed in terms of the Bravais-Miller indices, then $2H + K + L$, $K - H + L$, and $L - 2K - H$ are all exactly divisible by 3. For most planes of a hexagonal lattice having small Bravais-Miller indices, $2H + K + L$, $K - H + L$, and $L - 2K - H$ are not exactly divisible by 3. When white x-rays are passed parallel to the 3-fold axis of calcite, and Bravais-Miller indices are assigned to the Laue spots by means of the gnomonic projection, the large majority of spots show $2H + K + L$,

$K - H + L$, and $L - 2K - H$, all exactly divisible by 3. We must assume therefore that the structure of calcite is based on a rhombohedral lattice. This limits us to space-groups D_{3d}^5 and D_{3d}^6.

Step 2. Now that we have settled upon a rhombohedral space-lattice for calcite, we must determine the number **n** of "molecules" in a unit-rhombohedron. Calcite cleaves into rhombohedra whose edges are ordinarily taken as the crystallographic axes. The interaxial angle is 101° 55′. Measurements on the cleavage faces by the Bragg method show an apparent lattice constant of 3.028×10^{-8} cm. We have already seen in our discussion of NaCl that, depending upon the actual crystal structure, this apparent spacing may be the actual spacing d or some exact fraction of it, d/n. We could, of course, follow the procedure used with NaCl and pretend that n is unity. It will be of interest, however, to follow the method used in the first complete determination of the structure of calcite by the Laue method.[3]

The volume of a rhombohedron whose lattice constant for planes parallel to the face is d and whose interaxial angles are 101° 55′ is $1.0963d^3$. If **n** is the number of "molecules" in this rhombohedron, M is the weight in grams of one chemical molecule (= molecular weight $\times$ 1.649×10^{-24}), and ρ is the density of calcite, then

$$1.0963d^3 = \mathbf{n}M/\rho$$

If, now, we use an edge of d/n instead of d, thus corresponding to the nth order of diffraction, we must write

$$1.0963\left(\frac{d}{n}\right)^3 = \frac{\mathbf{n}M}{\rho n^3}$$

In this equation we do not know the values of either **n** or n, but we do know that they both must be integers.

$$\frac{n^3}{\mathbf{n}} = \frac{M}{1.0963\rho(d/n)^3}$$

$$\frac{n^3}{\mathbf{n}} = \frac{1.649 \times 10^{-24} \times 100}{1.0963 \times 2.710 \times (3.028 \times 10^{-8})^3} = 2.00$$

Assuming various integers for n and **n**, we arrive at the following values of $n^3/\mathbf{n}$:

n	**n** = 1	**n** = 2	**n** = 3	**n** = 4	**n** = 5
1	1	0.50	0.33	0.25	0.20
2	8	4.00	2.67	2.00	1.60
3	27	13.50	9.00	6.75	5.40

Evidently $n^3/\mathbf{n}$ corresponds to a second-order diffraction from the faces of a rhombohedron which contains four "molecules."

It can be readily shown, however, that such a unit of structure as we have described, with the interaxial angles of 101° 55′, cannot be correct. When a diffraction pattern is made with, say, 50-kilovolt white x-rays, calculations of $2d \sin \theta$ (see Bragg's law, Chap. I) show that values of $n\lambda$ are obtained which are less than are permitted by the quantum equation

$$\lambda_{\text{min.}} = \frac{12{,}336 \times 10^{-8}}{V}$$

where V is the number of volts employed across the x-ray tube.* We therefore must find a new unit of structure, related to the first, for which the calculated values of $n\lambda$ will be at least as great as those permitted by the quantum equation. Trial shows that this may be obtained by using a rhombohedron whose edges are the face-diagonals of the original rhombohedron (see Fig. 1). It may be shown that the volume of the new unit of structure is one half that of the old. Since the cleavage rhombohedron contained four "molecules," the new rhombohedron must contain two. We must therefore find places, if possible on D^5_{3d} or D^6_{3d} for two Ca, two C, and six O.

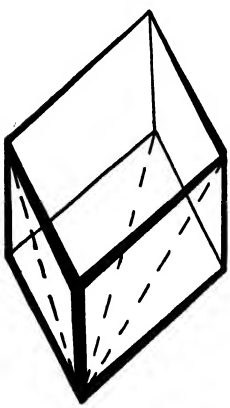

FIG. 1.—Full lines, one-eighth of the cleavage rhombohedron of calcite. Dashed lines, one corner of the new rhombohedron which gives possible values of λ. See also Fig. 9 of Chap. II for a view of the new rhombohedron inscribed in the actual cleavage rhombohedron.

Using the type of notation employed in our study of NaCl, Table I shows the various groupings of equivalent positions and shows whether, in the light of Table XXXVIII of Appendix III, they are compatible with space-groups D^5_{3d} or D^6_{3d}. Of the 30 types of equivalent positions listed in Table I, only five survive the test of Table XXXVIII of Appendix III. They are:

For D^5_{3d}:

(1)	Ca (or C), 2;	C (or Ca), 2;	O, 6
(2)	Ca (or C), 2;	C (or Ca), 1-1;	O, 6
(3)	Ca (or C), 2;	C (or Ca), 2;	O, 3-3
(4)	Ca (or C), 2;	C (or Ca), 1-1;	O, 3-3

For D^6_{3d}:

(5)	Ca (or C), 2;	C (or Ca), 2;	O, 6

* $\lambda_{\text{min.}} = \dfrac{hc}{eV \times 10^8}$

where $\lambda_{\text{min.}}$ = the minimum possible wave length in centimeters.
$h = 6.547 \times 10^{-27}$ erg sec.
$c = 3 \times 10^{10}$ cm. per second.
$e = 1.591 \times 10^{-20}$ abs. e.m.u. of charge.
V = volts across x-ray tube = $10^8 \times V$ abs. e.m.u. of potential.

Reference to Wyckoff's Tables[7] shows that these five types of equivalent positions lead to the following atomic coordinates:

(1)	Ca (or C),	$u_1u_1u_1$;	$\bar{u}_1\bar{u}_1\bar{u}_1$	
	C (or Ca),	$u_2u_2u_2$;	$\bar{u}_2\bar{u}_2\bar{u}_2$	
	O,	$u_30\bar{u}_3$;	$\bar{u}_30u_3$;	$0u_3\bar{u}_3$
		$\bar{u}_3u_30$;	$u_30\bar{u}_3$;	$0\bar{u}_3u_3$;
or		$u_3\bar{u}_3\frac{1}{2}$;	$\bar{u}_3\frac{1}{2}u_3$;	$\frac{1}{2}u_3\bar{u}_3$
		$\bar{u}_3u_3\frac{1}{2}$;	$u_3\frac{1}{2}\bar{u}_3$;	$\frac{1}{2}\bar{u}_3u_3$
or		u_3u_3v;	u_3vu_3;	vu_3u_3
		$\bar{u}_3\bar{u}_3\bar{v}$;	$\bar{u}_3\bar{v}\bar{u}_3$;	$\bar{v}\bar{u}_3\bar{u}_3$
(2)	Ca (or C),	$u_1u_1u_1$;	$\bar{u}_1\bar{u}_1\bar{u}_1$	
	C (or Ca),	000;	$\frac{1}{2}\frac{1}{2}\frac{1}{2}$	
	O,	as in (1)		
(3)	Ca (or C),	$u_1u_1u_1$;	$\bar{u}_1\bar{u}_1\bar{u}_1$	
	C (or Ca),	$u_2u_2u_2$;	$\bar{u}_2\bar{u}_2\bar{u}_2$	
	O,	$00\frac{1}{2}$;	$0\frac{1}{2}0$;	$\frac{1}{2}00$
		$\frac{1}{2}\frac{1}{2}0$;	$\frac{1}{2}0\frac{1}{2}$;	$0\frac{1}{2}\frac{1}{2}$
(4)	Ca (or C),	$u_1u_1u_1$;	$\bar{u}_1\bar{u}_1\bar{u}_1$	
	C (or Ca),	000;	$\frac{1}{2}\frac{1}{2}\frac{1}{2}$	
	O,	$00\frac{1}{2}$;	$0\frac{1}{2}0$;	$\frac{1}{2}00$
		$\frac{1}{2}\frac{1}{2}0$;	$\frac{1}{2}0\frac{1}{2}$;	$0\frac{1}{2}\frac{1}{2}$
(5)	Ca (or C),	$\frac{1}{4}\frac{1}{4}\frac{1}{4}$;	$\frac{3}{4}\frac{3}{4}\frac{3}{4}$	
	C (or Ca),	000;	$\frac{1}{2}\frac{1}{2}\frac{1}{2}$	
	O,	$\frac{1}{4}\frac{3}{4}\frac{3}{4}$;	$\frac{3}{4}\frac{3}{4}\frac{1}{4}$;	$\frac{3}{4}\frac{1}{4}\frac{3}{4}$
		$\frac{3}{4}\frac{1}{4}\frac{1}{4}$;	$\frac{1}{4}\frac{1}{4}\frac{3}{4}$;	$\frac{1}{4}\frac{3}{4}\frac{1}{4}$
or		$u\bar{u}0$;	$\bar{u}0u$;	$0u\bar{u}$
$\frac{1}{2}-u, u+\frac{1}{2}, \frac{1}{2}$;		$u+\frac{1}{2}, \frac{1}{2}, \frac{1}{2}-u$;		$\frac{1}{2}, \frac{1}{2}-u, u+\frac{1}{2}$

Step 3. The Laue pattern shows that, except for a few weak spots, all spots due to diffracted beams of the first order correspond to planes with one even and two odd indices. This indicates an atomic configuration which is closely related to a body-centered structure. Of the four types of coordinates listed above for D_{3d}^5, type (4) is obviously most closely related to a body-centered structure. It is pictured in Fig. 2. Such a structure would contain a network in which each C (or Ca) would be surrounded by six equidistant O situated at the centers of the faces of the rhombohedron, and by twelve other equidistant O situated at the centers of the edges. Each of the six O would be held jointly by two C (or Ca) spaced equally on each side of it. Each of the twelve O would be held jointly by four C (or Ca) spaced equally around it in a plane. Such a structure finds no justification in chemistry, for, although there

is plenty of chemical evidence for the existence of the CO_3^{--} ion, there is absolutely no chemical evidence for a continuous network of C and O. If type (4) of the D_{3d}^5 coordinates must be discarded for chemical reasons, it is easy to see that types (1), (2), and (3) must also be discarded. Although these structures may be discarded solely on chemical grounds,

TABLE I.—GROUPINGS OF EQUIVALENT POSITIONS FOR Ca, C, AND O IN CALCITE

Ca (or C)	C (or Ca)	O	Compatible with	
			D_{3d}^5	D_{3d}^6
2	2	6	Yes	Yes
2	2	4-2	No	No
2	2	4-1-1	No	No
2	2	3-3	Yes	No
2	2	3-2-1	No	No
2	2	3-1-1-1	No	No
2	2	2-2-2	No	No
2	2	2-2-1-1	No	No
2	2	2-1-1-1-1	No	No
2	2	1-1-1-1-1-1	No	No
2	1-1	6	Yes	No
2	1-1	4-2	No	No
2	1-1	4-1-1	No	No
2	1-1	3-3	Yes	No
2	1-1	3-2-1	No	No
2	1-1	3-1-1-1	No	No
2	1-1	2-2-2	No	No
2	1-1	2-2-1-1	No	No
2	1-1	2-1-1-1-1	No	No
2	1-1	1-1-1-1-1-1	No	No
1-1	1-1	6	No	No
1-1	1-1	4-2	No	No
1-1	1-1	4-1-1	No	No
1-1	1-1	3-3	No	No
1-1	1-1	3-2-1	No	No
1-1	1-1	3-1-1-1	No	No
1-1	1-1	2-2-2	No	No
1-1	1-1	2-2-1-1	No	No
1-1	1-1	2-1-1-1-1	No	No
1-1	1-1	1-1-1-1-1-1	No	No

it is interesting to note that they would have had to have been abandoned anyway as soon as a quantitative study had been made of the intensities of the spots of the Laue pattern. This disposes of space-group D_{3d}^5 and leaves us with only the two sets of coordinates for space-group D_{3d}^6 listed above under (5).

Type (5) gives fixed positions for Ca (or C) and for C (or Ca) but gives us two alternatives for the coordinates of O. The first of these

alternatives gives us fixed positions for the O also. If we place the Ca^{++} at ¼¼¼ and ¾¾¾, Eq. (1) becomes*

$$R^2 = X^2 + Y^2$$

$$= \left\{N_{Ca^{++}}\left[\cos 2\pi n\left(\frac{h}{4}+\frac{k}{4}+\frac{l}{4}\right)+\cos 2\pi n\left(\frac{3h}{4}+\frac{3k}{4}+\frac{3l}{4}\right)\right]\right.$$
$$+ N_{C^{++++}}\left[\cos 2\pi n(0)+\cos 2\pi n\left(\frac{h}{2}+\frac{k}{2}+\frac{l}{2}\right)\right]$$
$$+ N_{O^{--}}\left[\cos 2\pi n\left(\frac{h}{4}+\frac{3k}{4}+\frac{3l}{4}\right)+\cos 2\pi n\left(\frac{3h}{4}+\frac{3k}{4}+\frac{l}{4}\right)\right.$$
$$+ \cos 2\pi n\left(\frac{3h}{4}+\frac{k}{4}+\frac{3l}{4}\right)+\cos 2\pi n\left(\frac{3h}{4}+\frac{k}{4}+\frac{l}{4}\right)$$
$$\left.\left.+ \cos 2\pi n\left(\frac{h}{4}+\frac{k}{4}+\frac{3l}{4}\right)+\cos 2\pi n\left(\frac{h}{4}+\frac{3k}{4}+\frac{l}{4}\right)\right]\right\}^2$$
$$+ \{\text{corresponding terms with sin substituted for cos}\}^2$$

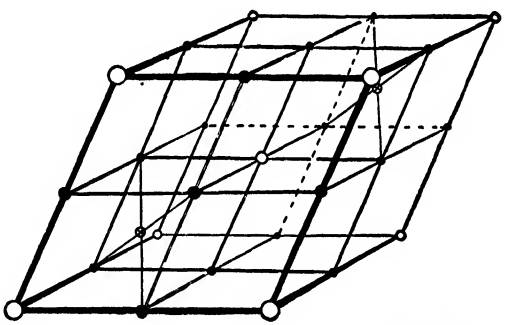

FIG. 2.—The structure calcite would have had if it had crystallized according to type (4) (see text). ⊗ represents Ca (or C); ○ represents C (or Ca); ● represents O.

Both the X- and the Y-terms of this expression become zero for all first-order diffracted beams (*i.e.*, if $n = 1$) when h, k, l are all odd or when one is odd and two are even. This result is inherent in the trigonometry of the equation and is independent of any assumptions we may make as to the values for $N_{Ca^{++}}$, $N_{C^{++++}}$, and $N_{O^{--}}$; it will be unaltered if we interchange the coordinates of Ca^{++} and C^{++++}. This set of coordinates must therefore stand or fall on the presence or absence of spots in the Laue pattern corresponding to planes having one odd and two even indices or all odd indices. Actual experiment shows a few weak first-order spots corresponding to planes having one odd and two even indices. It is necessary, therefore, to discard the first alternative for the coordi-

* The calcium, carbon, and oxygen of calcite are represented by Ca^{++}, C^{++++}, and O^{--}, respectively. This is in accordance with modern chemical theories of the electron nature of chemical combinations. Similar charges are assumed on these atoms in Chap. XIV in calculating the indices of refraction of calcite.

nates of O^{--} in D^6_{3d}. This leaves us with only one possible set of coordinates. We shall, therefore, calculate the intensities of our diffracted beams for these remaining coordinates in order to justify completely our final solution of the crystal structure of calcite.

For the second alternative of coordinates of (5) our intensity equation becomes (if Ca^{++} is at $\frac{1}{4}\frac{1}{4}\frac{1}{4}$ and $\frac{3}{4}\frac{3}{4}\frac{3}{4}$):

$$
\begin{aligned}
R^2 &= X^2 + Y^2 \\
&= \Bigg\{ N_{Ca^{++}} \left[\cos 2\pi n\left(\frac{h}{4} + \frac{k}{4} + \frac{l}{4}\right) + \cos 2\pi n\left(\frac{3h}{4} + \frac{3k}{4} + \frac{3l}{4}\right) \right] \\
&\quad + N_{C^{++++}} \left[\cos 2\pi n(0) + \cos 2\pi n\left(\frac{h}{2} + \frac{k}{2} + \frac{l}{2}\right) \right] \\
&+ N_{O^{--}} \Bigg[\cos 2\pi n(hu - ku + 0) + \cos 2\pi n(-hu + 0 + lu) \\
&+ \cos 2\pi n(0 + ku - lu) + \cos 2\pi n\left(\frac{h}{2} - hu + ku + \frac{k}{2} + \frac{l}{2}\right) \\
&+ \cos 2\pi n\left(hu + \frac{h}{2} + \frac{k}{2} + \frac{l}{2} - lu\right) + \cos 2\pi n\left(\frac{h}{2} + \frac{k}{2} - ku + lu + \frac{l}{2}\right) \Bigg] \Bigg\}^2 \\
&+ \{\text{corresponding terms with sin substituted for cos}\}^2
\end{aligned}
$$

The last three subterms in each of the two terms $N_{O^{--}}$ [. . .] can each be written as the functions of the difference of two angles as follows:

$$
\begin{aligned}
&\cos 2\pi n\left[\left(\frac{h}{2} + \frac{k}{2} + \frac{l}{2}\right) - (hu - ku)\right] \\
&\quad = \cos 2\pi n\left(\frac{h}{2} + \frac{k}{2} + \frac{l}{2}\right) \cos 2\pi n(hu - ku) \\
&\quad + \sin 2\pi n\left(\frac{h}{2} + \frac{k}{2} + \frac{l}{2}\right) \sin 2\pi n(hu - ku)
\end{aligned}
$$

$$
\begin{aligned}
&\cos 2\pi n\left[\left(\frac{h}{2} + \frac{k}{2} + \frac{l}{2}\right) - (lu - hu)\right] \\
&\quad = \cos 2\pi n\left(\frac{h}{2} + \frac{k}{2} + \frac{l}{2}\right) \cos 2\pi n(lu - hu) \\
&\quad + \sin 2\pi n\left(\frac{h}{2} + \frac{k}{2} + \frac{l}{2}\right) \sin 2\pi n(lu - hu)
\end{aligned}
$$

$$
\begin{aligned}
&\cos 2\pi n\left[\left(\frac{h}{2} + \frac{k}{2} + \frac{l}{2}\right) - (ku - lu)\right] \\
&\quad = \cos 2\pi n\left(\frac{h}{2} + \frac{k}{2} + \frac{l}{2}\right) \cos 2\pi n(ku - lu) \\
&\quad + \sin 2\pi n\left(\frac{h}{2} + \frac{k}{2} + \frac{l}{2}\right) \sin 2\pi n(ku - lu)
\end{aligned}
$$

$$\sin 2\pi n\left[\left(\frac{h}{2}+\frac{k}{2}+\frac{l}{2}\right)-(hu-ku)\right]$$
$$=\sin 2\pi n\left(\frac{h}{2}+\frac{k}{2}+\frac{l}{2}\right)\cos 2\pi n(hu-ku)$$
$$-\cos 2\pi n\left(\frac{h}{2}+\frac{k}{2}+\frac{l}{2}\right)\sin 2\pi n(hu-ku)$$

$$\sin 2\pi n\left[\left(\frac{h}{2}+\frac{k}{2}+\frac{l}{2}\right)-(lu-hu)\right]$$
$$=\sin 2\pi n\left(\frac{h}{2}+\frac{k}{2}+\frac{l}{2}\right)\cos 2\pi n(lu-hu)$$
$$-\cos 2\pi n\left(\frac{h}{2}+\frac{k}{2}+\frac{l}{2}\right)\sin 2\pi n(lu-hu)$$

$$\sin 2\pi n\left[\left(\frac{h}{2}+\frac{k}{2}+\frac{l}{2}\right)-(ku-lu)\right]$$
$$=\sin 2\pi n\left(\frac{h}{2}+\frac{k}{2}+\frac{l}{2}\right)\cos 2\pi n(ku-lu)$$
$$-\cos 2\pi n\left(\frac{h}{2}+\frac{k}{2}+\frac{l}{2}\right)\sin 2\pi n(ku-lu)$$

When these expanded expressions are substituted in our equation for R^2 it becomes evident that if all the indices are odd, or if one of them is odd and two are even, then (considering $n = 1$),

$$R^2 = 0 + \{2N_{O^{--}} - [\sin 2\pi u(h-k) + \sin 2\pi u(l-h) + \sin 2\pi u(k-l)]\}^2 \quad (2)$$

and the diffracted beam will be present but weak in intensity. This agrees with the experimental facts. When the indices are all even, or two odd and one even, then (considering $n = 1$),

$$R^2 = \{2N_{C^{++++}} \pm 2N_{Ca^{++}} + 2N_{O^{--}} [\cos 2\pi u(h-k) + \cos 2\pi u(l-h) + \cos 2\pi u(k-l)]\}^2 + 0$$

When $(h + k + l)$ is divisible by 4, the sign of $N_{Ca^{++}}$ is positive and the diffracted beam will be strong; but, if $(h + k + l)$ is only divisible by 2, the sign of $N_{Ca^{++}}$ is negative and the diffracted beam will be considerably weaker. This again agrees with the experimental facts. If Ca^{++} is placed at 000 and $\frac{1}{2}\frac{1}{2}\frac{1}{2}$, then $N_{C^{++++}}$ and $N_{Ca^{++}}$ must be interchanged in the above equations. In this case the calculated intensity does not fit the experimental data for the {111} planes.

Our second alternative for coordinates in D^6_{3d} with Ca^{++} at $\frac{1}{4}\frac{1}{4}\frac{1}{4}$ and $\frac{3}{4}\frac{3}{4}\frac{3}{4}$ is therefore the only set of coordinates which is completely consistent with the experimental data, and we are justified in assigning to calcite the coordinates

Ca^{++},	$\frac{1}{4}\frac{1}{4}\frac{1}{4}$;	$\frac{3}{4}\frac{3}{4}\frac{3}{4}$	
C^{++++},	000;	$\frac{1}{2}\frac{1}{2}\frac{1}{2}$	
O^{--},	$u\bar{u}0$;	$\bar{u}0u$;	$0u\bar{u}$
$\frac{1}{2}-u, u+\frac{1}{2}, \frac{1}{2}$;	$u+\frac{1}{2}, \frac{1}{2}, \frac{1}{2}-u$;		$\frac{1}{2}, \frac{1}{2}-u, u+\frac{1}{2}$

The structure represented by the above coordinates is shown in Fig. 3.

Aided by considerations of a purely chemical nature, and by a qualitative study of the intensities of the various diffracted x-ray beams, the theory of space-groups has given us very definite coordinates for the positions of Ca^{++} and C^{++++}. With respect to the coordinates of the O^{--} we are not so fortunate, for the theory of space-groups has left us with an undetermined parameter u. We must now attempt to evaluate u by a quantitative study of the intensities of some of the diffracted beams.

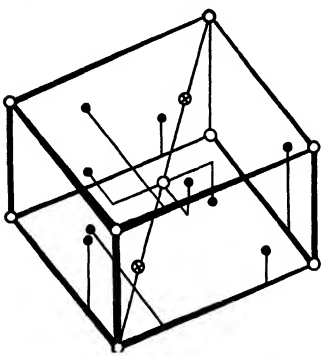

FIG. 3.—The structure of calcite. ⊗ represents Ca^{++}; ○ represents C; ● represents O.

We have seen from our calculations of intensity [see Eq. (2)] that the diffracted beams are due entirely to O^{--} for planes whose indices are all odd or are one odd and two even. For such planes the amplitude of the waves in the diffracted beam is

$$A \propto \sqrt{I} \propto R = 2N_{O^{--}} [\sin 2\pi u(h-k) + \sin 2\pi u(l-h) + \sin 2\pi u(k-l)] \quad (3)$$

TABLE II.—OXYGEN PLANES IN CALCITE WHICH ARE ORIENTED TO GIVE SPOTS IN THE LAUE PATTERN

(*a*) Spots present			(*b*) Spots absent		
Plane	Relative spacing	Curve No. (Fig. 4*a*)	Plane	Relative spacing	Curve No. (Fig. 4*b*)
$02\bar{1}$	0.436	1	$13\bar{1}$	0.325	1
$24\bar{1}$	0.254	2	540	0.224	2
052	0.244	2	$35\bar{1}$	0.206	3
$\bar{3}\bar{4}2$	0.202	3	$26\bar{1}$	0.179	4
610	0.196	3	$55\bar{1}$	0.179	5
896	0.175	1	$\bar{4}43$	0.154	6
$\bar{7}20$	0.174	3	085	0.149	7
$46\bar{1}$	0.173	4	$75\bar{1}$	0.149	8
$\bar{6}01$	0.173	5			
$\bar{2}45$	0.170	5			
294	0.156	4			
$\bar{7}02$	0.139	7			
$28\bar{1}$	0.137	6			

A tabulation is therefore made of all such planes which are so situated in the crystal that their diffracted beams, if any, would hit the photographic film and thus contribute to the Laue pattern. In the tabulation they are sorted out into two groups (see Table II*a* and *b*) according to

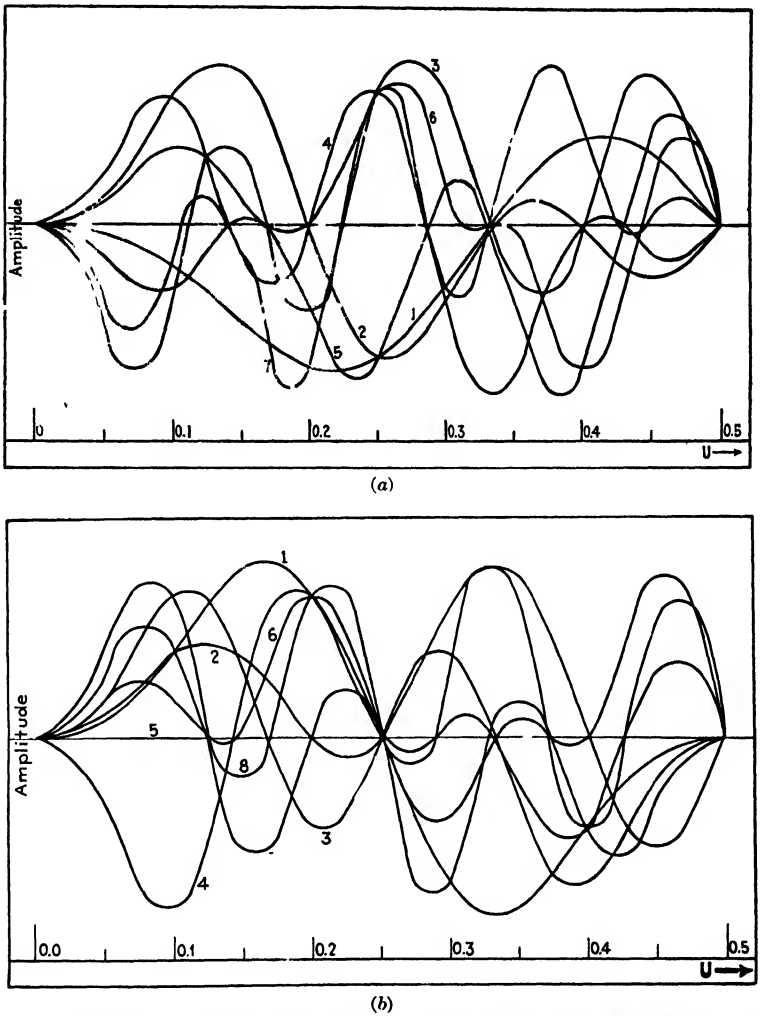

FIG. 4.—Intensities for calcite for successive values of u. (*a*) Spots present; (*b*) spots absent. (*Wyckoff.*[8])

whether or not they actually do show spots in the Laue pattern. Successive values of u are systematically substituted into Eq. (3) for each plane of Table II, and the calculated amplitudes are plotted as in Fig. 4. An inspection of Fig. 4*a* and *b* shows that only in the immediate neighborhood of $u = 0.23 - 0.29$ will *all* the planes of Table II*a* show a measura-

ble intensity of diffracted beams. The optimum is at $u = 0.25$. Only at $u = 0.24 - 0.26$ can all the planes of Table IIb show substantially zero intensity. At $u = 0.25$ these planes show actually zero intensity. Of course there is nothing in the nature of our calculations to prevent us from assuming for O^{--} the symmetrical positions corresponding to $u = 0.75$, but such an assumption would place O^{--} near Ca^{++} and would destroy the CO_3^{--} ion which is demanded by chemistry. We are therefore justified in assuming that, if Eqs. (14) and (16) of Chap. IV hold at all, $u = 0.25$.

Our final coordinates for calcite are therefore

Ca^{++},	$\frac{1}{4}\frac{1}{4}\frac{1}{4}$;	$\frac{3}{4}\frac{3}{4}\frac{3}{4}$	
C^{++++},	000;	$\frac{1}{2}\frac{1}{2}\frac{1}{2}$	
O^{--},	0.25, $\overline{0.25}$, 0;	$\overline{0.25}$, 0, 0.25;	0, 0.25, $\overline{0.25}$
	0.25, 0.75, 0.50;	0.75, 0.50, 0.25;	0.50, 0.25, 0.75

These coordinates are illustrated in detail in Fig. 13 of Chap. V.

DETERMINATION OF THE STRUCTURE OF TRICALCIUM ALUMINATE BY THE POWDER METHOD

Tricalcium aluminate ($3CaO.Al_2O_3$) is known to be optically isotropic, thus showing that its crystals have cubic symmetry. It is said to melt incongruently at 1535°C. giving a melt of the two oxides with an excess of CaO. No method is known by which crystals of tricalcium aluminate can be grown of such size as to permit of goniometric measurements. This necessitates the use[9] of a very general method of the application of the theory of space-groups to the powder method of x-ray crystal analysis.

X-ray diffraction patterns of the powder of tricalcium aluminate show strong lines characteristic of a body-centered cube, of edge $a = 3.812$Å., and, in addition, three weak lines corresponding to interplanar spacings of 3.1Å., 2.20Å., and 1.79Å. Experiment shows that these extra lines are not due to impurities but clearly belong to the diffraction pattern of tricalcium aluminate. They may be derived from a cube whose edge is twice that corresponding to the body-centered cubic pattern. The interpretation of the crystal structure of tricalcium aluminate therefore resolves itself into a search for those structures which can quantitatively account for the body-centered cubic pattern and for the three faint lines mentioned above. The first step is the determination of the number of "molecules" per unit-crystal cell.

The Number of "Molecules" per Unit-cell.—Since tricalcium aluminate can be made only in a finely divided and relatively impure condition, a precision measurement of its density is not possible. An approximation sufficiently close for the determination of the number of "molecules" per unit-cell may be made, however, by observing the behavior of the sub-

stance in liquids of various densities. In the original work, the observations were made by filling a fine capillary tube with a suspension of the powder in a mixture of methylene iodide and mesitylene of previously determined density. A petrographic microscope was mounted with its optical axis horizontal, and the tube containing the suspension was mounted vertically on the microscope stage. With a liquid whose density was 2.89, most of the tricalcium aluminate particles moved downward, and those of the chief impurity, $3CaO.5Al_2O_3$, moved upward. Complete separation could not be obtained because of the mechanical union between particles due to the sintering process by which the material was made from CaO and Al_2O_3. A partial separation of the two was obtained by centrifuging the suspension. The relatively pure $3CaO.Al_2O_3$ thus obtained was dried and used in subsequent determinations. This powder was found to fall in a liquid of density 2.94 and to rise in one of density 3.07. In a liquid of density 3.005 the particles went up and down in about equal numbers. The density of $3CaO.Al_2O_3$ is therefore between 2.94 and 3.07 and is probably very close to 3.00. The number of molecules per unit-cube ($a = 3.812$Å.) is given by the density and molecular weight as 0.373 ± 0.004. This is very nearly equal to $\frac{3}{8} = 0.375$. No other common fraction whose numerator and denominator are small integers comes within the precision of the data. Since the number of "molecules" in a unit-cell must be a whole number, it is evident that the edge of the unit-cell must be a multiple of 3.812Å. A cube of twice these dimensions (*i.e.*, $a = 7.624$Å.) would contain three "molecules." A smaller cell cannot possibly contain a whole number of "molecules" without conflicting with the x-ray data. Furthermore, there are no data from the diffraction patterns which require that it be larger. This means that for crystallographic purposes the formula of tricalcium aluminate should be $9CaO.3Al_2O_3$. The three faint lines mentioned above might be accounted for quantitatively within the precision of the data by assuming that they are caused by first-order diffraction from (2 1 1), second-order diffraction from (1 1 1), and third-order diffraction from (1 1 0), respectively. It will appear later that all three can be accounted for in this way.

The Crystal Structure.—Since the body-centered cubic pattern from the tricalcium aluminate is on the basis of a cube of one-half the dimensions of the unit-cell, it must be considered to be essentially an accidental result of the atomic arrangement within the unit-cell and, as such, it imposes no symmetry limitations upon the cell as a whole. Since no crystals large enough for symmetry observations or Laue photographs could be made, none of the usual methods for establishing the space-group is available. This means that every possible arrangement of the atoms consistent with the cubic symmetry must be considered as a possibility until it is shown to be in conflict with known facts or data.

The procedure used in writing down the possible arrangements is essentially the same as that used by Wyckoff in his treatment of calcite,[8] except that the process is greatly complicated by the fact that all cubic space-groups must be considered and that there are many more atoms to place in the unit-cell. In considering the possible combinations of groups of equivalent points occupied by a given kind of atom, it is obviously necessary to consider only those numbers which represent groups of equivalent points in cubic symmetry, namely, 1, 2, 3, 4, 6, 8, 12, and 16. Furthermore, those which do not have variable parameters, namely, 1, 2, and 3, need not be considered more than once. Bearing these limitations in mind, the possible combinations for the six Al ions are found to be 6 all alike, 4 of one kind and 1 each of the two others, 4 of one kind and 2 of another, 3 of one kind and 3 of another, and 3 of one kind 2 of another and 1 of another. The possible combinations for Al are, then, 6, 4-1-1, 4-2, 3-3, and 3-2-1. Reference to the summary table of equivalent points in the various space-groups of the cubic system (Appendix III) shows that all of these are possible except the last. The 3-2-1 combination is impossible because there is no one cubic space-group which contains arrangements of both two and three equivalent points.

A similar treatment of the nine positions required for the Ca ions leads to the combinations 8-1, 6-3, 4-3-1-1, and 4-4-1. Each combination for Al must now be considered with each combination for Ca, and the space-groups compatible with both are written down. As may be seen in Table III, the entire list includes only five space-groups. This whole process is then repeated for the possible combinations for the eighteen O^{--} ions. The results are listed in Table IV. Although there are only five space-groups involved, there are so many combinations possible within each space-group that the total number of possible arrangements is very large. For instance, if Ca is taken at 8*c* and 1*a*,* and Al at 6*a*, there are over 30 configurations of O possible. Since Al may also be at 6*b*, 6*c*, or 6*d*, this number is increased 4-fold. Placing Ca at 8*c* and 1*b* again doubles this figure. Such a systematic procedure involves a number of duplications, but it was followed rigidly in the original investigation to lessen the chances of error. The total number of possibilities tabulated was about 1,500. It is found that most of these possibilities can be eliminated by a consideration of the packing-sizes of the ions involved (see Chap. XIII) and of the space available in the unit-crystal. Ionic dimensions have been published by W. L. Bragg[10] and by the author.[11] According to Bragg the packing-radii are Ca^{++} = 2.1Å., Al^{+++} = 1.45Å., and O^{--} = 0.6Å. The corresponding values from Chap. XIII are Ca^{++} = 1.4Å., Al^{+++} = 0.9Å., and O^{--} = 1.0Å. These latter values will be used in our study of tricalcium aluminate for two reasons: first, that they give the distance from Al to O in Al_2O_3 as 1.9Å., in agreement with

* These arrangements are expressed in the code used by Wyckoff (reference 7).

the published data of Bragg; and second, that they give a smaller total distance for Ca + O and for Ca + Al, so that they tend to retain certain of the possibilities which would have been thrown out on the basis of Bragg's values. Thus any error introduced by our limited knowledge of the packing-dimensions of ions is clearly on the safe side. The procedure of finding whether or not space is available in a given configuration is greatly facilitated by drawing each of the arrangements of equiva-

TABLE III.—SPACE-GROUPS POSSIBLE FOR VARIOUS ARRANGEMENTS OF CA AND AL

Combinations for calcium	Aluminum at 6	Aluminum at 4-1-1	Aluminum at 4-2	Aluminum at 3-3
8-1	T_h^1, O^1, O_h^1	None	None	T_h^1, O_h^1, O
6-3	T^1, T_h^1, T_d^1, O^1, O	T^1, T_d^1	None	None
4-3-1-1	T^1, T_d^1	None	None	None
4-4-1	T^1, T_d^1	None	None	T^1, T_d^1

TABLE IV.—SPACE-GROUPS POSSIBLE FOR VARIOUS ARRANGEMENTS OF O WITH COMBINATIONS OF CA AND AI ALREADY FOUND POSSIBLE

Combinations for oxygen	Ca and Al					
	6-8-1	6-6-3	6-4-3-1-1	6-4-4-1	8-3-3-1	4-4-3-3-1
12-6	$T_h^1O^1O_h^1$	$T_h^1T^1T_d^1O^1O_h^1$	$T^1T_d^1$	$T^1T_d^1$	$T_h^1O^1O_h^1$	$T^1T_d^1$
12-4-1-1	None	$T^1T_d^1$	None	None	None	None
12-3-3	$T_h^1O^1O_h^1$	None	None	$T^1T_d^1$	None	None
8-8-1-1	None	$T_h^1O^1O_h^1$	None	None	None	None
8-6-3-1	$T_h^1O^1O_h^1$	$T_h^1O^1O_h^1$	None	None	None	None
6-6-6	$T_h^1O_h^1O^1$	$T^1T_h^1T_d^1O^1O_h^1$	$T^1T_d^1$	$T^1T_d^1$	$T_h^1O^1O_h^1$	$T^1T_d^1$
6-6-3-3	$T_h^1O^1O_h^1$	None	None	$T^1T_d^1$	None	None
6-4-4-3-1	None	$T^1T_d^1$	None	$T^1T_d^1$	None	None
6-6-4-1-1	None	$T^1T_d^1$	None	None	None	None

There were no possibilities with oxygen at 16-2, 16-1-1, 12-4-2, 8-8-2, 8-6-4, 8-6-2-2, 8-4-4-2, 8-4-4-1-1, 6-6-4-2, or 6-4-3-3-1-1.

lent positions involved on tracing-cloth. In this way any combination of arrangements can be superimposed and viewed against a bright light, and the ions to be placed along any one dimension of the cube can be picked out readily.

As an example of this procedure, consider the structure in which Ca is at 8*c* and 1*a*, Al at 3*a* and 3*b*, and O at 6*a* and 12*d*. This places ½Ca, 1 O, and ½Al along half the cube-edge. This requires a space of

$$1.4 + 2.0 + 0.9 = 4.3\text{Å}.$$

where only 3.8Å. are available. The structure is obviously an impossibility if the ions have anything like the packing-radii assigned to them

above. In making these eliminations, the packing-dimensions assumed for the ions are not to be regarded as strictly inflexible. No structure should be eliminated unless the available distance involved is exceeded by at least 10 per cent. This procedure eliminates all but about 40 of the original 1,500 possible structures. It remains to eliminate as many of these 40 as possible on the basis of x-ray evidence. Among the arrangements allowed by the ionic dimensions are a number of duplications, but these are best carried through as a check. In general, each of these structures actually represents a number of possibilities which cannot be distinguished experimentally because of the similar dimensions and scattering power of Al^{+++} and O^{--} ions. In the present state of our knowledge of diffracting power, we are hardly justified in distinguishing between Al^{+++} and O^{--} on x-ray data alone. It is therefore to be assumed that interchanging places between the six Al^{+++} ions and six of the O^{--} ions has no effect on the diffracting power of the crystal planes. Were this assumption not made, the number of structures to receive individual examination would be much larger than 40.

In the original work,[9] after it had been decided that the unit-cell must have a length of 7.624Å., repeated attempts were made to detect a first-order diffraction from the (1 0 0) planes for $d = 7.624$Å. These attempts gave uniformly negative results. This fact serves to eliminate a considerable number of otherwise possible structures without an intensity calculation. Disregarding the structure factor (Chap. X) because of lack of data we shall take the diffracting power of a plane as proportional to the total number of electrons in the ions which are situated in that plane. The diffracting powers of (1 0 0) planes are then calculated for all the 40 structures. Those whose (2 0 0) planes are obviously much too low in diffracting power to cut out the first order from $d_{100} = 7.624$Å. are discarded at once. However, because of the lack of definite knowledge of the correct basis for calculating diffracting powers, no structures should be discarded on this basis unless the (2 0 0) planes have less than three-fourths the diffracting power of the (1 0 0) planes. Repeated attempts to find experimental evidence of a second-order diffraction from $d_{100} = 7.624$Å. have given negative results. This eliminates a few additional structures because it is inherent in these structures that the ions are distributed in the space between the (1 0 0) and (2 0 0) planes in such a way as to produce unavoidably such a second-order diffraction.

When all possible eliminations have been made by simple inspection of (1 0 0) planes, there remain only 18 structures, of which nine are duplicates of the other nine. For instance, the structure having Ca at 8*c* and 1*a*, Al at 6*d*, and O at 6*b* and 12*d* may be transformed into the structure having Ca at 8*c* and 1*b*, Al at 6*a*, and O at 6*c* and 12*e* by merely changing the origin of coordinates from a corner of the unit-cube to its

body-center. From this point on, we combine the duplicates, leaving nine structures for which intensity calculations must be made. In those cases where two arrangements differ only in having one variable parameter more or less (for instance, 12*e* and 12*n*), only the more general arrangement will be considered. Similarly, the combination of 6*b* and 6*c* with u_1 and u_2 will be used instead of the special case represented by 12*f*.

In making the intensity calculation the customary assumption is made that the amplitude of the radiation scattered by a given plane is proportional to the electron population of that plane. This population is determined in the usual manner on the basis of $C^{---} = 10$, $Al^{+++} = 10$, and $Ca^{++} = 18$. The resultant amplitude from a given form is taken as the vector sum of the amplitude from the individual cooperating planes. This is determined by the graphical addition of vectors in the same manner as the addition of alternating currents which have a known phase difference. The intensity of the resultant beam is calculated from the formula*

$$I = R^2 f \left(\frac{d}{n}\right)^m \qquad \text{[see Eq. (5), of Chap. VI]}$$

where R is the resultant amplitude, f is the number of families of planes of the form, n is the order of diffraction, and d is the fundamental spacing of the form, taking the edge of the unit-cube as unity and regarding the unit-cell as being simple cubic.

* Because of our inexact knowledge of diffracting power this equation can be used only to show qualitatively the relative intensities of diffraction. The simpler the plane form to which it is applied the more reliable are the results. It may be used quite successfully for the (1 0 0) planes and seems to apply for the (1 1 0) planes. For the (1 1 1) planes the packing-radii of the ions are so large in comparison with the interplanar spacing that the calculated results can only be depended upon to show that a line is present or absent in the diffraction pattern. There is a tendency to make the diffracted beam of orders, higher than the first, abnormally weak. For this reason the formula shows whether the second and fourth orders of (1 1 1) are present and whether the first and third orders are absent, but it does not give the relative intensity of the second and fourth orders. (See Chap. X for a discussion of intensities.)

It is well known that certain crystals act as though the resultant amplitude of the diffracted beam depends upon the square root of the electron population. Attempts made to repeat the above calculations on this basis show that in no case is it possible to retain a structure which had been rejected in the original calculations.

Bragg uses $m = 2.0$; Wyckoff uses $m = 2.35$; McKeehan uses $m = 3.0$. None of these seems to be entirely satisfactory. Table V was calculated using $m = 2$, merely for the sake of convenience in making the large number of calculations required. It is clear that Table V could have been made to show greater *apparent* agreement by using a different value for m, but it does not follow that such a change would have increased the probability of the correctness of our ultimate solution. Exact agreement between the experimental and the calculated intensities can only be had in terms of structure factors as is described in Chaps. X and XI.

These calculations show clearly that six of the nine structures are quite incompatible with the x-ray data. For example, the structure with Ca at 8*c* and 1*a*, Al (or O) at 3*a* and 3*b*, O (or Al) at 6*d*, and O at 12*d* give a calculated intensity of 380 for the first order of d_{100} = 7.624Å. and 257 for the fourth order, even when such parameters are used as to give the weakest possible first order and the strongest possible fourth order. Since, experimentally, the first order is absent and the fourth order is strong, this structure is in direct conflict with the experimental data and must be discarded. Similar calculations on the (1 0 0) planes for the rest of the nine structures eliminate all but three.

TABLE V.—CALCULATED AND OBSERVED INTENSITIES FOR THE MOST PROBABLE STRUCTURE OF TRICALCIUM ALUMINATE

Line		Calculated intensity	Observed intensity
100	first order (d_{100} = 7.624)	75	Absent
100	second order	0.1	Absent
100	third order	14.1	Absent
100	fourth order	1,750	Strong
110	first order	26	Absent
110	second order	1,420	Very, very strong
110	third order	80	Very faint
110	fourth order	1,500	Weak
111	first order	163*	Absent
111	second order	1,067*	Weak
111	third order	69*	Absent
111	fourth order	552*	Faint
211	first order	4,754*	Weak
211	second order	735*	Very strong

* Note statements in the text as to the weight to be put on numerical results for these planes.

In the case of the three remaining structures it is necessary to make intensity calculations for the first four orders of the (1 0 0), (1 1 0), and (1 1 1) planes. These calculations have been made for a large number of different values for the variable parameters which were allowed by the space available for the ions and by the symmetry requirements of the atomic arrangements. The best fit in intensities is found in the structure illustrated in Fig. 5 in which Ca is at 8*c* and 1*a*, Al at 3*a* and 3*b*, and O at 6*d* and 12*f*.* The calculated intensities are shown in Table V. It will be noted that they indicate the presence of the three faint lines mentioned at the beginning of this discussion.

As was mentioned previously, it is not possible to distinguish with certainty between Al and O ions on the basis either of dimensions or of

* The presence of Al at 3*a* and 3*b* leaves room for O at 6*b* and 6*c* only at a point halfway between 3*a* and 3*b*. This changes 6*b* and 6*c* into the special case of 12*f*.

diffracting power. The assignment of certain of the positions in Fig. 5 to Al and of other positions to O was made on the basis of electrostatic considerations. For instance, in Fig. 5 the x-ray data would permit Al to be at 6*d* and six of the eighteen O at 3*a* and 3*b*. However, since there are O ions at 12*f*, we would then have five O ions in a row along a direction parallel to the edge of the cube (d_{100} = 7.624Å.). Such an arrangement is highly improbable from electrostatic considerations. Similarly, the Al might have been placed at 6*b* (or 6*c*) with the O at 3*a*, 3*b*, and 6*c* (or 6*b*). This also places five O in direct contact with one another and is therefore a highly improbable structure Furthermore, there is some

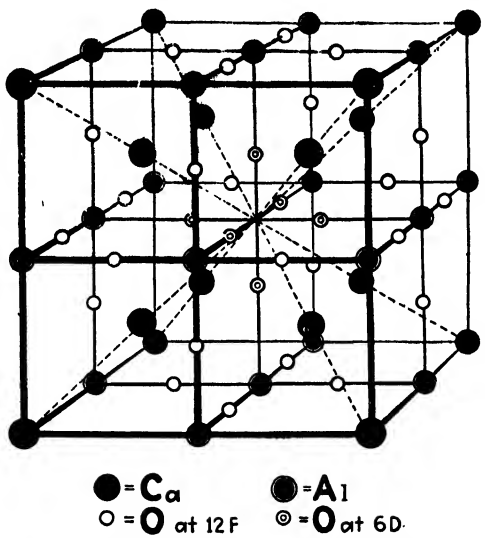

FIG. 5.—The most probable structure of tricalcium aluminate. ● represents Ca^{++}; ● represents Al^{+++}; ○ represents O^{--} at 12*f*; ◎ represents O^{--} at 6*d*.

theoretical basis for expecting that Al^{+++} would have a somewhat greater equivalent scattering power than O^{--}, especially in the higher orders and from forms of small spacing. If this be true, the Al at 3*a* and 3*b* would cause a fainter (111) second-order diffraction than the calculated value given in Table V. This would give a still better match with the experimental data.

It has already been stated in a footnote that, although the theory of space-groups permits a variable parameter for 12*f*, the dimensions of Al^{+++} and O^{--} ions fix this parameter in Fig. 5 at u = 0.25. Arrangements 6*d* and 8*c* have variable parameters. The best intensity match is obtained when u for Ca^{++} at 8*c* = 0.24 and u for O^{--} at 6*d* = 0.31. Intensity calculations show that these parameters are not particularly critical, especially in the case of O^{--} at 6*d*, which may well be somewhat closer to Al at 3*a*. It may well be that, if we knew enough about the diffracting powers of Ca^{++} and O^{--}, both values of u would come out 0.25.

The two other structures which were mentioned as possibilities both have Ca at 8*c* and 1*a*. One has 6*a*, 6*b*, 6*c*, and 6*d* for Al^{+++} and O^{--}, while the other has them at 6*a*, 6*b*, $6b_2$, and 6*d*. These two structures are closely related, since 6*c* may be derived from 6*b* by a single rotation of 90°. While the calculated intensities of these two structures are somewhat less satisfactory than those of the one shown in Fig. 5, the degree of reliability of the laws of scattering with complex crystals is so uncertain that they must be considered as possible structures. It will be shown in Chap. XIX that the same general chemical conclusions can be drawn from all three structures.

It will help the student to solve other crystal structures if he will make the drawings described above and work out the complete solution to the structure of tricalcium aluminate.

SUMMARY

We have shown, using examples from both the Laue and the powder methods, how the theory of space-groups may be used in the solution of crystal structure. Our illustrations have included sodium chloride, calcite, and tricalcium aluminate. These have provided us with a case in which definite ionic coordinates were found at once and a case which left us with an undetermined parameter which had to be evaluated in terms of the intensities of the various diffracted beams. We have dealt with the simple case where the theory of space-groups, aided by a knowledge of the external symmetry of the crystal, gave us only a few alternatives from which to choose and with a case which started out with 1,500 possibilities. We have had examples of definite solutions of crystal structures and an example of a partial solution which leaves us with three physically possible alternatives one of which is more probable chemically than the other two.

These illustrations have applied specifically to the Laue and to the powder methods. Similar applications to the Bragg and the rotating-crystal methods should be obvious.

References

1. A. E. H. Tutton, "Crystallography and Practical Crystal Measurement," Vol. I, p. 677, The Macmillan Company, New York, 1922.
2. K. F. Herzfeld and A. Hettisch, *Zeit. Physik*, **38**, 1 (1926).
3. A. P. Honess, "The Nature, Origin, and Interpretation of Etch Figures on Crystals," p. 32, John Wiley & Sons, Inc., New York, 1927; and private communication of unpublished observations.
4. A. H. Compton and R. L. Doan, *Proc. Nat. Acad. Sci.*, **11**, 598 (1925).
5. J. Thibaud, *Compt. rend.*, **182**, 55 (1926).
6. R. W. G. Wyckoff, "The Structure of Crystals," pp. 212–217, Chemical Catalog Company, New York, 1924.
7. R. W. G. Wyckoff, The Analytical Expression of the Results of the Theory of Space-Groups, *Carnegie Inst. Pub.* 318 (1930).

8. R. W. G. WYCKOFF, *Amer. Jour. Sci.*, **50**, 317 (1920).
9. F. A. STEELE and W. P. DAVEY, *Jour. Amer. Chem. Soc.*, **51**, 2283 (1929); *Zeit. Kryst.*, **73**, 17 (1930).
10. W. L. BRAGG, *Phil. Mag.*, **40**, 169 (1920).
11. W. P. DAVEY, *Phys. Rev.*, **21**, 716 (1923); *Chem. Rev.*, **2**, 349 (1926); *Gen. Elec. Rev.*, **29**, 274 (1926). See also Chap. XII.

CHAPTER X

STRUCTURE FACTOR*

In Chaps. IV, V, and VI we discussed in some detail the intensity of the x-ray beams diffracted by a crystal. We found that, if in a crystal there were more planes of a given family than were required by the simplest structure typical of that crystallographic system, then the extra planes would greatly impair the intensity of the diffracted beam or even reduce it to zero. For instance, we found that the {1 1 1} planes of diamond come in pairs (see Fig. 2 of Chap. III and Fig. 4 of Chap. V) such that there is interleaved with the periodic spacing of the {1 1 1} planes a second set of {1 1 1} planes which divides the periodic spacing, $d_{1\,1\,1}$, into two portions which stand in the ratio of 3:1. This was found to reduce the intensity of the first order of diffraction from the {1 1 1} planes of diamond and to destroy the second order of diffraction entirely. Other instances of interleaving of planes were found in the case of zinc blende (ZnS) and fluorite (CaF_2). The effect of the interleaving of planes of Na^+ and Cl^-, K^+ and Cl^-, K^+ and I^-, etc., in the alkali halides was thoroughly discussed in Chaps. V and VI.

EFFECT OF ATOMIC STRUCTURE ON THE INTENSITY OF THE DIFFRACTED BEAMS

In all of the above discussions one important approximation was made; each atom or ion was assumed to diffract like a single point whose diffracting ability was proportional to the atomic or ionic number. It would have been more in accordance with our pictures of the mechanism of diffraction if we had assumed that, when x-rays are diffracted, the actual diffracting centers are the electrons which compose the extranuclear portions of the atoms in the crystal. Whether we assume these electrons to be stationary (static-atom theory in some form or other) or whether we assume them to be in motion in definite orbits around the nucleus (Bohr-Sommerfeld theory, etc.), or whether we take some one of the newer pictures of atomic structure, in any case it is hard to escape the conclusion that the x-rays diffracted from one electron must be some-

* The phrases "atomic structure factor" and "molecular structure factor" (often abbreviated in this chapter to "structure factor" in accordance with common usage) have to do entirely with the effect of the internal structure of atoms (or ions or molecules) on the intensities of the diffracted x-ray beams. These terms should not be confused with an older use in the literature of the phrase "structure factor" which referred to the decrease in intensity of diffracted x-ray beams caused by the positions of atoms (or ions) in the unit-crystal.

what out of phase with the x-rays diffracted by some other electron in the same atom. The total intensity of any beam of x-rays diffracted by a crystal would, then, be expected to depend not only upon the configuration of atoms in the crystal but also upon the distribution of electrons in the atoms of which the crystal is composed.

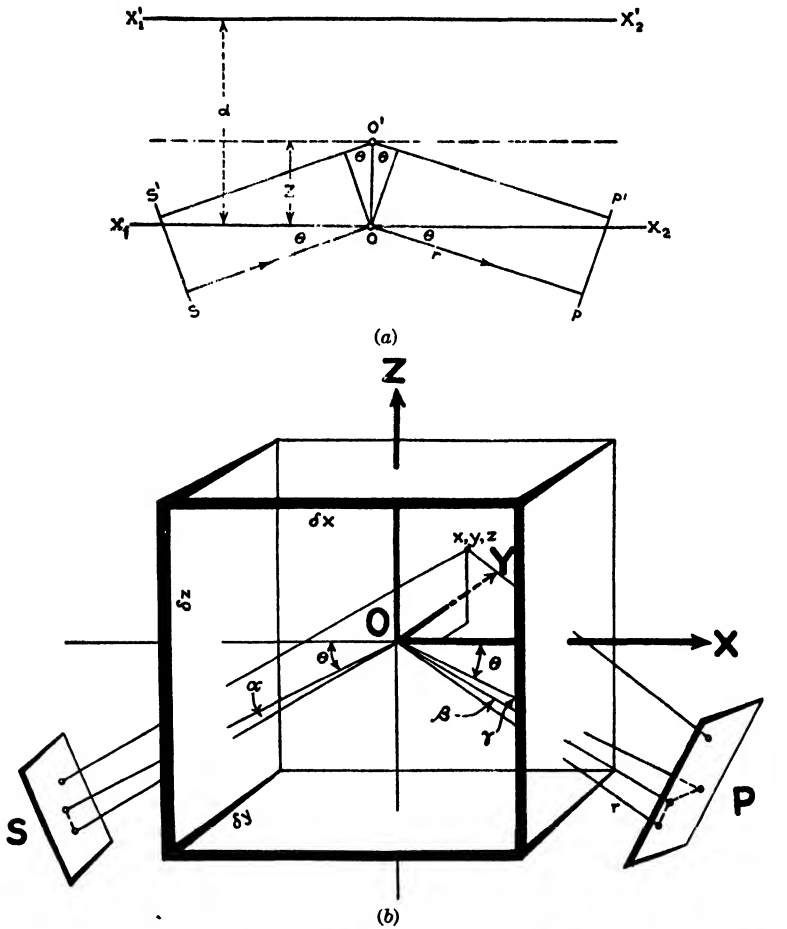

FIG. 1 (*a*) and (*b*).—Effect of the finite size of atoms and of mosaic structure on the amplitude of a diffracted wave.

In the case of the most frankly mechanical pictures of atomic structure, such as the static-atom theory, the layers of electrons would have the effect of interleaving the periodic spacing with the small interplanar spacings of the layers of electrons of which the atoms are supposed to be built up. In the case of less frankly mechanical pictures of atomic structure, we still have to do, for each family of atomic planes in the crystal, with the probability that an electron will be found at a distance

z above or below a geometrical plane passed through the centers of the atoms. Since the second viewpoint is more general in its nature than the first, it will be taken as the basis of our calculations.[1] After we have discussed the effect of the distribution in space of the electrons in the atoms of a crystal, we shall discuss how we can use this sort of information to determine, from the x-ray diffraction data, the probable places in a crystal where electrons are clustered together. This, in turn, can be interpreted directly in terms of the location of atoms, *i.e.*, in terms of crystal structure.

Structure Factor.—In Fig. 1*a*, let X_1X_2 be the mid-plane of a layer of atoms in a crystal, let SS' be the wave front of a plane-polarized incident beam of x-rays whose electric vector is perpendicular to the plane SOP, and let the x-ray beam be diffracted to the plane PP' according to Bragg's law, $n\lambda = 2d \sin \theta$. If, now, all the electrons of each atom were in the mid-plane X_1X_2 (for instance, the electron at O), then the amplitude of the diffracted wave at PP' would be the sum of the amplitudes of all the wavelets from all the individual electrons. We shall call the amplitude of each wavelet A_0. But in the actual case an electron may be at the point O' located a distance z above the plane X_1X_2, and this would increase the length of the path of the x-ray beam by $2(z \sin \theta)$. The amplitude of the wavelet at PP' diffracted by the electron at O' would no longer be given by A_0 but would be given by*

$$A_e = A_0 \cos \left(\frac{2\pi}{\lambda} \cdot 2z \sin \theta \right) \tag{1}$$

* When waves are to be added which are out of phase with each other, their amplitudes may be expressed in terms of some arbitrary standard of phase. The algebraic sum of the components of amplitude, expressed in this way, gives the amplitude of the resultant wave. A consideration of the elementary equations of wave motion, such as may be found in any text on physical optics, shows that Eq. (1) gives the contribution A_e, which the wavelet from O' makes to the amplitude of the resultant wave at PP'. It will be found that if the wavelet from O' is out of phase with the wavelet from O by an amount expressed in circular measure as Δ, then

$$A_e = A_0 \cos \Delta$$

But the phase angle, Δ, is related to the whole wave length, expressed as 2π in circular measure, by the proportion

$$\frac{\Delta}{2\pi} = \frac{2z \sin \theta}{\lambda}$$

so that

$$\Delta = \frac{2\pi}{\lambda} \cdot 2z \sin \theta$$

Therefore

$$A_e = A_0 \cos \left(\frac{2\pi}{\lambda} \cdot 2z \sin \theta \right)$$

In order to facilitate cross reference, the symbols used in this discussion correspond in general to those used in "X-rays and Electrons" by A. H. Compton, D. Van Nostrand Company, New York.

We may assume that the probability that any given electron will be above the plane X_1X_2 at a height between z and $z + dz$ is proportional to dz and to some function of z which we shall call $p(z)$; *i.e.*, the probability is proportional to $p(z)\,dz$. The probable contribution of any one electron to the total amplitude of the diffracted wave is therefore

$$\bar{A}_e = A_0 \int_{-a}^{+a} p(z) \cos\left(\frac{4\pi z}{\lambda} \sin\theta\right) dz \tag{2}$$

where a is the maximum value of z which the electron could have and still "belong" to its own atom. The amplitude of a wave diffracted from a whole atom of Z electrons will be

$$A = Z\bar{A}_e = ZA_0 \int_{-a}^{+a} p(z) \cos\left(\frac{4\pi z}{\lambda} \sin\theta\right) dz = A_0 F \tag{3}$$

where

$$F \equiv Z \int_{-a}^{+a} p(z) \cos\left(\frac{4\pi z}{\lambda} \sin\theta\right) dz \tag{4}$$

F is called the "structure factor" of the atom. The number F denotes the ratio of the amplitude of the wave scattered by the actual atom to the amplitude which would have been found if all the electrons had been concentrated on the mid-plane. We must now see how this quantity F comes into our experimental data for the intensity of the rays diffracted by a crystal, so that we may use these measured intensities in quantitative investigations of crystal structure.

Calculation of "Integrated Reflection."—In preparation for our study of the ways in which the structure factor can be used in crystal analysis, we shall first calculate the amplitude (and from this the intensity) of x-rays diffracted by a very small crystal. Consider a crystal fragment of size $\delta x\ \delta y\ \delta z$ (Fig. 1*b*) such that it contains only a few unit-crystals. This crystal fragment may be considered to be one of the blocks in the mosaic structure of the crystal. Then we may assume that, if it is oriented to the x-ray beam to give nearly the correct angle of diffraction θ, required by Bragg's law for some atomic plane, the rays diffracted by one atom will be substantially in phase with the rays diffracted by any other atom in the same plane, and the phases of rays diffracted by atoms in successive planes will differ by approximate multiples of 2π. For simplicity, we shall assume that the X-, Y-, and Z-axes of the crystal fragment are at right angles to each other, that the units of measure along all three axes are equal, and that the crystal structure is of the simplest possible type; in other words, we shall assume a simple cubic crystal. This means that each unit-crystal "contains" one atom. Let the x-ray beam make a grazing angle of incidence $(\theta + \alpha)$ with some

atomic plane,* say the (0 0 1), and let the corresponding grazing angle of diffraction be $(\theta + \beta, \gamma)$ where α and β are measured in the plane *SOP*, and γ is measured at right angles to the plane *SOP*. If an x-ray wave front is diffracted by both *O* and the point *xyz*, then the difference in path length is (neglecting second-order terms):

$$x(\beta - \alpha) \sin \theta + y\gamma + z\{2 \sin \theta + (\alpha + \beta) \cos \theta\}$$

It is evident from Fig. 1*a* that, if the diffracted waves from *O* and *O'* are to meet in phase, $2z \sin \theta$ must equal an exact number of wave lengths. The only significant difference in the path lengths of the waves from *O* and the point *xyz* of Fig. 1*b* is therefore

$$x(\beta - \alpha) \sin \theta + y\gamma + z(\alpha + \beta) \cos \theta$$

If Δ is the phase difference between the two waves, then

$$\frac{\Delta}{2\pi} = \frac{x(\beta - \alpha) \sin \theta + y\gamma + z(\alpha + \beta) \cos \theta}{\lambda}$$

so that

$$\Delta = \frac{2\pi}{\lambda}\{x(\beta - \alpha) \sin \theta + y\gamma + z(\alpha + \beta) \cos \theta\} \tag{5}$$

If we write for convenience,

$$\begin{aligned} a &= (\beta - \alpha) \sin \theta \\ b &= \gamma \\ c &= (\alpha + \beta) \cos \theta \end{aligned}$$

* In the case of perfect crystals whose size is large compared with the wave length of x-rays, the grazing angle of incidence must equal the grazing angle of diffraction and $n\lambda/2d$ must be exactly equal to sin θ. It is inherent in the derivations of Bragg's law (Chap. I) that crystal fragments, such as δx, δy, δz of Fig. 1*b*, which are only a few wave lengths on a side, may have a grazing angle of incidence which differs slightly from θ. This angle may be expressed as $(\theta + \alpha)$, where α is a very small angle lying in the same plane as θ. The diffracted beam may not only emerge at an angle slightly different from θ, but it may even lie somewhat off the plane of θ. It may be expressed as $(\theta + \beta, \gamma)$, where β is a small angle in the plane of θ, and γ is a small angle in a plane perpendicular to the plane of θ.

The difference in path length caused by moving the diffracting electron from *O* to the point *xyz* may be found approximately as the algebraic sum of the components of *x*, *y*, and *z* along the path of the x-ray beam. These are (remembering that for very small angles the sine is approximately equal to the angle expressed in radians, and the cosine is approximately unity):

(1) $x \cos (\theta + \alpha) - x \cos (\theta + \beta)$
$= x(\cos \theta \cos \alpha - \sin \theta \sin \alpha) - x(\cos \theta \cos \beta - \sin \theta \sin \beta)$
= (approx.) $x(\beta - \alpha) \sin \theta$

(2) $y \sin \gamma$ = (approx.) $y\gamma$

(3) $z \sin (\theta + \alpha) + z \sin (\theta + \beta)$
$= z(\sin \theta \cos \alpha + \cos \theta \sin \alpha) + z(\sin \theta \cos \beta + \cos \theta \sin \beta)$
= (approx.) $z[2 \sin \theta + (\alpha + \beta) \cos \theta]$

then

$$\Delta = \frac{2\pi}{\lambda}(ax + by + cz)$$

If, now, the crystal contains n atoms per cubic centimeter (for a simple cubic crystal this is the equivalent of n unit-crystals per cubic centimeter), then we shall have $n(dx\,dy\,dz)$ atoms in an infinitesimal volume $dxdydz$] and the amplitude of the wavelet which it diffracts will be [from Eq. (3), $nA_0Fdxdydz$. But this wavelet will be out of phase with the resultant wave by a phase angle Δ, so that the contribution which this infinitesimal volume makes to the resultant wave is

$$dA = nA_0F \cos \Delta\, dxdydz$$

The whole crystal fragment whose volume is $\delta x\delta y\delta z$ will therefore diffract an x-ray beam with an amplitude

$$A_1 = nA_0F \int_{-\frac{\delta z}{2}}^{\frac{\delta z}{2}} \int_{-\frac{\delta y}{2}}^{\frac{\delta y}{2}} \int_{-\frac{\delta x}{2}}^{\frac{\delta x}{2}} \cos \Delta\, dxdydz \tag{6}$$

$$= nA_0F \int_{-\frac{\delta z}{2}}^{\frac{\delta z}{2}} \int_{-\frac{\delta y}{2}}^{\frac{\delta y}{2}} \int_{-\frac{\delta x}{2}}^{\frac{\delta x}{2}} \cos \left\{\frac{2\pi}{\lambda}(ax + by + cz)\right\} dxdydz$$

$$A_1 = nA_0F \frac{\sin \xi}{\xi} \frac{\sin \eta}{\eta} \frac{\sin \zeta}{\zeta} \delta x\delta y\delta z \tag{7}*$$

$$*\int^{\delta z}\int^{\delta y}\int^{\delta x} \cos \left\{\frac{2\pi}{\lambda}(ax + by + cz)\right\} dxdydz$$

$$= \int^{\delta z}\int^{\delta y} \frac{\lambda}{2\pi a}\left[\sin \frac{2\pi}{\lambda}(ax + by + cz)\right]_{-\frac{\delta x}{2}}^{\frac{\delta x}{2}} dydz$$

$$= \int^{\delta z}\int^{\delta y} \frac{\lambda}{2\pi a}\left\{\sin \frac{2\pi}{\lambda}\left(\frac{a\delta x}{2} + by + cz\right) - \sin \frac{2\pi}{\lambda}\left(-\frac{a\delta x}{2} + by + cz\right)\right\} dydz$$

$$= \int^{\delta z}\int^{\delta y} \frac{\lambda}{\pi a}\left\{\sin \frac{\pi}{\lambda}a\delta x\right\}\left\{\cos \frac{2\pi}{\lambda}(by + cz)\right\} dydz$$

$$= \int^{\delta z} \frac{\lambda^2}{2\pi^2 ab}\left\{\sin \frac{\pi}{\lambda}a\delta x\right\}\left[\sin \frac{2\pi}{\lambda}(by + cz)\right]_{-\frac{\delta y}{2}}^{\frac{\delta y}{2}} dz$$

$$= \int^{\delta z} \frac{\lambda^2}{2\pi^2 ab}\left\{\sin \frac{\pi}{\lambda}a\delta x\right\}\left\{\sin \frac{2\pi}{\lambda}\left(\frac{b\delta y}{2} + cz\right) - \sin \frac{2\pi}{\lambda}\left(-\frac{b\delta y}{2} + cz\right)\right\} dz$$

$$= \int^{\delta z} \frac{\lambda^2}{\pi^2 ab}\left\{\sin \frac{\pi}{\lambda}a\delta x\right\}\left\{\sin \frac{\pi}{\lambda}b\delta y\right\}\left\{\cos \frac{\pi}{\lambda}cz\right\} dz$$

$$= \frac{\lambda^3}{\pi^3 abc}\left\{\sin \frac{\pi}{\lambda}a\delta x\right\}\left\{\sin \frac{\pi}{\lambda}b\delta y\right\}\left\{\sin \frac{\pi}{\lambda}c\delta z\right\}$$

$$= \frac{\sin \frac{\pi}{\lambda}a\delta x}{\frac{\pi}{\lambda}a} \cdot \frac{\sin \frac{\pi}{\lambda}b\delta y}{\frac{\pi}{\lambda}b} \cdot \frac{\sin \frac{\pi}{\lambda}c\delta z}{\frac{\pi}{\lambda}c}$$

(Footnote continued at the bottom of page 298.)

where

$$\xi = \pi a\frac{\delta x}{\lambda} = \pi(\beta - \alpha)\frac{\delta x}{\lambda}\sin\theta$$

$$\eta = \pi b\frac{\delta y}{\lambda} = \pi\gamma\frac{\delta y}{\lambda}$$

$$\zeta = \pi c\frac{\delta z}{\lambda} = \pi(\alpha + \beta)\frac{\delta z}{\lambda}\cos\theta$$

The intensity of a wave of amplitude A_1 is proportional to the square of its amplitude, *i.e.*,

$$I_1 = \frac{c}{8\pi}A_1^2$$

where c is the velocity of light. In terms of Eq. (7), the intensity of the beam diffracted in the direction $(\theta + \beta, \gamma)$ is

$$I_1 = \frac{cn^2A_0^2F^2}{8\pi}\left\{\frac{\sin\xi}{\xi}\cdot\frac{\sin\eta}{\eta}\cdot\frac{\sin\zeta}{\zeta}\delta x\delta y\delta z\right\}^2 \tag{8}$$

Experimentally it will not do merely to set an ionization chamber at what we suppose to be the correct angle for diffraction and then assume that the ionization current which we obtain represents the true intensity of the diffracted beam. Because of the mosaic structure which exists to a greater or less extent in all crystals (see Chaps. I and XII) the angles of incidence and of diffraction for a given crystal are not quite sharp. In order to measure the true intensity we may avail ourselves of the scheme of opening the slits in front of the ionization chamber as far as possible so as to include all values of β, γ and then rotating the crystal at a uniform rate ω so as to include all values of incidence $\theta \pm \alpha$ for the various blocks in the mosaic in the immediate neighborhood of the diffracting angle θ. The ionization current is then a measure of the total energy diffracted by the crystal at angles approximating θ. It requires a time $d\alpha/\omega$ for the crystal to go with the angular velocity ω from the angular position α

---

which may be written

$$\frac{\sin\xi}{\xi}\cdot\frac{\sin\eta}{\eta}\cdot\frac{\sin\zeta}{\zeta}\delta x\delta y\delta z$$

where ξ, η, and ζ have the meaning given in Eq. (7).

It should be noted that the derivation of Eqs. (6) and (7) is hardly rigorous, since it assumes (1) that the atoms are continuously distributed at the rate $n(dx\,dy\,dz)$ although we are really thinking of a small volume containing discrete atoms, and (2) that each atom is so small that phase differences between its parts can be taken care of by putting $nA_0F\,dx\,dy\,dz$ for the amplitude from the element $dx\,dy\,dz$ although in Chap. XIII we show evidence for atoms of such size that their domains touch at absolute zero.

to the position $\alpha + d\alpha$ so that the total energy received by the ionization chamber is

$$W_1 = \int_{-\infty}^{\infty} P_1 \frac{d\alpha}{\omega}$$

where P_1 is the energy received by the ionization chamber in unit-time. This energy-per-unit-time, or "power," is obviously (see Fig. 1*b*)

$$P_1 = \int_{-\infty}^{\infty} r d\beta \int_{-\infty}^{\infty} r d\gamma I_1$$

so that

$$W_1 = \int\int_{-\infty}^{\infty} \int \frac{r^2}{\omega} I_1 d\alpha d\beta d\gamma \tag{9}$$

Substituting Eq. (8) into Eq. (9) we have*

---

* The variables ξ, η, ζ must be defined in terms of α, β, γ. This may be done by substitution as follows:

$$\xi = \pi \frac{\delta x}{\lambda} \sin\theta(\beta - \alpha) = k_1(\beta - \alpha)$$

$$\eta = \pi \frac{\delta y}{\lambda} \gamma = k_2 \gamma$$

$$\zeta = \pi \frac{\delta z}{\lambda} \cos\theta(\alpha + \beta) = k_3(\alpha + \beta)$$

$$d\xi = k_1(d\beta - d\alpha)$$

$$d\zeta = k_3(d\beta + d\alpha)$$

$$\frac{d\xi}{k_1} - \frac{d\zeta}{k_3} = -2d\alpha; \text{ i.e., } -d\alpha = \frac{d\xi}{2k_1} - \frac{d\zeta}{2k_3}$$

$$d\beta = \frac{d\xi}{2k_1} + \frac{d\zeta}{2k_3}$$

$$d\gamma = \frac{d\eta}{k_2}$$

Then the integration may be performed as follows:

$$\int\int_{-\infty}^{\infty} \int \frac{\sin^2\xi}{\xi^2} \cdot \frac{\sin^2\eta}{\eta^2} \cdot \frac{\sin^2\zeta}{\zeta^2} d\alpha d\beta d\gamma$$

$$= \int\int_{-\infty}^{\infty} \int \frac{\sin^2\xi}{\xi^2} \cdot \frac{\sin^2\eta}{\eta^2} \cdot \frac{\sin^2\zeta}{\zeta^2} \left| J \frac{\alpha, \beta, \gamma}{\xi, \eta, \zeta} \right| d\xi d\eta d\zeta$$

$$J = \begin{vmatrix} \frac{\partial\alpha}{\partial\xi} & \frac{\partial\beta}{\partial\xi} & \frac{\partial\gamma}{\partial\xi} \\ \frac{\partial\alpha}{\partial\eta} & \frac{\partial\beta}{\partial\eta} & \frac{\partial\gamma}{\partial\eta} \\ \frac{\partial\alpha}{\partial\zeta} & \frac{\partial\beta}{\partial\zeta} & \frac{\partial\gamma}{\partial\zeta} \end{vmatrix} = \begin{vmatrix} -\frac{1}{2k_1} & \frac{1}{2k_1} & 0 \\ 0 & 0 & \frac{1}{k_2} \\ \frac{1}{2k_3} & \frac{1}{2k_3} & 0 \end{vmatrix}$$

$$J = \frac{1}{4k_1k_2k_3} + \frac{1}{4k_1k_2k_3} = \frac{1}{2k_1k_2k_3}$$

The integral therefore corresponds to the standard form

$$a\int_{-\infty}^{\infty} \frac{\sin^2 x}{x^2} dx = a\pi$$

The triple integral is therefore

$$\int\int_{-\infty}^{\infty} \int = \frac{\pi^3}{2k_1k_2k_3} = \frac{\lambda^3}{2\sin\theta\cos\theta\delta x\delta y\delta z}$$

$$W_1 = \int\int_{-\infty}^{\infty} \int \frac{cr^2n^2A_0^2F^2}{8\pi\omega} \left\{ \frac{\sin \xi}{\xi} \cdot \frac{\sin \eta}{\eta} \cdot \frac{\sin \zeta}{\zeta} \delta x \delta y \delta z \right\}^2 d\alpha d\beta d\gamma$$

$$= \frac{cr^2n^2A_0^2F^2\delta x^2\delta y^2\delta z^2}{8\pi\omega} \int\int_{-\infty}^{\infty} \int \frac{\sin^2 \xi}{\xi^2} \cdot \frac{\sin^2 \eta}{\eta^2} \cdot \frac{\sin^2 \zeta}{\zeta^2} d\alpha d\beta d\gamma$$

$$= \frac{cr^2n^2A_0^2F^2\delta x^2\delta y^2\delta z^2}{8\pi\omega} \cdot \frac{\lambda^3}{2 \sin \theta \cos \theta \cdot \delta x \delta y \delta z}$$

$$W_1 = \frac{cr^2n^2A_0^2F^2\lambda^3}{8\pi\omega \sin 2\theta} \delta x \delta y \delta z \tag{10}$$

Equation (10) expresses the energy received by the ionization chamber in terms of the quantity A_0 which, it will be remembered from the discussion of Fig. 1, is the amplitude of a wavelet at PP' after having been diffracted by an electron at O. It would suit our purpose better to express this energy in terms of the intensity, I_s, at the point O of Fig. 1, of the incident beam coming from the original source of x-rays. Electromagnetic theory shows that the amplitude A_0 at PP' is related to the amplitude, A_s, of the beam which is incident on the electron at O by means of the equation

$$A_0 = A_s \frac{e^2}{mrc^2} \tag{11}$$

when the electric vector is perpendicular to the plane SOP. In this equation, e and m are the charge and mass of the electron; c is the velocity of light; and r is shown in Fig. 1. Substituting Eq. (11) into Eq. (10), and remembering that $\delta x \delta y \delta z$ is the volume, δV, of the crystal fragment of Fig. 1, we have

$$W_1 = \frac{cA_s^2}{8\pi} \cdot \frac{e^4}{\omega m^2c^4} \cdot \frac{n^2F^2\lambda^3}{\sin 2\theta} \cdot \delta V$$

But $cA_s^2/8\pi$ is the intensity I_s of the beam incident on the crystal fragment at O, so that

$$W_1 = \frac{I_s e^4}{\omega m^2c^4} \cdot \frac{n^2F^2\lambda^3}{\sin 2\theta} \cdot \delta V \tag{12}$$

So far we have considered only an x-ray beam which is polarized with the electric vector perpendicular to the plane SOP of Fig. 1. If, instead, we take a beam which is polarized with the electric vector parallel to the plane SOP, then the component of the amplitude acting through an angle 2θ would be $A_s \cos 2\theta$. The corresponding energy would be $W_2 = W_1 \cos^2 2\theta$. If, instead of considering the x-ray energy to be concentrated into a polarized beam, we consider the same quantity of energy to exist in an unpolarized beam, we have

$$W = \frac{W_1 + W_2}{2} = \frac{1}{2} W_1(1 + \cos^2 2\theta) \tag{13}$$

By combining Eqs. (12) and (13) for the general case of an unpolarized beam, we have

$$W = \frac{I}{2\omega} \cdot \frac{e^4}{m^2c^4} \cdot \frac{n^2F^2\lambda^3}{\sin 2\theta}(1 + \cos^2 2\theta)\delta V \tag{14}$$

In investigating the structure of crystals by the structure-factor method it would be ideal to be able to use conveniently the *efficiency of diffraction* of x-rays by the crystal planes under investigation. This would necessitate: (1) a measurement of the rate at which energy is received by the crystal; (2) a measurement of the rate at which energy is diffracted by the crystal; and (3) an expression of the ratio of (2) to (1). Equation (14) does not lend itself directly to such an ideal statement. It can, however, be put easily into a form which will do about as well, for we can get from it the quantity $W\omega/I$ in which I can, in special cases, be made to yield a value for the rate at which energy is delivered to the crystal. $W\omega$ is the average rate at which energy is diffracted by the crystal times the angle through which the crystal is turned, so that $W\omega/I$ is proportional to

$$\frac{\text{The average rate at which energy is diffracted by the crystal}}{\text{The intensity of the incident beam}}$$

This quotient is given the technical name of "integrated reflection" ρ.

$$\rho = \frac{W\omega}{I} = \frac{1}{2}n^2\lambda^3F^2\frac{e^4}{m^2c^4} \cdot \frac{1 + \cos^2 2\theta}{\sin 2\theta}\delta V \tag{15}$$

In this equation, W is the total energy diffracted by a crystal fragment (Fig. 1) of volume δV while it is turned past the nominal diffracting angle θ at a uniform angular velocity ω. I is the intensity of the unpolarized incident beam; n is the number of atoms per cubic centimeter in the crystal fragment (in this special case of a simple cubic crystal, n is numerically equal to the number of unit-crystals per cubic centimeter); λ is the wave length of x-rays employed; e is the charge on the electron; m is the mass of the electron; c is the velocity of light; and the structure factor F is defined by Eq. (4).

In Eq. (15), the factor

$$\frac{1}{2}n^2\lambda^3F^2\frac{e^4}{m^2c^4}\frac{1 + \cos^2 2\theta}{\sin 2\theta} \tag{15a}$$

is called Q, so that

$$\rho = \frac{W\omega}{I} = Q\delta V \tag{16}$$

It was stated above that in special cases the value of the intensity I of the incident beam could be converted into a value of the rate at which energy is received by the crystal, *i.e.*, into the "power" of the

incident beam. Three special cases are of interest: (1) the incident beam passes through a single crystal or an agglomerate of similarly oriented tiny crystals and the diffracted beam is measured on the emergent side; (2) the incident beam is diffracted (or, as the literature has it, "reflected") from the surface of a single crystal; (3) the incident beam is diffracted by a mass of powdered crystal in which the fragments have a random orientation. We shall take up these three cases in succession.

1. Diffraction of a Transmitted Ray by a Single Crystal.—In Fig. 2 let *abcd* represent an irregular, "imperfect" crystal whose face covers

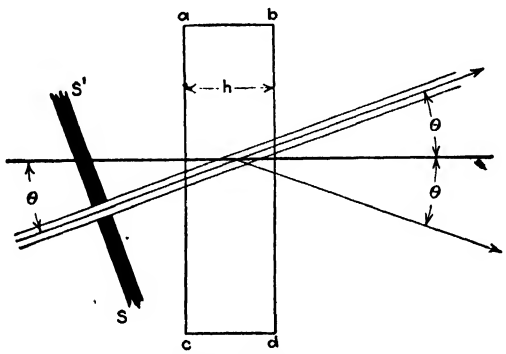

FIG. 2.—Diffraction of transmitted x-rays from a single crystal.

considerable area, or, what is practically the same thing, a mass of small crystals having almost exactly the same orientation. When this is irradiated by x-rays through the slit SS', then, if the area of the slit opening is $\mathfrak{A}$ and the thickness of the crystal is h, the volume of the crystal irradiated is $\mathfrak{A}h/\cos\theta$. This corresponds to the δV of Eq. (16). Equation (16) therefore gives

$$\rho = \frac{W\omega}{I} = Q\frac{\mathfrak{A}h}{\cos\theta}$$

as the integrated reflection for the fictitious case of a diffracting crystal which absorbs no x-rays. In any real crystal, absorption reduces this value by the factor

$$e^{-\mu(h \sec\theta)}$$

where e = base of natural logarithms.

μ = coefficient of absorption.

$h \sec\theta$ = length of the path of the x-rays in the crystal (see Fig. 2).

The actual integrated reflection is therefore

$$\frac{W\omega}{I} = Q\mathfrak{A}h \sec\theta e^{-\mu(h \sec\theta)} \qquad (17)$$

Since the intensity I is the rate at which energy is received on a unit-area, the intensity of the incident beam of Fig. 2 can obviously be translated

into the rate at which energy is received (*i.e.*, the power) by the diffracting point under consideration in the interior of the crystal by the relation

$$P = I\bar{A}e^{-\mu(h \sec \theta)}$$

so that

$$\frac{W\omega}{P} = Qh \sec \theta \tag{18}$$

2. Diffraction of a "Reflected" Ray by a Single Crystal.—Let Fig. 3 represent the case in which x-rays enter some given face of a crystal and the diffracted rays emerge from the same face, *i.e.*, in the language of the literature, the rays are "reflected from the crystal face." Consider the

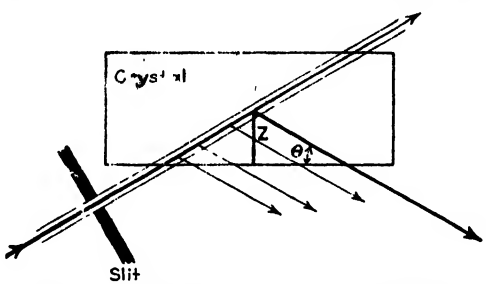

FIG. 3.—Diffraction of x-rays from a surface.

x-ray beam diffracted at a depth z inside the surface. Then Eq. (16) becomes

$$\frac{W\omega}{I} = Q\int_0^\infty \bar{A} \csc \theta e^{-2\mu z \csc \theta} dz$$

where $\int_0^\infty \bar{A} \csc \theta dz$ is the volume δV, and $e^{-2\mu z \csc \theta}$ represents the decrease in intensity due to absorption. The integration gives

$$\frac{W\omega}{I} = \frac{Q\bar{A}}{2\mu} \tag{19}$$

In the case of reflection, the power P of the incident beam is usually determined in terms of the rate at which energy is received at the surface of the crystal. This requires that the crystal be removed, the area $\bar{A}$ of the slit measured, and the intensity I of the x-rays determined. Obviously for this case,

$$P = I\bar{A}$$

and Eq. (19) becomes

$$\frac{W\omega}{P} = \frac{Q}{2\mu} \tag{20}$$

It should be noted that at the diffracting angle the coefficient of absorption is considerably larger than that measured under ordinary conditions, and attempts to measure its actual value usually end by

reasoning in a circle. For this reason case 2 is the least satisfactory of the three cases under consideration.

3. Diffraction by Powdered Crystals.—In Fig. 4 let a monochromatic x-ray beam travel in the direction SOX, and let it meet a mass of powdered crystal at O. Let a reference sphere $SNAXC$ be drawn with O as its center, and let the great circle ABC be perpendicular to SOX. If some crystal fragment at O is oriented so that some family of planes can diffract the x-ray beam along the line OS', its normal must lie in the plane of the

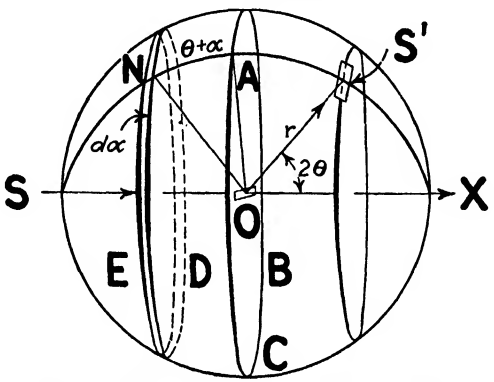

FIG. 4.—Diffraction of x-rays from a powder.

great circle $SNAS'X$. If the crystal fragment is so small as to compare in size with the crystal of Fig. 1*b* whose volume was δV, then the normal ON must make an angle $\theta + \alpha$ with the plane ABC; *i.e.*, it must make an angle $\theta + \alpha$ with OA. α is very small in comparison with θ.

The diffracting power of a randomly oriented crystal fragment will depend, in part, upon the probability that the angle NOA will lie between $\theta + \alpha$ and $\theta + (\alpha + d\alpha)$. This probability will depend upon the ratio of the solid angle subtended by the belt NED to the solid angle subtended by the surface of the whole sphere. Since the belt has an infinitesimal width $NOd\alpha$, it may be considered as a cylinder of radius $NO \sin SON = NO \cos(\theta + \alpha)$, so that its area is $2\pi(NO)^2 \cos(\theta + \alpha)d\alpha$. It therefore subtends an angle $2\pi \cos(\theta + \alpha)d\alpha$ from the center O. The whole sphere subtends a solid angle 4π so that the probability that the normal to a single plane-family in a randomly oriented crystal fragment will lie between $\theta + \alpha$ and $\theta + (\alpha + d\alpha)$ is

$$\frac{2\pi \cos(\theta + \alpha)d\alpha}{4\pi} = \frac{1}{2}\cos(\theta + \alpha)d\alpha$$

Since α is very small, this is very closely equal to

$$\tfrac{1}{2} \cos \theta d\alpha$$

In the case of an actual crystal fragment this probability is increased by a factor f which is the number of plane-families in the form under con-

sideration [see Eq. (5) of Chap. VI]. Depending upon the system of crystallization and the form, f may be 1, 2, 3, 4, 6, 8, 12, or 24.

In the discussion of Fig. 1*b* we found that the power P_1 diffracted to the ionization chamber by a single plane-family in the crystal is

$$P_1 = \int_{-\infty}^{\infty} r d\beta \int_{-\infty}^{\infty} r d\gamma I_1$$

The probable power $\bar{P}_1$ diffracted by a randomly oriented crystal powder is therefore*

$$\begin{aligned} \bar{P}_1 &= \int_{-\infty}^{\infty} P_1 \cdot \tfrac{1}{2} f \cos\theta d\alpha \\ &= \tfrac{1}{2} f \cos\theta \int\int_{-\infty}^{\infty} \int r^2 I_1 d\alpha d\beta d\gamma \end{aligned} \tag{21}$$

In the same manner that we obtained Eq. (12) from Eq. (9), we have, from Eq. (21),

$$\bar{P}_1 = \frac{1}{2} f \cos\theta \cdot \frac{I_s e^4}{m^2 c^4} \cdot \frac{n^2 F^2 \lambda^3}{\sin 2\theta} \cdot \delta V \tag{22}$$

Just as in Eq. (14) we introduced the polarization factor $\frac{1}{2}(1 + \cos^2 2\theta)$, so Eq. (22) becomes

$$\frac{\bar{P}}{I} = \frac{1}{4} f \cos\theta \, n^2 F^2 \lambda^3 \cdot \frac{e^4}{m^2 c^4} \cdot \frac{1 + \cos^2 2\theta}{\sin 2\theta} \cdot \delta V \tag{23}$$

If we represent, as before,

$$\frac{1}{2} n^2 F^2 \lambda^3 \cdot \frac{e^4}{m^2 c^4} \cdot \frac{1 + \cos^2 2\theta}{\sin 2\theta}$$

by Q, then

$$\frac{\bar{P}}{I} = \frac{1}{2} Q f \cos\theta \cdot \delta V \tag{24}$$

In Eq. (24), $\bar{P}$ is the probable value of the power diffracted in a cone whose apex is O and whose semiapex angle is 2θ.

Let the x-rays be measured by an ionization chamber whose slit is at S' of Fig. 4. Let the length of the slit be l, and let l be small in comparison with $r \sin 2\theta$, where r is the distance from the crystal to the ionization chamber (see Fig. 1*b*). If the slit is wide enough to take in all the angle α on each side of θ at which there is any measurable diffracted beam, then the power received by the ionization chamber is

$$P_s = \bar{P} \frac{l}{2\pi r \sin 2\theta}$$

* Since the diffracted beam is of negligible intensity except for very small values of α, it is permissible to use $-\infty$ and ∞ as the limits of integration.

If $\mathfrak{A}$ is the area of the slit which delimits the incident beam SO, then the power of the incident beam is

$$P = \mathfrak{A}I$$

so that I of Eq. (24) is $P/\mathfrak{A}$. Then Eq. (24) becomes

$$\frac{P_s}{P} = \frac{l}{2\pi\mathfrak{A}r \sin 2\theta} \cdot \frac{Q}{2} f \cos\theta \cdot \delta V \tag{25}$$

Since

$$\frac{\cos\theta}{\sin 2\theta} = \frac{1}{2 \sin\theta}$$

it follows that

$$\frac{P_s}{P} = \frac{flQ\delta V}{8\pi\mathfrak{A}r \sin\theta} \tag{26}$$

Reference to "X-rays and Electrons" by A. H. Compton and to the article by W. L. Bragg and J. West [*Zeit. Kryst.*, 69, 123 (1928)] will be facilitated by the following table:

This chapter	Compton	Bragg and West*
Eq. (15)	(5.16)	(4)
Eq. (17)	.....	(6)
Eq. (18)	(5.18)	...
Eq. (20)	(5.20)	(5)
Eq. (24)	(5.21)	(7)

* Bragg and West write for $\mathfrak{A}I$ of Eq. (17) the symbol I. This I corresponds to the P_t of Compton's equation (5.25). θ of Eq. (24) is misprinted as 2θ in Bragg and West's article.

Effect of Extinction.—All of the key equations given above involve the quantity Q, and through Q they involve the structure factor F of Eq. (4). It would seem, therefore, that, if we merely made the measurements indicated by $W\omega/P$ or $\bar{P}/I$ or P_s/P, then, knowing all the other constants in the appropriate equation, we should be able to calculate F. We could even imagine ourselves going a step farther. Using NaCl as an illustration we could imagine ourselves drawing a graph in which F is plotted against the glancing angle θ for some plane (hkl). Such a graph for the (1 0 0) planes would represent the combined intensity effect of $Na^+ + Cl^-$; for the odd-order diffraction from planes like (1 1 1) it would represent $Cl^- - Na^+$. Half the sum of the ordinates of the two curves would enable us to draw a curve in which F for Cl^- alone is plotted against θ, and this in turn would enable us to draw a similar "atomic F curve" for Na^+. From these two atomic F curves and a knowledge of the crystal structure of NaCl we could expect to predict the relative intensities of every x-ray beam diffracted by NaCl. There are, however, two difficulties to be overcome in the case of single crystals.

These difficulties have to do with the effect on the intensities of the diffracted beams of (1) temperature and (2) primary and secondary extinction (see Chap. I).

1. Not only has the theoretical value of the constant B in Debye's equation [Eq. (18) of Chap. I] been a subject for debate, but experimental values of B are complicated by the fact that the lattice parameters of a crystal change with temperature so that we cannot measure the Debye factor apart from this expansion. The experimental measurements of intensities give a series of values F_{hkl} which are characteristic of the crystal at the temperature of the experiment. We have seen that in order to compare these observed values with calculated values of F_{hkl} we need to have, for the plane (hkl), F values for the individual kinds of atoms (or ions) of which the crystal is composed. In order to take account of temperature, each of these atomic F curves should be corrected for the effect of heat motion on that particular kind of atom (or ion). Bragg and West recommend either of two procedures in actual practice: (*a*) use atomic F curves for atoms at rest and expect that at high angles the observed values will fall off from the calculated values; or (*b*) make empirical temperature corrections in the F curves.* Similar temperature corrections may be made in Eq. (24) for the case of a powdered crystal.

2. We have seen in Chap. I that perfect crystals have, at the diffracting angle for a given wave length, a coefficient of absorption which is many times greater than that measured in the ordinary way. In the case of one experiment by Bragg, James, and Bosanquet the increase was 140-fold. This effect was called "primary extinction." We have also seen that ideally imperfect crystals would permit of appreciable diffraction at greater depths below the surface because the interior is shielded only by those crystal fragments which happen to be at the correct angle for diffraction. The loss in intensity due to this partial shielding was called "secondary extinction." Probably a powdered crystal with a maximum ultimate particle-diameter of 250 atomic diameters† is the only really ideally imperfect crystal. If a crystal could be ground to this fineness, this would probably be one of the best ways of getting around the difficulties caused by primary extinction, except that, of course, we would no longer be working with a single crystal. This means that, if we take this way out of our difficulties, we must save it for the

* This second method looks like reasoning in a circle. Experience shows, however, that the calculated atomic coordinates do not change much with small changes in F, so that any reasonable correction in the right direction is an aid and gives a final result with a negligible error. Methods (*a*) and (*b*) really differ in degree and not in kind: (*a*) represents a qualitative correction made mentally; (*b*) represents a semiquantitative correction made in the graph itself.

† For most "imperfect" crystals this ultimate particle-size may be approximated by grinding to an apparent particle-size of 10^{-3} cm.

last operation in our experimental work. The cleavage faces of all actual single crystals are perfect enough to show a little primary extinction and are imperfect enough to show a great deal of secondary extinction. If, however, the face is ground and polished, it usually becomes sufficiently imperfect to be classed as an almost ideally imperfect crystal face. This is probably the most practical way of avoiding primary extinction. A third way out of the difficulty is to take advantage of the fact that primary extinction becomes very small in the case of beams diffracted with low intensities, for instance, at large angles of diffraction, *i.e.*, beams of higher orders of diffraction from planes of low indices or beams from planes of high indices. This way of getting around the difficulty is used when the crystals to be examined are too small to have their possible faces ground and polished.

Secondary extinction produces the same effect as an increase in the coefficient of absorption of the crystal. It has been shown by Darwin[1] that for the weaker lines of a diffraction pattern this effect can be allowed for in Eqs. (17), (19), and (20) by using $(\mu + gQ)$ instead of μ. The value of the constant g must be determined for each individual crystal. Using units of area such that $\bar{A}$ is unity,* Eq. (19) becomes

$$\rho = \frac{Q}{2\mu} \tag{27}$$

where ρ is the true integrated reflection that would have been observed if there had been no secondary extinction. Then

$$\rho' = \frac{Q}{2(\mu + gQ)} \tag{28}$$

where ρ' is the actual integrated reflection found by experiment. Equation (17) becomes

$$\rho' = Qte^{-(\mu+gQ)t} \tag{29}$$

where $t = h \sec \theta$, *i.e.*, t is the length of the path of the x-ray beam inside the crystal.

This may be written

$$\log Q - \log \frac{\rho'}{t} = t(\mu + gQ) \tag{30}$$

This is the equation of a straight line which expresses the relation of $\log \rho'/t$ to t. $\log Q$ is the intercept of the line on the axis of $\log \rho'/t$, and $(\mu + gQ)$ is the slope of the line.

If, now, the face of a single crystal is ground down bit by bit and if ρ' is measured for each successive thickness, we can plot $\log \rho'/t$ against t.

*This can be done, in effect, by dividing the "constant" of the ionization chamber by the area of its slit measured in sq. cm.

The slope of this line should be the effective coefficient of absorption $(\mu + gQ)$ for the crystal with which we are working. Since we know both μ and Q we can solve for g. This assumes that the degree of perfection of the crystal face remains unaltered during the successive grinding operations. The graph of $\log \rho'/t$ *vs.* t is only a straight line for those crystals for which this assumption holds true. Presumably the chance of getting a straight line would be increased by etching the crystal face instead of grinding it. In case a straight line is obtained we can substitute Eq. (27) into (28), obtaining

$$\rho' = \frac{\rho}{1 + 2g\rho}$$

Then

$$\rho = \frac{\rho'}{1 - 2g\rho'} \tag{31}$$

Equation (31) now enables us to find the "true," that is, the theoretical, value ρ of the integrated reflection in terms of the experimental value ρ'.

When the graph of $\log \rho'/t$ *vs.* t is not a straight line, *i.e.*, when the crystal is made more imperfect by the grinding operation, we must do the best we can with some method of approximation. For instance, we can take some family of planes whose arrangement we feel fairly sure of by reason of other considerations (Laue method, Bragg method, powder method, etc.), and from this arrangement we can calculate a theoretical value of F_{hkl}. By means of F_{hkl} we can calculate the corresponding values of Q and ρ. By substituting this calculated value of ρ and the experimentally measured value of ρ' into Eq. (31) we can get a fair approximation for g which may be used in finding the structure of the crystal. If this new structure happens to involve some minor adjustments in the structure of the atomic plane with which we started, we can use the more exact structure to give us a second approximation of g which may be used, in turn, to give a more exact solution of the whole crystal structure.

THE PROBABLE DISTRIBUTIONS OF ELECTRONS IN A CRYSTAL

We have so far discussed the meaning of the term "structure factor"; we have seen how it comes into the theoretical expressions for "integrated reflection"; and we have found how to avoid certain pitfalls due to temperature and to extinction. We must now see how we can use structure factor to help us determine the probable places in a crystal where electrons are clustered together, for this can be interpreted directly

in terms of the locations of atoms, *i.e.*, in terms of crystal structure. So far, three methods for doing this have appeared in the literature:

1. The method of the empirical equation.
2. The method of trial and error.
3. The method of the Fourier's series.

Each of these will be taken up in turn.

1. The Method of the Empirical Equation.—A. H. Compton[1] equated Eq. (20) to Bragg's empirical equation for the normal decrease in the intensity of a diffracted beam as the angle of diffraction is increased.[2] This gives

$$\frac{W\omega}{P} = \frac{Q}{2\mu} = C\frac{1 + \cos^2 2\theta}{\sin^2 \theta}e^{-B\sin^2\theta} \tag{32}$$

where C depends upon the energy and wave length of the incident x-ray beam and on the nature of the crystal. Since, from Eq. (15*a*),

$$Q = \frac{1}{2}n^2\lambda^3F^2\frac{e^4}{m^2c^4}\frac{1 + \cos^2 2\theta}{\sin 2\theta}$$

we have

$$F^2 = \frac{4\mu}{n^2\lambda^3}\cdot\frac{m^2c^4}{e^4}\cdot C\cdot\frac{\sin 2\theta}{\sin^2\theta}\cdot e^{-B\sin^2\theta}$$

$$F^2 = \frac{8\mu}{n^2\lambda^3}\cdot\frac{m^2c^4}{e^4}\cdot C\cdot\cot\theta\cdot e^{-B\sin^2\theta}$$

When θ is small, $e^{-B\sin^2\theta}$ approximates unity. Remembering that for small angles cot θ approximates $1/\sin\theta$, we have

$$F = \left\{\frac{8\mu}{n^2\lambda^3}\cdot\frac{m^2c^4}{e^4}\cdot C\right\}^{\frac{1}{2}}\left\{\frac{1}{\sin\theta}\right\}^{\frac{1}{2}}$$

But, by Eq. (4),

$$F = Z\int_{-a}^{+a} p(z)\cos\left(\frac{4\pi z}{\lambda}\sin\theta\right)dz$$

so that

$$Z\int_{-a}^{+a} p(z)\cos\left(\frac{4\pi z}{\lambda}\sin\theta\right)dz = \left\{\frac{8\mu}{n^2\lambda^3}\cdot\frac{m^2c^4}{e^4}\cdot C\right\}^{\frac{1}{2}}\left\{\frac{1}{\sin\theta}\right\}^{\frac{1}{2}}$$

$$F = Z\int_{-a}^{+a} p(z)\cos\left(\frac{4\pi z}{\lambda}\sin\theta\right)dz = K\left\{\frac{1}{\sin\theta}\right\}^{\frac{1}{2}} \tag{33}$$

This approximate equation has several possible types of solutions but all lead to absurd results except one, namely

$$p(z) = bz^{-\frac{1}{2}} \tag{34}$$

where b is a constant. In so far as this approximate equation holds at all, it indicates for each atom an electron density which is inversely proportional to the square root of the distance from the center of the

atom. This implies an infinite radius to every atom. The fact that such a picture of atomic structure seems to be inconsistent with well-established theories does not prevent the "method of the empirical equation" from being useful. F curves calculated by this method for chlorine agree well with experimental F curves. Presumably the method would apply still better to atoms of higher atomic number.

Thomas[3] has proposed other equations which, although they are not empirical, can be interpreted to mean that each atomic nucleus is sur-

TABLE I.—STANDARD F CURVE FOR THE THOMAS MODEL OF Cs ($N = 55$)

$\frac{\sin\theta}{\lambda} \times 10^{-8}$	F_{Cs}
0.0	55.0
0.1	50.7
0.2	43.8
0.3	37.6
0.4	32.4
0.5	28.7
0.6	25.8
0.7	23.2
0.8	20.8
0.9	18.8
1.0	17.0
1.1	15.6
1.2	14.5
1.3	13.2
1.4	12.3
1.5	11.3
1.6	10.4
1.7	9.6
1.8	9.2
1.9	8.6
2.0	8.1

rounded by a continuous "electron atmosphere" which decreases in intensity as the distance from the nucleus is increased. His method may therefore be mentioned appropriately at this point. Thomas assumes (1) that in the six-dimensional space for the motion of an electron the electrons are distributed uniformly at the rate of two for each h^3 of six-dimensional volume; (2) that the potential V in each atom is a function of the distance r from the nucleus and is determined by the nuclear charge and by the distribution of electrons. The constants in his equation are determined by the atomic number N. Thomas has calculated the atomic F curve for cesium ($N = 55$). His calculated results are given in Table I. Like the Compton "empirical atom," the Thomas atom can hardly represent the actual facts at any great distance from the nucleus so that it gives us no picture of the probable location of the outmost electrons of an atom. This defect is not troublesome, however,

for the energy of the x-rays scattered by the outmost electrons largely cancels out by interference. These electrons, therefore, really contribute very little to the atomic F curve.* Evidently the higher the atomic number, the better the Thomas atom approximates the facts in the immediate neighborhood of the nucleus. Agreement with experiment is sufficiently close for atoms of atomic number greater than 25 and is fairly good for the lighter atoms.

From Thomas' standard F curve for Cs given in Table I it is possible to calculate F curves for other atoms, since† tables similar to Table I may be made for any atom of atomic number N by using

$$\left(\frac{\sin\theta}{\lambda}\right)_N = \left(\frac{\sin\theta}{\lambda}\right)_{Cs}\left(\frac{N}{55}\right)^{1/3}$$

and

$$F_N = F_{Cs}\left(\frac{N}{55}\right)$$

The Thomas F curve for iron ($N = 24$) is compared with the experimental curve of Claassen[4] in Table II.

TABLE II.—COMPARISON OF THOMAS' F CURVE FOR IRON WITH RESULTS OF EXPERIMENTS

$\frac{\sin\theta}{\lambda} \times 10^{-8}$	0.0	0.1	0.2	0.3	0.4	0.5	0.6	0.7	0.8	0.9	1.0
Experimental (Claassen).....	..	22.6	17.0	14.0	12.0	10.7	9.4	8.2	6.9	...	...
Calculated (Thomas).....	24	23.1	19.1	15.7	13.4	11.7	10.1	8.8	7.8	7.1	6.3

2. The Method of Trial and Error.—We may write Eq. (4) in the form

$$F = Z\int_{-\frac{d}{2}}^{\frac{d}{2}} p(z)\cos\left(4\pi\frac{z}{\lambda}\sin\theta\right)dz \qquad (4)$$

where $d/2$ is half the interplanar spacing. $d/2$ is the largest possible

* It is this fact that makes it practically impossible to be sure of the difference between the F curves for atoms and the F curves for the corresponding ions.

† Let r_0 be the distance measured from the nucleus of the Cs atom, Z_0' the total charge of both nucleus and extranuclear electrons within a sphere of radius r_0, and ψ_0 the potential at the distance r_0 from the nucleus. Then Thomas' equations show that the corresponding quantities, r, Z', ψ, for an atom of atomic number N are:

$$r = r_0\left(\frac{55}{N}\right)^{1/3}$$

$$Z' = Z_0'\left(\frac{N}{55}\right)$$

$$\psi = \psi_0\left(\frac{N}{55}\right)^{4/3}$$

$$\frac{\text{Electron density at } r}{\text{Electron density at } r_0} = \left(\frac{N}{55}\right)^{4/3}$$

value of a of Eq. (4) which would have any meaning if we are to retain our current picture of an impenetrable atom. There is nothing to prevent us from using some other limits of integration such as $-r$ and r as long as r does not exceed $d/2$.

Let us assume that, for the atoms of any given chemical element, the electrons are arranged at random on the surfaces of spherical shells of radii $r_1, r_2, r_3, \ldots, r_p$; and let the number of electrons on the various shells be $m_1, m_2, m_3, \ldots, m_p$. Then, in any plane of atoms in a crystal, the common center of these spherical shells will be on the mid-plane of the atomic layer (X_1X_2 of Fig. 1a). If we consider a sufficiently large number of atoms, the average effect for any one shell will be the same as though the m_s electrons were uniformly distributed over the surface of that shell. We shall continue to represent by $p(z)$ the probability that a given electron in the shell will be found at a distance z from the mid-plane of the atomic layer. If the shell contains m_s electrons, the probability that *some* electron will be found at a distance z is $m_s p(z)$. For a given value of z this probability is a definite quantity so that $p(z)$ becomes a constant $= c$, and $m_s p(z) = m_s c$. Since we have assumed that we have 100 per cent probability that the electron is between the limits $[-r < z < r]$, it follows that

$$\int_{-r}^{r} c\,dz = 1$$

i.e., that

$$c = \frac{1}{2r} \text{ and } m_s p(z) = m_s \frac{1}{2r}$$

Equation (4) therefore becomes, for any one shell of electrons,

$$\begin{aligned} F &= m_s \int_{-r_s}^{r_s} \frac{1}{2r} \cos\left(4\pi \frac{z}{\lambda} \sin\theta\right) dz \\ &= m_s \int_{-r_s}^{r_s} \frac{\cos\left(4\pi \frac{z}{\lambda} \sin\theta\right)}{\frac{8\pi r_s}{\lambda} \sin\theta} d\left(4\pi \frac{z}{\lambda} \sin\theta\right) \\ &= m_s \left[\frac{\sin\left(4\pi \frac{z}{\lambda} \sin\theta\right)}{\frac{8\pi r_s}{\lambda} \sin\theta}\right]_{-r_s}^{r_s} \\ &= m_s \left[\frac{\sin\left(4\pi \frac{r_s}{\lambda} \sin\theta\right)}{4\pi \frac{r_s}{\lambda} \sin\theta}\right] \end{aligned}$$

For the whole atom, therefore, we have

$$F = \sum_{1}^{p} m_s \frac{\sin\left(4\pi\frac{r_s}{\lambda}\sin\theta\right)}{4\pi\frac{r_s}{\lambda}\sin\theta} \tag{35}$$

The accepted values of m for successive shells (as of 1926) are given for about half of the chemical elements in Vol. I, page 49, of the "International Critical Tables." Corresponding values for the rest of the elements may be guessed in terms of those given in the table. We may therefore start with some substance whose structure is well known by other methods, assume values of m_s in the light of the "International

TABLE III.—*F* CURVES FOR THE THOMAS AND HARTREE MODELS OF ATOMS

$\frac{\sin\theta}{\lambda} \times 10^{-8}$		0.0	0.1	0.2	0.3	0.4	0.5	0.6	0.7	0.8	0.9	1.0	1.1	1.2	1.3
K, $N = 19$	Hartree	19	16.3	13.4	10.7	8.9	7.7	7.1	6.4	5.9	5.3	4.8	4.3	3.7	3.3
	Thomas	19	16.5	13.3	10.8	9.2	7.9	6.7	5.9	5.2	4.7	4.2	3.7	3.3	...
Cl, $N = 17$	Hartree	18	15.2	11.5	9.3	8.1	7.2	6.5	5.8	5.1	4.4	3.8	3.3	2.9	...
	Thomas	17	14.6	11.6	9.5	8.1	6.9	5.8	5.1	4.5	4.0	3.5	3.1	3.0	...
Al, $N = 13$	Hartree	10	9.6	8.6	7.5	6.4	5.2	4.1	3.3	2.7	2.3	1.9	1.7	1.5	1.4
	Thomas	13	11.0	8.5	7.0	5.8	4.9	4.2	3.6	3.2	2.8	2.5	2.2	2.0	1.8
Na, $N = 11$	Hartree	10	9.5	8.2	6.7	5.2	4.1	3.2	2.6	2.2	2.0	1.8	1.6	1.5	...
	Thomas	11	9.2	7.1	5.6	4.7	3.9	3.3	2.8	2.5	2.2	1.9	1.7	...	...

Critical Tables," and then find by trial the values of r_s which best fit the x-ray data. We may then hope to use these values of m_s and r_s for these atoms (or ions) in the crystals of other substances. A much more elegant method has been proposed by D. R. Hartree.[5] He calculates by the methods of wave mechanics the probable structures of the atoms (or ions) of which the crystal is composed. This leads directly to the data needed for calculating atomic (or ionic) *F* curves. The basis of Hartree's calculations lies considerably beyond the scope of this book. For details the reader must be referred first to texts on wave mechanics and then to Hartree's original articles. It will be sufficient to state that atomic *F* curves based on Hartree's models agree quite satisfactorily (within 5 per cent) with experimental curves if we take into account extinction, zero-point energy, and thermal agitation. Atomic *F* curves

for potassium, chlorine, aluminum, and sodium are given in Table III for both the Thomas and Hartree models. Even for these light atoms the agreement is probably well within the errors introduced by extinction and thermal agitation. It is perhaps not too much to say that any atomic model which gives a high electron density near the center will give a more or less usable atomic F curve.

3. The Method of Fourier's Series.—This method was first used by W. H. Bragg[6] and was later refined and improved by William Duane[7] and A. H. Compton.[8] It has been used in its final form by many investigators of whom the first was R. J. Havighurst.[9] The method may be visualized by reviewing the analogous case in optics known as the Abbe diffraction theory of microscopic vision.[10] Light from an illuminated object may be regarded as being the resultant of all the diffraction patterns of all orders which the object can produce and which are permitted by the conditions of the illumination. In order that a lens may give a truthful picture of an illuminated object, the aperture of the lens must be wide enough to transmit the whole of the diffraction pattern. If the aperture is decreased so that only a portion of the diffraction pattern is transmitted, the image will differ from the true image. It will look like some fictitious object which could give off only those diffracted beams which actually pass the lens. If the structure of the object is too fine, or if the aperture of the lens is too narrow, none of the diffraction pattern will be transmitted and no structure can be seen no matter how great the magnification may be.

The following may serve to make this clear. It deals with experiments by A. B. Porter[11] which were originally intended for demonstrating that the images of periodic structures as seen by the naked eye are really due to diffracted light. Porter concentrated light from an arc lamp on a pinhole in an opaque screen. Some distance from this pinhole was a wire gauze having about 30 wires to the centimeter, set so that its wires were horizontal and vertical. Immediately next to the gauze was a lens which focused the light on a cardboard screen about 30 cm. distant. The light therefore traveled from the pinhole through the gauze and through the lens to the cardboard screen. A diffraction pattern was found on the cardboard screen. It consisted of a central image and eight groups of spectra (each group containing all the orders of spectra) extending radially from the central image. Two of these groups lay in a horizontal line, two in a vertical line, two formed a straight line at 45° to the horizontal and the remaining two formed a straight line at right angles to the third pair. These last two pairs are considered to be spectra of spectra and are found whenever a light source is observed through a pair of crossed gratings. Porter then cut small holes in the cardboard screen. Each of these let through to his eye some small portion of the diffraction pattern. The effect observed depended upon

the size of the hole. If the hole was only large enough to let through the central image, then he could not see the image of the wire gauze. If the hole was in the form of a long narrow slit so placed as to let through the central image and the horizontal pair of groups of spectra, then he could see only the vertical wires of the gauze. If this slit was turned so as to let through only the central image and the vertical pair of groups of spectra, then he could see only the horizontal wires of the gauze. If he turned the slit through 45° so as to let through the central image and one of the pairs of diagonal groups of spectra, then he saw no vertical or horizontal wires but, instead, a fictitious set of diagonal wires which ran perpendicular to the length of the slit. If these fictitious wires had been real they would have produced primary spectra exactly like the "spectra of spectra" which were actually present.

We have a similar situation in the examination of a crystal by means of the diffraction of x-rays. The x-rays are scattered by the unit-crystal with different efficiency in different directions, and all the information which we can gain as to the structure of the unit-crystal is contained in these scattered x-rays. Instead of recording on the retina of the eye (or on the photographic plate of a camera) the image formed by the recombination of the light waves, we must measure the intensity of the x-rays which are scattered in certain directions permitted by the crystal lattice and then interpret our data as best we can by computation. In visual observation the phases of the waves scattered in various directions play an important part in the formation of the final image. In crystal analysis we cannot use these phase differences experimentally, for we have nothing in x-ray work which corresponds to the lens of our eye or of a camera; we can only make independent measurements of the intensities of the scattered waves in the directions in which the crystal diffracts them.* This is the real reason why we cannot, in general, build up by calculation a true image of the unit-crystal analogous to the image of a small body seen under a microscope. Instead of giving us a true image our calculations tend to give us a picture of the atom which may be as badly distorted as some of those in Porter's experiments. Porter's experiments could not tell us whether the wire gauze had (*a*) wires running vertically and horizontally, (*b*) wires running diagonally, or (*c*) some wires running vertically, some horizontally, and some diagonally. But in any case, the points of intersection of the wires could be located definitely. In a crystal there are no stretched wires, but the mean positions of the atoms correspond to the intersections of wires in Porter's gauze. It is reasonable to assume, therefore, that even though our

* In the case of the simplest crystals having high symmetry, this difficulty can be avoided by making certain assumptions. In the case of the more complicated crystals still other assumptions must be made which, in the long run, amount to making the method of Fourier analysis into a type of trial-and-error method.

pictures of the electron configurations in the atoms in a given crystal may be considerably distorted, the uncertainty of our calculated image does not extend to the average location of the atoms in the crystal.

The method of the Fourier's series offers a convenient means of making the necessary calculations. Any Fourier analysis rests upon the fact that a portion of a graph, taken between finite limits, can be expressed approximately as the sum of a series of sine or cosine curves such as

$$A_0 + A_1 \cos \alpha + A_2 \cos 2\alpha + A_3 \cos 3\alpha + \cdots$$

The degree of approximation depends only upon the number of terms taken in the series. Since every atomic F curve is bounded at each end by finite limits which are set by the nature of the experiments, it follows that an atomic F curve can be represented by a Fourier's series such as the one given above. Our study of the use of the Fourier's series in interpreting F curves will, therefore, consist in evaluating the constants A and α and in interpreting the terms of the series into the language of atomic structure and into pictures analogous to those of Porter's experiments.

The discussion at the beginning of this chapter, based on Fig. 1, assumed a simple cubic crystal. This assumption will be continued in the following discussion.*

We shall write Eq. (4) in the form

$$F = Z \int_{-\frac{a}{2}}^{\frac{a}{2}} p(z) \cos \left(4\pi \frac{z}{\lambda} \sin \theta \right) dz \tag{36}$$

where $a/2$ is half the interplanar spacing under consideration,† and

* This discussion may be made to apply to any cubic crystal as follows. We learned in Chap. VIII that a space-group consists of an array of point-groups hung on a space-lattice. This point of view may be extended by considering all cubic crystals to be based on a simple cubic lattice. Then a body-centered cube might be thought of as having pairs of points associated with each point of the simple cubic lattice; a face-centered cube might be thought of as having a group of four points associated with each point of a simple cubic lattice; etc. Other possible changes will be obvious which will make the discussions of this chapter apply to still other crystal systems.

† The use of the limits $-a/2$ and $a/2$ assumes that each atom is a separate entity and that there is no interpenetration between adjacent atoms. This assumption really makes the method of the Fourier series a sort of trial-and-error method or even a sort of empirical method. It is the necessity for this type of assumption that keeps the method of the Fourier series from being a perfectly general and direct method of crystal analysis by which the structure of a crystal might be determined by purely x-ray data.

It hardly needs to be pointed out that the assumption of non-interpenetrating atoms is consistent with all of our fundamental ideas of physics and chemistry; in fact modern chemistry and physical chemistry would be meaningless without it.

where Z now represents the total number of electrons in the whole group of atoms associated with a single lattice point. Bragg's law tells us that*

$$\frac{\sin\theta}{\lambda} = \frac{n'}{2a}$$

so that, in Eq. (36), $4\pi\frac{z}{\lambda}\sin\theta$ becomes $2\pi n'\frac{z}{a}$. Then the structure factor corresponding to the n'th order of diffraction may be written

$$F_{n'} = Z\int_{-\frac{a}{2}}^{\frac{a}{2}} p(z)\cos\left(2\pi n'\frac{z}{a}\right)dz \tag{37}$$

In this equation $Zp(z)$ represents the number of electrons per unit height. It is this quantity which we must express, to the necessary degree of approximation, by a Fourier cosine series.

$$Zp(z) = A_0 + A_1\cos 2\pi\frac{z}{a} + A_2\cos 4\pi\frac{z}{a} + \cdots + A_n\cos 2\pi n'\frac{z}{a} + \cdots \tag{38}$$

This may be written

$$Zp(z) = A_0 + \sum_1^\infty{}_r A_r\cos\left(2\pi r\frac{z}{a}\right) = \sum_0^\infty{}_r A_r\cos\left(2\pi r\frac{z}{a}\right) \tag{39}$$

Substituting Eq. (39) into (37), we have

$$F_{n'} = \int_{-\frac{a}{2}}^{\frac{a}{2}}\sum_0^\infty{}_r A_r\cos\left(2\pi r\frac{z}{a}\right)\left(\cos 2\pi n'\frac{z}{a}\right)dz$$

In the general case,† integration between the limits $-a/2$ and $a/2$ yields a series of terms each of which is zero. In the special case in which $r = n'$, we have

* In the following discussion n' will be used to represent the order of diffraction. The n of Eq. (6) represents the number of atoms per cubic centimeter.

† This integral corresponds to the standard form,

$$\int\cos mx\cos nx dx = \frac{\sin(m-n)x}{2(m-n)} + \frac{\sin(m+n)x}{2(m+n)}$$

When $m = n$, this form of the integral breaks down. For this limiting form,

$$\int\cos^2 mx dx = \frac{1}{m}\left\{\frac{1}{2}mx + \frac{1}{4}\sin 2mx\right\}$$

$$F_{n'} = \int_{-\frac{a}{2}}^{\frac{a}{2}} A_n \cos^2\left(2\pi n'\frac{z}{a}\right)dz$$

$$F_{n'} = \left[A_{n'}\frac{a}{2\pi n'}\left(\pi n'\frac{z}{a} + \frac{1}{4}\sin 4\pi n'\frac{z}{a}\right)\right]_{-\frac{a}{2}}^{\frac{a}{2}}$$

$$F_{n'} = \tfrac{1}{2}aA_{n'}$$

$$A_{n'} = \frac{2}{a}F_{n'} \qquad (40)$$

Equation (40) enables us to use the experimental values of the atomic F curves direc y in Eq. (38). This gives us the "density distribution"

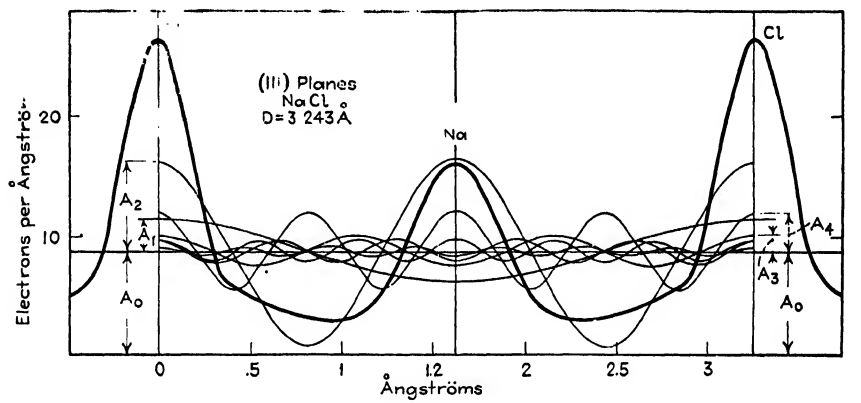

FIG. 5.—Graphical summation corresponding to Eq. (41).

of electrons, $Zp(z)$, by means of a series, each term of which has the form

$$\frac{2}{a}F_{n'}\cos 2\pi n'\frac{z}{a}$$

These terms may be plotted as cosine curves with A_0 as the base line of the ordinates $Zp(z)$. The sum of all these cosine curves may be found graphically and corresponds to

$$Zp(z) = A_0 + \frac{2}{a}\sum_{1}^{\infty} F_{n'}\cos 2\pi n'\frac{z}{a} \qquad (41)$$

This is illustrated in Fig. 5 which represents the data for F_1, F_2, F_3, etc., as given by Bragg, James, and Bosanquet[1] for the (1 1 1) planes of NaCl

($a = 3.243$Å.).* The value of the ordinate A_0 may be found as follows:

$p(z)\,dz$ is the probability that some one electron will be at a height between z and $z + dz$ above the mid-plane of the layer of the atoms under consideration in the crystal.† Then $\int_{-\frac{a}{2}}^{\frac{a}{2}} p(z)\,dz$ expresses the probability that the electron is between $a/2$ and $-a/2$, *i.e.*, that the electron is in the atom at all. Since, however, we have made the fundamental assumption that each atom is a separate entity and that adjacent atoms do not interpenetrate, it follows that this probability must be unity, *i.e.*,

$$\int_{-\frac{a}{2}}^{\frac{a}{2}} p(z)\,dz = 1 \tag{42}$$

Substituting $p(z)$ from Eq. (39) into (42) we have

$$1 = \int_{-\frac{a}{2}}^{\frac{a}{2}} p(z)\,dz = \frac{A_0}{Z}a + \frac{1}{Z}\sum_1^\infty{}_r \int_{-\frac{a}{2}}^{\frac{a}{2}} A_r \cos 2\pi r\frac{z}{a}dz$$

$$1 = \frac{A_0 a}{Z} + 0$$

$$A_0 = \frac{Z}{a} \tag{43}$$

Equation (41) therefore becomes

$$P_z = Z\,p(z) = \frac{Z}{a} + \frac{2}{a}\sum_1^\infty F_{n'} \cos 2\pi n'\frac{z}{a} \tag{44}$$

If we grant the fundamental assumption made in connection with Eqs. (36) and (42), then Eq. (44) gives the number of electrons in a unit-cube between the heights z and $z + dz$ above the mid-plane of the layer of atoms under consideration.

This assumption can hardly be avoided, for without it we should have had an infinite number of solutions of the Fourier series. It is forced upon us by our inability to determine the phase relationships between the scattered x-ray beams. In our ignorance of these phase relationships our fundamental assumption seems to be the only way in which we can tie down the Fourier series so as to obtain a single, definite solution. If it had not been for the necessity of making this assumption, we might have hoped to find not only the structure of the crystal but also the

* The exact form of the resultant curve will depend upon the number of terms used in the Fourier series. The larger the number of terms, the more nearly the resultant curve will approximate the real distribution of electrons. Corresponding experiments may be made with Porter's apparatus for the diffraction of visible light.

† See discussion leading to Eq. (2).

structure of the individual atoms in the crystal. The necessity for making this assumption definitely closes the door to such a hope except under certain advantageous conditions which will be taken up in Chap. XVI. The results of our fundamental assumption appear in Fig. 5, which necessarily shows the electrons clustered in groups. Small groups, identified by low peaks, represent atoms (or ions) of low atomic (or ionic) number; larger groups of electrons, identified by higher peaks, represent atoms (or ions) of higher atomic (or ionic) number. Thus, in Fig. 5, the low peak of the resultant curve represents the Na^+ of NaCl; the high peaks represent the Cl^-. The ordinates are very closely in the ratio of 10:18, but the nature of the data and the limited number of terms used in the Fourier series make it impossible to distinguish with any certainty between atoms and ions by methods such as we have described. Further discussion of this point must be postponed until we reach Chaps. XIII and XIX. The equivalent of Eq. (44) has also been obtained by Duane[1] and Havighurst[1] from the standpoint of the quantum theory of diffraction. The fundamental assumption made in this chapter is also found in their derivation, but it is stated in a somewhat different form.

For further discussion of the method of Fourier series, the reader is referred to two articles by A. L. Patterson[12] in *Zeitschrift für Krystallographie* (1930).

SUMMARY

We have considered the x-ray wavelets diffracted by the individual electrons in the atoms of a crystal and have studied the phase differences between these wavelets caused by the space configurations of these electrons. We have found that these phase differences cause a decrease in the intensity of the diffracted beam which can be expressed in terms of a quantity called the "structure factor." We have taken account of the variables which affect the intensity of the beam and have seen how the structure factor can be used as a powerful tool in determining the structure of crystals. It remains to clarify these ideas in terms of actual examples. This will be done in the following chapter.

References

1. The first part of this chapter is based on the following:
P. Debye, *Ann. Physik*, **43**, 49 (1913).
C. G. Darwin, *Phil. Mag.*, **27**, 315, 675 (1914); **43**, 800 (1922).
W. H. Bragg, *Phil. Trans. Roy. Soc. London*, **215**, 253 (1915).
A. H. Compton, *Phys. Rev.*, **9**, 29; **10**, 95 (1917).
W. L. Bragg, R. W. James, and C. H. Bosanquet, *Phil. Mag.*, **41**, 309; **42**, 1 (1921); **44**, 433 (1922).
Wm. Duane, *Proc. Nat. Acad. Sci.*, **11**, 489 (1925).
R. J. Havighurst, *Proc. Nat. Acad. Sci.*, **11**, 502, 506 (1925); *Phys. Rev.*, **29**, 1 (1927).
W. L. Bragg, C. G. Darwin, and R. W. James, *Phil. Mag.*, **1**, 897 (1926).

J. M. Bijvoet, *Chem. Weekblad*, **24**, 574 (1929).
G. E. M. Jauncey and W. D. Claus, *Phys. Rev.*, **31**, 717; **32**, 12 (1928).
G. E. M. Jauncey, *Chem. Rev.*, **5**, 437 (1928).
W. L. Bragg and J. West, *Zeit. Kryst.*, **69**, 118 (1928).
W. L. Bragg, *Inst. intern. physique Solvay*, V^me conseil, 1927, 1 (1928)
A. L. Patterson, *Zeit. Kryst.*, **76**, 177, 187 (1930).
See also A. H. Compton, "X-rays and Electrons," D. Van Nostrand Company, New York, 1926.

2. W. H. Bragg, *Phil. Mag.*, **27**, 881 (1914).
3. L. H. Thomas, *Proc. Cambridge Phil. Soc.*, **23**, 5, 542 (1927).
4. A. Claassen, *Proc. Phys. Soc. London*, **38**, 5, 482 (1926).
5. D. R. Hartree, *Proc. Cambridge Phil. Soc.*, **24**, 89, 111 (1928); *Proc. Roy. Soc.*, **A, 118**, 334 (1928).
6. W. H. Bragg, *Phil. Trans. Roy. Soc. London*, **A, 215**, 253 (1915).
7. Wm. Duane, *Proc. Nat. Acad. Sci.*, **11**, 489 (1925).
8. A. H. Compton, "X-rays and Electrons," pp. 151–161, D. Van Nostrand Company, New York, 1926.
9. R. J. Havighurst, *Proc. Nat. Acad. Sci.*, **11**, 502 (1925).
10. See any standard text on physical optics such as R. W. Wood, "Physical Optics," The Macmillan Company, New York, 1911.
11. Porter's experiments are referred to in R. W. Wood, "Physical Optics," p. 224, The Macmillan Company, New York, 1911. Some of the theory is discussed in A. B. Porter, *Phys. Rev.*, **20**, 386 (1905); *Phil. Mag.*, **11**, 154 (1906).
12. A. L. Patterson, *Zeit. Kryst.*, **76**, 177, 187 (1930).

CHAPTER XI

APPLICATIONS OF THE STRUCTURE-FACTOR METHOD

We have studied in the previous chapter how the structure of a crystal may be solved in terms of a quantity called the "structure factor." So powerful is this method of crystal analysis that W. L. Bragg has stated that, once given a crystal of sufficient size so that its exterior symmetry can be determined, the structure of that crystal can be unraveled completely no matter how complex it may be. It is not often given to one man to have played so important a part both in the early stages of a subject and in its final reduction to a routine tool of research. Not only does the fundamental law of x-ray diffraction by a crystal bear his name, but the foundations and a large part of the finished form of the structure-factor method are due to him and his associates. It is not inappropriate, then, that the illustrations which we shall take up of the application of this method to crystal analysis come from his laboratory.

THE STRUCTURE OF DIOPSIDE, $CaMg(SiO_3)_2$

Experimental Data.—The structure of diopside, $CaMg(SiO_3)_2$, has been worked out by Warren and Bragg[1] by means of the trial-and-error scheme mentioned in Chap. X. This material has been shown by Wyckoff and Merwin[2] to belong to the monoclinic space-group C_{2h}^6 with four molecules per unit-crystal. The axial angle is 74° 10′ and the axial lengths* are $a = 9.71$Å., $b = 8.89$Å., and $c = 5.24$Å. The location of the axes of symmetry and the points of inversion for C_{2h}^6 are shown in Fig. 1. There are four independent sets of symmetry centers, and each set is represented four times in the unit-crystal. The (0 0 1) face, in terms of Warren and Bragg's axes, is centered. The symmetry plane perpendicular to the b-axis is a glide-plane with a translation $c/2$. The 2-fold axes of symmetry are labeled C in Fig. 1.

The fundamental experimental data consist of values of the apparent "integrated reflection" ρ' which can be translated into values of the true integrated reflection ρ. These values of ρ can be translated, in turn,

* Warren and Bragg have followed the ordinary usage of crystallography in naming the three axes a, b, and c of Fig. 1. In terms of the terminology of Chaps. II and VIII and of Wyckoff ("Analytical Expression of the Results of the Theory of Space-groups"), a and c are in the directions of the X- and Y-axes; b is in the direction of the Z-axis. It should be remembered that a plane which would be called (5 6 2) on the basis of Warren and Bragg's coordinates would be the (5 2 6) plane on the basis of Wyckoff's coordinates. For convenience of reference to Warren and Bragg's article, their axes will be used in this discussion.

into values of the structure factor F_{hkl}. It is with the various values of F_{hkl} that the structure-factor method of crystal analysis must deal, so that we must build up from ρ' to ρ and then from ρ to F_{hkl}.

Values of ρ' were determined by Warren and Bragg for several hundred sets of indices $(h\,k\,l)$. In the case of the a, b, and c faces of the crystal, direct measurements of ρ' were calibrated to give the true integrated reflection ρ in terms of the integrated reflection from the (4 0 0) planes of a standard crystal of NaCl for which ρ was 1.09×10^{-6}. Rhodium

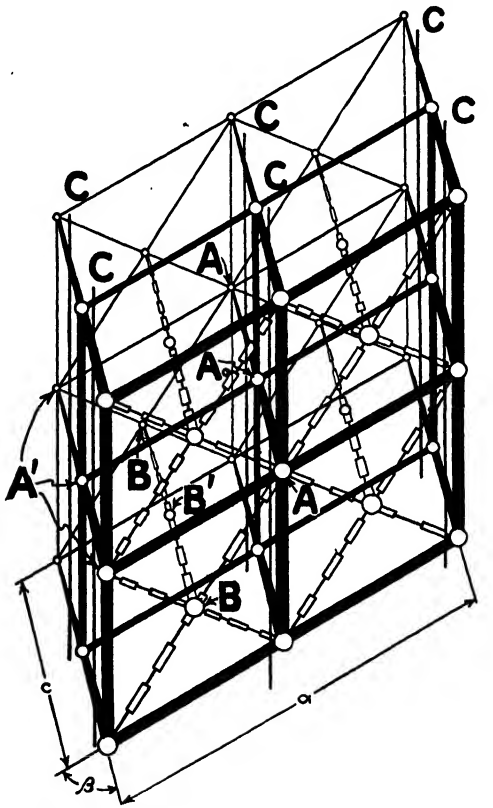

FIG. 1.—The axes of symmetry and the points of inversion of space-group C_{2h}^{6}.

K_α radiation ($\lambda = 0.614$Å.) was used. Values of ρ were found for other indices as follows: Sections of diopside were cut perpendicular to the a-, b-, and c-axes, with thicknesses 0.064, 0.107, and 0.210 cm., respectively. The face of each of these thin sections was therefore perpendicular to an important zone axis. Each cut face was used in setting up the crystal to measure the intensities of the diffracted beams for the various planes passing through that zone axis. This may be illustrated in terms of the section cut perpendicular to the b-axis. The section of crystal was mounted so that the cut face was vertical, *i.e.*, so that

the b-axis was horizontal. It was rotated about the b-axis until some plane $(h0l)$, normal to the cut face, also became vertical. Then, by setting the crystal section and the ionization chamber at the proper angles, measurements were taken rapidly of the intensities of the diffracted beams of various orders. The crystal section was then rotated again about the b-axis until some other plane $(h0l)$, normal to the cut face, became vertical, and again measurements were made of the intensities of the diffracted beams. This procedure was repeated for other planes $(h0l)$ until all had been used. These measurements of intensity were not related in any simple way to the apparent integrated reflection ρ', but at least the factors which connected these two types of values varied in a continuous way with the glancing angle. The intensity measurements were therefore translated into measurements of ρ' in terms of a calibration from the $(h00)$ and $(00l)$ planes whose ρ' had been measured directly at the beginning of the investigation.

Before the structure factor F for each of these planes can be calculated, ρ' must be changed into the corresponding true integrated reflection ρ. It was pointed out in Chap. X [Eq. (31)] that ρ can be expressed in terms of the experimental value ρ by an equation of the form

$$\rho = \frac{\rho'}{1 - 2g\rho'}$$

For these experiments, $g = 1.06 \times 10^4$.* It should be remembered that the resulting values of ρ are only approximate and will lead to approximate values of F_{hkl}. Fortunately, the values of F_{hkl} are very sensitive to slight changes in atomic coordinates so that approximate measurements of F_{hkl} (accuracy of the order of 20 per cent) lead to a rather high degree of accuracy in the determination of atomic coordinates.

Warren and Bragg calculated the values of F_{hkl} from the experimental data of ρ' by a combination of Eqs. (15a), (27), and (31) of Chap. X. These three equations give†

$$\rho = \frac{\rho'}{1 - 2g\rho'} = \frac{Q}{2\mu} = \frac{\frac{1}{2}n^2\lambda^3F^2\frac{e^4}{m^2c^4} \cdot \frac{1 + \cos^2 2\theta}{\sin 2\theta}}{2\mu} \tag{1}$$

* This value of g was estimated by Warren and Bragg from a preliminary analysis of diffractions around the [0 1 0] zone of the crystal. They found it possible to determine, to a high degree of approximation, the positions of the atoms when projected on the (0 1 0) plane, without taking extinction into account. In those cases where ρ' was large, values of F_{hkl} were calculated for this structure and were compared with those calculated directly from the experimentally determined values of ρ'. The two sets of values for F_{hkl} were made to agree by picking a suitable value for g.

† Equation (15) of Chap. X was based on a *simple* unit of structure, *i.e.*, one atom per unit-crystal. For a more complicated structure such as diopside the structure factor F must be expressed in terms of all the atoms per unit-crystal.

in which n = number of unit-crystals per cubic centimeter
= the reciprocal of the volume of the unit-crystal
= $1/435 \times 10^{24}$
$\lambda = 0.614 \times 10^{-8}$ cm. (K_α of rhodium)
$e = 4.774 \times 10^{-10}$ abs. e.s.u.
$m = 8.994 \times 10^{-28}$ g.
$c = 3 \times 10^{10}$ cm. per second.
$\mu = 12.8$ cm^{-1} for K_α of rhodium (by direct measurement).

Using these values, Eq. (1) can be condensed to the form

$$\rho = \frac{\rho'}{1 - 2g\rho'} = 0.189F^2\frac{1 + \cos^2 2\theta}{\sin 2\theta} \cdot 10^{-8} \qquad (2)$$

Warren and Bragg found that the cut specimens mentioned above gave diffracted beams as follows:

Indices $(0kl)$, ... k even.
Indices $(h0l)$, ... h and l both even.
Indices $(hk0)$, ... $h + k$ even.

This is consistent with Wyckoff and Merwin's data which placed diopside in the holohedral monoclinic space-group C_{2h}^6. Values of ρ' and of $\pm F_{hkl}$

TABLE I.—VALUES OF F_{h00}, F_{0k0}, and F_{00l}, CALCULATED FROM ρ' BY MEANS OF EQ. (2)

sin θ	Indices	$\rho' \times 10^6$	$\pm F$ calculated from ρ'	F calculated from structure
0.0658	(200)	....	.....	− 11
0.0691	(020)	9.0	19	+ 26
0.1219	(002)	60. ?	>140*	−175
0.1316	(400)	3.0	15	+ 16
0.1382	(040)	....	.....	− 7
0.1974	(600)	31.0	100	+114
0.2073	(060)	28.0	94	− 91
0.2438	(004)	34.0	136	+107
0.2632	(800)	21.0	76	+ 69
0.2764	(080)	....	.....	− 23
0.3290	(1000)	11.5	56	+ 56
0.3455	(0100)	12.5	65	+ 66
0.3657	(006)	3.4	29	− 48
0.3948	(1200)	....	.....	− 5
0.4146	(0120)	3.0	29	+ 36
0.4606	(1400)	8.0	58	+ 56
0.4876	(008)	3.7	38	+ 47
0.5264	(1600)	....	.....	+ 5
0.5922	(1800)	1.0	22	+ 21

* Value uncertain because of high extinction.

calculated from them by Eq. (2) for the a, b, and c faces and for the $(0kl)$, $(h0l)$, and $(hk0)$ planes are given in Tables I, II, III, and IV. These tables also give, for purposes of reference, the corresponding values of F_{hkl} calculated by Warren and Bragg from their final structure for diopside.

Table V shows empirical atomic F values for Mg, Ca, O, and Si, for various values of sin θ. These values were arrived at from work

TABLE II.—VALUES OF F_{0kl} CALCULATED FROM ρ' BY MEANS OF EQ. (2)

sin θ	Indices	$\rho' \times 10^6$	$\pm F$ calculated from ρ'	F calculated from structure
0.0922	(021)	21.4	44	−42
0.1400	(022)	28.4	75	+59
0.1513	(041)	29.6	82	−96
0.1844	(042)	24.0	72	+56
0.1942	(023)	Weak	Small	−10
0.2189	(061)	14.0	50	+52
0.2292	(043)	13.1	50	+51
0.2406	(062)	25.0	88	+87
0.2534	(024)	Weak	Small	+11
0.2766	(063)	9.3	44	−35
0.2800	(044)	....	.....	− 9
0.2832	(081)	3.5	25	+30
0.3022	(082)	3.9	28	+30
0.3123	(025)	....	.....	+10
0.3200	(064)	....	.....	−17
0.3316	(083)	....	.....	−10
0.3345	(045)	3.1	26	−36
0.3685	(065)	3.2	29	+24
0.3688	(084)	Weak	Small	−27
0.3714	(026)	....	.....	+ 2
0.4115	(085)	....	.....	+ 4
0.4200	(066)	Weak	Small	+21
0.4483	(047)	2.2	26	+30

on other silicates. The bottom line of the table gives the F value that all the atoms in a unit-crystal would have had if they had all diffracted the x-rays with the same phase. Comparison of these values with the actual values for the same sin θ in Tables I, II, III, and IV shows how markedly the resultant amplitude is cut down by interference.

Bird's-eye View of the Analysis.—We now have at hand the necessary fundamental data with which to make our analysis. In making this analysis we cannot impose any arbitrary limitations on the structure of our crystal except those set by its exterior symmetry, cleavage, etch

figures, etc. We must follow as general a scheme as possible. This means that, if possible, we should make our first attack on some one or more parameters which we can determine independently of the others by means of some sort of symmetry considerations. Once this has been done, the analysis of the remaining parameters will be found to have been much simplified.

TABLE III.—VALUES OF F_{h0l} CALCULATED FROM ρ' BY MEANS OF EQ. (2)

sin θ	Indices	$\rho' \times 10^6$	$\pm F$ calculated from ρ'	F calculated from structure
0.1212	(202)	19.1	46	+ 44
0.1529	(20$\bar{2}$)	31.0	88	− 85
0.1530	(402)	28.6	80	−117
0.2017	(602)	26.0	82	−105
0.2021	(40$\bar{2}$)	35.5	128	− 99
0.2344	(204)	Weak	Small	− 6
0.2424	(404)	21.9	77	+ 85
0.2579	(802)	5.7	32	− 30
0.2585	(60$\bar{2}$)	....	.....	0
0.2687	(604)	14.7	59	+ 96
0.2693	(20$\bar{4}$)	2.1	19	+ 22
0.3058	(40$\bar{4}$)	22.3	90	+ 84
0.3060	(804)	....	.....	− 6
0.3179	(1002)	8.1	44	− 69
0.3184	(80$\bar{2}$)	10.0	51	− 51
0.3524	(60$\bar{4}$)	Weak	Small	+ 21
0.3530	(206)	5.0	36	− 42
0.3532	(406)	13.3	49	− 48
0.3636	(606)	3.6	30	− 27
0.3790	(100$\bar{2}$)	12.0	63	− 75
0.3882	(20$\bar{6}$)	....	.....	− 4
0.4042	(80$\bar{4}$)	3.8	33	+ 31
0.4206	(40$\bar{6}$)	13.0	72	− 71
0.4587	(60$\bar{6}$)	....	.....	− 14
0.4688	(408)	Weak	Small	+ 22
0.4734	(208)	....	.....	+ 20

Figure 1 shows four symmetry centers A, A', B, B' and four 2-fold axes C. Wyckoff and Merwin found four "molecules" of $CaMgSi_2O_6$ per unit-crystal. This gives us four Ca and four Mg to place in each unit-crystal. We may therefore start our analysis of the structure by assuming that Ca and Mg lie at the symmetry centers A, A', B, and B', or that they are associated with the 2-fold axes C or are associated with A, A', B, B' and C. Of course. this assumption must be justified

later in terms of the end results of the analysis, but, if we once grant this assumption provisionally, the rest of our analysis of the structure falls naturally into four steps, namely, finding in projection on the *a-c* plane,

TABLE IV.—VALUES OF F_{hk0} CALCULATED FROM ρ' BY MEANS OF EQ. (2)

sin θ	Indices	$\rho' \times 10^6$	$\pm F$ calculated from ρ'	F calculated from structure
0.0477	(110)	....	.....	− 8
0.0954	(220)	22.8	48	− 64
0.1040	(310)	32.8	76	+ 80
0.1084	(130)	2.5	12	+ 16
0.1431	(330)	18.2	49	+ 81
0.1480	(420)	5.6	22	− 22
0.1525	(240)	2.7	16	+ 9
0.1675	(510)	21.8	61	− 65
0.1755	(150)	27.6	82	− 92
0.1908	(440)	14.8	48	− 48
0.1934	(530)	9.2	36	+ 49
0.1982	(350)	16.2	53	− 65
0.2080	(620)	2.6	18	− 19
0.2168	(260)	6.8	31	+ 44
0.2323	(710)	9.5	40	+ 44
0.2385	(550)	Weak	Small	+ 8
0.2438	(170)	....	.....	+ 1
0.2520	(730)	....	.....	+ 5
0.2608	(370)	Weak	Small	− 4
0.2862	(660)	Weak	Small	− 6
0.2867	(750)	23.8	92	−112
0.2920	(570)	7.4	40	+ 41

TABLE V.—ATOMIC F VALUES FOR Mg, Ca, O, AND Si
(Empirical results of Warren and Bragg[1]) $\lambda = 0.614$

sin θ	0.1	0.2	0.3	0.4	0.5	0.6
Magnesium	9.3	6.6	4.3	2.8	1.9	1.2
Calcium	15.1	10.6	7.7	5.9	4.5	3.6
Oxygen	6.6	3.3	1.8	0.9	0.5	0.3
Silicon	10.2	7.6	5.6	4.0	2.8	2.0
4(Ca + Mg + 2Si + 6O)	338	209	136	88	60	42

(*a*) possible locations for Si, (*b*) possible locations for Ca and Mg, (*c*) possible locations for O, and (*d*) finding in projection on the *a-b* plane the probable locations of Si, Ca, Mg, and O.

a. It is evident from Fig. 1 that planes which include the symmetry axes C and points corresponding to A, A', B, and B' must have Miller indices $(h\,0\,l)$ for which h and l are multiples of 4. This means that, if our assumption is is correct, all the Ca and Mg lie exactly on planes such as (4 0 0), (4 0 4), (0 0 4), (8 0 0), (8 0 4), (4 0 $\bar{4}$), (12 0 0), (4 0 8), (16 0 0),

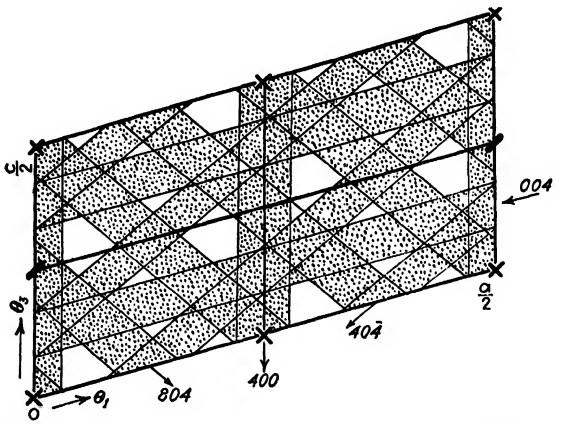

FIG. 2.—Projection on the (0 1 0) plane of some of the regions forbidden to Si. (Only one-fourth the base of the unit-crystal is shown.)

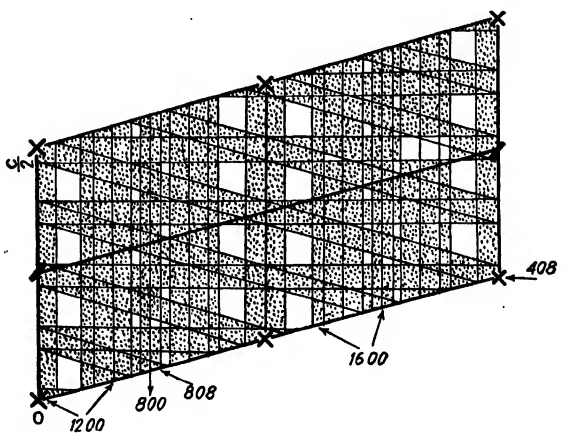

FIG. 3.—Projection on the (0 1 0) plane of other regions forbidden to Si. (Only one-fourth the base of the unit-crystal is shown.)

etc. With Ca and Mg fixed with reference to planes $(4n_1, 0, 4n_2)$, we can study the values of F for these planes as an aid in locating the eight Si and twenty-four O. If the base (a-c plane) is divided into four equal portions each of side $a/2$, $c/2$, the symmetry of the crystal requires that the projected atomic positions in each portion must be the same.*

* Planes of the form $(h\,0\,l)$ in the crystal above one of these quarter portions of the base are represented by lines on the base. Volumes between parallel $(h\,0\,l)$ planes are

Each observed value of F_{h0l}* must be explained by contributions from four Ca, four Mg, eight Si, and twenty-four O. Since the Ca and Mg atoms are assumed to lie exactly on the plane, we know their contributions to F_{h0l} from Table V. It is now possible to map out projected areas on the base (corresponding to volumes in the crystals) which cannot possibly be occupied by Si no matter where the O atoms are placed. For instance, if the observed value of F_{h0l} is very small, and if the Ca and Mg atoms by themselves outweigh any possible negative contribution which the O atoms could make (even though they all diffracted in phase), then it must follow that the Si atoms cannot make any positive contribution to F_{h0l}. We can represent this by marking off on the base a series of strips which represent regions forbidden to Si. (See Figs. 2 and 3, each of which represents only one-fourth of the (0 1 0) plane of the unit-crystal.) By considering in this way several planes in succession, we can limit the possible areas corresponding to Si atoms in one-fourth the crystal to the small regions marked 1, 2, 3, 4, 1′, 2′, 3′, 4′ of Fig. 4. This gives us on each quarter of the (0 1 0) plane eight unforbidden areas in which to put two Si atoms. We have eight Si atoms to place in each unit-crystal. The theory of space-groups (see Chap. VIII) permits C_{2h}^6 to have five sets of atomic coordinates for the special case of four equivalent points and one set for the general case of eight equivalent points.

(*a*)	$\frac{1}{4}00$;	$\frac{3}{4}00$;	$\frac{1}{4}\frac{1}{2}\frac{1}{2}$;	$\frac{3}{4}\frac{1}{2}\frac{1}{2}$
(*b*)	$\frac{1}{4}0\frac{1}{2}$;	$\frac{3}{4}0\frac{1}{2}$;	$\frac{1}{4}\frac{1}{2}0$;	$\frac{3}{4}\frac{1}{2}0$
(*c*)	$\frac{1}{4}\frac{1}{4}\frac{1}{4}$;	$\frac{3}{4}\frac{3}{4}\frac{1}{4}$;	$\frac{3}{4}\frac{1}{4}\frac{3}{4}$;	$\frac{1}{4}\frac{3}{4}\frac{3}{4}$
(*d*)	$\frac{3}{4}\frac{3}{4}\frac{3}{4}$;	$\frac{1}{4}\frac{1}{4}\frac{3}{4}$;	$\frac{1}{4}\frac{3}{4}\frac{1}{4}$;	$\frac{3}{4}\frac{1}{4}\frac{1}{4}$
(*e*)	$00u$;	$\frac{1}{2}0\bar{u}$;	$0\frac{1}{2}\ u+\frac{1}{2}$;	$\frac{1}{2}\frac{1}{2}\ \frac{1}{2}-u$
(*f*)	xyz;	$\bar{x}\bar{y}\bar{z}$;	$x+\frac{1}{2}, y, z$;	$\frac{1}{2}-x, \bar{y}, \bar{z}$;
	$x, y+\frac{1}{2}, z+\frac{1}{2}$;	$\bar{x}, \frac{1}{2}-y, z+\frac{1}{2}$;	$x+\frac{1}{2}, y+\frac{1}{2}, \frac{1}{2}-z$;	
		$\frac{1}{2}-x, \frac{1}{2}-y, \frac{1}{2}-z$		

Of these, only the coordinates of (*f*) fit any of the regions permitted by Fig. 4, and these fit any of the pairs of regions permitted by Fig. 4. As a starting point in the analysis, Warren and Bragg arbitrarily pick 4 and 4′ as the projection of the Si atoms on the (0 1 0) plane.†

b. We have assumed so far that Ca and Mg atoms are at *A*, *A*′, *B*, *B*′, or *C*. Our choice of positions may be limited by considering

represented in projection by areas on the base. Shaded areas in Figs. 2, 3, and 4 should be interpreted as representing volumes between planes perpendicular to the paper. These figures all represent only one-fourth of the base.

* The signs of the observed values of *F* are unknown.

† In general, there is no reason for picking 4 and 4′ instead of 1 and 1′, 2 and 2′, or 3 and 3′. Whatever pair we start with, it is still necessary to investigate the other three possibilities. A solution of the crystal structure can not be regarded as complete until it has been shown that (*a*) a certain pair of positions will account for the experimental data and (*b*) no other pair of positions will account for the data.

the F values for $(h\,0\,l)$ planes for which h and l are not multiples of 4. For instance, the observed F values for $(4\,0\,\bar{6})$ are very nearly equal to the maximum values permitted by Table V. The lines corresponding to these planes are shown for one-fourth of the crystal in Fig. 4. If, now, the Si atoms are at 4 and 4′ of Fig. 4, then a Ca or Mg at A, A', B, or B' would reduce the value of F seriously for the $(4\,0\,\bar{6})$ planes. This leaves, by climination, position C. Quantitative confirmation of this conclusion will be given later in a detailed study of F for still other $(4n_1,\ 0,\ 4n_2)$ planes. It will turn out that the Ca and Mg atoms occupy crystallographically equivalent positions. These may be arrived at in the projection of Fig. 4 by going a distance $a/4$ from the center of the Si pair in a direction parallel to the a-axis.

c. We now are ready to consider the O atoms. Table I shows that the experimentally observed value of F_{400} is very small, ± 15. Succes-

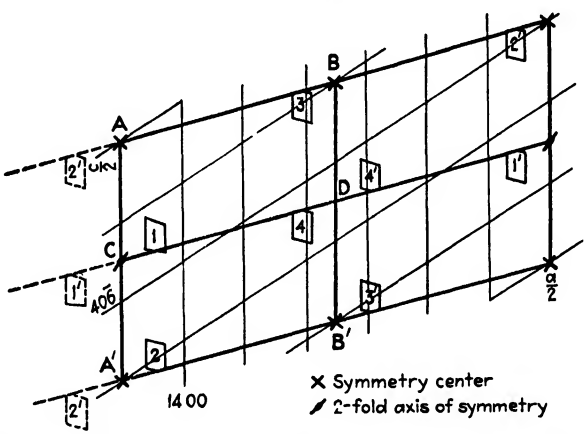

FIG. 4.—Projection on the (0 1 0) plane of regions permitted to Si. (Only one-fourth the base of the unit-crystal is shown).

sive (4 0 0) planes for one-fourth of the crystal are shown in Fig. 4 by the lines AA' and BB'. Since Ca and Mg are assumed to be (in projection) at positions corresponding to C, and since the Si are at positions 4 and 4′, they must all make strong contributions to F_{400}. The sum of these contributions must be almost completely balanced out by the O atoms, so that F_{400} may be reduced to ± 15. This places them about halfway between successive (4 0 0) planes.

d. If we once grant that the foregoing conclusions can be verified by a detailed study of the data, then we are ready to complete the analysis of the (0 1 0) plane. The approximate coordinates of the O atoms parallel to the a-axis are known, and their c-coordinates can be found by trial and error. It will be found that the only coordinates which give good agreement around the [0 1 0] axis are those shown in projection on the (0 1 0) plane in Fig. 7. Each O comes at a distance of

1.5Å. from a rotation axis. We have already placed the Mg and Ca atoms on 2-fold axes of symmetry, and we have located the projection of the Si atoms on the (0 1 0) plane.

e. Our bird's-eye view of the analysis will be completed with a description of the structure. The unit-crystal contains four 2-fold axes. On each of these we must place, like beads on a string, one Ca, one Mg, and three pairs of O atoms. Each pair of O atoms will be placed so that one of the atoms lies on one side of the axis and the other at an equal distance on the other side. The O pair, then, simulates a dumb-bell placed with its handgrip perpendicular to a 2-fold axis of the crystal. In order to preserve the symmetry, the Ca, Mg, and O atoms must be threaded similarly on two of the four axes and in the reverse direction on the other two. Using the interatomic distances for O — O, Ca — O, and Ca — Mg, usually found in silicates,* it appears that there is just room for these atoms along the *b*-axis. Only two arrangements of atoms are possible: (*a*) Ca — Mg — 2 O — 2 O — 2 O, and (*b*) Ca — 2 O — 2 O — Mg — 2 O, with the order reversed on alternate 2-fold axes. The first of these must certainly be discarded on chemical grounds, so that only alternative (*b*) is left.

Since we know the locations of the 2-fold axes in the crystal, and since we know the locations of the *b*-axes which pass through the Si atoms, we can express the whole structure of diopside in terms of these locations and two other parameters. The first of these fixes the location of some one of the atoms on the 2-fold axes; the second fixes the location of the Si atoms along their *b*-axes. These two additional parameters can be determined easily by trial and error.

The atomic coordinates just described represent a first approximation to the final values. A second approximation may be made to improve the agreement between the experimental and calculated values of F_{hkl}. The final coordinates as found by Warren and Bragg give the agreement listed in Tables I, II, III, and IV. Closer agreement is hardly necessary because of the large variations in F_{hkl} caused by small changes in lattice parameters. We are now ready to take up a detailed study of the experimental data to see how the above bird's-eye view can be arrived at.

Detailed Study of the Data. *a. Indices* $(4n_1, 0, 4n_2)$.—Figures 2, 3, and 4 show only a fourth of the (0 1 0) base of the unit-crystal. The total value of F_{h0l} is, of course, four times that due to the portion shown in these figures. The projection of nine planes $(4n_1, 0, 4n_2)$ on (0 1 0) will be considered. For one plane, a detailed discussion will be given by way of illustration. The discussion for the rest will be given by means of symbols.

* It will appear in Chap. XIII that these distances are considerably different from the sum of the packing-radii found in the elements or in binary compounds of the ionic type.

The diffracted beam from the (8 0 4) planes is too weak to measure. The sum of the contributions of the various atoms to the value of F_{804} must therefore be close to zero. No matter whether the four Ca and four Mg atoms lie, in the projection on the (0 1 0) plane of Fig. 4, on points corresponding to A, A', B, or B' or on points corresponding to C, they will lie exactly on the plane (8 0 4). They will therefore contribute their full atomic F values toward F_{804}. Interpolated atomic F values from Table V for $\sin\theta = 0.3060$ show that these four Ca and four Mg atoms contribute an amount equal to +47 toward F_{804}. The eight Si atoms will contribute some value between +44 and −44, depending upon where they are placed. The twenty-four O atoms will contribute some value between +41 and −41. It is evidently not possible for the Si atoms to contribute +44, for even a contribution of −41 from the O atoms would still leave a large and easily measurable positive value of F_{804}. But actually F_{804} is negligibly small. If the Si atoms in this plane contribute any positive value at all to F_{804}, the O atoms cannot possibly reduce the F_{804} to less than +6. Evidently the Si atoms cannot be in any position which would cause them to make any positive contribution to F_{804}. This does not, however, forbid positions for the Si atom such that they can make a negative contribution to F_{804} which, together with an appropriate contribution from the O atoms, would balance out the +47 from the Ca and Mg atoms and make F_{804} negligibly small. The (8 0 4) planes are therefore drawn as in Fig. 2, and parallel strips are shaded to show the projections on (0 1 0) of regions corresponding to positive contributions from Si atoms to F_{804}. These represent regions forbidden to the Si atoms.

The width and location of each shaded area are determined by the following considerations. The atomic F factor takes care of the loss in intensity of the diffracted beam of x-rays due to the spatial structure of the atom, on the assumption that the atomic center lies on the crystallographic plane (see Chap. X). But we have seen that, although the Ca and Mg atoms lie on the $(4n_1, 0, 4n_2)$ plane, the Si atoms do not. Since the Si atoms lie off the crystallographic plane, the x-ray wavelets which they diffract will not be in phase with the wavelets from the Ca and Mg atoms. This necessitates an additional factor, $\cos\phi$, where

$$\frac{\phi}{2\pi} = \frac{\text{distance from the center of the Si atom to the plane } (4n_1, 0, 4n_2)}{\text{interplanar spacing between two successive } (4n_1, 0, 4n_2) \text{ planes}}$$

This factor changes the intensity which the Si atoms would have contributed if they had been exactly on the $(4n_1, 0, 4n_2)$ plane into the intensity which they really contribute in their actual positions in the crystal. Each of the Si atoms in the unit-crystal therefore contributes $F_{Si}\cos\phi$ to the diffracted beam. The eight Si atoms in the unit-crystal contribute $8F_{Si}\cos\phi$. F_{Si} may be found by interpolation from Table V,

using the value for sin θ demanded by Table III for the diffraction of RhK rays from the plane $(4n_1, 0, 4n_2)$. The value of cos ϕ must be estimated in terms of the discussion already given involving the experimental values of the structure factor F_{h0l} and the values of $4F_{Ca}$, $4F_{Mg}$, $8F_{Si}$, and $24F_O$.* The estimated limiting values of cos ϕ for the (8 0 4) planes are given below along with similar estimates for other $(4n_1, 0, 4n_2)$ planes.

(4 0 0)

$$\begin{aligned} \pm F_{400} &= 15 \\ 4F_{Ca} + 4F_{Mg} &= +87 \\ 8F_{Si} &= 74 \\ 24F_O &= 130 \end{aligned}$$

It is improbable that $1.0 > \cos\phi > 0.8$ is permitted for Si. The evidence is not conclusive, and that afforded by (12 0 0) which covers the same area is more reliable.

(0 0 4)

$$\begin{aligned} \pm F_{004} &> 75\dagger \\ 4F_{Ca} + 4F_{Mg} &= +59 \\ 8F_{Si} &= 54 \\ 24F_O &= 60 \end{aligned}$$

At a conservative estimate, $-0.8 > \cos\phi > -1.0$ is forbidden to Si, and the forbidden range is greatly extended if extinction is fully allowed for.

(4 0 $\bar{4}$)

$$\begin{aligned} \pm F_{40\bar{4}} &> 69 \\ 4F_{Ca} + 4F_{Mg} &= +47 \\ 8F_{Si} &= 44 \\ 24F_O &= 41 \end{aligned}$$

$-0.4 > \cos\phi > -1.0$ is forbidden to Si.

(8 0 4)

$$\begin{aligned} \pm F_{804} &= 0 \\ 4F_{Ca} + 4F_{Mg} &= +47 \\ 8F_{Si} &= 44 \\ 24F_O &= 41 \end{aligned}$$

$1.0 > \cos\phi > 0$ is definitely forbidden to Si and even -0.13 may be forbidden.

* The estimates given for cos ϕ by Warren and Bragg[1] differ from those given by Bragg and West[3] from the same data. It is an interesting commentary on the dependability of the structure-factor method that there is only a negligible difference between the end results obtained from the two sets of estimates. The estimates of Warren and Bragg are used in this chapter. The values of cos ϕ are taken to only one decimal place.

† Values of F_{hkl} uncorrected for extinction have been used in this series because the extinction correction depends upon this analysis. The corrected value of F_{004} is 136.

(12 0 0)

$$\begin{aligned} \pm F_{12\,0\,0} &= 0 \\ 4F_{Ca} + 4F_{Mg} &= +36 \\ 8F_{Si} &= 32 \\ 24F_{O} &= 22 \end{aligned}$$

$1.0 > \cos\phi > 0$ is forbidden to Si.

(4 0 8)

$$\begin{aligned} \pm F_{4\,0\,8} &= 0 \\ 4F_{Ca} + 4F_{Mg} &= +28 \\ 8F_{Si} &= 26 \\ 24F_{O} &= 19 \end{aligned}$$

$1.0 > \cos\phi > 0$ is forbidden to Si.

(8 0 8)

$$\begin{aligned} \pm F_{8\,0\,8} &= 0 \\ 4F_{Ca} + 4F_{Mg} &= +27 \\ 8F_{Si} &= 24 \\ 24F_{O} &= 12 \end{aligned}$$

$1.0 > \cos\phi > 0$ is forbidden to Si.

(16 0 0)

$$\begin{aligned} \pm F_{16\,0\,0} &= 0 \\ 4F_{Ca} + 4F_{Mg} &= +24 \\ 8F_{Si} &= 21 \\ 24F_{O} &= 10 \end{aligned}$$

$1.0 > \cos\phi > 0$ is forbidden to Si

The shaded areas of Figs. 2 and 3 show, in projection on the (0 1 0) plane, the regions forbidden to Si for one-fourth the unit-crystal. They exclude all except the small regions marked 1, 2, 3, 4, 1′, 2′, 3′, and 4′ in Fig. 4.

Detailed Study of the Data. *b. Complete Analysis of the Projection on Plane* (0 1 0).—We have seen that space-group C_{2h}^{6} provides for the possibility of eight equivalent positions, corresponding to 1, 1′, or 2, 2′, or 3, 3′, or 4, 4′ of Fig. 4. The theory of space-groups does not, however, help us in choosing which of these pairs of positions corresponds to the projection on the (0 1 0) plane of the positions of the Si atoms. In the most general type of analysis we should expect to have to try each pair in turn and see whether it enables us to account for the various $F_{h\,k\,l}$ values of Tables I, II, III, and IV. A favorable outcome of the analysis on the assumption of Si at some one pair of positions would not mean that the Si atoms had been definitely located; it would still be necessary to show, if possible, that none of the other pairs of positions shown in Fig. 4 satisfy the data. Since trial shows that the regions corresponding to 4, 4′ do enable us to account for the various $F_{h\,k\,l}$ values, we shall use them to illustrate the details of the method. It will appear later that in the case of diopside we can make a short-cut and eliminate positions corre-

sponding to 1 and 1′, 2 and 2′, and 3 and 3′ without having to repeat our whole analysis for these positions.

On the assumption that the Si atoms are in positions corresponding, in projection, to 4 and 4′ of Fig. 4 we shall determine the areas on the (0 1 0) plane corresponding to the positions of the Ca, Mg, and O atoms, using for the purpose $F_{4\,0\,0}$, $F_{2\,0\,0}$, $F_{4\,0\,\bar{6}}$, and $F_{14\,0\,0}$.

(4 0 0)

$$\begin{aligned} \pm F_{4\,0\,0} &= 15 \\ 4F_{Ca} + 4F_{Mg} &= +87 \\ 8F_{Si} &= 74 \\ 24F_{O} &= 130 \end{aligned}$$

Since the Si atoms do not lie exactly on the (4 0 0) planes, their contribution to the intensity of the diffracted beam will not be $8F_{Si} = 74$ but will be $8F_{Si} \cos\phi = 74 \cos\phi$, where (scaling off from Fig. 4.)

$$\frac{\phi}{2\pi} = \frac{\text{distance from the center of the Si atom to the (4 0 0) plane}}{\text{distance between successive (4 0 0) planes}}$$

Figure 4 shows that, if the projected position of the Si atom at 4 is measured from the line AA', then ϕ lies between the limits 289° and 319°. If it is measured from the line BB', it lies between 71° and 41°.

$$\begin{aligned} \cos 289° &= \cos 71° = +0.326 \\ \cos 319° &= \cos 41° = +0.755 \end{aligned}$$

It follows that the eight Si atoms whose positions correspond in projection to 4 and 4′ of Fig. 4 make a contribution to $F_{4\,0\,0}$ between +24 and +56. The O atoms must therefore all lie in projection in a strip approximately half way between AA' and BB'; otherwise they could not balance out the large positive contribution from Ca + Mg + 2Si. This means that the O atoms will occur in coordinates (*f*) of space-group C_{2h}^{6}. In order to account for twenty-four O atoms we must have three values of x, three of y, and three of z in the set of coordinates (*f*) of this space-group.

(2 0 0)

$$\begin{aligned} F_{2\,0\,0} &= 0 \\ 4F_{Ca} &= \pm 68 \\ 4F_{Mg} &= \pm 42 \\ 8F_{Si} &= 84 \\ 24F_{O} &= 192 \end{aligned}$$

The eight Si atoms in positions corresponding to 4 and 4′ contribute an amount between −83 and −75 (origin at *O* of Figs. 2 and 3). The O atoms, approximately halfway between AA' and BB', are in such a position that their contribution is small. The Ca contribution must therefore be positive. We have already assumed that Ca must be at *A*, or *A′*, or *B*, or *B′*, or *C*, or *D*. The required positive contribution to

F_{200} permits the Ca atoms to be at A or A' or C. There is a strong probability that Mg is also at A or A' or C.

(4 0 $\bar{6}$)

$$\begin{aligned} \pm F_{40\bar{6}} &= 72 \\ 4F_{Ca} &= \pm 22 \\ 4F_{Mg} &= \pm 10 \\ 8F_{Si} &= 30 \\ 24F_{O} &= 17 \end{aligned}$$

$F_{40\bar{6}}$ is nearly the maximum amount permitted by

$$4F_{Ca} + 4F_{Mg} + 8F_{Si} + 24F_{O}.$$

With Si atoms at 4 and 4', Ca and Mg atoms must support them by being at C or D. Position D for Ca is definitely eliminated by (2 0 0). Hence the Ca and Mg must be at C.

(14 0 0)

$$\begin{aligned} \pm F_{1400} &= 58 \\ 4F_{Ca} &= \pm 20 \\ 4F_{Mg} &= \pm 9 \\ 8F_{Si} &= 26 \\ 24F_{O} &= 14 \end{aligned}$$

The planes (14 0 0) are shown in Fig. 4. The value of F_{1400} is nearly the sum of $4F_{Ca} + 4F_{Mg} + 8F_{Si} + 24F_{O}$. This agrees with a position for Si, in projection, in the areas 4 and 4', and C for Ca, and makes it almost certain that Mg is also at C and not at D.

Warren and Bragg then examined the whole series of (h 0 l) "reflections" at high angles where the contribution of the O atoms is small. The conclusion that both Ca and Mg atoms are at C was confirmed, and the positions of the Si atoms in the areas 4 and 4' were fixed more definitely.

Granting the positions of the Ca, Mg, and Si atoms in Fig. 4, we can now fix the three typical O atoms. The positions finally arrived at are shown in the projection on the plane (0 1 0) in Fig. 7. In order to get any general agreement between calculated and observed values of F_{h0l} such as that shown in Table III, it is readily shown that two O atoms must be close together at O_1' and O_2 (Fig. 7), and the third near O_3. The precise determination of the positions of O_1' and O_2 is a refinement made at a later stage in the analysis when values of F_{hk0} and F_{0kl} are being considered.

Detailed Study of the Data. *c. Projections on the a-b Plane.*—It is highly improbable that a Si pair is centered about C of Fig. 4, for this would place the atoms on a 2-fold cyclic axis of symmetry so that both Si atoms would lie in a plane parallel to the (0 1 0) plane. Such an arrangement would place the two atomic centers within 1.25Å. of each other, a distance which is obviously too small for atoms having a packing-radius

(see Chap. XIII) of at least 1.17Å. It has been proved that if we assume the Si atoms to be centered about points corresponding to D in Fig. 4, then the Ca and Mg atoms are at C. Similarly, if the Si pairs are centered about A or B, the Ca and Mg atoms will be at B or A, respectively. A consideration of planes $(h\,0\,l)$ cannot decide between these alternatives, since in the projection there is nothing to distinguish points A, A', B, B', C, or D.

The following discussion of the values of $F_{0\,2\,0}$, $F_{0\,4\,0}$, $F_{2\,2\,0}$, and $F_{2\,4\,0}$, all of which are small, will show that the Ca and Mg atoms both lie on the 2-fold axis at C and not at the centers of symmetry AA' or BB' of Figs. 1 and 4. By definitely placing the Ca and Mg atoms at C, we shall have confirmed our original assumption that Si atoms are at 4 and 4′ of Fig. 4, thus making it unnecessary for us to repeat our whole analysis for the other positions permitted to Si by Fig. 4.

The atomic coordinates will be defined with reference to the center of symmetry marked O in Figs. 2 and 3. It is the point A_0 in Fig. 1. If an atom has coordinates x, y, z, measured parallel to the axes a, b c, respectively, then phase coordinates* may be defined:

$$\theta_1 = 360° \frac{x}{a}$$

$$\theta_2 = 360° \frac{y}{b}$$

$$\theta_3 = 360° \frac{z}{c}$$

Projections on the plane (0 0 1) are shown in Figs. 5 and 6. If an atom is in the general position corresponding to the coordinates C_{2h}^6 (f) of

* The location of the Si and O atoms may be pictured most easily in our minds in terms of the rectilinear coordinates x, y, and z, parallel respectively to the a-, b-, and c-axes of the crystal. These coordinates are expressed as the fraction of the distances a, b, and c which would have to be traveled to go from the origin of coordinates to the atom. Such a viewpoint does not lend itself readily to calculations of the amplitude of the resultant of the x-ray beam diffracted from the various atoms. We have already seen that these component amplitudes must be multiplied by the cosine of the phase angle of the wavelet before they may be added together. The coordinates of the Si and O atoms may be expressed for this purpose in angular measure if we write 2π or 360° for each of the interplanar spacings a, b, and c, *i.e.*, if we take the (1 0 0), (0 1 0), and (0 0 1) planes in turn as the standard of phase angle. Then the coordinate x would be expressed as

$$x = \frac{\theta_1}{360} a$$

where θ_1 is the phase coordinate corresponding to x. Similarly

$$y = \frac{\theta_2}{360} b$$

$$z = \frac{\theta_3}{360} c$$

Wyckoff's tables, and if its a- and b-coordinates are expressed as θ_1 and θ_2, the contribution of all eight atoms of C_{2h}^6 (f) in the unit-crystal to the x-ray beam diffracted from ($hk0$) is determined by the factor

$$8 \cos (h\theta_1) \cos (k\theta_2)$$

when $h + k$ is even. If $h + k$ is odd, the factor is zero (see value of s in Appendix III).

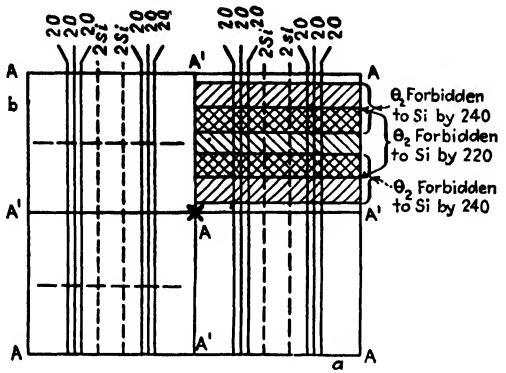

FIG. 5.—Projection of the structure of diopside on the (001) plane if Ca and Mg atoms are at A and A'. (Unlike Figs. 2, 3, and 4, Fig. 5 shows the projection for the whole unit-crystal.)

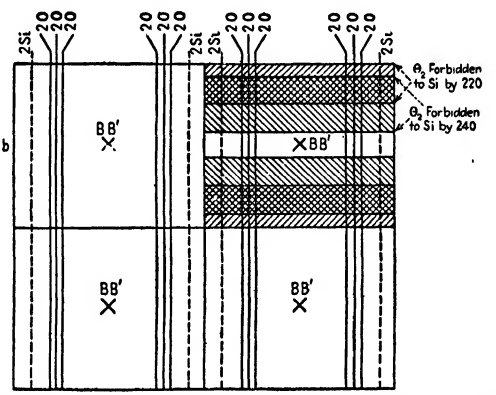

FIG. 6.—Projection of the structure of diopside on the (001) plane if Ca and Mg atoms are at BB'. (Unlike Figs. 2, 3, and 4, Fig. 6 shows the projection of the whole unit-crystal.)

We are to decide whether the Ca and Mg atoms lie, in projection in Fig. 4, at AA', BB', or C. We shall assume at first that they are at AA' of Fig. 4. The lettering is identical for Figs. 4 and 5. Referring to Fig. 5, the Si atoms must then lie somewhere on the dotted lines and the O atoms on the groups of vertical lines. The θ_1-coordinates of the O and Si atoms would have, in this case, the values given below, but their θ_2-coordinates would be unknown.

Si, $\theta_1 = 76°$; $\theta_2 = \theta_2'$
O_1, $\theta_1 = 136°$; $\theta_2 = \theta_2''$
O_2, $\theta_1 = 51°$; $\theta_2 = \theta_2'''$
O_3, $\theta_1 = 56°$; $\theta_2 = \theta_2''''$

(220)
$$\pm F_{220} = 48$$
$$4F_{Ca} + 4F_{Mg} = +99$$
$$8F_{Si} = 84$$

The contribution to F_{220} of the twenty-four O atoms is given by the factor

$$8(\cos 272° \cos 2\theta_2'' + \cos 102° \cos 2\theta_2''' + \cos 112° \cos 2\theta_2'''')$$

The value of this factor lies between +4.9 and −4.9 (rounded off to ±5), whatever the values of θ_2; *i.e.*, the twenty-four O atoms cannot produce a greater effect than five atoms in phase. The maximum contribution of the O atoms is therefore $\pm 5 \times 6.6 = \pm 33$. Ca and Mg give full positive contributions to the (220) plane. Therefore the contribution of the Si atoms ($= 84 \cos 152° \cos 2\theta_2'$) must be negative, *i.e.*, $270° > 2\theta_2' > 90°$.

$135° > \theta_2' > 45°$ is forbidden to Si.

(240)
$$\pm F_{240} = 16$$
$$4F_{Ca} + 4F_{Mg} = +81$$
$$8F_{Si} = 70.4$$
Maximum value of $24F_O = \pm 23.5$

Ca and Mg give full positive contributions to the (240) plane. The Si contributions ($= 70.4 \cos 152° \cos 4\theta_2'$) must have a large negative value, conservatively estimated at a value between −40 and −63.

$0.6 > \cos 4\theta_2' > -1.0$ is forbidden to Si.
$77° > \theta_2' > 13°$ is forbidden to Si.
$167° > \theta_2' > 103°$ is forbidden to Si.

The regions forbidden to Si by (220) and (240) are shown in projection on the (001) plane in Fig. 5. Evidently the Si atoms must lie, in projection, close to the lines AA'.

(020)
$$\pm F_{020} = 19$$
$$4F_{Ca} + 4F_{Mg} = 108.8$$
$$24F_O = 187$$

Because of their positions near AA', the Si atoms make practically their maximum positive contribution, *i.e.*, +88. It follows that all O atoms must be placed, in projection, approximately halfway between the lines AA', *i.e.*, θ_2'', θ_2''', and θ_2'''' must be approximately 90°.

(040). With O atoms halfway between lines AA', all atoms would make large positive contributions to F_{040} which should therefore be one of

the most powerful beams diffracted by the crystal. Actually it is too small to observe. A position of Ca and Mg atoms at the centers A, A' is therefore definitely excluded. It will be noticed that the conclusion depends upon weak diffracted beams and is therefore independent of extinction corrections.

A similar argument excludes positions of the Ca and Mg atoms at centers BB' (see Fig. 6). If Ca and Mg were at BB' they would give full contributions to F_{020}, F_{040}, F_{220}, and F_{240}. Hence an identical course

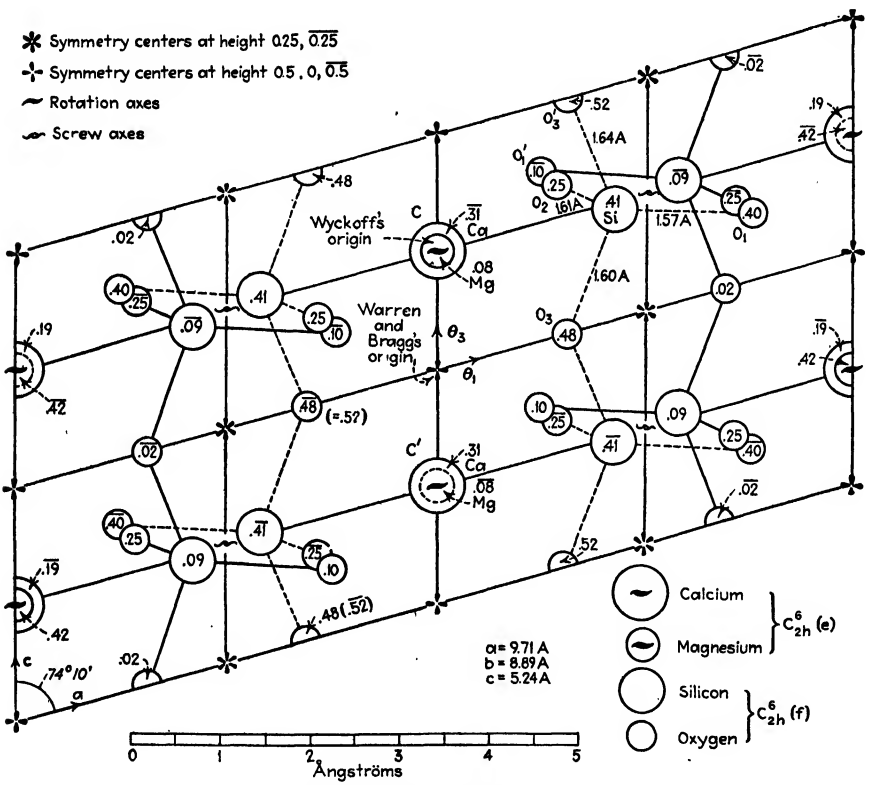

FIG. 7.—Projection of diopside structure on plane (0 1 0).

of reasoning from the values F_{220} and F_{240} would lead to positions of the Si atoms near the horizontal line $BB' - BB'$. Such positions are incompatible with the small values of F_{020} and F_{040}.

The only remaining possibility is that the Ca and Mg atoms lie on the 2-fold axes corresponding to C of Figs. 1 and 4. The observed values of F_{hk0} and F_{0kl} are to be explained by assigning θ_2-coordinates to Ca and Mg atoms as well as to the Si and O atoms. The structure depends upon 14 parameters, one each for Ca and Mg, and three each for Si, O_1, O_2, and O_3.

Detailed Study of the Data. *d. Completion of the Analysis.*—The foregoing analysis has shown that Ca and Mg atoms lie on 2-fold axes, and the θ_1- and θ_3-coordinates have been found. It remains to determine the θ_2-coordinates of all the atoms, *i.e.*, the coordinates parallel to the *b*-axis. The projection upon the (0 1 0) plane of the structure finally settled upon for the entire unit-crystal is shown in Fig. 7.* The point used by Warren and Bragg as the origin of coordinates is marked in the figure. It is one of the centers of symmetry in the crystal. The θ_2-coordinates finally determined are represented by the numbers within the circles denoting the atomic positions; these numbers represent fractions of the *b*-axis. For instance 0.50 denotes an atom at the top of the unit-crystal (θ_2 180°), $\overline{0.50}$ denotes an atom at the bottom ($\theta_2 = -180°$). The atomic positions in the projection, combined with these numbers, will make the symmetry elements evident. It is this series of numbers which are to be found by the present stage of the analysis.

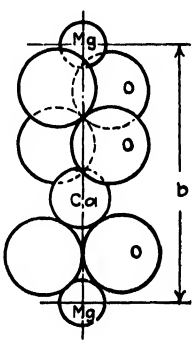

FIG. 8.—Type of arrangement around the 2-fold axis.

It will be seen in Fig. 7 that the O atoms are grouped in pairs around 2-fold axes. For instance, the oxygen atoms marked O_1', O_2, O_3 are at a distance of about 1.5Å. from the symmetry axis marked *C*, and each atom has a companion on the opposite side of the axis. If the centers of the two O which compose a "pair" are joined by an imaginary line, then the O atoms would look like the weights of a dumb-bell with the imaginary line forming the grip. The symmetry axis marked *C* is the perpendicular bisector of this imaginary line. The axis may be regarded, then, as having a Ca atom, aMg atom, and three pairs of O atoms threaded on it within a length *b* which is 8.9Å. Assuming that the O atoms are arranged dumb-bell fashion, in pairs, we have the following alternatives:

Mg,	2O,	Ca,	2O,	2O,	(Mg)
Mg,	2O,	2O,	Ca,	2O,	(Mg)
Mg,	Ca,	2O,	2O,	2O,	(Mg)

Of these the last is highly improbable on chemical grounds. The first two are evidently duplicates which differ only in the direction of listing. They are shown diagrammatically in Fig. 8.

The sizes of atoms under various chemical conditions will be discussed in Chap. XIII. It is sufficient to say here that W. L. Bragg and his associates have found it useful to assume that in silicates the distance between adjacent centers O — O is 2.7 to 2.9Å.; Ca — O is 2.35Å.; Mg — O is 2.10Å. If these atoms were threaded on to the axis so that

* The relation of the points in Fig. 7 to the space-group coordinates already given will be taken up later.

all the O pairs were in the same plane, there would not be room for them along the *b*-axis. The over-all distance may be shortened by allowing the two adjacent pairs of O atoms to fit into each other, forming a tetrahedral arrangement. When this is done, the distance in which the group repeats itself is found by calculation to be 9Å.—a close correspondence with $b = 8.9$Å. It will be clear that the orientation of the O pairs around the axis does not affect this result as long as the pairs occurring together are allowed to fit into each other.

It can be seen, in Fig. 7, that two pairs of O atoms, O_1' and O_2, have nearly the same orientation. The third pair, O_3, is set in a position transverse to the other two. Since there is only just room to stack the atoms along the *b*-axis within the prescribed limit of 8.9Å., it is probable that the arrangement is one or the other of the following:

(*a*) Mg, $2O_1'$ or $2O_2$, Ca, $2O_2$ or $2O_1'$, $2O_3$, (Mg)

or

(*b*) Mg, $2O_1'$ or $2O_2$, Ca, $2O_3$, $2O_2$ or $2O_1'$, (Mg)

It could hardly be

(*c*) Mg, $2O_3$, Ca, $2O_1'$ or $2O_2$, $2O_2$ or $2O_1'$, (Mg)

since this arrangement demands a much longer *b*-axis by not allowing the two successive O pairs to fit together. Since the projected positions O_1' and O_2 are closely the same, we have, broadly speaking, a simple alternative between (*a*) and (*b*); either the O pairs on either side of Mg have the same orientation (*a*), or they are placed transversely (*b*).

Besides the question already raised in connection with O atoms, there is the question of how the arrangements of Ca and Mg are placed relatively to each other on the symmetry axes *C* and *C'*. The one is derived from the other by an inversion at the origin (Fig. 7), and a movement of the one group as a whole along the axis *C* involves a corresponding movement of the other group in the opposite direction along *C'*. A single coordinate, for instance θ_2, for the Ca ion determines the position of the groups. In considering the possibilities, Warren and Bragg found it helpful to take two general alternatives: either a Ca atom on the symmetry axis *C* comes opposite a single O pair on *C'*, or it comes opposite a double O pair. Other arrangements can be considered as being merely distortions of one or the other of these alternatives.

Finally, the θ_2-coordinates of the Si atoms must be found. The general features of the whole structure are thus determined by two coordinates parallel to the *b*-axis, one for the group $CaMgO_6$ and the other for the Si pair, and by a choice between the alternatives (*a*) and (*b*) given in the discussion of the O atoms. Some 60 values of F_{hk0} and F_{0kl} are available for the analysis. Warren and Bragg used trial-

and-error methods to narrow down the possibilities and arrived at approximate values for the coordinates. In their trials they made use of interatomic distances to rule out configurations which were obviously impossible.

The process of making final adjustments to the coordinates is somewhat tedious but quite straightforward. At high glancing angles the O

TABLE VI.—THE POSITIONS OF ATOMIC CENTERS OF Ca, Mg, AND O ALONG THE *C*-AXIS OF FIG. 7
(See also Fig. 8)

Atom	Relative distance from origin along *b*-axis	Distance from origin along *b*-axis, Ångströms
Ca	$\bar{0}\ \bar{31}$	$y = -2.72$
$2O_1'$	$0.1\bar{0}$	$y = -0.89$
Mg	0.08	$y = +0.71$
$2O_2$	0.25	$y = +2.22$
$2O_3$	0.48	$y = +4.27$
(Ca)	(0.69)	$(y = +6.17 = 8.89 - 2.72)$

atoms contribute very little to F_{hkl}, and a knowledge of their approximate positions is sufficient to enable their contributions to be assayed with sufficient accuracy. These beams diffracted at high angles provide therefore suitable material for adjusting the positions of Ca, Mg, and Si. It is always possible to find diffracted beams which are sensitive to slight movements of one atom and insensitive to the other two. These

TABLE VII.—ATOMIC COORDINATES FOR DIOPSIDE x, y, AND z ARE MEASURED PARALLEL TO THE a-, b-, AND c-AXES RESPECTIVELY

Atom	θ_1	θ_2	θ_3	x	y	z
Ca	0°	−110°	90°	0.00Å	−2.72Å	1.31Å
Mg	0	30	90	0.00	0.71	1.31
Si	76	148	85	2.05	3.66	1.24
O_1	136	145*	50	3.67	3.57	0.73
O_2	51	90	115	1.38	2.22	1.68
O_3	56	173	0	1.51	4.27	0.00

* θ_2 for O_1', is −35° thus giving for O_1', $y = -0.89$ (see Table VI).

are used to fix more closely the coordinates of the important atom. When Ca, Mg, and Si have been fixed, the reflections at small glancing angles are used to determine the coordinates of the O atoms. It is more difficult to estimate these latter values. Warren and Bragg estimate the probable error in coordinates to be 0.05Å.

The relative positions in space found in this way for the various atoms have been shown already in Fig. 7. Table VI shows, in their order along

the axis C, the positions of the atomic centers of Ca, Mg, and O. In this connection see also Fig. 8. It will be noted that the two O pairs on either side of Mg are approximately parallel (O_1' and O_2), and that the two pairs between Mg and Ca form a tetrahedral group (O_2 and O_3). The Ca atom on axis C' at a height 0.31 is opposite to the two O pairs on axis C (O_2 at 0.25 and O_3 at 0.48). The coordinates assigned to the atoms are given in Table VII.

The O and Si atoms at θ_1, θ_2, and θ_3 are each multiplied into a group of eight atoms by the symmetry elements of the crystal. The contribution to F_{hkl} by these eight atoms is the product of the atomic F value by the factor

$$8 \cos\left(l\frac{\pi}{2} - h\theta_1 - l\theta_3\right) \cos\left(l\frac{\pi}{2} + k\theta_2\right)$$

when $h + k$ is even. The factor is zero when $h + k$ is odd.

A Ca or Mg atom at θ_2 is multiplied into a group of four atoms in the unit-crystal by the symmetry elements of the crystal. The contribution to F_{hkl} by these four atoms is the product of the atomic F value by the factor

$$4 \cos\left(l\frac{\pi}{2} + k\theta_2\right)$$

Calculated and observed values of F_{hkl} are given in Tables I, II, III, and IV. In general the agreement is satisfactory. There are a few cases where it is not so good, for instance, in the case of F_{604} and F_{330}. These discrepancies do not tend to cast doubt on the structure or on the experimental measurement; they are due to the fact that in these cases small errors in the coordinates produce larger errors in the calculated atomic contributions to F_{hkl}. In the exceptional case where all these contributions have the same sign, and where all the atoms are in sensitive positions, the total error in the computed value of F_{hkl} may be large. For instance, in the case of F_{330}, a movement of the Si atom in the b-direction of 0.01 b alters F_{330} by ± 10.

The point which Warren and Bragg used as the origin of coordinates in the unit-crystal is so marked in Fig. 7. The various points on this figure will be found to correspond to Wyckoff's coordinates for C_{2h}^6 if the origin is taken at a point ($a = 0$, $b = 0$, $c = \frac{1}{4}$) and if the X-axis is taken along the c-direction and the Y-axis along the a-direction. The Ca and Mg atoms lie on $C_{2h}^6(e)$. All the other atoms lie on $C_{2h}^6(f)$. This places the eight Si atoms on the eight general positions and gives three sets of positions of eight each for the twenty-four O atoms. The parameters along the Z-axis (Warren and Bragg's b-axis) are marked on the circles which represent the various atoms. It will be seen that these

conform rigorously to Wyckoff's coordinates so that they automatically provide for the proper points of inversion and axes of symmetry.

The version of the analysis originally published by Warren and Bragg made no mention of Wyckoff's atomic coordinates for the space-group C_{2h}^6. The reader has doubtless noticed places in the foregoing where the labor of the analysis could have been lessened considerably if a frank use of these coordinates had been made. Such use, however, would have defeated the purpose of the original article, namely, to show by a special example how the structure of a complicated crystal may be arrived at by using, by trial-and-error methods, the information obtained from values of F_{hkl} and of the contribution to F by each atom, supplemented only when necessary by a knowledge of the symmetry of the crystal.

THE STRUCTURE OF TOPAZ, $[Al(F,OH)]_2SiO_4$

The structure of topaz has been worked out by two students of W. L. Bragg—N. A. Alston and J. West[4]—by means of the structure-factor method using a combination of the trial-and-error scheme and of the Fourier analysis scheme. The chemical properties of topaz may be represented by the formula $[Al(F,OH)]_2SiO_4$, the fluorine being replaced by hydroxyl in amounts which vary from crystal to crystal. It crystallizes in the orthorhombic system. It is sometimes reported in the literature as having the symmetry of the $D_{2h}(=V_h)$ point-group and sometimes as having the symmetry of the C_{2v} point-group. Etch figures suggest the V_h point-group.[5] The pyroelectric and piezoelectric properties suggest the C_{2v} point-group, but these properties are weak, often vary in direction, and are often regional even in the same crystal. Alston and West assume that just as the chemical composition of a mineral may be represented by a simple formula which is seldom rigorously satisfied by actual specimens, so the structure of some crystals may be represented by an arrangement of atoms conforming to the symmetry requirements of a certain crystallographic class, although, owing to small distortions of no real significance caused by the physical and chemical conditions of formation, the actual arrangement in any particular specimen belongs more strictly to a point-group of lower symmetry. This may be expected to apply more especially to crystals whose crystallographic class is in doubt. Topaz apparently provides a good example of such a crystal, and the fundamental structure may properly be regarded as possessing holohedral symmetry, *i.e.*, as having the symmetry of point-group V_h.

The Unit-cell and Space-group.—The unit-crystal, which contains four molecules of $[Al(F,OH)]_2SiO_4$ has the dimensions

$$a = 4.44_1\text{Å}.$$
$$b = 8.78_3\text{Å}.$$
$$c = 8.37_8\text{Å}.$$

giving the axial ratios

$$a:b:c = 0.5285:1:0.9540$$

These agree to within less than 1 part in 9,000 with the axial ratios accepted by crystallographers. The uncertainty, already indicated, which exists with regard to the crystal class of topaz, leads to a difficulty in the determination of the space-group. An analysis of the usual six rotation photographs taken about the three rectangular axes in turn as

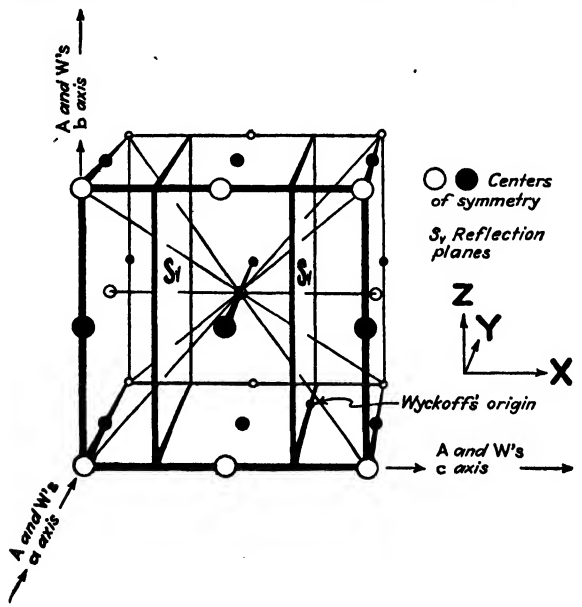

FIG. 9.—Space-group V_h^{16}.

axis of rotation, supplemented by an examination for weak reflections with the ionization spectrometer, results as follows:

1. Planes (hkl); all types present. The lattice is therefore simple orthorhombic.
2. Planes ($hk0$); all types present.
3. Planes ($h0l$); only those present for which ($h + l$) is even.
4. Planes ($0kl$); only those present for which k is even.

Comparing 3 and 4 with the tables for the orthorhombic system in Appendix III, and remembering that in those tables h and k can be systematically interchanged, it is found that topaz must belong either to space-group C_{2v}^9 or to space-group V_h^{16}. The presence or absence of lines in the diffraction pattern cannot alone distinguish between these two space-groups. The difference in the two space-groups lies in the exclusive possession by V_h^{16} of reflection planes and centers of symmetry. The reflection planes are parallel to the (0 0 1) face, and the centers of symmetry occupy the corners, body-center, edge-centers, and face-

centers of the unit-crystal. These symmetry elements are shown in Fig. 9, using Alston and West's choice of coordinates. These coordinates are related to Wyckoff's[6] as follows:

Wyckoff's origin is at Alston and West's $3a/4$, 0, $3c/4$; his X-axis is Alston and West's c; his Y-axis is Alston and West's a; his Z-axis is Alston and West's b. As a result of the operations of the symmetry machines in space-group V_h^{16}, an atom is converted into eight equivalent atoms if it is in the general position of V_h^{16}, *i.e.*, if it is one of the atoms whose coordinates correspond to $V_h^{16}(d)$ in Wyckoff's tables. If an atom lies on a center of symmetry it will be one of four equivalent atoms corresponding to Wyckoff's $V_h^{16}(a)$ or $V_h^{16}(b)$. If an atom lies on a reflection plane, its coordinates will correspond to Wyckoff's $V_h^{16}(c)$. Space-group C_{2v}^9 has no special positions, and each atom must lie on one of the four equivalent general positions corresponding to Wyckoff's $C_{2v}^9(a)$.

In view of the character of the crystallographic data,[5] Alston and West commenced their analysis with the assumption that the correct space-group is V_h^{16}. This procedure was later justified by the final results. They chose one of the centers of symmetry as their origin of coordinates and expressed the location of the various atoms in phase coordinates such as were used in the discussion of diopside. For convenience of reference their procedure will be followed here. Accordingly, if the rectangular coordinates of an atom in the general position,[6] (d) of V_h^{16}, are x, y, z, measured parallel to the axes a, b, c, respectively, then the phase coordinates are

$$\theta_1 = 2\pi\frac{x}{a}$$

$$\theta_2 = 2\pi\frac{y}{b}$$

$$\theta_3 = 2\pi\frac{z}{c}$$

and the coordinates of the eight equivalent atoms (using Alston and West's origin and axes) are

$\theta_1, \theta_2, \theta_3;$	$(\theta_1 - \pi), (\pi - \theta_2), (\theta_3 - \pi)$
$\theta_1, \theta_2, (\pi - \theta_3);$	$(\pi - \theta_1), (\pi + \theta_2), \theta_3$
$\bar{\theta}_1, \bar{\theta}_2, \bar{\theta}_3;$	$(\pi - \theta_1), (\theta_2 - \pi), (\pi - \theta_3)$
$\bar{\theta}_1, \bar{\theta}_2, (\theta_3 - \pi);$	$(\theta_1 - \pi), (\bar{\theta}_2 - \pi), \bar{\theta}_3$

The structure factor $F_{g_{hkl}}$ of this group of eight atoms for an x-ray beam diffracted by a plane (hkl) is

$$F_{g_{hkl}} = F_a \Sigma \cos (h\theta_1 + k\theta_2 + l\theta_3)$$

where F_a is the structure factor for a single atom. In the case under consideration the summation is taken over the eight atoms, so that the equation reduces to

$$F_{g_{hkl}} = 8F_a \cos\left[h\theta_1 + (h+k)\frac{\pi}{2}\right] \cos\left[k\theta_2 + (h+k+l)\frac{\pi}{2}\right] \cos\left[l\theta_3 + l\frac{\pi}{2}\right] \quad (3)$$

In the case of a group of four atoms corresponding to $V_h^{16}(a)$, (b), or (c), the factor 8 must, of course, be replaced by a factor 4. The structure factor for the whole unit-crystal is

$$F_{hkl} = \Sigma F_{g_{hkl}} \quad (4)$$

where the summation is taken over all the sets of equivalent atoms in the crystal. Numerical values of F_{hkl} must be deduced from the quantitative experimental data.

Bird's-eye View of the Analysis.—In addition to the usual rotation photographs, used for the determination of the space-group and for a qualitative survey of the various diffracted x-ray beams, Alston and West made direct measurements of the integrated reflection from the faces (100), (010), (001), (110), (011), and (101) ground on the crystal. They estimated the integrated reflections of still other faces from slips of topaz, using the technique described in the discussion of Eq. (30) of Chap. X. All these measurements supplied the numerical values of F_{hkl} necessary to the quantitative analysis of the structure of the crystal.

The intensities of the diffracted beams indicated that although the crystal was not "ideally imperfect," nevertheless it was definitely of the mosaic type. Equation (1) was therefore applicable. As a result of a detailed examination of diffraction from the (001) planes, the value of g in Eq. (1) was estimated by trial-and-error methods as 0.60×10^4. The other constants of Eq. (1) are as follows:

n = number of unit-crystals per cubic centimeter
= reciprocal of the volume of the unit-crystal
$$= \frac{1}{4.641 \times 8.783 \times 8.378 \times 10^{-24}} = 2.929 \times 10^{21}.$$
$\lambda = 0.614 \times 10^{-8}$ cm. (K_α of rhodium).
$e = 4.774 \times 10^{-10}$ abs. e.s.u.
$m = 8.994 \times 10^{-28}$ g.
$c = 3 \times 10^{10}$ centimeters per second.
$\mu = 7.1$ cm.$^{-1}$

Equation (1) therefore becomes

$$\rho = \frac{\rho'}{1 - 1.20\rho' \times 10^4} = 5.544F^2\frac{1 + \cos^2 2\theta}{\sin 2\theta} \times 10^{-9} \quad (5)$$

where ρ' is the observed intensity, and ρ is the intensity after correction for extinction. If we had neglected to take account of extinction, Eq. (5) would have been replaced by

TABLE VIII.—STRUCTURE-FACTOR DATA FOR TOPAZ

Indices	sin θ	$\frac{1+\cos^2 2\theta}{\sin 2\theta}$	ρ'	F_{hkl}	ρ	F_{hkl} from experimental data	F_{hkl} calculated from structure	F_{hkl} calculated for ideally perfect crystal
(200)	0.132	7.37	9.7	15.4	10.9	16.4	11.3	98
(400)	0.265	3.41	23.6	35.4	32.9	41.8	− 47.9	493
(600)	0.397	2.01	13.8	35.2	16.6	38.6	− 43.9	453
(800)	0.529	1.34	0	0	0	0	1.1	0
(1000)	0.662	1.02	2.4	20.6	2.5	21.0	18.0	161
(020)	0.070	14.6	15.2	13.7	18.6	15.2	18.5	81
(040)	0.140	6.95	52.5	36.9	142.0	60.6	66.0	562
(060)	0.210	4.50	7.0	16.8	7.6	17.5	− 13.8	114
(080)	0.27[illegible]	3.22	28.0	41.0	42.2	48.8	64.0	617
(0100)	0.34[illegible]	2.43	12.0	29.9	14.0	32.3	− 37.0	338
(0120)	0.41[illegible]	1.87	0.5	6.9	0.5	6.9	− 12.7	17
(0140)	0.489	1.50	0	0	0	0	3.9	0
(0160)	0.549	1.23	5.5	28.4	5.9	29.7	28.5	282
(0130)	0.643	1.08	0.6	10.0	0.6	10.0	− 3.4	55
(002)	0.073	13.11	7.0	9.8	7.6	10.2	14.0	39
(004)	0.147	6.60	13.0	18.9	15.4	20.6	22.1	147
(006)	0.220	4.25	68.0	53.8	367.5	124.4	−144.9	1162
(008)	0.293	3.03	0.5	5.5	0.5	5.5	− 10.9	12
(0010)	0.367	2.28	1.9	12.2	2.0	12.6	− 19.7	64
(0012)	0.440	1.75	9.2	30.8	10.3	33.1	45.0	342
(0014)	0.514	1.40	0.8	10.2	0.8	10.2	− 2.8	36
(0016)	0.587	1.15	0.9	11.9	0.9	11.9	10.1	50
(0018)	0.660	1.04	1.5	16.2	1.5	16.2	− 18.4	100
(110)	0.075	12.9	16.7	15.3	20.9	17.1	11.3	95
(220)	0.150	6.45	53.8	38.8	152.0	65.1	− 68.8	615
(330)	0.224	4.14	1.6	8.3	1.6	8.3	10.5	28
(440)	0.299	2.95	8.0	22.1	8.9	23.3	34.4	190
(550)	0.374	2.20	2.3	13.7	2.4	14.0	17.7	70
(660)	0.459	1.63	0.9	10.0	0.9	10.0	11.6	34
(770)	0.524	1.34	1.2	12.7	1.2	12.7	− 7.8	56
(880)	0.598	1.15	0.3	6.9	0.3	6.9	8.5	17
(990)	0.673	1.02	0.4	8.4	0.4	8.4	5.1	28
(101)	0.076	.....	0	0	0	0	− 1.3	0
(202)	0.151	.....	0	0	0	0	− 1.3	0
(303)	0.227	4.10	70.0	55.5	437.5	139.0	137.6	1250
(404)	0.302	.....	0	0	0	0	− 1.0	0
(505)	0.378	.....	0	0	0	0	− 6.5	0
(606)	0.454	1.66	8.0	29.5	8.9	31.1	40.3	307
(707)	0.529	.....	0	0	0	0	− 1.1	0
(808)	0.605	.....	0	0	0	0	− 6.6	0
(909)	0.681	.....	0	0	0	0	5.7	0
(022)	0.101	9.80	43.4	28.3	83.5	39.3	− 53.1	334
(044)	0.203	4.60	15.0	24.3	18.3	26.8	39.5	236
(066)	0.304	2.88	0.7	6.6	0.7	6.6	4.9	17
(088)	0.405	1.97	6.2	23.9	6.8	25.1	− 36.9	208
(01010)	0.506	1.41	2.8	18.9	2.9	19.3	16.7	125
(01212)	0.608	1.10	0.6	9.9	0.6	9.9	− 11.4	35

$$\rho' = 5.544F'^2\frac{1 + \cos^2 2\theta}{\sin 2\theta} \times 10^{-9} \qquad (6)$$

Table VIII gives for each of 47 planes the values of ρ' calculated from the underlying experimental data, and the corresponding values of F', ρ, and F. The table also gives for each of these planes the value of F_{hkl} calculated from the structure finally deduced for topaz, and, for purpose of comparison, states what the value of F_{hkl} would have been if the crystal had been an "ideally perfect" crystal. We are now ready to retrace the steps of Alston and West in finding a structure for topaz which will give computed structure factors, F_{hkl}, corresponding as closely as possible to those in column 7 of Table VIII.

The unit-crystal contains four molecules of $[Al(F,OH)]_2SiO_4$, so that locations have to be found for eight Al, four Si, eight F(or OH) and sixteen O. If we adopt for topaz the ionic sizes which Bragg and his associates have found useful in dealing with silicates, it is found that the volume available for O and F (or OH)* is such that these ions must be closely packed together. This leaves the resulting interstices for the Al and Si.

Examples of close-packed arrangements have been found in several of the silicates. We must now find which type of close-packing exists in topaz; when the form which the configuration takes in any particular case is known, the subsequent analysis is greatly simplified. The two best known types of close-packing are the face-centered cubic and the hexagonal close-packed. Although, of these, the hexagonal close-packed is consistent with the symmetry requirements of V_h^{16} and, curiously enough, explains in detail the whole of the diffracted beams from the (0 0 1) face, it can be shown by the data from other planes not to represent the true configuration of O and F atoms. The discrepancy between the experimental results and those to be expected from the hexagonal arrangement is too great for it to be worth while to regard the structure as a distorted form of such packing. The "close-packing" must, then, be of some other type. It therefore seems best first to locate the Al and Si atoms directly and then to find the exact type of close-packed arrangement of O and F (or OH) consistent with the positions of the Al and Si.

Symmetry considerations help us to some extent. Since there are only four Si atoms in the unit-crystal, they must occupy one of the two sets of symmetry centers of Fig. 9 or must lie on the reflection planes S_v of Fig. 9. If we suppose (as seems to be the case for all $-SiO_4$ compounds) that each Si is surrounded by four O atoms arranged tetrahed-

* Alston and West have, as a convenient approximation, treated the O and F (or OH) as identical when considering dimensional relationships. Following them, we shall collectively refer to both in such cases as O atoms or simply as "negative ions."

rally,* we must place the Si on the reflection planes, and, because of the symmetry of the tetrahedron, two of the O atoms must lie on the reflection plane, the other two being situated symmetrically on each side of it. We thus have two sets of four O atoms on the reflection planes and one set of eight in the general position. If in addition we give dimensions to the tetrahedra, we automatically give a value to the c-coordinate of the O atom in the general position. There remain the Al and F (or OH). Symmetry requirements would permit the Al atoms to consist of one set of eight in the general position or two sets of four in the special positions. A similar argument applies in the case of the F (or OH). However, since the intensities of the diffracted beams of higher orders are due mainly to the positive ions Al and Si, we must place the Al in the general position in order to explain the strong diffraction from (0 0 12) and (0 0 18) and the weak diffraction from (0 0 14) and (0 0 16). A similar qualitative consideration of the diffracted beams of lower order requires the F (or OH) to be placed in the general position.

Summarizing we have

Element	Number of atoms	Code symbol	Position	Number of parameters
Al	8	Al	General position	3
O	8	G_1	General position	3
F (or OH)	8	G_2	General position	3
O	4	R_1	Reflection planes	2
O	4	R_2	Reflection planes	2
Si	4	Si	Reflection planes	2

The solution of the structure thus requires the evaluation of fifteen parameters.

The Analysis in Detail. The (0 0 1) Planes.—Figure 9 shows that the simplest set of planes to examine is the (0 0 1), since only three parameters (the c-coordinates of Al, G_1, and G_2) are to be determined. Let us consider the Al and Si atoms and the higher order diffractions (column 4 of Table VIII). Since the origin is taken at a center of symmetry, and since the Si atoms lie on reflection planes [Wyckoff's coordinates $V_h^{16}(c)$], the c-coordinate of our typical Si atom is $\theta_3 = 90°$.

* This assumption is a convenience in describing the process of analysis. It is not a necessity in the analysis itself. A qualitative consideration of the higher orders of diffraction from the (1 0 0), (0 1 0), and (1 0 1) faces would have avoided the use of this assumption as such.

As a first approximation we can neglect, for the high orders, both the effect of extinction. and the contribution from the negative ions* (see Table V). We must therefore fix the positions of the Al atoms so that the structure factor $F_{0\,0\,l}$ due to all the Al and Si atoms is substantially equal to that calculated from the observed intensities ρ' with no correction for extinction (column 5 of Table VIII). In this way we are led to assign a preliminary value $\theta_3 = 30°$ to the c-coordinate of the typical Al atom. The fact that $F_{0\,0\,18}$ has nearly its maximum value is good evidence for the correctness of our estimate.

We may now consider G_1 and G_2. Since we know definitely that $\theta_3 = 90°$ for Si, R_1 and R_2, and since we have estimated the value of θ_3 for Al, we can find the contribution made by these atoms to the structure factor corresponding to each of the diffracted beams from the $(0\,0\,l)$

TABLE IX.—THE COORDINATES FOR TOPAZ

	x	y	z	θ_1	θ_2	θ_3
Aluminum (Al)	−0.49Å.	1.15Å.	0.67Å.	− 38°	47°	29°
Silicon (Si)	−1.93	0.49	−2.09	−150	20	−90
Oxygen (R_1)	−1.29	0.10	2.09	−100	4	90
Oxygen (R_2)	0.39	2.20	2.09	30	90	90
Oxygen (G_1)	1.03	−0.10	0.74	80	−4	32
Fluorine (G_2)	−1.93	2.20	0.51	−150	90	22

planes (column 5 of Table VIII). Thus we can find the contribution due to G_1 and G_2 alone. Although the values of the contributions estimated in this way will be too small (no correction for extinction having been made), they lead to approximate values of $\theta_3 = 30°$ for both G_1 and G_2. These values might have been roughly anticipated by a consideration of ionic sizes. Conversely, our result may be taken as evidence that the accepted ionic sizes for silicates are applicable to the present crystal. It will be noticed that the provisional set of c-coordinates causes the periodicity of the (0 0 6), (0 0 12), and (0 0 18) planes to be unity. For these planes the waves diffracted from all the atoms in the unit-crystal are in phase. We must now introduce the correction g of Eq. (1) so that our values of $F_{0\,0\,l}$ will contain the correction for extinction. This is done by trial and error, giving various values to g and readjusting the c-coordinates of Al, G_1, and G_2 until the most satisfactory general agreement is obtained between the experimental $F_{0\,0\,l}$ and calculated $F_{0\,0\,l}$ (columns 7 and 8 of Table VIII). In this way we not only can obtain the final set of coordinates given in Table IX, but we also obtain the value of g for use in Eq. (1), *i.e.*, we obtain Eq. (5). This enables us to correct for

* Of these negative ions, R_1 and R_2 lie on the reflecting planes [Wyckoff's coordinates $V_h^{16}(c)$]; G_1 and G_2 are in the general positions [Wyckoff's $V_h^{16}(d)$] in between the reflection planes, each with its own values of the adjustable parameters.

extinction all the experimental data from the other faces and thus complete column 7 of Table VIII. As a result we need from now on to deal with only column 7.*

The Analysis in Detail. The a- and b-coordinates.—The first step, as before, is to fix the a- and b-coordinates (θ_1 and θ_2) of the Al and Si atoms by a consideration of diffracted beams of higher order. The experimental values of F_{1000} and F_{0160} (column 7 of Table VIII) indicate that the x-rays scattered from the positive ions are very nearly in phase. This reduces considerably the number of possible positions for the Al and Si atoms, and the number is still further reduced by a consideration of the weak (800), (0120), and (0180) diffractions and by a consideration of the (101), (202), (303), . . , (909) planes. The ($l0l$) series has a very simple character and is of great assistance in the general analysis. For example, the 4th fraction from the (303) plane is similar to that from the (006) which has almost the same spacing. We know that the rays scattered from the (006) plane are very nearly in phase, so we assume the same to apply to the (303) plane also. By trial, using the above planes in particular, and the ($hk0$) planes in general, the possible positions for the Al and Si atoms can be reduced to a few alternatives.

It remains to decide between these alternatives and to fix the positions of the negative ions, *i.e.*, O and F (or OH). For this purpose it is convenient to consider the projection of the whole structure on the reflection plane since the c-coordinates of all the atoms are known. At the beginning we assumed a tetrahedron of O atoms to surround each Si atom, and this assumption has so far been consistent with the data which we have considered. We shall assume a length of 2.5Å. as the probable lower limit to the edge of this tetrahedron and shall consider the projections of these tetrahedra on the reflection plane. A set of approximate a- and b-coordinates can now be obtained for all the atoms in the unit-crystal by (1) considering in turn the alternative arrangements of the Al and Si atoms and (2) imagining the projected tetrahedra to rotate, in the plane of projection, about the Si atoms in such a way as to account for the more important diffractions [*e.g.*, (303)] when the F atoms (or OH) are placed in the available spaces.†

* If the space-group had been C_{2v}^9 instead of V_h^{16}, there would have been nine parameters to evaluate instead of three. Since it is the c-axis of topaz which some consider polar, Alston and West carried out a quantitative examination of the ($0\,0\,l$) planes assuming C_{2v}^9. They found, within the accuracy of the data, the same arrangement (especially for Al and Si) as that described above, assuming V_h^{16}. They regarded this as further justification for adopting V_h^{16} in the subsequent analysis.

† This rough analysis could have been further facilitated by the assumption of a group of six negative ions systematically arranged about each Al atom or by a frank use of Wyckoff's coordinates. As in the case of diopside, such a procedure would have defeated the purpose of the work, namely, to illustrate as fully as possible the use of the structure factor F_{hkl}.

With this complete, but approximate, set of coordinates before us, it is a comparatively simple matter to readjust the various parameters until the most satisfactory numerical agreement is reached between the observed and calculated values of F_{hkl} (columns 7 and 8 of Table VIII). The final set of coordinates, found in this way by Alston and West, is given in Table IX. They consider that the probable error in Table IX is of the order of 0.05Å.

It appears from Table IX (see also Fig. 13) that four O atoms surround each Si, and four O and two F (or OH) surround each Al. The assumption of an SiO_4 group was made in the preliminary rough analysis, but

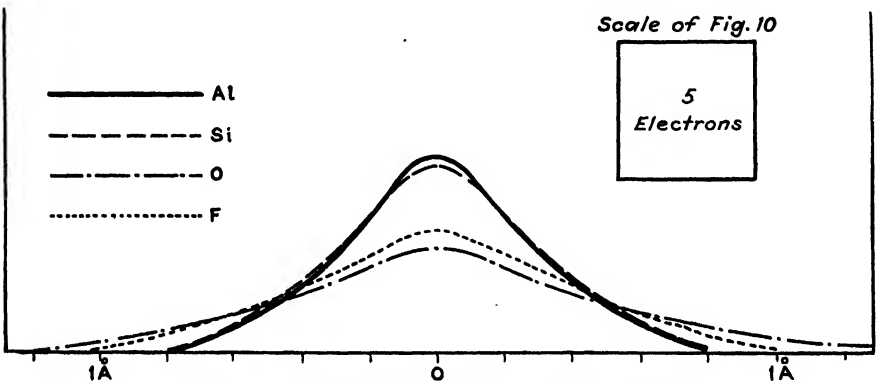

FIG. 10.—Atomic $Zp(z)$ curves for Al, Si, O, and F.

following Alston and West in the detailed analysis we considered the effect of interchanging the O and F (or OH) in order to make our analysis as general as possible. In so far as it is possible in so complex a crystal to distinguish between O and F (or OH) with their similar F curves, it would seem that the original assumption was justified and that the SiO_4 group has a physical existence in topaz.

Fourier Analysis of the (100), (010), and (001) Planes.—Equation (44) of Chap. X was derived for the case of a simple cubic crystal. Since topaz has centers of symmetry, the same equation will apply without change. It is repeated here as Eq. (7) for purposes of easy reference,

$$Zp(z) = \frac{Z}{a} + \frac{2}{a}\sum_{n=1}^{n=\infty} F_n \cos\left(2\pi n \frac{z}{a}\right) \qquad (7)$$

where F_n is the structure factor for the nth order of diffraction from the crystal planes under consideration, a is the interplanar spacing, Z is the number of electrons per unit-crystal, and z is the height, above the mid-plane, at which the electron density is to be determined.

The numerical values of the coefficients F_n are calculated directly from the measured intensities of the diffracted beams (column 4 of Table VIII). The signs of these coefficients are, however, in general not so easily determined; it is usually necessary to have a rough knowledge of the structure from some other investigation. There are three other difficulties which may arise in the application of Eq. (7) to a particular case: (1) In order to avoid false detail in the calculated distribution of electrons, the series should contain as large a number of terms as possible. This was brought out in Fig. 5 of Chap. X. (2) The series should be sharply convergent so as to be applicable within the experimental range. This will normally be the case when the heat motion is large. Where the convergence is not sufficiently rapid, we may make it so by multiplying each term by a factor of the form $e^{-B \sin^2 \theta}$ [see Eq. (18) of Chap. I]; this is equivalent to finding the distribution of electrons at a temperature higher than that at which the experimental results were obtained. This makes the electron distribution appear more diffuse; the atoms seem to occupy larger volumes and the curves which represent the electron distribution are flatter. (3) Since the Fourier analysis gives equal consideration to all the quantitative data, it yields an excellent pictorial summary of the data, provided all the values of F_{hkl} are equally reliable. Unfortunately for some crystals in which the extinction is large and the correction for it uncertain, the F values (and therefore the Fourier coefficients) corresponding to the very strong diffractions are not known so accurately as those corresponding to the weaker diffracted beams. In such cases the Fourier analysis may be a little misleading, and the trial-and-error method used in the earlier discussion of topaz is to be preferred since it treats each diffracted beam individually. Generally speaking, the Fourier analysis of certain crystal planes does assist the investigator to arrive at a more accurate and self-consistent set of parameters by suggesting small alterations in the atomic positions which have already been located approximately by some other method.

Figure 10 gives the atomic $Zp(z)$ curves for Al, Si, O, and F. These curves were obtained by a comparison of the data for topaz with curves for beryl which had been studied previously[7] by means of a Fourier analysis. They represent for each atom the electron density at various distances along a line drawn through the atomic center. Figures 11*a*, *b*, and *c* give the experimental and the best synthetic $Zp(z)$ curves (F curves) for the (1 0 0), (0 1 0), and (0 0 1) planes, respectively, of topaz. We know from the trial-and-error analysis of topaz the approximate positions of the various atoms in the unit-crystal. In the light of this knowledge we can make a suitable distribution, in both number and position, of curves from Fig. 10 along the horizontal axes of Figs. 11*a*, *b*, and *c*. From these we can construct a curve representing their sum. The final set of atomic positions to be adopted is that which gives the

best agreement between the upper pair of curves in Figs. 11*a*, *b*, and *c*. The dotted curves are the synthetic curves; the full-line curves are the experimental curves.

Further details of the Fourier analysis of crystals may be found in articles by W. Duane,[8] R. J. Havighurst,[9,10] W. L. Bragg,[11] and A. L. Patterson.[12]

Discussion of the Structure of Topaz.—Figure 12 shows the structure of topaz as seen along the *a*-axis. The O and F (or OH) atoms are found

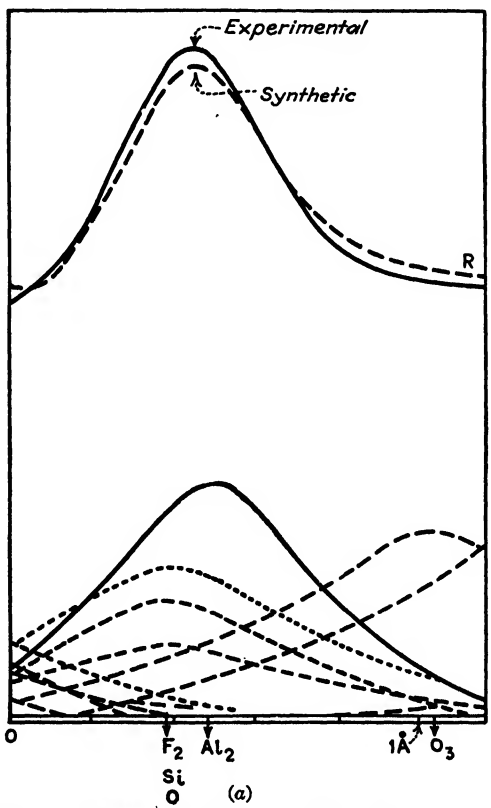

FIG. 11.—(*a*) Calculated and observed $Zp(z)$ curves for (100). (010), and (001) planes of topaz.

to be arranged in a form of close-packing which belongs exclusively to neither the cubic nor the hexagonal type. As in other silicates, each Al^{+++} ion is surrounded by six negative ions, and each Si^{++++} ion is surrounded by four negative ions. Chemical considerations point to a group of four O^{--} ions around each Si^{++++}, and we shall therefore interpret negative ions to mean O^{--} ions. This leaves four O^{--} and two F^{-} (or OH^{-}) ions for the Al^{+++}. The distribution of the Al^{+++} and Si^{++++} in space is such that they are as far apart as is permitted by space-group

V_h^{16}. The structure explains the perfect cleavage parallel to (001) and the less perfect cleavage parallel to (101).

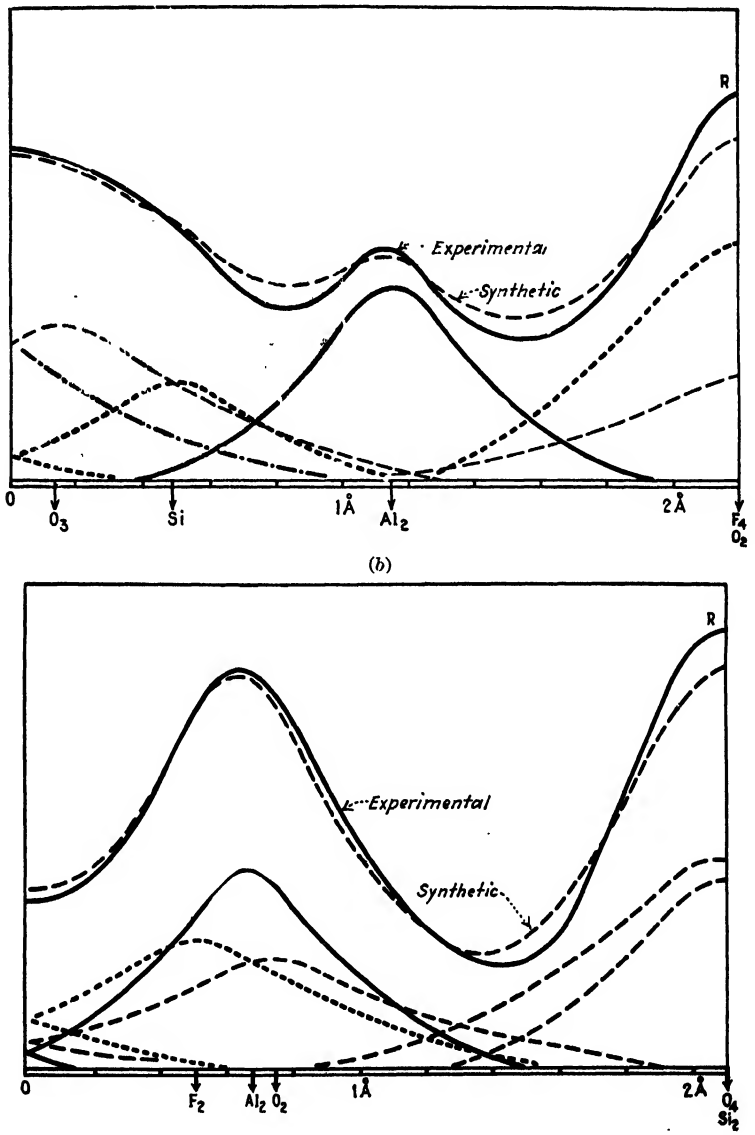

FIG. 11.—(b) (c) Calculated and observed $Zp(z)$ curves for (100). (010), and (001) planes of topaz.

Figure 13*a* shows the configuration of atoms in the hexagonal type of close-packing as viewed along the hexagonal (*i.e.*, *Z*-) axis. Figure 13*b*

shows the corresponding cubic close-packing as viewed along the cube-diagonal. Figure 13*c* shows a close approximation to the topaz close-packing as viewed along the *b*-axis (Wyckoff's *Z*-axis) of the crystal.

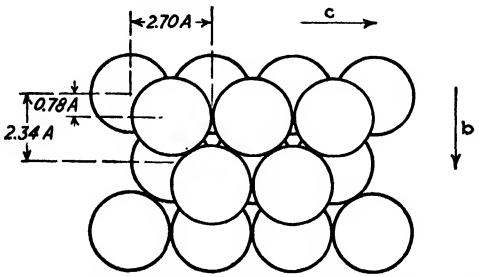

FIG. 12.—Structure of topaz as seen along the *a*-axis.

Figure 13*c* is somewhat "idealized," retaining only those slight distortions which assist in making visible a layer of atoms otherwise hidden. The exact locations of the atoms with respect to each other may be found by reference to R_1, R_2, G_1, and G_2 of Table IX. Certain dimensional

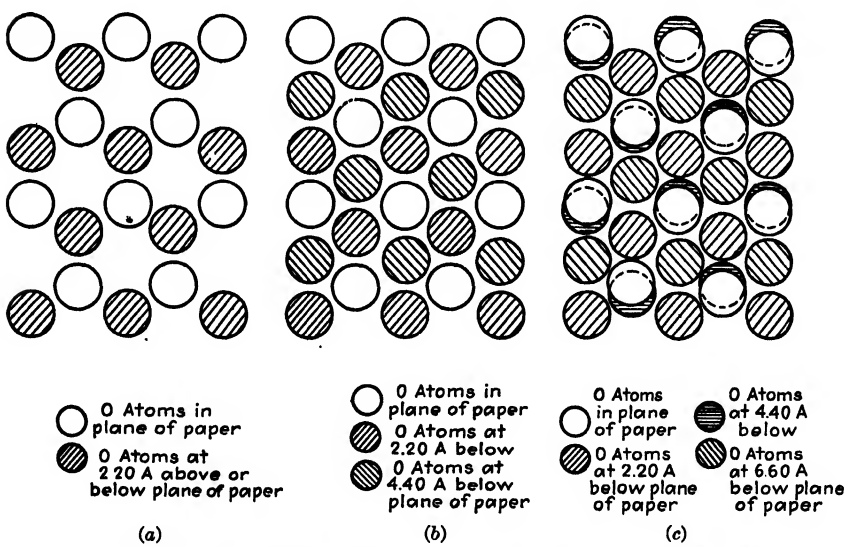

FIG. 13.—(*a*) Hexagonal close-packing; (*b*) cubic close-packing; (*c*) topaz close-packing.

relations applicable to all three figures will be clear from Fig. 12 which represents two layers of O ions (radius 1.35Å.) in close-packing.

A consideration of Figs. 13*a*, *b*, and *c* will show that all three arrangements consist of ordered collections of tetrahedral and octahedral groups of negative ions. It is within these groups that the smaller positive ions (such as Si^{++++} and Al^{+++}) are found in actual crystals. It will be noticed that the individual layers (parallel to the plane of the paper) are identical

in all three cases. The difference between the three figures is to be found in the way in which the successive layers form a sequence. Thus in Fig. 13*a* the planes of atoms are so disposed relative to each other that, beginning with any layer, every *third* layer is exactly under the first [if we look in a direction perpendicular to the layers, *i.e.*, along the hexagonal (*Z*-) axis]. In Fig. 13*b* it is every *fourth* layer that is directly above the first (if we look perpendicular to the layers, *i.e.*, along the cube-diagonal).

In Fig. 13*c* the succession of planes is less simple. If we begin with the layer in the plane of the paper, the first, second, and third layers

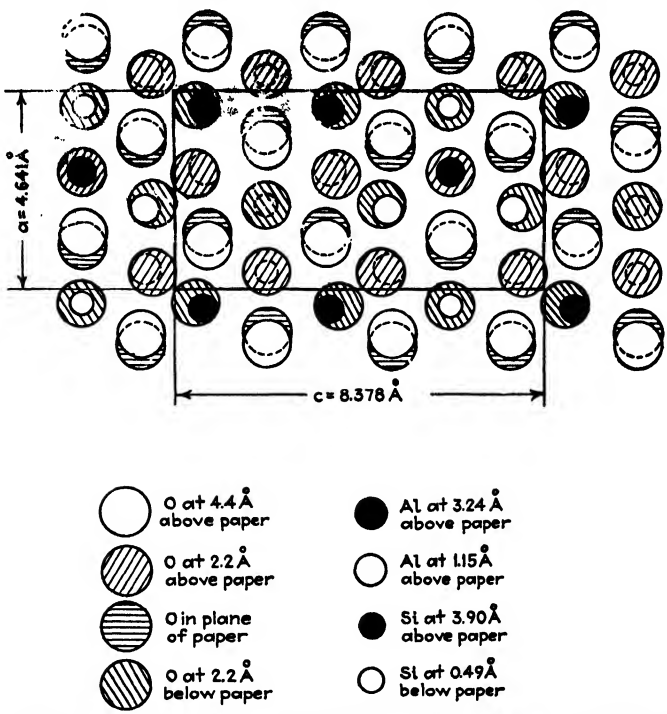

FIG. 14.—Negative ions of topaz. The *b*-axis (Wyckoff's *Z*) is perpendicular to the paper. The distance between layers of atoms parallel to the paper is 2.21A.

below the paper are as in Fig. 13*a*. But the fourth layer departs from the sequence to be expected from Fig. 13*a* in such a way as to cause the second, third, and fourth layers to resemble the arrangement in Fig. 13*b*. The fifth layer again falls under the first, and the series begins again. To some extent, therefore, we may regard the arrangement in topaz as a combination of the hexagonal and cubic forms. We may, however, also regard it as a more complicated form of hexagonal close-packing, for just as the sequence of layers 1, 2, and 3 resembles Fig. 13*a*, so does the sequence of layers 3, 4, and 5. Reference to the symmetry elements

of space-group V_h^{16} shows that there is a screw axis parallel to the b-axis with a translation of $b/2$. It is just this relation that appears between the two sequences.

SUMMARY

We have shown, using examples from the publications of W. L. Bragg and his coworkers, how the structures of even complicated crystals may be found from a knowledge of their exterior symmetries and of the intensities of diffracted beams of different orders from a large number of planes. The structure-factor method is seen to be an extension and refinement of the Bragg method outlined in Chap. V. Of the various possible subdivisions of the method, that of trial and error is apparently the most useful especially in the case of crystals having complicated structures. For such crystals the Fourier series is helpful in increasing the precision to which the various parameters may be determined, after a first approximation has been obtained by trial and error. The use of the Fourier series in determining directly, for simple crystals, the distribution of scattering power (atomic dimensions) will be taken up in Chap. XIII.

References

1. B. Warren and W. L. Bragg, *Zeit. Kryst.*, **69**, 168 (1928).
2. R. W. G. Wyckoff and H. E. Merwin, *Amer. Jour. Sci.*, **9**, 379 (1925).
3. W. L. Bragg and J. West, *Zeit. Kryst.*, **69**, 118 (1928).
4. N. A. Alston and J. West, *Zeit. Kryst.*, **69**, 149 (1928).
5. A. P. Honess, "Nature, Origin, and Interpretation of Etch Figures on Crystals," John Wiley & Sons, Inc., New York, 1927.
6. R. W. G. Wyckoff, Analytical Expression of the Results of the Theory of Space-groups (2d ed.) *Carnegie Inst. Pub.* 318.
7. W. L. Bragg and J. West, *Proc. Roy. Soc.*, **111**, 691 (1926).
8. Wm. Duane, *Proc. Nat. Acad. Sci.*, **11**, 489 (1925).
9. R. J. Havighurst, *Proc. Nat. Acad. Sci.*, **11**, 502 (1925).
10. R. J. Havighurst, *Proc. Nat. Acad. Sci.*, **11**, 507 (1925).
11. W. L. Bragg, *Proc. Roy. Soc.*, **123**, 537 (1929).
12. A. L. Patterson, *Zeit. Kryst.*, **76**, 177, 187 (1930).

CHAPTER XII

THE MECHANISM OF CRYSTAL GROWTH AND ITS CONSEQUENCES

We have seen in Chaps. I, X, and XI the importance of the mosaic structure of crystals. Perfection in single crystals is so rare that we may confidently assume imperfection to be their normal state. It will be of interest, therefore, to examine the various ways in which crystals may be grown in the hope of finding mechanisms of crystal growth which will lead easily to the mosaic type rather than to the perfect type of structure. If any such mechanism is to have real value it must necessitate the existence of demonstrable crystal properties which are distinct from the data which lead to the mechanism. The present chapter deals, therefore, not only with the evidence leading up to a picture of the mechanism of crystal growth but also with the consequences of that mechanism in determining certain of the properties of crystals.

THE GROWTH OF CRYSTALS

There are, in general, four ways of growing crystals: (1) from the vapor, (2) from the melt, (3) from solution, and (4) from less stable crystals in contact with the growing crystal in a continuous solid. We shall take up each of these in turn.

1. Growth from the Vapor.—If the vapor of a substance is allowed to come in contact with a cold surface it will condense to form a solid. X-ray evidence in the case of nickel[1] shows that, if the surface is at a sufficiently low temperature, this solid material is amorphous. If the surface is at a high enough temperature, the solid material is crystalline. It is only rarely in actual practice that vapors are condensed at low enough temperatures to give truly amorphous solid condensates. For each substance we may imagine a critical temperature below which it is almost impossible to obtain a crystalline deposit. The higher the temperature above this limit, the more readily will the deposit crystallize. In the case of nickel the amorphous condensate may be obtained on a surface cooled with water. If the surface is heated to 400°C. a deposit is readily obtained, which is composed of small crystals. An amorphous layer 10^{-5} cm. thick apparently is sufficiently insulating so that the latent heat from further condensation of nickel raises the surface temperature enough to yield crystals.

These facts can be explained if we make three simple assumptions:

a. Atoms of nickel which hit a sufficiently cool surface do not bounce off elastically but remain on that surface. In other words, every atom which hits the surface "condenses." If it evaporates subsequently it must have gained from neighboring atoms enough kinetic energy to overcome the energy of its cohesion to its neighbors. This assumption is identical with that made by Langmuir[2] to explain certain of his data on evaporation and condensation.

b. If the temperature of the condensing surface is low enough, every atom which hits the surface must stay practically in the place where it hits. If the temperature of the condensing surface is high enough, it is assumed that each condensed atom can migrate on the surface like a molecule of a two-dimensional gas until it happens to find some spot where it can help to build up a crystal. In such a spot the potential energy of the atom would be at a minimum and its chance of further migration would be vanishingly small. This assumption is apparently necessary in order to make it possible to grow crystals of nickel in the neighborhood of 400°C. Such temperatures are much too low to permit the evaporation of any appreciable number of atoms from the surface,* so that evaporation alone cannot rid the surface of improperly situated atoms whose locations do not fit the positions demanded by the crystal structure of nickel.

c. When a crystalline surface has once been formed, newly condensed atoms have only to move two or three atomic diameters to find appropriate stations in the structure. If the condensing atoms could be made to impinge uniformly on the crystalline surface, we might expect to grow very perfect crystals. It is, however, inherent in the kinetic theory of gases that the atoms must hit the surface in irregular groups much like the pitter-patter of rain on a roof. Although, on the average, as many atoms will hit on one portion of the surface as on any other portion, we must assume that the distribution from instant to instant will be very non-uniform. This leads inevitably to minute imperfections in the crystals so that what appears at first to be a single crystal is really a mosaic of tiny crystals having almost exactly the same orientation. If we grant this picture, we should expect to grow reasonably perfect crystals from vapor only at exceedingly slow rates of condensation at temperatures close enough to the melting point to permit all imperfections to be wiped out by the migration of atoms within the crystal. Such conditions are not usually found in practice. Even if ideal thermal conditions are realized, minute traces of impurities in the vapor will tend to deposit in patches here and there on the surface

* According to the "International Critical Tables," Vol. III, p. 205, nickel has a vapor pressure of only 10^{-3} cm. of mercury at 1250°C. At 400°C. it should have a vapor pressure of the order of 10^{-16} cm. of mercury.

FIG. 1.—Spectroscopically pure zinc grown from the vapor. (*Courtesy of New Jersey Zinc Company.*)

in layers one molecule (or atom or ion) thick. These layers of impurity will tend to foul the surfaces of the patches, thus limiting the growth of the crystal to small separate portions of the surface.* It would seem, therefore, that, in general, when a crystal is grown from vapor an approximation to the "ideally imperfect" state mentioned in Chap. X is really the normal state of the crystal.

Under exceptional circumstances, not easily controlled in the laboratory, the tendency for some parts of the surface to grow faster than other

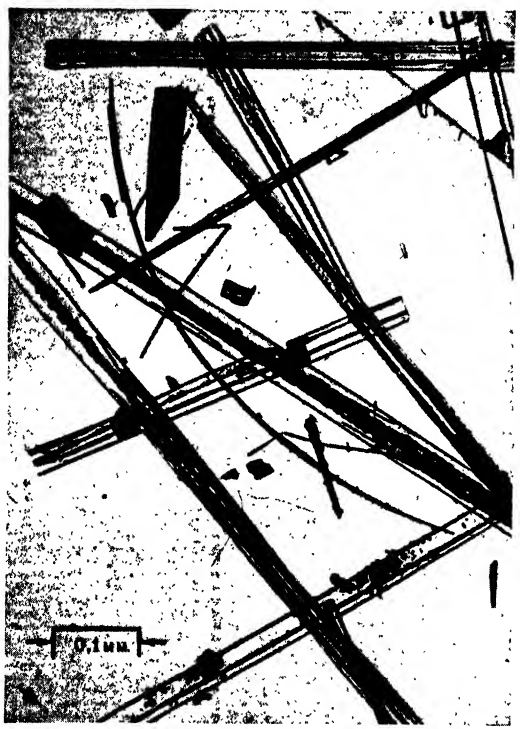

(*a*)

FIG. 2.—(*a*) Special laboratory samples of zinc oxide. (*Courtesy of New Jersey Zinc Company.*)

parts becomes especially great. Macroscopic needles or even finlike projections are sent out in advance of the growing surface. This is illustrated by Figs. 1 to 4 inclusive which were kindly furnished by H. M. Cyr and L. C. Copeland of the Research Laboratory of the New Jersey Zinc Company. Figure 1*a* shows a single-crystal stem of spectroscopically pure zinc grown from the vapor which shows several small fins and two large fins projecting from the sides of the stem. Larger fins are seen projecting from the end. In the original specimen these fins

* A possible mechanism which is capable of explaining this effect will be described later in this chapter.

can be seen to occur at angles which are related to the crystal symmetry of zinc. The angular relationships are brought out more plainly in another specimen of spectroscopically pure zinc shown in Fig. 1*b*. The

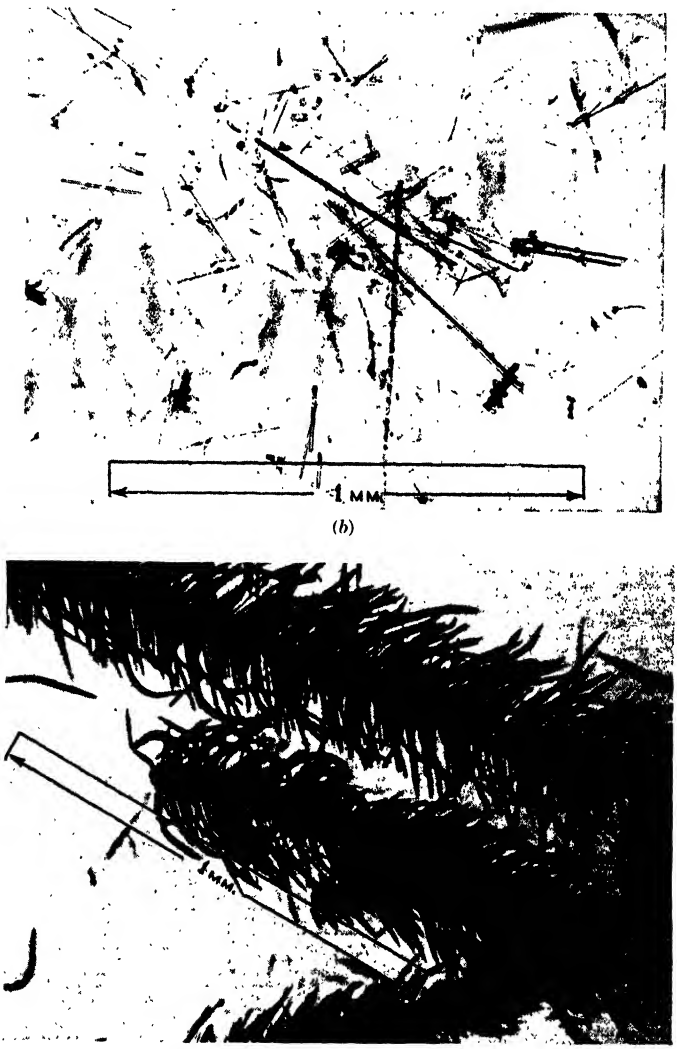

FIG. 2.—(*b*) (*c*) Special laboratory samples of zinc oxide. (*Courtesy of New Jersey Zinc Company.*)

axes of the projections obviously come out from the main stem at angles of 30°. Figure 1*c* shows still another specimen in which the projections come out at angles of 60°. Angles of 30° and 60° are characteristic of the hexagonal close-packed structure of zinc. Figure 1*c* also shows,

growing out from the primary projections, secondary projections of smaller size. The photomicrographs of certain laboratory samples of zinc oxide shown in Figs. 2*a* and *b* show many examples of spinelike growths projecting from the sides of the crystals. Figure 2*c* shows other

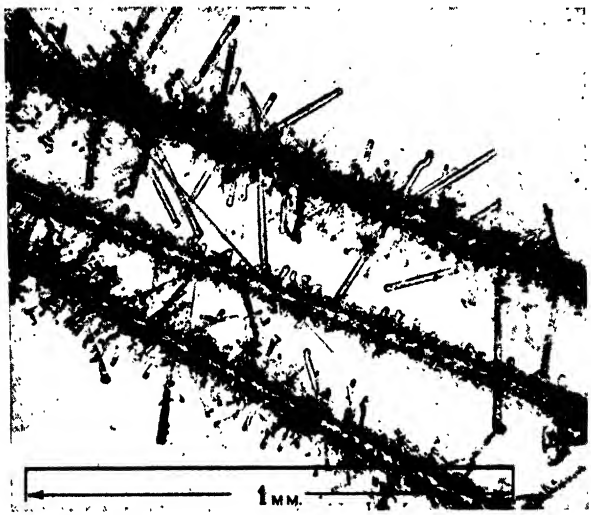

FIG. 3.—Primary and secondary needles on laboratory zinc oxide. (*Courtesy of New Jersey Zinc Company.*)

special samples of zinc oxide with a profusion of needles growing from the main stem. Figures 3 and 4 show primary needles growing on the main stem and the smaller secondary needles growing on the primary needles.

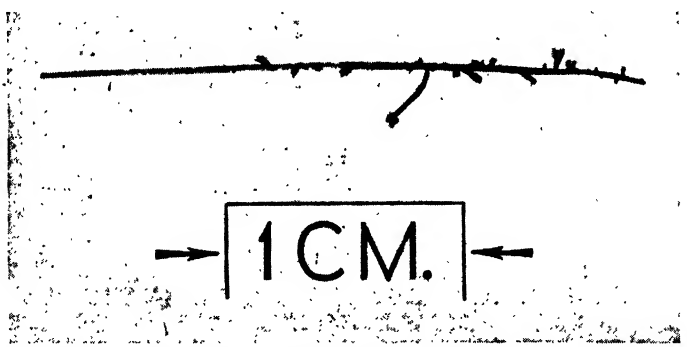

FIG. 4.—Primary and secondary needles on zinc oxide found in the cinder dump. (*Courtesy of New Jersey Zinc Company.*)

These photographs all show special, exaggerated instances which tend to confirm our third assumption. They appear to show on a large scale the consequence of the same sort of "group growth" on a crystal face which the kinetic theory of gases forced us to assume on a submicroscopic scale. Apparently, imperfection is the normal state of a

crystal grown from the vapor. We shall soon see that imperfection is the normal state of all crystals no matter by what process they have been grown.

2. Growth from the Melt.—Growth of crystals from the melt does not take place simultaneously in all parts of the liquid. Either a seed crystal is present and growth proceeds out from this seed, or spontaneous nuclei of crystallization are formed, each of which acts as a seed.

a. We may feel safe in assuming that the molecules* in the melt wander about with almost random motion. This implies that there is a chance of several molecules colliding together in just the configuration to form the beginning of a unit-crystal. In the simplest possible case, if the temperature is high enough, these molecules will have enough thermal energy to part company in spite of the crystal forces holding them together;† *i.e.*, above the melting point the chance of disaggregation exceeds the chance of aggregation. We are tempted at first to assume that below the melting point the chance of aggregation exceeds the chance of disaggregation and that at the melting point the two chances are equal.[3] Closer study of the forces, acting between molecules, shows that this simple picture must be somewhat modified. These modifications are of such a nature as to make it possible not only to account for a sharp freezing point in the presence of a trace of the solid but also to account for the possibility of undercooling in the absence of the solid.

If a seed crystal is placed in a perfectly insulated‡ melt at its freezing point, the crystal will neither melt nor grow. If, however, the heat insulation is not quite perfect, the environment of the melt will act as a slight heat-sink and the seed crystal will grow without any measurable change in the temperature of the melt. This is because molecules which are systematically oriented and marshaled in a crystal are held together by forces which are more or less chemical in their nature. The potential energy of such a system is therefore less than that of a chaotic arrangement such as the melt would have. The energy thus liberated is the latent heat of crystallization and is numerically equal to the latent heat of fusion. It is this energy which must be absorbed by the heat-sink. If *C*

* In this discussion the word molecules will be used as a convenient general term to include molecules, ions, and atoms.

† In growing a crystal from the vapor, a molecule which collides with the crystal surface is held by the forces of cohesion which are characteristic of the crystal. In growing a crystal from the melt, the apparent forces tending to hold the molecules on the surface are equal to the difference between the real forces of cohesion and the forces between these molecules and the surrounding liquid. This difference in the sizes of the resultant forces accounts for some of the differences in the pictures of the mechanisms of crystal growth in the two cases.

‡ The effect of perfect insulation may be obtained by keeping the material around the melt at the same temperature as the melt itself so that the melt neither gains nor loses heat. It is assumed that the melt is somewhat above the room temperature.

represents the cohesive force of the macroscopic seed crystal, L the forces between the liquid and the surface of the crystal, and D the forces tending to disintegrate the crystal due to thermal agitation, then the temperature at which the seed crystal can grow is an infinitesimal amount lower than the temperature for which

$$(C - L) = D \tag{1}$$

For a given material, then, the temperature at which a seed crystal can grow is definitely fixed. This temperature is defined as the freezing point of the melt.*

The difficulty of starting spontaneous crystallization may be explained as follows: Let us consider at first a melt made up of the simplest kind of molecules, for instance, a metal whose molecules are monatomic. In order to form a spontaneous nucleus, several molecules in the melt must collide together in the configuration which is characteristic of the crystal of that substance. In the melt such nuclei are probably made and broken up continually.† In the case of an embryo nucleus made up of only three or four molecules, a given molecule is not held to the group by as many immediate neighbors as would have held it if it has been a part of a "flat" surface of a massive crystal. This means that the cohesive forces of the newly formed spontaneous nucleus cannot be quite so large as the quantity C of Eq. (1). If we define the melting point in terms of Eq. (1), it follows from this picture that, *at the melting point*, the average tendency for disaggregation of spontaneous nuclei exceeds the average tendency for aggregation so that a spontaneous nucleus has no chance of persisting long enough to grow. In order that growth of the spontaneous nucleus may begin, it is necessary to undercool the melt below its freezing point. In other words, we must lower the temperature [and therefore

* Many cases of so-called spontaneous crystallization without undercooling are really started by extremely fine seed crystals which enter the melt from the air. The difficulty encountered in crystallizing anhydrous glycerine (freezing point 17.9°C.) is proverbial; yet the story is told of a laboratory in a cool climate which, having once produced crystals of glycerine, had difficulty in keeping any of its stock fluid. Tutton relates[4] a story told at a meeting of the Royal Society, of how a newly synthesized compound could not be crystallized for several days even under what should have been optimum conditions. After the compound had been manufactured for some time, the air of the laboratory became contaminated with spontaneous nuclei formed from the dust of the dried material and scattered by the daily handling of the material in the laboratory. After these nuclei were formed there was no further difficulty in crystallizing the material. Apparently we must assume that "crystal germs of the most common crystallized substances, of no larger size than bacteria, are floating about in our atmosphere, ready at any time to drop into our solutions and, if the latter are in the proper receptive condition, to set them crystallizing."

† This picture is consistent with the data on the diffraction of x-rays by liquids (see Chap. XVI).

the value of Φ of Eq. (1)] until the nucleus can persist long enough for some other molecule to collide with it at some point so close to the correct spot that the molecule can migrate easily to its proper location. According to this picture a thoroughly melted liquid cannot crystallize spontaneously unless it is cooled below its freezing point. The amount of undercooling necessary should be a property of the substance to be crystallized.

The case of less symmetrical molecules, such as those of organic substances, is complicated by the additional consideration that, in order to form a spontaneous nucleus, several molecules must not only collide to form the correct configuration of *molecules*, but their orientations must be such as to give also the correct configuration of *atoms*. Such a restriction greatly decreases the chance of forming spontaneous nuclei and therefore tends to decrease the concentration of nuclei in the melt. This effect may be partly compensated by the longer life of the nuclei, caused by the increase in resistance to disaggregation resulting from the large number of atoms which serve as points of attachment between molecules in a nucleus. At first sight it would seem that the net effect of these two opposing tendencies should largely determine the amount of undercooling possible for a given substance. It is conceivable, however, that not only in complicated substances, but even in simple substances like metals, the resistance to disaggregation may be so strong as to bring in still another effect. When a material is melted without raising the temperature perceptibly above the melting point, small crystal fragments the size of spontaneous nuclei may slough off from the crystal and float around in the melt for long periods.* The effect should be that of greatly increasing the concentration of nuclei and thus of promoting crystallization of the melt at the freezing point when the proper heat-sink is brought into play. This increase in concentration of effective nuclei should increase the chance of a molecule from the melt colliding with a nucleus at the proper place and with the proper orientation. In other words, it should be difficult to undercool a material which has been

* This hypothesis is consistent with the experimental results of A. Goetz.[5] He found that the orientation of single crystals of bismuth, grown from a single seed in the melt, depends upon *orientation of the portion of the seed which has just melted* rather than upon the orientation of the unmelted portion. This effect disappears when the bismuth is heated 10°C. above its "melting point." It is as though the "melted" portion of the seed contained sloughed-off crystal fragments from the mosaic. A. Mueller [*Proc. Roy. Soc.*, **127**, 417 (1930)] directed a fine beam of x-rays on some molten paraffin very near the surface of a crystal of the same substance. For a small range of temperature above the melting point the diffraction pattern showed that there was still a considerable amount of orientation among the molecules. Apparently the crystal dissolves in "sheets" of molecules. It is interesting to note, too, that Traube and v. Behren have found[6] that, when a crystal is dissolved into an almost saturated solution, ultramicroscopic particles can be found which persist for some time before being dissolved to a true molecular dispersion.

melted, without raising the temperature appreciably above the melting point. If, however, the liquid is strongly heated to bring it considerably above the melting point, the sloughed-off crystal fragments should all disintegrate, thus bringing down the concentration of effective nuclei to the normal value for that material. In view of the difficulties in crystallization caused by the necessity for molecular orientation, the reduction in the concentration of nuclei by heating should greatly increase the possibility of undercooling.*

It is evident from the above discussion that, except for mechanical inclusions, impurities can be included in the body of the crystal, only if the size and shape of the molecules of the impurity are such as to permit them to fit easily into the structure of the crystal and if, besides, the chemical forces between the crystal and the impurity are at least equal to C of Eq. (1). This will be taken up more fully in Chap. XVIII. It will be sufficient for our present purposes merely to point out that the ordinary practice of purification of materials by slow crystallization of a part of the melt is consistent with the picture of crystallization which we have presented here. It is a consequence of the picture that, if a melt is cooled slowly enough from one end, the impurities tend to concentrate in the last portion to crystallize. If crystallization proceeds too rapidly, so that crystal nuclei appear throughout the whole body of the liquid, then the impurities must concentrate at the grain boundaries. If crystallization is still more rapid, some of the impurities must concentrate at the boundaries of the mosaic of which each macroscopic crystal is composed. These predictions from the theory are consistent with the results of metallurgical practice.

b. Now that we have seen, both in the case of a seed crystal and in the case of a spontaneous nucleus, how crystallization starts, we must take up the manner in which the seed or the nucleus grows to form a finished crystal from the melt. The following experiment[9] will serve as an illustration of the process. A test tube is filled with lump photographic hypo ($Na_2S_2O_3.5H_2O$) and is heated over a bunsen burner to melt the hypo. With a little practice this can be done without losing much of the water of crystallization. At first the molten hypo will appear cloudy, but in a few seconds a clear transparent liquid is obtained. A large watch glass is warmed by dipping it into boiling water and is then quickly mounted so that it can be illuminated properly from below. The molten hypo is poured into the watch glass, and a single crystal of hypo is

* This picture is really a detailed expansion of that given by Othmer[3] and Tammann.[7] Another picture given by Richards[8] differs from this primarily (*a*) in substituting a foreign adsorbent for the crystal fragments sloughed off from the melting solid and (*b*) in substituting a portion of the melt adsorbed on the foreign adsorbent for the oriented molecules which we have pictured as colliding with the crystal fragments or with true spontaneous nuclei. In both these pictures the forces called into play by orientation take the whole matter out of the field of thermodynamics.

immersed in the melt at the center of the watch glass. It is best to handle this single crystal with warm, chemically clean, dry tweezers. Very soon small needles will be seen projecting out from the surface of the crystal. Under favorable conditions of illumination it may be seen that these needles lie in three directions which are definitely oriented to the axes of the crystal. They tend to form a three-dimensional meshwork with liquid hypo in the interstices. If the volume of material, rate of cooling, and conditions of illumination are all favorable, these needles may be seen to grow still other needles on their sides so that the original meshwork becomes the frame for a very much finer meshwork.

It is easy to imagine[9] this process repeating itself to give a whole succession of such meshes each finer than that from which it is hung, so that we are tempted to assume the existence of an ultimate three-dimensional meshwork of such fineness that it could not be seen even with a microscope. Eventually the whole mass of liquid becomes crystallized, and, if the conditions of the experiment have been favorable, a large "single" crystal of hypo is obtained. When we remember the marked changes in volume which most materials undergo in solidification, we are led to assume that the last traces of liquid to crystallize out must yield solid material which is under considerable strain. These strains may even be thought of as distorting the fine meshwork so as to change slightly the orientation of the tiny crystal fragment which this meshwork encloses. This distortion will, of course, be increased by the sharp temperature gradients due to the local liberation of the latent heat of solidification. Such a picture leads us at once to the conclusion that crystals grown at any reasonable rate from the melt must have a mosaic structure and that an approximation to an "ideally imperfect" state is really the normal state of such a crystal.

It is to be expected that, for very slow rates of crystal growth, the space between the primary needles will be filled in with solid crystal almost as rapidly as the needles grow, so that the needles should be practically obliterated. We should, therefore, expect crystals grown very slowly from the melt to appear as smooth-faced polyhedra. If the rate of growth of the primary and secondary needles is in excess of the rate of growth of crystals from the intervening melt, then the crystals should grow as dendrites. We should therefore expect a dendritic structure in crystals grown rapidly from the melt. Both these predictions are consistent with ordinary experience.

For most materials, even if large ideally perfect single crystals could be grown easily from the melt, they would probably not stay perfect. This may be illustrated by the case of some single crystals of copper grown by the author from the melt in an atmosphere of hydrogen. The crucible containing the molten copper was lowered very slowly (0.005 in. per minute) through a vertical furnace 2 ft. in length. Each

part of the newly formed crystal was therefore kept very near to its melting point for a long time, thus giving it every chance to be as perfect as possible. Copper crystals about the size of a lead pencil, formed in this way, could hardly support their own weight when held horizontally from one end. The act of deformation changed the bent portion of the rod from a single crystal to a multitude of small crystals each having a mosaic structure.

The ease with which these single crystals of copper can be deformed is also shown by the following. The crystal axes of a somewhat larger specimen were determined by x-ray methods (see Chap. XVII), and the crystal was then slowly sawed by hand and carefully dressed up with a fine file so as to give it faces corresponding to the cube faces of the crystal. Care was taken throughout the whole procedure to keep from bending or deforming the specimen. Only light cuts were taken so that the distortion of the interior should be a minimum and so that there should be no appreciable temperature rise due to too rapid expenditure of energy. After the cube faces had been put on the specimen in this way further x-ray tests were made to check the correctness of the faces. The surface of the specimen was found to be polycrystalline. The specimen had to be etched off to a depth of $\frac{1}{16}$ in. before x-ray evidence could be found that the remainder was a single crystal. That the effect is not confined to soft metals like copper may be shown by the fact that, before the author could determine the orientation of a polished slab cut from a quartz crystal, it was necessary to etch off the thin polycrystal surface which had been formed by the polishing operation. It is evident that only in the case of the most rigid materials can we hope to grow from the melt approximations to ideally perfect single crystals and maintain them as such.

Probably the reason why the three most perfect crystals reported in the literature (see Chap. I) are samples of diamond and calcite lies in the extraordinary rigidity of one and in the mechanical protection afforded the other by Nature. Most natural crystals either have grown under such conditions as to favor the mosaic type of structure or have been subjected to geologic forces which have introduced imperfections by mechanical means.

3. Growth from Solution.—*a.* Figure 5 is a schematic temperature-concentration diagram for a typical solution. The solubility curve connects points at which "saturation" is found. If the temperature and concentration of such a solution are such as to give a point on the solubility curve, then a crystal of the solute suspended in the solution will neither grow nor dissolve. If the temperature and concentration of the solution are changed to correspond to a point situated to the right of the solubility curve, the crystal will dissolve. If the temperature and con-

centration are made to correspond to a point at the left of the solubility curve, the crystal will grow at the expense of the solute in the solution. If no seed crystal is allowed to enter the solution, it may be cooled to a second temperature-concentration condition shown by the "supersolubility curve." Passing to the left of this curve, crystallization proceeds spontaneously and the crystals come down in a "labile shower," corresponding to the familiar "precipitate" of the analytical chemist.

The situation is exactly like that described for growth from the melt, except that the presence of a solvent introduces the concentration of the solution as a variable along with the temperature. Bearing this slight complication in mind the theory of growth of crystals from the melt can be translated directly into a theory for growth from solution. The saturation curve connects freezing points of the solute at various concentrations. The supersolubility curve connects temperatures of maximum undercooling of the solute at various concentrations. Solution therefore becomes almost synonymous with melting, precipitation with freezing, and supersaturation with undercooling. In dealing with solutions, however, we cannot speak of the freezing point or melting point of the solute alone; we must regard the temperature of saturation as representing the freezing or melting point of the solute *dispersed in contact with solvent* in a solution of some definite concentration. We must similarly restrict our statements in connection with supersaturation.

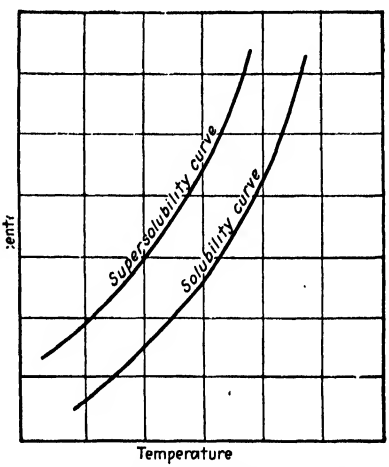

FIG. 5.—Temperature-concentration diagram of a typical solution.

There is every reason to believe that the mechanism of crystal growth from solution corresponds almost exactly to that described for growth from the melt. The growth of needles from the surface of the seed is, however, only an assumption in this case. The assumption is based on analogy with crystallization from the melt and does not necessitate needles large enough to be seen with the microscope. This picture leads us, then, to the conclusion that imperfection is the natural state for a crystal grown from solution, even when it is grown at a reasonably slow speed. Probably natural crystals of calcite, requiring thousands of years to grow, represent the closest possible approximation to ideally perfect crystals that can be grown from solution.

b. We are accustomed to the fact that the unbalanced forces at the surface of a droplet of liquid have a component parallel to the surface so

that they tend to give the droplet a spherical shape. Even when the surface tension is very small, the surfaces of droplets of ordinary liquids are rounded because these liquids have no rigidity of shape. In the case of a crystal in contact with the melt, either the surface forces or the rigidity, or both, may have large values. If the strength of the crystal is in excess of the strength of the surface forces the crystal will be polyhedral in shape. If the strength of the crystal is less than the strength of the surface forces, the crystal must have a rounded exterior. The interfacial tension between the solid and the melt does not necessarily decrease with temperature at the same rate as does the strength of the solid material. The result is that in some cases the same material may assume a polyhedral or a spheroidal form depending upon the temperature at which the crystal is grown. In such cases the required freezing temperature may be obtained experimentally by crystallizing the material from a solution. For instance,[10,11] if copper is crystallized from a copper-bismuth melt containing 50 per cent copper by weight, most of the copper crystallizes out between 900° and 800°C. If the melt contains only 25 per cent copper, most of the copper crystallizes out between 800° and 700°C. Still lower concentrations of copper in solution in the bismuth crystallize out at still lower temperatures. The interfacial tension between the solid copper and the melt decreases so much more slowly with temperature rise than does the rigidity of shape that copper crystals grown from the 50 per cent solution all have rounded exteriors (see Fig. 6). The 25 per cent solution yields a large number of copper crystals with polyhedral exteriors and a few with rounded exteriors. Still lower concentrations of copper yield nothing but polyhedral forms. Similar results may be shown by crystallizing beryllium from silver[12,13] or aluminum[12,14] or FeSi from iron.[10,15] Surface effects such as have been described will certainly increase still further the tendency toward a mosaic structure in a crystal grown from solution.

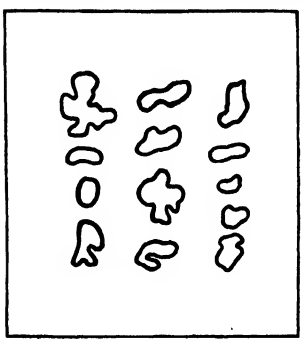

FIG. 6.—Typical rounded outlines of copper crystals grown from a bismuth solution at 800 to 900°C. Others may be found on p. 31 of reference 8.

c. Von Weimarn[16] has shown that the size of the crystals obtained by spontaneous crystallization from pure solutions is a function of the solubility, degree of supersaturation, and viscosity of the solution. Let S represent the solubility of the solute, let P be the degree of supersaturation (*i.e.*, the number of gram-molecules of the solute which must be removed from 1 liter (l.) of solution to reduce it to saturation), and let η be the coefficient of viscosity of the solution. Then the perfection and particle size of the crystals of precipitate are determined by the dispersion coefficient δ, which is defined by the equation

$$\delta = \frac{P}{S^{\eta}} \qquad (2)$$

When δ is very small, crystallization is very slow and the crystals would probably be very perfect. The time required to grow a sizable crystal would, however, probably be measured in geologic units rather than in hours or days. When δ is very large, the number of spontaneous nuclei is so great that practically the whole solute is in the form of nuclei and the mass forms a so-called "amorphous jelly." This is illustrated in Table I which gives some of v. Weimarn's results on $BaSO_4$ precipitated from mixtures of aqueous solutions of barium thiocyanate and manganous

TABLE I.—EFFECT OF δ ON NATURE OF $BaSO_4$ PRECIPITATE

Equivalent concentration of reagents	P, grams per cubic centimeter	δ	Nature of precipitate
0.00005–0.0001	0–0.0006	0–3	No visible precipitate in a year. Microcrystals expected after several years
0.00014–0.0017	0.0006–0.0096	3–48	Slow precipitation at $\delta = 8$ Suspension stage at $\delta = 25$ Complete separation in months to hours
0.0017–0.75	0.0096–4.38	48–21,900	Precipitation in a few seconds at $\delta = 48$ Instantaneous precipitation with crystal skeletons and needles at $\delta > 48$ At $\delta = 21{,}900$, crystals so small as to be barely visible
0.75–3	4.38–17.51	21,900–87,500	Immediate formation of so-called "amorphous precipitate"
3–7	17.51–40.9	87,500–204,500	Clear jelly

sulphate. The greater the degree of supersaturation, *i.e.*, the faster the precipitation of solute, the more nearly do we approach the amorphous-jelly type of precipitate. Since the amorphous jelly has almost none of the characteristics which we associate with a crystal we may make the generalization that the faster a solute is precipitated the less perfect the crystals will be. It would seem from Table I that even for reasonably slow speeds of crystallization in the laboratory, imperfection is the normal state of a crystal.

4. Growth in Solids.—*a.* It is inconceivable that two crystals having different orientations should meet in the body of a solid without having at the interface a thin layer of molecules whose positions represent a compromise between the locations demanded by one of the crystals and those

demanded by the other. This thin semidisorganized layer is the crystal analyst's substitute for the "amorphous intercrystalline cement" which has been postulated by many metallurgists.* This conception of a semidisorganized intercrystalline layer leads at once to a picture of the mechanism of the growth of a crystal in a pure solid at the expense of its neighbors. In order that crystal growth may occur in a pure solid it would be necessary for one of the crystals to align the molecules† of this intercrystalline layer according to the pattern set by its own orientation. This in turn would produce a new intercrystalline layer which would have to be formed at the expense of the less favorably oriented crystal. The molecules of this newly disorganized layer would then have to be aligned to conform to the pattern of the growing crystal and the whole cycle would have to be repeated over and over again until the less favorably oriented crystal disappears.

In ordinary metallurgical practice it often happens that a mass of metal is heated to encourage crystal growth. It is not often that solid crystalline materials of this sort are pure enough for the simple mechanism which we have just described to represent the actual facts. We have seen that when substances crystallize from a melt, the "insoluble" impurities tend to crystallize last, *i.e.*, they tend to collect at the intercrystalline boundaries. It is obvious that these impurities will tend to form a mechanical barrier to crystal growth.[10] To form such a barrier the amount of impurity need be only an extremely small percentage of the total, for it only has to be well scattered through a thin layer at the crystal boundary. In terms of this picture, in order to enable a crystal of a material of ordinary over-all purity to grow at the expense of its neighbors, two conditions must be fulfilled: (1) the intercrystalline boundary must be punctured in some way in order to bring pure crystals in contact with each other, and (2) the mass must then be heated above some characteristic temperature range such that the molecules in the punctured areas become mobile enough to align themselves in accordance with the demands of the crystal which is to grow. This is consistent with the ordinary metallurgical experience that crystal growth in metals is facilitated by hammering, swaging, or passing the metal between rolls, followed by heating the deformed metal above some characteristic temperature. Mechanical working cannot destroy or remove the impurities from an intercrystalline layer; it can only

* Since the potential energy of the atoms or molecules in such a disorganized layer must be greater than the potential energy of the systematically arranged atoms of a crystal, it is to be expected that etching reagents will, in general, strongly attack the intercrystalline boundaries. This offers at once a rational explanation for many of the facts of intercrystalline corrosion.

† In the case of most metals, the word "molecule," as used here, becomes synonymous with "atom."

change the distribution of the impurities so that here and there the layer is punctured. The invading crystal therefore cannot advance along a continuous front but must be thought of as sending out needle-like shoots or sprouts through the punctured portions of the intercrystalline layer. The spaces between these needle-like projections must be filled in as well as possible by realigning the molecules of the invaded crystal through growth from the sides of the needles. Such a picture is so nearly like that which we had for the growth of crystals from the melt that we feel justified in the conclusion that imperfection is the natural state of crystals grown in mechanically deformed solids. This conclusion is consistent with the ordinary experience of crystal analysts.

b. Certain materials show allotropic forms, *i.e.*, they exhibit more than one crystal form, each one of which is stable over a definite temperature range. A familiar example is the case of high-purity iron which changes reversibly from the face-centered cubic γ form to the body-centered cubic α form at 903.5° ± 2°C. X-ray examination fails to show any amorphous range between the high- and low-temperature forms of an allotropic material. This must mean that allotropic changes do not require molecules* to move past each other. Small motions of translation, sometimes accompanied by motions of rotation of the molecules, must be sufficient to enable an allotropic substance to change from one of its crystal forms to the other. This condition appears to be always fulfilled. The case of γ- and α-Fe will serve to illustrate the point. It was stated in Chap. II that a body-centered cube may be considered as a face-centered tetragonal prism with an axial ratio of $1/\sqrt{2}$. The face-diagonal of the body-centered cube becomes the edge of the base of the face-centered tetragonal prism. The altitude of the body-centered cube is identical with the altitude of the face-centered tetragonal prism. It would be natural to assume that this would offer a mechanism for the transition. There is, however, still another way by which the transition may be made from a face-centered to a body-centered cube, and it turns out that this second way gives a structure which has less potential energy than the first.

R. F. Mehl and D. W. Smith have shown[17] that when γ-Fe changes to α-Fe the (1 1 0) planes of the α-Fe form parallel to the (1 1 1) planes of the γ-Fe, and that the [1 1 1] direction in the α-Fe coincides with the [1 1 0] direction of the γ-Fe. Inspection of a model of a face-centered cube shows that its (1 1 1) planes are composed of equilateral triangles. The sides of these equilateral triangles lie in the [1 1 0] directions. In γ-Fe the length of the sides of the triangles is about 2.55Å. at the transition temperature. Inspection of a model of a body-centered cube shows

* For purposes of brevity the word "molecules" will be used here to represent not only true molecules and the atoms of metals but also ions such as the CO_3^{--} ion in calcite and aragonite or the NH_4^+ ion in ammonium chloride.

that its (1 1 0) planes may be considered to be made up of isosceles triangles whose bases lie in the [1 0 0] direction and whose legs lie in the [1 1 1] directions. One of the legs of each isosceles triangle in α-Fe must therefore coincide in direction with one side of an equilateral triangle of the parent γ-Fe. In α-Fe the length of the legs of the isosceles triangle is about 2.51Å. at the transition temperature. The base of the triangle is about 4.10Å. The transition from γ- to α-Fe is therefore accomplished with only a negligible motion of two out of three atoms at the corners of each triangle. The third atom has to move a distance which is of the order of one atomic diameter. Evidently any mosaic structure in the original crystal has a good chance of persisting in the new crystal. Indeed, there should be a good chance that additional strains would form which would even cause new crystal boundaries so that the new crystals would, in such cases, be smaller in size than the old crystals. Such a break-up of crystals during allotropic change (as from γ- to α-Fe) is of common occurrence in metallurgy.

c. In metallurgical work it frequently happens that substance B may be "dissolved" in solid solution in substance A above some definite temperature, but below that temperature individual solid phases separate out which are either A and the ionic compound A_xB_y or a solid solution of B in A and a solid solution of A in B. This involves much greater atomic motion than the processes which we have so far considered. Obviously atoms of B can travel through the body of the metal only by taking advantage of interstices between the atoms of A. It cannot be assumed that the compound A_xB_y, as such, travels through the metal; the interstices between atoms of A are hardly large enough, even at high temperatures. The effect of travel of A_xB_y can, however, be obtained solely through the migration of B plus slight motions of the atoms of A. It will be shown in Chap. XVIII that there is good reason for assuming all the atoms of B in a solid solution to be combined with A to form "molecules" of the ionic compound A_xB_y. It will be shown, too, that the apparent migration of A_xB_y can be accounted for if we assume that, when each B^- ion* migrates, it returns the valence electron which it has borrowed from an adjacent atom of A on one side and that it borrows a valence electron from another atom of A on the other side. Each ion of B^- is thus always a part of an ionic "molecule" of A_xB_y, but it is not always combined with the same A^+. In this way, although only ions of B^- travel through the metal A, each one is at any instant a real part of some "molecule" of A_xB_y. If this picture is accepted, a discussion of the effect of migration of the B^- ion will, in general, serve to explain both the formation of crystals of A_xB_y and the formation of crystals of solid solution A-in-B, or B-in-A.

* This statement is worded in terms of B being the negative ion. The changes in wording when A is the negative ion will be obvious.

It is evident that, if an ion B^- is to move from the left side to the right side of an atom (or ion) of A, (1) the heat motion must happen to cause all the atoms (or ions) of A lying to the right of B^- to move simultaneously away from each other, leaving a hole through which B^- can pass, and (2) at the same time the heat motion of B^- must happen to move it in the direction of the hole.* The number of accidental opportunities of this sort per second will decrease as the temperature is decreased, partly because the average motion of the atoms is slower, and partly because a smaller fraction of the openings formed will be large enough in diameter. If, in their random wanderings, two ions of B^- find themselves in the correct configuration with each other and with the ions of A to conform to the crystal structure of A_xB_y, then, if this configuration represents a decrease in the potential energy of the system, the configuration will tend to be stable enough to persist. If now a third ion of B^- migrates to the correct position with respect to the other two, the configuration tends to become still more stable. This process is repeated until a crystal of A_xB_y is formed. It is not to be assumed, however, that this crystal will be "perfect." Its very method of formation involves the chance of atoms of A being enclosed as impurities in the crystal, thus causing local distortions which would give the effect of mosaic structure. If the configuration of A_xB_y does not represent a sufficient decrease in the potential energy of the system, ions of B^- will tend to migrate off until they happen to meet other ions of B^-. If the resulting crystal† of B represents a decrease in the potential energy of the system, the crystal will tend to be stable enough to persist and it will grow if other ions of B^- happen to migrate to it. Since the migration of both A and B will be haphazard, the crystal of B will not be entirely free of A. Stray atoms of A may become enclosed mechanically in the crystal of B. These will exist as ions of molecules of A_xB_y so that what we have called a crystal of B is really a crystal of a "solid solution of A (*i.e.*, A_xB_y) in B." Similarly, laggard ions of B^- will be left enclosed as A_xB_y in a "solid solution of B (*i.e.*, A_xB_y) in A." This picture is consistent with ordinary metallurgical experience. It will be shown in Chap. XVIII that these dissolved ions will introduce enormous strains in the crystal. These highly localized strains can only result in a mosaic type of structure.

SECONDARY CRYSTAL STRUCTURE

We have now discussed the various important methods of crystal growth, and in every case we have come to the same conclusion, namely, that imperfection is the natural state of a crystal. We have seen that,

* See Chap. XVIII.

† When such energy conditions exist, then if two B^- ions meet, each must return its extra valence electron to A so that atoms of B exist in contact with each other.

for crystals grown from the vapor or from the melt,* these imperfections may be pictured as being due to the formation of a skeleton of needle-like growths which is later filled in with solid crystalline material. We must now try to find, in the very nature of the crystalline state, (1) some reason for the existence of such a skeleton and what its probable spacing is, and (2) the effect of such skeletons on the physical properties of crystals.

1. The Nature of the Skeletal Structure (Zwicky "Pi" Planes).—We need first to satisfy ourselves that there are spots on the surface of a crystal from which growth may take place with comparative ease. The following line of reasoning will show that this is indeed the case. We have already seen that surface-tension effects are present in crystals. Estimates of internal pressure and measurements on the surface tension of molten metals and molten salts at their freezing temperatures lead us to believe that these surface-tension forces in crystals are very large. We have seen that these forces may even be large enough, under the proper circumstances, to force a crystal to abandon its polyhedral shape in favor of a spheroidal shape. The surface of a crystal must therefore be assumed to be under a heavy stress. It is inherent in the very nature of surface tension that this stress must decrease with the depth below the surface. Consider, for purposes of illustration, a minute seed crystal of an alkali halide such as NaCl.† The surface tension must tend to bring the surface Na^+ and Cl^- ions closer together on the cube face, thus decreasing the lattice parameter at the surface. Evidently, the surface cannot contract as a whole, for, since the effect decreases with the depth below the surface, the smaller lattice parameter of the top layer would bring, at definite intervals, an ion in the top layer directly above an ion of the same sign in the next lower layer. Such an impossible situation would be avoided if the surface were contracted in patches of substantially the same size, with crevices separating the patches. The linear size L of such a patch can be calculated by the method of Zwicky[18] as‡

$$L = 100\frac{a_0}{\gamma} \tag{3}$$

* We have seen that there is good reason for assuming this same picture to hold also for growth from solution. Growth from the solid comes into the present discussion only to a minor extent, for the original crystals in the solid were formed either from the vapor, or from the melt or from solution.

† The picture given here may be generalized so as to apply to a metal by assuming the valence electrons to occupy positions in the crystal structure. The positive metallic ions would correspond to the Na^+ ions and the valence electrons would correspond to the Cl^- ions. It will appear in later chapters that this sort of picture has considerable justification. Of course each substance will have its own characteristic dimensions for its crevices.

‡ These calculations are identical with those made by Zwicky (*loc. cit.*) in the course of a much less detailed discussion. The reader is referred to Zwicky's articles in the *Physical Review* and in the *Proceedings of the National Academy of Sciences* for a presentation of his point of view.

where a_0 is the length in Ångströms of the edge of the unit-crystal of NaCl and γ is the percentage of contraction in the lattice parameter at the surface. Zwicky has shown[19] that, when a crystal of NaCl is put under tension along its length, it suffers a lateral contraction which may be as large as 5.4 per cent. (Lennard-Jones has shown[20] that the lateral contractions of all the alkali halides are of the order of 6 per cent.) We shall assume, therefore, that the stress perpendicular to the surface of our seed crystal of NaCl is accompanied by a contraction γ at the surface of 5.4 per cent of the normal lattice parameter. Then Eq. (3) becomes

$$L = 100\frac{5.6}{5.4} = 100\text{Å., approx.} \tag{4}$$

That is, if the surface of a newly deposited film of crystalline NaCl is to avoid having ions of the same sign directly over each other, it must be broken up by crevices which are not more than 100Å. apart. Since there is no reason why these crevices must be closer together, we shall assume that they have a substantially regular spacing of about 100Å. Such a surface should be one possessing minimum free energy.

Crevices of this sort will extend into the crystal to a rather definite depth which we assume to be that at which the surface tension effect is no longer detectable. This depth may be calculated for NaCl as follows:[18] Let ϵ be the decrease in surface energy due to the contraction in 1 sq. cm. of surface. Then if the area of a single patch is S, the decrease in energy associated with the contraction is $S\epsilon$. Let S' represent the area of surface in the crevice which is formed at the expense of the energy $S\epsilon$. Then, since the energy used up in making the crevice must come from the surface energy, we have

$$S\epsilon = S'\sigma$$

where σ is the surface tension of the NaCl. Calculation on the basis of the ionic nature of NaCl gives ϵ a value of about 220 ergs per square centimeter. The related value of σ for solid NaCl is found* to be 156 ergs per square centimeter. If we assume that the surface tension decreases uniformly with the depth below the surface, we have an *average* value $\sigma/2 = 78$, so that $220S$ must equal $78S'$. Within the precision of the calculations we may say that $S = \frac{1}{3}S'$. Now the length L of one side of a patch was found to be about 100Å., so that $S = (100)^2$ sq. Å. Since there are four crevice surfaces per patch, the total length of the

* $\sigma = 0.12\frac{e^2}{a_0{}^3}$, where e is the electronic charge and a_0 is the lattice parameter of the crystal of NaCl. Then

$$\sigma = 0.12\frac{(4.77 \times 10^{-10})^2}{(5.6 \times 10^{-8})^3} = 156 \text{ ergs per square centimeter}$$

For molten NaCl at 800°C.,

$\sigma = 100$ ergs per square centimeter, approximately

crevice per patch is $4L = 400$Å. The area of the crevice surface associated with each patch must therefore be $S' = 400d$, where d is the depth in Ångströms of the crevice. Since S is approximately equal to $\frac{1}{3}S'$, we have

$$(100)^2 = \frac{400d}{3}$$

so that d is in the neighborhood of 75Å.

We therefore have the picture that by the time a seed crystal of NaCl has grown to be several hundred atomic diameters across, its surface is covered with a square network of crevices which are approximately 100Å. apart and about 75Å. deep. Obviously the width of each crevice must be at least the packing-diameter of a Na^+ or Cl^- ion. This picture is perhaps too simple. It is not to be expected that these crevices will be entirely empty. Near the top we must expect to find here and there stray ions of Na^+ and Cl^- attempting to bridge across from one wall of the crevice to the other. There is no reason to suppose that these ions occur at any definite spacing with respect to each other, but, wherever such a stray ion does exist, its exact position will be determined by the electrostatic forces between it and its neighbors on the walls of the crevice. These stray ions then would act as poor attempts at bridges here and there across the crevices. They would give the crystal as a whole somewhat more strength across the crevices than if they were entirely absent.

In order to facilitate further discussion of the effect of these crevices, we shall assume that the surfaces of the patches on the seed crystal all lie in a horizontal plane. At the center of each patch, the ions are pulled equally in all horizontal directions by the adjacent ions on all sides. As we go closer and closer to a crevice we finally reach a region where the electrostatic pulls are not exactly balanced; the total pull toward the crevice is less than the total pull toward the center of the patch. The horizontal interionic spacing will therefore be smaller and smaller the closer we come to a crevice, and the potential energy between adjacent ions will therefore become less and less. Similarly, on the surface of a crevice, the vertical interionic spacings will be smaller and smaller the closer we come to the surface of the patch, and the potential energy must become less and less. Ions at the corners formed by the intersection of two crevices with the surface of the patch will have the least potential energy of all; they will be closest to their neighbors. As the seed crystal grows vertically it is to be expected, then, that growth will take place most readily at these corners, for the newly arrived ions will be most tightly held at such points. This should result in a primary crystal growth along a vertical needle-like skeleton, with a subsequent filling in on the surface of the patch. This filling in should occur most

rapidly at the edges formed by the intersections of the crevices with the top surface of the seed crystal, because of the relative closeness of packing of adjacent ions along these edges. The central portion of the patch should be the last to be filled in. Obviously, a height will at last be reached such that a horizontal crevice will be formed to relieve the distortion along the surfaces of the vertical crevices. The argument in this case is identical with the argument which originally led us to assume the existence of vertical crevices,* with one exception. At the moment of forming the horizontal crevice we have at each corner of each of the original patches a vertical needle extending above the general level of the patch. When the horizontal crevice is formed, these projecting needles should determine the orientation of the new crystal fragment which will grow above the horizontal crevice. The orientation of the new growth above the crevice will therefore differ from that below it only by reason of some small accidental tilting of the projecting needles at the moment of forming the horizontal crevice.

We have, then, arrived at a theoretical picture of the growth of the NaCl seed crystal which requires the final "single crystal" to be really a mosaic of crystal fragments, all having nearly the same orientation, having practically the same size and shape, and being separated by crevices of substantially uniform spacing. Generalizing this picture so as to make it apply to other salts and to metals, we may think of the structure of a "single crystal" as being a lattice-work of points (such as is described by the theory of space-groups) on which is superimposed a coarser structure represented by the crevices.† Following the terminology of Zwicky,[18,21] we shall call the planes of the finer structure "p-planes" and the walls of the crevices which outline the coarser structure "π-planes." Since each crevice must have two walls, it is evident that π-planes must come in pairs. We may call the crevices "π-crevices." Just as the spacing of the p-planes is a characteristic of the material of which the crystal is composed, so the spacing of the π-crevices must be a definite characteristic of the material.

It is not to be expected that the surface forces which we have so far considered are the only forces tending to form crevices in a crystal. For instance we have neglected entirely thermal strains caused by the fact that the latent heat of solidification is given up *at the surface* of the growing crystal. This heat must be taken away mainly by conduction through the crystal itself so that, as the crystal is built up, it is subjected to rather

* Since the horizontal distances between the original vertical crevices are about 100Å., and since our calculations have shown that the depth of a crevice is about 75Å., it is evident that the horizontal crevices from the four sides of a given patch will all meet, thus giving a continuous horizontal crevice.

† This type of picture is consistent with all the x-ray data on the degree of imperfection of crystals and leads directly to the outstanding mechanical and crystallographic properties of crystalline materials.

large local strains. These strains should tend to alter somewhat the orientations of the crystal fragments which compose the mosaic, causing slight irregularities in the walls of the π-planes, thus giving rise to "supercrevices." Zwicky has shown[22] that electrostatic considerations also point to the existence in a "single crystal" of a structure still coarser than that of the π-planes. The walls of these supercrevices we may call "II-planes" and the supercrevices themselves "II-crevices." According to Zwicky's calculations they may have a spacing as large as 5000Å. or possibly even 20,000Å., depending upon the material of which the single crystal is composed. Apparently the supercrevices whose walls constitute the II-planes are of somewhat greater width than the crevices which we have called π-crevices.

The picture of II-planes and of π-crevices is almost entirely a theoretical picture. There is at present no direct experimental evidence of their existence and it is hard to see how there ever can be. Because of the changes in the density of a crystal from point to point along the edges (and faces) of the mosaic, and because of the small width of the π-crevices in comparison with the width of the mosaic units, x-ray diffraction from the π-planes (*i.e.*, from the spacings of the mosaic units as a whole) should be of almost zero intensity. The only real indirect evidence for the existence of π-crevices lies in the intensities of the x-ray beams diffracted from the p-planes of crystals. It will be remembered from Chap. X that the data on the intensities of diffracted x-ray beams show that most crystals are almost "ideally imperfect." This imperfection of structure is, of course, consistent with the idea of π-crevices but does not require them to be regularly spaced. There does seem to be considerable indirect evidence for the existence of II-planes and II-crevices. This evidence will now be outlined, using the assumption that the distances between II-crevices are substantially equal. If this assumption is not made, the picture becomes somewhat less elegant, but the conclusions to be drawn will not be seriously altered. In such a case the few changes in wording required will be obvious.

2. Consequences of π-planes and II-planes.—*a.* From the standpoint of crystal growth no substance can be regarded as being really pure, for, if an impurity is present only to the extent of a few parts per million, it may still affect the crystal growth by concentrating on the growing surface. Most ordinary materials contain impurities in amounts ranging from a fraction of 1 per cent up to several per cent. We may imagine these ions (or atoms or molecules) of impurity to collide with the growing surface in exactly the same manner as the ions (or atoms or molecules) of the crystallizing material. The chemical bond between the impurity and the crystallizing material may be (1) weaker than, (2) equal to, or (3) stronger than that between adjacent ions (or atoms or molecules) of the crystallizing material. (1) If the bond is weaker, the impurity will have

a greater chance of leaving the surface than will the ions (or atoms or molecules) of the crystallizing material. The impurity will therefore be present mostly in the form of material entrapped in the π-crevices, in the Π-crevices, or in the intercrystalline boundaries. Only a fraction of it will be left to foul the growing surface and retard crystal growth. (2) If the bond is practically equal, the impurity will enter into the structure of the p-planes after the manner of the alums. (3) If the bond is stronger, either the impurity will remain on the growing surface, fouling it so as to retard growth, or the impurity will leave the growing surface, taking with it that portion of the surface material with which it has combined, and in such a case it must tend to concentrate at the π-planes, at the Π-planes, and at the crystal boundaries.

When an impurity tends to deposit on the growing surface of a crystal, deposition must occur most strongly near the corners and edges of the patches, for these are the places where the potential energy becomes least. But these are exactly the places which are, according to our picture, the regions of fastest crystal growth. In other words, an impurity tends to foul the growing surface in such a way as to retard crystal growth most effectively. If it were not for diffusion of the impurity from regions of higher to regions of lower concentration, there would be little chance of having any unfouled surface. When, however, the impurity adjacent to one group of patches is deposited on the growing surface, the region above the surface finds itself with a lower concentration of the impurity than its surroundings. The impurity at once tends to diffuse into these impoverished regions, thus reducing the chance of some other, adjacent, group of patches becoming fouled. These comparatively clean groups of patches, therefore, will be able to grow more rapidly than their fouled neighbors, thus forming macroscopic needles. Of course, since these needles tend to grow sideways as well as in the direction of their length, the sides become covered with patches bounded by Π-crevices. A discussion similar to the above shows that the sideways growth will eventually become a matter of sending out secondary needles, and that these finally must send out tertiary needles, etc.* It may be assumed that all these macroscopic needles predicted by theory represent the actual needles of Figs. 1, 2, 3, and 4 and the needles described in the experiment with sodium hyposulphite. A similar line of reasoning may be applied to the dendritic structures so familiar to metallurgists.

b. Consider an undistorted "single crystal," and let its apparent orientation be known from goniometer or x-ray measurements. It is

* This needle-like skeleton corresponds to the "lineages" of M. J. Buerger[23] except that it is brought out in this discussion that the ultimate needles of which each large needle is composed can hardly avoid having transverse crevices. It is only fair to Professor Buerger, however, to add that, although he accepts "lineages," he does not accept the idea of mosaic structure and of the π-planes which that structure implies.

a consequence of the mechanism of growth which we have described that the individual fragments which compose the mosaic differ only slightly in orientation from each other. Any given set of atomic planes will appear to pass through one crystal fragment, across the π-plane, and through the next crystal fragment with hardly a perceptible break. This is illustrated in Fig. 7*a*. It may be assumed that for such a crystal the orientation is also preserved across the boundaries of the Π-planes. Such crystals may be expected to be mechanically weak.

The large spacings between adjacent π-planes and the still larger spacings between adjacent Π-planes will offer good opportunities for

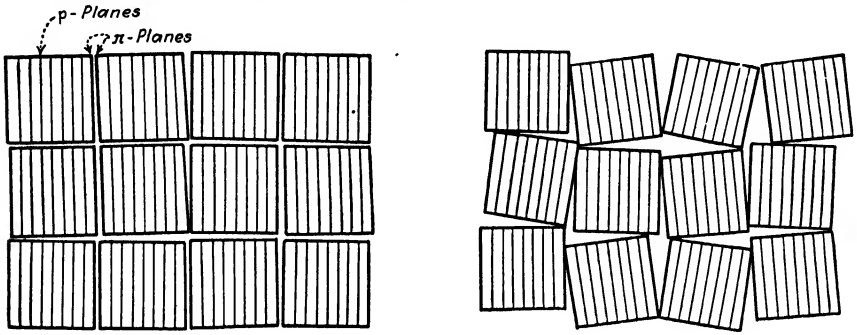

(*a*) (*b*)

FIG. 7.—(*a*) p-planes and π-planes in an undistorted crystal; (*b*) p-planes and π-planes in a distorted crystal.

slip. Slip must occur first between the planes of greatest spacing, *i.e.*, between the Π-planes. This gives a reasonable explanation for the well-known fact that in metals the slip bands have spacings which are rather exact multiples of the smallest spacing between bands. Since the direction of slip does not, in general, coincide with the direction of pull, torques will be set up which will tend to give somewhat different orientations to adjacent portions of the single crystal. The Π-planes would be pretty well wrecked, and each portion of the single crystal would be jammed crossways against its neighbors. In a very real sense the original single crystal may be said to have been broken up into a large number of smaller ones. This is consistent with the ordinary experience of x-ray investigators. Slip must then take place between the planes of next greatest spacing, *i.e.*, between the π-planes in each portion of the crystal. The torques set up will tend to rotate the fragments of which the mosaic is composed so that they will no longer look like Fig. 7*a* but will be like Fig. 7*b*. Further slip can take place only between the p-planes. This is not likely to take place because of the closeness of the spacing. Before slip will take place between the p-planes, it is to be expected that rupture will occur along the line of the wrecked Π-planes or π-planes.

If we adopt this picture of slip, we have not only explained at once why metals show block slip rather than a continuous shear but we have made it necessary for the block slip to occur in small finite increments. The picture requires that slip must occur first between the two weakest Π-planes. Slip will proceed until the plane becomes wrecked at some point by the jamming of the π-plane structure of which its walls are composed. Slip must then start in the next weakest Π-crevice. This process must continue until finally the process is taken up by the weakest π-crevice. In other words, slip must be a step-by-step process. Experiment shows that this is actually the case. Joffé and Ehrenfest and later Miss Klassen have shown[24,25] that shear in zinc and in rock salt progresses

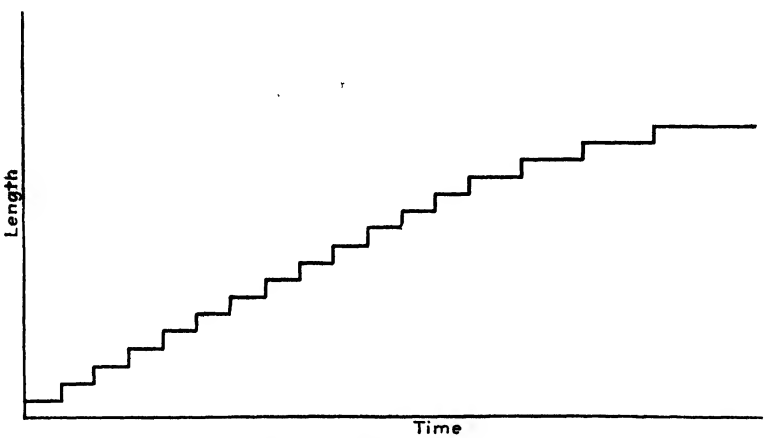

FIG. 8.—Step-by-step slip.

in small jumps. The magnitude of the jumps remains constant to within 10 per cent for thousands of jumps. The initial time interval between successive jumps depends upon the difference between the applied load and the elastic limit, but for a given shearing stress it gradually increases until the jumps finally cease. The effect is illustrated in Fig. 8 which is taken from Joffé's "The Physics of Crystals" (McGraw-Hill Book Company, Inc., New York, 1928).

It is well known that slip ordinarily occurs in the direction of those p-planes which have the greatest interplanar spacing. Our discussion of slip has therefore implied that the π-planes and the Π-planes lie parallel to those p-planes which have the greatest interplanar spacing in the crystal. An examination of our discussion of the formation of π-planes shows that this is implied there, too, for crevices may be expected to form most easily along the largest interplanar spacings of the growing crystal.*

* This in turn implies that the normal direction of crystal growth is perpendicular to the slip planes in an orthogonal crystal. Cases in which growth appears to be in some other direction may really be examples of a zigzag growth perpendicular to members of the family of slip planes.

Obviously, as the weakest Π-planes and π-planes are wrecked in succession so that they can no longer slip, the tensile strength of the crystalline material must increase, *i.e.*, the crystal must strain-strengthen. The only way to avoid strain-strengthening would be to keep the material at such a temperature that the wrecked planes can repair themselves as a result of the high atomic mobilities associated with thermal agitation. The picture which has been given for the mechanism of slip explains strain-stiffening also, for Joffé has shown by x-ray methods[24] that, when a single crystal is bent beyond the elastic limit, it really suffers a large number of minute shears of the block-slip type. Since the tensile properties of materials are pictured as depending upon the Π-planes and π-planes, it is not surprising that the tensile strength of a crystal cannot be calculated from the electrostatic forces between the ions in the p-planes. As would be expected, the actual tensile strength of a crystal is always considerably smaller than that calculated from the p-planes.

We have seen under part *a* that, next to the intercrystalline boundaries, the crevices between the Π-planes and between the π-planes offer the most favorable place for the deposit of impurities during crystallization. The idea may be expanded beyond the meaning ordinarily attached to the word "impurity." When, by reason of an appropriate thermal history, an alloy "precipitates out" a new phase, then this new phase will tend to collect at the crystal boundaries and in the crevices between the Π-planes, and between the π-planes, provided only that the atoms have sufficient freedom of motion to permit the necessary migration. The presence of the new phase between the Π-planes and between the π-planes must, of course, act to bridge over these crevices in an irregular fashion thus tending to tie the side walls together and making slip more difficult. This offers a simple and apparently adequate explanation of the strengthening of metals by the precipitation of a new phase. The effect of carbon in the strengthening of steels comes to mind at once as an illustration. Metallurgists will find many other examples in ordinary metallurgical practice.

c. The theory has indicated that at the edges formed by the intersections of π-planes the molecules are especially close together, thus forming structures of minimum potential energy, and that the spacing (and therefore the potential energy) between molecules increases as we go from the edges toward the center of a patch. Because of the lower potential energy, the melting point of the edge portions must be somewhat above the melting point of the main body of the patches. When a crystal is brought just barely up to its melting point, we may assume that the bonding of the Π-planes is first loosened, but the structure cannot melt down because of the rigidity of the blocks of which it is composed; the material merely becomes soft. Similarly, it cannot melt when the bonds between the π-planes are loosened. Finally, the centers of the patches

must melt out, leaving the edges of the patches to slough off without melting. A similar statement could be made of the edges formed by the intersection of the Π-planes. These unmelted "edges" correspond to the sloughed-off portions mentioned in our discussion of the growth of crystals from the melt. We therefore have a theoretical explanation* of the experiments of Goetz[5] and of Traube and v. Behren[6] which have already been referred to, and the experiments of Richards[8] in which it was shown that the whole material does not become a truly homogeneous liquid until a temperature is reached which is appreciably above the melting point. We also have a rational explanation for the results of Boydston,[26] who found that the electromotive forces of oriented bismuth crystals do not disappear at the melting point but continue until the "liquid" is heated appreciably above the melting point. Applications of the theory of sloughing to the ordinary melting operations of the metallurgical industries will be at once obvious to all metallurgists.

d. The same considerations of potential energy that we have already used in part serve to explain the action of etching reagents. An etching agent must attack first the regions of highest potential energy. It must therefore attack readily, not only the intercrystalline boundaries, but also the centers of the patches, before it attacks the edges next to the π-planes and the π-planes themselves. Similarly, we must expect that it will attack the Π-planes last. It is not surprising, then, that strongly etched crystals will show etching pits. We may assume that the boundaries of the etching pits are parallel to the Π-planes and therefore to the π-planes and to the p-planes of greatest interplanar spacings. If this picture is granted, we have a theoretical basis for the technique of Honess[27] in determining crystal symmetries by means of a careful study of etch figures. Goetz[28] has found the etching pits of bismuth to be characterized by steps which are separated either by a definite spacing or by a simple multiple of that spacing. He finds this fundamental distance to be $1.4 \pm 0.2 \times 10^{-4}$ cm. Since this is the correct order of magnitude for the distance between pairs of Π-planes, he has published his data as offering possible confirmation of the existence of a secondary structure in crystals. In the opinion of the author, Goetz' work offers one of the strongest pieces of *direct* experimental evidence in favor of the existence of Π-planes.†

* This explanation offers a somewhat different point of view from that given by Goetz, who apparently assumes that the sloughed-off portions represent whole patches.

† R. B. Barnes[29] has shown by infra-red absorption measurements that, if large crystals of rock salt are made plastic by soaking in water and are then taken out and dried superficially, they contain considerable water in the interior. This water can be removed by heating 24 hr. at 150°C. Different crystals showed this property to different degrees. If it could be shown by x-ray methods that the more permeable the crystal the more nearly ideally imperfect it is, we would have an excellent piece of direct evidence for the existence of π-planes or of Π-planes.

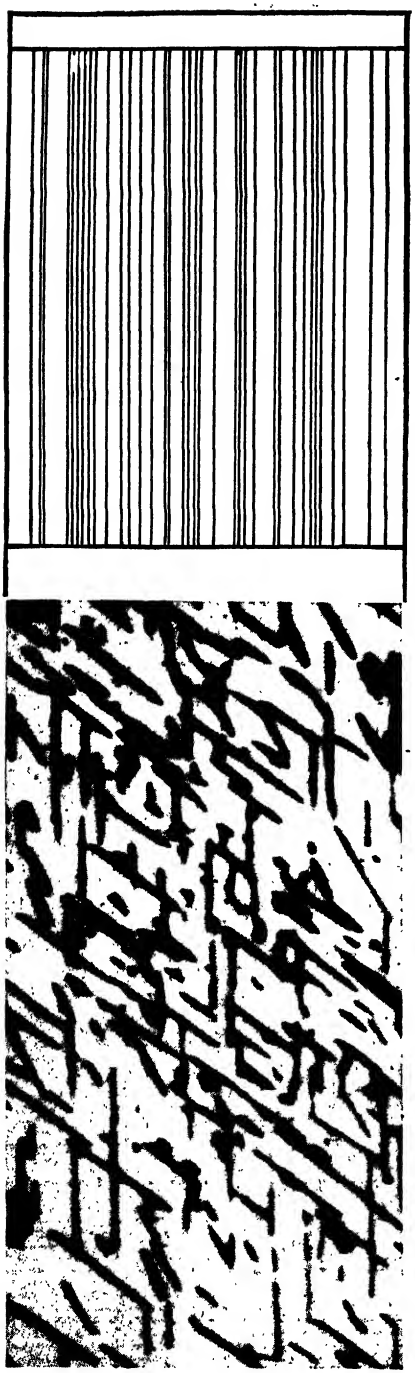

FIG. 9.—Regular spacing of segregate structures of Widmanstätten type.

e. We have already built up the picture that, when a new phase is precipitated in an alloy, it will tend to concentrate itself at crystal boundaries and in the crevices between pairs of π-planes and pairs of Π-planes, if only the atoms have sufficient mobility to permit the necessary migration. If, however, the new phase finds that the crevices between the Π-planes and between the π-planes are already filled, then the new phase must crystallize as best it can in islands within the matrix. These islands correspond to the well-known segregate structures of the Widmanstätten type. It has been pointed out by Mehl and his associates[30,31,32] that these islands are most likely to be formed so that some p-plane of the new phase lies parallel to a p-plane of the matrix having approximately the same interatomic distances. All the islands in a single crystal must therefore take the form of thin plates and must have the same orientation within the limits set by the mosaic structure. When the nucleus of such a crystal island is once formed, the region in its immediate neighborhood becomes impoverished with respect to the new phase. Migration will therefore occur from surrounding regions where the concentration is still *relatively* high.

Since the crevices between the Π-planes are already filled with other material, migration cannot take place readily across the Π-planes. A somewhat similar

barrier must exist between each pair of π-planes, but because of the narrower width of the π-crevices the barrier will not be so difficult to overcome. We must expect, then, that migration toward the nucleus of each crystal island will be limited to that portion of the new phase which lies within the volume bounded by the nearest II-planes. There is therefore a very high degree of probability that there will be only one crystal island of the new phase in each of these volumes.* In other words, the average spacing between crystal islands should be substantially uniform. It should be the same as the spacings between adjacent II-crevices projected in a direction perpendicular to the length of the crystal islands.† Figure 9 shows that these predictions are correct. Through the courtesy of the New Jersey Zinc Company, the photomicrograph is taken from the paper of Fuller and Rodda[33] on Segregate Structures of the Widmanstätten Type Developed from Solid Solutions of Copper in Zinc. The photomicrograph was taken from a single-crystal specimen whose plane of polish was such as to give symmetrical orientations of the Widmanstätten figures. Lines were drawn showing the planes of all the traces having a given orientation. Because of the small area of surface (less than 0.9 sq. cm.) shown in the photomicrograph, it is not to be expected that every II-plane will be represented in Fig. 9 by a segregate structure line. It is evident, however, that the smallest spacings are all of substantially the same width and that the larger spacings are fairly exact multiples of this smallest width, as demanded by the theory. Calculation shows that the fundamental distance apart in the specimen is of the order of 5×10^{-5} cm. Because of the effect of the orientation of the plane of polish, and because of the mutual orientations of the planes upon which the segregate structures are found, only the order of magnitude of this distance is of any real significance. It is interesting to note that the spacing found here is of the same order of magnitude (one-third as large) as that found in the Goetz etching experiments on bismuth.

SUMMARY

We have taken up systematically the experimental evidence as to the growth of crystals (1) from the vapor, (2) from the melt, (3) from solution, and (4) from the solid and have discussed the physical conditions which are associated with each. In every case we found imperfection to be the natural state of a crystal. This conclusion is consistent with the mosaic

* This is really a special form of the theory of rhythmic precipitation in which the limits of diffusion are set by the II-crevices instead of by the concentration of solute.

† Dr. R. F. Mehl has pointed out to the author that not all materials will precipitate out from the same material in the same crystallographic direction. This should not, however, prevent the II-planes from determining the average spacing between crystal islands by setting limits on the diffusion which is tied up with rhythmic precipitation.

structures, mentioned in Chaps. I, X, and XI, which seems to be required by the intensity data of diffracted x-rays. Following the general lines of the theory of Zwicky, we have built up in detail a theoretical picture of the growth of crystals such that the imperfections are inherent in the structure and such that the ordinary properties of materials (such as manner of crystal growth, tensile properties, segregation of impurities, properties of the melt, etch figures, and Widmanstätten figures) follow as natural corollaries.

References

1. L. R. Ingersoll and S. S. DeVinney, *Phys. Rev.*, **26**, 86 (1925).
2. I. Langmuir, *Phys. Rev.*, **8**, 149 (1916); *Proc. Nat. Acad. Sci.*, **3**, 141 (1917).
3. P. Othmer, *Zeit. anorg. Chem.*, **91**, 209 (1915).
4. A. E. H. Tutton, "The Natural History of Crystals," E. P. Dutton & Co., Inc., New York, 1924.
5. A. Goetz, *Phys. Rev.*, **35**, 193 (1930).
6. J. Traube and W. v. Behren, *Zeit. phys. Chem.*, **138, A**, 85 (1928).
7. G. Tammann, "Aggregatzustände," Chap. IX, L. Voss, Leipzig, 1922 (English translation by R. F. Mehl, D. Van Nostrand Company, New York, 1925).
8. T. W. Richards, *Jour. Amer. Chem. Soc.*, **54**, 479 (1932).
9. W. P. Davey, *Phys. Rev.*, **29**, 206 (1927).
10. G. Tammann, "A Text-book of Metallurgy," Chemical Catalog Company, New York, 1925.
11. The constitution diagram may be found in "International Critical Tables," Vol. II, p. 427, McGraw-Hill Book Company, Inc., New York, 1927.
12. G. Oesterheld, *Zeit. anorg. Chem.*, **97**, 27 (1916).
13. The constitution diagram may be found in "International Critical Tables," Vol. II, p. 421, McGraw-Hill Book Company, Inc., New York, 1927.
14. The constitution diagram may be found in "International Critical Tables," Vol. II, p. 402, McGraw-Hill Book Company, Inc., New York, 1927.
15. The constitution diagram may be found in "International Critical Tables," Vol. II, p. 453, McGraw-Hill Book Company, Inc., New York, 1927.
16. P. P. v. Weimarn, "Grundzüge der Dispersoidchemie," T. Steinkopf, Dresden, 1911.
17. R. F. Mehl and D. W. Smith, *Tech. Pub.* 521, Iron and Steel Div., A.I.M.E., 1934.
18. F. Zwicky, *Proc. Nat. Acad. Sci.*, **15**, 253, 816 (1929).
19. F. Zwicky, *Phys. Zeit.*, **24**, 131 (1923).
20. J. E. Lennard-Jones and B. M. Dent, *Proc. Roy. Soc.*, **121**, 247 (1928).
21. F. Zwicky, *Phys. Rev.*, **40**, 63 (1932).
22. F. Zwicky, *Phys. Rev.*, **38**, 1772 (1931).
23. M. J. Buerger, *Amer. Mineral.*, **17**, 177 (1932).
24. A. F. Joffé, "The Physics of Crystals," McGraw-Hill Book Company, Inc., New York, 1928.
25. M. W. Klassen, *Jour. Russ. Phys.-chem. Soc.* (1927). Referred to in reference 24.
26. R. W. Boydston, *Phys. Rev.*, **30**, 911 (1927).
27. A. P. Honess, "Nature, Origin, and Interpretation of Etch Figures on Crystals," John Wiley & Sons, Inc., New York, 1927.
28. A. Goetz, *Proc. Nat. Acad. Sci.*, **16**, 99 (1930).
29. R. B. Barnes, *Phys. Rev.*, **43**, 82 (1933).

30. R. F. Mehl and C. S. Barrett, *Trans. A.I.M.E.*, Inst. Met. Div., **93**, 78 (1931).
31. R. F. Mehl and O. T. Marzke, *Trans. A.I.M.E.*, Inst. Met. Div., **93**, 123 (1931).
32. R. F. Mehl, C. S. Barrett, and F. N. Rhines, *Trans. A.I.M.E.*, Inst. Met. Div., **99**, 203 (1932).
33. M. L. Fuller and J. L. Rodda, *Trans. A.I.M.E.*, Inst. Met. Div., **104**, 116 (1933).

CHAPTER XIII

THE PACKING-SHAPES AND PACKING-SIZES OF ATOMS AND IONS

We have seen in Chaps. IX and XI that a knowledge of the packing-dimensions of atoms and ions may be quite useful in solving the structure of crystals. The packing-size and packing-shape of an atom or ion are not to be confused with its "actual" size and shape. The actual shape and size of an atom or ion depend upon the configuration of the electrons and upon the various interelectronic distances in the atom. If we happen to be thinking in terms of strictly physical or mathematical figures of speech, we may express the actual size of an atom in terms of the characteristic dimensions of the orbits of its outmost electrons. If, instead, we prefer the less general but more easily visualized chemical figures of speech, we may express the actual size of an atom in terms of the dimensions of the framework of some type of static atom.* It is possible that these two pictures are really only two viewpoints of the same fundamental picture, for calculations based on one necessarily give identical answers with calculations based on the other.[1] The packing-shape and packing-size of an atom may or may not be simply related to its actual size and shape. In the simplest cases, the packing-volume may be visualized as being merely the actual volume plus a proper portion of the space between adjacent atoms. In other cases the picture is rendered much more difficult of interpretation by the mechanism of chemical combination. For instance, if two atoms share electrons with each other, it is sometimes difficult to say where one atom ends and the other one begins. On the other hand it would impose a serious limitation on our ability to visualize crystal structures if we could not picture any given crystal as being made up of building blocks packed tightly together, each building block containing an individual atom or ion. These imaginary building blocks may be called "atomic domains" (or "ionic domains"). The high incompressibility of solids indicates that each atom (or ion) must stay inside its own "domain." In other words, the atomic (or ionic) domains are to be considered as being impenetrable at absolute zero when subjected to ordinary pressures. To the crystal analyst the shapes of these atomic domains in any given crystal are the "packing-shapes" of the atoms which compose that crystal, and the dimensions of the atomic

* In either case there is implied the assumption that electrons occupy definitely defined volumes, an assumption which may be open to serious question.

domains are the "packing-dimensions" of the atoms. These shapes and dimensions are the only atomic (or ionic) shapes and dimensions with which the crystal analyst is concerned, the only ones which may be derived directly from his experimental data.

It is not to be assumed that the packing-shape or packing-dimensions of a given atom (or ion) will be identical under various physical and chemical conditions. Since the centers of adjacent Ca^{++} ions are closer together in CaO than are the centers of adjacent atoms of Ca in calcium, it is evident that the ionic domain of Ca^{++} in CaO is smaller than the atomic domain of Ca. It is not even to be assumed that an ion retains the same packing-dimensions in different states of chemical combination. In other words, there is no *a priori* reason why the packing-dimensions of Ca^{++} in CaO should be identical with those of Ca^{++} in CaS or in $CaCl_2$. There is, however, a body of experimental evidence which indicates strongly that within a given class of chemical compounds a given ion tends to retain about the same packing-size and packing-shape. We have already taken advantage of this body of experience in Chap. IX in the case of tricalcium aluminate and in Chap. XI in the case of diopside and topaz. It will therefore be worth our while to take up in detail the shapes and sizes of the atomic and ionic domains of various elements and the experimental evidence on which these shapes and sizes are based.

THE PACKING-SHAPES AND PACKING-SIZES OF ATOMS FROM CRYSTAL STRUCTURE DATA*

Spherical and Spheroidal Atomic Domains.—Many elements crystallize with a face-centered cubic structure. Since a face-centered cube is one of the two alternative closest packings for spheres, it is only natural to ascribe a spherical shape† to the atomic domains of these elements.[2,3] Such elements are Ne, Ar, Kr, Xe, Cu, Ag, Au, Ca, Al, β-Tl, Ce, Pb, Th, γ-Fe, α-Co, Ni, Rh, Pd, Ir, Sr, Pt. Each atom is symmetrically surrounded by 12 others. At any given temperature, the distance between the centers of adjacent atoms is the "distance of closest approach" of these atoms for that temperature. At temperatures above absolute zero, this distance ought really to be thought of as being composed of three segments. The two end segments would be the true radii of the domains of the two atoms at the given temperature. The middle segment would

* It is realized that the shapes of atomic and ionic domains pictured in this chapter will appear to the reader to be very crude, as indeed they are. They are at best only approximations which have the virtue of representing a useful viewpoint. The text will be found, however, to fulfill the aim set forth in the preface, namely, to put the reader in possession of knowledge such that he can read the literature further by himself whenever he needs to.

† The argument is not greatly altered if some close approximation to a sphere (such as a dodecahedron) is substituted for the sphere. It would probably be impossible to detect the difference because of rotations accompanying the heat motion.

TABLE I.—RADII OF SPHERICAL ATOMIC DOMAINS

Element	Purity, per cent	Radius, Ångströms	Temperature	Data published by
Ne	?	1.60	Slightly above boiling He	de Smedt, Keesom, and Mooy
Ar	?	1.92	Slightly above boiling H_2	Simon and v. Simson
Kr	?	1.97	Boiling H_2	Keesom and Mooy
Xe	?	2.18	Liquid air	Natta and Nasini
Cu	99.9 99.99	1.2755 1.272	18° C. Room	Owen and Yates* Davey
Ag	99.9 99.999	1.4415 1.442	18° C. Room	Owen and Yates* Davey
Au	Spectroscopically pure 99.999	1.4389 1.437	18° C. Room	Owen and Yates* Davey
Mg	?	1.59	Room	Hull
Ca	?	1.97	Room	Hull
Sr	?	2.18	Room	King
Al	99.6 99.97	1.4286 1.430	18° C. Room	Owen and Yates* Davey
β-Tl	?	1.71	Room	Seikito
Ce	?	1.82	Room	Hull
Pb	99.9 99.96	1.7464 1.740	18° C. Room	Owen and Yates* Davey
Th	?	1.77	Room	Hull
γ-Fe	?	1.27	Room	Westgren
α-Co	Electrolytic	1.257	Room	Hull
Ni	99.9 99.548	1.2427 1.237	Room Room	Private communication from E. R. Jette Davey
Rh	S.P.	1.3419	18° C.	Owen and Yates*
Pd	S.P.	1.3726	18° C.	Owen and Yates*
Ir	99.8	1.3545	18° C.	Owen and Yates*
Pt	S.P. 99.995	1.3844 1.383	18° C. Room	Owen and Yates* Davey

* Also private communication from E. R. Jette.

represent the mean separation of these atomic domains due to their thermal agitation. Ordinarily, however, it is more convenient to consider the middle segment as being included in the radii of the atomic domains. In other words, at a given temperature, half the distance of closest approach is taken as the radius of the atomic domain at that temperature. Table I gives the packing radii of spherical atoms, determined from material of the highest obtainable purity.

The other alternative closest packing for spheres is the hexagonal close-packed structure when the axial ratio is 1.633. Co and Ce are

TABLE II.—RADII OF SPHEROIDAL ATOMIC DOMAINS AT ROOM TEMPERATURE

Element	Purity, per cent	Axial ratio	Equatorial radius, Ångströms	Axial radius, Ångströms	Data published by
Be	?	1.58	1.141	1.104	McKeehan
Zn	99.993	1.8563	1.3300	1.5117	Private communication from M. L. Fuller (New Jersey Zinc Co.)
Cd	S.P.	1.8864	1.4868	1.7167	Private communication from M. L. Fuller
α-Tl	?	1.59	1.73	1.69	Seikito
Ti	99.9	1.590	1.475	1.436	Patterson
Zr	?	1.589	1.611	1.568	Van Arkel
Hf	?	1.565	1.600	1.533	Van Arkel
Re	?	1.616	1.376	1.362	Goldschmidt
Ru	?	1.586	1.347	1.309	Barth and Lunc
Os	?	1.584	1.362	1.321	Barth and Lune

the only elements which are able to crystallize with this structure whose axial ratio is definitely accepted to be exactly 1.633. Both of these elements are also found with the face-centered cubic structure. There is some justification for including Mg among the hexagonal close-packed metals with spherical atoms. It is listed in crystallographic tables as having an axial ratio of 1.624, but the experimental and calculated readings of interfacial angles do not agree precisely. The published x-ray data seem to fit an axial ratio of 1.633 about as well as 1.624. In any case, even if the accepted value of 1.624 is correct, the Mg atom cannot

differ by more than about ¾ per cent from a true sphere. Unlike Co and Ce, Mg has never been found in the face-centered cubic form.

The other elements which crystallize with the hexagonal close-packed structure have axial ratios ranging from 1.58 to 1.89. Since the axial ratios of Be, α-Tl, Ti, Zr, Hf, Re, Ru, and Os are less than 1.633, their atomic domains are considered to be oblate spheroids.[3] The atomic domains of Zn and Cd are assumed to be prolate spheroids since their axial ratios are larger than 1.633. All these atomic domains are therefore given two radii which are half the major and minor axes of the spheroid. The equatorial radius is half the distance of closest approach of atomic centers in the direction of the hexagonal (*X*-, *Y*-, and *F*-) axes

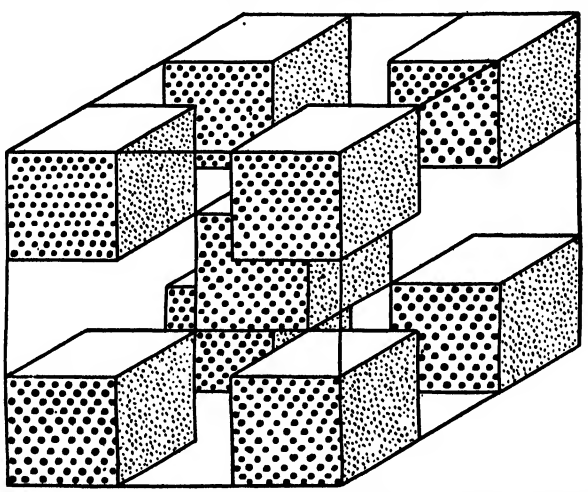

FIG. 1.—Unit body-centered cube made up of cubic atomic domains.

of the crystal. The other, which we shall call the axial radius, is the radius of the spheroid along the orthogonal (*Z*-) axis of the crystal.* Radii of this sort for spheroidal atoms at room temperature are listed in Table II.

Cubic Atomic Domains.—The elements Li, Na, K, Rb, Cs, Ba, V, Cb, Ta, Cr, Mo, W, and α-Fe, each crystallize on a body-centered cubic lattice. It is a characteristic of this lattice that each atom is symmetrically surrounded by eight other atoms. This is the closest packing for equal numbers of spheres of equal radius having opposite electric charges, but the ordinary physical and chemical properties of these elements hardly justify a picture of half the atoms positively charged and half negatively charged. A picture of the shape of the atomic domains of

* Hull[3] lists, instead, the two distances of closest approach of atoms. One of these is the same as the equatorial radius. The other is intermediate between this and the axial radius. The axial radius is obviously the equatorial radius multiplied by $C/1.633$, where C is the axial ratio.

these elements which has been found free from objection so far has been proposed by Hull.[3] Since the eight points of contact may be symbolized

TABLE III.—DIMENSIONS OF CUBIC ATOMIC DOMAINS AT ROOM TEMPERATURE

Element	Purity, per cent	Edge of cubic atomic domain, Ångströms	Half body-diagonal of cubic atomic domain, Ångströms	Data published by
Li	?	1.75	1.52	Posenjak
Na	?	2.15	1.86	Posenjak
K	Baker Chemical Company Lot No. 52827	2.666	2.309	Posenjak
Rb	?	2.81	2.43	Simon and Vohsen
Cs	?	3.02	2.61	Simon and Vohsen
Ba	?	2.507	2.171	King and Clark
V	?	1.505	1.304	Hägg
Cb	?	1.65	1.43	Meisel
Ta	99.8	1.6557	1.4339	Owen and Iball
Cr	99.8	1.436	1.244	Patterson
Mo	99.5	1.552	1.344	Owen and Iball
	99.8	1.571	1.360	Davey
W	99.9	1.5796	1.3680	Owen and Iball
	99.999	1.577	1.366	Davey
α-Fe	99.9	1.4303	1.2387	Owen and Yates; Greiner and Jette
	99.937	1.427	1.236	Davey

by the eight corners of a cube, he pictured these atomic domains as having a cubic shape.* If such a picture is adopted, we must assume that

* The difference between spherical and cubic shapes of atomic domains may be regarded, if we wish, as more a difference in degree than in kind. In discussions of the theory of atomic structure use is made of the probability that a given electron will find itself in some definite position in the atom. If the eight electrons in the outmost "completed shell" of an atom have a high degree of probability of finding themselves at the corners of an imaginary cube, then the atomic domain might be represented by a cube with its corners somewhat rounded. If we decrease the degree of probability that the electrons are, at any one instant, at cube corners we necessarily

tunnels of square cross-section are inherent in the very structure of a body-centered cubic crystal of an element. It is evident from Fig. 1 that the cross-section of such a tunnel must be equal to the cross-section of a cubic atomic domain. It will appear later that such a picture fits in remarkably well with certain metallurgical data.* Table III lists the dimensions of these cubic atomic domains at room temperature, both in terms of the edge of the cube and in terms of half the body-diagonal of the cube, *i.e.*, half the distance of closest approach of atomic centers.

Tetrahedral Atomic Domains.—The elements C, Si, Ge, and gray Sn, each crystallize in a diamond cubic structure. This causes each atom to be symmetrically surrounded by four others. These four points of contact may be symbolized by picturing the atomic domains to be tetrahedral in shape. Two dimensions of the tetrahedron are significant: the length of the edge of the tetrahedron and the distance from the center of the tetrahedron to one of the four corners, *i.e.*, half the distance of closest approach of atomic centers. These dimensions are listed in Table IV.

TABLE IV.—DIMENSIONS OF TETRAHEDRAL ATOMIC DOMAINS AT ROOM TEMPERATURE

Element	Purity, per cent	Edge of tetrahedral atomic domain, Ångströms	Distance from center of tetrahedral atomic domain to vertex, Ångströms	Data published by
C	Diamond	1.259	0.771	Ehrenberg
Si	99.79	1.9154	1.172	Private communication from E. R. Jette
Ge	?	1.99	1.22	Hull
Sn gray	?	2.28	1.40	Biji and Kolkmeyer

Other Shapes of Atomic Domains.—Frozen Hg[4], black P[5], As[6], Sb[6], and Bi[6] crystallize as rhombohedra which may be regarded as distorted cubes. At present the sizes and shapes of the atomic and molecular domains of these elements are relatively unimportant. Oxygen *molecules* crystallize on a body-centered orthorhombic lattice.[7] From the dimensions of the unit body-centered orthorhombic crystal it may be calculated that the distance of closest approach of oxygen molecules is 3.76Å. Sulphur at room temperature apparently crystallizes by molecules in space-group V_h^{24} of the orthorhombic system.[8] Selenium and tellurium apparently crystallize by molecules of Se_3 and Te_3 on

increase the degree of rounding off the corners of the atomic domain. An extreme case of this would obviously yield a spherical atomic domain.

* The body-centered cubic structure is the closest packing for octrahedra, but such a shape for the atomic domains would lack the tunnels at room temperature.

a simple triangular lattice[9] which is such as to yield nearly a rhombohedral lattice of atoms.[10] Below 35.5°K., nitrogen crystallizes* as molecules of N_2 on space-group T^4. This may be visualized as a face-centered cube with the center of gravity of a N_2 molecule at each lattice point and with all the individual atoms lying on cube faces.[11] The diameter of the spherical *molecular* domain of N_2 is 4.00Å. It is interesting to note[11] that CO also crystallizes by molecules on space-group T^4, with 4.00Å. as the distance of closest approach of the molecules. This agreement in both structure and dimensions is strictly in accordance with the predictions of the Lewis-Langmuir theory of atomic structure.

OTHER ESTIMATES OF SHAPES AND SIZES OF ATOMS

It is interesting to note that as early as 1873 Maxwell estimated the size of molecules to be of the order of 0.001 wave length of visible light.[12] Lunnon[13] lists a total of 21 methods, exclusive of crystal structure, which have been proposed at one time or another for estimating the sizes of atoms and ions. As might be expected, these various methods imply many viewpoints as to what it is that may be called the "size" of an atom. For instance, some involve ideas as to the dimensions of electron orbits, while others involve the diameter of a cloud of material surrounding (and possibly attached to) an atom or ion. Five of the methods mentioned by Lunnon apply to atoms rather than to ions, and seem to give definite enough results to warrant notice. They are (1) atomic volume; (2) viscosity of gases; (3) Van der Waals' equation and its modifications; (4) atomic structure theory; (5) ionizing potential. To these we may add a sixth, the composite physico-chemical method of Sirk, and a seventh, the method of the atomic-structure factor. It will be interesting to take up, too, some calculations and lines of reasoning which depend for their success upon assumptions as to the shape of atoms.

1. The Method of Atomic Volumes.—The atomic volume of a "monatomic" element is defined as its atomic weight divided by its density. The volume of an individual atom of the element may be found by dividing the atomic volume by the Loschmidt (Avogadro) number and multiplying this quotient by a factor, v, which represents the fraction of the total volume actually occupied by atoms. The value assigned to the factor v will depend upon the shape assumed for the atomic domain and upon the configuration of atoms in the crystal. For instance, if we consider the atomic domain to be spherical, v would be 0.52 for a

* Vegard also reports [*Science*, **77**, 588 (1933)] a β form of nitrogen, stable above 35.5°K., with a hexagonal close-packed structure. The axial ratio is such as to make the molecular domain practically spherical. Instead of interpreting the structure in terms of coalesced atoms, he mentions the alternative explanation of molecules rotating in the crystal.

simple cube, 0.68 for a body-centered cube, and 0.74 for a face-centered cube. If, instead, we consider the atomic domain to be cubic, v would be unity for a simple cube and 0.50 for a body-centered cube. The radius of a sphere whose volume is V is $\sqrt[3]{\frac{3}{4\pi}V}$, the edge of a cube of volume V is $\sqrt[3]{V}$, and its half body-diagonal is $\frac{\sqrt{3}}{2}\sqrt[3]{V}$.

Apparently argon is the only solidified inert gas for which the density has been measured by other than x-ray methods. Simon and Kippert[14] state that the density at 76°K. is 1.505. This density gives a radius for a spherical Ar atomic* domain of 1.97Å. in good agreement with the value of 1.92Å. shown in Table I from x-ray methods. Of course it would have been just as good a check on the two types of measurement of radii if we had compared the experimentally determined value of the density of argon with that calculated from the crystal-structure data. Similar agreement may be found in the case of other monatomic face-centered cubic elements.†

2. The Method of Viscosity of Gases.—If we assume that the atomic domains of the inert gases are spheres, their mean radii in the act of collision may be calculated from viscosity data by means of the equation[13,15,16]

$$\pi r^2 = \frac{0.087\rho V}{n\eta\left(1 + \frac{S}{T}\right)}$$

where r = radius of atomic domain (*i.e.*, mean radius in act of collision).
ρ = density of gas.
V = mean molecular velocity.
n = number of atoms per cubic centimeter.
η = coefficient of viscosity.
S = Sutherland's constant.[17]
T = absolute temperature.

Radii obtained in this way are:[18] Ne, 1.17Å.; Ar, 1.43; Kr, 1.58; Xe, 1.75. Comparison with Table I shows that these radii for Ne and Ar are about three-fourths of the x-ray radii; the radii for Kr and Xe are about four-fifths of the x-ray radii. It should be noted, however, that radii calculated from viscosities relate to the atomic domains alone; those calculated from x-ray data include also the equivalent half-spacing between atoms at the temperature for which the data were taken.

* Both methods of calculating the size of the atomic domain contain an assumption as to the shape of the atomic domain. This assumption enters into both calculations in the same way so that, whatever shape is assumed, the agreement as to the size of the atomic domains still remains.

† "International Critical Tables," Vol. I, pp. 103–104 and 340–341, McGraw-Hill Book Company, Inc., New York, 1927.

When we consider the smallness of the attractive forces* between the atoms of these elements, we conclude that the difference between the values for the two types of radii is not unreasonable.

3. The Method of the Equation of State.—The value of the covolume b in Van der Waals' equation may be interpreted as being the volume of the molecular domain. If we assume the domains of the monatomic gases to be spherical, we can arrive at once at values for their radii. Lunnon gives[13] radii apparently calculated from values of b collected by Pease[19] for the inert gases. They agree with those of method 2 and are subject to the same comments. The radii are: Ne, 1.18Å.; Ar, 1.46; Kr, 1.57; Xe, 1.71.

4. The Method of Atomic Structure.—This method may be illustrated by the work of Turner[20] who has calculated the radii of the various possible electron orbits of the alkali metals from the frequencies of light in their characteristic spectra. The distance from the nucleus to the most distant part of the outmost orbit in the normal atom may be considered to be a radius for the normal atom itself. This will, of course, be different from the radius of the atomic domain as determined by the packing of atoms in a crystal. Turner's end results are compared with the x-ray results in Table V. It will be noticed that his atomic radii are practically 1½ times the half-distance of closest approach of the atomic domains.

TABLE V.—COMPARISON BETWEEN TURNER'S RESULTS FOR RADII OF VALENCE-ELECTRON ORBITS AND RADII OF ATOMIC DOMAINS

Element	Radius of valence-electron orbit, Ångströms	Half body-diagonal of cubic atomic domain, Ångströms (see Table III)	Ratio
Li	2.38	1.52	1.57
Na	2.72	1.86	1.46
K	3.45	2.31	1.49
Rb	3.61	2.43	1.49
Cs	3.94	2.61	1.51

There are two obvious ways of explaining this discrepancy: (*a*) by dismissing it as a temperature effect, and (*b*) by assuming a special kind of interpenetration of atoms.

a. Not only is the atom alone out in space during the time that the spectroscopic data are obtained, but it is also at an elevated temperature. Data on ionic structure factors show that ions actually expand with rise of temperature,[47] so that it is reasonable to assume that atoms

* The volume coefficient of expansion of liquid Ar is 0.004 at 90°K., whereas for chlorine at 233°K. it is only 0.002 and for sulphur at 388–407°K. only 0.0004. This must mean that at least in *liquid* Ar the atoms are comparatively far apart. Presumably much the same conditions obtain in solid Ar near its melting point.

show the same property. It may be expected, however, that the radii of such expanded valence-electron orbits will be roughly proportional to the radii of the corresponding atomic domains as found from a study of crystals. Table V shows that this is indeed the case.

b. Since we do not know much about the expansion of atoms (as distinguished from the increase in distance between them), it will be interesting to speculate on what conclusions we must draw if we disregard atomic expansion. Since we have on the average, for monovalent atoms, two valence electrons per unit body-centered cube, we can only retain cubic symmetry by relating either the orbits or the mean positions of these valence electrons to the body-diagonals of the unit-cubes. The structure is complete for eight adjacent unit-cubes* and requires the use of such diagonals that "no two of the diagonals in any four cubes whose centers are in one plane are parallel or intersect."† Apparently, if we are to adopt at room temperatures radii such as Turner's and at the same time retain the correct crystal symmetry and the correct lattice parameter, we must imagine each valence electron to have an orbit which lies partly in one atom and partly in an adjacent atom.

In any case, since it is with the atomic domain at room temperature that the crystal analyst has to do rather than with the size of the atom under spectroscopic conditions, he may perhaps be pardoned if he contents himself with showing merely that the atomic-structure calculations yield results which are roughly proportional to the sizes of the corresponding atomic domains.

In Chap. XV we shall have occasion to calculate various properties of the alkali metals. These calculations will be based on the assumption that the valence electrons occupy fixed positions in the crystal in the same sense that atoms do. In accordance with the results of the theory of space-groups they will be placed on the appropriate body-diagonals of the unit-cube, midway between adjacent atoms.‡

5. The Method of Ionizing Potentials.—It is a consequence of the theory of the Bohr type of atom that the radius of the circular orbit of the single electron in a hydrogen atom is

* *I.e.*, unit-cubes as determined by x-ray diffraction methods in terms of *atoms* alone.

† If we choose to consider the valence electron to rotate about the nucleus instead of about a point on the body-diagonal of the unit-cube, then this may be interpreted as meaning (1) that the plane of the orbit is constrained to be such as to include the body-diagonal of the unit-cube, and (2) that the possible positions assigned by the theory of space-groups are the intersections of the orbits with the body-diagonals. It is easier, however, for the crystal analyst to think of the valence electrons as having definite mean positions in the crystal lattice just as the positive ions (atoms minus their valence electrons) do. It will appear later that there is considerable justification for this point of view.

‡ Any other location on the body-diagonal would be the equivalent of assuming equal numbers of positively and negatively charged metallic ions, an assumption which we have already found reason to reject.

$$r = \frac{e^2}{\text{energy of the electron}} = \frac{e^2}{eV} = \frac{e}{V}$$

where e is the charge on the electron and V is the ionizing potential of the atom. If this simple sort of formula could be applied directly to the atoms of other elements, we would have at once the law that the radius of an atom is inversely proportional to its ionizing potential.[21,22] A similar conclusion can be drawn for the chemist's static atom.[1,23] Actually it is not so simple. The additional electrons in the atoms of elements other than hydrogen alter the electrostatic forces, and the equation becomes more complicated. This means that the atomic radii may be expected to be only approximately proportional to the reciprocal of the ionizing potential. The approximation should be best in the case of the monovalent elements whose atomic structure is so simple that they may be replaced by a point positive charge and a single electron, *i.e.*, the alkali metals. Trial shows that even here the product of the ionizing potential* and the "radius" from Table III is not constant to within 10 per cent of the mean. But here again we must recognize that the radius of the orbit of the valence electron is not the radius of the atomic domain. B. Davis[24] has proposed that the product of the radius of the atomic domain and a quantity $(I - R)$ should be approximately constant, where I is the ionizing potential of an atom and R its radiation potential. This gives a more constant product than that of Eve and Saha.[21,22] Anderson[25] has calculated the approximate radii of the orbits of the valence electrons of the alkali-metal vapors on the assumption that the ionizing potential is one-half the calculated potential of a point on the orbit of the valence electron and that the distribution of the electrons in the kernel of the atom is that given by Bury and Bohr. His values are compared with the distances of closest approach in the crystal

TABLE VI.—RADII OF ATOMS OF ALKALI-METAL VAPORS FROM IONIZING POTENTIALS

Element	"Radius" from ionizing potential, Ångströms	Half body-diagonal of cubic atomic domain, Ångströms
Li	1.379	1.52
Na	1.80	1.86
K	2.21	2.31
Rb	2.45	2.43
Cs	2.695	2.61

in Table VI. The agreement is probably accidental. The distance of closest approach includes the mean distance between the true atomic

* See Landolt-Börnstein (1923) or "International Critical Tables," Vol. VI, pp. 70–72.

domains, and Anderson's calculations evidently yield an orbit for the valence electron which just fits into this space.

6. The Composite Physico-chemical Method (Sirk's Method).—This method[26] combines the values of four specific constants,

T_K = critical temperature in degrees Kelvin.
D = density at the boiling point.
λ = internal heat of vaporization in calories per gram.
M = molecular weight.

with the value of the Loschmidt (Avogadro) number*

$$L = 6.061 \times 10^{23}.$$

in such a way as to yield the radius of the molecule. Since the density and molecular weight are involved, it is evident that this method yields a radius of the molecular domain. Except for the fact that this method deals with the properties of boiling liquids, this radius should correspond to the half-distance of closest approach in the crystalline form.

Sirk arrives at the molecular radius in the following way: The surface tension of a substance may be considered[27,28] as being composed of two parts, one of which vanishes at absolute zero and the other of which is relatively independent of molecular motion. Debye finds[29] that this second portion which we shall call S may be expressed as

$$S = \frac{3\pi}{8} \cdot \frac{\alpha\tau^2 n^2}{d^4} \tag{1}$$

where α and τ are molecular constants, n is the number of molecules per unit volume, and d is the molecular diameter. From this it is evident that S varies with the temperature only because it varies directly with n^2. Since n varies as $1/V$, we may write

$$\frac{S}{S_0} = \frac{V_0^2}{V^2} \tag{2}$$

where S_0 and S are, now the temperature-insensitive portion of the surface tension at absolute zero and the boiling point, and V_0 and V are the molecular volume at absolute zero and the boiling point.

$$V = \frac{M}{D} \text{ and } V_0 = \frac{M}{D_0}$$

It is this use of the molecular volume which causes Sirk's method to give the dimensions of the atomic domain.

Following the classical treatment of Ramsay and Eötvös, we have for S_0,

$$S_0 = 2.1\left(\frac{T_K}{V_0^{2/3}}\right) \tag{3}$$

*Sirk used $L = 6.23 \times 10^{23}$. His results have been recalculated in terms of the accepted value.

Debye obtains the latent heat of evaporation in c.g.s. units per gram-molecule as

$$\Lambda = \frac{6\pi}{5} \cdot \frac{\alpha r^2}{d^5} \cdot n^2 V \tag{4}$$

Eliminating α, r^2, and n^2 from Eqs. (1) and (4) we have

$$d = 3.2\frac{SV}{\Lambda} \tag{5}$$

By the use of Eqs. (2) and (3) we may eliminate S from Eq. (5), giving

$$d = 6.72\frac{T_K}{\Lambda} \cdot \frac{V_0^{1/3}}{V} \tag{6}$$

or, since $\Lambda = .18M\lambda \times 10^7$ and $V = M/D$,

$$d = 1.61 \times 10^{-7}\left(\frac{T_K D V_0^{1/3}}{M^2\lambda}\right) \tag{7}$$

Sirk has calculated diameters, and therefore radii, for several gases. Of these we have available x-ray data for Ar, N_2, CO, and O_2. We shall use the case of the monatomic element Ar as an example of Sirk's applica-

TABLE VII.—COMPARISON OF SIRK'S DIAMETERS WITH DISTANCES OF CLOSEST APPROACH

Element	Sirk's diameter, Ångströms	Distance of closest approach, Ångströms
Ar	3.6	3.84 (reference 30)
N_2	3.9	4.00 (reference 11)
CO	3.9	4.00 (reference 11)
O_2	3.6	3.76 (reference 7)

tion of Eq. (7). Since it has been shown[30] by x-ray methods that Ar crystallizes on a face-centered cubic lattice, *i.e.*, the closest packing of spheres, we have that*

$$V_0 = \frac{1}{\sqrt{2}}Ld^3$$

Equation (7) therefore becomes

$$d \times 10^8 = \sqrt[3]{0.192\frac{M^2\lambda}{T_K D}}$$

* Consider a face-centered cube of edge a and therefore of volume a^3. Since it contains four atoms, the "atomic volume" is $\frac{1}{4}a^3$. The actual diameter of each atom, considered as a sphere, is $\frac{1}{2}a\sqrt{2}$ and its actual volume is therefore $\frac{1}{6}\pi(a/\sqrt{2})^3$. Therefore the actual volume is, within the precision of the rest of the data, $1/\sqrt{2} \times$ atomic volume.

For Ar this gives a diameter of 3.6Å. at the boiling point, 87°K. This is to be compared with the value of 3.84Å. at 85°K. from Table I. Considering the relative indirectness of Sirk's method, and the experimental difficulties involved in the exact determination of some of the quantities required by Eq. (7), the agreement is remarkably close. Sirk's diameters are compared in Table VII with the distances of closest approach in crystals.

7. Wollan[31] has calculated from the x-ray scattering by gaseous neon a curve for the density of distribution of electrons along the radius of a neon atom. His curve extrapolates to zero very close to a radius of 1.6Å., corresponding to the value shown in Table I from the lattice parameter of solid neon.

8. Consequences of Spherical Shape of Atomic Domains.—In the foregoing discussion we have really been considering the volumes of atomic domains. In order to arrive at those linear measurements which we have called radii, etc., we have had to assume a shape for each atomic domain. It will therefore be of interest to cite two different lines of reasoning which depend for their success upon the correctness of our assumptions as to the shapes of the atomic domains. The first of these will deal with temperatures of fusion, the second with diffusion in metals.

a. The melting point of an element which has a spherical atomic domain should depend upon the over-all expansion of the element to such an extent that the effects of cohesive forces are of secondary importance. This may be shown as follows:[32] The (1 1 1) planes of a face-centered cubic crystal and the (0 0 · 1) planes of a hexagonal close-packed crystal have their atomic centers at the vertices of equilateral triangles. If we assume that the atomic domains are spheres, then at absolute zero these spheres should be in contact with each other and a single plane would appear as shown by the circles in Fig. 2. The next layer immediately above this plane will have its atoms above the black spots of Fig. 2. If a solid body such as copper, with a structure like this, is to become liquid, it must evidently expand sufficiently to enable the atomic domains in the layer just above the paper to pass through the "valleys" between the atomic domains in the plane of the paper. It may be calculated readily that, for the case of atoms at rest, this expansion must be 4½ per cent along each cube-edge.

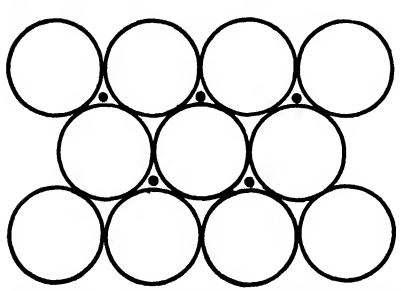

Fig. 2.—(1 1 1) planes of a face-centered cube at absolute zero.

But in the actual case this expansion is the result of a random heat motion such that Maxwell's distribution law may be applied. Examination of a face-centered cubic model shows that at each corner of the

cube a tetrahedron is formed by the atoms at the centers of the adjacent faces and the atom at the corner. Examination shows further that if, of the four tetrahedra which meet at a common point on the exterior cube face of the crystal, one is expanded enough to permit an atomic domain to slide out of its position, then all four tetrahedra will be able to disintegrate.* If this condition obtains at every such meeting place of tetrahedra on the crystal surface, the surface will slough off, *i.e.*, the surface will melt. Since each unit-cube contains eight tetrahedra, this

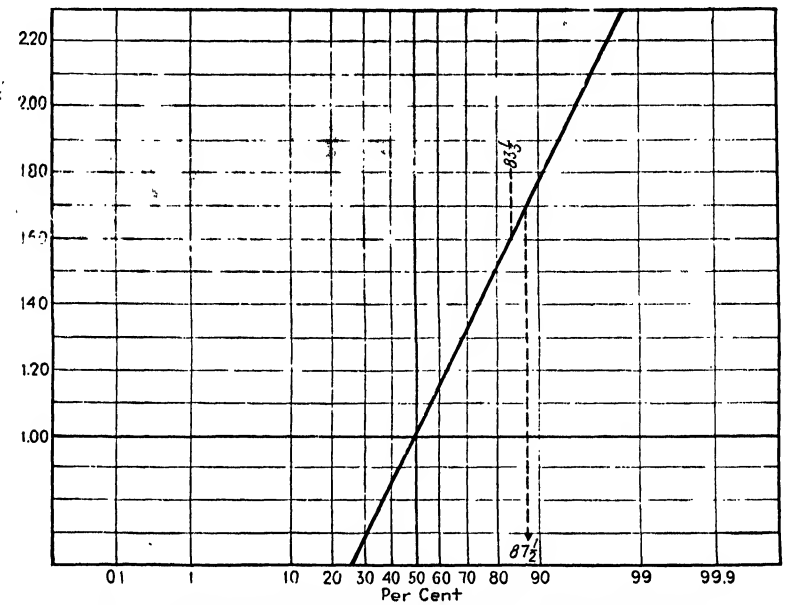

FIG. 3.—Maxwell's distribution law plotted on probability paper.

means that, on the average, 12½ per cent of the tetrahedra belonging to the surface unit-cubes must expand by at least as much as 4½ per cent of their 0°K. size. This, in turn, means that 12½ per cent of all the tetrahedra in the whole crystal must experience such a critical expansion. This leaves, at the melting temperature, 87½ per cent of the tetrahedra with expansions below the critical 4½ per cent. Figure 3 shows the Maxwell distribution law plotted on probability paper (see Chap. VI for a description of this kind of coordinate paper). According to the graph, if 87½ per cent of the tetrahedra are still below some critical expansion, then the most probable expansion is only 1.0/1.7 of the critical value. Therefore a gross linear expansion of $1.0/1.7 \times 4.5 = 2.6$ per cent above the dimensions at absolute zero is a prerequisite to the melting of a face-centered cubic crystal made up of spherical atomic domains.

* This may be seen easily if the model is held with the (1 1 1) planes horizontal.

Added to this will be the expansion of the true atomic domains themselves and the slight additional expansion occurring while (and if) the atoms take up additional heat energy to overcome the forces of cohesion.

Coefficients of expansion for face-centered cubic metals over various temperature ranges may be found in Landolt and Börnstein's "Tabellen," Vol. II, pages 1217 to 1219 (1923). These data go to low enough temperatures so that we may feel fairly safe in extrapolating to 0°K. Taking these data as they appear in the "Tabellen," we arrive at the following total expansions from 0°K. to the melting point for metals which we have assumed to have spherical atomic domains:* Ag, 2.3; Mg, 2.4; Al, 2.4; Ni, 2.9; Cu, 2.4 per cent.† There is, however, considerable doubt as to the correctness of the coefficients listed near the melting points, partly because of the mechanical weakness of such metals near their melting points and partly because of the effect of oxidation. A careful measurement[33] in hydrogen of the total expansion of copper from room temperature to the melting point gave values which, when added to those from the "Tabellen" for lower temperatures, indicate a total expansion in copper of 2.9 per cent from 0°K. to the melting point. Not only is this large enough to take care of the necessary geometry described above, but it also gives a not unreasonable margin to take care of cohesion and atomic expansion. Presumably similar measurements on pure Ag, Mg, and Al would make similar changes in the final results. Marked changes in the data for Ni are not to be expected in view of the well-known resistance of Ni to oxidation.

If the atomic domains of these metals had not been assumed to be spherical (or at least some close approximation to spheres), the results of our calculations would have been quite different. For instance, suppose we had considered the metals listed in Table I to have had cubic atomic domains. Then there would have been no geometrical limits imposed upon the expansion as the metal was heated up to the melting point. The only limit to the melting temperature for cubic crystals whose atomic domains are cubic must be set by the forces of cohesion. In other words, for a pure metal, belonging to the cubic system, whose atomic domains are cubic, the total expansion from 0°K. is not the most important prerequisite for fusion; the temperature of melting should depend primarily upon the ultimate tensile strength. Tensile-strength data

* If we had assumed spherical atomic domains for elements having the body-centered cubic structure, the expansion necessary to permit the melting would have been $1.0/1.6 \times 50 = 31$ per cent of the dimensions at 0°K. Data on Mo and Ta [A. G. Worthing, *Phys. Rev.*, **28**, 190 (1926)] and on W ("International Critical Tables," Vol. II, p. 462) give expansions from 0°K. to the melting point of 2.0, 2.45, and 1.7 per cent, respectively. Obviously we cannot by any stretch of the imagination consider these atomic domains to be spherical.

† The case of γ-Fe is complicated by the fact that we never have pure Fe in the γ state either at 0°K. or at the melting point.

for the face-centered cubic metals Cu, Ag, Au, Al, Pb, Ni, and Pt, given in the "International Critical Tables" (Vol. II, pages 478 *ff.*) show no relation between tensile strength and melting temperature. Evidently the atomic domains of face-centered cubic metals can not be cubic.

In contrast to the face-centered cubic metals, we find that for the body-centered cubic metals the greater the tensile strength the higher is the melting point. This is brought out in Table VIII, which lists along with the alkali metals the best data available for Fe,* Mo, Ta, and W

TABLE VIII.—DEPENDENCE OF MELTING POINT ON COHESIVE FORCES FOR PURE METALS HAVING CUBIC ATOMIC DOMAINS

Element	Melting point	Ultimate tensile strength, kilograms per square centimeter
Fe	1535° C.	29.6*
Mo	2620	70
Ta	2850	93
W	3370	150–420

* Depending upon heat treatment. The low values given in "International Critical Tables" are for annealed electrolytic iron which probably corresponds in condition most closely with the other metals listed.

(see "International Critical Tables," Vol. II, pages 478, 592). There is evidently considerable justification for considering these atomic domains to have a cubic shape, and none† for considering them to have a spherical shape.

b. It has already been mentioned that if we assume the atoms of body-centered cubic metals to have cubic atomic domains, then it follows that body-centered cubic crystals are traversed by tunnels whose square cross-section is equal to that of the cubic atomic domains.‡

* Fe is included in this table because it has the body-centered cubic structure both at the melting temperature (δ-Fe) and at the temperature of the tensile strength data (α-Fe).

† See preceding footnote in connection with the expansion of Mo, Ta, and W from 0°K. to the melting point.

‡ It might seem at first sight as though permeability of pure iron to hydrogen would furnish a crucial test of this picture. In α-Fe at room temperature the tunnels should be 1.43×10^{-8} cm. square (Table III). They are therefore too small for molecular hydrogen (effective diameter 2.4Å.[34]) to pass through. If we assume an effective diameter of 1.2Å. for a single atom of hydrogen, then we should expect iron to be permeable to atomic hydrogen at room temperature. It is true that iron is impermeable to molecular hydrogen and that it is permeable to nascent, *i.e.*, atomic, hydrogen.[35,36] But unfortunately for a crucial test of the existence of tunnels, there is considerable evidence[37] (some of which will be touched upon in a later chapter) that the atomic hydrogen unites chemically with the iron to form an iron hydride. This would, of course, cause the hydrogen atom to lose its valence electron to some iron atom in its neighborhood. The resulting H^+ ion, consisting of only a single

It is a well-known fact that it is extremely difficult, if not impossible, in a vacuum to cause carbon to leave a crystal of graphite and diffuse through a block of α iron. But it is easy to get atomic carbon on the surface of iron by the decomposition of CO, CH_4, NaCN, or other organic matter, and carbon thus obtained diffuses readily through the α iron if the temperature is high enough. There is such a wealth of evidence as to the existence of the compound Fe_3C that we can hardly imagine the migrating carbon to be in any other form than that of an ion.* Because of its size, C^{----} cannot be expected to travel through the "normal" tunnels of the iron at room temperature (1.4 Å.sq.). At such temperatures it is only when some portion of a tunnel next to a C^{----} ion has opened up sufficiently that the ion can move another step.† With increasing temperature the chance of a wide enough opening increases. If we plot the reciprocal of the absolute temperature against the logarithm of the rate of migration, we should get a straight line. This line should have a much greater slope in the case of a body-centered cubic metal than in the case of a face-centered cubic metal. That this is so is indicated even in the case of hydrogen. The $1/T$ *vs.* log-rate curve for hydrogen in iron rises steeply over the temperature corresponding to α iron, shows a sudden drop at the A_3 point, and then rises at a much smaller rate over the temperatures corresponding to γ iron.

Obviously, according to this picture, the Si^{----} ion, because of its larger size, should require higher temperatures or longer times than C^{----} to show the same diffusion effects in iron. Also we should expect that C^{----} ought to diffuse through Mo or W somewhat more readily than through Fe because of the larger dimensions of the tunnels. These conclusions are in accord with metallurgical experience. Without the picture of tunnels it would seem difficult to account for the speed of migration of carbon and silicon in iron and similar metals at temperatures so far from the melting point and at the same time to account for the practical absence of migration at room temperature.

---

proton of negligible dimensions, should be able to travel freely and with considerable rapidity through the crystals of the iron. Presumably the valence electron should travel along from atom to atom of the iron keeping pace with the H^+ ion. Experiment shows that the H^+ ion recaptures its valence electron on the emergent face of the metal and combines with some other atom of hydrogen thus giving H_2 once more. Enough hydrogen can be diffused through a sheet of iron in this way to give a perceptible reading on a pressure gauge on the emergent side of the iron. This picture leads us to believe that the transfer of hydrogen is not limited to metals which have tunnels, for the H^+ ion should be able to travel through any metal which is capable of holding its valence electron. Experiment shows that this is indeed the case.

* Even in "molecular," *i.e.*, electron-sharing, compounds of carbon we seem compelled to assume that the shared electrons are much farther from the carbon nucleus than they are from the nucleus of the other element. This assumption is made use of in Chap. XIV and is brought up again in Chap. XIX.

† See discussion of the Maxwell distribution law in connection with Fig. 3.

We have, then, considerable justification for our pictures of spherical and cubic atomic domains and for the dimensions assigned to them. Equally convincing arguments could be brought forward, if space permitted, in favor of the spheroidal and tetrahedral shapes of other atomic domains. It will be sufficient to say that organic chemistry, both of carbon and of silicon compounds, would be difficult to understand except in terms of tetrahedral atoms. The shapes and sizes assigned to atomic domains give us a set of pictures in terms of which we can more readily interpret those directive fields of force which bind atoms together and which have so much to do with the properties of elements. It is only natural to assume that, if similar pictures could be made of the various ionic domains, our ideas of ionic compounds would be similarly clarified. The remainder of this chapter will deal with various attempts which have been made in this direction.

THE PACKING-SHAPES AND PACKING-SIZES OF IONS

There are two ordinary ways by which two elements may be held together in chemical combination.* One is by the direct transfer of valence electrons from the atoms of one element to the atoms of the other element. This method produces "ionic" compounds in which the crystal of the solid is made up not of atoms but of ions. When crystals of this sort are dissolved in water, the resulting solutions are electrically conducting. When these crystals are fused, they conduct by ionic conduction and the compound may be decomposed by electrolysis. All simple inorganic salts and all oxides and sulphides of metals with a valence of one or two are supposed to be of this sort. It is a characteristic of these compounds that they crystallize in such a way that each ion of one element is surrounded by ions of the other element, symmetrically placed and equally spaced. In NaCl each Na^+ is surrounded by six Cl^-. Three of these Cl^- form an equilateral triangle above the Na^+, and three form an equilateral triangle below it. Each Cl^- is similarly surrounded by six Na^+. In CsCl each Cs^+ is in the center of a cube of Cl^-, and each Cl^- is similarly surrounded by eight Cs^+. In $CaCO_3$ the rhombohedral crystal may be thought of as a distorted NaCl cube in which Ca^{++} replaces Na^+ and CO_3^{--} replaces Cl^-. Other illustrations may be found in any résumé of crystal-structure data.

The second method produces "molecular" (*i.e.*, electron-sharing) compounds and "radicals." These include the oxides of elements such as Si, Al, Cr, Fe, with a valence of three or more, many organic crystals, and such radicals as NO_3^-, CO_3^{--}, SO_3^{--}, etc. It is true that we may think of one of the components as having given up its valence electrons to the other (for instance, in Chap. VI we have already considered SiO_2 to be made up of Si^{++++} and two O^{--}, and we shall do so again in Chap. XIV);

* See Chap. XIX for a discussion of five types of chemical combination.

still, the end result is different from a truly ionic compound in that the two components seem to be more definitely attached to each other. For example, very pure Al_2O_3 is not a good electrical conductor even when strongly heated. When an NO_3^{--} radical is dissolved in water, the N and three O do not wander apart as separate ions. These compounds are characterized by the fact that they crystallize with the "molecule" or "radical" as a unit. In SiO_2 each Si has two O which are closer to it than to any other Si; in Al_2O_3 three O form an equilateral triangle with one Al immediately above the center of the triangle and a second Al immediately below; the CO_3^{--} group has an equilateral triangle of O with a C in the center of the triangle.

The packing-size and the packing-shape of an atom in the crystal of a compound are, in general, quite different from what we have found in our previous discussion for the same atom in the crystal of the element, and the packing-shape and packing-dimensions in a molecular compound have no necessary direct connection with what we find for the same atom in an ionic compound. If an element can have more than one valence, the ion may be expected to have a different packing-size and shape for each valence. The packing-radii of atoms when sharing electrons are hardly as definite as the radii of true ions, for it is largely a matter of interpretation where the positive atom is supposed to end and the negative atom to begin. We shall therefore take up first the shapes and sizes of the domains of true ions.

Shapes of Alkali and Halogen Ionic Domains.—Just as it was possible to assign definite shapes to the domains of atoms, in the same way it is possible to assign shapes to various ions on the basis of their crystal structures. For instance CsI has a body-centered cubic structure with Cs^+ at the corners of each unit-cube and I^- at the center. This is the closest packing for equal numbers of positively and negatively charged spheres of approximately equal size. We are therefore tempted at once to assume that the domains of Cs^+ and I^- are spherical in shape. Such a packing-shape is about what we might have expected of an ion of such high ionic number if it were not for the commonly accepted picture that the I^- (or Cs^+) has only eight electrons in its outmost shell. Possibly the ionic domain of I^- (or Cs^+) represents a compromise between a sphere and a cube. The spherical picture would appear to gain considerable support from the experimental data. The distances of closest approach of Cs^+ and I^- in CsI and of Cs^+ and Br^- in CsBr are measured along the body-diagonals of the unit-cubes of the crystals. In RbBr and RbI the corresponding distances are measured parallel to the edges of the unit-cubes. This gives us two directions which are 54° 30′ apart. If, now, we use the chemical symbol to represent the distance from the center of an ionic domain to the point of contact with an adjacent atomic domain we have, by experiment,[38]

$$(Cs^+ + I^-) = 3.947 \pm 0.004\text{Å}.$$
$$(Cs^+ + Br^-) = 3.713 \pm 0.004\text{Å}.$$
$$(Rb^+ + I^-) = 3.662 \pm 0.004\text{Å}.$$
$$(Rb^+ + Br^-) = 3.434 \pm 0.004\text{Å}.$$

Then

$$(Cs^+ + I^-) - (Cs^+ + Br^-) = I^- - Br^- = 0.234 \pm 0.008\text{Å}.$$

measured along the body-diagonal of the unit-cube;

$$(Rb^+ + I^-) - (Rb^+ + Br^-) = I^- - Br^- = 0.228 \pm 0.008\text{Å}.$$

measured parallel to the edge of the unit-cube.

It is hard to imagine that these differences in distance could be identical within the precision of the data if the two ionic domains were not substantially spherical.* With this much direct evidence of the spherical shape of the I^- ionic domain, we can probably assume safely that the domain of Cs^+ is also spherical, for Cs^+ has the same number of extranuclear electrons as I^- and the two ions differ in nuclear charge by only 2 per cent from the mean.

We have made the implied assumption in the foregoing that the ionic domain of Br^- is also substantially spherical. We might continue the reasoning that was so successful in the case of Cs^+ and I^- and argue that the ionic domain of Rb^+ is also spherical. We could then compare the corresponding data for CsI, CsCl, RbI, and RbCl with the following results:

$$(Cs^+ + I^-) - (Cs^+ + Cl^-) = 0.392 \pm 0.008\text{Å}.$$

measured along the body-diagonal of the cube;

$$(Rb^+ + I^-) - (Rb^+ + Cl^-) = 0.377 \pm 0.007\text{Å}.$$

measured parallel to the cube-edge.

Here we see that the agreement in the two directions is again within the possible experimental error. Similar calculations for CsI, CsCl, KI, and KCl agree even more closely, so that we are tempted at once to assign spherical ionic domains to Cs^+, Rb^+, K^+, I^-, Br^-, and Cl^-.

We must be prepared, however, to permit slight departure from sphericity as long as the changes do not alter the characteristic dimensions of the ionic domain too greatly. For instance we could substitute for a sphere a cube with well-rounded corners. If the corners were rounded off sufficiently, the cube would become a sphere with six small flat spots which could not be distinguished from a true sphere within the

* For instance, if the ionic domains had both been cubic in shape, the differences would have had to be in the ratio of 1.00:0.58. A compromise between the spherical and cubic shapes will be proposed later.

precision of Table IX.* There is a great deal to be said in favor of such a picture. Both the chemist's static-atom picture and the physicist's kinetic atom give to these ions certain of the characteristics of a cube. There is no trouble in imagining a set of well-rounded corners for a "cubic" ionic domain enclosing a kinetic type of ion, and even the most enthusiastic supporter of the chemist's static-atom picture would hardly deny that the "positions" assigned to the electrons represent more than mean positions of vibrating† electrons. We may, therefore, perhaps be pardoned if we assume in connection with our crude mechanical pictures of "domains" that the alkali and halogen ionic domains are essentially spherical in shape with possibly six flat spots on the sphere to make it simulate a cube. It might not be amiss to assume that the flat spots are less pronounced in the case of Cs^+ and I^- than in the case of ions of lower ionic number.

ZnO crystallizes with the Zn^{++} in a hexagonal close-packed lattice. Each O^{--} lies at the center of a tetrahedron of Zn^{++}. ZnS (sphalerite) has the Zn^{++} in a face-centered cubic lattice with each S^{--} in the center of a tetrahedron of Zn^{++}. This is taken to mean that the domain of Zn^{++} is essentially spherical and that the ionic domains of O^{--} and S^{--} may be relatively small. We thus have the interesting picture that, when an atom of Zn loses two valence electrons to become an ion, the domain changes from the spheroidal shape of Zn to the spherical shape of Zn^{++}.

Radii of Ionic Domains from X-ray Data.—No matter what picture of atomic structure we adopt, it is evident that the electrostatic forces inside of a "metallic" atom will be altered by the subtraction of each valence electron, with the result that the positive ion must be smaller than the neutral atom. The greater the number of valence electrons which are subtracted, the greater will be the change in the electrostatic forces and the smaller will the positive ion become. Similarly, a negative ion must be larger than the corresponding neutral atom; and the greater the valence of the element, the more will the negative ion swell beyond the size of the neutral atom. When an attempt is made to determine the absolute sizes of these ions from crystal-structure data, it is at once found that the data give only $n - 1$ equations with which to determine n ionic radii. These $n - 1$ equations alone, therefore, will not enable us to calculate *radii* but only *differences between radii*. These differences

* Let a true sphere and a cube of the same volume have a common center. The diameter of the sphere is 1.24 times the length of the cube-edge. Now let the sphere be sliced off at six points opposite the six faces of the cube in such a way as to bring each flat spot to the mid-point between the cube face and the end of the diameter of the sphere. The decrease in volume in going from the true sphere to the sphere with six flat spots is only of the order of 6 per cent.

† Or, according to one of the early pictures, rotating about the body-diagonals of the cubic domain.

are listed in Table IX. The data[39,40,41] are all in terms of NaCl = 2.814Å. as a standard. It will be noticed that, if we exclude Li^+, Na^+, and F^-, these differences are constant for any two ions to within the precision of

TABLE IX.—DIFFERENCES IN DISTANCE OF CLOSEST APPROACH OF IONS IN ALKALI HALIDES*

	Iodide	Bromide	Chloride	Fluoride
Cs	3.947 ± 0.004Å.	3.713 ± 0.004Å.	3.555 ± 0.004Å.	3.00Å.
Rb	3.662 ± 0.004	3.434 ± 0.003	3.285 ± 0.003	2.81
Diff.	0.285 ± 0.008	0.279 ± 0.007	0.270 ± 0.007	0.19
Cs	3.947 ± 0.004	3.713 ± 0.004	3.556 ± 0.004	3.004 ± 0.003Å.
K	3.525 ± 0.004	3.285 ± 0.003	3.138 ± 0.003	2.664 ± 0.003
Diff.	0.422 ± 0.008	0.428 ± 0.007	0.418 ± 0.007	0.340 ± 0.006
Cs	3.947 ± 0.004	3.713 ± 0.004	3.566 ± 0.004	3.004 ± 0.003
Na	3.231 ± 0.003	2.968 ± 0.003	2.814	2.310 ± 0.002
Diff.	0.716 ± 0.007	0.745 ± 0.007	0.752 ± 0.004	0.694 ± 0.005
Cs	3.947 ± 0.004	3.713 ± 0.004	3.566 ± 0.004	3.004 ± 0.003
Li	3.01 ± 0.01	2.745 ± 0.003	2.566 ± 0.003	2.007 ± 0.002
Diff.	0.94 ± 0.01	0.968 ± 0.007	1.000 ± 0.007	0.997 ± 0.005

	Cæsium	Rubidium	Potassium	Sodium	Lithium
I	3.947 ± 0.004	3.662 ± 0.004	3.525 ± 0.004	3.231 ± 0.003	3.01 ± 0.01
Br	3.713 ± 0.004	3.434 ± 0.004	3.285 ± 0.003	2.968 ± 0.003	2.745 ± 0.003
Diff.	0.234 ± 0.008	0.228 ± 0.008	0.240 ± 0.007	0.263 ± 0.006	0.26 ± 0.01
I	3.947 ± 0.004	3.662 ± 0.004	3.525 ± 0.004	3.231 ± 0.003	3.01 ± 0.01
Cl	3.555 ± 0.004	3.285 ± 0.003	3.138 ± 0.003	2.814	2.566 ± 0.003
Diff.	0.392 ± 0.008	0.377 ± 0.007	0.387 ± 0.007	0.417 ± 0.003	0.44 ± 0.01
I	3.947 ± 0.004	3.66	3.525 ± 0.004	3.231 ± 0.003	3.01 ± 0.01
F	3.004 ± 0.003	2.81	2.664 ± 0.003	2.310 ± 0.002	2.007 ± 0.002
Diff.	0.943 ± 0.007	0.85	0.861 ± 0.007	0.921 ± 0.005	1.00 ± 0.01

* Data revised from *Phys. Rev.*, **21**, 143 (1923), except RbF, which is from *Naturwissenschaften*, **14**, 477 (1926).

the data. In other words, contrary to what might have been expected, the radii of these ions are at least approximately independent of their state of chemical combination. The fact that this is obviously untrue

for Li^+, Na^+, and F^- makes it seem likely that more precise data would show slight changes in the values for the other ions. In our present state of knowledge it is sufficient to say that Cs^+, I^-, Rb^+, Br^-, K^+, and Cl^- are so much more constant in size than Li^+, Na^+, and F^- that we may consider them to act like rigid objects.

In order that we may advance from differences between radii to the radii themselves, it is necessary to make some plausible assumption which will furnish an additional equation. Several such assumptions are to be found in the literature. The most plausible of these is furnished by the x-ray diffraction patterns themselves.[38] When the diffraction patterns of the alkali halides are examined, it is found that Cs^+ and I^- have, as nearly as can be determined, equal diffracting power. Rb^+ with Br^-, and K^+ and Cl^-, respectively, also seem to have equal diffracting power. These three pairs are the only ones among the alkali halides for which this is so. A glance at the periodic table shows that each pair lies adjacent to an inert gas, and that each of the ions of each pair contains the same number of electrons as the adjacent neutral atom of the inert gas. The theory of diffraction leads us to believe that the only way in which equal numbers of electrons can show equal diffracting power is for them to be arranged similarly in atomic domains of equal volume. If our data on equality of diffracting power were quite reliable we would have three independent equations:

$$\text{Radius of } Cs^+ = \text{radius of } I^-$$
$$\text{Radius of } Rb^+ = \text{radius of } Br^-$$
$$\text{Radius of } K^+ = \text{radius of } Cl^-$$

An actual trial shows that these equations are approximately true, for they give fairly consistent values of ionic radii in spite of having two more equations than are needed.* That they are not anything more than good approximations may be shown as follows: The periodic table would tempt us to make a fourth equation, similar to the other three, stating the equality of radii of Na^+ and F^-. But in this case the x-ray evidence clearly shows that the 10 electrons in Na^+ do not have the same diffracting power as the 10 in F^- and that therefore their radii are probably different. This is not surprising when we remember that the 10 electrons in F^- are pulled inward by a nuclear charge of 9, while in Na^+ they are pulled in by a charge of 11. It would therefore seem as though the other pairs of ions should not be of exactly equal radius. This is confirmed by Table IX

* These assumptions give the following radii:

$Cs^+ \geq 1.974\text{Å}. \geq I^-$
$Rb^+ \geq 1.717\text{Å}. \geq Br^-$
$K^+ \geq 1.569\text{Å}. \geq Cl^-$

A similar assumption gives

$Na^+ \geq 1.155\text{Å}. \geq F^-$

which shows that $Cs^+ - Rb^+$ is not equal to $I^- - Br^-$ and that $Cs^+ - K^+$ is not quite equal to $I^- - Cl^-$. Since the ions Cs^+ and I^- have the highest atomic numbers of any of the alkali and halogen ions, we shall assume that the best approximation will be had by considering that their radii are equal to each other and therefore that each has a radius equal to one-half the distance of closest approach of Cs^+ and I^- in CsI. This assumption, together with the differences listed in Table IX, gives us the ionic radii of Table X. It should be noted that, since Cs^+ is probably

TABLE X.—RADII OF DOMAINS OF ALKALI AND HALOGEN IONS ON THE ASSUMPTION THAT $Cs^+ = I^-$

Cs^+	1.974×10^{-8} cm.	I^-	1.974×10^{-8} cm.
Rb^+	1.696	Br^-	1.740
K^+	1.348	Cl^-	1.589
Na^+		F^-	
in NaI	1.257	in CsF	1.030
in NaBr	1.231	in RbF	.....
in NaCl	1.225	in KF	1.116
in NaF	<1.15	in NaF	>1.15
Li^+			
in LiI	1.03		
in LiBr	1.01		
in LiCl	0.98		
in LiF	<0.86		

a little smaller than I^-, the radii listed for the alkali ions all represent upper limits, while those listed for the halogen ions represent lower limits.

The same type of reasoning which led us to assume that the radii of the domains of Cs^+ and I^- were substantially equal would lead us to assume that, to a lesser degree of approximation, the domains of Ba^{++} and Te^{--} may be considered equal. BaTe crystallizes with the NaCl type of structure. The edge of the unit-cube containing four BaTe is 6.986 ± 0.002Å.[42] This gives, according to the assumption made above,

$$Ba^{++} \geq 1.746\text{Å}. \geq Te^{--}$$

Similar assumptions for SrSe, CaS, and MgO would give

$$Sr^{++} \geq 1.558\text{Å}. \geq Se^{--}$$
$$Ca^{++} \geq 1.421\text{Å}. \geq S^{--}$$
$$Mg^{++} \geq 1.05\text{Å}. \geq O^{--}$$

Just as we found more definite values for the radii of the alkali and halogen ionic domains by considering $Cs^+ = I^-$, so we may hope to arrive at more definite values for the radii of the domains of the ions of the

alkali earths and of the oxygen series by considering $Ba^{++} = Te^{--}$. The lattice parameters given in the literature for compounds in the $A^{++}B^{--}$ class are given in Table XI. Approximate radii calculated from

TABLE XI.—LATTICE PARAMETERS FOR $A^{++}B^{--}$ CLASS OF COMPOUNDS OF THE ALKALI EARTHS

BaTe	6.986Å.	V. M. GOLDSCHMIDT, *Zeit. Kryst.*, **69**, 411 (1929)
BaSe	6.616	M. K. SLATTERY, *Phys. Rev.*, **21**, 22 (1923)
BaS	6.35	S. HOLGERSSON, *Zeit. anorg. Chem.*, **126**, 179 (1923)
BaO	5.50	V. M. GOLDSCHMIDT, *Naturwissenschaften*, **14**, 477 (1926)
SrTe	6.48	V. M. GOLDSCHMIDT, *Naturwissenschaften*, **14**, 477 (1926)
SrSe	6.234	M. K. SLATTERY, *Phys. Rev.*, **21**, 22 (1923)
SrS	5.86	S. HOLGERSON, *Zeit. anorg. Chem.*, **126**, 179 (1923)
SrO	5.10	T. A. WILSON, *Phys. Rev.*, **31**, 305 (1928)
CaTe	6.345	I. OFTEDAL, *Zeit. phys. Chem.*, **128**, 154 (1927)
CaSe	5.914	W. P. DAVEY, *Phys. Rev.*, **21**, 213 (1923)
CaS	5.686	W. P. DAVEY, *Phys. Rev.*, **21**, 213 (1923)
CaO	4.790	W. P. DAVEY, *Phys. Rev.*, **21**, 213 (1923) See also: I. OFTEDAL, *loc. cit.*
MgTe*	$a = 4.52$ $c = 8.33$	W. ZACHARIASEN, *Zeit. phys. Chem.*, **128**, 417 (1927)
MgSe	5.452	E. BROCH, *Zeit. phys. Chem.*, **127**, 446 (1927)
MgS	5.190	E. BROCH, *Zeit. phys. Chem.*, **127**, 446 (1927)
MgO	4.203	L. PASSERINI, *Gazz. chim. ital.*, **59**, 144 (1929)

* Wurtzite type. All others are NaCl type.

Table XI are listed in Table XII. Inasmuch as the purity of the specimen is not known in most cases, the results are rather open to suspicion, but at any rate they will serve to give an idea of the general size of the

TABLE XII.—APPROXIMATE RADII OF IONIC DOMAINS OF THE ALKALI EARTHS AND OF THE OXYGEN SERIES

Ba^{++} 1.746×10^{-8} cm.	Te^{--} 1.746×10^{-8} cm.
Sr^{++} 1.55	Se^{--} 1.56
Ca^{++} 1.39 – 1.42	S^{--} 1.42 – 1.5
Mg^{++} 1.01 – 1.22	O^{--} 0.97 – 1.09

radii of these ionic domains. Since O^{--} should be larger than Mg^{++}, we are tempted to accept the limiting values of $O^{--} = 1.09$Å. and $Mg^{++} = 1.01$Å. for the correct radii of the ionic domains in MgO.*

Just as we found variable radii for the ionic domains of Li^+ and F^-, so we find variable radii for Mg^{++} and O^{--} and even for Ca^{++} and S^{--}.

* It is interesting to note that this value for the packing-radius of the O^{--} is consistent with the fact that the oxygen-to-oxygen distance in carbonates is 2.18Å.

This was to have been expected. Certainly the radius of an ionic domain should depend upon the nearness of the ion to other ions, especially to those of opposite sign. The higher the valence and the smaller the size of the ion, the more marked should be the effect. The wonder is not that the domains of these small ions show variations in size from compound to compound but rather that the larger ionic domains show as much constancy of size as they do. It was this possibility of variation in size which led us in Chap. IX to allow a leeway of 10 per cent in the sizes of ionic domains when fitting them into a crystal structure.

Using the radius of Te^{--} from Table XII and the lattice parameters of FeTe,[43] we find that the radius of the ionic domain of ferrous iron is $Fe^{++} \geq 0.85$ Å.

It is not known how far this method can be extended in calculating the dimensions of ionic domains, but probably its reliability decreases rapidly as the valence of the ions is increased. The next step would seem to be to consider $In^{+++} \geq Sb^{---}$ in InSb, $Ga^{+++} \geq As^{---}$ in GaAs,

TABLE XIII.—APPROXIMATE RADII OF TRIVALENT IONS OF THE Al AND P SERIES

$In^{+++} \geq$	1.39×10^{-8} cm.	$\geq Sb^{---}$
$Ga^{+++} \geq$	1.22	$\geq As^{---}$
$Al^{+++} \geq$	1.17	$\geq P^{---}$

and $Al^{+++} \geq P^{---}$ in AlP. The data in the literature[44] lead to the values given in Table XIII. These radii are able to predict the interionic spacings of GaSb and GaP to within about 2 per cent. The difficulty of getting pure enough materials to make any higher precision worth while will be apparent to any one who has ever tried it. Even if the data in Table XIII are taken to really represent the dimensions of the ionic domains in the compounds mentioned, it is not to be assumed that the same ions have the same dimensions in other compounds. We must remember that the ions we are now dealing with have a complex and possibly variable structure which is reflected in the dimensions of their domains. For instance, if we are to trust the data in the literature at all, then the lattice parameters of FeSb[45] would indicate that the radius of the ionic domain of ferric iron is $Fe^{+++} \geq 1.27$Å. Such a result is obviously absurd when we remember that the domain of Fe^{+++} should not only be smaller than that of Fe but also that it should be even smaller than that of Fe^{++}. It is evident, then, that we have gone as far as we dare in assigning dimensions to ionic domains in terms of measurements of lattice parameters. We must find some other basis on which to make further estimates. Such a basis may be found in the theory of Chap. X.

In Chap. X it was shown that, if we had sufficient knowledge of the intensities of diffracted beams of various orders from a given crystal, we might hope to arrive at a fairly definite idea of the concentration of

electrons at different distances along the radii of the atoms (or ions) composing the crystal. If curves expressing the results of such calculations are drawn, it is found that they indicate more or less definite "dimensions" for the atoms (or ions). In reading such curves care must be taken to include the whole of the atom (or ion) and not merely to include the most obvious portion immediately surrounding the center. When such precautions are taken, the ionic-structure-factor results agree remarkably well with the packing-dimensions given above.

Some of the pioneer work on the atomic-structure factor was done by R. J. Havighurst,[46] who has published graphs of the electron densities in various directions for KI. His graph for the direction perpendicular

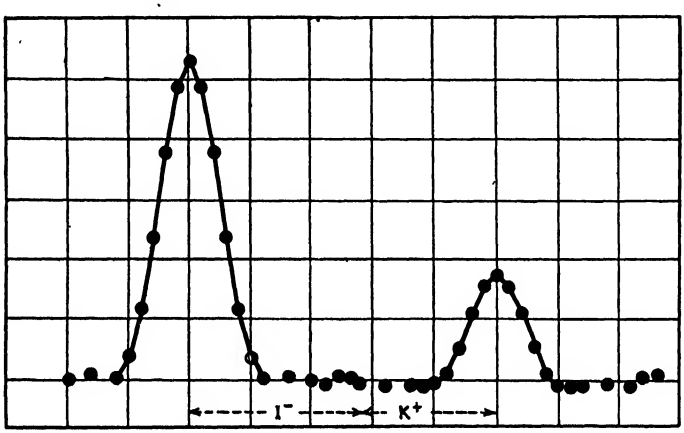

FIG. 4.—Havighurst's graph for electron distributions in KI perpendicular to the (1 0 0) planes.

to the (1 0 0) planes is reproduced here as Fig. 4. This graph indicates that 56 per cent of the $K^+ - I^-$ distance "belongs" to the I^- ion and that 44 per cent "belongs" to the K^+ ion. This gives dimensions of 1.97Å. and 1.55Å., respectively, for the domains of I^- and K^+.* The corresponding packing-radii from Table X are 1.974Å. and 1.548Å. The graphs for the (1 1 1) and (1 1 0) planes are considerably harder to interpret. Apparently the radius for I^- perpendicular to the (1 1 1) plane is, within the error of reading the graph, 16 per cent of 12.2Å. = 1.95Å. The radius perpendicular to the (1 1 0) plane seems to be somewhere between 1.59Å. and 2.49Å. Within the error of reading the graphs there would seem to be considerable justification for our picture of a substantially spherical I^- ion which we arrived at from a discussion of lattice parameters. It is interesting to note that the graphs seem to show that, perpendicular to the (1 0 0) planes, the K^+ and I^- ionic domains "touch,"

* These electron distributions are for ions at room temperature. We assume therefore that the graph shows electron distributions such that the domains are comparable with those considered in Table X.

but that perpendicular to the (1 1 0) and (1 1 1) planes there is a free space between the domains. This is to be expected in terms of substantially spherical domains.

Havighurst also gives graphs for the electron distribution in NaCl. His graph for the distribution perpendicular to the (1 0 0) planes is reproduced here as Fig. 5. This graph shows that Na^+ requires 45 per cent of the $Na^+ - Cl^-$ distance and that Cl^- requires 55 per cent. This gives the ionic domain of Na^+ a radius of 1.26Å. and of Cl^- a radius of 1.55Å. The corresponding packing-radii from Table X are 1.22Å. and 1.59Å. The graph for electron distribution perpendicular to the (1 1 1) planes shows that Cl^- requires 18 per cent of 9.75Å. = 1.75Å. Since this is greater than 1.55Å. and less than $1.55\sqrt{3}$Å., the ionic domain of Cl^-

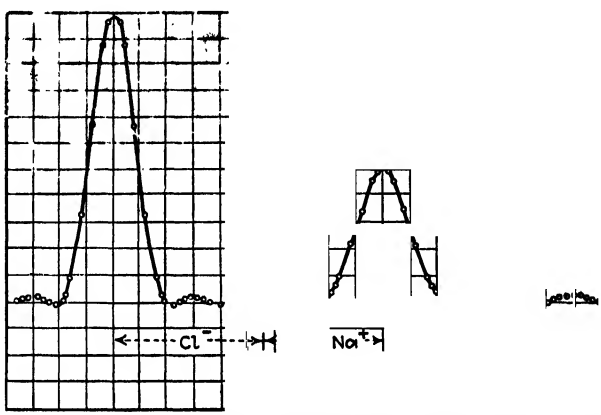

FIG. 5.—Havighurst's graph for electron distributions in NaCl perpendicular to the (1 0 0) planes.

would seem to be a cube with rounded corners, *i.e.*, a sphere with flattened spots. This again is in accord with the picture which we found as a result of our study of lattice parameters.

A similar graph plotted by James and Firth[47] for 290°C. yields radii of 2.14Å. and 2.72Å. for Na^+ and Cl^-, respectively, in a direction perpendicular to the (1 1 1) planes. On the assumption that these ions are not far from cubic, this would correspond to radii perpendicular to the (1 0 0) planes of 1.24Å. and 1.57Å., respectively. The agreement is about as good as could be expected when it is remembered that not only were the temperatures different from Havighurst's but even the equations for the calculations of electron density differed somewhat. It is interesting to note that Havighurst finds[48] that the electron-distribution curves indicate that Na^+ in NaF is a little smaller than Na^+ in NaCl. This is in agreement with Table X.

Wollan[31,49] has investigated the electron distributions in MgO. Using the radial distribution scheme of Duane and Havighurst, he finds

for Mg^{++} a radius of 1.25Å., and for O^{--} a radius of 1.05Å. Using Compton's equation for calculating the electron distribution above a plane in the crystal, he arrives at a graph for the [1 1 1] direction which nowhere reaches down to the zero of electron density. We must now make a choice between two possible assumptions. Either we may accept the x-ray intensity measurements as representing nothing but the diffraction of a single wave length of x-rays, or else we may assume that, since only a ZrO_2 filter was used with Mo rays, the diffraction of MoK_α was superimposed upon a background of scattered "white" x-rays. If we make the first assumption, we are at once tempted to extrapolate the Mg^{++} and O^{--} humps down to the zero of electron density in such a way as to make the areas under each of the humps correspond to the ionic number 10. The distance between the intercepts of the extrapolated curves would then represent the "diameters" of the ions. For all planes in the crystal such an interpretation would show overlapping atoms. But, if we are to retain any idea of impenetrability of ionic (or atomic) domains (*i.e.*, any idea of low compressibility of solids), we ought to have at least one direction in the crystal for which the ions do not overlap. This contradiction makes it hard to retain the first of the alternative assumptions. If, instead, we take the second assumption, we must do as we have already done by implication in Figs. 4 and 5, *i.e.*, we must allow for the scattered white x-rays by taking the lowest part of the electron-distribution curve as our base line of intensity. Such an interpretation shows for Mg^{++} a radius of

$$0.24 \times 4.21 \times \sqrt{3}$$

in a direction perpendicular to the (1 1 1) planes, and for O^{--} in the same direction a radius of $0.26 \times 4.21 \times \sqrt{3}$. Assuming that these ionic domains are nearly cubic in shape this would give radii perpendicular to the (1 0 0) plane of about 1.01Å. for Mg^{++} and 1.09Å. for O^{--}. The corresponding values from Table XII are: Mg^{++}, from 1.01 to 1.22Å.; and O^{--}, from 0.97 to 1.09Å.

Landé[50] has made a very interesting assumption, namely, that the Li^+ ion, being composed of only a positive nucleus and two K electrons, is negligible in size and therefore fits into the chinks between the I^- ions. He therefore takes half the distance of closest approach of adjacent I^- ions in LiI as the upper limit of the radius of I^-. He then obtains the values for the radii of the other alkali and halogen ions by subtraction from the distances of closest approach in the crystals of the alkali halides. The lattice parameters used by Landé have since been shown to be considerably in error. His results have therefore been recalculated for Table XIV. It will be noted that all his radii for the domains of negative ions are to be taken as upper limits. They are all larger than the corresponding values of Table X. His radii for the domains of positive

ions are all to be taken as lower limits. They are all smaller than the corresponding values of Table X. The two tables are therefore completely consistent with each other.

Radii of Iopic Domains from Compressibility Data.—Richards[51] has made a very interesting assumption in terms of which ionic radii may be calculated. The "molecular volume" (molecular weight divided by density) of an alkali halide is less than the sum of the "atomic volumes" of the alkali and halogen from which it is made. He assumes that this contraction is related to the compressibilities of the elements involved. For each of the halogens he plots the contraction in volume which occurs during chemical combination with the various alkalies against the compressibilities of the alkali metals. Each of these curves

TABLE XIV.—RADII OF ALKALI AND HALOGEN IONS ON THE ASSUMPTION THAT THE RADIUS OF I⁻ IS NEGLIGIBLE

Ion	Radius
Cs^+	≤ 1.82Å.
Rb^+	≤ 1.44
K^+	≤ 1.40
Na^+	$\leq 1.07 - 1.10$*
I^-	≥ 2.13
Br^-	≥ 1.90
Cl^-	≥ 1.74
F^-	$\geq 1.19 - 1.27$†

* Depending upon the halogen with which it is combined.
† Depending upon the alkali with which it is combined.

is extrapolated to zero abscissa to give the contraction which the halogen might be expected to experience if it were combined with an imaginary incompressible alkali. The difference between this extrapolated value and the atomic volume of the halogen is, then, the "ionic volume" and is proportional to the actual volume of the halogen ion. For instance, the atomic volume of Cl is

$$\frac{\text{Atomic weight}}{\text{Density}} = \frac{35.46}{1.412} = 25.1$$

The contraction of Cl for zero abscissa is 12.5. This gives 12.6 for the ionic volume of Cl^-. The ionic volumes of Br^- and I^- are similarly determined as 17.6 and 23.7, respectively. Since each gram-atom contains 6.062×10^{23} atoms, the volumes of these halogen ions can be expressed at once in cubic centimeters, *i.e.*;

$$Cl^- = 20.8 \times 10^{-24} \text{ cc.},$$
$$Br^- = 29.0 \times 10^{-24} \text{ cc.},$$
$$I^- = 39.1 \times 10^{-24} \text{ cc.}$$

In order to go from the volumes of these ionic domains to their radii we must make some assumption as to their shape. If the domains were

cubic and the crystal had a structure like NaCl* the distance of closest approach would be parallel to the cube-edge and the radius of the halogen would be $0.50\sqrt[3]{V}$, where V is the volume. If, instead, the domains

TABLE XV.—COMPARISON OF RADII OF HALOGEN IONIC DOMAINS BY COMPRESSIBILITY METHOD AND BY LATTICE-PARAMETER METHOD

Ion	Radii by compressibility method			Radii by crystal structure method
	Sphere	Cube	Average	
Cl^-	1.70+ Å.	1.38− Å.	1.54Å.	1.59Å.
Br^-	1.91+	1.55−	1.73	1.74
I^-	2.10+	1.70−	1.90	1.97

were true spheres of volume V, the radius would be $0.62\sqrt[3]{V}$. We have seen that we may consider these ionic domains as being spheres with six flat spots, or, what is the same thing, as cubes with well-rounded corners. The true radius will therefore lie somewhere between $0.50\sqrt[3]{V}$ and $0.62\sqrt[3]{V}$. Table XV shows that the radii from crystal-structure data are not far from halfway between these two limits.

Radii of Ionic Domains from Optical Data.—From a consideration of molar refractive indices of crystals, Wasastjerna[51] has arrived at the

TABLE XVI.—EMPIRICAL RADII OF IONIC DOMAINS FROM OPTICAL DATA

Cs^+	1.75Å.	I^-	2.19Å.
Rb^+	1.50	Br^-	1.92
K^+	1.30	Cl^-	1.72
Na^+	1.01	F^-	1.33
		O^{--}	1.32
		S^{--}	1.69

empirical radii for ionic domains listed in Table XVI. It will be noted that his values agree very closely with those of Landé given in Table XIV.

IONIC SIZES IN TERMS OF LATTICE ENERGIES

Up to this point, the term "ionic domain" has been used in this chapter to include not only the actual domain itself but also a portion of the interionic volume. This extended meaning has been justified by the fact that it gives a set of dimensions for various ions such that, if the radii of A^{n+} and B^{n-} are added together, we get an approximation (within 10 per cent) to the distance of closest approach of ionic centers of A^{n+} and B^{n-} in the crystal. Information of this sort has already been found useful in previous chapters. It would be possible to arrive with even more certainty at the same sort of result if we knew the dimensions of the

* Actually it is impossible to pack equal numbers of cubes of two different sizes to give an NaCl lattice. For such a lattice the corners of the cubes would have to be well rounded.

actual ionic domains and if, in addition, we had some way of accounting for the free interionic distances. Born[53] and Pauling[54,55] have made calculations of this sort. We shall take up briefly the calculations of Pauling since they are especially well suited to our purpose.

Pauling uses as his starting point the well-known equation* of Born for the lattice energy of an ionic crystal:

$$\Phi = -\frac{z^2e^2A}{r} + \frac{B}{r^n} \tag{1}$$

where Φ = crystal energy per "molecule."
ze = charge on an ion (z = valence).
r = a characteristic distance between ionic centers in the crystal.
A (the Madelung constant) and B = constants for a given crystal.

For any given arrangement of ions in the crystal, A may be calculated from the laws of electrostatics and B is chosen so that at equilibrium r will have the value R found experimentally for the given crystal. Since at equilibrium

$$\frac{d\Phi}{dr} = 0$$

we obtain from Eq. (1)

$$B = \frac{z^2e^2A}{n} \cdot R^{n-1} \tag{2}$$

Equation (1) can therefore be written in the form

$$U = -\frac{z^2e^2A}{R}\left(1 - \frac{1}{n}\right) \tag{3}$$

where U is the crystal energy at equilibrium. Measurements of compressibilities show that for the alkali halides the value of n is in the neighborhood of 9.

By applying the perturbation theory of quantum mechanics, Pauling shows that the potential energy of two ions M and X, situated a distance r_{MX} apart, is approximately

$$\varphi = \frac{z_M z_X e^2}{r_{MX}} + \beta_{MX} \cdot \frac{(r_M + r_X)^n}{r_{MX}} \cdot B_0 \tag{4}$$

in which r_M and r_X are "standard radii" characteristic of the ions M and X, B_0 is a constant for all ions, and β_{MX} has values which depend upon the model assumed for the ions. B_0 has a value of unity when M and X are univalent ions of opposite sign, a value of 0.75 when they are both

* For the purposes of this chapter equations are merely stated without going into the details of their derivation. Pauling's derivation[54] is expressed in the symbols of quantum mechanics and should be studied by all those who have had the necessary training.

univalent negative ions, and a value of 1.25 when they are both univalent positive ions. If we have a compound MX, whose crystal structure is of the NaCl type, then each ion is surrounded by 6 ions of opposite sign and 12 ions of the same sign. If we neglect all the rest of the ions in the crystal, it may be shown that

$$B = B_0\{(r_+ + r_-)^n f(g)\} \tag{5}*$$

where B and B_0 are the same as in Eqs. (1) and (4), r_+ and r_- are the radii of M^+ and X^-, respectively, and $f(g)$ is a function of (1) the number of closest anion-cation, cation-cation, and anion-anion contacts per "molecule" of MX, and (2) a quantity which has to do with the geometry of the crystal.

From Eq. (2) we have

$$R = \left(\frac{nB}{z^2e^2A}\right)^{\frac{1}{n-1}} \tag{6}$$

By substituting (5) in (6), we have

$$R = \left(\frac{nB_0}{z^2e^2A}\right)^{\frac{1}{n-1}}(r_+ + r_-)^{\frac{n}{n-1}}\{f(g)\}^{\frac{1}{n-1}} \tag{7}$$

If now, the values of the constant, and of the r_+ and r_- are so chosen that, for the special case† where r_+/r_- is 0.75, R becomes equal to $(r_+ + r_-)^{\frac{n}{n-1}}$, then Eq. (7) becomes, for a crystal of the NaCl type,

$$R = (r_+ + r_-)^{\frac{n}{n-1}} \cdot F(\rho) \tag{8}$$

where ρ is the "radius ratio" r_+/r_-, and where

$$F(\rho) = \left\{\frac{(1+\rho)^n + \beta_{++}(\sqrt{2}\rho)^n + \beta_{--}(\sqrt{2})^n}{(1.75)^n + \beta_{++}(\sqrt{2}\cdot 0.75)^n + \beta_{--}(\sqrt{2})^n}\right\}^{\frac{1}{n-1}} \tag{9}$$

may be considered as being a correction factor which shows how the interionic distance in NaCl-type crystals depends upon the radius ratio ρ. This dependence is shown graphically in Fig. 6.

We have already seen from Table IX that the interionic distances in the alkali halide series are not strictly additive; there were small deviations in the case of Na^+ and F^- and pronounced deviations in the case of Li^+. Presumably, more accurate measurements of lattice parameters would have disclosed less striking but definite, small deviations in the case of the larger ions also. If in a binary compound, crystallizing like NaCl, one of the two ions is small enough, the departure from the additive

* This is Eq. (18) of reference 54.

† This really means that we are making $F(\rho)$ of Eq. (9) arbitrarily equal to unity when ρ is 0.75. This is evident by an inspection of Fig. 6.

law has a simple mechanical explanation.[50,55] Imagine equal numbers of spheres of two sizes, packed together in the NaCl arrangement. Let one set of spheres be kept unaltered, and let the diameters of the spheres of the other set be reduced step by step. It will be found that when the diameters of the small spheres are reduced to 41.4 per cent of that of the large spheres (*i.e.*, if ρ is made 0.414), the large spheres will come in contact with each other. Further reduction of the diameters of the small spheres cannot bring the larger spheres closer together, for they are already in contact with each other. As the small spheres are made still smaller and smaller in diameter they will lie more and more loosely in the spaces left by the large spheres. This would cause the distance between

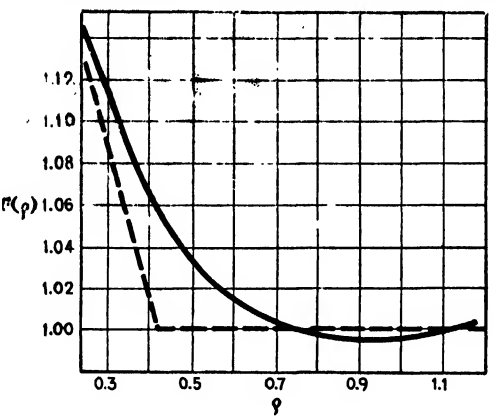

FIG. 6.—The variation of $F(\rho)$ with ρ (solid line). The broken line shows the form of the function for solid spheres, *i.e.*, when n is infinity.

centers of adjacent large and small spheres to be in excess of that required by the additive law, by a factor shown by the dotted line of Fig. 6.

Pauling has pointed out[56] that, in the case of actual ionic crystals, the additive law should fail for values of ρ considerably larger than $\rho = 0.414$. There are two reasons for this: (1) The large ions will act like still larger spheres because of the separation produced by the repulsion of like charges; (2) in the case of Li^+ the second term of Eq. (1) becomes of importance near the "edge" of the ion thus introducing still a second repulsive force which acts between the Li^+ and the halogen ion. The solid line of Fig. 6 was made to accord with this view by making $F(\rho)$ equal to unity for $\rho = 0.75$ in Eq. (9). The correction factor $F(\rho)$ for the distance of closest approach of oppositely charged ions then becomes substantially unity when ρ is larger than 0.70. For values of ρ smaller than 0.70 the correction factor is larger than that shown by the dashed line.

If some value (or set of values) is assumed for n in Eq. (8) (Pauling assumes a uniform value of $n = 9$), and if $F(\rho)$ is considered to be known from Fig. 6, then we can set up simultaneous equations in which the

values of R are related to the radii r_+ and r_- of the "true" domains of the alkali and halogen ions. As in the discussion of Tables IX and X, we have here one more unknown quantity than we have equations, and some plausible additional equation must be found. Pauling chooses, on theoretical grounds, the equation

$$\rho = \frac{r_+}{r_-} = \frac{Z_{X^-} - S_{X^-}}{Z_{M^+} - S_{M^+}} \tag{10}$$

where Z_{M^+} and Z_{X^-} are the actual nuclear charges and S_{M^+} and S_{X^-} are the "screening constants" of the two ions M^+ and X^-; *i.e.*, $Z - S$ is the "effective" nuclear charge. He takes the calculated values of this ratio for the case of K^+ and Cl^- and for Rb^+ and Br^- and thus finds values for r_{K^+}, r_{Cl^-}, r_{Rb^+}, and r_{Br^-}. Values for the remaining alkali and halogen ions come out at once from the simultaneous equations. He thus obtains a self-consistent set of radii for the true ionic domains which, when used with Eqs. (8) and Fig. 6, give close to the correct distance of closest approach of M^+ and X^- in crystals of the NaCl type. When the simultaneous equations are used for CsCl, CsBr, and CsI (none of which are of the NaCl type), the radii obtained for Cs^+ and I^- are the radii which these ions would have had if CsI had had the NaCl structure.

The radii of the true domains of the alkali and halogen ions, calculated in this way, are listed in Table XVII.

It should be emphasized at this point that all ionic radii listed in this chapter represent approximations of one sort or another. The approximations on which several of the previous tables are based have already been stated. The fundamental approximations and assumptions on which Table XVII is based are: (*a*) Eq. (1); (*b*) Eq. (4); (*c*) the simplifications leading to Eq. (5); (*d*) the assumption that $F(\rho)$ will equal unity for $\rho = 0.75$; (*e*) the use of a single value, namely 9, for n, instead of a different n for each salt;* (*f*) equality of ρ with the inverse ratio of the

* The various values proposed for n by Born, Herzfeld, and Pauling are:[56]

	Born	Herzfeld	Pauling
NaCl	7.84	9.1	8
NaBr	8.61	9.5	8.5
NaI	8.45	....	9.5
KF	....	7.9	8
KCl	8.86	9.7	9
KBr	7.78	10.0	9.5
KI	9.31	10.5	10.5
RbBr	....	10.0	10
RbI	....	11.0	11

Since $\frac{n}{n-1}$ appears in the exponent of Eq. (8), variations in n will make considerable variations in the values assigned to r_+ and r_-.

TABLE XVII.—PAULING'S RADII FOR THE "TRUE" IONIC DOMAINS

Cs^+	1.434Å.	I^-	1.867Å.
Rb^+	1.294	Br^-	1.702
K^+	1.173	Cl^-	1.589
Na^+	0.873	F^-	1.225
Li^+	0.574		

TABLE XVIII.—CALCULATED AND OBSERVED INTERIONIC DISTANCES IN THE ALKALI HALIDES (PAULING'S METHOD)

Salt	$\rho = r_+/r_-$	$F(\rho)$ [Eq. (9)]	$(r_+ + r_-)\sqrt[n-1]{n} = (r_+ + r_-)1.116$	R calculated from Eq. (8)	R observed*
LiF	0.68	1.042	1.936	1.971	2.007 2.009
LiCl	0.39	1.082	2.382	2.577	2.566 2.566
LiBr	0.337	1.094	2.522	2.760	2.745 2.745
LiI	0.307	1.111	2.729	3.032	3.01 3.025
NaF	0.713	1.002	2.302	2.306	2.310 2.310
NaCl	0.550	1.023	2.756	2.819	2.814 2.814
NaBr	0.513	1.029	2.898	2.982	2.968 2.981
NaI	0.468	1.041	3.108	3.235	3.231 3.231
KF	0.958	0.995	2.675	2.662	2.664 2.664
KCl†	0.738	1.001	3.136	3.139	3.138 3.140
KBr	0.689	1.005	3.281	3.297	3.285 3.293
KI	0.629	1.010	3.493	3.528	3.535 3.526
RbF	1.057	0.997	2.827	2.819	2.81 2.815
RbCl	0.815	0.997	3.291	3.281	3.285 3.268
RbBr†	0.760	0.999	3.436	3.433	3.434 3.434
RbI	0.693	1.004	3.650	3.665	3.662 3.663
CsF	1.171	0.999	2.994	2.991	3.00 3.005
CsCl	0.903	0.995	3.471	3.454	(3.555) (3.560)
CsBr	0.843	0.996	3.618	3.603	(3.713) (3.715)
CsI	0.769	0.999	3.832	3.829	(3.947) (3.95)

* The upper value is from Table IX. The lower value is that chosen by Pauling.[55]
† Starting points for calculation of Table XVII.

effective nuclear charges. These approximations are justified because of the simplification which they entail. Anyhow, it is of more importance to the crystal analyst to have a consistent set of radii for true domains which can be used in an equation than to have true radii. In fact, since each electron and each proton exerts an influence over an infinite distance, there may be no true radii of true ionic domains.

For convenience of reference the calculated and observed distances of closest approach for the alkali halides are listed in Table XVIII. In this table the second column gives the radius ratio ρ, calculated for each salt from Table XVII; the third column gives $F(p)$ from Fig. 6 for each of the values of ρ; the fourth column gives the value which the distance of closest approach R, would have had if this distance had been independent of the radius ratio; the fifth column gives the final value of the distance of closest approach after the corrective factor $F(\rho)$ has been taken into account; the experimental value of the distance of closest approach is given in the last column. The agreement is close enough for all practical purposes in crystal analysis.

Still another set of radii, based on much the same sort of considerations has been proposed by Zachariasen.[57]

SIZES AND SHAPES OF ATOMS WHEN IN NON-POLAR (ELECTRON-SHARING) COMBINATION

It is easy to find the shape of radicals like NO_3^-, CO_3^{--}, etc., for the answer is contained in the solution of the structure of the crystals which they help to build. For instance, in all alkali nitrates the simplest structure for NO_3^- which fits the data consists of an equilaterial triangle with an oxygen atom at each corner and a nitrogen atom at the center. The CO_3^{--} radical has a similar structure (see Q, Fig. 13 of Chap. V). Similarly the shapes of other radicals can be determined whenever sufficient crystal-structure data can be found. This is also true of "molecular compounds" such as SiO_2, Al_2O_3, Fe_2O_3, Cr_2O_3, and crystals of most organic substances. SiO_2 is an elbow-shaped molecule (see Fig. 23 of Chap. VI). Oxides having the composition M_2O_3 have the three oxygen atoms at the corners of an equilateral triangle. One atom of the metal is immediately above the center of this triangle, and the other is immediately below it. The three oxygen atoms evidently "belong" to the two atoms of the metal, for they are closer to them than to any other atoms of metal in the crystal. Similarly, the metal atoms are closer to their own three oxygens than to any other oxygen atoms in the crystal.*

* It will be shown in Chap. XIX that such a structure may be taken as evidence of the absence of a polar (*i.e.*, ionic) structure. For non-polar compounds the "molecule" is a real physical entity. For instance, Al_2O_3 does not electrolyze readily; even up close to its melting point it is a good insulator. Quartz is a good insulator at room

In all of these, however, there is no way of telling, from a study of lattice parameters alone, how much of the interionic space belongs to one atom and how much to the other atom. In calculating the radii of ionic domains it was found that the lattice parameters alone always gave one equation fewer than there were unknown quantities. Our discussion of ionic radii obtained by various methods was really, therefore, a discussion of attempts to find a suitable additional equation and a comparison of the results obtained by the use of the various equations that have been proposed. In the case of the radicals and molecular crystals the lattice parameters also give one equation fewer than there are unknown quantities, and there is a noticeable scarcity of assumptions on which to base an additional equation. In the absence of an additional equation an infinite number of radii could be proposed, any given set of which would be mutually consistent. In the early days of crystal analysis W. L. Bragg proposed a semiempirical set of radii for the domains of atoms in molecular compounds and in radicals,[59] based on the assumption that in FeS_2 the iron atoms are in contact with each other and that the sulphur atoms fit into the chinks between iron atoms. In the absence of any other data at the time, he proposed the same radii for atoms in the ionic state until better values could be found. Unfortunately his radii were adopted uncritically by many people in a way that was not intended, and he has since withdrawn those values.[60]

In a study of $MgAl_2O_4$, Bragg and Brown suggest[61] that the distance of closest approach of oxygen atoms in such a compound is of the order of 2.7Å., thus giving a radius of 1.3$_5$Å. From this, approximations to the domains of other atoms could of course be estimated by subtraction from the proper lattice distances. Bragg and Brown emphasize the danger in such computations because of the lack of constancy of the size of the atomic domain.

It is evident that the data of atomic-structure-factor studies of nonpolar compounds would give information as to the radii of the atoms

temperature because at such temperatures it, too, is molecular, not ionic. There is this difference, however, between quartz and alumina. The alumina remains molecular up to its melting point; quartz does not. At room temperature the Si in quartz is not very much closer to its "own" oxygens than to the oxygens of its neighbors. The greater vibration path at higher temperatures permits the Si to get close to the oxygens belonging to its neighbors, so that the molecular nature of the crystal is lost and it acts like an ionic conductor.

Even in the case of molecular combination, however, we must not take the phrase "electron-sharing" too literally. There seems to be less true "sharing" of electrons than was at first supposed. We can hardly think any longer of the shared electrons being owned equally by the two atoms. It will appear in Chap. XIV that in CO_3^{--} we must think of the carbon as having given up practically all claim to its four outmost electrons—they belong almost entirely to the oxygen so that CO_3^{--} would really be $[C^{++++}O_3^{--}]$. This is consistent with the data of organic chemistry on molecular rearrangements.[58]

which compose them. Such data have already been given in Figs. 10 and 11 of Chap. XI.[62] These indicate that the radius of the domain of oxygen in molecular compounds is of the order of 1.2 or 1.3Å. This is in agreement with the estimate of Bragg and Brown.[61]

SUMMARY

We have discussed the distinction between actual atoms (and ions) and their packing-domains. We have distinguished between the "true" domain (which is separated from its neighbors by an amount depending upon the absolute temperature) and the fictitious domain (called simply the "domain" for convenience) which is in contact with its neighbors at the temperature of the experiment. The fictitious domains have the merit that, in the simplest cases, they yield a good enough approximation to the distance of closest approach by simple addition.

We have outlined the various methods of investigating the shapes and characteristic dimensions of the domains of the atoms of the elements and have found them to be all in essential agreement. We have outlined also the methods for finding the shapes and sizes of ionic domains in the single case of binary compounds and have again found substantial agreement within the limitations of the various methods. We have pointed out in a general way the nature of the calculations and approximations necessary to find usable semiempirical radii for the true ionic domains and have shown how to use such radii to compute the distance of closest approach of oppositely charged ions in a binary compound. Finally, we have discussed the problem of the sizes of the domains of atoms in non-polar compounds.

It has appeared that the discussions of all x-ray methods for estimating ionic radii center about the search for an additional equation, not based on lattice parameters, which must be included in our calculations in order to arrive at definite numerical results. These additional equations are based on widely different assumptions the nature of which depends largely upon the type of training and upon the direction of the scientific interest of each investigator. The purpose of this chapter will have been realized, (1) if the reader has gained a vision both of the crude mechanical pictures and of the polished quantum theory on which the various assumptions have been based, and (2) if he has been stimulated to use both the pictures and the theory as a basis for the interpretation of data in other fields.

References

1. W. P. Davey, *Jour. Franklin Inst.*, **197**, 439, 629 (1924).
2. M. Born, *Verh. deut. phys. Ges.*, **20**, 230 (1918).
3. A. W. Hull, *Proc. Amer. Inst. Elec. Eng.*, **38**, 1171 (1919); *Jour. Franklin Inst.*, **193**, 189 (1922).
4. L. W. McKeehan and P. P. Cioffi, *Phys. Rev.*, **19**, 444 (1922).

5. G. Linck and H. Jung, *Zeit. anorg. allgem. Chem.*, **147**, 288 (1925).
6. A. J. Bradley, *Phil. Mag.*, **47**, 657 (1924).
7. J. C. McLennan and J. O. Wilhelm, *Phil. Mag.*, **3**, 383 (1927).
8. H. Mark and E. Wigner, *Zeit. phys. Chem.*, **111**, 398 (1924).
9. M. K. Slattery, *Phys. Rev.*, **25**, 333 (1925).
10. A. J. Bradley, *Phil. Mag.*, **48**, 477 (1924).
11. L. Vegard, *Zeit. Physik*, **58**, 497 (1929); **61**, 185 (1930); *Nature*, **124**, 267, 337 (1929).
12. C. Maxwell, *Nature* (Aug. 14, 1873).
13. R. G. Lunnon, *Proc. Phys. Soc. London*, **38**, 93 (1925).
14. F. Simon and F. Kippert, *Zeit. phys. Chem.*, **135**, 113 (1928).
15. S. Chapman, *Phil. Trans. Roy. Soc. London*, **A, 216**, 279 (1915).
16. A. O. Rankine, *Phil. Mag.*, **42**, 601 (1921).
17. W. Sutherland, *Phil. Mag.*, **36**, 507 (1893).
18. A. R. Rankine, *Proc. Roy. Soc.*, **98**, 560 (1921)
19. R. N. Pease, *Jour. Amer. Chem. Soc.*, **43**, 991 (1921).
20. L. A. Turner, *Astrophys. Jour.*, **58**, 176 (1923).
21. A. S. Eve, *Nature*, **107**, 552 (1921).
22. M. N. Saha, *Nature*, **107**, 682 (1921).
23. J. J. Thomson, The Electron in Chemistry, *Jour. Franklin Inst.* (1923).
24. B. Davis, *Proc. Nat. Acad. Sci.*, **8**, 61 (1922).
25. S. H. Anderson, *Phys. Rev.*, **20**, 200 (1922).
26. H. Sirk, *Phys. Zeit.*, **25**, 545 (1924); *Zeit. phys. Chem.*, **114**, 114 (1925); *Phil. Mag.*, **49**, 708 (1925).
27. E. Madelung, *Phys. Zeit.*, **14**, 729 (1913).
28. M. Born and R. Courant, *Phys. Zeit.*, **14**, 731 (1913).
29. P. Debye, *Phys. Zeit.*, **21**, 178 (1920).
30. F. Simon and C. v. Simson, *Zeit. Physik*, **25**, 160 (1924).
31. E. O. Wollan, *Rev. Mod. Phys.*, **4**, 205 (1932).
32. W. P. Davey, *Phys. Rev.*, **27**, 819 (1926).
33. T. A. Wilson and W. P. Davey, *Phys. Rev.*, **27**, 819 (1926).
34. S. Dushman, *Gen. Elec. Rev.*, **18**, 1042 (1915).
35. T. S. Fuller, *Trans. Amer. Electrochem. Soc.*, **32**, 247 (1917).
36. C. A. Edwards, *Jour. Iron Steel Inst. (London)*, **110**, 9 (1924).
37. W. R. Ham, *Amer. Inst. Min. Eng.* (New York meeting) (February, 1933).
38. W. P. Davey, *Phys. Rev.*, **18**, 102 (1921); **22**, 211 (1923).
See also independent work of:
Fajans, Grimm, and Herzfeld, *Zeit. Physik*, **2**, 299, 309 (1920).
39. W. P. Davey, *Phys. Rev.*, **21**, 143 (1923).
40. R. J. Havighurst, E. Mack, and F. C. Blake, *Jour. Amer. Chem. Soc.*, **46**, 2368 (1924).
41. R. W. G. Wyckoff and E. Posenjak, *Jour. Wash. Acad. Sci.*, **13**, 393 (1923).
42. V. M. Goldschmidt, *Zeit. Kryst.*, **69**, 411 (1929).
43. I. Oftedal, *Zeit. phys. Chem.*, **132**, 208 (1928).
44. V. Goldschmidt, *Skrift. Norsk. V. Akad., Oslo* (1926).
45. W. F. deJong and H. W. V. Williams, *Physica*, **7**, 74 (1927).
46. R. J. Havighurst, *Proc. Nat. Acad. Sci.*, **11**, 502, 507 (1925).
47. R. W. James and E. Firth, *Proc. Roy. Soc.*, **117**, 62 (1927).
48. R. J. Havighurst, *Phys. Rev.*, **29**, 1 (1927).
49. E. O. Wollan, *Phys. Rev.*, **35**, 1019 (1930).
50. A. Landé, *Zeit. Physik.*, **1**, 191 (1920).
51. T. W. Richards, *Jour. Amer. Chem. Soc.*, **36**, 2417 (1914); **43**, 1584 (1921); **45**, 422 (1923).

52. J. A. Wasastjerna, *Soc. Sci. Fenn. Comm. Phys. Math.*, **38**, 1 (1923). See also W. L. Bragg, *Phil. Mag.*, **2**, 258 (1926).
53. M. Born, *Zeit. Physik*, **1**, 221 (1920).
54. L. Pauling, *Jour. Amer. Chem. Soc.*, **50**, 1036 (1928).
55. L. Pauling, *Zeit. Kryst.*, **67**, 377 (1928).
56. L. Pauling, *Jour. Amer. Chem. Soc.*, **49**, 765 (1927).
57. W. H. Zachariasen, *Zeit. Kryst.*, **80**, 137 (1931).
58. F. C. Whitmore, *Jour. Amer. Chem. Soc.*, **54**, 3274 (1932).
59. W. L. Bragg, *Phil. Mag.*, **40**, 169 (1920).
60. W. L. Bragg, *Nature*, **116**, 249 (1925).
61. W. L. Bragg and G. B. Brown, *Proc. Roy. Soc.*, **110**, 34 (1926).
62. N. A. Alston and J. West, *Zeit. Kryst.*, **69**, 149 (1928).

CHAPTER XIV

THE REFRACTION OF LIGHT BY CRYSTALS

If we could know enough about the fundamental properties of matter, we ought to be able to calculate all the physical and chemical properties of any given crystalline material. The calculation of each of the properties of a crystal requires, in general, a knowledge of some or all of the following:

1. The structure of the crystal.
2. The various interatomic (or interionic) distances in the crystal.
3. The details of the mosaic structure (π-planes, Π-planes, etc.)
4. The inner structure of the atoms (or ions) which compose the crystal.
5. A method of calculating the energy of the crystal lattice.

We have already learned in Chaps. IV to XI inclusive how to determine 1 and 2. In Chap. XII we went part of the way toward 3. A study of atomic (and ionic) structure factors, of optical emission spectra and of the chemical properties of atoms and ions goes a long way toward 4. Item 5 does not seem so simple, and we shall therefore postpone it until the next chapter. In this chapter we shall take up the calculation of the optical properties of crystals, for such calculations can be made in terms of 1 and 2 with the aid of additional quantities which, although they depend ultimately on 4 and 5, can be determined in semi-empirical fashion without direct reference to 4 and 5. In other words, the optical properties of a crystal can be calculated by considering each atom (or ion) as a unit with very little reference to the internal architecture of the atoms (or ions) themselves.

The calculation chosen is that of W. L. Bragg[1] on the optical constants of calcite and aragonite. These minerals are both $CaCO_3$, but their crystal structures are different.[2,3,4] It is well known that both of these crystals are birefringent, *i.e.*, the degree with which they can bend a beam of polarized light depends upon the orientation of the crystal with respect to the plane of polarization of the light. It is generally assumed in physical chemistry that the optical properties of a compound may be calculated if only we know the optical properties of each of its components. This is approximately true in the case of isotropic substances, *e.g.*, jellies, solutions, and crystals belonging to the cubic system. Bragg makes the additional assumption that in all other crystalline solids the crystal structure must also be taken into account, for in a crystal the arrangement of atoms markedly affects the forces acting between them.

The customary procedure in the case of isotropic substances is to picture the electric vector in a beam of polarized light as pulling the electrons of the various atoms in one direction and pushing the corresponding protons in the opposite direction. In this way each atom is thought of as becoming an "electric doublet," *i.e.*, it acts like a tiny rod with a plus charge at one end and a minus charge at the other. The change in the strength of the electrostatic field (electric polarization) in a definite small volume, caused by the doublets thus formed, is then calculated by considering the effect of such doublets arranged in a hit-or-miss fashion in the isotropic substance. Such a calculation may be expected to apply to the case of a substance crystallizing in the cubic system, for all three directions are necessarily equivalent. It will not apply, however, even approximately, to substances crystallizing in other systems, and for these the configuration of atoms in the crystal has to be taken into account. Bragg has made the necessary calculations for calcite and aragonite, taking into account the arrangement of the atoms in the crystals, and (within the degree of approximation to which the assumptions hold for isotropic substances) these calculations lead at once to the correct values for the indices of refraction of the crystals.

INDEX OF REFRACTION OF ISOTROPIC MEDIA

It is reasonable to assume that, if a substance is placed between two charged electrodes so that a constant electrostatic field is imposed on it, all the electrons in the atoms* of that substance will be pulled over slightly toward the positive electrode and all the protons will similarly be shifted over toward the negative electrode. Let s be the distance which is now assumed to exist between the center of gravity of the negative charges and the center of gravity of the positive charges in a given atom. This distance will be proportional to the strength E' of the electrostatic field in which the atom finds itself and to the charge e on each electron and proton. It will depend, too, upon the magnitude of the electrostatic forces between the electrons and protons in the atom. It will be assumed that this restoring force is independent of the orientation of the atom, and this force will be included, for any given kind of atom, in the factor of proportionality. We may therefore write

$$s = E'e\lambda \tag{1}$$

where λ is characteristic of the atom under consideration. The factor λ may be defined as the displacement per unit force on the atom. It is the elastic yield of the atom to the polarizing force. If Eq. (1) is written

$$E'e = \frac{s_1}{\lambda_1} = \frac{s_2}{\lambda_2} \tag{2}$$

* For the sake of brevity, the word atom is used in the first part of this chapter to mean atom (or ion).

the expression s/λ may be interpreted as representing the strength of the doublet.

Let $\bar{E}$ be the average value of the strength of the electrostatic field (due to the charge on the electrodes) throughout the whole substance which has been placed between the electrodes. Since the dielectric constant of a vacuum is, by definition, unity, the increase in the field strength caused by the presence of the material substance is $(K-1)\bar{E}$, where K is the dielectric constant of the substance. This change in the field strength is called the "polarization per unit volume" and is designated by P. Assume that in each cubic centimeter of the substance there are N_1 atoms having a displacement constant λ_1 and therefore an electric moment s_1e; N_2 atoms of displacement constant λ_2 and electric moment s_2e; etc. Then

$$\begin{aligned}(K-1)\bar{E} = P &= N_1 s_1 e + N_2 s_2 e + \cdots \\ &= N_1 \frac{s_1}{\lambda_1}\lambda_1 e + N_2 \frac{s_2}{\lambda_2}\lambda_2 e + \cdots \\ &= E' N_1 e^2 \lambda_1 + E' N_2 e^2 \lambda_2 + \cdots \end{aligned} \tag{3}$$

Now consider some single atom located at a point A, for example. There will be some doublets so close to it that they may be regarded as making individual contributions to the strength of the electrostatic field at A. Other doublets, more remote, may be regarded as being so far from this point that they act with their neighbors to give the effect of a substantially uniform electrostatic field. The field strength E' which acts on any individual atom in an isotropic substance represents the average strength $\bar{E}$ of the field imposed by the charged electrodes plus the effect of these more remote doublets. The additional effect of the doublets which are near the atom at A may be determined as follows: Let a sphere be drawn with A as a center and with a radius large enough to reach to the more remote doublets mentioned above, and let all the doublets inside this sphere be removed. On one side of A the surface of the sphere acts as though it were covered with a continuous coating of positive electricity; on the other side of A it will act as though it had a continuous coating of negative electricity. It may be shown that the field due to these charged halves of the sphere is $\frac{1}{3}P$. If the substance between the electrodes is isotropic, the average effect of the doublets inside such a sphere is zero. The net effect is that the total electric field acting at the point A is now

$$E'e = \frac{s_1}{\lambda_1} = \frac{s_2}{\lambda_2} = \cdots = (\bar{E} + \frac{1}{3}P)e \tag{4}$$

Equation (3) must therefore be altered to read

$$\begin{aligned} P &= (\bar{E} + \tfrac{1}{3}P)N_1 e^2 \lambda_1 + (\bar{E} + \tfrac{1}{3}P)N_2 e^2 \lambda_2 + \cdots \\ &= (\bar{E} + \tfrac{1}{3}P)\Sigma N e^2 \lambda \\ &= E' \Sigma N e^2 \lambda \end{aligned} \tag{5}$$

or

$$K - 1 = \frac{P}{\bar{E}} = \frac{P}{E' - \frac{1}{3}P}$$
$$= \frac{E' \cdot \Sigma Ne^2\lambda}{E'(1 - \frac{1}{3}\Sigma Ne^2\lambda)}$$
$$= \frac{\Sigma Ne^2\lambda}{1 - \frac{1}{3}\Sigma Ne^2\lambda} \tag{6}$$

Equation (6) will still hold true if the field across the electrodes is an alternating field such as would be produced by the electric vector of a light wave, except that near all resonance frequencies the value of λ will depend upon the frequency of the field. Equation (6) may be made more useful for our purposes by means of the well-known principle that, if the dielectric constant of a substance is measured for fields of the same frequency as the light which we happen to use, then that dielectric constant is inversely proportional to the square of the velocity of light in that substance. Remembering that the ratio of the velocity of light in a vacuum to the velocity in a given substance is the index of refraction of that substance we have,

$$\frac{K_{\text{substance}}}{K_{\text{vacuum}}} = \frac{(\text{velocity of light in vacuum})^2}{(\text{velocity of light in substance})^2} = n^2$$

Since the dielectric constant of a vacuum is, by definition, unity, we can replace K in Eq. (6) by n^2, giving

$$n^2 - 1 = \frac{\Sigma Ne^2\lambda}{1 - \frac{1}{3}\Sigma Ne^2\lambda} \tag{7}$$

If M is the molecular weight of the substance and ρ is its density, then the quantity $\frac{n^2 - 1}{n^2 + 2} \cdot \frac{M}{\rho}$ is approximately a constant which is substantially independent of the physical state of the substance, provided it is isotropic. It is called the "molecular refractivity" of the substance and is denoted by R.* From Eq. (7) we have at once

$$\frac{M}{\rho} \cdot \frac{n^2 - 1}{n^2 + 2} = R = \frac{1}{3}\frac{M}{\rho} \cdot \Sigma Ne^2\lambda \tag{8}$$

Now N_1, N_2, etc., represent the number of atoms of kinds (1), (2), etc., per cubic centimeter. $N_1\frac{M}{\rho}$, $N_2\frac{M}{\rho}$, etc., are therefore the number of atoms per gram-molecule and may be represented by aN_0, bN_0, etc., where N_0 is the Avogadro number. In terms of N_0, Eq. (8) becomes

$$R = a(\tfrac{1}{3}N_0e^2\lambda_1) + b(\tfrac{1}{3}N_0e^2\lambda_2) + \cdots$$
$$= aA_1 + bA_2 + \cdots \tag{9}$$

where A_1, A_2, etc., are the atomic refractivities.* On the basis of their

* I_1, I_2, etc., would represent the ionic refractivities of Ca^{++}, O^{--}, etc.

optical properties in isotropic substances it is possible to assign values for the refractivities for the atoms and ions of many elements, and the molecular refractivity of a compound is approximately the sum of the atomic (or ionic) refractivities of its constituents, provided only that the substance is isotropic.

INDEX OF REFRACTION OF NON-ISOTROPIC MEDIA

So far we have assumed that the immediate neighbors of any given atom were situated around it in an entirely haphazard fashion. Although not so arranged in the case of crystals of cubic symmetry, the mathematics of cubic crystals is such as to lead to essentially the same result. This is not the case for non-cubic crystals. The net electrostatic field at a point due to the more closely situated atoms is no longer zero. It must be calculated in terms of the relative positions of these atoms (or ions) and the distance between them as given by crystal analysis.

Consider an atom situated at the origin of coordinates, and let one of the doublets in its immediate neighborhood have coordinates x, y, z, so that it is at a distance

$$r = \sqrt{x^2 + y^2 + z^2}$$

from the origin. The x-component of the field which it sets up at the origin is, in Heaviside units,

$$\frac{\mu_x}{4\pi r^3} \cdot \frac{3x^2 - r^2}{r^2} + \frac{\mu_y}{4\pi r^3} \cdot \frac{3xy}{r^2} + \frac{\mu_z}{4\pi r^3} \cdot \frac{3xz}{r^2} \tag{10}$$

where μ_x, μ_y, and μ_z are its components of polarization. Fields of this sort from each doublet in the neighborhood are superimposed on the field which we considered in the case of isotropic substances, so that the simple form of Eq. (4) must be replaced by a group of equations of the form

$$\left.\begin{aligned} \frac{s_1}{\lambda_1} &= \left(\bar{E} + \frac{1}{3}P\right)e + (a_1 s_1 e + a_2 s_2 e + \cdots)e \\ \frac{s_2}{\lambda_2} &= \left(\bar{E} + \frac{1}{3}P\right)e + (b_1 s_1 e + b_2 s_2 e + \cdots)e \end{aligned}\right\} \tag{11}$$

The new terms $a_n s_n e$ give the changes to the field which have been contributed by doublets of strength $s_n e$. All doublets of a given kind situated at a distance r from the origin of coordinates are included in the same term. For instance, if for the doublets of strength $s_1 e$ the components of polarization are $\mu_x = s_1 e$, $\mu_y = 0$, $\mu_z = 0$; then Eq. (10) gives the value of a_1 as

$$a_1 = \sum_{r_0}^{r_1} \frac{1}{4\pi r^3} \cdot \frac{3x^2 - r^2}{r^2} \tag{12}$$

In general, μ_y and μ_z will not be zero, but the error introduced will be small and can be allowed for in numerical calculations if desired.

The equations illustrated by Eq. (11) may be written in the form

$$\frac{s_1}{\lambda_1} = \left(\bar{E} + \frac{1}{3}P\right)e + \left(\frac{s_1}{\lambda_1}a_1e^2\lambda_1 + \frac{s_2}{\lambda_2}a_2e^2\lambda_2 + \cdots\right) \qquad (11a)$$

Calculations based on values for a_1, a_2, etc., given by Eq. (12), and on values for λ_1, λ_2, etc., given by atomic refractivities, give values for the second parentheses which are small (± 0.2 for calcite and aragonite) in comparison with ($\bar{E} + \frac{1}{3}P$), so they may be represented by a corrective factor thus:

$$\left.\begin{aligned} \frac{s_1}{\lambda_1} &= C_1\left(\bar{E} + \frac{1}{3}P\right)e \\ \frac{s_2}{\lambda_2} &= C_2\left(\bar{E} + \frac{1}{3}P\right)e \\ &\cdots\cdots\cdots\cdots \end{aligned}\right\} \qquad (13)$$

For non-isotropic media, Eq. (5) therefore becomes

$$P = C_1(\bar{E} + \tfrac{1}{3}P)N_1e^2\lambda_1 + C_2(\bar{E} + \tfrac{1}{3}P)N_2e^2\lambda_2 + \cdots$$

and Eq. (7) becomes

$$n^2 - 1 = \frac{C_1N_1e^2\lambda_1 + C_2N_2e^2\lambda_2 + \cdots}{1 - \frac{1}{3}(C_1N_1e^2\lambda_1 + C_2N_2e^2\lambda_2 + \cdots)} \qquad (14)$$

We are now ready to consider calcite and aragonite and to compare their indices of refraction as calculated by Eq. (14) with the results of experiment.

STRUCTURE AND OPTICAL PROPERTIES OF CALCITE AND ARAGONITE

The rhombohedron of calcite has been shown in Chaps. V and IX to have a distorted NaCl structure. When a calcite crystal, bounded by its cleavage planes, is placed so that its short body-diagonal is vertical, the structure may be thought of as being made up of three interpenetrating simple triangular lattices. The arrangement of atoms, looking down vertically upon such a crystal, is shown in Fig. 1. The CO_3^{--} group is equally spaced from each of three Ca^{++} ions below and three Ca^{++} ions above. The oxygens lie midway between one of the lower Ca^{++} and one of the upper Ca^{++}.

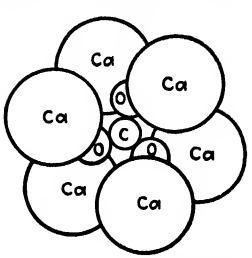

FIG. 1.—Arrangement of atoms in calcite, looking along the short diagonal of the rhombohedron. (*Bragg.*)

Although aragonite belongs to the orthorhombic system, the positions of the Ca^{++} and CO_3^{--} are very nearly what they would have been if the structure had been triangular close-packed. The arrangement of atoms, looking along

the Z-axis of the prism is shown in Fig. 2. Here again the CO_3^{--} group is equally spaced from each of three Ca^{++} ions below and three Ca^{++} ions above, but now each oxygen lies midway between three Ca^{++} ions.

When the electric vector of a polarized light wave is parallel to the planes of CO_3^{--} in calcite, the index of refraction,* ω, is 1.658; when it is perpendicular to these planes the index of refraction, ϵ, is 1.486. If aragonite had true hexagonal symmetry, it, too, would have two indices of refraction, one ω with the electric vector perpendicular to the CO_3^{--} planes (*i.e.*, parallel to the Z-axis) and a second ϵ with the electric vector parallel to the CO_3^{--} planes (*i.e.*, in the plane of the X- and Y-axes). But since the symmetry of aragonite is only pseudo-hexagonal and is actually that of the orthorhombic system, it has three indices of refraction. These are: $\alpha = 1.530$ when the electric vector is parallel to the pseudo-hexagonal Z-axis; $\beta = 1.681$ when it is parallel to the orthorhombic (pseudo-orthohexagonal) X-axis; and $\gamma = 1.686$ when the electric vector is parallel to the Y-axis. Aragonite, therefore, is not far from being a uniaxial crystal with $\omega = 1.683$, and $\epsilon = 1.530$.

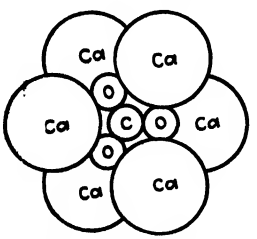

FIG. 2.—Arrangement of atoms in aragonite, looking along the Z-axis. (*Bragg.*)

Values found in the literature[5] for the ionic refraction of calcium, carbon, and oxygen indicate that the calcium ions ($I_{Ca^{++}} = 1.99$) are responsible for only about 15 per cent of the total refractivity of calcite. Assuming that the molecular volume of $CaCO_3$ in calcite† is

$$\frac{M}{\rho} = 36.13$$

the expression $Ne^2\lambda$ in Eq. (14) becomes [see Eqs. (8) and (9)]

$$Ne^2\lambda = 3\frac{\rho}{M}I_{Ca^{++}} = 0.165 \qquad (15)$$

for the calcium ions in calcite. The corresponding molecular volume in aragonite is 34.01, giving a value for $Ne^2\lambda$ of 0.175. The rest of the refractivity is to be accounted for by the carbon and oxygen. It remains, therefore, to apportion the remainder between the carbon and the

* For the D line of sodium.

† This value is the one recorded by Groth and used by Bragg. The actual density of calcite is 2.71, which gives a molecular volume of 36.93 and a value for $Ne^2\lambda$ for Ca^{++} of 0.162. The final value of N (calculations of the first approximation) on this basis is 1.459 as compared with Bragg's value of 1.468. Since the difference is of the same order of magnitude as that caused by the uncertainty in $I_{O^{--}}$, there is little point in trying to correct Groth's value for the molecular volume. In any case, it would hardly affect the values for the differences in the corresponding indices for calcite and aragonite. As Bragg has pointed out, it is these differences that are most important.

oxygen. Wasastjerna has shown that ions and molecules of the type XO_3 have nearly identical refractivities. For instance: $R_{Al_2O_3} = 10.6$; $R_{SO_3^{--}} = 10.8$; $R_{NO_3^-} = 10.4$; $R_{CO_3^{--}} = 11.1$. It is evident, therefore, that most of the refractivity is due to the three oxygens and that the element to which they are directly combined in the crystal has but little effect. This fits in very well with the theories published by Lewis, Langmuir, Kossel, and others, in which they picture each of the three oxygens as having two extra electrons so that for our purposes they may be considered as acting like negatively charged ions. In the case of the CO_3^{--} radical, this leaves the carbon with only its positive nucleus and the two K electrons. The effect of such a C^{++++} should be very small in comparison with that of the three O^{--} ions. On this basis the refractivity of O^{--} must be a little less than $11.1/3 = 3.7$. If, instead, we use the value from NO_3^-, it must be a little less than $10.4/3 = 3.5$. Bragg assumes that the allowance for C^{++++} should be such as to give 3.30 for the refractivity of O^{--}. For oxygen the value of $Ne^2\lambda$ in Eqs. (14) and (15) is, then,

$$3 \cdot \frac{3 \times 3.30}{36.13} = 0.822 \text{ in calcite,}$$

and

$$3 \cdot \frac{3 \times 3.30}{34.01} = 0.873 \text{ in aragonite}$$

where N is, as in Eq. (3), the number of atoms (in this case oxygen ions) per cubic centimeter.

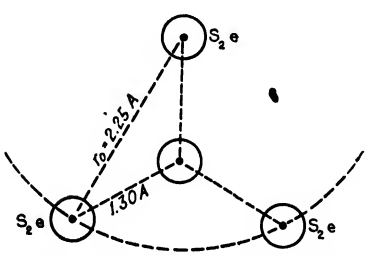

FIG. 3.—Diagram of CO_3^{--} group. The electric vector is perpendicular to the plane of the diagram (extraordinary ray for calcite). (*Bragg.*)

Confining our attention for the present to calcite, we now have the following values ready to substitute in Eq. (14):

For Ca^{++}, $N_1e^2\lambda_1 = 0.165$
For O^{--}, $N_2e^2\lambda_2 = 0.822$
For C^{++++}, $N_3e^2\lambda_3 = 0$

[*i.e.*, it is considered to be negligible in Eq. (14) or in an equation of this type]. These are all calculated on the basis of the number of ions per cubic centimeter because our original equations, such as Eq. (3), were based on a volume of 1 cc.

It remains to find values for the coefficients C_1 and C_2. Since the refractivity of Ca^{++} is small, there will be but little error introduced into the final answer by calling C_1 unity. The value assigned to C_2 for the oxygen terms will depend upon how far we wish to carry our approximations in finding the radius of the sphere mentioned in the derivation of

Eqs. (4) and (11). The roughest possible approximation, short of blindly calling C_2 equal to unity so as to give the sphere a radius of zero, is to consider a sphere which is so small as to take in only the three O^{--} ions of a single CO_3^{--} group; *i.e.*, r in Eq. (12) equals x. If in Fig. 3 the electric vector is perpendicular to the plane of the CO_3^{--} group, then the polarization of each O^{--} is given by Eqs. (11a) and (12) in terms of s_2/λ_2. In Eq. (12) r is 2.25×10^{-8} cm., and since the X-axis is in the direction of the electric vector of the light wave, $x = 0$. In Eq. (11a), therefore, $a_2 = \dfrac{-1}{4\pi r_0^3}$ for each of the two oxygen ions at the circumference of the sphere. The negative sign indicates that the polarization represented by this term opposes that of the $(\bar{E} + \frac{1}{3}P)e$ term Equation (13) now becomes

$$\begin{aligned} \frac{s_2}{\lambda_2} &= \left(\bar{E} + \frac{1}{3}P\right)e + \frac{s_2}{\lambda_2}a_2 e^2\lambda_2 \\ &= \left(\bar{E} + \frac{1}{3}P\right)e - \frac{s_2}{\lambda_2} \cdot \frac{2}{4\pi r_0^3} \cdot e^2\lambda_2 \\ &= \left(\frac{1}{1 + \dfrac{e^2\lambda_2}{2\pi r_0^3}}\right)\left(\bar{E} + \frac{1}{3}P\right)e \end{aligned} \tag{16}$$

The factor $\dfrac{1}{1 + \dfrac{e^2\lambda_2}{2\pi r_0^3}}$ is the C_2 of Eqs. (13) and (14). The numerical value of this factor may be found by an equation like (15),

$$N_2 e^2\lambda_2 = 3\frac{\rho}{M}I_{O^{--}} = 3.30 \times 3\frac{\rho}{M}$$

Since

$$\frac{M}{\rho}N_2 = N_0 = \text{Avogadro's constant} = 6.062 \times 10^{23}$$

and since

$$\tfrac{1}{3}N_0 e^2\lambda_2 = 3.30$$

we have

$$e^2\lambda_2 = 1.63 \times 10^{-23}$$

and

$$\frac{e^2\lambda_2}{2\pi r_0^3} = \frac{1.63 \times 10^{-23}}{2\pi(2.25)^3 \times 10^{-24}} = 0.228$$

C_2 is therefore

$$\frac{1}{1.228} = 0.815$$

We are now ready to substitute all our numerical values in Eq. (14). Such a substitution gives

$$n^2 - 1 = \frac{0.165 + (0.815 \times 0.822)}{1 - \frac{1}{3}\{0.165 + (0.815 \times 0.822)\}} = 1.155 \qquad (17)$$

or

$$n = 1.468$$

Since the electric vector was assumed in Fig. 3 to be perpendicular to the plane of the CO_3^{--} group, n will be the index of refraction for the extraordinary ray. The experimental value is 1.486. In view of the crude assumptions made in the calculations the agreement is very satisfactory.

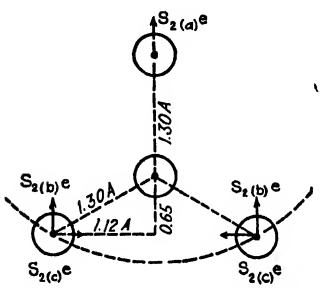

FIG. 4.—Diagram of CO_3^{--} group. The electric vector is parallel to the line joining the carbon to one of the oxygens (ordinary ray for calcite). (*Bragg.*)

In Fig. 4 the electric vector lies in the plane of the CO_3^{--} group and is in the direction of a line joining the carbon to one of the oxygens. This fixes the X-axis. The two oxygen ions on the circumference of the sphere have coordinates

$$x = 1.95 \times 10^{-8} \text{ cm.}$$
$$y = 1.125 \times 10^{-8} \text{ cm.}$$
$$z = 0$$

There will now be three s_2/λ_2 equations corresponding to the three sets of arrows in Fig. 4. We shall assume that the elastic properties of O^{--} ions are the same along all three coordinates so that λ_2 will be the same in all three equations. The three s_2 values, however, will be different since the field strengths differ. Thus

$$\frac{s_{2(a)}}{\lambda_2} = \left(\bar{E} + \frac{1}{3}P\right)e + 2 \cdot \frac{1}{4\pi r_0^3}\left(\frac{3 \times (1.95)^2 - (2.25)^2}{(2.25)^2} s_{2(b)}e + \frac{3 \times (1.125) \times 1.95}{(2.25)^2} s_{2(c)}e\right)e$$

$$= \left(\bar{E} + \frac{1}{3}P\right)e + \frac{1}{4\pi r_0^3}(2.50 s_{2(b)}e + 2.60 s_{2(c)}e)e$$

$$\frac{s_{2(b)}}{\lambda_2} = \left(\bar{E} + \frac{1}{3}P\right)e + \frac{1}{4\pi r_0^3}(1.25 s_{2(a)}e - s_{2(b)}e)e$$

$$\frac{s_{2(c)}}{\lambda_2} = \frac{1}{4\pi r_0^3}(1.30 s_{2(a)}e - 2 s_{2(c)}e)e$$

Solving these three simultaneous equations we have

$$\frac{s_{2(a)}}{\lambda_2} = 1.36\left(\bar{E} + \frac{1}{3}P\right)e$$

$$\frac{s_{2(b)}}{\lambda_2} = 1.07\left(\bar{E} + \frac{1}{3}P\right)e$$

$$\frac{s_{2(c)}}{\lambda_2} = 0.103\left(\bar{E} + \frac{1}{3}P\right)e$$

The mean polarization in the direction of the electric vector of the light wave is

$$\frac{(s_{2(a)} + 2s_{2(b)})}{3\lambda_2} = 1.17\left(\bar{E} + \frac{1}{3}P\right)e$$

A corresponding calculation for Fig. 5 leads to the same value for the coefficient of $(\bar{E} + \frac{1}{3}P)e$. This is as it should be, because of the symmetry of the CO_3^{--} group.

We are now ready to substitute the following values in Eq. (14):

For Ca^{++}, $N_1e^2\lambda_1 = 0.165$; $C_1 = 1.00$
For O^{--}, $N_2e^2\lambda_2 = 0.822$; $C_2 = 1.17$
For C^{++++}, $N_3e^2\lambda_3 = 0$ (*i.e.*, considered to be negligible).

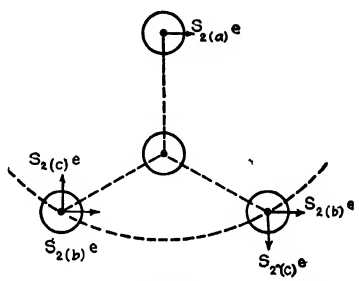

FIG. 5.—Diagram of CO_3^{--} group. The electric vector is parallel to the line joining the two oxygens. (*Bragg.*)

This gives a calculated value for n in calcite of 1.676. Since the electric vector of the light wave is in the plane of the CO_3^{--} group, this should correspond to the index of refraction for the "ordinary" ray. The test value is 1.658. Here again the agreement is good when the rough approximations on which the calculations were based are considered.

These calculations may be refined by using a sphere of larger radius around each oxygen so as to include a larger number of neighboring ions. Such a computation ought, strictly, to take into account the effect of O^{--} on Ca^{++}, Ca^{++} on O^{--}, Ca^{++} on Ca^{++}, and O^{--} on O^{--}. If the radius of the sphere is increased from 2.25×10^{-8} cm. to 6.00×10^{-8} cm., each sphere in calcite would include 42 neighboring ions. In aragonite it would include 50. The uncertainty in the value for the ionic refractivity of oxygen makes it seem unwarranted to go through such a calculation without introducing certain simplifying assumptions. Bragg points out three assumptions of this sort, *viz:*

1. Components of polarization not in the direction of the field are negligible except in the case of the two nearest oxygen ions. This assumption is justified by the previously determined value for $s_{2(c)}/\lambda_2$ in calcite.

2. The effect of Ca^{++} on O^{--} is negligible. Bragg's computations show that this assumption affects the accuracy only in and beyond the third decimal place.

3. For Ca^{++} the constant C is unity.

In Eq. (16) the two oxygen ions on the surface of the sphere of radius 2.25×10^{-8} cm. introduced a term

$$-\frac{s_2}{\lambda_2}\cdot\frac{2}{4\pi r_0^2}\cdot e^2\lambda_2.$$

If the radius of the sphere is increased to 4.50×10^{-8} cm., additional ions are brought in whose effect is of the opposite sign, thus decreasing the value of the negative term. If the radius of the sphere is further increased to 5.5×10^{-8} cm., the additional ions add a negative quantity to the previous result. If the sphere is increased to a radius of 6.0×10^{-8} cm., a small positive quantity is added. In other words, increasing the radius of the sphere adds alternately positive and negative quantities which rapidly decrease in amount with increasing radius. For a radius of 6.0×10^{-8} cm., Eq. (16) becomes

$$\frac{s_2}{\lambda_2} = \left(\overline{E} + \frac{1}{3}P\right)e - \frac{s_2}{\lambda_2}\cdot\frac{1.52}{4\pi r_0^3}e^2\lambda_2 \qquad (18)$$

The variations in the second term of Eq. (18) caused by further slight increases in the radius of the sphere are of the order of 10 to 15 per cent so that the variations in the calculated indices of refraction are of the order of one or two in the second decimal place. Using a radius of 6.0×10^{-8} cm., we have the following values for C_2 in Eq. (14):

Calcite:

1. Polarization perpendicular to the plane of the CO_3^{--} group, $C_2 = 0.847$.
2. Polarization parallel to the plane of the CO_3^{--} group, $C_2 = 1.100$.

Aragonite:

1. Polarization perpendicular to the plane of the CO_3^{--} group (*i.e.*, parallel to the Z-axis and corresponding to the α index of refraction), $C_2 = 0.874$.
2. Polarization parallel to the X-axis and corresponding to the β index of refraction, $C_2 = 1.118$.
3. Polarization parallel to the Y-axis and corresponding to the γ index of refraction, $C_2 = 1.100$.

The corresponding refractive indices are given in Table I. The agreement between the calculated and observed values is considerably

TABLE I.—COMPARISON BETWEEN CALCULATED AND OBSERVED INDICES OF REFRACTION FOR CALCITE AND ARAGONITE

	Calculated		Observed
	$r = 2.25$Å.	$r = 6.00$Å.	
Calcite	$\epsilon = 1.468$ $\omega = 1.676$	$\epsilon = 1.488$ $\omega = 1.631$	$\epsilon = 1.486$ $\omega = 1.658$
Aragonite	$\alpha = 1.503$ $\beta = 1.730$ $\gamma = 1.730$ $\frac{\beta+\gamma}{2} = 1.730$	$\alpha = 1.538$ $\beta = 1.694$ $\gamma = 1.680$ $\frac{\beta+\gamma}{2} = 1.687$	$\alpha = 1.530$ $\beta = 1.681$ $\gamma = 1.686$ $\frac{\beta+\gamma}{2} = 1.683$

better for the larger radius of the sphere and is clearly within the limit of error mentioned above. It is to be expected that a further increase would iron out most of the remaining differences and even make the calculated value of γ larger than that of β.

INTERIONIC SPACINGS FROM OPTICAL CALCULATIONS

In the light of the preceding calculations it is possible to make some interesting inferences as to interatomic spacings in certain crystals. For instance, by assuming a succession of values for the distance between the O^{--} ions in calcite it is possible to compare the calculated values of the indices of refraction with the values determined by test. It is more convenient to compare the values for the "ionic birefringence" of O^{--}, which are found as follows: The ordinary "molecular birefringence" is found as the difference, $R_\omega - R_\epsilon$, between the molecular refractivity, R_ω, for the ordinary refractive index and the corresponding molecular refractivity, R_ϵ, for the extraordinary refractive index. The expression for molecular refractivity is given in Eq. (8). The ionic refractivities, R_ω' and R_ϵ', of CO_3^{--} are found by subtracting the ionic refractivity of the metal ion from R_ω and R_ϵ. Assuming the effect of C^{++++} to be negligible, this gives the ionic birefringence of O^{--} as $R_\omega' - R_\epsilon'$. If we assume that the metal ion contributes about equally to both R_ω and R_ϵ, then $R_\omega' - R_\epsilon'$ is approximately equal to $R_\omega - R_\epsilon$.

Table II gives Bragg's values[6] for $R_\omega' - R_\epsilon'$ for assumed $C^{++++} - O^{--}$ spacings in calcite. The experimental value of $R_\omega' - R_\epsilon'$ is 2.94. It is evident that the $C^{++++} - O^{--}$ distance is between 1.20 and 1.30 $\times 10^{-8}$ cm.; interpolation gives $1.24^5 \times 10^{-8}$ cm. From x-ray diffraction data W. H. Bragg estimated this distance as between 1.24 and 1.34. Wyckoff, using the Laue method, estimated it[3] as being close to 1.24. This illustration shows the possibilities in using optical data to supplement the ordinary data of x-ray diffraction in determining the structure of crystals. For instance, $NaNO_3$ has the same sort of structure as calcite,[7,8] but the molecular birefringence is greater in the ratio of 4.83:2.94. Table II would seem to indicate that this means that the O^{--} ions are closer together in the NO_3^- group than they are in the CO_3^{--} group. W. L. Bragg has made calculations similar to those in Table II for $NaNO_3$

TABLE II.—DEPENDENCE OF IONIC BIREFRINGENCE UPON INTERIONIC DISTANCES

d	R_ω'	R_ϵ'	$R_\omega' - R_\epsilon'$ $(= R_\omega - R_\epsilon)$
1.00×10^{-8} cm.	13.55	6.75	6.80
1.10	12.21	7.48	4.73
1.20	11.33	8.01	3.32
1.30	10.89	8.39	2.50

using Wasastjerna's value of 0.75 for the ionic refractivity of Na^+. His calculations show that the distance between N^{+++++} and O^{--} ions of a single NO_3^- group is 1.09×10^{-8} cm. This is consistent with the current pictures of the ionic structure of NO_3^- and CO_3^{--}, for the three O^{--} ions should be more strongly attracted by N^{+++++} than by C^{++++}.

Similar calculations on the birefringence of Al_2O_3 lead Bragg to assign $1.45 - 1.48 \times 10^{-8}$ cm. as the distance from each O^{--} ion to the center of the equilateral triangle on which it is situated. This is to be compared with 1.45×10^{-8} cm. as indicated by x-ray diffraction. It is interesting to note that this gives a packing-radius of 1.04 Å. to O^{--} in agreement with Table XII of Chap. XIII.

SUMMARY

Using calcite and aragonite as examples, we have seen how it is possible to calculate the indices of refraction of crystals from a knowledge of the configurations and spacings of atoms (or ions) in crystals. Conversely, we can use the index of refraction of a crystal to determine some of its lattice parameters. This was done by making the assumption that $CaCO_3$ is composed of Ca^{++}, C^{++++}, and three O^{--}, but without any further assumptions as to the inner architecture of these ions. Similar calculations lead to correct lattice parameters for $NaNO_3$, and Al_2O_3.

These calculations are tedious to make, but they place us, as scientists, one step nearer the goal of building a picture of Nature from which we can predict all her properties.

References

1. W. L. Bragg, *Proc. Roy. Soc.*, **105**, 370 (1924); **106**, 346 (1924).
2. W. L. Bragg, *Proc. Roy. Soc.*, **89**, 248 (1914); **105**, 16 (1924).
3. R. W. G. Wyckoff, *Amer. Jour. Sci.*, **50**, 317 (1920); **9**, 145 (1925).
4. W. H. Bragg, *Phil. Trans. Roy. Soc. London*, **215**, 253 (1915).
5. J. A. Wasastjerna, *Soc. Sci. Fenn. Comm. Phys. Math.*, **1**, 37 (1923).
6. W. L. Bragg, *Proc. Roy. Soc.*, **106**, 346 (1924).
7. W. L. Bragg, *Proc. Roy. Soc.*, **89**, 468 (1914).
8. R. W. G. Wyckoff, *Phys. Rev.*, **16**, 149 (1920).

CHAPTER XV

THE CALCULATION OF LATTICE ENERGIES

In Chap. XIV we calculated the optical constants of crystals on the assumption that we could treat atoms (or ions) as units without reference to their internal structure. We shall now calculate some of the other properties of materials on the basis of the simplest possible sort of structure for the atoms of which they are composed. Having thus obtained a point of view in terms of which we may think of the ultimate source of these properties, we are ready to point out the path for the more complicated cases and to indicate a short-cut in the path which helps to make the actual computation less laborious.

It would seem at first sight that the outstanding physical properties of a substance could be expressed in terms of the forces between its atoms and in terms of the forces which hold together the atoms themselves. Actually, our calculations will be in much more usable form if they are made in terms of energy rather than force. In calculating the potential energy of an atom it is necessary first to assume a simple structure for the atom which is consistent with the known facts and then to assume a law of force between the component parts of the atom. The two assumptions to be made may or may not be correct; at any rate they must not be inconsistent with any known fact. Their ultimate justification must lie in the degree of accuracy of the predictions which may be made in consequence of making these particular assumptions. In terms of these two assumptions and the known configuration of atoms in the crystal, the potential energy of a metallic ion and of a valence electron may be calculated. This makes it possible to calculate many properties such as the compressibility, surface tension, and threshold of the photoelectric effect. It is the purpose of this chapter to give the basis for the assumptions which must be made and to show in detail how some of these calculations may be carried out.

THE POTENTIAL ENERGY OF AN ATOM IN A CRYSTAL

It is universally accepted that an atom of an element is composed of a positively charged nucleus which is surrounded by electrons whose number is such as to neutralize the nuclear charge completely, thus giving a net electric charge of zero to the atom as a whole. Most of the mass of the atom resides in its nucleus; for instance, the mass of the nucleus of a hydrogen atom is 1,845 times as great as the mass of its electron. Most

of the other physical properties of an atom, and all its chemical properties, are supposed to be caused by the number and configuration of its electrons. If the electrons are stationary, and if the ordinary inverse-square law of electrostatics is assumed to hold for intra-atomic distances, it is easy to calculate that the repulsive force of the electrons against each other is less than the attractive force between these electrons and the positive nucleus. This leaves us four alternatives:

1. We must consider the inmost electrons to be in contact with the positive nucleus and the remainder of the electrons to be nested in close contact in one or more outer layers, something like the grains of corn in a pop-corn ball.
2. We must arbitrarily assign such a structure to the nucleus as will produce a non-uniform field of force in the atom.
3. We must assume a modification of Coulomb's inverse-square law for small distances.
4. We must introduce a new repulsive force for the electrons.

The first alternative can hardly be accepted in the light of existing experimental data. We have already seen that the atoms of the elements pack in crystals like solid elastic bodies of one shape or another. If these atoms contained electrons in contact with each other, pop-corn-ball fashion, the only straight paths through a crystal would lie in those natural voids which might be inherent in the crystal structure. It is well known from the work of Geiger[1] that α particles from radioactive substances can travel in straight lines through metal foil. The stopping power of a pop-corn-ball atom for an α particle would have to depend, therefore, primarily upon the crystal structure of the element. Actually it seems to depend[2] only upon the square root of the atomic weight. In other words, the stopping power of an atom depends upon the mass of its nucleus, not upon the way the atom groups itself with other like atoms to form a crystal. This would seem to require an atomic architecture quite different from the pop-corn-ball type.

The second alternative is to assume a nuclear structure, such that in certain directions the attractive force of the nucleus on any given electron will be decreased. If the shape of such a field of force could be so made as to enable electrons to find positions of stable equilibrium, the problem would be solved. But as soon as we have admitted that in certain directions the attractive force between the nucleus and an electron may be less than that required by Coulomb's law, we are dealing with a special case of the third possible alternative. We shall therefore pass at once to a consideration of that alternative.

The most obvious modification of Coulomb's law would be to superimpose upon the inverse-square law a sine or cosine law with a decrement. If the decrement were large enough to leave only the inverse-square law at points outside the atom, the modified law would satisfy the existing experimental data. A simple modification, and one which lends itself

more readily to numerical calculation, has been proposed by J. J. Thomson[3] and by I. Langmuir.[4] According to their assumption, if, in an atom of atomic number N, an electron with a charge e is at a distance r from a positive nucleus of charge Ne, then the force between them is

$$F = Ne^2\left(\frac{1}{r^2} - \frac{c}{r^3}\right) \tag{1}$$

This gives a law which degenerates into the ordinary inverse-square law at a distance determined by the value of c.

The fourth alternative is one proposed by Bohr.[5] If the electrons are imagined to rotate in orbits about the positive nucleus, the effect of their centrifugal forces would be added to the Coulomb repulsive forces between the various electrons. If the linear velocity of each electron in its orbit is properly adjusted to the radius of its orbit, the centrifugal force will be just enough to keep the electron from traveling in toward the nucleus. Definite values are assigned to the radii and therefore to the velocities of the electrons by additional assumptions which need not be discussed here.

Since these last two alternatives are both attempts to find forces which will keep the electrons of an atom from falling in toward the positive nucleus, it is inevitable that the inverse-cube correction applied to Coulomb's law should give the same numerical result as the centrifugal forces of the Bohr atom. Any refinements to these various theories of atomic structure can hardly make any very great changes in the sort of calculations which we are about to make. It is therefore permissible to make our calculations on the basis of either hypothesis, for the results from one may be applied quantitatively at once to the other, at least to a first approximation. Since the calculations are very much easier in the case of the inverse-cube hypothesis, we shall follow the lead of J. J. Thomson[3] and make them on that basis.

For the sake of simplicity we shall limit ourselves at first to univalent metals, *i.e.*, to those which have only a single valence electron. Although no element crystallizes in a simple cubic lattice, it is the easiest structure to visualize. We shall therefore illustrate the method by first calculating the potential energy of a fictitious univalent metal crystallizing in a simple cubic lattice. In doing this it will simplify the work to assume at first that only the Coulomb inverse-square forces exist. The result so obtained can then be corrected to include the inverse-cube forces.

For the sake of simplicity, we shall assume that all the electrons of the atom, except the valence electrons, lie so close to the positive nuclei that the net effect is the same as though these electrons and the nuclei were replaced by single positive charges. Our simplified atoms therefore each consist, in effect, of only a single positive charge and a single valence electron. Imagine the valence electrons to lie at the corners of a simple

cubic lattice, such as is shown in Fig. 1,* and let the positive charges lie at the body-centers of these cubes. Then these positive charges will themselves lie at the corners of a simple cubic lattice. Our fictitious univalent element will therefore have a simple cubic structure whether we consider only the valence electrons or whether we consider only the remainder of the atom. If such a lattice is extended to infinity in all directions, each electron will be shared equally by eight cubes. Each simple cube of electrons will contain eight-eighths electrons and will have a single positive charge at its center. There will therefore be an average of one valence electron for each of the positive charges which we have used to represent the remainder of the univalent atom. To be sure, no one valence electron can be said to "belong" to any one particular atom, but this constitutes no objection to the model, for such a communal possession of valence electrons introduces nothing which is inconsistent with any known physical or chemical data.†

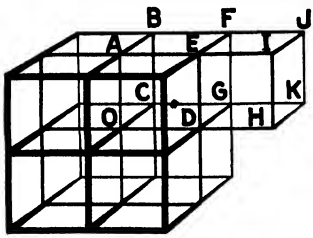

FIG. 1.—Simple cubic lattice of valence electrons of a fictitious univalent element.

Our problem is to find the potential energy of such an "atom" (metallic ion plus its valence electron) in a simple cubic crystal. This will be done in two steps, first finding the energy of the valence electron, then finding that of the metallic ion. The sum of these will be the energy of the atom. Let us choose the electron O of Fig. 1. On the basis of a purely inverse-square law of force, the potential energy of the electron is

$$e^2 \sum \left(\frac{1}{r}\right)$$

where the summation is taken over all the charges in the crystal. Thomson finds that, if the charges associated with each unit-cube in Fig. 1 are considered together, the summation comes out in the form of a rapidly converging series. He therefore calculates the various terms of such a series until they become negligibly small.

It is evident from Fig. 1 that there are eight identically similar cubes which have the point O in common. Each of these has electrons at three points like A, C, and D, whose distances from O are the edge a of the unit-cube. The coordinates of A are $(0,0,1)$ a; of C, $(0,1,0)$ a;

* In connection with his studies of the properties of crystals (see especially p. 1779 of reference 6), Zwicky,[6] too, is led to assume that the valence electrons of elements occupy definite positions in the crystal lattice.

† If by some stretch of the imagination we suppose each valence electron to be tied to one definite metallic ion, even then we would have to consider our fictitious element as having a simple cubic structure, for the "atoms" would repeat their positions in space in such a way that, considered as points, they would lie on a simple cubic lattice.

of D, $(1,0,0)$ a. The distance from O to A may be expressed as $(\sqrt{0^2+0^2+1^2})\,a$. Since only one-eighth of the electron at A belongs to the cube $OABCDEFG$, the contribution of A from that cube to the potential energy of O is

$$\frac{1}{8}\left(\frac{1}{\sqrt{0^2+0^2+1^2}}\right)\frac{e^2}{a}=\frac{1}{8}\cdot\frac{e^2}{a}$$

A, C, and D, together, then contribute $\frac{3}{8}\cdot e^2/a$. Similarly the electrons at the three points B, E, and G contribute

$$\frac{3}{8}\left(\frac{1}{\sqrt{1^2+1^2+0^2}}\right)\frac{e^2}{a}=\frac{3}{8\sqrt{2}}\cdot\frac{e^2}{a}$$

and the electron at F contributes

$$\frac{1}{8}\left(\frac{1}{\sqrt{1^2+1^2+1^2}}\right)\frac{e^2}{a}=\frac{1}{8\sqrt{3}}\cdot\frac{e^2}{a}$$

The coordinates of the positive charge at the center of the cube are $\frac{1}{2}, \frac{1}{2}, \frac{1}{2}$. Its contribution to the potential energy of the electron at O is therefore

$$-\left(\frac{1}{\sqrt{(\frac{1}{2})^2+(\frac{1}{2})^2+(\frac{1}{2})^2}}\right)\frac{e^2}{a}$$
$$=-\frac{2}{\sqrt{3}}\cdot\frac{e^2}{a}$$

The whole cube therefore contributes

$$\left(\frac{3}{8}+\frac{3}{8\sqrt{2}}+\frac{1}{8\sqrt{3}}-\frac{2}{\sqrt{3}}\right)\frac{e^2}{a}$$

and the eight cubes meeting at O contribute a potential energy

$$\left(3+\frac{3}{\sqrt{2}}+\frac{1}{\sqrt{3}}-\frac{16}{\sqrt{3}}\right)\frac{e^2}{a}=-3.53894\frac{e^2}{a}$$

to the electron at O.

There are 24 cubes like $DEFGHIJK$. The positive nuclei at the centers of these cubes have as coordinates the successive permutations of

$$(\pm\tfrac{1}{2},\ \pm\tfrac{1}{2},\ \pm\tfrac{3}{2})a$$

Each of these nuclei therefore contributes

$$-\left(\frac{1}{\sqrt{(\frac{1}{2})^2+(\frac{1}{2})^2+(\frac{3}{2})^2}}\right)\frac{e^2}{a}=-\frac{2}{\sqrt{11}}\cdot\frac{e^2}{a}$$

to the potential energy of the electron at O. The electrons at the corners contribute the following from the cube: $DEFGHIJK$.

D: $$\frac{1}{8}\left(\frac{1}{\sqrt{1^2+0^2+0^2}}\right)\frac{e^2}{a} = \frac{1}{8}\cdot\frac{e^2}{a}$$

E and G each: $$\frac{1}{8}\left(\frac{1}{\sqrt{1^2+1^2+0^2}}\right)\frac{e^2}{a} = \frac{1}{8\sqrt{2}}\cdot\frac{e^2}{a}$$

F: $$\frac{1}{8}\left(\frac{1}{\sqrt{1^2+1^2+1^2}}\right)\frac{e^2}{a} = \frac{1}{8\sqrt{3}}\cdot\frac{e^2}{a}$$

H: $$\frac{1}{8}\left(\frac{1}{\sqrt{2^2+0^2+0^2}}\right)\frac{e^2}{a} = \frac{1}{16}\cdot\frac{e^2}{a}$$

I and K each: $$\frac{1}{8}\left(\frac{1}{\sqrt{2^2+1^2+0^2}}\right)\frac{e^2}{a} = \frac{1}{8\sqrt{5}}\cdot\frac{e^2}{a}$$

J: $$\frac{1}{8}\left(\frac{1}{\sqrt{2^2+1^2+1^2}}\right)\frac{e^2}{a} = \frac{1}{8\sqrt{6}}\cdot\frac{e^2}{a}$$

The cube $DEFGHIJK$ therefore contributes a total of $-0.003743e^2/a$ toward the potential energy of the electron at O. All 24 of these cubes contribute a total of $-0.089832e^2/a$.

Table I shows results of similar calculations for 30 types of cubes in the lattice of the fictitious univalent simple cubic element. It is evident that for cubes whose centers are not too close to the origin the final results group themselves into clusters of positive and negative values which practically cancel each other out up to the fourth decimal place. Limiting ourselves to cubes whose centers are less than $5a$ from the origin, we have a total potential* of

$$(-3.675 + 0.066)\frac{e^2}{a} = -3.609\frac{e^2}{a}$$

on the assumption that only inverse-square forces are present.

The potential energy of the electron due to the inverse-cube forces will be proportional to $\frac{e^2}{r^2}$, *i.e.*, it will be equal to $k\frac{e^2}{r^2}$ where k is the proportionality constant. The reason for introducing the inverse-cube forces was to decrease the effect of the inverse-square forces. Since the inverse-square energy is negative in sign, it is evident that k must be positive. The total potential energy of the electron at O, Fig. 1, is therefore

$$\left(-\frac{3.609}{a} + \frac{k}{a^2}\right)e^2$$

* The fourth and fifth columns are carried out to six decimal places because we are dealing with a multiple of a *difference*. This is justifiable because the decimal fractions represent common fractions which are known from solid geometry. Our final answer is expressed only to three decimal places because of the uncertainty introduced by using only a small number of cubes.

If we neglect any effect of temperature, the structure of our fictitious element will be stable if the quantity in the parentheses is a minimum,

TABLE I.—POTENTIALS OF VARIOUS TYPES OF CUBES IN LATTICE OF FICTITIOUS UNIVALENT ELEMENT

Type of coordinates of metallic ion at center of cube*	Square of distance from origin to center of cube	Number of equivalent cubes of type listed in column 1	Potential of valence electrons per cube $\times a/e^2$	Potential of metallic ion per cube $\times a/e^2$	Resultant potential of all cubes of type listed in column 1
½½½	¾	8	+0.712334	−1.154701	−3.53894 e^2/a
½½3/2	1¼	24	+0.599280	−0.603623	−0.08983 e^2/a
½3/2 3/2	1¾	24	+0.460283	−0.458831	+0.03485 e^2/a
3/2 3/2 3/2	2¼	8	+0.386346	−0.384900	+0.01157 e^2/a
½½5/2	2¾	24	+0.383747	−0.384900	−0.02767 e^2/a
½3/2 5/2	3¼	48	+0.338098	−0.338062	+0.00173 e^2/a
½3/2 3/2	3¾	24	+0.305269	−0.304997	+0.00653 e^2/a
½½7/2	4¼	24	+0.280154	−0.280056	+0.00235 e^2/a
½3/2 5/2	4¾	24	+0.260527	−0.260378	+0.00358 e^2/a
3/2 3/2 5/2	5¼	8	+0.231041	−0.230940	+0.00081 e^2/a
½½9/2	5¼	24	+0.279760	−0.280056	−0.00710 e^2/a
½3/2 7/2	5¾	48	+0.260302	−0.260378	−0.00365 e^2/a
½3/2 3/2	6¼	24	+0.244354	−0.244339	+0.00036 e^2/a
½½9/2	7¼	48	+0.230959	−0.230940	+0.00091 e^2/a
½3/2 5/2	8¼	48	+0.219571	−0.219529	+0.00202 e^2/a
½5/2 5/2	9¼	24	+0.201049	−0.201008	+0.00098 e^2/a
½½11/2	9¼	24	+0.201026	−0.201008	+0.00043 e^2/a
½½7/2	10¼	24	+0.193373	−0.193347	+0.00062 e^2/a
½½5/2	12¼	24	+0.180360	−0.180334	+0.00062 e^2/a
½½½	14¼	8	+0.164975	−0.164959	+0.00013 e^2/a
3/2 3/2 3/2	8¼	24	+0.219432	−0.219529	−0.00228 e^2/a
3/2 3/2 3/2	9¼	48	+0.209613	−0.209657	−0.00211 e^2/a
3/2 3/2 3/2	9¼	24	+0.200992	−0.201008	−0.00038 e^2/a
3/2 5/2 3/2	10¼	48	+0.193343	−0.193347	−0.00019 e^2/a
3/2 5/2 3/2	11¼	48	+0.186508	−0.186501	+0.00034 e^2/a
3/2 5/2 5/2	13¼	24	+0.174754	−0.174741	+0.00031 e^2/a
3/2 7/2 3/2	13¼	48	+0.174747	−0.174741	+0.00029 e^2/a
3/2 3/2 3/2	13¼	48	+0.169648	−0.169638	+0.00048 e^2/a
3/2 3/2 5/2	15¼	48	+0.160656	−0.160644	+0.00058 e^2/a
3/2 3/2 3/2	16¼	24	+0.156657	−0.156652	+0.00012 e^2/a

* The coordinates of the eight electrons associated with a given metallic ion may be found by adding successively to these coordinates the following: ½, ½, ½; ½, ½, −½; ½, −½, ½; −½, ½, ½; −½, −½, ½; −½, ½, −½; ½, −½, −½; −½, −½, −½.

i.e., if the first differential of that quantity is equal to zero. This gives us the equation

$$\frac{3.609}{a^2} - \frac{2k}{a^3} = 0$$

or

$$k = \frac{3.609}{2}a$$

The total potential energy of the electron at O, Fig. 1, is therefore

$$\text{P.E.}_{\text{electron}} = \left(-\frac{3.609}{a} + \frac{3.609a}{2a^2}\right)e^2 \tag{2a}$$

so that

$$\text{P.E.}_{\text{electron}} = -\frac{3.609}{2a}e^2 \tag{2}$$

But O was any electron in the crystal of our fictitious element which was far enough below the surface to be surrounded by all the cubes used in our calculations. A glance at the coordinates of the centers of these cubes shows that, in order that our calculations may be strictly applicable, the electron must lie at least four atoms below the surface.

We have so far assumed, with Thomson, that the ordinary Coulomb's law force was weakened by a subtractive inverse-cube term. Equation (2a) for the potential energy therefore contains two terms, one of which contains the inverse square of the length of the side of the unit-cube. Suppose that instead of an inverse-cube term in the force equation we had used an inverse-nth term. It is easy to show that the constant k would become

$$k = \frac{3.609}{n-1}a^{n-2}$$

and Eq. (2) would become

$$\begin{aligned}\text{P.E.}_{\text{electron}} &= \left(-\frac{3.609}{a} + \frac{3.609a^{n-2}}{(n-1)a^{n-1}}\right)e^2 \\ &= -\left(\frac{n-2}{n-1}\right)\left(\frac{3.609}{a}\right)e^2\end{aligned} \tag{3}$$

which differs from Eq. (2) by a constant factor whose value depends upon the value of n. If therefore our final calculated results differ from those of experiment, we shall expect that, for any given crystal structure, they will differ by a constant factor. For the present we shall continue our calculations on the basis $n = 3$.

In the original description of the crystal structure of our fictitious element it was brought out that the positive ions of this element resided on exactly the same sort of a lattice as the electrons. If we had wished, we could have drawn Fig. 1 with the lines of the simple cubic framework passing through the positive ions. This would have given a simple cubic lattice of positive ions with an electron at the center of each cube. Then a calculation identical with that which has just been carried out would have given us the potential energy of a positive ion. But the total energy of the atom is the sum of the energies of its positive ion and of its valence electron. Therefore if the single atom of our fictitious element is at least four atoms below the surface, its energy is

$P.E._{atom} = -3.609e^2/a$. In a unit-volume of N atoms the effect of each atom on every other atom is considered. Each atom is thus counted twice and contributes effectively $-1.804e^2/a$ to the P.E. of the unit-volume.

Similar calculations have been made by J. J. Thomson and Miss I. Woodward[3] for elements which crystallize so that their positive ions lie on body-centered cubic, face-centered cubic, and diamond cubic lattices. These calculations apply directly to elements whose positive ions have a simple type of architecture, *i.e.*, which resemble the inert gases. They do not seem to apply to elements whose positive ions have a more complex structure (such as Cu), and this may mean that we cannot apply to such elements Thomson's simplifying assumption that the positive ion may be considered as merely a positive charge concentrated at a point. As examples of elements whose positive ions resemble the atoms of the inert gases we may cite the univalent elements Li, Na, and K, which crystallize as body-centered cubes; the bivalent element Ca and the trivalent element Al, which are face-centered cubic; and the quadrivalent element C, which in the diamond is diamond cubic.

In each case it is necessary for the purpose of the calculations to assign positions in the lattice to the valence electrons. Where two or more sets of positions are possible, each with the requisite symmetry, it is found that they all give results of the correct order of magnitude, but that some one simple configuration of valence electrons gives results that agree much more closely with the data of experiment than do any of the others. Such a configuration is naturally chosen as representing the "correct" configuration in terms of the static-atom (Lewis-Langmuir) picture of atomic architecture. As has already been stated, the picture thus obtained may be expressed later more or less completely in terms of any other picture of atomic structure if we so desire.

For a univalent body-centered cubic element, such as Na, the positive ions are, of course, to be thought of as being situated at the points of a body-centered cubic lattice. This gives eight-eighths-plus-one positive ions per unit-cube. Since we thus have two positive ions per unit-cube, we must have two valence electrons per unit-cube. These are pictured by Thomson as lying along a single body-diagonal of each unit-cube.* In order to preserve the cubic symmetry of the crystal, these diagonals are so chosen that "in a cube built up of eight such small cubes no two of the diagonals in any four whose centers are in one plane are parallel or intersect." These diagonals are shown in Fig. 2. It is a consequence of this configuration that any two unit-cubes which meet only at one corner have their valence electrons on parallel body-diagonals. Miss Woodward

* By compressing the metallic ion into a single point charge and by placing the valence electrons halfway between these point charges, we avoid the difficulties associated with Turner's calculations referred to in Chap. XIII.

finds* that the effective energy of an atom of a monovalent element having such a structure is $-2.015e^2/a$. As before, it is assumed that the atom is below the surface of the crystal. Since in a body-centered cubic crystal there are two atoms per unit cube, the potential energy per unit-crystal is $-4.03e^2/a$.

For a univalent face-centered cube the structure is assumed to be like that of ZnS (Fig. 9 of Chap. V). The positive metallic ions take the place of the Zn^{++} and the electrons take the place of the S^{--}. The effective energy per atom is $-2.78e^2/a$. Since there are four atoms per unit-cube, the potential energy per unit-cube is $-11.12e^2/a$.

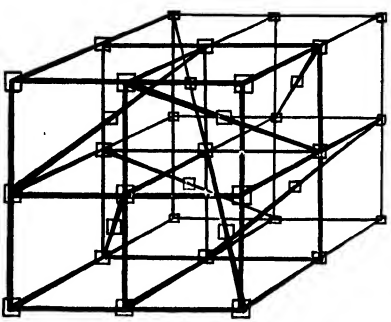

FIG. 2.—Configuration of body diagonals on which J. J. Thomson supposes the valence electrons to lie for the alkali metals.

The structure of a bivalent face-centered cubic element like Ca is considered to be like that of CaF_2 with the valence electrons occupying the positions of the F^- (Figs. 10 and 11 of Chap. V). For such a configuration, Thomson finds that the effective energy of an atom is $-8.92e^2/a$. Since a face-centered cube contains four atoms, the potential energy of the unit-cube is $-35.68e^2/a$.

In a trivalent face-centered cubic element like Al, Thomson assumes two of the valence electrons to lie as in the case of Ca. The third has the same relation to the Al^{+++} ion that Cl^- has to Na^+ in NaCl. This gives an effective energy for such an atom of $-14.24e^2/a$. The potential energy of the unit crystal is therefore $-56.96e^2/a$.

Since a unit-cube of diamond contains eight atoms, it is necessary to find positions in the unit-cube for 32 valence electrons. Thomson assumes that one of these is situated at each of the middle points of the edges of the unit-cube of the diamond, and one at the body-center of the unit-cube. This gives an NaCl structure between four C^{++++} ions and four valence electrons and may be considered to break up the unit-cube into eight smaller cubes. He then puts a valence electron at the center of each of the faces of these small cubes. Four of the small cubes already have a C^{++++} at the body-center. He puts a valence electron at the body-centers of the other four. Using this rather arbitrary structure† he finds that it gives an effective energy of $-21.15e^2/a$ per atom or $-169.2e^2/a$ per unit-cube, provided only that we deal with atoms sufficiently far below the surface.

* The results are expressed here in somewhat different form from that used by J. J. Thomson and Miss Woodward.[3]

† The structure given by the theory of space-groups is discussed in Chap. XIX. It would probably give results rather similar to those given here.

Remembering that

$$e = 4.774 \times 10^{-10} \text{ abs. e.s.u. of charge}$$

and that

$$300 \text{ volts} = 1 \text{ abs. e.s.u. of potential}$$

we may express the potential energy of any unit-crystal in terms of the number of volts required to give a single electron that same amount of energy. For a body-centered cube this voltage is

$$-\frac{300 \times 4.03 \times 4.774 \times 10^{10}}{a} \text{ volts} \qquad (4)$$

where a is, as before, the edge of the unit-cube. This enables us to calculate the voltages for Li, Na, K, Rb, and Cs from the known values of a. The values of these voltages for the alkali metals are summarized in Table II.

TABLE II.—ELECTRON VOLTAGE CORRESPONDING TO ENERGY OF UNIT-CRYSTAL

Element	a from direct x-ray data	P.D./e in volts	P.D./e in volts; using values for a calculated from the density
Li	3.50×10^{-8} cm.	16.5	16.4
Na	4.30×10^{-8}	13.4	13.5
K	5.20×10^{-8}	11.1	10.9
Rb*	5.73×10^{-8}	10.1	10.2
Cs*	6.16×10^{-8}	9.3	9.3

* Instead of the lattice parameters found from x-ray data (Chap. XIII) values of a are used which are calculated from the density on the basis of a body-centered cubic structure. This gives for Rb (density 1.532) a parameter $a = 5.73 \times 10^{-8}$ cm. instead of 5.62 as found by Simson and Vohsen. We have, similarly, for Cs (density 1.87) a parameter $a = 6.16 \times 10^{-8}$ cm. instead of 6.05 as found by Simson and Vohsen.

PHYSICAL DATA CALCULATED FROM LATTICE POTENTIALS

Compressibility of Elements.—The work required to compress a unit-cube so that its side is decreased from a to $(a - \delta a)$ is

$$W_1 = \text{P.E.}\left(\frac{\delta a}{a}\right)^2 \qquad (5)$$

where P.E. is the potential energy of the unit-cube. Since there are $1/a^3$ unit-cubes per cubic centimeter, the work of compression per cubic centimeter is

$$W = \text{P.E.}\left(\frac{\delta a}{a}\right)^2\left(\frac{1}{a^3}\right) \qquad (6)$$

The change in the volume of a solid while undergoing compression is proportional to the pressure applied and to the original volume, so that

$$\text{Pressure} = k\left(\frac{\delta V}{V}\right)$$

where V is the volume and k is the constant of proportionality and is called the "bulk modulus." The quantity $1/k$ is called the "compressibility." If W is the work done in compressing each cubic centimeter of material, then the total work for V cc. is

$$WV = \tfrac{1}{2} \text{ pressure} \times \delta V$$

$$= \frac{1}{2}k\frac{\delta V}{V}\delta V$$

Then

$$W = \frac{1}{2}k\left(\frac{\delta V}{V}\right)^2$$

Since

$$\frac{\delta V}{V} = 3\frac{\delta a}{a}$$

we have

$$W = \frac{9}{2}k\left(\frac{\delta a}{a}\right)^2 \tag{7}$$

Combining Eqs. (6) and (7),

$$k = \frac{2}{9}\text{P.E.}\left(\frac{1}{a}\right)^3 \tag{8}$$

For univalent body-centered cubic materials this becomes

$$k = \frac{2}{9} \times 4.03\frac{e^2}{a^4} \tag{9}$$

This equation enables us to calculate the values for the bulk modulus k given in Table III for Li, Na, K, Rb, and Cs.

TABLE III.—BULK MODULI OF THE ALKALI METALS

Element	Calculated	Experimental
Li	0.136×10^{12}	0.114×10^{12}
Na	0.060×10^{12}	0.065×10^{12}
K	0.028×10^{12}	0.032×10^{12}
Rb*	0.019×10^{12}	0.025×10^{12}
Cs*	0.014×10^{12}	0.016×10^{12}

* See note under Table II.

All these results for the bulk moduli of the alkali metals are compared in this table with Prof. T. Richard's experimental values. When it is remembered that Eq. (9) contains no adjustable constants and that the

calculations are based on the crude assumption that the positive ion may be considered as a single positive charge concentrated at a point, the agreement is quite striking. Similar results for polyvalent elements are given in Table IV.

Calculations show that the moduli of all the alkali metals are not far from what they would have been if they had had a simple cubic structure. This is consistent with the fact that the directive forces which give these metals a definite crystal structure are rather small. For instance, Li tends to lose its crystalline characteristics considerably below its melting

TABLE IV.—BULK MODULI OF POLYVALENT ELEMENTS

Element	Calculated	Experimental
Ca $a = 5.56 \times 10^{-8}$ cm.	0.189×10^{12}	0.182×10^{12}*
Al $a = 4.046 \times 10^{-8}$ cm.	1.08×10^{12}	0.78×10^{12}*
C (Diamond) $a = 3.56 \times 10^{-8}$ cm.	5.27×10^{12}	6.2×10^{12}†

* Richards.
† Adams.

point.[7] It is not to be expected that other metals will show a similar freedom from the effect of crystal structure.

Calculations such as we have just made give results for Cu, Ag, and Au which are much larger than the experimentally determined values. These are the univalent metals whose positive ions are supposed to bear no structural resemblance to the atoms of the inert gases. This seems to indicate that for these metals the positive ion cannot be considered as a geometrical point in making our calculations. It is as though these metals had relatively incompressible positive ions. We have already seen that the ions of the alkali metals pack in the crystals of their halides as though they were relatively incompressible. But these ionic domains are much smaller than the domains of the corresponding neutral atoms so that we may assume that the relatively great compressibility of the alkali metals is caused by the valence electron being spaced some little distance from the border of the domain of the positive ion.* A study of models of crystals makes it easy to assume that this distance is probably relatively small for the univalent face-centered cubic metals. If this assumption is correct, it would be necessary to take into account in the calculations the structure of the positive ion in the case of Cu, Ag, and Au.

* Note that this conclusion is not consistent with the calculations of Turner (Chap. XIII). The consistency is hardly improved by adopting the language of the Bohr type of atom.

A similar situation arises in the case of the alkali halides. Here we seem to have the domains of two relatively incompressible ions in contact at absolute zero. At room temperature they are assumed to be not quite in contact. These salts should therefore have much smaller compressibilities (larger bulk moduli) than can be calculated on the basis of replacing the actual ions by simple point charges. Unpublished calculations of Miss I. Woodward, taking into account an assumed structure of the ions, are reported[3] to have given fair agreement between the calculated and experimental values for the alkali halides.

The Photoelectric Effect.—If W_1 is the work required to expel an electron from a unit-crystal, and if W_2 is the work required to expel a metallic ion from the unit-crystal, then

$$\text{P.E.} = \tfrac{1}{2}(W_1 + W_2)$$

where P.E. is the potential energy of the unit-crystal. Assuming that W_1 is a constant fraction of the total energy,

$$W_1 = \alpha(\text{P.E.}) = \frac{\alpha}{2}(W_1 + W_2)$$

The difference in W_1 for sodium and potassium is the contact difference of potential for these metals. Then from Table II this contact difference of potential is

$$\alpha(13.5 - 10.9) = 2.6\alpha = 0.4 \text{ volt}$$

This gives

$$\alpha = 0.15$$

Therefore the work required to ionize an atom from a unit-crystal of an alkali metal is

Li	2.46 volts
Na	2.03
K	1.63
Rb	1.53
Cs	1.41

Since these voltages give the minimum energy required for electron emission, they may be translated by means of the quantum equation to give the maximum wave length to which these metals will be photoelectric. These calculated results should be slightly in error because the photoelectric effect is a surface effect, whereas the potential energies of Table II were calculated only for unit-crystals four or more atoms below the surface.

It is difficult to determine experimentally what is the longest wave length to which a given metal is photoelectric because for these limiting wave lengths the intensity of the photoelectric effect is very small.

Curves of data on the variation of intensity of the photoelectric effect with the wave length of the exciting light are available for Li, Na, and K in the solid state. Of these, the shape of the curves for Li and Na is given with some detail. Results taken from these curves are compared in Table V with the results that have been calculated in the foregoing. That the values from the curve are only approximate is well shown by the fact that the author's reading for the quantum voltage from the graph for sodium is 2.03, while Richardson estimates 2.1 volts from the

TABLE V.—CALCULATED AND EXPERIMENTAL VALUES FOR MAXIMUM WAVE LENGTH WHICH WILL PRODUCE A PHOTOELECTRIC EFFECT

Element	Calculated minimum voltage to liberate electron	Maximum λ for photoelectric effect, calculated from quantum relation	Maximum λ for photoelectric effect from experiment	Ratio
Li	2.46	5,000Å.	4,500Å.	1.11
Na	2.03	6,100Å.	5,500Å.	1.11

TABLE VI.—CONSTANCY OF RATIO BETWEEN CALCULATED MAXIMUM WAVE LENGTH FOR THE PHOTOELECTRIC EFFECT AND EXPERIMENTAL WAVE LENGTH FOR MAXIMUM PHOTOELECTRIC EFFECT

Element	Calculated minimum voltage to liberate an electron	Calculated maximum λ for photoelectric effect	Experimental λ for maximum photoelectric effect	Ratio
Li	2.46	5,000Å.	2,800Å.	0.56
Na	2.03	6,100Å.	3,400Å.	0.56
K	1.63	7,600Å.	4,400Å.	0.58
Rb	1.53	8,100Å.	4,800Å.	0.59

photoelectric effect and 2.6 volts from the thermionic effect. Data are easily available[8,9] on the wave length to which the first four of the alkali metals show a maximum photoelectric effect. If our voltages as calculated are at all correct, we might expect them to be a constant fraction of the quantum voltage corresponding to the maximum photoelectric effect. That this is so is shown in Table VI.

A USEFUL SHORT-CUT

The calculation of lattice potentials of elements has been gone into rather thoroughly in the foregoing, using as a basis three assumptions: (1) that the valence electrons of an element occupy definite positions in the crystal lattice; (2) that the positive ion of the element may be considered to be a point charge; (3) that the law of electrostatics between unlike charges can be modified as in Eq. (1). If the reader has attempted

to repeat the calculations leading to Tables III and IV, he has been impressed with their tediousness. If he tries to repeat the calculations of Miss Woodward on the alkali halides, he will find his task doubly laborious, for he will need to account for the effect of each of the electrons in the outmost shell of each kind of ion. This in turn involves assumptions as to the internal architecture of these ions.

A great deal of the work of such calculations can be obviated in the case of alkali halides by assuming (1) that each ion is replaced by a point charge, and (2) that the combined effect of the positive and negative charges in each ion can be expressed by replacing Eq. (1) by the equation[10,11]

$$F = (Ne)^2\left(\frac{1}{r^2} - \frac{c}{r^{n+1}}\right) \qquad (10)^*$$

where Ne is the charge on an ion, F is the force between adjacent ions of opposite sign, r is the distance between centers of ions, and $n + 1$ is a number of the order of 9, 10, 11, and even up to 15, depending upon the ion and its state of chemical combination. The energy equation corresponding to Eq. (10) is, of course,

$$\Phi = -(Ne)^2\frac{A}{r} + \frac{B}{r^n} \qquad (11)$$

where Φ is the crystal energy per "molecule."

Since at equilibrium

$$\frac{d\Phi}{dr} = 0 \text{ and } r = r_0,$$

we have

$$\frac{d\Phi}{dr} = 0 = \frac{(Ne)^2A}{r^2} + \frac{(-nB)}{r^{n+1}}$$

so that

$$B = \frac{(Ne)^2A}{n}r^{n-1}$$

Therefore, if the crystal is to be in a stable state, the crystal energy per molecule must be

$$U = -\frac{(Ne)^2A}{r_0}\left(1 - \frac{1}{n}\right) \qquad (12)$$

An energy equation of this general sort may be made the starting point for a number of interesting calculations on chemical stability,

* In Eq. (1) we were dealing with the force between an ion and a single electron so that the coefficient was $(e)\ (Ne) = Ne^2$. In Eq. (10) we are dealing with the force between two ions so that the coefficient must be $(Ne)\ (Ne) = (Ne)^2$.

magnetic susceptibility, size of atomic and ionic domains, lattice constants, compressibility, cohesive forces,* and a whole host of thermodynamic calculations which belong to a text on thermodynamics rather than to a text on crystal structure.† Many of the other calculations[12] are best taken up in connection with a detailed study of quantum mechanics, so that they, too, would be beyond the scope of this book.

Although equations of the general type of (10), (11), and (12) are most often used in connection with the crystals of compounds, it is of course

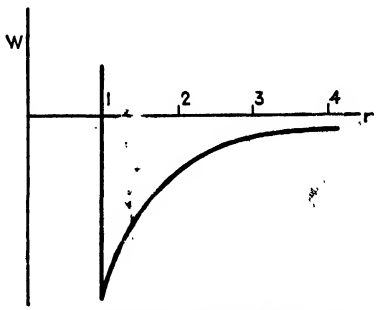

FIG. 3.—Inverse power law of interatomic energy with distance.

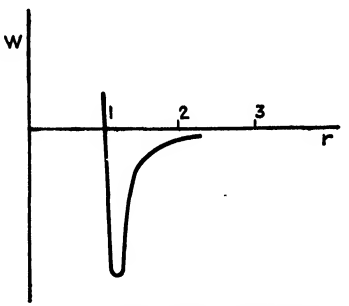

FIG. 4.—Modified inverse power law of interatomic energy with distance.

possible to use them for metals. This is done by assuming, as was done at the beginning of this chapter, that the metal is really an ionic compound in which the negative ions are the valence electrons. In fact, Eq. (1) may be regarded as a special case of Eq. (10) in which $n + 1 = 3$. This does not mean that we must necessarily "believe" that the valence electrons of metals actually occupy definite places in the crystal lattice, but it does mean that, for the sake of making any calculations at all, we assume them to *act as though* they occupy definite mean positions.

R. H. Canfield has made some interesting calculations on the stability of crystal lattices of elements. His assumptions differ from those of Eqs. (10), (11), and (12) in that he treats the whole atom as a unit without any separation of the valence electrons. The reader is referred to the original paper[13] for the details of the calculations. The end results are that, if atomic domains are rigid spheres which attract each other according to some inverse power of the distance between them, they must pack to form either face-centered cubic or hexagonal close-packed crystals. Such an energy law is illustrated in Fig. 3. If on the other hand the atoms of an element are to pack in body-centered cubic crystals, the energy law must be modified as shown in Fig. 4.

* Calculations on cohesive forces deal only with p-planes, not with π-planes or Π-planes (see Chap. XII), and do not therefore check with the results of experiments on tensile strength.

† A good review of crystal energies of ionic compounds and of their thermodynamic applications has been published by J. Sherman.[11]

SUMMARY

The calculation of each of the properties of a crystal requires, in general, a knowledge of some or all of the following:

1. The structure of the crystal.
2. The various interatomic (or interionic) distances in the crystal.
3. The details of the mosaic structure.
4. The inner structure of the atoms (or ions) which compose the crystal.
5. A method of calculating the energy of the crystal lattice from items 1, 2, and 4.

For a given crystal those properties which do not depend upon 3 may be calculated from a quantitative knowledge of the energy of the crystal. In a few cases the calculations have been gone into in some detail in order to emphasize the basis on which such calculations must ultimately rest. A short-cut in the calculations has been pointed out and references have been given by which the reader who has the necessary training may follow the subject farther. A second type of short-cut has been pointed out by which certain general results may be obtained without a knowledge of items 1, 2, or 4.

References

1. H. GEIGER, *Proc. Roy. Soc.*, **83**, 492 (1910).
2. W. H. BRAGG and R. D. KLEEMAN, *Phil. Mag.*, **10**, 318 (1905). See also J. L. GLASSON, *Phil. Mag.*, **43**, 477 (1922).
3. J. J. THOMSON, *Phil. Mag.*, **43**, 721 (1922); "The Electron in Chemistry," Franklin Institute, 1923. See also W. P. DAVEY, *Jour. Franklin Inst.*, **197**, 439, 629 (1924) and MISS I. WOODWARD, *Phil. Mag.*, **47**, 992 (1924).
4. I. LANGMUIR, *Science*, **53**, 290 (1921); **54**, 497 (1921). See also M. BORN, "Der Aufbau der Materie," Julius Springer, Berlin, 1922.
5. N. BOHR, *Zeit. Physik*, **9**, 1 (1922); *Ann. Physik*, **71**, 228 (1923), etc.
6. F. ZWICKY, *Phys. Rev.*, **38**, 1772 (1931).
7. C. C. BIDWELL, *Phys. Rev.*, **27**, 381 (1926).
8. W. H. SOUDER, *Phys. Rev.*, **8**, 310 (1916).
9. H. S. ALLEN, "Photoelectricity," Longmans, Green & Co., New York, 1913.
10. J. E. LENNARD-JONES and P. A. TAYLOR, *Proc. Roy. Soc.*, **109**, 476 (1925).
11. J. SHERMAN, *Chem. Rev.*, **11**, 93 (1932).
12. M. BORN and A. LANDÉ, *Ver. deut. phys. Ges.*, **20**, 210 (1918); "Atomtheorie des festen Zustandes," 2d ed., Leipzig, 1923.
    J. A. WASASTJERNA, *Soc. Sci. Fenn. Comm. Phys. Math.*, **1**, 38 (1923).
    L. PAULING, *Zeit. Kryst.*, **67**, 377 (1928); *Jour. Amer. Chem. Soc.*, **50**, 1036 (1928), etc.
    W. H. ZACHARIASEN, *Zeit. Kryst.*, **80**, 137 (1931).
    P. P. EWALD, *Ann. Physik*, **64**, 253 (1921).
    C. N. WALL, *Phys. Rev.*, **36**, 1243 (1930).
13. R. H. CANFIELD, *Phys. Rev.*, **35**, 530 (1930).

CHAPTER XVI

THE DIFFRACTION OF X-RAYS BY AMORPHOUS MATERIALS

In Chap. XII it was shown that the molecules of a liquid are to be thought of as continually building up crystal nuclei which are in turn continually torn apart by thermal agitation. It is to be expected then, that, if a liquid is subjected to a beam of monochromatic x-rays, diffracted beams will be found which correspond to these temporary nuclei. Similarly, it is to be expected that the jellies and the glasses, which may be considered for our purposes to be undercooled liquids, will contain structures corresponding to crystal nuclei and that they, too, will show x-ray diffraction effects. In monatomic gases, since each atom acts almost as an independent entity, it is to be expected that x-rays will be diffracted because of the internal structure of the atoms. In other words, all the so-called "amorphous states of matter" should possess enough regularity of structure to show some traces of diffraction effects with x-rays. It will therefore be worth while to take up each of the amorphous states of matter in turn, from the standpoint of x-ray diffraction.

LIQUIDS

The Cybotactic State.—X-ray diffraction effects in liquids were known experimentally[1,2,3,4,5,6,7,8,9] before the existence of temporary nuclei in liquids was generally recognized. Data are now available for about 250 liquids.[10,11,12,13,14,15]* The outstanding experimental facts to be explained may be summarized as follows:

1. The scattered x-ray beam does not decrease regularly with angle as would be the case for ordinary light scattered by a fog. Instead it shows, for a single wave length of x-rays, almost zero intensity except for one or more broad but distinct bands (called "halos"), each of which falls between definite angular limits. These limits depend upon the nature of the liquid and upon its temperature.

2. If, for a given wave length of x-rays, the half-angular limits are substituted for θ in Bragg's law, values of d are obtained which are of the correct order of magnitude for the separation of the centers of molecular domains for the temperature and pressure of the experiment.

3. For the so-called "straight-chain" aliphatic compounds two halos of different intensity are found. They are called the "primary"

* These references by no means exhaust the literature. They are picked so as to give a convenient picture of the type of data available. In this connection see also Chap. XIX.

and the "secondary" halo. The position of the secondary halo depends upon the number of carbon atoms in the chain, *i.e.*, upon the length of the chain. If the half-angular limits are substituted for θ in Bragg's law, the values of d are directly proportional to the number of carbons per molecule. For a normal paraffin the length of the chain comes out to be

$$L = (1.24n + 2.70) \times 10^{-8} \text{ cm.}$$

where n is the number of carbon atoms. The term 2.70 may be interpreted as the sum of the space used by the terminal hydrogens and the intermolecular spacing. The length associated with each carbon atom in a paraffin is therefore about 1.24Å. Since the distance of closest approach of carbon atoms in diamond is 1.50Å., it is assumed that the carbons must be arranged in a zigzag or in a spiral.

4. For straight-chain aliphatic compounds the primary, or principal, halo shows angular limits which are substantially independent of the number of carbon atoms per molecule. Since item 3 gives a value of d which has been associated with the length of the molecule, item 4 is open to the interpretation of relating to the molecular diameter.

5. Items 3 and 4 are consistent with measurements of the molecular dimensions of saturated normal fatty acids as measured[16] by the water-spreading method in that they show constant molecular diameters and increasing molecular lengths as the number of carbons in the chain is increased.

6. The primary and secondary halos for normal saturated fatty acids in the liquid state give spacings in Bragg's law which are similar to (but not exactly equal to) those found for the corresponding solids.

7. When branched-chain hydrocarbons are tested, three halos are found, corresponding to the three characteristic dimensions of a branched molecule.

8. For branched-chain hydrocarbons, one halo corresponds to an interplanar spacing greater than that for the principal halo of the straight chain of the same number of carbons. Another halo corresponds to a d smaller than for the secondary halo of the straight chain of the same number of carbons.

9. The half-angular limits of the primary halos, and therefore the corresponding values of d from Bragg's law, are practically identical for normal saturated paraffins and their normal alcohols.

If we accept the picture of liquids given in Chap. XII* the explanation of the above facts is simple. We have only to use the ideas of the powder method of crystal analysis given in Chap. VI. The temporary crystal nuclei take the place of the fragments of the powdered crystal

* G. W. Stewart[17] has used the word "cybotaxis" (space arrangement) to express the existence of temporary crystal nuclei in a liquid.

except that they are many times smaller. This extreme smallness of size is shown in the rapid decrease in intensity of diffraction as the angle is increased, so that liquids can show only one, two, or at most three, spacings. The extreme breadth of the halos might be interpreted as meaning that the temporary nuclei are so small as not to fulfill completely the conditions for Bragg's law. The breadth might also be interpreted as meaning that, even if the temporary nuclei were large enough to satisfy Bragg's law from the standpoint of dimensions, they would probably have somewhat variable interplanar spacings because, during the short time of their existence, they would hardly have time to relieve the strains and inhomogeneities incident to their rapid growth. The breadth of the halo should depend upon the wave length used and upon the shape of the diffracting particle. If the particle crystallizes in the cubic system and is a cube containing m^3 unit-cubes each of edge a, then the breadth of the halo should be[18]

$$B = \frac{2}{\cos\bar{\theta}}\left(\frac{\log_e 2}{\pi}\right)^{1/2}\frac{\lambda}{ma}$$

where B = breadth of the halo at half-intensity.

$\bar{\theta}$ = grazing angle of incidence between the x-ray beam and the diffracting plane of atoms. It is measured as the angle for maximum intensity of the halo. $2\bar{\theta}$ is the angle of bending of the x-ray beam and is Laue's X_h.

λ = wave length of x-rays used.

For particles crystallizing in other systems or with other shapes the corresponding formulas are much more difficult of derivation and, in some cases, apparently impossible.

The intensity of a given halo should depend not only upon the wave length (and the other quantities, such as angle of diffraction and width of the halo, which are connected with wave length) but also upon the temperature.[19] If the intensity of a halo is plotted against the angle of diffraction, the peaks shift toward smaller angles as the temperature is raised. Such a shift would correspond, in terms of Bragg's law, to an expansion of the lattices of the temporary nuclei. When a liquid shows halos corresponding to more than one interplanar spacing, it is found that all the peaks do not necessarily shift alike. Skinner finds[19] that, in general, the liquids fall into two classes. For class I a rise in temperature is accompanied by (*a*) a decrease in the height of the principal peak (*i.e.*, a decrease in the intensity of the principal diffracted beam), and (*b*) a linear increase in the breadth of the halo. For class II, a rise in temperature is accompanied by (*a*) an increase in the height of the principal peak and (*b*) a much smaller linear increase in the breadth of the halo than for class I. The percentage change in peak width per degree change in temperature is about five times as great for liquids

of class I as for class II. For both classes of liquids the x-ray scattering at small angles (*i.e.*,. between the zero beam and the first halo) increases as the temperature is raised. This increase is greater for liquids of class II. There is no abrupt change in the height of the peak at the boiling point.

Skinner's data for the peaks are shown in Table I. Prof. J. G. Aston[20] suggests that there is a possibility of a chemical distinction between the two classes of liquids of Table I, such that molecules of liquids belonging to class I have only the carbon grouping

$$-C-C-C-, \quad \text{or} \quad -C=C-C-,$$

whereas those of class II have the grouping

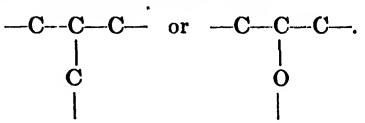

The suggestion seems reasonable for two reasons: (1) Higher temperatures by increasing the mobility of the molecules would increase the rate of collision and therefore would increase the chance of formation of temporary crystal nuclei. Although the side chains should decrease the chance of molecules meeting with the correct orientation to form nuclei, still those nuclei which do happen to form should persist at higher temperatures due to the extra attachments afforded by the side chains. (2) Because of the strong three-dimensional effect of the side chains, x-ray diffraction effects are likely to be stronger in class II than in the case of class I for temporary nuclei of the same general dimensions. It might easily be that (1) and (2) together would lead to an increase in the intensity of diffraction with increase in temperature, provided the temperatures used do not exceed some limit which should be characteristic of the substance. If Aston's suggestion turns out to be correct, x-ray diffraction effects at different temperatures may be of considerable use in work on the constitution of fractions from petroleums.

The Chaotic State.—We have seen in Chap. XII that the tendency toward disaggregation in a liquid should increase with rise of temperature. It is to be expected, then, that for each liquid substance there must be a temperature above which temporary crystal nuclei will persist for only extremely short times. The net effect should be, as far as x-ray diffraction is concerned, the same as if the concentration of temporary nuclei were greatly decreased. Any possible diffraction effect from the non-nuclear portion of the liquid would therefore become of relatively greater importance. It is interesting to note, therefore, that, theoretically, diffraction effects are to be expected from that portion of a liquid which happens at a given instant to be non-nuclear.

Kinetic theory indicates that the distribution of the molecules in any small volume of a liquid cannot be absolutely uniform as in the case of a perfect crystal. The density of matter in the liquid must fluctuate from

TABLE I.—EFFECT OF CHANGE OF TEMPERATURE ON DIFFRACTION FROM LIQUIDS

Liquid	Class	Temperature	d_1 (Secondary peak)	d_2 (Principal peak)	d_3	Percentage change in intensity of peak		
						d_1	d_2	d_3
Mesitylene	II	23° C	.....Å.	6.00Å.	3.96Å.	.....	+18.0	−42.3
		154	.....	6.92	3.96			
4-Hydroxyl 1.3 dimethyl benzene	II	2[illegible]	14.[illegible]	5.10	3.86	+80.0	+ 5.1	−30.0
		200	13.6	5.75	3.82			
2-Hydroxyl 1.4 dimethyl benzene	II	[illegible]	17.1	5.76	3.79	.....	+12.7	−37.8
		200	.....	6.17	3.92			
Naphthalene	II	80	.....	5.17	....	.....	+ 4.7	.....
		210	.....	5.76	....			
Phenol	II	43	12.7	4.73	....	−38.0	+ 2.8	.....
		180	12.7	4.92	....			
Benzene	I	26	.....	4.64	....	.....	− 1.1	.....
		80	.....	4.80	....			
Cyclohexane	I	28	.....	5.08	....	.....	−14.0	.....
		80	.....	5.24	....			
Di-*n*-propyl carbinol	II	24	10.2	4.87	4.35	− 6.7	+18.9	.....
		153	10.2	4.87	....			
Heptylic acid	I	28	17.7	4.64	....	+18.5	−12.2	.....
		193	18.5	4.80	....			
Tertiary butyl alcohol	II	27	8.51	4.80	....	−37.7	+ 9.8	.....
		80	8.88	4.90	....			
Lauryl alcohol	I	27	22.7	4.54	....	− 2.4	− 5.6	.....
		140	24.0	4.80	....			
Octane	I	27	.....	4.54	....	.....	− 7.3	.....
		120	.....	4.70	....			
2.7 Dimethyl octane*	I	27	.....	4.75	....	.....	−10.3	.....
		150	.....	5.17	....			
2.2.4 Trimethyl pentane	II	27	.....	5.67	....	.....	+ 0.5	.....
		92	.....	5.91	....			

* This seems, according to Skinner's published data, to be an exception to the generalization made in the text.

place to place, and the character of the distribution will be influenced by thermal agitation and other factors. If we were dealing with the scattering of visible light, we could, because the wave lengths are large in

comparison with the sizes of molecular domains, confine our attention to the total quantity of matter present in volumes which are too small to be observed under the microscope but which are big enough to contain a large number of molecules. For purposes of discussion, let this small volume be a cube whose edge is L. Then, if ρ_0 is the average density of the liquid, the density in any small region such as the cube under consideration will be

$$\rho = \rho_0 + \Delta$$

where Δ is the fluctuation in density. The work done in compressing the fluid in the small volume L^3 so that its density is increased by Δ is

$$W = \frac{L^3}{2}\left(\frac{\Delta}{\rho_0}\right)^2 \frac{1}{\beta} \tag{1}$$

where β is the isothermal compressibility of the liquid. Equating this to $RT/2N$, we have for the mean square of the fluctuation in density

$$\Delta^2 = {\rho_0}^2 \frac{RT\beta}{NL^3} \tag{2}$$

where R is the gas constant, T the absolute temperature, and N the Avogadro constant.*

The very mechanism postulated by the kinetic theory would require that a condition of abnormal density must move from place to place in the liquid as a sort of irregular wave of compression or rarefaction. It is, therefore, not too much of a stretch of the imagination to picture a liquid as being continuously traversed by irregular waves which resemble high-frequency sound waves. As a convenient mathematical device[21] these may be resolved by a Fourier analysis into a set of fictitious plane sound waves of different wave lengths. Assuming equipartition of energy, Δ of Eq. (1) may then be replaced by its equivalent,

$$\Delta = \Sigma_l \Sigma_m \Sigma_n B_{l\,m\,n} \cos 2\pi \frac{lx}{2L} \cos 2\pi \frac{my}{2L} \cos 2\pi \frac{nz}{2L} \tag{3}$$

where l, m, and n are positive integers, and where x, y, and z are coordinates of any point lying within the volume L^3, *i.e.*, $0 < x < L$, $0 < y < L$, $0 < z < L$. The potential energy in the sound wave whose amplitude is $B_{l\,m\,n}$, integrated over the volume L^3, is

$$\text{P.E.} = \frac{L^3}{16} \cdot \frac{B^2_{l\,m\,n}}{{\rho_0}^2} \cdot \frac{1}{\beta} \tag{4}$$

Applying the Boltzmann principle to a "wave" of amplitude $B_{l\,m\,n}$, we have for the thermodynamic probability of the average work,

* Δ will be positive as often as negative.

$$\overline{W} = C \exp. \left\{ \frac{-N}{RT} \cdot \frac{L^3}{16} \left(\frac{B_{l\,m\,n}}{\rho_0} \right)^2 \frac{1}{\beta} \right\} dB_{l\,m\,n} \qquad (5)^*$$

where C is a constant.

In the foregoing application of the Fourier analysis it was tacitly assumed that, except for the fluctuations in density due to temperature, the liquid could be regarded as a uniform continuum. In dealing with the scattering of x-rays by a liquid this assumption no longer holds, for the diameters of the molecular domains are of the same order of magnitude as the wave lengths of the x-rays. The Fourier analysis must therefore be applied to the determination of the actual distribution of matter in the liquid. The result of the analysis will depend on the manner in which the molecules (or rather the total of the electrons composing the molecules) are dispersed in space. Since we are dealing with liquids at such temperatures that temporary crystal nuclei exist for only negligible lengths of time, we must expect to find a continuous distribution of intermolecular spacings with a most probable spacing equal, or nearly equal, to the mean distance between the centers of adjacent molecular domains. The following discussion will show that this expectation is justified.

Imagine[9] in the liquid a cube the length of whose edge is normally a_0. If at any instant it is distended or compressed into a cube of edge a_1, the work done is

$$W = \frac{a_0^3}{2} \left(1 - \frac{a_1^3}{a_0^3} \right)^2 \frac{1}{\beta} \qquad (6)$$

where β is, as before, the isothermal compressibility of the liquid. Actually the thermal agitation might cause the cube to change shape as well as to change volume. For simplicity we shall assume that the angles always remain right angles, so that the original cube may be distorted into a rectangular parallelepiped whose three edges may be either longer or shorter than a_0. There is only one chance in eight that the length of all the edges would all be greater (or all less) than a_0. The average work corresponding to a change in the length of an edge from a_0 to a_1 may therefore be taken as

$$\overline{W} = \frac{a_0^3}{16} \left(1 - \frac{a_1^3}{a_0^3} \right)^2 \frac{1}{\beta} \qquad (7)$$

and its thermodynamic probability in accordance with the Boltzmann principle is

$$\overline{W} = A \exp. - \left\{ \frac{N}{RT} \cdot \frac{a_0^3}{16} \left(1 - \frac{a_1^3}{a_0^3} \right)^2 \frac{1}{\beta} \right\} da_1 \qquad (8)$$

* This gives for the mean square of the amplitude,

$$\frac{1}{8} \overline{B}^2_{l\,m\,n} = \rho_0^2 \frac{RT\beta}{NL^3}$$

Since $\overline{\Delta}^2 = \frac{1}{8} \overline{B}^2_{l\,m\,n}$, this reduces to Eq. (2).

where A is a constant. If a_1 is taken to represent a "wave length" in the Fourier analysis of the distribution of matter in the liquid, Eq. (8) is the formula for the "distribution of intensity in the structural spectrum."[9] Equation (8) gives a peak at the wave length $a_1 = a_0$ and the intensity falls off rapidly on either side of the peak.* In other words, we now identify the length a_0 of our hypothetical structural cube with the most probable distance between the centers of adjacent molecular domains. If $\mathbf{n}$ is the number of molecules per cubic centimeter, then a_0 must be proportional to $1/\sqrt[3]{\mathbf{n}}$, *i.e.*, $a_0 = k(\mathbf{n})^{-1/3}$. The value of the constant k will depend upon the temperature, pressure, and shape of the molecular domain. Raman and Ramanathan[9] find that it ranges from 0.8 to 1.0.

We have now arrived at the conclusion that at any instant most of the molecules are pretty regularly spaced after all. The only physical difference between the chaotic state in a liquid and the cybotactic state appears to be that (1) in the chaotic state the molecules have a random orientation, whereas in the cybotactic state the orientation forces are nearly as strong as in a true crystal, and (2) in the chaotic state the intermolecular spacings may be expected to be a little larger than in the cybotactic state. It is a consequence of (1) that in the chaotic state there is only a single length which has any great significance in x-ray diffraction, whereas in the cybotactic state two or even three lengths may be significant. The transition from the cybotactic to the chaotic state with rise in temperature is brought out in Table I which shows two cases in which a liquid loses a diffraction peak in going from room temperature to higher temperatures.

Since we have assumed equipartition of energy in all the foregoing, it follows that all the structural "waves" in the liquid have the same amplitude. The intensity of x-rays diffracted by a liquid at various angles, 2θ (and therefore, from Bragg's law, from a spacing $d = \frac{n\lambda}{2 \sin \theta}$), will depend only upon the probability of the existence of that spacing in the liquid. The equation for the intensity of the halo diffracted from a chaotic liquid will therefore resemble in form Eq. (8) and may be written,[9]

$$I = C_1 \exp. - \left\{ \frac{N}{RT} \cdot \frac{a_0^3}{16} \left(1 - \frac{a_1^3}{a_0^3} \right)^2 \frac{1}{\beta} \right\} \tag{9}$$

where a_1 is given by Bragg's law as $n\lambda = 2a_1 \sin \theta$. It should be noted

* This may be interpreted to mean that we are now dealing with real periodicities in the distribution of matter and not merely with fictitious mathematical periodicities as in the discussion of Eq. (5). These structural waves pass through the fluid in all directions, and we might write instead of Eq. (8) a more appropriate equation,

$$\overline{W} = B \exp. - \left\{ \frac{N}{RT} \cdot \frac{a_0^3}{16} \left(1 - \frac{a_1^3}{a_0^3} \right)^2 \frac{1}{\beta} \right\} da \, d\Omega$$

where B is another constant and $d\Omega$ is the elementary solid angle.

that the efficiency of diffraction will diminish so markedly with the angle, 2θ, of bending of the x-rays, that the order of diffraction n is unity for most experiments.

Figure 1 compares Eq. (9) with the experimental data of Hewlett[6] on the scattering of x-rays by benzene.* The similarity of form for the theoretical and experimental curves, together with the fact that only one peak was found experimentally, makes it look as though a large fraction

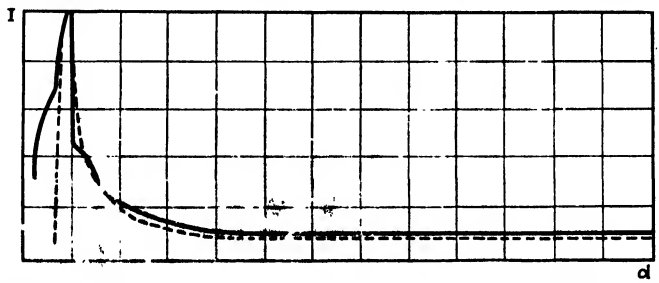

FIG. 1. Comparison of Eq. (9) with experimental data from benzene. Broken line, Eq. (9); solid line, Hewlett's data.

of the benzene in Hewlett's experiments at 26°C. was in the chaotic state. This is not surprising when it is remembered that 26°C. is, on the absolute scale, 6/7 of the way up to the boiling point and a little over half the way to its critical point.

GELS AND GLASSES

Gels.—X-ray diffraction effects in gels correspond in a general way to those in liquids, except that in the case of gels the results are complicated by the fact that fibers may be produced by stretching. This fibering action is shown by the fact that the halo produced by the stretched gel is no longer uniform in intensity around its circumference. Instead, the halo tends to concentrate itself in spots or arcs. These arcs have, of course, the same radius of curvature as the original halo. The intensity of the arcs is greater than that of the original halo, and the intensity in the spaces between the arcs is less than that in the original halo. From the location of the arcs, certain conclusions can be drawn as to the orientation of the fibers, using the technique of Chap. XVII.†

A study of the "particle-size" of the micellæ of a gel may be attempted in terms of the width of its halo. The photographic record of the halo is photometered (or the readings of an ionization chamber are taken) and

* Hewlett's data for benzene have been confirmed by Skinner.[19] Equation (9) could have been matched just as well against the principal peak of any of the substances listed in Table I by merely using a different value of a_0.

† Many interesting examples of x-ray diffraction in gels may be found in "Applied X-Rays," by G. L. Clark (McGraw-Hill Book Company, Inc., 2d ed., 1932). To repeat them here would be beyond the purpose of this book as stated in the preface.

expressed by a graph in which intensity is plotted against distance across the halo. The "width" is measured on this graph as the distance between the two ordinates (one on each side of the peak) whose height is half that of the peak. This half-width is then inserted in some equation[22,23,24,25,26,27,28,29] which gives the particle-size, provided certain conditions are satisfied. Since very few investigators have made any effort to meet all these experimental conditions in the case of a gel, their choice of an equation would seem to a casual observer to have been often rather an act of faith. Probably in most cases for gels, most of the formulas would give results somewhere around the correct order of magnitude.* X-ray results on the size of micellæ should always be accompanied by a statement of the formula used and of the extent to which its conditions have been fulfilled. The direct study of gels by x-rays is, then, confined to (1) the fibering effect, (2) a measurement of the diameter and half-width of the halo or halos, and (3) such calculations of the size of micellæ as the optimism of the investigator happens to permit.

In isolated cases the study of the fibering effect in gels and related materials can be made to yield valuable results. It has been useful in a study of cotton.[31] Rubber is especially interesting in this connection. Although it can hardly be called a true gel, since it has not been shown to be a two-phase system, yet it resembles a true gel in its action toward x-rays in that it gives distinct halos. Because of the great extensibility of rubber, these halos lend themselves readily to a study of the fibering effect. A detailed résumé of one such study will be worth while here as an example of the indirect uses which can be made of x-ray diffraction effects.

It has been shown[32] that, when rubber is subjected at room temperature to a standard stretching cycle such as is shown in Table II, the fibering does not take place instantaneously but that there is a time lag (see graph *A* of Fig. 2) between the act of stretching and the completion of fibering. Obviously the structure of rubber must be such as to account for this time lag. Of the various structures that have been proposed from time to time, only two seemed to be suitable: (*a*) a random distribution of tangled molecules (or molecular complexes), and (*b*) long molecular complexes (so-called "beta" rubber) coiled like rattlesnakes with

* In the case of solid particles of colloidal size, these various formulas involve one or more of the following assumptions: uniform particle-size; distribution of particle-sizes according to some assumed law; some assumed external shape of particles; some assumed degree of opacity to x-rays; a truly crystalline state of the particles without strains or flaws; some particular crystal system (usually the cubic system). Apparently most of the published results on solids depending upon the use of some one of the formulas are open to the suspicion that the assumptions have not been met. Exception must be made in the few cases where the results have been checked by some other means.[30]

"alpha" rubber (shorter complexes) filling in the vacant spaces. Additional work was therefore done[33] on the effect of possible variables on the time lag in the hope of finding data which would lead to a single

TABLE II.—STRETCHING CYCLES FOR EXPERIMENTS ON FIBERING OF RUBBER

Condition of sample *i.e.*, portion of cycle	Duration of portion of cycle, seconds	
	Standard cycle	Special cycle
Stretched (510%)	5.0	5.0
Relaxing	0.5	0.5
Relaxed	0.5	3.2
Stretching	0.5	0.5

Rubber was vulcanized only for the necessary toughness and contained only a minimum amount of inorganic material; composition: pale crepe, 90.0 parts; mineral rubber, 3.0 parts; sulphur, 1.5 parts; accelerator, 0.5 part; anti-oxidant, 1.0 part; zinc oxide, 2.5 parts.

picture. The results found, and their interpretation in terms of pictures (*a*) and (*b*), are as follows:

1. The effect of temperature was found to be small up to 30°C. (see graphs *A*, *B*, *C*, *D*, *E* of Fig. 2). At 35°C. the standard cyclic stretching of Table II produced almost no fibering (see graph *F* of Fig. 2). An

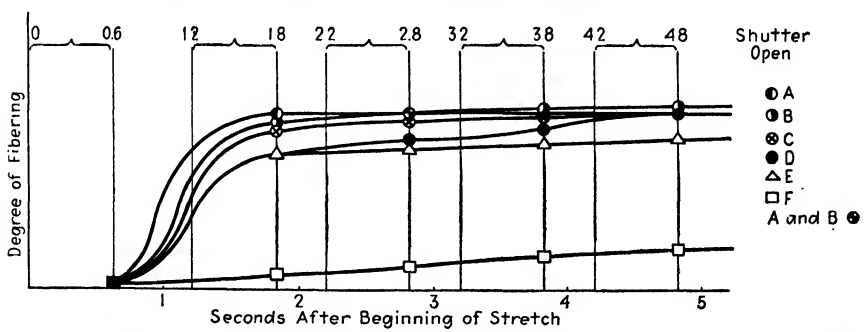

FIG. 2.—Time lag of fibering at different temperatures. *A*. Temperature, 15°C. Time of relaxation, 0.6 sec. *B*. Temperature, 15°C. Time of relaxation, 2.0 sec. *C*. Temperature, 25°C. Time of relaxation, 0.6 sec. *D*. Temperature, 27°C. Time of relaxation, 0.6 sec. *E*. Temperature, 30°C. Time of relaxation, 0.6 sec. *F*. Temperature, 35°C. Time of relaxation, 0.6 sec.

effort was then made to fix the non-fibering state at room temperature by heating the rubber rapidly to 55°C., stretching it 510 per cent, keeping it at 55°C. for a few minutes (long times were avoided to prevent chemical changes), chilling it rapidly to room temperature, and then immediately subjecting it to the standard stretching cycle of Table II. The specimen acted at room temperature as though no heat treatment had been

attempted. This must mean that the physical nature of the rubber had not been fundamentally altered by heating, but that at 55°C. the heat vibrations merely prevented that extreme degree of alignment necessary for an x-ray fiber pattern. This tempts us at once to imagine the stretched rubber as a collection of stretched elastic strings. Heating would tend to make the strings vibrate transversely. Because of the different degrees of loading and tension of these vibrating strings by the other molecules (or fibers) around them, no two strings would have the same period of vibration. As soon as the tendency for these strings to vibrate out of phase with each other becomes greater than the tendency of the cohesive forces to produce substantially perfect alignment of parallel strings, the fiber pattern should disappear. As soon as the rubber is cooled to the point where this tendency becomes less than the sideways forces associated with alignment, the fibering should again predominate. This must mean in terms of picture (*a*) that the ends of the tangled molecules are not loosened from their anchorages by a temperature of 55°C., otherwise the tangles would disappear permanently with heating. In terms of picture (*b*) we must assume that heating does not destroy the elastic properties of the spirals.

2. It was found that if specimens were given the standard stretching cycle for about four weeks, the time lag disappeared. Specimens were therefore used for only two weeks each. Some of these samples were kept in a box, free from light, for a year and were then once more put on the standard stretching cycle. They acted exactly like fresh samples, except that they required a somewhat higher percentage of stretch. Similar unused samples kept in similar fashion for the same length of time showed no change whatever. It was as though the combination of age and stretching history had produced some change such as oxidation. In terms of picture (*a*), if a considerable number of molecules should undergo such a change, it is possible that their shape would be altered in such a fashion that they could no longer slide over each other so easily and that they would thus resist the fibering process. If picture (*b*) is adopted, we assume that the chemical change must distort the long "beta" spirals so that they are more resistant to stretching.

3. It was found that the rubber was completely relaxed in less than 0.5 sec., so that the tangling process must be very rapid. According to (*a*), this would mean that the ends pulled from the tangle in the direction of the force must snap back into the tangle when the stretching force is released. This requires a mechanism for producing the force which causes the return of the stretched molecule (or fiber) to the tangle. Such a mechanism is implied in the picture of the tangle itself. Each molecule (or fiber) must have other molecules (or fibers) looped about it in random fashion. Some of these loops will have a direction roughly perpendicular to the axis of the molecule (or fiber) under consideration.

The applied force would straighten out the molecules (or fibers) which happen to be parallel to the force, but this very process would produce a tension in the loops which are roughly perpendicular to the molecules (or fibers) which have been pulled out straight. When the applied force is released, this sideways pull would snap the lined-up molecules (or fibers) back into the tangle. Obviously this process could take place rapidly. In terms of picture (*b*) the coils must have a random orientation. The applied force would tend to straighten out those spirals of "beta" rubber which happen to be correctly oriented. In this picture the force which resists the stretching lies entirely within the molecule itself, while in (*a*) the restoring force is furnished largely by the inter-

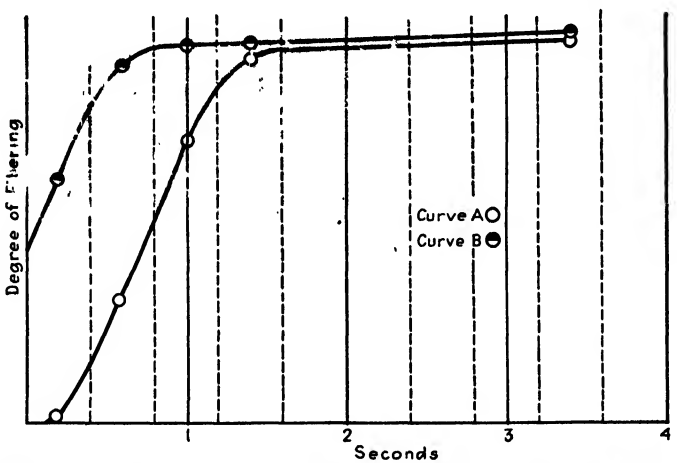

FIG. 3.—Effect of rate of stretch upon the time lag of fibering. Curve *A*, standard rate of stretch; curve *B*, slow rate of stretch.

action of several molecules (or fibers). According to (*b*), relaxation would result in the collapse of the long spiral "beta" molecules (or fibers). This could be a rapid process, limited only by the damping effect of the so-called "alpha" rubber.

4. No difference could be found in the time lag of fibering whether the rubber was held stretched for 2 sec. (standard cycle of Table II) or for 5 sec. (special cycle of Table II). This result is equally consistent with both the (*a*) and (*b*) pictures.

5. When the time for the stretching part of the cycle was increased, it was found that the apparent time lag was greatly decreased as shown in Fig. 3. This probably means that a considerable part of the fibering took place continuously during the time of the slow stretching so that, by the time the stretching portion of the cycle was completed, most of the fibering had occurred.

If the data are to be explained in terms of picture (*a*), we must assume that stretching pulls out molecules (or molecular complexes)

from the tangle and aligns them in the direction of stretch. For a slow rate of stretching, the lining-up and the untangling process are about complete at the end of the stretching process. Expressed in terms of the mechanism given under item 3, the stretching out of the loose ends of the molecules (or complexes) and the straightening out in the tangle have both taken place when the maximum stretch is reached. For the rapid rate of stretching, the untangling process does not occur until after the maximum stretch. The loose ends are aligned by this time, but the untangling has not taken place. We may assume that these loose ends are overstretched and that this excess strain is relieved by the untangling process after the over-all stretching is completed. According to this picture, we cannot expect fibering until after the untangling has occurred.

The effect of the rate of stretching may also be explained in terms of picture (*b*). In this case, fibering would consist of two processes: first, the stretching out of the "beta" molecules (or complexes); and, second, the expulsion of the "alpha" molecules (or complexes). For a slow rate of stretching, these two processes could occur simultaneously. As a result, the fiber pattern would show up strongly just at the end of the stretching process. The rapid stretching would allow the "beta" rubber to be stretched out first, and this would then be followed by the expulsion of the "alpha" rubber. Such a picture is able to explain the time lag and its change with the rate of stretching. The chief difficulty is that it does not explain what sort of a process the "alpha" rubber must go through so that it interferes with the fibering before expulsion and does not do so after expulsion—it does not provide a place for the "alpha" rubber to go. The tangle picture is not open to this objection for it allows the "alpha" and "beta" (less and more polymerized) rubber to act alike.

Apparently, neither picture (*a*) nor picture (*b*) alone can explain easily and directly the whole behavior of rubber toward the time lag of fibering. If it were not for the high extensibility of rubber, the data would seem to point to the tangle type of picture, for such a picture does not require a place where the "alpha" rubber may go without interfering with the fibering. On the other hand, it is hard to imagine stretching something resembling a tangled piece of string before the untangling operation has commenced. This difficulty may be avoided if we assume rubber to be a tangle of spiral molecules, much as is shown in Fig. 4*a*. This would make it possible to overstretch the untangled ends of a molecule (Fig. 4*b*) and have the overstretched ends relax as the tangle is pulled out (Fig. 4*c*). The fibering is evidently in the direction of the applied force and will occur only for those fibers whose ends are aligned pretty much in the direction of that force. We may assume that, when the tangle is stretched, the tangle is not completely unraveled; the other molecules will still be looped around those molecules which take part in the fibering.

These other molecules will also have their spirals stretched out but will have no opportunity to align themselves accurately so that they can not contribute to the fiber structure.* They do, however, make possible the forces necessary to reestablish the tangle after the external forces of stretching are removed. It is assumed of course that the loose ends align themselves rapidly, but that straightening out the tangle requires more time. Such a picture is equivalent to combining picture (*a*) with a part of picture (*b*), but it avoids the complications incident to distinguishing between "alpha" and "beta" rubber and it avoids the poor

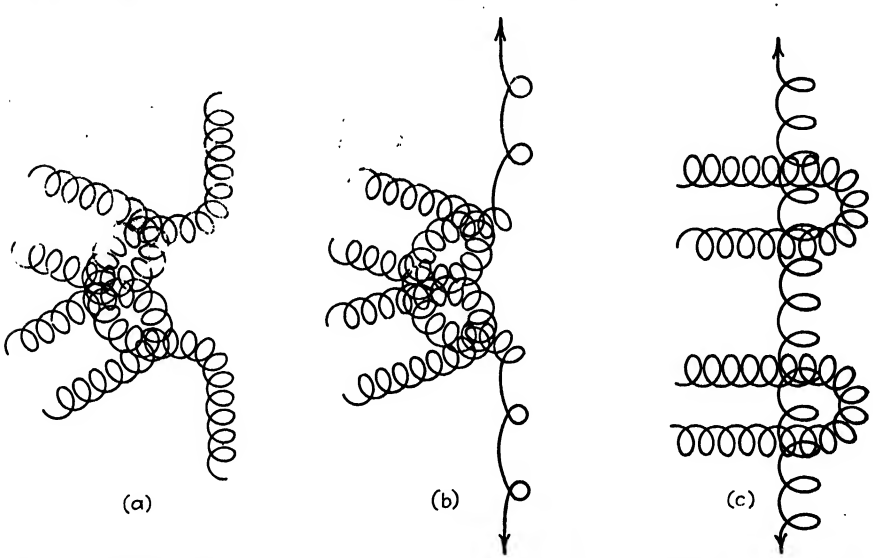

FIG. 4.—Idealized structure of rubber for (*a*) the relaxed state, (*b*) immediately after stretching, (*c*) at the end of the time lag.

mechanics of stretching straight strings by over 500 per cent. There will be, therefore, both intermolecular and intramolecular forces brought into play in the stretching and fibering processes. By retaining the coiled-spring structure this combined picture not only explains the time-lag data but is consistent with the spiral structure found by Hauser[34] from a detailed consideration of the arcs of the fiber pattern. We might express our picture of the structure of rubber in more general language by saying that rubber appears to be an aperiodic network of coiled (or zigzag) molecular complexes which, by stretching, can be made periodic in the direction of the stretch.

It will be noted that the foregoing discussion differs from previous discussions in this book in that the conclusions do not follow directly from x-ray data. In this case the x-ray data serve to put severe restric-

* If they could so contribute, we should have fibering in three dimensions, *i.e.*, a crystal.

tions at every step of an argument which is based primarily on the mechanical and time-lag properties of rubber, so that by *indirect* use of x-ray diffraction data we have arrived at a reasonable, unambiguous result.

Glasses.—The glasses offer another instance where x-ray diffraction halos may be used to limit a discussion based largely on other considerations. Glasses really come under the classification of undercooled liquids. It is not surprising, then, that they show the halos characteristic of liquids. Only when they devitrify do their diffraction patterns take on the characteristics which we have learned to associate with crystals.

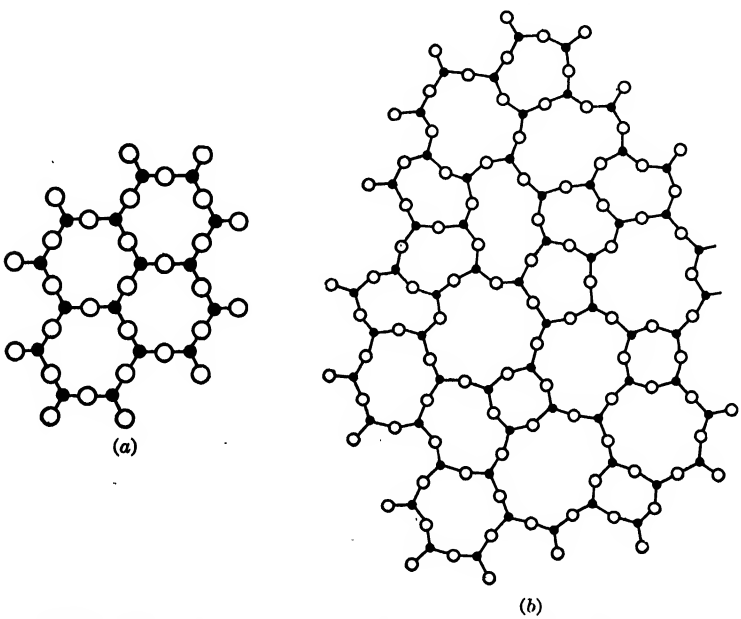

FIG. 5.—(*a*) Two-dimensional analog of a crystal of A_2B_3. (*b*) Two-dimensional analog of a glass of A_2B_3. (*Zachariasen.*)

The presence of the halo, or halos, indicates clearly that for a given glass there are one or more characteristic ranges of atomic or molecular spacings. The absence of a true crystal diffraction pattern indicates such a lack of periodicity of structure that we may assume that no two atoms are structurally equivalent. At the same time we must remember that the same type of physical and chemical forces must be present inside (and between) the molecules in a glass that are present after the glass has devitrified and has assumed the crystalline state.

Zachariasen has proposed[35] a type of structure for the glasses which meets these conditions. He assumes that (1) the individual molecules (or ions) composing the glass are identical with those in the corresponding crystalline material, (2) the individual molecules (or ions) are arranged

together in a network which is just irregular enough to prevent any atom from being equivalent to any other atom, and (3) this aperiodic network is intimately related to the periodic network of the crystalline state. This may be illustrated in two dimensions for a fictitious substance A_2B_3 by means of Fig. 5*a* and *b*. In Fig. 5*a*, each A is adjacent to two B's in such a way that the B — A — B angle is 120°. The network is periodic, *i.e.*, it reproduces itself in terms of a fundamental unit of structure. Figure 5*b* shows how the same B — A — B angles can be built up into an aperiodic network such as Zachariasen postulates for the corresponding glass. Of course, in actual glasses the network would have to be in three dimensions.

Since most ordinary simple glasses are oxides, we may take up further details in terms of oxides alone. The changes in wording for other simple glasses will be obvious. Crystal analysis shows that in all crystalline oxides A_mO_n the oxygens may be thought of as lying at the corners of polyhedra with the atoms of A at the centers of the polyhedra. In terms of Zachariasen's third assumption, these same polyhedra should persist in the vitreous state. The necessary three-dimensional linking could be effected by the sharing of corners between different polyhedra. The energy of the network would depend (1) upon the nature of the polyhedra of oxygen, and (2) upon the way in which the polyhedra are linked together. We may use silica as a concrete example. In low quartz the elbow-shaped molecules of SiO_2 (Chap. VI) are so arranged as to place each silicon at the center of what is practically a tetrahedron of oxygens. The relative orientation of two "tetrahedra" with a common corner will be the same throughout the entire crystal. Not only is the angle of the "elbow" constant for the SiO_2 molecules, but the angle between adjacent elbows of SiO_2 will be identical throughout the crystal. In vitreous silica the angle of the elbows remains constant, but the elbows themselves will no longer make identical angles with each other. In fact the angles between adjacent elbows may vary within rather wide limits. Obviously the energy of the configuration of molecules in vitreous silica cannot be much greater than that of crystal quartz. Otherwise for molecules of such simple shape the rate of devitrification would be appreciable and it would not be possible to seal two pieces of silica tubing together in the oxyhydrogen flame without serious crystallization.

Only certain types of oxides can form aperiodic networks of only slightly higher energy content than the corresponding crystals. For instance, the two-dimensional analogue of a fictitious crystal of AO is shown in Fig. 6. Each oxygen is symmetrically surrounded by three A's, and each A is symmetrically surrounded by three oxygens. No two-dimensional glass of AO can be formed therefore which does not have a much higher energy content and such a rapid devitrification rate that for practical purposes we may say that the glass cannot exist. Similar

studies in three dimensions have led Zachariasen to propose the following four rules for finding whether or not a given oxide can exist in the form of a stable glass: (1) an oxygen atom must not be linked to more than two atoms of A; (2) the number of oxygen atoms surrounding atoms of A must be small; (3) the oxygen polyhedra must share corners with each other, not edges or faces; (4) at least three corners in each oxygen polyhedron must be shared. Oxides of the type A_2O and AO do not satisfy these requirements under any conditions. Requirements (1), (3), and (4) are satisfied (*a*) by A_2O_3, if the oxygens form triangles around each atom of A; (*b*) by AO_2 and A_2O_5, if the oxygens form tetrahedra around each atom of A; (*c*) by AO_3, A_2O_7, and AO_4, if the oxygens form octahedra around each atom of A. There remains rule (2) to be satisfied. This means that we must find a limit for the number of oxygens surrounding each atom of A. Since there seems to be no evidence of any vitreous oxide of the type AO_3, A_2O_7, or AO_4, it is assumed that only oxygen triangles and tetrahedra agree with rule (2). An exhaustive study of the simple oxides shows that, with this interpretation of rule (2), it can be predicted which simple oxides can exist in the vitreous state and which can exist only in the crystalline state.*

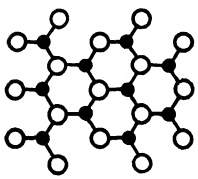

FIG. 6.—Two-dimensional analog of a crystal of AO. (*Zachariasen.*)

These rules are a direct result of a line of reasoning which is limited and bounded at every step by the necessity of maintaining a definite interatomic spacing in an aperiodic structure, and this limitation is imposed by the x-ray diffraction halos of glasses. This indirect use of x-ray data guides us to a picture of the structure of glasses which is consistent with their known properties. For instance:

1. The isotropic character of glass follows as a consequence of the absence of symmetry in the network. The atomic arrangement is *statistically* the same in all directions unless external fields of sufficient intensity are present.

2. The lack of a definite melting point follows as a consequence of the different energy required to detach each atom in an aperiodic network.

3. The lack of a definite, simple, chemical formula for a polyoxide glass follows as a consequence of the aperiodic network which offers no opportunity for chemical compounds in the ordinary sense of the word.

4. The transparency of glasses follows from the extended three-dimensional aperiodic networks just as the transparency of the corresponding crystals follows from their extended three-dimensional periodic networks.

The hypothesis of an aperiodic network in an undercooled liquid, such as a glass, is remarkably similar to the hypothesis of the cybotactic

* For polyoxide glasses, Zachariasen proposes the following rules: "An oxide glass may be formed, (1) if the sample contains a high percentage of cations which are surrounded by oxygen triangles or by oxygen tetrahedra, (2) if these triangles or tetrahedra share only corners with each other, (3) if some oxygen atoms are linked to only two such cations and do not form further bonds with any other cations."

state in real liquids and lends further support to the pictures of the nature of liquids and of the mechanism of crystal growth given in Chap. XIII.

GASES

We have taken up x-ray diffraction effects in amorphous materials caused by temporary nuclei in liquids and by the networks which are assumed to exist in gels. There remains the effect of the structure of the atoms themselves on the scattering of x-rays. This effect can be studied without the complication introduced by closely adjacent atoms by studying the x-ray scattering effects of the atoms of the inert gases. Such a study has been made by A. H. Compton[36] who has set up equations for the scattering of a single wave length of x-rays by helium. He has

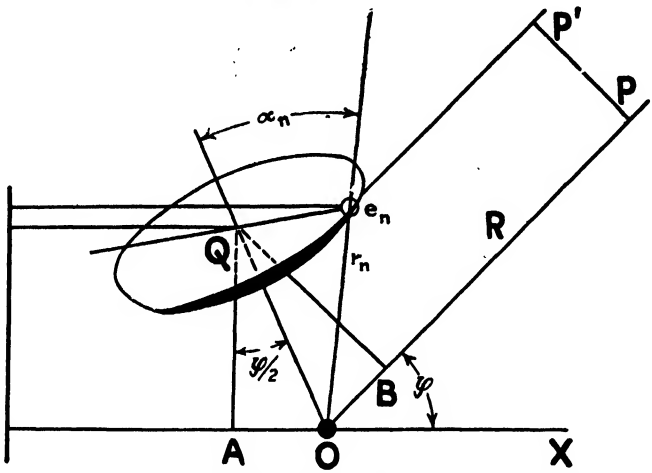

FIG. 7.—Scattering of monochromatic x-rays by an atom of an inert gas.

applied his equations to the experimental work of C. S. Barrett[37] and finds that the curve so obtained agrees well with the theoretical curve calculated by L. Pauling[38] from wave mechanics. The following is adapted from Compton's published article,[36] using the same symbols for purposes of easy reference. The reader will be interested to compare portions of this discussion with that given in Chap. IX for the scattering effect of individual atoms (or ions) in crystals.

Even if we were unwilling to accept the physicist's picture of electrons spinning about an atomic nucleus, and if we insisted upon confining ourselves to the chemist's static-atom picture, we should still be compelled to express the following discussion in terms of random positions of the electrons in their respective "orbits," for there is no *a priori* reason to suppose that the atoms of an inert gas have anything but random orientation with respect to one another. We shall therefore use as a starting point an atom containing Z electrons whose distances from the nucleus

are, respectively, $r_1, r_2, r_3, \ldots, r_s$ and whose angular distribution with reference to the nucleus is absolutely random. In Fig. 7 let O be the nucleus of such an atom, and let e_n represent the position at some instant of the nth electron in its orbit as it spins about the axis OQ of the atom. Then the line e_nO, joining the electron with the nucleus, makes an angle α_n with the axis OQ. Let an x-ray beam of wave length λ pass in the direction of OX. The portion of the beam which hits the electron e_n will set it into forced vibration and will cause it to send out scattered waves. Let us confine ourselves to some one direction in these scattered waves, say the direction of OP and e_nP' which make an angle ϕ with the direction of the incident beam. If, now, the nucleus O had been an electron the scattered wave which it sent out would have had, at some arbitrary point P on the line OP, an electric vector whose amplitude we shall call A_e and whose phase angle we shall call δ. Then the electric vector at P', due to x-rays scattered by the electron e_n, will be

$$E_r = A_e \cos\left\{\delta - \left(\frac{2\pi}{\lambda}\right)2r_n \cos \alpha_n \sin \frac{\phi}{2}\right\} \tag{10}$$

where $2r_n \cos \alpha_n \sin \frac{\phi}{2}$ is the total difference in path between the ray scattered from e_n and the ray scattered from O.* Representing

$$\frac{4\pi r_n}{\lambda} \cos \alpha_n \sin \frac{\phi}{2}$$

by x_n, we may write Eq. (10) in the form

$$E_n = A_e \cos (\delta - x_n) \tag{11}$$

The total electric vector due to all the electrons in the atom is

$$E = \sum_1 E_n = A_e \sum_1 \cos (\delta - x_n) \tag{12}$$

We shall choose our starting point for the measurement of time so that

$$\delta = 2\pi\nu t = pt$$

where p is the phase frequency of the incident wave.

Equation (12) gives for the electric vector at the instant t,

*Since the plane containing e_n and Q is perpendicular to OQ at Q, we have from Huygens' principle that the phase of the wave scattered from e_n to the plane PP' will be the same as if the electron were at Q. But the distance to the plane PP' from Q is greater than that from O by the distance AOB.

$$E = A_e \sum_1^Z \cos(pt - x_n)$$
$$= A_e \sum_1^Z (\cos pt \cos x_n + \sin pt \sin x_n) \tag{13}$$

Since the intensity of the scattered wave at this instant is proportional to the square of its amplitude we may write, using b as the proportionality constant,

$$I_i = bA_e^2 \left\{ \sum_1^Z (\cos pt \cos x_n + \sin pt \sin x_n) \right\}^2 \tag{14}$$

When Eq. (14) is averaged over a complete cycle from $t = 0$ to $t = 2\pi/p$, all the terms in the summation disappear except those of the form

$$\cos x_m \cos x_n + \sin x_m \sin x_n$$

The average intensity for the whole cycle is therefore

$$I_\alpha = \tfrac{1}{2} bA_e^2 \sum_1^{'Z} {}_m \sum_1^Z {}_n (\cos x_m \cos x_n + \sin x_m \sin x_n) \tag{15}$$

as long as we maintain the orientation α.

For a single electron Eq. (15) becomes

$$I_e = \tfrac{1}{2} bA_e^2 \tag{16}*$$

so that Eq. (15) may be written

$$I_\alpha = I_e \sum_1^Z \sum_1^Z (\cos x_m \cos x_n + \sin x_m \sin x_n) \tag{17}$$

We must now average this intensity over all possible angles α_n. The probability that any α will lie between α and $\alpha + d\alpha$ is, for random orientation, $\frac{1}{2} \sin \alpha d\alpha$. We may express x_n [see Eq. (11)] briefly by $z_n \cos \alpha_n$, where $z = \frac{4\pi r_n}{\lambda} \sin \frac{\phi}{2}$. Similarly we may express x_m by $z_m \cos \alpha_m$. Using these values for x_m and x_n, we have from Eq. (17)

* For unpolarized x-rays,[39]

$$I_e = \frac{Ie^4}{2m^2R^2c^4}(1 + \cos^2 \phi)$$

where I = intensity of the primary beam traversing the electron.
e = charge on the electron.
m = mass of the electron.
c = velocity of light.
R = distance OP in Fig. 7.

$$dI_\alpha = I_e\left\{\sum_1^Z\sum_1^Z{}_{m\neq n}\tfrac{1}{4}[\cos(z_m\cos\alpha_m)\cos(z_n\cos\alpha_n) + \sin(z_m\cos\alpha_m)\sin(z_n\cos\alpha_n)]\sin\alpha_m\sin\alpha_n d\alpha_m d\alpha_n + \sum_1^Z \tfrac{1}{2}[\cos^2(z_n\cos\alpha_n) + \sin^2(z_n\cos\alpha_n)]\sin\alpha_n d\alpha_n\right\} \quad (18)$$

Equation (18) must now be integrated over all values of α_m and α_n, giving for electrons arranged at fixed distances $r_1, r_2, r_3, \ldots$, from the nucleus, and with random orientation about the nucleus,

$$I_r = I_e\left\{Z + \sum_1^Z\sum_1^Z{}_{m\neq n}\frac{\sin z_m}{z_m}\frac{\sin z_n}{z_n}\right\} \quad (19)$$

We are now ready to take up for a moment the special case of the helium atom. We assume, provisionally, that the helium atom has two electrons outside its nucleus, that they are both at the same distance, $r = a$, from the center, *i.e.*, that we have a Bohr type of atom, and that they both have random orientation. We may write Eq. (19) in the form

$$S \equiv \frac{I_r}{ZI_e} = 1 + \frac{1}{Z}\sum_1^Z\sum_1^Z{}_{m\neq n}\frac{\sin z_m \sin z_n}{z_m z_n} \quad (20)$$

For helium Eq. (20) becomes

$$S = 1 + \left(\frac{\sin z_a}{z_a}\right)^2 \quad (21)$$

The solid line of Fig. 8 shows a graph of Eq. (21). For purposes of com-

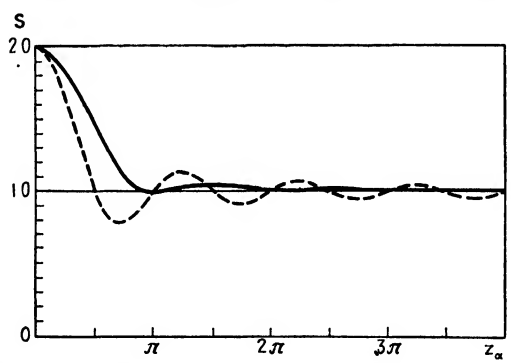

FIG. 8.—Relative scattering per electron for an atom of two electrons. Solid line, both electrons at radius a and random orientation; broken line, electrons at opposite ends of diameter $2a$. (*Compton.*)

parison the scattering by two electrons at opposite ends of a diameter $2a$ is shown by the dashed line according to the equation[40]

$$S = 1 + \frac{\sin 2z_a}{2z_a} \quad (22)$$

Going back once more to the general case, the probability that any one electron will lie between r and $r + dr$ is proportional to dr and to some function of r which we shall call $u(r)$. This probability may, then, be expressed by $u(r)\,dr$. If this probability is the same for every electron, then, [see Eq. (19)],

$$dI_e = I_e\left\{Z + \sum_1^Z \sum_1^Z{}_{m\neq n} \frac{\sin kr_m \sin kr_n}{k^2 r_m r_n} u(r_m)u(r_n)dr_m dr_n\right\} \tag{23}$$

where

$$k \equiv \frac{z_m}{r_m} = \frac{4\pi}{\lambda} \sin \frac{\phi}{2} \tag{24}$$

Since we have assumed that $u(r_m)$ is the same for all electrons, the integral of Eq. (22) may be written:

$$I_e = I_e Z + I_e \sum_1^Z \sum_1^Z{}_{m\neq n}\left\{\int_0^a u(r) \frac{\sin kr}{kr} dr\right\}^2 \tag{25}$$

in which a is the maximum radius of the atom.

Since $\sum_1^Z \sum_1^Z{}_{m\neq n} 1 = Z^2 - Z$, we may write Eq. (25) in the form:

$$I_e = I_e Z + I_e(Z^2 - Z)\left\{\int_0^a u(r) \frac{\sin kr}{kr} dr\right\}^2 \tag{26}$$

The relative scattering per electron is therefore

$$S = \frac{I_e}{ZI_e} = 1 + (Z - 1)\left\{\int_0^a u(r) \frac{\sin kr}{kr} dr\right\}^2 \tag{27}$$

Equation (19) gave the intensity of x-rays scattered by the electrons of an atom on the assumption that the electrons were always at fixed distances from the nucleus (Bohr type of atom). Equation (27) gives the corresponding intensity for the case of a continuous radial distribution.*

Since we have assumed in the derivation of Eq. (27) that the electrons have a spherically symmetrical distribution about the nucleus, we may use a Fourier sine or cosine series to express the probability that an electron will lie between r and $r + dr$. We may therefore substitute in Eq. (27) the following:†

* Equation (26) indicates that I_e is always at least as large as $I_e Z$, since the second term is always positive. Similarly, S in Eq. (27) is always greater than unity. This is not so, however, for the S of Eq. (22) which represents[39] the case of electrons at a fixed distance $2a$ from each other.

† This same sort of series was used in Chap. X except that it was at that time expressed as a cosine series.

$$u(r) = A_1 \sin \frac{\pi r}{a} + A_2 \sin \frac{2\pi r}{a} + \cdots + A_n \sin \frac{n\pi r}{a} \tag{28}$$

where a is an assumed maximum radius. This gives

$$S = 1 + (Z - 1)\left[\sum_1^\infty {}_n \int_0^a \frac{A_n}{k} \sin\left(\frac{n\pi r}{a}\right) \sin (kr)\, dr\right]^2 \tag{29}$$

We now have to evaluate the constants represented by A_n. This may be done by the following scheme. In the summation of terms in Eq. (29) all the integrals except the nth vanish if $k = n\pi/a$, *i.e.*, by Eq. (24), if

$$n\lambda = 2(2a) \sin \frac{\phi}{2} \tag{30}$$

where a is the assumed maximum radius (radius of the "true" atomic domain). This gives

$$S_n = 1 + (Z - 1)\left[\frac{1}{4} \frac{a^2}{k^2} A_n{}^2\right] \tag{31}$$

so that

$$A_n = \pm \frac{2k}{a} \sqrt{\frac{S_n - 1}{Z - 1}} \tag{32}$$

By using successive values of n we can determine each of the coefficients $A_1, A_2, A_3, \ldots, A_n$ of Eq. (28) and thus find a value for $u(r)$. The value assumed for a is quite arbitrary. If it is made larger, then the successive values of k become smaller and the series approaches the Fourier integral

$$u(r) = r \int_0^\infty B \sin (\pi r x) dx \tag{33}$$

in which

$$x \equiv \frac{n}{a} = \frac{4 \sin \frac{\phi}{2}}{\lambda} \text{ [see Eq. (30)]} \tag{34}$$

and

$$B \equiv A_x a = 2\pi x \sqrt{\frac{S_x - 1}{Z - 1}} \tag{35}$$

If, instead of finding the most probable position of a single electron, we wish to find the probable number of electrons between r and $r + dr$, we may multiply Eq. (28) by Z, the number of electrons per atom, thus:

$$U(r) = Z\, u(r) = Zr \sum_1^\infty A_n \sin \frac{n\pi r}{a} \tag{36}*$$

* This equation may be compared with the corre ponding equation for crystals as follows:

Imagine a probability curve in which the average linear density of electrons at a distance z from the middle of an atomic layer in the crystal is plotted against z. Let

or, instead, we may multiply Eq. (33) by Z, thus:

$$U(r) = Z\,u(r) = Zr\int^{\infty} B \sin(\pi r x)dx \tag{37}$$

The foregoing derivation started out with the assumption that we were dealing with monatomic gases. We are now ready to compare our equations with the results of experiment. Helium and hydrogen

---

the peak of the probability curve be at a height P. Then, if there are $U\,dr$ electrons between r and dr, they will contribute to P,

$$dP = U\,dr\,u(z) \tag{a}$$

where $u(z)$ is the probability that each of these electrons is at a height z from the middle of the atomic layer. In the discussion of the method of trial and error in Chap. X it was shown that $u(z) = 1/2r$ for electrons distributed at random on the surface of a sphere so that

$$dz = \frac{1}{2r}U\,dr$$

$$U\,dr = 2r\,dP \tag{b}$$

These electrons, then, contribute to the probability curve an element of height dP and of breadth $2z = 2r$, the diameter of the shell. Using the value of P given by Eq. (39) of Chap. X and remembering that

$$dP = -\frac{dP}{dz}dz = -\frac{dP}{dz}dr$$

we have

$$-\frac{dP}{dz} = \frac{2\pi}{D}\left\{A_1 \sin 2\pi\frac{z}{D} + 2A_2 \sin 2\pi\frac{2z}{D} + \cdots\right\} \tag{c}$$

where D is the interplanar spacing.

Equation (40) of Chap. X gives, in the terminology of this footnote,

$$A_n = \frac{2F_n}{D}$$

so that Eq. (*b*) becomes

$$U\,dr = 8\pi\frac{r}{D^2}\sum_1^{\infty} nF_n \sin 2\pi n\frac{r}{D}\,dr \tag{d}$$

which is to be compared with Eq. (36). The two equations become identical if

$$ZrA_n = 2\pi\frac{r}{a^2}nF_n \tag{e}$$

in which $a = \frac{1}{2}D$. (Note that this is the a of Chap. XVI not of Chap. X.)

Remembering that

$$D = 2a = \frac{n\lambda}{2\sin\frac{\phi}{2}}$$

and that

$$k = \frac{4\pi}{\lambda}\sin\frac{\phi}{2},$$

Eqs. (*e*) and (32) give

$$F_n = Z\left\{\frac{S_z - 1}{Z - 1}\right\}^{\frac{1}{2}} \tag{f}$$

which is to be compared with Eq. (35).

both have two electrons per molecule, but in the case of hydrogen we may assume that they are far enough apart to act independently of each other, *i.e.*, to give a scattering which is practically just twice the scattering of an isolated electron. Any difference in the amount of scattered x-rays between that found for H_2 and that found for He would be accounted for on the basis of interference phenomena between the two electrons of the He atom. For H_2, then, S_{H_2} of Eq. (27), *i.e.*, the relative scattering per electron, is unity. For He the value of S_{He} in Eq. (27) will be the factor by which S_{H_2} must be multiplied to equal S_{He}. C. S. Barrett has published[37] data on the scattering of H_2 and He at 20°, 30°, 40°, 60°, and at still larger angles to the incident x-ray beam. At angles of 60° and above, the scattering from H_2 and He was identical so that for these angles S_{He} is unity. At 40°, S_{He} is 1.025; at 30° it is 1.08; at 20° it is 1.26. We must find some way of telling what the results would be at still smaller angles. This is done[36] as follows: At very small angles from the incident beam we may assume that the phase difference

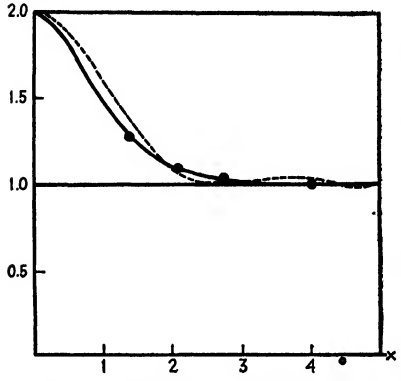

FIG. 9.—Solid line, relative scattering by He; circles are Barrett's data. Broken line, calculated scattering by Bohr type of He atoms. (*Compton.*)

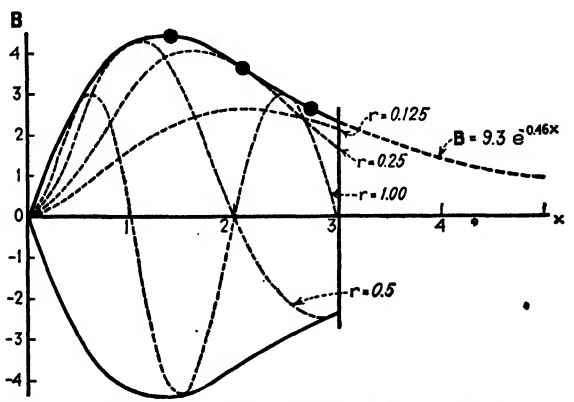

FIG. 10.—Solid line, B vs. x curve. Dotted line, Φ_1 vs. x curves. The circles represent Barrett's data.

between the beams scattered by the two electrons will be negligibly small. Equation (27) indicates that, at 0°, $S_{He} = 2$. For small values of scattering angle the phase differences will be small quantities of the first order of smallness, but the differences in amplitude, which are propor-

tional to the cosines of these phase differences,* will depend only upon quantities of the second order of smallness. The S_{He} curve must therefore, according to theory, leave the S_{He} coordinate (angle = 0°) in a direction practically perpendicular to the S_{He} coordinate for an atom of finite extent. Adding this information to that of Barrett, we can draw a pretty accurate curve of S_{He} vs. angle of scattering. In order to fit in with the equations more conveniently, Fig. 9 is plotted by Compton as S_{He} vs. x [see Eq. (34) for definition of x].†

Equation (35) enables us to transform Fig. 9 into the B vs. x curve shown by the solid line of Fig. 10. Values of B from this curve are necessary in arriving at values for $U(r)$ in Eq. (37) An extrapolation of the solid line of Fig. 10 would make B gradually approach zero for large values of x. Trial shows that the final value of $U(r)$ is not much affected by the exact shape of the extrapolated portion of the curve, as long as it decreases slowly and continuously. The extrapolated portion is so obviously like a portion of an exponential curve that we may write for that portion

$$B = be^{-ax} \qquad [x > x_1] \tag{38}$$

where x_1 is the value of x at the junction of the solid and the extrapolated portions of the curve. In order that the two portions may join and be continuous, we have two conditions to meet, namely,

$$a = -\left(\frac{1}{B}\frac{dB}{dx}\right)_{x_1} \tag{39}$$

and

$$b = B_1 e^{ax_1} \tag{40}$$

Having now the values of B for various values of x we can substitute in Eq. (37) and find $U(r)$, the probable number of electrons at a radius r from the center of the atom. This means that we must evaluate the integral $\int_0^\infty B \sin(\pi r x)dx$ in Eq. (37). For convenience of reference let us call this integral Φ. It can be separated into two parts: one, Φ_1, dealing with the solid part of the curve; and the other, Φ_2, dealing with the extrapolated part of the curve.

* Find the maximum value of E in Eq. (13) for small values of x_n. This maximum is unaffected by x_n but is reduced by terms containing x_n^2.

† The dotted line of Fig. 9 shows the intensity of scattered rays from helium calculated from Eq. (21). (It is the same curve as the solid line of Fig. 8.) The differences between the solid and the dotted lines of Fig. 9 are greater than the probable experimental error. Apparently the only way to reconcile the data with a Bohr atom would be to assume that the differences were due to (*a*) lack of complete monochromatism of Barrett's x-rays and (*b*) the presence of the Compton effect.

$$\Phi_1 = \int_0^{x_1} B \sin(\pi r x) dx \tag{41}$$

$$\Phi_2 = \int_{x_1}^{\infty} B \sin(\pi r x) dx \tag{42}$$

Φ_1 may be found graphically by plotting $B \sin(\pi r x)$ for various values of r (see the dotted lines in Fig. 10) and integrating with a planimeter. Φ_2 may be found by substituting Eq. (38) in Eq. (42) and integrating. This gives

$$\Phi_2 = B_1 \frac{a \sin(\pi r x_1) + \pi r \cos(\pi r x_1)}{a^2 + \pi^2 r^2}$$

in which, from Fig. 10, $x_1 = 3$, $B_1 = 2.36$ and $a = 0.46$. Compton's final values of Φ_1 and Φ_2 and of

$$U(r) = Zr \int_0^{\infty} B \sin(\pi r x) dx$$

are given in Table III.

TABLE III.—COMPTON'S CALCULATED VALUES OF $U(r)$ FOR VARIOUS VALUES OF r

r	Φ_1	Φ_2	$\Phi = \Phi_1 + \Phi_2$	$U(r) = Zr\Phi$
0.125Å.	5.75	1.64	7.39	1.85
0.25	8.16	−0.42	7.74	3.87
0.5	3.14	−0.35	2.79	2.79
1.0	0.86	−0.70	0.16	0.32

We are now ready to plot $U(r)$ vs. r, thus getting a plot of the probable electron distribution in the heliufn atom. Such a plot is shown by the solid line in Fig. 11. This plot is in excellent agreement with the distribution calculated by Pauling[38] from wave mechanics in spite of the fact that there are no arbitrary constants by which the two plots might be "fitted" together. We are therefore tempted to assume, not the definite electron orbits of Bohr, but the "probable distribution" of orbital radii of wave mechanics.

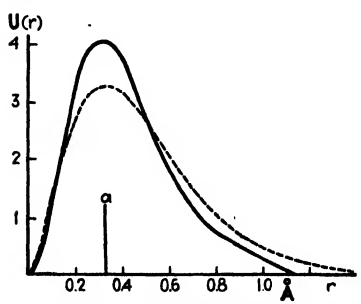

FIG. 11.—Radial electron distribution in helium. Solid line from Table III. Broken line, Pauling's calculation from wave mechanics. a = radius of Bohr orbits.

SUMMARY

We have taken up the x-ray diffraction effects in amorphous materials. We have found confirmation for our ideas of temporary nuclei (Chap. XII) in the diffraction halos from liquids, and we have seen some little evidence that these temporary nuclei become less and less important as

the temperature is raised above the melting point. We have learned that, even when a liquid is considerably above its melting point, there is a most probable spacing between molecules for which the peak of the probability curve is rather sharp.

We have discussed the sort of information which may be obtained by the indirect application of x-ray diffraction data in gels and glasses.

Finally, we have discussed the diffraction effect in gases due to the most probable distribution of electrons in the atoms themselves and have found that, at least in the simplest cases, we can arrive at some fairly definite ideas of atomic structure.

References

1. W. Friedrich, *Phys. Zeit.*, **14**, 317 (1913).
2. E. Hupka, Die Interferenz der Röntgenstrahlen, *Sammlung Vieweg*, **18**, 62 (1914).
3. P. Ehrenfest *Proc. Roy. Soc. Amsterdam*, **17**, 1184 (1914–1915).
4. P. Debye and P. Scherrer, *Nachr. Ges. Wiss. Göttingen* (1916).
5. E. Hückel, *Phys. Zeit.*, **22**, 561 (1921).
6. C. W. Hewlett, *Phys. Rev.*, **20**, 702 (1922).
7. G. E. M. Jauncey, *Phys. Rev.*, **20**, 405 (1922).
8. R. W. G. Wyckoff, *Amer. Jour. Sci.*, **5**, 455 (1923).
9. C. V. Raman and K. R. Ramanathan, *Proc. Indian Assoc. Cult. Sci.*, **8**, 127 (1923). See also Zernike and Prins, *Zeit. Physik*, **41**, 184 (1927).
10. C. M. Sogani, *Ind. Jour. Phys.*, **1**, 357 (1927); **2**, 97 (1927).
11. G. W. Stewart and R. M. Morrow, *Phys. Rev.*, **30**, 232 (1927).
12. J. R. Katz, *Zeit. Physik*, **45**, 97 (1927); *Zeit. angew. Chem.*, **41**, 329 (1928).
13. G. W. Stewart and E. W. Skinner, *Phys. Rev.*, **31**, 1 (1928).
14. R. M. Morrow, *Phys. Rev.*, **31**, 10 (1928).
15. G. W. Stewart, *Phys. Rev.*, **31**, 1, 174 (1928); **32**, 153 (1928).
16. I. Langmuir, *Jour. Amer. Chem. Soc.*, **39**, 1848 (1917), etc.
17. G. W. Stewart, *Phys. Rev.*, **32**, 558 (1928).
18. M. v. Laue, *Zeit. Kryst.*, **46**, 115 (1926).
19. E. W. Skinner, *Phys. Rev.*, **36**, 1625 (1930). See also F. H. W. Noll, *Phys. Rev.*, **42**, 336 (1932).
20. J. G. Aston, private communication.
21. A. Einstein, *Ann. Physik*, **35**, 679 (1911).
22. P. Debye, in R. Zigmondy's "Kolloidchemie" and quoted by many authors, for instance: P. P. Ewald, "Handbuch der Physik," Vol. XXIV, p. 362, Julius Springer, Berlin, 1927.
23. J. Waller, *Zeit. Physik*, **17**, 398 (1923).
24. M. v. Laue, *Zeit. Kryst.*, **64**, 115 (1926).
25. A. L. Patterson, *Zeit. Kryst.*, **66**, 637 (1928).
26. J. Hengstenberg, *Zeit. Kryst.*, **69**, 271 (1928).
27. J. Hengstenberg and H. Mark, *Zeit. Kryst.*, **70**, 283 (1929).
28. R. Brill and H. Pelzer, *Zeit. Kryst.*, **72**, 398 (1929).
29. G. L. Clark, "Applied X-rays," 2d ed. p. 339, McGraw-Hill Book Company, Inc., New York, 1932.
30. G. H. Cameron, *Physics*, **3**, 57 (1932).
31. G. L. Clark, *Ind. Eng. Chem.*, **22**, 474 (1930).
32. M. F. Acken, W. E. Singer, and W. P. Davey, *Ind. Eng. Chem.*, **24**, 54 (1932).
33. J. D. Long, W. E. Singer, and W. P. Davey, *Ind. Eng. Chem.*, **26**, 543 (1934).

34. E. A. HAUSER, *Ind. Eng. Chem.*, **19**, 169 (1927).
35. W. H. ZACHARIASEN, *Jour. Amer. Chem. Soc.*, **54**, 3841 (1932).
36. A. H. COMPTON, *Phys. Rev.*, **35**, 925 (1930).
37. C. S. BARRETT, *Phys. Rev.*, **32**, 22 (1928).
38. L. PAULING, *Proc. Roy. Soc.*, **114**, 181 (1927).
39. J. J. THOMSON, "Conduction of Electricity through Gases," 2d ed., p. 325, Cambridge University Press (Eng.), 1906.
A. H. COMPTON, "X-rays and Electrons," p. 60, D. Van Nostrand Company, New York, 1926.
40. P. DEBYE, *Ann. Physik*, **46**, 809 (1915).
A. H. COMPTON, "X-rays and Electrons," p. 72, D. Van Nostrand Company, New York, 1926.

CHAPTER XVII

THE ORIENTATION OF CRYSTALS

In many cases the industrial usefulness of a given specimen of metal depends not only on the way in which its atoms are arranged in crystals but also on the dimensions and the orientations of those crystals. Most crystal dimensions of metallurgical importance can be found with the aid of the microscope. The order of magnitude of the dimensions of the smallest crystal fragments can sometimes be found from x-ray studies, using equations similar to those referred to in Chap. XVI.[1,2,3,4,5,6,7,8] There remains, then, the determination of the orientations of individual crystals and of the distribution of orientations in a group of crystals.

ORIENTATION OF SINGLE CRYSTALS

Optical Methods.—When the faces of a single crystal are well formed, all that is necessary, of course, is to mount the crystal in a goniometer and to determine the angles between the faces in the usual way. From these measurements, and from a knowledge of the crystal structure of the material, the orientation can be calculated directly.

When single crystals are grown from the melt in cylindrical or conical molds, the crystal faces are all concealed by the shape of the mold. If such a crystal is carefully machined to a cylindrical shape and etched, the crystal faces disclose their presence by a change in luster as the crystal is rotated. This is because what appears to be a smoothly etched surface is really a series of ultramicroscopic steps caused by preferential etching along definite crystallographic directions. Such an etched cylindrical crystal can be mounted in an ordinary goniometer so that when the cylinder is rotated about its own axis the prolongation of the axis of the goniometer always lies in the surface of the cylinder. The collimating telescope and the observation telescope are then set at less than 90° to each other and both are trained on the same element of surface of the cylindrical specimen. The crystal is thus illuminated by a pencil of light of known direction. The crystal is then rotated about its own axis until the velvet-like luster is seen in the observation telescope. This means that the crystal is now in such an orientation that the "steps" on the etched portion are able to reflect the incident beam into the telescope. The normal to the reflecting planes must therefore bisect the angle between the incident and reflected beams, so that the orientation of the reflecting steps is known. The reflecting line on the crystal is marked with a spot of ink and the crystal is rotated until another reflec-

tion is found, and so on for a complete rotation of the crystal. The observation telescope is then moved to catch a sharper angle of reflection and the foregoing procedure is repeated. All the elements of surface previously marked should show reflecting planes at the same relative orientations as before, and there is the possibility of finding new reflecting planes whose steps are at such an angle that during the first trial the reflections were blocked out. If necessary, the cylindrical crystal is then given a new axis of rotation and the above procedure is repeated, but in many cases the data from the first set-up will be sufficient. The orientation of the crystal is then determined in terms of the known crystal structure of the material and the reflection data.

X-ray Methods. *a. Monochromatic Method.*—In cases where optical methods cannot be used, it is necessary to use x-ray methods to determine

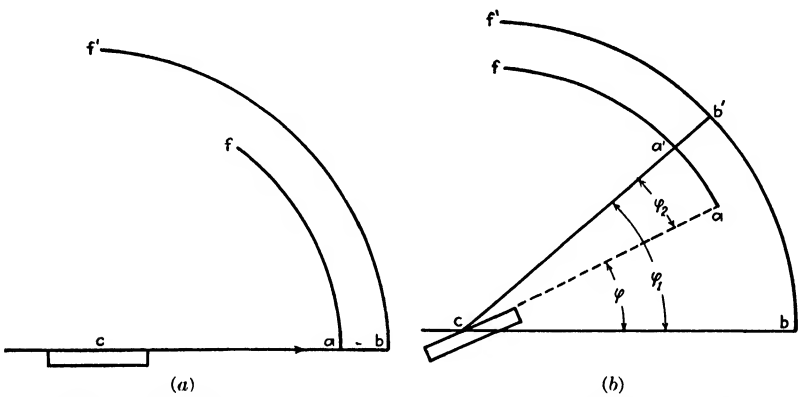

FIG. 1.—Schematic diagram of apparatus for monochromatic x-ray method. (*a*) At end of oscillation, (*b*) during an oscillation.

the axes of a single crystal. There are in general two types of x-ray methods. The first uses some known single wave length. The second uses "white" x-rays. The monochromatic method was developed by the author[9] to determine the orientations of single crystals of copper. It has the advantage that crystals may be used of any thickness or of any opacity to the x-rays. It has the disadvantage that it gives only the orientation at the surface. This disadvantage may be turned into an advantage (at the expense of some little labor) by etching the surface off layer by layer and determining the orientation of each new surface. Such a procedure enables the investigator to follow changes in orientation due to thermal gradients occurring during the growth of the crystal, etc. The crystal *c* is mounted on an oscillating table represented by the plane of the paper in Fig. 1, so that the axis of oscillation lies in some face of the crystal and coincides with some zone axis of the crystal (found by trial and error, if necessary). Mounted on the edge of this same oscillating table is a strip of photographic film *f*, bent into an arc of a circle

whose center is on the axis of oscillation. Just off the oscillating table is a stationary strip of photographic film f'. The x-ray beam is made monochromatic by filtering as in the case of the powder method (Chap. VI).

The crystal is now adjusted on the oscillating table so that at the end of each oscillation the incident x-ray beam just grazes the face of the crystal. The photographic record of this undeviated beam thus forms a reference point a on film f and a reference point b on f', so that the orientation of the crystal may be expressed in terms of its zero position. The oscillating table is now made to move back and forth by some suitable mechanism over an angle such as to permit diffraction from such planes of the crystal as may cross at the axis of oscillation.* The stationary film f' records the upper half of a rotation pattern (see Chap. VII). But for every line, such as b' or f', there must be a corresponding line a' on film f whose position is determined by the angle through which the crystal was turned at the instant diffraction occurred. This angle will be the difference between the angles subtended from c by the arcs bb' and aa' of Fig. 1*b*, *i.e.*,

$$\phi = \phi_1 - \phi_2 \tag{1}$$

Since the structure of the crystal is already known from previous studies, the film f' discloses the indices of the diffracting planes passing through the zone axis, *i.e.*, passing through the axis of oscillation. The film f discloses the orientation of each of these planes. In the general case the crystal is then remounted so that some other zone axis coincides with the axis of oscillation, and a second pair of photographic films is used as in the foregoing. A study of these two pairs of films is sufficient to determine the orientation of the single crystal. The details of such a study are given here briefly for ready reference.

The zero beam will always produce an image on the film f' at the point b. Since, however, the film f' records the upper half of a rotation diagram, we cannot assume that a given diffracted beam will lie in the plane cbb' of Fig. 1. In the general case it will make an angle χ with the plane cbb'. This is brought out in Fig. 2, which shows, in perspective, the stationary film f' and a diffracted beam cB'.†

In order to express the orientation of the crystal we must know the angles 2θ, ϕ_1, ϕ_2, and $B'bb'$. We must therefore find a way to express these angles in terms of distances which we can measure on the films f and f' or on the apparatus itself. This may be done as follows:[10] Pass a plane through bB tangent to the cylindrical stationary film f'. The plane

* Planes cannot be used which make too great an angle with the face of the crystal since they offer too much absorption to the x-rays.

† The line cb' shows where the diffracted beam would have gone if we had had the simple conditions of Fig. 1 with all the diffracted beams in the plane of the oscillating table and with $\phi_1 = 2\theta$.

of the oscillating table, which cuts the film f' in the arc bb', cuts the tangent plane in the straight line bb''. The diffracted beam cB' hits the tangent plane at B'', and the projection cb' of the diffracted beam on the plane of the oscillating table hits the tangent plane at b''. The angle

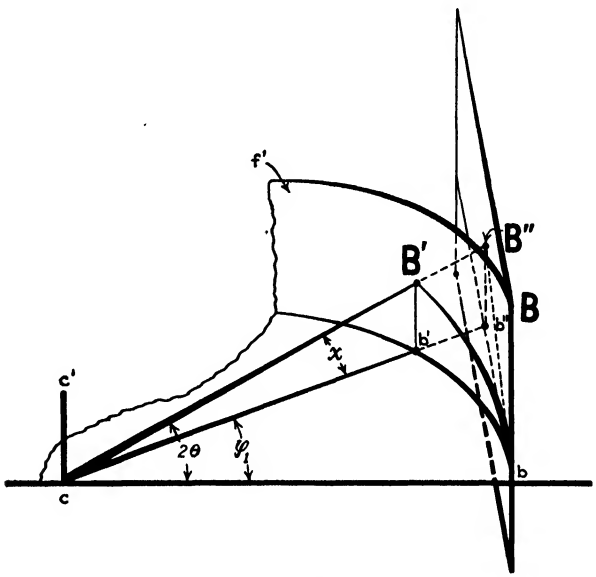

FIG. 2.—The stationary film (f' of Fig. 1) shown in perspective. The plane of the paper in Fig. 1 is shown here as the plane cbb'. The film f' forms a cylindrical surface perpendicular to the plane cbb' with cc' as the axis of the cylindrical surface.

$\alpha' = B''bb''$ is the measure of the cylindrical angle $\alpha = B'bb'$. We have therefore for the stationary film f',

$$\tan \chi = \frac{B'b'}{cb'} = \frac{B'b'}{cb} \tag{2}$$

$$\phi_1 = \frac{bb'}{cb'} = \frac{bb'}{cb} \tag{3}$$

$$\tan \alpha = \tan B'bb' = \frac{\tan \chi}{\sin \phi_1} \tag{4}*$$

* From Fig. 2, since $B'b'$ and $B''b''$ are both perpendicular to the plane of the oscillating table,

$$\tan \alpha' = \frac{B''b''}{b''b} \tag{a}$$

$$\tan \phi_1 = \frac{b''b}{cb} \tag{b}$$

$$\tan \chi = \frac{B''b''}{cb''} \tag{c}$$

$$cb'' = \frac{cb}{\cos \phi_1} \tag{d}$$

Substituting (*d*) in (*c*):

Similarly, for the oscillating film f we have

$$\tan \chi = \frac{B_1'b_1'}{cb_1'} = \frac{B_1'b_1'}{cb_1} \tag{5}$$

$$\phi_2 = \frac{b_1b_1'}{cb_1'} = \frac{b_1b_1'}{cb_1} \tag{6}$$

Besides, we have

$$\cos 2\theta = \cos \chi \cos \phi_1 \tag{7}$$

We are therefore in a position to express the orientation of the single crystal in terms of quantities which can be measured readily and directly, provided only that we have succeeded in pairing off the spots on f and f' correctly. In some cases this can be done directly because of some peculiarity in the appearance of the spots. In other cases we must look for identical values of tan χ from Eqs. (2) and (5). In all cases we must be sure that the final pairing of spots is consistent with a single orientation of the known structure for the crystal under examination. If desired, the orientation of the various planes may then be plotted[10] on a stereographic net (see technique described later on in this chapter), so that the orientations of the principal planes may be read off at a glance. In most cases for single crystals, however, it is sufficient to mark the significant crystallographic directions on the crystal itself.

It should be noted that the monochromatic method offers a very sensitive test for the perfection of a crystal surface. A relatively small amount of strain will almost wipe out the spots in the oscillating film f, without interfering with the clarity of the spots on the stationary film f'. Even in the case of a rigid material like quartz the distortions on the surface due to polishing were sufficient, in one specimen examined by the author, to wipe out the oscillating pattern entirely. It was restored by etching the polished surface with hydrofluoric acid.

b. "White" X-ray Method.—This type of x-ray method for determining the orientation of single crystals follows the general scheme of the Laue method of crystal analysis (Chap. IV). The "white" x-rays are passed through the crystal, and the Laue pattern is obtained. If a large number of crystals are to be examined, it is probably most convenient to make a standard set of Laue patterns for known orientations and then determine the unknown orientation by comparison. Such standard patterns for body-centered and face-centered cubic crystals have been

---

$$\tan \chi = \frac{B''b'' \cos \phi_1}{cb} \tag{e}$$

Substituting (*b*) and (*e*) in (*a*):

$$\tan \alpha' = \tan \alpha = \frac{\tan \chi \cdot cb}{\cos \phi \cdot cb \cdot \tan \phi_1}$$

$$= \frac{\tan \chi}{\cos \phi_1 \tan \phi_1} = \frac{\tan \chi}{\sin \phi_1} \tag{4}$$

published by Majima and Togino[11] for a systematic set of orientations with 5° intervals up to 45° for the X-axis and similar 5° intervals up to 45° for the Y-axis. Interpolation to 1° should not be difficult. If only a limited number of crystals are to be examined, it is probably easiest to make successive trial settings of the crystal in order to get finally a zone axis (preferably a principal axis) parallel to the x-ray beam. The gnomonic rotation net (Figs. 15 and 16 of Chap. IV) may be used to reduce the number of settings, and the gnomonic projection itself will show by its symmetry when a zone axis is exactly parallel to the x-ray beam.

PREFERRED ORIENTATION OF POLYCRYSTAL MATERIAL

When metals are subjected to mechanical working, such as rolling, the individual crystals tend to break up into smaller crystals. This breaking up is accompanied by motions of rotation such that most of the crystal fragments fall into a system or systems of preferred orientations which bear definite angular relations to the surface of the specimen. In rolled metals the crystals may orient themselves with respect to the axis of the rolls or to the rolling direction or both. Since we must deal with a large number of crystals of varying orientation, Bragg's law requires the use of a known single wave length. Since we must determine orientations with respect to three dimensions, we must use a pinhole-slit system so as to get a sharp pencil of x-rays. Our problem is, then, twofold: (*a*) we must adapt the technique of the powder method (Chap. VI) to the determination of the angular limits of the preferred orientations and to the determination of the degree of preferment between these limits, and (*b*) we must find a way of expressing the experimental results in usable form. We shall take up each of these in turn.

DETERMINATION OF PREFERRED ORIENTATION AND DEGREE OF PREFERMENT

If a specimen of metal is mounted as in Fig. 3, it will diffract x-rays to the upper portion of the photographic film F. The lower portion of

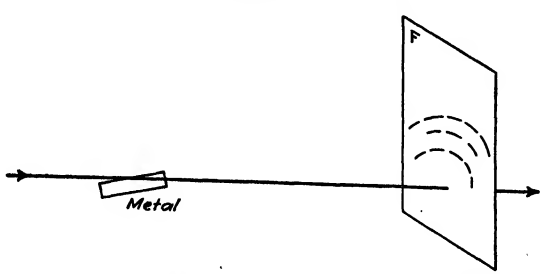

FIG. 3.—Diffraction of x-rays from rolled metal.

the film will be shadowed by the specimen and, except in the case of thin foils, will show no diffraction pattern. If the crystals of the metal are

small enough in size and have random orientations, the diffraction pattern will consist of smooth continuous rings whose limits will be set only by the shadow of the specimen. If the crystals are somewhat larger, the rings will not be smooth but will be made up of small spots (each spot representing diffraction from a single crystal) uniformly distributed over the ring. If, however, the crystals are not randomly oriented, the rings will not be uniform in intensity from point to point along their lengths. Each ring will tend to concentrate itself in spots or arcs. These arcs have, of course, the same radius of curvature that the original ring would have had. The intensity of the arcs is greater than the intensity which the ring would have had, and the intensity in the spaces between the arcs is less than the intensity which the ring would

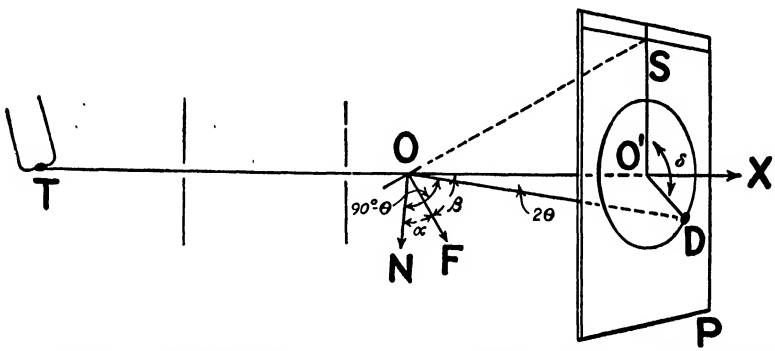

FIG. 4.—Diagram for Bozorth's calculations of preferred orientation (x-rays transmitted through specimen).

have had. In favorable cases the intensity between the arcs drops to practically zero. The higher the degree of preferment of orientation, the shorter will be the arcs. When the arcs are so short as to be only spots, the monochromatic pinhole pattern may be interpreted easily by a geometrical calculation based on the angular relationships of the planes in the crystal and the spots on the diffraction pattern. An example of this is the work of Bozorth[12] on the preferred orientations of crystals of electrodeposited metals. The specimens of metal which he investigated were so thin that he passed the x-ray beam through the body of the specimen as shown in Fig. 4. (The interpretation of the following in terms of Fig. 3 will be obvious.) The x-ray beam TX cuts the sample at O and hits the photographic film P at O'. OF is the normal to the surface of the specimen on the side from which the x-ray beam emerges. ON is the normal to some family of planes which diffracts the beam to D. The reference line $O'S$ lies in the plane of P and in the plane $O'OF$ and is drawn on the side of OO' opposite to OF. Then

$$\cos \alpha = \cos \beta \sin \theta + \sin \beta \cos \theta \cos \delta \qquad (8)$$

The value of θ is known from the crystal structure and the wave length of the x-rays, and δ is measured on the photographic film. β can best be found from

$$\tan \beta = \frac{OO'}{O'S} \tag{9}$$

where OO' is calculated from the measured distances $O'D$ and from the

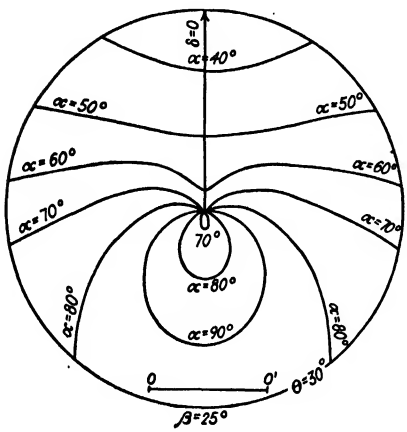

FIG. 5.—δ as a function of θ for $\beta = 25°$.

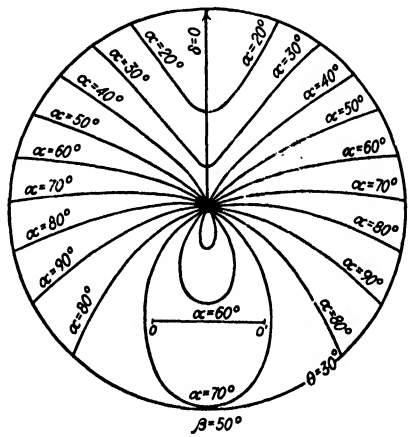

FIG. 6.—δ as a function of θ for $\beta = 50°$.

values of θ calculated from Bragg's law, and where $O'S$ is the distance from O' to the edge of the shadow cast by the specimen.

The crystallographic plane (hkl) which coincides with the specimen surface is determined with the aid of a chart and a table. The chart is constructed for the chosen value of β. A different chart is required for each angle of inclination of the foil to the x-ray beam. For some arbitrary value of α a curve is drawn giving δ as a function of θ. In this curve, δ is plotted in azimuth and θ is plotted radially so that a line of constant θ is a circle of radius OO' tan 2θ. (Such a circle represents the Hull-Debye-Scherrer ring produced by x-rays diffracted from crystal planes inclined at an angle θ to the incident beam.) The chart is completed by drawing δ *versus* θ curves for other values of α. Values of α are taken 10° apart to facilitate interpolation. Figures 5, 6, and 7 show such charts for $\beta = 25°$, $\beta = 50°$, and $\beta = 75°$. In using them, they

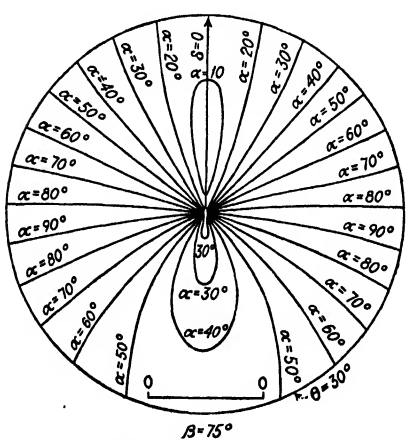

FIG. 7.—δ as a function of θ for $\beta = 75°$.

should be copied at such a size that OO' is equal to the distance in the actual experiment from the sample to the photographic film. After the

TABLE I.—ANGLES BETWEEN VARIOUS PLANES OF SIMPLE INDICES IN THE CUBIC SYSTEM

(h k l)	(h k l)	Values of α, the angle between (h k l) and (h k l)						
100	100	0° 0′	90° 0′					
	110	45° 0′	90° 0′					
	111	54° 44′						
	210	26° 34′	63° 26′	90° 0′				
	211	35° 16′	65° 54′					
	221	48° 11′	70° 32′					
	310	18° 26′	71° 34′	90° 0′				
	311	25° 14′	72° 27′					
	320	33° 41′	56° 19′	90° 0′				
	321	36° 43′	57° 42′	74° 30′				
110	110	0° 0′	60° 0′	90° 0′				
	111	35° 16′	90° 0′					
	210	18° 26′	71° 46′	71° 34′				
	211	30° 0′	54° 44′	73° 13′	90° 0′			
	221	19° 28′	45° 0′	76° 22′	90° 0′			
	310	26° 34′	47° 52′	63° 26′	77° 5′			
	311	31° 29′	64° 46′	90° 0′				
	320	11° 19′	53° 58′	66° 54′	78° 41′			
	321	19° 6′	40° 54′	55° 28′	67° 48′	79° 0′		
111	111	0° 0′	70° 32′					
	210	39° 14′	75° 2′					
	211	19° 28′	61° 52′	90° 0′				
	221	15° 41′	54° 44′	78° 54′				
	310	43° 5′	68° 35′					
	311	29° 30′	58° 31′	79° 58′				
	320	61° 17′	71° 19′					
	321	22° 12′	51° 53′	72° 1′	90° 0′			
210	210	0° 0′	36° 52′	53° 8′	66° 25′	78° 28′	90° 0′	
	211	24° 6′	43° 5′	6° 47′	79° 29′	90° 0′		
	221	26° 34′	41° 49′	53° 24′	63° 26′	72° 39′	90° 0′	
	310	8° 8′	58° 3′	45° 0′	64° 54′	73° 34′		
	311	19° 17′	47° 36′	66° 8′	82° 15′			
	320	7° 7′	29° 45′	41° 55′	60° 15′	68° 9′	75° 38′	82° 53′
	321	17° 1′	33° 13′	53° 18′	61° 26′	70° 13′	83° 8′	90° 0′
211	211	0° 0′	33° 33′	48° 11′	60° 0′	70° 32′	80° 24′	
	221	17° 43′	35° 16′	47° 7′	65° 54′	74° 12′	82° 12′	
	310	25° 21′	49° 48′	58° 55′	75° 2′	82° 35′		
	311	19° 8′	42° 24′	60° 30′	75° 45′	90° 0′		
	320	25° 9′	37° 37′	55° 33′	63° 5′	83° 30′		
	321	10° 54′	29° 12′	40° 12′	49° 6′	56° 56′		
		70° 54′	77° 24′	83° 44′	90° 0′			
221	221	0° 0′	27° 16′	38° 57′	63° 37′	83° 37′	90° 0′	
	310	32° 31′	42° 27′	58° 12′	65° 4′	83° 57′		
	311	25° 14′	45° 17′	59° 50′	72° 27′	84° 14′		
	320	22° 24′	42° 18′	49° 40′	68° 18′	79° 21′	84° 42′	
	321	11° 29′	27° 1′	36° 42′	47° 41′	63° 33′	74° 30′	
		79° 44′	84° 53′					
310	310	0° 0′	25° 51′	36° 52′	53° 8′	72° 33′	84° 16′	
	311	17° 33′	40° 17′	55° 6′	67° 35′	79° 1′	90° 0′	
	320	15° 15′	37° 52′	52° 8′	74° 45′	84° 58′		
	321	21° 37′	32° 19′	40° 29′	47° 28′	53° 44′	59° 32′	
		65° 0′	75° 19′	85° 9′	90° 0′			
311	311	0° 0′	35° 6′	50° 29′	62° 58′	84° 47′		
	320	23° 6′	41° 11′	54° 10′	65° 17′	75° 28′	85° 12′	
	321	14° 46′	36° 19′	49° 52′	61° 5′	71° 12′	80° 44′	
320	320	0° 0′	22° 37′	46° 11′	62° 31′	67° 23′	72° 5′	90° 0′
	321	15° 30′	27° 11′	35° 23′	48° 9′	53° 37′	58° 45′	63° 36′
		92° 45′	77° 9′	85° 45′	90° 0′			
321	321	0° 0′	21° 47′	31° 0′	38° 13′	44° 25′	50° 0′	60° 0′
		64° 37′	69° 4′	73° 24′	81° 47′	85° 54′		

chart has been enlarged to the proper size, the photographic film is placed over it and the proper value of α is read off for each "spot" on

each diffraction ring. A table is now written up, giving the angles between various planes of simple indices. Table I is such a table, calculated by Bozorth for the cubic system. For the diffraction ring from planes (h k l) the planes ($h\,k\,l$) are found for which the angles given in the table are equal to the values of α found from the chart. By repeating this procedure for each of the rings of the diffraction pattern, the plane ($h\,k\,l$) which coincides with the surface of the specimen is finally found.

The foregoing may be illustrated in terms of one of Bozorth's experiments with an electrolytic foil of nickel. The foil was mounted with $\beta = 50°$. The values of α found from the chart of Fig. 6 are given in the second column of Table II. A search through Table I shows that the values of α for ($h\,k\,l$) = (2 1 1) are the only ones which give even approximate agreement with the values found from the chart.* These values of α for (2 1 1) are listed in the third column of Table II. It is therefore

TABLE II.—BOZORTH'S RESULTS FOR ELECTROLYTIC NICKEL FOIL

Diffracting planes n(h k l)	α from Fig. 6	α for ($h\,k\,l$) = (2 1 1) from Table I
(1 1 1)	61°, 90°	19° 28′, 61° 52′, 90°
2(1 0 0)	36°, 66°	35° 16′, 65° 54′
2(1 1 0)	30°, 55°, 73°, 90°	30°, 54° 44′, 73° 13′, 90°

concluded that the (2 1 1) family of planes in the nickel foil was practically parallel to the surface of the specimen.

Methods such as the foregoing are of difficult application when the degree of preference is low, or when, instead of a single preferred orientation, a system of orientations exists in the metal. In such cases it is often easier to use a cut-and-try method developed by the author.[13,14]† In outlining this method we shall assume: (1) that two diffraction patterns were taken, one of which was taken so that a plane perpendicular to the sheet of metal and including the incident beam also includes the direction of rolling, *i.e.*, in abbreviated language, "the incident beam is in the direction of rolling"; (2) that the second pattern was taken with the "incident beam perpendicular to the direction of rolling"; and (3) that one of these patterns shows continuous rings and that the other shows arcs. The changes in wording necessary in the following will be obvious in the case of both patterns showing arcs.

A silver print is made of the pattern which shows the arcs, care being taken that the print is a true "positive" without reversal of the right- and left-hand sides. All determinations of preferred orientations by this

* Column 3 of Table II shows one plane not shown in column 2. This is due to the limitations imposed on the diffraction by the angles β and θ.

† A thorough study of this method will give the reader the necessary mental bias for studying pole figures.

method are best made with the aid of positive prints, no work being done on the original negative. The diffraction rings are numbered consecutively in ink on the positive print, the separate arcs in each ring being distinguished by subscripts. From a knowledge of (1) the x-ray wave length used, (2) the specimen-film distance, (3) the diameter of the diffraction rings, and (4) the crystal structure of the specimen, the Miller indices are calculated for the atomic planes in the specimen corresponding

FIG. 8.—Zinc lattice model and mounting.

to each diffraction ring. These indices are tabulated along with the numbers of the rings to which they belong. In this description the planes will be called by the number of the ring which they produce in order to avoid a number of long cumbersome phrases.

A large model of the crystal lattice of the metal undergoing examination is constructed with balls and rods (Fig. 8). The balls are preferably spaced three to four inches apart, and they must be carefully placed so that the model has the true proportions of the crystal lattice which it represents. The model is mounted on an adjustable mounting such as is shown in Fig. 9, or it is attached to a double set of gimbals. The

positive print mentioned above is mounted in a vertical position at a convenient height, and the model is set up in front of it as shown in Fig. 9. A string is stretched from a vertical support to the model so that its direction is perpendicular to the plane of the positive print. This string represents the incident x-ray beam. It is maintained perpendicular to the print throughout the whole interpretation process. The position of the model may be adjusted without causing slack in the string if a stout rubber band is tied to one end. In some cases it is convenient to replace the string by a narrow elastic tape.

The fact that the other diffraction pattern has continuous rings shows that we have random orientation of our model about an axis perpendicular

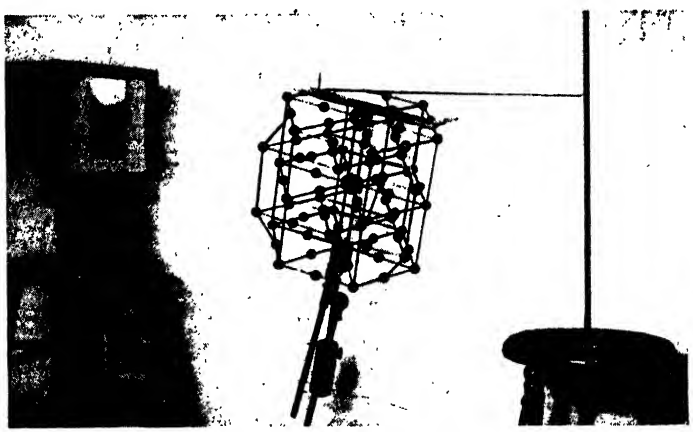

FIG. 9.—Arrangement of apparatus for the interpretation of a pattern of rolled zinc.

to the string. The fact that the diffraction pattern which we have just mounted up in front of the model has detached arcs shows that we have preferred orientations about an axis parallel to the string. The model is now turned to such a position that the atomic plane corresponding to ring 1 is at the correct angle to the string to account for diffraction to the center of some one arc of ring 1. The degree of deviation in the actual sample from the median orientation as represented by the model may be found by simple calculation from the length and the radius of the arc on the diffraction pattern.

We have now fixed the median location of plane 1, but we have not found how this plane is oriented about an axis perpendicular to itself. The model is therefore rotated about an imaginary line normal to plane 1 until a second tilt about an axis perpendicular to the string places plane 2 at the correct angle for diffraction to an arc on ring 2. (It must be remembered that there are no restrictions as to the angle of tilt about the axis perpendicular to the string because the other diffraction pattern shows continuous rings.) It must be possible to account for the total

degree of deviation from the median orientation for the arc in ring 2 in terms of (1) a random orientation about an axis perpendicular to the string and (2) the degree of deviation for the arc used in ring 1. If this cannot be done, we have four possibilities: (1) there are two preferred orientations such that certain arcs overlap; (2) two differently oriented planes of this same family can produce overlapping rings when the degree of deviation is taken into account; (3) two families of planes happen to have the same interplanar spacing (this can be found by direct calculation from the crystal lattice); (4) we have tried to correlate the wrong pair of arcs in rings 1 and 2.

When an orientation of the model is found which will account for one pair of arcs in rings 1 and 2, the model must be examined to see whether other members of the same families of planes can (taking the degree of deviation into account) produce arcs in their respective rings. It is obvious that, if we have the correct median orientation of our model, no arcs will be possible except those actually found in the diffraction pattern. Remembering (1) that we may have *any* angle of tilt about an axis perpendicular to the string, and (2) that we may tilt the model about an axis parallel to the string to the extent permitted by the degree of deviation of the arc in ring 1, we must now investigate rings 3, 4, 5, etc. In every case we must check back by means of the degree of deviation to make sure that we have started with the right pair of arcs in rings 1 and 2.

If it turns out that all the rings on the diffraction pattern can thus be accounted for, and that there are no theoretical arcs not shown on the diffraction pattern, then we have found in our rolled sheet a single preferred orientation, with a known degree of deviation, about an axis parallel with the string, and this preferred orientation must coexist with a random orientation about an axis perpendicular to the string. If, on the other hand, it turns out that we can account for all the theoretical arcs associated with this preferred orientation, but we have some arcs left over on our diffraction pattern which have not been accounted for, then we must cross off those already accounted for and repeat the above technique on the remaining arcs in the hope of finding a second preferred orientation coexisting with the one already found. In order to determine completely the preferred orientations of the metal, it is now necessary to repeat the above procedure with still other pairs of diffraction patterns taken with known orientations of the specimen. This will be evident when we take up the subject of pole figures.

We are now ready to illustrate the foregoing method by giving in detail a study[14] of two diffraction patterns of rolled zinc.* The specimen

* It is not to be inferred that all sheet zinc will give, with all kinds of rolling technique, orientations of the type described here. The orientations obtained will depend upon many factors which are beyond the scope of this chapter. The results

had been hot rolled from 0.5 to 0.1 in. (12.5 to 2.5 mm.) and then cold rolled from 0.1 to 0.006 in. (2.5 to 0.15 mm.) in thickness.

With the x-ray beam grazing the surface of the specimen at an angle of 10°, two x-ray patterns were taken. In the first case (Fig. 10) the x-ray beam was perpendicular to the rolling direction, and in the second case (Fig. 11) the x-ray beam was in the plane formed by the rolling

FIG. 10.—Rolled zinc—x-ray beam perpendicular to rolling direction.

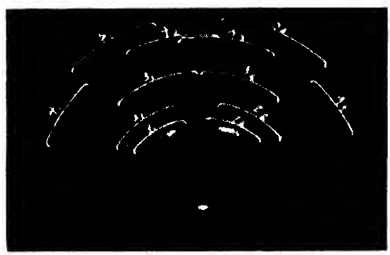

FIG. 10*a*.—Pattern of Fig. 10, marked to indicate the arcs.

direction and the normal to the rolling plane, *i.e.*, in abbreviated language, the x-ray beam was "in the direction of rolling." As in the case of the general description of the method given above, one of the patterns showed arcs and one showed continuous rings.

The model, pattern, and string were set up, as previously described (see Fig. 9), and the model mounting was tilted away from the pattern so that the base of the mounting made an angle of 10° with the string. The model was attached to a series of clamps such that it could be rotated about the central hexagonal axis of the model or rotated about two axes perpendicular to, and parallel with, the string. Any of these motions could be made independently of the others. The base of the mounting corresponded to the surface of the specimen. With the pattern (which was taken with the x-ray beam perpendicular to the rolling direction) in place, the model was oriented so that the basal plane (0 0 · 1) made the proper angle for reflection on an intermediate point of the arc 1_2 (see Fig. 10*a*). This was done by satisfying two conditions: (1) the string (always perpendicular to the positive print of the diffraction pattern) must make an angle (determined by Bragg's law) of 8.3° with the basal, *i.e.*, the (0 0 · 1) plane, and (2) the string must be in the plane defined by

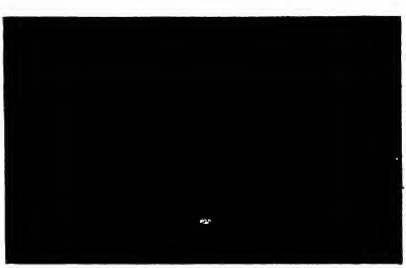

FIG. 11.—Rolled zinc—x-ray beam in rolling direction.

described here are from one sample only and are given only as a concrete example of the application of the method.

the center of the arc 1_2 and the normal to the $(00\cdot1)$ plane of the model. This normal was represented by a brass rod mounted in a strip of wood which was laid on the $(00\cdot1)$ plane of the model. When the correct position of the $(00\cdot1)$ plane was found, the model was locked in position on the hinged mounting (Figs. 8 and 9). Two rubber bands having hooks at each end were fastened to the model in such a way as to define the $(10\cdot1)$ plane. Rotation of the model about the hexagonal axis, *i.e.*, the normal to the $(00\cdot1)$ plane, brought this $(10\cdot1)$ plane into proper position to "reflect" in the 2_1 arc. From this step on, the only adjustment of the model was to rotate it about the rolling direction, *i.e.*, about an axis perpendicular to the string, always maintaining the same relation to the rolling direction as was fixed by the first two steps of the procedure. This rotation may be of any angle since, from Fig. 11, a random orientation exists about the rolling direction. The $(00\cdot1)(2)$, $(10\cdot0)$, and $(00\cdot1)(4)$ reflections do not show in Fig. 11. It was found by manipulation of the model that the absence of these two reflections was consistent with the system of orientations tentatively decided upon above.

By rotating the model about the rolling direction a few degrees, the model was brought in position to reflect from the $(10\cdot2)$ plane on one of the intermediate spots of 3_1. In a similar manner two $(10\cdot3)$ planes could be brought to reflect on arcs 4_2 and 4_4. No $(11\cdot0)$ planes (whose diffraction rings, if present, would have been coincident with those of the $(10\cdot3)$ planes) could be found which would reflect, no matter how much the model was rotated about the rolling direction. An intermediate spot on the arc 5_2 could also be accounted for. It was not thought wise to consider the $(11\cdot2)$ arc, since it was very poorly defined. This process was twice repeated from the beginning, except that the starts were made from each of the two extremities of arc 1_2. In this manner the corresponding extremities of arcs 2_1, 3_1, 4_2, 4_4, and 5_2 could be accounted for. It is allowable to assume that every spot in these arcs could be accounted for by the system of orientations limited by the extremities of these arcs.

If the model is rotated about the rolling direction so that it points downward instead of upward, or is turned 180° in the rolling plane about a normal to the rolling plane (these rotations accomplish the same result), the model is then in a position to account for arcs 1_1, 2_2, 3_2, 4_3, and 5_1. This was carried out exactly as described for the other arcs, taking three spots on each arc. Arcs from the $(10\cdot0)$ plane on Fig. 10 and the $(00\cdot1)(2)$, $(10\cdot0)$ and $(00\cdot1)(4)$ planes on Fig. 11 do not appear. This was found to be consistent with the system of orientations defined by the arcs which do appear.

The variation from one end of each of the arcs 1_1 and 1_2 to the other end of each is 36°. The position of the model at the mean of these is such that the hexagonal axis makes an angle of 61° with the rolling

direction and such that an X-axis (edge of one of the hexagonal bases) is perpendicular to the rolling direction. The system of orientations, therefore, which exists in this specimen of rolled zinc, is such that the hexagonal axis is at an angle of $61 \pm 18°$ with the rolling direction. There is no preferred orientation with respect to the rolling plane. Crystals exist at any position about the rolling direction, so long as their hexagonal axes have the proper relation to the rolling direction. Similar studies of other pairs of diffraction patterns taken with known orientations of the specimen will serve to define the preferred orientation completely.

For further studies of pairs of diffraction patterns the reader is referred to an article by Hollabaugh and Davey[15] in which all the steps are given in considerable detail.*

POLE FIGURES†

Now that we have gained a general idea of how preferred orientations may be determined, we must take up some method of expressing them graphically. The most convenient method is that of F. Wever[16,17] in which the stereographic projection (Chap. IV) is used. It lends itself well to this purpose, for it enables us to chart within the area of a circle of finite radius all possible orientations which can occur within a solid angle subtended by a hemisphere. Such a stereographic representation of preferred orientations is called a "pole figure" (Flächenpolfigur). It has the advantage of simplifying the work of interpretation of diffraction patterns in that the patterns do not necessarily have to be studied in pairs as in the cut-and-try method just described, but the results from each single film may be recorded on the chart as the investigation proceeds.‡ When the metal is thin enough to permit, both "reflection" and "transmission" monochromatic pinhole diffraction patterns may be employed to advantage.

The whole subject of pole figures is easiest explained in terms of a concrete example. As such an example we shall take a certain specimen of rolled zinc alloy§ which had the crystal structure of pure zinc, *i.e.*, hexagonal close-packed. From the metal strip, which was 0.040 in. (0.1 cm.) thick, a thin section 0.002 to 0.003 in. (0.005 to 0.007 cm.)

* These experiments of Hollabaugh and Davey represent the unusual case in which the purpose of the experiment is gained without having to determine completely the preferred orientation in all directions.

† This portion of the chapter was written by M. L. Fuller of the Research Laboratory of the New Jersey Zinc Company.

‡ From this standpoint the use of pole figures may be considered to be not only a method of expressing orientation data but also a method of interpreting the data.

§ The orientations found in this particular metal strip are not to be interpreted as being characteristic of all rolled zinc alloys, since the orientation differs with different rolling treatments.

TABLE III.—TABULATION OF DIFFRACTION PATTERNS TAKEN FOR POLE FIGURES

Type of pattern	Angle between incident x-ray beam and		
	Rolling plane	Rolling direction	Across-rolling direction
Reflection	8°	90°	...
Reflection	8°	50°	...
Reflection	8°	40°	...
Transmission	90°	...	...
Transmission	50°	90°	...
Transmission	28°	...	90°

thick was prepared by etching. This thin section was selected from a position approximately midway between the surface and the center of

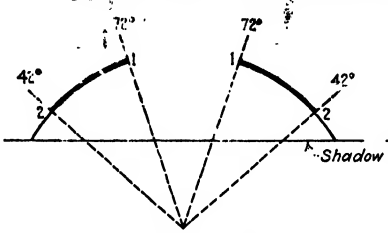

FIG. 12.—Basal plane (0 0 · 1) diffraction arcs. X-ray beam 8° to rolling plane, 90° to rolling direction.

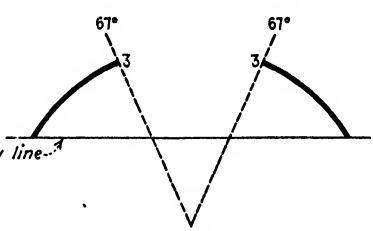

FIG. 13.—Basal plane (0 0 · 1) diffraction arcs. X-ray beam 8° to rolling plane, 50° to rolling direction.

the strip. (Obviously, for a complete study of the orientations present, sections from still other positions in the strip would have had to be

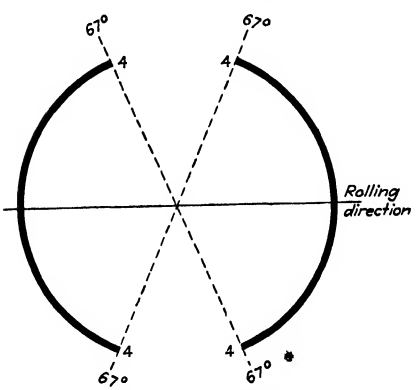

FIG. 14.—Basal plane (0 0 · 1) diffraction arcs. X-ray beam 90° to rolling plane.

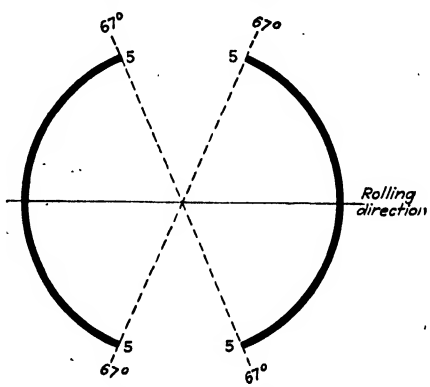

FIG. 15.—Basal plane (0 0 · 1) diffraction arcs. X-ray beam 50° to rolling plane, 90° to rolling direction.

prepared.) For the study of this particular thin section, x-ray pinhole patterns were prepared as listed in Table III, using MoK_α rays. Figures 12 to 16 are diagrammatic reproductions of the basal plane (0 0 · 1) arcs on

five of the diffraction patterns. One pattern (x-ray beam 40° to rolling direction and 8° to the rolling plane) had no basal "reflections" and hence is not reproduced.

The stereographic projection is carried out by means of a stereographic net.[18] The net is reproduced in Fig. 17. The principle of the stereographic projection has already been discussed in detail in Chap. IV. The net of Fig. 17 gives the stereographically projected great and small circles for every 2°. If the projection is drawn on tracing-paper while the net is in place beneath the paper, the points can be plotted more readily than when a stereographic ruler is used. From a completed projection the angular relationship between the points can be read easily with the aid of the net. Figure 18 results from plotting the data from Figs. 12 to 16 with the aid of the net of Fig. 17. The projected crystal plane is the basal plane (0 0 · 1), which is perpendicular to the principal axis of the hexagonal close-packed structure. The projection is made on the plane which includes the normal to the rolling plane and the transverse (or "across rolling") direction, *i.e.*, the rolling direction is normal to the plane of the diagram.

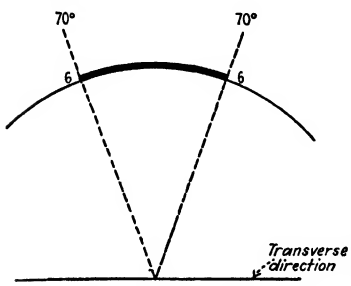

FIG. 16.—Basal plane (0 0 · 1) diffraction arcs. X-ray beam 28° to rolling plane, 90° to transverse (or "across rolling") direction.

The cross-hatched areas on Fig. 18 include all the orientations found in the specimen. The areas which are doubly cross-hatched have a denser crystal population than the singly cross-hatched areas, as shown by the intensities of the diffracted beams. To define the orientations present in the specimen rigorously, the pole figure for an additional crystal plane would be required. It so happens, however, that in this case the crystals occupy all possible positions of rotation about the basal plane normal as an axis. This can be deduced readily from the lengths of the arcs of the other diffraction rings on the x-ray patterns.

Figure 19 shows the same pole figure as that of Fig. 18 with the method of plotting indicated. Aside from the pole figure itself, which can be readily distinguished by reference to Fig. 18, the following code has been used:

Dashed Lines.—Traces of imaginary planes through the metal sheet to which the incident x-ray beam was perpendicular.

Dotted Lines.—Loci of orientations definitely found to be absent since the corresponding x-ray "reflections" are not found on the x-ray patterns.

Light Full Lines.—Loci of orientations definitely indicated to be present by the x-ray patterns.

Heavy Full Lines.—Same as light full lines except that the crystal population in these loci are denser than in those indicated by light full lines.

Points Indicated by Small Circles.—Points plotted from the measurements on the x-ray patterns. The numbers adjacent to these points correspond to the similarly numbered points in the x-ray patterns of Figs. 12 to 16.

Figure 12 furnishes the points 1 and 2 on the pole figure of Fig. 19. This pattern was obtained by causing the x-ray beam to be incident on the specimen at a grazing angle of 8° to the rolling plane and perpendicular to the rolling direction. Since the grazing angle of incidence for the

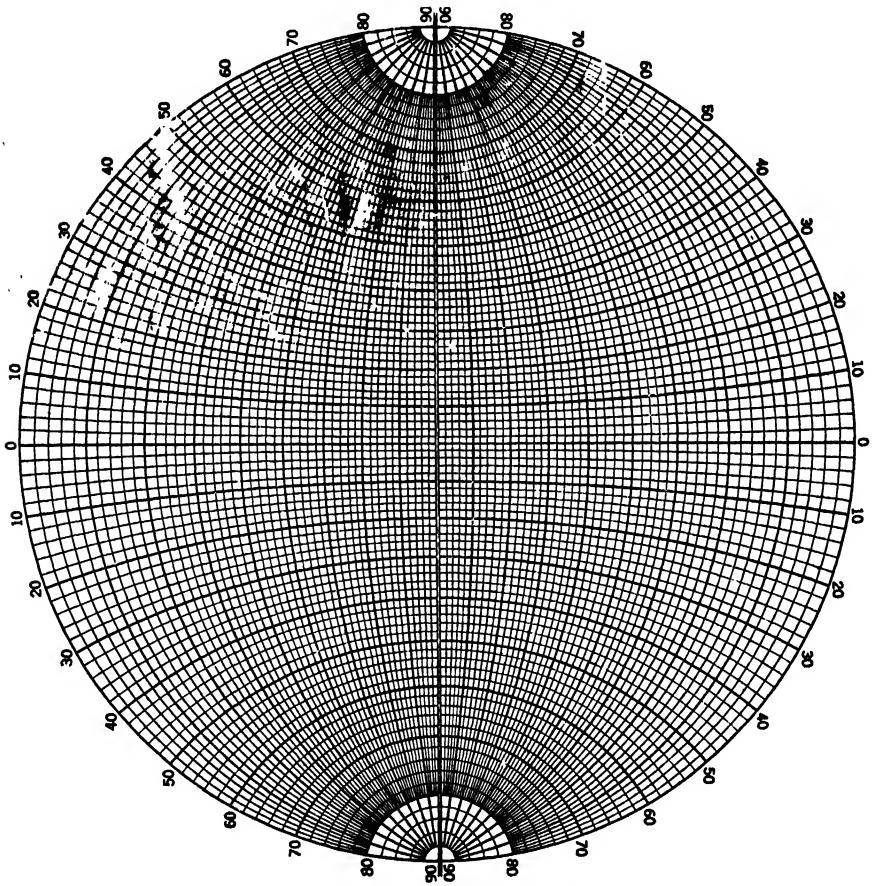

FIG. 17.—Stereographic net.

basal plane (0 0 · 1) reflections is 8° (using MoK_α x-rays), it is evident that all basal planes reflecting are approximately parallel to the transverse or across rolling direction. The plotting of the orientation on the pole figure on the basis of this approximation is allowable when the precision of measurements on the x-ray pattern is considered. It should be noted that with a "reflection" pattern the angular range of measurable orientations is limited by the "shadow" of the specimen on the x-ray

pattern. The dotted lines *A*-1 are loci of orientations indicated to be absent by the x-ray pattern of Fig. 12. Densely populated loci of orientations are indicated by the heavy lines 1-2 and less densely populated loci by the extension of the lines 1-2 to the limit imposed by the shadow line on the x-ray pattern.

Figure 13 which is a "reflection" pattern taken with the x-ray beam at 8° to the rolling plane and 50° to the rolling direction supplies the points 3. The plotting is similar to that of Fig. 12 except that it is not on the great circle *A*-1-2-2-1-*A* (perpendicular to the plane of projection) but is on the great circles *A*-3-3-*A* which make angles of 50° to the plane of projection.

Figure 14 is a transmission pattern obtained by making the incident x-ray beam perpendicular to the rolling plane. This pattern gives rise

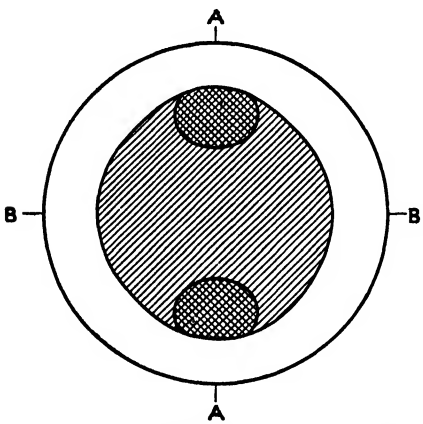

FIG. 18.—Basal plane (00.1) pole figure from a rolled zinc alloy. *AA*, direction normal to rolling plane; *BB*, transverse (or across rolling) direction.

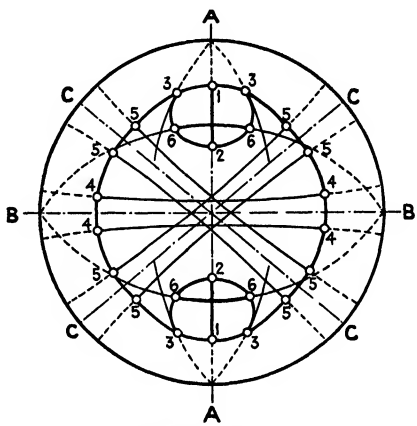

FIG. 19.—Basal plane (00·1) pole figure from rolled zinc alloy, illustrating projection method.

to the points 4. The two small circles 4-4 are the 8° small circles about the normal direction as a polar axis and are the loci of all orientations which, if present, can possibly give basal plane reflections on the pattern of Fig. 14. As before, the dotted and full lines of the figure indicate the orientations definitely found to be absent and present, respectively.

Figure 15, which is a transmission pattern exposed with the incident x-ray beam at 50° to the rolling plane and at 90° to the rolling direction, gives the orientations on the small circles 5-5. The lines *C*-*C* are the traces of the equatorial planes of the 8° small circles 5-5. The equatorial planes *C*-*C* make angles of 40° to the rolling plane *B*-*B*.

Figure 16, which is a transmission pattern obtained with the incident x-ray beam at 28° to the rolling plane and at 90° to the transverse direction, furnishes the points 6. Because of the narrowness of the angular range 6-6, it was considered sufficiently accurate to plot these

orientations on the great circles *B*-6-6-*B* rather than on small circles as was done with the two previously discussed transmission patterns. Absorption of the diffracted x-rays in the specimen, in the exposure of this pattern, permitted only half of the pattern to be recorded. The basal plane reflections recorded are those from basal planes at approximately 36° to the rolling plane and not those from basal planes approximately 20° to the rolling plane. These considerations show that the great circles *B*-6-6-*B* should be the loci of plotting. The planes of these great circles make angles of 54° to the rolling plane. Orientations corresponding to the extension of the arcs 6-6 were indicated by the x-ray pattern, but the extremities of these arcs were not accurately measurable as in the case of the points 6.

It is assumed that regions between the linear loci of orientations found to be present are also occupied by crystal orientations in the metal specimen. Orientations are probably present in the specimen corresponding to all points on the cross-hatched areas of Fig. 18. Experience has shown that the foregoing method of plotting orientation pole figures is sufficiently precise for the practical evaluation of orientation anisotropy in rolled metal. The pole figure furnishes an excellent orientation diagram for the study of the mechanical deformation of polycrystal metal and for the study of the relation between crystal orientation and the directional properties of the worked metal.

SUMMARY

We have discussed both the methods of determining the orientations of single crystals and the methods of finding preferred orientation in polycrystal material. In the case of single crystals we took up (*a*) an optical method, (*b*) a monochromatic x-ray method, and (*c*) a "white" x-ray method. In the case of polycrystal materials we took up (*a*) Bozorth's method (most applicable when the degree of preference is high), (*b*) a cut-and-try method (tedious but foolproof) which gives the proper mental atmosphere for the pole figure method, and (*c*) the method of pole figures. In addition to forming the basis of a method for determining preferred orientations, pole figures form a useful way of expressing the results of experiments on preferred orientation, no matter which of the above methods is used. The pole figures have the advantage, too, that they indicate at once whether or not additional data must be obtained in order to determine a system of preferred orientation completely.

References

1. P. DEBYE, *Ann. Physik*, **49**, 1 (1914).
2. J. WALLER, *Zeit. Physik*, **17**, 398 (1923).
3. M. v. LAUE, *Zeit. Kryst.*, **64**, 115 (1926).
4. A. L. PATTERSON, *Zeit. Kryst.*, **66**, 637 (1928).

5. J. HENGSTENBERG, *Zeit. Kryst.*, **69**, 271 (1928).
6. J. HENGSTENBERG and H. MARK, *Zeit. Kryst.*, **70**, 283 (1929).
7. R. BRILL and H. PELZER, *Zeit. Kryst.*, **72**, 398 (1929).
8. G. L. CLARK, "Applied X-rays," 2d ed., p. 339, McGraw-Hill Book Company, Inc., New York, 1932.
9. W. P. DAVEY, *Phys. Rev.*, **23**, 764 (1924).
10. T. A. WILSON, *Gen. Elec. Rev.*, **31**, 612 (1928).
11. M. MAJIMA and S. TOGINO, *Sci. Papers, Inst. Phys. Chem. Research, Tokyo*, **7**, 75, 259 (1927).
12. R. M. BOZORTH, *Phys. Rev.*, **26**, 390 (1925).
13. H. B. DEVORE and W. P. DAVEY, *Phys. Rev.*, **31**, 160 (1928).
14. W. P. DAVEY, C. C. NITCHIE, and M. L. FULLER, *A.I.M.E. Tech. Pub.* 243 (1929); *Trans. A.I.M.E.*, Inst. Met. Div., p. 557 (1930).
15. C. B. HOLLABAUGH and W. P. DAVEY, *Metals and Alloys*, **2**, 245, 302 (1931).
16. F. WEVER, *Zeit. Physik*, **28**, 69 (1924).
17. F. WEVER, *Trans. A.I.M.E.*, Inst. Met. Div., p. 51 (1931).
18. A. HUTCHINSON, *Mineralog. Mag.*, **15**, 93 (1908).

CHAPTER XVIII

SOLID SOLUTIONS

CRITERIA FOR THE EXISTENCE OF SOLID SOLUTIONS

The characteristic property of a solution is that the solute and solvent become so intimately intermingled that the solution appears to be quite homogeneous even under the highest power microscope. Of course, no solution is homogeneous if we think in terms of atomic or molecular distances, but if we limit ourselves to distances which we can actually see with the aided or unaided human eye, a solution is homogeneous.* In other words, a solution must consist of more than one component, but it must all be a single phase. When the solvent is a liquid, it is easy to tell whether or not more than one phase is present. Usually we have only to look at it and see whether it is clear and homogeneous, or to filter it and see whether we can separate out a second phase. In case of doubt we can see whether or not the rise in the boiling point, lowering of the freezing point, etc., are less than would be expected for a truly molecular dispersion.†

When the solvent is a solid (*i.e.*, when we have a "solid solution"), all such methods fail except the method of the lowering of the melting point,‡ and even that must be used with extreme caution. We have, however, two other possible methods of attack which are based on the fact that we are dealing with crystalline solids: (*a*) we may polish and etch the surface of the specimen and see whether we can find a second

* Strictly speaking, we must limit ourselves to distances much smaller than this if we are to distinguish between true solutions and colloidal solutions.

† H. K. Ward finds [*Jour. Chem. Phys.*, **2**, 153 (1934)] that x-ray diffraction rings may be used to advantage.

‡ In metallurgical work the melting (or freezing) point is often detected by an arrest in a heating (or cooling) curve caused by the absorption (or liberation) of the latent heat of fusion. This is a sensitive method for finding melting (or freezing) points. The method is extended to the detection of changes in the phases (*e.g.*, "solution" or "precipitation") of a solid solute when the temperature is raised (or lowered). When the phase transformation is fast enough so that appreciable amounts of heat are absorbed (or liberated) per second, the method is sensitive and, when used in connection with data from the microscope and from x-ray diffraction, leads to temperature-constitution diagrams which show at once the limits of solid solubility at equilibrium. When the transformation is sluggish, it must be followed in an adiabatic calorimeter, otherwise it may be overlooked entirely. The chances for errors of technique and of interpretation may be appreciated if one follows the literature of some well-known constitution diagrams (such as Fe-C or Zn-Al) from the earliest down to provisional diagrams such as in "International Critical Tables."

phase under the microscope; or (*b*) we may use x-ray methods in the effort to detect crystals of a second phase. If a second phase is present in considerable amount and is composed of crystals of appropriate size and of random orientation, then it is usually easy to show (using the simple technique of the powder method) two diffraction patterns superimposed upon each other—one from each of the solid phases. If, however, the crystals of a second phase are extremely small or are very imperfect, they may be represented in the diffraction pattern by only one, two, or three lines and even these may be broad and indistinct in outline. If the crystals of a second phase are preferentially oriented as in the case of Fig. 9 of Chap. XII, then the simple technique of the powder method may not be sufficient and it may be necessary to oscillate the specimen.

If no second phase can be found, it may be assumed tentatively that the components with which we started are in solution. In such a case the diffraction pattern will resemble that of the solute material except that the lattice parameters may be somewhat altered.* The higher the concentration of the solute in the solution the greater is the change in the lattice parameters. It is assumed that, within the limits of concentration set by the solid solubility of the solute in the solvent, this change in lattice parameter is a continuous function of the concentration of the solute. It will be noted that, in accordance with the definition of the word "solution," the basic evidence for the existence of a given solid solution is entirely negative, *i.e.*, the evidence is based on the inability of the experimenter to demonstrate the presence of a second phase. Such evidence is obviously weak and must always be accepted with caution. In interpreting the data in the literature on solid solutions we must always ask ourselves whether a slight change in experimental technique, either in the preparation of the specimen or in the x-ray examination (more favorable wave length, different mounting of the specimen, time of exposure, etc.) might not have enabled the experimenter to have demonstrated the existence of a second phase. We must, besides, always allow for the possibility that a second phase is present but is not in such a state as to show an appreciable diffraction pattern.† A change in the lattice parameter of the solute, although it is always found in solid solutions when the concentration is sufficiently great, is not basic evidence of solid solution. It is really only a signpost,

* This change in lattice parameter reminds us at once of the well-known fact, mentioned in most elementary textbooks on physical chemistry, that in liquid solutions the volume of the solution is not, in general, exactly equal to the sum of the volumes of the solvent and of the solute.

† For instance, it may be present in crystals of colloidal size. In the case of martensitic steel the Fe_3C crystals have not been definitely demonstrated by x-ray methods although Lucas[1] has photographed them with the aid of an extremely high-power microscope.

actually empirical, but well supported by theory, as will be shown later in this chapter.

The fact that, in any given instance, the burden of proof rests with the experimenter who appears to have found a solid solution is well illustrated by the following: Data may be found in the literature[2] which seem to show several instances of two metals, A and B, with the same type of crystal structure, which are mutually soluble in all proportions with an almost straight-line change in lattice parameter from 100 per cent A to 100 per cent B. That this may not be the actual state of affairs is shown in Fig. 1, which gives the data of Holgersson and Sedström[3] on the Cu-Pd alloys. If the only compositions investigated had been those represented by the points marked in Fig. 1, the Cu-Pd system would undoubtedly have been recorded as being still one more instance of con-

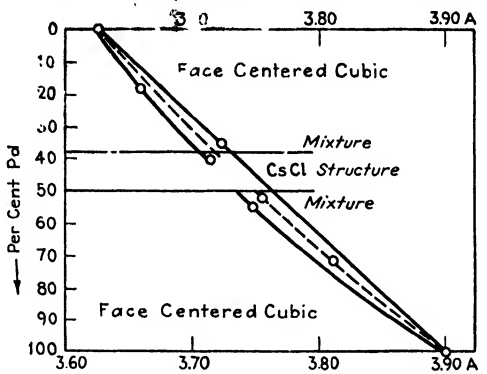

FIG. 1.—Data of Holgersson and Sedström on the Cu-Pd system.

tinuous solubility with a face-centered cubic structure whose parameter changes progressively from that of 100 per cent Cu to that of 100 per cent Pd. Fortunately, however, Holgersson and Sedström included in their experiments an alloy whose composition was 45.5 atomic per cent Pd and 54.5 atomic per cent Cu. This showed instead of the face-centered cubic diffraction pattern a body-centered pattern. This represented, of course, the existence of a new phase. The intensities of the lines in the diffraction pattern were what would have been expected for a compound Cu-Pd with Cu at the corners of the unit-cube and Pd at the body-center.* This makes us somewhat skeptical of the graphical representations of the data in the literature for other similar systems of alloys and makes us feel that careful work would possibly uncover still other examples of the same sort.

When one metal† is in solid solution in another of different crystal structure, the one which determines the crystal structure is called the

* Or, of course, Pd at the corners and Cu at the body-center.

† It is easiest to discuss solid solutions of one chemical element in another in terms of metals, for the metals are the outstanding examples of crystalline elements which

"solvent." For instance, cobalt may be either face-centered cubic or hexagonal close-packed; α-Fe is body-centered cubic. But since an alloy of 80 weight per cent cobalt is body-centered cubic,[4] it is assumed that the iron is the solvent up to 80 per cent cobalt. Zinc (hexagonal close-packed) dissolves in copper (face-centered cubic) up to about 40 per cent zinc, while copper dissolves in zinc up to about 1.8 per cent copper.[5] It is a general rule that, if A has the ability to go into solid solution in B, then B can go into solid solution in A, but the degree of solid solubility of A in B is no criterion of the degree of solubility of B in A. It is also a general rule that, if A and B have different crystal structures and if A is soluble in B (and therefore B in A), then, when A and B reach the proportions shown by the solubility limits, either they form a definite intermetallic compound or they form a eutectic mixture.* Probably instances of intermetallic compounds would be still more numerous in the x-ray literature if it were not for the difficulty, inseparable from the limitations of the solid state, of obtaining equilibrium conditions.

When it has once been established that a two-component system has only a single phase, so that it may rightfully be classed as a solid solution, it remains to determine whether the molecules (or atoms or ions) of the solute lie in between the molecules (or atoms or ions) of the solvent or whether they replace them in the crystal lattice. This may be done by comparing the density of the solid solution, determined by ordinary physical methods, with the density calculated with the aid of the lattice parameter of the solid solution. If the solution is interstitial, the calculated density must be found as

$$D = \frac{n_1 M_1 + n_2 M_2}{V} \times 1.649 \times 10^{-24}$$

where n_1 = number of molecules (or atoms or ions) of solvent in the unit of structure of the pure solvent.

n_2 = average number of molecules (or atoms or ions) of solute material in the unit of structure, calculated from the concentration of the solid solution.

M_1 = molecular (or atomic or ionic) weight of the solvent.

M_2 = molecular (or atomic or ionic) weight of the solute.

V = volume of the unit of structure of the solid solution.

If the solution is of the substitutional type, the calculated density is easiest found as

---

can be obtained in quantity in a reasonable state of purity. The use of still purer metals will make our knowledge of solid solutions much more definite.

* That is, two different crystalline phases intimately mixed together.

$$D = \frac{n \times 1.649 \times 10^{-24}}{\left(\frac{a}{M_1} + \frac{b}{M_2}\right)V}$$

where a and b are the weight-fractions of the solvent and solute, respectively, and n is the number of molecules (or atoms or ions) per unit of structure.

THEORY OF SOLID SOLUTION

Because of the very nature of the definition of the word "solution," our discussion of methods of detecting solid solutions has implied the crude picture of a mechanical dispersion of molecules (or atoms or ions) of the solute in the solvent. Assuming, now, that we have at hand a number of solid solutions, detected in accordance with the above discussion, we must examine their properties closely to find the clues which will enable us to build up a more complete picture of the physical and chemical states of the solute and solvent. Such a picture should enable us to see why some solids are soluble in a given second solid and why some others are not, and it should predict, at least in a general way, the characteristic physical and chemical properties of solid solutions. It will simplify our discussion if we take up first the simple case of liquid solutions and then add the additional complications imposed upon solid solutions by the crystalline state.

As early as 1904, Jones and Getman[6] found that the depression of the freezing point of water by cane sugar pointed to the picture of a hydration of the sugar molecules* in the solution. Callender[7] gave the same explanation for the abnormally high osmotic pressures of solutions of cane sugar.[8] The subject of solutions was examined from the standpoint of energy transfer in 1910 by Garver[9] who concluded that there must be some sort of a chemical bond between a solute and its solvent. One example out of several of Garver's lines of reasoning will be given. Suppose that an aqueous solution is merely a mechanical dispersion of n gram-molecules of solute in N gram-molecules of the solvent water. Then in a dilute solution, if the solute and solvent water are both at a common temperature before solution, the heat-energy contribution from the solute is small in comparison with that from the solvent water, and the kinetic energy E of the molecules of the solvent may, with only negligible error, be considered as being distributed among the molecules of the solution. This gives an average energy per gram-molecule of solvent water of $E/N = E_1$ and an average energy per gram-molecule of solution of $\frac{E}{N+n} = E_2$. Since the kinetic energy of the molecules is directly proportional to the absolute temperature,

* There can be no complications here due to the electrostatic interaction of positive and negative ions such as we have in the case of concentrated solutions of electrolytes.

$$\frac{E_1}{E_2} = \frac{N + n}{N} = \frac{T_1}{T_2}$$

If we apply this equation to the case of 1 gram-molecule of cane sugar dissolved in 1 l. (55.6 gram-molecules) of water at 20°C., we have

$$\frac{55.6 + 1}{55.6} = \frac{293}{T_2}$$

This gives $T_2 = 288°K.$, *i.e.*, the temperature drop due to the act of solution should be about 5°C. Actually the heat absorbed is 800 cal. so that the 1,000 g. of water would have to cool off only 0.8°C. Suppose, on the other hand, that we regard $N + n$ as our unknown quantity. Then we have

$$\frac{N + n}{55.6} = \frac{293}{292.2}$$

This gives $N + 1 = 55.8$ so that out of our original 55.6 gram-molecules of water only 54.8 gram-molecules are left. Obviously this can be accounted for by assuming a chemical combination (hydration) between the sugar and the water.

The data of the "International Critical Tables" can be used to give still other calculations which indicate the existence of chemical action between the solute and the solvent in a solution. If a solution is merely a mechanical dispersion of molecules of a solute in a solvent, then the energy needed to dissolve one mole of solute should be equal to the heat required to change the solute into a gas whose volume and temperature are the same as the volume and temperature of the solution. For a liquid solute this energy input would be $(L - W)$, where L is the molar latent heat of vaporization of the solute at the temperature of the solution and at a pressure of 1 atmosphere, and W is the mechanical work done in compressing this vapor to the volume of the solution. The quantity $(L - W)$ is, of course, always positive. Values for L can be found for various organic compounds in Vol. V of the "International Critical Tables." For instance, for glycol at 197°C., L is

$$800 \times 62 = 49{,}600 \text{ kilojoules* per gram-molecule.}$$

At room temperature it should be somewhat larger. If 1 gram-molecule of glycol at 20°C. is dissolved in $22.4 \times {}^{293}\!/_{273}$ l. of water, W is zero and the quantity of solution is so large that the solution may be regarded for our purposes as being practically infinitely dilute. The experimental facts are that, instead of our having to put in 49,600 kilojoules to cause the gram-molecule of glycol to dissolve, it dissolves spontaneously in

* One kilojoule = 239.2 g.-cal.$_{20°C.}$ = 0.948 B.t.u.$_{60°F.}$

the water with the evolution of 7.1 kilojoules of heat. This represents the spontaneous evolution of enough energy to supply the 49,600 kilojoules required on the basis of a mere mechanical dispersion of glycol molecules in the water and, besides, an additional 7.1 kilojoules.* The source of this energy must lie in the glycol-water system itself, so that we are forced to assume that the solvent has lost potential energy to the extent of almost 50,000 kilojoules per gram-molecule of glycol. The only way we can imagine such a release of energy from inside the system is to assume some sort of chemical reaction between the glycol and the water.

The chemical state of the components in a liquid solution may be shown directly by electrolytic methods. Kremann and v. Rehenburg[10] were able to electrolyze molten binary metallic alloys. Of course any metal that might be deposited on the electrodes would tend to melt off again, so that all they could do was to balance the electrolytic effect against the back diffusion. In order to overcome this difficulty, they electrolyzed for some time and then suddenly chilled the whole melt, thus preserving in the frozen state the conditions which they had during electrolysis. That they succeeded is shown by the fact that as the current density was raised in the experiment the divergence in composition approached a maximum. An alloy of 39 per cent Zn, 61 per cent Sb, electrolyzed at 620°C. with a current density of 7.6 amp. per square millimeter gave a maximum difference in composition between the two electrode areas of 75 per cent. The Sb migrated to the anode and was therefore the negative ion. This is consistent with the positions of the two metals in the periodic table. When an alloy of 58 per cent Bi and 42 per cent Pb was electrolyzed at 240°C. and at a current density of 10 amp. per square millimeter, the Bi tended to concentrate at the anode. This again is consistent with the periodic table. In a 33 per cent Na amalgam at 240°C. and at a current density of 7 amp. per square millimeter, the Hg migrated to the anode and the effect amounted to 9 per cent Na. The alloy 70 per cent K and 30 per cent Na is liquid at room temperature. Kremann and v. Rehenburg electrolyzed it at 100°C. in a glass capillary 1 mm. in diameter. The electrodes were of copper, and the current density was varied from 1.4 to 7.17 amp. per square millimeter in successive experiments. After electrolysis had continued for 4 hr., the capillary was chilled and cut into short lengths. Analysis of the contents of each section showed that the concentration of Na was increased at the anode and that of the K was increased at the cathode. When the current density was 1.4 amp. per square millimeter, the change in concentration of the K was about 10 per cent; at 4.45 amp. per square

* The reader will find in Vol. V of the "International Critical Tables" the data for a multitude of similar calculations, both for aqueous and for non-aqueous solutions.

millimeter, it was 24.5 per cent; at 7.17 amp. per square millimeter, it was 32.5 per cent. When even Na and K show evidence of ionization when in solution in each other, it is hard to keep from making the generalization that the components of all liquid solutions are in some sort of chemical combination with each other. Of course this does not mean that the law of definite proportions can always be demonstrated, especially in the sense in which it is explained to students in elementary chemistry.* It does mean that we must assume the forces acting between solvent and solute to be chemical in their nature and the energies involved to be truly chemical energies. We may even go so far as to assume that, instead of a tendency to produce a mechanical dispersion of molecules (or atoms or ions) of A in B, we have a tendency to produce a mechanical dispersion of "molecules" of the compound A_xB_y in B. In other words, when A is dissolved in B, we may assume that we have a weak chemical reaction corresponding to

$$xA + yB \longleftrightarrow A_xB_y$$

The mass action law demands the presence of a little A along with the compound A_xB_y and these two together are to be considered as forming the real solute which is dispersed in B.†‡

If we once accept this picture in the case of liquid solutions, it is evident that we must carry it over to the case of solid solutions.§ That chemical combination of this sort exists in solid solutions is shown directly by the experiments of Hanawalt[12] who studied the palladium-hydrogen

* In the first place, the concentration of solute in the crystals of solvent is not given by the over-all proportions of solute and solvent. This may be explained by the work of Phillips and Brick[11] who were led to assume that the solubility in the crystal depends upon the grain size, *i.e.*, upon the area available at the grain boundaries. In some cases we may assume besides that the mass-action constant is such as to require a considerable excess of one component. In other cases we may be compelled to speak of secondary valence effects. In any case, in order that the law of definite proportions may be applied, we must consider it in terms of isolated molecules (or atoms or ions) of solute, not in terms of the total masses of solute and solvent. This may be illustrated by a so-called "aqueous" solution of CO_2, which undoubtedly contains H_2CO_3 dissolved in the water. The H_2CO_3 can be decomposed merely by pumping off CO_2 from above the solution, and the law of definite proportions must be applied to each individual molecule of CO_2 which combines with the water.

† In the following, the word "solute" will be reserved for the material which was originally added to the solvent, *i.e.*, when A is added to B to make a solid solution of A plus A_xB_y in B, A will be called the solute.

‡ This point of view receives strong experimental support from the studies of G. W. Stewart [*Jour. Chem. Physics*, **2**, 147 (1934)] on x-ray diffraction effects in solutions of LiCl in normal alcohols. He finds definite evidence that a portion of the solvent is bound to the ions of the solute.

§ The arguments against this type of picture can be found in nearly any textbook on metallography. Most of them are founded on data or depend upon certain viewpoints which seem to the author to be open to question.

system.* He found that his experiments on the characteristic absorption of x-rays, together with his experiments on the lattice parameters of these solid solutions, could be interpreted easily by assuming that he had, not a solid solution of hydrogen, but a solid solution of PdH in palladium. That is, some of the points on the palladium lattice were occupied by "molecules" of PdH. When half the points were so occupied, he had the well-known compound Pd_2H. This interpretation is consistent with the data of Coehn[13] who found that, when he passed an electric current through a palladium wire in which hydrogen was dissolved, the diffusion of hydrogen was greater in the "direction of the current" than in the direction of flow of electrons. Evidently at least a portion of the hydrogen was present as H^+ in the solid solution.

Hanawalt's conclusions are also consistent with Ham's interpretation[14] of the mechanism of diffusion of hydrogen through thin metal sheets. Using well-established principles of the kinetic theory of gases, Ham has worked over the data of Borelius[15] on the flow of hydrogen through thin sheets of platinum or nickel together with additional data of his own on the flow of hydrogen through welded sheets one face of which was platinum and the other face nickel. He found that, if he expressed the rate of flow of hydrogen through the sheet in terms of the pressure p_0 of molecular hydrogen at the inlet face of the sheet, then p_0 entered into his equations in the form of $p_0^{1/2}$. Ham accounted for the necessity of using the square root of the intake pressure by assuming that $p_0^{1/2}$ was proportional to the pressure of hydrogen at some plane, parallel to the face of the metal sheet, situated inside the metal near the inlet face. This led him to use the mass-action law for a reaction of the first order. The mass-action law gives us three, and only three, alternatives, namely,

$$(a)\quad H_2 \longleftrightarrow 2H$$
$$(b)\quad H_2 \longleftrightarrow H_2^+ + \epsilon^-$$
$$(c)\quad H_2 \longleftrightarrow 2H^+ + 2\epsilon^-$$

where ϵ^- represents an electron.

* The length of the edge of the unit face-centered cube of palladium (99.66 per cent pure) is 3.885Å. Hanawalt found that, when he dissolved hydrogen in pure palladium, the edge of the unit-cube became 4.017Å. or larger, but the x-ray diffraction pattern was still that of a face-centered cube. No lattice parameters were found between 3.885Å. and 4.017Å. if impurities were absent, but parameters of 4.017Å. or greater could be found depending upon the concentration of hydrogen. Solutions with a lattice parameter greater than 4.017Å. shrank continuously on aging with loss of hydrogen until the value of 4.017 was reached no matter whether the solid solution was kept at 20°, 50°, 70°, or 90°C. When the palladium was impure (containing Cu, Fe, Si), it was possible to get solid solutions of hydrogen over the whole range, giving continuous variations in the values of the edge of the unit-cube from 3.885Å. to beyond 4.017Å.

The first of these must be discarded because it involves no ionization of hydrogen and is therefore inconsistent with the fact, already recorded in the literature,[16] that the metal picks up an electrostatic charge in the presence of hydrogen. Alternative (*b*) must be discarded since it does not lead to the correct exponent of p_0, when pressure is used as an index of concentration. This leaves us with only alternative (*c*), namely,

$$H_2 \longleftrightarrow 2H^+ + 2\epsilon^-$$

which obviously accounts for the exponent of p_0* and accounts qualitatively for the electrostatic charge on the metal. Obviously, the ionization of the hydrogen implies the formation of an ionic compound with the solvent metal.

As still further confirmation of the picture of chemical reaction between the solvent and the solute of a solid solution it is interesting to note that Mehl and Mair[17] have used the degree of compressibility of metallic solid solutions as a criterion of chemical combination between the solute and the solvent metal. They compared the experimentally measured compressibilities of solid solutions of metals with calculated values based on the compressibilities of the solvent and solute. They found that the discrepancies between the experimental and calculated values were greater the more the solvent and solute differed in chemical type, and that in every case where numerical data were available the experimental values of compressibility were smaller than the calculated values. They interpreted this to mean that the solute and solvent were in each case compressed together by chemical forces so that externally applied compressive forces had less effect than if the solid solutions had been mere mechanical dispersions of atoms.†

* When pressure is used as an index of concentration in the mass-action-law equation, it is evident that the term $2\epsilon^-$ disappears since electrons exert no pressure.

† Experiments by Phelps and Davey[18] on solid solutions of aluminum (99.971 per cent) in pure silver (made by reduction of Baker's Analyzed C. P. $AgNO_3$) showed that the densities of the solid solutions were less than could be calculated on the basis of merely substituting atoms of Al for atoms of Ag in the crystal lattice. This was interpreted to mean that, instead of a mechanical dispersion of Al atoms in the Ag lattice, there was present a dispersion of "molecules" of Ag_3Al or even of submicroscopic (so small, indeed, that they could not show diffraction patterns under the conditions of the experiments) crystals of the intermetallic compound Ag_3Al whose low density would account for the low over-all densities of the solid solutions. Barrett[19] was, however, unable to confirm these results in spite of long and careful annealing on certain of his specimens. This may mean that either Barrett or Phelps and Davey had some unrecognized error in their experiments, or it may mean that Barrett did not succeed in growing submicroscopic aggregates of Ag_3Al. At the time this is written, there is no way, short of time-consuming repetition of the whole set of experiments, of deciding between these two alternatives. The result is that we cannot, with certainty, use the published data on discrepancies in density as an aid to the study of solid solutions.

If we accept the picture of chemical combination between solvent and solute, we have at once a qualitative explanation of the well-known fact that the electrical conductivity of metallic solid solutions is considerably less than that of the pure solvent metal. If the solute is in chemical combination with the solvent, an appreciable fraction of the valence electrons (which carry the electric current) are tied up to the negative ions of the solid solution. In other words, except at high temperatures, the compound of solute and solvent acts like a nonconductor of electricity. The valence electrons of the uncombined solvent can no longer travel directly along the potential gradient; they must travel around the molecules (or even submicroscopic crystals) of the chemical compound. The effect is as though the cross-section of the conductor were decreased and its length increased. Such a result would hardly have been predicted on the basis of a mere mechanical dispersion of solute in solvent.

Our picture gives us a reasonable explanation of the experimental fact that, in general, the lattice parameter of a solid solution is either larger or smaller than that of the pure solid solvent. This can be illustrated in terms of metallic solid solutions which have already been mentioned. If a "molecule" of compound merely replaces an atom of the solvent metal and is larger than the atom which it replaces, then of course the lattice parameter will be increased. This was the case in Hanawalt's experiments in which a molecule of PdH replaced an atom of Pd in the crystal lattice. The effect needs only to be mechanical—merely a matter of pushing atoms of solvent metal a little farther away from each other in the neighborhood of the "molecule" of the compound. If, instead, the solute and solvent tend to form an ionic intermetallic compound,* the electrostatic forces between adjacent ions will tend to pull them closer together. If the combined volume of the compressed ions is less than that of the atoms of solvent metal whose places they occupy, then the effective lattice parameter is decreased. This is illustrated by the case of solid solutions of palladium in copper (see Fig. 1) or of aluminum in silver. The two-dimensional analogy is shown in Fig. 2. The chains of solvent metal, held together by cohesive forces, would transmit the pull from the ions to the rest of the crystal. The effect would be comparable to the pull of a rope tied around a bundle. Just as the bundle is put under compression, so the crystal of solvent metal is put under compression. Similarly, if the combined volume of the compressed ions is greater than that of the atoms of solvent metal whose places they occupy, then the lattice parameter is increased. This is illustrated by the case of solid solutions of copper in

* That is, in the same sense that NaCl is ionic (see Chap. XIX). In many cases the ionic nature of intermetallic compounds is much more complicated. This is brought out in the discussion of Hume-Rothery's rule in Chap. XIX.

palladium (see Fig. 1). The situation is now much as in the case of the Pd-H system, and the necessary changes in wording of the foregoing and the changes in Fig. 2 will be obvious. Irrespective of whether the lattice parameter is increased or decreased, the regions near the ions would be distorted and so would produce little or no x-ray diffraction pattern. This is consistent with the experimental fact that the diffraction pattern of the solvent metal becomes weaker as the percentage of solute is increased. The portion of the crystal of solvent metal midway between "molecules" of intermetallic compound would show

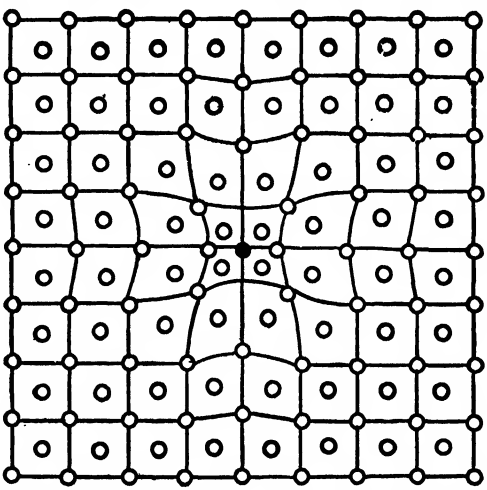

FIG. 2.—Two-dimensional analogy of a solid solution of A in B (*i.e.*, of A_xB_y in B) in the completely disaggregated state.

either a smaller lattice parameter due to the compression or a larger parameter due to the expansion, again agreeing with the results of experiment.

Our picture of solid solution offers a simple mechanism for the experimental facts of the "precipitation" of an intermetallic compound* from solid solution.[18] This will be illustrated by the case of Ag_3Al. (Fe_3C or any similar compound might have been used equally well). According to our picture we should expect the aluminum in solid solution in silver to be in the form of Al^{---} and we should expect every Al^{---} to be accompanied by three Ag^+ to give Ag_3Al. We may assume that, if the Al^{---} migrates in the crystal, it can hand back a valence electron to one Ag^+ and pick up one from a neutral Ag in its path. In this way, although we should always have the Al^{---} as part of Ag_3Al, it is not necessary to picture migrations for anything except the Al^{---}. If, during migration, two or more Al^{---} happen to fall into the correct spatial relationship for the lattice of Ag_3Al, they will tend to stay there. If, now, a third and

* A short discussion of intermetallic compounds is given in Chap. XIX.

a fourth Al^{---} happen to fall into the correct positions with respect to the first two, they will have a still greater tendency to remain, so that tiny aggregates of Ag_3Al can be built up. In general these aggregates will be too small to give an x-ray diffraction pattern. Since the presence of these tiny particles of Ag_3Al cannot be demonstrated either by x-rays or by the microscope, we must classify the alloy as a solid solution; the existence of the second phase is here a matter of theory, not of demonstrable fact. The final size of the aggregates will be the result of two opposing tendencies: (1) a tendency toward disaggregation, which should be a function of the temperature, and (2) a tendency toward aggregation which should be a function of the concentration of Al^{---}. Therefore at a given temperature and a given concentration of Al^{---}, a definite proportion of the Al^{---} will necessarily be in ionic dispersion in the silver, and the rest of the Al^{---} will be in the tiny aggregates of Ag_3Al. As the concentration of Al^{---} is increased, more and more of the silver will be in the form of Ag_3Al and will not contribute to the diffraction pattern of the compressed silver. More and more time should therefore be required to obtain diffraction patterns of the solid solution as the percentage of aluminum is increased. This is in agreement with the experimental facts. As the concentration of Al^{---} is still further increased, the tendency toward aggregation should become so large that the aggregates of Ag_3Al should begin to show diffraction patterns of their own. The existence of the second phase is now no longer a matter of theory but is a demonstrable fact. The alloy is manifestly no longer homogeneous and therefore the alloy as a whole is no longer to be called a solid solution. As the diffraction patterns of silver continue to decrease in intensity due to the high percentage of Ag_3Al, the patterns of Ag_3Al should increase in intensity. Here again the predictions of the theory are in accord with the facts of experiment. The two-dimensional analogy for these aggregates of Ag_3Al is shown in Fig. 3. It is not to be assumed that the crystals of the new phase, Ag_3Al, will be perfect. In the first place, we learned in Chap. XII that the precipitate will tend to form first along the grain boundaries of the silver and in the Π-crevices so that they will have the best possible chance of picking up such impurities as may happen to be present. In the second place there is the probability that, as ions of Al^{---} cluster together with their fellows and with Ag^{+}, some neutral atoms of silver will remain mechanically enclosed in the Ag_3Al crystal. Of course, this imperfection of the crystals of the precipitate adds still more to the difficulties of the crystal analyst in demonstrating by x-ray methods the existence of a second phase in a suspected "solid solution."

So far we have discussed the chemical conditions which must be satisfied in order that we may have a solid solution. There remains to be discussed what physical conditions (*e.g.*, size and shape of atomic and ionic domains) must also be satisfied. These physical conditions

can be visualized most clearly in the case of mix-crystals and will therefore be treated under that heading.

Mix-crystals.—We have seen both in the case of liquid solutions and in the case of solid solutions that there is a good reason for assuming the forces involved to be chemical in their nature. So far, the solid solutions which we have studied have had chemical elements as solute and solvent. It will be of interest to see how our picture will apply to the special case of solid solution in which both solute and solvent are ionic compounds. Standard classroom examples of such solid solutions are the system AgCl-NaCl or the system $HgBr_2$-HgI_2. It will be noticed that in both

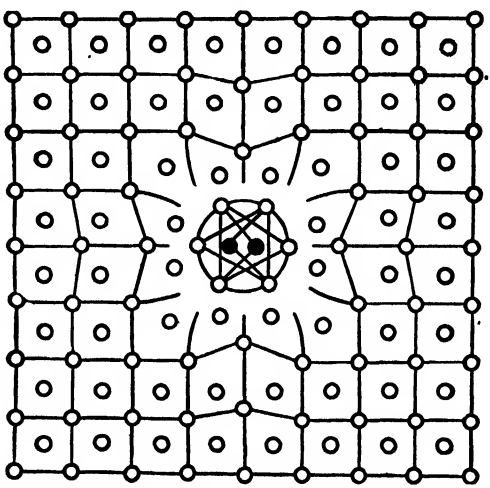

FIG. 3.—Two-dimensional analogy of a solid solution of A in B (*i.e.*, of A_xB_y in B) in a partially aggregated state.

of these examples we are dealing with two ionic salts which have a common ion. Although the common ion is not a requirement, most of the best known solid solutions of one ionic salt in another contain a common ion. Solutions of this type were called by German investigators "Mischkristalle." The word was mistranslated as "mixed crystals" and the error has persisted in the literature. A better translation would have been "crystals composed of mixtures," or briefly "mix-crystals." When two salts have a common ion and both have the same crystal structure, it is not possible (except on the basis of proportions) to distinguish between the solute and the solvent. In such cases the chemical nature of the solid solution is easily recognized. For instance, in the system AgCl-NaCl it makes no chemical difference to a Cl^- ion whether it is symmetrically surrounded by six Ag^+, or by six Na^+, or by $n Ag^+$ and $(6 - n)Na^+$. Obviously the chemical conditions for solution are already satisfied. The act of solution involves, therefore, only the heat required to equal the mechanical work of diffusing the ions of one salt among the

ions of the other. This heat corresponds to the heat required by a gas expanding against a small external force.* The heat of solid solution for a mix-crystal should therefore be either negligibly small or positive.† That this is so is shown in Table I.

Granting that we have the proper chemical prerequisites for solid solution, there remains the geometrical prerequisite as to whether the sizes and shapes of the ionic domains are such as to permit the mix-

TABLE I.—HEATS OF SOLUTION FOR VARIOUS MIX-CRYSTALS

System	Heat of solution, calories	References [quoted by G. Bruni, *Chem. Rev.*, **1**, 345 (1925)]
$KClO_3$-$KMnO_4$	0	*a*
$FeSO_4$-$CdSO_4$	0 or +	*a*
KCl-NaCl	2,100	*b*
KBr-NaBr	1,400	*b*
KI-NaI	1,250	*b*
KCl-RbCl	+	*c*
KCl-KBr	220	*d*
KBr-KI	390	*d*
KCl-KI	551	*d*
$NaNO_3$-$NaNO_2$	400	*e*
$NaNO_3$-KNO_3	0	*f*, *g*

[a] SOMMERFELD, *Zeit. phys. Chem.*, **36**, 754 (1901).
[b] KURNAKOW and ZEMCZUZNY, *Zeit. anorg. Chem.*, **52**, 186 (1907).
[c] ZEMCZUZNY and RAMBACH, *Zeit. anorg. Chem.*, **65**, 403 (1910).
[d] BRUNI and AMADORI, *Atti ist. Veneto*, **71**, 51 (1911).
[e] BRUNI and MENEGHINI, *Gazz. chim. ital.*, **40**, 1 (1910).
[f] ZAWIDSKI and SCHAZZER, *Kosmos*, **35**, 498 (1910).
[g] AMADORI, *Atti ist. Veneto*, **72**, 451 (1912).

crystal to form. It seems reasonable to suppose that two ionic compounds would dissolve most easily in solid solution in each other if their ionic domains were of the same size and shape. It is easy to insure the same shape of ionic domains, for we have only to pick ionic compounds which have the same type of crystal structure, for instance, NaCl and AgCl. We cannot hope to find the same size of domains for the ions of two different chemical elements, but we can choose ions whose domains cover a definite range of sizes. In this way we can hope to find out how closely the sizes of the two ionic domains must approximate each other in order that mix-crystals may form. This was done by Havighurst, Mack, and Blake.[20] Since they worked with salts with a common ion,

* The heat of vaporization hardly enters into the calculation in the case of mix-crystals. For instance, each Ag^+ ion in AgCl is symmetrically surrounded by six Cl^- ions; when AgCl is in solid solution in NaCl, each Ag^+ ion is still surrounded by six Cl^- ions.

† Positive according to the rational convention of signs. Negative according to the egocentric convention.

they were able to use the difference between the lattice parameters as measures of the difference in radii of the domains of the other ions. They found that, if two such salts had lattice parameters a_1 and a_2 and if they had a similar crystal structure, then mix-crystals could be formed, if

$$\delta = \frac{a_1 - a_2}{\frac{1}{2}(a_1 + a_2)} < 0.05$$

In other words, given two ionic compounds with a common ion, the two non-common ions are sufficiently similar for the salts to form mix-crystals if,[20,21] (1) the shapes of the domains of the non-common ions are identical, and (2) the difference between the radii of the domains of the non-common ions is not more than 5 per cent of the average of the lattice parameters of the two salts.

Much the same sort of rule must apply to solid solutions of the substitutional type of one metal in another except that probably we should use the ionic domain of the solute metal and the atomic domain of the solvent metal. Unfortunately we know almost nothing about the sizes of the negative ionic domains of metals.

It was stated at the beginning of this section that, although a common ion is customary in mix-crystals, it is not necessary. It is the degree of similarity in size and shape of the ionic domains that decides whether or not a mix-crystal can be formed. For instance[21] $BaSO_4$ and $KMnO_4$ form well-defined mix-crystals together. Similarly NaBr or NaCl (but not RbBr which has too large a lattice parameter) may be seeded with freshly cleaved RbS.[21]

Mix-crystals are sufficiently simple in structure so that it is possible to study quantitatively the change in the lattice parameter of the solvent caused by the presence of the solute. For such cases, Havighurst, Mack, and Blake[20] propose the general equation for cubic crystals:

$$a^n = a_1^n + (a_2^n - a_1^n)x$$

where a = edge of the unit cube of the solid solution.
a_1 = edge of the unit cube of the solvent.
a_2 = edge of the unit cube of the solute.
x = mole fraction of the solute.

When $n = 8$ or 3, this becomes the special case of Grimm and Herzfeld's formula.[22] When $n = 3$ or 1, it becomes the special case of Vegard's formula.[23] Havighurst, Mack, and Blake find that their data favor $n = 3$. If this is correct, it makes an easy interpretation of their equation in terms of the volumes of the unit-cubes of solution, solvent and solute.

It is to be assumed that the ions of the same sign in a mix-crystal are arranged together in an absolutely random fashion. If, for example, we could examine a mix-crystal of AgCl-NaCl and if we could plot the

frequency with which two, three, four, etc., Ag^+ ions (or Na^+ ions) occupy adjacent positive points in the lattice, we would obtain a probability curve. If we found the frequency of clustering to be much in excess of this, we should assume at once, either that the molten salts had been incompletely mixed together before being frozen, or that at the temperature of the solid they were insoluble in each other. In such a case, we should be able to demonstrate the presence of AgCl and NaCl by their characteristic diffraction patterns. On the other hand, there is no evidence that Ag^+ and Na^+ tend to become uniformly distributed in the crystal. Such a condition would give regular, periodic spacings of $Ag^+ - Ag^+$ and of $Na^+ - Na^+$. These periodic spacings should, in turn, give rise to faint new lines in the diffraction pattern of the solid solution. Such lines have never been found for a mix-crystal.[24] They have been found in the case of: (*a*) 0.25Si + 0.75Fe,*[25] corresponding to a possible chemical compound Fe_3Si; (*b*) 0.5Pd + 0.5Cu, which we have already recognized as the chemical compound PdCu; (*c*) 0.25Au + 0.75Cu,[26] which we shall learn in Chap. XIX to consider as a chemical compound. In general, a tendency toward a truly uniform distribution of a solute in a solvent is evidence of definite chemical combination. It cannot occur in mix-crystals where the chemical prerequisites for solid solution have already been met by the very nature of the solvent and solute.

Mechanism of Diffusion in Solid Solutions.—There are two ways in which we may picture the diffusion of a solid solute through a solid solvent. The first of these has already been hinted at in Chaps. XII and XIII. In terms of the kinetic theory we picture each of the molecules (or atoms or ions) to be in random motion within a limited region. It is a result of the randomness of these motions that a given group of adjacent molecules (or atoms or ions) will at one instant be clustered close together and at some other instant will be separated by relatively large distances. If, now, in a group containing several molecules (or atoms or ions) of the solvent and one molecule (or atom or ion) of solute, the molecules of solvent should happen to move apart from each other, and if at the same instant the molecule of solute should happen to be moving in the direction of the opening, and if it should happen at the next instant that the molecules of solvent should come close to each other again immediately behind the molecule of solute—if all this succession of chance occurrences should take place—then the molecule of solute would have diffused by one step. Jeffries has calculated[27] the number of vibrations necessary, on the average, for an atom (ion) of copper to travel one atomic diameter in nickel. Copper diffuses into

* The author was informed by John S. Marsh that the "superlattice" lines may be found over a wide range of concentrations down to 12.5 atomic per cent Si. In this connection see Fig. 5*b* of Chap. VI.

nickel at the rate of 0.025 cm. in 140 hr. at 1000°C., or about two atomic diameters per second. The rate of thermal vibration of the atoms is somewhat in excess of 10^{12} times per second. It is evident, then, that, if the copper could travel in a straight line in the nickel, it would have to make one step for every 500,000,000,000 vibrations. Even if the actual zigzag path of the copper ion were such that only one step out of 500 could be effective in the forward diffusion of the copper, we would still have the stupendous figure of 1,000,000,000 vibrations for a step of a single atomic diameter. The number of vibrations per step for carbon in iron is about $\frac{1}{200}$ that for copper in nickel. It is evident, then, that the process of diffusion is a relatively sluggish process. The only ways in which diffusion can be hastened, according to this picture, are (*a*) by increasing the number of vibrations per second, *i.e.*, by raising the temperature, or possibly (*b*) by expanding the crystal lattice through the action of some second solute. Both of these conclusions seem to be in accord with ordinary metallurgical experience.

This simple picture of the mechanism of diffusion cannot be more than an approximation to reality, for it does not lead to the experimental fact[28] that diffusion is more sluggish in metals of low symmetry than in metals of high symmetry. A theory of diffusion put forward by Langmuir[29] overcomes this difficulty. Langmuir assumes that a whole row of atoms can move lengthwise in a crystal over a distance of at least one atomic diameter. Since every atom must, by the very nature of crystal structure, lie simultaneously in a large number of such rows, we have a possible picture of the diffusion process. If one row containing an atom (ion) of solute happened to move by one atomic diameter, and if, while it was at rest in this new position, another row containing the same atom moved in some other direction, then the atom would have suffered a net change in position of one step in a diagonal direction. The chance of diffusion of the atom would then depend upon (1) the chance that the first row will move as much as an atomic diameter, (2) the chance that the first row will stand still at such a place that the atoms once more fit into the crystal structure, (3) the chance that the second, intersecting, row will move as much as an atomic diameter at the time the first row is standing still. Rosenhain has described the successive movements of "upwards of one row, horizontally of another, horizontally of another again, and downwards of the fourth" as a "sort of puss-in-the-corner game with very limited rules." It is easy to guess that the degree of probability of diffusion is no greater on this theory than on the one first described. It has the advantage that the motion of a whole row will be easier the more closely packed it is (*i.e.*, the more important the zone axis is), or, what amounts to the same thing, the greater the spacing between the centers of atoms of adjacent rows. This requires diffusion to take place most readily along the directions of the most important

zone axes. Since the number of zone axes of a given form is greater in crystals of high symmetry, it follows that the rate of diffusion should be greater the higher the symmetry of the solvent material.

SUMMARY

We have discussed the criteria for the existence of solid solutions and have found that the burden of proof of solid solution rests upon the experimenter. We have discussed the evidence for the chemical nature of the forces which are responsible for the act of solution and have arrived at a picture of solid solution which seems to correlate the available experimental data. This picture differs from that which will be found in the literature and in most textbooks on metallography. We have found that mix-crystals form a special case under our picture of solid solution, and we have used the data from mix-crystals to discover some clues as to the geometrical condition which must be satisfied before we can have a solid solution. Finally, we have discussed the mechanism of diffusion by which molecules (or atoms or ions) can come to equilibrium in a solid solution.

References

1. F. F. Lucas, *Trans. Amer. Soc. Steel Treating*, **6**, 669 (1924).
2. "International Critical Tables," Vol. I, pp. 345–351, McGraw-Hill Book Company, Inc., New York.
3. S. Holgersson and E. Sedström, *Ann. Physik*, **75**, 143 (1924).
4. M. R. Andrews, *Phys. Rev.*, **18**, 245 (1921).
5. W. M. Peirce, *Trans. A.I.M.E.*, **68**, 767 (1922).
6. H. C. Jones and F. H. Getman, *Amer. Chem. Jour.*, **32**, 308 (1904).
7. H. L. Callender, *Proc. Roy. Soc.*, **80**, 466 (1908).
8. The Earl of Berkeley and E. G. J. Hartley, *Proc. Roy. Soc.*, **73**, 436 (1904); *Trans. Roy. Soc.*, **206**, 481 (1906).
9. M. M. Garver, *Jour. Phys. Chem.*, **14**, 260 (1910); **15**, 20 (1910).
10. R. Kremann and R. G. v. Rehenburg, *Zeit. phys. Chem.*, **110**, 559 (1924).
11. A. Phillips and R. M. Brick, *Jour. Franklin Inst.*, **215**, 557 (1933).
12. J. D. Hanawalt, *Phys. Rev.*, **33**, 444 (1929).
13. A. Coehn, *Naturwissenschaften*, **11**, 183 (1928); *Zeit. Elektrochemie*, **35**, 676 (1929).
14. W. R. Ham, paper presented at February, 1933, meeting of the A.I.M.E.; also *Jour. Chem. Phys.*, **1**, 476 (1933).
15. G. Borelius and S. Lindblom, *Ann. Physik*, **82**, 201 (1927).
16. O. W. Richardson, "Emission of Electricity from Hot Bodies," Longmans, Green & Co., New York, 1921.
17. R. F. Mehl and B. J. Mair, *Jour. Amer. Chem. Soc.*, **50**, 55 (1928).
18. R. T. Phelps and W. P. Davey, *Trans. A.I.M.E.*, Inst. Met. Div., **99**, 234 (1932).
19. C. S. Barrett, *Metals and Alloys*, **4**, 63 (1933).
20. R. J. Havighurst, E. Mack and F. C. Blake, *Jour. Amer. Chem. Soc.*, **47**, 29 (1925).
21. H. G. Grimm, *Zeit. Elektrochemie*, **30**, 467 (1924).
22. H. G. Grimm, and K. F. Herzfeld, *Zeit. Physik*, **16**, 77 (1923).
23. L. Vegard, *Zeit. Physik*, **5**, 17 (1921).
24. M. v. Laue, *Ann. Physik*, **78**, 167 (1925).
25. G. Tammann, *Ann. Physik*, **79**, 81 (1926).

26. E. Bain, *Chem. Met. Eng.*, **26**, 655 (1922); **28**, 65 (1923).
27. Z. Jeffries, Third Annual Lecture, A.I.M.E., Inst. Met. Div.; *Trans. A.I.M.E.*, **70**, 303 (1924).
28. W. Rosenhain, *Trans. Inst. Metals*, **30**, 3 (1923).
29. Quoted by Z. Jeffries (reference 27) and by W. Rosenhain, Thirteenth May Lecture, Institute of Metals, *Jour. Inst. Metals*, **30**, 3 (1923).

CHAPTER XIX

CHEMICAL INFORMATION TO BE GAINED FROM CRYSTAL-STRUCTURE STUDIES

In previous chapters we have frequently had occasion to mention specific items of chemical information which had a direct bearing on the subject of crystal structure. We shall now look at the other side of the picture and shall attempt to collect some of the chemical information which may be gained from a study of crystals. It is hoped that the topics to be discussed and the illustrations used may enable the student to read the chemical literature more easily and may help him make intelligent chemical applications of crystal-structure technique.

TYPES OF CHEMICAL COMBINATION

a. **Molecular Compounds.**—The basis of chemistry lies in the distinction between elements and compounds and in the law that compounds contain definite proportions of their component elements. In the early days of chemistry this gave rise to the simple picture that compounds were made up of units, called "molecules," and that each molecule was made up of atoms of the component elements. At the time this simple picture was first suggested, it was not regarded as being anything more than a speculation with only a shadowy foundation in experimental fact. It was taken more and more seriously as more data became available until finally it became universally accepted as a working hypothesis. It was recognized, however, that the evidence for the picture was indirect and that exceptions had to be made at least in the case of aqueous solutions of electrolytes. The methods of crystal analysis offered for the first time a very direct type of evidence in connection with this problem. It is now possible, if we once grant the atomic nature of the elements, to find whether or not the atoms in a compound are grouped together in definite proportions in physical entities which may therefore be called molecules.

It turns out that not all compounds have their atoms so grouped as to show the existence of molecules, but apparently all non-electrolytes are molecular in structure. Such compounds are said to be "molecular," "non-polar," or "homopolar" compounds. Of the crystalline inorganic compounds which are molecular, the best known are Fe_2O_3, Al_2O_3, Cr_2O_3, SiO_2, and SnI_4.* Crystal analysis of the first three of these

* Others are Ga_2O_3, Ti_2O_3, and V_2O_3 with the same structure as Fe_2O_3.

Ice is undoubtedly molecular since the ion-product constant of water is so small; but the x-ray diffraction effects from hydrogen are so small that the crystal-structure data hardly constitute direct evidence of molecular grouping.

indicates that three oxygens lie at the corners of an equilateral triangle with one of the two metal atoms immediately above and the other immediately below the center of the triangle. The whole crystal is made up of a succession of groups of this sort, so that the three oxygens are somewhat closer to the two metals atoms of their own group than they are to the metal atoms of adjacent groups. In other words, the three oxygens "belong" to the two metal atoms in the manner suggested by the chemical formula. If we adopt the picture that the atoms in molecules of this sort are held together by sharing their valence electrons, then it follows that these materials should have no free electrons with which to conduct electricity in the way that metals do and because of the size of the molecules they should not be able to conduct by the actual transport of material in the way that electrolytes do. It is interesting to note in this connection that Al_2O_3 is a good insulator even at temperatures near its melting point and that it shows no tendency to electrolyze.

The structure of quartz has already been discussed in Chap. VI. The molecule is shaped like a bent arm with the silicon at the elbow and an oxygen at the hand and at the shoulder. At room temperature the two oxygens are slightly closer to their "own" silicon than to the other silicons in the neighborhood, so that at ordinary temperatures quartz may be said to be made up of real molecules. The difference in distance is small enough, however, so that at elevated temperatures the heat motion will cause a large number of oxygens at any given instant to be closer to the silicons of some other molecule than they are to their own silicons. At such temperatures the word "molecule" ceases to have any meaning for quartz beyond an indication of the stoichiometrical proportions of oxygen and silicon. Quartz changes, then, from a molecular compound to an ionic compound (see section *b*) when the temperature is raised sufficiently. This gives a rational explanation for the fact that quartz is a good insulator at room temperature and a relatively good conductor near its melting point.

The structure of SnI_4 is not one of simple groupings of SnI_4 as one might expect. Instead, this compound seems to crystallize with a face-centered cubic distribution of the complex molecule $(SnI_4)_2$.

The inorganic radicals such as SO_3^{--}, SO_4^{--}, NO_3^{-}, CO_3^{--}, etc., are real crystallographic entities so that they are regarded as having a "molecular" type of structure. In the case of the CO_3^{--} ion the shape and dimensions are quite accurately known both from crystal-structure measurements (Chap. IX) and from optical calculations (Chap. XIV). The oxygens are symmetrically placed about the central carbon atom and are closer to it than to the adjacent Ca and C atoms. The same sort of statement applies to the NO_3^{-} ion, and presumably applies to the other inorganic radicals like SO_3^{--}, SO_4^{--}, etc. It is as though the central atoms "shared" their valence electrons with the oxygens except

that the shared electrons seem to be closer to the oxygens than to the central atom, giving somewhat the effect of an ionic cluster. This picture is consistent with the intensity measurements of x-ray diffraction (Chaps. V and IX), with the optical calculations of Chap. XIV, and with the data on radicals in organic chemistry (see reference 58 of Chap. XIII).

Except for the salts of simple acids (*e.g.*, sodium acetate), all crystalline organic compounds which have been investigated so far by crystal-structure methods show the presence of real molecules. The sizes and shapes of the molecular domains of the fatty acids[1,2,3,4,5] agree fairly well with those predicted by the water-spreading methods of Langmuir[6] and Adam[7] except that the effective lengths of the molecules are about 10 per cent smaller. This will be discussed more fully later on in this chapter.

b. Ionic Compounds.—The crystal structure of NaCl has already been discussed in Chaps. I, V, VI, and IX. If a model of the NaCl structure is built, it is seen at once that each sodium is symmetrically surrounded by six chlorines all equally spaced from it, and each chlorine is similarly surrounded by six equally spaced sodiums. There is nothing in the crystal structure of NaCl to indicate that a given sodium is tied up more tightly to one chlorine than to any other of the six which surround it. In other words, there is no evidence whatever in the crystal-structure data in favor of the existence of a molecule of sodium chloride. This does not mean that sodium chloride is not a definite chemical compound. In a sodium chloride crystal of infinite extent there must be as many sodiums as chlorines so that, on a statistical basis, the law of definite proportions is obeyed. Even though the law cannot be applied in its original sense to the individual sodiums and to the individual chlorines, sodium chloride is entitled to be classed as a compound by reason of its statistical obedience to the law.

The crystal certainly contains no "molecules" except in the stoichiometric sense. It is therefore not a molecular compound. All the well-known electrolytic evidence from aqueous solutions of NaCl and from molten (and even from solid) NaCl points to the ionic state of the sodium and of the chlorine of which it is composed. It is therefore only natural for compounds of this type to be called "ionic," "polar," or "heteropolar" compounds. It is interesting to note in this connection that Hengstenberg has found[8] direct evidence from x-ray studies that solid KCl is composed of ions not atoms. He distorted a KCl crystal by placing a strong electrostatic field (20 kv. on a crystal 0.35 mm. thick, and 18 kv. on a crystal 0.20 mm. thick) across the two opposite (1 0 0) faces while the crystal was diffracting MoK_β rays. He found that the intensity of the tenth-order diffracted beam from the (0 1 0) planes was altered by 2 and 5 per cent, respectively, for the two samples which he

used. This change in intensity agrees with the distortion calculated on the basis of a uniform fall of potential across a crystal composed of ions rather than of atoms.

Ionic compounds are not confined to crystals of the NaCl-KCl type. For instance, in CsCl each Cs^+ is symmetrically surrounded by eight Cl^- and each Cl^- is symmetrically surrounded by eight Cs^+. All the arguments used to show that NaCl is ionic in its nature apply also to CsCl. From what has already been stated, it is evident that we may lay down the generalization that a crystalline compound is ionic if every positive ion in the crystal is symmetrically surrounded by negative ions and if every negative ion is symmetrically surrounded by positive ions. In applying this generalization, the sign of an ion may be determined by the relative position of the element in the periodic table without attempting actual experiments in electrolysis. For instance it would be hard to electrolyze CaO even in the laboratory, but it has the same crystal structure as NaCl and the periodic table leaves no doubt as to which element is the positive ion and which is the negative ion. On this basis we can class nearly all inorganic oxides and sulphides as ionic compounds, for instance Cu_2O, CuO, Ag_2O, ZnO, CdO, ZnS, CdS, etc. The crystal structures of inorganic salts such as the alkali and alkali-earth halides, the sulphates, nitrates, and carbonates, show that they, too, can be listed as being ionic compounds. All intermetallic compounds whose crystal structures have been investigated so far have turned out to be ionic compounds, thus falling in with the picture given in Chap. XVIII. Even the 0.25 Au-0.75 Cu alloy investigated by Bain[9] turns out to fulfill the criterion for an ionic compound. He found that, after he had heated the so-called "solid" solution for a long time close to the melting point, the Au and Cu had migrated so that the Au was at the corners of the face-centered cube and the Cu at the centers of the faces. This caused each Au to be symmetrically surrounded by twelve Cu at a distance* of $a/\sqrt{2}$ and caused each Cu to be symmetrically surrounded by four Au at a distance of $a/\sqrt{2}$.

c. Geometrical Compounds.—Intermetallic compounds seem to obey the law of definite proportions more because of the requirements of the solid geometry of crystal lattices than because of any positive valences which they may show in the formation of oxides, salts, etc., or because of any negative valences which may be predicted by atomic-structure theories. Out of a total of about 150 intermetallic compounds listed by Tammann[10] only 35 are consistent with the saline valences of the component metals. Not only do we find compounds in the literature such as CuPd, Ag_3Al, and Ni_2Mg, but we even find $NaZn_{12}$, $NaCd_5$, KZn_{12}, $FeZn_7$, $Cu_{12}Zn$, $CuZn_{12}$, and $Cu_{31}Sn_8$. The geometrical nature of some of these compounds suggests that possibly the valence electrons

* The edge of the unit-cube is represented by a as usual.

of the component elements may occupy definite positions in the crystal lattice. In previous chapters we have already seen evidence which is consistent with this picture. The picture is rendered still more probable

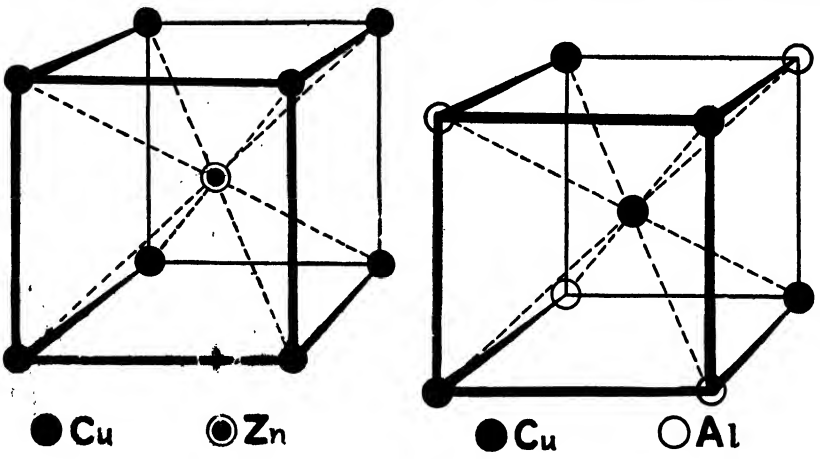

(*a*) (*b*)

FIG. 1.—(*a*) Unit-cube of CuZn; (*b*) one-eighth of unit-cube of Cu_3Al.

by Hume-Rothery's rule[11] that, for binary intermetallic compounds of the same type of crystal structure, the ratio

$$\frac{\text{Number of valence electrons per unit of structure}}{\text{Number of atoms per unit of structure}}$$

is constant.* This rule may be illustrated by the following examples. The intermetallic compounds which represent the β-phases of the Cu-Zn, Cu-Al, and Cu-Sn systems of alloys all have the type of crystal structure illustrated in Fig. 1. Their chemical formulas are CuZn, Cu_3Al, and Cu_5Sn, thus giving Hume-Rothery ratios of

$$\frac{1+2}{1+1}=\frac{3}{2}, \qquad \frac{3+3}{3+1}=\frac{6}{4}, \qquad \frac{5+4}{5+1}=\frac{9}{6}$$

respectively. The γ-phases of the same three systems show the compounds $Cu_{36}Al_{16}(=Cu_9Al_4)$, $Cu_{20}Zn_{32}(=Cu_5Zn_8)$, and $Cu_{31}Sn_8$,† all of which have the same crystal structure. Their Hume-Rothery ratios are:

$$\frac{9+12}{9+4}=\frac{21}{13}, \qquad \frac{5+16}{5+8}=\frac{21}{13}, \qquad \frac{31+32}{31+8}=\frac{63}{39}=\frac{21}{13}$$

* We have already seen in Chap. XV that there is some justification for thinking of crystals of the metallic elements as having definite space-group positions for the valence electrons. A Hume-Rothery type of compound may be pictured similarly as having two metallic elements symmetrically placed on some of the points of a structure with the valence electrons from both metals occupying the remaining points.

† $Cu_{31}Sn_8$ is only 0.8 weight per cent Sn off from Cu_4Sn; and this phase is often given that formula. Actually a bronze of composition 4Cu + Sn is not homogeneous. It is homogeneous at about 1 weight per cent higher in Sn content.

In 1933, there were 35 binary intermetallic alloys known in which up to three intermediate phases were met with which were structurally similar to the β-, γ-, and ϵ-phases of the Cu-Zn system. The characteristic values for the Hume-Rothery ratio are:

(*a*) $\frac{3}{2}$ for phases with the body-centered cubic lattice of β-brass or with the cubic lattice assigned in the literature to β-manganese, with 20 atoms in the unit-cube. Such phases will all be called β-phases.

(*b*) $2\frac{1}{13}$ for phases with the cubic lattice of γ-brass with 52 atoms in the unit-cube. Such phases will all be called γ-phases.

(*c*) $\frac{7}{4}$ for phases with the hexagonal close-packed lattice of ϵ-brass. Such phases will all be called ϵ-phases.

Hume-Rothery's ratio may be written

$$\frac{mx + ny}{x + y} = k$$

where x is the number of atoms of the first component in the chemical formula of the binary intermetallic compound, y is the number of atoms of the second component, m is the number of valence electrons per atom of the first component, and n is the number of valence electrons per atom of the second component.

This equation may be solved for the ratio

$$\frac{x}{y} = \frac{k - n}{m - k}$$

Since $\frac{x}{y}$ is positive, $\frac{k - n}{m - k}$ must also be positive. This requires either that $m > k > n$ or that $n > k > m$. The following conclusions may be drawn from these inequalities:[12]

(1) β-, γ-, and ϵ-structures are not to be expected in binary intermetallic alloys if both components have the same number of valence electrons.

(2) A β-, γ-, or ϵ-structure is to be expected in binary intermetallic alloys if the one component has less and the other component more than $\frac{3}{2}$, $2\frac{1}{13}$, or $\frac{7}{4}$ valence electrons, respectively.

(3) Since the characteristic values of concentrations of valence electrons lie between the same two consecutive integers, it follows that in alloys in which one of the three structures referred to is met with, both other structures should be expected too. This accounts for the frequent coexistence of β-, γ-, and ϵ-structures.

(4) Since the lower and upper limits for the values of concentration of valence electrons are one and two, it follows that a β-, γ-, or ϵ-structure is to be expected in binary intermetallic alloys if the one component has not more than one valence electron and the other component has not less than two valence electrons.

Figure 1*a* shows that[13,14] CuZn clearly fulfills the criteria for an ionic compound: each Cu is symmetrically surrounded by eight Zn, and each Zn is symmetrically surrounded by eight Cu. In the case of Cu_3Al,

matters are a little more complicated.* Each Al is symmetrically surrounded by six Cu at a distance $a/2$ and by eight Cu at a distance $\frac{a\sqrt{3}}{4} = 0.433a$; each Cu at the edge-centers of the unit-cube is symmetrically surrounded by six Al at a distance $a/2$ and by eight Cu at a distance $\frac{a\sqrt{3}}{4}$; each Cu on a body-diagonal of the unit-cube is surrounded by four Al and by four Cu, all at a distance of $\frac{a\sqrt{3}}{4}$. In spite of the complicated structure it is evident from Fig. 1 that the structures of CuZn and Cu_3Al are closely related and that Cu_3Al is definitely ionic. Apparently no one has yet succeeded in getting the Cu and Sn of Cu_5Sn to diffuse uniformly enough to their equilibrium positions to give a good strain-free crystal. The x-ray data, therefore, are as yet unable to demonstrate anything except that the crystal is apparently body-centered cubic.

d. Secondary-valence (Wernerian) Compounds.—We now have to deal with a type of chemical combination which is quite inconsistent with our ordinary freshman-chemistry ideas of valence.† As a typical example we may take potassium chloroplatinate (K_2PtCl_6). When dissolved in water, this substance shows the presence of K^+ ions and of $PtCl_6^{--}$ ions as though we might write the reaction, according to the old Arrhenius theory,

$$K_2PtCl_6 \longleftrightarrow 2K^+ + PtCl_6^{--}$$

The $PtCl_6^{--}$ ion is very stable, since the concentration of Cl^- or of Pt^{++++} in the solution is vanishingly small. This means that the $PtCl_6^{--}$ must appear as a group in the crystal in such a manner that throughout its whole history each Pt "atom" is attached to precisely the same six Cl "atoms." The departure from the ordinary principles of valence is evident when it is realized that this compound is the end member of the following series of seven compounds, all of which are well known:

(1) $[Pt(NH_3)_6]Cl_4$, Hexammine-platé chloride
(2) $[Pt(NH_3)_5\ Cl]\ Cl_3$, Chloro-pentammine-platé chloride
(3) $[Pt(NH_3)_4\ Cl_2]Cl_2$, Dichloro-tetrammine-platé chloride
(4) $[Pt(NH_3)_3\ Cl_3]Cl$, Trichloro-triammine-platé chloride
(5) $Pt(NH_3)_2\ Cl_4$, Tetrachloro-diammine platinum

* Ag_3Al is said to have a structure similar to that of β-manganese, but in view of the doubt attached[15] to the published structure for β-manganese, it is best not to speculate too much. Until more work is done, it is probably best to picture Ag_3Al in terms of Cu_3Al.

† That these compounds are rarely mentioned in freshman texts is not due to their unimportance or to any infrequency of occurrence but rather to the necessity of confining elementary courses to the simplest possible and most systematic sort of subject matter.

(6) $K[Pt(NH_3)\ Cl_5]$, Potassium pentachloro-ammine plateate
(7) $K_2[Pt\ Cl_6]$, Potassium hexachloro plateate

The fifth member of this series does not ionize. All the rest of these compounds ionize in such a way that the group within the brackets appears as one ion. It is evident that the second, third, and fourth members of this series must crystallize in such a way that the complex radical remains intact, otherwise a mixture of two or more of the series would result when one of them is redissolved. Similarly the complex ion of the sixth member of the series must remain intact in the crystal, otherwise it would yield a mixture of the fifth and seventh on solution. It is a natural extrapolation to assume that the two end members of the series are equally stable.

The known valences of Pt and Cl can hardly explain the tenacity with which the (NH_3) groups are held in the ions. Werner[17,18,19,20] advanced the hypothesis that these ions are composed of a central atom (in this case platinum), surrounded by a shell of the other atoms or radicals or molecules which compose the ion. This picture is called the "Wernerian," or "coordination," or "secondary-valence" theory. Werner assigns to each possible central atom one or more "coordination numbers" which represent the number of chemical entities which it can attach to itself. For instance, the coordination number for platinum is six. Those groups in coordination positions which are electrically neutral (*e.g.*, NH_3), and the acid groups or atoms in excess of the primary valence of the central atom, are supposed to be held to the central atom by secondary-valence bonds, while the acid groups within the primary valence of the central atom (together with the groups outside which are necessary to secure the electrical neutrality of the "molecule" as a whole) are supposed to be held by ordinary primary-valence forces. Thus, for the first member of the series listed above, all six (NH_3) are supposed to be held by secondary-valence forces and the four primary valences of Pt are satisfied by the four Cl^- ions outside the complex ion. For the second member, five (NH_3) are pictured as being held by secondary-valence forces; the Cl^- in the complex ion completes the number of *six* in the shell surrounding the Pt, and accounts for one of the primary valences of the Pt, leaving three primary valences for the three Cl^- ions outside the complex ion. When we get to the fifth member of the series, the two (NH_3) are pictured as being held by secondary-valence forces, and the four Cl^- not only complete the requirement of six chemical entities in the shell around the Pt but they also account for the four primary valences of the Pt so that the molecule is neutral, and therefore complete, without additional Cl^- ions.* The sixth member of the series

* This member of the series is evidently, then, a "molecular" compound. It is listed under "secondary-valence" compounds because of the (NH_3) groups. The

has only one (NH_3) to be held by secondary-valence forces. The four primary valences of the Pt are accounted for by four Cl^- in the complex ion, and the required number of six satellites for the Pt is obtained by attaching a fifth Cl^- by means of secondary-valence forces. This fifth Cl^- gives the complex ion a net negative charge of one unit, thus enabling it to hold one K^+ ion outside the complex ion. The seventh member of the series has all six of the coordination positions filled by Cl^-, thus giving the complex ion a net negative charge of two, thus enabling it to hold two K^+ outside the ion. Werner assumed that, in case the negative groups are in excess of the primary valences of the central atom, the primary-valence forces are distributed uniformly over the entire number, leaving the group negative as a whole. Thus in $K[Pt(NH_3)Cl_5]$ it is supposed that the five chlorines are all equivalent. In the case of $K_2[PtCl_6]$ it is assumed by the Wernerian theory that all six chlorines are symmetrically arranged about the Pt so that they are all equivalent.

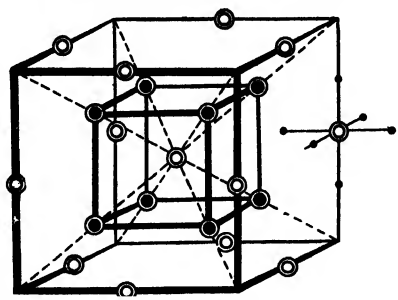

FIG. 2.—The $K_2[PtCl_6]$ structure. The black-centered circles represent the K^+ ions and the white-centered circles represent the Pt of the $[PtCl_6]^{--}$ ions. The whole complex ion is shown only in the case of the Pt at the extreme right where the six chlorines are shown as small solid circles.

The crystal structure of $K_2[PtCl_6]$ and of similar compounds[21,22] offers a truly remarkable confirmation of Werner's theory. This is illustrated in Fig. 2. There are four "molecules" per unit-cube. The space-group is O_h^5 and the atomic coordinates are:

K (at Wyckoff's 8*e*)

$$\begin{array}{llll} \tfrac{1}{4}\tfrac{1}{4}\tfrac{1}{4}; & \tfrac{1}{4}\tfrac{3}{4}\tfrac{3}{4}; & \tfrac{3}{4}\tfrac{1}{4}\tfrac{3}{4}; & \tfrac{3}{4}\tfrac{3}{4}\tfrac{1}{4} \\ \tfrac{3}{4}\tfrac{3}{4}\tfrac{3}{4}; & \tfrac{1}{4}\tfrac{1}{4}\tfrac{3}{4}; & \tfrac{1}{4}\tfrac{3}{4}\tfrac{1}{4}; & \tfrac{3}{4}\tfrac{1}{4}\tfrac{1}{4} \end{array}$$

Pt (at Wyckoff's 4*b*)

$$000; \quad \tfrac{1}{2}\tfrac{1}{2}0; \quad \tfrac{1}{2}0\tfrac{1}{2}; \quad 0\tfrac{1}{2}\tfrac{1}{2}$$

Cl (at Wyckoff's 24*a*)

$$\begin{array}{lll} u00; & 0u0; & 00u \\ \bar{u}00; & 0\bar{u}0; & 00\bar{u} \end{array}$$

and three sets of similar points clustered around

$$\tfrac{1}{2}\tfrac{1}{2}0; \quad \tfrac{1}{2}0\tfrac{1}{2}; \quad 0\tfrac{1}{2}\tfrac{1}{2}$$

The parameter u is 0.24_5 so that the six Cl are distant $0.24a$ from the

other members of the series are evidently "ionic" compounds. They are classed as secondary-valence compounds because of the nature of their complex ions.

nearest Pt and 0.35a from the nearest K. The complex ion $[PtCl_6]$ is therefore a real crystallographic entity as predicted by Werner's theory. It will be noted, too, that the predictions of the theory are fulfilled in that the chlorines are symmetrically placed about the platinum. There is therefore a rational geometrical explanation for the fact that the coordination number of platinum is 6. It is to be expected on this basis that the coordination numbers for other atoms at the centers of other complex ions will be limited to numbers with crystallographic significance, *i.e.*, 2, 3, 4, 6, 8, 12,* etc. Wyckoff[22] lists over 50 secondary-valence compounds, any one of which would have served instead of $K_2[PtCl_6]$ as an example of the correctness of Werner's theory. In some the complex ion is positive, in others negative; for instance, $[Cr(NH_3)_5(H_2O)](ClO_4)_3$ and $K_2[Pt(SCN)_6]$. In still other cases, both ions are complex; for instance, $[Co(NH_3)_4(H_2O)_2][Co(CN)_6]$ or $[Ni(H_2O)_6][SiF_6]$. A familiar example of a compound built on the coordination number 2 is $CsCl_2I$, which crystal analysis shows[24] to be really $Cs[ICl_2]$.† An interesting sidelight on the atomic nature of chlorine in this compound is furnished by the structure and dimensions of the unit-crystal. The unit-crystal is rhombohedral with Cs-Cl-I-Cl-Cs, all strung along the long body-diagonal. The distance from the center of one Cs to the center of the I nearest to it in the chain is 6.102Å. If we assume that the cesium and the iodine are in the ionic state, we may use the ionic packing-radii of Chap. XIII to give $Cs^+ + I^- = 3.947$Å. This leaves 2.155Å. for the packing-diameter of each chlorine along the long body-diagonal of $CsCl_2I$. Reference to Chap. XIII shows that this is much too small for the packing-diameter of a chlorine ion, which is 3.178Å., so that presumably the chlorine is in the form of a neutral atom. Unfortunately there are no crystal-structure measurements on solid Cl_2 which might give us an atomic packing-diameter to compare with the diameter 2.155Å. We

* Other numbers like 7 can sometimes be made to look like true coordination numbers by reason of some chemical quirk which adds one to a crystallographically significant number. For instance, ammonium fluozirconate is ordinarily given the formula $(NH_4)_3ZrF_7$. Crystal analysis shows that it has a structure[23] in which half of the negative ions are F^- and half are $[ZrF_6]^{---}$, so that its chemical formula should be written $(NH_4)_3[ZrF_6]F$, or even $NH_4F \cdot (NH_4)_2[ZrF_6]$.

† It does not require much imagination to extend the idea of coordination numbers beyond the point where it is of much practical use. For instance the coordination number 3 has been assigned by some to the carbon in the CO_3^{--} radical. Similarly, 4 has been assigned to the sulphur in the SO_4^{--} radical. The Werner theory, applied to these radicals, predicts the fact, found experimentally from crystal analysis, of a symmetrical grouping of oxygens about a central atom and emphasizes the fact, established experimentally by crystal analysis, that all the oxygens in $NaNO_3$, or $CaCO_3$, etc., are identical in their properties and that all the oxygens in Na_2SO_4 are identical in their properties, *i.e.*, that the alkali ions are "bonded" to the negative radical as a whole and are not attached to particular individual oxygens. A more legitimate use of the coordination number 4 is found in compounds like $K_2[PtCl_4]$.

can, however, make the atomic state of the chlorine look plausible by the following ratios:

$$\frac{\text{Packing-diameter of Cl in } CsCl_2I^{24}}{\text{Packing-diameter of } Cl^- \text{ ion (Chap. XIII)}} = \frac{2.155}{3.178} = 0.678$$

$$\frac{\text{Packing-diameter of atomic I in } I_2^{25}}{\text{Packing-diameter of } I^- \text{ ion (Chap. XIII)}} = \frac{2.70}{3.95} = 0.684$$

The results of crystal analysis have so completely confirmed the theory of Werner that the principle of coordination numbers is now taken as a basic principle in the explanation of complex ions and is even used as a short-cut by crystal analysts in the solution of complex structures. In this connection the reader is referred to a summary by Bragg[26] of the work of himself and his students on complex silicates and to an article by Pauling[27] on the principles which determine the structure of complex ionic crystals.

e. **Mixed Ionic Compounds.**—We took up in Chap. IX the structure of tricalcium aluminate ($3CaO \cdot Al_2O_3$). Examination of the structure[28] shows no crystallographic evidence of a formula like $Ca_3(AlO_3)_2$. There is no indication of those groups which might have been expected to be present, such as CaO, AlO_3, Al_2O_3, Al_2O_6, etc. The ionic nature of the compound is evident from the following symmetry considerations. Every O at Wyckoff's 12*f* is midway between two Al at 3*a* and 3*b*, and every O at 6*d* is equidistant from four Ca at 8*c*. Similarly, every Al at 3*a* is equidistant from four O at 12*f*; every Al at 3*b* is equidistant from four O at 12*f*; every Ca at 1*a* is equidistant from twenty-four O at 12*f*; every Ca at 8*c* is (within the error of experiment) equidistant from six O at 12*f*. Every Al at 3*b* is equidistant from two Ca at 1*a* and is also equidistant from eight Ca at 8*c*. Similarly, every Ca at 1*a* is equidistant from six Al at 3*b*, and every Ca at 8*c* is (within the error of experiment) equidistant from three Al at 3*a* and from three Al at 3*b*. Tricalcium aluminate certainly has no grouping which would justify its name. It is evidently not a molecular compound, nor does it fall under the simple classification of an ionic compound as discussed in section *b*. Its structure is distinctly different from that of crystals containing complex ions, for, instead of having a complex ion to act as a crystallographic entity, each Ca, Al, and O acts as a crystallographic unit. Apparently then tricalcium aluminate must be regarded as the representative of a fifth class of chemical combination. Since it looks more like a symmetrical mixture of ions than anything else, it has been called a "mixed ionic" compound. So far, tricalcium aluminate is the only compound of this sort.*

* The structure of $LiIO_3$ is reported[29] to show the oxygens midway between the Li and the I, thus making it look like a mixed ionic compound. This must certainly be in error because the chemical evidence demands a real IO_3^- ion.

VARIATE ATOM EQUIPOINTS

In our discussion of the theory of space-groups (Chaps. VIII and IX) we assumed that crystallographically equivalent points must also be chemically equivalent. Evidently such an assumption represents only an ideal state of affairs. In our discussion of topaz (Chap. XI) we found that F could be replaced by OH in certain parts of the crystal, and in our study of solid solutions it appeared that in mix-crystals one ion of the solute could take the place of any ion of solvent of the same sign. We must therefore recognize definitely that the ideal condition does not always exist and that, at least for certain equivalent groups of compounds, it is not necessary to have chemically identical atoms (or ions) at crystallographically equivalent points. Several examples of this departure from the ideal condition have been listed by Barth.[30]

The spinels[22,31] have the general formula X_2YO_4 and the crystallographic unit of structure has eight "molecules." It has ordinarily been assumed that not only do the thirty-two O atoms lie on crystallographically equivalent points, but that the sixteen X atoms and the eight Y atoms, respectively, are also situated on equivalent points. This assumption seems to be consistent with the data on the intensity of diffracted x-ray beams in the case of some of the spinels, for instance, Al_2ZnO_4, Al_2MgO_4, Al_2NiO_4, Al_2CoO_4, Al_2FeO_4, Al_2MnO_4. For all these the space-group is O_h^7, and the atomic coordinates are:

X (at Wyckoff's 16*c*)

$\frac{1}{8}\frac{3}{8}\frac{7}{8}$; $\frac{7}{8}\frac{1}{8}\frac{3}{8}$; $\frac{3}{8}\frac{7}{8}\frac{1}{8}$; $\frac{3}{8}\frac{5}{8}\frac{3}{8}$; $\frac{1}{8}\frac{5}{8}\frac{1}{8}$; $\frac{1}{8}\frac{1}{8}\frac{5}{8}$; $\frac{5}{8}\frac{1}{8}\frac{1}{8}$; $\frac{5}{8}\frac{5}{8}\frac{5}{8}$
$\frac{7}{8}\frac{3}{8}\frac{1}{8}$; $\frac{1}{8}\frac{7}{8}\frac{3}{8}$; $\frac{3}{8}\frac{1}{8}\frac{7}{8}$; $\frac{5}{8}\frac{3}{8}\frac{3}{8}$; $\frac{7}{8}\frac{5}{8}\frac{7}{8}$; $\frac{7}{8}\frac{7}{8}\frac{5}{8}$; $\frac{5}{8}\frac{7}{8}\frac{7}{8}$; $\frac{3}{8}\frac{3}{8}\frac{5}{8}$

Y (at Wyckoff's 8*f*)

000; $0\frac{1}{2}\frac{1}{2}$; $\frac{1}{2}\frac{1}{2}0$; $\frac{1}{2}0\frac{1}{2}$; $\frac{1}{4}\frac{1}{4}\frac{1}{4}$; $\frac{3}{4}\frac{3}{4}\frac{1}{4}$; $\frac{1}{4}\frac{3}{4}\frac{1}{4}$; $\frac{1}{4}\frac{3}{4}\frac{3}{4}$

O (at Wyckoff's 32*b*)

uuu;	$u\bar{u}\bar{u}$;	$\bar{u}u\bar{u}$;	$\bar{u}\bar{u}u$
$\frac{1}{4}-u, \frac{1}{4}-u, \frac{1}{4}-u$;		$\frac{1}{4}-u, u+\frac{1}{4}, u+\frac{1}{4}$;	
$u+\frac{1}{4}, \frac{1}{4}-u, u+\frac{1}{4}$;		$u+\frac{1}{4}, u+\frac{1}{4}, \frac{1}{4}-u$	

and three sets of eight similar points about

$$\tfrac{1}{2}\tfrac{1}{2}0,\ \tfrac{1}{2}0\tfrac{1}{2},\ 0\tfrac{1}{2}\tfrac{1}{2}$$

The value of u is close to $\frac{3}{8}$.

These coordinates place the O at the corners of tetrahedra which have Y at the center. In terms of the Werner theory, the coordination number of Y is four so that the O grouping is independent of the valence of *Y*. This leads to typical complex ions when a radical such as $(CN)'$

is substituted for O, for instance in $K_2[Zn(CN)_4]$.* There are, however, still other spinels for which such a picture is inconsistent with the x-ray intensity data. For instance, in the case of Fe_2MgO_4, the calculated intensities agree with the experimental data only if we assume that eight of the Fe atoms are structurally equivalent at Wyckoff's 8*f* and that the other eight Fe plus the eight Mg occupy crystallographically equivalent points at Wyckoff's 16*c*. This would change the formula to $(MgFe)FeO_4$. Other examples are $(MgGa)GaO_4$, $(MgIn)InO_4$, $(TiMg)MgO_4$, $(TiFe)FeO_4$, and $(SnZn)ZnO_4$. It should be emphasized that the two kinds of atoms at Wyckoff's 16*c* have no orderly arrangement with respect to each other; these atoms distribute themselves on the lattice positions of 16*c* quite at random just as in the case of similarly charged ions in a mix-crystal.

Posenjak and Barth report[32] variate atom equipoints for the cubic modification of $LiFe_2O_4$ (lithium ferrite). The diffraction pattern shows that the unit-cube contains one "molecule" of $Li_2Fe_2O_4$. The oxygens occupy the four equivalent points 4*b*, while the iron and lithium must occupy the four equivalent points 4*c*. The large difference in the scattering power of iron and lithium makes it possible to arrive at the definite conclusion that the same set of equivalent positions is occupied by the two chemically different elements. The distribution of iron and lithium in this set of equipoints is not regular, *i.e.*, there are not always two of each cation present in the unit-cube. The distribution is one of chance and must comply with the requirement that an equal number of each of the cations is always present within a relatively small space. As in the case of the $(MgFe)FeO_4$ spinel, the conception of the unit-cell loses its traditional chemical significance and becomes strictly a geometrical conception. The unit-cube of lithium ferrite has a meaning only as an idealized "average" assemblage of ions in space. The unit-cube of lithium ferrite, considered in this way, resembles the well-known NaCl structure (4*b* for Cl^- and 4*c* for Na^+), in which O^{--} replaces Cl^- and a hit-and-miss mixture of Li^+ and Fe^{+++} replaces the Na^+. If only the Li^+ and Fe^{+++} ions had occupied definite positions symmetrically located with respect to each other and to the positions of the oxygens, the compound would have been mixed-ionic.

By applying this picture of variate atom equipoints, Barth has been able[33] to find the structures of sodalite $Na_8Al_6Si_6O_{24}Cl_2$, noselite $Na_8Al_6Si_6O_{24}\cdot SO_4$, and hauyne $(Na, Ca)_{4-8}Al_6Si_6O_{24}\cdot(SO_4)_{1-2}$ in which the six Al and six Si occupy variate equipoints. The solution of these structures shows that there can be no "extra" ions, without fixed positions, wandering around in the structure as has been claimed by Jaeger.[34] Other com-

* There is no justification in the crystal structure of spinels for the way in which their chemical formulas are usually written (for instance, $MgAl_2O_4$) nor for the chemical names usually applied to them (for instance, magnesium aluminate).

pounds showing variate atom equipoints are gehlenite,[35] $Ca_2Al(AlSi)O_7$; ammonium-oxy-fluoro-molybdate,[36] $(NH_4)_3MoO_3F_3$; potassium cyanate,[37] KCNO; and[38] $Co(NH_3)_5(H_2O)(SO_4)I$.

CONTRIBUTIONS OF CRYSTAL STRUCTURE TO ORGANIC CHEMISTRY

Ever since the first structural formula was written, it has been the creed of organic chemists that the properties of the materials with which they work must be attributed to the shapes and sizes of their component atoms and to the arrangement of those atoms in space. Structural formulas represent hypothetical configurations of atoms which are consistent with the results of chemical and physical experiments. Because these structural formulas show an atomic configuration in only two dimensions, they have been universally recognized as being only workable fictions, which, however well they may represent the chemical properties of substances, have no necessary exact relation to the true positions of the atoms in the molecules. In a few cases attempts have been made to include the third dimension. Outstanding examples of this are to be found in the three-dimensional formulas assigned to methane and ethane on the basis of a tetrahedral carbon atom, and in the stereo formulas of the three kinds of tartaric acid. The x-ray study of crystals is gradually giving us quite an extensive set of three-dimensional formulas which are backed by such a strong array of experimental evidence that we feel justified in accepting them as close approximations to reality.

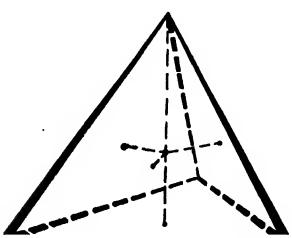

FIG. 3.—Tetrahedral shape of the carbon atom.

We have already seen in Chap. XIII that we must picture the atomic domain of carbon as being tetrahedral in shape. This is in complete agreement with all the chemical evidence, and we may consider the organic chemist's picture of a tetrahedral carbon atom to be on a sure foundation. There is no clue, however, as to whether the four valence electrons of the carbon atom are "attached" at the vertices of the tetrahedron or at the centers of the faces (see Fig. 3). The reason for this lies in the fact that the angles subtended at the center by the vertices of the tetrahedron are the same as the angles subtended by the face-centers, 109° 28′. It is only a matter of words, therefore, whether we say that the four valence electrons have mean positions at the centers of the faces of the tetrahedron or whether we say that their mean positions lie at the vertices of a second tetrahedron inscribed in the first so that the four vertices of the second tetrahedron coincide with the face-centers of the first. The essential thing is that carbon atoms pack in crystals practically as though they were tetrahedra, *i.e.*, they have four points 109° 28′ apart which cannot be distinguished from each other. The dis-

tance of closest approach of carbon atoms in diamond is 1.542×10^{-8} cm. In graphite it is 1.50×10^{-8} cm. In order to make certain figures in this section appear more stereoscopic, the carbon atoms will be represented by circles whose radii correspond to 0.75×10^{-8} cm. The interpretation of these circles in terms of tetrahedra will in all cases be sufficiently obvious.

The Paraffin Series.[39]—The ordinary structural formulas for the paraffins, and for the acids and esters derived from them, show the carbon atoms as lying along a straight line. Such a picture is not consistent with the x-ray data. We have already seen in Chap. XVI that the liquid paraffins tend to show three-dimensional molecules, and this is confirmed by work with the corresponding solids.[1,2,3,4,5] Two of these dimensions are, within experimental error, identical for all the saturated

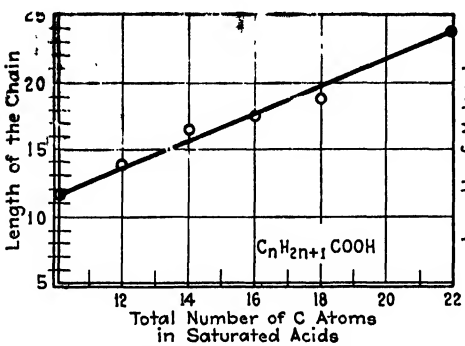

FIG. 4.—Lengths of molecules of saturated fatty acids. (*Müller.*)

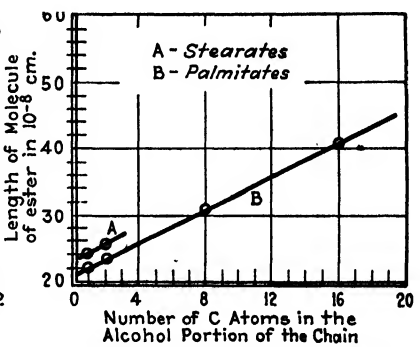

FIG. 5.—Lengths of molecules of esters of palmitic and stearic acids. (*Shearer.*)

paraffins so far tested. The third dimension varies rather systematically with the number of carbon atoms in the molecule. This is interpreted to mean that all the saturated fatty acids and their esters have practically the same cross-section but that the length of the chain depends upon the number of carbon atoms in it. The cross-section is greater than would be expected on the basis of a straight chain of carbon atoms each 1.5×10^{-8} cm. in "diameter." It is hard to imagine that the hydrogen atoms (the smallest in the whole list of elements) could account for this discrepancy in cross-section. The discrepancy in the cross-section makes it seem necessary to assume that the carbon chain is in zigzags. This assumption is strengthened by the fact that the chains are considerably shorter than the distances calculated by multiplying the "diameter" of carbon by the number of carbons in a chain. The lengths found experimentally by Müller[1] for the chains of various acids are given in Fig. 4.* The data indicate that the molecules are paired end to end.

* Langmuir[6] measured the lengths of the molecules of palmitic and stearic acids in terms of their spreading on water. His values are higher than those of Müller by

Data by Shearer[2] for the lengths of the molecules of various esters of palmitic and stearic acids are given in Fig. 5. The data show that the increase in the length of the alcohol averages $1.22_5 \times 10^{-8}$ cm. for each CH_2 group. This is to be contrasted with an average increase of 1.02×10^{-8} cm. per CH_2 group for the fatty acids of Fig. 4.

Müller and Shearer[3] have considered three possibilities in connection with the lengths of the chains, namely, (1) a zigzag or spiral structure, (2) a chain sloped at an angle to the planes for which measurements were made, (3) a slope of one angle for the acid end of an ester and a slope of a larger angle for the alcoholic end. There is considerable to be said in favor of the last two types of explanation and considerably more in favor of the first. It will be of interest to follow the lead of Müller and Shearer[3] and of Langmuir[6] and take up the zigzag spiral point of view in detail with the aid of Fig. 6. In Fig. 6*a* all the carbon atoms lie in the same plane. The arrangement is identical with that chain of atoms in diamond in the (1 1 0) plane which runs parallel to the (1 0 0) plane.

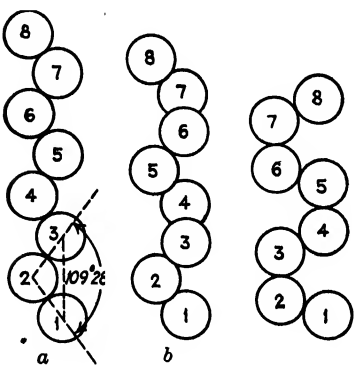

FIG. 6.—Theoretically possible carbon chains. *a* corresponds to the saturated alcohols. *b* seems to have no counterpart in aliphatic compounds. *c* corresponds to the free saturated fatty acids. (*Müller and Shearer.*)

Since the atomic domains are tetrahedral in shape, the angle 1 2 3 is taken as 109° 28′. The distance 1 2 or 2 3 is equal to the "diameter" of carbon, *i.e.*, 1.50×10^{-8} cm. The vertical length along the chain which is contributed by each carbon atom is half the distance 13. It is

$$1.50 \times 10^{-8} \sin \frac{109° 18'}{2} = 1.22 \times 10^{-8} \text{ cm.}$$

This agrees with the experimental value for the average increase per carbon atom for the alcohols as measured in the esters of saturated acids. It is therefore assumed that the carbons in the chains of saturated alcohols have the configuration of Fig. 6*a*. It should be noted that the model requires all the carbons to produce the same increment in length. This agrees with Fig. 5 which gives on a single straight line data for both odd- and even-numbered alcohols.

Figure 6*b* represents a spiral of tetrahedral carbon atoms. It is evident that it does not represent the experimental facts, since the incre-

---

x-ray methods. Adam's values[7] for myristic and behenic acids are also higher. This is perhaps as close an agreement as might be expected because of the experimental conditions inherent in the water-spreading method.

ment in length per atom is 1.12×10^{-8} cm., which is about halfway between the experimental values for the alcohols and for the saturated fatty acids. Although this configuration is theoretically possible for carbon atoms, for some reason it does not appear in either diamond or graphite.

Figure 6c shows a third possible configuration which actually occurs in diamond. Atoms 1, 2, and 3 are related to each other as in Fig. 6*a*. Atoms 4, 5, and 6 are also like the corresponding atoms in Fig. 6*a*, but atom 4 is joined on to a different tetrahedral face of 3 in *c* than in *a*. Each pair of atoms contributes 2.0×10^{-8} cm. to the length of the chain. The average increment in length per atom, 1.0×10^{-8} cm., is, within the experimental error, identical with the average increment per atom for the saturated fatty acids of Fig. 4. Of each pair of atoms in Fig. 6c, one contributes 1.5×10^{-8} cm. and the other contributes 0.5×10^{-8} cm. This again agrees with the experimental facts, for, if the lengths of the odd-numbered acids had been plotted in Fig. 4, their graph would have been parallel to the graph of the even-numbered acids but would have been a little above it. The difference between the acids containing an odd and an even number of carbon atoms is interesting. It is well known that similar differences are found in their melting points. Also, the even-numbered acids are common in nature, but the odds are very rare. It would therefore appear that there is a stronger tendency to add two carbon atoms to the acid chain rather than only one.

The x-ray investigations of the paraffin series, in so far as structural formulas are concerned, may be illustrated in terms of an ester like propyl butyrate. The ordinary structural formula is

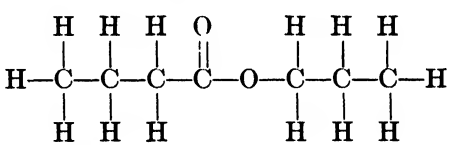

If the interpretation of Müller and Shearer is correct, the carbons should be written

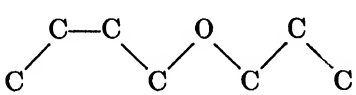

Each end carbon has three H atoms attached at angles of 109° 28′ from the line joining the end carbon to the next neighboring carbon. The hydrogen atoms of the CH_2 groups would be one above and one below the plane of the paper at angles determined by the tetrahedral carbon atoms. The additional oxygen atom of the carboxyl group would likewise not lie in the plane of the paper. There is of course the possibility that the molecule may have a bend in it at the linkage oxygen.

It has already been mentioned that the x-ray data for saturated fatty acids show the molecules to occur in pairs as though the two carboxyl

groups were in contact. Similar results are found for the unsaturated fatty acids. In other words the natural state of the aliphatic acids, when free from water, is one of association with $n = 2$. In this connection it is interesting to remember that the molecular weight of acetic acid, measured in terms of the depression of the freezing point of benzene, is *twice* the formula weight.

Müller and Shearer have investigated the two isomers, erucic acid and brassidic acid. Each of these contains twenty-two carbon atoms. There is one double bond, similarly placed, in each acid. The x-ray results are consistent with the structural formulas of Fig. 7. Since the

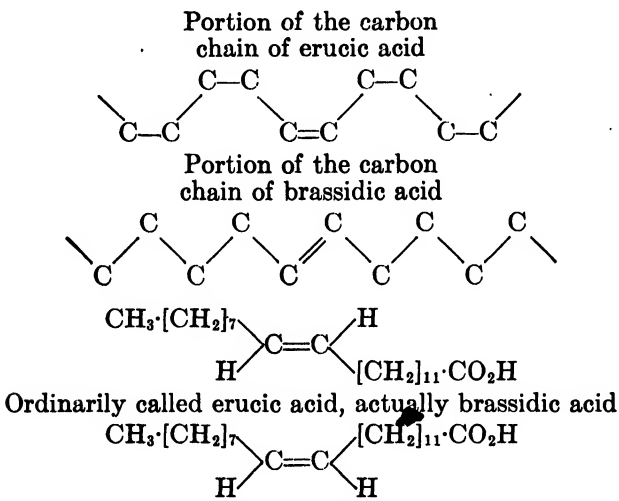

FIG. 7.—Structural formulas for erucic and brassidic acids.

material ordinarily known to organic chemists as brassidic acid has a chain 12×10^{-8} cm. longer than the chain of the substance which they call erucic acid, it is evident that the structure corresponding to Fig. 6*a* is the brassidic acid. As is brought out in Fig. 7, this requires the ordinary structural formulas for these two acids to be interchanged. It would seem that if Müller and Shearer's zigzag interpretation is correct, there is a possibility for isomers of the simple chain compounds which cannot be predicted on the basis of their ordinary structural formulas. The data show that natural saturated alcohols correspond to Fig. 6*a* and that natural saturated acids correspond to Fig. 6*c*. It should therefore be possible by the oxidation of natural alcohols to make acids corresponding to Fig. 6*a* and similarly by reduction of natural acids to make alcohols corresponding to Fig. 6*c*.

The chains of the saturated hydrocarbons are apparently[40] like those of the alcohols except that they are stretched in the ratio of 1.3:1.2.

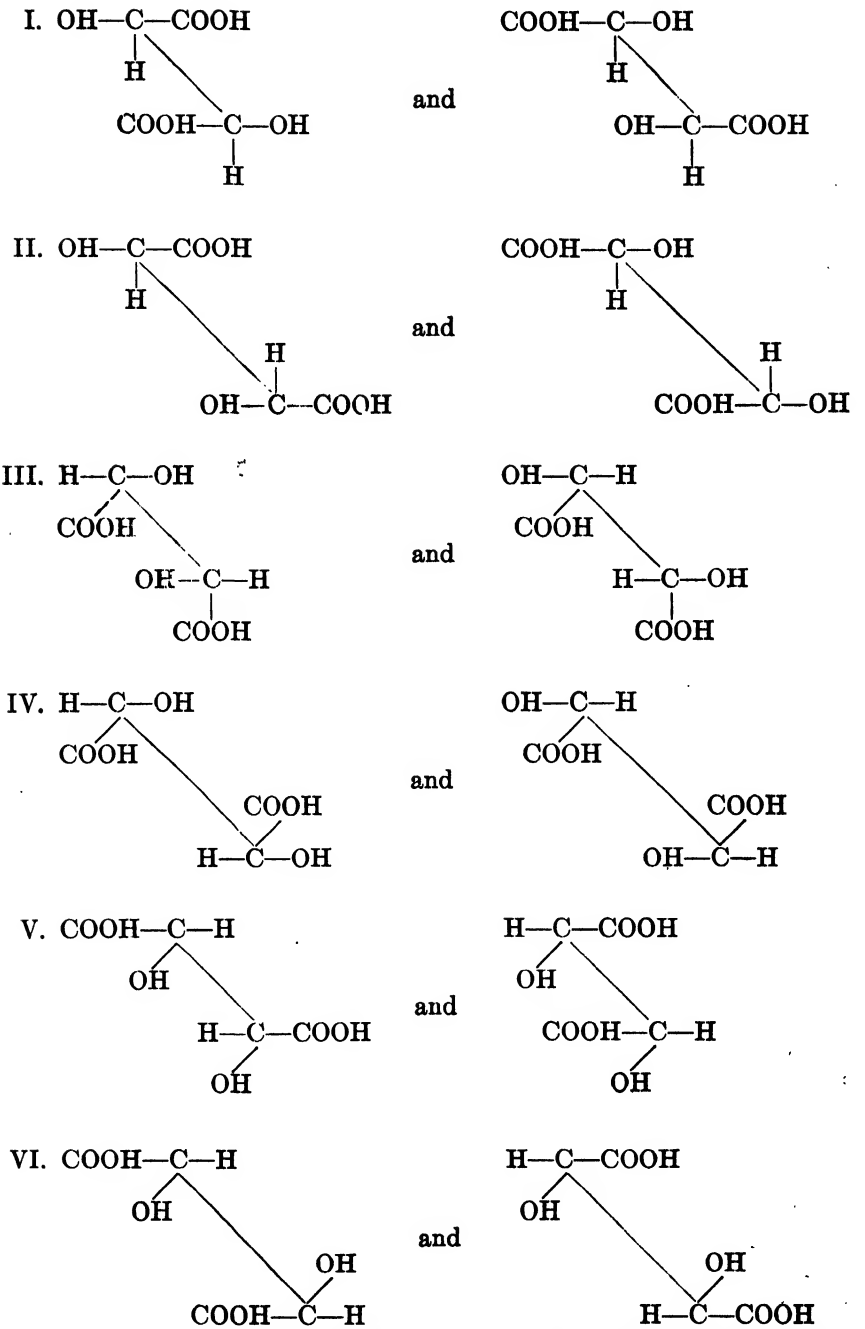

FIG. 8.—Possible molecular structures of dextro- and lævotartaric acids permitted by their chemical properties.

The reason for this stretching is not clear. It may possibly have to do with the purity of the specimens used.

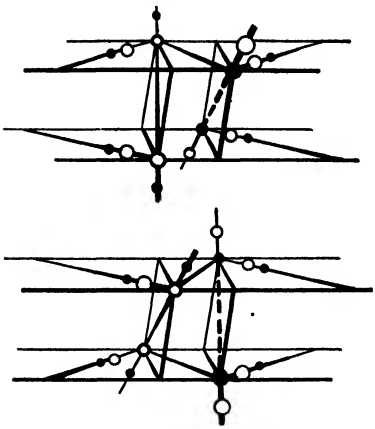

FIG. 9.—Astbury's solution of the crystal structure of dextro- and lævo-tartaric acids.

Since almost every elementary textbook in organic chemistry gives so-called "stereo formulas" for dextro- and lævotartaric acids, it will be interesting to see what the real stereo formulas are. The possible relationships between the atoms permitted by the chemical properties of tartaric acid are shown in Fig. 8. Astbury's analysis[41] of the crystal structure shows the atomic configurations of Fig. 9. The second arrangement in Fig. 8 is the two-dimensional counterpart of Fig. 9. It is assumed that the spiral arrangement of carbon atoms is a characteristic of the tartaric acid molecule but that the spiral arrangement of the OH groups is imposed by the crystal. In solution, then, the OH radicals would be free to set themselves at other angles to the carbon atoms, and these new angles do not need to be rigorously constant, at least in very dilute solutions. All this is consistent with the data on the optical activity of tartaric acid. Those who are interested in the optical activity of organic crystals will find Astbury's article[41] worth close study.

The Benzene Series.—The structure of the benzene ring has been a matter of discussion among organic chemists for some time. It will therefore be of interest to review briefly the x-ray data on the subject. W. H. Bragg has pointed out[42] that both diamond and graphite are made up of rings each of which contains six carbon atoms. A single ring might be assumed to represent the structure of benzene; two with a common side might represent the basic structure of naphthalene; etc. We therefore have the possibility of two competing models of the benzene ring, one patterned after the structure of diamond and one patterned after the structure of graphite. The six-sided rings in diamond are illustrated in Fig. 10. Atoms *A*, *B*, *C*, *D*, *E*, *F* alone could represent a benzene ring, while *A*, *B*, *C*, *D*, *E*, *F*, *G*, *H*, *I*, *J* could represent a naphthalene

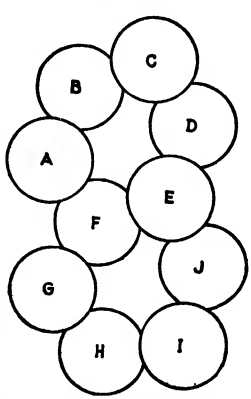

FIG. 10.—Ring structure of diamond.

ring. It is seen that the rings resemble hexagons except that they are puckered to give three atoms on one level and three on a parallel but higher level. If, on the other hand, we pattern our model of the benzene ring after the hexagons in graphite, the two planes of three carbons each so nearly coincide that we have practically a plane figure.

X-ray patterns have been taken of benzene[43,44,45,46,47] and of a large number of benzene derivatives such as hexachlorbenzene, hexabrombenzene, *p*-nitrobenzene, *m*-dinitrobenzene, hexamethyl benzene, etc. The interpretation of these patterns has proved difficult, and satisfactory atomic positions have been found only for hexamethyl benzene. Benzene itself crystallizes with its molecules on space-group V_h^{15}, with four molecules per unit orthorhombic prism. The positions of the individual atoms have not been determined from the diffraction patterns. Table VIII of Appendix III shows that the molecules in V_h^{15} must possess a center of symmetry. This offers no basis for deciding which type of ring benzene has, for it is consistent with both the diamond and the graphite ring. The choice between the two models must therefore be made in terms of the structure of hexamethyl benzene $[C_6(CH_3)_6]$. Hexamethyl benzene crystallizes[48] on a triclinic lattice (space-group C_i^1), with $\alpha = 44° 27'$, $\beta = 116° 43'$, $\gamma = 119° 34'$; $a = 9.01$, $b = 8.92$, $c = 5.34$Å. The atomic coordinates for carbon are

$$xyz; \quad \bar{x}\bar{y}\bar{z}$$

where x, y, and z have the following values:[22]

	x	y	z
In benzene ring	0.18_9	0.10_8	0
	0.08_1	0.18_9	0
	-0.10_8	0.08_1	0
In methyl group	0.37_8	0.21_6	0
	0.16_2	0.37_8	0
	-0.21_6	0.16_2	0

These coordinates give a six-sided figure of the same shape and size as the hexagon in graphite. The C–C distance in the ring is 1.42×10^{-8} cm. and is, within experimental error, the same for all the carbons in the ring. The distance between the center of a carbon in the ring and the center of a carbon in the CH_3 radical is 1.54×10^{-8} cm. This may be taken to indicate that the valences differ from those inside the ring itself. The C–C distances in the ring of saturated cyclohexane are said to be[22] 1.54×10^{-8} cm., thus showing the effect of having saturated the ring. Naphthalene and anthracene were first reported[49,50] to have the diamond type of hexagonal rings such as are shown in Fig. 10, but later measurements[51,52] seem to show definitely that the rings are of the flat graphite

type. It would seem, then, to be pretty well established that the actual structure of the benzene ring does not differ appreciably from the two-dimensional hexagon of the organic chemist. Only when the carbon valences become completely saturated, do we find[22] the puckered ring analogous to the saturated aliphatic alcohol chains.

Rubber, Cellulose, Etc.—We have already seen in Chap. XVI how the data of x-ray diffraction can be used to point out the probable nature of the fibers in rubber. Still other experiments combining the technique of the powder method (Chap. VI) with the technique for the study of orientation (Chap. XVII), and sometimes aided by the indirect methods of Chap. XVI, have contributed largely to our knowledge of cellulose and its compounds. Similar methods have been used, too, in studying the polymerization of oils and of synthetic plastics. To cover the subject adequately would require much more space than is available here and would require a duplication of material published in satisfactory form elsewhere. If the present book has succeeded in the aims set forth in the preface, the student who is especially interested in the study of cellulose should now be prepared to read without difficulty Meyer and Mark's "Der Aufbau der Hochpolymeren organischen Naturstoffe"[53] and the x-ray section of Hess's "Chemie der Cellulose."[54] Some of the important final conclusions as of the year 1932 are given in Clark's "Applied X-rays."[55] Astbury's "Fundamentals of F bre Structure" (Oxford University Press, 1933) gives a remarkably clear elementary account of the structures of the common textile fibers.

MOLECULAR SYMMETRIES

It is evident that we could learn a great deal about an organic compound if we could compare directly the organic chemist's structural formula for that compound with the symmetry of the molecule as found by crystal-analysis methods. We are able to do this with the aid of Tables I to XXXII of Appendix III. We have already had a little foretaste of this in the case of benzene, where the information was of possibly a negative sort. There are plenty of examples where the information is positive.

In Tables I to XXXII of Appendix III the fifth column lists the number n of completely asymmetric molecules required for a given space-group. The seventh column lists the degree of symmetry p (2-fold, 3-fold, etc.), which a molecule may have and still be compatible with that space-group. If the molecules of a compound have a p-fold symmetry, then the unit-crystal no longer requires n molecules but n/p instead to fit into the space-group. The last column of these tables lists the centers, planes, and axes of symmetry which such molecules will have. In other words, the second, third, fourth, and fifth columns of these tables show the ways in which Nature builds up symmetrical

crystals from completely asymmetric material; the fifth, seventh, and eighth columns show how crystals with precisely the same symmetry characteristics can be built up out of a smaller number of more symmetrical building blocks. It must be understood that p refers to the molecular symmetry *as it is found in the crystal.** This symmetry may or may not be the same in the non-crystalline state. An example of this has already been mentioned in the discussion of the tartaric acids.

The following comments[55] on molecular symmetries as listed in Appendix III will make the tables more easily understood and more readily useful.

1. Monoclinic System.—This system is particularly important from the standpoint of molecular symmetry since so many organic substances are monoclinic. Organic molecules are often completely asymmetric or have only 2-fold symmetry. Obviously, the lower the symmetry of the molecule, the more likely it is to crystallize in a system of low, rather than in one of high, order of symmetry. Since the monoclinic tables (Tables III, IV, V) of Appendix III are based on the convention that the axis of symmetry of the crystal is the b-axis (Y-axis), it follows that the plane of symmetry is (0 1 0). Therefore, in column eight of these tables wherever we find the symbol 2-A we may interpret it to mean "a 2-fold axis of symmetry perpendicular to the (0 1 0) planes." Similarly the symbol P may be read "a plane of symmetry parallel to the (0 1 0) planes."

2. Orthorhombic System.—In the C_{2v} class (Table VII) the Z-axis is taken parallel to the 2-fold axis of symmetry, and there are therefore either planes of symmetry or glide-planes of symmetry parallel to the (1 0 0) and (0 1 0) planes but not to the (0 0 1). Wherever we find the symbol "2-A," we may interpret it to mean "a 2-fold axis of symmetry perpendicular to the (0 0 1) plane." Similarly the symbol 2P's intersecting in 2-A may be read "two planes of symmetry parallel to the (1 0 0) and (0 1 0) planes, intersecting in a 2-fold axis perpendicular to the (0 0 1) plane." In the V and V_h classes (Tables VI and VIII), all three axes are interchangeable. Where the tables give (for instance, V^3 in Table VI) $s = \frac{1}{2}$ for (1 0 0) and (0 1 0) and the symbol 2-A $\perp$ (0 0 1),

* A sharp distinction must be made between molecular and ionic compounds. For instance, we cannot apply the values for p to the case of an alkali halide like NaCl, for we have no true molecules of NaCl which we can localize and treat as separate entities built together with suitable relative orientations. If we assume that the structure of NaCl (space-group O_h^5) possesses 48-fold symmetry we cannot argue from the fact that there are four molecules per unit-cube that each stoichiometric "molecule" has $^{19}\frac{2}{4} = 48$-fold symmetry, nor can we say that each stoichiometric "molecule" has, in the crystal, the full symmetry of class O plus a center of symmetry at the point of intersection of the axes, *i.e.*, full symmetry of class O_h". The symmetry of space-group O_h^5 belongs to the *whole* crystal of the ionic compound NaCl but not to its stoichiometric "molecules."

we may interpret it to mean also "if $s = \frac{1}{2}$ for (1 0 0) and (0 0 1), then the possible molecular symmetry is given by a 2-fold axis perpendicular to (0 1 0)"; or "if $s = \frac{1}{2}$ for (0 1 0) and (0 0 1), then the possible molecular symmetry is given by a 2-fold axis perpendicular to (1 0 0)."

In every molecular compound in the orthorhombic system which has been completely investigated, the unit-crystal appears to contain the minimum number of molecules. If we arbitrarily assume that this is always the case, then we may, to a limited extent, determine the molecular symmetry. Astbury and Yardley give the following illustration: Assume an orthorhombic crystal, of unknown class, for which s is $\frac{1}{2}$ for all planes where $(h + k + l)$ is odd.

(*i*) In terms of our hypothesis, it follows that if density measurements show that the unit-crystal contains sixteen molecules, the space-group must be V_h^{25} and the molecules must be asymmetric.

(*ii*) If the unit-crystal contains eight molecules, the following arrangements are all possible:

(*a*) Space-group V_h^{25}; 2-fold molecular symmetry—a plane of symmetry parallel to (1 0 0), (0 1 0), or (0 0 1) in the crystal, or a center of symmetry. X-ray measurements cannot decide absolutely between these two elements of symmetry, nor can they decide, in the case of the plane of symmetry, to which of the three axial planes this plane in the molecule is parallel.

(*b*) Space-group V^{5}; molecule asymmetric.

(*c*) Space-group V^{9}; molecule asymmetric.

(*d*) Space-group C_{2v}^{20}; molecule asymmetric.

(*iii*) If the unit-crystal contains four molecules, the following arrangements are all possible:

(*a*) Space-group V_h^{25}; 4-fold molecular symmetry—two planes of symmetry parallel to any two axial planes of the crystal, and with these two symmetry planes intersecting in a 2-fold axis which is perpendicular to the third axial plane of the crystal.

(*b*) Space-group V^{8}; 2-fold molecular symmetry—a 2-fold axis perpendicular to any one of the three axial planes of the crystal.

(*c*) Space-group V^{9}; molecular symmetry as in (*b*).

(*d*) Space-group C_{2v}^{20}; 2-fold molecular symmetry—a plane of symmetry parallel to (1 0 0) or (0 1 0) in the crystal.

(*iv*) If the unit-crystal contains only two molecules, the following arrangements are all possible:

(*a*) Space-group V_h^{25}; 8-fold molecular symmetry—three planes of symmetry parallel to (1 0 0), (0 1 0), and (0 0 1) of the crystal, intersecting in three 2-fold axes.

(*b*) Space-group V^{8}; 4-fold molecular symmetry—three mutually perpendicular 2-fold axes.

(*c*) Space-group C_{2v}^{20}; 4-fold molecular symmetry—two planes of symmetry parallel to (1 0 0) and (0 1 0) of the crystal and with these two symmetry planes intersecting in a 2-fold axis.

(*v*) There cannot be only one molecule per unit-crystal in this case as the fundamental lattice is Γ_o'''.

As Astbury and Yardley point out, the example cited may be extreme, but it illustrates the inherent limitations of the method. The choice of

molecular symmetry can, of course, be narrowed down further, or even made absolute, if by some means (such as by a study of the exterior symmetries of the crystal, etch figures, or some directional physical property of the crystal) we can manage to eliminate certain of the space-groups from consideration.

3. Tetragonal System.—It was shown in Chaps. II, III, and IV and again in Table II of Chap. VIII that the tetragonal lattice Γ_t may be regarded as being either a simple tetragonal lattice $\Gamma_t(a)$ (corresponding to the simple orthorhombic lattice Γ_o), or as an end-centered tetragonal lattice $\Gamma_t(b)$ (*i.e.*, with the square faces centered, corresponding to the end-centered or side-centered orthorhombic lattice Γ_o'. Similarly it was shown that Γ_t' may be regarded at will as being a face-centered tetragonal lattice $\Gamma_t'(a)$ (corresponding to Γ_o''), or a body-centered tetragonal lattice (corresponding to Γ_o'''). For each of these two lattices the various crystal forms may be described according to either alternative, so that both are given in the tetragonal tabulations of Appendix III except for the space-groups derived from $D_{2d}(= V_d)$. In the $D_{2d}(= V_d)$ class the axial planes are always taken as bisecting the angles between the symmetry planes of the crystal, so that only one of the alternatives is possible with Γ_t and only one with Γ_t'. To avoid confusion the example of Astbury and Yardley is followed in Appendix III, and the orthorhombic lattice with which the actual tetragonal lattice may be compared is inserted in parentheses in the space-lattice column. In order to facilitate reference to Astbury and Yardley[55] $\Gamma_t(a)$ and $\Gamma_t'(b)$ are listed in Appendix III as the "first alternatives" of Γ_t and Γ_t', respectively. $\Gamma_t(b)$ and $\Gamma_t'(a)$ are listed as the "second alternatives."

In classes S, C_4, and C_{4h} the possible molecular symmetry is the same for both alternatives (1) and (2) in each space-group. In classes C_{4v}, D_4, and D_{4h}, the possible molecular symmetry, as stated in the table, applies only to (1). In order to apply it to (2), $\{1\,0\,0\}$ must be changed throughout into $\{1\,1\,0\}$ and $\{1\,1\,0\}$ into $\{1\,0\,0\}$. Another point to be watched carefully is that in the tetragonal system the form $\{1\,0\,0\}$ includes both the $(1\,0\,0)$ and $(0\,1\,0)$ planes. Similarly the $\{0\,k\,l\}$ includes both the $(0\,k\,l)$ and the $(h\,0\,l)$ planes. In other words the $\{1\,0\,0\}$ and $\{0\,1\,0\}$ are indistinguishable from each other. For example $C_{4v}(1)$ reads, "s is $\frac{1}{2}$ for $\{0\,k\,l\}$ if $(k + l)$ is odd; possible molecular symmetry 2-$A \perp \{0\,0\,1\}$, $P \parallel \{1\,1\,0\}$ or 2 P's $\parallel \{1\,1\,0\}$ intersecting in 2-A." This means that not only is $s = \frac{1}{2}$ for all planes in the $\{0\,k\,l\}$ zone if $(k + l)$ is odd, but also for all planes in the $\{h\,0\,l\}$ zone for which $(h + l)$ is odd; also, corresponding to any molecule having in itself a plane of symmetry parallel to $(1\,1\,0)$, there is a second molecule whose plane of symmetry is parallel to $(1\,\bar{1}\,0)$. If in this group the molecule has two planes of symmetry intersecting in a 2-fold axis, those planes will be parallel to $(1\,1\,0)$ and $(1\,\bar{1}\,0)$, respectively.

we may interpret it to mean also "if $s = \frac{1}{2}$ for (1 0 0) and (0 0 1), then the possible molecular symmetry is given by a 2-fold axis perpendicular to (0 1 0)"; or "if $s = \frac{1}{2}$ for (0 1 0) and (0 0 1), then the possible molecular symmetry is given by a 2-fold axis perpendicular to (1 0 0)."

In every molecular compound in the orthorhombic system which has been completely investigated, the unit-crystal appears to contain the minimum number of molecules. If we arbitrarily assume that this is always the case, then we may, to a limited extent, determine the molecular symmetry. Astbury and Yardley give the following illustration: Assume an orthorhombic crystal, of unknown class, for which s is $\frac{1}{2}$ for all planes where $(h + k + l)$ is odd.

(*i*) In terms of our hypothesis, it follows that if density measurements show that the unit-crystal contains sixteen molecules, the space-group must be V_h^{25} and the molecules must be asymmetric.

(*ii*) If the unit-crystal contains eight molecules, the following arrangements are all possible:

(*a*) Space-group V_h^{25}; 2-fold molecular symmetry—a plane of symmetry parallel to (1 0 0), (0 1 0), or (0 0 1) in the crystal, or a center of symmetry. X-ray measurements cannot decide absolutely between these two elements of symmetry, nor can they decide, in the case of the plane of symmetry, to which of the three axial planes this plane in the molecule is parallel.

(*b*) Space-group V^{3}; molecule asymmetric.

(*c*) Space-group V^{9}; molecule asymmetric.

(*d*) Space-group C_{2v}^{20}; molecule asymmetric.

(*iii*) If the unit-crystal contains four molecules, the following arrangements are all possible:

(*a*) Space-group V_h^{25}; 4-fold molecular symmetry—two planes of symmetry parallel to any two axial planes of the crystal, and with these two symmetry planes intersecting in a 2-fold axis which is perpendicular to the third axial plane of the crystal.

(*b*) Space-group V^{8}; 2-fold molecular symmetry—a 2-fold axis perpendicular to any one of the three axial planes of the crystal.

(*c*) Space-group V^{9}; molecular symmetry as in (*b*).

(*d*) Space-group C_{2v}^{20}; 2-fold molecular symmetry—a plane of symmetry parallel to (1 0 0) or (0 1 0) in the crystal.

(*iv*) If the unit-crystal contains only two molecules, the following arrangements are all possible:

(*a*) Space-group V_h^{25}; 8-fold molecular symmetry—three planes of symmetry parallel to (1 0 0), (0 1 0), and (0 0 1) of the crystal, intersecting in three 2-fold axes.

(*b*) Space-group V^{8}; 4-fold molecular symmetry—three mutually perpendicular 2-fold axes.

(*c*) Space-group C_{2v}^{20}; 4-fold molecular symmetry—two planes of symmetry parallel to (1 0 0) and (0 1 0) of the crystal and with these two symmetry planes intersecting in a 2-fold axis.

(*v*) There cannot be only one molecule per unit-crystal in this case as the fundamental lattice is Γ_0'''.

As Astbury and Yardley point out, the example cited may be extreme, but it illustrates the inherent limitations of the method. The choice of

molecular symmetry can, of course, be narrowed down further, or even made absolute, if by some means (such as by a study of the exterior symmetries of the crystal, etch figures, or some directional physical property of the crystal) we can manage to eliminate certain of the space-groups from consideration.

3. Tetragonal System.—It was shown in Chaps. II, III, and IV and again in Table II of Chap. VIII that the tetragonal lattice Γ_t may be regarded as being either a simple tetragonal lattice $\Gamma_t(a)$ (corresponding to the simple orthorhombic lattice Γ_o), or as an end-centered tetragonal lattice $\Gamma_t(b)$ (*i.e.*, with the square faces centered, corresponding to the end-centered or side-centered orthorhombic lattice Γ_o'. Similarly it was shown that Γ_t' may be regarded at will as being a face-centered tetragonal lattice $\Gamma_t'(a)$ (corresponding to Γ_o''), or a body-centered tetragonal lattice (corresponding to Γ_o'''). For each of these two lattices the various crystal forms may be described according to either alternative, so that both are given in the tetragonal tabulations of Appendix III except for the space-groups derived from $D_{2d}(= V_d)$. In the $D_{2d}(= V_d)$ class the axial planes are always taken as bisecting the angles between the symmetry planes of the crystal, so that only one of the alternatives is possible with Γ_t and only one with Γ_t'. To avoid confusion the example of Astbury and Yardley is followed in Appendix III, and the orthorhombic lattice with which the actual tetragonal lattice may be compared is inserted in parentheses in the space-lattice column. In order to facilitate reference to Astbury and Yardley[55] $\Gamma_t(a)$ and $\Gamma_t'(b)$ are listed in Appendix III as the "first alternatives" of Γ_t and Γ_t', respectively. $\Gamma_t(b)$ and $\Gamma_t'(a)$ are listed as the "second alternatives."

In classes S, C_4, and C_{4h} the possible molecular symmetry is the same for both alternatives (1) and (2) in each space-group. In classes C_{4v}, D_4, and D_{4h}, the possible molecular symmetry, as stated in the table, applies only to (1). In order to apply it to (2), $\{1\,0\,0\}$ must be changed throughout into $\{1\,1\,0\}$ and $\{1\,1\,0\}$ into $\{1\,0\,0\}$. Another point to be watched carefully is that in the tetragonal system the form $\{1\,0\,0\}$ includes both the $(1\,0\,0)$ and $(0\,1\,0)$ planes. Similarly the $\{0\,k\,l\}$ includes both the $(0\,k\,l)$ and the $(h\,0\,l)$ planes. In other words the $\{1\,0\,0\}$ and $\{0\,1\,0\}$ are indistinguishable from each other. For example $C_{4v}(1)$ reads, "s is $\frac{1}{2}$ for $\{0\,k\,l\}$ if $(k + l)$ is odd; possible molecular symmetry 2-$A \perp \{0\,0\,1\}$, $P \parallel \{1\,1\,0\}$ or 2 P's $\parallel \{1\,1\,0\}$ intersecting in 2-A." This means that not only is $s = \frac{1}{2}$ for all planes in the $\{0\,k\,l\}$ zone if $(k + l)$ is odd, but also for all planes in the $\{h\,0\,l\}$ zone for which $(h + l)$ is odd; also, corresponding to any molecule having in itself a plane of symmetry parallel to $(1\,1\,0)$, there is a second molecule whose plane of symmetry is parallel to $(1\,\bar{1}\,0)$. If in this group the molecule has two planes of symmetry intersecting in a 2-fold axis, those planes will be parallel to $(1\,1\,0)$ and $(1\,\bar{1}\,0)$, respectively.

Under the eighth column of the tables (headed "possible molecular symmetry") will be found occasional references to a 4-fold alternating axis. This is not a type of symmetry that is likely to occur often, but it should be kept in mind because of its probable existence in compounds such as $C[(C \cdot dXYZ)_2(C \cdot lXYZ)_2]$ and $(CHC \cdot dXYZ)_2(CHC \cdot lXYZ)_2$. Another still more complicated type of symmetry, referred to in the D_{2d} and D_{4h} classes, is the full D_{2d} symmetry. This consists of two perpendicular planes of symmetry intersecting in a 4-fold alternating axis. This means that there will be also two 2-fold axes of symmetry perpendicular to the 4-fold alternating axis and bisecting the angles between the planes. In the D_{2d} class the planes must always be parallel to the $\{1\,1\,0\}$ by convention. In the D_{4h} they may be parallel to the $\{1\,1\,0\}$ or the $\{1\,0\,0\}$.

4. Cubic System.—In the cubic system the form $\{h\,k\,0\}$ includes all the three axial zones, just as the form $\{1\,0\,0\}$ includes all three axial planes. This must be remembered in using Tables XVI to XX of Appendix III. Where we read, as in T_h^2, "$s = \frac{1}{2}$ for $\{hk0\}$, if $(h + k)$ is odd; possible molecular symmetry 2-$A \perp \{1\,0\,0\}$, etc.," we must remember that s will equal $\frac{1}{2}$ for the whole $\{hk0\}$ form, *i.e.*, $(1\,2\,0)$, $(0\,1\,2)$, $(2\,0\,\bar{1})$, $(0\,1\,0)$, $(0\,0\,1)$, etc.; that is, s will be $\frac{1}{2}$ for any plane in an axial zone if the sum of the indices is odd. Also if the molecule itself has a 2-fold axis, then for each molecule whose axis is perpendicular to the $(1\,0\,0)$, for instance, there will be two other molecules whose axes are perpendicular to $(0\,1\,0)$ and $(0\,0\,1)$ respectively. In the space-group T_h^6, s is listed as $\frac{1}{2}$ for the planes $(hk0)$ if h is odd. This includes of course $(hk0)$ if h is odd, $(0kl)$ if k is odd, and $(h0l)$ if l is odd.

In the case in which the possible molecular symmetry is stated to be "2 P's $\parallel \{1\,0\,0\}$ and $\{1\,1\,0\}$ intersecting in 2-$A \perp \{1\,1\,0\}$," any one molecule might have, for example, two planes parallel to $(1\,0\,0)$ and $(0\,\bar{1}\,1)$ intersecting in a 2-fold axis perpendicular to $(0\,1\,1)$, in which case there would be two other molecules the direction of whose symmetry elements could be found by rotation through $2\pi/3$ and $4\pi/3$, respectively, about a 3-fold axis perpendicular to $\{1\,1\,1\}$; but no molecule can exist whose two planes are parallel to $(1\,0\,0)$ and $(1\,0\,\bar{1})$, say, since these two planes would intersect in a 2-fold axis which would be perpendicular to $\{1\,0\,0\}$ instead of $\{1\,1\,0\}$.

Illustrations of the Symmetries of Molecules and Atoms.—It is easy to imagine the value of the foregoing to an organic chemist. Many examples of molecular symmetries may be found in the summary of the crystal structures of organic compounds in Wyckoff's "Structure of Crystals,"[22] so that they need not be repeated here. It may be of interest, however, to see what we can bring out about the symmetries of inorganic molecules and of the atoms of the elements.

Al_2O_3* crystallizes on space-group D_{3d}^6 with two molecules per unit-rhombohedron. This requires a value of six for p of Table XXV of Appendix III. The molecular symmetry requires either "three 2-fold axes of symmetry intersecting in a 3-fold axis of symmetry which is perpendicular to $\{1\,1\,1\}$," or "one 3-fold axis of symmetry perpendicular to $\{1\,1\,1\}$, plus a center of symmetry." The first of these two alternatives fits our description of an Al_2O_3 molecule very well. We have described the molecule as an equilateral triangle of oxygens with one Al immediately above and one immediately below the center of the triangle. The line joining the two Al atoms is evidently a 3-fold axis of symmetry which is perpendicular to the plane of the three oxygens. In the plane of the three oxygens a line joining the center of any given oxygen with the center of the triangle is evidently a 2-fold axis of symmetry. Three of these are possible. This completes the requirements for the first alternative. The second alternative, which demands a center of symmetry, would require the Al to be surrounded by six oxygens, three above and three below, with the equilateral triangles of each set at exactly equal distances from the Al and rotated 180° with respect to each other. This requirement cannot be met, for the lattice parameters of Al_2O_3 show that the two sets of triangles do not lie at exactly the same distances from the Al. If they had been so spaced, Al_2O_3 would have been an ionic compound and we should have been at a loss to explain its insulating value at high temperatures.

"Low" quartz crystallizes on space-group D_3^4 or D_3^6 depending on whether it is "left-handed" or "right-handed" quartz. It has three molecules per unit-crystal. The value of p of Table XXII of Appendix III is therefore 2. The molecular symmetry requires a 2-fold axis perpendicular to $\{1\,1\,\bar{2}\,0\}$. We have already found occasion to describe the low temperature form of quartz as an elbow lying in the basal plane of the hexagonal crystal. Reference to Figs. 21 and 22 of Chap. VI shows that a line bisecting the angle of the elbow is, in every case, perpendicular to some member of the $\{1\,1\,\bar{2}\,0\}$ form. This bisector is a 2-fold axis of symmetry for the SiO_2 molecule. The symmetry requirements are still met if, as suggested in Chap. VI, the molecule is rotated slightly about this 2-fold axis so as to place one oxygen in a $(1\,1\,\bar{2}\,0)$ plane slightly above that of the silicon and the other oxygen in a plane correspondingly lower than that of the silicon.

CBr_4, CI_4, SnI_4, $ZrCl_4$, and GeI_4, all crystallize on space-group T_h^6 with eight molecules per unit-cube. This makes p of Table XVIII of Appendix III equal to 3. The molecule must have one 3-fold axis of symmetry perpendicular to each of the four members of the $\{1\,1\,1\}$ form. This requirement leads at once to a tetrahedral distribution of the four halogens with the metal atom at the center. Si and Pb are the only

* Similar statements can be made for Fe_2O_3, Cr_2O_3, Ga_2O_3, Ti_2O_3, and V_2O_3.

other members of this chemical family in the periodic table. They seem to have no solid inorganic compounds of the form RX_4, but they form the solid compounds $Si(C_6H_5)_4$ and $Pb(C_6H_5)_4$. These belong to space-group $V_d^4 (= D_{2d}^4)$ and show a tetrahedral distribution of C_6H_5 groups about the central atom of Si or Pb.* All this is just what we should have expected from the fact that these elements all lie in the carbon column of the periodic table, and we are strengthened in our assumption of Chap. XIII that C, Si, etc., have tetrahedral atomic domains. It remains to get direct evidence from the crystals of the elements themselves. This is legitimate not only on the basis of a static-atom picture with definite positions in the lattice for the valence electrons, but also on the basis of any other picture which permits the valence electrons to have a "most probable" or "mean" position.

Diamond† crystallizes on Wyckoff's cubic 8(*f*), with eight atoms per unit-cube. Only the cubic space-groups O^4, T_h^4, and O_h^7 permit Wyckoff's 8(*f*). Tables XVI to XX of Appendix III show that if space-groups O^4 or T_h^4 are to have eight atoms of carbon per unit-cube, then the atoms themselves must have the full symmetry of T. Similarly, if space-group O_h^7 is to have eight atoms of carbon per unit-cube, then the atoms themselves must have the full symmetry of T_d. It turns out that in the special case of eight atoms per unit-cube, these two symmetries become identical. This may be visualized easily by using Table XXXVII of Appendix III and Wyckoff's coordinates. Table XXXVII of Appendix III shows that, up to a limit of 32 points (*i.e.*, eight atoms with four valence electrons each) per unit-cube, O^4, T_h^4, and O_h^7 all permit:

Two sets of 8 points, each with definitely fixed coordinates, [Wyckoff's 8(*f*) and 8(*g*)]. Evidently there are not enough points to take care of 32 valence electrons.

Two sets of 16 points, each with definitely fixed coordinates, [Wyckoff's 16(*b*) and 16(*c*)]. This would indicate two groups of valence electrons of 16 electrons each. The two groups are identical except that 16(*c*) is displaced from 16(*b*) by a translation of $\frac{1}{2}\frac{1}{2}\frac{1}{2}$.

One set of 32 points [Wyckoff's 32(*b*)] with one undetermined parameter.

Either of the last two of these alternatives is, then, theoretically possible no matter which of the three space-groups we happen to pick. Wyckoff's 32(*b*) may be interpreted as putting the four valence electrons of each carbon atom at the corners of a tetrahedron, with adjacent tetrahedra placed corner to corner in such a way that adjacent corners lie on a line joining the centers of the two tetrahedra. This is completely consistent with the static atom picture of atomic structure advocated by

* Nothing is shown about the symmetry of the C_6H_5 group.

† Precisely similar statements can be made for Si, Ge, and gray Sn. Somewhat similar, but more complicated, statements can be made for Pb. We might picture the atomic domain of Pb as being practically a sphere with four valence electrons tetrahedrally arranged.

G. N. Lewis and M. Huggins. If, instead, we put half the valence electrons on Wyckoff's 16(*b*) and half on 16(*c*) we have a peculiar arrangement of tetrahedra. The valence electrons situated on 16(*b*) form tetrahedra whose centers correspond to the positions of the atoms in diamond. These tetrahedra have only a single electron at the places where the tetrahedra meet. The valence electrons situated on 16(*c*) form similar tetrahedra which are displaced from the first set by an amount $\frac{1}{2}\frac{1}{2}\frac{1}{2}$. If this second set of tetrahedra had contained, in addition, the nuclei and *K* electrons of carbon, they would have changed each diamond cube into eight body-centered cubes. In the absence of these nuclei and *K* electrons it is highly improbable from electrostatic considerations that the second set of tetrahedra would be exactly equal in size to the first. But Wyckoff's 16(*b*) and 16(*c*) require exact equality of size of the two sets of tetrahedra so that, even apart from any possible x-ray evidence, the structure is untenable. We are therefore compelled by the theory of space-groups to place the "most probable," or "mean" positions of the valence electrons of the carbon atoms in diamond on Wyckoff's 32(*b*). The "shape" of the carbon atom is therefore tetrahedral, agreeing with the shape of the atomic domain as found in Chap. XIII and with the crystal structure of the compounds of carbon and its close relatives in the periodic table.*

When we add all this evidence to the mass of evidence offered by organic chemistry, we feel safe in saying that, even though atoms are too small to be seen with the most powerful microscope, the tetrahedral shape of the carbon atom is one of the most firmly established facts known to science.

SUMMARY

We have taken up the various types of chemical combination as shown by crystal-structure data and have found evidence for five types: (*a*) molecular, (*b*) ionic, (*c*) geometrical, (*d*) secondary valence, (*e*) mixed-ionic. All compounds and radicals belonging to types (*c*), (*d*), or (*e*) may be regarded as special cases of (*a*) or (*b*). Types (*c*) and (*e*) seem to differ only in that the negative ions are electrons in (*c*) whereas they are O^{--} ions in (*c*).

We have discussed, under the title of Variate Atom Equipoints, the departures which certain complex crystals may make from the ordinary simple law that crystallographically equivalent points must always contain chemically equivalent atoms (or ions).

We have discussed the contributions of crystal analysis to both organic and inorganic chemistry and have made considerable use of Tables I to XXXII of Appendix III in a discussion of molecular symmetries.

* This agreement lends considerable plausibility to the assumption, made here and in previous chapters, that the valence electrons of an element occupy definite mean positions in the crystal structure.

References

1. A. Müller, *Jour. Chem. Soc.*, **123**, 2043 (1923).
2. G. Shearer, *Jour. Chem. Soc.*, **123**, 3152 (1923).
3. A. Müller and G. Shearer, *Jour. Chem. Soc., London*, **123**, 3156 (1923).
4. J. Trillat, *Compt. rend.*, **180**, 1320, 1485, 1838 (1925).
5. J. Trillat, *Ann. Physik*, **6**, 1 (1926).
6. I. Langmuir, *Proc. Nat. Acad. Sci.*, **3**, 251 (1917). See also *Jour. Amer. Chem. Soc.*, **39**, 1848 (1917).
7. N. K. Adam, *Proc. Roy. Soc. London*, **101**, 452 (1922).
8. J. Hengstenberg, *Zeit. Physik*, **58**, 345 (1929).
9. E. Bain, *Chem. Met. Eng.*, **26**, 655 (1922); **28**, 65 (1923).
10. G. Tammann, "A Text Book of Metallography" (English translation by Dean and Swenson), Chemical Catalog Company, New York, 1925.
11. W. Hume-Rothery, *Jour. Inst. Metals*, **35**, 313 (1926).
12. H. Perlitz, *Jour. Chem. Phys.*, **1**, 335 (1933).
13. A. F. Westgren and G. Phragmen, *Trans. Faraday Soc.*, **25**, 379 (1929).
14. A. F. Westgren and G. Phragmen, *Metallwirtschaft*, **7**, 700 (1928).
15. "International Critical Tables," Vol. I, p. 340, McGraw-Hill Book Company, Inc., New York, 1926.
16. H. Mark and E. Pohland, *Zeit. Kryst.*, **62**, 103 (1925).
17. A. Werner, "Neuere Anschauungen auf dem Gebiete der anorganischen Chemie," 4th ed., Vieweg, Braunschweig, 1920.
18. F. Ephraim, "Anorganische Chemie," T. Steinkopf, Leipzig, 1923.
19. R. Schwartz, "The Chemistry of the Inorganic Complex Compounds," John Wiley & Sons, Inc., New York, 1923.
20. F. A. Steele, *Gen. Elec. Rev.*, **32**, 552 (1929).
21. P. Scherrer and P. Stoll, *Zeit. anorg. Chem.*, **121**, 319 (1922).
22. R. W. G. Wyckoff, "The Structure of Crystals," 2d ed., Chemical Catalog Company, New York, 1931.
23. O. Hassel and H. Mark, *Zeit. Physik*, **27**, 89 (1924).
24. R. W. G. Wyckoff, *Jour. Amer. Chem. Soc.*, **42**, 1100 (1920).
25. P. M. Harris, E. Mack, and F. C. Blake, *Jour. Amer. Chem. Soc.*, **50**, 1583 (1928).
26. W. L. Bragg, *Zeit. Kryst.*, **74**, 237 (1930).
27. L. Pauling, *Jour. Amer. Chem. Soc.*, **51**, 1010 (1929).
28. F. A. Steele and W. P. Davey, *Jour. Amer. Chem. Soc.*, **51**, 2283 (1929).
29. F. A. Barta and W. H. Zachariasen, *Phys. Rev.*, **37**, 1626 (1931).
30. T. F. W. Barth, *Fortschritte Mineral. Krist. Petrog.*, **17**, 25 (1932).
31. T. F. W. Barth and E. Posenjak, *Jour. Wash. Acad. Sci.*, **21**, 255 (1931).
32. E. Posenjak and T. Barth, *Phys. Rev.*, **38**, 2234 (1931).
33. T. F. W. Barth, *Zeit. Kryst.*, **83**, 405 (1932).
34. F. M. Jaeger, *Trans. Faraday Soc.*, **25**, 320 (1929).
35. F. Machatschki, *Centralbl. Mineral., Geol.*, A, 278 (1930).
36. L. Pauling, *Jour. Amer. Chem. Soc.*, **46**, 2738 (1924).
37. S. B. Hendricks and L. Pauling, *Jour. Amer. Chem. Soc.*, **47**, 2904 (1925).
38. O. Hassel, *Norsk. Geol. Tids.*, **10**, 33 (1928).
39. W. P. Davey, *Chem. Rev.*, **6**, 143 (1929). Good résumés of the structures of organic crystals may be found in R. W. G. Wyckoff, "The Structure of Crystals," 2d ed., Chemical Catalog Company, New York, 1931.
    S. B. Hendricks, *Chem. Rev.*, **7**, 431 (1930), and in the Referate, *Zeit. Kryst.*
40. A. Müller and Saville, *Jour. Chem. Soc. London*, **127**, 559 (1926).

41. W. T. Astbury, *Proc. Roy. Soc.*, **102**, 506 (1923).
42. W. H. Bragg, *Proc. Phys. Soc., London*, **34**, 33 (1921); *Jour. Chem. Soc. London*, **121**, 2766 (1922).
43. B. Broome, *Phys. Zeit.*, **24**, 124 (1923).
44. E. D. Eastman, *Jour. Amer. Chem. Soc.*, **46**, 917 (1924).
45. B. Broome, *Zeit. Kryst.*, **62**, 325 (1925).
46. E. G. Cox, *Nature*, **122**, 401 (1928).
47. G. Bruni and G. Natta, *Rec. trav. chim.*, **48**, 860 (1929).
48. K. Lonsdale, *Proc. Roy. Soc.*, **123**, 494 (1929); *Trans. Faraday Soc.*, **25**, 352 (1929).
49. W. H. Bragg, *Proc. Phys. Soc. London*, **35**, 167 (1923).
50. J. M. Robertson, *Proc. Roy. Soc.*, **125**, 542 (1929).
51. J. M. Robertson, *Nature*, **125**, 456 (1930).
52. K. Banerjee, *Nature*, **125**, 456 (1930); *Ind. Jour. Phys.*, **4**, 557 (1930).
53. K. Meyer and H. Mark, "Der Aufbau der Hochpolymeren organischen Naturstoffe," Akademische Verlagsgesellschaft, 1930.
54. K. Hess, "Chemie der Cellulose," Akademische Verlagsgesellschaft, 1928.
55. G. L. Clark, "Applied X-rays," 2d ed., McGraw-Hill Book Company, Inc., New York, 1932; see also *Ind. Eng. Chem.*, **21**, 128 (1929).
56. W. T. Astbury and K. Yardley, *Phil. Trans. Roy. Soc. London*, **224**, 221 (1924).

APPENDIX I*

X-RAY TUBES, TRANSFORMERS, AND ACCESSORIES

A. X-RAY TUBES FOR CRYSTAL ANALYSIS†

Coolidge Tube.—The Coolidge tube consists of a highly evacuated glass bulb, into the opposite ends of which are sealed a tungsten-filament cathode and a metal anticathode or target. Figure 1 shows a diagram of the molybdenum-target tube used in the General Electric x-ray diffraction apparatus.

In the operation of the tube the filament is heated by a low-voltage electric current and thus becomes a source of thermal electrons. A high voltage is impressed across the two electrodes of the tube, and the electrons emitted by the filament are driven at a high velocity against the target. The resulting bombardment of the target material by high-speed electrons causes the target to emit x-rays. The electron stream is confined to the face of the target as closely as possible by means of the focusing effect of a concave molybdenum cup surrounding the filament.

Control of the space current in the x-ray tube for a given voltage is entirely by regulation of the filament-heating current. Great care is taken in the construction of the tube to remove as much residual gas as possible from the glass and metal parts of the tube. A tube which becomes gassy is erratic in operation and ultimately will draw an excessive current and be uncontrollable.

The Coolidge tube may be operated on alternating current if the target is kept cool enough to prevent the emission of thermal electrons from it. This is accomplished by direct water-cooling or by conduction of the heat generated at the target through the copper anode arm to an external set of radiating fins. The former method of cooling requires that either the anode end of the tube be at ground potential or the cooling system be insulated. Operation with water-cooling and self-rectification is the usual method for x-ray diffraction units.

* By M. L. Fuller, investigator in spectroscopy and crystal structure, Research Division, New Jersey Zinc Company, Palmerton, Pa.

† It is perhaps only fair to warn the reader against the purchase of certain European made tubes. Some of the best known continental European firms have sold defective tubes to their American customers and then have refused either to replace the tubes or to refund the purchase price except under extraordinary pressure. It is much safer to buy tubes from reputable American manufacturers.—W.P.D.

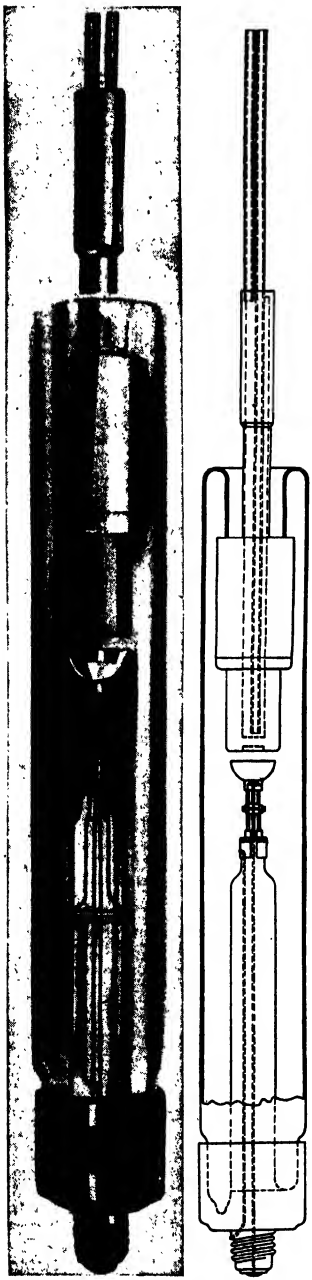

FIG. 1.—Diagram of Coolidge-type tube used in General Electric apparatus. (*Courtesy of General Electric x-ray Corporation.*)

An excellent account of the details of design and construction of Coolidge tubes is given by Terrill and Ulrey.[1]

Gas-discharge Tube.—A gas-discharge tube is usually constructed entirely of metal, with the exception of a glass or porcelain insulator which insulates the high-potential cathode from the metal parts of the tube which are usually at ground potential. The cathode consists of a concave aluminum mirror which focuses the electron stream on the target. The x-rays leave the tube through openings covered with thin aluminum foil. The gas-discharge tube is operated under a partial vacuum of air of the order of 0.01 mm. of mercury, which vacuum is controlled during the operation of the tube by a vacuum pumping system. Positive ions present in the gas are driven against the aluminum cathode by means of the impressed high voltage and liberate from it negative electrons which are then driven against the target giving rise to x-rays.

Most workers prefer to construct their own gas-discharge tubes, and descriptions of such tubes may be found in the literature. The principal feature of an x-ray tube with aluminum-foil windows, which permits it to be used where the glass Coolidge tube cannot be used, is in the production of long-wavelength x-rays such as those produced from copper and iron targets. This long-wavelength radiation is efficiently transmitted by thin aluminum-foil windows (0.01 mm. thick) but is highly absorbed by the walls of an ordinary glass x-ray tube. Thin windows of pyrex glass or of Corning 707 BM glass may be used instead of aluminum foil if desired.

Metal x-ray tubes are constructed so that the metallic body of the tube is at the same potential as the target. This permits the target to be mounted very close to the aluminum-foil windows. The result is that the specimen and photographic film may be

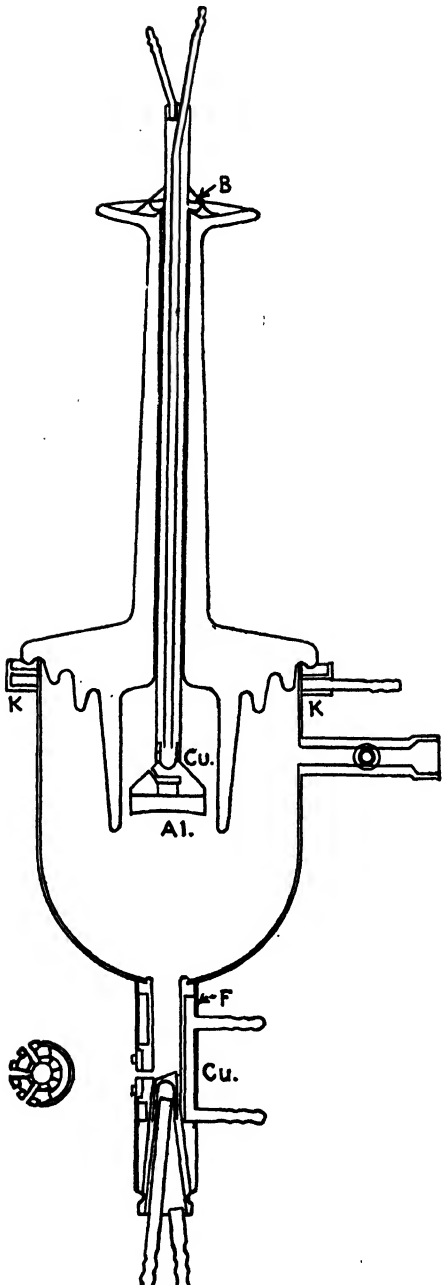

FIG. 2.—Diagram of Hadding-Siegbahn-type gas-discharge tube.

brought very close to the target, making much shorter exposure times than those required with ordinary glass Coolidge-type tubes. Rugged metal construction and effective water-cooling enable metal gas-discharge tubes to operate at high currents which further aids in reducing exposure time. A copper-target tube will produce x-ray patterns in much less exposure time than molybdenum-target tubes.

Offsetting these apparent advantages in exposure time of gas-discharge tubes over Coolidge-type tubes is the difficulty of maintaining satisfactory operation without the attention of an operator. With a Coolidge-type tube, up to 12 exposures may be made in a 24-hr. period without the attention of an operator, whereas the average production of patterns of similar type will be considerably less per day with a gas-type tube with three windows. This estimate assumes operation of the tube only during the normal working day and considers the time spent in repairing and adjusting the apparatus, etc.

The essential advantages of the metal gas-discharge tube over the glass Coolidge type of tube are:

1. Ability to produce long-wave-length x-rays with which x-ray diffraction effects from crystals of large interplanar spacing may be studied (particularly organic compounds) without contaminating the target with tungsten from the filament.
2. Ease with which targets of various materials and special construction may be inserted and removed.
3. Short exposure time in special cases where the diffraction apparatus requires the attention of the operator or where the specimen undergoing examination alters during the course of a longer exposure.
4. General adaptability for experimental purposes of metal construction.

Figure 2 shows a diagram of the essential features of a Hadding-Siegbahn-type tube. The details of assembly and operation of this tube will be discussed in a later section of this Appendix.

Filament-cathode Metal Tubes.—The filament-cathode metal tube is similar in construction to the metal gas-discharge tube. The former differs from the latter in that a heated tungsten-filament cathode is used instead of a cold aluminum cathode. The tube must be operated at a vacuum high enough to prevent the production of electrons by positive-ion bombardment. The tube then operates like a Coolidge tube. In the filament-cathode metal tube no air-leak device is needed to maintain the proper amount of rarefied air in the tube as in the gas-discharge tube. This simplification of operation is offset by the difficulty of maintaining the necessary high vacuum in a metal tube and the frequent replacement of tungsten filaments. This type of tube has the same advantages due to metal construction which were set forth for the gas-discharge tube. It is more frequently used in spectroscopic investigations than in crystal-diffraction studies. Figure 3 is a sectional view of a filament-cathode tube designed by Siegbahn.

B. X-RAY POWER UNITS

Transformers.—High-voltage transformers for x-ray power units should be purchased from reputable American manufacturers in order to make sure that they will stand up under American climates and American conditions. It is false economy to purchase an inferior transformer or one that does not have an adequate current voltage rating. It is well to have a transformer of higher capacity than appears to be needed

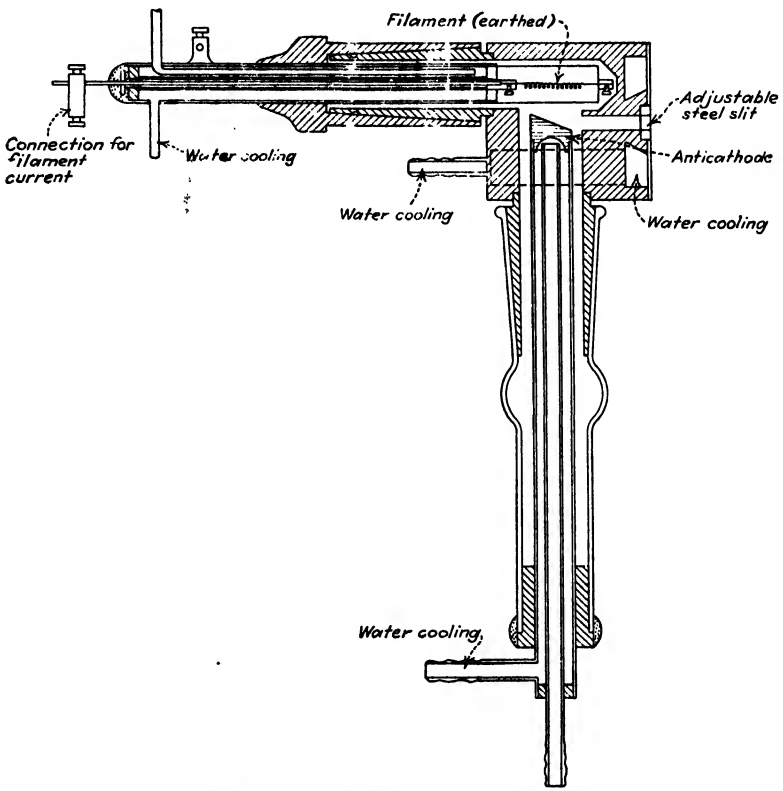

FIG. 3.—Diagram of Siegbahn-type filament cathode tube.

when setting up an x-ray power unit. In experimental work of this kind unforeseen demands for higher voltage or higher current are usually met eventually.

Transformers for gas-discharge tubes should have primary windings of higher resistance than is usual in transformers. This added resistance may be in the winding itself or may be supplied by an external series resistance. With such a resistance in the circuit, excessive withdrawal of current in gas-discharge tubes due to sudden release of gas from the tube walls is immediately counteracted by a drop in voltage. The result

of these effects is a more steady operation of the tube without danger of overloading the transformer.

The minimum excitation potentials of the K radiation of the commonly used target materials, molybdenum, copper, and iron, are 20.0, 8.86, and 7.10 kv., respectively. For a given set of conditions only that portion of the voltage wave which is above the minimum excitation voltage of the radiation desired will be effective in producing that radiation. The intensity of x-rays produced in an x-ray tube is approximately proportional to the square of the applied voltage and linearly proportional to the current. For the foregoing reasons the higher the voltage wave used, the greater will be the intensity of the x-rays produced. On the other hand the use of too high a voltage will result in the production of a strong continuous radiation having a pronounced peak near the short-wave-length limit. The short waves in the continuous spectrum will become objectionable through fogging of the photographic film by diffuse scattered radiation and sometimes by the production of a diffraction halo corresponding to the peak in the continuous radiation referred to above. Filtering will not remove these short wave lengths sufficiently if the voltage is too high. The production of continuous radiation is much greater with the high-atomic-weight targets than with the low-atomic-weight targets.

The optimum voltage for the operation of molybdenum-target tubes is about 40 kv. peak and for copper- and iron-target tubes about 50 kv. peak. In the production of a strong continuous radiation for the Laue method a tungsten target operating at 60 to 65 kv. peak is most commonly used.

Rectifying and Non-rectifying X-ray Tubes.—Coolidge tubes, in which provision is made for keeping the anticathode cool, operate self-rectifying. The self-rectifying x-ray tube allows current to pass only when the heated filament is the negative electrode. Coolidge tubes not provided with anticathode-cooling, and gas-discharge tubes, must be provided with direct current. Filament-cathode metal tubes, such as the Siegbahn tubes previously described, will operate self-rectifying if a sufficiently good vacuum is maintained. The reason that this type will not always operate self-rectifying is that it is difficult to obtain in a metal x-ray tube a vacuum high enough to prevent the tube acting partially as a gas-discharge tube. It is only with the greatest of care in manufacture that a glass Coolidge tube is sufficiently outgassed to prevent the flow of an inverse current. Rectification of the alternating-current output of the transformer is accomplished by one of two types of rectifiers. The one type is the high-voltage vacuum-tube rectifier. The other type is the rotating-switch or mechanical rectifier.

Vacuum-tube Rectification.—The high-voltage vacuum-tube rectifier consists of a highly evacuated glass bulb into opposite ends of which

are sealed two electrodes. The one electrode is a tungsten filament and the other a metal plate. In operation the filament is heated by a low-voltage current and thus the tube acts as a valve permitting current to pass only when the filament is the negative electrode. These tubes are constructed so as to withstand the no-load high voltage of the inverse wave. Sufficient filament-heating current is supplied to transmit the high-voltage current in the "useful" direction with very little drop in voltage across the vacuum tube. The filament current is varied and hence the current-carrying capacity of the tube is varied by varying the voltage applied to the filament. This is accomplished by either an autotransformer or a series resistance or both.

There are various ways of connecting vacuum-tube rectifiers in x-ray-tube circuits. The three methods most generally used for x-ray-diffraction work will be described. Only circuits which permit the anode of

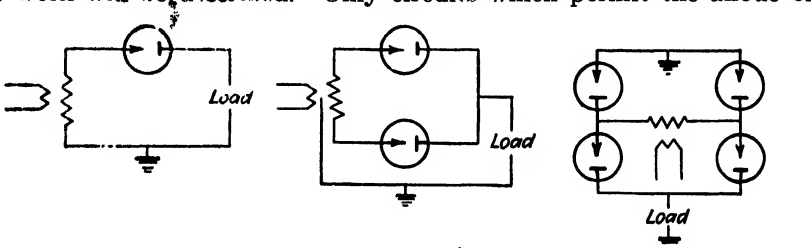

(a) (b) (c)

FIG. 4(a) Single-tube half-wave circuit. (b) Two-tube full-wave circuit. (c) Four-tube full-wave circuit.

the x-ray tube to be grounded are shown since this is the usual method for crystal-analysis x-ray apparatus. The simplest scheme is shown in Fig. 4*a*. In the wiring diagrams shown, the arrowhead represents the filament of the rectifier tube. One rectifier tube is used, but only half-wave rectification can be obtained. The full voltage of the transformer is applied across the x-ray tube. The rectifier must be able to withstand the full no-load voltage of the transformer. Using two vacuum tubes, full-wave rectification can be obtained according to the diagram of Fig. 4*b*. Only half of the full voltage of the transformer, however, is applied across the x-ray tube. The rectifier tubes must be able to stand the full transformer voltage or twice that of the x-ray tube. If the anode is to be grounded, full-wave rectification and full transformer voltage across the x-ray tube can only be obtained by using four rectifier tubes connected as shown in Fig. 4*c*. The rectifiers must be able to stand the full no-load voltage of the transformer. Full-wave, full-voltage rectification with two tubes, using condensers in the circuit, can be accomplished. Such an arrangement, however, does not permit the grounding of the anode of the x-ray tube.

The three methods described will furnish the x-ray tube with a unidirectional current, but the voltage will fluctuate from zero to the

peak value of the wave. The current flowing at voltages below the critical excitation potential of the x-rays used will be useless in the production of x-rays but will have a heating effect which is undesirable. A constant-potential direct current can be obtained with kenotron rectification if (1) the voltage supplied to the transformer has a frequency of 500 cycles or more and (2) condensers of sufficient capacity are connected in the circuit to smooth out the ripples in the fluctuating voltage. At present no method of crystal analysis requires a constant voltage. A very excellent description of methods used to obtain constant-potential direct current is given by Terrill and Ulrey.[1]

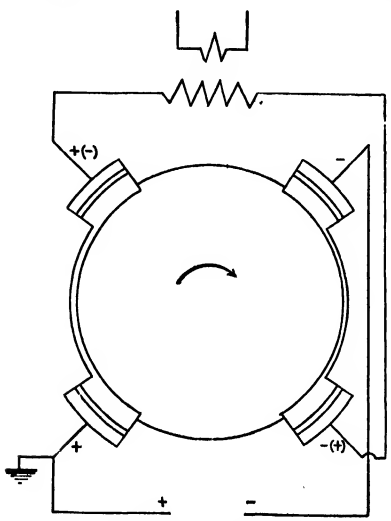

FIG. 5.—Diagram of rotating-switch rectifier circuit.

Rotating-switch Rectification.—The rotating-switch rectifier automatically connects the one or the other terminal of the transformer to the x-ray tube so that the x-ray tube receives a unidirectional current.

The rectifier consists of four moving contacts mounted 90° from each other on the shaft of a synchronous motor and four stationary contacts mounted about $\frac{1}{16}$ in. outside the path of revolution of the moving contacts and 90° apart from each other. The moving contacts are mounted either on four arms or on a bakelite disk. The power supply to the synchronous motor is the same as that to the primary of the transformer. An indicating device must be used to show whether the synchronous motor is connected correctly (or incorrectly) to the line, in order to make sure that the x-ray tube will receive voltage of the right polarity. A wiring diagram for this type of rectifier is shown in Fig. 5. Full-wave rectification is obtained. The contacts are made in an arc of such length that only the upper portion of the voltage wave is utilized. Thus the low-voltage portion of the wave, which is not effective in producing x-rays but does produce heating of the apparatus, is not used. The resultant current is a pulsating unidirectional current. Actually, however, it is not possible to cut out the undesirable portion of the wave form sharply, since there is always much sparking over before and after a moving contact meets a stationary contact.

The mechanical rectifier is rugged and dependable and requires very little attention. Its operation is accompanied by a great deal of noise. No make of rotating-switch rectifier is noiseless since in all types there is

necessarily sparking between the moving and stationary contacts with the resultant noise, but the noise can be reduced by enclosing the rectifier unit in a sound-deadening cabinet.

The advantages of vacuum-tube rectification are:

1. Silent operation.
2. No bearings to be oiled.
3. Easily adapted to constant-potential outfits.

The disadvantages of vacuum-tube rectification are:

1. Uncertain life of vacuum tubes involving replacements; hence, an upkeep cost.
2. Unless condensers are used, both the low non-useful voltage and the high useful voltage are supplied to the x-ray tube.
3. Adjustment of filament current required from time to time.

The advantages of rotary-switch rectification are:

1. Practically no upkeep cost.
2. Very little to get out of order, and adjustment very infrequent.
3. Utilization of high-voltage portion of wave only.

The disadvantages of rotary-switch rectification are:

1. Noisy operation.
2. Not adaptable to constant-potential circuits since the rotary switch cannot be operated at the high frequency (500 cycles) required for constant-potential direct-current condenser circuits.

Control Units.—Where it is desirable to vary the voltage applied to the Coolidge type of x-ray tube an autotransformer is desirable. The primary of the autotransformer is connected to the power source, and the secondary of the autotransformer is connected to the primary of the high-potential transformer. With gas-discharge tubes, a series resistance is desirable in connection with voltage control for reasons already given.

In Coolidge-tube circuits the amount of current passing through the tube is varied by varying the heating current of the filament. A series resistance in the filament circuit is used for this purpose. Such current control is also used in the metal tubes having hot filaments.

The tube current in gas-discharge-tube circuits depends on the gas pressure in the tube. In the operating range of pressures an increase of pressure is accompanied by an increase of current and *vice versa*. The regulation of the gas pressure or degree of vacuum will be discussed in a later section.

Stabilizers.—Filament-tube circuits usually include a current-stabilizer relay. When, due to the formation of gas within the tube or for other reasons, the tube draws a heavier current, the stabilizer automatically decreases the filament-heating current. The reduction of the filament-heating current then lowers the x-ray-tube current at which

point the normal filament is again supplied, etc. The resultant of this cycle of operations is a very steady current through the x-ray tube. One well-known type of stabilizer accomplishes this control of the filament current by means of a current relay which automatically opens and closes short-circuiting contacts across a resistance in series with the filament.

Stabilization of gas-discharge-tube currents is obtained by automatic vacuum-regulating devices to be described later under section C.

C. OPERATION OF UNITS

Coolidge Tubes.—The operation of Coolidge tubes may be gathered from what has already been said. Space current in the x-ray tube is readily controlled by regulation of the filament-heating current, stable operation is assured by the use of a reliable stabilizer, and flexibility of voltage requirements is obtained with one of the usual control units.

Ultimately a Coolidge-type tube which has been sealed off from the pump will fail by becoming gassy or by the puncturing of the glass walls of the tube. In order to avoid excessive current withdrawals, caused by a gassy condition, every control unit should be provided with a suitable circuit-breaker for opening the circuit when the primary current of the transformer becomes excessive. It is often possible to renew a gassy tube by the following procedure: Reduce the filament current to such a point that the tube will draw a small current steadily. Slowly increase the filament current until the tube draws its normal current steadily. This series of increases of filament current may have to be extended over a period of 10 to 50 hr. before steady operation is attained. In several cases this treatment was applied two or three times to the same tubes, thus increasing the lives of the tubes several-fold. Tube puncturing seems to happen almost accidentally, and it is usually impossible to assign a definite cause for a given tube failure by puncturing. The best that can be done to prevent it is to keep the tube clean and free from dust and to support the tube in such a way that no sharp points are near it. Little trouble will be had with filaments burning out if the filament current does not exceed that specified as a safe limit by the manufacturer.

Tube life is very variable and may be as short as two or three hundred hours or as long as several thousand hours.* The usual failure of Coolidge tubes is by gassing. The gas is liberated from the glass walls of the tube by the bombardment of stray electrons or by slow leaks either through pinholes in the glass or (more probably) by diffusion of gases through some of the metal parts. The number of stray electrons is very much increased as the tube current or voltage is increased. An important advance has been made recently, by W. P. Davey, in the design

* The minimum life should be about 1,000 hr.—W.P.D.

of tubes for the General Electric x-ray diffraction apparatus. By mounting the cathode and target much closer together than had hitherto been the practice, the number of electrons which leave the cathode and are not absorbed by the target is very much reduced. In the laboratory of the New Jersey Zinc Company a tube of this type ran for 15,000 hr. of practically continuous operation before it failed. Not once during its life did it show a gassy condition. Similar long lives have been reported for this type of tube elsewhere. The average life of 14 tubes of the former type, previously used in this laboratory, was 450 hr. Only two of the 14 tubes ran more than 1,000 hr.

Gas-discharge Tubes and Accessories.—The operation of gas-discharge tubes is often quite difficult. These difficulties may be overcome by proper attention to the technique of setting up the apparatus and by the use of the proper auxiliary devices to maintain steady operation automatically. Unfortunately, very little has been published in English concerning gas-discharge-tube technique. The discussion which follows applies particularly to the Hadding-Siegbahn type of gas-discharge tube but applies in general to any gas-discharge tube.

The normal operating vacuum for this type of tube is of the order of 0.01 mm. of mercury. Small leaks in soldered and sealing-wax joints, filtration of air through the aluminum-foil windows, and the liberation of gas from the interior walls of the tube make it necessary to maintain the optimum vacuum with a vacuum pump. The pump must be a high-speed pump consisting of some form of mercury-vapor pump with a backing pump. A pump may be able to produce the necessary vacuum when no discharge is passing through the tube, but as soon as the high voltage is applied the liberation of gas within the tube is often more than the pumps can handle. In order to make this preliminary outgassing as short as possible, a pumping system of large capacity should be used. The ordinary Cenco Hyvac oil pump with a mercury-vapor pump is sufficient under most conditions. In order to have a greater margin of capacity the larger Cenco Megavac pump with a mercury-vapor pump is recommended, however. The Cenco Hypervac pump, which has recently been placed on the market, has sufficient pumping capacity to be used without a mercury-vapor pump. A high-capacity pumping system is a most valuable asset to a gas-discharge-tube set-up.

The usual high-vacuum technique in the connection of the pump to the x-ray tube should be followed. Essential features to be remembered are: (1) Large-diameter connecting tubing. (2) Absence of sharp or frequent bends in the line between x-ray tube and mercury-vapor pump. (Make this line as short and direct as possible.) (3) In making sealing-wax joints the following procedure is recommended: Heat the parts to be joined and while they are hot coat them with sealing wax by rubbing a rod of wax over them until the parts are covered with a thin layer of

wax. Keeping the joint warm, apply softened sealing wax until a thick enough layer of wax is built up around the joint to make a strong and rigid joint. Ordinary red sealing wax may be made less likely to crack and less likely to pull away from the glass by the addition of about 5 per cent of dibutyl phthalate. For the glass-to-metal joint, which connects the x-ray tube to the pumping line, the German manufactured picein wax is recommended. This wax adheres to metal better than sealing wax does. (4) In the pumping line a rubber tubing or flexible metal tube connection should be inserted to permit adjustment of the position of the x-ray tube without disturbing the vacuum pumping apparatus. Heavy-walled rubber tubing especially designed for vacuum connections has been found to be entirely satisfactory. When stretched over glass tubing for a length of about 1 in. and fastened with two wire constrictions, a sufficiently vacuum-tight joint may be made.

After the preliminary outgassing operation the vacuum pumps will produce too high a vacuum in the x-ray tube. The pressure in the tube will then be too low for satisfactory operation. In order to restore the pressure to the optimum, it is necessary to introduce a controllable air leak. In the Hadding tube two tubulatures are provided. To one is connected the vacuum pumping system and to the other the air leak.

The setting up of a satisfactory air leak is likely to be the most troublesome part of the whole assembly. Most air-leak valves have the difficulty that they are hard to adjust, small adjustments in the valves making large differences in the flow of air. In general a valve will be easier to adjust if the backing pressure on the valve is less than atmospheric (10 to 150 mm. of mercury). This is accomplished in one of two ways. The inlet to the valve is connected to the line between the backing pump and the mercury pump or to a large bottle (about 2 l.) of air at reduced pressure. The choice of either method will depend on the backing pressure required.

G. L. Clark[2] describes a ground-glass needle valve which he has used in his laboratory. G. W. C. Kaye[3] in his book, "High Vacua," gives a diagram and description of a metal needle valve. Several European manufacturers supply needle valves for this purpose. Dodge and Dunbar[4] describe a valve which they used in pressure work which may be adapted as an air-leak valve. It consists of a piston fitting into a cylinder. Resistance to flow depends on the area of contact between the piston and cylinder. Adjustment is obtained by moving the piston within the cylinder. Using the Dodge and Dunbar valve, it has been found most satisfactory to have the valve at one setting in general and to regulate the flow of air by varying the backing pressure on the valve. A 2-l. bottle of air at about 30 mm. of mercury pressure used as a backing pressure will not leak sufficiently into the x-ray tube to require restoration of the 30-mm. pressure more than once or twice a day. The pressure in

the bottle is brought back to 30 mm. by allowing air to enter through a stopcock with a capillary opening.

No air-leak device, however stable its own operation may be, will maintain a uniform pressure within the x-ray tube. The liberation of gas within the x-ray tube is erratic and causes pressure variations which the vacuum pumping system is unable to smooth out. A rise in pressure is accompanied by an increase in current which entails a corresponding drop in voltage when the primary circuit of the transformer has a proper resistance. A decrease in pressure produces the opposite effect on the current and voltage.* The regulation of the pressure within the x-ray tube and hence the regulation of the voltage across the tube is accomplished by a voltage vacuum regulator. Several voltage regulators for gas-discharge x-ray tubes have been described. They regulate the vacuum by a form of automatic valve in the vacuum pumping line. The adjustment of this valve is controlled by the variations in voltage across the x-ray tube. Bozorth,[5] of the Bell Telephone Laboratories, has described such a regulator. Haworth,[6] of the same laboratory, has described a more compact and less cumbersome regulator which is being used in the Bell Telephone Laboratories instead of the Bozorth regulator. White,[7] and Wyckoff and Lagsdin[8] have also published descriptions of voltage regulators.

Figure 6 shows a diagram of the Haworth voltage regulator. This diagram is reproduced through the courtesy of F. E. Haworth, of the Bell Telephone Laboratories, Inc., who has supplied us with his original drawing. The regulator is connected in the vacuum pumping line between the x-ray tube and the pumps as indicated on the diagram. Not shown in the diagram is a solenoid which fits around the lower tube of the regulator and actuates the laminated iron armature within the lower tube. The aluminum cylinder floats in the mercury, and suspended from the aluminum cylinder is the iron armature. The solenoid may be connected through a variable resistance across the primary of the high-potential transformer. In control units having a voltmeter intended to give an indication of the high-potential voltage of the transformer, the solenoid may be connected across its terminals. The latter connection gives more sensitive regulation. When the voltage across the x-ray tube becomes too high, meaning too low a pressure in the x-ray tube, the action of the solenoid on the armature causes the beveled glass-tube elbow to be immersed partially or entirely in the mercury thus reducing the pumping speed and permitting the pressure in the x-ray tube to rise. A decrease in voltage causes the regulator to increase the pumping speed. The normal position of the glass tube will be such that it is partially immersed

* The variations in pressure to which reference is made are those within the range of operating pressures. Obviously an increase in pressure may be of such an amount that no current will pass.

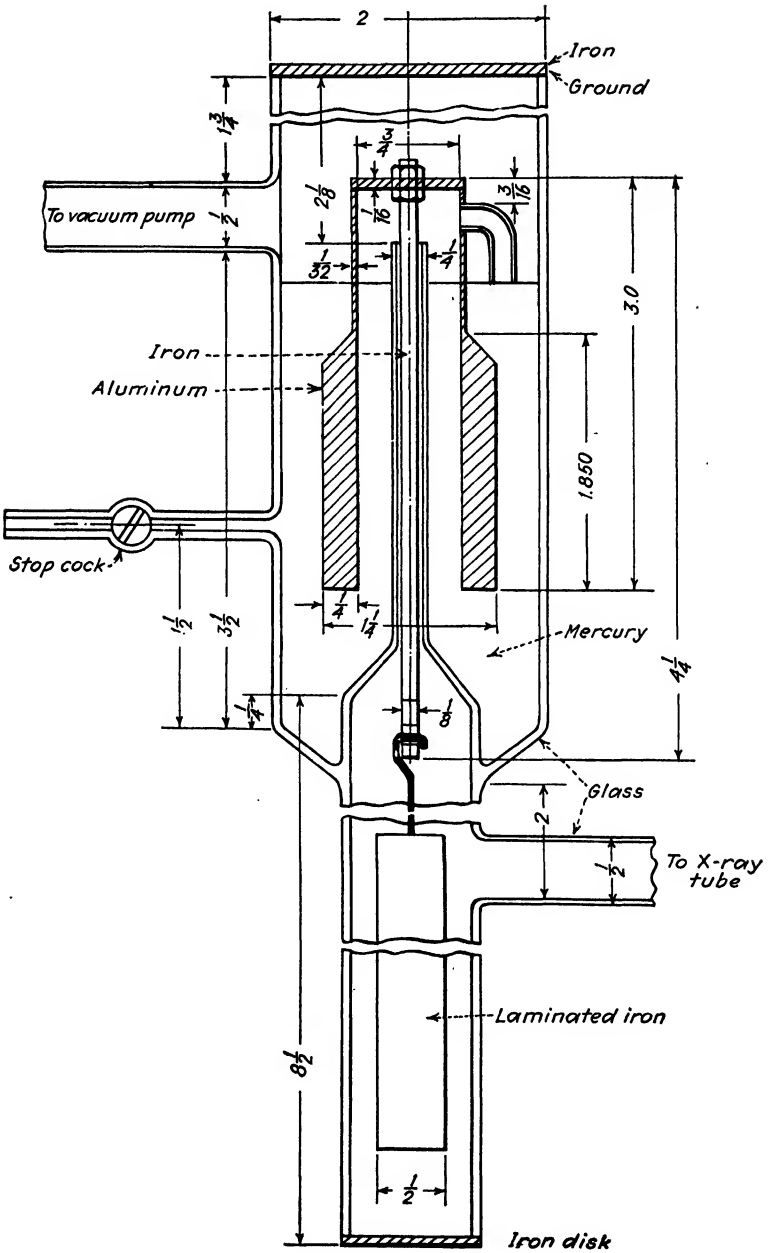

FIG. 6.—Haworth voltage regulator.

in the mercury to such a level that a pumping speed sufficient to maintain the optimum pressure in the x-ray tube is obtained. Adjustment of the regulator for the desired conditions is made by regulating the resistance in series with the solenoid or by changing the level of the solenoid.

Other details of the Haworth regulator, useful in the actual construction and use of this type of regulator, are as follows:

Solenoid.—One and one-half pounds of No. 30 double silk-covered wire wound on a brass spool for a length of 3 in. The turns should be insulated from the brass spool with sheet mica.

Armature.—Silicon-steel strips 6- by ½-in., built up to make an armature 6- by ½- by ½-in. The strips should be insulated from one another with thin mica. Do not use lacquer or varnish insulation between the strips since this type of insulation is a constant source of vapors in the vacuum system.

Lead Pieces.—Iron disks fastened to the upper and lower ends of the regulator with picein wax are better than fused-glass seals since dissassembly of the regulator is made easier. Adjustment of the regulator for the particular x-ray unit will probably require hanging of a suitable lead weight to the bottom of the armature.

By-pass.—In the preliminary outgassing period when starting operation of the x-ray tube, the regulator does not permit sufficient pumping speed to reduce the time required for outgassing to a minimum. The introduction of a by-pass tube in parallel with the regulator makes greater pumping speed available during the outgassing period. When the optimum vacuum in the x-ray tube has been reached the by-pass tube may be dispensed with by closing a glass stopcock which is included in the by-pass tube. The regulator will then take care of itself. By using a voltage regulator and an air leak very constant voltage and current conditions can be maintained for an entire day without adjustment.

Focusing of the Cathode Beam.—The cathode beam must be properly focused on a small area of the target if intense x-rays of uniform intensity are to be passed through the several slit systems which may be mounted outside the tube.

In the gas-discharge tube the focusing of the cathode ray depends on the following factors: (1) radius of curvature of the cathode, (2) distance between cathode and target, (3) pressure of the gas in the tube, and (4) shape and material of the body of the x-ray tube and the electrostatic fields produced thereby.

Clay[9] has experimented in some detail with the first three of these factors in connection with the Shearer tube. With any type of tube it is a matter of experimentation to determine the proper radius of curvature and distance. Clay recommends a radius of curvature of 2 cm. and a cathode-to-target distance of 3 to 4 cm. In the laboratory of G. L. Clark, the optimum radius of curvature of the aluminum cathode of the smaller Hadding-Siegbahn tube was found to be 3½ cm. when placed in the x-ray tube so that it is inside of the cup of the porcelain insulator. In the laboratory of the New Jersey Zinc Company, the optimum radius of curvature of the aluminum cathode of the larger Hadding-Siegbahn-type tube was found to be 5.4 cm. and the cathode-to-target distance

approximately 12.5 cm. The general rule is that the radius of curvature of the cathode is about one-half the distance between cathode and target. Properly focused, the cathode ray will etch a spot about 2 mm. in diameter on the face of the target after several days running.

In order to bring the focal spot to the center of the target face the central radius of the concave cathode must be properly aligned with the axis of the tube. In the Hadding tube this may be done conveniently as follows: An arrangement is constructed to fit on the end of the porcelain insulator, which holds three set screws bearing on the cathode-cooling tube (which runs through the center of the porcelain insulator). The cathode tube is free to move on the inside of the x-ray tube and pivoted at the end of the porcelain insulator. The alignment of the cathode tube can now be adjusted by the regulation of the set screws. When picein wax is used to make the cathode-tube porcelain-insulator seal, this adjustment can be made without destroying the seal since the wax is soft enough to stand a small amount of movement. Test the focus as follows: A pinhole in a lead plate is mounted about 1 cm. outside the window of the x-ray tube. The image of the pinhole, viewed with a fluorescent screen held about 5 to 10 cm. from this pinhole, should be of symmetrical intensity with the brightest portion at the center if proper focus has been obtained. An improperly focused tube will give an image with a bright spot off to one side of the center.

Cooling of the Tube.—The wax joints, the target, and the cathode require cooling. In the Hadding tube the wax joint from insulator to the metal bowl of the tube, the aluminum window mounting, and the target are cooled through suitable water-circulating chambers from the laboratory water supply.

The cooling of the cathode-tube-to-insulator wax joint and the cooling of the cathode necessitate an insulated cooling system since these parts are at high potential. The most commonly used system is that of the circulation of water from an insulated reservoir through the cathode tube and back to the reservoir. The flow from reservoir to x-ray tube is by gravity and from x-ray tube to reservoir by a compressed-air lift. A description of such a system has been published.[10] In cases where an elevated insulated reservoir cannot be installed, the cooling medium must be circulated from reservoir to x-ray tube by a small insulated centrifugal pump. The pump is connected by means of a bakelite shaft to a grounded electric motor. If necessary, a coil of copper tubing is inserted between the x-ray tube and the reservoir to dissipate the heat in the cooling liquid.

Arrangement of Apparatus.—The disposition of the several units comprising the gas-discharge tube set-up is a matter of considerable flexibility and will depend upon the particular laboratory conditions which have to be met. A compact, electrically safe arrangement has been

described by G. L. Clark.[2] The intended position of operation of the Hadding-type tube is with the porcelain insulator and high-potential cathode uppermost. The tube will function equally well, however, if it is used with the high-potential end down. The latter arrangement is the one used by Clark. The tube is mounted on a table top with the porcelain insulator projecting underneath the table through an opening in the table top. Underneath the table is the electrical apparatus. The advantages of this arrangement are, first, compactness and, second, protection of the operator from high-voltage shock. The high-voltage equipment is out of the way and may be easily screened to avoid accident. The alternative arrangement requires floor space for both the electrical power

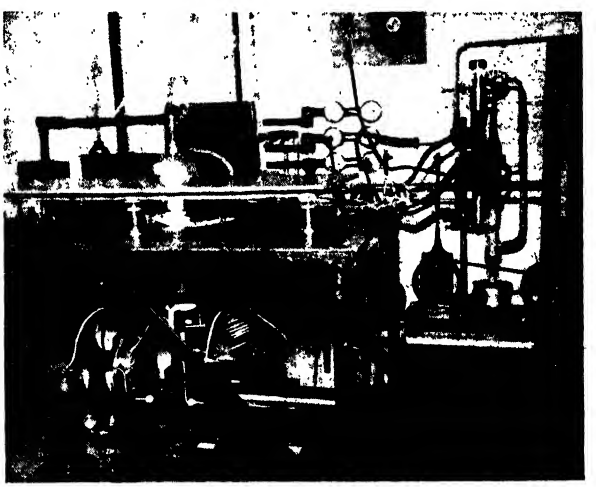

FIG. 7.—Photograph of Hadding-Siegbahn-type tube set-up. (*Courtesy of New Jersey Zinc Company.*)

plant and the x-ray-tube table, with a high-voltage overhead conductor to connect the two units.

Figure 7 shows a photograph of the Hadding-Siegbahn-type unit in the laboratory of the New Jersey Zinc Company. The arrangement is the inverted-tube type. A rotating-switch rectifier mounted on top of an oil-filled water-cooled transformer forms the high-voltage direct-current power plant. This unit was installed in a pit 2 ft. below the floor level. The electrical unit is enclosed in a sound-deadening cabinet through the cover of which projects the high-potential post. On top of the cabinet are mounted the insulated oil-cooling system for the cathode, the milliammeter, and the sphere gap. Electrical connections are made with ¼-in. copper tubing which prevents most of the corona loss present when small-diameter-wire connectors are used. A grounded iron table stands over the entire electrical unit. The open sides of the table are encased in wire mesh. The wire mesh affords protection to

the operator from contact with the high potential and prevents interference with local radio reception from the rotating-switch rectifier. In Fig. 7 two of the wire screens are removed in order to show the equipment below the table more clearly. All the high-voltage equipment is thus enclosed, and everything on top of and around the iron table is at ground potential. The air-leak device is on the left of the x-ray tube, and the vacuum pumping equipment and voltage regulator are on the right. An autotransformer control unit is used to regulate the primary voltage.

D. TECHNIQUE OF ASSEMBLY AND DISASSEMBLY OF THE HADDING-TYPE TUBE

The concave aluminum cathode becomes pitted after about 75 to 125 hr. of operation. This pitting seems to be unavoidable. A pitted cathode is roughened over the entire surface, and in the center a deep, crater-like pit is formed. The focus of the cathode ray is impaired by the pitting, and exposure times become noticeably larger. In order to replace the cathode with a new one, the porcelain insulator must be removed. The porcelain insulator of the Hadding tube rests in an annular channel at the rim of the metal bowl of the x-ray tube. The joint is made mechanically rigid and vacuum-tight by filling the channel with picein wax. The wax is most conveniently melted by passing steam through the water jacket underneath the channel. The cathode is threaded on to the end of the cathode cooling tube and may usually be removed without moving the cooling tube. If removal of the cooling tube becomes necessary another picein joint at the outer end of the porcelain insulator must be melted.

The inside of the metal bowl of the tube and the inside of the porcelain insulator should be cleaned whenever the tube is opened. There will be deposited on these parts a powdered layer of sputtered metals (representing all the metals present in the x-ray tube) and carbonaceous matter from stopcock grease and sealing wax. If allowed to accumulate, this material becomes a constant source of gas. The production of gas in this way may become so large that the vacuum pumps are not capable of producing the optimum vacuum in the x-ray tube.

The target is mounted on a conical plug which is inserted in a corresponding conical receiver at the end of the neck of the metal part of the tube. The cones should not be lubricated with stopcock grease. The outside of the cone joint should be sealed with picein wax to insure vacuum tightness.

The openings in the neck of the tube from which the x-rays proceed are 3 mm. in diameter. Thin aluminum foil about 0.01 mm. thick is sealed over these openings. The seal is best made with picein wax. Heat the neck of the tube by passing steam through the appropriate

water jacket. Paint a thin ring of wax about 7 mm. inside diameter and 10 mm. outside diameter around the 3-mm. opening. Then apply a 12-mm. square of aluminum foil over the opening. A brass disk is furnished with the tube to clamp the foil in place. This disk should not be tightened until the wax is cool enough so that the wax will not run into the opening of the x-ray tube. On the Hadding-type tube three such windows, at angles of 75° with each other, are furnished.

E. FILAMENT-CATHODE METAL TUBES

The technique of operation of these tubes may be inferred from what has already been said concerning them and from the discussions of the operating technique of the Coolidge-type and gas-discharge-type tubes. The filament-cathode metal tube must be continuously connected to a vacuum pumping system. The vacuum should be as high as possible. With a sufficiently high vacuum the operation of this type of tube is similar to that of the Coolidge-type tube. A discussion of the construction of this type of tube, the preparation of tungsten filaments, and details of operation may be found in "Spectroscopy of X-rays" by Manne Siegbahn.

F. VOLTAGE AND CURRENT MEASUREMENTS

An exact determination of the voltage applied to the x-ray tube in crystal-structure investigations is not necessary. Indeed the exact determination is very difficult. A sphere-gap measurement is the usual method of determining voltage. In the case of a self-rectifying Coolidge-type tube, a sphere gap placed in parallel with the tube will give an indication of the peak voltage of the inverse wave. The voltage of the no-load inverse wave is of course much higher than the voltage of the useful portion of the wave. In order to make a sphere-gap measurement on a self-rectifying-tube set-up, an equivalent load, such as another x-ray tube, must be placed in the circuit in such a way as to draw current from the inverse wave, or a vacuum-tube rectifier must be placed in series with the spark-gap so as to permit the gap to measure only the useful half waves. Under such conditions an accurate measurement of the peak voltage may be obtained. For crystal-structure determinations it is usually sufficient to have a knowledge of the transformer ratio. In a gas-discharge-tube circuit, a sphere gap for measuring peak voltage will work quite satisfactorily because gas tubes will operate properly only on unidirectional voltage. A sphere gap is indispensable as a guide to the operating conditions of the gas type of tube.

Any sphere-gap voltage measurement of a wave form of fluctuating voltage will be an indication of the peak voltage only. Of two voltage waves having the same sphere-gap voltage, wide difference in wave forms will make a large difference in ability to produce x-rays. Hence,

two x-ray circuits operating at the same sphere-gap voltage may be very different from the standpoint of the production of x-rays. Comparison of such circuits must be based on oscillograph measurements. For crystal-structure investigations, however, the sphere-gap measurements are in general quite satisfactory. In any given circuit a reproducible indication of operating voltage is sufficient rather than an absolute knowledge of the voltage. Directions for the construction of sphere gaps and calibration tables for their use may be found in handbooks of electrical engineering.

Milliammeters for the measurement of x-ray-tube current must be of a rugged, well shielded construction. They should be protected against sudden surges. They may be connected in the high voltage or in the grounded side of the circuit.

G. X-RAY PROTECTION

Harmful effects of x-ray exposure on operators of x-ray equipment should be guarded against. Short exposures to intense x-ray beams may produce an x-ray burn. An x-ray burn is very painful and has, in addition to the characteristics of ordinary burns, the property of penetrating deeply into the burned member and of not making itself evident until after many days have elapsed. Prolonged exposure to weak x-rays has a cumulative effect which may result in a harmful decrease in the white and red corpuscles in the blood. X-ray exposure may also cause sterility.

A few simple rules should be followed to avoid these harmful physiological effects.

1. Do not expose any portion of the body to the direct beam from the x-ray tube.
2. When it is necessary to view a beam of x-rays with a fluorescent screen, a piece of lead glass should be placed between the operator and the screen.
3. X-ray diffraction apparatus not otherwise shielded should be shielded with sheets of lead. This shielding protects those working near the apparatus from exposure to scattered radiation.
4. The apparatus should be so shielded that sensitive photographic materials may be stored in the same room. In fact, all unexposed photographic films should be stored in a cool place near the x-ray apparatus, without any additional protection beyond that used in connection with the apparatus itself.

"If it isn't safe for a photographic film, it isn't safe for you."

Mutscheller [*Am. J. Roentgenology*, **13**, 65 (1925)] has determined that, on the basis of 200 working hours per month, the safe limit of x-ray dosage is 1×10^{-5} "*r*-units" per second. At this rate it would take 12 years to total a dose such that, if received at one sitting, a reddening of the skin would appear three weeks after the exposure.

The English X-ray and Radium Protection Committee requires a minimum of 1.5 mm. of lead shielding or equivalent for protection against x-rays generated at 70 kv. For 100 kv. a minimum of 2.0 mm. of lead is required.

The United States Bureau of Standards has issued a 26-page booklet entitled "X-ray Protection." Although it is written from the standpoint of the medical practitioner rather than from the standpoint of the crystal analyst, obvious changes in wording will make the rules apply to x-ray diffraction work. The booklet may be obtained from the Superintendent of Documents, Washington, D.C., for 10 cents.

References

1. TERRILL and ULREY, "X-ray Technology," D. Van Nostrand Company, New York, 1930.
2. G. L. CLARK, *Ind. Eng. Chem.*, **20**, 1386–1390 (1928).
3. G. W. C. KAYE, "High Vacua," Longmans, Green & Co., Ltd., London, 1927.
4. DODGE and DUNBAR, *Jour. Amer. Chem. Soc*, **49**, 595 (1927).
5. R. M. BOZORTH, *Jour Amer. Chem. Soc.*, **49**, 971 (1927).
6. F. E. HAWORTH, *Jour. Optical Soc. Amer. and Rev. Sci. Instr.*, **19**, 79 (1929).
7. F. N. WHITE, *Jour. Sci. Instr.*, **7**, 99–100 (1930).
8. R. W. G. WYCKOFF and J. B. LAGSDIN, *Radiology*, **15**, 42 (1930).
9. R. E. CLAY, *Proc Phys. Soc. London*, **40**, 221–223 (1928).
10. G. GREENWOOD, *Jour. Optical Soc. Amer. and Rev. Sci. Instr.*, **19**, 150–151 (1929).

APPENDIX II

SEMILOGARITHMIC CHARTS FOR USE WTH THE POWDER METHOD[1]

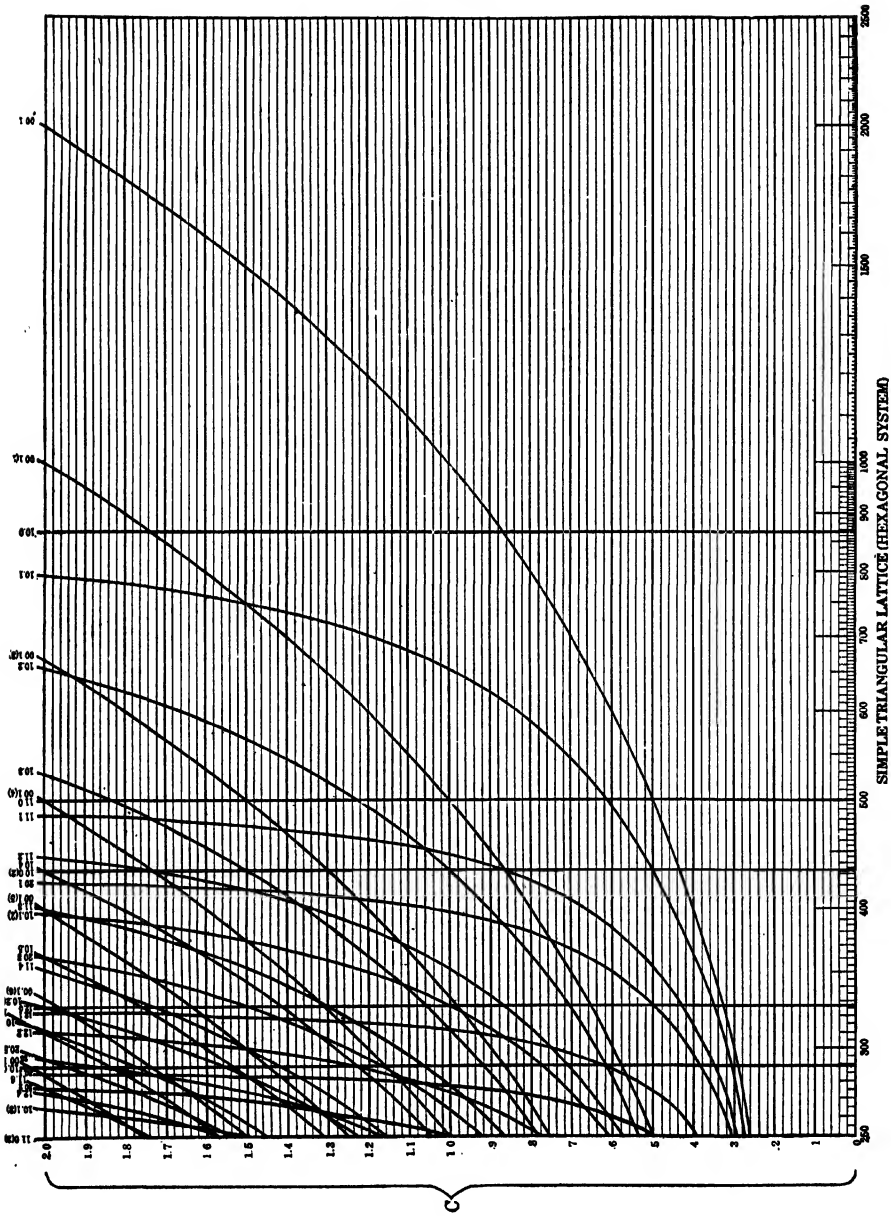

FIG. 1.—Simple triangular lattice (hexagonal system).

[1] Figures in this appendix are from Fairbanks, "Laboratory Investigation of Ores," McGraw-Hill Book Company, Inc., 1928.

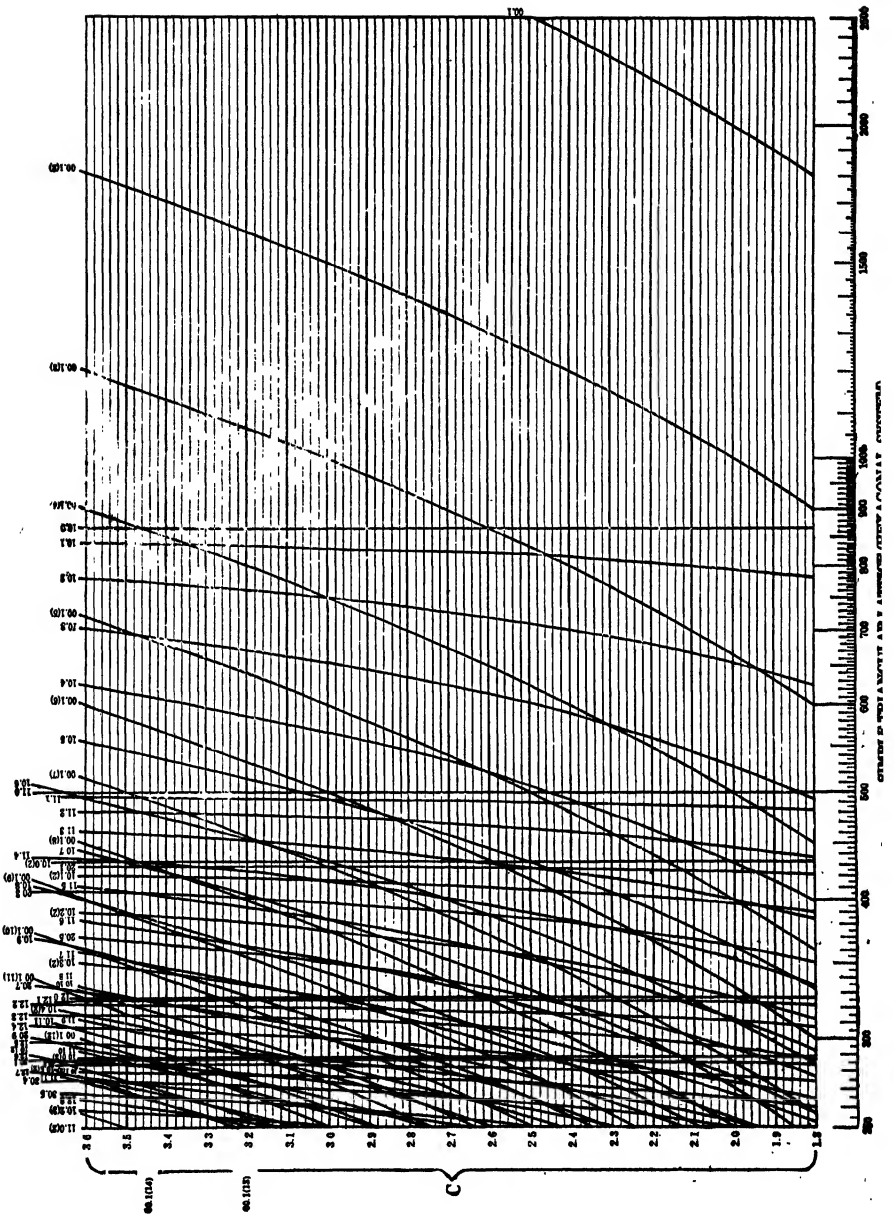
C

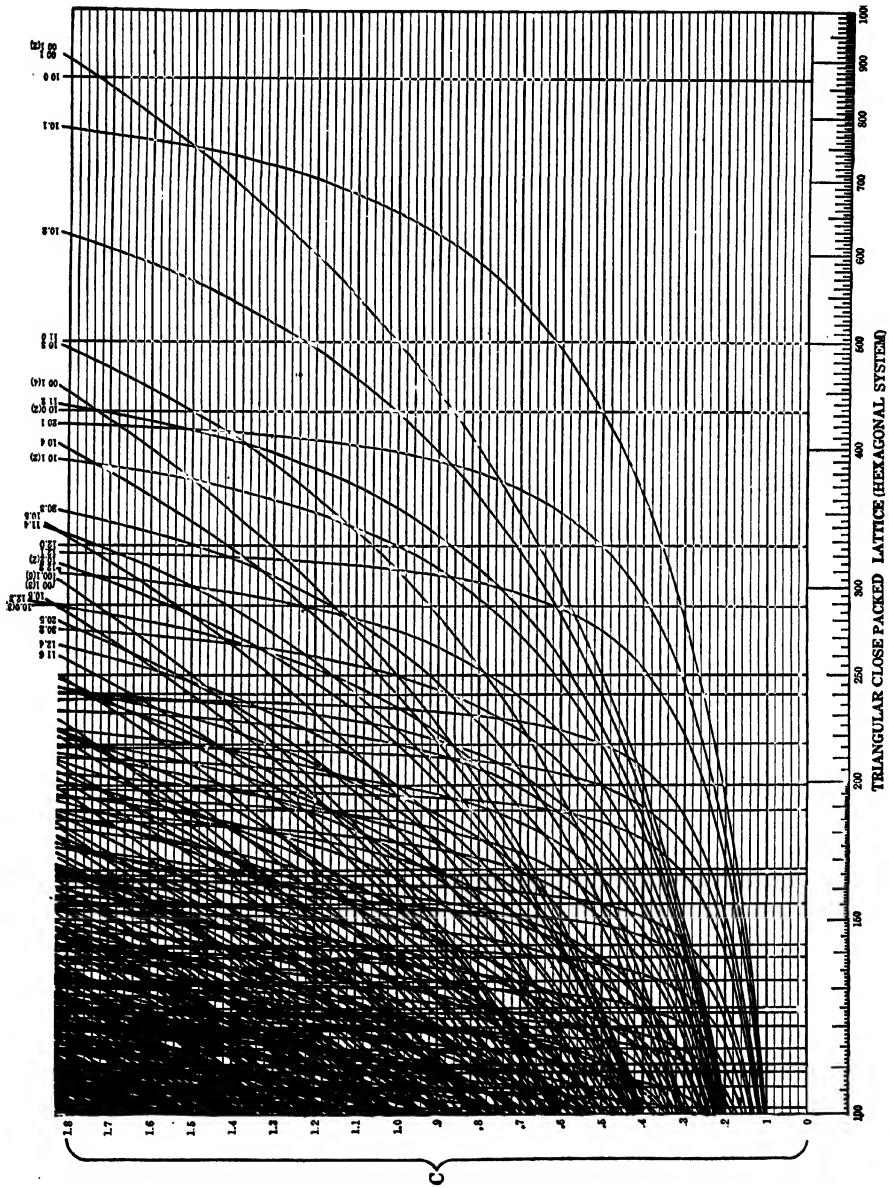

FIG. 3.—Hexagonal close-packed structure (hexagonal system).

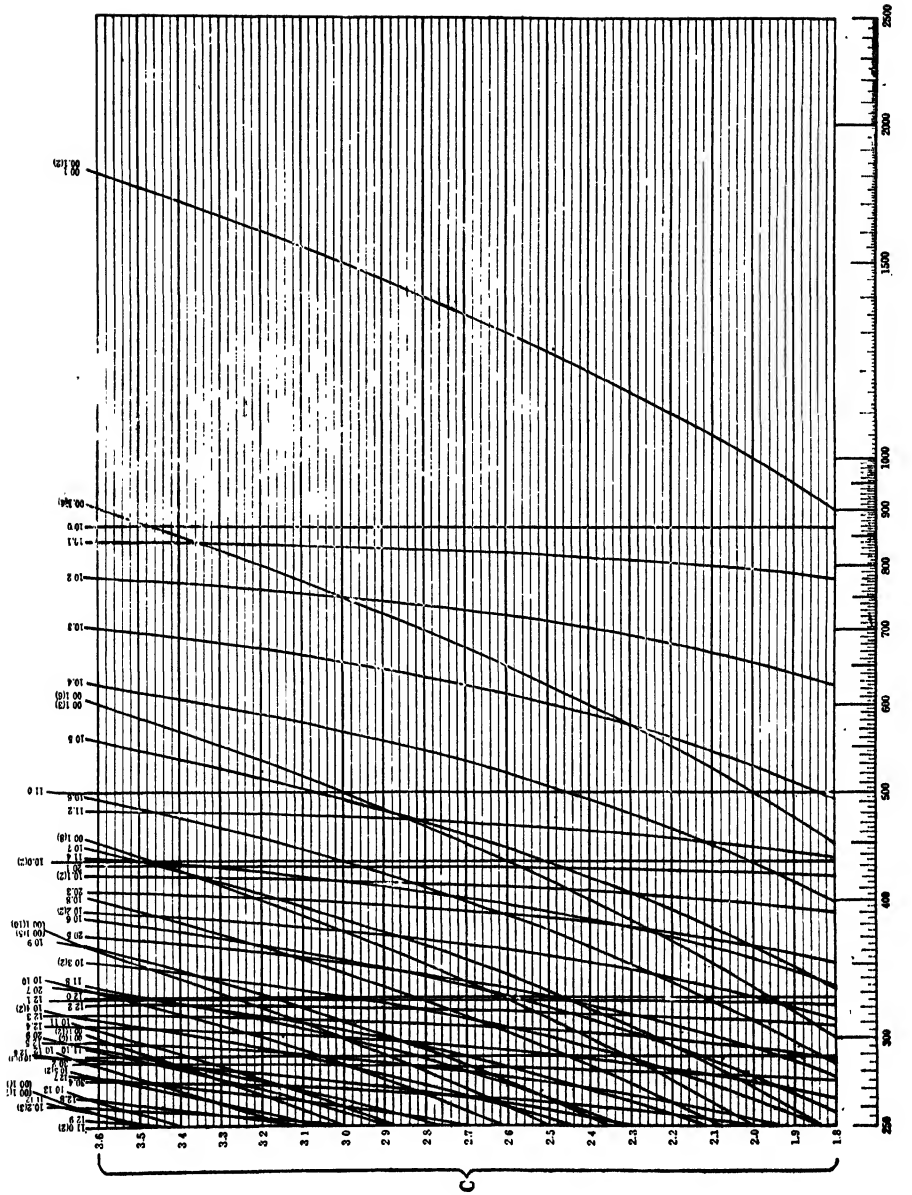
C
3.6
3.5
3.4
3.3
3.2
3.1
3.0
2.9
2.8
2.7
2.6
2.5
2.4
2.3
2.2
2.1
2.0
1.9
1.8
250
300
400
500
600
700
800
900
1000
1500
2000
2500

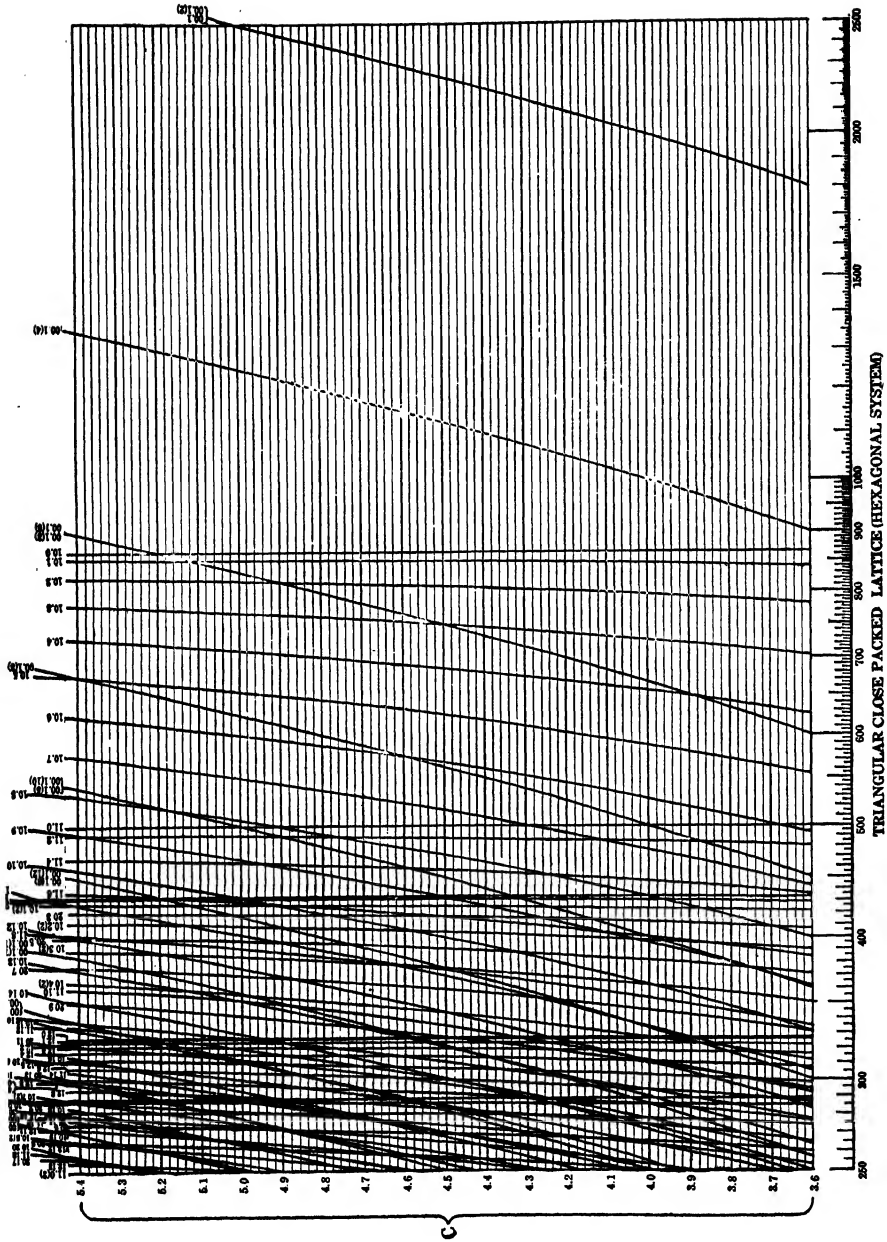

FIG. 5.—Hexagonal close-packed structure (hexagonal system).

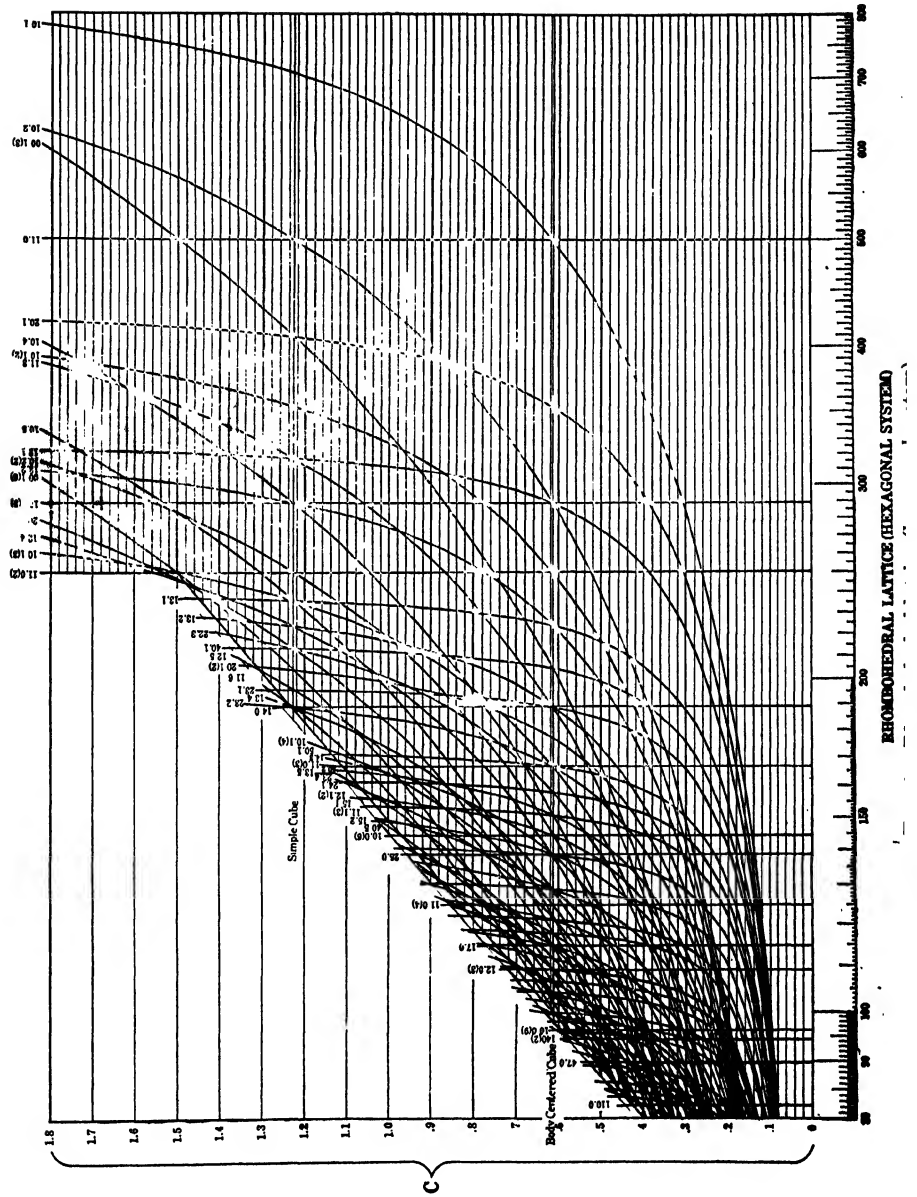
RHOMBOHEDRAL LATTICE (HEXAGONAL SYSTEM)
Simple Cube
Body-Centered Cube
C

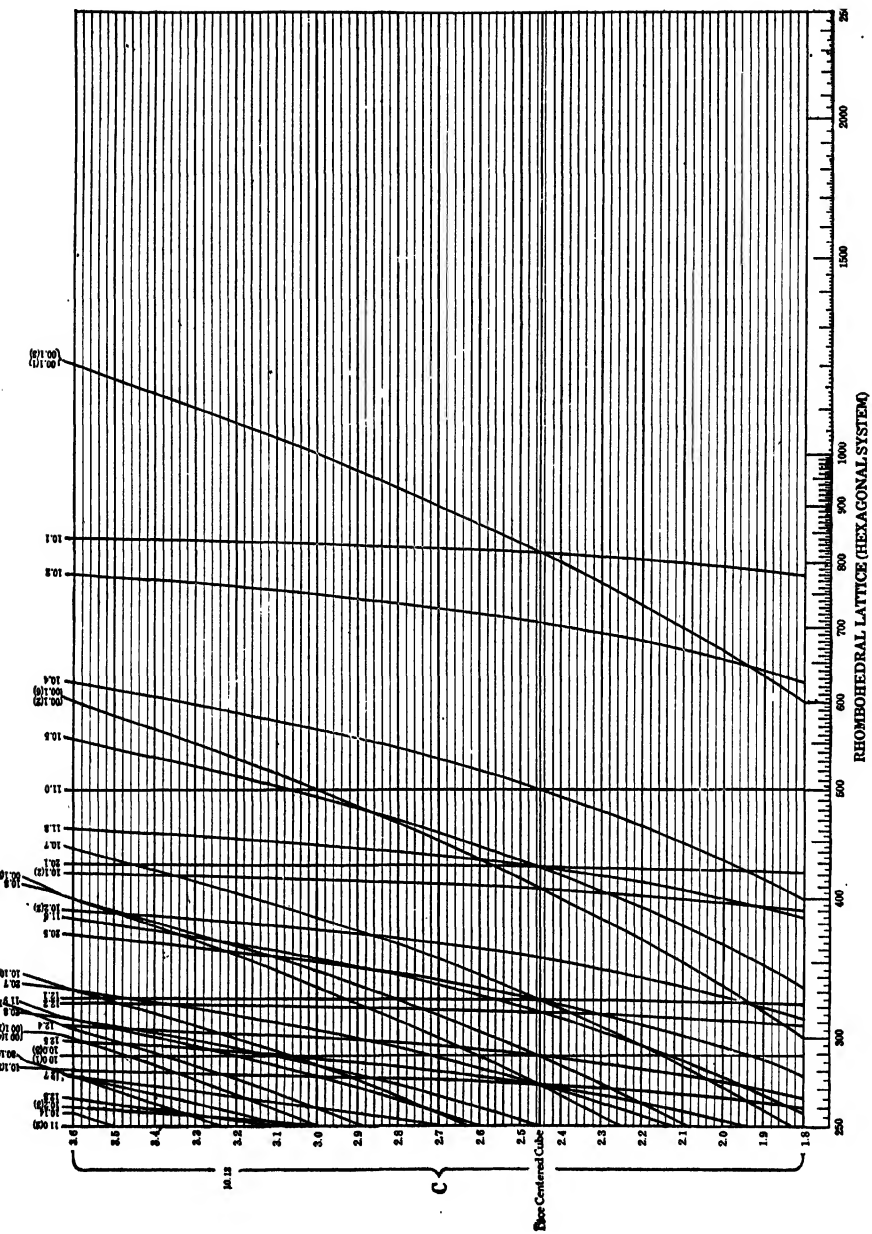

Fig. 7. Rhombohedral lattice (hexagonal system).

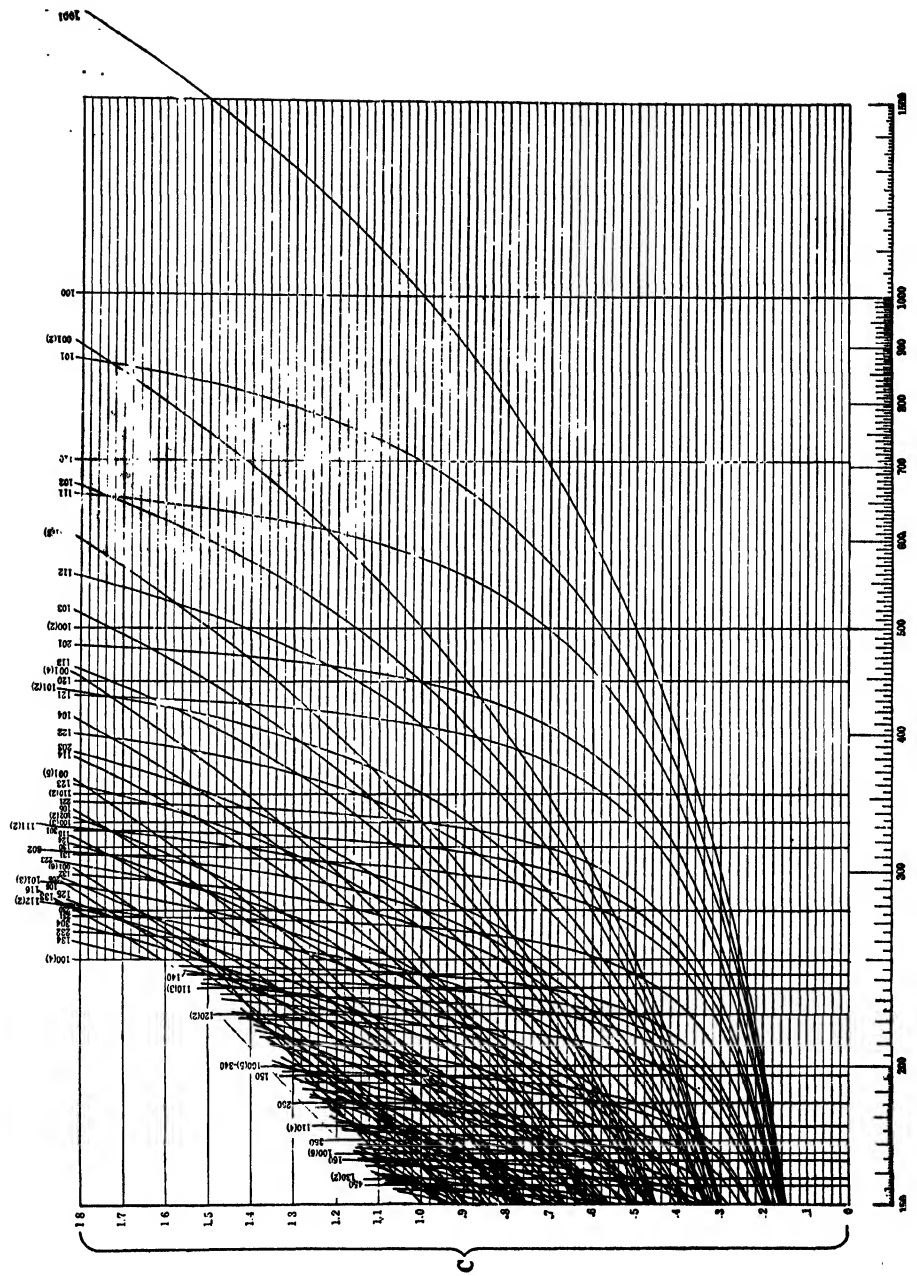

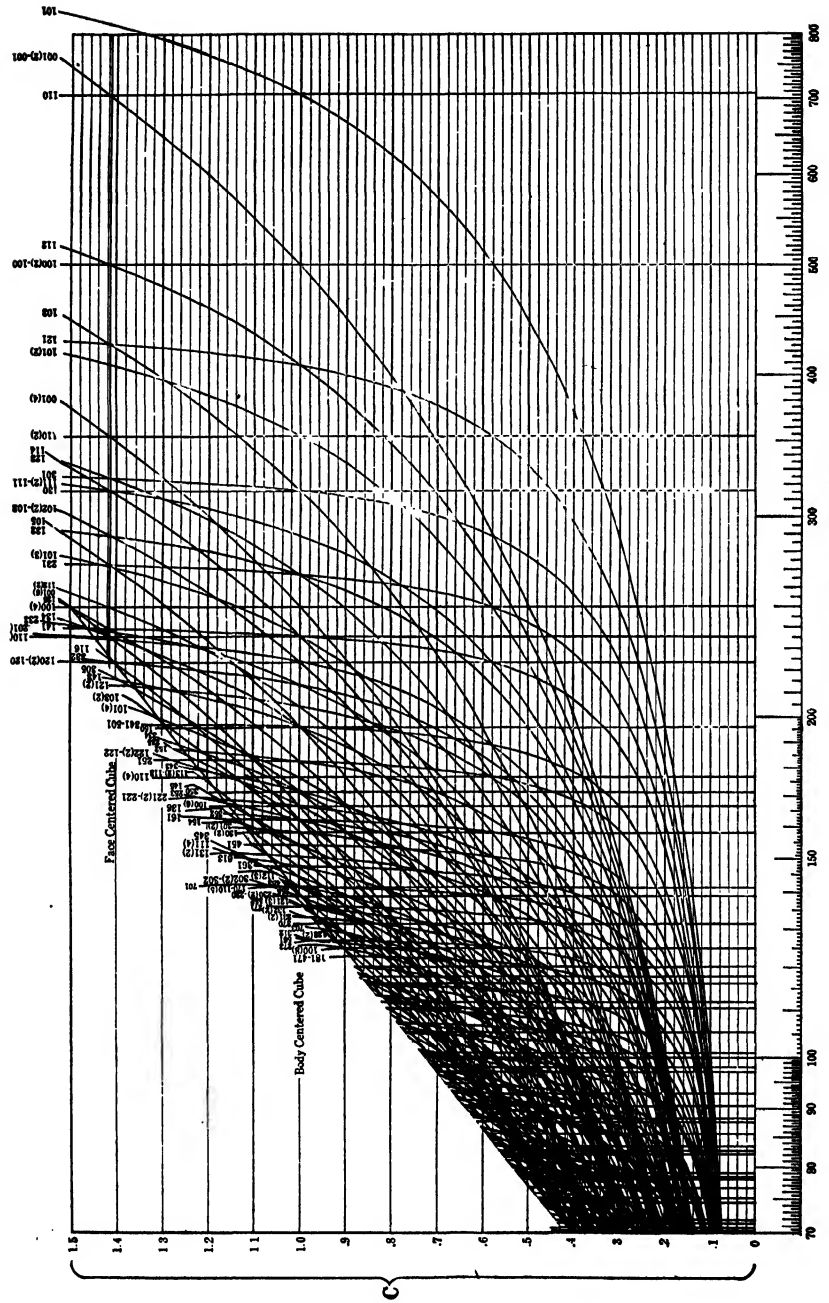

FIG. 9.—Body-centered tetragonal lattice.

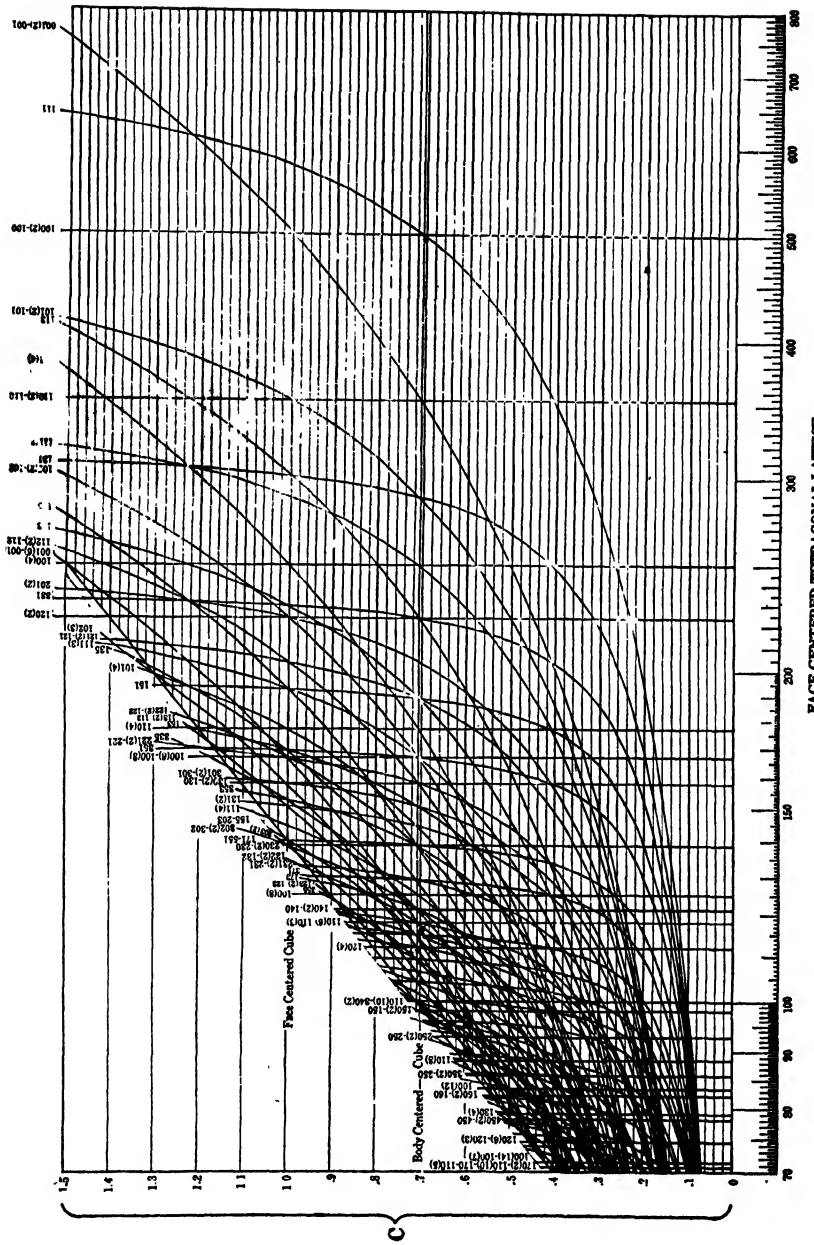

FIG. 10.—Face-centered tetragonal lattice.

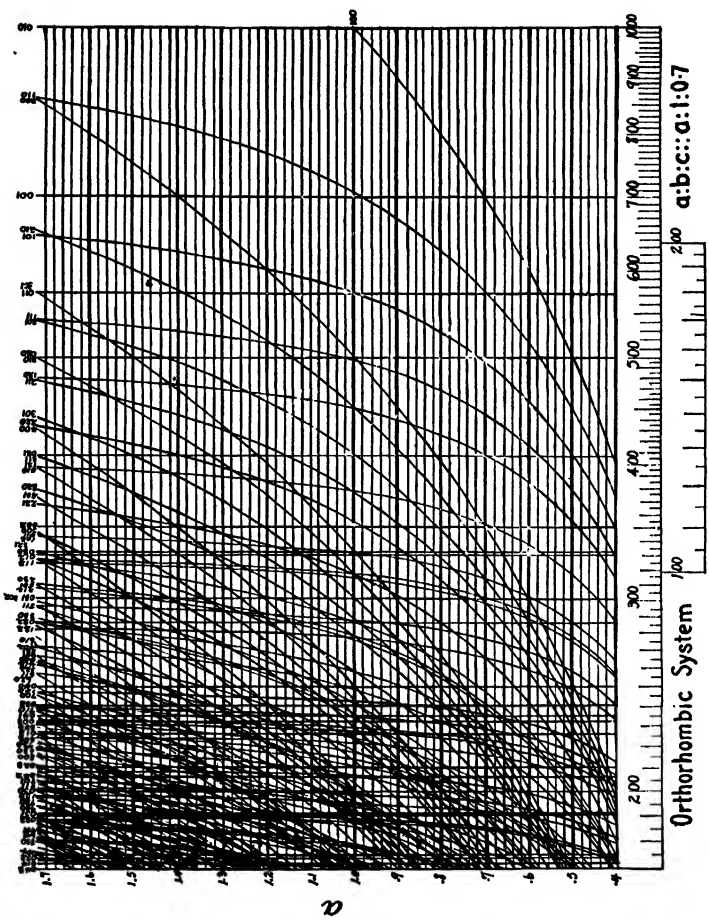

FIG. 11.—Orthorhombic system, $a:b:c::a:1:0.7$.

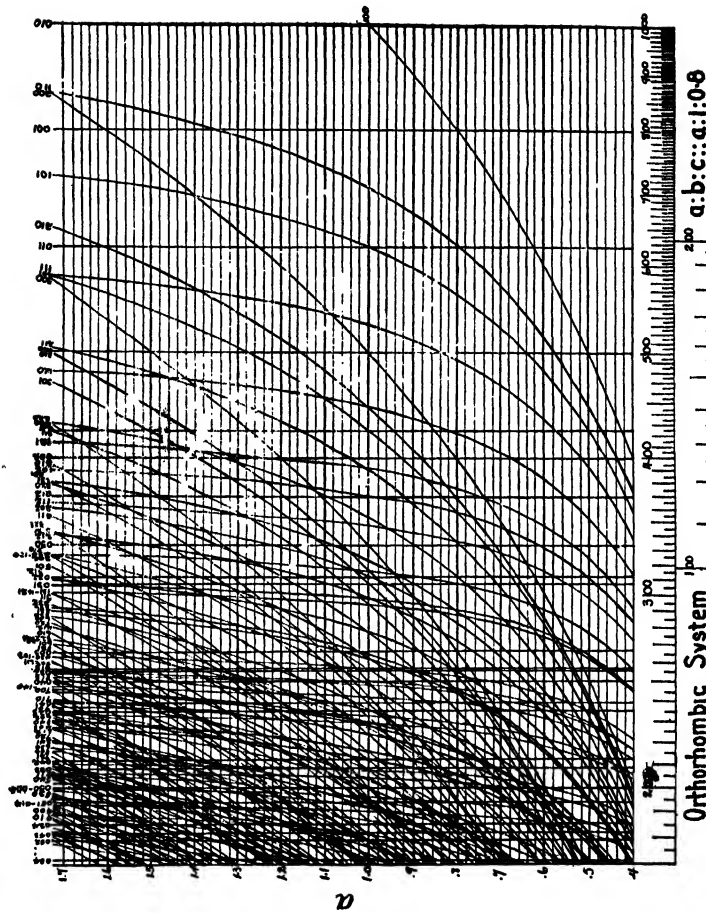

FIG. 12.—Orthorhombic system, $a:b:c::a:1:0.8$.

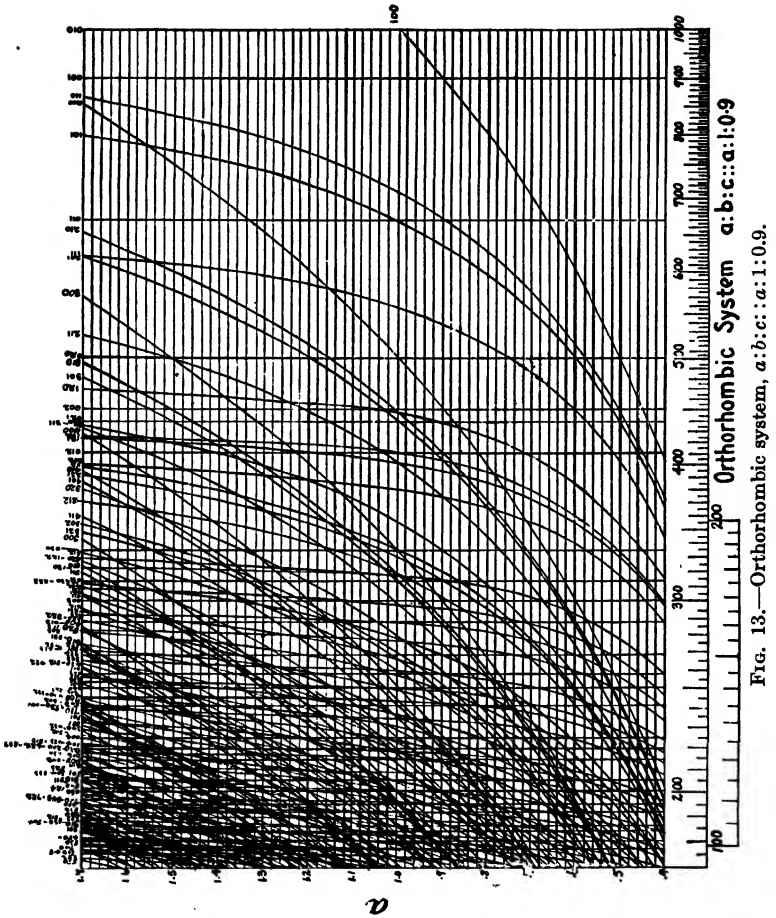

FIG. 13.—Orthorhombic system, $a:b:c::a:1:0.9$.

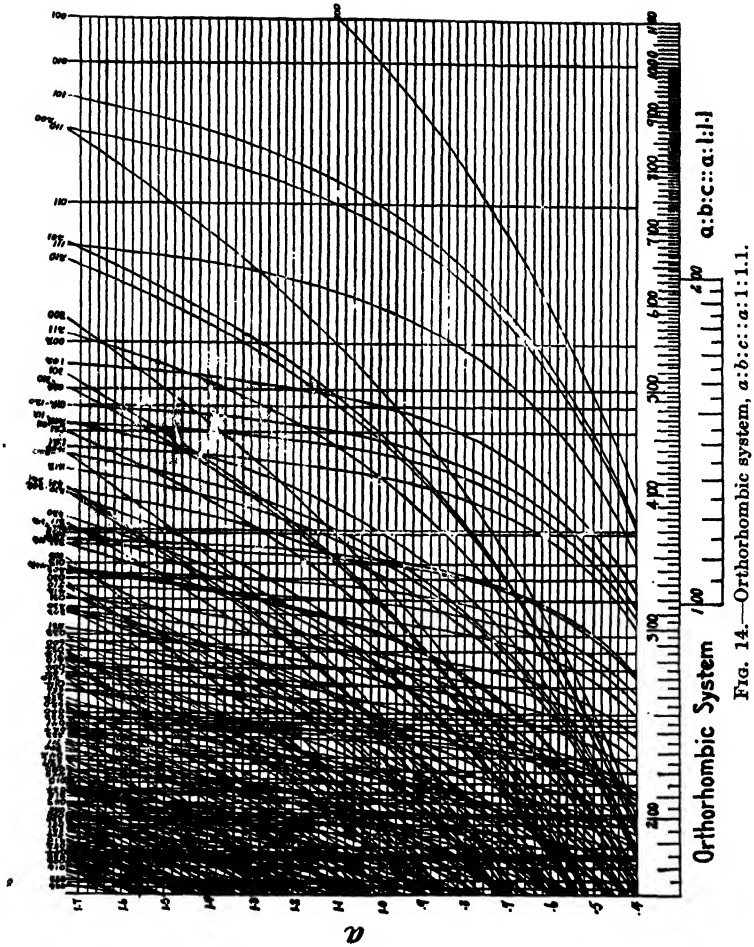

FIG. 14.—Orthorhombic system, $a:b:c::a:1:1.1$.

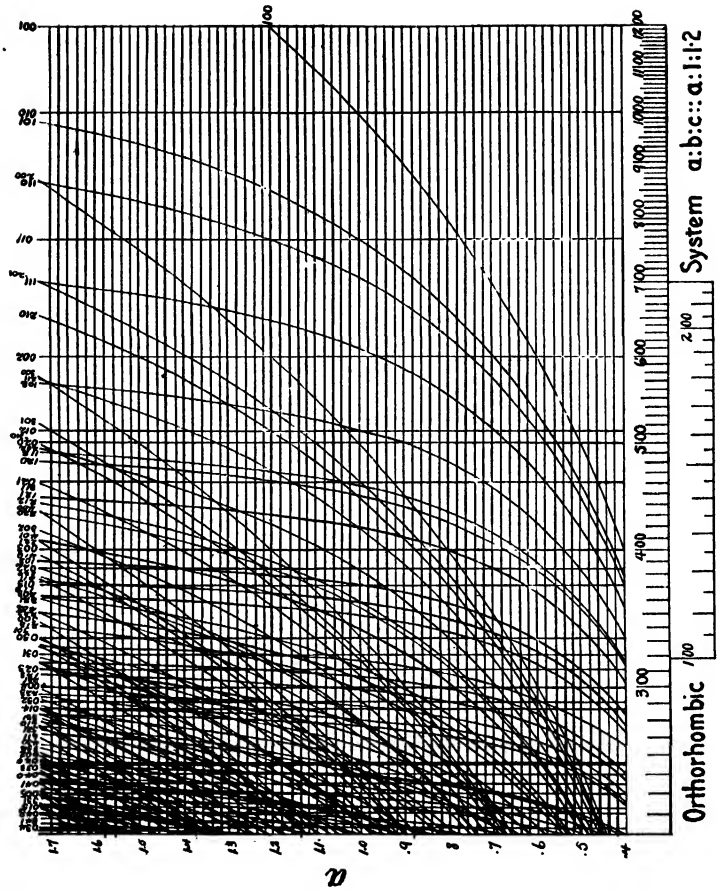

FIG. 15.—Orthorhombic system, $a:b:c::a:1:1.2$.

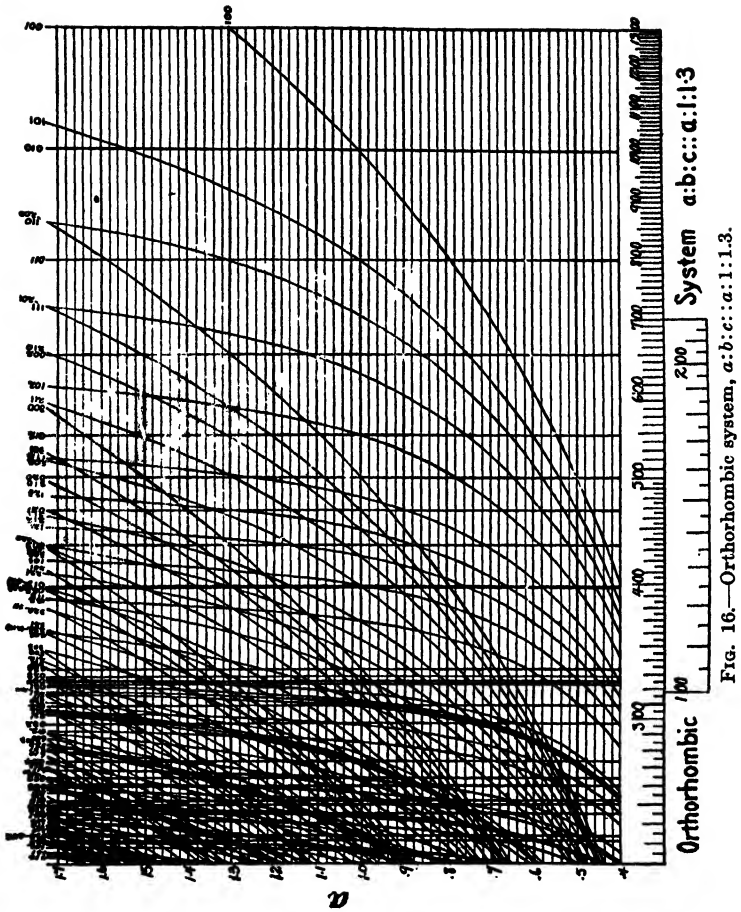

FIG. 16.—Orthorhombic system, $a:b:c::a:1:1.3$.

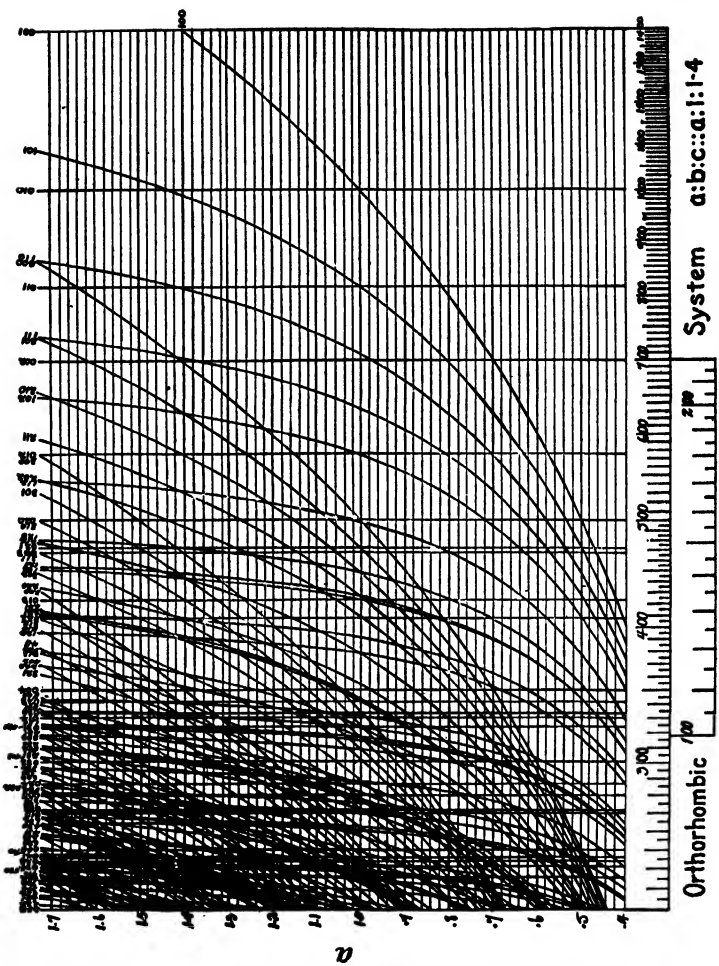

FIG. 17.—Orthorhombic system, $a:b:c::a:1:1.4$.

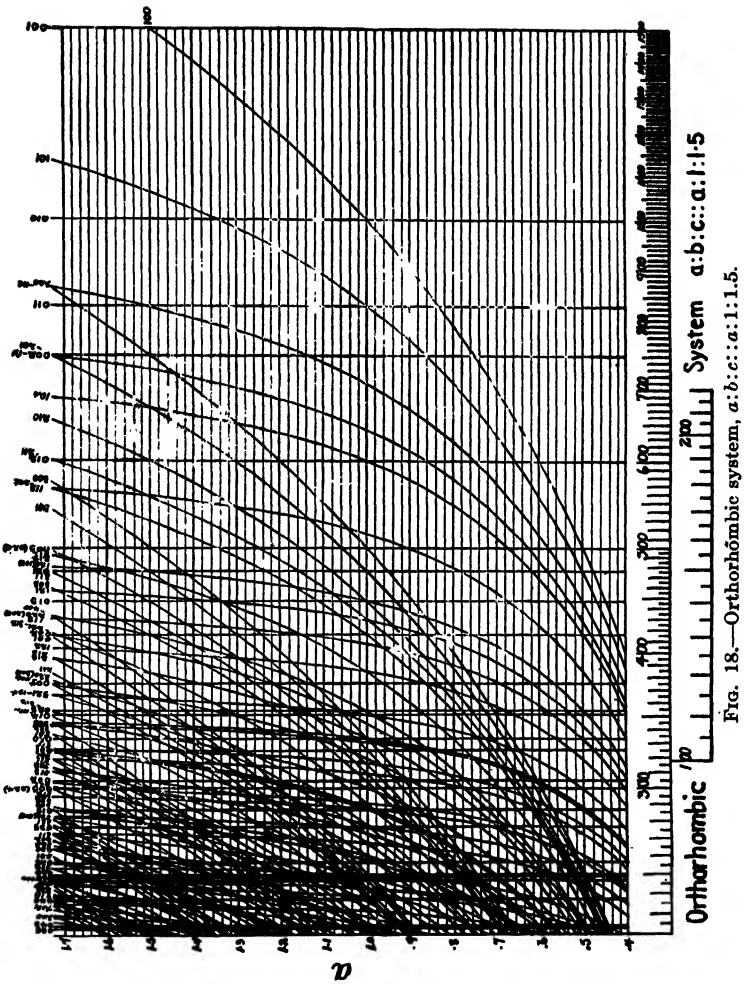

FIG. 18.—Orthorhombic system, $a:b:c::a:1:1.5$.

APPENDIX III

TABLES

THE 230 SPACE-GROUPS LISTED ACCORDING TO THE CRYSTAL SYSTEMS TO WHICH THEY BELONG

ABBREVIATIONS

S.G.	space-group
S.L.	space-lattice
n	number of asymmetric molecules per unit-prism
c	periodicity of planes (see Chap. III)
p	molecular symmetry. n/p is the number of molecules of symmetry p per unit-prism
C	center of symmetry
P	plane of symmetry
2-A	2-fold axis of symmetry
3-A	3-fold axis of symmetry
4-A	4-fold axis of symmetry
6-A	6-fold axis of symmetry
4a-A	4-fold alternating axis of symmetry
Deriv.	derivation of the space-group

A brief discussion of these tables is given in Chaps. VIII and XIX, to which reference should be made. To avoid confusion with the various parentheses necessary to the tabulations, braces are used around all Miller indices irrespective of whether they refer to plane-families or to forms of plane-families. This practice conforms to the tables of Astbury and Yardley on which Tables I to XXXII are largely based. The symbols used in showing the derivation of the space-groups conform to those used by Wyckoff. The interpretation of the eighth column of these tables to the case of atoms of elements and to the case of ions is taken up in Chap. XIX.

A. *Triclinic System.*

I. Triclinic hemihedry; Asymmetric

No.	S.G.	Deriv.	S.L.	n	s
1	C_1^1	C_1, Γ_{tr}	Γ_{tr}	1	Always 1

II. Triclinic holohedry; Centrosymmetric

No.	S.G.	Deriv.	S.L.	n	s
2	C_i^1	C_i, Γ_{tr}	Γ_{tr}	2	Always 1

B. *Monoclinic System.*

For convenience of reference to Astbury and Yardley these tables for the monoclinic system follow the ordinary convention of crystallography which chooses the Y-axis as the axis of symmetry and the (0 1 0) plane as the plane of symmetry. This places the Y-axis at right angles to the X-Z plane. This convention is different from the one adopted in Chaps. II and III which chooses the Z-axis as the one perpendicular to the plane of the other two. To make the portions of Chaps. II and III which deal with the monoclinic lattice read in accordance with the ordinary convention,

Y-axis	must be substituted for	Z-axis
Z-axis	must be substituted for	Y-axis
l/C	must be substituted for	k
k	must be substituted for	l/C
μ	must be substituted for	ν
ν	must be substituted for	μ

III. Monoclinic hemihedry; Equatorial

No.	S.G.	Deriv.	S.L.	n	s
3	C_s^1	Γ_m, S_h	Γ_m	2	Always 1
4	C_s^2	Γ_m, $S_h(\tau)$	Γ_m	2	(a) ½ for $\{h\,0\,l\}$ if h is odd (b) ½ for $\{h\,0\,l\}$ if l is odd (c) ½ for $\{h\,0\,l\}$ if $(h+l)$ is odd
5	C_s^3	Γ_m', S_h	Γ_m' (*cf.* Γ_o''') (*cf.* Γ_o') (*cf.* Γ_o'), (*cf.* Γ_o'')	4 4 4 8	(a) ½ for $\{h\,k\,l\}$ if $(h+k+l)$ is odd (b_1) ½ for $\{h\,k\,l\}$ if $(k+l)$ is odd (b_2) ½ for $\{h\,k\,l\}$ if $(h+k)$ is odd (c) ½ for $\{h\,k\,l\}$ if $(h+k)$ or $(k+l)$ or $(h+l)$ is odd
6	C_s^4	Γ_m', $S_h(\tau)$	Γ_m'	4 8	(a)(b_1)(b_2) Same as C_s^3*; also ½ for all $\{h\,0\,l\}$ (c) Same as $C_s^3(c)$ also ¼ for $\{h\,0\,l\}$ if $(h+l)$ is odd, and ½ for $\{h\,0\,l\}$ if $(h+l)$ is even

* This is to be interpreted to mean "same as C_s^3 (a)(b_1)(b_2) respectively."

	p	Possible molecular symmetry	No.
	—	None	1

	p	Possible molecular symmetry	No.
	2	C	2

	p	Possible molecular symmetry	No.
	2	P	3
	—	None	4
	2	P	5
	—	None	6

IV. Monoclinic hemimorphic hemihedry; Digonal polar

No.	S.G.	Deriv.	S.L.	n	s
7	C_2^1	Γ_m, $A(\pi)$	Γ_m	2	Always 1
8	C_2^2	Γ_m, $A(\pi, \tau_z)$	Γ_m	2	½ for {0 1 0}
9	C_2^3	Γ_m', $A(\pi)$ = Γ_m', $A(\pi, \tau_z)$	Γ_m'	4 8	$(a)(b_1)(b_2)$ Same as C_s^3 (c) Same as C_s^3

V. Monoclinic holohedry; Digonal equatorial

No.	S.G.	Deriv.	S.L.	n	s
10	C_{2h}^1	C_2^1, S_h	Γ_m	4	Always 1
11	C_{2h}^2	C_2^2, S_h	Γ_m	4	½ for {0 1 0}
12	C_{2h}^3	C_2^3, S_h	Γ_m'	8 16	$(a)(b_1)(b_2)$ Same as C_s^3 (c) Same as C_s^3
13	C_{2h}^4	C_2^1, $S_h(\tau)$	Γ_m	4	$(a)(b)(c)$ Same as C_s^2
14	C_{2h}^5	C_2^2, $S_h(\tau)$	Γ_m	4	$(a)(b)(c)$ Same as C_s^2; also ½ for {0 1 0}
15	C_{2h}^6	C_2^3, $S_h(\tau)$	Γ_m'	8 16	$(a)(b_1)(b_2)$ Same as C_s^4 (c) Same as C_s^4

C. *Orthorhombic System.*

VI. Orthorhombic enantiomorphic hemihedry; Digonal holoaxial

No.	S.G.	Deriv.	S.L.	n	s
16	V^1 or Q^1	C_2^1, C_2^1, C_2^1	Γ_o	4	Always 1
17	V^2	C_2^1, C_2^1, C_2^2	Γ_o	4	½ for {0 0 1}
18	V^3	C_2^2, C_2^2, C_2^1	Γ_o	4	½ for {1 0 0} and {0 1 0}
19	V^4	C_2^2, C_2^2, C_2^2	Γ_o	4	½ for {1 0 0}, {0 1 0} and {0 0 1}
20	V^5	C_2^3, C_2^3, C_2^2	$\Gamma_o'(a)$	8	½ for {0 0 1}; ½ for $\{hkl\}$ if $(h + k)$ is odd
21	V^6	C_2^3, C_2^3, C_2^1	$\Gamma_o'(a)$	8	½ for $\{hkl\}$ if $(h + k)$ is odd
22	V^7	C_2^3, C_2^3, C_2^3	Γ_o''	16	½ for $\{hkl\}$ if $(h + k)$ or $(k + l)$ or $(h + l)$ is odd

	p	Possible molecular symmetry	No.
	2	2-A	7
	—	None	8
	2	2-A	9

	p	Possible molecular symmetry	No.
	2 4	2-A; P 2-A $\perp$ P	10
	2	P; C	11
	2 4	2-A; P; C 2-A $\perp$ P	12
	2	2-A; C	13
	2	C	14
	2	2-A; C	15

	p	Possible molecular symmetry	No.
	2 4	2-A $\perp$ {100}, {010} or {001} 3 mutually $\perp$ 2-A's	16
	2	2-A $\perp$ {100} or {010}	17
	2	2-A $\perp$ {001}	18
	—	None	19
	2	2-A $\perp$ {100} or {010}	20
	—	Same as V^1	21
	—	Same as V^1	22

VI. (*Concluded*)

No.	S.G.	Deriv.	S.L.	n	s
23*	V^8	C_2^3, C_2^3, C_2^3	Γ_o'''	8	½ for $\{hkl\}$ if $(h+k+l)$ is odd
24*	V^9	C_2^3, C_2^3, C_2^3	Γ_o'''	8	Same as V^8

* These two space-groups differ in the distribution of their axes. For details see Wyckoff, "Analytical Expression of the Results of the Theory of Space-groups."

VII. Orthorhombic hemimorphic hemihedry; Didigonal polar

No.	S.G.	Deriv.	S.L.	n	s
25	C_{2v}^1	C_2^1, $S = C_2^1, S_1$	Γ_o	4	Always 1
26	C_{2v}^2	C_2^2, $S = C_2^2, S_1(\tau_z)$	Γ_o	4	½ for $\{0kl\}$ if l is odd
27	C_{2v}^3	C_2^1, $S(\tau_z)$	Γ_o	4	½ for $\{h0l\}$ if l is odd ½ for $\{0kl\}$ if l is odd
28	C_{2v}^4	C_2^1, $S(\tau_x)$	Γ_o	4	½ for $\{h0l\}$ if h is odd
29	C_{2v}^5	C_2^2, $S(\tau_x)$	Γ_o	4	½ for $\{h0l\}$ if h is odd ½ for $\{0kl\}$ if l is odd
30	C_{2v}^6	C_2^1, $S(\tau_x+\tau_z)$	Γ_o	4	½ for $\{h0l\}$ if $(h+l)$ is odd ½ for $\{0kl\}$ if l is odd
31	C_{2v}^7	C_2^2, $S(\tau_x+\tau_z)$	Γ_o	4	½ for $\{h0l\}$ if $(h+l)$ is odd
32	C_{2v}^8	C_2^1, $S_m(\tau_x)$	Γ_o	4	½ for $\{h0l\}$ if h is odd ½ for $\{0kl\}$ if k is odd
33	C_{2v}^9	C_2^2, $S_m(\tau_x)$	Γ_o	4	½ for $\{h0l\}$ if h is odd ½ for $\{0kl\}$ if $(k+l)$ is odd
34	C_{2v}^{10}	C_2^1, $S_m(\tau_x+\tau_z)$	Γ_o	4	½ for $\{h0l\}$ if $(h+l)$ is odd ½ for $\{0kl\}$ if $(k+l)$ is odd
35	C_{2v}^{11}	C_2^1, S_d	$\Gamma_o'(a)$	8	½ for $\{hkl\}$ if $(h+k)$ is odd
36	C_{2v}^{12}	C_2^2, S_d	$\Gamma_o'(a)$	8	Same as C_{2v}^{11}; also ½ for all $\{0kl\}$
37	C_{2v}^{13}	C_2^1, $S_d(\tau_z)$	$\Gamma_o'(a)$	8	Same as C_{2v}^{11}; also ½ for all $\{0kl\}$ and $\{h0l\}$
38	C_{2v}^{14}	C_2^2, S	$\Gamma_o'(b)$	8	½ for $\{hkl\}$ if $(k+l)$ is odd

	p	Possible molecular symmetry	No.
	—	Same as V^1	23
	2	2-$A \perp$ {100}, {010} or {001}	24

	p	Possible molecular symmetry	No.
	2 4	$P \parallel$ {100} or {010} Two P's intersecting in 2-A	25
	2	$P \parallel$ {010}	26
	2	2-A	27
	2	2-A; $P \parallel$ {100}	28
	—	None	29
	2	2-A	30
	2	$P \parallel$ {100}	31
	2	2-A	32
	—	None	33
	2	2-A	34
	2 4	2-A; $P \parallel$ {100} or {010} Two P's intersecting in 2-A	35
	2	$P \parallel$ {010}	36
	2	2-A	37
	—	Same as C_{2v}^1	38

VII. (*Concluded*)

No.	S.G.	Deriv.	S.L.	n	s
39	C_{2v}^{15}	C_2^2, $S(\tau_z)$	$\Gamma_o'(b)$	8	Same as C_{2v}^{14}; also ½ for all $\{0kl\}$
40	C_{2v}^{16}	C_2^2, $S(\tau_x)$	$\Gamma_o'(b)$	8	Same as C_{2v}^{14}; also ½ for all $\{h0l\}$
41	C_{2v}^{17}	C_2^2, $S(\tau_x + \tau_z)$	$\Gamma_o'(b)$	8	Same as C_{2v}^{14}; also ½ for all $\{0kl\}$ and $\{h0l\}$
42	C_{2v}^{18}	C_2^2, S	Γ_o''	16	½ for $\{hkl\}$ if $(h+k)$ or $(k+l)$ or $(h+l)$ is odd
43	C_{2v}^{19}	C_2^2, $S_m\left(\frac{\tau_x+\tau_z}{2}\right)$	Γ_o''	16	Same as C_{2v}^{18}; also ¼ for $\{h0l\}$ if $(h+l)$ is odd ½ for $\{h0l\}$ if $(h+l)$ is even ¼ for $\{0kl\}$ if $(k+l)$ is odd ½ for $\{0kl\}$ if $(k+l)$ is even
44	C_{2v}^{20}	C_2^2, S_d	Γ_o'''	8	½ for $\{hkl\}$ if $(h+k+l)$ is odd
45	C_{2v}^{21}	C_2^2, $S_d(\tau_z)$	Γ_o'''	8	Same as C_{2v}^{20}; also ½ for all $\{h0l\}$ and $\{0kl\}$
46	C_{2v}^{22}	C_2^2, $S_d(\tau_x)$	Γ_o'''	8	Same as C_{2v}^{20}; also ½ for all $\{h0l\}$

VIII. Orthorhombic holohedry; Didigonal equatorial

No.	S.G.	Deriv.*	S.L.	n	s
47	V_h^1	V^1, S_h = V^1, I	Γ_o	8	Always 1
48	V_h^2	V^1, I_m	Γ_o	8	½ for $\{0kl\}$ if $(k+l)$ is odd ½ for $\{h0l\}$ if $(h+l)$ is odd ½ for $\{hk0\}$ if $(h+k)$ is odd
49	V_h^3	V^1, I_w	Γ_o	8	½ for $\{0kl\}$ if l is odd ½ for $\{h0l\}$ if l is odd
50	V_h^4	V^1, I_g	Γ_o	8	½ for $\{0kl\}$ if k is odd ½ for $\{h0l\}$ if h is odd ½ for $\{hk0\}$ if $(h+k)$ is odd
51	V_h^5	V^2, I	Γ_o	8	½ for $\{h0l\}$ if l is odd

	p	Possible molecular symmetry	No.
	2	2-A; $P \parallel \{010\}$	39
	2	2-A; $P \parallel \{100\}$	40
	2	2-A	41
	—	Same as C_{2v}^{11}	42
	2	2-A	43
	—	Same as C_{2v}^{1}	44
	2	2-A	45
	2	2-A; $P \parallel \{100\}$	46

	p	Possible molecular symmetry	No.
	2 4 8	$P \parallel \{100\}$, $\{010\}$, or $\{001\}$ Two P's intersecting in 2-A Three P's intersecting in three 2-A's	47
	2 4	2-$A \perp \{100\}$, $\{010\}$, or $\{001\}$; C Three mutually $\perp$ 2-A's.	48
	2 4	2-$A \perp \{100\}$, $\{010\}$, or $\{001\}$; $P \parallel \{001\}$ 2-$A \perp P \parallel \{001\}$; three mutually $\perp$ 2-A's	49
	—	Same as V_h^2	50
	2 4	2-$A \perp \{100\}$; $P \parallel \{100\}$ or $\{001\}$ 2-$A \perp P \parallel \{100\}$; two P's $\parallel \{100\}$ and $\{001\}$ intersecting in 2-A	51

VIII. (*Continued*)

No.	S.G.	Deriv.*	S.L.	n	s
52	V_h^6	V^2, I_m	Γ_o	8	½ for $\{0kl\}$ if $(k+l)$ is odd ½ for $\{h0l\}$ if h is odd ½ for $\{hk0\}$ if $(h+k)$ is odd
53	V_h^7	V^2, I_a	Γ_o	8	½ for $\{h0l\}$ if $(h+l)$ is odd ½ for $\{hk0\}$ if h is odd
54	V_h^8	V^2, I_k	Γ_o	8	½ for $\{0kl\}$ if k is odd ½ for $\{h0l\}$ if l is odd ½ for $\{hk0\}$ if k is odd
55	V_h^9	V^3, I	Γ_o	8	½ for $\{0kl\}$ if k is odd ½ for $\{h0l\}$ if h is odd
56	V_h^{10}	V^3, I_m	Γ_o	8	½ for $\{0kl\}$ if l is odd ½ for $\{h0l\}$ if l is odd ½ for $\{hk0\}$ if $(h+k)$ is odd
57	V_h^{11}	V^3, I_k	Γ_o	8	½ for $\{h0l\}$ if h is odd ½ for $\{hk0\}$ if k is odd
58	V_h^{12}	V^3, I_w	Γ_o	8	½ for $\{0kl\}$ if $(k+l)$ is odd ½ for $\{h0l\}$ if $(h+l)$ is odd
59	V_h^{13}	V^3, I_g	Γ_o	8	½ for $\{hk0\}$ if $(h+k)$ is odd
60	V_h^{14}	V^3, I_f	Γ_o	8	½ for $\{0kl\}$ if l is odd ½ for $\{h0l\}$ if $(h+l)$ is odd ½ for $\{hk0\}$ if k is odd
61	V_h^{15}	V^4, I	Γ_o	8	½ for $\{0kl\}$ if k is odd ½ for $\{h0l\}$ if l is odd ½ for $\{hk0\}$ if h is odd
62	V_h^{16}	V^4, I_g	Γ_o	8	½ for $\{0kl\}$ if $(k+l)$ is odd ½ for $\{h0l\}$ if h is odd
63	V_h^{17}	V^5, I	$\Gamma_o'(a)$	16	Same as V^5; also ½ for all $\{h0l\}$
64	V_h^{18}	V^5, I_a	$\Gamma_o'(a)$	16	Same as V^5; also ½ for all $\{h0l\}$ and $\{hk0\}$
65	V_h^{19}	V^6, I	$\Gamma_o'(a)$	16	Same as V^6

	p	Possible molecular symmetry	No.
	2	2-A ⊥ {100} or {010}; C	52
	2 4	2-A ⊥ {100} or {010}; P ∥ {100} 2-A ⊥ P ∥ {100}	53
	—	Same as V_h^6	54
	2 4	2-A ⊥ {001}; P ∥ {001} 2-A ⊥ P ∥ {001}	55
	2	2-A ⊥ {001}; C	56
	2	2-A ⊥ {001}; P ∥ {100}; C	57
	—	Same as V_h^9	58
	2 4	P ∥ {100} or {010}; C Two P's ∥ {100} and {010} intersecting in 2-A	59
	—	Same as V_h^{10}	60
	2	C	61
	2	P ∥ {001}; C	62
	2 4	2-A ⊥ {100}; P ∥ {100} or {001}; C Two P's ∥ {100} and {001} intersecting in 2-A; 2-A ⊥ P ∥ {100}	63
	2 4	2-A ⊥ {100} or {010}; P ∥ {100}; C 2-A ⊥ P ∥ {100}	64
	2 4 8	2-A ⊥ {001}; P ∥ {100}, {010}, or {001} Two P's intersecting in 2-A; 2-A ⊥ P ∥ {001} Three P's intersecting in three 2-A's	65

VIII. (*Concluded*)

No.	S.G.	Deriv.*	S.L.	n	s
66	V_h^{20}	V^6, I_m	$\Gamma_o'(a)$	16	Same as V^6; also ½ for all $\{0kl\}$ and $\{h0l\}$
67	V_h^{21}	V^6, I_a	$\Gamma_o'(a)$	16	Same as V^6; also ½ for all $\{hk0\}$
68	V_h^{22}	V^6, I_f	$\Gamma_o'(a)$	16	Same as V^6; also ½ for all $\{0kl\}$, $\{h0l\}$, and $\{hk0\}$
69	V_h^{23}	V^7, I	Γ_o''	32	Same as V^7
70	V_h^{24}	V^7, I_m	Γ_o''	32	Same as V^7; also ¼ for $\{0kl\}$ if $(k+l)$ is odd ½ for $\{0kl\}$ if $(k+l)$ is even ¼ for $\{h0l\}$ if $(h+l)$ is odd ½ for $\{h0l\}$ if $(h+l)$ is even ¼ for $\{hk0\}$ if $(h+k)$ is odd ½ for $\{hk0\}$ if $(h+k)$ is even
71	V_h^{25}	V^8, I	Γ_o'''	16	Same as V^8.
72	V_h^{26}	V^8, I_w	Γ_o'''	16	Same as V^8; also ½ for all $\{0kl\}$ and $\{h0l\}$
73	V_h^{27}	V^9, I	Γ_o'''	16	Same as V^8; also ½ for all $\{0kl\}$, $\{h0l\}$, and $\{hk0\}$
74	V_h^{28}	V^9, I_y	Γ_o'''	16	Same as V^8; also ½ for all $\{hk0\}$

* See Fig. 12, Chap. VIII.

D. *Tetragonal System.**

IX. Tetragonal tetartohedry; Tetragonal polar

No.	S.G.	Deriv.	S.L.	n	s
75	C_4^1	$A(\pi/2)$, Γ_t	Γ_t (Γ_o) (Γ_o')	4 8	1) Always 1 2) ½ for $\{hkl\}$ if $(h+k)$ is odd

* Note that $\{100\}$ includes both the (100) and (010) planes; similarly $\{0kl\}$ includes both the $(0kl)$ and $(h0l)$ planes. Therefore, "½ for $\{0kl\}$" means "½ for $(0kl)$ or $(h0l)$." (See p. 247.)

	p	Possible molecular symmetry	No.
	2	2-A ⊥ {100}, {010}, or {001}; P ∥ {001}	66
	4	Three mutually ⊥ 2-A's; 2-A ⊥ P ∥ {001}	
	2	2-A ⊥ {100}, {010}, or {001}; P ∥ {100} or {010}	67
	4	Two P's ∥ {100} and {010} intersecting in 2-A; three mutually ⊥ 2-A's; 2-A ⊥ P ∥ {100}; 2-A ⊥ P ∥ {010}	
	2	2-A ⊥ {100}, {010}, or {001}; C	68
	4	Three mutually ⊥ 2-A's	
	2	2-A ⊥ {100}, {010}, or {001}; P ∥ {100}, {010}, or {001}	69
	4	Two P's intersecting in 2-A; 2-A ⊥ P ∥ {100}, {010}, or {001}	
	8	Three P's intersecting in three 2-A's	
	2	2-A ⊥ {100}, {010}, or {001}; C	70
	4	Three mutually ⊥ 2-A's	
	2	P ∥ {100}, {010} or {001}; C	71
	4	Two P's intersecting in 2-A	
	8	Three P's intersecting in three 2-A's	
	2	2-A ⊥ {100}, {010}, or {001}; P ∥ {001}; C	72
	4	Three mutually ⊥ 2-A's; 2-A ⊥ P ∥ {001}	
	2	2-A ⊥ {100}, {010}, or {001}; C	73
	2	2-A ⊥ {100} or {010}; P ∥ {100} or {010}	74
	4	2-A ⊥ P ∥ {100} or {010}; two P's ∥ {100} and {010} intersecting in 2-A	

	p	Possible molecular symmetry*	No.
	2	2-A ⊥ {001}	75
	4	4-A ⊥ {001}	

* Applies to both case 1 and case 2.

IX. (*Concluded*)

No.	S.G.	Deriv.	S.L.	n	s
76	C_4^3	$A(\pi/2, \tau_z/2)$, Γ_t	Γ_t (Γ_o) (Γ_o')	4 8	1) ¼ for {0 0 1} 2) ¼ for {0 0 1}; ½ for $\{h\,k\,l\}$ if $(h+k)$ is odd
77	C_4^3	$A(\pi/2, \tau_z)$, Γ_t	Γ_t (Γ_o) (Γ_o')	4 8	1) ½ for {0 0 1} 2) ½ for {0 0 1}; ½ for $\{h\,k\,l\}$ if $(h+k)$ is odd
78	C_4^4	$A(\pi/2, 3\tau_z/2)$, Γ_t	Same as C_4^3 but in the opposite rotatory sense, therefore identical data		
79	C_4^5	$A(\pi/2)$, Γ_t'	Γ_t' (Γ_o'') (Γ_o''')	16 8	1) ½ for $\{h\,k\,l\}$ if $(h+k)$, $(k+l)$, or $(h+l)$ is odd 2) ½ for $\{h\,k\,l\}$ if $(h+k+l)$ is odd
80	C_4^6	$A(\pi/2, \tau_z/2)$, Γ_t'	Γ_t' (Γ_o'') (Γ_o''')	16 8	1) Same as C_4^5 1); also ¼ for {0 0 1} 2) Same as C_4^5 2); also ¼ for {0 0 1}

X. Tetragonal tetartohedry of the second sort; Tetragonal alternating

No.	S.G.	Deriv.	S.L.	n	s
81	S_4^1	C_2^1, $\overline{A}$	Γ_t (Γ_o) (Γ_o')	4 8	1) Always 1 2) Same as C_4^1, 2) *i.e.*, ½ for $\{h\,k\,l\}$ if $(h+k)$ is odd
82	S_4^2	C_2^2, $\overline{A}$	Γ_t' (Γ_o'') (Γ_o''')	16 8	1) Same as C_4^5 1) *i.e.*, ½ for $\{h\,k\,l\}$ if $(h+k)$, $(k+l)$, or $(h+l)$ is odd 2) Same as C_4^5 2) *i.e.*, ½ for $\{h\,k\,l\}$ if $(h+k+l)$ is odd

XI. Tetragonal enantiomorphic hemihedry; Tetragonal holoaxial

No.	S.G.	Deriv.	S.L.	n	s
83	D_4^1	C_4^1, U_o	Γ_t (Γ_o) (Γ_o')	8 16	1) Always 1 2) Same as S_4^1 2)
84	D_4^2	C_4^1, U_o	Γ_t (Γ_o) (Γ_o')	8 16	1) ½ for {1 0 0} 2) Same as S_4^1 2); also ½ for {1 1 0}
85	D_4^3	C_4^2, U_o	Γ_t (Γ_o) (Γ_o')	8 16	1) ¼ for {0 0 1} 2) Same as S_4^1 2); also ¼ for {0 0 1}
86	D_4^4	C_4^2, U_o	Γ_t (Γ_o) (Γ_o')	8 16	1) ¼ for {0 0 1}; ½ for {1 0 0} 2) Same as S_4^1 2); also ¼ for {0 0 1}; ½ for {1 1 0}

	p	Possible molecular symmetry*	No.
	—	None	76
	2	2-A ⊥ {001}	77
			78
	—	Same as C_4^1	79
	—	Same as C_4^3	80

*Applies to both case 1 and case 2.

	p	Possible molecular symmetry*	No.
	2 4	2-A ⊥ {001} 4a-A ⊥ {001}	81
	—	Same as S_4^1	82

* Applies to both case 1 and case 2.

	p	Possible molecular symmetry†	No.
	2 4 8	2-A ⊥ {100}, {110}, or {001} 4-A ⊥ {001}; three intersecting 2-A's ⊥ {100} and {001} Four 2-A's ⊥ {100} and {110} intersecting in 4-A ⊥ {001}	83
	2 4	2-A ⊥ {001} or {110} 4-A ⊥ {001}; three intersecting 2-A's ⊥ {110} and {001}	84
	2	2-A ⊥ {100} or {110}	85
	2	2-A ⊥ {110}	86

† This column of the table applies only to case 1. Make the substitution {110} ⇄ {100} whe applying this column to case 2.

XI. (*Concluded*)

No.	S.G.	Deriv.	S.L.	n	s
87	D_4^5	C_4^3, U_a	Γ_t (Γ_o) (Γ_o')	8 16	1) ½ for {001} 2) Same as S_4^1 2); also ½ for {001}
88	D_4^6	C_4^3, U_c	Γ_t (Γ_o) (Γ_o')	8 16	1) ½ for {100} and {001} 2) Same as S_4^1 2); also ½ for {001} and {110}
89	D_4^7	C_4^4, U_a	Same as D_4^3 but in opposite rotatory sense, therefore identical data		
90	D_4^8	C_4^4, U_c	Same as D_4^4 but in opposite rotatory sense, therefore identical data		
91	D_4^9	C_4^5, U_a	Γ_t' (Γ_o'') (Γ_o''')	32 16	1) Same as S_4^2 1) 2) Same as S_4^2 2)
92	D_4^{10}	C_4^6, U_a	Γ_t' (Γ_o'') (Γ_o''')	32 16	1) Same as S_4^2 1); also ¼ for {001} 2) Same as S_4^2 2); also ¼ for {001}

XII. Tetragonal paramorphic hemihedry; Tetragonal equatorial

No.	S.G.	Deriv.	S.L.	n	s
93	C_{4h}^1	C_4^1, I	Γ_t (Γ_o) (Γ_o')	8 16	1) Always 1 2) Same as S_4^1 2)
94	C_{4h}^2	C_4^2, I	Γ_t (Γ_o) (Γ_o')	8 16	1) ½ for {001} 2) Same as S_4^1 2); also ½ for {001}
95	C_{4h}^3	C_4^1, I_1	Γ_t (Γ_o) (Γ_o')	8 16	1) ½ for $\{hk0\}$ if $(h+k)$ is odd 2) Same as S_4^1 2); also ½ for all $\{hk0\}$
96	C_{4h}^4	C_4^3, I_1	Γ_t (Γ_o) (Γ_o')	8 16	1) ½ for {001}; ½ for $\{hk0\}$ if $(h+k)$ is odd 2) Same as S_4^1 2); also ½ for all {001} and $\{hk0\}$
97	C_{4h}^5	C_4^5, I	Γ_t' (Γ_o'') (Γ_o''')	32 16	1) Same as S_4^2 1) 2) Same as S_4^2 2)
98	C_{4h}^6	C_4^6, I_1	Γ_t' (Γ_o'') (Γ_o''')	32 16	1) Same as S_4^2 1); also ¼ for {001}; ¼ for $\{hk0\}$ if $(h+k)$ is odd; ½ for $\{hk0\}$ if $(h+k)$ is even 2) Same as S_4^2 2); also ¼ for {001}; ½ for all $\{hk0\}$

	p	Possible molecular symmetry†	No.
	2	2-A ⊥ {100}, {110}, or {001}	87
	4	Three intersecting 2-A's, either ⊥ {110} and {001} or ⊥ {100} and {001}	
	2	2-A ⊥ {001} or {110}	88
	4	Three intersecting 2-A's ⊥ {001} and {110}	
			89
			90
	2	2-A ⊥ {100}, {110}, or {001}	91
	4	4-A ⊥ {001}; three intersecting 2-A's ⊥ {110} and {001}	
	8	Four 2-A's ⊥ {100} and {110} intersecting in 4-A ⊥ {001}	
	2	2-A ⊥ {100}, {110}, or {001}	92
	4	Three intersecting 2-A's ⊥ {100} and {001}	

† This column of the table applies only to case 1. Make the substitution {110} ⇄ {100} when applying this column to case 2.

	p	Possible molecular symmetry*	No.
	2	2-A ⊥ {001}; P ∥ {001}	93
	4	4-A ⊥ {001}; 2-A ⊥ P ∥ {001}	
	8	4-A ⊥ P ∥ {001}	
	2	2-A ⊥ {001}; P ∥ {001}	94
	4	2-A ⊥ P ∥ {001}	
	2	2-A ⊥ {001}; C	95
	4	4-A ⊥ {001}; 4a-A ⊥ {001}	
	2	2-A ⊥ {001}; C	96
	4	4a-A ⊥ {001}	
	—	Same as C_{4h}^1	97
	—	Same as C_{4h}^4	98

* Applies to both case 1, and case 2.

XIII. Tetragonal hemimorphic hemihedry; Ditetragonal polar

No.	S.G.	Deriv.	S.L.	n	s
99	C_{4v}^{1}	C_4^1, S_s	Γ_t (Γ_o) (Γ_o')	8 16	1) Always 1 2) Same as S_4^1 2)
100	C_{4v}^{2}	C_4^1, S_c	Γ_t (Γ_o) (Γ_o')	8 16	1) ½ for $\{0kl\}$ if k is odd 2) Same as S_4^1 2); also ½ for $\{hhl\}$ if h is odd
101	C_{4v}^{3}	C_4^3, S_s	Γ_t (Γ_o) (Γ_o')	8 16	1) ½ for $\{0kl\}$ if l is odd 2) Same as S_4^1 2); also ½ for $\{hhl\}$ if l is odd
102	C_{4v}^{4}	C_4^3, S_c	Γ_t (Γ_o) (Γ_o')	8 16	1) ½ for $\{0kl\}$ if $(k+l)$ is odd 2) Same as S_4^1 2); also ½ for $\{hhl\}$ if $(h+l)$ is odd
103	C_{4v}^{5}	C_4^1, $S_s(\tau_z)$	Γ_t (Γ_o) (Γ_o')	8 16	1) ½ for $\{0kl\}$ and $\{hhl\}$ if l is odd 2) Same as S_4^1 2); also ½ for all $\{0kl\}$ ½ for $\{hhl\}$ if l is odd
104	C_{4v}^{6}	C_4^1, $S_c(\tau_z)$	Γ_t (Γ_o) (Γ_o')	8 16	1) ½ for $\{0kl\}$ if $(k+l)$ is odd ½ for $\{hhl\}$ if l is odd 2) Same as S_4^1 2); also ½ for all $\{0kl\}$ ½ for $\{hhl\}$ if $(h+l)$ is odd
105	C_{4v}^{7}	C_4^3, $S_s(\tau_z)$	Γ_t (Γ_o) (Γ_o')	8 16	1) ½ for $\{hhl\}$ if l is odd 2) Same as S_4^1 2); also ½ for all $\{0kl\}$
106	C_{4v}^{8}	C_4^3, $S_c(\tau_z)$	Γ_t (Γ_o) (Γ_o')	8 16	1) ½ for $\{0kl\}$ if k is odd ½ for $\{hhl\}$ if l is odd 2) Same as S_4^1 2); also ½ for all $\{0kl\}$ ½ for $\{hhl\}$ if h is odd
107	C_{4v}^{9}	C_4^5, S_s	Γ_t' (Γ_o'') (Γ_o''')	32 16	1) Same as S_4^2 1) 2) Same as S_4^2 2)
108	C_{4v}^{10}	C_4^5, $S_s(\tau_z)$	Γ_t' (Γ_o'') (Γ_o''')	32 16	1) Same as S_4^2 1); also ½ for all $\{hhl\}$ 2) Same as S_4^2 2); also ½ for all $\{0kl\}$
109	C_{4v}^{11}	C_4^5, S_c	Γ_t' (Γ_o'') (Γ_o''')	32 16	1) Same as S_4^2 1); also ¼ for $\{0kl\}$ if $(k+l)$ is odd ½ for $\{0kl\}$ if $(k+l)$ is even 2) Same as S_4^2 2); also ¼ for $\{hhl\}$ if l is odd ½ for $\{hhl\}$ if $l = 2x$ where x is even or zero 1 for $\{hhl\}$ if $l = 2x$ where x is odd

	p	Possible molecular symmetry†	No.
	2 4 8	$P \parallel \{100\}$ or $\{110\}$ Two P's $\parallel \{100\}$ intersecting in 2-A Four P's $\parallel \{100\}$ and $\{110\}$ intersecting in 4-A	99
	2 4	$P \parallel \{110\}$ 4-$A \perp \{001\}$; 2P's $\parallel \{110\}$ intersecting in 2-A	100
	2 4	2-$A \perp \{001\}$; $P \parallel \{110\}$ Two P's $\parallel \{110\}$ intersecting in 2-A	101
	—	Same as C_{4}^{3}	102
	2 4	2-$A \perp \{001\}$ 4-$A \perp \{001\}$	103
	—	Same as C_{4v}^{5}	104
	2 4	$P \parallel \{100\}$ Two P's $\parallel \{100\}$ intersecting in 2-A	105
	2	2-$A \perp \{001\}$	106
	2 4 8	$P \parallel \{100\}$ or $\{110\}$ Two P's $\parallel \{110\}$ intersecting in 2-A Four P's $\parallel \{100\}$ and $\{110\}$ intersecting in 4-A	107
	2 4	$P \parallel \{100\}$ 4-$A \perp \{001\}$; two P's $\parallel \{100\}$ intersecting in 2-A	108
	2 4	$P \parallel \{110\}$ Two P's $\parallel \{110\}$ intersecting in 2-A	109

† This column of the table applies only to case 1. Make the substitution $\{110\} \rightleftarrows \{100\}$ whe applying this column to case 2.

XIII. (*Concluded*)

No.	S.G.	Deriv.	S.L.	n	s
110	C_{4v}^{12}	C_4^6, $S_o(\tau_z)$	Γ_t' (Γ_o'')	32	1) Same as S_4^2 1); also ¼ for $\{0kl\}$ if $(k+l)$ is odd ½ for $\{0kl\}$ if $(k+l)$ is even ½ for all $\{hhl\}$
			(Γ_o''')	16	2) Same as S_4^2 2); also ½ for all $\{0kl\}$ ¼ for $\{hhl\}$ if l is odd ½ for $\{hhl\}$ if $l = 2x$ where x is even or zero 1 for $\{hhl\}$ if $l = 2x$ where x is odd

XIV. Tetragonal hemihedry of the second sort; Ditetragonal alternating

No.	S.G.	Deriv.	S.L.	n	s
111	$D_{2d}^1 = V_d^1$	V^1, S_d	Γ_t (Γ_o)	8	Always 1
112	D_{2d}^2	V^1, $S_d(\tau_z)$	Γ_t (Γ_o)	8	½ for $\{hhl\}$ if l is odd
113	D_{2d}^3	V^3, S_d	Γ_t (Γ_o)	8	½ for $\{100\}$
114	D_{2d}^4	V^3, $S_d(\tau_z)$	Γ_t (Γ_o)	8	½ for $\{100\}$; ½ for $\{hhl\}$ if l is odd
115	D_{2d}^5	V^6, S_d	Γ_t (Γ_o')	16	Same as S_4^1 2)
116	D_{2d}^6	V^6, $S_d(\tau_z)$	Γ_t (Γ_o')	16	Same as S_4^1 2); also ½ for $\{hhl\}$ if l is odd
117	D_{2d}^7	V^6, $S_{d_1}\left(\frac{\tau_x+\tau_y}{2}\right)$	Γ_t (Γ_o')	16	Same as S_4^1 2); also ½ for $\{hhl\}$ if h is odd
118	D_{2d}^8	V^6, $S_{d_1}\left(\frac{\tau_x+\tau_y}{2}+\tau_z\right)$	Γ_t (Γ_o')	16	Same as S_4^1 2); also ½ for $\{hhl\}$ if $(h+l)$ is odd
119	D_{2d}^9	V^7, S_d	Γ_t' (Γ_o'')	32	Same as S_4^2 1)

	p	Possible molecular symmetry†	No
	—	Same as C_{4v}^8	110

† ↑ is column of the table applies only to case 1. Make the substitution {110} ⇄ {100} when applying this column to case 2

	p	Possible molecular symmetry	No.
	2	2-A ⊥ {100} or {001}; P ∥ {110}	111
	4	Two P's ∥ {110} intersecting in 2-A; Three mutually ⊥ 2-A's	
	8	Two P's ∥ {110} intersecting in 4a-A ⊥ {001}	
	2	2-A ⊥ {100} or {001}	112
	4	Three mutually ⊥ 2-A's; 4a-A ⊥ {001}	
	2	2-A ⊥ {001}; P ∥ {110}	113
	4	Two P's ∥ {110} intersecting in 2-A; 4a-A ⊥ {001}	
	2	2-A ⊥ {001}	114
	4	4a-A ⊥ {001}	
	2	P ∥ {110}	115
	4	Two P's ∥ {110} intersecting in 2-A	
	8	Two P's ∥ {110} intersecting in 4a-A ⊥ {001}	
	—	Same as D_{2d}^2	116
	—	Same as D_{2d}^2	117
	—	Same as D_{2d}^2	118
	2	2-A ⊥ {100}; P ∥ {110}	119
	4	Two P's ∥ {110} intersecting in 2-A	
	8	Two P's ∥ {110} intersecting in 4a-A ⊥ {001}	

XIV. (*Concluded*)

No.	S.G.	Deriv.	S.L.	n	s
120	D_{2d}^{10}	V^7, $S_d(\tau_s)$	Γ_t' (Γ_o'')	32	Same as S_4^2 1); also ½ for all $\{hhl\}$
121	D_{2d}^{11}	V^8, S_d	Γ_t' (Γ_o''')	16	Same as S_4^2 2)
122	D_{2d}^{12}	V^9, $S_d\left(\frac{\tau_x}{2}, \frac{\tau_y}{2}, \frac{\tau_z}{2}\right)$	Γ_t' (Γ_o''')	16	Same as S_4^2 2); also ¼ for $\{hhl\}$ if l is odd ½ for $\{hhl\}$ if $l = 2x$ where x is even or zero 1 for $\{hhl\}$ if $l = 2x$ where x is odd

XV. Tetragonal holohedry; Ditetragonal equatorial

No.	S.G.	Deriv.	S.L.	n	s
123	D_{4h}^1	D_4^1, I	Γ_t (Γ_o) (Γ_o')	16 32	1) Always 1 2) Same as S_4^1 2)
124	D_{4h}^2	D_4^1, I_w	Γ_t (Γ_o) (Γ_o')	16 32	1) ½ for $\{0kl\}$ if l is odd ½ for $\{hhl\}$ if l is odd 2) Same as S_4^1 2); also ½ for all $\{0kl\}$; ½ for $\{hhl\}$ if l is odd
125	D_{4h}^3	D_4^1, I_g	Γ_t (Γ_o) (Γ_o')	16 32	1) ½ for $\{hk0\}$ if $(h+k)$ is odd ½ for $\{0kl\}$ if k is odd 2) Same as S_4^1 2); also ½ for all $\{hk0\}$; ½ for $\{hhl\}$ if h is odd
126	D_{4h}^4	D_4^1, I_m	Γ_t (Γ_o) (Γ_o')	16 32	1) ½ for $\{hk0\}$ if $(h+k)$ is odd ½ for $\{0kl\}$ if $(k+l)$ is odd ½ for $\{hhl\}$ if l is odd 2) Same as S_4^1 2); also ½ for all $\{hk0\}$ and $\{0kl\}$ ½ for $\{hhl\}$ if $(h+l)$ is odd
127	D_{4h}^5	D_4^2, I	Γ_t (Γ_o) (Γ_o')	16 32	1) ½ for $\{0kl\}$ if k is odd 2) Same as S_4^1 2); also ½ for $\{hhl\}$ if h is odd

	p	Possible molecular symmetry	No.
	—	Same as D_{2d}^2	120
	2	2-A ⊥ {100} or {001}; P ∥ {110}	121
	4	Two P's ∥ {110} intersecting in 2-A	
		Three mutually ⊥ 2-A's; 4a-A ⊥ {001}	
	8	Two P's ∥ {110} intersecting in 4a-A ⊥ {001}	
	2	2-A ⊥ {100} or {001}	122
	4	4a-A ⊥ {001}	

	p	Possible molecular symmetry†	No.
	2	P ∥ {100}, {110}, or {001}	123
	4	Two P's ∥ {100} intersecting in 2-A	
		Two P's ∥ {001} and {100} intersecting in 2-A	
		Two P's ∥ {001} and {110} intersecting in 2-A	
	8	Three P's ∥ {100} and {001} intersecting in three 2-A's	
		Four P's ∥ {100} and {110} intersecting in 4-A	
	16	Four P's ∥ {100} and {110} intersecting in 4-A; P ∥ {001}	
	2	2-A ⊥ {100}, {110} or {001}; P ∥ {001}	124
	4	4-A ⊥ {001}; three intersecting 2-A's ⊥ {100} and {001}; 2-A ⊥ P ∥ {001}	
	8	4-A ⊥ P ∥ {001}; four 2-A's ⊥ {100} and {110} intersecting in 4-A ⊥ {001}	
	2	2-A ⊥ {100} or {110}; P ∥ {110}	125
	4	4-A ⊥ {001}; two P's ∥ {110} intersecting in 2-A; 2-A ⊥ P ∥ {110}	
	8	Four 2-A's ⊥ {110} and {100} intersecting in 4-A ⊥ {001}; full D_{2d} symmetry (P ∥ {110})	
	2	2-A ⊥ {100}, {110} or {001}; C	126
	4	4-A ⊥ {001}; three intersecting 2-A's ⊥ {100} and {001}; 4a-A ⊥ {001}	
	8	Four 2-A's ⊥ {100} and {110} intersecting in 4-A ⊥ {001}	
	2	P ∥ {110} or {001}	127
	4	4-A ⊥ {001}; two P's ∥ {110} intersecting in 2-A; two P's ∥ {001} and {110} intersecting in 2-A	
	8	4-A ⊥ P ∥ {001}; three P's ∥ {110} and {001} intersecting in three 2-A's	

† This column of the table applies only to case 1. Make the substitution {110} ⇄ {100} when applying this column to case 2.

XV. (*Continued*)

No.	S.G.	Deriv.	S.L.	n	s
128	D_{4h}^{6}	D_4^2, I_w	Γ_t (Γ_o)	16	1) ½ for $\{0\,k\,l\}$ if $(k+l)$ is odd ½ for $\{h\,h\,l\}$ if l is odd
			(Γ_o')	32	2) Same as S_4^1 2); also ½ for all $\{0\,k\,l\}$ ½ for $\{h\,h\,l\}$ if $(h+l)$ is odd
129	D_{4h}^{7}	D_4^2, I_g	Γ_t (Γ_o) (Γ_o')	16 32	1) ½ for $\{h\,k\,0\}$ if $(h+k)$ is odd 2) Same as S_4^1 2); also ½ for all $\{h\,k\,0\}$
130	D_{4h}^{8}	D_4^2, I_m	Γ_t (Γ_o)	16	1) ½ for $\{h\,k\,0\}$ if $(h+k)$ is odd ½ for $\{0\,k\,l\}$ and $\{h\,h\,l\}$ if l is odd
			(Γ_o')	32	2) Same as S_4^1 2); also ½ for all $\{h\,k\,0\}$ and $\{0\,k\,l\}$ ½ for $\{h\,h\,l\}$ if l is odd
131	D_{4h}^{9}	D_4^5, I	Γ_t (Γ_o) (Γ_o')	16 32	1) ½ for $\{h\,h\,l\}$ if l is odd 2) Same as S_4^1 2); also ½ for all $\{0\,k\,l\}$
132	D_{4h}^{10}	D_4^5, I_w	Γ_t (Γ_o) (Γ_o')	16 32	1) ½ for $\{0\,k\,l\}$ if l is odd 2) Same as S_4^1 2); also ½ for $\{h\,h\,l\}$ if l is odd
133	D_{4h}^{11}	D_4^5, I_g	Γ_t (Γ_o)	16	1) ½ for $\{h\,k\,0\}$ if $(h+k)$ is odd ½ for $\{0\,k\,l\}$ if k is odd ½ for $\{h\,h\,l\}$ if l is odd
			(Γ_o')	32	2) Same as S_4^1 2); also ½ for all $\{h\,k\,0\}$ and $\{0\,k\,l\}$ ½ for $\{h\,h\,l\}$ if h is odd
134	D_{4h}^{12}	D_4^5, I_m	Γ_t (Γ_o)	16	1) ½ for $\{h\,k\,0\}$ if $(h+k)$ is odd ½ for $\{0\,k\,l\}$ if $(k+l)$ is odd
			(Γ_o')	32	2) Same as S_4^1 2); also ½ for all $\{h\,k\,0\}$ ½ for $\{h\,h\,l\}$ if $(h+l)$ is odd

	p	Possible molecular symmetry†	No.
	2	2-A ⊥ {110} or {001}; P ∥ {001}	128
	4	4-A ⊥ {001}; three intersecting 2-A's ⊥ {110} and {001}; 2-A ⊥ P ∥ {001}	
	8	4-A ⊥ P ∥ {001}	
	2	2-A ⊥ {110}; P ∥ {100} or {110}	129
	4	Two P's ∥ {100} intersecting in 2-A 2-A ⊥ P ∥ {110}	
	8	Four P's ∥ {100} and {110} intersecting in 4-A; full D_{2d} symmetry (P ∥ {100})	
	2	2-A ⊥ {001} or {110}; C	130
	4	4-A ⊥ {001}; three intersecting 2-A's ⊥ {001} and {110}; 4a-A ⊥ {001}	
	2	2-A ⊥ {110}; P ∥ {100} or {001}	131
	4	Two P's ∥ {100} intersecting in 2-A Two P's ∥ {001} and {100} intersecting in 2-A	
	8	Three P's ∥ {100} and {001} intersecting in three 2-A's; full D_{2d} symmetry (P ∥ {100})	
	2	2-A ⊥ {100} or {001} P ∥ {110} or {001}	132
	4	Two P's ∥ {110} intersecting in 2-A Two P's ∥ {001} and {110} intersecting in 2-A 2-A ⊥ P ∥ {001} Three intersecting 2-A's ⊥ {100} and {001}	
	8	Three P's ∥ {110} and {001} Full D_{2d} symmetry (P ∥ {110})	
	2	2-A ⊥ {100}, {001}, or {110}; C	133
	4	Three intersecting 2-A's ⊥ {100} and {001} Three intersecting 2-A's ⊥ {110} and {001} 4a-A ⊥ {001}	
	2	2-A ⊥ {100}, {001} or {110}; P ∥ {110}	134
	4	Three intersecting 2-A's ⊥ {100} and {001} Three intersecting 2-A's ⊥ {110} and {001} Two P's ∥ {110} intersecting in 2-A; 2-A ⊥ P ∥ {110}	
	8	Full D_{2d} symmetry (P ∥ {110})	

† This column of the table applies only to case 1. Make the substitution {110} ⇄ {100} when applying this column to case 2.

XV. (*Continued*)

No.	S.G.	Deriv.	S.L.	n	s
135	D_{4h}^{13}	D_4^6, I	Γ_t (Γ_o) (Γ_o')	16 32	1) ½ for $\{0\,k\,l\}$ if k is odd ½ for $\{h\,h\,l\}$ if l is odd 2) Same as S_4^1 2); also ½ for all $\{0\,k\,l\}$ ½ for $\{h\,h\,l\}$ if h is odd
136	D_{4h}^{14}	D_4^6, I_w	Γ_t (Γ_o) (Γ_o')	16 32	1) ½ for $\{0\,k\,l\}$ if $(k+l)$ is odd 2) Same as S_4^1 2); also ½ for $\{h\,h\,l\}$ if $(h+l)$ is odd
137	D_{4h}^{15}	D_4^6, I_g	Γ_t (Γ_o) (Γ_o')	16 32	1) ½ for $\{h\,k\,0\}$ if $(h+k)$ is odd ½ for $\{h\,h\,l\}$ if l is odd 2) Same as S_4^1 2); also ½ for all $\{h\,k\,0\}$ and $\{0\,k\,l\}$
138	D_{4h}^{16}	D_4^6, I_m	Γ_t (Γ_o) (Γ_o')	16 32	1) ½ for $\{h\,k\,0\}$ if $(h+k)$ is odd ½ for $\{0\,k\,l\}$ if l is odd 2) Same as S_4^1 2); also ½ for all $\{h\,k\,0\}$ ½ for $\{h\,h\,l\}$ if l is odd
139	D_{4h}^{17}	D_4^9, I	Γ_t' (Γ_o'') (Γ_o''')	64 32	1) Same as S_4^2 1) 2) Same as S_4^2 2)
140	D_{4h}^{18}	D_4^9, I_w	Γ_t' (Γ_o'') (Γ_o''')	64 32	1) Same as S_4^2 1); also ½ for all $\{h\,h\,l\}$ 2) Same as S_4^2 2); also ½ for all $\{0\,k\,l\}$

	p	Possible molecular symmetry†	No.
	2	2-A ⊥ {001} or {110}; P ∥ {001}	135
	4	Three intersecting 2-A's ⊥ {110} and {001}	
		2-A ⊥ P ∥ {001}	
		4a-A ⊥ {001}	
	2	2-A ⊥ {001}; P ∥ {110} or {001}	136
	4	Two P's ∥ {110} intersecting in 2-A	
		Two P's ∥ {001} and {110} intersecting in 2-A	
		2-A ⊥ P ∥ {001}	
		4a-A ⊥ {001}	
	8	Three P's ∥ {110} and {001} intersecting in three 2-A's	
	2	2-A ⊥ {110}; P ∥ {100}; C	137
	4	Two P's ∥ {100} intersecting in 2-A	
	8	Full D_{2d} symmetry (P ∥ {100})	
	2	2-A ⊥ {001} or {110}; P ∥ {110}	138
	4	Three intersecting 2-A's ⊥ {110} and {001}	
		Two P's ∥ {110} intersecting in 2-A	
		2-A ⊥ P ∥ {110}; 4a-A ⊥ {001}	
	2	P ∥ {100}, {110} or {001}	139
	4	Two P's ∥ {110} intersecting in 2-A	
		Two P's ∥ {001} and {100} intersecting in 2-A	
		Two P's ∥ {001} and {110} intersecting in 2-A	
	8	Three P's ∥ {110} and {001} intersecting in three 2-A's	
		Four P's ∥ {100} and {110} intersecting in 4-A	
		Full D_{2d} symmetry (P ∥ {110})	
	16	Four P's ∥ {100} and {110} intersecting in 4-A	
		P ∥ {001}	
	2	2-A ⊥ {100} or {110}; P ∥ {100} or {001}	140
	4	4-A ⊥ {001}	
		Two P's ∥ {100} intersecting in 2-A	
		Two P's ∥ {001} and {100} intersecting in 2-A	
		2-A ⊥ P ∥ {100}	
	8	Four 2-A's ⊥ {100} and {110} intersecting in 4-A ⊥ {001}	
		4-A ⊥ P ∥ {001}	
		Three P's ∥ {100} and {001} intersecting in three 2-A's	
		Full D_{2d} symmetry (P ∥ {100})	

† This column of the table applies only to case 1. Make the substitution {110} ⇄ {100} when applying this column to case 2.

XV. (*Concluded*)

No.	S.G.	Deriv.	S.L.	n	s
141	D_{4h}^{19}	D_4^{10}, I_g	Γ_i' (Γ_o'')	64	1) Same as S_4^2 1); also ¼ for $\{h\,k\,0\}$ if $(h+k)$ is odd ½ for $\{h\,k\,0\}$ if $(h+k)$ is even ¼ for $\{0\,k\,l\}$ if $(k+l)$ is odd ½ for $\{0\,k\,l\}$ if $(k+l)$ is even
			(Γ_o''')	32	2) Same as S_4^2 1); also ½ for all $\{h\,k\,0\}$ ¼ for $\{h\,h\,l\}$ if l is odd ½ for $\{h\,h\,l\}$ if $l = 2x$ where x is even or zero 1 for $\{h\,h\,l\}$ if $l = 2x$ where x is odd
142	D_{4h}^{20}	D_4^{10}, I_m	Γ_i' (Γ_o'')	64	1) Same as S_4^2 1); also ¼ for $\{h\,k\,0\}$ if $(h+k)$ is odd ½ for $\{h\,k\,0\}$ if $(h+k)$ is even ¼ for $\{0\,k\,l\}$ if $(k+l)$ is odd ½ for $\{0\,k\,l\}$ if $(k+l)$ is even ½ for all $\{h\,h\,l\}$
			(Γ_o''')	32	2) Same as S_4^2 2); also ½ for all $\{h\,k\,0\}$ and $\{0\,k\,l\}$ ¼ for $\{h\,h\,l\}$ if l is odd ½ for $\{h\,h\,l\}$ if $l = 2x$ where x is even or zero 1 for $\{h\,h\,l\}$ if $l = 2x$ where x is odd

E. *Cubic System.*

XVI. Cubic tetartohedry; Tesseral polar

No.	S.G.	Deriv.	S.L.	n	s
143	T^1	V^1, A_3	Γ_c	12	Always 1
144	T^2	V^7, A_3	Γ_c'	48	½ for $\{h\,k\,l\}$ if $(h+k)$ or $(k+l)$ or $(h+l)$ is odd
145	T^3	V^8, A_3	Γ_c''	24	½ for $\{h\,k\,l\}$ if $(h+k+l)$ is odd
146	T^4	V^4, A_3	Γ_c	12	½ for $\{1\,0\,0\}$
147	T^5	V^9, A_3	Γ_c''	24	Same as T^3

	p	Possible molecular symmetry†	No.
	2	2-A ⊥ {100} or {110}; P ∥ {110}	141
	4	2-A ⊥ P ∥ {110}	
		Two P's ∥ {110} intersecting in 2-A	
	8	Full D_{2d} symmetry (P ∥ {110})	
	2	2-A ⊥ {100}, {001} or {110}; C	142
	4	Three intersecting 2-A's ⊥ {100} and {001}	
		4a-A ⊥ {001}	

† This column of the table applies only to case 1. Make the substitution {110} ⇄ {100} when applying this column to case 2.

	p	Possible molecular symmetry	No.
	2	2-A ⊥ {100}	143
	3	3-A ⊥ {111}	
	12	Three 2-A's ⊥ {100} intersecting in 3-A ⊥ {111} (*i.e.*, full symmetry of class T)	
	—	Same as T^1	144
	—	Same as T^1	145
	3	3-A ⊥ {111}	146
	2	2-A ⊥ {100}	147
	3	3-A ⊥ {111}	

XVII. Cubic enantiomorphic hemihedry; Tesseral holoaxial

No.	S.G.	Deriv.	S.L.	n	s
148	O^1	T^1, U	Γ_c	24	Always 1
149	O^2	T^1, U_m	Γ_c	24	½ for {1 0 0}
150	O^3	T^2, U	Γ_c'	96	Same as T^2
151	O^4	T^2, U_m	Γ_c'	96	Same as T^2; also ¼ for {1 0 0}
152	O^5	T^3, U	Γ_c''	48	Same as T^3
153	O^6	T^4, U_1	Γ_c	24	¼ for {1 0 0}
154	O^7	T^4, U_2	Same as O^6 but in opposite rotatory sense		
155	O^8	T^5, U	Γ_c''	48	Same as T^3; also ¼ for {1 0 0}

XVIII. Cubic paramorphic hemihedry; Tesseral central

No.	S.G.	Deriv.	S.L.	n	s
156	T_h^1	T^1, I	Γ_c	24	Always 1
157	T_h^2	T^1, I_m	Γ_c	24	½ for $\{hk0\}$ if $(h + k)$ is odd
158	T_h^3	T^2, I	Γ_c'	96	Same as T^2

	p	Possible molecular symmetry	No.
	2	2-A ⊥ {110}	148
	3	3-A ⊥ {111}	
	4	4-A ⊥ {100}	
	24	Six 2-A's ⊥ {110} plus three 4-A's ⊥ {100} all intersecting in a point through which pass four 3-A's ⊥ {111} (*i.e.*, full symmetry of class O)	
	2	2-A ⊥ {100} or {110}	149
	3	3-A ⊥ {111}	
	12	Full symmetry of class T	
	—	Same as O^1	150
	—	Same as O^2	151
	—	Same as O^1	152
	2	2-A ⊥ {110}	153
	3	2-A ⊥ {111}	
therefore identical data			154
	2	2-A ⊥ {100} or {110}	155
	3	3-A ⊥ {111}	

	p	Possible molecular symmetry	No.
	2	P ∥ {100}	156
	3	3-A ⊥ {111}	
	4	Two P's ∥ {100} intersecting in 2-A	
	24	Three mutually ⊥ P's ∥ {100} with four 3-A's ⊥ {111} passing through point of intersection (*i.e.*, full symmetry of class T_h)	
	2	2-A ⊥ {100}	157
	3	3-A ⊥ {111}	
	6	3-A ⊥ {111}; C	
	12	Full symmetry of class T	
	2	2-A ⊥ {100}; P ∥ {100}	158
	3	3-A ⊥ {111}	
	4	Two P's ∥ {100} intersecting in 2-A	
	24	Full symmetry of class T_h	

XVIII. (*Concluded*)

No.	S.G.	Deriv.	S.L.	n	s
159	T_h^4	T^2, I_m	Γ_c'	96	Same as T^2; also ¼ for $\{h\,k\,0\}$ if $(h+k)$ is odd ½ for $\{h\,k\,0\}$ if $(h+k)$ is even
160	T_h^5	T^3, I	Γ_c''	48	Same as T^3
161	T_h^6	T^4, I	Γ_c	24	½ for $\{h\,k\,0\}$ if h is odd
162	T_h^7	T^5, I	Γ_c''	48	Same as T^3; also ½ for all $\{h\,k\,0\}$

XIX. Cubic hemimorphic hemihedry; Ditesseral polar

No.	S.G.	Deriv.	S.L.	n	s
163	T_d^1	T^1, S_d	Γ_c	24	Always 1
164	T_d^2	T^2, S_d	Γ_c'	96	Same as T^2
165	T_d^3	T^3, S_d	Γ_c''	48	Same as T^3
166	T_d^4	T^1, $S_d(\tau)$	Γ_c	24	½ for $\{h\,h\,l\}$ if l is odd
167	T_d^5	T^2, $S_d(\tau)$	Γ_c'	96	Same as T^2; also ½ for all $\{h\,h\,l\}$
168	T_d^6	T^3, $S_d(\tau)$	Γ_c''	48	Same as T^3; also ¼ for $\{h\,h\,l\}$ if l is odd ½ for $\{h\,h\,l\}$ if $l = 2x$ where x is even or zero 1 for $\{h\,h\,l\}$ if $l = 2x$ where x is odd

	p	Possible molecular symmetry	No.
	—	Same as T_h^2	159
	2	$P \parallel \{100\}$	160
	3	3-$A \perp \{111\}$	
	4	Two P's $\parallel \{100\}$ intersecting in 2-A	
	6	3-$A \perp \{111\}$; C	
	24	Full symmetry of class T_h	
	3	3-$A \perp \{111\}$	161
	6	3-$A \perp \{111\}$; C	
	2	2-$A \perp \{100\}$	162
	3	3-$A \perp \{111\}$	
	6	3-$A \perp \{111\}$; C	

	p	Possible molecular symmetry	No.
	2	$P \parallel \{110\}$	163
	4	Two P's $\parallel \{110\}$ intersecting in 2-A	
	6	Three P's $\parallel \{110\}$ intersecting in 3-$A \perp \{111\}$	
	24	Six P's $\parallel \{110\}$ intersecting in four 3-A's $\perp \{111\}$ plus three 2-A's $\perp \{100\}$, all intersecting in the same point (*i.e.*, full symmetry of class T_d)	
	—	Same as T_d^1	164
	—	Same as T_d^1	165
	2	2-$A \perp \{100\}$	166
	3	3-$A \perp \{111\}$	
	12	Full symmetry of class T	
	—	Same as T_d^4	167
	2	2-$A \perp \{100\}$	168
	3	3-$A \perp \{111\}$	

XX. Cubic holohedry; Ditesseral central

No.	S.G.	Deriv.	S.L.	n	s
169	O_h^1	O^1, I	Γ_c	48	Always 1
170	O_h^2	O^1, I_m	Γ_c	48	½ for $\{h\,k\,0\}$ if $(h+k)$ is odd ½ for $\{h\,h\,l\}$ if l is odd
171	O_h^3	O^2, I	Γ_c	48	½ for $\{h\,h\,l\}$ if l is odd
172	O_h^4	O^2, I_m	Γ_c	48	½ for $\{h\,k\,0\}$ if $(h+k)$ is odd
173	O_h^5	O^3, I	Γ_c'	192	Same as T^2
174	O_h^6	O^3, I'	Γ_c'	192	Same as T^2; also ½ for all $\{h\,h\,l\}$
175	O_h^7	O^4, I_m	Γ_c'	192	Same as T^2; also ¼ for $\{h\,k\,0\}$ if $(h+k)$ is odd ½ for $\{h\,k\,0\}$ if $(h+k)$ is even
176	O_h^8	O^4, I_m'	Γ_c'	192	Same as T^2; also ½ for all $\{h\,h\,l\}$ ¼ for $\{h\,k\,0\}$ if $(h+k)$ is odd ½ for $\{h\,k\,0\}$ if $(h+k)$ is even
177	O_h^9	O^5, I	Γ_c''	96	Same as T^3

	p	Possible molecular symmetry	No.
	2	$P \parallel \{100\}$ or $\{110\}$	169
	4	Two P's $\parallel \{100\}$ and $\{110\}$ intersecting in 2-$A \perp \{110\}$	
	6	Three P's $\parallel \{110\}$ intersecting in 3-$A \perp \{111\}$	
	8	Four P's $\parallel \{100\}$ and $\{110\}$ intersecting in 4-$A \perp \{100\}$	
	48	Full symmetry of class O, plus C at point of intersection of axes (*i.e.*, full symmetry of class O_h)	
	2	2-$A \perp \{110\}$	170
	3	3-$A \perp \{111\}$	
	4	4-$A \perp \{100\}$	
	6	3-$A \perp \{111\}$; C	
	24	Full symmetry of class O	
	2	2-$A \perp \{110\}$; $P \parallel \{100\}$	171
	3	3-$A \perp \{111\}$	
	4	Two P's $\parallel \{100\}$ intersecting in 2-A	
	24	Full symmetry of class T_h	
	2	$P \parallel \{110\}$	172
	4	Two P's $\parallel \{110\}$ intersecting in 2-A	
	6	Three P's $\parallel \{110\}$ intersecting in 3-$A \perp \{111\}$	
	12	Three P's $\parallel \{110\}$ intersecting in 3-$A \perp \{111\}$; C	
	24	Full symmetry of class T_d	
	—	Same as O_h^1	173
	2	2-$A \perp \{110\}$; $P \parallel \{100\}$	174
	3	3-$A \perp \{111\}$	
	4	4-$A \perp \{100\}$	
		Two P's $\parallel \{100\}$ intersecting in 2-A	
	24	Full symmetry of class O; full symmetry of class T_h	
	—	Same as O_h^4	175
	2	2-$A \perp \{100\}$ or $\{110\}$	176
	3	3-$A \perp \{111\}$	
	6	3-$A \perp \{111\}$; C	
	12	Full symmetry of class T	
	2	$P \parallel \{100\}$ or $\{110\}$	177
	4	Two P's $\parallel \{100\}$ and $\{110\}$ intersecting in 2-$A \perp \{110\}$	
	6	Three P's $\parallel \{110\}$ intersecting in 3-$A \perp \{111\}$	
	8	Four P's $\parallel \{100\}$ and $\{110\}$ intersecting in 4-$A \perp \{100\}$	
	12	Three P's $\parallel \{110\}$ intersecting in 3-$A \perp \{111\}$; C	
	48	Full symmetry of class O_h	

XX. (*Concluded*)

No.	S.G.	Deriv.	S.L.	n	s
178	O_h^{10}	O^8, I	Γ_o''	96	Same as T^3; also ½ for all $\{hk0\}$ ¼ for $\{hhl\}$ if l is odd ½ for $\{hhl\}$ if $l = 2x$ where x is even or zero 1 for $\{hhl\}$ if $l = 2x$ where x is odd

F. *Hexagonal System.*

(*a*) Rhombohedral division.

XXI. Rhombohedral tetartohedry; Trigonal polar

No.	S.G.	Deriv.	S.L.	n	s
179	C_3^1	$A(2\pi/3)$, Γ_h	Γ_h	3	Always 1
180	C_3^2	$A(2\pi/3, 2\tau_z/3)$, Γ_h	Γ_h	3	⅓ for $\{0001\}$
181	C_3^3	$A(2\pi/3, 4\tau_z/3)$, Γ_h	Same as C_3^2 but in opposite rotatory sense,		
182	C_3^4	$A(2\pi/3)$, Γ_{rh}	Γ_{rh}	3	Always 1

XXII. Rhombohedral enantiomorphic hemihedry; Trigonal holoaxial

No.	S.G.	Deriv.	S.L.	n	s
183	D_3^1	C_3^1, U_a	Γ_h	6	Always 1
184	D_3^2	C_3^1, U_a	Γ_h	6	Always 1
185	D_3^3	C_3^2, U_a	Γ_h	6	⅓ for $\{0001\}$
186	D_3^4	C_3^2, U_a	Γ_h	6	⅓ for $\{0001\}$
187	D_3^5	C_3^3, U_a	Same as D_3^3 but in opposite rotatory sense,		
188	D_3^6	C_3^3, U_a	Same as D_3^4 but in opposite rotatory sense,		
189	D_3^7	C_3^4, U_a	Γ_{rh}	6	Always 1

	p	Possible molecular symmetry	No.
	2 3 6	2-A ⊥ {100} or {110} 3-A ⊥ {111} 3-A ⊥ {111}; C	178

	p	Possible molecular symmetry	No.
	3	3-A ⊥ {0001}	179
	—	None	180
therefore identical data			181
	3	3-A ⊥ {111}	182

	p	Possible molecular symmetry	No.
	2 3 6	2-A ⊥ {10$\bar{1}$0} 3-A ⊥ {0001} Three 2-A's ⊥ {10$\bar{1}$0} intersecting in 3-A ⊥ {0001}	183
	2 3 6	2-A ⊥ {11$\bar{2}$0} 3-A ⊥ {0001} Three 2-A's ⊥ {11$\bar{2}$0} intersecting in 3-A ⊥ {0001}	184
	2	2-A ⊥ {10$\bar{1}$0}	185
	2	2-A ⊥ {11$\bar{2}$0}	186
therefore identical data			187
therefore identical data			188
	2 3 6	2-A ⊥ {1$\bar{1}$0} 3-A ⊥ {111} Three 2-A's ⊥ {1$\bar{1}$0} intersecting in 3-A ⊥ {111}	189

XXIII. Rhombohedral hemimorphic hemihedry; Ditrigonal polar

No.	S.G.	Deriv.	S.L.	n	s
190	C_{3v}^{1}	C_3^1, S_s	Γ_h	6	Always 1
191	C_{3v}^{2}	C_3^1, S_a	Γ_h	6	Always 1
192	C_{3v}^{3}	C_3^1, $S_s(\tau_z)$	Γ_h	6	½ for $\{m0\bar{m}l\}$ if l is odd
193	C_{3v}^{4}	C_3^1, $S_a(\tau_z)$	Γ_h	6	½ for $\{mm\overline{2m}l\}$ if l is odd
194	C_{3v}^{5}	C_3^4, S_a	Γ_{rh}	6	Always 1
195	C_{3v}^{6}	C_3^4, $S_a(\tau_z)$	Γ_{rh}	6	½ for $\{hhl\}$ if l is odd

XXIV. Hexagonal tetartohedry of the second sort; Hexagonal alternating

No.	S.G.	Deriv.	S.L.	n	s
196	C_{3i}^{1}	C_3^1, I	Γ_h	6	Always 1
197	C_{3i}^{2}	C_3^4, I	Γ_{rh}	6	Always 1

XXV. Rhombohedral holohedry; Dihexagonal alternating

No.	S.G	Deriv.	S.L.	n	s
198	D_{3d}^{1}	D_3^1, I	Γ_h	12	Always 1
199	D_{3d}^{2}	D_3^1, I'	Γ_h	12	½ for $\{mm\overline{2m}l\}$ if l is odd

	p	Possible molecular symmetry	No.
	2	$P \parallel \{11\bar{2}0\}$	190
	6	Three P's $\parallel \{11\bar{2}0\}$ intersecting in 3-A	
	2	$P \parallel \{10\bar{1}0\}$	191
	3	3-$A \perp \{0001\}$	
	6	Three P's $\parallel \{10\bar{1}0\}$ intersecting in 3-A	
	3	3-$A \perp \{0001\}$	192
	3	3-$A \perp \{0001\}$	193
	2	$P \parallel \{1\bar{1}0\}$	194
	6	Three P's $\parallel \{1\bar{1}0\}$ intersecting in 3-A	
	3	3-$A \perp \{111\}$	195

	p	Possible molecular symmetry	No.
	2	C	196
	3	3-$A \perp \{0001\}$	
	6	3-$A \perp \{0001\}$; C	
	2	C	197
	3	3-$A \perp \{111\}$	
	6	3-$A \perp \{111\}$; C	

	p	Possible molecular symmetry	No.
	2	2-$A \perp \{10\bar{1}0\}$; $P \parallel \{10\bar{1}0\}$	198
	4	2-$A \perp P \parallel \{10\bar{1}0\}$	
	6	Three P's $\parallel \{10\bar{1}0\}$ intersecting in 3-A	
		Three 2-A's $\perp \{10\bar{1}0\}$ intersecting in 3-$A \perp \{0001\}$	
	8	3-$A \perp \{0001\}$	
	12	Three P's $\parallel \{10\bar{1}0\}$ plus three 2-A's $\perp \{10\bar{1}0\}$ all intersecting in 3-$A \perp \{0001\}$	
	2	2-$A \perp \{10\bar{1}0\}$; C	199
	3	3-$A \perp \{0001\}$	
	6	Three 2-A's $\perp \{10\bar{1}0\}$ intersecting in 3-$A \perp \{0001\}$; 3-$A \perp \{0001\}$; C	

XXV. (*Concluded*)

No	S.G.	Deriv.	S.L.	n	s
200	D^3_{3d}	D^2_3, I	Γ_h	12	Always 1
201	D^4_{3d}	D^2_3, I'	Γ_h	12	½ for $\{m0\bar{m}l\}$ if l is odd
202	D^5_{3d}	D^7_3, I	Γ_{rh}	12	Always 1
203	D^6_{3d}	D^7_3, I'	Γ_{rh}	12	½ for $\{hhl\}$ if l is odd

(*b*) Hexagonal division.

XXVI. Trigonal paramorphic hemihedry; Trigonal equatorial

No.	S.G.	Deriv.	S.L.	n	s
204	C^1_{3h}	C^1_3, S_h	Γ_h	6	Always 1

XXVII. Trigonal holohedry; Ditrigonal equatorial

No.	S.G.	Deriv.	S.L.	n	s
205	D^1_{3h}	D^1_3, S_h	Γ_h	12	Always 1
206	D^2_{3h}	D^1_3, S_m	Γ_h	12	½ for $\{m0\bar{m}l\}$ if l is odd

	p	Possible molecular symmetry	No.
	2	2-$A \perp \{11\bar{2}0\}$; $P \parallel \{11\bar{2}0\}$	200
	4	2-$A \perp P \parallel \{11\bar{2}0\}$	
	6	Three P's $\parallel \{11\bar{2}0\}$ intersecting in 3-A	
	12	Three P's $\parallel \{11\bar{2}0\}$ plus three 2-A's $\perp \{11\bar{2}0\}$ all intersecting in 3-$A \perp \{0001\}$	
	2	2-$A \perp \{11\bar{2}0\}$; C	201
	3	3-$A \perp \{0001\}$	
	6	Three 2-A's $\perp \{11\bar{2}0\}$ intersecting in 3-$A \perp \{0001\}$ 3-$A \perp \{0001\}$; C	
	2	2-$A \perp \{1\bar{1}0\}$; $P \parallel \{1\bar{1}0\}$	202
	4	2-$A \perp P \parallel \{110\}$	
	6	Three P's $\parallel \{110\}$ intersecting in 3-A	
	12	Three P's $\parallel \{1\bar{1}0\}$ plus three 2-A's $\perp \{1\bar{1}0\}$ all intersecting in 3-$A \perp \{111\}$	
	2	2-$A \perp \{1\bar{1}0\}$; C	203
	3	3-$A \perp \{111\}$	
	6	Three 2-A's $\perp \{1\bar{1}0\}$ intersecting in 3-$A \perp \{111\}$ 3-$A \perp \{111\}$; C	

	p	Possible molecular symmetry	No.
	2	$P \parallel \{0001\}$	204
	3	3-$A \perp \{0001\}$	
	6	3-$A \perp P \parallel \{0001\}$	

	p	Possible molecular symmetry	No.
	2	$P \parallel \{0001\}$ or $\{11\bar{2}0\}$	205
	4	Two P's $\parallel \{0001\}$ and $\{11\bar{2}0\}$ intersecting in 2-A	
	6	Three P's $\parallel \{11\bar{2}0\}$ intersecting in 3-A	
	12	Three P's $\parallel \{11\bar{2}0\}$ intersecting in 3-$A \perp P \parallel \{0001\}$	
	2	2-$A \perp \{10\bar{1}0\}$; $P \parallel \{0001\}$	206
	3	3-$A \perp \{0001\}$	
	6	3-$A \perp P \parallel \{0001\}$ Three 2-A's $\perp \{10\bar{1}0\}$ intersecting in 3-$A \perp \{0001\}$	

XXVII. (*Concluded*)

No.	S.G.	Deriv.	S.L.	n	s
207	D_{3h}^{3}	D_3^2, S_h	Γ_h	12	Always 1
208	D_{3h}^{4}	D_3^2, S_m	Γ_h	12	$\frac{1}{2}$ for $\{mm\overline{2m}l\}$ if l is odd

XXVIII. Hexagonal tetartohedry; Hexagonal polar

No.	S.G.	Deriv.	S.L.	n	s
209	C_6^1	$A(\pi/3)$, Γ_h	Γ_h	6	Always 1
210	C_6^2	$A(\pi/3, \tau_z/3)$, Γ_h	Γ_h	6	$\frac{1}{6}$ for {0001}
211	C_6^3	$A(\pi/3, 5\tau_z/3)$, Γ_h	Same as C_6^2 but in opposite rotatory sense,		
212	C_6^4	$A(\pi/3, 2\tau_z/3)$, Γ_h	Γ_h	6	$\frac{1}{3}$ for {0001}
213	C_6^5	$A(\pi/3, 4\tau_z/3)$, Γ_h	Same as C_6^4 but in opposite rotatory sense,		
214	C_6^6	$A(\pi/3, \tau_z)$, Γ_h	Γ_h	6	$\frac{1}{2}$ for {0001}

XXIX. Hexagonal enantiomorphic hemihedry; Hexagonal holoaxial

No.	S.G.	Deriv.	S.L.	n	s
215	D_6^1	C_6^1, U_a	Γ_h	12	Always 1
216	D_6^2	C_6^2, U_a	Γ_h	12	$\frac{1}{6}$ for {0001}
217	D_6^3	C_6^3, U_a	Same as D_6^2 but in opposite rotatory sense,		

	p	Possible molecular symmetry	No.
	2	$P \parallel \{0001\}$ or $\{10\bar{1}0\}$	207
	3	3-$A \perp \{0001\}$	
	4	Two P's $\parallel \{0001\}$ and $\{10\bar{1}0\}$ intersecting in 2-A	
	6	3-$A \perp P \parallel \{0001\}$	
		Three P's $\parallel \{10\bar{1}0\}$ intersecting in 3-A	
	12	Three P's $\parallel \{10\bar{1}0\}$ intersecting in 3-$A \perp P \parallel \{0001\}$	
	2	2-$A \perp \{11\bar{2}0\}$; $P \parallel \{0001\}$	208
	3	3-$A \perp \{0001\}$	
	6	3-$A \perp P \parallel \{0001\}$	
		Three 2-A's $\perp \{11\bar{2}0\}$ intersecting in 3-$A \perp \{0001\}$	

	p	Possible molecular symmetry	No.
	2	2-$A \perp \{0001\}$	209
	3	3-$A \perp \{0001\}$	
	6	6-$A \perp \{0001\}$	
	—	None	210
therefore identical data			211
	2	2-$A \perp \{0001\}$	212
therefore identical data			213
	3	3-$A \perp \{0001\}$	214

	p	Possible molecular symmetry	No.
	2	2-$A \perp \{0001\}$, $\{10\bar{1}0\}$, or $\{11\bar{2}0\}$	215
	3	3-$A \perp \{0001\}$	
	4	Three mutually $\perp$ 2-A's	
	6	6-$A \perp \{0001\}$; three 2-A's $\perp \{10\bar{1}0\}$ intersecting in 3-$A \perp \{0001\}$	
	12	Six 2-A's $\perp \{10\bar{1}0\}$ and $\{11\bar{2}0\}$ intersecting in 6-$A \perp \{0001\}$	
	2	2-$A \perp \{10\bar{1}0\}$ or $\{11\bar{2}0\}$	216
therefore identical data			217

XXIX. (*Concluded*)

No.	S.G.	Deriv.	S.L.	n	s
218	D_6^4	C_6^4, U_a	Γ_h	12	⅓ for {0001}
219	D_6^5	C_6^5, U_a	Same as D_6^4 but in opposite rotatory sense,		
220	D_6^6	C_6^6, U_a	Γ_h	12	½ for {0001}

XXX. Hexagonal paramorphic hemihedry; Hexagonal equatorial

No.	S.G.	Deriv.	S.L.	n	s
221	C_{6h}^1	C_6^1, S_h	Γ_h	12	Always 1
222	C_{6h}^2	C_6^6, S_h	Γ_h	12	½ for {0001}

XXXI. Hexagonal hemimorphic hemihedry; Dihexagonal polar

No.	S.G.	Deriv.	S.L.	n	s
223	C_{6v}^1	C_6^1, S_a	Γ_h	12	Always 1
224	C_{6v}^2	C_6^1, $S_a(\tau_z)$	Γ_h	12	½ for $\{m0\bar{m}l\}$ if l is odd ½ for $\{mm\bar{2}ml\}$ if l is odd
225	C_{6v}^3	C_6^6, S_a	Γ_h	12	½ for $\{m0\bar{m}l\}$ if l is odd
226	C_{6v}^4	C_6^6, $S_a(\tau_z)$	Γ_h	12	½ for $\{mm\bar{2}ml\}$ if l is odd

	p	Possible molecular symmetry	No.
	2	2-A $\perp$ {0001}, {10$\bar{1}$0}, or {11$\bar{2}$0}	218
	4	Three mutually $\perp$ 2-A's	
therefore identical data			219
	2	2-A $\perp$ {10$\bar{1}$0} or {11$\bar{2}$0}	220
	3	3-A $\perp$ {0001}	
	6	Three 2-A's $\perp$ {10$\bar{1}$0} intersecting in 3-A $\perp$ {0001}	
		Three 2-A's $\perp$ {11$\bar{2}$0} intersecting in 3-A $\perp$ {0001}	

	p	Possible molecular symmetry	No.
	2	2-A $\perp$ {0001}; P $\parallel$ {0001}	221
	3	3-A $\perp$ {0001}	
	4	2-A $\perp$ P $\parallel$ {0001}	
	6	6-A $\perp$ {0001}; 3-A $\perp$ P $\parallel$ {0001}	
	12	6-A $\perp$ P $\parallel$ {0001}	
	2	P $\parallel$ {0001}; C	222
	3	3-A $\perp$ {0001}	
	6	3-A $\perp$ P $\parallel$ {0001}; 3-A $\perp$ {0001}; C	

	p	Possible molecular symmetry	No.
	2	P $\parallel$ {10$\bar{1}$0} or {11$\bar{2}$0}	223
	4	Two P's $\parallel$ {10$\bar{1}$0} and {11$\bar{2}$0} intersecting in 2-A	
	6	Three P's $\parallel$ {11$\bar{2}$0} intersecting in 3-A	
	12	Six P's $\parallel$ {11$\bar{2}$0} and {10$\bar{1}$0} intersecting in 6-A	
	2	2-A $\perp$ {0001}	224
	3	3-A $\perp$ {0001}	
	6	6-A $\perp$ {0001}	
	2	P $\parallel$ {10$\bar{1}$0}	225
	3	3-A $\perp$ {0001}	
	6	Three P's $\parallel$ {10$\bar{1}$0} intersecting in 3-A	
	2	P $\parallel$ {11$\bar{2}$0}	226
	6	Three P's $\parallel$ {11$\bar{2}$0} intersecting in 3-A	

XXXII. Hexagonal holohedry; Dihexagonal equatorial

No.	S.G.	Deriv.	S.L.	n	s
227	D^1_{6h}	D^1_6, I	Γ_h	24	Always 1
228	D^2_{6h}	D^1_6, I'	Γ_h	24	½ for $\{m0\bar{m}l\}$ if l is odd ½ for $\{mm\bar{2m}l\}$ if l is odd
229	D^3_{6h}	D^6_6, I	Γ_h	24	½ for $\{m0\bar{m}l\}$ if l is odd
230	D^4_{6h}	D^6_6, I'	Γ_h	24	½ for $\{mm\bar{2m}l\}$ if l is odd

	p	Possible molecular symmetry	No.
	2	$P \parallel \{0001\}$, $\{10\bar{1}0\}$ or $\{11\bar{2}0\}$	227
	4	Two P's $\parallel \{0001\}$ and $\{10\bar{1}0\}$ intersecting in 2-A	
		Two P's $\parallel \{0001\}$ and $\{11\bar{2}0\}$ intersecting in 2-A	
		Two P's $\parallel \{10\bar{1}0\}$ and $\{11\bar{2}0\}$ intersecting in 2-A	
	6	Three P's $\parallel \{11\bar{2}0\}$ intersecting in 3-A	
	8	Three mutually $\perp$ P's $\parallel \{0001\}$, $\{10\bar{1}0\}$, and $\{11\bar{2}0\}$ intersecting in three 2-A's	
	12	Three P's $\parallel \{11\bar{2}0\}$ intersecting in 3-$A \perp P \parallel \{0001\}$	
		Six P's $\parallel \{10\bar{1}0\}$ and $\{11\bar{2}0\}$ intersecting in 6-A	
	24	Six P's $\parallel \{10\bar{1}0\}$ and $\{11\bar{2}0\}$ intersecting in 6-$A \perp P \parallel \{0001\}$	
	2	2-$A \perp \{0001\}$, $\{10\bar{1}0\}$ or $\{11\bar{2}0\}$; $P \parallel \{0001\}$	228
	3	3-$A \perp \{0001\}$	
	4	Three mutually $\perp$ 2-A's	
		2-$A \perp P \parallel \{0001\}$	
	6	6-$A \perp \{0001\}$; 3-$A \perp P \parallel \{0001\}$	
		Three 2-A's $\perp \{10\bar{1}0\}$ intersecting in 3-$A \perp \{0001\}$	
	12	6-$A \perp P \parallel \{0001\}$	
		Six 2-A's $\perp \{10\bar{1}0\}$ and $\{11\bar{2}0\}$ intersecting in 3-$A \perp \{0001\}$	
	2	2-$A \perp \{10\bar{1}0\}$; $P \parallel \{0001\}$ or $\{10\bar{1}0\}$	229
	3	3-$A \perp \{0001\}$	
	4	Two P's $\parallel \{0001\}$ and $\{10\bar{1}0\}$ intersecting in 2-A	
		2-$A \perp P \parallel \{10\bar{1}0\}$	
	6	3-$A \perp P \parallel \{0001\}$	
		Three P's $\parallel \{10\bar{1}0\}$ intersecting in 3-A	
	12	Three P's $\parallel \{10\bar{1}0\}$ intersecting in 3-$A \perp P \parallel \{0001\}$	
		Three P's $\parallel \{10\bar{1}0\}$ plus three 2-A's $\perp \{10\bar{1}0\}$ all intersecting in 3-$A \perp \{0001\}$	
	2	2-$A \perp \{11\bar{2}0\}$; $P \parallel \{0001\}$ or $\{11\bar{2}0\}$	230
	4	Two P's $\parallel \{0001\}$ and $\{11\bar{2}0\}$ intersecting in 2-A	
		2-$A \perp P \parallel \{11\bar{2}0\}$	
	6	Three P's $\parallel \{11\bar{2}0\}$ intersecting in 3-A	
	12	Three P's $\parallel \{11\bar{2}0\}$ intersecting in 3-$A \perp P \parallel \{0001\}$	
		Three P's $\parallel \{11\bar{2}0\}$ plus three 2-A's $\perp \{11\bar{2}0\}$ all intersecting in 3-$A \perp \{0001\}$	

TABLES XXXIII TO XXXIX

Tables XXXIII to XXXIX give a summary of the kinds of configurations of points which can be obtained from each of the space-groups and give the number of each kind which can be obtained. In these tables the numbers at the tops of the columns represent the number of possible equivalent positions, and the numbers in the body of each column give the number of possible configurations, followed in parentheses by the number of variable parameters permitted. For instance, 1(0) indicates a special case of only one possible configuration with no variable parameters; 2(1) indicates that we have our choice of either (or both) of two configurations each of which has one variable parameter.

These tables are identical with those found at the end of Wyckoff's "Analytical Expression of the Results of the Theory of Space-groups." The data given in these tables may be derived from Tables I to XXXII in this Appendix, using the method outlined at the end of Chap. VIII.

TABLE XXXIII.—TRICLINIC SYSTEM

S. G.	1	2
1. C_1^1	1(3)	....
2. C_i^1	8(0)	1(3)

TABLE XXXIV.—MONOCLINIC SYSTEM

S.G.	1	2	4	8
3.				
C_s^1	2(2)	1(3)	....	....
C_s^2	....	1(3)	....	....
C_s^3	....	1(2)	1(3)	....
C_s^4	....	....	1(3)	....
4.				
C_2^1	4(1)	1(3)	....	....
C_2^2	....	1(3)	....	....
C_2^3	....	2(1)	1(3)	....
5.				
C_{2h}^1	8(0)	4(1); 2(2)	1(3)	....
C_{2h}^2	....	4(0); 1(2)	1(3)	....
C_{2h}^3	....	4(0)	2(0) 2(1) 1(2)	1(3)
C_{2h}^4	....	4(0); 2(1)	1(3)	....
C_{2h}^5	....	4(0)	1(3)	....
C_{2h}^6	....	....	4(0); 1(1)	1(3)

TABLE XXXV.—ORTHORHOMBIC SYSTEM

S.G.	1	2	4	8	16	32
6.						
V^1	8(0)	12(1)	1(3)	.....	....	....
V^2	....	4(1)	1(3)	.....	.....	....
V^3	....	2(1)	1(3)	.....	..... .	....
V^4	....	.....	1(3)	.....	.....	....
V^5	....	.....	2(1)	1(3)	.....	....
V^6	....	4(0)	7(1)	1(3)	.....	....
V^7	....	.....	4(0)	6(1)	1(3)	....
V^8	....	4(0)	6(1)	1(3)	.....	....
V^9	...	....	3(1)	1(3)	.....	....
7.						
C^1_{2v}	4'1)	4(2)	1(3)	.....	.....	....
C^2_{2v}	..	2(2)	1(3)	.....	.....	....
C^3_{2v}	...	4(1)	1(3)	.....	.....	....
C^4_{2v}	...	2(1); 1(2)	1(3)	.....	.....	....
C^5_{2v}	....	.....	1(3)	.....	.....	....
C^6_{2v}	....	2(1)	1(3)	.....	.....	....
C^7_{2v}	....	1(2)	1(3)	.....	....	....
C^8_{2v}	....	2(1)	1(3)	.....	.....	....
C^9_{2v}	....	.....	1(3)	.....	.....	....
C^{10}_{2v}	....	2(1)	1(3)	.....	.....	....
C^{11}_{2v}	....	2(1)	1(1); 2(2)	1(3)	.....	....
C^{12}_{2v}	....	.....	1(2)	1(3)	.....	....
C^{13}_{2v}	....	.....	3(1)	1(3)	.....	. ..
C^{14}_{2v}	....	2(1)	3(2)	1(3)	.....	....
C^{15}_{2v}	....	.....	2(1); 1(2)	1(3)	.....	....
C^{16}_{2v}	....	.....	1(1); 1(2)	1(3)	.....	....
C^{17}_{2v}	....	.....	1(1)	1(3)	.....	....
C^{18}_{2v}	....	.....	1(1)	1(1); 2(2)	1(3)	....
C^{19}_{2v}	....	.....	.....	1(1)	1(3)	....
C^{20}_{2v}	. ..	2(1)	2(2)	1(3)	.....	....
C^{21}_{2v}	....	.....	2(1)	1(3)	.....	....
C^{22}_{2v}	....	.....	1(1); 1(2)	1(3)	.....	....
8.						
V^1_h	8(0)	12(1)	6(2)	1(3)	.....	....
V^2_h	....	4(0)	2(0); 6(1)	1(3)	.....	....
V^3_h	....	8(0)	8(1); 1(2)	1(3)	.....	....
V^4_h	...	4(0)	2(0); 6(1)	1(3)	.....	....
V^5_h	....	4(0); 2(1)	2(1); 3(2)	1(3)	.....	....
V^6_h	....	.....	2(0); 2(1)	1(3)	.....	....
V^7_h	....	4(0)	3(1); 1(2)	1(3)	.....	....
V^8_h	....	.....	2(0); 3(1)	1(3)	.....	....
V^9_h	....	4(0)	2(1); 2(2)	1(3)	.....	....
V^{10}_h	....	.....	2(0); 2(1)	1(3)	.....	....

TABLE XXXV.—(*Concluded*)

S.G.	1	2	4	8	16	32
8. (*Continued*)						
V_h^{11}	....	.....	2(0) 1(1) 1(2)	1(3)	.....	....
V_h^{12}	....	4(0)	2(1); 1(2)	1(3)	.....	....
V_h^{13}	....	2(1)	2(0); 2(2)	1(3)	.....	....
V_h^{14}	....	.....	2(0); 1(1)	1(3)	.....	....
V_h^{15}	....	.....	2(0)	1(3)	.....	....
V_h^{16}	....	.....	2(0); 1(2)	1(3)	.....	....
V_h^{17}	....	.....	2(0); 1(1)	1(0) 1(1) 2(2)	1(3)	....
V_h^{18}	....	.....	2(0)	1(0) 2(1) 1(2)	1(3)	....
V_h^{19}	....	4(0)	2(0); 6(1)	1(1); 4(2)	1(3)	....
V_h^{20}	....	.....	6(0)	5(1); 1(2)	1(3)	....
V_h^{21}	....	.....	6(0); 1(1)	5(1); 2(2)	1(3)	....
V_h^{22}	....	.....	2(0)	2(0); 4(1)	1(3)	....
V_h^{23}	....	.....	2(0)	4(0); 3(1)	3(1); 3(2)	1(3)
V_h^{24}	....	.....	.....	2(0)	2(0); 3(1)	1(3)
V_h^{25}	....	4(0)	6(1)	1(0); 3(2)	1(3)	....
V_h^{26}	...	.....	4(0)	1(0) 4(1) 1(2)	1(3)	....
V_h^{27}	....	.....	.....	2(0); 3(1)	1(3)	....
V_h^{28}	....	.....	4(0); 1(1)	2(1); 2(2)	1(3)	....

TABLE XXXVI.—TETRAGONAL SYSTEM

S.G.	1	2	4	8	16	32
9.						
C_4^1	2(1)	1(1)	1(3)	.....	.....	....
C_4^2	....	.....	1(3)	.....	.....	....
C_4^3	....	3(1)	1(3)	.....	.....	....
C_4^4	....	.....	1(3)	.....	.....	....
C_4^5	....	1(1)	1(1)	1(3)	.....	....
C_4^6	....	.....	1(1)	1(3)	.....	....
10.						
S_4^1	4(0)	3(1)	1(3)	.....	.....	....
S_4^2	....	4(0)	2(1)	1(3)	.....	....
11.						
D_4^1	4(0)	2(0); 2(1)	7(1)	1(3)	.....	....
D_4^2	....	2(0); 1(1)	3(1)	1(3)	.....	....

TABLE XXXVI.—(*Continued*)

S.G.	1	2	4	8	16	32
11. (*Continued*)						
D_4^3	....	.....	3(1)	1(3)	.....	....
D_4^4	....	.....	1(1)	1(3)	.....	....
D_4^5	....	6(0)	9(1)	1(3)	.....	....
D_4^6	....	2(0)	4(1)	1(3)	.....	....
D_4^7	....	.....	3(1)	1(3)	.....	....
D_4^8	....	.....	1(1)	1(3)	.....	....
D_4^9	....	2(0)	2(0); 1(1)	5(1)	1(3)	....
D_4^{10}	....	.....	2(0)	4(1)	1(3)	....
12.						
C_{4h}^1	4(0)	2(0); 2(1)	1(1); 2(2)	1(3)	.....	....
C_{4h}^2	....	6(0)	3(1); 1(2)	1(3)	.....	....
C_{4h}^3	....	2(0); 1(1)	2(0); 1(1)	1(3)	.....	....
C_{4h}^4	....	2(0)	2(0); 2(1)	1(3)	.....	....
C_{4h}^5	....	2(0)	2(0); 1(1)	1(0) 1(1) 1(2)	1(3)	....
C_{4h}^6	....	.....	2(0)	2(0); 1(1)	1(3)	....
13.						
C_{4v}^1	2(1)	1(1)	3(2)	1(3)	.....	....
C_{4v}^2	....	2(1)	1(2)	1(3)	.....	....
C_{4v}^3	....	2(1)	1(1); 1(2)	1(3)	.....	....
C_{4v}^4	....	1(1)	1(1); 1(2)	1(3)	.....	....
C_{4v}^5	....	2(1)	1(1)	1(3)	.....	....
C_{4v}^6	....	1(1)	1(1)	1(3)	.....	....
C_{4v}^7	....	3(1)	2(2)	1(3)	.....	....
C_{4v}^8	....	.....	2(1)	1(3)	.....	....
C_{4v}^9	....	1(1)	1(1)	2(2)	1(3)	....
C_{4v}^{10}	....	.....	2(1)	1(2)	1(3)	....
C_{4v}^{11}	....	.....	1(1)	1(2)	1(3)	....
C_{4v}^{12}	....	.....	.....	1(1)	1(3)	....
14.						
V_d^1	4(0)	2(0); 2(1)	5(1); 1(2)	1(3)	.....	....
V_d^2	....	6(0)	7(1)	1(3)	.....	....
V_d^3	....	2(0); 1(1)	1(1); 1(2)	1(3)	.....	....
V_d^4	....	2(0)	2(1)	1(3)	.....	....
V_d^5	....	4(0)	3(1)	2(1); 2(2)	1(3)	....
V_d^6	....	.....	4(0)	5(1)	1(3)	....
V_d^7	....	.....	4(0)	4(1)	1(3)	....
V_d^8	....	.....	4(0)	4(1)	1(3)	....
V_d^9	....	.....	4(0)	2(1)	2(1); 1(2)	1(3)
V_d^{10}	....	.....	.....	4(0)	4(1)	1(3)
V_d^{11}	....	2(0)	2(0); 1(1)	3(1); 1(2)	1(3)	....
V_d^{12}	....	.....	2(0)	2(1)	1(3)	....

TABLE XXXVI.—(*Concluded*)

S.G.	1	2	4	8	16	32
15.						
D^1_{4h}	4(0)	2(0); 2(1)	7(1)	5(2)	1(3)	....
D^2_{4h}	....	4(0)	2(0); 2(1)	4(1); 1(2)	1(3)	....
D^3_{4h}	....	4(0)	2(0); 2(1)	4(1); 1(2)	1(3)	....
D^4_{4h}	....	2(0)	2(0); 1(1)	1(0); 4(1)	1(3)	....
D^5_{4h}	....	4(0)	4(1)	3(2)	1(3)	....
D^6_{4h}	....	2(0)	2(0); 1(1)	2(1); 1(2)	1(3)	....
D^7_{4h}	....	2(0); 1(1)	2(0); 1(1)	2(1); 2(2)	1(3)	....
D^8_{4h}	....	.....	2(0); 1(1)	1(0): 2(1)	1(3)	....
D^9_{4h}	....	6(0)	7(1)	1(1); 3(2)	1(3)	....
D^{10}_{4h}	....	4(0)	2(0); 4(1)	3(1); 2(2)	1(3)	....
D^{11}_{4h}	....	.....	4(0)	1(0); 5(1)	1(3)	....
D^{12}_{4h}	....	2(0)	4(0); 1(1)	5(1); 1(2)	1(3)	....
D^{13}_{4h}	....	.....	4(0)	3(1); 1(2)	1(3)	....
D^{14}_{4h}	....	2(0)	2(0); 3(1)	1(1); 2(2)	1(3)	....
D^{15}_{4h}	....	2(0)	2(1)	1(0); 1(1) 1(2)	1(3)	....
D^{16}_{4h}	....	.....	4(0); 1(1)	3(1); 1(2)	1(3)	....
D^{17}_{4h}	....	2(0)	2(0); 1(1)	1(0); 4(1)	1(1); 3(2)	1(3)
D^{18}_{4h}	....	.....	4(0)	1(0); 3(1)	2(1); 2(2)	1(3)
D^{19}_{4h}	....	.....	2(0)	2(0); 1(1)	2(1); 1(2)	1(3)
D^{20}_{4h}	....	.....	.....	2(0)	1(0); 3(1)	1(3)

TABLE XXXVII.—CUBIC SYSTEM

S.G.	1	2	3	4	6	8	12	16	24	32	48	64	96	192
16.														
T^1	2(0)	....	2(0)	1(1)	4(1)	....	1(3)	....	....	....	....	....	....	....
T^2	....	....	....	4(0)	....	....	....	1(1)	2(1)	....	1(3)	....	....	....
T^3	....	1(0)	....	....	1(0)	1(1)	2(1)	....	1(3)	....	....	....	....	....
T^4	....	....	....	1(1)	....	....	1(3)	....	....	....	....	....	....	....
T^5	....	....	....	....	....	1(1)	1(1)	....	1(3)	....	....	....	....	....
17.														
O^1	2(0)	....	2(0)	....	4(1)	1(1)	2(1)	....	1(3)	....	....	....	....	....
O^2	....	1(0)	....	2(0)	3(0)	1(1)	5(1)	....	1(3)	....	....	....	....	....
O^3	....	....	....	2(0)	....	1(0)	....	....	1(0) 1(1)	1(1)	3(1)	....	1(3)	....
O^4	....	....	....	....	....	2(0)	....	2(0)	....	1(1)	2(1)	....	1(3)	....
O^5	....	1(0)	....	....	1(0)	1(0)	1(0) 2(1)	1(1)	2(1)	....	1(3)	....	....	....
O^6	....	....	....	2(0)	....	1(1)	1(1)	....	1(3)	....	....	....	....	....
O^7	....	....	....	2(0)	....	1(1)	1(1)	....	1(3)	....	....	....	....	....
O^8	....	....	....	....	....	2(0)	2(0)	1(1)	3(1)	....	1(3)	....	....	....

TABLE XXXVII.—(*Concluded*)

S.G.	1	2	3	4	6	8	12	16	24	32	48	64	96	192
18.														
T_h^1	2(0)	....	2(0)	....	4(1)	1(1)	2(2)	....	1(3)	....	....	....	....	....
T_h^2	....	1(0)	....	2(0)	1(0)	1(1)	2(1)	....	1(3)	....	....	....	....	....
T_h^3	....	....	....	2(0)	....	1(0)	....	....	1(0)	1(1)	1(1)	....	1(3)	....
									1(1)		1(2)			
T_h^4	....	....	....	....	....	2(0)	....	2(0)	....	1(1)	1(1)	....	1(3)	....
T_h^5	....	1(0)	....	....	1(0)	1(0)	2(1)	1(1)	1(2)	....	1(3)	....	....	....
T_h^6	....	....	....	2(0)	....	1(1)	....	....	1(3)	....	....	....	....	....
T_h^7	....	....	....	....	....	2(0)	....	1(1)	1(1)	....	1(3)	....	....	....
19														
T_d^1	2(0)	....	2(0)	1(1)	2(1)	....	1(1)	....	1(3)	....	....	....	....	....
							1(2)							
T_d^2	....	....	....	4(0)	....	....	....	1(1)	2(1)	....	1(2)	....	1(3)	....
T_d^3	....	1(0)	....	....	1(0)	1(1)	1(0)	....	1(1)	....	1(3)	....	....	....
							1(1)		1(2)					
T_d^4	....	1(0)	....	....	3(0)	1(1)	3(1)	....	1(3)	....	....	....	....	....
T_d^5	....	....	....	....	....	2(0)	....	....	2(0)	1(1)	2(1)	....	1(3)	....
T_d^6	....	....	....	....	....	....	2(0)	1(1)	1(1)	....	1(3)	....	....	....
20.														
O_h^1	2(0)	....	2(0)	....	2(1)	1(1)	3(1)	....	3(2)	....	1(3)	....	....	....
O_h^2	....	1(0)	....	....	1(0)	1(0)	1(0)	1(1)	2(1)	....	1(3)	....	....	....
							1(1)							
O_h^3	....	1(0)	....	....	3(0)	1(0)	3(1)	1(1)	1(1)	....	1(3)	....	....	....
									1(2)					
O_h^4	....	1(0)	....	2(0)	1(0)	1(1)	1(0)	....	2(1)	....	1(3)	....	....	....
							1(1)		1(2)					
O_h^5	....	....	....	2(0)	....	1(0)	....	....	1(0)	1(1)	3(1)	....	2(2)	1(3)
									1(1)					
O_h^6	....	....	....	....	....	2(0)	....	....	2(0)	....	2(1)	1(1)	1(1)	1(3)
													1(2)	
O_h^7	....	....	....	....	....	2(0)	....	2(0)	....	1(1)	1(1)	....	1(1)	1(3)
													1(2)	
O_h^8	....	....	....	....	....	....	....	1(0)	....	2(0)	1(0)	1(1)	2(1)	1(3)
O_h^9	....	1(0)	....	....	1(0)	1(0)	1(0)	1(1)	2(1)	....	1(1)	....	1(3)	....
							1(1)				2(2)			
O_h^{10}	....	....	....	....	....	....	....	2(0)	2(0)	1(1)	2(1)	....	1(3)	....

TABLE XXXVIII.—HEXAGONAL SYSTEM
Rhombohedral Division

S.G.	1	2	3	4	6	12
21.						
C_3^1	3(1)	.....	1(3)	....	.....	....
C_3^2	....	.....	1(3)	....	.....	....

TABLE XXXVIII.—(*Concluded*)

S.G.	1	2	4	8	16	32
21. *Continued.*						
C_3^3	....	.....	1(3)	....	.....	....
C_3^4	1(1)	.....	1(3)	....	.....	....
22.						
D_3^1	6(0)	3(1)	2(1)	....	1(3)	....
D_3^2	2(0)	2(1)	2(1)	....	1(3)	....
D_3^3	....	.....	2(1)	....	1(3)	....
D_3^4	....	.....	2(1)	....	1(3)	....
D_3^5	....	.....	2(1)	....	1(3)	....
D_3^6	....	.....	2(1)	....	1(3)	....
D_3^7	2(0)	1(1)	2(1)	....	1(3)	....
23.						
C_{3v}^1	3(1)	.....	1(2)	....	1(3)	....
C_{3v}^2	1(1)	1(1)	1(2)	....	1(3)	....
C_{3v}^3	....	3(1)	....	....	1(3)	....
C_{3v}^4	....	2(1)	....	....	1(3)	....
C_{3v}^5	1(1)	....	1(2)	....	1(3)	....
C_{3v}^6	....	1(1)	....	....	1(3)	....
24.						
C_{3i}^1	2(0)	2(1)	2(0)	....	1(3)	....
C_{3i}^2	2(0)	1(1)	2(0)	....	1(3)	....
25.						
D_{3d}^1	2(0)	2(0); 1(1)	2(0)	1(1)	2(1); 1(2)	1(3)
D_{3d}^2	....	4(0)	....	2(1)	1(0); 1(1)	1(3)
D_{3d}^3	2(0)	2(1)	2(0)	....	2(1); 1(2)	1(3)
D_{3d}^4	....	2(0)	....	2(1)	1(0); 1(1)	1(3)
D_{3d}^5	2(0)	1(1)	2(0)	....	2(1); 1(2)	1(3)
D_{3d}^6	....	2(0)	....	1(1)	1(0); 1(1)	1(3)

TABLE XXXIX.—HEXAGONAL SYSTEM

Hexagonal Division

S.G.	1	2	3	4	6	8	12	24
26.								
C_{3h}^1	6(0)	3(1)	2(2)	.....	1(3)	....	.....	....
27.								
D_{3h}^1	6(0)	3(1)	2(1)	.....	3(2)	....	1(3)	....
D_{3h}^2	....	6(0)	....	3(1)	1(1); 1(2)	....	1(3)	....
D_{3h}^3	2(0)	2(0); 1(1)	2(1)	1(1)	3(2)	....	1(3)	....
D_{3h}^4	....	4(0)	....	2(1)	1(1); 1(2)	....	1(3)	....

TABLE XXXIX.—(*Concluded*)

S.G.	1	2	3	4	6	8	12	24
28.								
C_6^1	1(1)	1(1)	1(1)	.....	1(3)	....	.....	....
C_6^2	....	.....	....	.....	1(3)	....	.....	....
C_6^3	....	.....	....	.....	1(3)	....	.....	....
C_6^4	....	.....	2(1)	.....	1(3)	....	.....	....
C_6^5	....	.....	2(1)	.....	1(3)	....	.....	....
C_6^6	....	2(1)	....	.....	1(3)	....	.....	....
29.								
D_6^1	2(0)	2(0); 1(1)	2(0)	1(1)	5(1)	....	1(3)	....
D_6^2	....	....	....	.. ..	2(1)	....	1(3)	....
D_6^3	....	....	....	.....	2(1)	....	1(3)	....
D_6^4	....	. . .. .	4(0)	.....	6(1)	....	1(3)	....
D_6^5	...	....	4(0)	.....	6(1)	....	1(3)	....
D_6^6	....	4(0)	....	2(1)	2(1)	....	1(3)	....
30.								
C_{6h}^1	2(0)	2(0); 1(1)	2(0)	1(1)	1(1); 2(2)	....	1(3)	....
C_{6h}^2	....	4(0)	....	2(1)	1(0); 1(2)	....	1(3)	....
31.								
C_{6v}^1	1(1)	1(1)	1(1)	.....	2(2)	....	1(3)	....
C_{6v}^2	....	1(1)	....	1(1)	1(1)	....	1(3)	....
C_{6v}^3	....	1(1)	....	1(1)	1(2)	....	1(3)	....
C_{6v}^4	....	2(1)	....	.....	1(2)	....	1(3)	....
32.								
D_{6h}^1	2(0)	2(0); 1(1)	2(0)	1(1)	5(1)	....	4(2)	1(3)
D_{6h}^2	....	2(0)	....	2(0); 1(1)	2(0)	1(1)	3(1); 1(2)	1(3)
D_{6h}^3	....	2(0)	....	2(0); 1(1)	1(0); 1(1)	1(1)	1(1); 2(2)	1(3)
D_{6h}^4	....	4(0)	....	2(1)	1(0); 1(1)	....	1(1); 2(2)	1(3)

TABLE XL.—THE SYMMETRY CHARACTERISTICS OF THE 32 POINT-GROUPS

(The typical chemical examples are taken from Tutton, "The Natural History of Crystals," E. P. Dutton & Co., Inc., New York)

Triclinic system: $a \neq b \neq c$; $\lambda \neq \mu \neq \nu$.

1. C_1 Hemihedry; Asymmetric.
   No symmetry.
   Calcium thiosulphate, $CaS_2O_3 \cdot 6H_2O$.
2. C_i Holohedry; Centrosymmetric.
   One 2-fold axis $\perp$ plane of compound symmetry.
   This is the equivalent of a center of symmetry.
   Copper sulphate, $CuSO_4 \cdot 5H_2O$.

TABLE XL.—(*Continued*)

Monoclinic system: $a \overset{=}{\neq} b \overset{=}{\neq} c$; $\lambda = \mu = 90°$; $\nu \neq 90°$*

$\lambda = \nu = 90°$; $\mu \neq 90°$†

3. C_s Hemihedry; Equatorial.
One plane of symmetry.
Potassium tetrathionate, $K_2S_4O_6$.

4. C_2 Hemimorphic hemihedry; Digonal polar.
One 2-fold axis.
Tartaric acid, $C_4H_6O_6$

5. C_{2h} Holohedry; Digonal equatorial.
One 2-fold axis $\perp$ plane of symmetry.
Potassium magnesium sulphate, $K_2Mg(SO_4)_2 \cdot 6H_2O$.

Orthorhombic system: $a \neq b \neq c$; $\lambda = \mu = \nu = 90°$.

6. $V = Q$ Enantiomorphic hemihedry; Digonal holoaxial.
Three mutually $\perp$ 2-fold axes.
Magnesium sulphate, $MgSO_4 \cdot 7H_2O$.

7. C_{2v} Hemimorphic hemihedry; Didigonal polar.
One 2-fold axis $\parallel$ two mutually $\perp$ planes of symmetry.
Ammonium magnesium phosphate, $NH_4MgPO_4 \cdot 6H_2O$.

8. $V_h = Q_h$ Holohedry; Didigonal equatorial.
Three mutually $\perp$ 2-fold axes, and three mutually $\perp$ planes of symmetry.
Potassium sulphate, K_2SO_4.

Tetragonal system: $a = b \neq c$; $\lambda = \mu = \nu = 90°$.

9. C_4 Tetartohedry; Tetragonal polar.
One 4-fold axis.
Lead molybdate, $PbMoO_4$.

10. S_4 Tetartohedry of the second sort; Tetragonal alternating.
One 4-fold axis $\perp$ plane of compound symmetry.
Only example known, $2CaO \cdot Al_2O_3 \cdot SiO_2$.

11. D_4 Enantiomorphic hemihedry; Tetragonal holoaxial.
One 4-fold axis $\perp$ plane containing four 2-fold axes.
Strychnine sulphate, $(C_{21}H_{22}N_2O_2) \cdot H_2SO_4 \cdot 6H_2O$

12. C_{4h} Paramorphic hemihedry; Tetragonal equatorial.
One 4-fold axis $\perp$ plane of symmetry.
Calcium tungstate, $CaWO_4$.

13. C_{4v} Hemimorphic hemihedry; Ditetragonal polar.
One 4-fold axis at the intersection of four planes of symmetry.
Iodosuccinimide, $C_4H_4O_2NI$.

14. $V_d = Q_d$ Hemihedry of the second sort; Ditetragonal alternating.
One 4-fold axis $\perp$ plane of compound symmetry; two mutually $\perp$ 2-fold axes lying in the plane of compound symmetry; two planes of symmetry intersecting in the 4-fold axis and bisecting the angles of the two 2-fold axes.
Potassium dihydrogen phosphate, KH_2PO_4.

15. D_{4h} Holohedry; Ditetragonal equatorial.
One 4-fold axis at the intersection of four planes of symmetry; one

* Convention of Chap. II.
† Convention of Appendix III.

TABLE XL.—(*Continued*)

plane of symmetry and four 2-fold axes all ⊥ the 4-fold axis.
Zircon, $ZrSiO_4$.

Cubic system: $a = b = c$; $\lambda = \mu = \nu = 90°$.

16. *T* Tetartohedry; Tesseral polar.
Three mutually ⊥ 2-fold axes, and four 3-fold axes equally inclined to them.
Barium nitrate, $Ba(NO_3)_2$.

17. *O* Enantiomorphic hemihedry; Tesseral holoaxial.
Three mutually ⊥ 4-fold axes; four 3-fold axes equally inclined to them; six 2-fold axes bisecting the angles between the 4-fold axes. No planes of symmetry.
Cuprite, Cu_2O.

18. T_h Paramorphic hemihedry; Tesseral central.
Three mutually ⊥ 2-fold axes; four 3-fold axes equally inclined to them; three planes of symmetry ⊥ the 2-fold axes.
Pyrites, FeS_2.

19. *T'* Hemimorphic hemihedry; Ditesseral polar.
Three mutually ⊥ 2-fold axes; four 3-fold axes equally inclined to them; six planes of symmetry bisecting angles corresponding to the angles between the 4-fold axes of class *O* or of class O_h.
Tetrahedrite, Cu_3SbS_3.

20. O_h Holohedry; Ditesseral central.
Three mutually ⊥ 4-fold axes; four 3-fold axes equally inclined to them; six 2-fold axes bisecting the angles between the 4-fold axes; three planes of symmetry ⊥ the 4-fold axes; six planes of symmetry bisecting the angles between the 4-fold axes.
Calcium fluoride, CaF_2; Sodium chloride, NaCl.

Hexagonal system:

Hexagonal axes:
$a = b \neq c$; $\lambda = \mu = 90°$; $\nu = 120°$.
Rhombohedral axes:
$a = b = c$; $\lambda = \mu = \nu \neq 90°$.

Rhombohedral division:

21. C_3 Rhombohedral tetartohedry; Trigonal polar.
One 3-fold axis of symmetry.
Sodium periodate, $NaIO_4 \cdot 3H_2O$.

22. D_3 Enantiomorphic hemihedry; Trigonal holoaxial.
One 3-fold axis ⊥ plane containing three 2-fold axes.
Quartz (low temperature form), SiO_2.

23. C_{3v} Hemimorphic hemihedry; Ditrigonal polar.
One 3-fold axis at intersection of three planes of symmetry.
Tourmaline, $H_6Na_2Fe_4B_6Al_3Si_{12}O_{63}$.

24. C_{3i} Hexagonal tetartohedry of the second sort; Hexagonal alternating.
One 3-fold axis which is also a 6-fold axis of compound symmetry.
Dioptese, CuH_2SiO_4.

25. D_{3d} Rhombohedral holohedry; Dihexagonal alternating.
One 3-fold axis at intersection of three planes of symmetry; three 2-fold axes in a plane ⊥ 3-fold axes.
Calcite, $CaCO_3$.

TABLE XL.—(*Concluded*)

Hexagonal division:

26. C_{3h} Trigonal paramorphic hemihedry; Trigonal equatorial.
One 3-fold axis ⊥ plane of symmetry.
No example known.

27. D_{3h} Trigonal holohedry; Ditrigonal equatorial.
One 3-fold axis at intersection of three planes of symmetry; the 3-fold axis is ⊥ three 2-fold axes lying in a plane of symmetry.
Silver hydrogen phosphate, Ag_2HPO_4.

28. C_6 Hexagonal tetartohedry; Hexagonal polar.
One 6-fold axis.
Strontium antimonyl tartrate, $Sr\,(SbO)_2(C_4H_4O_6)_2$.

29. D_6 Enantiomorphic hemihedry; Hexagonal holoaxial.
One 6-fold axis ⊥ plane containing six 2-fold axes.
$(C_4H_4O_6)_2(SbO)_2Ba \cdot KNO_3$.

30. C_{6h} Paramorphic hemihedry; Hexagonal equatorial.
One 6-fold axis ⊥ plane of symmetry.
Apatite, $Ca_5F(PO_4)_3$.

31. C_{6v} Hemimorphic hemihedry; Dihexagonal polar.
One 6-fold axis at intersection of six planes of symmetry.
Greenockite, CdS.

32. D_{6h} Hexagonal holohedry; Dihexagonal equatorial.
One 6-fold axis at intersection of six planes of symmetry; the 6-fold axis is ⊥ six 2-fold axes lying in a plane of symmetry.
Beryl, $Be_3Al_2(SiO_3)_6$.

TABLE XLI.—TWO HUNDRED THIRTY SPACE-GROUPS ACCORDING TO THE ZURICH NOTATIONS*

C_1^1	$P1$	C_{2v}^6	Pnc	D_2^5	$C222_1$
C_i^1	$P\bar{1}$	C_{2v}^7	Pmn	D_2^6	$C222$
C_s^1	Pm	C_{2v}^8	Pba	D_2^7	$F222$
C_s^2	Pc	C_{2v}^9	Pna	D_2^8	$I222$
C_s^3	Cm	C_{2v}^{10}	Pnn	D_2^9	$I2_12_12_1$
C_s^4	Cc	C_{2v}^{11}	Cmm		
		C_{2v}^{12}	Cmc	D_{2h}^1	$Pmmm$
C_2^1	$P2$	C_{2v}^{13}	Ccc	D_{2h}^2	$Pnnn$
C_2^2	$P2_1$	C_{2v}^{14}	Amm	D_{2h}^3	$Pccm$
C_2^3	$C2$	C_{2v}^{15}	Abm	D_{2h}^4	$Pban$
		C_{2v}^{16}	Ama	D_{2h}^5	$Pmma$
C_{2h}^1	$P2/m$	C_{2v}^{17}	Aba	D_{2h}^6	$Pnna$
C_{2h}^2	$P2_1/m$	C_{2v}^{18}	Fmm	D_{2h}^7	$Pmna$
C_{2h}^3	$C2/m$	C_{2v}^{19}	Fdd	D_{2h}^8	$Pcca$
C_{2h}^4	$P2/c$	C_{2v}^{20}	Imm	D_{2h}^9	$Pbam$
C_{2h}^5	$P2_1/c$	C_{2v}^{21}	Iba	D_{2h}^{10}	$Pccn$
C_{2h}^6	$C2/c$	C_{2v}^{22}	Ima	D_{2h}^{11}	$Pbcm$
				D_{2h}^{12}	$Pnnm$
C_{2v}^1	Pmm	D_2^1	$P222$	D_{2h}^{13}	$Pmmn$
C_{2v}^2	Pmc	D_2^2	$P222_1$	D_{2h}^{14}	$Pbcn$
C_{2v}^3	Pcc	D_2^3	$P2_12_12$	D_{2h}^{15}	$Pbca$
C_{2v}^4	Pma	D_2^4	$P2_12_12_1$	D_{2h}^{16}	$Pnma$
C_{2v}^5	Pca				

* *Zeit. Kryst.*, **76**, 542 (1931).

TABLE XLI.—(*Continued*)

D_{2h}^{17}	$Cmcm$	C_4^6	$I4_1$	D_{4h}^6	$P4/mnc$
D_{2h}^{18}	$Cmca$			D_{4h}^7	$P4/nmm$
D_{2h}^{19}	$Cmmm$	C_{4h}^1	$P4/m$	D_{4h}^8	$P4/ncc$
D_{2h}^{20}	$Cccm$	C_{4h}^2	$P4_2/m$	D_{4h}^9	$P4/mmc$
D_{2h}^{21}	$Cmma$	C_{4h}^3	$P4/n$	D_{4h}^{10}	$P4/mcm$
D_{2h}^{22}	$Ccca$	C_{4h}^4	$P4_2/n$	D_{4h}^{11}	$P4/nbc$
D_{2h}^{23}	$Fmmm$	C_{4h}^5	$I4/m$	D_{4h}^{12}	$P4/nnm$
D_{2h}^{24}	$Fddd$	C_{4h}^6	$I4_1/a$	D_{4h}^{13}	$P4/mbc$
D_{2h}^{25}	$Immm$			D_{4h}^{14}	$P4/mnm$
D_{2h}^{26}	$Ibam$	D_{2d}^1	$P\bar{4}2m$	D_{4h}^{15}	$P4/nmc$
D_{2h}^{27}	$Ibca$	D_{2d}^2	$P\bar{4}2c$	D_{4h}^{16}	$P4/ncm$
D_{2h}^{28}	$Imma$	D_{2d}^3	$P\bar{4}2_1m$	D_{4h}^{17}	$I4/mmm$
C_3^1	$C3$	D_{2d}^4	$P\bar{4}2_1c$	D_{4h}^{18}	$I4/mcm$
C_3^2	$C\bar{3}$	D_{2d}^5	$C\bar{4}2m$	D_{4h}^{19}	$I4/amd$
C_3^3	$C3_1$	D_{2d}^6	$C\bar{4}2c$	D_{4h}^{20}	$I4/acd$
C_3^4	$R3$	D_{2d}^7	$C\bar{4}2b$		
		D_{2d}^8	$C\bar{4}2n$	C_{5h}^1	$C\bar{6}$
C_{3i}^1	$C\bar{3}$	D_{2d}^9	$F\bar{4}2m$		
C_{3i}^2	$R\bar{3}$	D_{2d}^{10}	$F\bar{4}2c$	C_6^1	$C6$
		D_{2d}^{11}	$I\bar{4}2m$	C_6^2	$C6_1$
C_{3v}^1	$C3m$	D_{2d}^{12}	$I\bar{4}2d$	C_6^3	$C6_5$
C_{3v}^2	$H3m$			C_6^4	$C6_4$
C_{3v}^3	$C3c$	C_{4v}^1	$P4mm$	C_6^5	$C6_2$
C_{3v}^4	$H3c$	C_{4v}^2	$P4bm$	C_6^6	$C6_3$
C_{3v}^5	$R3m$	C_{4v}^3	$P4cm$		
C_{3v}^6	$R3c$	C_{4v}^4	$P4nm$	C_{6h}^1	$C6/m$
		C_{4v}^5	$P4cc$	C_{6h}^2	$C6_3/m$
D_3^1	$H32$	C_{4v}^6	$P4nc$		
D_3^2	$C32$	C_{4v}^7	$P4mc$	D_{3h}^1	$C\bar{6}m2$
D_3^3	$H3_12$	C_{4v}^8	$P4bc$	D_{3h}^2	$C\bar{6}c2$
D_3^4	$C3_12$	C_{4v}^9	$I4mm$	D_{3h}^3	$H\bar{6}m2$
D_3^5	$H3_22$	C_{4v}^{10}	$I4cm$	D_{3h}^4	$H\bar{6}c2$
D_3^6	$C3_22$	C_{4v}^{11}	$I4md$		
D_3^7	$R32$	C_{4v}^{12}	$I4cd$	C_{6v}^1	$C6mm$
				C_{6v}^2	$C6cc$
D_{3d}^1	$H\bar{3}m$	D_4^1	$P42$	C_{6v}^3	$C6cm$
D_{3d}^2	$H\bar{3}c$	D_4^2	$P42_1$	C_{6v}^4	$C6mc$
D_{3d}^3	$C\bar{3}m$	D_4^3	$P4_12$		
D_{3d}^4	$C\bar{3}c$	D_4^4	$P4_12_1$	D_6^1	$C62$
D_{3d}^5	$R\bar{3}m$	D_4^5	$P4_22$	D_6^2	$C6_12$
D_{3d}^6	$R\bar{3}c$	D_4^6	$P4_22_1$	D_6^3	$C6_52$
		D_4^7	$P4_32$	D_6^4	$C6_42$
S_4^1	$P\bar{4}$	D_4^8	$P4_32_1$	D_6^5	$C6_32$
S_4^2	$I\bar{4}$	D_4^9	$I42$	D_6^6	$C6_32$
		D_4^{10}	$I4_12$		
C_4^1	$P4$			D_{6h}^1	$C6/mmm$
C_4^2	$P4_1$	D_{4h}^1	$P4/mmm$	D_{6h}^2	$C6_3/mcc$
C_4^3	$P4_2$	D_{4h}^2	$P4/mcc$	D_{6h}^3	$C6/mcm$
C_4^4	$P4_3$	D_{4h}^3	$P4/nbm$	D_{6h}^4	$C6/mmc$
C_4^5	$I4$	D_{4h}^4	$P4/nnc$		
		D_{4h}^5	$P4/mbm$	T^1	$P23$
				T^2	$F23$
				T^3	$I23$

TABLE XI.I.—(*Concluded*)

T^4	$P2_13$	T_d^2	$F\bar{4}3m$	O^7	$P4_33$
T^5	$I2_13$	T_d^3	$I\bar{4}3m$	O^8	$I4_13$
		T_d^4	$P\bar{4}3n$		
T_h^1	$Pm3$	T_d^5	$F\bar{4}3c$	O_h^1	$Pm3m$
T_h^2	$Pn3$	T_d^6	$I\bar{4}3d$	O_h^2	$Pn3n$
T_h^3	$Fm3$			O_h^3	$Pm3n$
T_h^4	$Fd3$	O^1	$P43$	O_h^4	$Pn3m$
T_h^5	$Im3$	O^2	$P4_23$	O_h^5	$Fm3m$
T_h^6	$Pa3$	O^3	$F43$	O_h^6	$Fm3c$
T_h^7	$Ia3$	O^4	$F4_13$	O_h^7	$Fd3m$
		O^5	$I43$	O_h^8	$Fd3c$
T_d^1	$P\bar{4}3m$	O^6	$P4_13$	O_h^9	$Im3m$
				O_h^{10}	$Ia3d$

APPENDIX IV

A GRAPHICAL PROJECTION METHOD OF DETERMINING THE COORDINATES OF CERTAIN POINT-GROUPS*

The various symmetry operations† for the 32 point-groups may be visualized easily by means of appropriate projections, thus facilitating the study of the point-groups by beginners. The scheme will be illustrated in terms of a few of the cubic, rhombohedral, and hexagonal point-groups. The point-group symbols used are those of reference (1).

CUBIC SYSTEM

Point-group T.—This point-group is arrived at by means of a 3-fold axis which is operated on by three 2-fold axes. The 3-fold axis corresponds to one of the four body-diagonals of a cube. The 2-fold axes correspond to the principal axes of a cube. The origin of coordinates is taken at the center of the cube and the three axes of reference pass through the centers of the cube faces. If the Z-axis of the cube is held vertical, and, if the cube is rotated so that the positive direction of the x-axis points somewhat diagonally toward the left of the observer, then the cube is in such a position as to give, by our method, the same sequence of coordinates as in reference (2). The cube in this position is shown in Fig. 1.

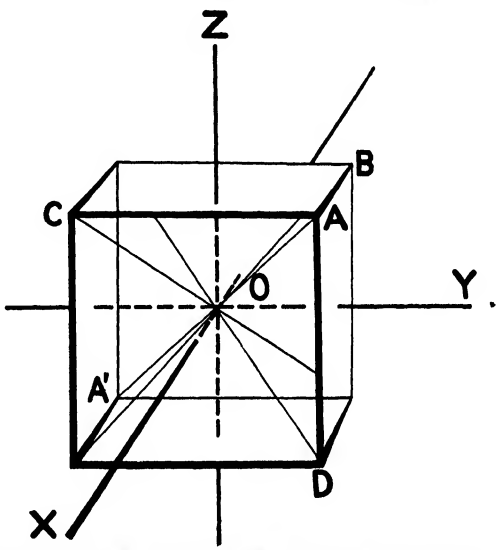

FIG. 1.—Cube showing axes of reference and 3-fold axes.

If, now, the observer looks along the body-diagonal from A to A', the cube will appear in projection on the (1 1 1) plane as in Fig. 2. That is, in the plane of the paper, the projection of the origin of coordinates

* D. MCLACHLAN and W. P. DAVEY, *Jour. Chem. Educ.*, **9**, 1953 (1932).

† R. W. G. WYCKOFF, The Analytical Expression of the Results of the Theory of Space-groups, *Carnegie Inst. Pub.* 318.

and of the points A and A' will all coincide at the center of the plane figure. The positive directions of the projections of the X-, Y-, and Z-axes will be 120° to each other. These projections will be called X', Y', and Z', respectively. The projection of the edge AB falls on $\overline{X}'$; that of AC falls on $\overline{Y}'$; that of AD on $\overline{Z}'$.

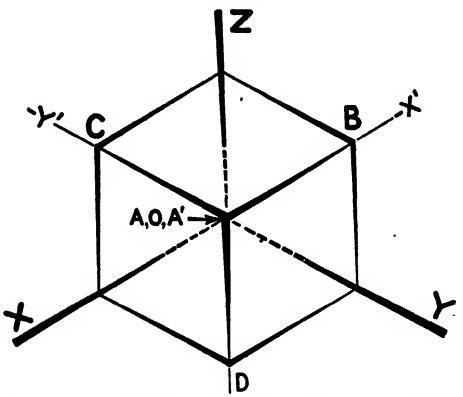

FIG. 2.—Projection of cube with (1 1 1) plane parallel to paper.

Draw a template as in Fig. 3 on tracing cloth or semitransparent paper showing, by dotted lines, the projections X', Y', and Z' in the positive directions of the X-, Y-, and Z- axes. On this template draw, in projection, the coordinates x, y, and z of the point P, and mark off the distances x and $2x$, y and $2y$, z and $2z$ along the X'-, Y'-, and Z'-directions, respectively. We shall follow the usual custom of considering the lengths x, y, and z to represent *distances* only. The sequence of the coordinates indicates the axes to which they refer. The coordinates of the 12 points corresponding to the point-group T may now be found as follows.

1, $A(2\pi/3)$, $A(4\pi/3)$.—Place the template on Fig. 2, passing a pin through the origin of coordinates of both the template and of Fig. 2. Make X', Y', and Z' of the template register with X', Y', and Z' of Fig. 2. Then, in projection on the (1 1 1) plane, the point P is in the initial position 1. Obviously its coordinates may be read off directly as x, y, z. The template in this position is shown in Fig. 4.

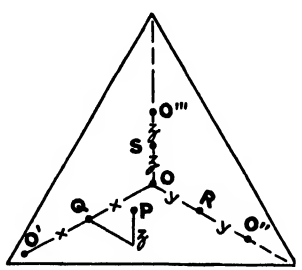

FIG. 3.—Template for cubic point-groups.

Rotate the template about the pin counterclockwise through an angle $2\pi/3$. This is the equivalent, in projection, of rotating the 3-fold axis AA' through $2\pi/3$. The new position is shown in Fig. 5. The new coordinates are, obviously, z, x, y. They may be found most easily by noting the path required to go from the pin at the origin of Fig. 2 to Q and then along the original Y- and Z-coordinates of the point P. (When negative directions of travel are found, they must be indicated by minus signs in the usual way.) The resultant distances along the X'-, Y'-, and Z'-directions must then be put in the proper sequence to show to which coordinates they refer. This course will be followed in this discussion.

Rotate the template counterclockwise about the pin through a second angle of $2\pi/3$. This is the equivalent, in the projection, of rotating the 3-fold axis AA' through a total angle of $4\pi/3$ from the initial position. The coordinates for the $A(4\pi/3)$ position of P are evidently y, z, x. The position of the template is shown in Fig. 6.

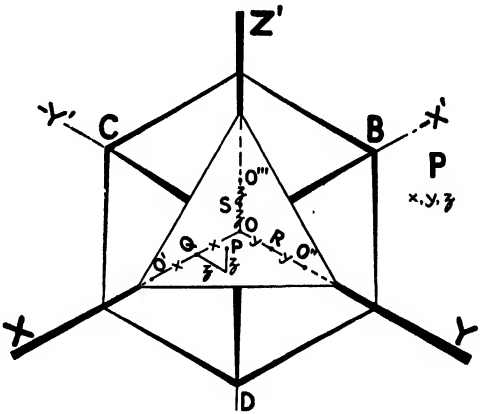

FIG. 4.—Template in initial position for the identity, 1.

U, $A_1(2\pi/3)$, $A_1(4\pi/3)$.—We must now rotate our original point $x\ y\ z$ through an angle π about the X-axis (Umklappung operation) and then repeat the 3-fold operations of symmetry. The Umklappung is done, in projection, by placing the template in the initial position (Fig. 4), inserting the pin through the point Q, and rotating the template 180°. This brings the point O' above the projection of the origin of Fig. 2, as shown in Fig. 7.

We are now ready to find the coordinates of the point P in the three positions *U*, $A_1(2\pi/3)$, and $A_1(4\pi/3)$, corresponding to the operation of the 3-fold axis. The template is already in position for the first of these. Using the type of procedure outlined under $A(2\pi/3)$, and noting that the origin of the cube is now as far on one side of Q as the original origin O is on the other, we find at once that the coordinates of the point P in the U position are $x, \bar{y}, \bar{z}$.

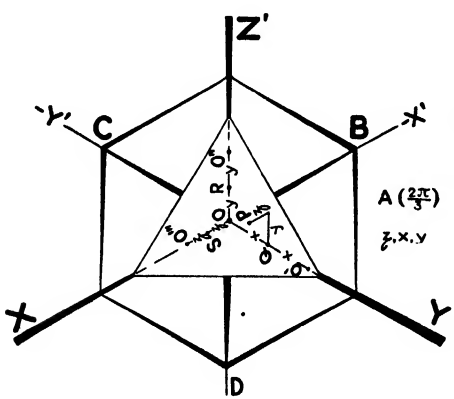

FIG. 5.—Template at $A\left(\frac{2\pi}{3}\right)$.

By transferring the pin to O' of the template (which lies over the origin of coordinates of Fig. 2), and rotating the template counterclockwise through $2\pi/3$ and $4\pi/3$, we may complete the operations of the 3-fold axes and find the coordinates of P for the positions $A_1(2\pi/3)$ and $A_1(4\pi/3)$, respectively. They are $\bar{z}, x, \bar{y}$ and $\bar{y}, \bar{z}, x$.

V, $A_2(2\pi/3)$, $A_2(4\pi/3)$.—To make, in projection, the Umklappung operation about the Y-axis, restore the template to its original position

as in Fig. 4, put the pin through R which lies at a distance y from O along the direction of Y'. Rotate the template 180° so that the point O'' lies above the origin of coordinates of Fig. 2. Transfer the pin to the point O''. We are now ready (see Fig. 8) to find the coordinates of V, $A_2(2\pi/3)$, and $A_2(4\pi/3)$. The origin of the cube is now as far on one side of R as the original origin O of the template is on the other, so that the coordinates of the point P for the position V are $\bar{x}, 2y\text{-}y, \bar{z} = \bar{x}, y, \bar{z}$. A counterclockwise rotation of $2\pi/3$ and $4\pi/3$ gives the coordinates of P for the positions $A_2(2\pi/3)$ and $A_2(4\pi/3)$, respectively. They are $\bar{z}, \bar{x}, 2y\text{-}y = \bar{z}, \bar{x}, y$ and $2y\text{-}y, \bar{z}, \bar{x} = y, \bar{z}, \bar{x}$.

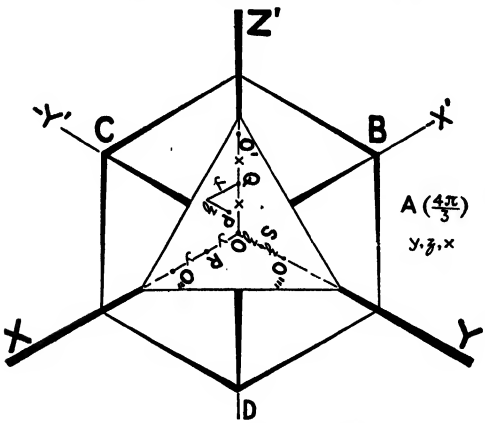

FIG. 6.—Template at $A\left(\frac{4\pi}{3}\right)$.

W, $A_3(2\pi/3)$, $A_3(4\pi/3)$.—Restore the template to its original position as in Fig. 4, and make the Umklappung operation about the Z-axis by putting the pin through S and rotating the template 180° so that the point O''' lies above the origin of coordinates of Fig. 2 (see Fig. 9). The coordinates of P in the W position are read off as $\bar{x}, \bar{y}, 2z\text{-}z = \bar{x}, \bar{y}, z$. Transfer the pin to O''' and operate the 3-fold axis, in projection, by counterclockwise rotations of $2\pi/3$ and $4\pi/3$. These give for the coordinates of P in the $A_3(2\pi/3)$ and $A_3(4\pi/3)$ positions, $2z\text{-}z, \bar{x}, \bar{y} = z, \bar{x}, \bar{y}$, and $\bar{y}, 2z\text{-}z, \bar{x} = \bar{y}, z, \bar{x}$, respectively. This completes the determination of the coordinates of the point P in all 12 of the equivalent positions of point-group T.

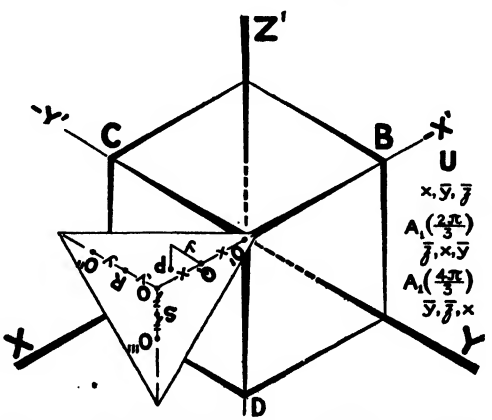

FIG. 7.—The template after Umklappung about the X-axis.

Point-group O.—The octohedral group has four 3-fold, three 4-fold, and six 2-fold axes arranged in the same manner as the body-diagonals, altitudes, and face-diagonals of a cube. The 2-fold axes U, V, W of point-group T are now 4-fold axes, so that to the operations 1, U in point-group T we must now add $B(\pi/2)$ and

$B(3\pi/2)$; to the operations 1, V we must add $B_1(\pi/2)$ and $B_1(3\pi/2)$; and to the operations 1, W we must add $B_2(\pi/2)$ and $B_2(3\pi/2)$, thus giving the following operations of the three 4-fold axes:

$$1,\ B\left(\frac{\pi}{2}\right),\qquad U,\ B\left(\frac{3\pi}{2}\right)$$
$$1,\ B_1\left(\frac{\pi}{2}\right),\qquad V,\ B_1\left(\frac{3\pi}{2}\right)$$
$$1,\ B_2\left(\frac{\pi}{2}\right),\qquad W,\ B_2\left(\frac{3\pi}{2}\right)$$

In addition we have six 2-fold axes whose operators are U_1, U_2, V_1, V_2, W_1, W_2.

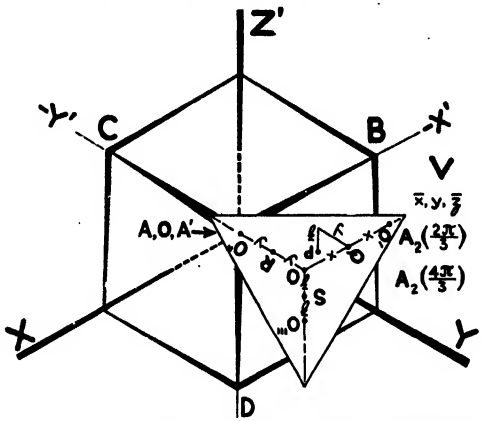

FIG. 8.—The template after Umklappung about the Y-axis.

Instead of starting from the original point for each of the 24 operations of O, it is simpler, in projection, to build up the 12 points of point-group T and then rotate T, as a whole, 180° about one of the 2-fold axes lying in the (1 1 1) plane of projection. The observer is now looking along the body-diagonal of the reference cube (Fig. 1) from A' toward A. In projection on the (1 1 1) plane he sees the reference cube, not as in Fig. 2, but with the X- and Y-axes interchanged and with the positive directions of all three axes reversed.

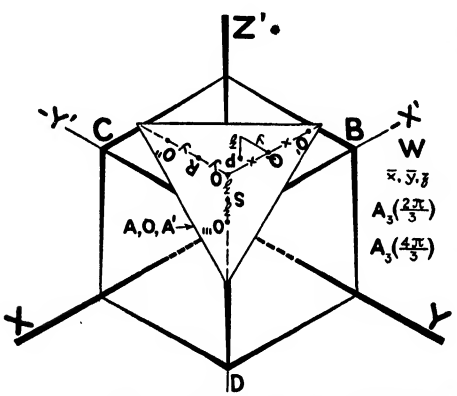

FIG. 9.—The template after Umklappung about the Z-axis.

If now, keeping this change of axes and signs in mind, all the operations of point-group T are repeated, the additional coordinates of point-group O will be found. They are:

$$\bar{y}, \bar{x}, \bar{z}; \qquad \bar{x}, \bar{z}, \bar{y}; \qquad \bar{z}, \bar{y}, \bar{x}$$
$$y, \bar{x}, z; \qquad \bar{x}, z, y; \qquad z, y, \bar{x}$$
$$-2y + y, x, z = \bar{y}, x, z; \quad x, z, -2y + y = x, z, \bar{y}; \quad z, -2y + y, x = z, \bar{y}, x$$
$$y, x, -2z + z = y, x, \bar{z}; \quad x, -2z + z, y = x, \bar{z}, y; \quad -2z + z, y, x = \bar{z}, y, x$$

These 12 coordinates, together with the 12 found for point-group T, complete the determination of the coordinates of the point P in all 24 equivalent positions of point-group O.

The application of the above technique to orthorhombic and tetragonal point-groups is obvious.

HEXAGONAL SYSTEM

Rhombohedra may be referred either to rhombohedral (distorted cubic) axes or to hexagonal axes. Figure 10 shows that, if a rhombohedron is held so that the observer looks along the trigonal axis, it will appear in projection on the (1 1 1) plane, with the projections X', Y', Z' of the rhombohedral axes 120° apart as in the case of a cube. At 30° to these projections may be seen the actual X_h-, Y_h-, and F_h- hexagonal axes. The hexagonal Z_h-axis lies perpendicular to the paper; it is the trigonal axis of the rhombohedron. The changes in technique necessary to make the procedure just described for cubic point-groups apply to rhombohedral point-groups are caused by the use of the hexagonal axes in the symmetry operations. These will be illustrated in terms of the C_3, D_3, C_{3v}, and C_{3i} point-groups. The illustrations may be followed more easily by making a separate drawing (Fig. 11) which shows the X'-, Y'-, and Z'-directions and the hexagonal X_h-axis.

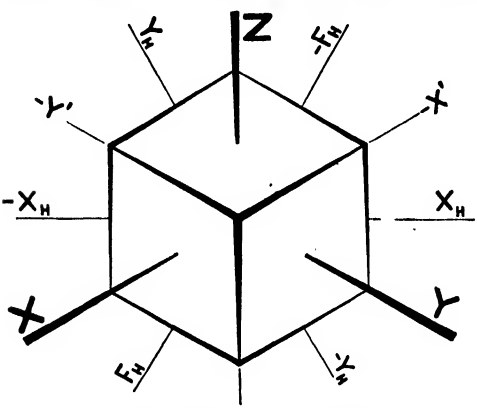

FIG. 10.—A rhombohedron projected along the trigonal axis on the (1 1 1) plane.

Point-group C_3.—By using the template of Fig. 12, and by duplicating exactly the procedure for 1, $A(2\pi/3)$, $A(4\pi/3)$ of point-group T, we arrive at the rhombohedral coordinates of C_3, namely:

$$x, y, z; \quad z, x, y; \quad y, z, x$$

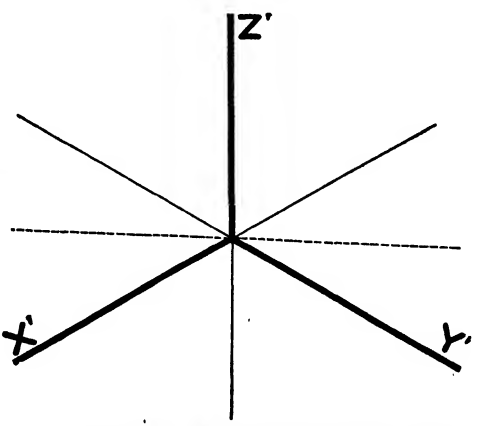

FIG. 11.—Projections for determining the coordinates of rhombohedral point-groups.

Point-group D_3.—This point-group contains the three points of C_3 and, in addition, three others obtained by an Umklappung operation (rotation of 180°) about one of the hexagonal axes X_h, Y_h, or F_h. Since all three of these hexagonal axes produce identical end results,

it is only necessary to illustrate the operation around one of them, say the X_h. The Umklappung operation will turn the rhombohedron upside down and will therefore present to the observer the projected axes X', Y', and Z' as shown in Fig. 13.

Applying the template of Fig. 12 to Fig. 13, we obtain the coordinates

$$\bar{y}, \bar{x}, z; \quad \bar{x}, z, \bar{y}; \quad z, \bar{y}, \bar{x}$$

These together with the three listed under C_3 are the coordinates of the point P for D_3.

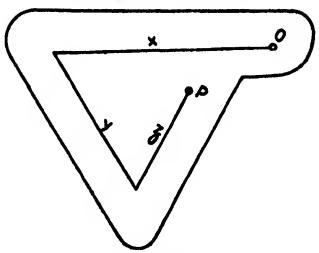

FIG. 12.—Template for rhombohedral point-groups.

Point-group C_{3v}.—This point-group may be obtained by adding to C_3 the operation of a vertical mirror passing through the hexagonal axis Z_h. There are two types of orientation possible for such a mirror: (*a*) it may pass through X_h, or Y_h, or F_h; or (*b*) it may bisect the angle between X_h and F_h, or X_h and Y_h, or Y_h and F_h. It may be shown that all of these orientations lead to identical configurations of points, and that those from type (*b*) differ from those of type (*a*) only in the viewpoint of the observer. Alternative (*b*) may be expressed by saying that the mirror lies in the direction of X', Y', or Z'. The coordinates of the points produced by the mirror can be obtained in the order tabulated by Wyckoff if we orient the mirror in the direction of Z'. The effect of such a mirror on Fig. 11 is shown in Fig. 14. The additional coordinates of C_{3v} may now be found directly by placing the template (Fig. 12) on Fig. 14 and repeating the operations already outlined for C_3. The coordinates thus found are

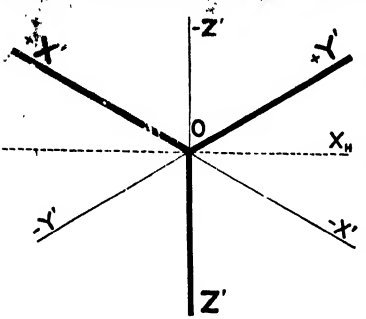

FIG. 13.—X', Y', and Z' after the rhombohedron has been rotated 180° about the X_h-axis (Umklappung).

$$y, x, z; \quad x, z, y; \quad z, y, x$$

These together with the three listed under C_3 are the coordinates of the point P for C_{3v}.

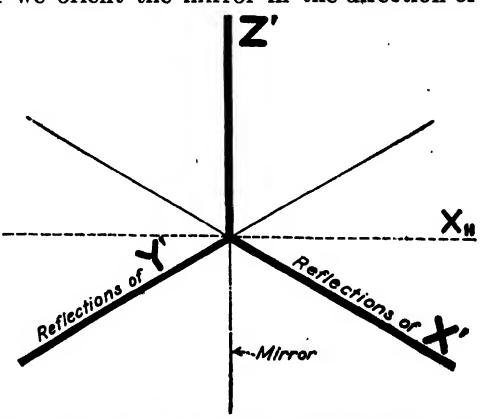

FIG. 14.—The effect on Fig. 11 of a vertical mirror placed in the direction of Z'.

Point-group C_{3i}.—The effect of the inversion operation may be found, in projection, by making

a new template such as is shown in Fig. 15. This template is applied to Fig. 11, and the procedure already outlined for C_3 is repeated except that it is necessary to write the coordinates for P' as well as for P. Such a procedure gives for P:

$$x, y, z; \quad z, x, y; \quad y, z, x$$

and for P'

$$\bar{x}, \bar{y}, \bar{z}; \quad \bar{z}, \bar{x}, \bar{y}; \quad \bar{y}, \bar{z}, \bar{x}$$

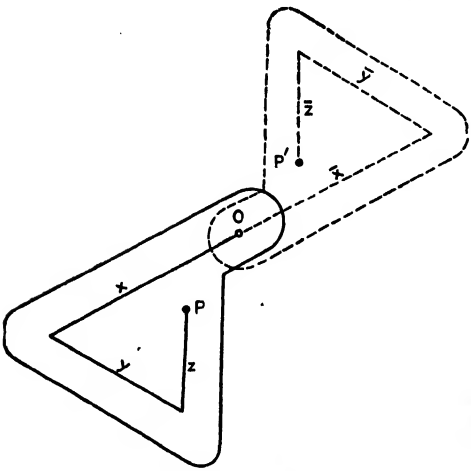

FIG. 15.—Template for use with inversions.

Point-group $D_{3d} = D_{3i}$.—This point-group may be found by adding to the procedure already described for D_3 that just described for the inversion.

Hexagonal Coordinates.—Those point-groups which are expressed most naturally by hexagonal coordinates (C_3, D_{3h}, C_6, D_6, C_{6h}, C_{6v}, D_{6h}) may be examined in projection by imagining the observer to look along the hexagonal Z_h-axis. All sense of perspective along the Z_h-axis is thus lost, and the point-group is seen projected in the plane of the X_h- and Y_h-axes. It is easy to keep track of whether the point P lies above or below the plane of the paper, *i.e.*, whether the Z_h- coordinate is positive or negative. The only difficulty which the beginner has is in finding the coordinates along the X_h- and Y_h-axes. The X_h distances which have to be used are x, x-y, y, $\bar{y}$, y-x, $\bar{x}$; the Y_h distances are also x, x-y, y, $\bar{y}$, y-x, $\bar{x}$. These may be marked off to scale on triangular coordinate paper for the values of x and y adopted for the point P. This gives a set of coordinates such as is shown in Fig. 16. The use of this type of triangular coordinate paper may be illustrated in terms of point-group D_6 as follows.

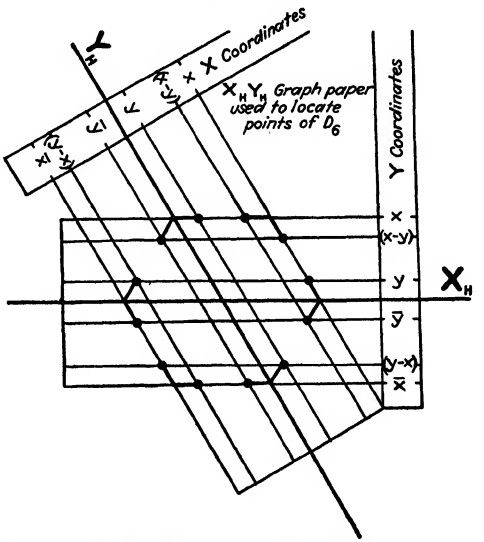

FIG. 16.—Hexagonal coordinates marked out in the X_h Y_h plane.

Imagine a template drawn to scale showing the point P at x, y, z. (If desired the Z_h-coordinate may be thought of as a pin stuck vertically into the template.) Clockwise rotation of this template in steps of 60° places the point P successively at x, y, z; $y, y\text{-}x, z$; $y\text{-}x, \bar{x}, z$; $\bar{x}, \bar{y}, z$; $\bar{y}, x\text{-}y, z$; $x\text{-}y, x, z$. Umklappung about the X_h- or F_h-axis produces the same result as Umklappung about the Y_h-axis. Restore the imaginary template to its original x, y, z position and perform the Umklappung operation about the Y_h-axis. This will place the point P at $\bar{x}, y\text{-}x, \bar{z}$. Now rotate the imaginary template in a clockwise direction in steps of 60°. The additional coordinates thus found are $x, y\text{-}x, \bar{z}$; $y, x, \bar{z}$; $x, x\text{-}y, \bar{z}$; $x\text{-}y, \bar{y}, \bar{z}$; $\bar{y}, \bar{x}, \bar{z}$.

The coordinates of equivalent positions of P have thus been found in the order listed by Wyckoff.

The application to the other hexagonal point-groups will be obvious from the above.

INDEX

D

H

I

N

O

P

Q

R